Edited by
Karl Esser

THE MYCOTA

A Comprehensive Treatise on Fungi
as Experimental Systems for Basic and Applied Research

Biology of the Fungal Cell VIII

Second Edition

Richard J. Howard and Neil A. R. Gow
Volume Editors

Springer

VISIT…

The Mycota

Edited by
K. Esser

The Mycota

I *Growth, Differentiation and Sexuality*
1st edition ed. by J.G.H. Wessels and F. Meinhardt
2nd edition ed. by U. Kües and R. Fischer

II *Genetics and Biotechnology*
Ed. by U. Kück

III *Biochemistry and Molecular Biology*
Ed. by R. Brambl and G. Marzluf

IV *Environmental and Microbial Relationships*
1st edition ed. by D. Wicklow and B. Söderström
2nd edition ed. by C.P. Kubicek and I.S. Druzhinina

V *Plant Relationships*
1st edition ed. by G. Carroll and P. Tudzynski
2nd edition ed. by H.B. Deising

VI *Human and Animal Relationships*
1st edition ed. by D.H. Howard and J.D. Miller
2nd edition ed. by A. Brakhage and P. Zipfel

VII *Systematics and Evolution*
Ed. by D.J. McLaughlin, E.G. McLaughlin, and P.A. Lemke†

VIII *Biology of the Fungal Cell*
Ed. by R.J. Howard and N.A.R. Gow

IX *Fungal Associations*
Ed. by B. Hock

X *Industrial Applications*
Ed. by H.D. Osiewacz

XI *Agricultural Applications*
Ed. by F. Kempken

XII *Human Fungal Pathogens*
Ed. by J.E. Domer and G.S. Kobayashi

XIII *Fungal Genomics*
Ed. by A.J.P. Brown

The Mycota

A Comprehensive Treatise
on Fungi as Experimental Systems
for Basic and Applied Research

Edited by K. Esser

VIII

Biology of the Fungal Cell
2nd Edition

Volume Editors:
R.J. Howard · N.A.R. Gow

With 86 Figures, 7 in Color, and 9 Tables

Springer

Series Editor

Professor Dr. Dr. h.c. mult. Karl Esser
Allgemeine Botanik
Ruhr-Universität
44780 Bochum, Germany

Tel.: +49 (234)32-22211
Fax.: +49 (234)32-14211
e-mail: Karl.Esser@rub.de

Volume Editors

Professor Dr. Richard J. Howard
DuPont Crop Genetics
Experimental Station E353
Powder Mill Road
Wilmington, DE 19880-0353, USA

Tel.: +1 (302)695-1494
Fax.: +1 (302)695-4509
e-mail: richard.j.howard@cgr.dupont.com

Professor Dr. Neil A.R. Gow
School of Medical Sciences
Institute of Medical Sciences
University of Aberdeen
Aberdeen AB25 2ZD, UK

Tel.: +44 (1224)555879
Fax: +44 (1224)555844
e-mail: n.gow@abdn.ac.uk

Library of Congress Control Number: 2007927884

ISBN 978-3-540-70615-1 Springer Berlin Heidelberg New York
ISBN 3-540-60186-4 1st ed. Springer Berlin Heidelberg New York

This work is subject to copyright. All rights are reserved, whether the whole or part of the material is concerned, specifically the rights of translation, reprinting, reuse of illustrations, recitation, broadcasting, reproduction on microfilm or in any other way, and storage in data banks. Duplication of this publication or parts thereof is permitted only under the provisions of the German Copyright Law of September 9, 1965, in its current version, and permissions for use must always be obtained from Springer-Verlag. Violations are liable for prosecution under the German Copyright Law.

Springer is a part of Springer Science+Business Media
springer.com
© Springer-Verlag Berlin Heidelberg 2001, 2007

The use of general descriptive names, registered names, trademarks, etc. in this publication does not imply, even in the absence of a specific statement, that such names are exempt from the relevant protective laws and regulations and therefore free for general use.

Editor: Dr. Dieter Czeschlik, Heidelberg, Germany
Desk editor: Dr. Andrea Schlitzberger, Heidelberg, Germany
Cover design: Erich Kirchner and WMXDesign GmbH, Heidelberg, Germany
Production and typesetting: LE-TEX Jelonek, Schmidt & Vöckler GbR, Leipzig, Germany

Printed on acid-free paper SPIN 11313472 31/3180 5 4 3 2 1 0

Karl Esser

(born 1924) is retired Professor of General Botany and Director of the Botanical Garden at the Ruhr-Universität Bochum (Germany). His scientific work focused on basic research in classical and molecular genetics in relation to practical application. His studies were carried out mostly on fungi. Together with his collaborators he was the first to detect plasmids in higher fungi. This has led to the integration of fungal genetics in biotechnology. His scientific work was distinguished by many national and international honors, especially three honorary doctoral degrees.

Richard J. Howard

(born 1952) studied hyphal growth and fungal cell structure during graduate work in the Department of Plant Pathology at Cornell University (USA). His M.S. thesis (1977) focused on the role of microtubules in hyphal tip growth. His Ph.D., completed in 1980, refined the technique of freeze substitution for the study of fungal cell ultrastructure. He received an NSF Postdoctoral Fellowship grant in the same year and worked with the human pathogen *Histoplasma capsulatum* at the Barnes Hospital medical campus of Washington University in St. Louis, MO (USA). In 1981 he accepted a research scientist position at the DuPont Experimental Station in Wilmington, DE (USA) where he conducted detailed studies of the rice blast pathogen *Magnaporthe grisea* and the cell biology of appressorium structure and function. Appointed in 2003 as a Research Fellow for Crop Genetics, his laboratory now serves as the core biological imaging center for DuPont's research and development interests.

Neil A. R. Gow

(born 1957) graduated from Edinburgh University and was a postgraduate at Aberdeen University. He was a postdoctoral fellow in Denver before returning to a faculty position at Aberdeen where he now holds a personal chair in Molecular Mycology. He is a founding member of the Aberdeen Fungal Group, which constitutes one of the single largest academic centres for medical mycology. He is the immediate Past President of the British Mycological Society and is a Vice President of the International Society for Human and Animal Mycology and holds fellowships of the Institute of Biology, the Royal Society of Edinburgh and the American Academy of Microbiology. He is currently the editor-in-chief of the journal *Fungal Genetics and Biology*. His research interest is in the growth, morphogenesis and pathogenesis of the human fungal pathogen *Candida albicans* and he has specific interests in the molecular genetics of cell wall biosynthesis in fungi and the directional growth responses of fungal cells as well as the virulence properties of medically important fungal species.

Series Preface

Mycology, the study of fungi, originated as a subdiscipline of botany and was a descriptive discipline, largely neglected as an experimental science until the early years of this century. A seminal paper by Blakeslee in 1904 provided evidence for selfincompatibility, termed "heterothallism", and stimulated interest in studies related to the control of sexual reproduction in fungi by mating-type specificities. Soon to follow was the demonstration that sexually reproducing fungi exhibit Mendelian inheritance and that it was possible to conduct formal genetic analysis with fungi. The names Burgeff, Kniep and Lindegren are all associated with this early period of fungal genetics research.

These studies and the discovery of penicillin by Fleming, who shared a Nobel Prize in 1945, provided further impetus for experimental research with fungi. Thus began a period of interest in mutation induction and analysis of mutants for biochemical traits. Such fundamental research, conducted largely with *Neurospora crassa*, led to the one gene: one enzyme hypothesis and to a second Nobel Prize for fungal research awarded to Beadle and Tatum in 1958. Fundamental research in biochemical genetics was extended to other fungi, especially to *Saccharomyces cerevisiae*, and by the mid-1960s fungal systems were much favored for studies in eukaryotic molecular biology and were soon able to compete with bacterial systems in the molecular arena.

The experimental achievements in research on the genetics and molecular biology of fungi have benefited more generally studies in the related fields of fungal biochemistry, plant pathology, medical mycology, and systematics. Today, there is much interest in the genetic manipulation of fungi for applied research. This current interest in biotechnical genetics has been augmented by the development of DNA-mediated transformation systems in fungi and by an understanding of gene expression and regulation at the molecular level. Applied research initiatives involving fungi extend broadly to areas of interest not only to industry but to agricultural and environmental sciences as well.

It is this burgeoning interest in fungi as experimental systems for applied as well as basic research that has prompted publication of this series of books under the title *The Mycota*. This title knowingly relegates fungi into a separate realm, distinct from that of either plants, animals, or protozoa. For consistency throughout this Series of Volumes the names adopted for major groups of fungi (representative genera in parentheses) are as follows:

Pseudomycota

Division:	Oomycota (*Achlya*, *Phytophthora*, *Pythium*)
Division:	Hyphochytriomycota

Eumycota

Division:	Chytridiomycota (*Allomyces*)
Division:	Zygomycota (*Mucor*, *Phycomyces*, *Blakeslea*)
Division:	Dikaryomycota
Subdivision:	Ascomycotina

Class:	Saccharomycetes (*Saccharomyces*, *Schizosaccharomyces*)
Class:	Ascomycetes (*Neurospora*, *Podospora*, *Aspergillus*)
Subdivision:	Basidiomycotina
Class:	Heterobasidiomycetes (*Ustilago*, *Tremella*)
Class:	Homobasidiomycetes (*Schizophyllum*, *Coprinus*)

We have made the decision to exclude from *The Mycota* the slime molds which, although they have traditional and strong ties to mycology, truly represent nonfungal forms insofar as they ingest nutrients by phagocytosis, lack a cell wall during the assimilative phase, and clearly show affinities with certain protozoan taxa.

The Series throughout will address three basic questions: what are the fungi, what do they do, and what is their relevance to human affairs? Such a focused and comprehensive treatment of the fungi is long overdue in the opinion of the editors.

A volume devoted to systematics would ordinarily have been the first to appear in this Series. However, the scope of such a volume, coupled with the need to give serious and sustained consideration to any reclassification of major fungal groups, has delayed early publication. We wish, however, to provide a preamble on the nature of fungi, to acquaint readers who are unfamiliar with fungi with certain characteristics that are representative of these organisms and which make them attractive subjects for experimentation.

The fungi represent a heterogeneous assemblage of eukaryotic microorganisms. Fungal metabolism is characteristically heterotrophic or assimilative for organic carbon and some nonelemental source of nitrogen. Fungal cells characteristically imbibe or absorb, rather than ingest, nutrients and they have rigid cell walls. The vast majority of fungi are haploid organisms reproducing either sexually or asexually through spores. The spore forms and details on their method of production have been used to delineate most fungal taxa. Although there is a multitude of spore forms, fungal spores are basically only of two types: (i) asexual spores are formed following mitosis (mitospores) and culminate vegetative growth, and (ii) sexual spores are formed following meiosis (meiospores) and are borne in or upon specialized generative structures, the latter frequently clustered in a fruit body. The vegetative forms of fungi are either unicellular, yeasts are an example, or hyphal; the latter may be branched to form an extensive mycelium.

Regardless of these details, it is the accessibility of spores, especially the direct recovery of meiospores coupled with extended vegetative haploidy, that have made fungi especially attractive as objects for experimental research.

The ability of fungi, especially the saprobic fungi, to absorb and grow on rather simple and defined substrates and to convert these substances, not only into essential metabolites but into important secondary metabolites, is also noteworthy. The metabolic capacities of fungi have attracted much interest in natural products chemistry and in the production of antibiotics and other bioactive compounds. Fungi, especially yeasts, are important in fermentation processes. Other fungi are important in the production of enzymes, citric acid and other organic compounds as well as in the fermentation of foods.

Fungi have invaded every conceivable ecological niche. Saprobic forms abound, especially in the decay of organic debris. Pathogenic forms exist with both plant and animal hosts. Fungi even grow on other fungi. They are found in aquatic as well as soil environments, and their spores may pollute the air. Some are edible; others are poisonous. Many are variously associated with plants as copartners in the formation of lichens and mycorrhizae, as symbiotic endophytes or as overt pathogens. Association with animal systems varies; examples include the predaceous fungi that trap nematodes, the microfungi that grow in the anaerobic environment of the rumen, the many insect-associated fungi and the medically important pathogens afflicting humans. Yes, fungi are ubiquitous and important.

There are many fungi, conservative estimates are in the order of 100,000 species, and there are many ways to study them, from descriptive accounts of organisms found in nature to laboratory experimentation at the cellular and molecular level. All such studies expand our knowledge of fungi and of fungal processes and improve our ability to utilize and to control fungi for the benefit of humankind.

We have invited leading research specialists in the field of mycology to contribute to this Series. We are especially indebted and grateful for the initiative and leadership shown by the Volume Editors in selecting topics and assembling the experts. We have all been a bit ambitious in producing these Volumes on a timely basis and therein lies the possibility of mistakes and oversights in this first edition. We encourage the readership to draw our attention to any error, omission or inconsistency in this Series in order that improvements can be made in any subsequent edition.

Finally, we wish to acknowledge the willingness of Springer-Verlag to host this project, which is envisioned to require more than 5 years of effort and the publication of at least nine Volumes.

Bochum, Germany
Auburn, AL, USA
April 1994

Karl Esser
Paul A. Lemke
Series Editors

Addendum to the Series Preface

In early 1989, encouraged by Dieter Czeschlik, Springer-Verlag, Paul A. Lemke and I began to plan *The Mycota*. The first volume was released in 1994, 12 volumes followed in the subsequent years. Unfortunately, after a long and serious illness, Paul A. Lemke died in November 1995. Thus, it was my responsibility to proceed with the continuation of this series, which was supported by Joan W. Bennett for Volumes X–XII.

The series was evidently accepted by the scientific community, because several volumes are out of print. Therefore, Springer-Verlag has decided to publish completely revised and updated new editions of Volumes I, II, III, IV, V, VI, and VIII. I am glad that most of the volume editors and authors have agreed to join our project again. I would like to take this opportunity to thank Dieter Czeschlik, his colleague, Andrea Schlitzberger, and Springer-Verlag for their help in realizing this enterprise and for their excellent cooperation for many years.

Bochum, Germany
February 2007

Karl Esser

Volume Preface to the Second Edition

A *place* for Fungi in our world has been well established. In the years since the early 1990s the body of evidence accumulating and defining these organisms as a separate Kingdom among life on earth has been (almost) universally accepted. On a molecular basis, there remain a few questions concerning the deep divides low in the branches of the evolutionary tree. And as one considers the mid- and finer branches, there will not likely be any shock waves big enough to rattle the tree or our thinking of the Fungi (e.g. Eumycota) as a distinct group of organisms – but there remains much to be done and learned. Certainly the work of phylogeneticists is not over, but especially, nor is that of cell biologists – far from it! Indeed the technological and conceptual advances made in fungal cell biology have been so rapid that a vast literature is being generated that explores how fungal cells grow and divide. Since the previous edition of this volume in this series was published these new methods in single-cell imaging, video microscopy, functional proteomics and gene expression have been widely applied to core questions related to fungal growth and development. The current edition incorporates the latest research using these new approaches and new perspectives that have been gained. It also adds new chapters in contemporary topics that have emerged in recent years to the areas that have been reviewed in the past as core areas of fungal cell biology.

What makes the fungal cell unique among eukaryotes and what features are shared? This volume addresses some of the most prominent and fascinating facets of questions as they pertain to the growth and development of both yeast and hyphal forms of fungi, beginning with subcellular components, then cell organization, polarity, growth, differentiation and beyond – to the cell biology of spores, biomechanics of invasive growth, plant pathogenesis, mycorrhizal symbiosis and colonial networks. Throughout this volume, structural, molecular and ecological aspects are integrated to form a contemporary look at the biology of the fungal cell.

Chapter 1 endeavors to *generate a new perspective and appreciation for the unique qualities of the endomembrane system in filamentous fungi*, as opposed to other eukaryotes and sometimes also yeast cells, by drawing connections between structural and molecular data. In filamentous fungi the tubular vacuole system is one component of the endomembrane system, as described in Chap. 2, which plays a most important role in transport – of nutrients, proteins and membrane elements – at the subcellular and intercellular level. The importance of these vacuolar tubules has generally not been widely appreciated but they *are now beginning to take their rightful place alongside vesicles as major mediators of cellular traffic*. Their vital role in intercellular traffic of late diverging fungi is dependent upon the perforate septation of hyphae that enables more complex multicellular differentiation. Chapter 3 offers a review of the Woronin body, an organelle unique to these "advanced" members of the Eumycota (i.e. not found among non-septate filamentous fungi) that is also indispensable in the formation of large multicellular structures. The ability of these fungi to establish tissues and large organs, and shared with animals and plants, is a consequence of Woronin body function in gating cell-to-cell movement and loss of contents upon cell injury and is thus of great evolutionary significance.

A molecular and genomic component to the analysis of each of these cellular constituents has been essential in bringing our current understanding to new levels. Similarly, these same tools provide a fresh insight into the most obvious manifestation of the fungal cell, the cell wall, and Chap. 4 includes additional impetus for new research efforts that go beyond the *Saccharomyces* model. This same message is delivered in Chaps. 5 and 6. Central to this volume, and to fungal cell biology, is the topic of growth as it relates to the polarity of yeast and hyphal cells. These two chapters review these aspects from different perspectives and thus provide a more comprehensive synthesis of the similarities and likely differences that underlie the biology of the major growth forms exhibited by cells of fungi. Chapter 7 continues these considerations with regard to the "pleomorphic" pathogen *Candida albicans*, an extremely important organism in human health as well as a model allowing the functional dissection of morphogenetic signaling pathways. The very recently discovered participation by *C. albicans*, and another important human pathogen *C. glabrata*, in mating processes led to additional findings as reviewed in Chap. 8 that point to a possible connection between the phenotypic switching processes of morphogenesis and pathogenesis, and an obvious practicality for understanding the biology of these growth forms and cellular events.

The biology of fungal cells that enable the pathogenesis of plants is reviewed in the following three chapters, from the very first stages of contact to the mechanisms of invasive hyphal growth and the various cell structures elaborated for this purpose. That hyphae can penetrate solid substances *is one of the defining characteristics of the fungi* – as pointed out in Chap. 10, this is important not only during plant pathogenesis, but in every interaction between fungal cells and their environment. The essential ecological role of certain fungi with the ability to form mycorrhizae, a sophisticated *symbiotic relationship between roots and these fungi that is one of the most prevalent associations in all terrestrial ecosystems*, is described in Chap. 12. Though obviously important, we still known very little about the biology of these plant–fungus interactions but, as you will read, many tools of contemporary cell biology are being applied to help fill these knowledge gaps. The final chapter of the volume concerns the form and function of interconnected, self-organized fungal networks typically occupying many square meters of space that are ubiquitous in nature but about which we also know quite little.

As a whole this volume offers many small windows through which the reader can appreciate both the unique and shared biology of the fungal cell as well as how and why these organisms represent remarkable and fascinating models for study.

Wilmington, Delaware, USA
Aberdeen, Scotland, UK
February 2007

Richard J. Howard
Neil A. R. Gow
Volume Editors

Volume Preface to the First Edition

Research in cell biology has exploded over the past decade, rendering impossible the task of mortals to stay abreast of progress in the entire discipline. Anyone interested in the biology of the fungal cell has most certainly noticed this trend, even in this fringe field of the larger subject. Indeed, to understand the biology of the fungal cell is to understand its interactions with the environment and with other cells, encompassing a tremendously broad array of subdisciplines. In fact, the Mycota represent one of the last, largely unexplored gold mines of biological diversity. From cellular morphogenesis to colony formation and pathogenesis, this volume provides examples of the breadth and depth of fungal cell biology. Of course, there are many topics that could not be addressed in such limited space, but no matter. Our primary aim has been to provide a selected sampling of contemporary topics at the forefront of fungal cell biology to facilitate the dissemination of information across and between the many enclaves of researchers who study fungal cell biology. These include cell biologists, cytologists, developmental biologists, ecologists, geneticists, medical mycologists, microbiologists, molecular biologists, plant pathologists, and physiologists – many of whom would never consider themselves *mycologists*, and what a pity. We hope that the current volume will, in some ways, serve to bridge the gaps and inequalities that exist between these mycologists and to unite their efforts toward the advancement of our science.

This volume is divided into two parts. The first part considers a sampling of *behavioral* topics – *how*, or in what manner and to what effect, do cells of fungi behave in various environments; how does environment influence cell biology; how do the cells affect their surroundings, animate and inanimate? Topics include invasive growth, a defining characteristic of the Mycota; controls of cell polarity and shape, and morphological changes that are essential for the virulence of many pathogenic fungi; and a detailed consideration of the ways in which groups of cells of the same species form an individualistic coordinated organism.

The second part of the volume looks at the fungal cell as a structural continuum – from proteins, e.g. hydrophobins, that manage patterns of growth and development in space, to extracellular matrices, molecular connections between extra- and intracellular domains, including the cytoskeleton, to the molecular patterns of genomes that dictate things we do not yet know exist. All of these topics are perfused by recent advances in molecular genetics and are written at a time when fungal genome databases are just becoming established as a tool for the future. We hope that this volume will not only demonstrate that fungal cell biology is useful in representing accessible systems for exploration of biological systems as a whole, but also in illuminating aspects of fungal biology that are unique and fascinating in their own right. We are challenged by an amazing universe of fungal cell biology waiting to be explored.

Wilmington, Delaware, USA
Aberdeen, Scotland, UK
March 2001

Richard J. Howard
Neil A. R. Gow
Volume Editors

Contents

1 The Endomembrane System of the Fungal Cell
T.M. Bourett, S.W. James, R.J. Howard 1

2 Motile Tubular Vacuole Systems
A.E. Ashford, W.G. Allaway 49

3 The Fungal Woronin Body
T. Dhavale, G. Jedd 87

4 A Molecular and Genomic View of the Fungal Cell Wall
F.M. Klis, A.F.J. Ram, P.W.J. De Groot 97

5 The Cytoskeleton and Polarized Growth of Filamentous Fungi
R. Fischer 121

6 Polarised Growth in Fungi
P. Sudbery, H. Court 137

7 Signal Transduction and Morphogenesis in Candida albicans
A.J.P. Brown, S. Argimón, N.A.R. Gow 167

8 Mating in Candida albicans and Related Species
D.R. Soll 195

9 Ions Regulate Spore Attachment, Germination, and Fungal Growth
B.D. Shaw, H.C. Hoch 219

10 Biomechanics of Invasive Hyphal Growth
N.P. Money 237

11 Cell Biology of Fungal and Oomycete Infection of Plants
A.R. Hardham 251

12 Fair Trade in the Underworld: the Ectomycorrhizal Symbiosis
F. Martin 291

13 Network Organisation of Mycelial Fungi
M. Fricker, L. Boddy, D. Bebber 309

Biosystematic Index 331

Subject Index 333

List of Contributors

W.G. Allaway
School of Biological Sciences, The University of Sydney, Sydney, NSW 2006, Australia

S.Argimón (e-mail: s.argimon@abdn.ac.uk)
School of Medical Sciences, University of Aberdeen,
Current address:
Department of Microbiology, Columbia University,
Hammer Building, 701 West 168th Street, New York, NY 10032

A.E. Ashford (e-mail: a.ashford@unsw.edu.au)
School of Biological Earth and Environmental Sciences,
The University of New South Wales, Sydney, NSW 2052, Australia

D. Bebber
Department of Plant Sciences, University of Oxford,
South Parks Road, Oxford, OX1 3RB, UK

L. Boddy
Cardiff School of Biosciences, Cardiff University,
Cardiff, CF10 3US, UK

T.M. Bourett (e-mail: timothy.m.bourett@cgr.dupont.com)
DuPont Crop Genetics, Wilmington, DE 19880-0353, USA

A.J.P. Brown (e-mail: al.brown@abdn.ac.uk)
School of Medical Sciences, Institute of Medical Sciences, University of Aberdeen,
Foresterhill, Aberdeen, AB25 2ZD, UK

H. Court
Department of Molecular Biology and Biotechnology, Sheffield University,
Western Bank, Sheffield S10 2TN, UK

T. Dhavale (e-mail: ns_tjdha@tll.org.sg)
Temasek Life Sciences Laboratory, National University of Singapore,
1 Research Link, Singapore 117604

R. Fischer (e-mail: reinhard.fischer@bio.uni-karlsruhe.de)
Max-Planck-Institute for terrestrial Microbiology,
Karl-von-Frisch-Str., D-35043 Marburg
and
University of Karlsruhe, Institute for Applied Biosciences, Dept. of Applied Microbiology,
Hertzstrasse 16, D-76187 Karlsruhe, Germany

M. Fricker (e-mail: mark.fricker@plants.ox.ac.uk)
Department of Plant Sciences, University of Oxford,
South Parks Road, Oxford, OX1 3RB, UK

N.A.R. Gow (e-mail: n.gow@abdn.ac.uk)
School of Medical Sciences, Institute of Medical Sciences, University of Aberdeen,
Foresterhill, Aberdeen, AB25 2ZD, UK

P.W.J. De Groot (e-mail: p.w.j.degroot@uva.nl)
Swammerdam Institute for Life Sciences, University of Amsterdam,
1018 WV Amsterdam, The Netherlands

A.R. Hardham (e-mail: adrienne.hardham@anu.edu.au)
Plant Cell Biology Group, Research School of Biological Sciences,
The Australian National University, Canberra, ACT 2601, Australia

H.C. Hoch
Department of Plant Pathology, Cornell University,
New York State Agricultural Experiment Station, Geneva, NY 14456

R.J. Howard (e-mail: richard.j.howard@cgr.dupont.com)
DuPont Crop Genetics, Wilmington, DE 19880-0353, USA

S.W. James (e-mail: sjames@gettysburg.edu)
Biology Department, Gettysburg College, Gettysburg, PA 17325, USA

G. Jedd (e-mail: gregory@tll.org.sg)
Temasek Life Sciences Laboratory, and Department of Biological Sciences,
National University of Singapore, 1 Research Link, Singapore

F.M. Klis (e-mail: f.m.klis@uva.nl)
Swammerdam Institute for Life Sciences, University of Amsterdam,
1018 WV Amsterdam, The Netherlands

F. Martin (e-mail: fmartin@nancy.inra.fr)
UMR INRA/UHP 1136 'Interactions Arbres/Micro-Organismes', IFR110,
Centre INRA de Nancy, 54280 Champenoux, France

N.P. Money (e-mail: moneynp@muohio.edu)
Department of Botany, Miami University, Oxford, OH 45056, USA

A.F.J. Ram (e-mail: ram@rulbim.leidenuniv.nl)
Institute of Biology, Clusius Laboratory, Leiden University,
2333 AL Leiden, The Netherlands

B.D. Shaw (e-mail: bdshaw@tamu.edu, hch1@cornell.edu)
Department of Plant Pathology and Microbiology, Program for the Biology
of Filamentous Fungi, 2132 TAMU, Texas A&M University, College Station
TX 77843, USA

D.R. Soll (e-mail: david-soll@uiowa.edu)
Department of Biological Sciences, The University of Iowa, Iowa City, IA 52242, USA

P. Sudbery (e-mail: P.Sudbery@shef.ac.uk)
Department of Molecular Biology and Biotechnology, Sheffield University,
Western Bank, Sheffield S10 2TN, UK

1 The Endomembrane System of the Fungal Cell

T.M. Bourett[1], S.W. James[2], R.J. Howard[1]

CONTENTS

I. **Introduction** 1
II. **Tools for Study of the Endomembrane System** 2
III. **Secretory Pathway** 24
A. Endoplasmic Reticulum 24
B. Golgi Apparatus 27
C. Exocytosis/Secretion 32
IV. **Endocytic Pathway: Plasma Membrane, Endocytosis, Endosomes, and Vacuoles** . . . 36
V. **Enigmatic Compartments** 39
VI. **Conclusions** 40
References 42

I. Introduction

The eukaryotic endomembrane system can be defined as all the organelles comprising both the endocytic and secretory pathways, including the endoplasmic reticulum (ER), Golgi apparatus, endosomes, multivesicular bodies, lysosomes, vacuoles, plasma membrane, and transport intermediates such as vesicles and microvesicles. These membrane-enclosed compartments form a complex intracellular system that can comprise a large percentage of the total cellular volume. To understand the interrelationships between these intracellular compartments it is helpful to consider how each might have evolved. One of the most significant advances in evolution from prokaryotes to eukaryotes was the development of extensive cellular compartmentalization (Stanier 1970), facilitated by the proliferation of internal membranes (Blobel 1980). This elaboration of internal membranes allowed for an organelle-based division of labor for the biochemistry that was previously restricted to the surface of prokaryotic cells (Becker and Melkonian 1996). This in turn allowed for the development of large cells with vastly reduced surface area:volume ratios – the average eukaryotic cell is 10^2–10^3 times greater in volume than prokaryotes (Dacks and Field 2004).

Intracellular compartments can be divided into three distinct topological groups: (1) the nucleus and cytosol, (2) mitochondria, and (3) organelles of the endomembrane system, based upon the predominant means of protein transport within each group (Blobel 1980): gated between the cytosol and nucleus via nuclear pores, transmembrane in the case of mitochondria, and mainly vesicle-mediated. Organelles are membrane-bounded compartments that contain specific chemistry. The protein constituents of each organelle define its structure and function. Since most proteins are synthesized in the cytosol, mechanisms exist for delivery of these proteins to the proper organelle. Therefore, an understanding of protein transport is inexorably connected with understanding the endomembrane system. In large part organelle homeostasis is controlled by limiting the flow of molecules both into and out of each compartment. Thus, to understand the workings of the eukaryotic cell it is fundamental to understand the defining biochemical activities for each organelle, how molecules move between them, and how the compartments are created and maintained. For the compartments that comprise the endomembrane system this is a daunting task considering all the interorganellar communication that occurs concurrently with the flow of biomaterials through the system. It is even more remarkable in fungal hyphae, perhaps the ultimate fast growing polarized eukaryotic cell. Cells of septate fungi can be upwards of 200 times longer than wide (and coenocytic Zygomyetes much longer than this) with a hyphal apex that extends a distance of up to four times the hyphal diameter every minute (Collinge and Trinci 1974; López-Franco et al. 1995).

While there is certainly much overlap in the strategies adopted by various eukaryotes, the

[1] DuPont Crop Genetics, Wilmington, DE 19880-0353, USA
[2] Biology Department, Gettysburg College, Gettysburg, PA 17325, USA

Biology of the Fungal Cell, 2nd Edition
The Mycota VIII
R.J. Howard and N.A.R. Gow (Eds.)
© Springer-Verlag Berlin Heidelberg 2007

endomembrane system of filamentous fungi has several singular structural features that set it apart from that of other higher eukaryotes. For example, the Golgi apparatus in filamentous fungi lacks stacks of membrane cisternae and does not disperse during mitosis. Also, there is a lack of structural evidence to support the existence of clathrin-coated vesicles, vectors that are responsible for the bulk of endocytosis and trans-Golgi network trafficking. Some of these differences appear to be shared between filamentous fungi and their yeast relatives while others are not (Tables 1.1–1.6). Whether these structural differences underlie significant functional differences remains to be answered and could perhaps be exploited in the design of control strategies against fungi, many of which have a significant negative impact upon humankind.

As we consider the endomembrane system of filamentous fungi, we unavoidably focus on the hyphal tip cell (Fig. 1.1) where the most obvious product of that system, polarized growth, is manifest. Additionally, in terms of morphology and ultrastructure, the hyphal tip cell is undoubtedly the most studied of all fungal cells. The overall distribution of endomembrane compartments related to the tip growth process is carefully orchestrated and maintained; and perturbation of the hyphal apex is evidenced by a rapid redistribution of cellular endomembrane components, particularly those associated with the Spitzenkörper. For further related discussion, the reader is referred to Chaps. 5 and 6 in this volume, respectively by Fischer, and by Sudbery and Court.

The present chapter was written in part to spur further inquiries in this area by bringing together disjointed sources of information. By emphasizing morphogenesis and structure we aim to draw connections between microscope-based structural knowledge and molecular data, and hope that this undertaking will generate a new perspective and appreciation for the unique qualities of the endomembrane system in filamentous fungi.

II. Tools for Study of the Endomembrane System

The discovery and manipulation of **fluorescent reporter molecules** has revolutionized cell biology and been exploited to study fungi (Cormack 1998; Lorang et al. 2001; Czymmek et al. 2005). Fluorescent protein tagging methods have aided greatly investigations of the endomembrane system of other eukaryotes (Hanson and Köhler 2001). These probes can be used to determine the subcellular distribution of a given molecule as well as assess its mobility and potential protein–protein interactions. In addition, fluorescent protein markers can be used to label specific compartments, monitoring their size, shape, mobility and time-resolved changes that occur during development or in response to environmental stimuli. For example, a yeast deletion library was used in conjunction with a background strain with a plasma membrane-targeted GFP to identify genes required for precise delivery of this protein to its proper destination (Proszynski et al. 2005). These types of studies could do much to advance our understanding.

Recent advances in gene targeting and the development of fusion PCR for gene-tagging have combined to make large-scale gene and genome manipulation feasible in *Neurospora crassa*, *Aspergillus nidulans*, and *A. fumigatus*. First, disruption of the non-homologous end joining DNA repair pathway (NHEJ), by deletion of the KU70 or KU80 genes, essentially eliminates the historically difficult problem of inefficient gene targeting in these fungi (Ninomiya et al. 2004; da Silva Ferreira et al. 2006; Krappman et al. 2006; Nayak et al. 2006). For example, in *A. nidulans* cells lacking KU70 or KU80, ~90% of transformants are

Table. 1.1. (on page 3–4) Endoplasmic reticulum proteins in fungi. *A. nidulans* (An) ER proteins were identified by tBlastn of the An genome (http://www.broad.mit.edu/annotation/genome/aspergillus_nidulans/) using *S. cerevisiae* (Sc) proteins. Sc proteins were obtained from Gene Ontology annotation for yeast endoplasmic reticulum (www.yeastgenome.org). Proteins were further defined by forward and reverse tBlastn and blastp between Sc and An genomes, tBlastn of An proteins against the An genome, and tBlastn and blastp of An and Sc proteins to all Fungal Genome Initiative (FGI) genomes (http://www.broad.mit.edu/annotation/fgi/)

Table. 1.2. (on page 5–7) Golgi proteins. *A. nidulans* (An) ER proteins were identified by tBlastn of the An genome (http://www.broad.mit.edu/annotation/genome/aspergillus_nidulans/) using *S. cerevisiae* (Sc) proteins. Sc proteins were obtained from Gene Ontology annotation for yeast golgi (www.yeastgenome.org). Proteins were further defined by forward and reverse tBlastn and blastp between Sc and An genomes, tBlastn of An proteins against the An genome, and tBlastn and blastp of An and Sc proteins to all Fungal Genome Initiative (FGI) genomes (http://www.broad.mit.edu/annotation/fgi/)

S. cerevisiae	*A. nidulans*		Other fungi[a]	
Endoplasmic reticulum membrane proteins				
SEC61 translocation complex				
SBH1, SBH2	AN0417	($8e^{-14}$, $5e^{-19}$)	Ci, Cg, Nc, Mg, Bc, Ss	($1e^{-110} \rightarrow 5e^{-08}$)
SSS1	AN4589	($2.6e^{-16}$)	Bc, Ss, Mg, Ci, Cg, Ro, Nc, Cn	($7e^{-25} \rightarrow 0.001$)
SEC61, SSH1	AN7721	($1e^{-123}$, $5e^{-50}$)	Ci, Ss, Nc,Cg, Mg,Cn, Ro, Bc	($0.0 \rightarrow 1e^{-119}$)
SEC63 pre-secretory protein translocation complex				
SEC62	AN6269	($4e^{-24}$)	Ci, Bc, Ss, Mg, Nc, Cg,Ro, Cn	($1e^{-146} \rightarrow 1e^{-25}$)
SEC63	AN0834	($5e^{-32}$)	Ci, Bc, Ss, Mg, Nc, Cg,Ro, Cn	($0.0 \rightarrow 6e^{-29}$)
SEC66	AN1442	($2e^{-09}$)	Ss, Nc, Cg, Mg, Ci, Bc, Cn, Ro	($1e^{-97} \rightarrow 1e^{-12}$)
SEC72	AN10987	($7e^{-07}$)	Ci, Nc, Mg, Cg, Bc, Ss,Ro, Cn	($2e^{-56} \rightarrow 3e^{-06}$)
Other ER membrane proteins				
VPS64 (*cytoplasm→ vacuole protein targeting*)	AN4632	($2e^{-18}$)	Ci, Nc, Ss, Mg, Bc, Cg, Ro	($1e^{-150} \rightarrow 9e^{-22}$)
HSD1 (*unknown function*)	AN3177	($1e^{-43}$)	Ci, Bc, Mg, Cg, Nc, Ss, Cn, Ro	($1e^{-122} \rightarrow 3e^{-15}$)
PHO86 (*packaging PHO84 into COPII vesicles*)	None		None	
NPL4 (*complex w/CDC48, UFD1*)	AN0295	($1e^{-127}$)	Ci., Ss, Cg, Bc, Nc, Mg, Ro, Cn	($0.0 \rightarrow 2e^{-88}$)
ERI1 (*GPI–GnT complex*)	AN8536	(0.74)	Mg, Bc, Nc, Ss, Cg, Ci	($1e^{-20} \rightarrow 1e^{-05}$)
CUE1 (*recruits UBC7, protein degradation*)	AN5900	(0.072)	Ci, Bc, Ss, Mg, Nc, Cg, Cn	($1e^{-44} \rightarrow 0.003$)
ERG28 (*interacts w/ERG6, -26, -27*)	AN5862	($8e^{-17}$)	Ci, Bc, Ss, Nc, Cg, Mg, Ro, Cn	($1e^{-30} \rightarrow 2e^{-06}$)
DER1 (*ER-associated protein degradation*)	Contig 109[b]	(0.010)	Nc, Mg, Ci	($3e^{-10} \rightarrow 3e^{-07}$)
CSG2 (*mannosylation*)	AN0674	(0.016)	Ci, Ss, Bc, Mg, Nc, Cg, Ro, Cn	($1e^{-109} \rightarrow 7e^{-11}$)
YET1, YET2, YET3 (Hu*BAP31 homolog*)	AN0819	(0.001, 0.028, $3e^{-13}$)	Ci, Nc, Cg, Mg, Ss, Bc, Ro	($5e^{-56} \rightarrow 1e^{-04}$)
STE14 (*farnesyl Cys-COOH methyltransferase*)	AN6162	($4e^{-45}$)	Ci, Nc, Cg, Mg, Ro, Bc, Cn, Ss	($6e^{-68} \rightarrow 2e^{-04}$)
BIG1 (*cell wall β-glucan content*)	AN5684	(2.4)	Bc, Ci, Ss, Mg, Cg, Nc	($3e^{-23} \rightarrow 2e^{-09}$)
ERD1 (*retention of luminal ER proteins*)	AN5682	($8e^{-07}$)	Nc, Mg, Cg, Ss Bc, Ci, Cn	($4e^{-94} \rightarrow 6e^{-11}$)
ERD2 (*binds HDEL motif in ER proteins*)	AN11226	($7e^{-42}$)	Ss, Bc, Nc, Ci, Mg, Cg, Cn, Ro	($6e^{-74} \rightarrow 1e^{-36}$)
Novel additional ERD2 homolog	AN4528	($2e^{-19}$)	Nc, Bc, Mg, Ss, Cg, Cn	($2e^{-70} \rightarrow 4e^{-24}$)
VPH2 (*vacuolar-ATPase assembly*)	None		None	
VMA21 (*vacuolar-ATPase assembly*)	AN2975[c]	–	Ss, Mg, Cg	($2e^{-05} \rightarrow 0.028$)
VMA22 (*vacuolar-ATPase assembly*)	AN4766[d]	–	Nc, Mg, Cg, Ci, Bc, Ro, Ss	($2e^{-18} \rightarrow 0.68$)
MCD4 (*GPI anchor synthesis*)	AN7049	($1e^{-140}$)	Ci, Bc, Cg, Nc, Ss, Mg, Ro	($0.0 \rightarrow 6e^{-51}$)
RCR1 (*chitin deposition in cell wall*)	AN1001	(0.41)	Ci, Cg, Nc, Ss, Mg, Bc, Ro	($1e^{-126} \rightarrow 1e^{-27}$)
KAR5 (*nuclear membrane fusion*)	AN1771	($2e^{-06}$)	Ci, Mg, Bc, Cg, Nc, Ss	($2e^{-30} \rightarrow 3e^{-06}$)
FRT1 (*calcineurin substrate*)	Not found		MGG_09764 ?	(0.79)
FRT2 (*interacts with FRT1*)	None		None	
Endoplasmic reticulum lumenal proteins				
ZRG17 (*possible zinc uptake function*)	AN1076	($1e^{-24}$)	Ci, Bc, Ss, Mg, Nc, Cg	($1e^{-130} \rightarrow 1e^{-81}$)
PGA2 (*maturation of GAS1, PHO8*)	AN0597[e]	–	Mg, Nc, Ci, Ss, Bc	($4e^{-06} \rightarrow 0.005$)
PGA3 (*maturation of GAS1, PHO8*)	AN6366	($3e^{-55}$)	Ci, Bc, Ss, Mg, Nc, Cg, Ro, Cn	($1e^{-135} \rightarrow 2e^{-72}$)
INP54 (*ptdins 4,5-bisphosphate-5-phosphatase*)	AN11023	($6e^{-06}$)	Ci, Ss, Mg, Nc, Cg, Bc, Ro	($7e^{-96} \rightarrow 5e^{-11}$)
Disulfide bond formation				
ERV2 (*PI 4,5-bisphosphate-5-phosphatase*)	AN3759	($5e^{-30}$)	Ci, Nc, Mg, Ss, Bc	($1e^{-44} \rightarrow 1e^{-35}$)
EPS1 (*PDI1-related protein*)	AN5970	($1e^{-05}$)	Ci, Ss, Bc, Cg, Nc, Mg, Ro	($0.0 \rightarrow 5e^{-32}$)
PDI1, EUG1 (*protein disulfide isomerase*)	AN7436	($3e^{-49}$, $6e^{-33}$)	Ci, Nc, Cg, Ss, Mg, Bc, Ro, Cn	($1e^{-179} \rightarrow 3e^{-73}$)

S. cerevisiae	*A. nidulans*		Other fungi[a]	
MPD1 (*inhibits CNE1 chaperone activity*)	AN0248	($5e^{-24}$)	Ci, Nc, Mg, Ss, Bc, Cg, Ro, Cn	($1e^{-112} \rightarrow 5e^{-17}$)
ER chaperones/unfolded protein response				
SHR3 (*ER packaging chaperone*)	AN1845	($6e^{-19}$)	Ci, Ss, Bc, Mg, Nc	($1e^{-58} \rightarrow 3e^{-11}$)
ERJ5 (*co-chaperone, DnaJ-like domain*)	AN5770	($3e^{-04}$)	Ci, Mg, Cg, Bc, Nc, Ss, Ro, Cn	($1e^{-102} \rightarrow 9e^{-06}$)
ORM1, ORM2 (*unfolded protein response*)	AN1933	($1e^{-42}$, $8e^{-25}$)	Ci, Cg, Ss, Bc, Mg, Nc, Cn, Ro	($7e^{-82} \rightarrow 1e^{-19}$)
ERO1 (*oxidative protein folding*)	AN1510	($4e^{-71}$)	Ci, Ss, Bc, Mg, Nc, Cg, Ro, Cn	($1e^{-179} \rightarrow 3e^{-51}$)
FES1 (*HSP70 nucleotide exchange factor*)	AN6543	($6e^{-28}$)	Cg, Mg, Ci, Nc, Ss, Bc, Ro, Cn	($6e^{-52} \rightarrow 2e^{-09}$)
LHS1 (*HSP70 family chaperone*)	AN0847	($2e^{-44}$)	Ci, Ss, Bc, Nc, Mg, Cg, Cn, Ro	($0.0 \rightarrow 3e^{-47}$)
SIL1 (*KAR2 nucleotide exchange factor*)	BC1G_08026.1[f]	($8e^{-12}$)	Bc, Cg, Nc, Mg	($8e^{-12} \rightarrow 5e^{-08}$)
KAR2/BiP (*ATPase, chaperone*)	AN2062	(0.0)	Ci, Bc, Ss, Nc, Mg, Cg, Ro, Cn	($0.0 \rightarrow 0.0$)
CPR5 (*ER cyclophilin*)	AN4467	($7e^{-41}$)	Cg, Nc, Ss, Ro, Ci, Bc, Mg	($9e^{-63} \rightarrow 9e^{-41}$)
HRD1 (*ubiquitin-protein ligase for ERAD*)	AN1488	($2e^{-24}$)	Ci, Ss, Bc, Cg, Nc, Mg, Cn	($0.0 \rightarrow 3e^{-35}$)
CNE1 (*calnexin, ER chaperone*)	AN3592	($2e^{-48}$)	Ci, Nc, Cg, Mg, Ss, Bc, Cn, Ro	($0.0 \rightarrow 2e^{-39}$)
HLJ1 (*co-chaperone for HSP40*)	AN4441	($5e^{-18}$)	Ss, Bc, Cg, Mg, Nc, Ci, Ro	($5e^{-78} \rightarrow 1e^{-21}$)
JID1 (*probable HSP40 co-chaperone*)	Contig 51[g]	($4e^{-10}$)	Ss, Bc, Nc, Ci, Mg, Ro	($5e^{-22} \rightarrow 0.007$)
YDJ1 (*DnaJ co-chaperone for HSP70, -90*)	AN2731	($1e^{-79}$)	Ci, Ss, Bc, Cg, Nc, Mg, Ro, Cn	($1e^{-165} \rightarrow 1e^{-91}$)
Other ER and ER-associated proteins				
SWR1 (*SWI2/SNF2-related ATPase*)	AN9077	(0.0)	Ci, Ss, Nc, Cg, Bc, Mg, Ro, Cn	($0.0 \rightarrow 0.0$)
SWC3 (*SWR1 complex*)	AN3834	(0.001)	Ci, Bc, Ss, Cg, Mg, Nc	($3e^{-47} \rightarrow 7e^{-26}$)
MSC1 (*unknown function*)	AN4940	($4e^{-26}$)	Ci, Nc, Mg, Bc, Ss, Cg, Cn	($1e^{-148} \rightarrow 5e^{-10}$)
MSC2 (*cation diffusion facilitator family*)	AN5347	($8e^{-47}$)	Ci, Nc, Ro, Bc, Mg, Ss, Cg, Cn	($1e^{-77} \rightarrow 7e^{-23}$)
MSC7 (*unknown function*)	AN6636	($1e^{-120}$)	Ci, Bc, Cg, Mg, Nc, Ss, Ro, Cn	($0.0 \rightarrow 6e^{-81}$)
SLC1 (1-acyl-glycerol-3-PO_4 acyltransferase)	AN6139	(0.0)	Ci, Cg, Nc, Bc, Ss, Mg, Cn, Ro	($1e^{-110} \rightarrow 1e^{-46}$)
ARE1, ARE2 (acyl-CoA:sterol acyltransferase)	AN4208	(0.0)	Ss, Mg, Nc, Ci, Cg, Bc, Cn	($1e^{-175} \rightarrow 4e^{-51}$)
Novel additional ARE1/2 homolog	AN6159[h]	($5.7e^{-21}$, $3e^{-30}$)	Ci, Ss, Bc, Cg, Nc, Mg, Ro, Cn	($1e^{-162} \rightarrow 1e^{-29}$)
MNL1 (α-mannosidase-like protein)	AN11163	(0.0)	Ci, Bc, Ss, Mg, Cg, Nc, Bc, Ro, Cn	($0.0 \rightarrow 2e^{-77}$)

[a] Listed are fungi in which one or more putative orthologs occur. Order of fungi and corresponding range of e-values indicate relative strength of homology to An sequence. Bc *Botrytis cinerea*, Cg *Chaetomium globosum*, Ci *Coccidioides immitis*, Cn *Cryptococcus neoformans*, Mg *Magnaporthe grisea*, Nc *Neurospora crassa*, Ro *Rhizopus oryzae*, Ss *Sclerotinia sclerotiorum*.

[b] Sc DER1 found an unnamed hypothetical ORF in An (contig 109, nt 132344–133047). Sc DER1 found putative orthologs in three other fungi; its closest relative is NCU00146 ($3e^{-10}$).

[c] Sc VMA21 did not find the An ortholog, but did find the putative Mg ortholog, MGG_09929 ($2e^{-05}$). MGG_09929, in turn, found Sc VMA21 ($1.6e^{-07}$) and the putative An ortholog, AN2975 (0.008).

[d] Sc VMA22 did not find the An ortholog, but did find the putative Ss ortholog, SS1G_13727 (e=11.0). SS1G_13727, in turn, found Sc VMA22 (0.097) and the putative An ortholog, AN4766 (3.1).

[e] Sc PGA2 did not find an An homolog, but did find the putative Ci ortholog, CIMG_00038.2 ($1e^{-04}$). CIMG_00038.2, in turn, found Sc PGA2, and a putative An ortholog, AN0597. The An gene did not find PGA2 in Sc, but found the same five putative orthologs in other fungi as were found by CIMG_00038.2.

[f] Sc SIL1 did not find an An homolog, but did find the putative Bc ortholog, BC1G_08026.1 ($8e^{-12}$). BC1G_08026.1, in turn, found Sc SIL1 ($1.3e^{-10}$) and putative orthologs in three other fungi, but not in *A. nidulans*.

[g] Sc JID1 found an unnamed hypothetical ORF in An (contig 51, nt 221952–222362). Sc JID1 found putative orthologs in other fungi; its closest relative is SS1G_11303 ($2e^{-10}$).

[h] Sc ARE1 and ARE2 are strongly related paralogs ($1.3e^{-155}$). The An ortholog of ARE1/ARE2 is AN4208 (0.0). Reciprocal blastp of the Sc genome finds ARE1 ($2.2e^{-67}$) and ARE2 ($4.2e^{-57}$). In addition, An possesses one paralog, AN6159, that shows moderate similarity to AN4208 ($2.3e^{-31}$), and to the Sc ARE1/2 paralogs ($5.7e^{-21}$ and $3e^{-30}$, respectively).

S. cerevisiae	*A. nidulans*		*Other fungi*[a]	
Golgi resident proteins				
ATX2 (*manganese homeostasis*)	AN6216	($8.5e^{-06}$)	Ci, Ss, Bc, Mg, Nc, Cg, Ro, Cn	($1e^{-116} \rightarrow 1e^{-35}$)
ARV1 (*intracellular sterol distribution*)	AN5868	($1.3e^{-09}$)	Ci, Nc, Ss, Cg, Bc, Mg	($4e^{-23} \rightarrow 3e^{-05}$)
AUR1 (*IPC synthase, sphingolipid synthesis*)	AN4991	(0.0)	Ci, Ss, Bc, Cg, Nc, Ro, Cn	($1e^{-129} \rightarrow 3e^{-64}$)
GDA1 (*guanosine diphosphatase, GDP → GMP*)	AN1082	(0.0)	Ci, Ss, Bc, Mg, Nc, Cg, Ro, Cn	($1e^{-151} \rightarrow 1e^{-76}$)
CCC1 (*vacuolar Fe^{2+}/Mn^{2+} transporter*)	AN3681	($3.5e^{-34}$)	Ci, Mg, Ss, Ro, Bc, Cg, Cn	($2e^{-72} \rightarrow 5e^{-17}$)
Novel *A. nidulans* CCC1 homolog	AN4990	($2.1e^{-31}$)	**None**[b]	
GEF1 (*chloride channel, Fe metabolism*)	AN2308	(0.0)	Ci, Ss, Nc, Cg, Mg, Bc, Cn, Ro	($0.0 \rightarrow 1e^{-159}$)
Novel additional GEF1 homologs[c]	AN6107	(0.0)	Ci, Nc, Ss, Mg, Bc, Cg, Cn, Ro	($0.0 \rightarrow 1e^{-119}$)
	AN6311	(0.0)	Ci, Mg, Cg, Nc, Ss, Bc, Cn, Ro	($0.0 \rightarrow 1e^{-105}$)
IMH1 (*vesicular transport, GRIP domain*)	AN2480	($9.4e^{-39}$)	Ci, Nc, Ss, Bc, Cg, Mg, Ro	($0.0 \rightarrow 6e^{-32}$)
LCB4, LCB5 (*sphingolipid long-chain base kinase*)	AN1176	(0.0)	Ci, Bc, Ss, Mg, Nc, Cg, Ro, Cn	($1e^{-144} \rightarrow 7e^{-43}$)
ANP1 (*retention of Golgi glycosyltransferases*)	AN10265	(0.0)	Ci, Ss, Mg, Cg, Nc, Bc, Ro	($1e^{-156} \rightarrow 6e^{-57}$)
VAN1 (*component of mannan polymerase I*)	AN4395	(0.0)	Ci, Mg, Cg, Bc, Nc, Ss, Ro	($1e^{-153} \rightarrow 8e^{-60}$)
MNN9 (*Golgi mannosyltransferase complex*)	AN7672	(0.0)	Ci, Bc, Ss, Nc, Mg, Cg	($1e^{-126} \rightarrow 1e^{-105}$)
MNN10 (*Golgi membrane mannosyltransferase*)	AN7562	(0.0)	Ss, Bc, Ci, Mg, Nc, Cg	($1e^{-132} \rightarrow 1e^{-110}$)
MNN11 (*Golgi mannosyltransferase complex*)	AN1969	($1.5e^{-22}$)	Ci, Cg, Nc, Ss, Mg, Bc	($4e^{-98} \rightarrow 1e^{-44}$)
HOC1 (α-*1,6-mannosyltransferase*)	AN4716	(0.0)	Ci, Ss, Nc, Bc, Mg, Cg, Cn	($1e^{-117} \rightarrow 8e^{-34}$)
MNN2 (α-*1,2-mannosyltransferase*)	AN6571	(0.0)	Ci, Bc, Ss, Mg, Nc, Cg, Ro, Cn	($1e^{-125} \rightarrow 6e^{-05}$)
MNN5 (α-*1,2-mannosyltransferase*)	AN6857	($4e^{-44}$)	Ci, Bc, Ss, Mg, Nc, Cg, Cn, Ro	($1e^{-138} \rightarrow 1e^{-14}$)
MNN1 (α-*1,3-mannosyltransferase*)	*AN6571*[d]	($9e^{-05}$)	Ci, Bc, Ss, Mg, Nc, Cg, Ro, Cn	($1e^{-125} \rightarrow 6e^{-05}$)
KRE6 (*integral membrane* β-*1,6 glucan synthase*)	AN10779	(0.0)	Ci, Bc, Ss, Cn	($0.0 \rightarrow 1e^{-115}$)
RSN1 (*membrane protein, unknown function*)	AN8069	(0.0)	Ci, Bc, Cg, Ss, Nc	($0.0 \rightarrow 1e^{-104}$)
DRS2 (*aminophospholipid translocase*)	AN6112	(0.0)	Ci, Bc, Cg, Nc, Mg, Ss, Ro, Cn	($0.0 \rightarrow 0.0$)
KEX1 (*killer toxin processing,TPA carboxypeptidase*)	AN10184	(0.0)	Ci, Ss, Nc, Mg, Bc, Cg, Cn, Ro	($0.0 \rightarrow 4e^{-43}$)
KEX2 (*Ca^{2+}-dependent Ser protease, proprotein convertase*)	AN3583	(0.0)	Ci, Bc, Ss, Cg, Nc, Mg, Cn, Ro	($0.0 \rightarrow 1e^{-155}$)
VRG4 (*Golgi GDP-mannose transporter*)	AN8848[e]	(0.0)	Ci, Bc, Ss, Mg, Nc, Cg, Ro, Cn	($1e^{-145} \rightarrow 8e^{-98}$)
HVG1 (*unknown function, similar to VRG4*)	AN9298[e]	(0.0)	**None**	
PSD2 (*phosphatidylserine decarboxylase*)	AN3188[f]	(0.0)	Ci, Ss, Cg, Mg, Bc, Cn, Ro	($0.0 \rightarrow 1e^{-145}$)
Novel additional PSD2 homolog	AN7989	(0.0)	Ci	($1e^{-102}$)
HUT1 (*UDP-galactose transport to GA lumen*)	AN4068	(0.0)	Ci, Ss, Bc, Mg, Nc, Cg, Ro, Cn	($1e^{-133} \rightarrow 2e^{-47}$)
GOT1 (*ER → GA transport?*)	AN10313	($1e^{-07}$)	Ci, Mg, Cg, Ss, Nc, Ro	($3e^{-26} \rightarrow 2e^{-09}$)
STE13 (*dipeptidyl aminopeptidase*)	AN2946	($1e^{-112}$)	Ss, Bc, Ci, Nc, Cg, Mg	($0.0 \rightarrow 0.0$)
PMR1 (*Ca^{+2}/Mn^{+2} P-type ATPase*)	AN7464	(0.0)	Ci, Ss, Bc, Mg, Nc, Cg, Cn, Ro	($0.0 \rightarrow 1e^{-122}$)
TUL1 (*RING-finger E3 ubiquitin ligase*)	AN1075	($1e^{-51}$)	Ci, Mg, Bc, Nc, Ss, Cg, Ro, Cn	($0.0 \rightarrow 4e^{-04}$)
YIF1 (*fusion of ER-derived COPII vesicles*)	AN6628	($1e^{-22}$)	Ci, Bc, Nc, Cg, Mg, Ss, Cn, Ro	($1e^{-129} \rightarrow 1e^{-19}$)
COY1 (*similar to mammalian CASP*)	AN0762	($3e^{-48}$)	Ci, Bc, Nc, Ss, Mg, Cg, Cn	($0.0 \rightarrow 2e^{-41}$)
SWH1, OSH2 (*oxysterol-binding protein*)	AN9063	($1e^{-123}$, $1e^{-160}$)	Bc, Nc, Ss, Mg, Ci, Cg, Ro	($0.0 \rightarrow 2e^{-51}$)
GMH1 (*interacts with GEA1, GEA2*)	AN3439	($7e^{-08}$)	Ci, Cn	($6e^{-52} \rightarrow 5e^{-05}$)

S. cerevisiae	*A. nidulans*		*Other fungi*[a]	
GVP36 (*unknown function*)	AN10743	($3e^{-30}$)	Ci, Mg, Ss, Cg, Bc, Ro, Cn	($1e^{-120} \rightarrow 1e^{-21}$)
SVP26 (*retention of early GA proteins*)	AN5788	($1e^{-40}$)	Ci, Nc, Bc, Mg, Ss, Cn, Ro	($6e^{-63} \rightarrow 3e^{-16}$)
BFR2 (*essential protein, secretion*)	AN7526	($3e^{-23}$)	Ci, Bc, Nc, Cg, Mg, Ro, Ss	($3e^{-90} \rightarrow 4e^{-08}$)
BUG1 (*unknown function*)	**None**		**None**	
CHS7 (*regulates CHS3 export from ER*)	AN1069	($3e^{-62}$)	Ci, Nc, Cg, Ss, Bc, Mg, Ro, Cn	($1e^{-129} \rightarrow 5e^{-54}$)
Novel additional CHS7 homolog	AN5152	($2e^{-08}$)	Ss, Nc, Ci, Cg, Bc, Mg, Ro	($1e^{-85} \rightarrow 5e^{-20}$)
TPO5 (*putative polyamine transporter*)	AN1061	($2e^{-57}$)	Ci, Mg, Ss, Nc	($0.0 \rightarrow 1e^{-98}$)
SBE2, SBE22 (*transport of cell wall components*)	AN3752	($7e^{-06}$, $5e^{-10}$)	Ss, Mg, Nc, Ci, Cg, Bc, Cn, Ro	($1e^{-111} \rightarrow 6e^{-13}$)
INP53 (*PI 4,5-bisphosphate phosphatase*)	AN8288	($1e^{-169}$)	Ss, Ci, Mg, Nc, Cg, Bc, Ro, Cn	($0.0 \rightarrow 6e^{-71}$)
YKL063C (*putative protein, unknown function*)	**None**		**None**	
YCR043C (*putative protein, unknown function*)	AN8720	($7e^{-49}$)	Bc, Ss, Cg, Mg, Nc	($5e^{-94} \rightarrow 1e^{-78}$)
YJL123C (*putative protein, unknown function*)	AN4024	($5e^{-12}$)	Ci, Ss, Bc, Nc, Cg, Mg, Cn, Ro	($1e^{-131} \rightarrow 1e^{-07}$)
Golgi protein retention				
VPS1 (*dynamin GTPase*)	AN8023	(0.0)	Ci, Ss, Cg, Nc, Mg, Ro, Cn	($0.0 \rightarrow 0.0$)
VPS13 (*homologous to human COH1*)	AN5579	(0.0)	Ss, Ci, Mg, Cg, Bc,Nc, Ro, Cn	($0.0 \rightarrow 1e^{-161}$)
Golgi to plasma membrane				
LST4 (*transport of GAP1 permease*)	**None**		**None**	
LST7 (*transport of GAP1 permease*)	AN4598	(0.0083)	Ci, Ss, Bc, Nc, Mg, Cg	($1e^{-129} \rightarrow 1e^{-11}$)
SEC14 (*P-inositol/P-choline transfer protein*)	AN4997	($4e^{-82}$)	Nc, Cg, Ss, Bc, Mg, Ci, Cn	($1e^{-25} \rightarrow 8e^{-26}$)
CHS5 (*chitin biosynthesis, CHS3 localization*)	AN8710	($3e^{-56}$)	Ci, Ss, Bc, Mg, Cg, Nc, Ro, Cn	($1e^{-115} \rightarrow 2e^{-19}$)
BCH2 (see Table 1.5)	AN3122	(0.003)	Ci, Cg, Ss, Nc, Mg, Bc, Ro, Cn	($0.0 \rightarrow 1e^{-73}$)
GORASP (Golgi postmitotic reassembly stacking protein)				
GRH1 (*hsGRASP55/65 homolog*)	AN11248[g]	($8e^{-18}$)	Ci, Ss, Mg, Cg, Bc, Nc, Ro, Cn	($2e^{-89} \rightarrow 7e^{-04}$)

[a] Listed are fungi in which one or more putative orthologs occur. Order of fungi and corresponding range of e-values indicate relative strength of homology to An sequence. Bc *Botrytis cinerea*, Cg *Chaetomium globosum*, Ci *Coccidioides immitis*, Cn *Cryptococcus neoformans*, Mg *Magnaporthe grisea*, Nc *Neurospora crassa*, Ro *Rhizopus oryzae*, Ss *Sclerotinia sclerotiorum*.

[b] AN4990 appears to represent a novel, expanded homolog of Sc CCC1 that occurs in *A. nidulans*, but not in the other fungal species in this study.

[c] The single Sc GEF1 Golgi chloride channel found three strongly conserved fungal homologs. By reciprocal blastp search each An protein found Sc GEF1 as the only significant hit (AN2308 $7.2e^{-108}$, AN6107 $1.1e^{-69}$, and AN6311 $4.4e^{-68}$). Each of these three exhibits strong homology with human chloride channel 3 protein (NP_001820, $7e^{-148} \rightarrow 3e^{-135}$).

[d] Other fungi appear to be missing an ortholog of the Sc MNN1 α-1,3-mannosyltransferase. MNN1 finds only one An protein, AN6571 ($9e^{-05}$). However, AN6571 appears to be the ortholog of the Sc MNN2 α-1,2-mannosyltransferase (0.0). Similarly, Sc MNN1 found no homologs by blastp of all fungi.

[e] AN8848 and AN9298 appear to represent a duplicated gene pair in *A. nidulans* that is not duplicated in the other fungal species in this study, with the possible exception of *R. oryzae*. The two An genes are very similar to each other (0.0). By reciprocal blastp, AN8848 shows strong conservation with Sc VRG4 ($1.5e^{-91}$) and HVG1 ($1.8e^{-72}$). By comparison, AN9298 is more diverged from Sc VRG4 ($1.5e^{-61}$) and HVG1 ($5e^{-55}$).

[f] AN7989 and AN3188 appear to represent paralogs that are also duplicated *C. immitis* (CIMG_02491 and CIMG_00068) but not in the other fungal species. The two An genes are very similar to each other (0.0).

[g] AN11248 (GRASP55/65 homolog) shares greater homology with human GORASPs 1 and 2 ($1e^{-26}$, $7e^{-23}$) than it does with Sc GRH1 ($8e^{-18}$).

S. cerevisiae	*A. nidulans*	*Other fungi*[a]
Golgins (tethering and organization of Golgi stacks in animals)		
Human golgins 1,-2,-3,-4,-5,-6,-7,-8a,-8b, -B1	**None**[h]	**None**
Human GOPC (*Golgi-associated PDZ and coiled-coil*)	**None**	**None**
Human GCC1 (GRIP and coiled-coil containing-1)	**None**	**None**

[h] Human golgins-1, -2, -3, -4, -5, -6, -7, -8a, -8b, and Golgin-B1 found weak hits ($\leq e^{-20}$) to large predicted proteins such as AN3906 (viral A-type inclusion protein repeat), AN3062 (similar to calmodulin-binding coiled-coil protein), AN5499 (TPR/MLP1/MLP2-like protein, which forms the central scaffold element of the nuclear pore basket), AN3437 (*ApsB*, anucleate primary stergimata protein B), AN4706 (myosin head, motor domain), and AN7443 (transient receptor potential ion channel). These *A. nidulans* proteins, in turn, found human restins, myosins, plectins, TPR/MLP1/MLP2, and sometimes golgins, at higher e-values.

correctly targeted and contain no additional ectopic integrations of the transforming DNA (Nayak et al. 2006). Even difficult genes can be readily deleted from NHEJ-deficient strains. For example, we were able to delete the *cdc7* gene within a recombinationally suppressed chromosomal region on LGVI of *A. nidulans*, in which the apparent genetic-to-physical distance was at least 7-fold expanded ($\geq$54 kb per map unit) relative to the average of ~8 kb per map unit. Repeated attempts using conventional strains failed to delete the locus, but in the *ΔnkuA* (ΔKU70) background ~15% of transformants (4 out of 30) were deleted for this gene (laboratory of S.W. James, unpublished data). Second, fusion PCR can be used to rapidly produce constructs for gene deletion, tagging, or promoter replacement. Two-way fusion PCR, or single-joint PCR, may be used to fuse any two DNA fragments, e.g., the coding region of a gene with an inducible promoter; and three-way fusion PCR can be used to make deletion constructs (Yang et al. 2004; Yu et al. 2004). Where the genome has been sequenced, fusion PCR obviates the need for DNA cloning; PCR-generated fusion constructs can be directly transformed into NHEJ-deficient host strains to delete, tag, or replace portions of genes. In *A. nidulans*, useful tagging cassettes are available 21 for tagging a gene's C-terminus with GFP or mRFP for in vivo cytological studies; and with the 15-amino-acid S-peptide for affinity purification of in vivo protein complexes (Yang et al. 2004). Publicly available cassettes, strains, libraries, and a host of other resources may be obtained via the Fungal Genetics Stock Center (University of Missouri, Kansas City; http://www.fgsc.net/). Together, these recent advances in gene targeting and gene manipulation make it possible to rapidly target every gene in a fungal genome (e.g., see Nayak et al.

Table. 1.3. (on page 8–11) COPII (ER → Golgi) and COPI (Golgi → ER) transport processes. *A. nidulans* (An) proteins were identified by tBlastn of the An genome (http://www.broad.mit.edu/annotation/genome/aspergillus_nidulans/) using Sc proteins. Sc proteins were obtained from Gene Ontology annotation for yeast (www.yeastgenome.org). Proteins were further defined by forward and reverse tBlastn and blastp between Sc and An genomes, tBlastn of An proteins against the An genome, tBlastn and blastp of An and Sc proteins to all Fungal Genome Initiative (FGI) genomes (http://www.broad.mit.edu/annotation/fgi/), and by phylogenetic trees using the neighbor-joining method excluding positions with gaps (http://www.ebi.ac.uk/clustalw/index.html)

S. cerevisiae	*A. nidulans*		*Other fungi*[a]	
ER → GA transport				
COPII coatomer complex				
SAR1 (*Arf GTPase SarA*)	AN0411	($4e^{-35}$)	Ss, Cg, Ro, Nc, Ci, Mg, Bc, Cn	($1e^{-70} \rightarrow 4e^{-28}$)
SEC13 (*COPII component*)	AN4317	($1e^{-82}$)	Ci, Nc, Cg, Mg, Ss, Bc, Ro, Cn	($1e^{-136} \rightarrow 6e^{-38}$)
SEC16 (*COPII vesicle coat*)	AN6615	($7e^{-22}$)	Ci, Bc, Ss, Nc, Mg	($0.0 \rightarrow 8e^{-55}$)
SEC23 (*GTPase activator of Sar1*)	AN0261	(0.0)	Ci, Ss, Cg, Bc, Mg, Ro, Cn, Nc	($0.0 \rightarrow 0.0$)
SEC24, SFB2 (*COPII vesicle coat*)	AN3720	(0.0, 0.0)	Mg, Cg, Nc, Ss, Bc, Ci, Cn, Ro	($0.0 \rightarrow 0.0$)
SFB3 (SEC24 family, COPII sorting)	AN3080	($8e^{-82}$)	Ss, Mg, Nc, Cg, Bc, Ro, Ci, Cn	($0.0 \rightarrow 2e^{-90}$)
SEC31 (*COPII vesicle coat*)	AN6257	($1e^{-102}$)	Ci, Ss, Mg, Bc, Nc, Cg, Ro, Cn	($0.0 \rightarrow 6e^{-86}$)
COPII-related functions				
EMP24 (*COPII vesicle membr protein*)	AN1154	($1e^{-27}$)	Ss, Bc, Mg, Ci, Cg, Mg, Cn	($3e^{-75} \rightarrow 2e^{-25}$)
EMP46, EMP47 (*COPII vesicle membr protein*)	AN7302	(0.010)	Nc, Ci, Cg,Mg, Bc, Ss, Ro	($2e^{-77} \rightarrow 2e^{-09}$)
ERP1, ERP5, ERP6 (*complex w/ERP2, EMP24*)	AN4446	($6e^{-37}$, $1e^{-34}$, $7e^{-15}$)	Ci, Ss, Cg, Nc, Bc, Mg, Cn, Ro	($2e^{-71} \rightarrow 2e^{-04}$)
ERP2, ERP3, ERP4 (*complex w/ERP1, EMP24*)	AN8194	($5e^{-05}$, $6e^{-09}$, $6e^{-05}$)	Ci, Cg, Ss, Bc, NC, Mg, Ro, Cn	($2e^{-83} \rightarrow 2e^{-36}$)
ERV25 (*complex with ERP1, ERP2, EMP24*)	AN4165	($1e^{-40}$)	Ci, Bc, Cg, Mg, Ss, Nc, Ro	($1e^{-74} \rightarrow 4e^{-17}$)
ERV14, ERV15 (*COPII vesicle protein*)	AN5195	($2e^{-30}$, $5e^{-19}$)	Mg, Ci, Bc, Cg, Nc, Ss, Ro, Cn	($2e^{-55} \rightarrow 5e^{-11}$)
ERV29 (*COPII vesicle protein*)	AN1117	($3e^{-27}$)	Ss, Nc, Mg, Cg, Ci, Ro, Cn	($1e^{-78} \rightarrow 4e^{-15}$)
ERV41 (*complex with ERV46*)	AN7679	($6e^{-24}$)	Ci, Ss, Bc, Mg, Nc, Cg, Cn	($1e^{-110} \rightarrow 2e^{-20}$)
ERV46 (*complex with ERV41*)	AN2738	($2e^{-42}$)	Ci, Nc, Ss, Mg.Cg. Ro, Bc, Cn	($1e^{-148} \rightarrow 8e^{-12}$)
BST1 (*GPI inositol deacylase*)	AN6702	($6e^{-71}$)	Ss, Bc, Nc, Cg, Ci, Mg, Ro, Cn	($0.0 \rightarrow 3e^{-41}$)
TRAPP complex (transport protein particle), ER → GA transport				
BET3	AN9086	($3e^{-50}$)	Mg, Nc, Ss, Ci, Cg, Bc, Cn, Ro	($3e^{-79} \rightarrow 1e^{-32}$)
BET5	AN8828	($8e^{-08}$)	Ss, Bc, Nc, Ci, Mg, Cg, Ro, Cn	($2e^{-46} \rightarrow 2e^{-11}$)
GSG1	AN7311	($1e^{-12}$)	Nc, Cg, Mg, Ci, Bc, Ss, Ro, Cn	($1e^{-151} \rightarrow 2e^{-25}$)
KRE11	**Not found**		**Not found**	
TRS120	AN6533	($2e^{-13}$)	Ci, Bc, Mg, Ss, Nc, Cg, Ro	($0.0 \rightarrow 3e^{-19}$)
TRS130	AN1038	($1e^{-07}$)	Bc, Nc, Ci, Mg, Ss, Cg, Cn, Ro	($0.0 \rightarrow 9e^{-23}$)
TRS20	AN11500	($2e^{-06}$)	Ci, Nc, Ss, Bc, Mg, Cg	($4e^{-52} \rightarrow 8e^{-14}$)
TRS23	Contig 129[b]	($2e^{-08}$)	Ci, Cg, Mg, Nc, Bc, Ss, Ro	($7e^{-21} \rightarrow 5e^{-08}$)
TRS31	AN6825	($6e^{-17}$)	Ci, Ss, Bc, Cg, Nc, Mg, Ro, Cn	($3e^{-53} \rightarrow 9e^{-13}$)
TRS33	AN10826	($2e^{-06}$)	Bc, Ci, Mg, Ro, Ss, Cg, Nc, Cn	($2e^{-48} \rightarrow 3e^{-18}$)
GA → ER transport				
COPI coatomer complex				
COP1 (RET1; *COP1* α *subunit*)	AN3026	(0.0)	Nc, Cg, Bc, Ss, Mg, Ci, Cn, Ro	($0.0 \rightarrow 0.0$)
SEC26 (*COP1* β *subunit*)	AN1177	($1e^{-142}$)	Cg, Mg, Nc, Bc, Ss, Ci, Cn, Ro	($0.0 \rightarrow 0.0$)
SEC27 (*COP1* β' *subunit*)	AN5972	(0.0)	Ss, Bc, Mg, Cg, Nc, Ro, Ci, Cn	($0.0 \rightarrow 0.0$)
SEC28 (*COP1* ε *subunit*)	AN0665	(0.022)	Ss, Bc, Cg, Mg, Ro, Cn	($1e^{-101} \rightarrow 7e^{-21}$)
SEC21 (*COP1* γ *subunit*)	AN4547	($1e^{-120}$)	Nc, Ss, Mg, Bc, Ci, Cg, Cn, Ro	($0.0 \rightarrow 1e^{-170}$)
GLO3 (*Arf-GAP*)	AN6033	($4e^{-19}$)	Ss, Mg, Nc, Ci, Bc, Cg, Cn, Ro	($1e^{-145} \rightarrow 4e^{-27}$)

S. cerevisiae	*A. nidulans*		*Other fungi*[a]	
RET2 (*COP1 δ subunit*)	AN0922	($2e^{-41}$)	Ci, Nc, Bc, Mg, Ss, Cg, Cn, Ro	($0.0 \rightarrow 4e^{-32}$)
RET3 (*COP1 ζ subunit*)	AN6080	($2e^{-32}$)	Ci, Mg, Bc, Cg, Nc, Ss, Ro, Cn	($1e^{-81} \rightarrow 5e^{-07}$)
DSL1 complex (COPI vesicle fusion with ER by stabilizing Use1p-Ufe1p-Sec20p SNARE complex; prohibits back-fusion of COPII vesicles with ER)				
DSL1 (*interacts with coatomer at ER target*)	AN9435[c]	–	Ci, Bc, Nc, Ss, Cg, Mg, Cn	($1e^{-154} \rightarrow 2e^{-04}$)
TIP20 (*fusion of COPI vesicles with ER*)	AN4884[d]	–	Ci, Mg, Nc, Bc, Cg, Ss, Ro, Cn	($0.0 \rightarrow 1e^{-39}$)
DSL3 (SEC39; *Q/t-SNARE stability at ER*)	AN4188	($2e^{-11}$)	Ci, Ss, Nc, Bc, Mg, Cg, Ro	($0.0 \rightarrow 1e^{-09}$)
GET complex (GA → ER retrieval of HDEL proteins)				
GET1	AN4342[e]	(0.056)	Mg, Ci, Ss, Bc, Nc, Cn, Cg, Ro	($2e^{-40} \rightarrow 3e^{-06}$)
GET2	**None**[f]		**None**	
GET3	AN2909[g]	($4e^{-80}$)	Ss, Bc, Nc, Mg, Ro, Ci, Cg, Cn	($1e^{-144} \rightarrow 2e^{-60}$)
Other GA → ER proteins				
VPS15 (*S/T kinase; regulates protein sorting*)	AN0576	($1e^{-123}$)	Ci, Ss, Mg, Nc, Cg, Bc, Cn, Ro	($0.0 \rightarrow 2e^{-45}$)
VPS34 (*PI3 kinase; vacuolar protein sorting*)	AN4709	($1e^{-161}$)	Ci, Ss, Bc, Mg, Nc, Cg, Ro, Cn	($0.0 \rightarrow 9e^{-92}$)
NEO1 (*GA → ER transport*)	AN6614	(0.0)	Ss, Bc, Nc, Cg, Mg, Ci, Cn, Ro	($0.0 \rightarrow 0.0$)
RER1 (*GA retrieval receptor for GA → ER*)	AN5915	($9e^{-26}$)	Ci, Cg, Nc, Mg. Ss, Bc, Cn, Ro	($1e^{-67} \rightarrow 3e^{-32}$)
TVP15 (*localizes with v-SNARE TLG2*)	AN10033	(0.54)	Mg, Ci, Nc, Cg, Bc, Ss, Ro, Cn	($2e^{-27} \rightarrow 0.072$)
TVP23 (*localizes with v-SNARE TLG2*)	AN3576	($5e^{-17}$)	Ci, Mg, Bc, Ss, Cg, Nc, Cn	($6e^{-49} \rightarrow 4e^{-06}$)
TVP38 (*localizes with v-SNARE TLG2*)	AN3579	($4e^{-23}$)	Ci, Bc, Ss, Mg, Nc, Cg, Cn, Ro	($2e^{-96} \rightarrow 9e^{-07}$)
UBP3 (*Ub protease, ER → GA → ER*)	AN5186	($1e^{-48}$)	Ci, Nc, Bc, Ss, Mg, Cg, Ro, Cn	($0.0 \rightarrow 2e^{-60}$)
BRE5 (*UBP3 protease cofactor*)	AN8268	($6e^{-04}$)	Ci, Ss, Cg, Bc, Mg, Nc, Ro, Cn	($6e^{-52} \rightarrow 6e^{-19}$)
SGM1 (*unknown function*)	AN1210	($3e^{-27}$)	Mg, Ci, Bc, Ss, Nc, Cg, Ro	($1e^{-103} \rightarrow 6e^{-12}$)
GTP-dependent regulators of COPII and COPI-mediated vesicle formation and transport				
ADP ribosylation factor family GTPases (ARFs)				
ARF1, ARF2 (*coated vesicle formation*)	AN1126	($1e^{-79}$, $7e^{-80}$)	Nc, Ro, Ci, Cg, Mg, Ss, Bc	($1e^{-72} \rightarrow 5e^{-57}$)
SAR1 (*ER → GA*)	AN0411	($4e^{-35}$)	Ss, Cg, Ro, Nc, Ci, Mg, Bc, Cn	($1e^{-70} \rightarrow 4e^{-28}$)
Novel fungal ARF GTPase[h] (ARF1)	An vs Sc AN5020 ($4e^{-59}$)	An vs Hs HsARF6 ($7e^{-72}$)	Mg, Ci, Ss, Bc, Cn, Nc, Ro	($3e^{-80} \rightarrow 6e^{-63}$)
ARF-like GTPases				
ARL1 (*membrane traffic regulation*)	AN5912	($5e^{-46}$)	Nc, Bc, Cg, Mg, Ci, Ss, Cn, Ro	($1e^{-67} \rightarrow 2e^{-33}$)
ARL3 (*recruits ARL1 to Golgi*)	AN0634	($4e^{-22}$)	Ci, Mg, Bc, Nc, Ss, Cg	($5e^{-85} \rightarrow 2e^{-32}$)
Novel additional ARF-like GTPases[h] (ARF1, ARL1)	An vs Sc AN3934 ($5e^{-13}$, $2e^{-07}$)	An vs Hs HsARL10 ($7e^{-56}$)	Bc, Ss, Cg, Ci, Nc, Mg, Ro	($2e^{-59} \rightarrow 8e^{-43}$)
Novel additional ARF-like GTPases[h] (ARF1, ARL1)	An vs Sc Contig 13[i] ($3e^{-19}$, $5e^{-15}$) [CIMG_03295 ($5.3e^{-34}$, $1.3e^{-37}$)]	An vs Hs HsARL2 ($1e^{-61}$)	Nc, Cg, Bc, Ss, Mg, Cn	($4e^{-66} \rightarrow 1e^{-34}$)

S. cerevisiae	*A. nidulans*		*Other fungi*[a]	
GTPase activating proteins for ARFs (ARF-GAPs)				
AGE1 (*secretory/endocytic pathways*)	AN4274	($1e^{-20}$)	Ci, Cg, Mg, Ss, Nc, Bc, Ro	($0.0 \rightarrow 2e^{-49}$)
AGE2 (*TGN transport*)	AN1931	($7e^{-20}$)	Ci, Bc, Ss, Cg, Nc, Mg, Cn, Ro	($1e^{-107} \rightarrow 1e^{-32}$)
GCS1 (*ER → GA transport*)	AN2222	($1e^{-48}$)	Ci, Mg, Ss, Bc, Cg, Nc, Cn	($3e^{-98} \rightarrow 2e^{-18}$)
GLO3 (*ER → GA transport*)	AN6033	($4e^{-19}$)	Ss, Mg, Nc, Ci, Bc, Cg, Cn, Ro	($1e^{-145} \rightarrow 4e^{-27}$)
Novel additional ARF-GAP[h] (AGE2)	An vs Sc 1629 ($1e^{-07}$)	An vs Hs HsSMAP1 ($8e^{-24}$) [ARF6 GAP]	Ci, Bs, Mg, Ss, Cg, Nc, Cn, Ro	($4e^{-83} \rightarrow 3e^{-17}$)
ARF guanine nucleotide exchange factors (ARF-GEFs)				
GGA1, GGA2 (γ-*adaptin, ARF1/2 regulator*)	AN5710	($8e^{-34}$, $2e^{-76}$)	Bc, Ss, Ci, Nc, Mg, Cg, Ro, Cn	($1e^{-154} \rightarrow 1e^{-36}$)
SYT1 (*vesicular transport*)	AN6120	($1e^{-19}$)	Ci, Bc, Ss, Nc, Mg, Cg, Cn	($0.0 \rightarrow 6e^{-50}$)
GEA1, GEA2 (*GA → ER*)	AN0112	($4e^{-113}$, $1e^{-76}$)	Ci, Ss, Mg, Nc, Cg, Bc, Cn, Ro	($0.0 \rightarrow 1e^{-108}$)
SEC7 (*ER → GA, intra-GA transport*)	AN6709	(0.0)	Ss, Cg, Nc, Mg, Ci, Ro, Cn	($0.0 \rightarrow 0.0$)
SEC12 (*ER → GA, SAR1 activator*)	AN0127?[j]		UMO2499, CNAG_01871, RO3G_09896	
YBL060W (*hypothetical ORF with a SEC7 domain*)	AN3438	($4e^{-12}$)	Ci, Ss, Mg, Cg, Nc, Bc, Ro, Cn	($0.0 \rightarrow 7e^{-32}$)

[a] Listed are fungi in which one or more putative orthologs occur. Order of fungi and corresponding range of e-values indicate relative strength of homology to An sequence, except for TRS23, ARF1/ARL1, and SYS1 comparisons (see footnotes b,i,k), below. Bc *Botrytis cinerea*, Cg *Chaetomium globosum*, Ci *Coccidioides immitis*, Cn *Cryptococcus neoformans*, Mg *Magnaporthe grisea*, Nc *Neurospora crassa*, Ro *Rhizopus oryzae*, Ss *Sclerotinia sclerotiorum*.

[b] Sc TRS23 found an unnamed hypothetical ORF in An (contig 129, nt 520998–521219), and found putative orthologs in other fungi, at e-values ranging from $7e^{-21} \rightarrow 5e^{-08}$ (Sc TRS23 vs all fungi).

[c] Sc DSL1 did not find an An homolog, but did find a weakly similar protein in Ro (RO3G_08898, e=0.014). RO3G_08898, in turn, found DSL1 in Sc (0.014) and potential orthologs in other fungi, with e-values ranging from $1e^{-14}$ (MGG_02443) to 0.072 (AN9435). MGG_02443.5 did not find Sc DSL1, and AN9435 found it as a distant hit ($e \geq 0.96$). However, the Ro, Mg, and An genes each found the human DSL1 homolog, ZW10, as the top hit ($6e^{-14}$, $3e^{-07}$ and $3e^{-06}$, respectively). Sc DSL1 did not find human ZW10, in blastp searches.

[d] Sc TIP20 did not find other fungal orthologs, but the human TIP20 homolog, RINT-1 (Rad50-interacting protein-1), did find the potential ortholog in An (AN4884, $1e^{-33}$) and other fungi. In turn, AN4884 found Sc TIP20 ($1.9e^{-06}$).

[e] GET1 is poorly conserved between Sc and An (0.056) and Sc and human (0.013), with relatively stronger conservation between An and human ($2e^{-11}$).

[f] Sc GET2 homologs do not exist in other fungi, as determined by iterative forward and reverse tBlastn of Sc and all fungal genomes and GenBank at e = 10. All fungal hits were $e \geq 2.9$. Weak fungal hits were tested by blastp analysis of Sc and An genomes.

[g] Sc GET3 found the putative ortholog in An (AN2909) and other fungi. AN2909 was the only hit at e = 1.0. AN2909 found Sc GET3 ($3e^{-86}$) + two additional weak, unrelated hits ($e \geq 0.34$). AN2909 found itself ($1e^{-179}$) + 6 additional weak, unrelated *A.nidulans* hits at $e \geq 2.6$. GET3 is strongly conserved from Sc to human, with greater similarity between the An and human orthologs ($8e^{-102}$) than between Sc and human ($7e^{-80}$) or Sc and An ($4e^{-80}$).

[h] One novel additional ARF, two additional ARLs, and one ARF-GAP expansion occur in An and other fungi. Shown are the closest Sc homologs (ARF1 and ARL1, AGE2), and the e-value for tblastn of the An genome using Sc ARF1 and ARL1 or AGE2. Also shown are the closest human homologs of the novel An proteins, and corresponding e-values from blastp of the Hs genome using the An proteins.

[i] Sc ARF1 and ARL1 found an unnamed hypothetical ORF in An (contig 13, nt 160799–161626). This An ORF found strong putative orthologs in other fungi; its closest relative is CIMG_03295 ($3e^{-70}$). Shown above are e-values for tBlastn search of all fungi using CIMG_03295.

S. cerevisiae	*A. nidulans*		*Other fungi*[a]	
Other ARF/ARL-associated proteins				
SYS1 (*ARL3 targeting to GA*)	Contig 84[k]	($1e^{-09}$)	Nc, Ci, Mg, Cg, Bc, Ss	($2e^{-08} \rightarrow 3e^{-04}$)
	NCU02294	($2e^{-08}$)		
MON2 (*endosomal, ARL1-interacting*)	AN3643	($4e^{-53}$)	Ci, Ss, Cg, Nc, Bc, Mg, Cn, Ro	($0.0 \rightarrow 1e^{-30}$)
SLO1 (*Golgi, ARL3-interacting*)	AN4502[l]	–	Ci, Bc, Ss, Nc, Mg, Cg, Cn, Ro	($1e^{-29} \rightarrow 0{,}52$)
IMH1 (*Endo → GA, GRIP domain*)	AN2480	($4e^{-36}$)	Ci, Nc, Ss, Bs, Mg, Cg, Ro	($0.0 \rightarrow 4e^{-31}$)
USO1 (*ER → GA SNARE complex*)	AN0706	($8e^{-39}$)	Bc, Ci, Ss, Mg, Nc, Cg	($0.0 \rightarrow 1e^{-168}$)
GMH1 (*GA, interacts with GEA1/2*)	AN3439	($7e^{-08}$)	Ci, Cn	($6e^{-52} \rightarrow 5e^{-05}$)

[j] Sc SEC12 and *S. pombe* SPO14 did not find other fungal orthologs. Instead, the human SEC12, PREB/SEC12 (NP_037520.1; Weissman et al. 2001) was used to find orthologs in *A. thaliana* (NP_680414.1) and *D. melanogaster* (AAL28195.1), which in turn were used to find the putative ortholog in *U. maydis*, UM02499. UM02499, in turn, found Sc SEC12 ($7e^{-09}$), *S. pombe* SPO14 ($8.5e^{-06}$), and found putative orthologs in Cn (CNAG_01871; $2e^{-46}$), Ro (RO3G_09896; $2e^{-26}$), and *Fusarium graminearum* (FG06652; $2e^{-06}$). These three, in turn, found *S. cerevisiae* SEC12 ($4.5e^{-16}$, 0.015, and 0.0074, respectively).

[k] Sc SYS1 found an unnamed hypothetical ORF in An (contig 84, nt 469956–470450). This An ORF found strong putative orthologs in other fungi; its closest relative is NCU02294 ($2e^{-40}$). Shown are the e-values for tBlastn search of all fungi using Sc SYS1.

[l] Sc SLO1 did not find other fungal orthologs, but the human SLO1 homolog, SCOCO (short coiled-coil protein, NP_115936), did find putative orthologs in other fungi, with e-values ranging from $7e^{-08}$ (RO3G _03250.1) to $6e^{-04}$ (CIMG_04540.2). The putative An ortholog, AN4502 found Sc SLO1 (0.053).

2006). A knockout project is currently underway in *N. crassa*, with ~800 genes deleted so far (Colot et al. 2006). Similar projects, along with microarray libraries and related technologies, are planned or under development for a variety of fungi (for current status, see http://www.fgsc.net/).

Tagging the C-terminus of certain endomembrane proteins, such as those requiring C-terminal prenylation, could be problematic and may, for example, necessitate the incorporation of a prenylation motif following the tag. Alternatively, tagging of the N-terminus would require, in many cases, that the tag be incorporated after the N-terminal cleavage site for the signal peptide.

The power of fluorescent reporters has been enhanced through the development of and advancements in imaging methodologies such as **laser scanning confocal** and **multiphoton microscopy** (König 2000; Zipfel et al. 2003; Czymmek 2005), making the use of these approaches even more attractive. However, an element of caution must also be employed. Controlling the level of expression of a fusion protein can alter its localization within the cell. In a worst-case non-lethal scenario the fusion is non-functional and targeted to the wrong intracellular location. Functional complementation of a mutant phenotype by the fusion protein is an important determinant of proper targeting, as is antibody-based ultrastructural confirmation that the fusion is going to the proper compartment (Hawes et al. 2001). Since it is rare to have the native promoter for a gene in hand, expression must be controlled by the judicious choice of a known promoter whose expression level in a given cell type is

Table. 1.4. (on page 12–16) SNAREs, RABs, RAB regulators, COGs, YIPs, and other SNARE mediators. *A. nidulans* (An) SNARE and SNARE-related proteins, COGs, and YIPs were identified by tBlastn and blastp using *S. cerevisiae* (Sc) proteins. Sc proteins were obtained from Gupta and Heath (2002), and from Gene Ontology annotation for yeast proteins (www.yeastgenome.org). An proteins were defined by forward and reverse tBlastn between Sc and An genomes (http://www.broad.mit.edu/annotation/genome/aspergillus_nidulans/), tBlastn and blastp of An proteins against the An genome, and tBlastn and blastp of An and Sc proteins to all Fungal Genome Initiative (FGI) genomes (http://www.broad.mit.edu/annotation/fgi/). *A. nidulans* (An) RABs were identified by tBlastn using *S. cerevisiae* (Sc) Rabs. Sc Rabs were obtained from Pereira-Leal and Seabra (2001). *ER* Endoplasmic reticulum, *GA* Golgi apparatus, *VA* vacuole, *HVS* homotypic vacuole sorting, *Endo* Endosome, *TGN* trans-Golgi network, *FUN* function unknown, *PM* plasma membrane, *PVC* prevacuolar compartment

S. cerevisiae	*A. nidulans*		Other fungi[a]	
Qa-SNAREs (Syntaxins, t-SNAREs)				
SED5 (*cis-Golgi, ER ↔ GA*)	AN9256	($3e^{-35}$)	Cg, Cn	(2.8 → 6.3)
TLG2 (*Endo → GA*)	AN2048	($2e^{-14}$)	Ss, Ci, Cg, Bc, Mg, Nc, Cn, Ro	($1e^{-107}$ → $8e^{-14}$)
PEP12, VAM3 (*vacuole, PVC*)	AN4416	($8e^{-18}$, $1e^{-11}$)	Ci, Ss, Mg, Cg, Nc, Ro	($6e^{-80}$ → $1e^{-12}$)
UFE1 (*ER membrane, GA → ER*)	AN6047[b]	(0.004)	Ci, Ss, Mg, Cg, Nc, Ro	($2e^{-25}$ → 0.023)
SSO1, SSO2 (*plasma membrane*)	AN3416	($1e^{-04}$, $2e^{-09}$)	Nc, Mg, Ci, Ss, Ro, Cn, Bc	($3e^{-32}$ → $7e^{-24}$)
Qb-SNAREs				
BOS1 (*ER membrane, ER → GA*)	Contig 112[c]	($5e^{-09}$)	Nc, Mg, Ci	($1e^{-16}$ → $4e^{-10}$)
SEC20 (*GA → ER*)	AN2969[d]		Ss, Cn, Nc, Ci	(0.001 → 0.68)
GOS1 (*Golgi transport*)	AN1229	($3e^{-25}$)	Ci, Bc, Mg, Ss, Cg, Nc	($1e^{-53}$ → $1e^{-33}$)
SEC9, SPO20 (*fusion with PM*)	AN2419	($3e^{-27}$, $5e^{-21}$)	Ci, Bc, Ss, Mg, Ro	($7e^{-79}$ → $1e^{-13}$)
VTI1 (*cis-Golgi, vacuolar sorting*)	AN1973	($3e^{-19}$)	Ci, Ss, Bc, Mg, Nc, Cg, Ro, Cn	($1e^{-60}$ → $1e^{-04}$)
Qc-SNAREs				
BET1 (*ER → GA transport*)	AN5127	($5e^{-19}$)	Nc, Cg, Mg, Ci, Bc, Ss	($1e^{-26}$ → $4e^{-05}$)
SFT1 (*intra-Golgi transport*)	AN10508[e]		Bc, Ss, Nc, Mg, Cg, Ro	($9e^{-22}$ → 0.11)
SYN8 (*endosomal*)	AN2169	($6e^{-05}$)	Ci, Ss, Bc, Mg, Nc, Cg, Ro, Cn	($1e^{-74}$ → $3e^{-10}$)
TLG1 (*endosome → GA*)	AN8171	($8e^{-11}$)	Ci, Ss, Bc, Mg, Nc, Cg, Cn	(0.0 → $2e^{-23}$)
VAM7 (*vacuole*)	AN4551	($4e^{-12}$)	Ci, Ss, Bc, Nc, Mg, Cg, Ro, Ss, Cn	($1e^{-100}$ → $2e^{-19}$)
USE1 (SLT1; *ER, GA → ER*)	AN0650[f]		Nc, Mg	(0.011, 0.70)
R-SNAREs (Synaptobrevins)				
SEC22 (*ER → GA → ER*)	Contig 110[g]	($7e^{-33}$)	Mg, Cg, Nc, Bc, Ss, Ci, Cn, Ro	($5e^{-43}$ → $4e^{-11}$)
SNC1, SNC2 (*GA → PM*)	AN8769	($2e^{-20}$, $6e^{-23}$)	Ci, Bc, Ss, Mg, Nc, Cn	($5e^{-23}$ → $7e^{-11}$)
YKT6 (*GA, Endo → VA, VA fusion*)	AN8488	($3e^{-32}$)	Ci, Ss, Bc, Cg, Nc, Mg, Ro, Cn	($1e^{-56}$ → $1e^{-09}$)
NYV1 (*vacuolar vesicle fusion*)	AN0571	($2e^{-10}$)	Ci, Ss, Bc, Nc, Mg, Cg, Ro, Cn	($2e^{-84}$ → $3e^{-09}$)
SNARE-binding Sm-like proteins (SNARE masters)				
SLY1 (*ER → GA, binds SED5p*)	AN2518	($3e^{-99}$)	Ss, Mg, Bc, Ci, Ro, Nc, Cg, Cn	(0.0 → $8e^{-95}$)
SEC1 (*exocytic vesicle docking/fusion*)	AN4724	($1e^{-45}$)	Mg, Ss, Bc, Ci, Cg, Nc, Cn, Ro	(0.0 → $2e^{-23}$)
VPS45 (*GA → PVC, early Endo, late GA*)	AN6531	($1e^{-102}$)	Ci, Bc, Nc, Ss, Mg, Cg, Cn, Ro	(0.0 → $8e^{-91}$)
SNARE mediators				
USO1 (*ER → GA transport*)	AN0706	($8e^{-39}$)	Bc, Ci, Ss, Mg, Nc, Cg, Cn	(0.0 → $4e^{-27}$)
PBI2 (*vacuolar fusion*)	AN5125[h]	–	Ro, Ss, Bc, Nc, Mg, Cg	($6e^{-05}$ → 0.54)
SWF1 (*palmitoyltransferase*)	AN1907	($5e^{-16}$)	Nc, Mg, Cg, Ss, Ci, Bc	($1e^{-76}$ → $1e^{-10}$)
SNX4 (*sorting nexin, Endo → GA*)	AN3584	($7e^{-69}$)	Ci, Bc, Ss, Mg, Nc, Cg, Ro, Cn	(0.0 → $7e^{-22}$)
ATG20, SNX41 (*Cyto → VA targeting*)	AN6351	($2e^{-33}$, $2e^{-11}$)	Ci, Ss, Nc, Cg, Mg, Ro, Bc, Cn	(0.0 → $2e^{-25}$)
VTC1 (*vacuolar transporter chaperone*)	AN1334	($8e^{-40}$)	Ci, Nc, Cg, Mg, Ss, Bc, Ro	($9e^{-50}$ → $6e^{-42}$)
SEC17 (*ER → GA, HVS*)	AN6267	($9e^{-37}$)	Ci, Bc, Ss, Mg, Cg, Nc, Ro, Cn	($1e^{-100}$ → $2e^{-20}$)
SEC18 (*ATPase, regulates SEC17*)	AN3098	(0.0)	Ci, Ss, Nc, Mg, Ro, Cn, Bc, Cg	(0.0 → $4e^{-30}$)

S. cerevisiae	*A. nidulans*		Other fungi[a]	
PTM1 (FUN, copurifies with TLG2p)	AN0063	($4e^{-35}$)	Ci, Bc, Mg, Nc, Cg, Ss, Ro, Cn	($3e^{-97} \rightarrow 9e^{-14}$)
SFT2 (*late GA transport*)	AN1297	($5e^{-10}$)	Nc, Mg, Ss, Ci, Bc, Cn	$7e^{-28} \rightarrow 4e^{-15}$)
DNA damage-inducible v-SNARE binding protein				
DDI1	AN6741	($6e^{-49}$)	Ci, Ss, Bc, Nc, Mg, Cg, Ro, Cn	($1e^{-122} \rightarrow 7e–^{37}$)
RAB family GTPases (SNARE activators)[i]				
YPT1 (*ER → GA transport, HsRAB1 homolog*)	AN4281	($9e^{-64}$)	Ss, Cg, Bc, Nc, Ro, Mg, Ci, Cn	($3e^{-83} \rightarrow 5e^{-47}$)
SEC4 (*vesicle → exocytosis*)	AN6974	($1e^{-56}$)	Ci, Cg, Mg, Ro, Cg, Ss, Nc, Cn	($5e^{-91} \rightarrow 5e^{-37}$)
YPT31, -32 (*intra-GA, vesicle budding, HsRAB11*)	AN0347	($3e^{-57}$)	Ss, Nc, Mg, Ro, Bc, Ci, Cg, Cn	($3e^{-80} \rightarrow 1e^{-59}$)
YPT51, -53 (*endocytosis, VA prot sorting, HsRAB5*)	AN4915[j]	($7e^{-45}$)	Ci, Cg, Bc, Ss, Nc, Mg, Ro	($1e^{-86} \rightarrow 2e^{-44}$)
YPT52 (*endocytosis, VA protein sorting, HsRAB5*)	AN3842[j]	($1e^{-35}$)	Ci, Cg, Ss, Mg, Bc, Ro, Nc	($4e^{-85} \rightarrow 8e^{-44}$)
YPT6 (*Endo → GA, HsRAB6*)	AN7602	($2e^{-52}$)	Ci, Bc, Ro, Ss, Mg, Cg, Nc	($3e^{-62} \rightarrow 2e^{-34}$)
YPT7 (*Endo → Endo, homotypic vac fusion, HsRAB7*)	AN0089	($2e^{-54}$)	Cg, Ss, Nc, Bc, Ro, Mg, Cn, Ci	($1e^{-82} \rightarrow 6e^{-43}$)
YPT10 (*vacuolar transport?*)	**None**		**None**	
YPT11 (*distribution of mitochondria*)	**None**		**None**	
Novel additional Rabs[k]				
Hs Rab2, Rab2B	AN5106	($2e^{-36}$, $7e^{-34}$)	Ci, Nc, Bc, Ss, Mg, Cg, Ro	($1e^{-66} \rightarrow 1e^{-28}$)
Hs Rab4b, Rab4A	AN9072	($9e^{-40}$, $7e^{-38}$)	Ci, Ss, Mg, Nc, Cg, Bc	($5e^{-91} \rightarrow 7e^{-64}$)
Hs Rab24	AN2474	($4e^{-30}$)	Ci, Ss, Mg, Bc , Cg, Nc, Cn	($1e^{-93} \rightarrow 2e^{-29}$)
Prenylation of RAB GTPases				
MRS6 (*Rab escort protein for YPT1 prenylation*)	AN8679	($7e^{-33}$)	Ci, Ss, Cg, Bc, Mg, Nc, Ro	($6e^{-47} \rightarrow 9e^{-05}$)
BET2 (β-*subunit, geranylgeranyltransferase*)	AN3747	($3e^{-83}$)	Ci, Cg, Mg, Bc, Nc, Ro, Ss, Cn	($1e^{-117} \rightarrow 1e^{-60}$)
BET4 (α-*subunit, geranylgeranyltransferase*)	AN1981	($1e^{-39}$)	Ci, Nc, Ss, Mg, Bc, Cn, Ro	($3e^{-93} \rightarrow 1e^{-10}$)
RAB-GAPs				
GYP1 (*GAP for YPT1, HsTBC1D22B*)	AN7444	($1e^{-83}$)	Cg, Ci, Nc, Bc, Mg, Ss, Ro, Cn	($1e^{-56} \rightarrow 3e^{-45}$)
GYP5 (*GAP for YPT1 and SEC4, HsRABGAP1*)	AN1980[l]	($5e^{-47}$)	Ci, Bc, Nc, Cg, Ss, Mg, Ro, Cn	($0.0 \rightarrow 6e^{-31}$)
GYL1 (*stimulates GYP5 activity onYPT1, HsTBC1D1*)	AN5407[l]	($6e^{-17}$)	Ci, Bc, Nc, Cg, Ss, Mg, Ro, Cn	($0.0 \rightarrow 6e^{-41}$)
GYP6 (*GAP for YPT6, HsTBC1D5*)	AN4537	(0.68)	Ci, Nc, Ss, Cg, Bc, Cn, Ro, Mg	($7e^{-77} \rightarrow 9e^{-14}$)
GYP7 (*GAP for YPT7, YPT1, YPT31/32, HsTBC1D15*)	AN6618	($3e^{-68}$)	Ci, Ss, Mg, Nc, Cg, Bc, Ro, Cn	($0.0 \rightarrow 2e^{-39}$)
GYP8 (*GAP for YPT1, SEC4, YPT31/32, HsTBC1D20*)	AN4036	($2e^{-08}$)	Ci, Nc, Bc, Mg, Cg, Ro, Cn, Ss	($5e^{-79} \rightarrow 1e^{-06}$)
MSB3, MSB4 (*GAP for SEC4, HsTBC1D8/1D9*)	AN10355	($9e^{-71}$, $2e^{-71}$)	Ci, Bc, Ss, Nc, Mg, Cg, Ro	($1e^{-146} \rightarrow 3e^{-51}$)
MDR1 (*GAP for YPT6, -31, SEC4, HsTBC1D8/1D9*)	AN11010	($1e^{-160}$)	Nc, Cg, Bc, Ss, Ci, Mg, Ro, Cn	($0.0 \rightarrow 1e^{-112}$)
Novel additional RAB-GAPs[m]	An vs Sc	An vs Hs		
(MDR1)	AN0573 ($2e^{-24}$)	HsTBC1D2B ($2e^{-34}$)	Ci, Ss, Mg, Nc, Cg, Cn, Ro	($0.0 \rightarrow 5e^{-20}$)
(GYP5)	AN3094 ($3e^{-12}$)	HsUSP6 N-terminal-like ($1e^{-24}$)	Ci, Ss, Cg,Mg, Nc, Cn, Ro	($1e^{-177} \rightarrow 2e^{-13}$)
(MDR1)	AN3752 ($3e^{-08}$)	HsTBC1D14($3e^{-47}$)	Ci, Bc, Mg, Nc, Ss, Cg, Cn, Ro	($0.0 \rightarrow 3e^{-27}$)

S. cerevisiae	*A. nidulans*		Other fungi[a]	
RAB-GEFs				
RIC1 (*with RGP1, GEF for YPT6*)	AN1283	(0.060)	Ci, Ss, Cg, Bc, Mg, Cn, Ro	($0.0 \rightarrow 2e^{-25}$)
RGP1 (*Golgi membrane exchange factor for YPT6*)	AN6289	($3e^{-06}$)	Ss, Mg, Bc, Cg, Nc, Ro, Cn	($1e^{-144} \rightarrow 1e^{-10}$)
VPS9 (*GEF for YPT51*)	AN3678	($2e^{-45}$)	Mg, Ss, Cg, Ci, Nc, Bc, Cn	($1e^{-136} \rightarrow 2e^{-44}$)
GDI1 (*GDP dissoc. inhibitor for SEC4/YPT family*)	AN5895	($1e^{-127}$)	Ci, Nc, Cg, Ss, Mg, Bc, Cn, Ro	($0.0 \rightarrow 1e^{-64}$)
Novel additional VPS9 domain proteins				
(VPS9)	AN5920	($5e^{-07}$)	Ci, Bc, Ss, Mg, Cg, Nc, Bc, Cn	($1e^{-147} \rightarrow 2e^{-11}$)
YML002W (uncharacterized hyp ORF)	AN1280	($3e^{-29}$)	Ci, Bc, Ss, Nc, Cg, Mg, Ro, Cn	($0.0 \rightarrow 3e-^{04}$)
Hs Rab6-interacting protein 1 (NP 056028)[n]	AN4349	($8e^{-15}$)	Ci, Ss, Cg, Nc, Mg, Bc, Ro	($0.0 \rightarrow 1e^{-35}$)
	AN0575	($1e^{-05}$)	Nc, Ss, Bc, Ci, Mg, Cg	($0.0 \rightarrow 0.0$)

[a] Listed are fungi in which one or more putative orthologs occur. Order of fungi and corresponding range of e-values indicate relative strength of homology to An sequence, except where noted. Bc, *Botrytis cinerea*; Cg, *Chaetomium globosum*; Ci, *Coccidioides immitis*; Cn, *Cryptococcus neoformans*; Mg, *Magnaporthe grisea*; Nc, *Neurospora crassa*; Ro, *Rhizopus oryzae*; Ss, *Sclerotinia sclerotiorum*.

[b] Sc UFE1 found four putative fungal orthologs by forward and reverse tblastn, with e-values ranging from $2e^{-09}$ (RO3G_11201) to 0.070 (CHGG_05038).

[c] Sc BOS1 found an unnamed hypothetical ORF in An (contig 1.112, nt 95072–95750), and found putative orthologs in three other fungi, with e-values ranging from $1e^{-16}$ to $4e^{-10}$.

[d] Sc SEC20 found no hits in An at e = 1.0. However, autocalled SEC20 orthologs were found in Ss (SS1G_04785; 0.001), Cn (CNAG_02135; 0.002), Nc (NCU00953; 0.006), and Ci (CIMG_07624; 0.68). CIMG_07624, in turn, found a putative An ortholog (AN2969, a hypothetical ORF, at an e-value of $3e^{-74}$).

[e] Sc SFT1 found no hits in An at e = 1.0. However, putative SFT1 orthologs were found in Mg (MGG_04953; 0.016), Bc (BC1G_05009; 0.53), and Ss (SS1G_02441; 0.90). MGG_04953 found a putative SFT1 ortholog in An (AN10508), with an e-value of $8e^{-17}$. AN10508, in turn, showed greatest homology to SFT1 and BET1 in Sc ($2.7e^{-07}$, $6.4e^{-06}$).

[f] Sc USE1 Sc found no hits in An at e = 1.0. However, putative USE1 orthologs were found in Nc (NCU00184; 0.011) and Mg (MGG_12919; 0.70). NCU00184 found a putative homolog in An (AN0650; $2e^{-22}$), but the An gene did not find USE1 or other SNAREs in Sc.

[g] Sc SEC22 found an unnamed hypothetical ORF in An (contig 110, nt 95603–96426), and found putative orthologs in other fungi.

[h] Sc PBI2 found no hits in An at e = 1.0, likely because it is a very short protein. However, putative PBI2 orthologs were found in other fungi. The Mg PBI2 ortholog, MGG_00164, found a putative An ortholog, AN5125 ($3e^{-05}$). In turn, AN5125 found Sc PBI2 ($3.1e^{-06}$).

[i] An RABs were defined by (1) presence of all five RAB family-specific sequences (RabF1 to RabF5), as described by Pereira-Leal and Seabra (2000, 2001), and (2) in all but two cases (AN7602 & AN9072) the occurrence of a putative C-terminal prenylation motif (XXCC, XCXC, XXC, or XXCX). Absence of a prenylation motif from AN7602 and AN9072 likely reflects errors in the automated annotation of the An genome, as both sequences appear orthologous to prenyl motif-containing genes in four or more other fungi. Orthology assignments were based on forward and reverse tBlastn between Sc, An, and Hs genomes, tBlastn of An RABs against the An genome, tBlastn of An and Sc RABs to all Fungal Genome Initiative (FGI) genomes, and by phylogenetic trees using the neighbor-joining method excluding positions with gaps, and including An Ras2 homologs (AN0182 and AN5832) as outliers (http://www.ebi.ac.uk/clustalw/index.html). e-values are from tBlastn of An genome with Sc RABs.

[j] Sc YPT51 (VPS21) and YPT53 are more closely related to each other ($4.3e^{-55}$, $1.6e^{-57}$) and to AN4915 ($2e^{-56}$, $2e^{-46}$) than to YPT52 ($5.8e^{-43}$, $5.3e^{-41}$) and AN3842 ($7e^{-50}$, $4e^{-44}$). YPT52, on the other hand, shows stronger homology to AN3842 ($4e^{-51}$) than to AN4915 ($2e^{-43}$).

[k] Sc orthologs of AN5106, AN9072, and AN2474 were not found, suggesting that these An genes may occupy new or novel functional niches. Hs genes indicate closest human homologs by forward and reverse tBlastn. AN5106 and AN9072 are most closely related to each other (e^{-23}). AN2474 clusters with AN5106 and AN9072 in neighbor-joining trees. e-values are from blastp of Hs genome using An proteins.

[l] GYP5 and GYL1 both show stronger homology to AN1980 ($5e^{-47}$, $1e^{-25}$) and weaker homology to AN5407 ($5.1e^{-30}$, $6e^{-17}$).

S. cerevisiae	*A. nidulans*		Other fungi[a]	
Conserved oligomeric Golgi complex (COG), cytosolic tethering complex, intra-Golgi vesicle-mediated transport				
COG1	AN6596[o]	–	Ci, Ss, Bc, Nc, Mg	($1e^{-123} \rightarrow 4e^{-59}$)
COG2	*AN8226*[o]	–	Ci, Ss, Cg, Bc, Mg, Nc, Cn	($3e^{-43} \rightarrow 2e^{-11}$)
COG3	AN4886	($5e^{-58}$)	Ci, Nc, Cg, Bc, Ss, Mg, Cn	($1e^{-163} \rightarrow 5e^{-13}$)
COG4	AN7462	($6e^{-44}$)	Ci, Ss, Bc, Cg, Mg, Cn, Ro	($0.0 \rightarrow 1e^{-16}$)
COG5	*AN8226*[o]	–	Ci, Ss, Cg, Bc, Mg, Nc, Cn	($3e^{-43} \rightarrow 2e^{-11}$)
COG6	AN10441	($2e^{-22}$)	Ci, Ss, Cg, Nc, Mg, Cn, Bc, Ro	($0.0 \rightarrow 5e^{-19}$)
COG7	AN5481[p]	(0.15)	Ci, Nc, Cg, Mg, Ss, Bc	($9e^{-29} \rightarrow 1e^{-08}$)
COG8	**Not found**[q]	–	Ro, Cn	
RUD3 (*interacts with COG3 & USO1*)	AN0186	($7e^{-18}$)	Ci, Ss, Cg, Bc, Nc, Mg	($3e^{-75} \rightarrow 4e^{-38}$)
YIP/YOS/YIF RAB-interacting proteins				
YIP1 (*COPII vesicle biogenesis*)	AN10878	($1e^{-33}$)	Ci, Bc, Mg, Cg, Nc, Ss, Ro	($1e^{-121} \rightarrow 1e^{-47}$)
YOP1 (*interacts with YIP1*)	AN2279[r]	($4e^{-30}$)	Ci, Ss, Bc, Nc, Cg, Mg, Ro, Cn	($1e^{-69} \rightarrow 6e^{-30}$)
Novel additional YOP1 homolog	AN6059[r]	($3e^{-12}$)	Ci, Bc, Cg, Nc, Ss, Mg, Cn, Ro	($2e^{-74} \rightarrow 2e^{-13}$)
YIP3 (*COPII, ER → GA transport*)	AN10724	($2e^{-43}$)	Bc, Mg, Ss, Nc, Cg, Cn, Ro	($7e^{-57} \rightarrow 4e^{-10}$)
YIP4 (*interacts with Rab GTPases*)	AN5926	($1e^{-13}$)	Ci, Bc, Ss, Mg, Nc, Ro, Cn, Cg	($6e^{-92} \rightarrow 4e^{-11}$)
YIP5 (*interacts with Rab GTPases*)	AN4017	($8e^{-15}$)	Ci, Ss, Bc, Nc, Cg, Mg, Ro, Cn	($1e^{-103} \rightarrow 4e^{-23}$)
YIF1 (*COPII, ER → GA transport*)	AN6628	($5e^{-30}$)	Ci, Bc, Nc, Cg, Mg, Ss, Cn, Ro	($1e^{-129} \rightarrow 1e^{-19}$)

[m] In addition to the eight orthologs of Sc RAB-GAPs, an additional three RAB-GAPs occur in An and other fungi. Shown are the closest Sc homologs (MDR1 and GYP5), and the e-value for tblastn of the An genome using Sc MDR1 or GYP5. Also shown are the closest human homologs of the novel An RAB-GAPs and corresponding e-values from blastp of the Hs genome using the An proteins.

[n] AN4349 and AN0575 have no homologs in Sc. These two genes contain DENN (AEX-3) domains characteristic of proteins involved in RAB-mediated processes. AN4349 and AN0575 show homology to human RAB6-interacting protein 1. Human RAB6IP1 finds only AN4349 and AN0575 ($8e^{-15}$, $1e^{-05}$) in *A. nidulans*, and no significant hits in *S. cerevisiae*. AN4349 finds Hs SBF1 ($6e^{-17}$) and Hs RAB6IP1 ($8e^{-15}$) as top hits by blastp. AN0575 is more divergent, in humans finding a variety of DENN/MADD-containing and other proteins ($4e^{-13} \rightarrow 1e^{-05}$), with RAB6IP1 as a more distant hit ($1e^{-05}$).

[o] Sc COG1, COG2, and COG5 did not find An orthologs at e = 10. Instead, the human COG1, -2, -5 were used to find potential An orthologs. The An orthologs, in turn, found the human genes. Note that Hs COG2 and Hs COG5 found the same An gene, AN8226 (0.81 and 0.005, respectively). AN8226 showed slightly greater similarity to Hs COG2 ($6e^{-10}$) than Hs COG5 ($8e^{-05}$).

[p] Sc COG7 shows weak homology to AN5481 (0.15). By reciprocal blastp, AN5481 shows weak similarity to MOT2 (0.41) and COG7 (0.85). These very weak homologies lead us to question whether AN5481 is a homolog of Sc COG7. Reciprocal blastp searches between Hs COG7 and AN5481 failed to reveal homology between the two genes.

[q] Sc COG8 finds two fungal COG8 homologs: RO3G_13059 ($8e^{-10}$) and CNAG_05498 ($3.9e^{-08}$). RO3G_13059, in turn, finds other putative fungal COG8 orthologs, including CNAG_05498 ($4e^{-44}$), NCU02974 ($2e^{-23}$), MGG_05624 ($3e^{-22}$), CIMG_03548 ($1e^{-21}$), SS1G_01629 ($5e^{-21}$), and CHGG_05908 ($1e^{-15}$). Human COG8 does not find the An ortholog, but also finds CNAG_05498 ($1e^{-43}$), RO3G_13059 ($3e^{-31}$), CIMG_03548 ($8e^{-09}$), MGG_05624 ($1e^{-07}$), NCU02974 ($2e^{-07}$), and SS1G_01629 ($4e^{-06}$).

[r] AN2279 is more closely related to Sc YOP1 ($4e^{-30}$) than is AN6059 ($3e^{-12}$). YOP1 and AN2279 both show strongest similarity to human Receptor Accessory Protein 5 (REEP5, NP_005660.3, $1e^{-22}$ and $9e^{-23}$ respectively), a protein that is deleted in some Familial Adenomatous Polyposis Coli cancers (Prieschl et al. 1996) and has been implicated in the function of odorant receptors (Saito et al. 2004) and also in Familial Glucocorticoid Deficiency (Clark et al. 2005). AN6059 shares greater homology with receptor expression enhancing protein 4 (REEP4, NP_079508, $3e^{-19}$), one of four other recently discovered human REEP paralogs (Clark et al. 2005).

[s] Sc YOS1 found an unnamed hypothetical ORF in An (contig 61, nt 141452–141694). Sc YOS1 found putative orthologs in other fungi; its closest fungal relative is BC1G_07235 (0.52, Sc YOS1 vs. all fungi).

understood. Overexpression is not necessarily undesirable, in that the additional labeling that is observed may provide information regarding the trafficking route for that protein. For example, overexpression of a sialyltransferase-GFP fusion in plant epidermal cells can lead to a distribution of the fusion protein throughout the entire Golgi stack, whereas under lower levels of expression the enzyme is restricted to the trans-face (Hawes and Satiat-Jeunemaitre 2005). Overexpression may also be required for microscopic detection if expression of the endogenous promoter is too low, as appears to be the case with the majority of gene products in the *Saccharomyces* genome (Natter et al. 2005).

Issues and uncertainties associated with overexpression may be less problematic in *A. nidulans*, where the widely used *alcA* alcohol dehydrogenase gene promoter permits flexible control over levels of expression, and where it is often possible to fine tune the expression of a protein based simply on the carbon source of the growth medium. In *Aspergillus*, the *alcA* alcohol dehydrogenase gene promoter is repressed strongly by glucose. Low

S. cerevisiae	*A. nidulans*		Other fungi[a]	
YOS1 (*COPII, ER → GA*)	Contig 61[s]	(0.067)	Bc, Ss, Mg	($0.52 \rightarrow 2.0$)
RTN1 (*reticulon, interacts with SEC6, YIP3*)	AN5404[t]	($6e^{-11}$)	Ci, Bc, Nc, Cg, Mg, Ss	($1e^{-69} \rightarrow 2e^{-61}$)
Novel additional RTN1-like	AN5648[t]	(0.41)	Ci, Ss, Bc, Mg, Cg, Nc, Cn, Ro	($1e^{-173} \rightarrow 3e^{-07}$)
RTN2 (*unknown function, similar to reticulon*)	**None**		**None**	

[t] An proteins show greatest homology in a reciprocal search to Sc RTN1 ($2.5e^{-08}$ for AN5404, 0.0029 for AN5648). However, they do not find each other in reciprocal *A. nidulans* blastp searches, suggesting that they may be unrelated or diverged. Sc RTN1 and AN5404 show greatest similarity to human reticulons. Surprisingly, however, Sc RTN1 shows stronger homology to the human reticulons ($3e^{-06} \rightarrow 8e^{-04}$) than does AN5404 (0.006), indicating that RTN1 orthologs in filamentous fungi and one basidiomycetous yeast have diverged away from those in mammals. Furthermore, the weak An RTN1 homolog, AN5648, does not find human reticulons, instead showing mild similarity to several functionally unrelated human proteins ($4e^{-07} \rightarrow 5e^{-05}$).

Table. 1.5. (on page 17–18) Clathrins, clathrin mediators, and dynamins in fungi. *A. nidulans* (An) proteins were identified by tBlastn and blastp using *S. cerevisiae* (Sc) proteins. Sc proteins were obtained from Gene Ontology annotation for yeast (www.yeastgenome.org). An proteins were defined by forward and reverse tBlastn and blastp between Sc and An genomes (http://www.broad.mit.edu/annotation/genome/aspergillus_nidulans/), tBlastn and blastp of An proteins against the An genome, tBlastn and blastp of An and Sc proteins to all Fungal Genome Initiative (FGI) genomes (http://www.broad.mit.edu/annotation/fgi/), and by phylogenetic trees using the neighbor-joining method excluding positions with gaps. In addition, fungal dynamins were analyzed by blastp of An proteins vs Hs genome, and by phylogenetic trees with Sc, An, and Hs proteins, using the neighbor-joining method excluding positions with gaps

Table. 1.6. (on page 19–22) Endosomal, vacuolar and exocytotic processes. *A. nidulans* (An) ER proteins were identified by tBlastn using *S. cerevisiae* (Sc) proteins. Sc proteins were obtained from Gene Ontology annotation for yeast endosome/vacuole (www.yeastgenome.org), and from Bowers and Stevens (2005). An proteins were defined by forward and reverse tBlastn and blastp between Sc and An genomes (http://www.broad.mit.edu/annotation/genome/aspergillus_nidulans/), tBlastn of An proteins against the An genome, and tBlastn and blastp of An and Sc proteins to all Fungal Genome Initiative (FGI) genomes (http://www.broad.mit.edu/annotation/fgi/). *MVB* Multivesicular body, *PM* plasma membrane, *PI-3-P* phosphatidylinositol 3-phosphate, *VA* vacuole

S. cerevisiae	*A. nidulans*		Other fungi[a]	
Clathrin vesicle coat				
CHC1 (*heavy chain*)	AN4463	(0.0)	Ci, Cg, Nc, Mg, Ro, Bc, Ss, Cn	(0.0 → 0.0)
CLC1 (*light chain*)	AN2050	($2e^{-10}$)	Bc, Ci, Ss, Cg, Nc, Mg	($3e^{-38}$ → $2e^{-26}$)
ENT3 (*clathrin recruitment, GA → Endo*)	AN3821	($1e^{-33}$)	Ss, Cg, Bc, Ci, Mg, Nc, Ro, Cn	($2e^{-56}$ → $7e^{-22}$)
ENT5 (*clathrin recruitment, GA → Endo*)	**None**		**None**	
Other clathrin-binding proteins				
ENT1, ENT2 (*endocytosis*)	AN3696	($1e^{-26}$, $5e^{-21}$)	Ci, Ss, Cg, Bc, Mg, Nc, Cn, Ro	($1e^{-159}$ → $1e^{-31}$)
ENT4 (*unknown function*)	**None**		**None**	
YAP1801, YAP1802 (*clathrin cage assembly*)	AN5224	($2e^{-12}$, $1e^{-19}$)	Ci, Cg, Bc, Nc, Mg, Ss, Cn, Ro	($1e^{-116}$ → $5e^{-22}$)
AP-1 adaptor complex				
APL2 (β-*adaptin*)	AN3029	($6e^{-73}$)	Ci, Ss, Nc, Ro, Bc, Cg, Mg	(0.0 → $1e^{-141}$)
APL4 (γ-*adaptin*)	AN4207	($3e^{-76}$)	Ci, Bc, Ss, Nc, Mg, Cg, Cn, Ro	(0.0 → $1e^{-101}$)
APS1 (σ-*subunit*)	AN7682	($4e^{-35}$)	Ci, Nc, Cg, Mg, Ss, Bc, Ro	($1e^{-63}$ → $8e^{-31}$)
APM1 (*Mu1-like subunit*)	AN8795	($7e^{-71}$)	Cg, Mg, Nc, Ss, Ci, Ro, Cn, Bc	(0.0 → $1e^{-108}$)
APM2 (*unknown function*)	**None**		**None**	
AP-2 adaptor complex				
APL1 (β-*adaptin*)	AN5950	($2e^{-51}$)	Nc, Cg, Ss, Bc, Cn, Ci, Ro	(0.0 → $9e^{-82}$)
APL3 (α-*adaptin*)	AN7016	($1e^{-73}$)	Ci, Bc, Nc, Mg, Ss, Cg, Ro	(0.0 → 0.0)
APS2 (σ-*subunit*)	AN0722	($7e^{-33}$)	Mg, Nc, Cg, Bc, Ci	($1e^{-63}$ → $3e^{-58}$)
APM4 (*Mu2-like subunit*)	AN7741	($3e^{-88}$)	Bc, Ss, Nc, Mg, Cg, Ci, Ro, Cn	(0.0 → $9e^{-94}$)
AP-3 alternative pathway complex				
APL5 (δ-*adaptin*)	AN8291	($7e^{-87}$)	Ci, Bc, Mg, Ss, Nc, Cg, Ro, Cn	(0.0 → $1e^{-37}$)
APL6 (β*3-like subunit*)	AN0165	($3e^{-62}$)	Ci, Ss, Bc, Nc, Cg, Mg, Ro, Cn	(0.0 → $5e^{-33}$)
APS3 (σ-*subunit*)	AN5519	($5e^{-29}$)	Ci, Cg, Mg, Bc, Nc, ss, Cn, Ro	($2e^{-70}$ → $4e^{-28}$)
APM3 (*Mu3-like subunit*)	AN5641	($5e^{-10}$)	Ci, Ss, Bc, Mg, Cg, Nc	($1e^{-119}$ → $8e^{-83}$)
Proteins associated with clathrin-coated vesicles				
AGE2 (*Arf GTPase, TGN*)	AN1931	($7e^{-20}$)	Ss, Ci, Bc, Cg, Nc, Mg, Cn, Ro	($1e^{-110}$ → $1e^{-32}$)
BCH1, BUD7, CHS6, FMP50 (*CHS1-ARF1 binding proteins, GA → PM export*)	AN3122	($6e^{-25}$, $2e^{-23}$, 0.053, 0.003)	Ci, Cg, Ss, Nc, Mg, Bc, Ro, Cn	(0.0 → $1e^{-73}$)
BSC6 (*function unknown*)	AN7147	($2e^{-23}$)	Nc, Ci, Bc, Cg, Ss, Mg	($5e^{-99}$ → $7e^{-86}$)
CPD1 (*cyclic nucleotide phosphodiesterase*)	**None**		**None**	
GYP6 *(GAP for Rab Ypt6*)	AN4537	(0.95)	Ci, Nc, Ss, Cg, Bc, Cn, Ro, Mg	($7e^{-77}$ → $9e^{-14}$)
LAA1 (*large AP-1 accessory protein*)	AN6598	($5e^{-18}$)	Bc, Nc, Mg, Cg, Ss, Ci, Ro, Cn	(0.0 → 0.0)
LDB19 (*function unknown, telomere length control?*)	AN0056	($1e^{-28}$)	Bc, Ss, Nc, Cg, Mg	($2e^{-98}$→$1e^{-60}$)
SCY1 (*putative kinase, suppressor of GTPase mutant*)	AN4322	($5e^{-56}$)	Ci, Ss, Bc, Cg, Nc, Mg, Cn, Ro	(0.0 → $7e^{-43}$)
TVP18 (*late Golgi integral membrane protein*)	Contig 84[b]	($1e^{-21}$)	Ss, Bc, Ci, Cg, Mg, Nc, Ro	($4e^{-22}$ → $2e^{-04}$)
YBL010C (*uncharacterized hypothetical ORF*)	**None**		**None**	
YEL048C (*uncharacterized hypothetical ORF*)	**None**		**None**	

S. cerevisiae	*A. nidulans*		Other fungi[a]	
YHL017W (*putative protein of unknown function*)	AN0063	($3e^{-28}$)	Ci, Bc, Mg, Nc, Cg, Ss, Ro	($3e^{-97} \rightarrow 2e^{-37}$)
YML037C (*putative protein of unknown function*)	**None**		**None**	
BinAmphiphysinRvs (BAR)-domain proteins (regulate early steps of endocytosis, formation of clathrin-coated vesicles at the plasma membrane)				
RVS161 (*amphiphysin-like lipid raft protein*)	AN8831	($5.8e^{-67}$)	Ci, Ss, Mg, Cg, Nc, Cn, Ro	($1e^{-114} \rightarrow 9e^{-52}$)
RVS167 (*homolog of amphiphysin*)	AN2516	($2.4e^{-107}$)	Ci, Ss, Mg, Nc, Cg, Cn, Bc, Ro	($1e^{-153} \rightarrow 6e^{-39}$)
GVP36 (*Golgi vesicle protein of unknown function*)	AN10743[c]	($1.6e^{-39}$)	Ci, Ss, Bc, Cg, Mg, Ro, Cn	($1e^{-144} \rightarrow 2e^{-49}$)
Novel additional BAR domain protein: Hs endophilin (*SH3-containing SH3GLB1*)	AN2277[c]	($3e^{-12}$)	Ci, Ss, Bc, Cg, Nc, Mg, Cn, Ro	($4e^{-94} \rightarrow 2e^{-33}$)
Dynamin GTPases and dynamin-related proteins				
	An vs Sc	An vs Hs[d]		
VPS1 (*vacuolar prot sorting*)	AN8023 (0.0)	DNM1L ($3e^{-159}$)	Ci, Ss, Cg, Nc, Ro, Mg	($0.0 \rightarrow 0.0$)
DNM1 (*mitochondrial fission, endocytosis*)	AN8874 (0.0)	DNM1L ($5e^{-180}$)	Ci, Mg, Ss, Bc, Nc, Cg, Ro	($0.0 \rightarrow e^{-131}$)
MGM1 (mitochondrial)	AN1093 ($1e^{-137}$)	DNM1 ($1e^{-59}$)	Ci, Ss, Bc, Mg, Nc, Cg, Ro, Cn	($0.0 \rightarrow e^{-154}$)
FZO1 (mitochondrial)	AN6897 ($5e^{-90}$)	**None**	Ci, Ss, Bc, Mg, Nc, Cg, Ro, Cn	($0.0 \rightarrow 0.0$)
Novel dynamin-related proteins[e]				
	An vs Sc	An vs Hs		
(DNM1)	AN1309 ($1.8e^{-19}$)	MX2, MX1 ($9e^{-30}$, $3e^{-27}$)	Mg, Ci, Nc, Cg, Bc, Ss	($e^{-166} \rightarrow e^{-77}$)
(VPS1)	AN10691 ($7.7e^{-23}$)	MX2, MX1 ($4e^{-33}$, $1e^{-31}$)	Ci, Nc, Cg, Bc, Mg, Ss	($e^{-169} \rightarrow 1e^{-79}$)
(DNM1)	AN1912 ($5.2e^{-21}$)	MX1, MX2 ($7e^{-31}$, $2e^{-29}$)	Ci, Bc, Ss, Cg, Nc, Mg	($e^{-172} \rightarrow 4e^{-47}$)
(VPS1)	AN5327 ($9.4e^{-30}$)	MX2, MX1 ($1e^{-33}$, $3e^{-30}$)	Nc, Cg, Bc, Ci	($e^{-106} \rightarrow 1e^{-54}$)
(DNM1)	AN1322 ($1.7e^{-05}$)	MX1, MX2 ($3e^{-16}$, $4e^{-15}$)	Cg, Bc, Mg, Ss	($1e^{-41} \rightarrow 5e^{-29}$)
(VPS1)	AN1648 ($1.5e^{-14}$)	DNM2 ($1e^{-15}$)	Nc, Mg, Cg, Cn, Ss	($2e^{-33} \rightarrow 2e^{-14}$)

[a] Listed are fungi in which one or more putative orthologs occur. Order of fungi and corresponding range of e-values indicate relative strength of homology to An sequence, except where noted. Bc *Botrytis cinerea*, Cg *Chaetomium globosum*, Ci *Coccidioides immitis*, Cn *Cryptococcus neoformans*, Mg *Magnaporthe grisea*, Nc *Neurospora crassa*, Ro *Rhizopus oryzae*, Ss *Sclerotinia sclerotiorum*.

[b] Sc TVP18 found an unnamed hypothetical ORF in An (contig 84, nt 252159–252599), and found putative orthologs in other fungi, at e-values ranging from $4e^{-22}$ to $2e^{-04}$.

[c] AN10743 and AN2277 appear to encode endophilin-related proteins, with e-values of $1e^{-10}$ and $3e^{-12}$ versus human SH3-containing and GRB2-like 1 (SH3GLB1). An e-value for AN2277 versus SH3GLB1 was obtained by blastp of the Hs genome. In a blastp of the Sc genome with AN2277, Sc RUD3 (interacts with COG3 and USO1, see Table 1.4) was the best, though very weak, hit (e = 0.03).

[d] e-values for human homologs are from blastp of Hs genome using An proteins.

[e] In addition to the four orthologs of Sc dynamins, an additional 6 dynamin-related proteins occur in *A. nidulans*. Shown are the closest Sc homologs (DNM1 or VPS1) and the e-value for tblastn of the Sc genome using An dynamins. Also shown are the closest human homologs of An dynamins and corresponding e-values from blastp of the Hs genome using An dynamins.

S. cerevisiae	*A. nidulans*		*Other fungi*[a]	
Lysosome-related functions				
MRL1 (*mannose-6-phosphate receptor*)	AN4095[b]	($1e^{-08}$)	Ss, Nc, Mg, Ci, Bc, Cg	($2e^{-50} \rightarrow 3e^{-27}$)
YOS9 (*similar to M6PR*)	AN1461[b]	($4e^{-10}$)	Ci, Bc, Ss, Mg, Cg, Nc, Ro, Cn	($1e^{-112} \rightarrow 9e^{-18}$)
CCZ1 (*vacuolar assembly, autophagy*)	**None**		**None**	
VTI1 (*v-SNARE*)	AN1973	($3e^{-19}$)	Ci, Ss, Bc, Mg, Nc, Cg	($1e^{-60} \rightarrow 4e^{-36}$)
ERS1 (H^+*-driven L-cystine transporter*)	AN0275	($3e^{-06}$)	Ci, Ss, Cg, Nc, Mg, Bc, Cn, Ro	($5e^{-99} \rightarrow 2e^{-15}$)
Endosomal sorting complexes required for transport (ESCRT)				
ESCRT-0 complex (endosome to lysosome targeting for degradation, sorting receptor for ubiquitinated cargo proteins at the MVB)				
VPS27 (*sorting ubiquitinated proteins*)	AN2071	($1e^{-57}$)	Ci, Bc, Nc, Mg, Cg, Ro, Ss, Cn	($1e^{-179} \rightarrow 1e^{-55}$)
HSE1 (*recycling of Golgi proteins*)	AN2066	($1e^{-30}$)	Ci, Bc, Cg, Ss, Nc, Mg, Ro, Cn	($1e^{-125} \rightarrow 1e^{-17}$)
ESCRT-I complex (ESCRT-0 binds ESCRT-I, ESCRT binds ubiquitinated cargo and recruits ESCRTs-II and -III)				
STP22	AN2521	($1e^{-05}$)	Ci, Mg, Nc, Ss, Bc, Cg, Cn, Ro	($2e^{-41} \rightarrow 1e^{-15}$)
VPS28	AN10129	($2e^{-37}$)	Ci, Bc, Mg, Nc, Cg, Ss, Ro, Cn	($1e^{-94} \rightarrow 1e^{-11}$)
SRN2	**None**		RO3G_05826 (0.16) but not other fungi	
ESCRT-II complex (increases membrane-binding of ESCRT-III by direct association with VPS20)				
VPS36	AN7037	($6e^{-24}$)	Ci, Nc, Ss, Bc, Mg, Cg, Cn	($0.0 \rightarrow 2e^{-14}$)
VPS25	Contig 61[c]	($6e^{-09}$)	Mg, Nc, Bc, Ss, Ci, Ro, Cn	($8e^{-59} \rightarrow 2e^{-05}$)
SNF8	AN7106	($4e^{-35}$)	Ci, Ss, Cg, Mg, Bc, Nc, Cn, Ro	($1e^{-106} \rightarrow 2e^{-33}$)
ESCRT-III complex (interacts with VPS4, -46, -60, VTA1, and BRO1)				
DID4	AN6898	($7e^{-41}$)	Bc, Ss, Nc, Mg, Ro, Cg, Ci, Cn	($2e^{-77} \rightarrow 2e^{-22}$)
SNF7	AN4240	($5e^{-16}$)	Bc, Ci, Ss, Mg, Nc	($3e^{-35} \rightarrow 5e^{-13}$)
VPS20	AN1365	($7e^{-17}$)	Ci, Bc, Ss, Mg, Cg	($6e^{-43} \rightarrow 7e^{-36}$)
VPS24	AN6920	($7e^{-32}$)	Ci, Bc, Ss, Nc, Mg, Cg, Ro, Cn	($2e^{-48} \rightarrow 2e^{-08}$)
YJL049W (*possible ESCRT-III family*)	AN7310	(0.013)	Mg, Bc, Nc, Ci, Ss, Cg	($9e^{-67} \rightarrow 9e^{-51}$)
Homotypic vacuole sorting (HOPS complex – docking and fusion at GA → Endo and Endo → VA)				
VPS16	AN6911	($5e^{-49}$)	Mg, Nc, Cg, Bc, Ss, Ci, Ro, Cn	($0.0 \rightarrow 1e^{-85}$)
VPS33 (*ATP-binding protein*)	AN2418	($1e^{-35}$)	Ci, Nc, Ss, Bc, Cg, Mg, Ro, Cn	($0.0 \rightarrow 1e^{-41}$)
VPS41 (*vacuolar membrane protein*)	AN4876	($4e^{-34}$)	Ci, Ss, Nc, Bc, Cg, Mg, Ro, Cn	($0.0 \rightarrow 6e^{-19}$)
PEP3 (*promotes vesicular docking/fusion*)	AN2266	($2e^{-64}$)	Ci, Ss, Mg, Nc, Cg, Bc, Ro, Cn	($0.0 \rightarrow 1e^{-71}$)
PEP5 (*complexes and acts with PEP3*)	AN2461	($2e^{-58}$)	Ci, Nc, Mg, Cg, Bc, Ro, Ss, Cn	($0.0 \rightarrow 1e^{-76}$)
VAM6 (*facilitates guanine nucleotide exchange on YPT7*)	AN10849	($1e^{-20}$)	Ss, Bc, Cg, Nc, Mg, Ci, Ro, Cn	($0.0 \rightarrow 7e^{-30}$)
Golgi-associated retrograde protein complex (GARP complex), recycling of proteins from late Endo → GA via Qc-SNARE TLG1				
VPS51	AN3015[d]	–	Ss, Bc	($0.0018, 3.7e^{-04}$)
VPS52	AN4014	($3e^{-32}$)	Cg, Bc, Nc, Ss, Mg, Ci, Cn, Ro	($1e^{-162} \rightarrow 3e^{-08}$)
VPS53	AN2736	($3e^{-62}$)	Ci, Bc, Ss, Mg, Nc, Cg, Cn, Ro	($0.0 \rightarrow 1e^{-20}$)
VPS54	AN7993	($2e^{-39}$)	Ci, Bc, Cg, Nc, Mg, Ss, Ro, Cn	($0.0 \rightarrow 5e^{-44}$)

S. cerevisiae	*A. nidulans*		*Other fungi*[a]	
Endosome to Golgi recycling (PEP8, VPS5, VPS17, VPS29, VPS35 form membrane-associated retromer complex)				
PEP8 (*subcomplex w/VPS29 and VPS35, cargo selection*)	AN3642	($2e^{-45}$)	Mg, Nc, Cg, Bc, Ci, Ss, Ro, Cn	($1e^{-148} \rightarrow 7e^{-69}$)
VPS17 (*promotes vesicle formation with VPS5*)	AN2224	($1e^{-72}$)	Ci, Ss, Bc, Cg, Mg, Nc, Cn	($0.0 \rightarrow 2e^{-29}$)
VPS29 (*subcomplex w/PEP8 & VPS35, cargo selection*)	AN1341	($5e^{-27}$)	Ci, Mg, Ss, Nc, Cg, Cn, Ro	($8e^{-66} \rightarrow 4e^{-27}$)
VPS35 (*subcomplex w/PEP8 & VPS29, cargo selection*)	AN4951	($1e^{-137}$)	Nc, Bc, Ss, Cg, Mg, Ro, Ci, Cn	($0.0 \rightarrow 1e^{-108}$)
VPS5 (*homolog of Hs Obesity-related gene receptor proteins*)	AN3594	($7e^{-27}$)	Ci, Bc, Ss, Nc, Cg, Mg, Ro, Cn	($1e^{-172} \rightarrow 6e^{-60}$)
RGP1, RIC1 (*RAB-GEFs*), YPT6 (*RAB GTPase*)	See Table 1.4			
Autophagy-specific phosphatidylinositol-3-kinase complex, required for autophagy, vacuolar protein sorting				
VPS15 (*myristoylated serine/threonine kinase*)	AN0576	($1e^{-144}$)	Ci, Ss, Mg, Nc, Cg, Bc, Cn, Ro	($0.0 \rightarrow 1e^{-130}$)
VPS30 (*forms membrane-assoc complex with ATG14*)	AN10213	($1e^{-40}$)	Ci, Bc, Ss, Mg, Nc, Cg, Ro, Cn	($1e^{-123} \rightarrow 3e^{-20}$)
VPS34 (*phosphatidylinositol-3-kinase*)	AN4709	($1e^{-167}$)	Ci, Bc, Ss, Mg, Cg,Nc, Ro, Cn	($0.0 \rightarrow 1e^{-177}$)
VPS38 (*binds VPS30, -34*)	**None**		**None**	
ATG14	**None**		**None**	
GPA1 (α-*subunit of G protein, activates VPS34*)	AN3090	($3e^{-58}$)	Ci, Nc, Ss, Cg, Bc, Ro	($1e^{-158} \rightarrow 4e^{-87}$)
Transport from early to late endosome				
RAV1 (*RAVE complex subunit, Vac ATPase assembly*)	AN0703	($2e^{-58}$)	Ci, Ss, Nc, Mg,Cg, Cn, Ro, Bc	($0.0 \rightarrow 3e^{-43}$)
Endosome to plasma membrane recycling				
RCY1 (*F box protein*)	AN10061	($1e^{-58}$)	Ci, Bc, Ss, Cg, Mg, Nc, Cn, Ro	($0.0 \rightarrow 2e^{-32}$)
Endosome transmembrane transport				
NHX1 (*endosomal Na+/H+ exchanger*)	AN2288	($1e^{-118}$)	Ci, Bc, Ss, Cg, Mg, Nc, Cn, Ro	($0.0 \rightarrow 5e^{-74}$)
PVC to Golgi pathway; multivesicular body sorting				
DID2 (= VPS46)	AN9396	($3e^{-21}$)	Ci, Cg, Cn, Nc, Bc, Mg	($4e^{-49} \rightarrow 0.024$)
NEO1, MON2	see Table 1.3			
GYP6, PEP12, SNX41	see Table 1.4			
ENT5	see Table 1.5			
HSE1, PEP8	see above, this table			
VPS4 (*AAA-ATPase, late endo → vac transport*)	AN3061	($1e^{-131}$)	Ss, Nc, Cg, Ci, Mg, Bc, Ro, Cn	($0.0 \rightarrow 3e^{-69}$)
VPS8 (*interacts with YPT51, vac prot localization*)	AN0244	($2e^{-53}$)	Ci, Bc, Ss, Nc, Mg, Cg, Ro, Cn	($0.0 \rightarrow 1e^{-134}$)
VPS13 (*peripheral membr prot, unknown function*)	AN5579	(0.0)	Ss, Ci, Mg, Cg, Bc, Nc, Ro, Cn	($0.0 \rightarrow 1e^{-161}$)
VPS55 (*late endo → vacuole trafficking*)	AN6546	($7e^{-12}$)	Ci, Cg, Nc, Ss, Bc, Mg, Cn	($4e^{-42} \rightarrow 1e^{-19}$)
VTA1 (*endosomal protein sorting, binds VPS4, -20, -60*)	AN0255	(0.49)	Ss, Ci, Nc, Mg, Bc, Cg, Cn, Ro	($4e^{-47} \rightarrow 0.003$)
BRO1 (*coordinates deubiquitination in MVB pathway*)	AN10788	($2e^{-45}$)	Cg, Ci, Bc, Ss, Nc, Ro, Cn	($0.0 \rightarrow 1e^{-111}$)
DOA4 (*ubiquitin hydrolase in late endo/prevacuolar*)	AN2072	($4e^{-57}$)	Ci, Ro, Cn, Mg, Cg, Nc, Bc	($0.0 \rightarrow 4e^{-49}$)
RIM20 (*PALA/AIP1 family, binds ESCRT-III SNF7*)	AN4351	($7e^{-56}$)	Nc, Mg, Ss, Cg, Bc, Ci, Ro, Cn	($0.0 \rightarrow 1e^{-34}$)
Late endosome; prevacuolar compartment (PVC)				
CDC50 (*endoomal protein, regulates cell polarity*)	AN5100	($2e^{-78}$)	Ci, Ss, Mg, Bc, Nc, Cg, Ro, Cn	($5e^{-84} \rightarrow 9e^{-29}$)
PIB1 (*RING type ubiquitin ligase, binds PI-3-P*)	AN9147[e]	($6e^{-12}$)	Cg, Mg, Ss, Bc, Nc	($1e^{-23} \rightarrow 7e^{-19}$)
PIB2 (*protein binding PI-3-phosphate*)	AN0627	($8e^{-07}$)	Ci, Nc, Ss, Mg, Bc, Cg	($1e^{-56} \rightarrow 3e^{-19}$)

S. cerevisiae	*A. nidulans*		*Other fungi*[a]	
STV1 (*subunit of vacuolar ATPase Vo domain*)	AN5606	(0.0)	Ss, Ci, Bc, Cg, Nc, Mg, Cn, Ro	(0.0 → 0.0)
CCZ1, DID2, NHX1, VPS55, MRL1	see above, this table			
SEC7 (*ARF-GEF*)	see Table 1.3			
VPS21 (YPT51), YPT52/53 (*RAB GTPases*)	see Table 1.4			
Endosome membrane				
TOR1 (*PIK-related protein kinase*)	AN5982	(0.0)	Ss, Ci, Mg, Bc, Cg, Nc, Ro, Cn	(0.0 → 0.0)
LST8 (*component of TOR signaling pathway*)	AN1335	($3e^{-90}$)	Ss, Nc, Bc, Cg, Mg, Ci, Cn, Ss	($2e^{-95}$ → $4e^{-25}$)
RSP5 (*ubiquitin protein ligase for MVB sorting*)	AN1339	(0.0)	Ss, Bc, Ci, Mg, Nc, Cg, Ro, Cn	(0.0 → $1e^{-120}$)
PEP7 (*adaptor for vesicle docking/fusion*)	AN3144	($7e^{-30}$)	Ci, Ss, Bc, Nc, Cg, Mg, Ro, Cn	(0.0 → $1e^{-05}$)
ENB1 (*ferric enterobactin transporter*)	AN8499	($2e^{-51}$)	Cg, Mg, Bc, Nc, Ci, Cn	($1e^{-61}$ → $2e^{-39}$)
EMP70, YDR107C (*predicted transmembrane protein*)	Contig 93[f]	($1e^{-133}$, $1e^{-130}$)	Nc, Cg, Bc, Ss, Ci, Cn, Ro	(0.0 → $1e^{-150}$)
Novel additional EMP70 homolog	AN5450[g]	($6e^{-69}$, $1e^{-70}$)	Ci, Nc, Ss, Bc, Mg, Cg, Cn, Ro	(0.0 → $2e^{-78}$)
Other vacuolar protein sorting				
PEP1, VTH1/2 (*type I sorting receptor – vac hydrolases*)	AN8880	($1e^{-176}$)	Ci, Bc, Ss, Nc, Cg,Mg, Cn, Ro	(0.0 → 0.0)
VPS3 (*sorting soluble vacuolar proteins*)	AN0763	($4e^{-06}$)	Ci, Bc, Ss, Nc, Cg, Mg	(0.0 → $1e^{-129}$)
VPS60 (*late endosome → vacuole transport*)	AN5632	($9e^{-30}$)	Ci, Bc, Ss, Cg, Nc, Cn, Mg, Ro	($2e^{-73}$ → $3e^{-26}$)
VPS62 (*cytoplasm → vacuole protein targeting*)	AN7454	($2e^{-49}$)	Ss, Bc, Nc, Ci, Cg	($1e^{-118}$ → $1e^{-67}$)
Novel additional VPS62 homolog	AN4807	($4e^{-46}$)	Bc, Ss, Ci	($2e^{-71}$ → $9e^{-64}$)
VPS64 (*cytoplasm → vacuole protein targeting*)	AN4632	($7e^{-19}$)	Ci, Mg, Nc, Bc, Ss, Cg, Cn, Ro	($1e^{-153}$ → $5e^{-24}$)
VPS66 (*unknown function in vac prot sorting*)	AN6345	($7e^{-08}$)	Ss, Ci, Cg, Nc, Mg, Ro, Cn	($3e^{-92}$ → $1e^{-08}$)
VPS68 (*vacuolar membr protein, unkn function*)	AN6544	($1e^{-33}$)	Ci, Nc, Bc, Cg, Ss, Mg, Ro, Cn	($3e^{-62}$ → $9e^{-21}$)
VPS70 (*unknown function in vac prot sorting*)	AN4018	($7e^{-89}$)	Ci, Cg, Ss, Bc, Nc, Mg, Ro	(0.0 → $1e^{-140}$)
VPS73 (*mitochondrial protein involved in VPS*)	**None**			
VPS74 (*unknown function in vac prot sorting*)	AN5705	($2e^{-97}$)	Ci, Ss, Mg, Cg, Nc, Bc, Ro, Cn	($1e^{-151}$ → $2e^{-93}$)
VPS75 (*unknown function in vac prot sorting*)	AN8170	($6e^{-04}$)	Ci, Ss, Nc, Mg, Bc, Cg	($2e^{-67}$ → $7e^{-33}$)
Components of the SWR1 complex that incorporate HTZ1 into chromatin; required for vacuolar protein sorting				
VPS71	AN2095	(0.002)	Ci, Cg, Mg, Nc, Bc, Cn	($9e^{-60}$ → $5e^{-05}$)
VPS72	AN0461	($6e^{-05}$)	Ci, Ss, Bc, Cg	($3e^{-18}$ → $3e^{-04}$)
Exocyst				
SEC3	AN0462	($3e^{-26}$)	Ss, Mg, Cg, Nc, Ci, Bc, Ro, Cn	(0.0 → $7e^{-19}$)
SEC5	AN1002	($1e^{-16}$)	Nc, Bc, Ci, Ss, Mg, Cg, Ro, Cn	(0.0 → $2e^{-09}$)
SEC6	AN1988	($5e^{-41}$)	Ci, Mg, Nc, Bc, Ss, Cg, Cn, Ro	(0.0 → $3e^{-47}$)
SEC8	AN11007	($1e^{-28}$)	Ci, Bc, Mg, Nc, Cg, Ss, Cn, Ro	(0.0 → $3e^{-14}$)
SEC10	AN8879	($2e^{-40}$)	Ci, Nc, Ss, Cg, Mg. Bc, Cn, Ro	(0.0 → $1e^{-22}$)
SEC15	AN6493	($3e^{-16}$)	Nc, Mg, Cg, Bc, Ci, Ss, Cn, Ro	(0.0 → $3e^{-17}$)
EXO70	AN6210	($4e^{-24}$)	Ci, Nc, Cg, Mg, Ss, Bc	(0.0 → $1e^{-132}$)
EXO84	AN0560	($8e^{-25}$)	Ci, Ss, Cg, Bc, Mg, Nc, Cn, Ro	(0.0 → $3e^{-04}$)
Exocytic SEC9-interacting proteins				
SRO7, SRO77 (*vesicle docking/fusion with PM*)	AN4980	($1e^{-101}$, $1e^{-107}$)	Ci, Bc, Nc, Mg, Cg, Ro, Bc	(0.0 → $1e^{-62}$)

S. cerevisiae	*A. nidulans*		*Other fungi*[a]	
Regulation of exocytosis				
SAC1 (*lipid phosphoinositide phosphatase*)	AN3841	($1e^{-115}$)	Ci, Bc, Ss, Nc, Cg, Mg, Cn, Ro	($0.0 \rightarrow 1e^{-75}$)
MSO1 (*secretory vesicle docking complex*)	**None**		**None**	
GYL1 (*RAB-GAP*) and others	see Table 1.4			

[a] Listed are fungi in which one or more putative orthologs occur. Order of fungi and corresponding range of e-values indicate relative strength of homology to An sequence. Bc *Botrytis cinerea*, Cg *Chaetomium globosum*, Ci *Coccidioides immitis*, Cn *Cryptococcus neoformans*, Mg *Magnaporthe grisea*, Nc *Neurospora crassa*, Ro *Rhizopus oryzae*, Ss *Sclerotinia sclerotiorum*.

[b] AN4095 and AN1461 show weak homology to human M6PR ($4e^{-11}$) and a human YOS9 relative ($2e^{-15}$).

[c] Sc VPS25 found an unnamed hypothetical ORF in An (contig 61, nt 354522–355120). VPS25 orthologs in other fungi were identified by tblastn of all fungi with the Mg ortholog, MGG_01031.

[d] Sc VPS51 found no hits in An at e = 10.0, likely because it is a very short protein. However, putative VPS51 orthologs were found in Ss (SS1G_11852.1, 0.0018) and Bc (BC1G_13961, 0.00037). BC1G_13961 found the putative An ortholog, AN3015 ($8e^{-26}$). In turn, AN3015 found Sc VPS51, but as a secondary hit with a high e-value (0.93).

[e] The An ortholog of Sc PIB1 appears to be a currently unnamed hypothetical ORF on contig 1.169, ~nt 269452–270600, which was incorporated as part of AN9147.2 in a previous annotation. Candidate PIB1 orthologs in other fungi were identified by tblastn with the Ci PIB1 ortholog, CIMG_04456. CIMG_04456 was identified by tblastn of all fungi using Sc PIB1 ($4e^{-10}$).

[f] Sc EMP70 found an unnamed hypothetical ORF in An (contig 93, nt 228960–231026). EMP70 putative orthologs in other fungi were identified by tblastn of all fungi with the Mg ortholog, MGG_07434.

[g] AN5450 is strongly related to human transmembrane 9 superfamily protein member-4, and -2 (TM9SF4, NP_055557 and TM9SF2, NP_004791), at e–values of $4e^{-122}$ and $3e^{-106}$, respectively.

basal expression occurs on glycerol and acetate, and increasing expression can be induced by, in order, ethanol + fructose (varying fructose concentration raises or lowers expression level), ethanol alone, and threonine (Waring et al. 1989). Levels of *alcA*-driven expression on glycerol are low enough that in some cases expression is not sufficient to fully complement a mutation. Conversely, while repression of an *alcA*-gene fusion by glucose is normally tight enough to prevent complementation of a corresponding mutation, the *alcA* promoter does leak slightly, with greater expression on minimal-glucose than on rich-glucose media (e.g., see James et al. 1999). In some cases, this differential leakiness can provide an additional and useful means of fine-tuning gene expression, especially in cases where the endogenous gene expresses at a very low level.

Fungi are eminently co-operative to both molecular and classic genetics. In combination with live cell imaging and fluorescent protein-tagged transformants, temperature-sensitive mutants and transient expression of gene products under the control of inducible promoters allow for the dissection of cell biological processes. These approaches are particularly useful where null mutations are lethal. In *A. nidulans* and *N. crassa*, for example, essential genes are commonly deleted from sheltered backgrounds containing an extra, inducible wild-type allele of the target gene. Issues of dosage and expression by the inducible copy, following deletion of the endogenous gene locus, may be mitigated in *N. crassa* by a recently introduced method for constructing minimally sheltered knockout mutants (Metzenberg 2005).

In this chapter, we use **comparative genomics** to delineate many components of the endomembrane system of *A. nidulans* and other fungi relative to the budding yeast *Saccharomyces cerevisiae*, with additional comparisons to human (Tables 1.1–1.6). Absent from this analysis are members of the signal recognition particle, and the complement of glycosyltransferases and related enzymes for N- and O-linked protein glycosylation, and secreted extracellular proteins. *S. cerevisiae* was chosen as the primary tool for comparison because the genome is very well annotated, and provides a robust ontology for genes of the endomembrane system (www.yeastgenome.org). *S. cerevisiae* also was selected for its relative simplicity, along with its phylogenetic relationship to filamentous fungi. That said, some caution is warranted in the use of this organism as a basis for comparison to other fungi, and in addition care must be

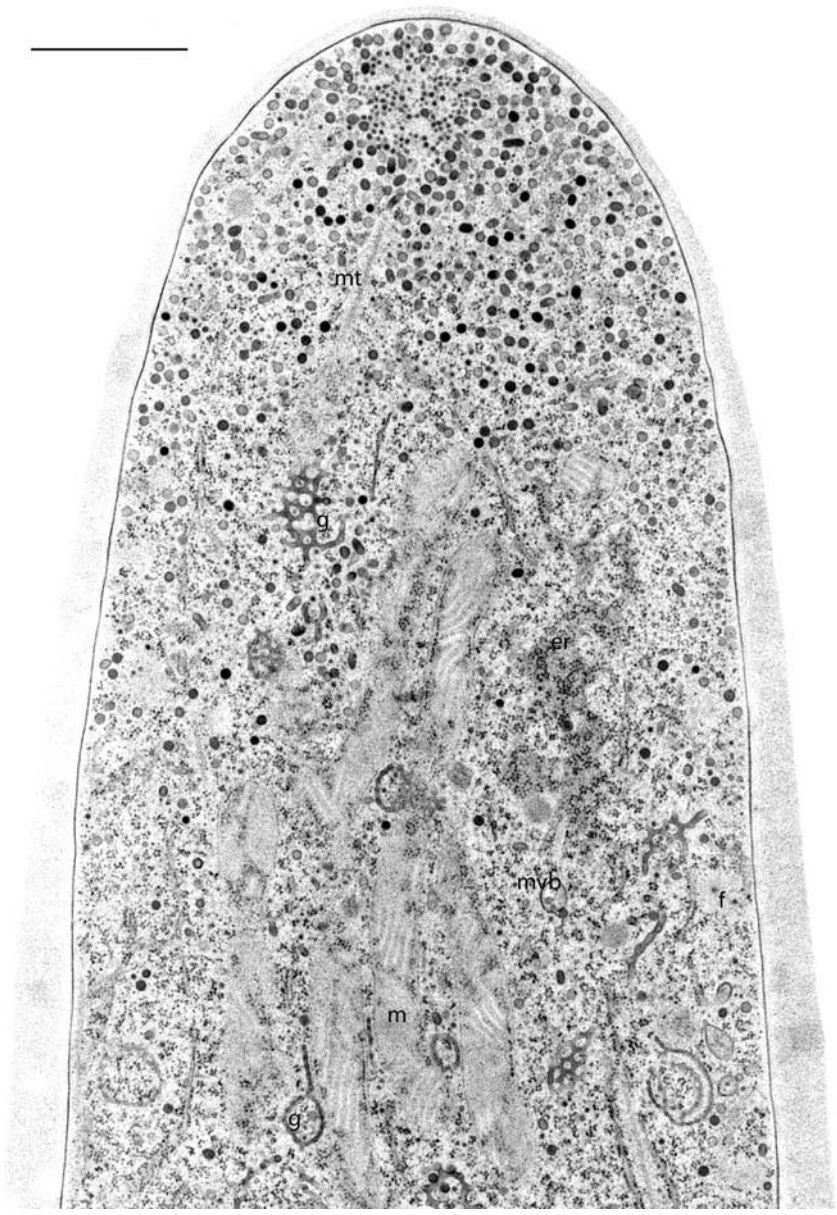

Fig. 1.1. The tip region of an *Aspergillus nidulans* hypha. Most organelles of the fungal endomembrane system can be observed in this near median longitudinal section. The mitochondria (*m*) in this preparation are marginally contrasted. *er* Endoplasmic reticulum, *f* filasome, g Golgi cisternum, *mvb* multivesicular body, *mt* microtubule. Freeze substitution preparation. *Bar* 1.0 µm

used when inferring cellular functions from comparative genomic approaches alone. Although comparative genomics has been used to assess subcellular distribution of various biomolecules and to compare cellular molecular machinery (Borkovich et al. 2004), sequence analysis is often less than conclusive (Hansen and Köhler 2001) and needs to be followed by concrete experimentation (Gupta and Heath 2002). For example, deletion of an *A. niger* ortholog of the essential *SEC4P* gene in *S. cerevisiae* required for proper vesicular transport was found not to be lethal (Punt et al. 2001). This functional difference could not have been gleaned by sequence comparison alone. It may be significant to note that comparative genomics has indicated that many components of the fungal cytoskeleton are more closely related to their respective animal molecules than to those found in *S. cerevisiae* (Xiang and Plamann 2003). There is a tendency for non-mycologists especially to lump filamentous fungi together with the yeast *S. cerevisiae* but this is ill advised and capricious. Furthermore, *S. cerevisiae* evolved by a whole-genome duplication event, followed by gene loss,

gene expansion, and gene-pair divergence, from an ancestor closely related to *Kluyveromyces waltii* (Kellis et al. 2004). Thus, it is no surprise that many fungi possess simpler and less redundant gene sets for many processes and pathways. This is true for *A. nidulans* and many other fungi, as we demonstrate in this chapter (Tables 1.1–1.6). In contrast, we discovered several endomembrane processes and gene families that have expanded relative to yeast. In some cases the expanded members show strong similarities to genes and their associated pathways in animals (e.g., Table 1.2, novel ERD2-related protein; Table 1.3, novel fungal ARF/ARL GTPases and ARF-GAP; Table 1.4, novel fungal RAB GTPases, RAB-GAPs, and RAB-GEFs; Table 1.5, novel fungal dynamin-related proteins and BAR domain protein).

As a general rule, two protein sequences were considered homologous at an expected value (e-value) ≤ 0.0001 (i.e., 10^{-4}). Choice of e-value cutoff for a significant Blast hit varies between 10^{-4} to 0.1 (e.g., see Claverie and Notredame 2003; Pevsner 2003; Buehler and Rashidi 2005), with the caveat that alignment between short homologs, especially those consisting of less than 100 amino acids, may generate e-values higher than the cutoff. Some endomembrane proteins reported herein are relatively short, less 100 amino acids, with correspondingly high e-values against putative *Aspergillus* orthologs (e.g., ERI1 and VMA21 in Table 1.1, PBI2 and YOS1 in Table 1.4). In several cases, we have reported potential homologs with e-values greater than 0.1.

Another major tool used to study the endomembrane system has been the **transmission electron microscope**, with fungi being among the first organisms to be studied (Bracker 1967, 1974; Bracker and Grove 1971). In the early days many new structures were described, many of which were later shown to be artifact (Heath and Greenwood 1970). The fine structure of most compartments of the endomembrane system was first described based on electron micrographs. The quality of the information has been improved through the adoption of the cryo-based methodology of ultrarapid freezing and **freeze substitution** (Howard and Aist 1979; Howard 1981; see also Chap. 2 in this volume). Much of the earliest "fungal" work was done on the öomycetes, organisms that since have been recognized as taxonomically separate from true fungi (Wainright et al. 1993); and ultrastructural differences such as those related to the Golgi apparatus bear this out (Bracker et al. 1996). The electron microscope continues to provide invaluable information in the form of high-resolution images, and molecular information can be obtained using immuno-based and other **affinity probes** such as lectins. The lectin concanavalin A (ConA) has been used as a general marker for the fungal endomembrane system for both light and electron microscopy (Bourett et al. 1993; Bourett and Howard 1994). ConA-labeled organelles include the plasma membrane, Golgi equivalents (see Sect. III.B.), transport vesicles and a class of tubular vacuoles, but not the ER (Fig. 1.2B). For discussion of additional probes, such as the fluorescent FM dyes, see Sect. IV..

Transmission electron microscope analyses can also be enhanced through the creation of three-dimensional renderings. While this three-dimensional information can be extracted from serial thin-section (e.g., Bourett and Howard 1994; Winey et al. 1995) or HVEM semi-thick section (e.g., Howard 1981) analysis, higher resolution images can be obtained using semi-thick sections and electron tomography methodologies (Ladinsky et al. 1999; O'Toole et al. 1999; Müller et al. 2000; Harris et al. 2005; Donohoe et al. 2006).

Biochemistry has also played a role in increasing our understanding of compartmentalization within the endomembrane system, especially in studies of *Saccharomyces cerevisiae* where good morphological data is often elusive. For example, it has proven to be very useful to analyze secreted proteins as they pass through successive compartments of the endomembrane system. If the secretory pathway is blocked by either treatment with a pharmacological agent or the introduction of a genetic lesion, then the normally secreted protein will accumulate at some location(s) within the cell. Through biochemical analysis the compartment where the accumulation occurred can be determined since the subcellular site for each sequential modification to the secreted protein has been established (Schekman 1992).

III. Secretory Pathway

A. Endoplasmic Reticulum

The ER has an essential role in both lipid and protein pathways as the site of biosynthesis of nearly all cellular membranes and transmembrane proteins regardless of the ultimate destination of these molecules. Luminal proteins destined

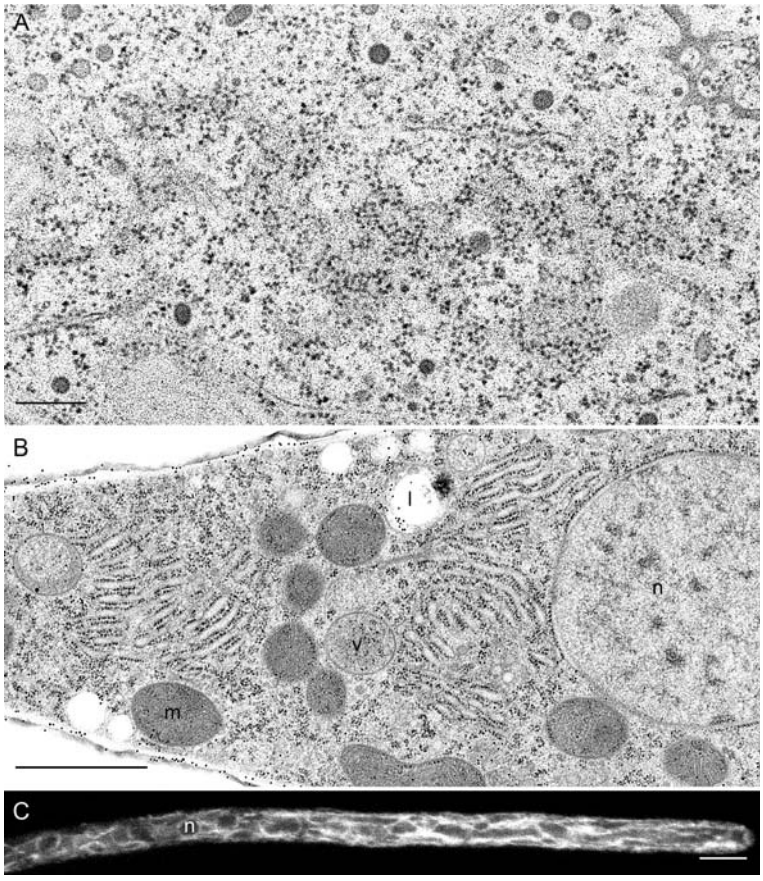

Fig. 1.2. Endoplasmic reticulum (ER) and nuclear envelope. **A** The ER in fungal cells is most often observed as sheets that, when tangentially sectioned, reveal a concentration of polysomes comprised of a spiral array of individual ribosomes as observed here in a vegetative hypha of *Aspergillus nidulans*. *Bar* 250 nm. **B** Note that the concanavalin A binding sites marked by gold particles are absent in this dilated ER in an apical conidial cell of *Magnaporthe grisea*. The continuity of the ER with the nuclear envelope is illustrated by the ribosome-studded outer membrane of the nuclear envelope. *l* Lipid body, *m* mitochondrion, *n* nucleus, *v* vacuole. *Bar* 1.0 µm. **C** ER in a living cell of a multinucleate *Fusarium verticillioides* hypha targeted with a fluorescent protein, using the KDEL ER-retention sequence. In this single optical laser scanning confocal section, the nuclear envelope is apparent as is the abundance of ER in this metabolically active tip cell. *n* Nucleus. *Bar* 5.0 µm. In **A**, **B**, cells were prepared by freeze substitution.

for the Golgi apparatus and vacuoles are initially co-translationally delivered into the ER lumen. In addition, the ER lumen serves to store calcium ions to be released into the cytosol upon induction via appropriate signaling (Estrada de Martin et al. 2005).

Though the ER is thought to represent a single interconnected membrane system (Voeltz et al. 2002), it can be subdivided into a collection of numerous functional domains (Staehelin 1997). In plants (Kèpés et al. 2005) and in *S. cerevisiae* (Preuss et al. 1991) the intracellular ER network is thought to represent a contiguous system forming both non-fenestrated sheets and variously branched tubules. The latter predominates at the cell periphery where the tubules are closely associated with, and may possess molecular links to, the plasma membrane (Lichtscheidl and Hepler 1996). The ER network in fungi exhibiting yeast-like growth may be more tubular and distributed toward the cell periphery (Preuss et al. 1991; Rossanese et al. 1999; Wedlich-Söldner 2002) compared to filamentous fungi where the ER appears commonly as cisternal sheets often stacked into parallel arrays and found throughout the radius of the fungal hypha (Fig. 1.2A–C). Then again, a prominent peripheral ER network has been described in a rust fungus (Hoch and Staples 1983a). In vegetative hyphae most ER is rough ER containing membrane-bound ribosomes arranged in polyribosomes obvious in sections tangential to the cisternal surface (Fig. 1.2A). It is less common to find extensive regions of smooth ER. Exceptions include the septal pore cap of basidiomycetes (Read and Beckett 1996; Müller et al. 1998, 2000) and the peripheral hyphal network described above (Hoch and Staples 1983a). The ER can exist as a mixture of rough and smooth ER. Transitional ER consists of smooth regions where translocation vectors are thought to form and facilitate the delivery of materials from the ER to the Golgi apparatus (Watanabe and Riezman 2004): these "*exit sites*" would be in proximity and juxtaposed to individual Golgi stacks. Thus, the transitional ER may play an integral role in the biogenesis and form of the Golgi apparatus

in *S. cerevisiae* (Watson and Stephens 2005) and perhaps also filamentous fungi. There appears to be little consistent evidence of any contiguity between fungal ER and Golgi compartments.

The ER may be highly dilated during specific stages of development, for example during the initial hydration of spores prior to germination (Fig. 1.2B). In phytopathogenic fungi the ER has been shown to undergo structural rearrangements during pathogenesis. For example, in haustoria of biotrophic fungi there is a shift toward a predominantly tubular system, termed the tubular–vesicular network (Mims et al. 2002), formed in response to cues from the host (Welter et al. 1988). This tubular–vesicular network appears to be a functional subcompartment of the ER based on an altered distribution of ER markers such as BIP- and HDEL-containing proteins (Bachem and Mendgen 1995).

The septal pore cap of basidiomycetes is contiguous with and thought to be derived from the ER (Bracker and Butler 1964). The plasma membrane is continuous between adjacent cells. Organelles can pass through the complex septal pore apparatus (Bracker and Butler 1964; Müller et al. 2000). Unless the pore is plugged there is cytoplasmic continuity.

The organization and dynamics of fungal ER have been studied by examining live cells expressing fluorescent proteins fused to the ER-resident chaperone BipA (Maruyama et al. 2006), or containing both an amino-terminal signal peptide and a carboxy-terminal H/KDEL ER-retention peptide (Fig. 1.2C; Suelmann et al. 1997; Fernández-Abalos et al. 1998; Wedlich-Söldner et al. 2002; Czymmek et al. 2005). To a limited extent the ER has also been examined using vital dyes such as ER Tracker and fluorophore-conjugated brefeldin A (Cole et al. 2000; Wedlich-Söldner et al. 2002; Maruyama et al. 2006). The ER was found to be a highly motile organelle.

In polarized fungal cells a non-random distribution of the organelles of the endomembrane system is maintained. The integrity of both the ER and Golgi apparatus of animal cells requires an intact microtubule cytoskeleton. In mammalian cells depolymerization of the microtubule cytoskeleton results in the fragmentation of the Golgi apparatus (Thyberg and Moskalewski 1999) and a gradual retraction of the ER from the cell periphery (Terasaki et al. 1986). Microtubules in animal cells are generally polarized with their minus ends oriented toward the centrosome and the plus ends closer to the cell periphery. The plus end-directed microtubule motor protein kinesin is required to maintain the ER distribution, and the minus end-directed dyneins are required for maintenance of the peri-nuclear Golgi distribution (Corthésy-Theulaz et al. 1992; Harada et al. 1998). In plants, microfilaments are required for Golgi mobility – though depolymerization of the actin cytoskeleton does not affect Golgi juxtaposition to exit sites of the ER, nor transport between the ER and Golgi (Brandizzi et al. 2002). In *Ustilago maydis* cytoplamic dynein and microtubules were shown to be required for ER motility but not for maintaining the basic ER organization (Wedlich-Söldner et al. 2002). In hyphal tip cells the Golgi cisternae are numerous and not restricted to a perinuclear distribution (e.g., Bourett et al. 1998; Fig. 1.1). Vacuole integrity in both *S. cerevisiae* (Klionsky et al. 1990) and *Ustilago maydis* (Steinberg et al. 1998) has been demonstrated to require functional microtubules. For further consideration of the fungal cell cytoskeleton, the reader is referred to Chaps. 2, 5, and 6 in this volume.

A comparative genomic analysis of various fungal species versus *S. cerevisiae* ER components is presented in Table 1.1. For the most part, ER-specific functions are highly conserved. A one-to-one correspondence of genes is evident, with some exceptions. Many of these exceptions are explained by the derivation of budding yeast from a whole-genome duplication event followed by retention of duplicate gene copies with or without functional divergence (Kellis et al. 2004). For example, the SEC61 translocation complex in *S. cerevisiae* has five components, including duplicates of the β- (SBH1, SBH2) and the channel-forming subunits (SEC61, SSH1; see www.yeastgenome.org). By comparison, *A. nidulans* possesses a single ortholog of each gene pair, and thus a total of three genes rather than five appear to comprise the SEC61 complex in this fungus. Similarly, the yeast YET1/YET2/YET3 genes, which encode homologs of human BAP31, are represented by a single *A. nidulans* ortholog. *A. nidulans* also possesses a single copy, respectively, of the duplicated *S. cerevisiae* protein disulfide isomerases, PDI1 and EUG1, and the ORM1/ORM2 components of the unfolded protein response. Conversely, filamentous fungi appear to lack homologs for several ER-specific yeast genes, including PHO86 (packaging of PHO84p into COPII vesicles), VPH2 (vacuolar ATPase assem-

bly), FRT1 (substrate of phosphatase calcineurin), and FRT2 (interacts with FRT1 to promote growth during pH and salt stress). Notably, all of these genes are dispensable in *S. cerevisiae*, and therefore these functions may have been lost during fungal evolution or may have evolved separately in some yeasts.

Filamentous fungi appear to possess novel, expanded functions involved in sterol biosynthesis (AN4208, AN6159), and in the retention of HDEL motif-containing, ER-resident proteins. Whereas *S. cerevisiae* contains a single ERD2 transmembrane protein that binds to HDEL motifs and regulates the retention of ER-specific proteins, *A. nidulans* encodes two proteins which have homology with ERD2 (AN11226, AN4528). AN11226 appears to be the ortholog of ERD2 and AN4528 has diverged substantially. The *A. nidulans* annotation identifies these as the two "ER lumen protein-retaining receptors" in this fungus. AN4528 is more similar to AN11226 ($8.7e^{-25}$) than to Sc ERD2 ($2.0e^{-19}$), and likely derived by duplication of AN11226 after the divergence of *S. cerevisiae* and filamentous fungal lineages. A comparison with the corresponding human receptors reveals two useful insights about the human and filamentous fungal genes. Humans possess three KDEL-specific receptors for retaining ER proteins (KDEL receptors -1, -2, -3). Interestingly, the three human receptors are much more closely related to each other ($1e^{-104} \rightarrow 1e^{-89}$) than they are to AN11226 ($4e^{-60} \rightarrow 4e^{-51}$) or to AN4528 ($2e^{-33} \rightarrow 2e^{-30}$), suggesting that all three human genes likely arose by duplications of a single ancestral ortholog related to AN11226 and ScERD2. Of greater interest to fungal biologists is the possibility that AN4528 has evolved into a novel, filamentous fungus-specific functional niche for endomembrane protein trafficking, and thus may offer a productive avenue for investigation.

B. Golgi Apparatus

The Golgi apparatus is perhaps the least understood of the organelles that comprise the fungal endomembrane system. It is the site where secretory products and plasma membrane resident proteins are packaged for delivery to the cell surface and other cargoes packaged in transit to vacuolar compartments. The Golgi can also be the endpoint for materials that enter the endocytic pathway. The classic view of the Golgi apparatus as a stable compartment (Dunphy and Rothman 1985) was questioned recently, with strong evidence that the Golgi may represent a dynamic continuum with the ER (Glick 2000; Hawes and Satiat-Jeunemaitre 2005). Unlike the ER, which persists throughout the cell cycle, the Golgi can be reconstituted in cells *de novo* though the fate of all Golgi-resident molecules during disassembly, e.g., during mitosis in mammalian systems (Lucocq et al. 1987; Colanzi et al. 2003), is not fully understood. It is clear that many Golgi molecules are reabsorbed into the ER during mitosis, while others such as some golgins are not (Seemann et al. 2002).

The structure of the Golgi apparatus in fungi is strikingly different from those found in higher plants and animals. The most salient difference is that *stacks* of flattened cisternae, or dictyosomes, are lacking in true fungi (Girbardt 1969; Grove and Bracker 1970; McLaughlin 1974; Howard 1981). Since **fungi lack dictyosomes**, choosing a terminology for Golgi-related structures is an issue. We have adopted the convention of Mollenhauer and Morré (1991). The term *Golgi apparatus* describes the sum total of all cisternae in a cell. Golgi cisternae – Golgi equivalents (Howard 1981) – are individual organelles, consist of a fenestrated sheet with tubular extensions that constitute recognizable and contiguous entities that are dispersed throughout the hypha. Cisternae often appear as fenestrated hollow spheres or sheets wrapped closely around mitochondria (Figs. 1.1, 1.3; see also Bracker and Grove 1971; Howard 1981; Newhouse et al. 1983). The width of cisternal tubules is generally uniform within such a sheet or sphere, but the width can vary between individual spheres and spheres with thin and wide cisternae can be found within the same cell (Howard 1981).

Putative fluorescence-labeled fungal Golgi has been reported in the literature. Spherical cisternae were observed in an *Aspergillus* transformant engineered to secrete a GFP-tagged glucoamylase when the secretory pathway was blocked (Khalaj et al. 2001). Wedlich-Söldner et al. (2002) used a GFP fusion to Ypt1p, a small GTPase associated with Golgi in yeast, to yield an apical fluorescence pattern in dikaryotic hyphae that extended to the apex proper. Based on electron microscope data, it seems unlikely that Golgi would be concentrated so close to the apex. Likewise, a GFP fusion to a presumed Golgi-resident 1,2-α-mannosyltransferase was used to create a putative Golgi reporter (Gilbert et al. 2006), but the

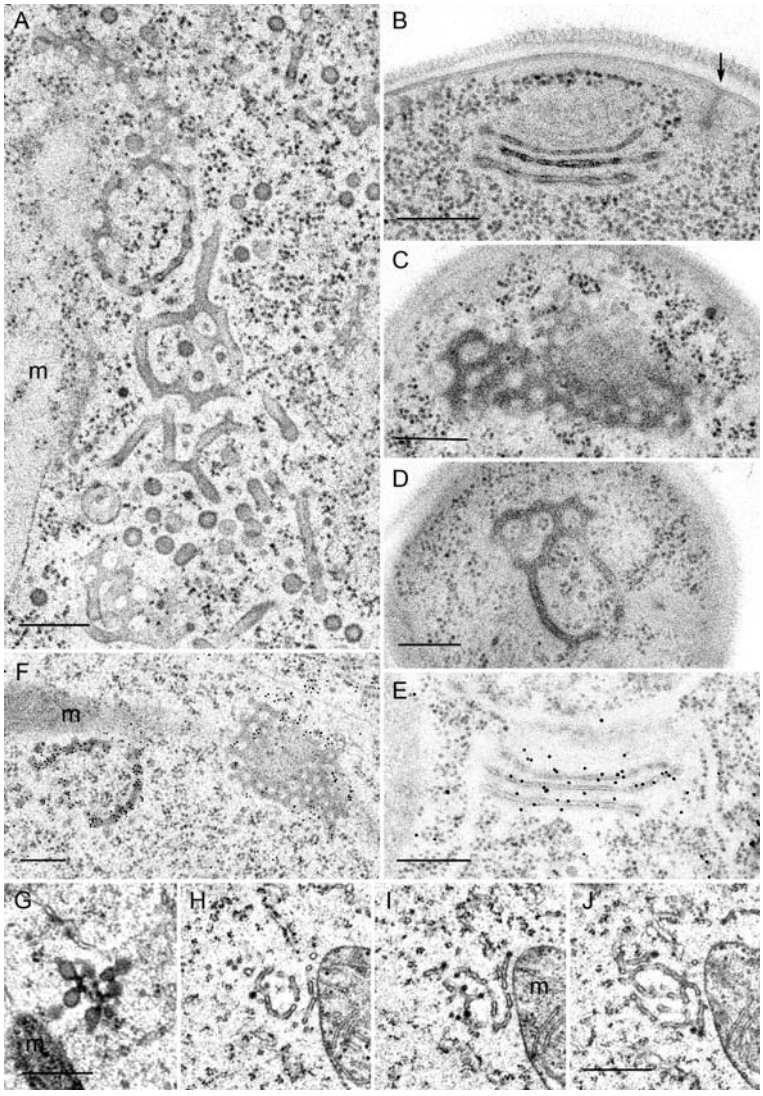

Fig. 1.3. Fungal Golgi. **A** Assemblages of tubular cisternae and a lack of cisternal stacks are the hallmarks of Golgi in filamentous fungi, observed in abundance and interspersed with vesicles in this hypha of *Aspergillus nidulans*. The width of tubules within a single cisternum is fairly uniform, but can differ between cisternae, as can the size and distribution of fenetrations. **B–E** Fenestrated cisternae are also observed in the yeast *Pichia pastoris*, but stacking of cisternae is evident (**B**, **E**). Con A binding sites are associated with cisternae of both yeast (*P. pastoris*, **E**) and filamentous fungi (*Trichoderma viride*, **F**). Golgi bodies in basidiomycetes are characterized by swollen peripheral terminations (*Helicobasidium mompa*, **G**). **H–J** Putative coated vesicles were observed in three consecutive sections from a hypha of *Helicobasidium mompa*. All specimens prepared by freeze substitution. *Arrow* Filasome-like structure associated with invagination of the plasma membrane, *m* mitochondrion. *Bars* 250 nm in **A–F**, 500 nm in **G–H**

results were not compelling. Putative fungal Golgi have also been described in whole mounts after labeling with fluorescently tagged succinylated concanavalin A (Bourett et al. 1993; see also Fig. 11.6C in this volume). At the TEM level, Con A-labeled entities included both spherical and linear structures of comparable width (see Figs. 3–8 in Bourett and Howard 1994).

Subtile structural differences have been noted between different groups of fungi. For example, the Golgi apparatus found in basidiomycetes is characterized by an interconnected cisternal network often terminating in characteristic swollen lobes (Fig. 1.3G; Hoch and Howard 1980; Hoch and Staples 1983a; Roberson and Fuller 1988; Welter et al. 1988; Swann and Mims 1991) and coated vesicles appear more common (Fig. 1.3H–J). A similar tubular system has been described in arbuscular mycorrhyizal hyphae (Bonfante et al. 1994), but has not been reported for ascomycetes. It is not clear whether these structural variations underlie significant functional differences.

Fungi are not the only eukaryotes with a Golgi apparatus lacking cisternal stacks. *Giardia* (Hehl and Marti 2004) and *Entamoeba* (Bredeston et al. 2005) for example have Golgi systems consisting of isolated stage-specific vesicles. Despite this minimal structural elaboration, it appears that these primitive eukaryotes still possess the basic molecular machinery required for compartmentalized separation of ER- and Golgi-related biochemistry and for the delivery of proteins and glycans to the

cell surface. Likewise the yeast *S. cerevisiae* also has been reported to lack Golgi stacks (Rossanese et al. 1999), though there are reports of some cisternal assemblages (Baba and Osumi 1987). Interestingly, other related yeasts including *Schizosaccharomyces pombe* (Ayscough et al. 1993) and *Pichia pastoris* (Fig. 1.3B–E) have been shown to possess elaborations ranging from parallel tubules to apparent stacks (Rambourg et al. 1995). Based on the distribution of a COPII coat protein known to be involved in ER to Golgi transport (Tang et al. 2005), it has been suggested that the lack of stacked Golgi cisternae in *S. cerevisiae* reflects a delocalized transitional ER system (Rossanese et al. 1999), whereas in *P. pastoris* the transitional ER is found in discrete patches juxtaposed to stacked Golgi cisternae. The lack of stacked Golgi cisternae may be a consequence of very rapid anterograde movement of membrane through the secretory pathway (Weber and Pitt 2001).

A unique property of the plant Golgi apparatus is its mobility (Boevink et al. 1998), an acto-myosin based phenomenon (Nebenführ et al. 1999), absent in animal cells and as yet unknown in filamentous fungi. While fluorescent proteins have been targeted to the Golgi apparatus in yeast (Wooding and Pelham 1998), this has not been done convincingly with filamentous fungi. All Golgi-resident enzymes described to date are integral membrane proteins. Information regarding their retention in the Golgi resides within a non-cleaved amino-terminal signal anchor sequence consisting of a transmembrane domain flanked by a short cytoplasmic tail and a lumenal stalk domain (Munro 1998). The sequence from an animal sialyltransferase molecule has been used to design a fluorescent protein-based probe for the Golgi compartment in plants (Boevink et al. 1998). Though sialic acid is not utilized by plants, the fluorescent reporter was delivered with fidelity to the Golgi compartment as confirmed by immunoelectron microscopy using an antibody raised against the GFP marker. Thus, though there is no consensus targeting sequence, recognition of these Golgi-retention sequences appears to be highly conserved across all eukaryotes (Saint-Jore et al. 2002).

As mentioned earlier, one of the hallmarks of the Golgi apparatus of filamentous fungi is the lack of stacked membrane cisternae. In animal cells **matrix proteins** exist that form a scaffold between cisternae of the Golgi body (Short et al. 2005), and phosphorylation of these scaffold proteins via mitosis-related protein kinases is followed closely by the characteristic fragmentation of the Golgi body during nuclear division (Shorter and Warren 2002). There is evidence from the work with golgins that Golgi matrix proteins serve not only to maintain the Golgi stacks but also to anchor cisternal-specific enzymes. In the absence of Golgi matrix proteins it may be that all the processing enzymes that perform Golgi functions are contained within a single cisternum, rather than each cisternum being responsible for sequestering a particular enzyme or subset. Though plant Golgi bodies are also believed to have similar matrix proteins (Latijnhouwers et al. 2005), specific mutations which affect Golgi localization of a CASP protein to the mammalian Golgi do not inhibit delivery to the plant Golgi apparatus (Renna et al. 2005).

We undertook a systematic search for golgins in filamentous fungi and found that these matrix proteins appear to be missing (Table 1.2). Forward and reverse tblastn and blastp searches of *A. nidulans* and human genomes produced no significant hits. Similarly, fungi appear to lack human homologs for GOPC (Golgi-associated PDZ, coiled-coil motif) and GCC1 (GRIP, coiled-coil domain containing-1). Conversely, however, both *S. cerevisiae* and filamentous fungi possess a potential ortholog of human GORASPs (GRASP55/65 family), which in animals are required for post-mitotic reassembly of Golgi stacks. In *S. cerevisiae,* GRH1 (GRASP65 homolog) plays a role in the spindle assembly checkpoint and displays two-hybrid genetic interactions with Golgi/ER components, such as CHO2 (phosphatidylethanolamine methyltransferase), ALG3 (dolichol-P-mannose dependent alpha-1,3-mannosyltransferase), and ERV14, involved with vesicle formation and incorporation of secretory cargo into COPII vesicles (Schuldiner et al. 2005). The *A. nidulans* homolog, AN11248 (GRASP55/65 homolog) shares greater homology with human GORASPs 1 and 2 than it does with Sc GRH1. Thus, some fungi may possess at least one of the genes required for the formation of Golgi stacks, though the actual function of AN11248 (and its orthologs in other fungi) remains open to investigation. These observations leave us wondering what is the functional advantage of the highly structured Golgi apparatus in higher eukaryotes? What is the penalty for the less-elaborated Golgi found in filamentous fungi?

In a manner similar to plants, fungi also utilize the Golgi apparatus to produce complex cell

wall polysaccharides. The mobility of plant Golgi observed in some cells may be reduced in others whose main function is to secrete cell wall polymers. In certain cell types it has been estimated that 80% of Golgi activity is devoted to the production of complex polysaccharides (Driouich et al. 1993). The situation in rapidly growing vegetative hyphae of filamentous hyphae may be similarly skewed in favor of polysaccharide production.

Much has been learned about plant and mammalian Golgi through the use of the fungal metabolite brefeldin A (BFA; Lippincott-Schwartz et al. 1989; Satiat-Jeunemaitre et al. 1996). In these systems BFA leads to a blockage of anterograde transport from the ER to the Golgi resulting in a disassembly of the Golgi apparatus and the redistribution of many of its components back to the ER – the retrograde pathway for retrieving ER markers from the Golgi is unaffected by BFA. Interestingly, though BFA had a negative effect on fungal growth, the Golgi cisternae of fungi were not disassembled and there was no redistribution of the Golgi marker ConA back into the ER (Bourett and Howard 1996; Satiat-Jeunemaitre et al. 1996), though BFA treatment did induce the proliferation/formation of membrane-enclosed compartments not observed in untreated cells (Fig. 1.7A).

A survey of Golgi-specific fungal genes reveals strong correspondence to *S. cerevisiae* (Table 1.2). Only two Golgi-specific proteins appear to be missing in other fungi – BUG1, function unknown, and LST4, required for the transport of Gap1p amino acid permease from the Golgi apparatus to the plasma membrane – and these are non-essential. Most fungi appear to possess a single ortholog corresponding to each of two *S. cerevisiae* gene-pair duplicates: SWH1/OSH2 and SBE2/SBE22. Several Golgi functions have undergone expansion in filamentous and other fungi. For example, the single *S. cerevisiae* GEF1 Golgi chloride channel has expanded to three genes, which are highly similar and well conserved across fungi. These genes and GEF1 are strongly related to metazoan voltage-gated chloride channels. In addition, filamentous fungi have undergone expansion of the *S. cerevisiae* CHS7 gene, of unknown function, involved in chitin biosynthesis by regulating Chs3p export from the ER. The *A. nidulans* ortholog, AN1069, shares much greater homology with *S. cerevisiae* CHS7 than does AN5152 (Table 1.2). The two *A. nidulans* genes share only moderate homology ($2e^{-26}$), suggesting the possibility that AN5152 has evolved to perform a novel, fungus-specific function. In addition, three Golgi functions have undergone expansion in a limited set of fungi: (1) *A. nidulans* appears to possess two homologs of *S. cerevisiae* CCC1 (vacuolar Fe^{2+}/Mn^{2+} transporter), whereas other fungi surveyed appear to possess a single ortholog, (2) *A. nidulans* also appears to differ from other fungi in possessing duplicated genes that correspond to *S. cerevisiae* VRG4 (Golgi GDP-mannose transporter), and (3) in *A. nidulans* and *C. immitis* but not in other fungi, we found gene-pair duplicates of *S. cerevisiae* PSD2 (phosphatidylserine decarboxylase).

It should be noted that numerous genes and proteins beyond those shown in Table 1.2 are associated with Golgi function. Because these additional components also play a role in other endomembrane processes, they are distributed within the subsequent four tables in this chapter.

Comparative genomic analysis of the structural trafficking machinery for ER-to-Golgi anterograde transport reveals almost complete conservation among the fungi (Table 1.3). For example, components of the COPII coatomer complex, transport protein particle (TRAPP) complex – a vesicle tethering complex that mediates membrane fusion – and associated COPII-related functions are fully conserved, with the exception that the non-essential *S. cerevisiae* TRAPP complex component KRE11 (TRAPP subunit involved in biosynthesis of cell wall β-glucans) is missing. The COPII machinery in many fungi is simpler, especially in comparison with *S. cerevisiae* genes encoding COPII-related functions, a number of which were retained and/or expanded in *S. cerevisiae* following whole-genome duplication (e.g., EMP46, -47; ERP1, -5, -6; ERP2, -3, -4; ERV14, -15).

Although the COPI structural machinery for Golgi to ER retrograde transport is also well conserved, several important COPI-related structural components are diverged or missing in filamentous fungi.

First, two out of three components of the Dsl1 vesicle tethering complex have diverged substantially. In *S. cerevisiae* the Dsl1 complex is composed of three indispensable peripheral membrane proteins (DSL1, TIP20, DSL3) that mediate Golgi to ER trafficking by facilitating the fusion of COPI vesicles with the ER through stabilization of the Use1p-Ufe1p-Sec20p SNARE complex; and by prohibiting back-fusion of COPII vesicles with ER (e.g. Andag and Schmitt 2003; Kamena and Spang 2004; Kraynack et al. 2005). A protein with marginal similarity

to *S. cerevisiae* DSL1 was found in one filamentous fungus, *R. oryzae*; and *S. cerevisiae* TIP20 did not find fungal orthologs. Because potential human homologs of DSL1 (ZW10, Zeste-white protein) and TIP20 (RINT-1, Rad50-interacting protein) were recently shown to function in transport between the ER and Golgi (Hirose et al. 2004), we used these human genes to locate candidate fungal orthologs (see Table 1.3).

Second, at least one component of the GET complex (Golgi to ER transport) appears to be missing from other fungi and one component has diverged. In *S. cerevisiae*, the GET complex consists of three structurally unrelated subunits that act in an ERD2-dependent manner to retrieve HDEL-containing ER-resident proteins from the Golgi to the ER (e.g., Schuldiner et al. 2005). The GET complex genes are non-essential in *S. cerevisiae* although the ERD2 protein, which binds to HDEL motif-containing proteins and on which the function of the GET complex depends, is essential. The GET3 *arsA* arsenite transporter is strongly conserved. Conversely, GET1 is poorly conserved and we were unable to detect homologs of GET2 in organisms other than ascomycetous yeasts (see Table 1.3). The apparent divergence in GET complex components in other fungi, combined with the expansion and divergence of a novel additional ERD2 homolog in other fungi (see Sect. III.A., above), suggests that retrieval processes for ER-resident proteins could differ in important ways from mechanisms in *S. cerevisiae*.

Our observations concerning the DSL1 and GET complexes reinforce and extend a consistent finding that endomembrane genes – indeed, as well as many other genes – in most fungi show greater similarity to animal genes than those of *S. cerevisiae*.

In addition to structural components of the COPI and COPII pathways, the regulatory G-protein machinery that controls anterograde and retrograde transport of vesicles and cargo between the ER and Golgi were examined. Vesicle trafficking between these compartments is controlled by a family of ADP ribosylation factor (ARF) and ARF-like (ARL) GTPases and their associated GTPase activating proteins (ARF-GAPs), guanine nucleotide exchange factors (ARF-GEFs), and other ARF/ARL-associated proteins (Table 1.3). These G proteins in large part control COPI- and COPII-coated vesicle formation and trafficking. *S. cerevisiae* possesses three ARFs and two ARLs that mediate four different, conserved processes. The ARFs, including SAR1 and functionally redundant ARF1/ARF2, mediate Golgi to ER transport and coated vesicle formation, respectively; and the ARL1 and ARL3 proteins mediate distinct steps in membrane trafficking at the Golgi apparatus. *A. nidulans* possesses single orthologs corresponding to the four conserved *S. cerevisiae* ARF/ARL functions and additionally possesses one novel, expanded ARF and two novel ARLs, for a total of three ARF and four ARL family members. The human genome, by comparison, has expanded to contain six ARFs and 11 ARLs. The human ARF proteins are subdivided into three classes, with three Class I (ARF1, -2, -3), two Class II (ARF4, -5), and a single Class III representative (ARF6). Whereas the *S. cerevisiae* ARFs correspond to human Class I orthologs, the novel *A. nidulans* ARF, AN5020, is strongly related to the human Class III ARF6. ARF6 is unique among human ARFs in that it localizes to the plasma membrane, where it plays a role in clathrin-mediated endocytosis by regulating the assembly of the AP2/clathrin coat (Paleotti et al. 2005). The two novel ARLs, represented by *A. nidulans* AN3934 and *C. immitis* CIMG_03295, appear to be orthologous with human ARL10 ($7e^{-56}$) and ARL2 ($1e^{-61}$), respectively. While little is known about human ARL2, human ARL10 is involved in trafficking processes for lysosomes (Bagshaw et al. 2006).

With respect to ARF-GAPs and ARF-GEFs, other fungi possess machinery similar but not identical to *S. cerevisiae* (Table 1.3). One additional novel ARF-GAP, represented by *A nidulans* AN1629, occurs in other fungi. Not surprisingly, AN1629 appears to be the ARF-GAP partner to the novel fungal ARF6 ortholog described above (AN5020). AN1629 shows only modest homology with *S. cerevisiae* AGE2 and much stronger homology with a human ARF-GAP for ARF6, stromal membrane-associated protein (NP_068759.2). Recently, this human ARF-GAP for ARF6 was shown to interact directly with clathrin to regulate clathrin-mediated endocytosis (Tanabe et al. 2005). The presence of an ARF6 and ARF6-GAP suggests that filamentous fungi possess more of the regulatory machinery needed for clathrin-mediated endocytosis than do ascomycetous yeasts (see also Tables 1.4, 1.5) and indicates that these novel ARF and ARF-GAP functions – though relatively ancient among eukaryotes – arose after the divergence of *S. cerevisiae* and other fungi.

We were interested to discover that while ARFs, ARLs, and ARF-GAPs have expanded, some fungi

appear to possess the same complement of ARF-GEFs as *S. cerevisiae*. While most *S. cerevisiae* ARF-GEFs have clear orthologs in other fungi, SEC12 orthologs were difficult to find, owing to their substantial divergence across eukaryotes and because they contain several WD40 repeat motifs, which are found in many diverse proteins. SEC12 is an essential gene in *S. cerevisiae* and serves as the GEF for the SAR1 GTPase, which is universally conserved among eukaryotes and required for ER to Golgi transport.

Although neither the *S. cerevisiae* SEC12 nor the *S. pombe* ortholog, SPO14, found homologs in filamentous fungi or a basidiomycetous yeast or humans, strong apparent orthologs of *S. cerevisiae* SEC12 occur in both *Candida lusitaniae* ($3e^{-51}$) and *C. guilliermondii* ($5e^{-46}$), indicating that SEC12 has remained conserved among some ascomycetous yeasts. By using SEC12 orthologs from human, plant, and fly, we were able to find the apparent ortholog in one dimorphic basidiomycete, *Ustilago maydis* (see Table 1.3). The *U. maydis* gene, in turn, found apparent orthologs in three other fungi. These, in turn, found *S. cerevisiae* SEC12. However, weaker candidate orthologs from additional fungi did not find SEC12 in *S. cerevisiae*, plants, or animals, indicating that in these species SEC12 has apparently diverged beyond detection.

In addition to the known ARF-GEFs in *S. cerevisiae*, we discovered that one uncharacterized hypothetical ORF (YBL060W) appears to contain a SEC7 domain characteristic of many ARF-GEFs and has a potential ortholog in *A. nidulans* (AN3438) and other fungi. The function of this and other fungal ARF-GEFs remains an open question.

C. Exocytosis/Secretion

Exocytosis is the vesicle-mediated delivery of materials to the outside of the cell and transmembrane proteins to the plasma membrane, especially glycosylated proteins that necessarily pass through the Golgi apparatus. Evidence such as microradiography studies of glucoamylase secretion in *Aspergillus niger* (Wösten et al. 1991) suggests that exocytosis is predominant at the hyphal tip. Fungal secretion has been exploited for industrial heterologous protein production and is important for many aspects of fungal biology. For example, a family of secreted aspartic proteinases has been shown to be a potent virulence factor in the animal pathogen *Candida albicans* (Schaller et al. 2005).

Interruption of fungal protein secretion inhibited plant pathogenesis by both *Colletotrichum lindemuthianum* (Siriputthaiwan et al. 2005) and *Magnaporthe grisea* (Gilbert et al. 2006). Interestingly in the latter, *M. grisea* transformants lacking a copy of the *MgAPT2* gene were not impaired in normal vegetative cell growth or sporulation.

In higher eukaryotes delivery of secretory vesicles to the plasma membrane with concurrent release of internal cargo can occur via either a constitutive or regulated secretory pathway: the latter is believed to be lacking in filamentous fungi (Weber and Pitt 2001). These two pathways utilize different vesicular machinery. Secretory vesicles are initiated at the trans-Golgi network concurrent with condensation of secretory proteins that may be acted upon by proteolytic enzymes. This proteolytic activity continues within the secretory vesicles and can serve to activate polypeptide cargoes such as hormones, neuropeptides, and hydrolytic enzymes. For hydrolytic enzymes, which can be secreted abundantly by fungi, one purpose of proteolytic processing is to prevent activation in compartments where activity might have harmful effects.

Fluorescent proteins have been exploited to examine secretion in filamentous fungi. Though attempts to use oligomeric reef coral fluorescent proteins to follow secretion have been unsuccessful (Bourett et al. 2002), secretion has been shown by other groups to be the default pathway when a signal peptide is employed without additional retention or vacuole targeting sequences (Gordon et al. 2000; Conesa et al. 2001; Masai et al. 2003). Secretion was evidenced by an accumulation of fluorescence signal at the hyphal apex and associated with incipient septa (Gordon et al. 2000). With these same transformants compartments of the endomembrane system were visualized when secretion was blocked by pharmacological agents or other treatments (Khalaj et al. 2001).

Most proteins in eukaryotic cells acquire N-linked core glycosylations co-translationally as they enter the ER through the protein translocators in the ER membrane. These core glycosylations appear to be highly conserved among all eukaryotes and are used by cells to assess whether proteins are properly folded (Cabral et al. 2001). Further modifications to the sugar residues occur in very precise subcompartments within the mammalian Golgi apparatus (Kornfeld and Kornfeld 1985). For example, it is known that the mannosidase I enzyme is active in the cis-Golgi and sialyl

residues are added to nascent glycoproteins within the trans-Golgi compartment. Filamentous fungi glycosylate proteins in distinctly different ways from those used by *S. cerevisiae* (Klionsky et al. 1990) or higher plant and animal cells (Hamilton et al. 2003). This can be problematic during expression of heterologous proteins by industrially important fungi unless glycosylation is genetically modified to a more mammalian type (Maras et al. 1999; Schmidt 2004).

Vesicles are a common feature of both secretion (see Figs. 1.1, 1.4) and protein transport between donor and target compartments of the endomembrane system. Inter-organelle protein transport associated with nuclei and mitochondria is not vesicle-mediated. Larger intermediary transport packages may also occur. The vesicle trafficking machinery has been the focus of computational genomic approaches in a range of eukaryotic organisms, including fungi (Tables 1.3, 1.4; Gupta and Heath 2002), to assess genetic conservation. From these studies it appears that the basic core machinery has been highly conserved. An increased complexity found in multicellular organisms has arisen through an elaboration of regulatory mechanisms such as the participation of more diverse Rab proteins and an expansion in tissue-specific members of each gene family (Bock et al. 2001; Table 1.4).

Membrane fusion between vesicles and destination compartments is highly complex and carefully regulated, involving a large variety of components. Among these are the soluble *N*-ethylmaleimide-sensitive factor attachment protein receptor (SNARE) proteins, a family of membrane-bound RAB GTPases and their requisite RAB-GAPs and RAB-GEFs, an array of compartment-specific proteins, RAB-activated vesicle-membrane tethering factors, and numerous accessory factors (reviewed by Pereira-Leal and Seabra 2001; Zerial and McBride 2001; Gupta and Heath 2002). Membrane fusion appears to initiate by the interaction of membrane-bound RAB GTPases with cognate tethering factors that act as a bridge between the vesicle membrane and the destination compartment. Modification/activation of the tethering factors by RAB GTPases allows SNARE proteins on the vesicle and target membranes to associate with each other and bring the membranes into proximity so that fusion can take place.

SNAREs comprise a large family of highly conserved, coiled-coil domain proteins that appear to mediate vesicle fusion throughout the endomembrane system. This is accomplished by the interaction of the coiled-coil domains between SNAREs associated with the vesicle (typically three v-SNAREs per vesicle) with one target SNARE (t-SNARE) on the target membrane. For a review of SNARE structure and function in *S. cerevisiae* and other fungi, see Burri and Lithgow (2004), Gupta and Heath (2002).

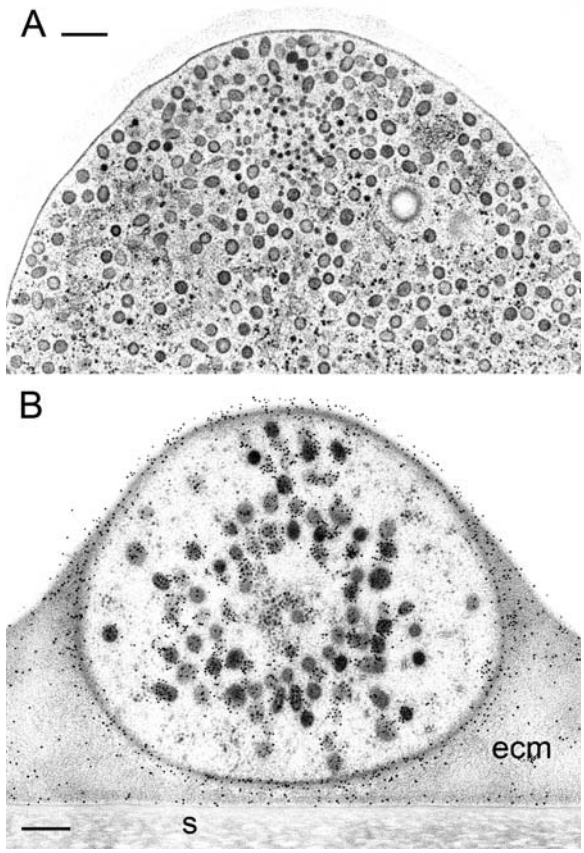

Fig. 1.4. The hyphal tip is a region containing an abundance of apical vesicles thought to be responsible for secretory activity and cell wall synthesis. **A** Near median longitudinal section of *Aspergillus nidulans* hypha. Note localized concentration of microvesicles. **B** Cross-section perpendicular to long axis of *Trichoderma viride* hypha, 400–500 nm behind the apex. Gold-tagged Con A binding sites are associated with apical vesicles that, when observed *en mass* by fluorescence-tagged Con A, embodies the Spitzenkörper (cf. Fig. 11.6C in this volume). Specimens prepared by freeze substitution. *ecm* Extracellular matrix, *s* substratum. *Bars* 500 nm

RAB subfamily GTPases are GPI-anchored membrane proteins, anchored through double prenylation via two C-terminal Cys residues, that act to recruit a wide array of RAB effectors onto their resident membrane. They control such

processes as vesicle formation, motility, and vesicle tethering prior to SNARE assembly.

Recent findings show that many of the RAB-tethering factors are organized into complexes that act in specific endomembrane pathways and compartments. These include the DSL1 and TRAPP (transport protein particle) complexes that mediate COPI and COPII vesicle fusion, respectively (see Table 1.3 and descriptions above), the conserved oligomeric Golgi (COG) complex (which mediates fusion of vesicles at the Golgi compartment), the Golgi-associated retrograde transport (GARP) and homotypic fusion and vacuole protein sorting (HOPS) complexes (which control vesicle fusion in the endosomal and vacuolar compartments, as well as the recycling of endosomal vesicles back to the trans-Golgi), and the exocyst (which mediates fusion of vesicles with the plasma membrane). For a review of vesicle tethering, see Whyte and Munro (2002).

With respect to SNARE and RAB proteins, our findings largely parallel those of Gupta and Heath (2002). The complement of SNARE proteins is highly conserved among all fungi surveyed (Table 1.4). For example, *A. nidulans* possesses one candidate SNARE ortholog for each of four redundant gene-pair duplicates in *S. cerevisiae* (PEP12/VAM3, SEC9/SPO20, SNC1/SNC2, SSO1/SSO2). Similarly, there is a one-to-one correspondence for SM-like SNARE-binding proteins ("SNARE masters") and other SNARE mediators (Table 1.4).

With respect to RAB family expansion in the filamentous fungi, fungi possess seven orthologs corresponding to the core of nine universally conserved *S. cerevisiae* RAB family members: YPT1, SEC4, YPT31/32, YPT51/52/53, YPT6, and YPT7 (Table 1.4). Other fungi appear to possess a single ortholog corresponding to the YPT31/32 paralogs and two homologs of the functionally interchangeable YPT51/52/53 paralogs.

For example, *S. cerevisiae* YPT51 (VPS21) and YPT53 are more closely related to each other and to *A. nidulans* AN4915 than to YPT52 and AN3842. YPT52, in contrast, shows stronger homology with AN3842 than AN4915. These relationships were supported by phylogenetic analysis using the neighbor-joining method (data not shown; see Table 1.4). With respect to fungal evolution, these observations suggest that YPT51 (AN4915) and YPT52 (AN3842) arose by duplication before the divergence of *S. cerevisiae* and other fungi, and that YPT51 and YPT53 arose by a second duplication following the divergence of these two lineages.

Consistent with Gupta and Heath (2002), homologs of *S. cerevisiae* YPT10 and YPT11 occur in some closely related ascomycetous yeasts, but not in the filamentous fungi and the basidiomycetous yeast surveyed in this study. However, these other fungi do possess three novel, expanded RAB family members not present in *S. cerevisiae* (Table 1.4). These novel fungal RABs correspond to RAB2, which occurs in mammals and *Arabidopsis*, and to RAB4 and RAB24, which occur in mammals but not *Arabidopsis* (Rutherford and Moore 2002). Gupta and Heath (2002) similarly reported the existence of RAB2 and RAB4 orthologs in three filamentous fungi, along with RAB18 orthologs in the basidiomycete *Phanerochaete chrysosporium*, but they did not detect RAB24 relatives. Thus, the three novel fungal RABs identified herein appear to represent orthologs of mammalian RABs that do not occur in *S. cerevisiae*.

The complement of RAB-GAPs and enzymes for prenylating RAB GTPases, have been highly conserved across fungi, with some expansion. Whereas *S. cerevisiae* appears to possess eight distinct RAB-GAP functions, with one functionally interchangeable pair (MSB3/MSB4), at least 11 distinct RAB-GAPs occur in *A. nidulans* and other fungi (Table 1.4).

Seven of the 11 *A. nidulans* genes appear to contain a TBC domain (AN11010, AN1980, AN10355, AN0573, AN5407, AN0281, AN3752), which is characteristic of some RAB-GAPs and also some genes that govern the spindle assembly checkpoint (Neuwald 1997). Among the three expanded *A. nidulans* RAB-GAPs, two have a TBC domain (AN0573, AN3752) and one appears to lack this domain (AN3094). Each of these three novel RAB-GAPs shows stronger homology with human than with *S. cerevisiae* RAB-GAPs (see Table 1.4). For example, AN0573 finds human TBC domain family member 2B (TBC1D2B, NP_055894), about which little is known, but which does not have an *S. cerevisiae* ortholog. AN3094 finds a potential RAB-GAP, USP6 N-terminal like protein (XP_943758), which is related to RN-Tre, a RAB5-specific GAP that interacts with both F-actin and actinin-4, an F-actin bundling protein (Lanzetti et al. 2004). The most divergent *A.nidulans* RAB-GAP, AN3752, shows strong homology with a human RABGAP, TBC1D14, which also has no corresponding *S. cerevisiae* ortholog. Thus, all three of these novel *A. nidulans* RAB-GAPs appear to have corresponding human orthologs.

RAB-GEFs have doubled in number between *S. cerevisiae* and other fungi (Table 1.4). *A. nidulans* and other fungi, for example, possess two additional, novel VPS9 domain proteins and two

RAB-GEFs which have homology with human RAB6-interacting protein 1. VPS9 in *S. cerevisiae* specifically stimulates the GEF exchange activity of YPT51 (mammalian RAB5 ortholog) to control protein trafficking and vesicle fusion at the late endosome and shares similarity with mammalian RAS inhibitors (Esters et al. 2001; Bowers and Stevens 2005).

Of three annotated VPS9 domain-containing proteins in *A. nidulans*, AN3678 shows strong homology with VPS9, and AN5920 exhibits considerably weaker homology (see Table 1.4). These *A. nidulans* proteins are weakly related to each other ($2e^{-12}$) and in human each shows greatest homology with RAB guanine nucleotide exchange factor 1 (RABGEF1), NP_055319.1 ($6e^{-29}$, $4e^{-11}$), which is a GEF for RAB5. The third *A. nidulans* protein, AN1280, is unrelated to *S. cerevisiae* VPS9 and the other two *A. nidulans* proteins, and contains both VPS9 and ankyrin repeat domains. Instead, AN1280 shows homology with a *S. cerevisiae* uncharacterized hypothetical ORF, YML002W ($3e^{-29}$), and in human to a novel VPS9 and ankyrin domain-containing protein, ankyrin repeat domain 27 (ANKYRD27, NP_115515, $3e^{-08}$). This protein, also known as VARP (VPS9, ankyrin repeat protein), is a recently discovered GEF for RAB21, a close relative of RAB5 that is involved in endosome dynamics (Zhang et al. 2006).

To summarize, we have discovered separate orthologs in *A. nidulans* and other fungi of the *S. cerevisiae* RAB5/RAB21 homologs YPT51/53 (AN4915) and YPT52 (AN3842), and similarly have found an expansion of *S. cerevisiae* VPS9, a GEF for YPT51. The considerable divergence between the *A. nidulans* VPS9 paralogs, AN3678 and AN5920 ($2e^{-12}$), suggests that AN5920 and its orthologs in other fungi may have evolved to fulfill a novel functional niche. Additionally, *A. nidulans* and other fungi appear to possess a novel, ankyrin repeat-containing RAB GEF for RAB21 that is present in humans but not *S. cerevisiae*.

The two remaining novel fungal RAB GEFs appear to be homologs of mammalian RAB6-interacting protein1 (RAB6IP1). As represented by AN4349 and AN0575, these are the only two *A. nidulans* genes bearing a DENN/AEX-3 domain (differentially expressed in neoplastic vs normal cells). This domain is characteristic of proteins involved in RAB-mediated processes, in particular mammalian RAB3 and RAB6IP1. DENN/AEX-3 proteins are also found in regulators of human MAP kinase pathways, such as MADD (a mitogen-activated protein kinase-activating protein containing death domain), ST5 (a suppressor of tumorigenicity), and in an unusual mammalian pseudo-phosphatase, SBF1 or SET (for Suvar3-9, enhancer-of-zeste, trithorax-binding factor 1), which is a growth regulator that contains a GEF homology domain (Firestein and Cleary 2001; Levivier et al. 2001). Beyond its role as a GDP dissociation inhibitor for RAB6 (Janoueix-Lerosey et al. 1995), little is known about RAB6IP1 and nothing is known concerning the role of DENN/AEX-3 domain proteins in fungi. Given that these proteins appear to be missing from *S. cerevisiae* and since in mammals DENN-GEF domain proteins function as growth regulators, some of which are implicated in oncogenic processes, there seems ample justification to use those other fungi as models for investigating these proteins.

Since many RABs are involved in local trafficking of vesicles between compartments, they must be continually retrieved and returned to their resident organelle. This is accomplished by RAB-GEFs, some or all of which act as GDP dissociation inhibitors (GDIs). These proteins act in RAB recycling, by extracting RAB-GDP from membrane to cytosol, and delivering the GDI-RAB-GDP complex back to the resident organelle where, upon dissociation of the GDI-RAB complex, RAB is integrated into the organelle membrane. The mechanism for targeting specific RAB GTPases to their resident organelles is poorly understood. However, growing evidence points to a group of eight integral membrane proteins, represented in *S. cerevisiae* by YIP1, -3, -4, -5, YOP1, YIF1, YOS1, and RTN1, that may act as GDI displacement factors (GDFs) to control the specific localization and integration of RABs to resident organelles through direct interaction with their cognate RABs. Specificity for a particular double-prenylated RAB may be conferred both by specific organelle localization of YIP/YOS/YIFs, and by combinatorial interactions among YIP/YOS/YIF proteins within particular compartments (reviewed by Geng et al. 2005).

The YIP/YOS/YIF family and the reticulons are well conserved, with distinct orthologs identifiable between *S. cerevisiae* and other fungi (Table 1.4). One *S. cerevisiae* reticulon-like protein, RTN2 (function unknown, similar to RTN1) appears to be missing in other fungi and two members of this group of proteins have expanded. First, *A. nidulans* and other fungi possess two YOP1 paralogs: AN2279 and AN6059. Second, *A. nidulans* and other fungi possess at least one and possibly two RTN1 (Reticulon-1) homologs, AN5404 and AN5648.

Finally, we considered the protein complexes that appear to act as tethering factors to facilitate RAB- and SNARE-mediated membrane fusion. Most tethering complexes are strongly conserved across eukaryotes, with little or no loss or expansion. This is particularly true for the post-Golgi tethering complexes, including the HOPS complex, the GARP complex, and the exocyst (see Table 1.6). This is also true of the DSL1 and TRAPP complexes (Table 1.3; discussed above) and the COG complex (Table 1.4), although some components of these latter three complexes appear to have diverged substantially for *S. cerevisiae* versus other fungi and human. The COG complex appears to be the most divergent tethering complex, with only three of eight subunits (COG3, -4, -6) showing good conservation between *S. cerevisiae* and other fungi (Table 1.4). We were unable to find *S. cerevisiae* orthologs of COG1, -2, -5, -8 in other fungi; and we are uncertain of the *A. nidulans* COG7 homolog. Instead, we were able to find *A. nidulans* COG1, -2, and -5 homologs by using the corresponding human COGs. As shown in Table 1.4, however, COG2 and COG5 each found a single *A. nidulans* gene, AN8226. Finally, although COG8 in *A. nidulans* could not be found using *S. cerevisiae* or human orthologs, likely COG8 orthologs were discovered in several other fungi.

IV. Endocytic Pathway: Plasma Membrane, Endocytosis, Endosomes, and Vacuoles

The plasma membrane of fungi, especially during the vegetative growth of saprophytic species, contains vast numbers of permeases and transporters to facilitate the uptake of macromolecules required to maintain what can often be prolific growth rates. The distribution of these plasma membrane resident molecules must be regulated, in part, through selective synthesis and turnover. Endocytosis provides a means for internalization of extracellular molecules including molecules involved with signaling, as well as plasma membrane proteins and lipids. The elaboration of internal membranes and the capacity for endocytosis allows eukaryotes to internalize macromolecules rather than just small metabolites. Furthermore, the existence of endosomal compartments facilitates further metabolism of macromolecules into forms that can be utilized by the organism. Compared with multicellular eukaryotes, perhaps fungi have a reduced or less-elaborated endosomal system, since at least saprophytic species may rely more on uptake of smaller metabolites following secretion of hydrolytic enzymes, following a strategy typical for bacteria and other prokaryotes. Perhaps this is necessary because many of the macromolecules endocytosed by animal cells would be too bulky to traverse the fungal cell wall, the porosity of which can limit all but very small molecules (Money 1990).

Clathrin-coated vesicles are often associated with endocytosis in higher eukaryotes and are considered requisite for receptor-mediated endocytosis (Robinson 1996). Coated pits are thought to be regions of receptor accumulation. Though fungi do possess a clathrin heavy-chain gene (Table 1.5), evidence for clathrin-coated pits and/or vesicles is scant (Caesar-Ton That et al. 1987). Nevertheless, there are several lines of evidence that support the existence of endocytosis in filamentous fungi (Read and Kalkman 2003). Perhaps the best evidence for the existence of endocytosis comes from observations of cells treated with the amphiphillic styryl dye FM 4-64 (Hoffman and Mendgen 1998; Fischer-Parton et al. 2000; Wedlich-Söldner et al. 2000). Furthermore, genetic and molecular studies in *S. cerevisiae* have established a role for clathrins and clathrin-adaptor proteins in vesicular transport from the late Golgi to endosomes. *S. cerevisiae* cells lacking the clathrin heavy chain (CHC1) are viable and secrete proteins normally. However, they exhibit a syndrome of defects in growth, mating, sporulation, endocytosis, late Golgi protein localization, and vesicle ultrastructure (reviewed by Bowers and Stevens 2005). In other fungi, the clathrin heavy chain is strongly conserved with *S. cerevisiae*, as is the ENT3 component of the clathrin recruitment machinery (Table 1.5). Conversely, however, the clathrin light chain is weakly conserved, sharing about the same homology with *S. cerevisiae* ($3.4e^{-14}$) and human ($7e^{-10}$). In addition, the ENT5 protein, which associates with the clathrin adaptor GGA1/2 (see Table 1.3), clathrin adaptor complex AP-1, and clathrin, appears to be missing in other fungi (Table 1.5). The AP-1, AP-2, and AP-3 adaptor complexes are strongly conserved between *S. cerevisiae* and other fungi, with no expansion and with the loss of only one AP-1 subunit, APM2. Between *S. cerevisiae* and other fungi, some loss and divergence has occurred in proteins known to be associated with clathrin-coated vesicles. For example, the four paralogous CHS5-ARF1 binding proteins (ChAPs) in *S. cere-*

visiae appear to be represented by a single ortholog in other fungi. In addition, *A. nidulans* and other fungi possess at least four BinAmphiphysin-Rvs (BAR)-domain proteins, which are involved in formation of clathrin-coated vesicles at the plasma membrane and are required for early steps in endocytosis (for a review, see McNiven and Thompson 2006). Two of these four genes encode amphiphysins and are highly conserved from *S. cerevisiae* to humans. The remaining two *A. nidulans* genes are endophilin-related and one of these appears to represent a novel, expanded function relative to *S. cerevisiae* (Table 1.5).

We discovered a surprisingly large number of dynamin GTPases and dynamin-related proteins in some species. Whereas *S. cerevisiae* possesses two dynamin GTPases involved in endomembrane transport (VPS1, DNM1) and two dynamin-related GTPases that function in mitochondria (MGM1, FZO1), *A. nidulans* and other fungi possess orthologs of these four plus at least six additional dynamin-related proteins (Table 1.5). It is an open question whether the conserved fungal dynamins and their novel, expanded counterparts function in vesicle scission by pinching off vesicles after budding. One of the six expanded dynamins does, however, share greatest homology with human Dynamin 2 (DNM2), which plays a role in endocytosis and has been linked to several important signaling pathways, and defects in which are associated with a degenerative muscle disease (Murph et al. 2003; Bhattacharya et al. 2005; Bitoun et al. 2005; Gorska et al. 2006). The remaining five of the six expanded fungal dynamins share strong homology with an interesting pair of human dynamins, myxovirus (influenza virus) resistance 1 and 2 (MX1, MX2). Both mammalian genes are induced by interferon-alpha during viral infection; and an antiviral and apoptosis-promoting activity has been demonstrated for MX1 (e.g., Peltekian et al. 2005; Gilli et al. 2006; Numajiri et al. 2006).

Flask-shaped invaginations of the plasma membrane resembling caveoli have been described in *S. cerevisiae* (Mulholland et al. 1994) and *P. pastoris* (Fig. 1.5F, G) but appear to be very rare in filamentous fungi. The caveolin genes are not present in the genomes of either *S. cerevisiae* or other fungi sequenced to date. For example, we were unable to find homologs of human caveolins 1, -2, and -3 in filamentous fungi and one basidiomycetous yeast. There is solid evidence that caveoli (Geli and Riezman 1998) and unknown cellular components (Damm et al. 2005) can be involved with non-clathrin facilitated endocytosis.

Filasomes (Fig. 1.5A–E; Howard 1980) are microvesicles with a fibrillar actin-containing (Hoch and Staples 1983b; Bourett and Howard 1991, see Srinivasan et al. 1996) non-clathrin coat, first described using the electron microscope (Hoch and Howard 1980; Howard 1980, 1981). In the vegetative hypha, filasomes are most numerous in the peripheral subapical region (Czymmek et al. 1996) and associated with particular fungal structures, such as the base of appressoria of certain phytopathogenic fungi and incipient septa, where rapid trans-cellular flux seems apparent (Swann and Mims 1991; see also Howard 1997). The requirement for an intact actin cytoskeleton for endocytosis has been firmly established in *S. cerevisiae* (Geli and Riezman 1998) and mutations to the single actin gene are lethal (Doyle and Botstein 1996). Filasomes, "putative cross-sectioned invaginations" (Mulholland et al. 1994), and "cortical actin patches" described in a number of fungal species may all be one-in-the-same organelle. Diligent application of cryofixation, with serial section or EM tomographic analysis, would seem necessary in addressing this question.

The early endosome is a compartment that functions as the main sorting station for molecules within the endocytic pathway, much like the cis- and trans-Golgi networks in higher eukaryotes sort molecules in the biosynthetic–secretory pathway. Early endosomes are important for recycling internalized receptors and transporters back to the cell surface or targeting them for degradation in a lytic vacuole. Endosomal compartments have been poorly defined for filamentous fungi, due in part to a lack of well characterized cell surface receptors and a dearth of decent electron microscope data. In a recent report, internalization of a tagged plasma membrane resident permease was used to identify presumed endosomal compartments (Higuchi et al. 2006). Putative endosomes have been identified in a number of fungi using FM4-64 (Wedlich-Söldner et al. 2000; Read and Hickey 2001; Atkinson et al. 2002). In *Ustilago maydis*, FM 4-64 stained peripheral vesicular entities that appeared to co-localize with a fusion protein between GFP and Yup1, a putative t-SNARE protein involved in membrane fusion, suggesting that the vesicles represent an early endosome compartment (Wedlich-Söldner et al. 2000). These putative endosomes were highly motile, showing bi-directional saltatory movements dependent upon a microtubule cytoskeleton. Mutations to

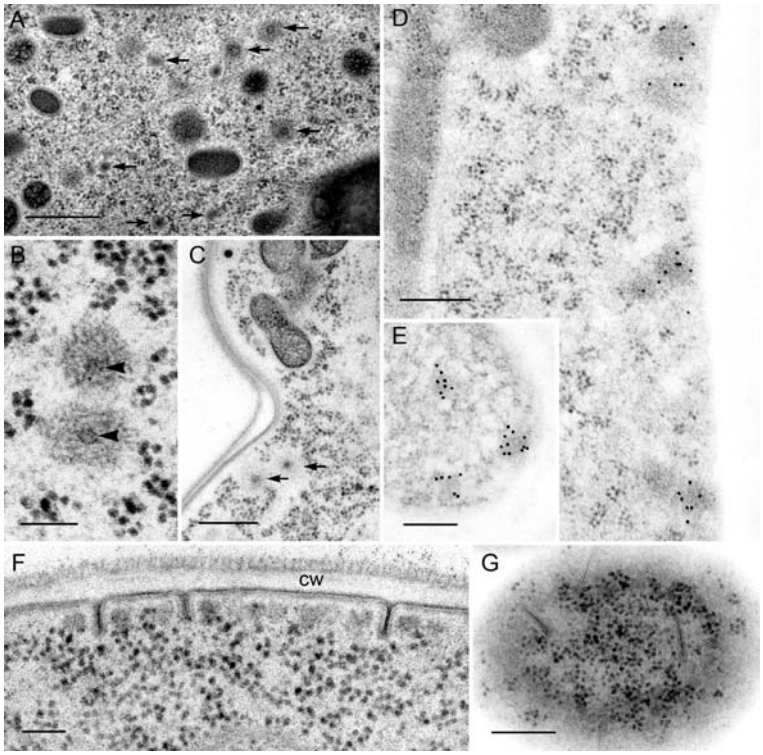

Fig. 1.5. **A**, **B** Endocytosis in filamentous fungi – here *Gilbertella persicaria* and *Magnaporthe grisea*, respectively – is believed to be facilitated by filament-coated microvesicles called filasomes (*arrows*) and not by clathrin-coated vesicles. **C** Filasomes also are found in yeast such as *Pichia*. Immunocytochemistry has demonstrated that the coat of filasomes contains actin in both *M. grisea* (**D**) and *P. pastoris* (**E**). In addition to filasomes the plasma membrane of yeast such as *Pichia* exhibits intriguing invaginations (**F**) that, superficially, resemble caveoli found in animal cells. **G** Sections tangential to the plasma membrane suggest that these invaginations may be more elongated and less strictly tubular. All specimens were prepared by freeze substitution. *cw* Cell wall. *Bars* 250 nm, except **A** (500 nm) and **B**, **F** (100 nm)

the *Yup 1* gene resulted in alterations in both cell morphology and cell wall deposition.

Another component of the endocytic pathway frequently observed in filamentous fungi is **multivesicular bodies** (MVBs). These are thought to represent an intermediary structure in the pathway between early and late endosomes (Pichler and Riezman 2004). MVBs are a common feature of the fungal cell, often associated with spindle pole bodies (Hoch and Staples 1983a; Swann and Mims 1991), sometimes appearing in high numbers prominently interspersed with astral microtubules during mitosis (O'Donnell 1994; Lü and McLaughlin 1995), and among secretory vesicles in cytoplasmic channels in *Gilbertella persicaria* (Fig. 1.6A) where they likely undergo bidirectional movement (R.J. Howard, unpublished data).

Fungal vacuoles are highly motile pleiomorphic structures and are thought to have several functions. They are involved with storage of cations and metabolites, serve as a regulator of cytosolic pH and for ion homeostasis and as a lytic compartment containing various hydrolytic enzymes (Klionsky et al. 1990). In plants, vacuoles can act both as a protein storage and lytic compartment. These two functional types of vacuole can be differentiated by the association of different sets of tonoplast intrinsic proteins (Johnson et al. 1989; Jauh et al. 1998; Reisen et al. 2003) and can be found within the same cell (Paris et al. 1996), suggesting that there is more than one mechanism to sort tonoplast-associated proteins (Brandizzi et al. 2004). Fungi are not known to store proteins in this way, and generally utilize trehalose, glycogen and lipids as reserves. Glycogen and lipids are found commonly in non-apical regions of hyphae and in spores, where they can be distinguished easily by electron microscopy. Fungal vacuoles have been visualized using carboxyfluorescein and related dyes (Stewart and Deacon 1995; Cole et al. 2000; Read and Hickey 2001), and tubular vacuoles have been shown to contain ConA-binding sites (Fig. 1.6B; Bourett et al. 1993). Fungal vacuoles are discussed in greater detail by Ashford and Allaway (Chap. 2 in this volume).

In animal systems, enzymes destined for the lytic lysosomal compartment are generally sorted in the trans-Golgi network with the aid of mannose-6-phosphate receptors, where they are packaged into clathrin-containing vesicles for delivery to the late endosome (Kornfeld 1990). Fungi do not utilize mannose-6-phosphate tags. At least in certain animal cell types, there is evidence to suggest that other mechanisms may exist to

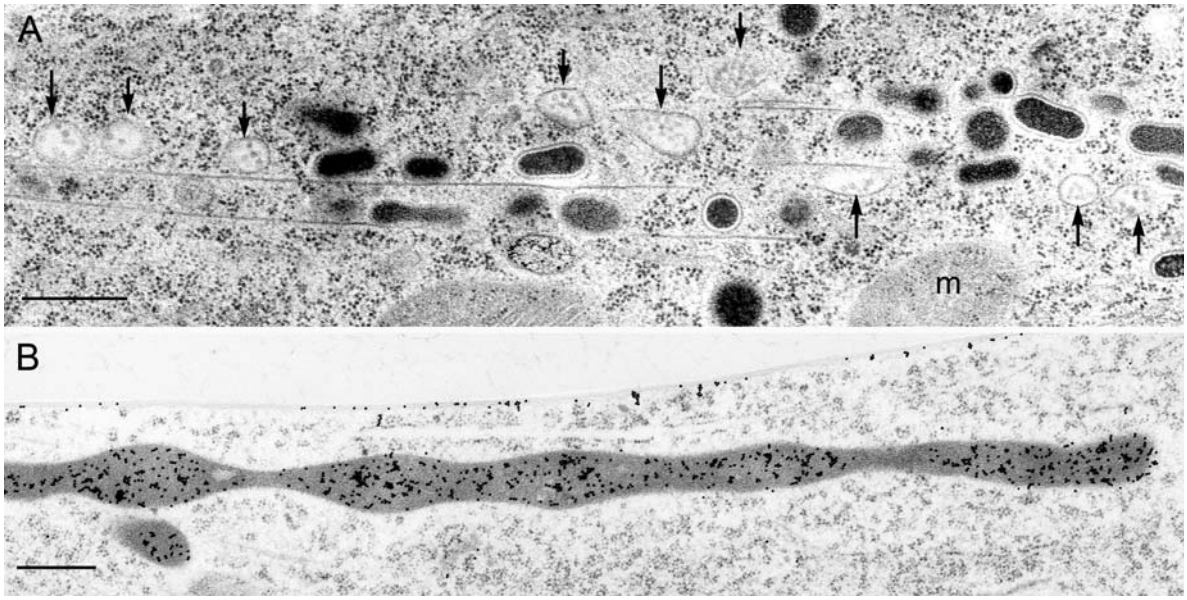

Fig. 1.6. Vacuoles and multivesicular bodies. **A** Multivesicular bodies are thought to be intermediate compartments between early and late endosomes and can be very abundant in hyphae (*arrows*) as illustrated here in *Gilbertella persicaria*. They are interspersed with microtubules and vesicles that exhibit bidirectional movement. **B** Fungal vacuoles are an assemblage of pleiomorphic entities that can exist as elongated tubular structures with Con A binding sites as illustrated here in *Magnaporthe grisea*. Specimens prepared by freeze substitution. *m* Mitochondrion. *Bars* 500 nm

target these enzymes to lysosomes (Lamaze and Schmid 1995) and perhaps these are utilized by fungi. *A. nidulans* and other fungi possess two genes with weak homology with *S. cerevisiae* MRL1 and YOS9 (Table 1.6). The *S. cerevisiae* genes appear to be distantly related to mammalian mannose-6-phosphate receptors. The *A. nidulans* genes show similarly weak homology with human M6PR and a YOS9 relative, and thus this pair of genes appears to be poorly conserved between ascomycetous yeasts, other fungi, and animals. We surveyed the large and varied complex of genes involved in post-Golgi vacuolar and endosomal sorting, endocytosis, and secretion (reviewed by Bowers and Stevens 2005). As shown in Table 1.6, the great majority of *S. cerevisiae* genes are conserved in other fungi, with little loss or expansion. These include all components of the HOPS, GARP, and exocyst vesicle-tethering complexes discussed above. Nearly all components of the four endosomal sorting complexes required for transport (ESCRT) complexes are conserved. These complexes are responsible for sorting ubiquitinated cargo proteins at the MVB. Also conserved are the accompanying components for protein ubiquitination, de-ubiquitination (RSP5, BRO1, DOA4), and synthesis of phosphatidylinositol 3-phosphate (PI3P) for recruitment and tethering of ESCRT-0 (VPS15, VPS34). Only two *S. cerevisiae* genes in this group appear to have expanded in other fungi. First, *S. cerevisiae* VPS62, a protein of unknown function that is involved in targeting cytoplasmic proteins to the vacuole, is related to two *A. nidulans* genes (Table 1.6). Neither of the *A. nidulans* genes is conserved in humans. Second, *A. nidulans* and other fungi possess two conserved homologs of an *S. cerevisiae* transmembrane protein, EMP70, the function of which is not known. These *A. nidulans* genes are strongly related to human transmembrane 9 superfamily protein member-4 and -2. Little is known about the cellular role of the human genes (Colland et al. 2004).

V. Enigmatic Compartments

Blocking the secretory pathway can lead not only to accumulation of the secretion products but also to cellular structures that may be very transient or absent in untreated cells. For example, Brefeldin A treatment of *Magnaporthe grisea* hyphae led to the accumulation of membrane-bounded structures of unusual morphology (Fig. 1.7A) that share

features with the septal pore cap found in basidiomycetes (Müller et al. 1998). Likewise, very similar structures were observed in infection hyphae of *M. grisea* produced *in planta* within infected leaves (Fig. 1.7B). The appearance of these structures may reflect structural changes in these highly metabolically specialized cells compared with the necrotrophic vegetative hyphae.

In transforming filamentous fungi with constructs designed for cytosolic expression of reef coral fluorescent proteins (Bourett et al. 2002), several transformants were discovered to sequester fluorescent proteins into a heretofore unreported subcellular compartment (Fig. 1.7C). These peripheral bodies seemed to underlie the plasma membrane, were highly flattened, often fenestrated, relatively static, and in greater numbers in distal cells relative to the apical cell. The latter is perhaps a reflection of the slow maturation of the reef coral fluorescent proteins and that there was no mature fluorescent protein in the apical cell. Similar compartments were also labeled when the reef coral fluorescent protein ZsGreen was targeted for either secretion or for retention in the ER (Bourett et al., unpublished data). However, in these transformants tubular entities were sometimes labeled in the subapical region of the apical cells (Czymmek et al. 2005).

VI. Conclusions

The Kingdom Fungi comprises perhaps 20% of the biodiversity on planet earth. As a taxonomic

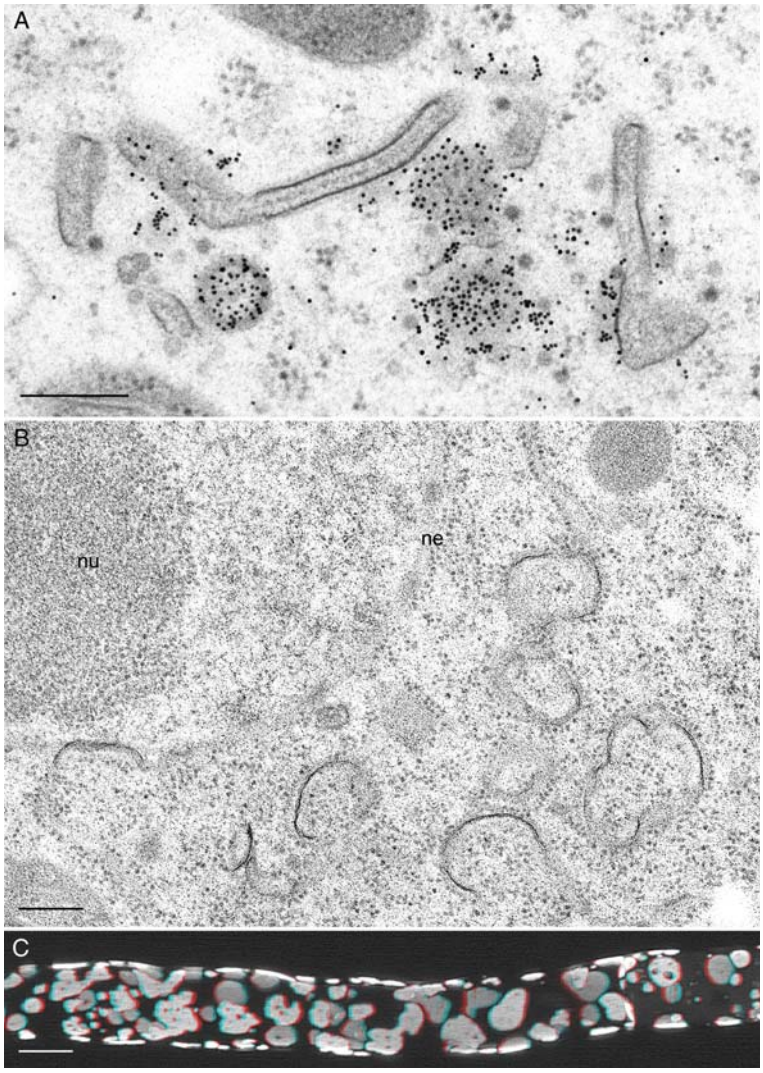

Fig. 1.7. Enigmatic compartments. **A** Unusual membrane-bounded organelles, lacking Con A binding sites (note gold markers), observed in *Magnaporthe grisea* only after brefeldin A treatment. **B** A similar compartment previously undescribed in vegetative hyphae was found to be prominent in *M. grisea* infection hyphae produced *in planta*. Note ribosomes associated with the surface of these structures. **C** Confocal light micrograph stereo rendering illustrating a fenestrated, flattened peripheral compartment observed in non-apical cells of a particular *Colletotrichum graminicola* transformant when the destabilized reef coral fluorescent protein ZsGreen was expressed in the cytosol. **A**, **B** Transmission electron microscope images from specimens prepared by freeze substitution. *ne* Nuclear envelope, *nu* nucleolus. *Bars* 250 nm. **C** Laser scanning confocal image of live specimen (red/green stereo anaglyph). *Bar* 5.0 μm

group they exhibit a number of subcellular traits which, as we have discussed, represent both distinguishing and enigmatic characteristics. The cellular processes by which these organisms acquire, process and utilize resources from their [our] environment for growth are of obvious significance. Yet, we have an incomplete understanding of the basics of the fungal endomembrane system. Many questions remain. By what primary mechanism does endocytosis occur? What is the nature and role of filasomes and are they present in all fungi? Why has the ultrastructure of endosomal compartments been so poorly characterized, and do these compartments function in receptor reuptake? What constitutes the Golgi? Why are there no stacks of Golgi cisternae? How does the fungal cell regulate and process secretory products? Why are Golgi cisternae so closely juxtaposed with mitochondria, and how is that association maintained? What is the relationship of the three dimensional organization of the endomembrane system to hyphal tip growth? Where on the cell surface does endocytosis take place?

Several hypotheses have been presented that require testing. For example, it has been suggested that the stack-less Golgi of *S. cerevisiae*, and presumably that of filamentous fungi and other "primitive eukaryotes," may represent a stage in the evolution of Golgi bodies which is followed by stacking, adhesion between the stacks via matrix proteins, and aggregation into a single peri-nuclear entity as seen in animal cells (Képes 2002). Additionally, some of the mysteries of the fungal endomembrane system may be shrouded by the transient nature of some of its components – perhaps a function of the metabolic state of the cell and, as we have mentioned, the manner in which cells are prepared for ultrastructural analysis.

Fungi are among the most tractable organisms for genetic manipulation and have proven to be very useful candidates to study a range of cell biology questions. In practical terms the ease by which they can be genetically engineered makes them ideally suited to approaches utilizing fluorescent protein fusions. Among the fluorescent probes that should be developed include those targeted to all compartments of the endomembrane system to allow further characterization and experimentation in live cells. There is a pressing need to develop such probes for the Golgi apparatus in particular, since this compartment is both enigmatic and arguably of centralmost importance. The molecular bioinformatics data included in Tables 1.1–1.6 are provided to aid in the design of such compartment-specific probes.

The role of clathrin in vesicle trafficking remains unresolved. Despite the presence of a highly conserved clathrin heavy-chain gene and the added discovery of novel fungal homologs of ARF6 GTPase and ARF-GAP for ARF6, clathrin-coated vesicles appear to be lacking in filamentous fungi (Fischer-Parton et al. 2000). In mammals ARF6 and ARF-GAP for ARF6 are known to regulate clathrin-mediated endocytosis, and these functions appear to be missing from the ascomycetous yeasts. We are left to ask very basic questions. By what molecular mechanism does endocytosis occur, and what about vesicle genesis from the trans-Golgi network? What constitutes the trans-Golgi network in fungi?

With the complete sequencing of the genome of numerous fungi and with it the ability to identify fungal homologues for many of the key genes in the endomembrane system of other eukaryotes, the next several years should prove to be a very exciting time for fungal cell biology. A complete understanding will demand the integration of genetic, molecular and structural approaches. Based on recent findings from the plant kingdom one might expect substantial overlap, but also many surprises. In this review, for example, it was demonstrated that, although the conservation of endomembrane components between *S. cerevisiae* and other fungi is considerable, a variety of intriguing expansions have occurred in the filamentous fungi and a basidiomycetous yeast. In most cases, these expansions are conserved in animals, although some appear to be specific to the group of fungi surveyed herein. In particular, fungal-specific expansions have occurred in proteins that likely function in retention of HDEL motif-containing ER proteins – in ER sterol biosynthesis; in the ARF and RAB GTPase families, with corresponding expansions of the associated GAP and GEF and YOP/RTN components, in a Golgi chloride channel, in vacuolar sorting and endosomal membrane components, in an endophilin, and in the dynamin GTPases, where a surprising array of six novel dynamin-related proteins was uncovered. Many of these novel, expanded components appear to have human counterparts, which in several cases have been implicated in heritable or acquired diseases. A better understanding of the fungal endomembrane system may well inform us about similar processes in more complex eukaryotes.

Note Since preparation of this chapter several additional fungi, including *Fusarium graminearum* and *Ustilago maydis*, have been added to the Broad Institute multi-fungi BLAST database.

Acknowledgements. We are grateful to Chris Hawes (Oxford Brookes University) for encouraging the undertaking of writing this chapter through his inspired work on the plant endomembrane system and for guidance during our initial bioinformatics queries and manuscript preparation. We also thank Jim Sweigard (Dupont) and Kirk Czymmek (University of Delaware) for enjoyable and fruitful collaborations and suggestions for the manuscript, and Kerry O'Donnell (USDA-ARS Peoria) for supplying the embedment of *Helicobasidium mompa* used to generate images in Fig. 1.3. We thank Martina Trovato, Gettysburg College student, for assistance in identifying *Aspergillus* SNARE family members.

References

Andag U, Schmitt HD (2003) Dsl1p, an essential component of the Golgi-endoplasmic reticulum retrieval system in yeast, uses the same sequence motif to interact with different subunits of the COPI vesicle coat. J Biol Chem 278:51722–51734

Atkinson HA, Daniels A, Read ND (2002) Live-cell imaging of endocytosis during conidial germination in the rice blast fungus, *Magnaporthe grisea*. Fungal Genet Biol 37:233–244

Ayscough K, Hajibagheri NMA, Watson R, Warren G (1993) Stacking of Golgi cisternae in *Schizosaccharomyces pombe* requires intact microtubules. J Cell Sci 106:1227–1237

Baba M, Osumi M (1987) Transmission and scanning electron microscopic examination of intracellular organelles in freeze-substituted *Kloeckera* and *Saccharomyces cerevisiae* yeast cells. J Electr Microsc Technique 5:249–261

Bachem U, Mendgen K (1995) Endoplasmic reticulum subcompartments in a plant parasitic fungus and in baker's yeast: differential distribution of lumenal proteins. Exp Mycol 19:137–152

Bagshaw RD, Callahan JW, Mahuran DJ (2006) The Arf-family protein, Arl8b, is involved in the spatial distribution of lysosomes. Biochem Biophys Res Commun 344:1186–1191

Becker B, Melkonian M (1996) The secretory pathway of protists: spatial and functional organization and evolution. Microbiol Rev 60:697–721

Bhattacharya R, Kang-Decker N, Hughes DA, Mukherjee P, Shah V, McNiven MA, Mukhopadhyay D (2005) Regulatory role of dynamin-2 in VEGFR-2/KDR- mediated endothelial signaling. FASEB J 19:1692–1694

Bitoun M, Maugenre S, Jeannet P-Y, Lacène E, Ferrer X, Laforêt P, Martin J-J, Laporte J, Lochmüller H, Beggs AH, Fardeau M, Eymard B, Romero NB, Guicheney P (2005) Mutations in dynamin 2 cause dominant centronuclear myopathy. Nat Genet 37:1207–1209

Blobel G (1980) Intracellular protein topogenesis. Proc Natl Acad Sci USA 77:1496–1500

Bock JB, Matern HT, Peden AA, Scheller RH (2001) A genomic perspective on membrane compartment organization. Nature 409:839–841

Boevink P, Oparka K, Santa Cruz S, Martin B, Betteridge A, Hawes C (1998) Stacks on tracks: the plant Golgi apparatus traffics on an actin/ER network. Plant J 15:441–447

Bonfante P, Balestrini R, Mendgen K (1994) Storage and secretion processes in the spore of *Gigaspora margarita* Becker & Hall as revealed by high-pressure freezing and freeze substitution. New Phytol 128:93–101

Borkovich KA, Alex LA, Yarden O, Freitag M, Turner GE, Read ND et al. (2004) Lessons from the genome sequence of *Neurospora crassa*: tracing the path from genomic blueprint to multicellular organism. Microbiol Mol Biol Rev 68:1–108

Bourett TM, Howard RJ (1991) Ultrastructural immunolocalization of actin in a fungus. Protoplasma 163:199–202

Bourett TM, Howard RJ (1994) Enhanced labelling of concanavalin A binding sites in fungal endomembranes using a double-sided, indirect method. Mycol Res 98:769–775

Bourett TM, Howard RJ (1996) Brefeldin A-induced structural changes in the endomembrane system of a filamentous fungus, *Magnaporthe grisea*. Protoplasma 190:151–163

Bourett TM, Picollelli MA, Howard RJ (1993) Post embedment labeling of intracellular concanavalin A-binding sites in freeze-substituted fungal cells. Exp Mycol 17:223–235

Bourett TM, Czymmek KJ, Howard RJ (1998) An improved method for affinity probe localization in whole cells of filamentous fungi. Fungal Genet Biol 24:3–13

Bourett TM, Sweigard JA, Czymmek KJ, Carroll A, Howard RJ (2002) Reef coral fluorescent proteins for visualizing fungal pathogens. Fungal Genet Biol 37:211–220

Bowers K, Stevens TH (2005) Protein transport from the late Golgi to the vacuole in the yeast *Saccharomyces cerevisiae*. Biochim Biophys Acta 1744:438–454

Bracker CE (1967) Ultrastructure of fungi. Annu Rev Phytopathol 5:343–374

Bracker CE (1974) The endomembrane system of fungi. Eighth Intl Congr Electron Microsc 2:558–559

Bracker CE, Butler EE (1964) Function of the septal pore apparatus in *Rhizoctonia solani* during protoplasmic streaming. J Cell Biol 21:152–157

Bracker CE, Grove SN (1971) Continuity between cytoplasmic endomembranes and outer mitochondrial membranes in fungi. Protoplasma 73:15–34

Bracker CE, Morré DJ, Grove SN (1996) Structure, differentiation, and multiplication of Golgi apparatus in fungal hyphae. Protoplasma 194:250–274

Brandizzi F, Snapp EL, Roberts AG, Lippincott-Schwartz J, Hawes C (2002) Membrane protein transport between the endoplasmic reticulum and the Golgi in tobacco leaves is energy dependent but cytoskeleton independent: evidence from selective photobleaching. Plant Cell 14:1293–1309

Brandizzi F, Irons SL, Johansen J, Kotzer A, Neumann U (2004) GFP is the way to glow: bioimaging of the plant endomembrane system. J Microsc 214:138–158

Bredeston LM, Caffaro CE, Samuelson J, Hirschberg CB (2005) Golgi and endoplasmic reticulum functions take place in different subcellular compartments of *Entamoeba histolytica*. J Biol Chem 280:32168–32176

Buehler LK, Rashidi HH (eds) (2005) Bioinformatics basics: applications in biological science and medicine, 2nd edn. Taylor and Francis, Boca Raton

Burri L, Lithgow T (2004) A complete set of SNAREs in yeast. Traffic 5:45–52

Cabral CM, Liu Y, Sifers RN (2001) Dissecting glycoprotein quality control in the secretory pathway. Trends Biochem Sci 26:619–624

Caesar-Ton That TC, Hoang-Van K, Turian G, Hoch HC (1987) Isolation and characterization of coated vesicles from filamentous fungi. Eur J Cell Biol 43:189–194

Clark AJ, Metherell LA, Cheetham ME, Huebner A (2005) Inherited ACTH insensitivity illuminates the mechanisms of ACTH action. Trends Endocrinol Metabol 16:451–457

Claverie J-M, Notredame C (2003) Bioinformatics for dummies. Wiley, New York

Colanzi A, Suetterlin C, Malhotra V (2003) Cell-cycle-specific Golgi fragmentation: how and why? Curr Opin Cell Biol 15:1–6

Cole L, Davies D, Hyde GJ, Ashford AE (2000) ER-Tracker dye and BODIPY-brefeldin A differentiate the endoplasmic reticulum and Golgi bodies from the tubular-vacuole system in living hyphae of *Pisolithus tinctorius*. J Microsc 197:239–248

Colland F, Jacq X, Trouplin V, Mougin C, Groizeleau C, Hamburger A, Meil A, Wojcik J, Legrain P, Gauthier J-M (2004) Functional proteomics mapping of a human signaling pathway. Genome Res 14:1324–1332

Collinge AJ, Trinci APJ (1974) Hyphal tips of wild-type and spreading colonial mutants of *Neurospora crassa*. Arch Microbiol 99:353–368

Colot HV, Park G, Turner GE, Ringelberg C, Crew CM, Litvinkova L, Weiss RL, Borkovich KA, Dunlap JC (2006) A high-throughput gene knockout procedure for *Neurospora* reveals functions for multiple transcription factors. Proc Natl Acad Sci USA 103:10352–10357

Conesa A, Punt PJ, van Luijk N, van den Hondel CAMJJ (2001) The secretion pathway in filamentous fungi: a biotechnological view. Fungal Genet Biol 33:155–171

Cormack B (1998) Green fluorescent protein as a reporter of transcription and protein localization in fungi. Curr Opin Microbiol 1:406–410

Corthésy-Theulaz I, Pauloin A, Pfeffer SR (1992) Cytoplasmic dynein participates in the centrosomal localization of the Golgi complex. J Cell Biol 118:1333–1345

Czymmek KJ (2005) Exploring fungal activity with confocal and multiphoton microscopy. In: Dighton J, Wicklow DT (eds) The fungal community. Dekker, New York, pp 307–329

Czymmek KJ, Bourett TM, Howard RJ (1996) Immunolocalization of tubulin and actin in thick-sectioned fungal hyphae after freeze-substitution fixation and methacrylate de-embedment. J Microsc 181:153–161

Czymmek KJ, Bourett TM, Howard RJ (2005) Fluorescent protein probes in fungi. Methods Microbiol 34:27–62

Dacks JB, Field MC (2004) Eukaryotic cell evolution from a comparative genomic perspective: the endomembrane system. Syst Assoc 68:309–334

Damm E-M, Pelkmans L, Kartenbeck J, Mezzacasa A, Kurzchalia T, Helenius A (2005) Clathrin- and caveolin-1*t*independent endocytosis: entry of simian virus 40 into cells devoid of caveolae. J Cell Biol 168:477–488

Donohoe BS, Mogelsvang S, Staehelin LA (2006) Electron tomography of ER, Golgi and related membrane systems. Methods 39:154–162

Doyle T, Botstein D (1996) Movement of yeast cortical actin cytoskeleton visualized in vivo. Proc Natl Acad Sci USA 93:3886–3891

Driouich A, Faye L, Staehelin LA (1993) The plant Golgi apparatus: a factory for complex polysaccharides and glycoproteins. Trends Biochem Sci 18:210–214

Dunphy WG, Rothman JE (1985) Compartmental organization of the Golgi stack. Cell 42:13–21

Esters H, Alexandrov K, Iakovenko A, Ivanova T, Thoma N, Rybin V, Zerial M, Scheidig AJ, Goody RS (2001) Vps9, Rabex-5 and DSS4: proteins with weak but distinct nucleotide-exchange activities for Rab proteins. J Mol Biol 310:141–156

Estrada de Martin P, Novick P, Ferro-Novick S (2005) The organization, structure, and inheritance of the ER in higher and lower eukaryotes. Biochem Cell Biol 83:752–761

Fernández-Ábalos JM, Fox H, Pitt C, Wells B, Doonan JH (1998) Plant-adapted green fluorescent protein is a versatile vital reporter for gene expression, protein localization and mitosis in the filamentous fungus, *Aspergillus nidulans*. Mol Microbiol 27:121–130

Firestein R, Cleary ML (2001) Pseudo-phosphatase Sbf1 contains an N-terminal GEF homology domain that modulates its growth regulatory properties. J Cell Sci 114:2921–2927

Fischer-Parton S, Parton RM, Hickey PC, Dijksterhuis J, Atkinson HA, Read ND (2000) Confocal microscopy of FM4-64 as a tool for analysing endocytosis and vesicle trafficking in living fungal hyphae. J Microsc 198: 246–259

Geli MI, Riezman H (1998) Endocytic internalization in yeast and animal cells: similar and different. J Cell Sci 111:1031–1037

Geng J, Shin MF, Gilbert PM, Collins RN, Burd CG (2005) *Saccharomyces cerevisae* Rab-GDI displacement factor ortholog Yip3p forms distinct complexes with the Ypt1 Rab GTPase and the reticulon Rtn1p. Eukaryot Cell 4:1166–1174

Gilbert MJ, Thornton CR, Wakley GE, Talbot NJ (2006) A P-type ATPase required for rice blast disease and induction of host resistance. Nature 440:535–539

Gilli F, Marnetto F, Caldano M, Sala A, Malucchi S, Capobianco M, Bertolotto A (2006) Biological markers of interferon-beta therapy: comparison among interferon-stimulated genes MxA, TRAIL and XAF-1. Mult Scler 12:47–57

Girbardt M (1969) Die Ultrastruktur der Apikalregion von Pilzhyphen. Protoplasma 67:413–441

Glick BS (2000) Organization of the Golgi apparatus. Curr Opin Cell Biol 12:450–456

Gordon CL, Archer DB, Jeenes JH, Doonan JH, Wells B, Trinci APJ, Robson GD (2000) A glucoamylase::GFP gene fusion to study protein secretion by individual hyphae of *Aspergillus niger*. J Microbiol Methods 42:39–48

Gorska MM, Cen O, Liang Q, Stafford SJ, Alam R (2006) Differential regulation of interleukin 5-stimulated signaling pathways by dynamin. J Biol Chem 281:14429–14439

Grove SN, Bracker CE (1970) Protoplasmic organization of hyphal tips among fungi: vesicles and Spitzenkörper. J Bacteriol 104:989–1009

Gupta GD, Heath IB (2002) Predicting the distribution, conservation, and functions of SNAREs and related proteins in fungi. Fungal Genet Biol 36:1–21

Hamilton SR, Bobrowicz P, Bobrowicz B, Davidson RC, Li H, Mitchell T, Nett JH, Rausch S, Stadheim TA, Wischnewski H, Wildt S, Gerngross TU (2003) Production of complex human glycoproteins in yeast. Science 301:1244–1246

Hanson MR, Köhler RH (2001) GFP imaging: methodology and application to investigate cellular compartmentation in plants. J Exp Bot 52:529–539

Harada A, Takei Y, Kanai Y, Tanaka Y, Nonaka S, Hirokawa N (1998) Golgi vesiculation and lysosome dispersion in cells lacking cytoplasmic dynein. J Cell Biol 141:51–59

Harris SD, Read ND, Roberson RW, Shaw B, Seiler S, Plamann M, Momany M (2005) Polarisome meets Spitzenkörper: microscopy, genetics, and genomics converge. Eukaryot Cell 4:225–229

Hawes C, Satiat-Jeunemaitre B (2005) The plant Golgi apparatus – going with the flow. Biochim Biophys Acta 1744:93–107

Hawes C, Saint-Jore CM, Brandizzi F, Zheng H, Andreeva AV, Boevink P (2001) Cytoplasmic illuminations: in planta targeting of fluorescent proteins to cellular organelles. Protoplasma 215:77–88

Heath IB, Greenwood AD (1970) The structure and formation of lomasomes. J Gen Microbiol 62:129–137

Hehl AB, Marti M (2004) Secretory protein trafficking in *Giardia intestinalis*. Mol Microbiol 53:19–28

Higuchi Y, Nakahama T, Shoji J-y, Arioka M, Kitamoto K (2006) Visualization of the endocytic pathway in the filamentous fungus *Aspergillus oryzae* using an EGFP-fused plasma membrane protein. Biochem Biophys Res Commun 340:784–791

Hirose H, Arasaki K, Dohmae N, Takio K, Hatsuzawa K, Nagahama M, Tani K, Yamamoto A, Tohyama M, Tagaya M (2004) Implication of ZW10 in membrane trafficking between the endoplasmic reticulum and Golgi. EMBO J 23:1267–1278

Hoch HC, Howard RJ (1980) Ultrastructure of freeze-substituted hyphae of the basidiomycete *Laetisaria arvalis*. Protoplasma 103:281–297

Hoch HC, Staples RC (1983a) Ultrastructural organization of the non-differentiated uredospore germling of *Uromyces phaseoli* variety *typica*. Mycologia 75:795–824

Hoch HC, Staples RC (1983b) Visualization of actin in situ by rhodamine-conjugated phalloin in the fungus *Uromyces phaseoli*. Eur J Cell Biol 32:52–58

Hoffmann J, Mendgen K (1998) Endocytosis and membrane turnover in the germ tube of *Uromyces fabae*. Fungal Genet Biol 24:77–85

Howard RJ (1980) An ultrastructural analysis of hyphal tip growth. PhD thesis, Cornell University, Ithaca

Howard RJ (1981) Ultrastructural analysis of hyphal tip cell growth in fungi: Spitzenkörper, cytoskeleton and endomembranes after freeze-substitution. J Cell Sci 48:89–103

Howard RJ (1997) Breaching the outer barrier cuticle and cell wall penetration. In: Carroll GC, Tudzynski P (eds) The Mycota, vol V, part A. Plant relationships. Springer, Berlin Heidelberg New York, pp 43–60

Howard RJ, Aist JR (1979) Hyphal tip cell ultrastructure of the fungus *Fusarium*: improved preservation by freeze-substitution. J Ultrastuct Res 66:224–234

James SW, Bullock KA, Gygax SE, Kraynack BA, Matura RA, MacLeod JA, McNeal KK, Prasauckas KA, Scacheri PC, Shenefiel HL, Tobin HM, Wade SD (1999) *nimO*, an *Aspergillus* gene related to budding yeast *Dbf4*, is required for DNA synthesis and mitotic checkpoint control. J Cell Sci 112:1313–1324

Janoueix-Lerosey I, Jollivet F, Camonis J, Marche PN, Goud B (1995) Two-hybrid system screen with the small GTP-binding protein Rab6. J Biol Chem 270:14801–14808

Jauh G-Y, Fischer AM, Grimes HD, Ryan CA Jr, Rogers JC (1998) δ-Tonoplast intrinsic protein defines unique plant vacuole functions. Proc Natl Acad Sci USA 95:12995–12999

Johnson KD, Herman EM, Chrispeels MJ (1989) An abundant, highly conserved tonoplast protein in seeds. Plant Physiol 91:1006–1013

Kamena F, Spang A (2004) Tip20p prohibits back-fusion of COPII vesicles with the endoplasmic reticulum. Science 304:286–289

Kellis M, Birren BW, Lander ES (2004) Proof and evolutionary analysis of ancient genome duplication in the yeast *Saccharomyces cerevisiae*. Nature 428:617–624

Képès F (2002) Secretory compartments as instances of dynamic self-evolving structures. Acta Biotheor 50:209–221

Képès F, Rambourg A, Satiat-Jeunemaître B (2005) Morphodynamics of the secretory pathway. Int Rev Cytol 242:55–120

Khalaj V, Brookman JL, Robson GD (2001) A study of the protein secretory pathway of *Aspergillus niger* using a glucoamylase–GFP fusion protein. Fungal Genet Biol 32:55–65

Klionsky DJ, Herman PK, Emr SD (1990) The fungal vacuole: composition, function, and biogenesis. Microbiol Rev 54:266–292

König K (2000) Multiphoton microscopy in life sciences. J Microsc 200:83–104

Kornfeld R, Kornfeld S (1985) Assembly of asparagine-linked oligosaccharides. Annu Rev Biochem 54:631–664

Kornfeld S (1990) Lysosomal enzyme targeting. Biochem Soc Trans 18:367–374

Krappman S, Sasse C, Braus GH (2006) Gene targeting in *Aspergillus fumigatus* by homologous recombination is facilitated in a nonhomologous end-joining-deficient genetic background. Eukaryot Cell 5:212–215

Kraynack BA, Chan A, Rosenthal E, Essid M, Umansky B, Waters MG, Schmitt HD (2005) Dsl1p, Tip20p, and the novel Dsl3(Sec39) protein are required for the stability of the Q/t-SNARE complex at the endoplasmic reticulum in yeast. Mol Biol Cell 16:3963–3977

Ladinsky MS, Mastronarde DN, McIntosh JR, Howell KE, Staehelin LA (1999) Golgi structure in three dimensions: functional insights from the normal rat kidney cell. J Cell Biol 144:1135–1149

Lamaze C, Schmid SL (1995) The emergence of a clathrin-independent pinocytic pathways. Curr Opin Cell Biol 7:573–580

Lanzetti L, Palamidessi A, Areces L, Scita G, Di Fiore PP (2004) Rab5 is a signalling GTPase involved in actin remodelling by receptor tyrosine kinases. Nature 429:309–314

Latijnhouwers M, Hawes C, Carvalho C (2005) Holding it all together? Candidate proteins for the plant Golgi matrix. Curr Opin Plant Biol 8:632–639

Levivier E, Goud B, Souchet M, Calmels TP, Mornon JP, Callebaut I (2001) uDENN, DENN, and dDENN: indissociable domains in Rab and MAP kinases signaling pathways. Biochem Biophys Res Commun 287:688–695

Lichtscheidl IK, Hepler PK (1996) Endoplasmic reticulum in the cortex of plant cells. In: Smallwood M, Knox JP, Bowles DJ (eds) Membranes: specialized functions in plants. BIOS, Abington, pp 337–365

Lippincott-Schwartz J, Yuan LC, Bonifacino JS, Klausner, RD (1989) Rapid redistribution of Goligi proteins into the ER in cells treated with brefeldin A: evidence for membrane cycling from Golgi to ER. Cell 56:801–813

López-Franco R, Howard RJ, Bracker CE (1995) Satellite Spitzenkörper in growing hyphal tips. Protoplasma 188:85–103

Lorang JM, Tuori RP, Martinez JP, Sawyer TL, Redman RS, Rollins JA, Wolpert TJ, Johnson KB, Rodriguez RJ, Dickman MB, Ciuffetti LM (2001) Green fluorescent protein is lighting up fungal biology. Appl Environ Microbiol 67:1987–1994

Lü H, McLaughlin DJ (1995) A light and electron microscopic study of mitosis in the clamp connection of *Auricularia auricular-judae*. Can J Bot 73:315–332

Lucocq JM, Pryde JG, Berger EG, Warren G (1987) A mitotic form of the Golgi apparatus in HeLa cells. J Cell Biol 104:865–874

Maras M, Die I van, Contreras R, Hondel CA van den (1999) Filamentous fungi as production organisms for glycoproteins of biomedical interest. Glycoconj J 16:99–107

Maruyama J, Kikuchi S, Kitamoto K (2006) Differential distribution of the endoplasmic reticulum network as visualized by the BipA-EGFP fusion protein in hyphal compartments across the septum of the filamentous fungus, *Aspergillus oryzae*. Fungal Genet Biol 43:642–654

Masai K, Maruyama J, Nakajima H, Kitamoto K (2003) In vivo visualization of the distribution of a secretory protein in *Aspergillus oryzae* hyphae using the Rnt-EGFP fusion protein. Biosci Biotechnol Biochem 67:455–459

McLaughlin DJ (1974) Ultrastructural localization of carbohydrate in the hymenium and subhymenium of *Coprinus*. Evidence for the function of the Golgi apparatus. Protoplasma 82:341–364

McNiven MA, Thompson HM (2006) Vesicle formation at the plasma membrane and trans-Golgi network: the same but different. Science 313:1591–1594

Metzenberg RL (2005) Construction of minimally-sheltered knockout mutants of *Neurospora crassa*. Fungal Genet Newslett 52:11–13

Mims CW, Rodriguez-Lother C, Richardson EA (2002) Ultrastructure of the host-pathogen interface in daylily leaves infected by the rust fungus *Puccinia hemerocallidis*. Protoplasma 219:221–226

Mollenhauer HH, Morré DJ (1991) Perspectives on Golgi apparatus form and function. J Electron Microsc Tech 17:2–14

Money NP (1990) Measurement of pore size in the hyphal cell wall of *Achlya bisexualis*. Exp Mycol 14:234–242

Mulholland J, Preuss D, Moon A, Wong A, Drubin D, Botstein D (1994) Ultrastructure of the yeast actin cytoskeleton and its association with the plasma membrane. J Cell Biol 125:381–391

Müller WH, Montijn RC, Humbel BM, van Aelst AC, Boon EJMC, van der Krift TP, Boekhout T (1998) Structural differences between two types of basidiomycete septal pore caps. Microbiology 144:1721–1730

Müller WH, Koster AJ, Humbel BM, Ziese U, Verkleij AJ, van Aelst AC, van der Krift TP, Montijn RC, Boekhout T (2000) Automated electron tomography of the septal pore cap in *Rhizoctonia solani*. J Struct Biol 131:10–18

Munro S (1998) Localization of proteins to the Golgi apparatus. Trends Cell Biol 8:11–15

Murph MM, Scaccia LA, Volpicelli LA, Radhakrishna H (2003) Agonist-induced endocytosis of lysophosphatidic acid-coupled LPA_1/EDG-2 receptors via a dynamin2- and Rab5-dependent pathway. J Cell Sci 116:1969–1980

Natter K, Leitner P, Faschinger A, Wolinski H, McCraith S, Fields S, Kohlwein SD (2005) The spatial organization of lipid synthesis in the yeast *Saccharomyces cerevisiae* derived from large scale green fluorescent protein tagging and high resolution microscopy. Mol Cell Proteomics 4:662–672

Nayak T, Szewczyk E, Oakley CE, Osmani A, Ukil L, Murray SL, Hynes MJ, Osmani SA, Oakley BR (2006) A versatile and efficient gene-targeting system for *Aspergillus nidulans*. Genetics 172:1557–1566

Nebenführ A, Gallagher LA, Dunahay TG, Frohlick, JA, Mazurkiewicz AM, Meehl JB, Staehelin LA (1999) Stop-and-go movements of plant Golgi stacks are mediated by the acto-myosin system. Plant Physiol 121:1127–1142

Neuwald AF (1997) A shared domain between a spindle assembly checkpoint protein and Ypt/Rab-specific GTPase-activators. Trends Biochem Sci 22:243–244

Newhouse JR, Hoch HC, MacDonald WL (1983) The ultrastructure of *Endothia parasitica*. Comparison of a virulent and a hypovirulent isolate. Can J Bot 61:389–399

Ninomiya Y, Suzuki K, Ishii C, Inoue H (2004) Highly efficient gene replacements in *Neurospora crassa* strains deficient for non-homologous end-joining. Proc Natl Acad Sci USA 101:12248–12253

Numajiri A, Mibayashi M, Nagata K (2006) Stimulus-dependent and domain-dependent cell death acceleration by an IFN-inducible protein, human MxA. J Interferon Cytokine Res 26:214–219

O'Donnell K (1994) A reevaluation of the mitotic spindle pole body cycle in *Tilletia caries* based on freeze-substitution techniques. Can J Bot 72:1412–1423

O'Toole ET, Winey M, McIntosh JR (1999) High-voltage electron tomography of spindle pole bodies and early mitotic spindles in the yeast *Saccharomyces cerevisiae*. Mol Biol Cell 10:2017–2031

Paleotti O, Macia E, Luton F, Klein S, Partisani M, Chardin P, Kirchhausen T, Franco M (2005) The small G-protein $Arf6_{GTP}$ recruits the AP-2 adaptor complex to membranes. J Biol Chem 280:21661–21666

Paris N, Stanley CM, Jones RL, Rogers JC (1996) Plant cells contain two functionally distinct vacuolar compartments. Cell 85:563–572

Peltekian C, Gordien E, Garreau F, Meas-Yedid V, Soussan P, Willams V, Chaix ML, Olivo-Marin JC, Brechot C, Kremsdorf D (2005) Human MxA protein participates to the interferon-related inhibition of hepatitis B virus replication in female transgenic mice. J Hepatol 43:965–972

Pereira-Leal JB, Seabra MC (2000) The mammalian Rab family of small GTPases: definition of family and subfamily sequence motifs suggests a mechanism for functional specificity in the Ras superfamily. J Mol Biol 301:1077–1087

Pereira-Leal JB, Seabra MC (2001) Evolution of the Rab family of small GTP-binding proteins. J Mol Biol 313:889–901

Pevsner J (2003) Bioinformatics and functional genomics. Wiley , Hoboken

Pichler H, Riezman H (2004) Where sterols are required for endocytosis. Biochim Biophys Acta 1666:51–61

Preuss D, Mulholland J, Kaiser CA, Orlean P, Albright C, Rose MD, Robbins PW, Botstein D (1991) Structure of the yeast endoplasmic reticulum: localization of ER proteins using immunofluorescence and immunoelectron microscopy. Yeast 7:891–911

Prieschl EE, Pendl GG, Harrer NE, Baumruker T (1996) The murine homolog of TB2/DP1, a gene of the familial adenomatous polyposis (FAP) locus. Gene 169:215–218

Proszynski TJ, Klemm RW, Gravert M, Hsu PP, Gloor Y, Wagner J, Kozak K, Grabner H, Walzer K, Bagnat M, Simons K, Walch-Solimena C (2005) A genome-wide visual screen reveals a role for sphingolipids and ergosterol in cell surface delivery in yeast. Proc Natl Acad Sci USA 102:17981–17986

Punt PJ, Seiboth B, Weenink XO, van Zeijl C, Lenders M, Konetschny C, Ram AF, Montijn R, Kubicek CP, van den Hondel CA (2001) Identification and characterization of a family of secretion-related small GTPase-encoding genes from the filamentous fungus *Aspergillus niger*: a putative *SEC4* homologue is not essential for growth. Mol Microbiol 41:513–525

Rambourg A, Clermont Y, Ovtracht L, Képès F (1995) Three-dimensional structure of tubular networks, presumably Golgi in nature, in various yeast strains: a comparative study. Anat Rec 243:283–293

Read ND, Beckett A (1996) Ascus and ascospore morphogenesis. Mycol Res 100:1281–1314

Read ND, Hickey PC (2001) The vesicle trafficking network and tip growth in fungal hyphae. In: Geitmann A, Cresti M, Heath IB (eds) Cell biology of plant and fungal tip growth. IOS, Amsterdam, pp 137–148

Read ND, Kalkman ER (2003) Does endocytosis occurr in fungal hyphae? Fungal Genet Biol 39:199–203

Reisen D, Leborgne-Castel N, Özalp C, Chaumont F, Marty F (2003) Expression of a cauliflower tonoplast aquaporin tagged with GFP in tobacco suspension cells correlates with an increase in cell size. Plant Mol Biol 52:387–400

Renna L, Hanton SL, Stefano G, Bortolotti L, Misra V, Brandizzi F (2005) Identification and characterization of AtCASP, a plant transmembrane Golgi matrix protein. Plant Mol Biol 58:109–122

Roberson RW, Fuller MS (1988) Ultrastructural aspects of the hyphal tip of *Sclerotium rolfsii* preserved by freeze substitution. Protoplasma 146:143–149

Robinson DG (1996) Clathrin-mediated trafficking. Trends Plant Sci 1:349–355

Rossanese OW, Soderholm J, Bevis BJ, Sears IB, O'Connor J, Williamson EK, Glick BS (1999) Golgi structure correlates with transitional endoplasmic reticulum organization in *Pichia pastoris* and *Saccharomyces cerevisiae*. J Cell Biol 145:69–81

Rutherford S, Moore I (2002) The *Arabidopsis* Rab GTPase family: another enigma variation. Curr Opin Plant Biol 5:518–528

Saint-Jore CM, Evins J, Batoko H, Brandizzi F, Moore I, Hawes C (2002) Redistribution of membrane proteins between the Golgi apparatus and endoplasmic reticulum in plants is reversible and not dependent on cytoskeletal networks. Plant J 29:661–678

Saito H, Kubota M, Roberts RW, Chi Q, Matsunami H (2004) RTP family members induce functional expression of mammalian odorant receptors. Cell 119:679–691

Satiat-Jeunemaitre B, Cole L, Bourett T, Howard R, Hawes C (1996) Brefeldin A effects in plant and fungal cells: something new about vesicle trafficking? J Microsc 181:162–177

Schaller M, Borelli C, Korting HC, Hube B (2005) Hydrolytic enzymes as virulence factors of *Candida albicans*. Mycoses 48:365–377

Schekman R (1992) Genetic and biochemical analysis of vesicular traffic in yeast. Curr Opin Cell Biol 4:587–592

Schmidt FR (2004) Recombinant expression systems in the pharmaceutical industry. Appl Microbiol Biotechnol 65:363–372

Schuldiner M, Collins SR, Thompson NJ, Denic V, Bhamidipati A, Punna T, Ihmels J, Andrews B, Boone C, Greenblatt JF, Weissman JS, Krogan NJ (2005) Exploration of the function and organization of the yeast early secretory pathway through an epistatic miniarray profile. Cell 123:366–368

Seemann J, Pypaert M, Taguchi T, Malsam J, Warren G (2002) Partitioning of the matrix fraction of the Golgi apparatus during mitosis in animal cells. Science 295:848–851

Short B, Haas A, Barr FA (2005) Golgins and GTPases, giving identity and structure to the Golgi apparatus. Biochim Biophys Acta 1744:383–395

Shorter J, Warren G (2002) Golgi architecture and inheritance. Annu Rev Cell Dev Biol 18:379–420

Silva Ferreira ME da, Kress MRVZ, Savoldi M, Goldman MHS, Härtl A, Heinekamp T, Brakhage AA, Goldman GH (2006) The *akuB*^{KU80} mutant deficient for nonhomologous end joining is a powerful tool for analyzing pathogenicity in *Aspergillus fumigatus*. Eukaryot Cell 5:207–211

Siriputthaiwan P, Jauneau A, Herbert C, Garcin D, Dumas B (2005) Functional analysis of *CLPT1*, a Rab/GTPase required for protein secretion and pathogenesis in the plant fungal pathogen *Colletotrichum lindemuthianum*. J Cell Sci 118:323–329

Srinivasan S, Vargas MM, Roberson RW (1996) Functional, organizational, and biochemical analysis of actin in hyphal tip cells of *Allomyces macrogynus*. Mycologia 88:57–70

Staehelin LA (1997) The plant ER: a dynamic organelle composed of a large number of discrete functional domains. Plant J 11:1151–1165

Stanier R (1970) Some aspects of the biology of cells and their possible evolutionary significance. In: Charles H, Knight B (eds) Organization and control in prokaryotic and eukaryotic cells. Cambridge University, Cambridge, pp 1–38

Steinberg G, Schliwa M, Lehmler C, Bölker M, Kahmann R, McIntosh JR (1998) Kinesin from the plant pathogenic fungus *Ustilago maydis* is involved in vacuole formation and cytoplasmic migration. J Cell Sci 111:2235–2246

Stewart A, Deacon JW (1995) Vital fluorochromes as tracers for fungal growth studies. Biotech Histochem 70:57–65

Suelmann R, Sievers N, Fischer R (1997) Nuclear traffic in fungal hyphae: in vivo study of nuclear migration and positioning in *Aspergillus nidulans*. Mol Microbiol 25:757–769

Swann EC, Mims CW (1991) Ultrastructure of freeze-substituted appressoria produced by aeciospore germlings of the rust fungus *Arthuriomyces peckianus*. Can J Bot 69:1655–1665

Tanabe K, Torii T, Natsume W, Braesch-Andersen S, Watanabe T, Satake M (2005) A novel GTPase-activating protein for ARF6 directly interacts with clathrin and regulates clathrin-dependent endocytosis. Mol Biol Cell 16:1617–1628

Tang BL, Wang Y, Ong YS, Hong W (2005) COPII and exit from the endoplasmic reticulum. Biochim Biophys Acta 1744:293–303

Terasaki M, Chen LB, Fujiwara K (1986) Microtubules and the endoplasmic reticulum are highly interdependent structures. J Cell Biol 103:1557–1568

Thyberg J, Moskalewski S (1999) Role of microtubules in the organization of the Golgi complex. Exp Cell Res 246:263–279

Voeltz GK, Rolls MM, Rapoport TA (2002) Structural organization of the endoplasmic reticulum. EMBO Rep 3:944–950

Wainright PO, Hinkle G, Sogin ML, Stickel SK (1993) Monophyletic origins of the metazoa: an evolutionary link with fungi. Science 260:340–342

Waring RB, May GS, Morris NR (1989) Characterization of an inducible expression system in *Aspergillus nidulans* using *alcA* and tubulin-encoding genes. Gene 79:119–130

Watanabe R, Riezman H (2004) Differential ER exit in yeast and mammalian cells. Curr Opin Cell Biol 16:350–355

Watson P, Stephens DJ (2005) ER-to-Golgi transport: form and formation of vesicular and tubular carriers. Biochim Biophys Acta 1744:304–315

Weber RWS, Pitt D (2001) Filamentous fungi *t* growth and physiology. In: Khachatourians GG, Arora DK (eds) Applied mycology and biotechnology, vol 1: agriculture and food production. Elsevier, New York, pp 13–54

Wedlich-Söldner R, Bölker M, Kahmann R, Steinberg G (2000) A putative endosomal t-SNARE links exo- and endocytosis in the phytopathogenic fungus *Ustilago maydis*. EMBO J 19:1974–1986

Wedlich-Söldner R, Schulz I, Straube A, Steinberg G (2002) Dynein supports motility of endoplasmic reticulum in the fungus *Ustilago maydis*. Mol Biol Cell 13:965–977

Weissman JT, Plutner H, Balch WE (2001) The mammalian guanine nucleotide exchange factor mSec12 is essential for activation of the Sar1 GTPase directing endoplasmic reticulum export. Traffic 2:465–475

Welter K, Müller M, Mendgen K (1988) The hyphae of *Uromyces appendiculatus* within the leaf tissue after high pressure freezing and freeze substitution. Protoplasma 147:91–99

Whyte JRC, Munro S (2002) Vesicle tethering complexes in membrane traffic. J Cell Sci 115:2627–2637

Winey M, Mamay CL, O'Toole ET, Mastronarde DN, Giddings Jr TH, McDonald KL, McIntosh JR (1995) Three-dimensional ultrastructural analysis of the *Saccharomyces cerevisiae* mitotic spindle. J Cell Biol 129:1601–1615

Wooding S, Pelham HRB (1998) The dynamics of Golgi protein traffic visualized in living yeast cells. Mol Biol Cell 9:2667–2680

Wösten HAB, Moukha SM, Sietsma JH, Wessels JGH (1991) Localization of growth and secretion of proteins in *Aspergillus niger*. J Gen Microbiol 137:2017–2023

Xiang X, Plamann M (2003) Cytoskeleton and motor proteins in filamentous fungi. Curr Opin Microbiol 6:628–633

Yang L, Ukil L, Osmani A, Nahm F, Davies J, De Souza CPC, Dou X, Perez-Balaguer A, Osmani SA (2004) Rapid production of gene replacement constructs and generation of a green fluorescent protein-tagged centromeric marker in *Aspergillus nudulans*. Eukaryot Cell 3:1359–1362

Yu J-H, Hamari Z, Han K-H, Seo J-A, Reyes-Dominguez Y, Scazzocchio C (2004) Double-joint PCR: a PCR-based molecular tool for gene manipulations in filamentous fungi. Fungal Genet Biol 41:973–981

Zerial M, McBride H (2001) Rab proteins as membrane organizers. Nat Rev Mol Cell Biol 2:107–117

Zhang X, He X, Fu X-Y, Chang Z (2006) Varp is a Rab21 guanine nucleotide exchange factor and regulates endosome dynamics. J Cell Sci 119:1053–1062

Zipfel WR, Williams RM, Webb WW (2003) Nonlinear magic: multiphoton microscopy in the biosciences. Nat Biotechnol 21:1369–1377

2 Motile Tubular Vacuole Systems

A.E. Ashford[1], W.G. Allaway[2]

CONTENTS

I. **Introduction** 49
II. **Vacuole Motility** 51
A. Visualisation of Vacuoles in Living Fungal Cells 51
B. Vacuole Probes and Electron Microscopy 55
C. Tubules or Vesicles? The Legacy of Classical Electron Microscopy 56
D. Changes in the Vacuole System with Development and Environment . . . 57
E. Fusion and Fission and the Generation of Tubular Networks; Lessons from Mitochondria 58
F. Mechanisms of Targeted Membrane Fusion 60
III. **Vacuole Motility and the Cytoskeleton** 61
IV. **Vacuolar Content** 64
A. Probing the Content of Individual Vacuoles 64
B. Probes, Vacuole pH and ATPase 67
V. **The Functions of Motile Vacuole Systems** . . 68
A. Transport in Vacuoles along Hyphae . . . 68
B. Vacuoles, Protein Targeting and the Endocytic Pathway 70
C. Vacuole Differentiation 73
D. The Vacuole as a Detoxifying Compartment 74
VI. **Conclusions** 76
References 76

I. Introduction

The tips of actively growing hyphae of mycelial fungi contain an extensive reticulum of motile interconnected tubules and spherical vacuoles. This is best seen in living cells labelled with fluorescent probes and viewed by either fluorescence or confocal microscopy (see Ashford et al. 2001). The system shows a range of morphologies, and the tubules exhibit several types of motility including tip extension and retraction, peristalsis-like motion and movement of varicosities. Tubular vacuoles are not artefacts of fluorochrome loading and can also be demonstrated in unlabelled cells by differential interference contrast microscopy (Hyde and Ashford 1997; Hyde et al. 1997). They do not survive chemical fixation but are preserved by freeze-substitution and are seen in virtually all fungal species that have been freeze-substituted (see Ashford 1998).

Motile tubular vacuole systems have been reported in representatives of all major fungal groups (Rees et al. 1994). They were first demonstrated in Australian isolates of the ectomycorrhizal fungus *Pisolithus tinctorius*[1] (Shepherd et al. 1993a, b) where they have been studied extensively. A similar motile vacuole system has now also been described in *Phanerochaete velutina*, a much faster growing saprotrophic basidiomycete which forms mycelial networks on the forest floor (Watkinson et al. 2005). Confocal microscopy of this fungus has enabled changes in the vacuole system as a whole to be correlated with growth and development, and rates of transfer of content between interconnected vacuole sub-compartments to be measured by fluorescence recovery after photobleaching (FRAP), indicating that the vacuole system is a feasible conduit for long-distance transport (Bebber et al. 2006; Darrah et al. 2006; see Sect. V.A.).

In both *Phanerochaete* and *Pisolithus* the vacuole system in the hyphal tip cells usually occurs as a tubular reticulum with some associated small spherical vacuoles and/or a series of larger, relatively immobile ovoid or spherical vacuoles, often obviously attached to the cell membrane and from which vacuolar tubules extend along microtubule tracks to interact and fuse with other large vacuoles or tubules (Cole et al. 1998; Darrah et al. 2006). The relative abundance of tubular and spherical components, and the motility of the system as a whole, vary according to cell age, position, hyphal growth rate and external conditions (see Sect. II.D.). In tip

[1] School of Biological Earth and Environmental Sciences, The University of New South Wales, Sydney, NSW 2052, Australia
[2] School of Biological Sciences, The University of Sydney, NSW 2006, Australia

[1] ITS data indicate that isolate 055 is *Pisolithus microcarpus* not *P. tinctorius* as was formerly thought (G Hyde pers. comm.).

Biology of the Fungal Cell, 2nd Edition
The Mycota VIII
R.J. Howard and N.A.R. Gow (Eds.)
© Springer-Verlag Berlin Heidelberg 2007

cells of actively growing hyphae a tubular reticulum may predominate or there may be a transition from a branched tubular system to a series of separate ellipsoid/spherical elements in the same cell, as shown in Fig. 2.1.

A different, less obviously motile form of tubular vacuole reticulum occurs in the hyphal tips of oomycetes (Allaway et al. 1997). An extensive tubular vacuole system with a different morphology from that found in basidiomycetes and oomycetes has been shown in two arbuscular mycorrhizal fungi, *Gigaspora margarita* and *Glomus intraradices* (Olsson et al. 2002; Uetake et al. 2002). In these two species the tubules are organised into long parallel arrays (Fig. 2.2) and their motility has not been established independent of cytoplasmic streaming. Nevertheless they form extensive connected networks and occur in both the extraradical and intercellular hyphae of the fungus in symbiosis with its higher plant partner, as well as in germ tubes. Their presence alters our view of potential mechanisms of nutrient transport in arbuscular mycorrhizal associations (see Ashford 2002; and Sect. V.A.).

Vacuoles also take on tubular form in *Saccharomyces cerevisiae*. Tubulation and motility mediate vacuole delivery into developing buds, thus ensuring that new buds receive their complement of vacuolar membrane and content from the parent cell, a process that has come to be known as vacuole inheritance. The tubulo-vesicular structures that are involved extend between parent and bud and are called segregation structures (Weisman and Wickner 1988; Gomes de Mesquita et al. 1991; Jones et al. 1997; Weisman 2003, 2006). When buds arise from a zygote a segregation structure emerges from each parent vacuole and these fuse in the bud, resulting in a distribution of content between all compartments. All vacuolar exchanges occur via these structures, since the parental vacuoles do not fuse within the zygote (Weisman and Wickner 1988; Weisman 2003, 2006). However the precise morphology of the segregation structure and the extent to which it is tubular or vesicular is confused in the literature (see Sect. II.C.).

The molecular biology of vacuole targeting and fusion in *Sac. cerevisiae* has been intensively investigated over the past decade and significant advances have been made. The elegant in vitro assay of homotypic vacuole fusion, in conjunction with the extensive knowledge of the yeast genome and the use of an array of mutants, has played a pivotal role (see Sect. II.F.). While the fundamental mechanisms of targeted membrane fusion are conserved amongst eukaryote cells (Wickner 2002), differences have arisen between *Sac. cerevisiae* and mycelial fungi, for example in the relationship between the cytoskeleton and vacuole motility (Stein-

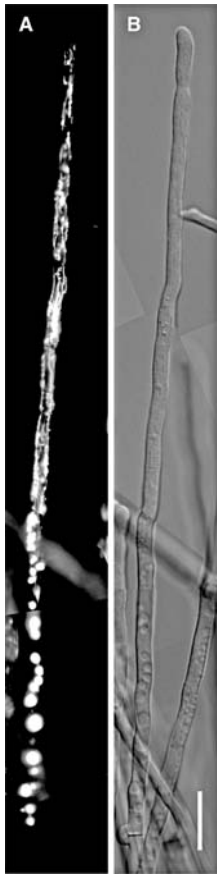

Fig. 2.1. Tubular vacuole system in the tip cell of a living *Pisolithus* hypha, showing the graduation in vacuolar form between the tip (*top*) and the first septum (*bottom*). **A** Montage of fluorescence images. There is a sparse network of vacuolar tubules near the tip. Tubular vacuoles are more abundant and the network more complex, with some small rounded vacuoles, further back from the tip. By about two-thirds of the way along the cell the vacuole system consists of medium-sized rounded vacuoles connected by tubules. Towards the extreme basal region of the cell there is a series of larger spherical vacuoles with few tubules. Labelled with carboxy-DFFDA, visualised by fluorescence microscopy. **B** Corresponding DIC montage. *Bar* 20 µm. Micrographs by R. Verma (from Ashford and Allaway 2002) by kind permission of Springer Science and Business Media

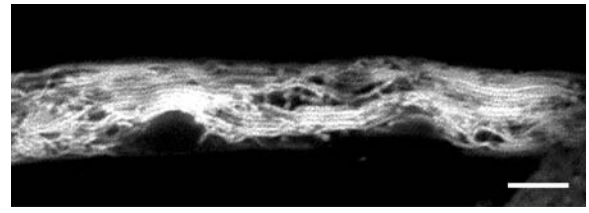

Fig. 2.2. Tubular vacuoles in a germ tube of the AM fungus *Gigaspora margarita* visualised in vivo with DFFDA and confocal microscopy. The tubular vacuoles differ from the typical basidiomycete system in that they often lie parallel to one another in bundles and occupy a large volume of the protoplast and are rarely connected with spherical vacuoles. Single optical slice of part of a hypha. *Bar* 5 µm. From Uetake et al. (2002) with permission of the New Phytologist Trust, copyright 2002

berg 2000). It therefore cannot be assumed that findings from molecular studies on yeast invariably apply in mycelial fungi. The two most likely candidates for use of molecular genetic tools in the study of vacuoles in mycelial fungi are *Aspergillus* and *Neurospora*, though it should be realised that these are representative of the growth form, but not necessarily lifestyles or taxonomic affinities across the breadth of the fungi. Species of both genera have a well developed tubular vacuole system (Rees et al. 1994; Hickey et al. 2005; Shoji et al. 2006).

Significant advances have been made in visualisation of the vacuole system in *Aspergillus oryzae* by expression of constructs of fusion products of enhanced green fluorescent protein (EGFP) and proteins targeted to vacuoles (Ohneda et al. 2002; Shoji et al. 2006). Shoji et al. (2006) have labelled vacuole membranes in *A. oryzae* via expression of fusion protein of EGFP and AoVam3p, a putative vacuolar t-SNARE. The work shows that *A. oryzae* also has a tubular vacuole system with very similar dynamic behaviour to that in *Phanerochaete* and *Pisolithus*. This approach offers new opportunities for molecular dissection of the various vacuolar and endosomal sub-compartments in mycelial fungi (see Sect. II.A.; and Chap. 1 in this volume).

In summary, although the role of vacuoles in storage, lysis and homeostasis is well established (Boller and Wiemken 1986; Klionsky et al. 1990; Jones et al. 1997), recent data indicate that fungal vacuoles are much more morphologically diverse and dynamic than was formerly thought. They are involved in molecular exchanges and transport, and their attributes are indicative of functional differentiation. The evidence upon which this is based is considered in more detail below.

II. Vacuole Motility

A. Visualisation of Vacuoles in Living Fungal Cells

Only by viewing labelled vacuoles in healthy living cells by video microscopy does one get a sufficient grasp of their complexity and motility to be able to monitor their interactions. The use of fluorescent probes in conjunction with fluorescence or confocal microscopy has become the approach of choice. In some cells, high levels of autofluorescence in vacuoles permit their visualisation without the need for fluorescent stains; for example the adenine-deficient *ade2* mutants of *Sac. cerevisiae* accumulate red pigments in their vacuoles that resist photobleaching and are sufficiently fluorescent to be useful in following vacuole dynamics during the yeast cell cycle (Weisman et al. 1987; Weisman 2003). In most cases, however, staining with fluorescent probes is required (Cole et al. 1997) and also, if possible, examination of unstained cells by phase contrast or differential interference contrast microscopy to determine the extent to which the probe might have affected cellular integrity and vacuole morphology (Hyde and Ashford 1997; Hyde et al. 1997).

Many stains such as neutral red, quinacrine and acridine orange accumulate in vacuoles because, like animal lysosomes, they are acidic compartments. LysoTracker and LysoSensor (Molecular Probes, Eugene, Ore., USA) are also acidic-organelle selective probes. They successfully stain yeast and plant vacuoles but also accumulate in other acidic compartments such as *trans* Golgi vesicles, endosomes and some coated vesicles. Fluorescent dyes offer several advantages over histochemical stains. They have high quantum efficiencies and can be detected at very low concentrations, minimising cell damage. In addition, they exhibit a range of excitation and emission spectra enabling dual- and even triple-labelling of different organelles, and their fluorescence has been used to measure a host of cellular events such as membrane potential, intracellular pH, concentrations of molecules such as glutathione and ions such as Ca^{2+} (Rost et al. 1995; Hyde 1998; Parton and Read 1998; Fricker et al. 2000; Meyer and Fricker 2000; Haugland 2001; Perisamy 2001).

Many fluorescent probes that label fungal vacuoles are available commercially. The "*Molecular Probes*" handbook (web edition at http://probes.invitrogen.com/handbook/) is an invaluable referenced resource, detailing the use of a large number of probes available for labelling organelles in living cells. Most vacuole probes are not specific and must be used in conjunction with other methods to confirm localisations. Those most commonly used include 6-carboxyfluorescein diacetate (6-CFDA), Oregon Green 488 carboxylic acid diacetate (carboxy-DFFDA), the thiol-reactive Cell Tracker reagents 7-amino-4-chloromethylcoumarin (CMAC) and 5-chloromethylfluorescein diacetate (CMFDA), and the styryl dyes N-(3-triethylammoniumpropyl)-4-(*p*-diethylaminophenyl-heximenyl)pyridinium dibromide (FM4-64) and MDY-64. The styryl probes label membranes and the others accumulate in

the vacuole lumen (Vida and Emr 1995; Cole et al. 1997, 1998; Zheng et al. 1998; Fischer-Parton et al. 2000). Vacuolar staining with 6-CFDA and carboxy-DFFDA is thought to occur as follows. As non-fluorescent esters, both molecules are readily transported across the plasma membrane. The acetate is removed by cytoplasmic esterases, converting each into the strongly fluorescent anionic forms (6-CF^-, carboxy-DFF^-), which are membrane-impermeant and sequestered into the vacuoles by organic anion transporters. This is based on the effects of probenecid, an organic anion transport inhibitor, on the subcellular distribution of fluorescence (see Cole et al. 1997). The chloromethyl dyes CMAC and CMFDA are thought to react with endogenous glutathione via a glutathione-S-transferase-mediated reaction to form a thiol-ether adduct. Glutathione transporters may facilitate transport of glutathione conjugates into the vacuole lumen. Reactions are discussed further in Sect. V.D.

"Membrane-impermeant" fluorescent probes such as Lucifer Yellow CH (LY-CH), initially developed to trace the endocytic pathway in animal cells (Swanson 1989), are internalised into vacuoles of yeasts with kinetics consistent with endocytosis (Riezman 1985; Basrai et al. 1990). However LY-CH is not a reliable indicator of endocytosis since it can move across the plasma membrane and vacuolar membranes via carrier-mediated mechanisms (Roszak and Rambour 1997; Aniento and Robinson 2005). Not all fungi accumulate LY-CH. For example *Pis. tinctorius* and *Neurospora crassa* do not internalise detectable amounts of either LY-CH or fluorescent dextrans, or accumulate these probes in vacuoles (Cole et al. 1997; Fischer-Parton et al. 2000). This may be because the probes do not cross the cell walls, as found in *Ustilago maydis* (Steinberg et al. 1998).

FM4-64 (Molecular Probes), another fluorescent probe widely used to demonstrate endocytosis, has also produced results that are equivocal. FM4-64 is an amphiphilic dye that is believed to be unable to cross membranes. It is thought to become inserted in the outer leaflet of the lipid bilayer of the plasma membrane when applied exogenously, and to fluoresce only when in a hydrophobic environment (Betz et al. 1992; Bolte et al. 2004). Fischer-Parton et al. (2000) found that it was the best of the three membrane selective dyes they tested, the other two being FM1-43 and TMA-DPH. FM4-64 is the dye currently preferred because of its brightness, good photostability and contrast, and low cytotoxicity. It is internalised in a time-, temperature- and energy-dependent manner consistent with endocytosis and ultimately labels the vacuolar membrane in *Sac. cerevisiae* (Vida and Emr 1995; Zheng et al. 1998), the germ tube of the rust fungus *Uromyces fabae* (Hoffmann and Mendgen 1998), germinating conidia of the rice blast fungus *Magnaporthe grisea* (Atkinson et al. 2002) and *N. crassa* (Fischer-Parton et al. 2000). In yeast, internalised FM4-64 labels small discrete fluorescent patches, likely to be endocytic intermediates, and later the vacuole membrane (Vida and Emr 1995). It is a preferred vacuole marker for yeast because it does not appear to affect growth rate or vacuole morphology and, in contrast to *ade2*, does not require a specific genotype (Weisman 2003). FM4-64 has been used to examine differences in vacuole and endosome morphology in various yeast mutants, to explore potential compartments of an endocytic pathway (Vida and Emr 1995; Gaynor et al. 1998) and to screen for mutants with abnormal vacuole morphology and dye localisation (Zheng et al. 1998). It has also been used in a membrane recycling assay (Wiederkehr et al. 2000), in homotypic vacuole fusion assays (Wang et al. 2002, 2003) and to follow vacuole inheritance (Wang et al. 1996). In *Neurospora* FM4-64 first labelled the plasma membrane, then spherical structures ~0.75 µm which might be "putative early endosomes", the Spitzenkörper and later the larger vacuoles (Fischer-Parton et al. 2000). Sequential labelling of cellular structures was broadly similar in *Magnaporthe* – plasma membrane labelling was followed by diffuse cytoplasmic staining, staining of apical vesicle clusters and punctate structures thought to be endosomes, then other structures and later vacuoles (Atkinson et al. 2002).

Though FM4-64 is a very useful marker for various cell compartments, inconsistencies in labelling in different cell types have plagued its use. Differences in the timing of internalisation may be explained by differences in growth rates (Bolte et al. 2004) and/or differences in wall permeability. This may explain why in *Pis. tinctorius*, which has a very slow growth rate, the plasma membrane, tonoplast and punctate structures became labelled with FM4-64 only after prolonged treatment and mainly in damaged cells (Cole et al. 1998). As with LY-CH uptake into cells does not necessarily indicate that endocytosis has occurred, since it is usually not possible to exclude transfer into endosome or vacuole membranes by other mechanisms (Fischer-Parton et al. 2000; see Read and Kalkman

2003 for a discussion). Inconsistencies in organelle labelling are also difficult to explain. For example inconsistencies between labelling of vacuoles with FM4-64 and LY-CH in *kin2* mutants of *Ustilago maydis* (Steinberg et al. 1998) suggest that the compounds do not both gain access to the vacuoles by the same process. Differences in the labelling patterns with FM4-64 and FM1-43, where mitochondria become labelled much more rapidly with the latter dye (Fischer-Parton et al. 2000), also require explanation in the context of endocytosis (Bolte et al. 2004). Furthermore FM4-64 labelling of Golgi bodies in cultured plant cells (Bolte et al. 2004) and of the Spitzenkörper (or apical vesicle clusters) in hyphal tips of many species (Fischer-Parton et al. 2000; Dijksterhuis 2003; Chap. 6 in this volume) shows that, even after short periods of time and well before vacuoles label, this dye labels more than a putative endocytic pathway.

More stable probes such as the Alexa dyes and developments in confocal laser scanning microscopy (see Fricker and Oparka 1999) offer higher sensitivity with less photobleaching. Further success in labelling membranes and organelles and studying cell processes depends on advances in both fields. However, many of the probes used to label vacuoles lack specificity and do not differentiate between the various vacuolar, vesicular and endosomal compartments. The introduction of green fluorescent protein (GFP) as a marker to monitor gene expression and protein distribution (Chalfie et al. 1994) has transformed the labelling of molecules and structures in a wide range of living cells, including those of fungi (Cormack 1998; Czymmek et al. 2002, 2005; Hickey et al. 2005; see also Chap. 1 in this volume). GFP has the potential to label any protein for which a gene construct can be made and, if fused with a peptide that targets a particular organelle, causes that organelle specifically to fluoresce. It has a wide range of applications (Fricker and Oparka 1999; Hanson and Köhler 2001; Chalfie and Kain 2006). The GFP chromophore does not require exogenous factors (except blue or UV light) to fluoresce and in most cases GFP addition does not appear to interfere with normal protein function. In spite of the initial difficulties in expressing constructs of the GFP gene in many organisms including mycelial fungi, modifications of the native gene by mutagenesis have improved expression (Cormack 1998; Fernández-Ábalos et al. 1998). Fluorescent proteins from other sources are also being used (Bourett et al. 2002): Fig. 2.3 shows labelled vacuoles in *Colletotrichum graminicola* hyphae expressing AmCyan, a reef-coral fluorescent protein. Gene modifications have also improved GFP brightness (Cubitt et al. 1995) and have produced variants with altered spectral properties, allowing multiple localisations (Haseloff 1999; Hawes et al. 2001; Czymmek et al. 2002), and the use of GFP in yeasts and mycelial fungi to monitor a variety of cellular events and structures has taken off.

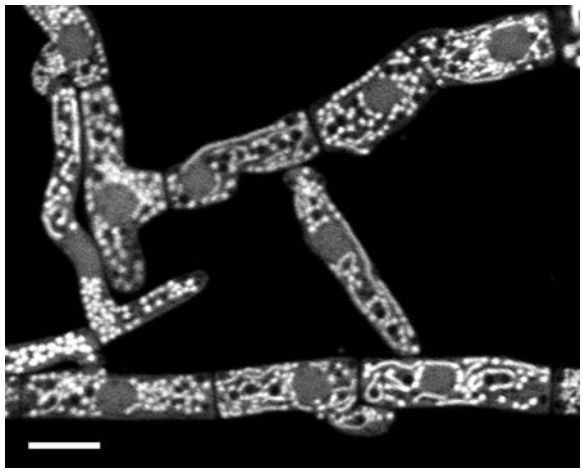

Fig. 2.3. Live *Colletotrichum graminicola* (hyphae about 7 µm wide) expressing the reef coral fluorescent protein AmCyan. Despite cytosolic expression these fluorescent proteins are often found sequestered in apparent tubular vacuoles in conidiophores and conidia. Micrograph by courtesy of T.M. Bourett (DuPont Crop Genetics, Wilmington, Del., USA)

Some examples of its use in *Sac. cerevisiae* are given below. Cowles et al. (1997) found that a GFP-fusion protein of alkaline phosphatase (ALP) was localised to vacuoles in wild-type cells but not in a mutant deficient in a key subunit of the AP-3 complex. In the mutant the GFP-ALP protein mislocalised into short tubules and vesicles, not to vacuoles, though FM4-64 staining showed that normal vacuoles are present indicating that an adaptor protein of the AP-3 complex is involved in targeting this enzyme from the Golgi to the vacuolar membrane. Visualisation of a fusion protein of GFP and the SNARE Snc1p that normally mediates exocytosis enabled demonstration of a distinct recycling pathway between the plasma membrane, Golgi and a compartment identified as an early endosome (Lewis et al. 2000). This discovery is based on redistribution of the GFP-fusion protein and its co-localisation with other compartment-specific proteins in mutants where Golgi function or exocytosis is blocked. Pan and Goldfarb (1998)

found that a fusion protein between GFP and Yeb3p (Vac8p) was located over the entire vacuole surface but became concentrated in bands between "clustered" vacuoles. Vac8p, a vacuolar membrane protein with multiple "armadillo repeats" (sites of protein–protein interaction) is involved in several processes, including vacuole movement and autophagy, and plays a key role in homotypic vacuole fusion and vacuole inheritance (Weisman 2003).

Kitamoto and colleagues have successfully expressed EGFP constructs of fusion proteins that target vacuoles in *Aspergillus oryzae*. Ohneda et al. (2002) made a construct of vacuolar carboxypeptidase Y, a hydrolase targeted to the vacuole lumen via the classical receptor-mediated vacuole protein sorting pathway from the Golgi in yeast (see Sect. V.B.). Vacuole labelling was sensitive to pH and required an alkaline growth medium for optimum fluorescence emission. The probe was localised in the lumen of large spherical vacuoles in basal regions, but tubules and ring structures stained when the transformant was growing over glass in minimal medium. They suggested that the latter are structures in the secretory pathway to vacuoles, but could not identify them definitively.

Another construct expressing a fusion protein of EGFP and the syntaxin AoVam3p has been localised to vacuolar membranes (Shoji et al. 2006). AoVam3p is the t-SNARE homologous to yeast Vam3p which localises to vacuole membranes (Wada et al. 1997) and plays an essential role in homotypic vacuole fusions in *Sac. cerevisiae* (see Sect. II.F.). In *A. oryzae* the expressed EGFP-AoVam3p localises to dynamic, pleiomorphic vacuolar networks. The behaviour and morphologies of the GFP-labelled vacuole networks are very similar to those in *Phanerochaete* and *Pisolithus*. Not only does this indicate that insertion of GFP did not impair vacuoles but it is further evidence that such vacuole behaviour is not due to loading of the lumen with probes. EGFP-AoVam3p also labelled small "punctate" structures. In contrast to the vacuoles these were CMAC-negative and were tentatively identified as late endosomes/prevacuolar compartments. AoVam3 is the only obvious homologue of both Vam3 and Pep12, and Shoji et al. (2006) propose it might be a t-SNARE for both compartments. However, as they note, this is not conclusive since there is overlap between these functions in yeast mutant complementation studies, as shown by Götte and Gallwitz (1997).

The selected examples given above illustrate the power and versatility of fluorescent labelling in living cells, especially if used in conjunction with molecular techniques. In many of the examples, labelling of several structures or processes simultaneously has been used to great effect. Dual labelling with "conventional" fluorescent probes targeting different organelles allows labelling of more than one organelle type simultaneously in the same cell. Vida and Emr (1995) used double labelling of vacuoles with CFCDA and FM4-64 in yeast to confirm that vacuoles were still present and had not lost their integrity in reconstitution experiments. A series of dual localisations, using carboxy-DFFDA, fluorescent BODIPY-brefeldin A and an ER-Tracker^{TM} dye allowed the tubular-vacuole system of *Pis. tinctorius* to be distinguished from the endoplasmic reticulum (ER) in living cells (Cole et al. 2000a, b). Localisations were supported by correlation with electron micrographs of freeze-substituted hyphae. Tubular vacuolar systems in *Pis. tinctorius* were also differentiated from mitochondria by dual labelling with 6-CFDA and rhodamine 123 (Ashford and Orlovich 1994). Similarly, the motile vacuole system in *Pha. velutina* was distinguished from the tubular mitochondrial system by dual labelling with Oregon Green and Rhodamine B (Watkinson et al. 2005). Dual localisation was also used with flow cytometry to isolate *Sac. cerevisiae* mutants that mislocalise vacuolar dyes (Zheng et al. 1998).

Dual and even multiple localisations of GFP-labelled structures, either with other GFP-labelled constructs or with "conventional" fluorescent probes, have produced some spectacular results. One such case is the ratiometric analysis between FM4-64 and GFP-constructs showing that the proteins and co-factors controlling the stages of vacuole fusion become concentrated in the vertex which forms at the edge of the zone of contact between vacuoles in a hierarchical manner (Wang et al. 2002, 2003; see Sect. II.F.). Another example is the multiple labelling of GFP-constructs of different proteins targeting various components simultaneously to demonstrate microtubule growth, assembly and movement of organelles along microtubules driven by both microtubule motors in *Ustilago maydis* (e.g. Lenz et al. 2006; and see Sect. III.). This list is not comprehensive, but it gives an idea of the value of the approach in the study of dynamic events in cells (see also Chaps. 1 and 5 in this volume).

Fluorescent probes are generally chosen for their low toxicity at the concentration required to visualise the target cellular event, and some spectacular images have been obtained of hyphae still rapidly growing after labelling with fluorescent probes (Hickey et al. 2002; Darrah et al. 2006, supplementary material). Nevertheless probes can cause damage and some are quite toxic. Damage to motile vacuole systems usually results in loss of their motility, broadening of vacuolar tubules and/or their conversion to a series of spherical vacuoles. Damage to vacuoles has been observed with fluorescent probes. For example $DiOC_6(3)$ treatment at concentrations which stain the ER may result in a broadening of vacuolar tubules, cessation of typical vacuolar movements and, ultimately, vacuole fragmentation (Ashford and Orlovich 1994). The report by Torralba and Heath (2002) that FM4-64 is toxic appears erroneous (Bolte et al. 2004). Shoji et al. (2006) report that FM4-64 did not affect growth rate or vacuole morphology in *Aspergillus oryzae* under their conditions; carboxy-DFFDA did not affect the growth rate of *Pha. velutina* when grown in slide culture (X.Y. Zhuang, D. Davies, A.E. Ashford, unpublished data). Damage is commonly seen when more than one probe is used as in dual localisations with FM4-64 and DFFDA (Read and Kalkman 2003). It is also seen after long treatments and at "high" concentrations (usually >50 µM). To avoid this, concentrations of the probe should be low, treatments short and irradiation minimised (Cole et al. 1997, 1998). An independent assessment of cellular integrity is mandatory, usually by comparison with unlabelled images viewed by DIC microscopy. In the case of GFP-constructs it is crucial that evidence is provided that the fusion protein really does substitute for the normal protein, i.e. that it functions normally and is targeted normally.

B. Vacuole Probes and Electron Microscopy

One of the major challenges in organelle labelling is the correlation of dye localisations in living cells with ultrastructure. As seen in Sect. II.A. many probes do not provide consistent labelling over a spectrum of cell types and conditions, and electron microscopy (EM) is often necessary to confirm the specificity of organelle labelling. This applies to all the most commonly used vacuole markers. It is also possible that localisation of GFP-fusion proteins may not be the same as that of wild-type protein (Hanson and Köhler 2001). EM is also needed to clarify the identity and morphology of new structures visualised with vital dyes, as there is usually insufficient resolution at the light microscope level. Conversely many tubular and vesicular structures seen at the EM level cannot be assigned to a functional organelle system without specific labelling. Markers are also needed to explore biochemical partitioning and differentiation within organelles such as vacuoles. This is not so much of a problem if specific immunocytochemical markers are used, since antibodies can be conjugated with fluorophores for light microscopy and electron-opaque markers for EM. It is, however, a problem if water-soluble dyes are to be retained in vacuoles. Several dyes such as LY-CH, CMAC and chloromethyl fluorescein diacetate (CMFDA) are aldehyde-fixable and have been used to some advantage (Oparka 1991; Haugland 2001; West et al. 2001). However, primary aldehyde fixation destroys the integrity of the vacuole system and alters its morphology, converting tubular components into isolated vesicles (for a discussion of this issue, see Sect. II in Ashford 1998) and so this approach cannot be used with vacuoles if credible results are to be obtained. Observations of continued membrane flow and other cellular changes during chemical fixation also cast doubt on its suitability for study of any interaction between membranes and membrane enclosed compartments (see Mersey and McCully 1978; McCully and Canny 1985; Hoch 1990). Furthermore it is usually not clear that the fluorochrome has been adequately captured in situ.

Methods such as low temperature freeze-drying or anhydrous freeze-substitution are more effective for retaining water-soluble fluorescent probes in situ (Canny and McCully 1986; Chandra and Morrison 1997). Hyde et al. (2003) were able to retain three probes (CMAC, CMFDA, carboxy-DFFDA) in the vacuole system during freeze-substitution into Spurr's resin without aldehyde fixation. They used the same anhydrous conditions as had been successful in retaining ions in test droplets (Orlovich and Ashford 1995). The best results were obtained with CMAC. Vacuole structure was well preserved but, though the probe was retained in the large vacuoles of most hyphae, tubules and small vacuoles were invisible and high background fluorescence suggested loss into the resin. In spite of these difficulties this approach still has promise and could be useful in localisation of other probes including some GFP-constructs. It may be possible to immobilise "fixable" probes and/or better stabilise antigens, as well as

achieve better cell preservation, by reaction with aldehydes during the substitution phase of freeze-substitution (Czymmek et al. 1996; see also Skepper 2000). Low-temperature methods are also very useful in optimising antigen survival for immunocytochemistry (Monaghan and Robertson 1990; Monaghan et al. 1998; Skepper 2000) and, for very small specimens such as hyphal tips, cryofixation is the best option for rapid membrane immobilisation and preservation of ultrastructure in a life-like state (see also Chaps. 1 and 11 in this volume).

The best approach currently for compartment labelling is immunocytochemistry of proteins (and other substances with reactive epitopes) specific to particular membrane domains or organelles, using freeze-substituted material. Excellent results have been obtained: for example, the localisation of clathrin in *Sac. cerevisiae* (Mendgen et al. 1995). It has been difficult to find appropriate probes to label vacuoles in mycelial fungi, but staining sections of freeze-substituted hyphae with the lectin concanavalin A, complexed with gold, has been very successful (Bourett et al. 1993; Bourett and Howard 1994). Large vacuoles and two different types of smooth cisternae are well labelled. The content of some vacuoles including tubular vacuoles is also labelled, as well as the membranes and content of multivesicular bodies. Using this approach with more specific probes, such as the many GFP-constructs of genes of known function now available for *Sac. cerevisiae*, there are endless possibilities to investigate the physical nature and interactions of the endocytic pathway, including the vacuole system. Techniques for correlation of GFP-labelling with electron microscopy by coupling anti-GFP antibodies with immunogold localisation (Luby-Phelps et al. 2003, and references therein) are available. If this approach is taken to investigate GFP localisation in vacuoles, or any processes involving membrane dynamics, aldehyde fixation should be avoided and freezing methods employed, such as freeze-substitution (see Sect. II.C.; also Chap. 1 in this volume). Use of freeze-substitution and 3-D reconstruction from serial sections of the mitochondrial system in budding pathogenic yeast cells (Yamaguchi et al. 2003, and references therein) shows the usefulness of this approach.

Various techniques involving freeze-substitution, followed by rehydration and treatment with wall-lysing enzymes, or butyl methyl methacrylate embedment and de-embedment, have been used for localisation of affinity probes in whole fungal cells by immunofluorescence (Czymmek et al. 1996; Hyde et al. 1999). The latter has been useful in labelling components of both the cytoskeleton and also the endomembrane system (Czymmek et al. 1996; Bourett et al. 1998; see Fig. 11.6C, E in this volume). This approach should be very valuable for visualisation of organelle systems in three dimensions by confocal microscopy, but it must be realised that there is a compromise between structural preservation and accessibility of probes to their reactive sites, and this must be carefully considered in any interpretation (Bourett et al. 1998; Skepper 2000).

C. Tubules or Vesicles? The Legacy of Classical Electron Microscopy

Electron microscopy has played a pivotal role in our understanding of cellular and subcellular structure and in allowing us to distinguish between organelles, based on their structure and staining reactions. The development of electron microscopy (EM) techniques led to the use of glutaraldehyde/osmium fixation as the most common preparative technique for cell fixation; and decades followed when many ultrastructural details were acquired. However it left an enduring legacy. It was then not (and still is not) fully appreciated that, in the preparation of these classical EM images, there is membrane flow during this slow chemical fixation process, which lasts for minutes and during which tubular structures are irreversibly converted into strings or clusters of vesicles (Mersey and McCully 1978; Wilson et al. 1990; Orlovich and Ashford 1993). In general vesicles will be over-represented and tubules under-represented in electron micrographs prepared by these methods. This problem is further exacerbated by the use of very thin sections without a 3-D reconstruction from a complete series. Though electron microscopy has moved on and preparative techniques have improved, this is still firmly embedded in the mindset of cell biologists. Vesicle trafficking is seen as central to exchange of material between compartments; see Abeliovich and Klionsky (2001) for a discussion of this issue. Tubule traffic is much less often considered and processes continue to be represented as occurring primarily via streams of vesicles, when in fact they may occur via tubules.

This legacy perhaps explains the confusion about the segregation structure in *Sac. cerevisiae*.

In the seminal paper by Weisman and Wickner (1988) on yeast vacuole inheritance, using the *ade2* strain which accumulates endogenous fluorophore in the vacuoles, the authors showed the segregation structures connecting vacuoles in the zygote with those in its developing bud. They initially described them as "vesicles or fluorescent trails", or "tracks" emanating from each major vacuole into the bud, and interpreted them as trails of vesicles. They concluded that bud vacuole formation entails vesicular traffic along a path between mother and bud vacuoles in both directions. However, given our current knowledge of tubular vacuoles from mycelial fungi and yeasts, the segregation structures would seem to be better interpreted as tubular extensions of the parent vacuole. Various images and descriptions consistent with the view that segregation structures are tubular can be found in the literature (see for example Gomes de Mesquita et al. 1991; Jones et al. 1993; Fig. 3A of Vida and Emr 1995; supplementary video images of Weisman 2003). However recent models of the segregation structure still represent this as comprising only vesicles (Tang et al. 2003). Weisman (2003) notes in her review that, in some video images and stills, the segregation structure appears tubular, while in others it appears as series of separate small vacuoles and there are many reports of "larger" segregation structures rapidly changing to a cluster of smaller vacuoles/vesicles. This is fully consistent with tubular vacuole behaviour as reported in mycelial fungi. Transformations of the same vacuole, from a tubule to "a series of linearly aligned small vacuoles", or the reverse, are seen commonly and can happen many times in succession. However the form and behaviour of vacuoles during these transformations in mycelial fungi suggests that they occur without fusion and fission and with no interruption of lumen continuity. Vacuoles that appear to be a series or cluster of separate vesicles are shown by electron microscopy of freeze-substituted hyphae to have a continuous lumen via tubular bridges of reduced diameter (see Figs. 4–7 of Shepherd et al. 1993a). A structure with this morphology containing fluorescent material is likely to appear as a series of separate vesicles in fluorescence microscopy if the fluorescent material in the bridges is below the level of detection and yet it will still have lumen continuity. This has implications for transport of vacuole content into the bud. Transfer by tubule is consistent with the rapid equilibration of non-*ade2* vacuoles in hybrid zygotes once the bud vacuole has acquired some fluorescent content from the vacuole of the *ade2* parent, without the need to invoke bi-directional transport of vesicles. Observations of yeast segregation structures at the ultrastructural level in serial sections of well preserved yeast cells should resolve this issue. Freeze-substitution preserves yeast cells well (Yamaguchi et al. 2003).

The concept of transport via tubules is steadily gaining support as a complement to vesicle transport; and the two processes are not seen to be mutually exclusive (de Figueiredo and Brown 1995; Mironov et al. 1997). Studies of organelles labelled with fluorescent probes in living cells have shown that tubule transport is commonplace. Of particular relevance are the prominence of tubule formation in Golgi dynamics and its similarities to vacuolar tubule transport (Cooper et al. 1990; Lippincott-Schwartz et al. 2000).

D. Changes in the Vacuole System with Development and Environment

The most useful information on the relationship between vacuole morphology and development has been obtained with *Pha. velutina*. Its fast rate of growth and the use of both time- and space-resolved confocal microscopy has enabled sequences of 3-D images to be constructed with minimum photobleaching as the hyphal tip grows (Darrah et al. 2006, supplementary material). It is important to differentiate this from the usual single-plane images (optical sections) captured in most time-resolved videos taken by confocal microscopy, where tubules and other structures move in and out of the plane of focus during the video. These are often difficult to interpret as key fusion or fission events may occur out of the plane of focus and, as in conventional EM, tubular structures may look like isolated vesicles/vacuoles if viewed in the transverse plane. This problem is avoided to some extent by use of fluorescence rather than confocal microscopy but the penalty is blur and poorer resolution. In addition videos are often too short to capture a full sequence of events because of photobleaching.

The picture that has emerged from work with the two basidiomycetes, *Pisolithus* and *Phanerochaete*, is that the vacuole system in tip cells of mycelial fungi is a dynamic, highly polarised structure. Polarisation of the vacuole system is also obvious among the Oomycota where an apical

filamentous vacuole network is contiguous with a large sub-apical vacuole that fills most of the cell volume (Allaway et al. 1997). In *Pisolithus* and *Phanerochaete* tubular vacuoles extend into the extreme hyphal tip as it grows and the whole vacuole system moves forward, so that vacuole zonation remains constant with time and its position maintained in relation to the extending apex. The tip cells of *Pisolithus* and *Phanerochaete* are relatively long and along their length several zones can be identified according to vacuole morphology, motility and distribution. There is typically a transition from a more tubular system, often with small ellipsoid or sperical vacuoles associated with it, to a series of larger less mobile vacuoles that are variously interconnected by tubules within the tip cell (Fig. 2.1). Vacuole systems with many tubular elements are also frequently seen in the second (penultimate) and third cells.

In general vacuoles become larger and more stationary (though still connected by tubules) with increasing distance from the hyphal tip both within the tip cell and, on a larger scale, within the mycelium as a whole. However, there is a lot of variability and non-motile vacuoles can become more motile, more tubular and more interconnected with changes in both external and internal conditions. Control of these processes is not well understood. We do know that in *Pisolithus* fresh medium promotes tubulation and motility (Hyde and Ashford 1997) and that cultures grown between cellophane sheets have a more extensive reticulum than those on an agar surface. A more reticulate system connecting small vacuoles was observed in *Aspergillus oryzae* in hyphae not in contact with nutrients, such as aerial hyphae and hyphae growing on a glass surface (Shoji et al. 2006). Changes in external levels of nutrients and salinity (R. Verma and A.E. Ashford, unpublished data) and exposure to elevated levels of heavy metals all have observable effects on tubular vacuole systems in mycelial fungi (Tuszynska 2006; Tuszynska et al. 2006). The usual effect is loss of tubules and reduction in motility. Cellular damage of various kinds readily converts a vacuolar reticulum into a series of larger non-motile vacuoles in both mycelial fungi and oomycetes (Allaway et al. 1997; Cole et al. 2000a, b; Tuszynska 2006; Tuszynska et al. 2006). Treatment with anti-microtubule drugs also suppresses vacuole tubulation and motility (Hyde et al. 1999). Many of these effects can be reversed on removal of the perturbing factor. In the Oomycota, recovery from a range of growth-inhibiting conditions is accompanied by a transient migration of vacuoles into hyphal tips, displacing tip cytoplasm. Only when cytoplasm has subsequently migrated back into the tip and displaced these vacuoles does the hypha resume growth (Bachewich and Heath 1999). It is clear that vacuole movements are independent of cytoplasmic streaming, suggesting that different regulatory mechanisms must be in operation.

In *Sac. cerevisiae*, vacuole motility and tubulation are closely tied in with the cell cycle. For example the segregation structures, and these include tubular elements (see Sect. II.C.), extend into young buds at the stage when the bud is about one-third of its final volume (Weisman and Wickner 1988; Gomes de Mesquita et al. 1991; Jones et al. 1993). Are the morphology and dynamics of the vacuole system in tip cells of mycelial fungal similarly correlated with the cell cycle? This would seem likely but there are no data to clarify this. Videos of *Phanerochaete* do, however, show a correlation between vacuole form and branching. There is a transformation of vacuoles in penultimate cells to a tubular, reticulate system more typical of that in rapidly growing apical cells, just prior to the formation of a branch (M. Tlalka, unpublished data). This deserves further investigation.

E. Fusion and Fission and the Generation of Tubular Networks; Lessons from Mitochondria

Since the last review (Ashford et al. 2001) there have been more reports of tubular vacuoles in plant as well as fungal cells, further supporting the view that vacuolar tubulation is a fundamental property of eukaryotic cells. As in fungi, plant tubular vacuoles are very susceptible to chemical fixation, which also causes them to transform irreversibly into clusters of vesicles (Mersey and McCully 1978; Wilson et al. 1990). In some cases tubular vacuoles are produced at particular stages in the cell cycle, as in guard cells (Palevitz and O'Kane 1981; Palevitz et al. 1981; Kutsuna and Hasezawa 2002) and in others apparently not (Lazzaro and Thomson 1996). Tubular lysosome networks, the compartments in animal cells considered to be their equivalent, are also found in some cell types and their tubules are also not well preserved by chemical fixation (Robinson et al. 1986; Swanson et al. 1987a,

b, 1992; Knapp and Swanson 1990; Robinson and Karnovsky 1991).

Other organelles also form tubular networks, either constitutively or at particular stages in the cell cycle. Such tubular networks, as exemplified by mitochondria, are very dynamic and are maintained by an equilibrium between opposing fusion and fission processes, controlled by three high molecular weight GTPases (Yaffe 1999; Shaw and Nunnari 2002; Westermann and Prokisch 2002). One is the dynamin-related GTPase Dnm1p which acts on the outer mitochondrial membrane to regulate fission (Shaw and Nunnari 2002). Fusion is regulated by two integral outer membrane proteins, Fzo1p and Ugo1p, and another protein, Mgm1p, that is thought to reside in the inner membrane (Wong et al. 2003). The loss of any of them causes fragmentation of mitochondrial tubular networks and some also affect mitochondrial inheritance; effects are reversible if expression is restored (Shepard and Yaffe 1999). Fzo1p is an integral GTPase protein of the mitochondrial outer membrane with its GTP-binding site projecting on the cytoplasmic side (Hermann et al. 1998; Yaffe 1999). In *Fzo1* and *ugo* mutants the tubular mitochondria fragment, presumably because fusion is blocked but fission continues (Shaw and Nunnari 2002). Mutations of the gene *DNM1* also disrupt the mitochondrial network, but in this case by interference with tubule fission (Bleazard et al. 1999). In the mutant the mitochondrial system collapses into a continuous planar network of interconnected tubules that lie along one side of the cell. Immunogold electron microscopy of cryosections shows that Dnm1p occurs at discrete sites at the tips of mitochondrial tubules and also along their sides. About one-third of these occur at constriction sites, suggesting that this protein may cause constriction at these sites, leading to tubule fission. Dnm1p antagonises the activity of Fzo1p; absence of Dnm1 prevents the fission and fragmentation that occurs with loss of Fzo1 activity, supporting a direct role for Dnm1p in fission (Bleazard et al. 1999; Shaw and Nunnari 2002). If Dnm1p acts like the dynamins that cause neck constriction and scission of coated pits to produce coated vesicles in endocytosis (Hinshaw and Schmid 1995; Takei et al. 1995; van der Bliek 1999; Takei and Haucke 2001), then it could bring about fission in mitochondrial tubules by a similar mechanism (Shepard and Yaffe 1999).

Membrane fusion and fission in yeast vacuoles also involve dynamin. In addition to Mgm1p and Dnm1p yeast cells have another dynamin-like protein, Vps1p. This protein was originally identified as involved in Golgi vesicle formation but was recently implicated in both the fusion and fission of yeast vacuoles (Peters et al. 2004). Deletion of *VPS1* results in enlarged vacuoles that have lost the ability to fragment in hypertonic media, consistent with a role for Vps1p in membrane scission. The localisation of Vps1p-GFP on vacuoles is non-uniform and different from that of SNAREs, tethering factors and Ypt7p Rab GTPase, all of which are reported to be distributed uniformly (Wang et al. 2002; Peplowska and Ungermann 2005). Vps1p-GFP distributes to foci in response to hypertonic stress and forms spiral/ring-like structures suggestive of dynamin. *Vps1* mutants are also deficient in homotypic vacuole fusion at the docking stage, indicating an involvement of Vps1p in fusion, that is further supported by its interaction with the t-SNARE Vam3p (Peters et al. 2004). Disruption of a homologue of *VPS1* encoding a dynamin-related protein in *Aspergillus nidulans* also results in highly fragmented vacuoles (Tarutani et al. 2001).

Dynamin is also implicated in the formation of membranous tubules in mycelial fungi. Tubular invaginations of the plasma membrane that are artificially induced when lysed nerve terminals are treated with GTPγS, a GTPase inhibitor, are coated with dynamin (Takei et al. 1995). The dynamin coat appears as a series of regularly spaced rings interpreted as a helix along the walls of tubules but not at their tips. Tubule tips in vivo are often capped with a clathrin-coated bud. These data indicate that dynamin is normally involved in fission of clathrin-coated vesicles from coated pits, but that GTPγS subverts this, causing the necks of coated pits to elongate into tubules rather than to separate. Dynamin-coated tubules can also be produced by incubation of protein-free liposomes with cytosol and purified dynamin, suggesting that dynamin alone is sufficient to produce tubules (Takei et al. 1998). In *Pis. tinctorius*, GTPγS causes a significant increase in both the number and length of vacuolar tubules (Hyde et al. 2002). This effect is antagonised by GDPβS and is consistent with involvement of a dynamin-like protein.

While fusion and fission can maintain equilibrium in tubular vacuole networks they do not explain the rapid extensions (and retractions) of individual tubules. Extensions of vacuolar tubules can occur for distances of at least 60 µm and the tubular vacuole network requires microtubules for its continued presence in hyphal tip cells (Hyde et al. 1999, 2002). Organelle transport to and from

hyphal tips in mycelial fungi is thought to involve microtubules and their motors (Steinberg 2000; see also Chap. 5 in this volume). It is tempting to speculate that extension of vacuolar tubules similarly occurs along microtubules driven by microtubule motors (see Sect. III.).

F. Mechanisms of Targeted Membrane Fusion

Molecular mechanisms of transport have hitherto been considered generally in the context that transport between intracellular compartments is accomplished primarily by vesicles (Rothman 1994). Vesicle fusion is a multi-step process involving priming, tethering, docking and finally fusion. It is well established that the specificity underlying vesicle docking and fusion resides in the specificity of receptor proteins on both target and vesicle membranes, called SNAREs (Rothman 1994), though these are not the only determinants (Gerst 1999; Mayer 1999, 2002; Pelham 1999a; Waters and Pfeffer 1999). SNAREs form complexes which hold together compatible membranes prior to their fusion. Vesicle-associated (or donor) SNAREs (v-SNAREs) interact specifically with their counterparts on the target membrane (t-SNAREs) to enable vesicle docking (Söllner et al. 1993a, b). Docking (not reversible) follows a tethering step that is reversible and involves compartment-specific Rab-GTPases as well as SNAREs (Waters and Pfeffer 1999; Mayer 2002). It is now clear that v- and t-SNAREs coexist on both vesicle and target membranes and the difference between vesicles and organelles is not always obvious (Pelham 1999a; Mayer 2002). This has led to a reclassification of SNAREs based on their structure and they are now called Q- and R-SNAREs (Fasshauer et al. 1998; Mayer 2002). This review uses the old nomenclature. SNAREs and associated proteins are highly conserved in eukaryotic cells and various *Sac. cerevisiae* gene products have been identified as homologues of mammalian SNAREs first found to be involved in synaptic vesicle fusion during nerve transmission. The field has been extensively reviewed (Ferro-Novick and Jahn 1994; Rothman 1994; Bennett 1995; Südhof 1995; Pfeffer 1996; Gerst 1999; Jahn and Südhof 1999; Mayer 1999, 2002; Pelham 1999a, b; Jahn et al. 2003; Ungar and Hughson 2003; see also Chap. 1 in this volume).

The in vitro assay developed to study fusion between similar "homotypic" vacuoles from *Sac. cerevisiae* indicates that these interact and fuse by mechanisms which parallel those that mediate vesicle priming, tethering, docking and fusion, i.e. heterotypic fusion (Nichols et al. 1997; Wickner and Haas 2000; Wickner 2002). The homotypic vacuole fusion assay uses two sets of vacuoles from mutant strains. One set is deficient in protease but contains the precursor to alkaline phosphatase and the other is alkaline-phosphatase deficient but protease active (Haas et al. 1994; Haas 1995). On fusion the pro-alkaline phosphatase is cleaved by the proteases to produce the active form of the enzyme. Alkaline phosphatase activity, which may be visualised in individual vacuoles, is the measure of fusion. Homotypic vacuole fusion shows that *cis* complexes of both v- and t-SNAREs exist on both the donor and recipient vacuole membranes and must first be dissociated to prime the vacuoles (Ungermann et al. 1998, 1999). This is ATP-hydrolysis-mediated and involves the action of Sec17p, (an α-SNAP), Sec18p (NSF protein, an ATP-driven chaperone) and LMA1 (its co-chaperone); all are SNARE regulators. Priming disassembles the *cis*-SNARE complex, releasing Sec17p from the vacuole membrane and activating the t-SNARE (Vam3p). The co-chaperone LMA1 stabilises the primed t-SNARE complex (Xu et al. 1998). Unless vacuoles are primed, contact will not result in fusion. Primed vacuoles that come into contact are initially tethered by a reversible reaction which requires Ypt7p, a small GTP-binding protein of the Rab/Ypt family of GTPases. The interaction becomes irreversible through association of the complementary SNAREs (Vam3p, Nyv1p) on the apposed membranes, forming a *trans*-v-t-SNARE complex, and the vacuoles are then "docked". The *trans*-SNARE pairing triggers release of calcium from the vacuole lumen leading to membrane fusion (Peters and Mayer 1998; Merz and Wickner 2004) but whether calmodulin is involved is in dispute (Starai et al. 2005). Purification of a functional vacuolar SNARE complex by its solubilisation in a yeast vacuole detergent extract and reconstitution to produce fusion competent proteoliposomes confirmed the role of SNAREs in fusion and showed that v- and t-SNAREs on the same vacuole membrane are fully functional (Sato and Wickner 1998).

Localisation of proteins involved in homotypic vacuole fusion at various stages of the process using GFP-constructs shows how the interacting proteins concentrate at the interfaces of clustered vacuoles, but only if the latter are first primed. Wada et al. (1997) showed by immunofluorescence that Vam3p, the t-SNARE involved in vacuole fusion, was localised in patches on yeast vacuole mem-

branes. Pan and Goldfarb (1998) found that constructs of Vac8p and GFP were localised over the entire surface of vacuoles but became concentrated at junctions where vacuoles were clustered. The GFP-fusion protein complemented defects in vacuole inheritance and fragmentation in mutants, showing that it was still functional. Wang et al. (2002, 2003) further showed that SNARE and other proteins became concentrated in a vertex ring that formed during vacuole tethering. Using confocal microscopy they followed the dynamics of homotypic fusion in vacuoles labelled by both FM4-64 and GFP-tagged Vph1p, an integral membrane protein (Wang et al. 2002, supplementary material). Where vacuoles that are primed contact one another a flattened boundary forms. At the edge of this boundary the vertex ring develops and the proteins involved in fusion accumulate there. Early in fusion the boundary membrane separates from non-boundary membrane at the vertex and is released into the vacuole lumen. This occurs within seconds. Once inside the fused vacuole the excised membrane breaks up into fragments, appears to vesiculate and makes repeated contact with the internal face of the fused vacuole limiting membrane; it is tempting to speculate that molecules are being re-inserted into the bounding membrane. This process differs from membrane invagination and scission as found in autophagy, and mutants deficient in such invagination are not affected in vacuole membrane internalisation during fusion. Using the ratio between FM4-64 fluorescence and the fluorescence of GFP-tagged proteins known to be involved in docking and fusion, Wang et al. (2003) were able to show that vertex ring formation is mediated by the Rab-GTPase Ypt7p at the tethering step of fusion and that enrichment of proteins in the vertex ring follows an orderly hierarchical progression.

As with vesicle fusion, protein-targeting and homotypic vacuole fusion in *Sac. cerevisiae* are areas of intensive research and more information on their molecular biology can be found in a large number of reviews (for example, see Jones et al. 1997; Klionsky 1998; Wendland et al. 1998; Gerst 1999; Götte and Lazar 1999; Jahn and Südhof 1999; Mayer 1999, 2002; Pelham 1999a; Wickner and Haas 2000; Seeley et al. 2002; Wickner 2002; Jahn et al. 2003; Weisman 2003, 2006; Starai et al. 2005).

In *Ustilago maydis* expression of the GFP construct of a putative t-SNARE Yup1p showed labelling in a range of small cellular structures as well as on membranes of larger spherical vacuoles (Wedlich-Söldner et al. 2000). The Yup1 protein shows most similarity with a subgroup of t-SNARES which include Vam7p, a protein involved in endosome-to-vacuole targeting as well as in homotypic vacuole fusion in yeast (Sato et al. 1998; Ungermann and Wickner 1998). Comparison of FM4-64 localisation in pulse chase experiments with that of GFP-Yup1p and studies with *Yup1* mutants suggest that it labels an endosomal compartment as well as vacuoles in *U. maydis* (Wedlich-Söldner et al. 2000).

SNARE-type mechanisms may also mediate specificity of targeting and docking at the tips of tubules. If this is the case, organelle linkages via tubules have the potential for delivery of specific content to specific compartments, depending on control of fusion and fission in time and space. Retrograde transport between organelles is known to operate via tubules and there is evidence that some retrograde transport is mediated by SNARE-type reactions (see Pelham 1999a). Tubules transfer whatever is in their lumen to a recipient vacuole by diffusion until the contents of both equilibrate (see Sect. V.A.), but they must be targeted to specific locations. The behaviour of tubule tips after first contact with larger vacuoles suggests a repeated exploration of the vacuole surface until exactly the right position is found before the tip locks on and fusion occurs. Such behaviour indicates some kind of recognition event and is suggestive of an array of molecules at the tubule tips equivalent to, or the same as, those that mediate homotypic vacuole fusion in the classical in vitro assays. However, this behaviour of tubule tips on the surface of larger vacuoles also suggests that targeting molecules on the latter may not be uniformly distributed, at least at the time of contact. It is tempting to speculate that this may be a role for dynamins via an interaction with SNAREs (see Sect. II.E.).

III. Vacuole Motility and the Cytoskeleton

Fungal hyphae have longitudinally oriented networks of overlapping microtubules that often lie close and parallel to long tubules of tubular vacuole networks in basidiomycetes (Allaway 1994; Czymmek et al. 1996; Hyde et al. 1999) and in some electron micrographs appear to be attached to them (Hyde et al. 1999; Ashford et al. 2001). Elongate tubules of the vacuolar reticulum of the oomycete

Saprolegnia ferax also show a similar close relationship with longitudinal microtubules (Allaway et al. 1997). In *Pis. tinctorius* depolymerisation of microtubules with two anti-microtubule reagents, oryzalin or nocodazole, resulted in the disappearance of vacuolar tubules and transformation of tubular vacuole systems into a series of non-motile spherical vacuoles (Hyde et al. 1999). The effects were dose-dependent and reversible on drug removal. Immunolocalization of α-tubulin showed the expected disruption of the longitudinally oriented microtubule system with oryzalin. In contrast the three anti-actin drugs tested (cytochalasins B, D, latrunculin B), at levels which destroyed the actin caps and plaques, did not affect the tubular vacuole system, except that tubular vacuole frequency at the extreme hyphal tip increased (Hyde et al. 1999). Thus, both maintenance of tubular vacuole morphology and tubule movement in *Pis. tinctorius* are dependent on microtubules. Vacuole formation and movement along hyphae are also affected by microtubule depolymerisation in other mycelial fungi. Herr and Heath (1982) found that some anti-microtubule drugs disrupted vacuole positioning and organelle motility in the germ tube of *Uromyces phaseoli*. Microtubule depolymerisation in *Saprolegnia ferax* also suppressed vacuolation in hyphae recovering from various types of perturbation (Bachewich and Heath 1999).

In *Neurospora crassa* Steinberg and Schliwa (1993) found that vacuolar fragments moved at about the same velocity as mitochondria ($1.8\pm0.8\ \mu m\ s^{-1}$) on tracks that they also shared with refractive spherical particles that moved faster ($3.2\pm1.0\ \mu m\ s^{-1}$). They reported that nocodazole treatment resulted in cessation of movement of the particles and mitochondria and disappearance of microtubules, with recovery on drug removal, while cytochalasin D had no visible effect on intracellular motility. They suggested that long-distance vectorial transport of several organelles including vesicular organelles, some of which are presumably vacuole fragments, occurs along the same tracks and that these are microtubules. More recently movement of compartments, identified as endosomes (see Sect. II.F.), along microtubules labelled by GFP-tagged α-tubulin has been demonstrated in *Ustilago maydis* (Wedlich-Söldner et al. 2000).

Do microtubules act merely as support structures, or are they the tracks along which vacuolar tubules move and are directed to specific locations, and do they generate the forces for tubule movement? Organelles are moved along microtubules by microtubule motors: kinesins mostly to the "plus" end, which has a high polymerisation rate, and dyneins towards the "minus" end (Hirokawa 1998; Steinberg 1998, 2000; Yamashita and May 1998; see also Chap. 5 in this volume). Both kinesin and dynein are known to be involved in the movement of endosomes and lysosomal tubules in vivo (Hollenbeck and Swanson 1990; Harada et al. 1998; Hirokawa 1998) and tubule extension from the Golgi apparatus requires a kinesin-like motor (Allan and Schroer 1999). Membrane tubule formation and the development of branched tubular networks have been observed in vitro when kinesin-coated giant vesicles are added to a network of immobilised microtubules (Koster et al. 2003). Membrane tubules have also been shown to extend by their attachment to the dynamic plus-ends of elongating microtubules (Waterman-Storer et al. 1995).

In *Ustilago maydis* germ tubes, the microtubule cytoskeleton is bipolar with its focus on the nuclear region. Microtubule plus ends elongate from the nuclear region towards growing hyphal tips and polymerisation in the other direction is much more rare (Schuchardt et al. 2005; Lenz et al. 2006). Since organelles commonly show bi-directional movement, this implies a need for activity of both microtubule motors. What evidence is there that microtubule motors are responsible for tubular vacuole motility? Kinesins and dyneins are both present in mycelial fungi (Steinberg 2000; Xiang et al. 2000; Schoch et al. 2003; see also Chaps. 5 and 6 in this volume). Phylogenetic analysis by Schoch et al. (2003) indicates ten kinesins in the four filamentous ascomycetes they studied compared with a smaller set in *Sac. cerevisiae* and *Schizosaccharomyces pombe*. Similarly Schuchardt et al. (2005) identified ten genes with predicted kinesin motor domains in *Ustilago maydis*. Two of the kinesins (Kin1, Kin3) are up-regulated in hyphal cells, compared with buds, and are essential for continued hyphal extension, which involves the forward progression of organelles. Mutants deficient in either of the genes have bipolar growth and are unable to produce hyphal filaments, but they do not show disruption of the microtubules, suggesting that Kin1 and Kin3 have essential roles in microtubule-based traffic towards hyphal tips. Kinesins have also been shown to be involved in formation of the large vacuoles in the basal region of *Ustilago maydis* hyphae (Steinberg et al. 1998) and *kin3* is the only *kin* mutant to produce abnormal vacuolated regions (Schuchardt et al. 2005). Kin3p is known to be involved in early endosome motility (Wedlich-Söldner et al.

2002). Mutations of the conventional kinesin gene *NKIN1* in *Nectria haematococca* show altered mitochondrial positioning compared to the wild type (Wu et al. 1998). This contrasts with the effects of mutation of the *NKIN* gene in *Neurospora crassa* which did not apparently affect vacuole motility and positioning, and a dynamic tubular vacuole system was still seen (Seiler et al. 1997, 1999).

Participation of dyneins in vacuole movement in mycelial fungi is also indicated by work with mutants. Maruyama et al. (2002) found that vacuole positioning was disrupted in an *arpA* null mutant of *Aspergillus oryzae*. Arp1p is an actin-related major structural protein of the dynactin complex, which is thought to regulate the attachment of cargo (vesicles and organelles) to dynein (Karki and Holzbaur 1999; Schroer 2004). Mutations of Arp1 abolish localisation of cytoplasmic dynein at hyphal tips. Seiler et al. (1999) also found alterations of vacuole distribution in a cytoplasmic dynein mutant of *Neurospora crassa*. In this case vacuoles accumulated at the tips of hyphae. More recently, Lenz et al. (2006) have shown that compartments identified as early endosomes move in both directions along microtubules that are oriented with their plus ends towards hyphal tips in *Ustilago maydis*. Analysis of mutants suggests that Kin3p and dynein act in concert to regulate long-distance transport of early endosomes. They further showed that dynein, dynactin and Lis (a dynein activator) all accumulate at the microtubule plus ends in the hyphal tips (an activity which itself is dependent on kinesin; Zhang et al. 2003). Here they remain as a reservoir of motors until they pick up a cargo of endosomes (Lenz et al. 2006). The dynein is then able to move in a retrograde direction with its cargo. This concept requires organelles to reach the tip before they can attach to dynein and be carried back in a retrograde direction. It contrasts with mammalian systems where kinesin and dynein motors are located on the same organelle. Earlier observations by Xiang et al. (2000) of the movement of fluorescent GFP-NudA labelled dynein to hyphal tips followed by retrograde movements in *A. nidulans* germlings indicated a similar process in mycelial fungi. However, it is difficult to see how such a mechanism alone could account for the diversity of motility seen in tubular vacuole systems.

Microtubules themselves undergo rapid directed motility (Steinberg et al. 2001). They glide along one another and the organisation of the microtubule-based cytoskeleton and its polarity depend on motor protein-based transport of assembled microtubules, a process that in *Ustilago maydis* is known to require both dynein and kinesin (Fink and Steinberg 2006; Straube et al. 2006). The model of "cut and run", where microtubules are enzymatically severed into shorter lengths that are mobile (Baas et al. 2005), would provide a motive force that fits well with observed tubular vacuole movements, especially if specific parts of the vacuole system are attached to such microtubule fragments. This activity is currently viewed as a means of reorganising the microtubule cytoskeleton but could equally well provide great flexibility of organelle movement. However, the extent to which movement of vacuoles (and other organelles) is due to their direct movement on microtubule tracks driven by motors, or due to gliding of microtubules along each other, remains to be seen.

Not all fungi depend primarily on microtubules for organelle movements. Though normal morphology of the *Sac. cerevisiae* vacuole system is reported to require microtubule integrity (Guthrie and Wickner 1988), movements of the tubular vacuoles of the yeast segregation structure do not. Their movements and those of other organelles during bud development occur on actin-based mechanisms that are reported to be similar to those that occur at the cell periphery of higher eukaryotes (Weisman 2006). Movement is driven by the myosin-V motor Myo2p, the product of *MYO2*, a gene essential for vacuole inheritance in yeast. The globular tail of Myo2p has a cargo-binding region specific for its attachment to vacuoles and this is distinct from the region specific for its attachment to secretory vesicles (see references in Weisman 2006). There are two tightly associated subdomains in the Myo2p tail that correlate with these two functions – and mutations in one subdomain that affect one do not affect the function of the other, and neither can function alone. There is evidence that microfilaments are also instrumental in mitochondrial movement in *Sac. cerevisiae* but not in *Sch. pombe* (reviewed by Westermann and Prokisch 2002).

A demonstrated involvement of microtubules does not exclude a role for actin filament-based motility in vacuole or other organelle movements. Interactions between the different components of the cytoskeleton are complex and many, and in other systems organelles appear to carry a complex assemblage of motor proteins that allow shifts from microtubule- to actin-based motility (reviewed by Allan and Schroer 1999; Brown 1999; Wu et al. 2006).

IV. Vacuolar Content

A. Probing the Content of Individual Vacuoles

The composition and state of the material inside vacuoles are important because they affect physiology and exchanges with the cytoplasm and, importantly in the context of this review, they determine what might undergo longitudinal transport in vacuoles. For example, it is important to know whether polyphosphate, known to be stored in vacuoles and thought to be the predominant form of P transferred, occurs in granules or as a dispersed form. What people think vacuoles contain, however, depends largely on technique and so this needs careful analysis.

With the light microscope in vivo, vacuoles of mycelial fungi usually appear clear under bright-field optics. Using fluorescent vacuolar dyes, vacuoles of live cells are typically filled uniformly with fluorescent material (Figs. 2.1, 2.4A; and see Figs. 1–3 in Cole et al. 1998; Uetake et al. 2002; Darrah et al. 2006), although there are sometimes non-fluorescent inclusions (e.g. Fig. 1d–f in Saito et al. 2006). Vacuole contents are usually seen to be uniform in *Sac. cerevisiae*, in vacuole-fluorescent (*ade*) mutants (Weisman et al. 1987; Weisman and Wickner 1988), or where fluorescent probes accumulate within vacuoles (e.g. Riezman 1985; Weisman et al. 1987; Zheng et al. 1998). Small membranous inclusions are clearly visible, however, in otherwise uniform yeast vacuoles following vacuole fusion (Wang et al. 2002, supplementary material, movies) or invagination of the bounding membrane (Müller et al. 2000). Under DIC optics, vacuoles of living mycelial fungi also usually appear clear, although occasional inclusions can be seen (Orlovich and Ashford 1993; Hyde and Ashford 1997; Bücking and Heyser 1999; Shoji et al. 2006). There is a special case, macroautophagy, where vacuoles contain

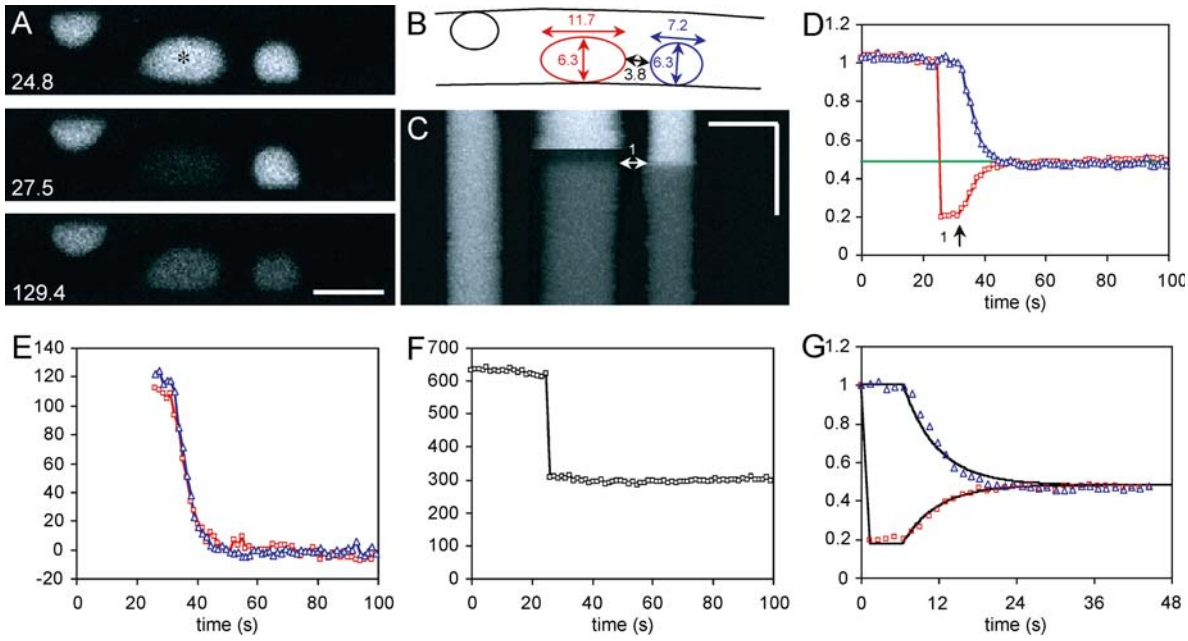

Fig. 2.4. FRAP measurement of longitudinal transport between rounded vacuoles interconnected by a tubule. The tubule, which formed between the middle and right-hand vacuoles, cannot be seen in this optical slice. **A** *top* Three vacuoles, with an *asterisk* indicating the vacuole that was to be photobleached, *centre* immediately after the middle vacuole had been photobleached, *bottom* after recovery. Times indicated are in seconds. **B** Dimensions (μm) of the middle and right-hand vacuoles and the tubular connection that formed between them. **C** Corresponding (x, t) image, *arrows* **1** indicate the inception of the tubular connection between the middle and right-hand vacuoles, about 7 s after photobleaching. **D** The intensity trace for the bleached vacuole (*red squares*) and its right-hand neighbour (*blue triangles*): the final position converged on the predicted equilibrium (*green line*). *Arrow* **1** as in **C**. All the material appearing in the bleached vacuole was matched by a symmetrical loss from its neighbour (**E**), maintaining mass conservation (**F**). Exchange between the two vacuoles was well described by a diffusion model (**G**, *solid lines*). *Bars* horizontal 10 μm, vertical 60 s. From Darrah et al. (2006) by permission of the American Society for Microbiology

often large, usually membranous, inclusions (Abeliovich and Klionsky 2001); this is dealt with separately in Sect. V.B.

Latest electron microscopy cryo-preparative methodology involves minimal chemical interference with the specimen, so that results are nearer to the in vivo state than achievable with chemical fixation (see Sect. II.B.). In ultrathin frozen sections in TEM, hyphal vacuole profiles appear to be uniformly filled with finely granular contents (Frey et al. 1997, 2000). In freeze-substitution TEM, the vacuole profiles of pathogenic yeasts *Cryptococcus neoformans* (Yamaguchi et al. 2002a) and *Exophiala dermatitidis* (Yamaguchi et al. 2002a, b, 2003; Biswas et al. 2003) – while heterogeneous possibly because of freezing damage – are mostly without inclusions. Freeze-substituted mycelial fungi typically show fine dispersed material in the vacuoles (Fig. 2.5A, B), with occasional inclusions (Fig. 2.5C; and see Orlovich and Ashford 1993; Cole et al. 1998; Ashford et al. 1999; Vesk et al. 2000). Bücking and Shachar-Hill (2005) reported electron-opaque granules as well as electron-lucent areas in vacuoles of freeze-substituted *Glomus intraradices*, but did not present micrographs. In freeze-dried tissue, however, electron-opaque aggregations in vacuoles have frequently been described and analysed (Frey et al. 1997; Bücking and Heyser 1999; Hauck et al. 2002; Paul et al. 2003). In chemically fixed hyphae polyphosphate occurs as electron-opaque vacuolar granules (e.g. Ashford et al. 1986; Bücking et al. 1998; Kottke et al. 1998). DIC observation of hyphae during chemical fixation, however, has shown that polyphosphate granules form during the chemical fixation procedure (Orlovich and Ashford 1993); observation of vacuolar inclusions in vivo and separate observation of polyphosphate granules after chemical fixation (Bücking and Heyser 1997, 1999) does not invalidate this result.

In summary, fungal vacuoles in vivo usually have uniform contents, with few inclusions except for membrane-enclosed vesicles (see Sect. V.C.). With minimal preparation damage they are also seen in TEM, usually to contain uniformly dispersed material with some membranous inclusions. This conclusion has been spectacularly corroborated in the elegant work of Saito et al. (2005, 2006), described briefly below. It is particularly important because of its consequences for transport within the fungal vacuole system (Sect. V.A.).

To identify the chemical nature of vacuolar contents, it would be preferable to make measurements in vivo. Probing fungal hyphae with microelectrodes could be a possibility, but is difficult because hyphae and their vacuoles are so small (c.f. Chap. V. in this volume). Analysis of cell fractions enriched in vacuoles (Martinoia et al. 1979; Vaughn and Davis 1981; Förster et al. 1998; Trilisenko et al. 2002) and NMR spectroscopy of whole tissue provide much valuable information but can only determine the average composition and metabolic activities of populations of vacuoles. NMR as applied to ectomycorrhizal fungi has been reviewed by Martin (1991). X-ray microanalysis and electron energy-loss spectroscopy can provide information about elemental composition of individual vacuoles. Essentially the comments in the above paragraphs apply to the preparation for these techniques, with yet further constraints (see Ashford et al. 2001). It is now well understood that chemical fixation changes membrane permeability from that in vivo and, in an aqueous environment, ion loss, redistribution and exchange all occur according to basic rules of chemistry. Localisations obtained after such preparative procedures are likely

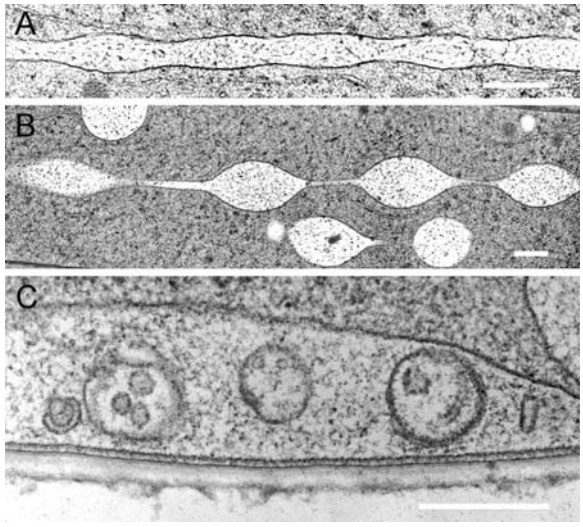

Fig. 2.5. Profiles of tubular vacuoles in TEM sections of freeze-substituted *Pisolithus* hyphae. **A** An elongate tubular vacuole, which was oriented parallel to the long axis of the hypha. Uniform dispersed contents. From Ashford and Orlovich (1994) copyright American Society of Plant Biologists, by permission. **B** Varicosities alternate with very narrow portions of a tubular vacuole, nearly parallel to the long axis of the hypha. Most of the contents are uniform. From Shepherd et al. (1993a) reproduced with permission of the Company of Biologists. **C** A vacuole closely appressed to the plasma membrane and cell wall. This vacuole contains multivesicular inclusions. From Cole et al. (1998) reproduced with permission from Elsevier. *Bars* 0.5 μm

to bear little relationship to those in living cells and must now always be disregarded. Cryopreparation is essential. Use of frozen-hydrated specimens can avoid element redistribution, but in frozen bulk specimens small vacuoles cannot be differentiated in analysis from surrounding cytoplasm. Ultrathin frozen sections are difficult to manage but in skilled hands give much better analytical resolution (Frey et al. 1997, 2000). To remove ice from frozen specimens by freeze-substitution, special care is required to avoid redistribution of ions: strictly anhydrous, non-polar reagents must be used, a water-attracting molecular sieve must be added to the substitution fluid and resin at all steps and the sections must be cut dry, kept dry and analysed as soon as possible (Canny and McCully 1986; Orlovich and Ashford 1995). In some cases freeze-drying has been employed before anhydrous substitution (Frey et al. 1997; Bücking et al. 1998) although shrinkage is clearly visible and brings detailed localisations into question.

So, what information about polyphosphate do we have from the most reliable modern techniques? In ultrathin frozen sections, hyphal vacuole contents average about 100–200 mmol P kg^{-1} DW by X-ray microanalysis (Frey et al. 1997, 2000). X-ray microanalysis after anhydrous freeze-substitution typically shows that fungal vacuoles are P-rich and may also contain large amounts of S (Orlovich and Ashford 1993; Cole et al. 1998; Ashford et al. 1999; Vesk et al. 2000). Histochemical and ^{31}P NMR data indicate that much of the P stored in vacuoles of actively growing mycelium and mycorrhizae occurs as polyphosphate, though the relative amounts of polyphosphate and orthophosphate vary according to growth conditions, the state of the hyphae and probably the fungal species (Ashford et al. 1986, 1994; Grellier et al. 1989; Gerlitz and Werk 1994; Martin et al. 1994; Gerlitz and Gerlitz 1997; Rasmussen et al. 2000; Ezawa et al. 2003; Viereck et al. 2004). Saito et al. (2005) developed an antibody technique to localise polyphosphate, based on a recombinant polyphosphate-binding domain of *Escherichia coli* exopolyphosphatase. They applied this to freeze-substituted sections of *Sac. cerevisiae* (Saito et al. 2005) and *Phialocephala fortinii*, a mycelial fungus (Saito et al. 2006). Using confocal microscopy with fluorescent antibody they demonstrated that polyphosphate is distributed throughout the vacuoles (Fig. 2.6A). With TEM and colloidal gold-labelled antibody, in yeast the polyphosphate was distributed throughout the vacuole, but it was not entirely uniform (Fig. 2.6B); in *P. fortinii*, label was generally uniform in any one vacuole profile, although there were unlabelled inclusions in some vacuoles (Fig. 2.6C,D).

In freeze-substituted hyphae of *Pis. tinctorius* P is co-localised in the vacuoles with K, but not with Ca, and is found dispersed throughout the vacuoles (Orlovich and Ashford 1993; Cole et al. 1998;

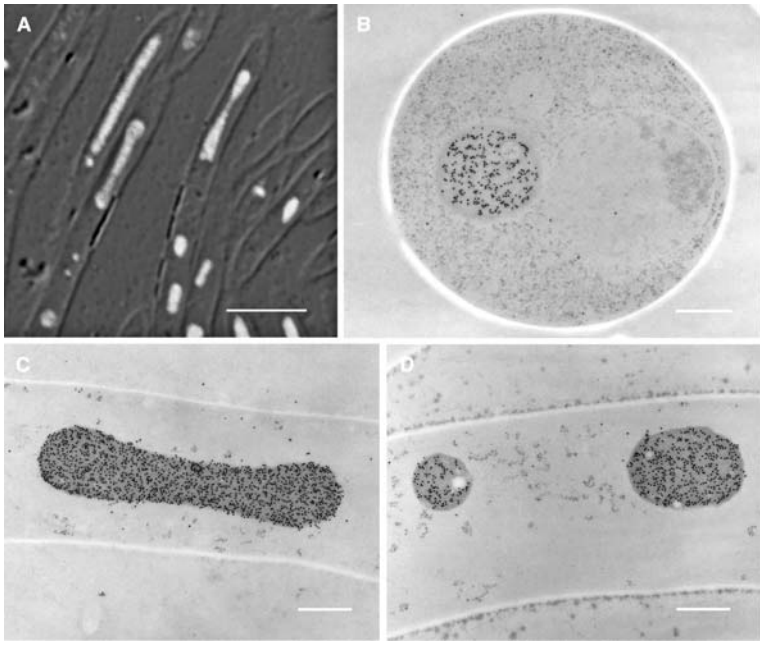

Fig. 2.6. Micrographs of the distribution of polyphosphate, labelled with PPBD-anti-Xpress antibody complex, followed by anti-mouse IgG antibody conjugated with Alexa 488 (**A**) or 10-nm colloidal gold (**B**, **C**, **D**). **A** Confocal microscope image showing dispersed polyphosphate in elongated vacuoles of *Phialocephala fortinii* hyphae. *Bar* 5 µm. **B** TEM of a section of a *Saccharomyces cerevisiae* cell: polyphosphate is again dispersed through the vacuole profile, although it is not completely uniform. *Bar* 0.5 µm. **C** TEM image of dispersed polyphosphate in an elongated vacuole profile of *P. fortinii*. *Bar* 0.5 µm. **D** *P. fortinii* vacuole profiles, labelled for polyphosphate, but also showing small unlabelled regions. *Bar* 0.5 µm. From Saito et al. (2005 by permission of the American Society of Microbiology (**B**) and Saito et al. (2006) by permission of the National Research Council of Canada (**A**, **B**, **C**))

Ashford et al. 1999; Vesk et al. 2000). In freeze-dried material Bücking and Heyser (1997, 1999) and Bücking et al. (1998) analysed vacuolar aggregations of material, finding Mg and K, but not Ca, co-localised with P. A biochemical approach has indicated that a biochemical approach has indicated that *Sac. cerevisiae* vacuoles Ca^{2+} occupies only a very small percentage of the binding-sites of polyphosphate (Dunn et al. 1994).

Nitrogen compounds are stored together with P in vacuoles. Association of polyphosphate with basic proteins and amino acids in vacuoles is well established in yeasts and mycelial fungi (Dürr et al. 1979; Cramer et al. 1980; Kanamori et al. 1982; Legerton et al. 1983; Kitamoto et al. 1988a, b; Klionsky et al. 1990; Young et al. 1993). *Sac. cerevisiae* and *N. crassa* both concentrate basic amino acids in the vacuole to higher levels than in the cytosol (Klionsky et al. 1990; Keenan et al. 1998). For example more than 95% of cellular arginine is located in the vacuole in *N. crassa* (Keenan et al. 1998). Several vacuolar permeases for transport of basic amino acids have been characterised in *Sac. cerevisiae* and *N. crassa* and at least three transport systems are involved in the transport of arginine across the vacuolar membrane in yeast (Opekarová and Kubín 1997). Proteins accumulated in vacuoles include hydrolytic enzymes. There exists a large body of literature on protein targeting to vacuoles, especially in *Sac. cerevisiae*, showing that it occurs by more than one pathway (see Sect. V.B.; see also Table 1.6 in this volume). The role of the vacuole in storage of nitrogen compounds supports a role for them in N transport as well as in P transport.

B. Probes, Vacuole pH and ATPase

Several methods are available to estimate the pH of vacuoles. These include nuclear magnetic resonance (NMR) spectroscopy and changes in the emission of fluorescent probes that have accumulated in vacuoles. Using ^{31}P-NMR spectroscopy Greenfield et al. (1987) estimated that the vacuolar pH was lower (pH 6.28±0.10) in *Sac. cerevisiae* stationary cells than that in cells in logarithmic growth (pH 6.58±0.14), compared with the respective cytoplasmic pH values of 7.19±0.05 and 6.97±0.12. Similarly^{15}N-NMR indicates a vacuolar pH of 6.1± 0.04 based on arginine resonance shifts (stored in the vacuole) and a cytoplasmic pH of 7.15±0.10 based on alanine and proline resonance shifts (Legerton et al. 1983).

Many fluorescent probes are available to measure pH (Haugland 2001). Those useful for vacuoles must be selectively accumulated in them and have the appropriate fluorescence characteristics. Useful probes include 5- or 6-carboxyfluorescein (5- or 6-CF), CDCF, 2′,7′-bis-(2-carboxymethyl)-5 (and -6)-carboxyfluorescein (BCECF), SNARF and carboxySNAFL (Tsien 1989; Davies et al. 1990; Haugland 2001). These are usually loaded into the cells as membrane-permeant esters. Ratio imaging and flow cytometry of wild-type *Sac. cerevisiae* cells loaded with 6-CF showed them to have an average vacuolar pH of 6.1, while a mutant deficient in vacuolar H^+-ATPase had an average vacuolar pH of 7.1 (Preston et al. 1989; Yamashiro et al. 1990). Dye ratio imaging allows analysis of the pH of individual vacuoles (Rost et al. 1995) – an important advantange as pH can vary between individual vacuolar compartments. This issue is not resolved by flow cytometry and NMR, which can only provide average values for vacuole populations. For example, the average pH for phosphate-storing vacuoles in ectomycorrhizal fungi as determined by ^{31}P NMR was pH 5.0, with a cytoplasm at pH 6.0–6.5 (Martin 1991). However, ratio imaging of 6-CF-loaded *Pis. tinctorius* vacuoles showed that the pH of the large vacuoles in tip cells ranged over pH 4.3–7.5 and in the penultimate cells pH 4.8–7.2. The modal pH values suggested a tendency for the vacuoles to become more acid as they aged (Rost et al. 1995).

All techniques indicate that vacuoles are more acid than the cytoplasm. Vacuole acidification plays a key role in ion transport, protein sorting, proteolytic processing and regulation of cytoplasmic pH (Stevens and Forgac 1997). The vacuolar H^+-ATPase (V-ATPase) is responsible for acidification of the vacuole lumen and for coupling energy release with transport across the vacuole membrane (Stevens and Forgac 1997; Nelson and Harvey 1999) and its activity is required for polyphosphate synthesis in yeast (Ogawa et al. 2000). The vacuolar H^+-ATPase of *Sac. cerevisiae* is the best characterised member of the V-type ATPase family (Uchida et al. 1985; Kane et al. 1989; Forgac 1999; Graham et al. 2000; Kane 2006) and the *N. crassa* enzyme appears to have a similar subunit composition (Margolles-Clark et al. 1999). The enzyme consists of a multisubunit complex (V_0) of integral and peripheral membrane proteins which, together, form the H^+ translocating channel. They are connected to a cytoplasmically located V_1 complex, which contains the ATP catalytic domain of six subunits and two or more stalk domains that connect the catalytic

headgroup with the membrane channel. Hydrolysis of ATP by the V_1 domain causes stalk rotation resulting in proton transport through the V_0 translocating channel (Kane 2006). Reversible disassociation of the V_1 and V_0 domains is one of several possible mechanisms for regulating V-ATPase activity and, hence, regulating vacuolar acidification (reviewed by Forgac 1999; Kane 2006). Antibodies to various *Sac. cerevisiae* V-ATPase subunits are commercially available (Haugland 2001). They have the potential to label vacuolar membranes in mycelial fungi. Specific, potent V-ATPase inhibitors such as bafilomycin A and concanamycin A, both macrolide antibiotics, have been instrumental in defining the relative roles of vacuolar and plasma membrane H^+-ATPases in cytoplasmic regulation in wild-type and various mutants of *N. crassa* (Bowman et al. 1997; Bowman and Bowman 2000). Bafilomycin and concanamycin are thought to inhibit the enzyme by binding largely to the c subunit of the V-ATPase complex and preventing rotation of the c subunits, a situation very similar to that between another macrolide antibiotic, oligomycin, and F_1F_0-ATP synthases, where the antibiotic also binds to c subunits at the interface with subunit a (Bowman et al. 1988, 2004; Bowman and Bowman 2002).

V. The Functions of Motile Vacuole Systems

Of the many diverse roles of vacuole systems in fungal cells we focus here on some aspects of function relevant to vacuole motility and differentiation.

A. Transport in Vacuoles along Hyphae

Motile tubular vacuole systems are obvious candidates to function as conduits for longitudinal transport along hyphae. The longitudinal arrangement of vacuolar tubules has been taken to imply that they have a role in longitudinal transport. The connection of larger vacuoles in older hyphae by tubules is well established and observations of movement of fluorochrome in varicosities along them are documented (see Fig. 3 of Cole et al. 1998). This led to the hypothesis that the vacuole compartment has a role to play in the transport of substances normally stored there, in particular P and N compounds (see reviews by Ashford and Orlovich 1994; Ashford 1998).

This idea is attractive because the vacuole can provide a conduit separate from the cytoplasm in which materials could be moved independently. However, demonstration of transport within the vacuole has been elusive until a recent report by Darrah et al. (2006). This work used FRAP, where a fluorochrome is locally bleached by irradiation, following which the reappearance of fluorescence due to a movement of fluorochrome from other areas is observed. Quantitative measurement of fluorescence allows calculation of fluorochrome concentration, microscopic measurement allows vacuolar volume to be calculated and, as a result, rates of movement of fluorochrome can be determined.

Darrah et al. (2006) applied carboxy-DFFDA to hyphae of rapidly growing cultures of *Pha. velutina*. The fluorochrome carboxy-DFF^- accumulates in rounded vacuoles connected by tubules. The vacuoles move about, join, separate and rejoin, as in other fungal species (cf. Shepherd et al. 1993a; Rees et al. 1994; Cole et al. 1998). After photobleaching, the movement of fluorochrome within large vacuoles takes place at a rate which is consistent with diffusion. Where vacuoles are connected by tubules, fluorochrome moves between them at rates also explicable by diffusion through narrow interconnecting tubes (Fig. 2.4). Disconnection of tubules stops the flow; reconnection allows it to begin again. All fluorochrome accumulating in a previously bleached vacuole can be accounted for by the loss of fluorochrome from its connected neighbour, indicating that transport through the connecting tubule is involved (Fig. 2.4F). Multiple connections and disconnections can be observed: the pathway for diffusion can be simple or complex depending on the local architecture of the vacuole system. Similar conclusions can be drawn for regions near the hyphal tip where the vacuoles consist mainly of small rounded compartments interconnected by tubules.

These observations provide clear evidence that a solute (in this case the fluorochrome carboxy-DFF^-) can move between vacuoles on a local scale by diffusion along the tubules that connect them. Darrah et al. (2006) extended their observations by computer modelling of longer strings of vacuoles and tubules. The models used a range of sizes of vacuoles and tubules, and frequencies of connection and disconnection, measured on living hyphae, with diffusion coefficients estimated from the FRAP measurements. The modelling indicated that, over a 2 mm length, diffusion within the vacuole system could be between 0.5% and 1.7% of the

rate that would occur if the whole hyphal lumen were available for diffusive transport. Using data from the literature for the supply of nitrogen compounds to growing hyphal tips, Darrah et al. (2006) calculated that diffusion within the vacuole system could be sufficient as a transport mechanism. It is not intended to imply that tubular vacuoles must actually be the main transport route for nitrogen compounds, but the calculation demonstrates that diffusion within tubular and larger vacuoles can be physiologically significant over millimeter scales (see also Bebber et al. 2006).

What are the consequences of diffusive transport in tubular vacuoles? Diffusion within a compartment depends on the diffusion coefficient, the concentration gradient and the dimensions of the compartment. It follows as a crucial consequence that, as long as the compartment remains intact, solutes inside it must move throughout it – indeed, they cannot be prevented from doing so. The tubular nature or tubular connections of vacuoles in hyphae therefore bring everything inside the vacuole to every part of the hypha. Tubules of the vacuole cross septa from cell to cell (e.g. Shepherd et al. 1993b) so the diffusive pathway extends beyond the individual cell. Where there is good information on the solute contents of vacuoles (see Sect. IV.A.) we can conclude that those solutes are transported throughout the connected system. Control of this movement of "everything that is inside" can be brought about by disconnection and reconnection of tubules or by movement of tubules and spherical vacuoles themselves within the hypha. The loading of materials at specific sites, and unloading elsewhere, then determines the direction of diffusion within the vacuolar system; and the rates of loading and unloading influence transport rates through altering the concentration gradients. It is noteworthy that transport by diffusion regulated in this way by loading and unloading can occur in opposite directions within the same vacuolar lumen – for example if, say, in a mycorrhizal fungus phosphate were loaded into the vacuolar system near the hyphal tip and unloaded where the hypha is nearer to the plant root, while plant-synthesised sugar were loaded into the vacuolar system at the base and unloaded wherever needed throughout the hypha, bidirectional diffusion of the two solutes would be taking place within the same vacuole. This capacity of the vacuole system to conduct everything that is inside it to everywhere the vacuole reaches places new emphasis on the need to understand the processes of vacuolar loading and unloading. If the vacuole is to function in this way the precise localisation of these processes is crucial. We need to work at finding out whether loading sites, either for vesicle fusion or for intrinsic membrane transport proteins, are so localised.

Because of the physical laws that govern it, diffusion within the vacuolar lumen has the greatest transport potential where the vacuole is large. However, the importance of tubular reticulum – the form of vacuole found in most hyphal tips – can now be understood. In these tip cells, cytoplasmic activities associated with growth and uptake are highly important and the cytoplasm accordingly occupies a large proportion of the cell volume. The tubular vacuolar reticulum, however, allows vacuolar diffusive transport to reach every part of the tip cells, including very close to the extreme tip, as the tubular reticulum moves along keeping pace with cell growth (see Sect. II.D.). The motility of the tubular vacuolar reticulum at the hyphal tip is significant in bringing the discrete vacuolar diffusive conduit to that area as well as in actually moving material by the motility itself. Motility, including peristalsis-like movements and movements of small rounded vacuoles along tubules (Cole et al. 1998), would be expected to increase the speed of transfer of contents over and above that of diffusion.

Vacuoles and vacuolar tubules provide for transport throughout all parts of the organism in an isolated compartment, so the concentrations of material undergoing this transport need have no effect on the cytoplasm along the way. This is important: in the above hypothetical example, the transport of phosphate (in any form) within the vacuole would have no effect on the energy charge of the cytoplasm; the transport of sugar would not affect metabolism.

Vacuolar diffusive transport operates in ways that differ significantly from vesicle-mediated transport. Within the vacuole, diffusion is nonspecific and may occur over long distances without necessitating much expenditure of energy along the pathway. Net diffusion can only occur down concentration gradients. The velocity of vacuolar diffusive transport is regulated both by the size and number of connecting tubule(s) and by the concentration gradient which depends on loading and unloading. Vacuolar tubules are under cytoskeletal control. Connection, disconnection, motility, extension and retraction (i.e. pleiomorphy) can regulate the vacuolar pathway. Transport in vacuolar tubules by diffusion can occur without

concomitant transfer of membrane. Targeting and precision of vacuolar tubules are, however, yet to be elucidated. Vesicle-mediated transport, in contrast, is often very specific, may go against concentration gradients, is influenced by both cytoplasmic streaming and the cytoskeleton, involves transfer of membrane as well as contents (and therefore requires membrane-retrieval mechanisms) and has special uptake, release and targeting mechanisms that are becoming understood. Another example that is consistent with this diffusion model of vacuolar function is the transfer of content in the yeast segregation structure (Weisman 2003).

In a cultured ectomycorrhizal association between *Pis. microcarpus* and *Eucalyptus pilularis*, Allaway and Ashford (2001) showed that tubular vacuoles were present throughout the extraradical mycelium and ectomycorrhizal structures, but they were unable to demonstrate that the vacuoles acted as a transport conduit. When the probe 6-CFDA was applied to sites at or near the growing hyphal front of extraradical mycelium, fluorescence accumulated at the site of application but was not detected elsewhere. There are several possible explanations for these negative results, including physiological status of the system and potential toxicity of the fluorochrome.

Arbuscular mycorrhizal (AM) fungi may be a special case in which tubular vacuoles are particularly important. Uetake et al. (2002) demonstrated extensive tubular vacuoles in vivo in many parts of the mycelium of *Gigaspora margarita*. Tubular vacuoles did not follow the same paths as the well known cytoplasmic streaming of small particles, lipid bodies and nuclei, although they were also longitudinal in orientation. Tubular vacuoles were abundant in germ-tubes and extra-radical hyphae cultured on onion seedlings. They were infrequently seen in intraradical hyphae, and arbuscules were too small for vacuoles within them to be discerned. Extensive tubular vacuoles have been observed in another arbuscular-mycorrhizal fungus, *Glomus intraradices*, grown on cultured carrot roots (Olsson et al. 2002; S.J. Nielsen, personal communication). In both these AM fungi, rounded vacuoles were also present and tubular vacuoles were fragile: some of the rounded vacuoles could be due to damage of tubular systems. These observations were made in vivo: again, they offer a strong contrast with the "standard" picture of the vacuoles in these fungi as demonstrated by electron microscopy after the introduction of structural artefacts by chemical fixation (c.f. Ashford 2002).

The significance of the extent of tubular vacuoles in AM fungi may lie in the obligately biotrophic nature of these organisms. They rely absolutely on the transport of sugars from the host root, while themselves taking up and transporting mineral nutrients to that root. Transport is therefore of even more crucial importance for these fungi than for others and the highly developed tubular vacuole system appears very suitable for this transport. As described above, diffusion within the extensive tubular vacuole system would transport materials everywhere in the hyphae and the rate and direction of movement would depend on sites and rates of loading and unloading. It is now time to re-evaluate the long-accepted story of AM fungal transport of nutrients, particularly P, in small rounded vacuoles by cytoplasmic streaming. Freeze-substitution and analysis of frozen sections of AM fungi are required. For further consideration of AM, see Chap. 12 in this volume.

B. Vacuoles, Protein Targeting and the Endocytic Pathway

Fungal vacuoles, like mammalian lysosomes, contain hydrolases and are lytic organelles (Klionsky et al. 1990). As such they are the final compartment of both protein sorting and endocytic pathways (Gruenberg and Maxfield 1995). These pathways have been systematically and intensively studied and various steps dissected by the use of mutants and other molecular approaches in *Sac. cerevisiae* (Wendland et al. 1998; Pelham 2002).

The endocytic pathway in yeast is considered to consist of three functionally distinct compartments, traditionally known as early endosomes, late endosomes and lysosomes (vacuoles), which act in concert and show both similarities and differences with those in animal cells (Pelham 2002). Late endosomes are closely associated with vacuoles and are often called "prevacuolar compartments" or "prevacuolar endosomes" (PVE). They are identified in yeast as the last sorting compartment before the vacuole at the intersection between the endocytic pathway and the classical carboxypeptidase Y (CPY) protein sorting pathway from the Golgi to vacuoles, a pathway followed by a number of vacuolar hydrolases including CPY (Vida et al. 1993). The PVE is recognised as the compartment that becomes enlarged in class E vacuole protein sorting (*vps*) mutants where a step in the vacuole protein sorting pathway is blocked (see Raymond

et al. 1992a; Vida and Emr 1995). Vacuolar hydrolases and endocytic markers both accumulate in this compartment in class E *vps* mutants (Rieder et al. 1996). The compartment contains the t-SNARE Pep12p whereas the t-SNARE on the vacuole membranes is Vam3p. Early endosomes, also called post-Golgi endosomes by Pelham (2002), relate to and recycle molecules with the plasma membrane. They contain a different subset of specific markers – including Tlg2p, another compartment-specific t-SNARE – and are involved in recycling molecules to the plasma membrane. There is also traffic between this compartment and the Golgi. Early endosomes also sort molecules that will travel further to vacuoles via late endosomes. These transient "sorting" compartments are tubular-vesicular. Sorting endosomes are viewed as separate from the "recycling" components of early endosomes, which are also tubular, and they mature within minutes into late endosomes, with a concomitant drop in pH (Maxfield and McGraw 2004). In fact eukaryote endocytic trafficking pathways are much more complex and endosomal compartments less stable over time than was formerly thought (Maxfield and McGraw 2004). This makes it more difficult to distinguish and clarify compartments of the endocytic pathway and the situation is reflected in the instability in their nomenclature.

Early information on compartments of the endocytic pathway in yeast was obtained by study of internalisation of α-factor and its receptor Ste2p. This mating pheromone passes through the endocytic pathway and sequentially accumulates in early and late endosomes before its degradation in the vacuole (Singer-Krüger et al. 1993; Wendland et al. 1998). Immunofluorescence of the α-factor receptor shows its accumulation also in a peripheral "early endocytic" compartment and later in a larger compartment near the vacuole (Hicke et al. 1997). Internalisation of positively charged nanogold particles by wild-type *Sac. cerevisiae* sphaeroplasts (protoplasts) has also been used to examine compartments of the endocytic pathway by electron microscopy (Prescianotto-Baschong and Riezman 1998). Gold particles are restricted to the plasma membrane at 0 °C, but on raising the temperature to 15 °C they are rapidly internalised first to small vesicles, then to peripheral vesicular/tubular compartments often with a horse-shoe shape and identified as early endosomes, later to multivesicular bodies and finally to the vacuoles. Multivesicular bodies (MVBs) are equated with late endosomes in *Sac. cerevisiae* (Piper and Luzio 2001; Shaw et al. 2003), though they may not represent the entire compartment. MVBs are formed as early endosomes mature by invagination of the limiting membrane into the lumen of the compartment to produce internal vesicles. During the process a subset of membrane proteins is sorted to these vesicles. It is clear from recent work that there are complex dynamic interactions between the limiting and internal membranes of MVBs (see Schmid and Sorkin 2002) and in freeze-substituted hyphae many MVBs are tubular not ovoid (L. Cole, D.A. Orlovich, A.E. Ashford, unpublished data). MVBs/late endosomes are reported to fuse directly with lysosomes in animal cells (Futter et al. 1996; Mullock et al. 1998) and vacuoles in yeast (Reggiori and Pelham 2001).

Much of the information about trafficking steps along the pathway and evidence for early and late endosomal compartments in *Sac. cerevisiae* comes from studies with mutants. For example, a mutant deficient in recycling (*rcy1*) has an early block in the endocytic pathway prior to the intersection with the vacuole sorting pathway (Wiederkehr et al. 2000). Mutation of *RCY1* leads to accumulation of an enlarged compartment that contains the t-SNARE Tlg1p and lies close to areas of cell expansion. The endocytic markers Lucifer Yellow, FM4-64 and Ste2p are all found in a similar enlarged compartment after their internalisation. This is identified as an early endosomal compartment. This compartment recycles membrane rapidly to the cell surface in *Sac. cerevisiae*, thus balancing high rates of membrane internalisation via endocytosis. The internalisation of the α-factor receptor Ste2p and other membrane proteins including transporters depends on their ubiquitination (Riezman 1998; Wendland et al. 1998; Hicke and Dunn 2003). The addition of ubiquitin acts as a signal in targeting membrane proteins into the endocytic pathway, not only at the plasma membrane internalisation step but also at later stages by targeting some proteins into the internal vesicles of multivesicular bodies (Hochstrasser 1996; Roth et al. 1998; Katzmann et al. 2001, 2002; Piper and Luzio 2001; Reggiori and Pelham 2001; Urbanowski and Piper 2001; Pelham 2002). The role of ubiquitylation in membrane targeting and transport is reviewed by Staub and Rotin (2006).

Although a lot of information about the molecular pathways for protein targeting and sorting and for endocytosis has been gained from genetic investigations in yeast (for recent reviews see Riezman 1998; Geli and Riezman 1998; Wendland et al.

1998; D'Hondt et al. 2000; Piper and Luzio 2001; Katzmann et al. 2002; Maxfield and McGraw 2004; Staub and Rotin 2006) we still do not have a clear picture of the precise morphological nature and dynamic activity of the compartments of the endocytic pathway (see Chap. 1 in this volume). In particular, information is lacking on the morphology of compartments, if and how this changes with time and their physical (as opposed to molecular) interactions. Images from vital dyes have the major shortcoming of limited resolution and work with them has not been well correlated with immunocytochemistry of cells that are well enough preserved to have a reliable ultrastructure (see Sect. II.B.). Most electron microscopy of yeast has been undertaken after aldehyde fixation. There is also controversy as to whether probes that are commonly used to demonstrate endocytosis enter cells only by endocytosis (see Sect. II.A.).

In mycelial fungi some form of membrane internalisation is to be expected for membrane retrieval, control of the plasma membrane surface area and to recycle receptors and signal molecules. However the massive secretion of vesicles by exocytosis during hyphal tip growth may not need to be compensated by an opposing high rate of endocytic activity because of the requirement for increase in plasma membrane surface area during tip extension (Torralba and Heath 2002). In contrast to yeast where there is good evidence for endocytosis from a range of molecular and structural work, in mycelial fungi evidence for endocytosis is largely based on the uptake of probes such as FM4-64, LY-CH or FITC-dextran with kinetics that are consistent with endocytosis (Fischer-Parton et al. 2000; Atkinson et al. 2002), coupled with a general assumption that all eukaryote cells have similar pathways. There is good ultrastructural evidence for some components of an endocytic pathway, such as multivesicular bodies in mycelial fungi, but not for others, such as clathrin-coated pits and coated vesicles, as would be expected if receptor-mediated endocytosis occurs as in animal cells (see Chap. 1 in this volume). Multivesicular bodies are common in hyphal tips of *Pis. tinctorius*, and in freeze-substituted cells they take the form of a tubular reticulum as well as the more typically described ovoid structures (L. Cole, D.A. Orlovich, A.E. Ashford, unpublished data). They can be distinguished from tubular vacuoles, which also contain membrane-enclosed vesicles, on both size and appearance. Profiles of MVB-like structures within larger vacuole profiles are shown in Fig. 2.5C. These are still surrounded by a single membrane, suggesting either fusion of the vacuole with a double-membrane structure or inclusion by direct invagination/budding of the vacuole bounding membrane; neither fits with the current concept of internalisation of MVBs. Lack of uptake of endocytosis markers such as LY-CH or fluorescent dextrans is not conclusive evidence against fluid-phase endocytosis since the cell walls may impede their access to the plasma membrane. Torralba and Heath (2002) found that the tips of growing *Neurospora* hyphae did not accumulate lanthanum and interpreted this as evidence for a lack of fluid phase endocytosis. In the case of *Neurospora* hyphae glutaraldehyde fixation was used. Lanthanum was excluded from Hartig net hyphae at the ectomycorrhizal interface in *Eucalyptus pilularis–Pis. tinctorius* ectomycorrhizas, but it permeated the cell walls and was in contact with the plasma membrane; in this case anhydrous freeze-substitution was used (Ashford et al. 1999; Vesk et al. 2000).

All three major compartments of the endosomal/lysosomal system in animal cells may form tubules and transport is not necessarily unidirectional nor is it mediated only by vesicles (Robinson et al. 1986; Swanson et al. 1987a, b, 1992; Hopkins et al. 1990; Knapp and Swanson 1990; Robinson and Karnovsky 1991; Tooze and Hollinshead 1991; Dunn and Maxfield 1992; Luo and Robinson 1992; Jahraus et al. 1994; Gruenberg and Maxfield 1995; Bryant et al. 1998). Retrograde traffic is essential for retrieval of a range of proteins including receptors and resident proteins of earlier compartments (de Figueiredo and Brown 1995; Bryant and Stevens 1998; Bryant et al. 1998) and such traffic is characteristically mediated by tubules. It has not been clear how motile tubular vacuole systems in mycelial fungi, as demonstrated by fluorochromes, relate to these animal cell compartments. Whether the tubular vacuole system in mycelial fungi as labelled by conventional fluorochromes is equivalent only to tubular lysosomes, or whether it also includes other parts of the endosomal pathway in fungi (Ashford and Orlovich 1994; Ashford 1998; Ashford et al. 2001) is still a matter of conjecture.

A major role for the vacuole is protein turnover and the vacuole contains both soluble and membrane-bound hydrolases. Several pathways of protein transport to the vacuole have been identified in *Sac. cerevisiae* (Bryant and Stevens 1998; Klionsky 1998). At least two occur via the Golgi (Conibear and Stevens 1998). One of them is the "classical" vacuole protein sorting (VPS)

pathway taken by the soluble vacuolar hydrolase CPY (also known as the CPY pathway) which passes through the pre-vacuolar compartment (Horazdovsky et al. 1995). The other is taken by alkaline phosphatase and Vam3p and does not have the Golgi to PVC vesicle-targeting mechanisms for entry into the prevacuolar compartment en route to the vacuole (Piper et al. 1997; Bryant et al. 1998). The latter pathway is clathrin-independent but is dependent on AP-3 adaptor proteins (Cowles et al. 1997; Odorizzi et al. 1998). Some proteins, including the enzyme aminopeptidase I, are taken up directly from the cytoplasm by a pathway known as the cytoplasm to vacuole (Cvt) pathway (Klionsky 1998; Khalfan and Klionsky 2002, Baxter et al. 2005). The enzyme is synthesised on cytosolic ribosomes and subsequently is found in membrane-enclosed compartments that are targeted to the vacuole (Scott et al. 1997). Under specific circumstances such as nitrogen or carbon starvation *Sac. cerevisiae* vacuoles degrade entire organelles and portions of the cytosol via macroautophagy as in mammalian cells. The process is reported to involve surrounding the structure or cytoplasm with a double membrane to produce an autophagosome which is then targeted to the vacuole (reviewed by Klionsky and Ohsumi 1999; Kim and Klionsky 2000; Abeliovich and Klionsky 2001). Direct invagination of the vacuole membrane leading to long tubules and their transformation into vesicles inside the vacuole lumen has also been observed in yeast and, after freeze-substitution, similar invaginations have been shown to contain cytosol (Müller et al. 2000). Both the Cvt pathway and the macroautophagy pathway have many features in common and overlap in function, but they display differences in kinetics, cargo specificity and vesicle size (Scott et al. 1996; Klionsky 1998; Khalfan and Klionsky 2002). In both cases fusion with the vacuole membrane involves the same SNARE complex as homotypic vacuole fusion (Khalfan and Klionsky 2002).

C. Vacuole Differentiation

There is very little information about precisely what individual vacuoles contain and the extent to which they might differ from one another in mycelial fungi. However there is evidence that higher plant cells have more than one functionally distinct vacuolar compartment and that these differ in pH and accumulation of fluorescent probes (Di Sansebastiano et al. 1998; Rogers 1998; Swanson et al. 1998). The view has been expressed that *Sac. cerevisiae* vacuoles are both morphologically and biochemically less diverse and may be less sophisticated in their organisation than those of other eukaryotes, in this case plants (Sato et al. 1997). The same may be true of mycelial fungi, but the varied morphology and dynamic exchanges of the *Pis. tinctorius* and *Pha. velutina* vacuole systems would suggest otherwise. The modelling of Darrah et al. (2006) shows the effect of the degree of isolation of individual vacuoles on rates of diffusive longitudinal transport.

Vacuoles frequently contain membranous inclusions. In images showing dynamics of vacuoles labelled with Vam3p-GFP-fusion protein, membranous vacuolar subcompartments can be seen (Shoji et al. 2006). Vacuole profiles in electron micrographs of freeze-substituted hyphae also commonly contain membrane-enclosed inclusions (Fig. 2.5C; see also Cole et al. 1998). In polyphosphate-labelling experiments with yeast and the mycelial fungus *Phialophora fortinii* it is obvious that the inclusions are negative whereas the rest of the vacuole profile labels for polyphosphate (Fig. 2.6D; see also Saito et al. 2005, 2006).

There are several processes by which membrane may be internalised into the lumen of vacuoles. Membrane fusion in yeast gives rise to internalised membrane fragments that subsequently appear to vesiculate and make repeated contact with the internal face of the vacuole bounding membrane (Wang et al. 2002, supplementary material). Direct invagination of the vacuole-bounding membrane also produces internal vesicles (Müller et al. 2000). Multivesicular bodies are targeted to vacuoles with which they are reported to fuse. Vacuoles would also contain single membrane-enclosed bodies derived from the Cvt and macroautophagy pathways if these pathways operate in mycelial fungi, as suggested for *Sac. cerevisiae* (reviewed by Abeliovich and Klionsky 2001; Khalfan and Klionsky 2002). The occurrence of internal membranous material derived from the vacuolar or late endosomal membranes and its degradation explains the occurrence of GFP fluorescence in the lumen of older vacuoles of Vam3p-GFP-labelled cells of *Aspergillus oryzae* (Shoji et al. 2006).

Large spherical/ovoid vacuoles are commonly associated with the plasma membrane with which they share a flattened interface, giving them a characteristic asymmetrical appearance (Cole et al. 1998; Darrah et al. 2006). There has

been no investigation into the nature of this vacuole/plasmamembrane interface but it is narrow and appears to exclude cytoplasm (Fig. 2.5C). It not only serves as an anchor for these larger vacuoles but also as a platform for movement; in a time-frame of minutes vacuoles are observed to roll slowly along the plasma membrane, while still maintaining their contact with its cytoplasmic surface (Cole et al. 1998). It is to be expected that cytoskeletal elements are involved in both the attachment to the plasma membrane and the observed motility. The common interface may also be a direct transport pathway from the external environment into vacuoles that essentially bypasses the cytoplasm.

D. The Vacuole as a Detoxifying Compartment

Sequestration of metal ions in vacuoles is thought to be a mechanism for their detoxification (Ramsay and Gadd 1997). Much of the early evidence for vacuolar accumulation of heavy metals based on X-ray microanalysis of element distribution (reviewed by Brunner 2001) is of material that has been chemically fixed or treated in such a way that it is subject to redistribution artefacts (see Sect. IV.A.). There are also problems with the differential extraction of cellular ion pools and analysis of cellular fractions (Ramsay and Gadd 1997). However, there are several more reliable indications of heavy metal accumulation in fungal vacuoles. For example *Sac. cerevisiae* mutants defective in vacuole formation or vacuole acidification show decreased accumulation of Zn, Mn, Co and Ni compared with wild-type cells, implying vacuolar sequestration and increased sensitivity to high concentrations of these metals (Ramsay and Gadd 1997). Three Zn^{2+} transporters have been found on the vacuole membrane of *Sac. cerevisiae* (MacDiarmid et al. 2000, 2002). Two of the yeast vacuole membrane transporters, Zrc1p and Cot1p, regulate influx into the vacuole and remove excess zinc from the cytoplasm. Both confer resistance to high zinc levels (reviewed by Eide 2003). The third, Zrt3p, is an efflux transporter that mobilises stored zinc to offset deficiency. They all belong to the cation diffusion facilitator (CDF) family of transporters. Together they regulate zinc storage in the vacuole and act in concert with both influx and efflux transporters at the plasma membrane to control zinc levels in the cytoplasm (MacDiarmid et al. 2000, 2002; Eide 2003). Ratiometric analysis with FuraZin-1, a fluorescent probe that accumulates in vacuoles, shows a rapid accumulation of zinc in the vacuoles when zinc-depleted cells encounter zinc, termed "zinc shock" (MacDiarmid et al. 2003). A gene encoding a putative Zn transporter thought to be involved in Zn homeostasis has also been found in *Glomus intraradices* but at present it is not clear where it is located (Gonzalez-Guerrero et al. 2005). There is also evidence of regulation of plasma membrane Zn influx transporters by endocytosis in mammalian cells (Kim et al. 2004; Wang et al. 2004).

Both zinc and nickel treatments caused disruption of the motile tubular vacuole system in hyphal tip cells of a *Paxillus involutus* strain isolated from a polluted soil (Tuszynska 2006; Tuszynska et al. 2006). This strain is likely to be more resistant to heavy metals than those from unpolluted sites. The effects of zinc and nickel on the vacuole system were characteristic of damage, such as loss of motility, widening of vacuolar tubules and their conversion to spherical, non-motile vacuoles. These effects were very similar to those caused by anti-microtubule drugs and were reversed on removal of the heavy metal. Both the degree of toxicity and the rate of recovery depended on the concentration of heavy metal applied and duration of exposure. The mitochondrial network was also affected. It fragmented indicating a general cytotoxic effect but vacuoles were more susceptible and less able to recover. Treatment with Ni^{2+} caused disruption of microtubules in *Paxillus involutus* (Tuszynska 2006), an effect also found in cultured animal cells (Gaskin et al. 1978; Lin and Chou 1990; Li et al. 1996a, b) and this could, at least in part, be responsible for the effects on vacuoles. Several toxic bivalent ions inhibit tubulin polymerisation and induce microtubule disassembly in vitro at low concentrations; and so the effect on microtubules may well be direct (Liliom et al. 2000). However, toxic ions like Ni^{2+} interfere with a range of cellular processes, including microfilament dynamics, and there are many potential sites of action that could produce this effect on vacuoles (DalleDonne et al. 1999).

The results with *Pax. involutus* have implications for nutrient transport. Disruption of the tubular components and loss of vacuole motility will disrupt any transport along the vacuolar conduit. All movement of PO_4^{3-}, K^+ and other cations, or N-containing molecules, along the vacuole system by diffusion (see Sect. V.A.) will be disrupted when heavy metals reach toxic levels. By the same token any heavy metals accumulated in vacuoles will be

isolated and not transported elsewhere. In these experiments the treatment was short-term and hyphae recovered but, unless hyphae are able to acclimate to long-term exposure, the loss of motile vacuoles has potentially serious implications for longitudinal nutrient transport.

There are also implications for zinc transport. Although vacuolar sequestration of zinc in *Pax. involutus* has not been firmly established, it is very likely. The short zinc exposures in the *Pax. involutus* experiments (minutes to hours) mimic a situation where cells in low zinc suddenly encounter much higher extracellular levels to produce the "zinc shock" phenomenon, a situation when zinc accumulates in yeast vacuoles (MacDiarmid et al. 2003). In *Sac. cerevisiae* it is thought that zinc can be accumulated to high levels in vacuoles and re-mobilised under zinc-deficient conditions (Eide 2006). Zinc, which is known to have very low soil mobility, is localised very patchily in soil, whether the soil is polluted or not. Though toxic at high levels, zinc is an essential micronutrient. Hyphae that encounter zinc and then survive and recover could transport accumulated zinc around the mycelial colony via the tubular vacuole system to hyphae where the soil zinc is deficient, while at the same time maintaining tight control of cytoplasmic zinc levels. Control of expression of vacuole efflux transporters like Zrt3p along the pathway, and at sites of accumulation and delivery, would be important and vacuole differentiation would be expected.

There is evidence for a glutathione-dependent detoxification pathway that involves vacuolar sequestration in fungi with similarities to that in plant cells (Coleman et al. 1997; Clemens and Simm 2003; Pócsi et al. 2004). Sequestration of metal ions by phytochelatins, small cysteine-containing peptides that are derived from glutathione (Rauser 1995), is the main mechanism for cadmium tolerance in *Sch. pombe* (reviewed by Clemens and Simm 2003; Clemens 2006). In *Sch. pombe* phytochelatin is synthesised from glutathione and its accumulation is triggered by metal ions, some of which form complexes with it. A homologue of *CAD1*, the gene that codes for phytochelatin synthase in *Arabidopsis thaliana*, has been found in *Sch. pombe* and mutants deficient in its synthesis are much more sensitive to Cd (Ha et al. 1999). The phytochelatin-Cd complex is transported into the vacuole by an ATP-binding cassette (ABC) transporter, Hmt1p (Ortiz et al. 1992, 1995). Once inside the vacuole it forms high molecular weight complexes by the addition of sulfide, apparently derived from cysteine sulfinate (reviewed by Pócsi et al. 2004). Detoxification by vacuolar sequestration also occurs via Cd/H^+ antiporters (Ortiz et al. 1995) and probably also by CDF proteins similar to those described above that sequester Zn^{2+} in *Sac. cerevisiae* (Paulsen and Saier 1997; Clemens and Simm 2003).

Transport into the vacuole as a glutathione-conjugate is probably a general pathway for removal of a range of endogenous and exogenous toxins from the cytosol in fungi and plants. Toxins may either spontaneously react with the SH group of glutathione or form glutathione-S-conjugates via glutathione-S-transferases. Glutathione-S-transferases, or gene sequences that code for similar proteins, have been found in a wide range of fungi including several mycelial fungi (Pócsi et al. 2004; McGoldrick et al. 2005; Shankar et al. 2006). *Sac. cerevisiae* does not express a phytochelatin synthase. However, it does have a glutathione-mediated pathway for detoxification. Glutathione is induced in the presence of Cd^{2+} and Cd-glutathione complexes are sequestered into the vacuole by the ABC transporter Ycf1p that mediates transport of glutathione and glutathione-conjugates into vacuoles (Li et al. 1996c, 1997; Sharma et al. 2002). The vacuolar accumulation of the characteristic red pigment used as a marker in studies of vacuole inheritance in *ade* mutants of *Sac. cerevisiae* (see Sect. II.A.), and also found in *Sch. pombe*, is due to the formation of glutathione conjugates by its toxic precursor and their transport to the vacuole (Chaudhuri et al. 1997; Sharma et al. 2002, 2003). Several glutathione-conjugate transporters – Ycf1p, Bpt1p and Bat1p – are involved in *Sac. cerevisiae* (Sharma et al. 2003). These show similarities to human multidrug resistance-associated proteins, many of which are Mg^{2+}-ATPases that are able to transport a broad range of apparently unrelated lipophilic compounds, including glutathione-conjugates and other large amphipathic anions. There is an inventory of *Sac. cerevisiae* ATP-binding cassette (ABC) transporters in Rea (1999).

Much less is known about glutathione detoxification pathways in mycelial fungi. It is especially important to clarify these pathways in mycorrhizal fungi because of their role as symbionts with forest trees and the current concerns about the relationship between forest decline and various forms of pollution. Levels of both glutathione and its precursor increase in Cd-stressed *Pax. involutus* hyphae (Courbot et al. 2004). Kinetic analysis of radiotracer desorption from mycelium indicates

$^{109}Cd^{2+}$ compartmentation in the vacuole (Blaudez et al. 2000). Compartmentation of Al in the vacuoles is also supported by shifts in resonances of peaks in ^{27}Al -NMR spectroscopy in the ectomycorrhizal fungus *Laccaria bicolor*, indicating that it forms complexes with the polyphosphate stored in these vacuoles (Martin et al. 1994). Polyphosphate with a very short chain length of about five residues is involved. Accumulation of the thiol-reactive Cell Tracker reagents (chloromethyl dyes) CMAC and CMFDA in the vacuoles of *Pis. tinctorius* is consistent with the presence of intracellular thiols and a glutathione-mediated transport pathway to the vacuole (Cole et al. 1997). The fact that many intracellular probes, targeted to or microinjected into the cytoplasm in mycelial and other fungi, end up in the vacuole (Fig. 2.3) could be attributed to mechanisms of detoxification via vacuolar accumulation by non-specific transporters. This possibility needs to be considered when fluorescent probes are used to evaluate ion activity and distribution.

VI. Conclusions

There is now sufficient evidence to indicate that the formation and motility of a tubular vacuole network are normal functions in the growing zone of mycelial fungi. There is also evidence that vacuolar content moves along these vacuolar tubules by diffusion – and that P and N, which vacuoles store, may be transported by this pathway. Modelling shows how transient interconnections within the vacuolar network could control both the frequency and the destinations of this transport. New data indicate that vacuolar tubules not only move material to new locations at a cellular level but also for longer distances and are likely to be involved in the transport of content, including nutrients, over these longer distances.

Systematic exploration of mutants deficient in specific activities has contributed significantly in investigating such processes as the delivery of protein to vacuoles, vacuole fusion and inheritance, and has further clarified the position of vacuoles as interacting compartments of both protein sorting and endocytic pathways. An understanding of the architecture and dynamism of these pathways has, however, lagged behind. The introduction of targeted fluorescent probes, especially GFP-constructs, has begun to rectify the problem but there is an urgent need to correlate observations in living cells with ultrastructure of well preserved material.

This review emphasises the importance of tubules. Evidence for transport via tubules continues to accumulate. The relative rates of fusion and fission control the extent of organelle tubulation but, equally, tubules are dependent on the cytoskeleton for their motility and support. Such processes not only control the distribution of organelles but are also seen to effect the transport of membrane and content at a cellular level. Organelle tubules are at last beginning to take their rightful place alongside vesicles as major mediators of cellular traffic. These concepts are seen to apply to vacuoles which readily form tubules in a wide range of organisms and under a wide range of conditions.

At the moment the major focus has been on molecular targeting in the yeast *Sac. cerevisiae*. Though many of the processes are conserved, because of differences seen between yeasts and other fungi, it is important to expand observations to include a greater range of fungi, especially those mycelial fungi that occupy very different ecological niches from yeast.

Acknowledgements. We are grateful to R. Verma for Fig. 2.1, Y. Kuga and K. Saito for Figs. 2.2, 2.6, T.M. Bourett for Fig. 2.3, M. Tlalka and M. Fricker for Fig. 2.4, and D.A. Orlovich for Fig. 2.5.

References

Abeliovich H, Klionsky DJ (2001) Autophagy in yeast: mechanistic insights and physiological function. Microbiol Mol Biol Rev 65:463–479

Allan VJ, Schroer TA (1999) Membrane motors. Curr Opin Cell Biol 11:476–482

Allaway WG (1994) Microtubules and the cytoplasmic motile tubular vacuole system in *Pisolithus tinctorius* hyphae. In: Stephenson AG, Kao T-H (eds) Pollen–pistil interactions and pollen tube growth. (Current topics in plant physiology, vol 12) American Society of Plant Physiology, Cambridge, Mass., pp 265–267

Allaway WG, Ashford AE (2001) Motile tubular vacuoles in extramatrical mycelium and sheath hyphae of ectomycorrhizal systems. Protoplasma 215:218–225

Allaway WG, Ashford AE, Heath IB, Hardham AE (1997) Vacuolar reticulum in oomycete hyphal tips: an additional component of the Ca^{2+} regulatory system? Fungal Genet Biol 22:209–220

Aniento F, Robinson DG (2005) Testing for endocytosis in plants. Protoplasma 226:3–11

Ashford AE (1998) Dynamic pleiomorphic vacuoles: are they endosomes and transport compartments in fungal hyphae? Adv Bot Res 28:119–159

Ashford AE (2002) Tubular vacuoles in arbuscular mycorrhizas. New Phytol 154:545–547

Ashford AE, Allaway WG (2002) The role of the motile tubular vacuole system in mycorrhizal fungi. Plant Soil 244:177–187

Ashford AE, Orlovich DA (1994) Vacuole transport, phosphorus, and endosomes in the growing tips of fungal hyphae. In: Stephenson AG, Kao T-H (eds) Pollen–pistil interactions and pollen tube growth. (Current topics in plant physiology, vol 12) American Society of Plant Physiology, Cambridge, Mass., pp 135–149

Ashford AE, Peterson RL, Dwarte D, Chilvers GA (1986) Polyphosphate granules in eucalypt mycorrhizas: determination by energy dispersive x-ray microanalysis. Can J Bot 64:677–687

Ashford AE, Ryde S, Barrow KD (1994) Demonstration of a short chain polyphosphate in *Pisolithus tinctorius* and the implications for phosphorus transport. New Phytol 126:239–247

Ashford AE, Vesk PA, Orlovich DA, Markovina A-L, Allaway WG (1999) Dispersed polyphosphate in fungal vacuoles of *Eucalyptus pilularis*/*Pisolithus tinctorius* ectomycorrhizas. Fungal Genet Biol 28:21–33

Ashford AE, Cole L, Hyde GJ (2001) Motile Tubular Vacuole Systems. In: Howard RJ, Gow NAR (eds) The Mycota, vol VIII. Biology of the fungal cell. Springer, Berlin Heidelberg New York, pp 243–265

Atkinson HA, Daniels A, Read ND (2002) Live-cell imaging of endocytosis during conidial germination in the rice blast fungus, *Magnaporthe grisea*. Fungal Genet Biol 37:233–244

Baas PW, Karabay A, Qiang L (2005) Microtubules cut and run. Trends Cell Biol 15:518–524

Bachewich C, Heath IB (1999) Cytoplasmic migrations and vacuolation are associated with growth recovery in hyphae of *Saprolegnia*, and are dependent on the cytoskeleton. Mycol Res 103:849–858

Basrai MA, Naider F, Becker JM (1990) Internalization of lucifer yellow in *Candida albicans* by fluid phase endocytosis. J Gen Microbiol 136:1059–1065

Baxter BK, Abeliovich H, Zhang X, Stirling AG, Burlingame AL, Goldfarb DS (2005) Atg19p ubiquitination and the cytoplasm to vacuole trafficking pathway in yeast. J Biol Chem 280:39067–39076

Bebber DP, Tlalka M, Hynes J, Darrah PR, Ashford A, Watkinson SC, Boddy L, Fricker MD (2007) Imaging complex nutrient dynamics in mycelial networks. In: Gadd GM, Watkinson SC, Dyer PS (eds) Fungi in the environment. (British Mycological Society Symposia, vol 25) Cambridge University, Cambridge, pp 1–21

Bennett MK (1995) SNAREs and the specificity of transport vesicle targeting. Curr Opin Cell Biol 7:581–586

Betz WJ, Mao F, Bewick GS (1992) Activity-dependent fluorescent staining and destaining of living vertebrate motor nerve terminals. J Neurosci 12:363–375

Biswas SK, Yamaguchi M, Norihide N, Takashima T, Takeo K (2003) Quantitative three-dimensional structural analysis of *Exophiala dermatitidis* yeast cells by freeze-substitution and serial ultrathin sectioning. J Electron Microsc 52:133–143

Blaudez D, Botton B, Chalot M (2000) Cadmium uptake and subcellular compartmentation in the ectomycorrhizal fungus *Paxillus involutus*. Microbiology 146:1109–1117

Bleazard W, McCaffery JM, King EJ, Bale S, Mozdy A, Tieu Q, Nunnari J, Shaw JM (1999) The dynamin-related GTPase Dnm1 regulates mitochondrial fission in yeast. Nat Cell Biol 1:298–304

Bliek AM van der (1999) Functional diversity in the dynamin family. Trends Cell Biol 9:96–102

Boller T, Wiemken A (1986) Dynamics of vacuolar compartmentation. Annu Rev Plant Physiol 37:137–164

Bolte S, Talbot C, Boutte Y, Catrice O, Read ND, Satiat-Jeunemaitre B (2004) FM-dyes as experimental probes for dissecting vesicle trafficking in living plant cells. J Microsc 214:159–173

Bourett TM, Howard RJ (1994) Enhanced labelling of concanavalin A binding sites in fungal membranes using a double-sided, indirect method. Mycol Res 98:769–775

Bourett TM, Picollelli MA, Howard RJ (1993) Postembedment labeling of intracellular concanavalin A-binding sites in freeze-substituted fungal cells. Exp Mycol 17:223–235

Bourett TM, Czymmek KJ, Howard RJ (1998) An improved method for affinity probe localization in whole cells of filamentous fungi. Fungal Genet Biol 24:3–13

Bourett TM, Sweigard JA, Czymmek KJ, Carroll A, Howard RJ (2002) Reef coral fluorescent proteins for visualizing fungal pathogens. Fungal Genet Biol 37:211–220

Bowman BJ, Bowman EJ (2002) Mutations in subunit c of the vacuolar ATPase confer resistance to bafilomycin and identify a conserved antibiotic binding site. J Biol Chem 277:3965–3972

Bowman EJ, Bowman BJ (2000) Cellular role of the V-ATPase in *Neurospora crassa*: analysis of mutants resistant to concanamycin or lacking the catalytic subunit A. J Exp Biol 203:97–106

Bowman EJ, Siebers A, Altendorf K (1988) Bafilomycin: a class of inhibitors of membrane ATPases from microorganisms, animal cells, and plant cells. Proc Natl Acad Sci USA 85:7972–7976

Bowman EJ, O'Neill FJ, Bowman BJ (1997) Mutations of *pma-1*, the gene encoding the plasma membrane H^+-ATPase of *Neurospora crassa*, suppress inhibition of growth by Concanamycin A, a specific inhibitor of vacuolar ATPases. J Biol Chem 272:14776–14786

Bowman EJ, Graham LA, Stevens TH, Bowman BJ (2004) The bafilomycin/concanamycin binding site in subunit c of the V-ATPases from *Neurospora crassa* and *Saccharomyces cerevisiae*. J Biol Chem 279:33131–33138

Brown SS (1999) Cooperation between microtubule- and actin-based motor proteins. Annu Rev Cell Dev Biol 15:63–80

Brunner I (2001) Ectomycorrhizas: their role in forest ecosystems under the impact of acidifying pollutants. Perspect Plant Ecol Evol Syst 4:3–12

Bryant NJ, Stevens TH (1998) Vacuole biogenesis in *Saccharomyces cerevisiae*: protein transport pathways to the yeast vacuole. Microbiol Mol Biol Rev 62:230–247

Bryant NJ, Piper RC, Weisman LS, Stevens TH (1998) Retrograde traffic out of the yeast vacuole to the TGN occurs via the prevacuolar/endosomal compartment. J Cell Biol 142:651–663

Bücking H, Heyser W (1997) Intracellular compartmentation of phosphorus in roots of *Pinus sylvestris* L. and the implications for transfer processes in ectomycorrhizae. In: Rennenberg H, Eschrich W, Zeiger H (eds) Trees – contributions to modern tree physiology. Backhuys, Leiden, pp 377–391

Bücking H, Heyser W (1999) Elemental composition and function of polyphosphates in ectomycorrhizal fungi – an X-ray microanalytical study. Mycol Res 103:31–39

Bücking H, Shachar-Hill Y (2005) Phosphate uptake, transport and transfer by the arbuscular mycorrhizal fungus *Glomus intraradices* is stimulated by increased carbohydrate availability. New Phytol 165:899–912

Bücking H, Beckmann S, Heyser W, Kottke I (1998) Elemental contents in vacuolar granules of ectomycorrhizal fungi measured by EELS and EDXS. A comparison of different methods and preparation techniques. Micron 29:53–61

Canny MJ, McCully ME (1986) Locating water-soluble vital stains in plant tissues by freeze-substitution and resin-embedding. J Microsc 142:63–70

Chalfie M, Kain SR (eds) (2006) Green fluorescent protein: properties, applications, and protocols, 2nd edn. Wiley–Interscience, Hoboken

Chalfie M, Tu G, Euskirchen G, Ward WW, Prasher DC (1994) Green fluorescent protein as a marker for gene expression. Science 263:802–805

Chandra S, Morrison GH (1997) Evaluation of fracture planes and cell morphology in complementary fractures of cultured cells in the frozen-hydrated state by field emission secondary electron microscopy: feasibility for ion localization and fluorescence imaging studies. J Microsc 186:232–245

Chaudhuri B, Ingavale S, Bachhawat AK (1997) *apd1*(+), a gene required for red pigment formation in *ade6* mutants of *Schizosaccharomyces pombe*, encodes an enzyme required for glutathione biosynthesis: a role for glutathione and a glutathione-conjugate pump. Genetics 145:75–83

Clemens S (2006) Evolution and function of phytochelatin synthases. J Plant Physiol 163:319–332

Clemens S, Simm C (2003) *Schizosaccharomyces pombe* as a model for metal homeostasis in plant cells: the phytochelatin-dependent pathway is the main cadmium detoxification mechanism. New Phytol 159:323–330

Cole L, Hyde G, Ashford AE (1997) Uptake and compartmentalisation of fluorescent probes by *Pisolithus tinctorius* hyphae: evidence for an anion transport mechanism at the tonoplast but not for fluid-phase endocytosis. Protoplasma 199:18–29

Cole L, Orlovich DA, Ashford AE (1998) Structure, function, and motility of vacuoles in filamentous fungi. Fungal Genet Biol 24:86–100

Cole L, Davies D, Hyde GJ, Ashford AE (2000a) ER-Tracker dye and BODIPY-brefeldin A differentiate the endoplasmic reticulum and Golgi bodies from the tubular vacuole system in living hyphae of *Pisolithus tinctorius*. J Microsc 197:239–248

Cole L, Davies D, Hyde GJ, Ashford AE (2000b) Brefeldin A affects growth, endoplasmic reticulum, Golgi bodies, tubular vacuole system, and secretory pathway in *Pisolithus tinctorius*. Fungal Genet Biol 29:95–106

Coleman JOD, Blake-Kalff MMA, Davies TGE (1997) Detoxification of xenobiotics by plants: chemical modification and vacuolar compartmentation. Trends in Plant Science 2:144–151

Conibear E, Stevens TH (1998) Multiple sorting pathways between late Golgi and the vacuole in yeast. Biochim Biophys Acta 1404:211–230

Cooper MS, Cornell-Bell AH, Chernjavsky A, Dani JW, Smith SJ (1990) Tubulovesicular processes emerge from trans-Golgi cisternae, extend along microtubules, and interlink adjacent trans-Golgi elements into a reticulum. Cell 61:135–145

Cormack B (1998) Green fluorescent protein as a reporter of transcription and protein localization in fungi. Curr Opin Microbiol 1:406–410

Courbot M, Diez L, Ruotolo R, Chalot M, Leroy P (2004) Cadmium-responsive thiols in the ectomycorrhizal fungus *Paxillus involutus*. Appl Environ Microbiol 70:7413–7417

Cowles CR, Odorizzi G, Payne GS, Emr SD (1997) The AP-3 adaptor complex is essential for cargo-selective transport to the yeast vacuole. Cell 91:109–118

Cramer CL, Vaughn LE, Davis RH (1980) Basic amino acids and inorganic polyphosphates in *Neurospora crassa*: independent regulation of vacuolar pools. J Bacteriol 142:945–952

Cubitt AB, Heim R, Adams SR, Boyd AE, Gross LA, Tsien RY (1995) Understanding, improving and using green fluorescent proteins. TIBS 20:448–455

Czymmek KJ, Bourett TM, Howard RJ (1996) Immunolocalization of tubulin and actin in thick-sectioned fungal hyphae after freeze-substitution fixation and methacrylate de-embedment. J. Microsc 181:153–161

Czymmek KJ, Bourett TM, Sweigard JA, Carroll A, Howard RJ (2002) Utility of cytoplasmic fluorescent proteins for live-cell imaging of *Magnaporthe grisea* in planta. Mycologia 94:280–289

Czymmek KJ, Bourett TM, Howard RJ (2005) Fluorescent protein probes in fungi. Methods Microbiol 34:27–62

DalleDonne I, Milzani A, Ciaparelli C, Comazzi M, Gioria MR, Colombo R (1999) The assembly of Ni^{2+}-actin: some peculiarities. Biochim Biophys Acta Gen Subj 1426:32–42

Darrah PR, Tlalka M, Ashford A, Watkinson SC, Fricker MD (2006) The vacuole system is a significant intracellular pathway for longitudinal solute transport in basidiomycete fungi. Eukaryot Cell 5:1111–1125

Davies JM, Brownlee C, Jennings DH (1990) Measurement of intracellular pH in fungal hyphae using BCECF and digital imaging microscopy Evidence for a primary proton pump in the plasmalemma of a marine fungus. J Cell Sci 96:731–736

D'Hondt K, Heese-Peck A, Riezman H (2000) Protein and lipid requirements for endocytosis. Annu Rev Genet 34:255–295

Di Sansebastiano G-P, Paris N, Marc-Martin S, Neuhaus J-M (1998) Specific accumulation of GFP in a non-acidic vacuolar compartment via a C-terminal propeptide-mediated sorting pathway. Plant J 15:449–457

Dijksterhuis J (2003) Confocal microscopy of Spitzenkörper dynamics during growth and differentiation of rust fungi. Protoplasma 222:53–59

Dunn KW, Maxfield FR (1992) Delivery of ligands from sorting endosomes to late endosomes occurs by maturation of sorting endosomes. J Cell Biol 117:301–310

Dunn T, Gable K, Beeler T (1994) Regulation of cellular Ca^{2+} by yeast vacuoles. J Biol Chem 269:7273–7278

Dürr M, Urech K, Boller T, Wiemken A, Schwencke J, Nagy M (1979) Sequestration of arginine by polyphosphate in vacuoles of yeast (*Saccharomyces cerevisiae*). Arch Microbiol 121:169–175

Eide DJ (2003) Multiple regulatory mechanisms maintain zinc homeostasis in *Saccharomyces cerevisiae*. J Nutr 133[Suppl 1]:1532S–1535S

Eide DJ (2006) Zinc transporters and cellular trafficking of zinc. Biochim Biophys Acta 1763:711–722

Ezawa T, Cavagnaro TR, Smith SE, Smith FA, Ohtomo R (2003) Rapid accumulation of polyphosphate in extraradical hyphae of an arbuscular mycorrhizal fungus as revealed by histochemistry and a polyhosphate kinase/luciferase system. New Phytol 161:387–392

Fasshauer D, Sutton RB, Brunger AT, Jahn R (1998) Conserved structural features of the synaptic fusion complex: SNARE proteins reclassified as Q- and R-SNAREs. Proc Natl Acad Sci USA 95:15781–15786

Fernández-Ábalos JM, Fox H, Pitt C, Wells B, Doonan JH (1998) Plant-adapted green fluorescent protein is a versatile vital reporter for gene expression, protein localization and mitosis in the filamentous fungus, *Aspergillus nidulans*. Mol Microbiol 27:121–130

Ferro-Novick S, Jahn R (1994) Vesicle fusion from yeast to man. Nature 370:191–193

Figueiredo P de, Brown W (1995) A role for calmodulin in organelle membrane tubulation. Mol Biol Cell 6:871–887

Fink G, Steinberg G (2006) Dynein-dependent motility of microtubules and nucleation sites supports polarization of the tubulin array in the fungus *Ustilago maydis*. Mol Biol Cell 17:3242–3253

Fischer-Parton S, Parton RM, Hickey PC, Dijksterhuis J, Atkinson HA, Read ND (2000) Confocal microscopy of FM4-64 as a tool for analysing endocytosis and vesicle trafficking in living fungal hyphae. J Microsc 198:246–259

Forgac M (1999) Structure and properties of the vacuolar (H^+)-ATPases. J Biol Chem 274:12951–12954

Förster C, Marienfeld S, Wilhelm R, Krämer R (1998) Organelle purification and selective permeabilisation of the plasma membrane: two different approaches to study vacuoles of the filamentous fungus *Ashbya gossypii*. FEMS Microbiol Lett 167:209–214

Frey B, Brunner I, Walther P, Scheidegger C, Zierold L (1997) Element localization in ultrathin cryosections of high-pressure frozen ectomycorrhizal spruce roots. Plant Cell Environ 20:929–937

Frey B, Zierold K, Brunner I (2000) Extracellular complexation of Cd in the Hartig net and cytosolic Zn sequestration in the fungal mantle of *Picea abies – Hebeloma crustuliniforme* ectomycorrhizas. Plant Cell Environ 23:1257–1265

Fricker MD, Oparka KJ (1999) Imaging techniques in plant transport: meeting review. J Exp Bot 50:1089–1100

Fricker MD, May M, Meyer AJ, Sheard N, White NS (2000) Measurement of glutathione levels in intact roots of *Arabidopsis*. J Microsc 198:162–173

Futter CE, Pearse A, Hewlett LJ, Hopkins CR (1996) Multivesicular endosomes containing internalised EGF-EGF receptor complexes mature and then fuse directly with lysosomes. J Cell Biol 132:1011–1023

Gaskin F, Kress Y, Brosnan C, Bornstein M (1978) Abnormal tubulin aggregates induced by zinc sulphate in organotypic cultures of nerve tissue. Neuroscience 3:1117–1125

Gaynor EC, Chen C-Y, Emr SD, Graham TR (1998) ARF is required for maintenance of yeast Golgi and endosome structure and function. Mol Biol Cell 9:653–670

Geli MI, Riezman H (1998) Endocytic internalization in yeast and animal cells: similar and different. J Cell Sci 111:1031–1037

Gerlitz TGM, Gerlitz A (1997) Phosphate uptake and polyphosphate metabolism of mycorrhizal and nonmycorrhizal roots of pine and of *Suillus bovinus* at varying external pH measured by in vivo ^{31}P-NMR. Mycorrhiza 7:101–106

Gerlitz TGM, Werk WB (1994) Investigations on phosphate uptake and polyphosphate metabolism by mycorrhized and nonmycorrhized roots of beech and pine as investigated by in vivo ^{31}P-NMR. Mycorrhiza 4:207–214

Gerst JE (1999) SNAREs and SNARE regulators in membrane fusion and exocytosis. Cell Mol Life Sci 55:707–734

Gomes de Mesquita DS, Ten Hoopen R, Woldringh CL (1991) Vacuolar segregation to the bud of *Saccharomyces cerevisiae*: an analysis of morphology and timing in the cell cycle. J Gen Microbiol 137:2447–2454

González-Guerrero M, Azcón-Aguilar C, Mooney M, Valderas A, MacDiarmid CW, Eide DJ, Ferrol N (2005) Characterization of a *Glomus intraradices* gene encoding a putative Zn transporter of the cation diffusion facilitator family. Fungal Genet Biol 42:130–140

Götte M, Gallwitz D (1997) High expression of the yeast syntaxin-related Vam3 protein suppresses the protein transport defects of a *pep12* null mutant. FEBS Lett 411:48–52

Götte M, Lazar T (1999) The ins and outs of yeast vacuole trafficking. Protoplasma 209:9–18

Graham LA, Powell B, Stevens TH (2000) Composition and assembly of the yeast H^+-ATPase complex. J Exp Biol 203:61–70

Greenfield NJ, Hussain M, Lenard L (1987) Effects of growth state and amines on cytoplasmic and vacuolar pH, phosphate and polyphosphate levels in *Saccharomyces cerevisiae*: a ^{31}P-nuclear magnetic resonance study. Biochim Biophys Acta 926:205–214

Grellier B, Strullu DG, Martin F, Renaudin S (1989) Synthesis in vitro, microanalysis and ^{31}P-NMR study of metachromatic granules in birch mycorrhizas. New Phytol 112:49–54

Gruenberg J, Maxfield FR (1995) Membrane transport in the endocytic pathway. Curr Opin Cell Biol 7:552–563

Guthrie BA, Wickner W (1988) Yeast vacuoles fragment when microtubules are disrupted. J Cell Biol 107:115–120

Ha S-B, Smith AP, Howden R, Dietrich WM, Bugg S, O'-Connell MJ, Goldsbrough PB, Cobbett CS (1999) Phytochelatin synthase genes from Arabidopsis and the yeast *Schizosaccharomyces pombe*. Plant Cell 11:1153–1163

Haas A (1995) A quantitative assay to measure homotypic vacuole fusion in vitro. Methods Cell Sci 17:283–294

Haas A, Conradt B, Wickner W (1994) G-protein ligands inhibit in vitro reactions of vacuole inheritance. J Cell Biol 126:87–97

Hanson MR, Köhler RH (2001) GFP imaging: methodology and application to investigate cellular compartmentation in plants. J Exp Bot 52:529–539

Harada A, Takei Y, Kanai Y, Tanaka Y, Nonaka S, Hirokawa N (1998) Golgi vesiculation and lysosome dispersion in cells lacking cytoplasmic dynein. J Cell Biol 141:51–59

Haseloff J (1999) GFP variants for multispectral imaging of living cells. In: Kay S, Sullivan K (eds) Methods in cell biology, vol 59. Academic, New York, pp 139–151

Hauck M, Paul A, Mulack C, Fritz, E, Runge M (2002) Effects of manganese on the viability of vegetative diaspores of the epiphytic lichen *Hypogymnia physodes*. Environ Exp Bot 47:127–142

Haugland RP (2001) Handbook of fluorescent probes and research chemicals, 8th edn. Molecular Probes, Eugene. Available at: http://probes.invitrogen.com

Hawes C, Saint-Jore CM, Brandizzi F, Zheng H, Andreeva AV, Boevink P (2001) Cytoplasmic illuminations: in planta targeting of fluorescent proteins to cellular organelles. Protoplasma 215:77–88

Hermann GJ, Thatcher JW, Mills JP, Hales KG, Fuller MT, Nunnari J, Shaw JM (1998) Mitochondrial fusion in yeast requires the transmembrane GTPase Fzo1p. J Cell Biol 143:359–373

Herr FB, Heath MC (1982) The effects of antimicrotubule agents on organelle positioning in the cowpea rust fungus *Uromyces phaseoli* var. *vignae*. Exp Mycol 6:15–24

Hicke L, Dunn R (2003) Regulation of membrane protein transport by ubiquitin and ubiquitin-binding proteins. Annu Rev Cell Dev Biol 19:141–172

Hicke L, Zanolari B, Pypaert M, Rohrer J, Riezman H (1997) Transport through the yeast endocytic pathway occurs through morphologically distinct compartments and requires an active secretory pathway and Sec18p/n-ethylmaleimide-sensitive fusion protein. Mol Biol Cell 8:13–31

Hickey PC, Jacobson DJ, Read ND, Glass NL (2002) Live-cell imaging of vegetative hyphal fusion in *Neurospora crassa*. Fungal Genet Biol 37:109–119

Hickey PC, Swift SR, Roca MG, Read ND (2005) Live-cell imaging of filamentous fungi using vital fluorescent dyes and confocal microscopy. Methods Microbiol 34:63–87

Hinshaw JE, Schmid SL (1995) Dynamin self-assembles into rings suggesting a mechanism for coated vesicle budding. Nature 374:190–192

Hirokawa N (1998) Kinesin and dynein superfamily proteins and the mechanism of organelle transport. Science 279:519–526

Hoch HC (1990) Preservation of cell ultrastructure by freeze-substitution. In: Mendgen K, Lesemann D-E (eds) Electron microscopy of plant pathogens. Springer, Berlin Heidelberg New York, pp 1–16

Hochstrasser M (1996) Ubiquitin-dependent protein degradation. Annu Rev Genet 30:405–439

Hoffmann J, Mendgen K (1998) Endocytosis and membrane turnover in the germ tube of *Uromyces fabae*. Fungal Genet Biol 24:77–85

Hollenbeck PJ, Swanson JA (1990) Radial extension of macrophage tubular lysosomes supported by kinesin. Nature 346:864–866

Hopkins CR, Gibson A, Shipman M, Miller K (1990) Movement of internalized ligand-receptor complexes along a continuous endosomal reticulum. Nature 346:335–339

Horazdovsky BF, DeWald DB, Emr SD (1995) Protein transport to the yeast vacuole. Curr Opin Cell Biol 7:544–551

Hyde GJ (1998) Calcium imaging: a primer for mycologists. Fungal Genet Biol 24:14–23

Hyde GJ, Ashford AE (1997) Vacuole motility and tubule-forming activity in *Pisolithus tinctorius* hyphae are modified by environmental conditions. Protoplasma 198:85–92

Hyde GJ, Cole L, Ashford AE (1997) Mycorrhiza movies. Mycorrhiza 7:167–169

Hyde GJ, Davies D, Perasso L, Cole L, Ashford AE (1999) Microtubules, but not actin microfilaments, regulate vacuole motility and morphology in hyphae of *Pisolithus tinctorius*. Cell Motil Cytoskeleton 42:114–124

Hyde GJ, Davies D, Cole L, Ashford AE (2002) Regulators of GTP-binding proteins cause morphological changes in the vacuole system of the filamentous fungus, *Pisolithus tinctorius*. Cell Motil Cytoskeleton 51:133–146

Hyde GJ, Davies DS, Cole L, Ashford AE (2003) Retention of fluorescent probes during aldehyde-free anhydrous freeze-substitution. J Microsc 210:125–130

Jahn R, Südhof TC (1999) Membrane fusion and exocytosis. Annu Rev Biochem 68:863–911

Jahn R, Lang T, Südhof TC (2003) Membrane fusion. Cell 112:519–533

Jahraus A, Storrie B, Griffiths G, Desjardins M (1994) Evidence for retrograde traffic between terminal lysosomes and the prelysosomal/late endosomal compartment. J Cell Sci 107:145–157

Jones EW, Webb GC, Hiller MA (1997) Biogenesis and function of the yeast vacuole. In: Pringle JR, Broach JR, Jones EW (eds) The molecular and cellular biology of the yeast *Saccharomyces*, vol 3. Cell cycle and cell biology. Cold Spring Harbor Laboratory, Cold Spring Harbor, pp 363–470

Jones HD, Schliwa M, Drubin DG (1993) Video microscopy of organelle inheritance and motility in budding yeast. Cell Motil Cytoskeleton 25:129–142

Kanamori K, Legerton TL, Weiss RL, Roberts JD (1982) Nitrogen-15 spin-lattice relaxation times of amino acids in *Neurospora crassa* as a probe of intracellular environment. Biochemistry 21:4916–4920

Kane PM (2006) The where, when and how of organelle acidification by the yeast vacuolar H^+-ATPase. Microbiol Mol Biol Rev 70:177–191

Kane PM, Yamashiro CT, Stevens TH (1989) Biochemical characterization of the yeast vacuolar H^+-ATPase. J Biol Chem 264:19236–19244

Karki S, Holzbaur ELF (1999) Cytoplasmic dynein and dynactin in cell division and intracellular transport. Curr Opin Cell Biol 11:45–53

Katzmann DJ, Babst M, Emr SD (2001) Ubiquitin-dependent sorting into the multivesicular body pathway requires the function of a conserved endosomal protein sorting complex, ESCRT-1. Cell 106:145–155

Katzmann DJ, Odorizzi G, Emr SD (2002) Receptor down-regulation and multivesicular-body sorting. Nat Rev Mol Cell Biol 3:893–905

Keenan KA, Utzat CD, Zielinski TK (1998) Isolation and characterization of strains defective in vacuolar or-

nithine permease in *Neurospora crassa*. Fungal Genet Biol 23:237–247

Khalfan WA, Klionsky DL (2002) Molecular machinery required for autophagy and the cytoplasm to vacuole targeting (Cvt) pathway in *S. cerevisiae*. Curr Opin Cell Biol 14:468–475

Kim BE, Wang F, Dufner-Beattie J, Andrews GK, Eide DJ, Petris MJ (2004) Zn^{2+}-stimulated endocytosis of the mZIP4 transporter regulates its location at the plasma membrane. J Biol Chem 279:4523–4530

Kim J, Klionsky DJ (2000) Autophagy, cytoplasm-to-vacuole targeting pathway, and pexophagy in yeast and mammalian cells. Annu Rev Biochem 69:303–342

Kitamoto K, Yoshizawa K, Ohsumi Y, Anraku Y (1988a) Dynamic aspects of vacuolar and cytosolic amino acid pools of *Saccharomyces cerevisiae*. J Bacteriol 170:2683–2686

Kitamoto K, Yoshizawa K, Ohsumi Y, Anraku Y (1988b). Mutants of *Saccharomyces cerevisiae* with defective vacuolar function. J Bacteriol 170:2687–2691

Klionsky DJ (1998) Nonclassical protein sorting to the yeast vacuole. J Biol Chem 273:10807–10810

Klionsky DJ, Ohsumi Y (1999) Vacuolar import of proteins and organelles from the cytoplasm. Annu Rev Cell Dev Biol 15:1–32

Klionsky DJ, Herman PK, Emr SD (1990) The fungal vacuole: composition, function, and biogenesis. Microbiol Rev 54:266–292

Knapp PE, Swanson JA (1990) Plasticity of the tubular lysosomal compartment in macrophages. J Cell Sci 95:433–439

Koster G, VanDuijn M, Hofs B, Dogterom M (2003) Membrane tube formation from giant vesicles by dynamic association of motor proteins. Proc Natl Acad Sci USA 100:15583–15588

Kottke I, Qian XM, Pritsch K, Haug I, Oberwinkler F (1998) *Xerocomus badius–Picea abies,* an ectomycorrhiza of high activity and element storage capacity in acidic soil. Mycorrhiza 7:267–275

Kutsuna N, Hasezawa S (2002) Dynamic organization of vacuolar and microtubule structures during cell cycle progression in synchronised tobacco BY-2 cells. Plant Cell Physiol 43:965–973

Lazzaro MD, Thomson WW (1996) The vacuolar-tubular continuum in living trichomes of chickpea (*Cicer arietinum*) provides a rapid means of solute delivery from base to tip. Protoplasma 193:181–190

Legerton TL, Kanamori K, Weiss RL, Roberts JD (1983) Measurements of cytoplasmic and vacuolar pH in *Neurospora* using nitrogen-15 nuclear magnetic resonance spectroscopy. Biochemistry 22:899–903

Lenz JH, Schuchardt I, Straube A, Steinberg G (2006) A dynein loading zone for retrograde endosome motility at microtubule plus-ends. EMBO J 25:2275–2286

Lewis MJ, Nichols BJ, Prescianotto-Baschong C, Riezman H, Pelham HRB (2000) Specific retrieval of the exocytic SNARE Snc1p from early yeast endosomes. Mol Biol Cell 11:23–38

Li W, Zhao Y, Chou I-N (1996a) Mg^{2+} antagonism on Ni^{2+}-induced changes in microtubule assembly and cellular thiol homeostasis. Toxicol Appl Pharmacol 136:101–111

Li W, Zhao Y, Chou I-N (1996b) Nickel (Ni^{2+}) enhancement of α-tubulin acetylation in cultured 3T3 cells. Toxicol Appl Pharmacol 140:461–470

Li Z-S, Szczypka M, Lu Y-P, Thiele DJ, Rea PA (1996c) The yeast cadmium factor protein (YCF1) is a vacuolar glutathione *S*-conjugate pump. J Biol Chem 271:6509–6517

Li Z-S, Lu Y-P, Zhen R-G, Szczypka M, Thiele DJ, Rea PA (1997) A new pathway for vacuolar cadmium sequestration in *Saccharomyces cerevisiae*: YCF1-catalyzed transport of bis(glutothionato)cadmium. Proc Natl Acad Sci USA 94:42–47

Liliom K, Wágner G, Pácz A, Cascante M, Kovács J, Ovádi J (2000) Organization-dependent effects of toxic bivalent ions Microtubule assembly and glycolysis. Eur J Biochem 267:4731–4739

Lin KC, Chou I-N (1990) Studies on the mechanisms of Ni^{2+}-induced cell injury: I. Effects of Ni^{2+} on microtubules. Toxicol Appl Pharmacol 106:209–221

Lippincott-Schwartz J, Roberts TH, Hirschberg K (2000) Secretory protein trafficking and organelle dynamics in living cells. Annu Rev Cell Dev Biol 16:557–589

Luby-Phelps K, Ning G, Fogerty J, Besharse JC (2003) Visualization of identified GFP-expressing cells by light and electron microscopy. J Histochem Cytochem 51:271–274

Luo Z, Robinson JM (1992) Co-localization of an endocytic marker and acid phosphatase in a tubular/reticular compartment in macrophages. J Histochem Cytochem 40:93–103

MacDiarmid CW, Gaither LA, Eide D (2000) Zinc transporters that regulate vacuolar zinc storage in *Saccharomyces cerevisiae*. EMBO J 19:2845–2855

MacDiarmid CW, Milanick MA, Eide D (2002) Biochemical properties of vacuolar zinc transport systems of *Saccharomyces cerevisiae*. J Biol Chem 277:39187–39194

MacDiarmid CW, Milanick MA, Eide D (2003) Induction of the *ZRC1* metal tolerance gene in zinc-limited yeast confers resistance to zinc shock. J Biol Chem 278:15065–15072

Margolles-Clark E, Tenney K, Bowman EJ, Bowman BJ (1999) The structure of the vacuolar ATPase in *Neurospora crassa*. J Bioenerg Biomembr 31:29–37

Martin FM (1991) Nuclear magnetic resonance studies of ectomycorrhizal fungi. In: Norris JR, Read DJ, Varma AK (eds) Techniques for the study of mycorrhiza. (Methods in microbiology, vol 23) Academic, London, pp 121–148

Martin F, Rubini P, Côté R, Kottke I (1994) Aluminium polyphosphate complexes in the mycorrhizal basidiomycete *Laccaria bicolor*: a ^{27}Al-nuclear magnetic resonance study. Planta 194:241–246

Martinoia E, Heck U, Boller T, Wiemken A, Matile PH (1979) Some properties of vacuoles isolated from *Neurospora crassa* slime variant. Arch Microbiol 120:31–34

Maruyama J, Nakajima H, Kitamoto K (2002) Observation of EGFP-visualized nuclei and distribution of vacuoles in *Aspergillus oryzae arpA* null mutant. FEMS Microbiol Lett 206:57–61

Maxfield FR, McGraw TE (2004) Endocytic recycling. Nat Rev Mol Cell Biol 5:121–132

Mayer A (1999) Intracellular membrane fusion: SNARES only? Curr Opin Cell Biol 11:447–452

Mayer A (2002) Membrane fusion in eukaryote cells. Annu Rev Cell Dev Biol 18:289–314

McCully ME, Canny MJ (1985) The stabilization of labile configurations of plant cytoplasm by freeze-substitution. J Microsc 139:27–33

McGoldrick S, O'Sullivan SM, Sheehan D (2005) Glutathione transferase-like proteins encoded in genomes of yeasts and fungi: insights into evolution of a multifunctional protein superfamily. FEMS Microbiol Lett 242:1–12

Mendgen K, Bachem U, Stark-Urnau M, Xu H (1995) Secretion and endocytosis at the interface of plants and fungi. Can J Bot 73:S640–S648

Mersey B, McCully ME (1978) Monitoring the course of fixation of plant cells. J Microsc 114:49–76

Merz AJ, Wickner WT (2004) Trans-SNARE interactions elicit Ca^{2+} efflux from the yeast vacuole lumen. J Cell Biol 164:195–206

Meyer AJ, Fricker MD (2000) Direct measurement of glutathione in epidermal cells of intact *Arabidopsis* roots by two-photon laser scanning microscopy. J Microsc 198:174–181

Mironov AA, Weidman P, Luini A (1997) Variations on the intracellular transport theme: maturing cisternae and trafficking tubules. J Cell Biol 138:481–484

Monaghan P, Robertson D (1990) Freeze-substitution without aldehyde or osmium fixatives: ultrastructure and implications for immunocytochemistry. J Microsc 158:355–363

Monaghan P, Perusinghe N, Müller M (1998) High-pressure freezing for immunocytochemistry. J Microsc 192:248–258

Müller O, Sattler T, Flötenmeyer M, Schwarz H, Plattner H, Mayer A (2000) Autophagic tubes: vacuolar invaginations involved in lateral membrane sorting and inverse vesicle budding. J Cell Biol 151:519–528

Mullock BM, Bright NA, Fearon CW, Gray SR, Luzio J (1998) Fusion of lysosomes with late endosomes produces a hybrid organelle of intermediate density and Is NSF dependent. J Cell Biol 140:591–601

Nelson N, Harvey WR (1999) Vacuolar and plasma membrane proton-adenosinetriphosphatases. Physiol Rev 79:361–385

Nichols BJ, Ungermann C, Pelham HRB, Wickner WT, Haas A (1997) Homotypic vacuolar fusion mediated by t- and v-SNAREs. Nature 387:199–202

Odorizzi G, Cowles CR, Emr SD (1998) The AP-3 complex: a coat of many colours. Trends Cell Biol 8:282–288

Ogawa N, DeRisi J, Brown PO (2000) New components of a system for phosphate accumulation and polyphosphate metabolism in *Saccharomyces cerevisiae* revealed by genomic expression analysis. Mol Biol Cell 11:4309–4321

Ohneda M, Arioka M, Nakajima H, Kitamoto K (2002) Visualization of vacuoles in *Aspergillus oryzae* by expression of CPY-EGFP. Fungal Genet Biol 37:29–38

Olsson PA, Aarle IM van, Allaway WG, Ashford AE, Rouhier H (2002) Phosphorus effects on metabolic processes in monoxenic arbuscular mycorrhiza cultures. Plant Physiol 130:1162–1171

Oparka KJ (1991) Uptake and compartmentation of fluorescent probes by plant cells. J Exp Bot 42:565–579

Opekarová M, Kubín J (1997) On the unidirectionality of arginine uptake in the yeast *Saccharomyces cerevisiae*. FEMS Microbiol Lett 152:261–267

Orlovich DA, Ashford AE (1993) Polyphosphate granules are an artefact of specimen preparation in the ectomycorrhizal fungus *Pisolithus tinctorius*. Protoplasma 173:91–102

Orlovich DA, Ashford AE (1995) X-ray microanalysis of ion distribution in frozen salt/dextran droplets after freeze-substitution and embedding in anhydrous conditions. J Microsc 180:117–126

Ortiz DF, Kreppel L, Speiser DM, Scheel G, McDonald G, Ow DW (1992) Heavy metal tolerance in the fission yeast requires an ATP-binding cassette-type vacuolar membrane transporter. EMBO J 11:3491–3499

Ortiz DF, Ruscitti T, McCue KF, Ow DW (1995) Transport of metal-binding peptides by HMT1, a fission yeast ABC-type vacuolar membrane protein. J Biol Chem 270:4721–4728

Palevitz BA, O'Kane DJ (1981) Epifluorescence and video analysis of vacuole motility and development in stomatal cells of *Allium*. Science 214:443–445

Palevitz BA, O'Kane DJ, Kobres RE, Raikhel NV (1981) The vacuole system in stomatal cells of *Allium*. Vacuole movements and changes in morphology in differentiating cells as revealed by epifluorescence, video and electron microscopy. Protoplasma 109:23–55

Pan X, Goldfarb DS (1998) *YEB3/VAC8* encodes a myristylated armadillo protein of the *Saccharomyces cerevisiae* vacuolar membrane that functions in vacuole fusion and inheritance. J Cell Sci 111:2137–2147

Parton RM, Read ND (1998) Calcium and pH imaging in living cells. In: Lacey AJ (ed) Light microscopy in biology – a practical approach. IRL, Oxford

Paul A, Hauck M, Fritz E (2003) Effects of manganese on element distribution and structure in thalli of the epiphytic lichens *Hypogymnia physodes* and *Lecanora conizaeoides*. Environ Exp Bot 50:113–124

Paulsen IT, Saier MH Jr (1997) A novel family of ubiquitous heavy metal ion transport proteins. J Membr Biol 156:99–103

Pelham HRB (1999a) SNAREs and the secretory pathway – lessons from yeast. Exp Cell Res 247:1–8

Pelham HRB (1999b) Intracellular membrane traffic: getting proteins sorted. (The Croonian lecture 1999) Philos Trans R Soc Lond Ser B 354:1471–1478

Pelham HRB (2002) Insights from yeast endosomes. Curr Opin Cell Biol 14:454–462

Peplowska K, Ungermann C (2005) Expanding dynamin: from fission to fusion. Nature Cell Biol 7:103–104

Perisamy A (ed) (2001) Methods in cellular imaging. Oxford University, Oxford

Peters C, Mayer A (1998) Ca^{2+}/calmodulin signals the completion of docking and triggers a late step of vacuole fusion. Nature 396:575–580

Peters C, Baars TL, Bühler S, Mayer A (2004) Mutual control of membrane fission and fusion proteins. Cell 119:667–678

Pfeffer SR (1996) Transport vesicle docking: SNAREs and associates. Annu Rev Cell Biol 12:441–461

Piper RC, Luzio JP (2001) Late endosomes: sorting and partitioning in multivesicular bodies. Traffic 2:612–621

Piper RC, Bryant NJ, Stevens TH (1997) The membrane protein alkaline phosphatase is delivered to the vacuole by a route that is distinct from the *VPS*-dependent pathway. J Cell Biol 138:531–545

Pócsi I, Prade RA, Penninckx MJ (2004) Glutathione, altruistic metabolite in fungi. Adv Microbiol Physiol 49:1–76

Prescianotto-Baschong C, Riezman H (1998) Morphology of the yeast endocytic pathway. Mol Biol Cell 9:173–189

Preston RA, Murphy RF, Jones EW (1989) Assay of vacuolar pH in yeast and identification of acidification-defective mutants. Proc Natl Acad Sci USA 86:7027–7032

Ramsay LM, Gadd GM (1997) Mutants of *Saccharomyces cerevisiae* defective in vacuolar function confirm a role for the vacuole in toxic metal ion detoxification. FEMS Microbiol Lett 152:293–298

Rasmussen N, Lloyd DC, Ratcliffe RG, Hansen PE, Jakobsen I (2000) ^{31}P NMR for the study of P metabolism and translocation in arbuscular mycorrhizal fungi. Plant Soil 226:245–253

Rauser WE (1995) Phytochelatins and related polypeptides. Structure, biosynthesis, and function. Plant Physiol 109:1141–1149

Raymond CK, Howald-Stevenson I, Vater CA, Stevens TH (1992a) Morphological classification of the yeast vacuolar protein sorting mutants: evidence for a prevacuolar compartment in class E *vps* mutants. Mol Biol Cell 3:1389–1402

Raymond CK, Roberts CJ, Moore KE, Howald I, Stevens TH (1992b) Biogenesis of the vacuole in *Saccharomyces cerevisiae*. Int Rev Cytol 139:59–120

Rea PA (1999) MRP subfamily ABC transporters from plants and yeast. J Exp Bot 50:895–913

Read ND, Kalkman ER (2003) Does endocytosis occur in fungal hyphae? Fungal Genet Biol 39:199–203

Rees B, Shepherd VA, Ashford AE (1994) Presence of a motile tubular vacuole system in different phyla of fungi. Mycol Res 98:985–992

Reggiori F, Pelham HRB (2001) Sorting of proteins into multivesicular bodies: ubiquitin-dependent and -independent targeting. EMBO J 20:5176–5186

Rieder SE, Banta LM, Kohrer K, McCaffery JM, Emr SD (1996) Multilamellar endosome-like compartment accumulates in yeast vps28 vacuolar protein sorting mutant. Mol Biol Cell 7:985–999

Riezman H (1985) Endocytosis in yeast: several of the yeast secretory mutants are defective in endocytosis. Cell 40:1001–1009

Riezman H (1998) Down regulation of yeast G protein-coupled receptors. Seminars Cell Dev Biol 9:129–134

Robinson JM, Karnovsky MJ (1991) Rapid-freezing cytochemistry: preservation of tubular lysosomes and enzyme activity. J Histochem Cytochem 39:787–792

Robinson JM, OkadaT, Castellot JJ Jr, Karnovsky MJ (1986) Unusual lysosomes in aortic smooth muscle cells: presence in living and rapidly frozen cells. J Cell Biol 102:1615–1622

Rogers JC (1998) Compartmentation of plant cell proteins in separate lytic and protein storage vacuoles. J Plant Physiol 152:653–658

Rost FWD, Shepherd VA, Ashford AE (1995) Estimation of vacuolar pH in actively growing hyphae of the fungus *Pisolithus tinctorius*. Mycol Res 99:549–553

Roszak R, Rambour S (1997) Uptake of Lucifer Yellow by plant cells in the presence of endocytotic inhibitors. Protoplasma 199:198–207

Roth AM, Sullivan DM, Davis NG (1998) A large PEST-like sequence directs the ubiquitination, endocytosis and vacuolar degradation of the yeast a-factor receptor. J Cell Biol 142:949–961

Rothman JE (1994). Mechanisms of intracellular protein transport. Nature 372:55–63

Saito K, Ohtomo R, Kuga-Uetake Y, Aono T, Saito M (2005) Direct labeling of polyphosphate at the ultrastructural level in *Saccharomyces cerevisiae* using an affinity of polyphosphate binding domain of *Escherichia coli* exopolyphosphatase. Appl Environ Microbiol 71:5692–5701

Saito K, Kuga-Uetake Y, Saito M, Peterson RL (2006) Vacuolar localization of phosphorus in hyphae of *Phialocephala fortinii*, a dark septate fungal root endophyte. Can J Microbiol 52:643–650

Sato K, Wickner W (1998) Functional reconstitution of Ypt7p GTPase and a purified vacuole SNARE complex. Science 281:700–702

Sato MH, Nakamura N, Ohsumi Y, Kouchi H, Kondo M, Hara-Nishimura I, Nishimura M, Wada Y (1997) The *AtVAM3* encodes a syntaxin-related molecule implicated in the vacuolar assembly in *Arabidopsis thaliana*. J Biol Chem 272:24530–24535

Sato TK, Darsow T, Emr SD (1998) Vam7p, a SNAP-25-like molecule, and Vam3p, a syntaxin homolog, function together in yeast vacuolar protein trafficking. Mol Cell Biol 18:5308–5319

Schmid SL, Sorkin AD (2002) Days and knights discussing membrane dynamics in endocytosis: meeting report from the Euresco/EMBL membrane dynamics in endocytosis, 6–11 October in Tomar, Portugal. Traffic 3:77–85

Schoch CL, Aist JR, Yoder OC, Turgeon BG (2003) A complete inventory of fungal kinesins in representative filamentous ascomycetes. Fungal Genet Biol 39:1–15

Schroer TA (2004) Dynactin. Annu Rev Cell Dev Biol 20:759–779

Schuchardt I, Aismann D, Thines E, Schuberth C, Steinberg G (2005) Myosin-V, kinesin-1, and kinesin-3 cooperate in hyphal growth of the fungus *Ustilago maydis*. Mol Biol Cell 16:5191–5201

Scott SV, Hefner-Gravink A, Morano KA, Noda T, Ohsumi Y, Klionsky DJ (1996) Cytoplasm-to-vacuole targeting and autophagy employ the same machinery to deliver proteins to the yeast vacuole. Proc Natl Acad Sci USA 93:12304–12308

Scott SV, Baba M, Ohsumi Y, Klionsky DJ (1997) Aminopeptidase I is targeted to the vacuole by a nonclassical vesicular mechanism. J Cell Biol 138:37–44

Seeley ES, Kato M, Margolis N, Wickner W, Eitzen G (2002) Genomic analysis of homotypic vacuole fusion. Mol Biol Cell 13:782–794

Seiler S, Nargang FE, Steinberg G, Schliwa M (1997) Kinesin is essential for cell morphogenesis and polarised secretion in *Neurospora crassa*. EMBO J 16:3025–3034

Seiler S, Platman M, Schliwa M (1999) Kinesin and dynein mutants provide novel insights into roles of vesicle traffic during cell morphogenesis in *Neurospora*. Curr Biol 9:779–785

Shankar J, Singh BP, Gaur SN, Arora N (2006) Recombinant glutathione-*S*-transferase a major allergen from *Alternaria alternata* for clinical use in allergy patients. Mol Immunol 43:1927–1932

Sharma KG, Mason DL, Liu G. Rea PA, Bachhawat AK, Michaelis S (2002) Localization, regulation, and substrate transport properties of Bpt1p, a *Saccharomyces cerevisiae* MRP-type ABC transporter. Eukaryot Cell 1:391–400

Sharma KG, Kaur R, Bachhawat AK (2003) The glutathione-mediated detoxification pathway in yeast: an analysis using the red pigment that accumulates in certain adenine biosynthetic mutants of yeasts reveals the involvement of novel genes. Arch Microbiol 180:108–117

Shaw JD, Hama H, Sohrabi F, DeWald DB, Wendland B (2003) PtdIns(3,5)P_2 is required for delivery of endocytic cargo into the multivesicular body. Traffic 4:479–490

Shaw JM, Nunnari J (2002) Mitochondrial dynamics and division in budding yeast. Trends Cell Biol 12:178–184

Shepard KA, Yaffe MP (1999) The yeast dynamin-like protein, Mgm1p, functions on the mitochondrial outer membrane to mediate mitochondrial ineritance. J Cell Biol 144:711–719

Shepherd VA, Orlovich DA, Ashford AE (1993a) A dynamic continuum of pleiomorphic tubules and vacuoles in growing hyphae of a fungus. J Cell Sci 104:495–507

Shepherd VA, Orlovich DA, Ashford AE (1993b) Cell-to-cell transport via motile tubules in growing hyphae of a fungus. J Cell Sci 105:1173–1178

Shoji J, Arioka M, Kitamoto K (2006) Vacuolar membrane dynamics in the filamentous fungus *Aspergillus oryzae*. Eukaryot Cell 5:411–421

Singer-Krüger B, Frank R, Crausaz F, Riezman H (1993) Partial purification and characterization of early and late endosomes from yeast. Identification of four novel proteins. J Biol Chem 268:14376–14386

Skepper J (2000) Immunocytochemical strategies for electron microscopy: choice or compromise. J Microsc 199:1–36

Söllner T, Bennett MK, Whiteheart SW, Scheller RH, Rothman JE (1993a) A protein assembly–disassembly pathway in vitro that may correspond to sequential steps of synaptic vesicle docking, activation and fusion. Cell 75:409–418

Söllner T, Whiteheart SW, Brunner M, Erdjument-Bromage H, Geromanos S, Tempst P, Rothman JE (1993b) SNAP receptors implicated in vesicle targeting and fusion. Nature 362:318–324

Stack JH, Horazdovsky BF, Emr SD (1995) Receptor-mediated protein sorting to the vacuole in yeast: roles for a protein kinase, a lipid kinase and GTP binding proteins. Annu Rev Cell Dev Biol 11:1–33

Starai VJ, Thorngren N, Fratti RA, Wickner W (2005) Ion regulation of homotypic vacuole fusion in *Saccharomyces cerevisiae*. J Biol Chem 280:16754–16762

Staub O, Rotin D (2006) Role of ubiquitylation in cellular membrane transport. Physiol Rev 86:669–707

Straube A, Hause G, Fink G, Steinberg G (2006) Conventional kinesin mediates microtubule-microtubule interactions in vivo. Mol Biol Cell 17:907–916

Steinberg G (1998) Organelle transport and molecular motors in fungi. Fungal Genet Biol 24:161–177

Steinberg G (2000) The cellular roles of molecular motors in fungi. Trends Microbiol 8:162–168

Steinberg G, Schliwa M (1993) Organelle movements in the wild type and wall-less fz;sg;os-1 mutants of *Neurospora crassa* are mediated by cytoplasmic microtubules. J Cell Sci 106:555–564

Steinberg G, Schliwa M, Lehmler C, Bölker M, Kahmann R, McIntosh JR (1998) Kinesin from the plant pathogenic fungus *Ustilago maydis* is involved in vacuole formation and cytoplasmic migration. J Cell Sci 111:2235–2246

Steinberg G, Wedlich-Söldner R, Brill M, Schultz I (2001) Microtubules in the fungal pathogen *Ustilago maydis* are highly dynamic and determine cell polarity. J Cell Sci 114:609–622

Stevens TH, Forgac M (1997). Structure, function and regulation of the vacuolar (H^+)-ATPase. Annu Rev Cell Dev Biol 13:779–808

Südhof TC (1995) The synaptic vesicle cycle: a cascade of protein-protein interactions. Nature 375:645–653

Swanson J (1989) Fluorescent labelling of endocytic compartments. Methods Cell Biol 29:137–151

Swanson J, Burke E, Silverstein SC (1987a) Tubular lysosomes accompany stimulated pinocytosis in macrophages. J Cell Biol 104:1217–1222

Swanson J, Bushnell A, Silverstein SC (1987b) Tubular lysosome morphology and distribution within macrophages depend on the integrity of cytoplasmic microtubules. Proc Natl Acad Sci USA 84:1921–1925

Swanson JA, Locke A, Ansel P, Hollenbeck PJ (1992) Radial movement of lysosomes along microtubules in permeabilized macrophages. J Cell Sci 103:201–209

Swanson SJ, Bethke PC, Jones RL (1998) Barley aleurone cells contain two types of vacuoles: characterization of lytic organelles by use of fluorescent probes. Plant Cell 10:685–698

Takei K, Haucke V (2001) Clathrin-mediated endocytosis: membrane factors pull the trigger. Trends Cell Biol 11:385–391

Takei K, McPherson PS, Schmid SL, De Camilli P (1995) Tubular membrane invaginations coated by dynamin rings are induced by GTP-γS in nerve terminals. Nature 374:186–190

Takei K, Haucke V, Slepnev V, Farsad K, Salazar M, Chen H, De Camilli P (1998) Generation of coated intermediates of clathrin-mediated endocytosis on protein-free liposomes. Cell 94:131–141

Tang F, Kauffman EJ, Novak JL, Nau JJ, Catlett NL, Weisman LS (2003) Regulated degradation of a class V myosin receptor directs movement of the yeast vacuole. Nature 422:87–92

Tarutani Y, Ohsumi K, Arioka M, Nakajima H, Kitamoto K (2001) Cloning and characterization of *Aspergillus nidulans vps*A gene which is involved in vacuolar biogenesis. Gene 268:23–30

Tooze J, Hollinshead M (1991) Tubular early endosomal networks in AtT20 and other cells. J Cell Biol 115:635–653

Torralba S, Heath IB (2002) Analysis of three separate probes suggests the absence of endocytosis in *Neurospora crassa* hyphae. Fungal Genet Biol 37:221–232

Trilisenko LV, Vagabov VM, Kulaev IS (2002) The content and chain length of polyphosphates from vacuoles of *Saccharomyces cerevisiae* VKM Y-1173. Biochemistry (Moscow) 67:592–596

Tsien RY (1989) Fluorescent indicators of ion concentrations. In: Taylor DL, Wang YL (eds) Fluorescence mi-

croscopy of living cells in culture, Part B. Quantitative fluorescence microscopy – imaging and spectroscopy. Methods Cell Biol 30X:127–156

Tuszynska S (2006) Ni^{2+} induces changes in the morphology of vacuoles, mitochondria and microtubules in *Paxillus involutus* cells. New Phytol 169:819–828

Tuszynska S, Davies D, Turnau K, Ashford A (2006) Changes in vacuolar and mitochondrial motility and tubularity in response to zinc in a *Paxillus involutus* isolate from a zinc-rich soil. Fungal Genet Biol 43:155–163

Uchida E, Ohsumi Y, Anraku Y (1985) Purification and properties of H^+-translocating, Mg^{2+}-adenosine triphosphatase from vacuolar membranes of *Saccharomyces cerevisiae*. J Biol Chem 260:1090–1095

Uemura T, Yoshimura SH, Takeyasu K, Sato MH (2002) Vacuolar membrane dynamics revealed by GFP-AtVam3 fusion protein. Genes Cells 7:743–753

Uetake Y, Kojima T, Ezawa T, Saito M (2002) Extensive tubular vacuole system in an arbuscular mycorrhizal fungus, *Gigaspora margarita*. New Phytol 154:761–768

Ungar D, Hughson FM (2003) SNARE protein structure and function. Annu Rev Dev Biol 19:493–517

Ungermann C, Wickner W (1998) Vam7p, a vacuolar SNAP-25 homolog, is required for SNARE complex integrity and vacuole docking and fusion. EMBO J 17:3269–3276

Ungermann C, Nichols BJ, Pelham HRB, Wickner W (1998) A vacuolar v-t-SNARE complex, the predominant form in vivo and on isolated vacuoles, is disassembled and activated for docking and fusion. J Cell Biol 140:61–69

Ungermann C, Fischer von Mollard G, Jensen ON, Margolis N, Stevens TH, Wickner W (1999) Three v-SNAREs and two t-SNARES, present in a pentameric cis-SNARE complex on isolated vacuoles, are essential for homotypic fusion. J Cell Biol 145:1435–1442

Urbanowski JL, Piper RC (2001) Ubiquitin sorts proteins into the intralumenal degradative compartment of the late-endosome/vacuole. Traffic 2:622–630

Vaughn LE, Davis RH (1981) Purification of vacuoles from *Neurospora crassa*. Mol Cell Biol 1:797–806

Vesk PA, Ashford AE, Markovina A-L, Allaway WG (2000) Apoplasmic barriers and their significance in the exodermis and sheath of *Eucalyptus pilularis–Pisolithus tinctorius* ectomycorrhizas. New Phytol 145:333–346

Vida TA, Emr SD (1995) A new vital stain for visualizing vacuolar membrane dynamics and endocytosis in yeast. J Cell Biol 128:779–792

Vida TA, Huyer G, Emr SD (1993) Yeast vacuolar proenzymes are sorted in the late Golgi complex and transported to the vacuole via a prevacuolar endosome-like compartment. J Cell Biol 121:1245–1256

Viereck N, Hansen PE, Jakobsen I (2004) Phosphate pool dynamics in the arbuscular mycorrhizal fungus *Glomus intraradices* studied by in vivo ^{31}P NMR spectroscopy. New Phytol 162:783–794

Wada Y, Nakamura N, Ohsumi Y, Hirata A (1997) Vam3p, a new member of syntaxin related protein, is required for vacuolar assembly in the yeast *Saccharomyces cerevisiae*. J Cell Sci 110:1299–1306

Wang F, Dufner-Beattie J, Kim B-E, Petris MJ, Andrews G, Eide DJ (2004) Zinc-stimulated endocytosis controls activity of the mouse ZIP1 and ZIP3 zinc uptake transporters. J Biol Chem 279:24631–24639

Wang L, Seeley ES, Wickner W, Merz AJ (2002) Vacuole fusion at a ring of vertex docking sites leaves membrane fragments within the organelle. Cell 108:357–369

Wang L, Merz AJ, Collins KM, Wickner W (2003) Hierarchy of protein assembly at the vertex ring domain for yeast vacuole docking and fusion. J Cell Biol 160:365–374

Wang Y-X, Zhao H, Harding TM, Gomes de Mesquita D, Woldringh CL, Klionsky DJ, Munn AL, Weisman LS (1996) Multiple classes of yeast mutants are defective in vacuole partitioning yet target vacuole proteins correctly. Mol Biol Cell 7:1375–1389

Waterman-Storer CM, Gregory J, Parsons SF, Salmon ED (1995) Membrane/microtubule tip attachment complexes (TACS) allow the assembly dynamics of plus ends to push and pull membranes into tubulovesicular networks in interphase *Xenopus* egg extracts. J Cell Biol 130:1161–1169

Waters MG, Pfeffer SR (1999) Membrane tethering in intracellular transport. Curr Opin Cell Biol 11:453–459

Watkinson SC, Boddy L, Burton K, Darrah PR, Eastwood D, Fricker MD, Tlalka M (2005) New approaches to investigating the function of mycelial networks. Mycologist 19:11–17

Wedlich-Söldner R, Bölker M, Kahmann R, Steinberg G (2000) A putative endosomal t-SNARE links exo- and endocytosis in the phytopathogenic fungus *Ustilago maydis*. EMBO J 19:1974–1986

Wedlich-Söldner R, Straube A, Friedrich MW, Steinberg G (2002) A balance of KIF1A-like kinesin and dynein organises early endosomes in the fungus *Ustilago maydis*. EMBO J 21:2946–2957

Weisman LS (2003) Yeast vacuole inheritance and dynamics. Annu Rev Genet 37:435–460

Weisman LS (2006) Organelles on the move: insights from yeast vacuole inheritance. Mol Cell Biol 7:243–252

Weisman LS, Wickner W (1988) Intervacuole exchange in the yeast zygote: a new pathway in organelle communication. Science 241:589–591

Weisman LS, Bacallao R, Wickner W (1987) Multiple methods of visualizing the yeast vacuole permit evaluation of its morphology and inheritance during the cell cycle. J Cell Biol 105:1539–1547

Wendland B, Emr SD, Riezman H (1998) Protein traffic in the yeast endocytic and vacuolar sorting pathways. Curr Opin Cell Biol 10:513–522

West CA, Chufa H, Su M, Swanson SJ, Mentzer SJ (2001) Aldehyde fixation of thiol-reactive fluorescent cytoplasmic probes for tracking migration. J Histochem Cytochem 49:511–517

Westermann B, Prokisch H (2002) Mitochondrial dynamics in filamentous fungi. Fungal Genet Biol 36:91–97

Wickner W (2002) Yeast vacuoles and membrane fusion pathways. EMBO J 21:1241–1247

Wickner W, Haas A (2000) Yeast homotypic vacuole fusion: a window on organelle trafficking mechanisms. Annu Rev Biochem 69:247–275

Wiederkehr A, Avaro S, Prescianotto-Baschong C, Haguenauer-Tsapis R, Riezman H (2000) The F-box protein Rcy1p is involved in endocytic membrane traffic and recycling out of an early endosome in *Saccharomyces cerevisiae*. J Cell Biol 149:397–410

Wilson TP, Canny MJ, McCully ME, Lefkovitch LP (1990) Breakdown of cytoplasmic vacuoles: a model of endomembrane rearrangement. Protoplasma 155:144–152

Wong ED, Wagner JA, Scott SV, Okreglak V, Holewinske TJ, Cassidy-Stone A, Nunnari J (2003) The intramitochondrial dynamin-related GTPase, Mgm1p, is a component of a protein complex that mediates mitochondrial fusion. J Cell Biol 160:303–311

Wu Q, Sandrock TM, Turgeon BG, Yoder OC, Wirsel SG, Aist JR (1998) A fungal kinesin required for organelle motility, hyphal growth, and morphogenesis. Mol Biol Cell 9:89–101

Wu X, Xiang X, Hammere JA III (2006) Motor proteins at the microtubule plus-end. Trends Cell Biol 16:135–143

Xiang X, Han G, Winkelmann DA, Zuo W, Morris NR (2000) Dynamics of cytoplasmic dynein in living cells and the effect of a mutation in the dynactin complex actin-related protein Arp1. Current Biol 10:603–606

Xu Z, Sato K, Wickner W (1998) LMA1 binds to vacuoles at Sec18p (NSF), transfers upon ATP hydrolysis to a t-SNARE (Vam3p) complex, and is released during fusion. Cell 93:1125–1134

Yaffe MP (1999) Dynamic mitochondria. Nat Cell Biol 1:E149–E150

Yamaguchi M, Biswas SK, Kita S, Aikawa E, Takeo K (2002a) Electron microscopy of pathogenic yeasts *Cryptococcus neoformans* and *Exophiala dermatitidis* by high-pressure freezing. J Electron Microsc 51:21–27

Yamaguchi M, Biswas SK, Suzuki Y, Furukawa H, Sameshima M, Takeo K (2002b) The spindle pole body duplicates in early G1 phase in the pathogenic yeast *Exophiala dermatitidis*: an ultrastructural study. Exp Cell Res 279:71–79

Yamaguchi M, Biswas SK, Suzuki Y, Furukawa H, Takeo K (2003) Three-dimensional reconstruction of a pathogenic yeast *Exophiala dermatitidis* cell by freeze-substitution and serial sectioning by electron microscopy. FEMS Microbiol Lett 219:17–21

Yamashiro CT, Kane PM, Wolczyk DF, Preston RA, Stevens TH (1990) Role of vacuolar acidification in protein sorting and zymogen activation: a genetic analysis of the yeast vacuolar proton-translocating ATPase. Mol Cell Biol 10:3737–3749

Yamashita RA, May GS (1998) Motoring along the hyphae – molecular motors and the fungal cytoskeleton. Curr Opin Cell Biol 10:74–79

Young N, Bullock S, Orlovich DA, Ashford AE (1993) Association of polyphosphate with protein in freeze-substituted sclerotia of *Sclerotinia minor*. Protoplasma 174:134–141

Zhang J, Li S, Fischer R, Xiang X (2003) Accumulation of cytoplasmic dynein and dynactin at microtubule plus ends in *Aspergillus nidulans* is kinesin dependent. Mol Biol Cell 14:1479–1488

Zheng B, Wu JN, Schober W, Lewis DE, Vida T (1998) Isolation of yeast mutants defective for localization of vacuolar vital dyes. Proc Natl Acad Sci 95:11721–11726

3 The Fungal Woronin Body

T. Dhavale[1], G. Jedd[1]

CONTENTS

I. The Fungal Hypha – Structure and Evolution 87
II. The Fungal Mycelium 88
III. Woronin Body Ultrastructure and Composition 88
IV. Woronin Body Function 90
V. Woronin Bodies Require a Solid Crystalline Core 91
VI. Woronin Body Genesis in Apical Hyphal Compartments 91
VII. Phylogenetic Distribution 93
VIII. The Woronin Body as Adaptation 93
IX. Conclusion and Future Perspective 94
References 94

I. The Fungal Hypha – Structure and Evolution

Along with plants and animals, the fungi comprise one of three eukaryotic kingdoms that independently evolved multicellular organization. Most fungi are composed of an interconnected network of cellular filaments – these filaments, or hyphae, are the *sine qua non* of the fungal kingdom – providing the cellular basis underlying unique aspects of the fungal lifestyle. Hyphae support the invasive growth of saprobes and pathogens, facilitate long-distance transport in symbiotic mycorrhizal fungi and through their aggregation form the basis for the development of multicellular reproductive structures (Alexopolous et al. 1996).

Hyphae grow through a continuous process of polarized tip-extension resulting in a tubular cell that can branch at its tip or laterally. These branches can further undergo a process of cell-to-cell fusion known as anastomosis and, ultimately, these processes combine to produce a syncytial network of interconnected cells known as the mycelium (Buller 1933a; Glass et al. 2004). The fungi are grouped into four distinct phyla on the basis of characteristic traits and differences in the nucleotide sequence of molecular markers (Bruns et al. 1992; Berbee and Taylor 2001; Lutzoni 2004). In the basal or early-diverging fungi, the Zygomycetes and Chytrids, vegetative hyphae are not interrupted by cell walls. In contrast the two remaining sister phyla, the Ascomycetes and Basidiomycetes (collectively referred to as dikaryomycetes, based on shared sexual physiology), are more recently evolved and their hyphae are interrupted at regular intervals by perforate cell walls known as septa (Fig. 3.1). The phylogenetic distribution of this character suggests that the perforate septum evolved in an ancestor common to the dikaryomycetes (Fig. 3.1 Berbee and Taylor, 2001) and this innovation may have favored the advent of septal pore-associated organelles such as the Woronin body, which is characteristic of Euascomycetes and the septal pore cap (SPC) found in certain Basidiomycetes (Bracker, 1967; Muller et al., 1998).

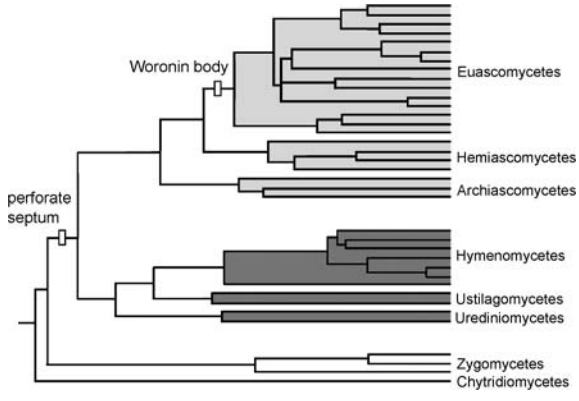

Fig. 3.1. Fungal phylogenetic tree with selected characters indicated. The phylogeny is based on 18S ribosomal RNA (modified from Berbee and Taylor 2001). Ascomycetes and Basidiomycetes are shaded *light gray* and *dark gray*, respectively. The inferred phylogenetic origin of the perforate septum and the Woronin body is indicated. The figure is presented as a working model

[1] Temasek Life Sciences Laboratory and Department of Biological Sciences, National University of Singapore, 1 Research Link, Singapore 117604

Biology of the Fungal Cell, 2nd Edition
The Mycota VIII
R.J. Howard and N.A.R. Gow (Eds.)
© Springer-Verlag Berlin Heidelberg 2007

II. The Fungal Mycelium

The fungal mycelium is a form of syncytial cellular organization that belies conventional definitions of the cell. In multicellular eukaryotes, cells can communicate with neighboring cells through a variety of conduits that allow the passage of selected macromolecules and organelles. These include gap junctions (Sosinsky and Nicholson, 2005) and tunneling nanotubules (Rustom et al., 2004) in animals and plasmodesmata in plants (Gallagher and Benfey, 2005). In contrast, the septal pore in fungal hyphae is unusually large and in some cases can provide a channel for the trans-cellular flow of protoplasm.

This phenomenon was first revealed by observations on the trans-cellular migration of vacuoles (Buller, 1933b). More recent experiments have shown that injected mineral oil also displays cell-to-cell movement in *Neurospora crassa* and because this material is unlikely to engage cellular motor proteins, this movement reflects the bulk flow of protoplasm (Lew, 2005). Other observations suggest that septal pores support long-distance transport: The fungal colony can be divided into two distinct zones; a peripheral growth zone where hyphal compartments contribute to tip-growth at the colonies leading edge and a central growth zone, where hyphae can continue to grow and accumulate biomass, but do not contribute to the colonies radial expansion (Trinci, 1971). These regions of the colony were experimentally defined by cutting hyphae at a defined distance from the growth front - the distance at which hyphal damage fails to inhibit growth of leading hyphae, defines the border between the peripheral and central growth zone. The peripheral growth zone in septate fungi is composed of many hyphal compartments and can be as wide as 1 cm (Trinci, 1971). While the precise role of sub-apical hyphae in supporting the tip growth of apical hyphae remains to be determined, it is likely that this contribution consists of tip-growth-associated factors such as secretory vesicles. Septal pores have also been shown to support long distance transport in the *mycorrhizal* Basidiomycete, *Pisolithus tinctorius*. In this system, motile-tubular vacuoles are responsible for the transport of nutrients such as phosphate throughout the mycelium. These tubular vacuoles can be seen forming transient connections via septal pores (Sheperd et al., 1993; Cole et al., 1998) and these observations provide an additional example of how septal pores can be used to facilitate long distance transport.

Early diverging fungi rarely exhibit septation, suggesting that this trait is not a prerequisite for the development of a fungal mycelium. However, several observations suggest that perforate septation supports complex forms of multicellularity absent in the basal fungi. In dikaryomycetes, the perforate septum provides the benefits afforded by cellular continuity while providing an intercellular channel, the septal pore, which can be gated, allowing hyphae to "cellularize" during differentiation and in response to hyphal damage, stress and aging. Moreover, the fungi with the most prominent and complex septal pore-associated organelles, the Hymenomycetes and Euascomycetes (Fig. 3.1), which contain septal pore caps (Bracker 1967; Muller et al. 1998) and Woronin bodies, respectively, also produce the largest and most complex multicellular fruiting bodies (Alexopolous et al. 1996), further suggesting that septate hyphae and associated organelles support complex forms of multicellular organization.

III. Woronin Body Ultrastructure and Composition

First reported by the Russian mycologist Michael Stepanovitch Woronin in the Euascomycete *Ascobolus pulcherrimus* (Woronin 1864; Buller 1933c), Woronin bodies were subsequently observed in many filamentous fungi, including plant and human pathogens (Markham and Collinge 1987). Their observation has thus far been confined to the Euascomycetes, suggesting that they arose in a common ancestor of this monophyletic group (Fig. 3.1). In thin-section transmission electron microscopy (TEM), Woronin bodies present a dense osmophilic core that is circumscribed by a tightly appressed unit membrane (Figs. 3.2, 3.3). In some cases the core structure has been observed in the matrix of peroxisomes, providing early evidence that Woronin bodies are produced from this organelle (Wergin 1973; Camp 1977). The core has a spheroidal morphology in the majority of species while in others, like *N. crassa*, it has the form of a hexagonal disk (Fig. 3.2). Protease digestion of hyphae embedded in thin sections first showed that the core is composed of protein (McKeen 1971; Hoch and Maxwell 1974). The overall size of Woronin bodies varies from around 100 nm to over 1 µm and this dimension is species-specific, always slightly exceeding the

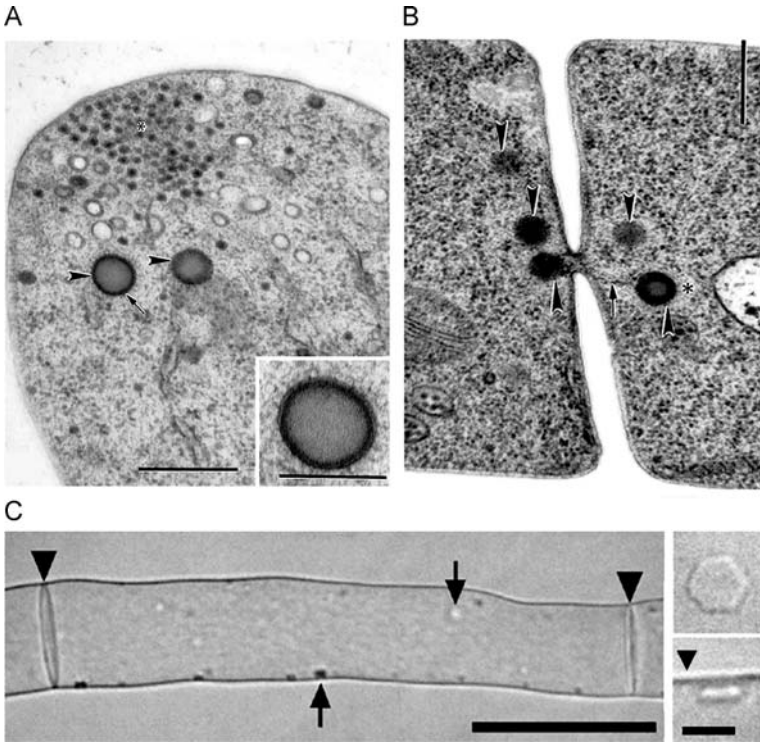

Fig. 3.2. Appearance and distribution of Woronin bodies in *Aspergillus nidulans* and *Neurospora crassa*. **A** Woronin bodies in the apical cell of *A. nidulans* by TEM. Two Woronin bodies (*arrowheads*) are observed in the vicinity of the Spitzenkörper (∗). *Bar* 250 nm. *Inset* Woronin body (identified by *arrow* in main image) shown magnified. *Bar* 125 nm. **B** Woronin bodies (*arrowheads*) at the *A. nidulans* septal pore (sub-apical region of hypha). *Arrow* indicates a mesh-like structure that appears to associate the Woronin body to the rim of the septal pore. *Bar* 250 nm. **C** Refractive Woronin bodies shown by light microscopy in *N. crassa*. *Left panel* Light microscopic view of a single sub-apical compartment of *N. crassa*, showing Woronin bodies associated with the cell cortex (*arrows*). *Bar* 20 µm. *Right panel* Magnified view of a Woronin body seen in face view (*top*) and in side view (*bottom*). *Arrowhead* Cell wall. *Bar* 2 µm. Parts **A** and **B** are adapted with permission from Momany et al. (2002)

inner diameter of the septal pore (Markham and Collinge 1987). In most species, the Woronin body is found in proximity to and on both sides of the septum (Fig. 3.2B) and can appear attached to the pore through a tether, which has the appearance of a mesh in TEM (Momany et al. 2002). The presence of a tether is further supported by experiments with laser tweezers: Woronin bodies pulled away from the septum have been observed recoiling to their original position upon release (Berns et al. 1992). In other species, such as *N. crassa*, the Woronin body is associated with the cell cortex, where it also appears to be sequestered as suggested by its exclusion from protoplasmic flow (Tey et al. 2005).

Woronin bodies were first purified from *N. crassa* through the combined use of differential and density gradient centrifugation (Jedd and Chua, 2000; Tenney et al., 2000). The *N. crassa* Woronin body can be seen as a refractive structure by light microscopy and this provided a convenient means of following the organelles distribution during its purification. Woronin body-enriched fractions contain an abundant 19 kDa protein, HEX-1, which was identified by protein sequencing and found to define a family of closely related proteins unique to Euascomycetes (Jedd and Chua, 2000; Tenney et al., 2000). In addition, HEX-1 shares weak homology to eIF-5A proteins (24% identity, 40% similarity, pBLAST 6e-07) and this provided the first hint of an evolutionary relationship between these two functions (Jedd and Chua, 2000). Antibodies to HEX-1 decorate

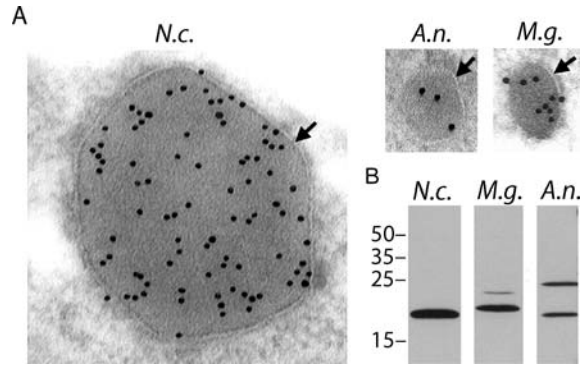

Fig. 3.3. Appearance and composition of Woronin bodies in three species of Euascomcyete. **A** Immuno-gold detection of HEX-1 in thin sections. Gold particles (10 nm) indicate binding of the HEX-1 specific antibody and prove the scale. *Arrows* Woronin body membrane. **B** Detection of HEX-1 by Western blotting. Size is indicated to the *left* (kDa). Note that both *Magnaporthe grisea* (*M. g.*) and *Aspergillus nidulans* (*A. n.*) exhibit two forms of the HEX-1 protein. *N. c. Neurospora crassa*

the matrix of the Woronin body (Fig. 3.3) in *N. crassa* (Jedd and Chua, 2000) *Aspergillus nidulans* (Momany et al., 2002), and *Magnaporthe grisea* (Soundararajan et al., 2004) and differential centrifugation revealed that HEX-1 exists in an extremely large and stable protein complex. *hex-1* and its orthologs all encode a consensus C-terminal peroxisome targeting signal (PTS-1), suggesting transport into the peroxisomal matrix. This was confirmed by experiments in the yeast *Saccharomyces cerevisiae* (Hemiascomycetes do not produce Woronin bodies), where *hex-1* expression results in the formation of hexagonal intra-peroxisomal protein assemblies displaying morphological similarity to the native Woronin body core. This also provided the first evidence that HEX-1 has the capacity to self-assemble and this was further confirmed by experiments demonstrating the ability of pure HEX-1 to self-assemble in vitro into characteristic hexagonal crystals (Jedd and Chua, 2000). Collectively, these results defined HEX-1 as a key structural determinant of the Woronin body core and demonstrated that Woronin bodies are indeed peroxisome derived.

Examination of *hex-1* in other species also revealed a process of alternative splicing between the first and second exon that produces two variant proteins differing by several kilodaltons at their N-terminus (Fig. 3.3). These two forms have been reported in *Magnaporthe grisea* (Soundararajan et al. 2004), *Aspergillus oryzae* (Maruyama et al. 2005) and *Trichoderma reesei* (Lim et al. 2001; Curach et al. 2004). All of these organisms produce a spheroidal Woronin body, as opposed to the hexagonal form produced by a single version of HEX-1 in *Neurospora crassa* (Figs. 3.2, 3.3; Jedd and Chua 2000). This correlation suggests that a co-complex of HEX-1 isoforms may determine the spheroidal morphology. One model predicts that the co-assembly of these isoforms may perturb crystal growth and consequently alter the shape of the resultant assemblage. This model is also consistent with observations documenting maturation of the spheroidal form from an early hexagonal intermediate (Wergin 1973). Alternatively, alternative splicing may control other aspects of Woronin body function (Soundararajan et al. 2004) and additional experiments are required to ascertain the precise function of *hex-1* splice-variants and whether these determine variation in Woronin body core-structure.

IV. Woronin Body Function

N. crassa Woronin bodies were first shown to occlude septal pores following hyphal damage that was induced by flooding with water or cutting with a razor blade (Trinci and Collinge, 1973). This function was further quantified in *Penicillium chrysogenum* where Woronin bodies were shown to rapidly plug 90% of septal pores within the vicinity of induced damage, whereas, only 5% were plugged in undamaged hyphae (Collinge and Markham, 1985). Electron microscopy further showed that material resembling the cell wall is deposited over the Woronin body septal-pore complex and new hyphal tips regenerate from the occluded septum (Trinci and Collinge, 1973), suggesting a pathway whereby septal pore occlusion is rapidly followed by plasma membrane re-sealing and the resumption of tip-growth.

The analysis of *hex-1* mutants in diverse Euascomycetes has shown that Woronin bodies execute a conserved function in damage-induced septal pore sealing. A *Neurospora hex-1* deletion mutant is devoid of visible Woronin bodies and the mutant presents a variety of phenotypes resulting from defects in cell damage-induced septal pore sealing: hyphae bleed protoplasm following mechanically induced cellular injury or hypotonic shock (Jedd and Chua 2000; Tenney et al. 2000) and, as a secondary consequence of this defect, mutants are also impaired in cellular regeneration following damage (Jedd and Chua 2000). In addition, aerial hyphae spontaneously lyse and bleed protoplasm, resulting in a greatly diminished capacity to produce asexual spores known as conidia (Jedd and Chua 2000; Tenney et al. 2000).

hex-1 mutants in *Magnaporthe grisea* (Soundararajan et al. 2004) and *Aspergillus oryzae* (Maruyama et al. 2005) also lack visible Woronin bodies and display defects consistent with the loss of damage-induced septal pore-plugging. Also, in *A. oryzae* Woronin bodies were labeled with the red fluorescent protein (RFP) and this allowed the three-dimensional imaging of septal pore-plugging in response to hypotonic shock (Maruyama et al. 2005).

In addition to defects in septal pore plugging, the *Magnaporthe hex-1* mutant is also defective in appressorium morphogenesis, invasive growth within the plant host and the mutant displays cell death in response to nitrogen starvation (Soundararajan et al. 2004). Nitrogen starvation

and *in planta* growth also appear to regulate the production of HEX1 splice-variants, favoring the use of a particular 3'-splice acceptor sequence (Soundararajan et al. 2004). Taken together, these results show that the Woronin body provides *Magnaporthe* with an important defense system in the context of *in planta* growth, and they further suggest that this system may be regulated – via alternate splicing – by nitrogen starvation (Soundararajan et al. 2004).

The demonstrated importance of Woronin bodies for *Magnaporthe* pathogenesis and the presence of *hex-1* orthologs in other pathogenic Euascomycetes (for example: *A. fumigatus*, *Coccidiodes immitis*, *Fusarium graminaeum*, *Botrytis cinerea*, *Chaetomium globosum*) suggest that this organelle may present an attractive target for the future development of novel fungicides.

V. Woronin Bodies Require a Solid Crystalline Core

Purified recombinant *N. crassa* HEX-1 spontaneously self-assembles into hexagonal crystals with the overall geometry of the *N. crassa* Woronin body and the structure of these crystals has been determined at a resolution of 1.8 Å (Yuan et al., 2003). The HEX-1 monomer has a two-domain structure consisting of mutually perpendicular antiparallel β-barrels (Fig. 3.4A; Yuan et al., 2003). Interestingly, this structure shares a similar domain architecture and overall fold with the structure of two archaebacterial eIF5-A proteins (Kim et al., 1998; Peat et al., 1998) (compare Fig. 3.4A,B and C). eIF-5A proteins are highly conserved and found from archaebacteria through eukaryotes and appear to function in mRNA transport or metabolism (Zuk and Jacobson, 1998; Rosorius et al., 1999). The observed structural homology coupled with a significant level of sequence homology (Fig. 3.4D) suggests that *hex-1* may have evolved from *eIF-5A* following gene duplication in the ancestral Euascomycete (see below).

The HEX-1 structure further reveals the basis of its self-assembly. HEX-1 monomers create a crystal lattice by associating via three intermolecular contacts called Group I, Group II and Group III. Association through Group I and II contacts results in the formation of a structural helical filament (Fig. 3.4D) and group III contacts crosslink these filaments, with each contacting 6 identical neighbors (Fig. 3.4E). This packaging produces the overall hexagonal symmetry of the native *N. crassa* Woronin body (compare Fig. 3.4C and Fig. 3.4E). Amino-acid residues mediating crystal lattice formation are conserved in HEX-1 orthologs and crystal contacts bury a degree of surface area (Group I; 1,299, Group II; 697 and Group III; 515 $Å^2$), comparable to that observed at other oligomeric interfaces (Henrick and Thornton, 1998; Yuan et al., 2003). Together, these observations suggest that the lattice structure observed in recombinant HEX-1 crystals may be a good model of the native Woronin body core.

Mutations disrupting crystal contact residues provided a direct test of the lattice model of Woronin body structure. A mutation disruption of the Group I contact (H39G) destroys the ability of HEX-1 to self-assemble in vitro and produces aberrant Woronin bodies possessing a soluble non-crystalline core in vivo. These vesicles grow to normal dimensions but fail to plug septal pores, as assessed by their inability to complement loss-of-function phenotypes, such as protoplasmic bleeding and defects in conidiation (Yuan et al. 2003). Taken together, these experiments demonstrate the significance of the HEX-1 crystal lattice to normal Woronin body function (Yuan et al. 2003). What specific aspect of fungal physiology might have selected for this property? Hyphae possess a measurable intracellular pressure that is associated with protoplasmic translocation (Lew 2005) and tip growth (Money and Harold 1992; Lew et al. 2004; Money et al. 2004). This intracellular turgor pressure needs to be resisted during septal pore sealing and may have provided the cellular condition favoring the evolution of HEX-1 crystallinity.

VI. Woronin Body Genesis in Apical Hyphal Compartments

Woronin bodies are found in all vegetative hyphae and are formed de novo, that is, without the division of a pre-existent Woronin body. Because Woronin bodies generally exceed septal pore diameter, it is unlikely that they are trafficked from sites of synthesis to sites of function and this further suggests that they are formed early in the process of hyphal growth. Consistently, Woronin bodies are present in the apical hyphal compartment, as first observed by light microscopy (Ternetz 1900; Buller 1933c)

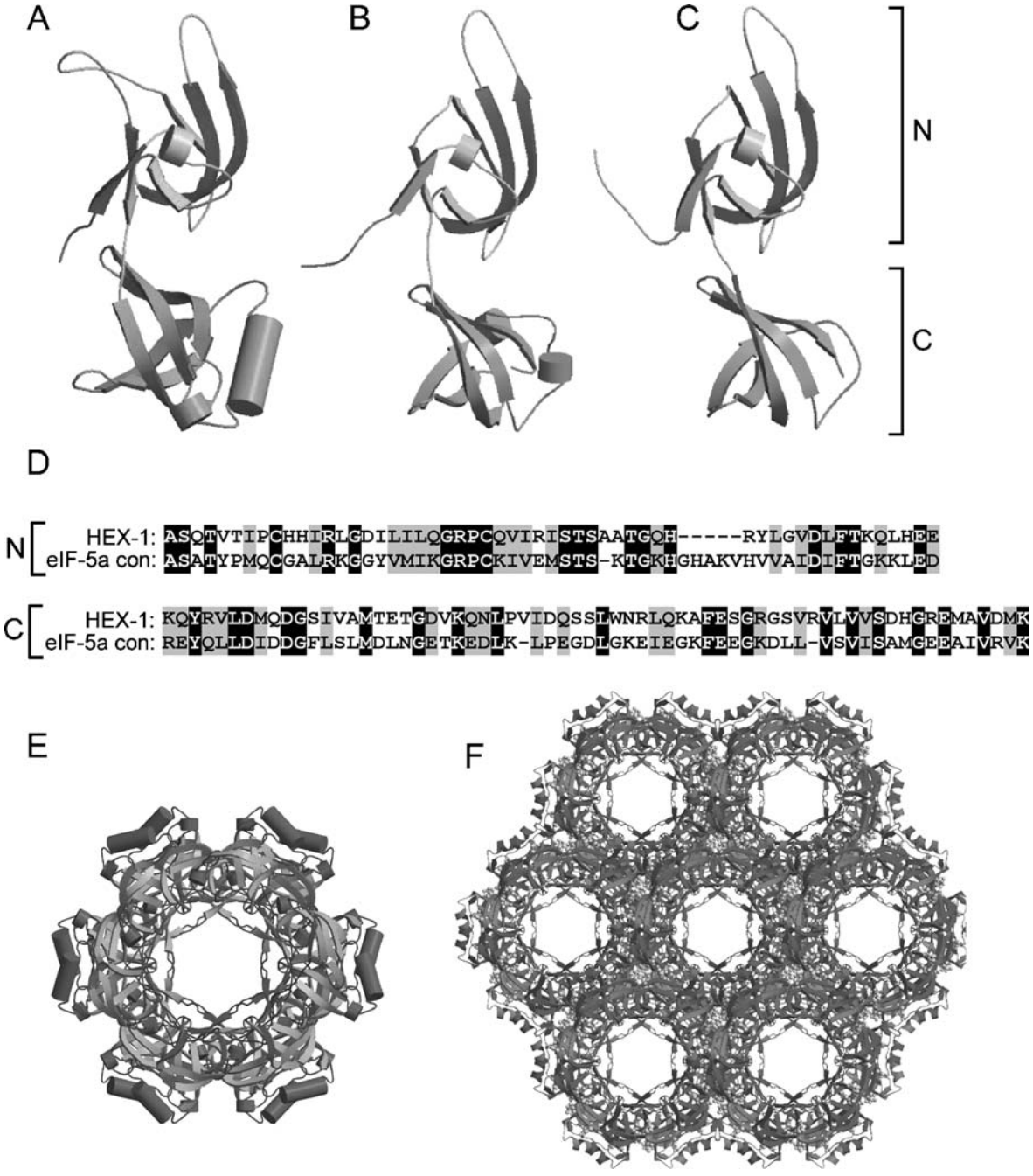

Fig. 3.4. Structure of HEX-1, eIF-5A and the HEX-1 crystal lattice. Overall structure of *N. crassa* HEX1 (**A**) and eIF-5A from *Pyrobaculum aerophilum* (**B**) and *Methanococcus jannaschii* (**C**). All three proteins are composed of two mutually perpendicular antiparallel β-barrels. The N-terminal (*N*) and C-terminal domains (*C*) are indicated at *right*. Beta sheets and alpha helical regions are depicted with *flat arrows* and *cylinders*, respectively. (**D**) HEX-1 shares sequence homology with eIF-5A proteins. The N- and C-terminal domains of *N. crassa* HEX-1 are aligned to the eIF-5A consensus sequence. Identical residues are *shaded black* and conserved residues are *shaded grey*. (**E**) HEX-1 monomers interact through alternating Group I and Group II contacts to produce a coiled filament that is viewed down the crystallographic *c-axis*. (**F**) Group III contacts associate these filaments to produce the hexagonal crystal lattice

and later by electron microscopy in a variety of Euascomycetes (Fig. 3.2A; Brenner and Carrol 1968; McClure et al. 1968; Collinge and Markham 1982; Momany et al. 2002). In addition, the distribution of Woronin bodies in *Aspergillus* germlings has been quantified by serial section TEM. In germlings that have undergone septation, fewer Woronin bodies are found at the hyphal tip, suggesting that septation may be associated with a process of retrograde transport of apical Woronin bodies and their targeting to the septum (Momany et al. 2002).

Time-lapse confocal microscopy in *Neurospora crassa* allowed the direct observation of Woronin body biogenesis in living hyphae. In apical cells, the Woronin body core is observed in the matrix of unusually large peroxisomes and this complex moves dynamically – generally in a tip-directed manner. Moving apical Woronin bodies undergo a process of maturation, involving membrane fission, and then begin to associate with the cell cortex roughly at the time of septation. These Woronin bodies are immobilized and excluded from forward protoplasmic flow. Thus, the continuous formation of Woronin bodies in apical compartments and their subsequent inheritance into sub-apical compartments through cortical association ensures that all compartments are endowed with a roughly uniform number of Woronin bodies (Tey et al. 2005).

What factors determine the localization of this process to apical cells? Expression of a fluorescent reporter protein from *hex-1* regulatory sequences revealed a tip-high fluorescent gradient that diminished towards sub-apical cells and this suggested that *hex-1* gene expression is polarized to apical compartment. To determine the spatial distribution of endogenous *hex-1* transcripts, a system was developed that fractionated the fungal colony grown on solid medium into zones corresponding to apical and increasingly sub-apical hyphal compartments (Tey et al. 2005). Using this system, endogenous *hex-1* transcripts were found to be specifically enriched at the leading edge of the fungal colony, while other transcripts were shown to accumulate in the colony interior (Tey et al. 2005). These experiments demonstrated the apical programming of hyphal gene expression and suggested a possible role for localized *hex-1* mRNA transcripts in the apical formation of the Woronin body. To test this model, the *hex-1* structural gene was expressed from the regulatory sequences of a transcript normally confined to the colony interior and, under these conditions, Woronin body formation was re-directed to the colony interior. Thus, the localization of *hex-1* transcripts is a key determinant of the localization of Woronin body formation. In this case, the apical programming of gene expression ensures that the first sub-apical compartment contains a complement of functional Woronin bodies (Tey et al. 2005).

VII. Phylogenetic Distribution

hex-1 orthologs have been identified in 17 Euascomycetes, including all seven with fully sequenced genomes (Jedd 2006). In all cases where sequence data is available, *hex-1* encodes a consensus PTS-1 and largely conserves crystal contact residues. In contrast, *hex-1* homologs are absent from the nine fully sequenced fungal genomes outside of the Euascomycetes[1]. This distribution conforms to the idea that *hex-1* arose in the ancestral Euascomycete (Fig. 3.1). An exception, however, may be found in the Archiascomycete *Neolecta*; most Archiascomycetes grow as yeast but some (e.g. *Taphrina* and *Neolecta*) are hyphal. *Neolecta* exhibits perforate septa, fruiting bodies, forcibly discharged asci and Woronin body-like organelles (Landvik et al. 2003), thus possessing numerous characters typical of the Euascomycetes. Low stringency Southern blotting has failed to detect a *hex-1* homolog in *Neolecta* (Hewitt and Jedd, unpublished data), suggesting a distinct evolutionary origin for its Woronin body-like organelle. However, it is possible that a highly divergent *hex-1* homolog may not be detected by this technique. Organelle purification and cloning of genes encoding resident proteins is crucial to resolving the origin of this Woronin body-like organelle. If a *hex-1* homolog indeed exists in *Neolecta*, then Woronin bodies may predate the ancestral Euascomycete. Alternatively, the Woronin body-like organelle in *Neolecta* may represent a convergent, evolutionarily independent, solution to Woronin body function.

VIII. The Woronin Body as Adaptation

Organelles associated with septal pores may be thought of as components of a highly adapted cel-

[1] These include yeast and filamentous Hemiascomycetes (*Saccharomyces cerevisiae* and *Ashbya gossypii*, respectively), an Archiascomycete (*Schizosaccharomyces pombe*), filamentous Hymenomyctes (*Coprinus cinereus*, *Phanerochaete chrysosporium*), an Ustilaginomycete (*Ustilago maydis*) and a Zygomycte (*Rhizopus oryzae*).

lular system. In one scenario, the evolution of the vegetative perforate septum in the common ancestor of the dikaryomycetes introduces selective pressure for the evolution of new supporting functions. One product of such selective pressure is the Woronin body, which exploited a pre-existent organelle, the peroxisome, for its formation and performs an adaptive function that is dependent on the septal pore (Jedd and Chua 2000; Tenney et al. 2000). Furthermore, a solid crystalline core of HEX-1 is essential for this function (Yuan et al. 2003) and can be seen as advantageous in the context of the turgor pressure characteristic of fungal hyphae (Buller 1933b; Money and Harold 1992; Bartnicki-Garcia et al. 2000; Money et al. 2004).

HEX-1 shares both sequence (Jedd and Chua 2000) and structural (Yuan et al. 2003) homology with eIF-5A proteins, suggesting that these functions may be related through gene duplication in the ancestral Euascomycete. eIF-5a proteins are ancient (found from the Archaea through eukaryotes) and highly conserved (Kyrpides and Woese 1998). They function in the cytoplasm and are involved in mRNA transport (Rosorius et al. 1999) or stability (Zuk and Jacobson 1998); and currently no evidence suggests that eIF-5a forms large protein complexes. Thus, *hex-1* may have evolved via the duplication of an ancestral eIF-5a followed by its acquisition of new functions. Consistently, residues that are conserved between HEX-1 and eIF-5a are largely those that determine the overall protein fold, suggesting that these residues were maintained in *hex-1* over time, while surface residues evolved to acquire new functions associated with peroxisome targeting and self-assembly (Yuan et al. 2003). This model conforms to the hypothesis that gene duplication and the subsequent acquisition of novel function can be associated with evolutionary transitions (Ohno 1970) and, in this light, it will be interesting to learn more about the nature and possible origins of additional genes associated with Woronin body function.

IX. Conclusion and Future Perspective

Woronin bodies define a peroxisomal function unique to the Euascomycetes and their biology is intimately associated with the fungal lifestyle. The structure of the Woronin body core is now understood at atomic resolution (Yuan et al. 2003) and the organelles biogenesis has defined a process of genetic differentiation in apical hyphal compartments (Tey et al. 2005). Important questions remain: (1) are Woronin bodies simply peroxisomes containing HEX-1 crystals, or do other proteins specifically contribute to Woronin body formation and function, as suggested by the organelles complex biology, (2) how is membrane resealing at the septal pore achieved and (3) what are the mechanisms controlling Woronin body genesis in apical hyphal compartments and inheritance by sub-apical compartments? The isolation of additional Woronin body-defective mutants should help answer these questions.

References

Alexopolous CJ, Mims CW, Blackwell M (1996) Introductory mycology. Wiley, Chichester

Bartnicki-Garcia S, Bracker CE, Gierz G, Lopez-Franco R, Lu H (2000) Mapping the growth of fungal hyphae: orthogonal cell wall expansion during tip growth and role of turgor. Biophys J 79:2382–2390

Berbee ML, Taylor JW (2001) Fungal molecular evolution: gene trees and geological time. In: McLaughlin DJ, McLaughlin EG, Lemke PA (eds) The Mycota, vol VII, part B. Systematics and evolution. Springer, Berlin Heidelberg New York, pp 229–245

Berns MW, Aist JR, Wright WH, Liang H (1992) Optical trapping in animal and fungal cells using a tunable, near-intrared titanium-sapphire laser. Exp Cell Res 198:375–378

Bracker CE (1967) Ultrastructure of fungi. Annu Rev Phytopathol 5:343–374

Brenner DM, Carrol GC (1968) Fine structural correlates of growth in hyphae of *Ascodesmis sphaerospora*. Journal of Bacteriology 95:658–671

Bruns TD, Vilgalys S, Barns D, Gonzalez DS, Hibbett DJ, Lane L, Simon S, Stickel TM, Szaro WG, Weisburg WG, Sogin ML (1992) Evolutionary relationships within the fungi:analyses of nuclear small subunit RNA sequences. Mol Phylogenet Evol 1:231–241

Buller AHR (1933a) The formation of hyphal fusions in the mycelium of the higher fungi. In: Buller AHR (ed) Researches on fungi, vol V. Longmans, London, pp 1–74

Buller AHR (1933b) The translocation of protoplasm through septate mycelium of certain Pyrenomycetes, Discomycetes and Hymenomycetes. In: Buller AHR (ed) Researches on fungi, vol V. Longmans, London, pp 75–167

Buller AHR (1933c) Woronin bodies and their movements. In: Buller AHR (ed) Researches on fungi, vol V. Longmans, London, pp 127–130

Camp RR (1977) Association of microbodies, Woronin bodies, and septa in intercellular hyphae of *Cymadothea trifolii*. Can J Bot 55:1856–1859

Cole L, Orlovick DA, Ashford AE (1998) Structure, function, and motility of vacuoles in filamentous fungi. Fungal Genet Biol 24:86–100

Collinge AJ, Markham P (1982) Hyphal tip ultrastructure of *Aspergillus nidulans* and *Aspergillus giganteus* and possible implications of Woronin bodies close to the hyphal apex of the latter species. Protoplasma 113:209–213

Collinge AJ, Markham P (1985) Woronin bodies rapidly plug septal pores of severed *Penicillium chrysogenum* hyphae. Exp Mycol 9:80–85

Curach NC, Te'o VS, Gibbs MD, Bergquist PL, Nevalainen KM (2004) Isolation, characterization and expression of the hex1 gene from *Trichoderma reesei*. Gene 331:33–140

Gallagher KL, Benfey PN (2005) Not just another hole in the wall: understanding intercellular protein trafficking. Genes Dev 19:189–195

Glass NL, Rasmussen C, Roca G, Read ND (2004) Hyphal homing, hyphal fusion and mycelial interconnectedness. Trends Microbiol 12:135–141

Henrick K, Thornton JM (1998) PQS: a protein quatrenary structure file server. Trends Biol Sci 23:358–361

Hoch HC, Maxwell DP (1974) Proteinaceous hexagonal inclusion in hyphae of *Whetzelinia sclerotiorum* and *Neurospora crassa*. Can J Microbiol 20:1029–1036

Jedd G (2006) Natural history of the fungal hypha: how Woronin bodies support a multicellular lifestyle. In: Gadd GM (ed) Fungi in the environment. Cambridge University, Cambridge

Jedd G, Chua NH (2000) A new self-assembled peroxisomal vesicle required for efficient resealing of the plasma membrane. Nature Cell Biol 2:226–231

Jennings DH, Thornton JD, Galpin MF, Coggins CR (1974) Translocation in fungi. Symp Soc Exp Biol 28:139–156

Kim KK, Hung LW, Yokota H, Kim R, Kim SH (1998) Crystal structures of eukaryotic translation initiation factor 5A from Methanococcus jannaschii at 1.8° resolution. Proc of the Natl Acad Sci USA 95:10419–10424

Kyrpides NC, Woese CR (1998) Universally conserved translation initiation factors. Proc Natl Acad Sci USA 95:224–228

Landvik S, Schumacher TK, Eriksson OE, Moss ST (2003) Morphology and ultrastructure of *Neolecta* species. Mycol Res 107:1021–1031

Lew RR (2005) Mass flow and pressure-driven hyphal extension in *Neurospora crassa*. Microbiology 151:2685–2692

Lew RR, Levina NN, Walker SK, Garrill A (2004) Turgor regulation in hyphal organisms. Fungal Genet Biol 11:1007–1015

Lim DB, Hains P, Walsh B, Bergquist P, Nevalainen H (2001) Proteins associated with the cell envelope of *Trichoderma reesei*: a proteomic approach. Proteomics 1:899–909

Lutzoni F, Kauff F, Cox JC, McLaughlin D, Celio G, Dentinger B, Padamsee M, Hibbett D, James TY, Baloch E, Grube M, Reeb V, Hofstetter V, Shcoch C, Arnold AE, Miadlikowska J, Spatafora J, Johnson D, Hambleton S, Crockett M, Shoemaker R, Sung G-H, Lücking R, Lumbsch T, O'Donnell K, Binder M, Diederich P, Ertz D, Gueidan C, Hansen K, Harris RC, Hosaka K, Lim Y-W, Matheny B, Nishida H, Pfister D, Rogers J, Rossman A, Schmitt I, Sipman H, Stone J, Sugiyama J, Yahr R, Vilgalys R (2004) Assembling the fungal tree of life: progress, classification, and evolution of subcellular traits. Am J Bot 91:1446–1480

Markham P, Collinge AJ (1987) Woronin bodies of filamentous fungi. FEMS Microbiol Rev 46:1–11

Maruyama J, Juvvadi PR, Ishi K, Kitamoto K (2005) Three-dimensional image analysis of plugging at the septal pore by Woronin body during hypotonic shock induced hyphal tip bursting in the filamentous fungus *Aspergillus oryza*e. Biochem Biophys Res Commun 331:1081–1088

McClure WK, Park D, Robinson PM (1968) Apical organization in the somatic hyphae of fungi. J Gen Microbiol 50:177–182

McKeen WE (1971) Woronin bodies in *Erysiphe graminis* DC. Can J Microbiol 17:1557–1563

Momany M, Richardson EA, Van Sickle C, Jedd G (2002) Mapping Woronin body position in *Aspergillus nidulans*. Mycologia 94:260–266

Money NP, Harold FM (1992) Extension growth of the water mold *Achlya*: interplay of turgor and wall strangth. Proc Natl Acad Sci USA 15:4245–4259

Money NP, Davis CM, Ravishankar JP (2004) Biochemical evidence for convergent evolution of the invasive growth process among fungi and oomycete water molds. Fungal Genet Biol 41:872–876

Muller WH, Montijn RC, Humbel BM, Aelst AC van, Boon EJMC, Krift TP van der, Boekhout T (1998) Structural differences between two types of basidiomycete septal pore caps. Microbiology 144:1721–1730

Ohno S (1970) Evolution by gene duplication. Springer, Berlin Heidelberg New York

Peat TS, Newman J, Waldo GS, Berendzen J, Terwilliger TC (1998) Structure of translation initiation factor 5A from Pyrobaculum aerophilum at 1.75° resolution. Structure 6:1207–1214

Rosorius O, Reichart B, Kratzer F, Heger P, Dabauvalle MC, Hauber J (1999) Nuclear pore localization and nucleocytoplasmic transport of eIF-5A: evidence for direct interaction with the export receptor CRM. J Cell Sci 112:2369–2380

Rustom A, Saffrich R, Markovic I, Walther P, Gerdes HH (2004) Nanotubular highways for intercellular organelle transport. Science 303:1007–1010

Shepherd VA, Orlovick DA, Ashford AE (1993) Cell-to-cell transport via motile tubules in growing hyphae of a fungus. J Cell Sci 105:1173–1178

Sosinsky GE, Nicholson BJ (2005) Structural organization of gap junction channels. Biochim Biophys Acta 1711:99–125

Soundararajan S, Jedd G, Li X, Ramos-Pamplona M, Chua NH, Naqvi NI (2004) Woronin body function in *Magnaporthe grisea* is essential for efficient pathogenesis and for survival during nitrogen starvation stress. Plant Cell 16:1564–1574

Tenney K, Hunt I, Sweigard J, Pounder JI, McClain C, Bowman EJ, Bowman BJ (2000) *hex-1*, a gene unique to filamentous fungi, encodes the major protein of the Woronin body and functions as a plug for septal pores. Fungal Genet Biol 31:205–217

Ternetz C (1900) Protoplasmabewegung und Fruchtkoperbildung bei *Ascophanus carneus*. Jahrb Wiss Bot 35:273–312

Tey WK, North AJ, Reyes JL, Lu YF, Jedd G (2005) Polarized gene expression determines Woronin body formation

at the leading edge of the fungal colony. Mol Biol Cell 16:2651–2659

Trinci APJ (1971) Influence of the width of the peripheral growth zone on the radial growth rate of fungal colonies on solid media. J Gen Microbiol 67:325–344

Trinci APJ, Collinge AJ (1973) Occlusion of septal pores of damaged hyphae of *Neurospora crassa* by hexagonal crystals. Protoplasma 80:57–67

Wergin WP (1973) Development of Woronin bodies from microbodies in *Fusarium oxysporum* f.sp. *lycopersici*. Protoplasma 76:249–260

Woronin M (1864) Zur Entwicklungsgeschichte der *Ascobolus pulcherrimus* Cr und eigiger Pezizen. Abh Senkenb Naturforsch Ges 5:333–344

Yuan P, Jedd G, Kumaran D, Swaminathan S, Shio H, Hewitt D, Chua NH, Swaminathan K (2003) A HEX-1 crystal lattice required for Woronin body function in *Neurospora crassa*. Nat Struct Biol 10:264–270

Zuk D, Jacobson D (1998) A single amino acid substitution in yeast eIF-5A results in mRNA stabilization. EMBO J 17:2914–2925

4 A Molecular and Genomic View of the Fungal Cell Wall

F.M. Klis[1], A.F.J. Ram[2], P.W.J. De Groot[2]

CONTENTS

I. **Introduction** 97
II. **Molecular Organization of the Cell Wall of the Budding Yeast *Saccharomyces cerevisiae* and the Fission Yeast *Schizosaccharomyces pombe*** 98
A. *Saccharomyces cerevisiae* 98
B. *Schizosaccharomyces pombe* 99
III. **The Cell Wall of Other Ascomycetes** 99
A. Many Ascomycetes Possess a Bi-Layered Wall 99
B. The Cell Wall of Some Dimorphic Ascomycetes 100
1. *Candida albicans* 100
2. *Exophiala (Wangiella) dermatitidis* . . 100
3. *Sporothrix schenckii* 101
4. *Blastomyces dermatitidis*, *Histoplasma capsulatum*, and *Paracoccidioides brasiliensis* 101
5. *Penicillium marneffei* 102
C. The Cell Wall of Some Mycelial Ascomycetes 102
1. *Fusarium oxysporum* 102
2. *Aspergillus* spp 103
3. *Neurospora crassa* 104
IV. **The Cell Wall of Some Basidiomycetous Fungi** 104
A. General 104
B. *Ustilago maydis* 104
C. *Trichosporon cutaneum* 105
D. *Cryptococcus neoformans* 105
V. **Covalently Linked Cell Wall Proteins** 106
A. GPI-Dependent Cell Wall Proteins and Non-GPI Cell Wall Proteins 106
B. Glycosylation 107
VI. **Synthesis of Cell Wall Polysaccharides** 108
A. β-1,3-Glucan 108
B. Chitin 108
C. α-1,3-Glucan 109
D. β-1,6-Glucan 109
E. β-1,4-Glucan 109
VII. **Cell Wall Construction Enzymes** 110
A. General 110
B. The Gas/Gel/Phr Family 110
C. The Crh Family 110
D. The Ecm33/Sps2 Family 110
E. The Bgl2 Family 110
F. The Dfg5/Dcw1 Family 111
VIII. **The Cell Wall Integrity Pathway** 111
IX. **Conclusions and Perspectives** 112
References 112

[1] Swammerdam Institute for Life Sciences, University of Amsterdam, 1018 WV Amsterdam, The Netherlands
[2] Institute of Biology, Clusius Laboratory, Leiden University, 2333 AL Leiden, The Netherlands

I. Introduction

The fungal cell wall is an essential organelle that accounts for 15–30% of the cellular dry weight and therefore represents a substantial metabolic investment for the cell. In return, possession of a cell wall makes it possible to withstand turgor pressures varying from about half a megapascal in normal cells up to eight megapascals in specialized cells, such as appressoria, which are used by some plant pathogens to penetrate plant cell walls (Howard et al. 1991). The wall also helps to maintain stable osmotic conditions inside the cell. Further, it maintains cell shape, allows morphogenesis, and protects the cell against physical damage. Other functions of the wall, such as adhesiveness and protection against desiccation, are related to the frequent presence of an external protein coat surrounding the skeletal part of the wall. *Saccharomyces cerevisiae* is the best-studied fungus to date and this raises the question in how far the cell wall biology of *Sac. cerevisiae* might be representative for other ascomycetous species, including mycelial fungi, and going one step further, whether it might also shed light on the cell wall biology of basidiomycetous fungi. To answer these and other similar questions, the increasing availability of fully sequenced fungal genomes is particularly helpful as it allows determining how well cell wall-related genes are conserved. In combination with biochemical studies on the cell walls of other fungi, this allows discussing the similarities and dissimilarities between the cell wall of *Sac. cerevisiae* and other fungi. Not surprisingly, this comparative analysis clearly shows that a single fungus cannot give all

Biology of the Fungal Cell, 2nd Edition
The Mycota VIII
R.J. Howard and N.A.R. Gow (Eds.)
© Springer-Verlag Berlin Heidelberg 2007

the answers and that we urgently need more model systems. However, despite the fact that sugar and polymer compositions of the fungal cell wall may vary widely, both quantitatively and qualitatively, we hope to convince you that, for the ascomycetous fungi and to a lesser extent for the basidiomycetes as well, *Sac. cerevisiae* may offer important clues of how to solve specific questions about the cell wall of your favorite fungus. For reasons of space we focus on ascomycetous and basidiomycetous fungi. The role of melanin or hydrophobins in cell wall biology is discussed in recent reviews (Wösten 2001; Gomez and Nosanchuk 2003; Linder et al. 2005). For older literature and different perspectives, the following reviews are useful (Wessels and Sietsma 1981; Ruiz-Herrera 1992; Sietsma and Wessels 1994; De Nobel et al. 2001).

II. Molecular Organization of the Cell Wall of the Budding Yeast *Saccharomyces cerevisiae* and the Fission Yeast *Schizosaccharomyces pombe*

A. *Saccharomyces cerevisiae*

Electron microscopic analysis of the cell wall of *Sac. cerevisiae* reveals a light-stained inner layer, representing the skeletal layer, consisting mainly of sugar polymers, and – depending on the technique used – a dark-stained or fibrillar outer layer, representing an external protein layer. In the budding yeast *Sac. cerevisiae* the major load-bearing polysaccharide of the inner layer is a moderately branched β-1,3-glucan, the nonreducing ends of which may act as acceptor sites for chitin and β-1,6-glucan. Its cell wall lacks α-1,3-glucan and β-1,4-glucan as found in many mycelial ascomycetes. The β-1,3-glucan forms a continuous, hydrogen-bonded, elastic network that is considerably stretched under normal osmotic conditions. This network acts as a scaffold for a protective outer layer of mannoproteins. The majority of cell wall proteins (CWPs) are GPI-dependent (GPI-CWPs; see also Sect. V.A.); they are linked through highly branched and thus water-soluble β-1,6-glucan chains to β-1,3-glucan, forming a CWP → β-1,6-glucan → β-1,3-glucan complex (Fig. 4.1; Lipke and Ovalle 1998; Yin et al. 2005; Klis et al. 2006). In addition, some proteins, the so-called *p*roteins with *i*nternal *r*epeats (PIR proteins; see also Sect. V.A.), are directly linked to the β-1,3-glucan network, probably through an ester linkage between a sugar hydroxyl group and the first glutamine residue in the amino acid sequence DGQJQ (where J is any hydrophobic acid; Ecker et al. 2006). GPI-dependent and PIR cell wall proteins can be differentially released from the cell wall by using HF-pyridine and mild alkali, respectively (Mrsa and Tanner 1999; De Groot et al. 2004). Chitin is normally present in low amounts and is mainly found in the form of a chitin ring in the neck of the mother cell, in the primary septum, and in bud scars. At these locations chitin may be present as a chitin → β-1,3-glucan complex or as free chitin (Kollar et al. 1995; Cabib and Duran 2005). Some additional chitin is found in the lateral walls where it is deposited after cytokinesis, mostly in the form of a CWP → [chitin →] β-1,6-glucan complex (Shaw et al. 1991; Kollar et al. 1997; Cabib and Duran 2005). In other words, the lateral walls of the growing bud generally do not contain chitin, demonstrating that chitin is not essential for the

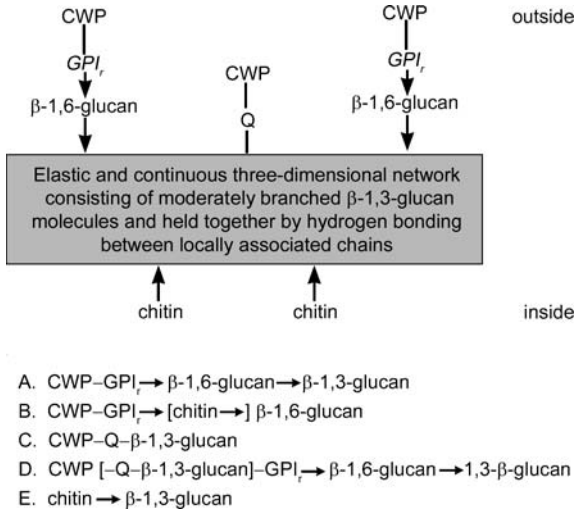

Fig. 4.1. Molecular organization of the cell wall of *Saccharomyces cerevisiae*. *Above* Molecular model of the cell wall. *Below* Covalently linked macromolecular complexes (*A–E*) in the cell wall. *CWP* Cell wall protein, *GPI* lipidless GPI remnant, *Q* the first glutamine residue in the characteristic DGQJQ sequence found in the repeats of PIR proteins and in some other CWPs and which is believed to be esterified to a hydroxyl group of β-1,3-glucan. *Arrows* point from the reducing end of a glycan to a nonreducing end of another glycan. Complex *A* is normally the most abundant. Complex *B* becomes more abundant in case of cell wall stress. Note that some GPI-modified cell wall proteins may also be linked through a DGQJQ sequence to β-1,3-glucan (Complex *D*). Complex *E* is mainly found in the lateral walls of the mother cell. Adapted from Klis et al. (2006). Copyright John Wiley & Sons Ltd, reproduced with permission

mechanical strength of the lateral walls in *Sac. cerevisiae*.

Cell wall construction and usage of specific cell wall macromolecules, including the cell wall proteins, are temporally and spatially controlled and closely coordinated with cell cycle progression, resulting in a mosaic-like cell wall (Caro et al. 1998; Rodriguez-Peña et al. 2002, Cabib and Duran 2005, Sumita et al. 2005; Smits et al. 2006). This is reflected by cell cycle-controlled expression of many cell wall proteins and putative assembly enzymes (Ram et al. 1995; Rodríguez-Peña et al. 2000; Klis et al. 2006; Smits et al. 2006). Septum formation, which requires the activation of a separate and largely autonomous construction program, is also tightly coordinated with the cell cycle (Roh et al. 2002).

B. *Schizosaccharomyces pombe*

In contrast to the wall of *Sac. cerevisiae*, the wall of *Schizosaccharomyces pombe* contains a considerable amount of α-1,3-glucan, but completely lacks chitin. The absence of chitin is consistent with the absence of members of the Crh1 family, which seem to be involved in the formation of the chitin → β-1,3-glucan complex (see below). In addition to β-1,3-glucan, α-1,3-glucan is also a major load-bearing polysaccharide (Kopecka et al. 1995; Hochstenbach et al. 1998; Katayama et al. 1999; Sugawara et al. 2004). Humbel and co-workers (2001) showed that the cell wall of *Sch. pombe* is also bi-layered, consisting of an outer, fibrillar layer, probably representing galactomannoproteins (Bush et al. 1974; Horisberger and Rouvet-Vauthey 1985), and an inner, light-staining layer, representing the skeletal layer. The inner, skeletal layer contains two types of fibrils, probably representing α-1,3-glucan and β-1,3-glucan (Kopecka et al. 1995). In addition, a highly branched β-1,6-glucan has been described (Sugawara et al. 2004; Magnelli et al. 2005). This β-1,6-glucan is believed to be covalently linked to the skeletal polysaccharide β-1,3-glucan (Manners and Meyer 1977) and seems to be preferentially located just below the external glycoprotein layer (Humbel et al. 2001). In addition, enzymatic digestion of β-1,6-glucan removes an amorphous layer from the external wall surface, suggesting that β-1,6-glucan interconnects the external protein layer to the underlying skeletal layer (Kopecka et al. 1995).

The protein believed to be responsible for the synthesis of α-1,3-glucan was identified as Ags1p, also known as Mok1p (Hochstenbach et al. 1998; Katayama et al. 1999); and homologues of this protein have been identified in many ascomycetous fungi (NCBI, http://www.ncbi.nlm.nih.gov/BLAST/; see also Sect. VI.C.). The presence of α-1,3-glucan in the wall raises the question if and how it might be connected to other cell wall macromolecules. Using hot dimethylsulfoxide (DMSO), Grün et al. (2005) were able to solubilize the cell wall of *Sch. pombe*. Size-fractionation of the solubilized molecules revealed the presence of three different subpopulations. α-1,3-Glucan was only found in the subpopulation with the smallest molecular size. As this subpopulation did not contain detectable amounts of proteins or other polysaccharides, α-1,3-glucan probably acts as an independent cell wall skeletal component. It is not yet known whether this observation may be generalized to other fungi that contain α-1,3-glucan in their walls. If so, it would considerably simplify attempts to develop a molecular model of their walls.

Consistent with how the proteins in the external glycoprotein layer in *Sac. cerevisiae* are attached to the stress-bearing polysaccharides, the available evidence indicates that also in *Sch. pombe* β-1,6-glucan acts as a flexible linker, connecting the glycoproteins in the external protein layer to β-1,3-glucan molecules. This would result in the putative cell wall protein–polysaccharide complex CWP → β-1,6-glucan → β-1,3-glucan. The three subpopulations identified by size-fractionation of DMSO-solubilized components may then represent in order of decreasing size: (1) a CWP–polysaccharide complex (CWP → β-1,6-glucan → β-1,3-glucan), (2) β-1,3-glucan, and (3) α-1,3-glucan.

III. The Cell Wall of Other Ascomycetes

A. Many Ascomycetes Possess a Bi-Layered Wall

A similar bi-layered wall as described above for baker's yeast and the fission yeast *Sch. pombe* has been observed in many other ascomycetous fungi, both in species that grow exclusively in the yeast or pseudohyphal form, in dimorphic species, and in mycelial species. Sometimes, the boundary between the inner skeletal layer and the outer fibrillar layer is more intensively stained than either of them, in which case some authors prefer to speak of a tri-layered wall. Examples

of fungi that have been shown to possess this particular cell wall organization and that grow exclusively in the yeast or pseudohyphal form are *Candida glabrata*, *Can. tropicalis*, *Hanseniaspora osmophila*, *Hansenula anomala*, *Kluyveromyces lactis*, *Pichia membranaefaciens*, *Sac. rouxii*, and *Trigonopsis variabilis* (Garrison 1981, 1985; Garrison and Arnold 1981; Uccelletti et al. 2000). Electron microscopic analysis has also revealed a bi-layered wall in several dimorphic ascomycetes such as the clinical fungi *Blastomyces dermatitidis*, *Can. albicans*, *Exophiala (Wangiella) dermatitidis*, *Histoplasma capsulatum*, and *Penicillium marneffei* (Garrison and Boyd 1973; Garrison 1985; Geis and Jacobs 1985; Kobayashi et al. 1985; Tokunaga et al. 1986; Biswas et al. 2003). Finally, some examples of mycelial ascomycetes, in which a bi-layered wall has been visualized, are *Aspergillus flavus*, *A. nidulans*, *Fusarium acuminatum*, *F. oxysporum*, *F. sulphureum*, *Neurospora crassa*, *Sclerotium rolfsii*, and *Trichophyton mentagrophytes* (Shatkin and Tatum 1959; Barran et al. 1975; Howard and Aist 1979; Roberson and Fuller 1990; Osumi et al. 1993; Heath 1994; Kurtz et al. 1994; Schoffelmeer et al. 1999; Hardham 2001; Jeong et al. 2004). The outer layer is easily overlooked. Successful visualization of the protein outer layer is highly dependent on the fixation and staining techniques used and as a result the outer layer may seem nonexistent (Garrison 1981).

Depending on growth conditions, an additional dark layer may be observed in *Sac. cerevisiae* located between the plasma membrane and the light-stained cell wall skeletal layer. However, the dark layer adjacent to the plasma membrane consists of soluble surface proteins such as invertase and acid phosphatase that are too large to pass the cell wall. These are lost during cell wall isolation and thus do not belong to the cell wall proper (De Nobel et al. 1989). Schoffelmeer and colleagues (1999) describe a similar situation in the mycelial, ascomycetous fungus *F. oxysporum*.

B. The Cell Wall of Some Dimorphic Ascomycetes

1. *Candida albicans*

The opportunistic human pathogen *Can. albicans* can grow in the yeast form and in the hyphal form and causes candidosis. There is ample evidence that the hyphal form of *Can. albicans* is fully comparable with that of mycelial fungi. For example, when growing in the hyphal form, it forms an authentic Spitzenkörper, which differs from the polarisome observed in the yeast form (Crampin et al. 2005). Pulse-labeling revealed that chitin is preferentially deposited in the hyphal tip of *Can. albicans* (Braun and Calderone 1978), similarly as for example in the mycelial fungus *A. nidulans* and in hyphal tips of germinating spores of the basidiomycete *Schizophyllum commune* (Katz and Rosenberger 1971; Sietsma and Wessels 1994). Furthermore, each septum contains a pore, allowing intercompartmental cytoplasmic flow (Gow and Gooday 1982). All the available morphological, biochemical and molecular–genetic evidence indicates that the molecular organization of the cell wall of *Can. albicans* in both the yeast and the hyphal form is based on the same principles as in *Sac. cerevisiae* and contains the same cell wall protein–polysaccharide complexes as baker's yeast (Tokunaga et al. 1986; Kapteyn et al. 1995, 2000; Müller 1999; De Groot et al. 2004). Evidence is emerging that this is also true for *Can. glabrata*, another human pathogen that only grows in the yeast form and is more closely related to *Sac. cerevisiae* (Frieman et al. 2002; Weig et al. 2004). Recently, it was shown for *Can. albicans* that the external protein layer of the wall masks the β-1,3-glucan layer, thereby preventing recognition of β-1,3-glucan by the extracellular domain of dectin-1, a phagocytic receptor protein in the plasma membrane that recognizes β-1,3-glucan (Gantner et al. 2005; Wheeler and Fink 2006). This masking is particularly efficient in hyphal cells, which do not form bud and birth scars. Although the global organization of the cell wall in *Candida* spp and *Sac. cerevisiae* is highly similar, this does not mean that they are identical. Important differences occur, which are highly relevant for the immune response to these fungi. For example, the carbohydrate side-chains of *Can. albicans* cell surface proteins contain β-1,2-linked mannose residues, which are absent in *Sac. cerevisiae* (Suzuki 1997; Trinel et al. 1997; Gemmill and Trimble 1999).

2. *Exophiala (Wangiella) dermatitidis*

E. dermatitidis is a clinical, dimorphic, black yeast and causes subcutaneous phaeohyphomycosis. Its cell wall is bi-layered with an internal skeletal layer and a fibrillar outer layer, which probably consists of galactomannoproteins (Geis and Jacobs 1985; Montijn et al. 1997; Biswas et al. 2003). Except for

the presence of some galactose, the sugar composition of its cell wall is similar to that of baker's yeast (Montijn et al. 1997). Both chitin and β-1,3-glucan are present, but similar to *Sac. cerevisiae* and *Candida* spp, α-glucan is lacking (Geis and Jacobs 1985). Furthermore, its wall also contains β-1,6-glucosylated cell wall proteins, which are resistant to extraction with hot SDS and can be released from the wall using a β-1,3-glucanase, and thus are probably covalently linked to the skeletal framework of the cell. These observations point to the presence of CWP → β-1,6-glucan → β-1,3-glucan complexes (Montijn et al. 1997). Interestingly, the wall of the hyphal form has a bi-layered structure as well, suggesting that it might also consist of galactomannoproteins covalently linked to the underlying skeletal framework (Geis and Jacobs 1985).

3. *Sporothrix schenckii*

Spo. schenckii is a dimorphic fungus that is responsible for sporotrichosis. At ambient temperature it grows in the soil as a mycelium but at 37 °C, for example when spores are inhaled into the lung, *Spo. schenckii* switches to the yeast form, a behavior that is called thermal dimorphism. The cell wall of the yeast form has been extensively studied (for a review, see Travassos 1985). The fungus has a widely extending fibrillar outer layer that strongly reacts with the lectin Concanavalin A, indicating the presence of α-linked mannose residues (Garrison 1985; Travassos 1985). Interestingly, sialic acid, which is probably protein-bound, is also an abundant cell surface component (Alviano et al. 1999). Both the yeast and hyphal walls contain about 7% chitin. They further contain glucose and mannose as major sugars, a substantial amount of rhamnose, probably in the form of rhamnomannan, and a trace of galactose, probably in the form of galactomannan. The hyphal walls also react strongly with Concanavalin A. Intriguingly, yeast and hyphal walls contain in addition to β-1,3-glucan and β-1,6-glucan some β-1,4-glucan, possibly linked to β-1,3-glucan as a β-1,4-glucan → β-1,3-glucan complex, as observed in *A. fumigatus* (Fontaine et al. 2000). There is no evidence for the presence of α-glucan. The linkage of cell wall proteins to the stress-bearing polysaccharides has not been investigated in detail in this fungus, but the presence of β-1,6-glucan and β-1,3-glucan is consistent with the presence of a CWP → β-1,6-glucan → β-1,3-glucan complex.

4. *Blastomyces dermatitidis*, *Histoplasma capsulatum*, and *Paracoccidioides brasiliensis*

B. dermatitidis, *H. capsulatum*, and *P. brasiliensis* are clinical fungi belonging to the family Onygenaceae and are the causative agents of blastomycosis, histoplasmosis, and paracoccidiomycosis, respectively. They normally grow in the soil in the mycelial form, but when conidia of mycelial fragments are inhaled by mammalian hosts, they start to grow in the yeast form (thermal dimorphism). The cell wall composition of *B. dermatitidis* is representative for this group (Kanetsuna and Carbonell 1971; Domer 1985; Nemecek et al. 2006). The compositions of the mycelial and yeast walls differ (Kanetsuna and Carbonell 1971). For example, the transition from mycelium to yeast is accompanied by a considerable increase in the level of α-1,3-glucan (Kanetsuna and Carbonell 1971; Domer 1985). In the hyphal wall the levels of α-1,3-glucan, β-1,3-glucan, and chitin are 14%, 34%, and 23%, respectively, but in the yeast wall these levels become 34%, 1%, and 37%, respectively (Kanetsuna and Carbonell 1971). Note, however, that according to Nemecek et al. (2006) the yeast wall contains 20% β-1,3-glucan. The yeast cell wall also contains some β-1,6-glucan (∼3%; Nemecek et al. 2006). Chitin is distributed uniformly over the cell surface and, in contrast to for example *Sac. cerevisiae* and *F. oxysporum* (see below), is apparently exposed at the cell surface as it can be stained with the fluorescently labeled lectin wheat germ agglutinin without any pretreatment of the wall (Brandhorst and Klein 2000; Nemecek et al. 2006). Interestingly, chitin effectively binds Bad1p (formerly Wi-1p), a 120-kDa adhesion protein that is specifically expressed in the yeast phase and is an important virulence factor (Klein and Jones 1994; Brandhorst and Klein 2000; Rooney et al. 2001; Brandhorst et al. 2003). It is a secretory protein with an authentic N-terminal signal peptide, but has no GPI-anchor addition signal and is apparently associated to the cell wall through noncovalent interactions. Remarkably, there is no evidence that it becomes glycosylated. The yeast and hyphal wall both contain only minor amounts of galactose and mannose, suggesting that the contribution of glycoproteins to the wall is limited.

In all three fungi, cell wall mutants have been isolated with lower or negligible levels of α-1,3-glucan (San-Blas and San-Blas 1977; Klimpel and Goldman 1988; Hogan and Klein 1994). These mutant strains proved to be less virulent

in a mouse model of infection. In addition, lowering the α-1,3-glucan levels in the wall of *H. capsulatum* by RNA interference of *AGS1*, which encodes an α-1,3-glucan synthase, also resulted in attenuated virulence (Rappleye et al. 2004). These observations strongly indicate that high α-1,3-glucan levels in the wall contribute to virulence, possibly by offering protection against the immune system. Recently, Reese and Doering (2003) showed that α-1,3-glucan in the wall of *Cryptococcus neoformans* mediates the anchoring of capsule material from *Cryptococcus* (see also Sect. IV.D.). Importantly, capsule material from *Cry. neoformans* binds to *H. capsulatum* cells as well, but only in strains containing α-1,3-glucan. This indicates that α-1,3-glucan is accessible at the outside of the cell wall and may mask other cell wall components. It might be interesting to determine whether dectin-1 is able to recognize β-1,3-glucan at the surface of living cells and to what extent (Gantner et al. 2005). For a more detailed discussion of the cell wall of *P. brasiliensis*, including a genomic comparison of the main players in cell wall synthesis, the reader is referred to Tomazett et al. (2005). The wall of another closely related temperature-controlled dimorphic pathogen, *Coccidioides immitis*, which causes coccidioidomycosis, is discussed in the reviews by Cole and Sun (1985) and by Cole and Hung (2001). For BLAST analysis against *H. capsulatum* genomic sequences, the reader is referred to http://genomeold.wustl.edu/blast/histo_client.cgi.

5. *Penicillium marneffei*

P. marneffei is another clinical fungus showing thermal dimorphism. It grows in the yeast form at body temperature and may cause lung disease (penicillosis). Immunogold labeling using an antiserum directed against the GPI protein Mp1p reveals its presence in the wall (Cao et al. 1998). In the hyphal wall it is present in a thin outer wall layer, suggesting that it might be covalently linked to the underlying skeletal layer, conceivably as a CWP → β-1,6-glucan → β-1,3-glucan complex. However, in the yeast wall it is distributed throughout the wall, including the inner layer, raising the question whether β-1,6-glucan might be present throughout the yeast wall. Importantly, homologues of Mp1p have been observed in *Aspergillus* spp (see below).

C. The Cell Wall of Some Mycelial Ascomycetes

1. *Fusarium oxysporum*

F. oxysporum is a soil inhabitant that causes vascular wilt. A special race of this fungus, called *F. oxysporum* f. *lycopersicae* causes wilt of tomatoes. Isolated walls from *F. oxysporum* f. *lycopersicae* still contain a considerable amount of protein after extraction with hot SDS (Schoffelmeer et al. 1999). These proteins carry both short and long carbohydrate side-chains that contain mannose, galactose, and glucuronic acid (Jikibara et al. 1992a, b, c). The presence of proteins is consistent with the presence of a prominent, dark-staining outer layer in electron micrographs and with the sensitivity to pronase of this layer (Howard and Aist 1979; Schoffelmeer et al. 1999). In addition, the cell surface of intact hyphae reacts strongly with the FITC-labeled lectin Concanavalin A, which recognizes α-linked mannose residues, whereas hyphae pretreated with pronase react only weakly (Schoffelmeer et al. 1999). The cell wall further contains substantial amounts of the skeletal components chitin, α-1,3-glucan, and β-1,3-glucan. Interestingly, prior pronase treatment of intact hyphae is required for effective labeling of chitin with FITC-labeled wheat germ agglutinin, indicating that the external protein layer masks chitin and is limiting cell wall permeability, as has also been shown for *Sac. cerevisiae* and *Can. albicans* (Zlotnik et al. 1984; De Nobel et al. 1990; Gantner et al. 2005).

Like in *Sac. cerevisiae*, digestion of the cell wall of *F. oxysporum* f. *lycopersicae* with β-1,3-glucanase releases β-1,3/1,6-glucosylated proteins, varying widely in molecular mass (Schoffelmeer et al. 1996). Treatment of the released protein with anhydrous HF, which specifically cleaves phosphodiester bonds such as the one present in the GPI remnant of GPI cell wall proteins (Kapteyn et al. 1996), results in the loss of all protein-bound β-glucans and the appearance of relatively discrete bands (Schoffelmeer et al. 1996). Direct treatment of isolated walls with anhydrous HF releases an abundant protein, suggesting that this might be a GPI-dependent cell wall protein. After cloning of the corresponding gene (*FEM1*), additional evidence was obtained that it encodes an authentic GPI-dependent cell wall protein:

1. The algorithm "big-PI Fungal Predictor" predicts that the amino acid sequence of Fem1p corresponds to an authentic GPI protein with

a C-terminal GPI addition signal (Eisenhaber et al. 2004).
2. It lacks basic amino acids in the region just preceding the predicted omega amino acid, to which the GPI anchor becomes attached, indicating that this protein is not retained in the plasma membrane (see also Sect. V.A.).
3. A C-terminally truncated form of Fem1p, which lacks the GPI anchor addition signal but still possesses the N-terminal signal peptide, is not incorporated in the wall, but instead secreted into the medium (Schoffelmeer et al. 2001).

Importantly, a PHI-BLAST search identifies homologous proteins in the ascomycetous fungi *Gibberella zeae*, *Neurospora crassa*, *Magnaporthe grisea*, and *Coc. immitis* (http://www.ncbi.nlm.nih.gov/BLAST/). These are also predicted to be authentic GPI proteins (big-PI Fungal Predictor; Eisenhaber et al. 2004). In summary, despite quantitative and qualitative differences in sugar and polymer composition between the walls of *F. oxysporum* f. *lycopersicae* and those of *Sac. cerevisiae*, the molecular organization of their walls shows remarkable similarities. In both fungi, the walls possess a prominent external protein layer that is covalently linked to the underlying skeletal layer and in both fungi GPI-dependent cell wall mannoproteins are found. Similar to *Sac. cerevisiae*, the wall of *F. oxysporum* seems to contain cell wall proteins linked through β-1,6-glucan to β-1,3-glucan (presumably in the form of a CWP → β-1,6-glucan → β-1,3-glucan complex). In view of the considerable amount of chitin in the wall of *F. oxysporum* and the observation that in the lateral walls of *Sac. cerevisiae* the CWP → [chitin →] β-1,6-glucan complex is preferred (Cabib and Duran 2005), this complex might also be present in the wall of *F. oxysporum*.

2. *Aspergillus* spp

A. niger is a common food contaminant. It is also an important industrial fungus used for example for the commercial production of citric acid and various enzymes. Its hyphal wall has been shown to contain the stress-bearing polysaccharides chitin (∼10%), α-1,3-glucan, and β-1,3-glucan (Blumenthal and Roseman 1957; Johnston 1965). In addition, it contains covalently attached proteins, which can be released from the wall by HF treatment (Damveld et al. 2005a, b), or by β-1,3-glucanase digestion and in that case carry a β-1,6-glucan epitope (Brul et al. 1997). These observations point to the existence of a CWP → β-1,6-glucan → β-1,3-glucan complex, which is also consistent with the presence of a gene encoding a homologue of ScKre6p (http://genome.jgi-psf.org/Aspni1/Aspni1.home.html). Alkali extraction releases both a galactomannan and a galactosaminogalactan from the hyphal wall (Bardalaye and Nordin 1976, 1977). As many ascomycetes possess protein-bound galactomannan, this suggests that the alkali-soluble galactomannan might be protein-bound as well.

Transmission electron microscopy of rapidly frozen, freeze-substituted hyphae of *A. flavus* and *A. fumigatus* shows a bi-layered wall about 35 nm thick with a fine, darkly stained outer layer, suggesting that this might be an external protein layer (Heath 1994; Kurtz et al. 1994). When the mycelium is grown in the presence of caspofungin, an inhibitor of β-1,3-glucan synthesis, both layers of the cell wall at the hyphal tips become much thicker, probably because a cell wall salvage mechanism is activated, including increased production of α-1,3-glucan (see also Sect. VIII.). Recently, an authentic GPI protein (big-PI Fungal Predictor; Eisenhaber et al. 2004) was identified in *A. flavus*, called Mp1p (Woo et al. 2003). Indirect immunofluorescence showed that Mp1p is present on the hyphal surface, suggesting that it is covalently linked to the skeletal framework of the wall. Immunogold labeling identified a homologue of Mp1p in the wall of *A. nidulans*, called MnnAp, where it was found distributed throughout the wall (Jeong et al. 2004). Interestingly, a PHI-BLAST search identifies homologues of this protein in various *Aspergillus* species (*A. fumigatus*, *A. kawachii*, *A. nidulans*, *A. niger*, *A. oryzae*), and in *P. marneffei* (http://www.ncbi.nlm.nih.gov/BLAST/).

The alkali-insoluble fraction of the cell wall of *A. fumigatus*, which accounts for about 40% of the cell wall dry weight, has been thoroughly analyzed (Fontaine et al. 2000). In their seminal paper Fontaine and co-workers identified three covalently linked polysaccharide complexes: (1) chitin → β-1,3-glucan, (2) galactomannan → β-1,3-glucan, and (3) β-1,3/1,4-glucan → β-1,3-glucan. In addition, a putative poly-N-acetylgalactosamine was identified. Although N-acetylgalactosamine was found in the alkali-insoluble fraction from *A. fumigatus*, it is probably equivalent to the alkali-soluble N-acetylgalactosamine-containing material identified in the walls of *A. nidulans* and *A. niger* (Bull

1970; Bardalaye and Nordin 1976) because in these studies more stringent alkali extraction conditions were used. The β-1,3/1,4-glucan in the wall of *A. fumigatus* is probably related to a similar fraction identified in the walls of *Spo. schenckii* (Travassos 1985; see also Sect. VI.E.). The alkali-insoluble fraction of the wall of *A. fumigatus* did not contain β-1,6-glucan, in contrast to the same cell wall fraction of *Sac. cerevisiae*, indicating that this polymer might be absent from the wall of *A. fumigatus*. In contrast, the genome of *A. fumigatus* contains a *ScKRE6* homologue (giving AfKre6p). *ScKRE6* encodes a Golgi-located, putative transglucosidase that plays a key role in the synthesis of β-1,6-glucan in *Sac. cerevisiae* (Roemer et al. 1993; Montijn et al. 1999). Possibly, AfKre6p and the Kre6p of *Sac. cerevisiae* have different functions, or alternatively expression of *KRE6* and formation of β-1,6-glucan are highly dependent on growth conditions. Unfortunately, the alkali-soluble fraction of the cell wall, which represents >50% of its total dry weight, has not been investigated in as much detail as the alkali-insoluble fraction. It largely consists of α-1,3-glucan, which is water-insoluble, but it also contains a water-soluble, macromolecular fraction that accounts for all the galactose and mannose of the wall and most of the protein, indicating that the water-soluble fraction contains galactomannoproteins (Hearn and Sietsma 1994). The alkali-soluble fraction also contains some glucan (5% of the wall dry weight), the precise nature of which has not been established, but might represent β-1,3/1,4-glucan similar to *Spo. schenckii*; see also Sect. VI.E.). It is claimed that the cell wall of *A. fumigatus* does not possess covalently-bound cell wall proteins (Latgé et al. 2005), but in view of the electron microscopic observations of the cell wall (Heath 1994; Kurtz et al. 1994) and the available biochemical evidence (Hearn and Sietsma 1994; see also Haido et al. 1998), this conclusion seems precipitate.

3. *Neurospora crassa*

The cell wall of *N. crassa* consists of two distinct layers: an outer fibrillar layer and an inner skeletal layer (Mahadevan and Tatum 1965, 1967). Alkali extraction removes the outer layer completely without affecting cell shape. The extract contains a protein–polysaccharide complex, which includes all of the galactosamine from the wall (∼10%; Edson and Brody 1976). The inner layer contains β-1,3-glucan and chitin (∼10%). There is no evidence for the presence of β-1,6-glucan in the wall, which is consistent with the absence of a homologue of ScKre6p (SGD; http://www.yeastgenome.org/; BLASTP vs fungi in comparison resources). This raises the question whether the wall protein layer might be linked directly to, for example β-1,3-glucan, without an intervening linker polysaccharide as in *Sac. cerevisiae*. Further genomic analysis indicates the presence of a ScCrh1p homologue, suggesting the presence of a chitin → β-1,3-glucan complex in the wall. Also an SpAgs1p homologue is present, raising the question whether the hyphal wall or walls from specialized cells might contain α-1,3-glucan. For a more extensive genomic view of cell wall biosynthesis in *N. crassa*, the reader is referred to Borkovich et al. (2004).

IV. The Cell Wall of Some Basidiomycetous Fungi

A. General

With some exceptions, our knowledge of the molecular architecture of the cell wall of basidiomycetous fungi is limited. Genomic analysis indicates that there is widespread use of a homologue of ScFks1p, the catalytic subunit of β-1,3-glucan synthase (Inoue et al. 1995; see also Sect. VI.A.), and ScGas1p, which is probably involved in processing the emerging β-1,3-glucan chains and incorporating them in the existing β-1,3-glucan network (Mouyna et al. 2000; see also Sect. VII.B.). Similarly, the formation of a chitin → β-1,3-glucan complex seems to be a general phenomenon. This is consistent with the presence of a ScCrh1 homologue in *Ustilago maydis* and *Cry. neoformans* (SGD, http://www.yeastgenome.org/; BLASTP vs fungi in comparison resources; see also Sect. VII.C.). A major difference with ascomycetous yeasts is that electron microscopic studies often reveal a multilayered wall with alternating regions of electron-dense and electron-translucent material (Garrison 1981; Depree et al. 1993). The cell wall of the yeast form of *U. maydis* forms an exception to this rule, as it is clearly bi-layered.

B. *Ustilago maydis*

U. maydis is a dimorphic fungus causing corn smut. Depending on the phase of the life cycle, it may

grow as a haploid budding yeast, or as a dikaryotic mycelium. Electron microscopic analysis of yeast walls reveals a light-stained, thick inner layer and a dark-stained, irregular outer layer; mycelial walls also possess a (thin) irregular, dark-stained outer layer, but in contrast to the yeast wall the inner part of the hyphal wall seems to be multilayered (Ruiz-Herrera et al. 1996). The chemical compositions of the hyphal and yeast walls are similar. Isolated, SDS-extracted yeast cell walls contain about 14% chitin, β-1,3-glucan, and xylose and mannose, possibly in the form of xylomannan. SDS-extracted walls still contain about 6% protein, indicating that also in *U. maydis* cell wall proteins may be covalently linked to cell wall polysaccharides (Ruiz-Herrera et al. 1996). Interestingly, some cell wall proteins can be liberated from isolated walls with β-1,3-glucanase, whereas others are released by chitinase. Collectively, these observations indicate that the dark-staining outer layer consists of glycoproteins linked to the inner skeletal layer of the wall, probably to β-1,3-glucan and chitin. It is not known whether the yeast walls also contain β-1,6-glucan, but the presence in the genome of a close homologue of ScKre6p suggests that this might be the case.

C. *Trichosporon cutaneum*

The genus *Trichosporon* includes several clinical yeasts. *T. cutaneum* (ATCC 20509) may grow in either yeast or mycelial form (Depree et al. 1993). The yeast cell wall consists of multiple layers varying in electron density (Depree et al. 1993). The available evidence indicates that there are four major components in the wall: a glucuronoxylomannan that may be protein-bound, α-1,3-glucan, β-1,3-glucan, and chitin. Autoclaving intact cells in neutral citrate buffer, which is a procedure often used to release (galacto)mannoproteins from ascomycetous fungi, releases a high-molecular-weight mannan, which consists of a 1,3-mannan backbone decorated with glucuronic acid and xylosyl residues (glucuronoxylomannan; GXM). Intriguingly, after partial purification by ion-exchange chromatography and gel filtration, the polysaccharide-containing fractions still contain about 7% protein, raising the question whether this polysaccharide might be covalently linked to protein or, alternatively, is bound to it by ionic interactions. In addition to GXM, the alkali-soluble fraction also contained a considerable amount of 1,3-linked glucose. As the alkali-soluble fraction was resistant to Zymolyase (a β-1,3-glucanase preparation), but sensitive to Novozyme (an enzyme preparation containing both β-1,3-glucanase and α-1,3-glucanase activity), the 1,3-linked glucose probably represents α-1,3-glucan. The alkali-insoluble fraction of the cell wall of *T. cutaneum*, which represents about 44% of the wall dry weight, contains chitin and β-1,3-glucan, suggesting the presence of a chitin → β-1,3-glucan complex in the wall (Depree et al. 1993).

D. *Cryptococcus neoformans*

Cry. neoformans is a soil fungus that has emerged as a major opportunistic pathogen in immunocompromised people. Genomic analysis shows that most of the genes involved in the synthesis of cell wall components are conserved between *Cry. neoformans* and ascomycetous fungi (Loftus et al. 2005). Its wall consists of two main layers, but in contrast to ascomycetous fungi the inner layer is darkly stained and has a lamellar appearance and the outer layer is lightly stained (Cassone et al. 1974; James et al. 1990). The wall is surrounded by an extensive and porous polysaccharide capsule, which is the major virulence factor of *Cry. neoformans* (Pierini and Doering 2001; Yamaguchi et al. 2002; Bose et al. 2003). Isolated, detergent-extracted cell walls of an acapsular mutant were found to be composed of 7% chitin, about 30% α-1,3-glucan, and a substantial amount of β-1,6-glucan, but surprisingly no evidence for the presence of β-1,3-glucan was obtained (James et al. 1990). The presence of β-1,6-glucan in the wall was confirmed by immunogold labeling and is consistent with the presence of a homologue of ScKre6p in *Cry. neoformans* (SGD; Feldmesser et al. 2000; http://www.yeastgenome.org/; BLASTP vs fungi in comparison resources). The (near) absence of β-1,3-glucan in the wall is consistent with the lack of staining by the fluorescent dye aniline blue, which preferentially stains β-1,3-glucan (Nicholas et al. 1994). In contrast, calcofluor white, which becomes attached to chitin, stained the cell wall uniformly, indicating that the cell wall is accessible to dyes and that chitin is distributed evenly over the wall. The (near) absence of β-1,3-glucan in the wall is also consistent with the relative resistance of *Cry. neoformans* to echinocandins, which inhibit the synthesis of β-1,3-glucan (Abruzzo et al. 1995). However, several observations seem to indicate that at least

some β-1,3-glucan might be present in the walls and might have been overlooked in the study by James et al. (1990). First, *Cryptococcus* contains a single copy of an *FKS1* homologue, the catalytic subunit of β-1,3-glucan synthase, and this gene seems to be essential for growth (Thompson et al. 1999). Second, *Cryptococcus* lysates contain β-1,3-glucan synthase activity (Maligie and Selitrennikoff 2005). Third, immunogold labeling with an antiserum directed against β-1,3-glucan results in a clear signal, although weaker than when using an antiserum directed against β-1,6-glucan (Feldmesser et al. 2000). Fourth, the genome contains a copy of a homologue of ScCrh1, which is proposed to be involved in connecting chitin to β-1,3-glucan (see Sect. VII.C.). Another virulence factor of *Cry. neoformans* is its capability to deposit melanin in the cell wall when supplied with exogenous substrates (Eisenman et al. 2005). Fascinatingly, there is evidence that the cell wall also contains sialylated glycoconjugates (Rodrigues et al. 2002).

The major component of the capsule is a glucuronoxylomannan (for reviews, see Bose et al. 2003; Small and Mitchell 1986). It consists of a α-1,3-mannan backbone decorated with glucuronic acid and xylosyl residues (GXMan). Another, minor component is an α-1,6-galactan with side-chains consisting of xylose, mannose and galactose residues (MXGal). How the cell constructs a capsule in space and in time was explored by Pierini and Doering (2001). Fascinatingly, α-1,3-glucan was shown to mediate the association between capsule material and the wall proper (Reese and Doering 2003; see also Sect. 4.). For further discussion of capsule biosynthesis and the enzymes involved, the reader is referred to Klutts et al. (2006).

V. Covalently Linked Cell Wall Proteins

A. GPI-Dependent Cell Wall Proteins and Non-GPI Cell Wall Proteins

As in other eukaryotic organisms, fungal GPI proteins follow the secretory pathway. GPI anchor addition takes place in the lumen of the ER, a step that is mediated by a transamidase complex that exchanges the C-terminal region of these proteins for a pre-formed glycosylphosphatidylinositol lipid membrane anchor (Fraering et al. 2001; Fontaine et al. 2004). Transport from the ER to the plasma membrane in *Sac. cerevisiae* is accompanied by lipid remodeling of the GPI anchor (Reggiori et al. 1997). BLAST searches indicate that many (but not all) genes involved in GPI anchor synthesis and transfer are highly conserved in ascomycetous and basidiomycetous fungi (SGD; http://www.yeastgenome.org/).

On an individual basis, potential fungal GPI proteins can be reliably identified using the GPI fungal bigPI Fungal Predictor server (Eisenhaber et al. 2004; http://mendel.imp.ac.at/gpi/fungi_server.html), whereas for genomic searches another powerful approach is available (De Groot et al. 2003). Not all fungal GPI proteins remain in the plasma membrane. A subset of GPI proteins becomes covalently bound to cell wall polysaccharides, a step which involves processing of their GPI anchor (Kollar et al. 1997). Many fungal cell wall proteins are indeed GPI proteins (Van der Vaart et al. 1995; Hamada et al. 1999; Schoffelmeer et al. 2001; Frieman et al. 2002; Woo et al. 2003; De Groot et al. 2004; Jeong et al. 2004; Weig et al. 2004; Yin et al. 2005). No GPI-dependent cell wall proteins have yet been identified in basidiomycetous fungi, but the cell wall of the yeast form of *U. maydis* seems a promising place to explore (see Sect. IV.B.). Unfortunately, there is no reliable algorithm available to differentiate between GPI proteins that are preferentially destined for the plasma membrane or for the cell wall, but the presence of basic amino acids in the region just preceding the omega amino acid (the C-terminal acid of the mature protein, to which the GPI anchor becomes attached) is an indication for its being preferentially retained in the plasma membrane (Caro et al. 1997; Hamada et al. 1999; Frieman and Cormack 2003).

The ScPIR proteins are non-GPI proteins and form a second class of covalently linked cell wall proteins (Fig. 4.1). They consist of an N-terminal signal peptide followed by a pro-peptide terminating in a dibasic motif, one or more repeats with the diagnostic subsequence DGQJQ (where J represents any hydrophobic amino acid), and a homologous C-terminal domain with a conserved cysteine pattern. As discussed above, the repeats are involved in linking PIR cell wall proteins through an alkali-sensitive linkage to β-1,3-glucan (Ecker et al. 2006). PIR cell wall proteins have been experimentally identified in *Sac. cerevisiae*, *Can. albicans*, *Can. glabrata*, and *Yarrowia lipolytica* (Mrsa et al. 1997; Kapteyn et al. 1999; Jaafar et al. 2003; Weig et al. 2004; Ecker et al. 2006), and are predicted to occur in other ascomycetous yeasts such

as *Debaryomyces hansenii*, *K. lactis*, and *Pichia angusta*, but not in *Sch. pombe* (SGD; BLASTP vs fungi; available at http://db.yeastgenome.org/). In some filamentous ascomycetes, such as *Blumeria graminis*, *Gibberella zeae*, *N. crassa*, and *M. grisea*, PIR-like proteins are also predicted to be present (De Groot et al. 2005); however, this is not the case for the sequenced species of the genus *Aspergillus*. The PIR-like proteins discovered in ascomycetous fungi differ significantly from their counterparts in ascomycetous yeasts. Unexpectedly, they seem to be authentic GPI proteins (big-PI Fungal Predictor; Eisenhaber et al. 2004); and, in agreement with this, the domain containing the conserved-cysteine pattern (in other words, the predicted activity domain) is situated in the N-terminal half of the protein upstream of the repeat units (De Groot et al. 2005). This suggests that they may be doubly linked to the cell wall skeletous framework, that is, through their GPI-anchor remnant and through their repeats, as also observed for ScCwp1 (Kapteyn et al. 2001).

It is important to keep in mind that the fungal cell wall may also contain noncovalently bound cell wall proteins such as the transglucosidase ScBgl2p, which strongly binds to β-1,3-glucan, and the adhesin Bad1p from *B. dermatitidis*, which strongly associates with chitin (Klebl and Tanner 1989; Brandhorst and Klein 2000). As these proteins possess a predicted N-terminal secretory peptide that is lacking in the mature proteins, they are believed to follow the secretory pathway. Fascinatingly, there are cell surface proteins that do not seem to follow the classic secretory pathway. For example, immunogold labeling of thin sections of fruiting bodies of *Coprinus cinerea* identified the presence of extracellular galectins. These are lectins that specifically bind to β-galactosides and are believed to contribute to interactions between hyphae (Boulianne et al. 2000). They do not possess the hallmarks of a secretory protein and they do not become glycosylated (Cooper et al. 1997). Furthermore, when the lectin Cgl2p was heterologously expressed in a *Sac. cerevisiae* mutant conditionally blocked in the classic secretory pathway, it was still exported to the cell surface at 37 °C, indicating that the mechanism for galectin export is not limited to the basidiomycete *Cop. cinerea* but also operates in ascomycetes, and second that galectin export does not require the classic export pathway (Boulianne et al. 2000). A nonconventional export pathway is also claimed for many other (abundant) cytosolic proteins in *Sac. cerevisiae* and *Can. albicans*, such as glycolytic enzymes, heat shock proteins, and elongation factors (for a review, see Nombela et al. 2006). Unfortunately, in many of the studies discussed relatively harsh extraction conditions were used to release cell surface proteins from living cells (Klis et al. 2007). This raises the question whether the extraction conditions themselves might be responsible for the presence of cytosolic proteins in the cell extracts, for example, by inducing apoptosis or cell leakage. The extraction procedure developed by Cappellaro et al. (1998) seems to be the mildest one available.

B. Glycosylation

Most fungal cell wall proteins are *N*- and *O*-glycosylated, and their carbohydrate side-chains often account for the bulk of their molecular mass (Dean 1999; Strahl-Bolsinger et al. 1999). Regrettably, it is rarely attempted to extract cell wall proteins intact, including their linkages to other cell wall components, by using recombinant cell wall-degrading enzymes or well defined mild chemical extraction methods. Mostly, isolated walls are extracted with hot alkali, which results in protein degradation and release of the (partially degraded) side-chains (Ahrazem et al. 2000), or by autoclaving intact cells in citrate buffer and precipitating the glycoproteins from the extract with the help of Fehling's reagent or Cetavlon (Nakajima and Ballou 1974; Jikibara et al. 1992b).

O-Glycosylation of serine and threonine residues in fungal glycoproteins is initiated in the endoplasmic reticulum by members of the protein mannosyl transferase (PMT) family (for a review, see Willer et al. 2003), which are highly conserved in both ascomycetous and basidiomycetous fungi (SGD; http://www.yeastgenome.org/; BLASTP vs fungi). *O*-Chains are often relatively short, but they may show nevertheless considerable structural variability (Gemmill and Trimble 1999; Lopes-Bezerra et al. 2006).

N-Glycosylation is also initiated in the endoplasmic reticulum and starts with the stepwise assembly of a lipid-linked 14-residue oligosaccharide and transfer of the sugar chain by the oligosaccharyltransferase complex to selected asparagine residues of nascent polypeptide chains (Knauer and Lehle 1999). After modification in the endoplasmic reticulum, *N*-chains are extended in the Golgi, which involves among others an α-1,6-mannosyl transferase complex. ScHoc1p, one of the subunits

of this complex, is highly conserved among ascomycetous fungi and to a lesser extent also in the basidiomycetes *Cry. neoformans* and *U. maydis*, indicating that extension of the core chain with α-1,6-mannosyl residues may widely occur. Decoration of the *N*-chain with other sugars also takes place in the Golgi.

N- and *O*-chains of *Sac. cerevisiae* consist (almost) exclusively of mannose residues. However, in other ascomycetous fungi additional sugars such as galactose (both in the pyranose and in the furanose form), glucose, glucuronic acid, rhamnose, and even sialic acids have been identified (Jikibara et al. 1992a, b, c; Alviano et al. 1999; Lopes-Bezerra et al. 2006).

The fungal cell wall often has an anionic character (Horisberger and Clerc 1988). The *N*- and *O*-chains of *Sac. cerevisiae* contain mannosylphosphate groups, which are responsible for the net negative charge of the cell wall proteins (Jigami and Odani 1999). ScMnn6 is believed to be a mannosylphosphate transferase contributing to the formation of phosphomannan. WU-BLAST2 (SGD; http://www.yeastgenome.org/) reveals that ScMnn6p is a highly conserved protein. Homologues are found in many ascomycetes such as *Candida* spp, *Aspergillus* spp, and *Sch. pombe*, and in the basidiomycetes *Cry. neoformans* and *U. maydis*. Also other substituents of protein-bound carbohydrate side-chains may confer an anionic character to the fungal cell surface, such as glucuronic acid residues, pyruvate conjugated to galactosyl residues, and presumably also sialyl residues (Nakayama et al. 1998; Alviano et al. 1999; Gemmill and Trimble 1999).

VI. Synthesis of Cell Wall Polysaccharides

A. β-1,3-Glucan

β-1,3-Glucan is an abundant stress-bearing polysaccharide of the cell wall in many ascomycetous and basidiomycetous fungi. Proteins involved in β-1,3-glucan synthesis in *Sac. cerevisiae* include the catalytic subunit (Fks1p) and a regulatory GTPase (Rho1p). GFP-tagged Fks1p in *Sac. cerevisiae* is found at the site of the incipient bud, at the tip of small buds, and at the cell surface of medium-sized buds, but not at the cell surface of the mother cells, suggesting that it may be endocytosed to restrict its function to certain areas and time-windows during the cell cycle (Utsugi et al. 2002). Later in the cell cycle, during cytokinesis it is transiently found at the cell neck. Staining with aniline blue, which specifically binds to noncrystalline β-1,3-glucan chains, resulted in uniform staining of the walls. All fungal genomes examined, including those of the basidiomycetous fungi *U. maydis* and *Cry. neoformans*, contain at least one Fks1p homologue. In *A. fumigatus*, a Rho1 protein copurifies with the Fks1 protein, indicating that the control of β-1,3-glucan synthase by Rho-related GTPases is well conserved (Beauvais et al. 2001). They further showed that aniline blue preferentially stains the hyphal tips, indicating that β-1,3-glucan synthesis takes place at the apex and that in the subapical region β-1,3-glucan becomes more crystalline, making it less accessible to the dye. As β-1,3-glucan is the major stress-bearing polysaccharide of many fungi, it is not surprising that in all fungi examined so far, deletion of the Fks gene(s) is lethal. Fks proteins are thus an obvious target for antifungal compounds. The echinocandins inhibit Fks proteins and several of them, such as caspofungin, micafungin, and anidulafungin, are now in clinical use (Kahn et al. 2006; Morrison 2006).

B. Chitin

Chitin, a nonbranched homopolymer of β-1,4-N-acetylglucosamine residues, is a characteristic stress-bearing polysaccharide of the fungal cell wall. In general, the cell wall of mycelial ascomycetes contains more chitin compared to yeasts. This is also reflected in the increased number of different chitin synthases found in mycelial ascomycetes. Fungal chitin synthases have been classified into six groups, according to their structural characteristics (reviewed by Munro and Gow 2001; Roncero 2002). The extensive studies by the group of Ohta and Horiuchi on chitin synthesis in *A. nidulans* clearly demonstrate that the different chitin synthases have both overlapping and distinct functions during the life cycle of *A. nidulans* (e.g. Fujiwara et al. 2000; Ichinomiya et al. 2002a, b, 2005; Yamada et al. 2005; Takeshita et al. 2006). The genomes of the basidiomycetous fungi *Cry. neoformans* and *U. maydis* both contain a large family of eight chitin synthase-encoding genes (Banks et al. 2005; Weber et al. 2006). Systematic analysis of the role and localization of the corresponding

proteins revealed that they are specifically required during different stages of growth and/or for plant infection (Weber et al. 2006). In mycelial asco- and basidiomycetes chitin synthases occur that possess a myosin motor-like domain. In *A. nidulans* and *U. maydis* these proteins are localized at the hyphal tips, suggesting a mechanism by which chitin synthases are directly transported to the hyphal tip via actin and actin-based motor proteins (Takeshita et al. 2006; Weber et al. 2006).

C. α-1,3-Glucan

Many fungal cell walls contain besides β-1,3-glucan and chitin a third structural component, namely α-1,3-glucan. α-1,3-Glucan usually contains some α-1,4-linked glucosyl residues, probably delineating separate building blocks (Grün et al. 2005). The polymer is lacking in *Sac. cerevisiae* and *Can. albicans*. The first α-1,3-glucan synthase was identified in *Sch. pombe* and is essential for vegetative growth (Hochstenbach et al. 1998). The enzyme (called Ags1p) is a plasma membrane protein and seems to be multifunctional (Konomi et al. 2003; Grün et al. 2005). The N-terminal domain is predicted to be localized outside the plasma membrane, where it is assumed to act as a transglucosidase, interconnecting α-glucan building blocks (Grün et al. 2005). The central, large intracellular loop of the protein is proposed to be the catalytic part of the enzyme, whereas the C-terminal part, which contains several transmembrane sequences, might be involved in the export of the α-glucan building blocks. In *Sch. pombe*, a family of five α-1,3-glucan synthase-encoding genes (*AGS1*/*MOK1*, *MOK11*, *MOK12*, *MOK13*, *MOK14*) has been identified (Katayama et al. 1999). In contrast to Ags1p/Mok1p, Mok12p, Mok13p, and Mok14p are dispensable for vegetative growth, but are involved in spore wall formation (García et al. 2006).

Most known genomes of mycelial ascomycetes contain genes encoding α-1,3-glucan synthases with a similar domain structure as described for *Sch. pombe*, except for the genomes of *Gibberella zeae* (anamorph *Fusarium graminarium*) and *Ashbya gossypii*, which seem to lack such genes. The number of α-1,3-glucan synthase-encoding genes varies, ranging from five in *A. niger* (Damveld et al. 2005b), three in *A. fumigatus* (Beauvais et al. 2005; Maubon et al. 2006), two in *A. nidulans* and *N. crassa*, and a single copy in *M. grisea*. α-1,3-Glucan is also present in basidiomycetes, such as *Cry. neoformans*, but *U. maydis* seems to lack *AGS1*-like genes in its genome.

D. β-1,6-Glucan

β-1,6-Glucan has been identified in the walls of Archi-, Hemi-, and Euascomycetes, indicating that it occurs widely. β-1,6-Glucan-possessing fungi include yeasts, such as *Sac. cerevisiae* and *Sch. pombe*, dimorphic species, such as *B. dermatitidis*, *Candida* spp, *E. dermatitidis*, and *Spo. schenckii*, and mycelial species, such as *A. niger* and *Penicillium variotii* (Manners et al. 1973; Travassos 1985; Brul et al. 1997; Montijn et al. 1997; Nemecek et al. 2006). As discussed above, it may not occur in the walls of all ascomycetes (Fontaine et al. 2000). As ScKre6p plays a crucial role in β-1,6-glucan synthesis (Roemer et al. 1993; Montijn et al. 1999), a WU-BLAST2 search (SGD; http://www.yeastgenome.org/) was performed with its amino acid sequence. This identified not only close homologues of ScKre6p among many ascomycetous fungi, but also in the genomes of the basidiomycetous fungi *U. maydis* and *Cry. neoformans*. The presence of β-1,6-glucan in the walls of *Cry. neoformans* was confirmed experimentally (see also Sect. IV.D.). The recently developed β-1,6-glucan synthase assay may provide a simple means to decide whether the synthesis of β-1,6-glucan is indeed as widespread as suggested by *in silico* analysis (Vink et al. 2004).

E. β-1,4-Glucan

The alkali-soluble and alkali-insoluble fractions of the cell wall of *Spo. schenckii* contain stretches of consecutive β-1,4-glucosyl residues (Travassos 1985); and in the alkali-insoluble fraction of the wall of *A. fumigatus* a β-1,3/1,4-glucan was identified (Fontaine et al. 2000). This indicates that fungal β-1,4-glucan synthases may exist. Consistent with this notion, some mycelial fungi possess homologues of CesA1p, which is the catalytic subunit of a plant cellulose synthase. When the amino acid sequence of the large cytosolic loop of this protein, which is predicted to be responsible for the catalytic activity, is subjected to a PSI-BLAST search (NCBI; http://www.ncbi.nlm.nih.gov/BLAST/), fungal homologues are identified in various *Aspergillus* spp, including *A. fumigatus*, and in *N. crassa*.

VII. Cell Wall Construction Enzymes

A. General

The various components of the fungal cell wall are either synthesized by separate enzyme complexes associated with the plasma membrane (e.g. β-1,3-glucan, β-1,3-glucan, chitin) or, as in the case of mannoproteins, they are synthesized intracellularly and then transported to the cell surface, where they are released. The location of β-1,6-glucan synthesis is still a matter of debate (Montijn et al. 1999; Humbel et al. 2001), but in *Sac. cerevisiae* it was shown that the linkage to proteins occurs extracellularly (Lu et al. 1995). The cell wall components of *Sac. cerevisiae* and the pathogenic yeasts *Can. albicans* and *Can. glabrata* are covalently attached to one another (Fig. 4.1). Consequently, the enzymes that connect these polymers have to be located at the extracellular face of the plasma membrane. To account for the five different interpolymeric linkages identified in *Sac. cerevisiae*, at least five different enzyme activities are required. None of these enzymes has been identified definitively, but there are several potential candidates. As we see below, the majority of them are GPI proteins.

B. The Gas/Gel/Phr Family

The Gas/Gel/Phr family is classified as glycosyl hydrolase (GH) family 72 in the carbohydrate-active enzyme database (*c*arbohydrate *a*ctive en*z*ymes, CAZY; http://afmb.cnrs-mrs.fr/CAZY; Coutinho and Henrissat 1999). It is a family of GPI proteins found in all sequenced fungi, including the basidiomycetes *U. maydis* and *Cry. neoformans*. Members of this family – isolated from *Sac. cerevisiae*, *Can. albicans*, and *A. fumigatus* – are able to hydrolyze β-1,3-glucan oligomers in vitro and to connect the newly created reducing end to a nonreducing end of another β-1,3-glucan oligomer (Mouyna et al. 2000; Carotti et al. 2004). This is consistent with a role in connecting β-1,3-glucan chains that are emerging from the plasma membrane to existing β-1,3-glucan chains in the cell wall.

C. The Crh Family

The Crh family, which belongs to GH family 16, also consists of GPI proteins and is widely distributed in ascomycetous and basidiomycetous fungi. Biochemical evidence for enzymatic activity of this family is still lacking, but several observations suggest that this family is involved in the formation of the chitin → β-1,3-glucan complex:

1. *Sac. cerevisiae* Crh1p and Utr2p/Crh2p colocalize with sites of chitin deposition (Rodríguez-Peña et al. 2000, 2002).
2. *CRH* deletion mutants have a defective cell wall (Rodríguez-Peña et al. 2000).
3. The GH 16 domain of Crh proteins is homologous to the catalytic domain of bacterial GH 16 members, including two conserved glutamates in the active site, which is reported to cleave β-1,4-glycosidic bonds adjacent to β-1,3-glycosidic bonds (Lloberas et al. 1988). As chitin is linked via a 1,4-bond to β-1,3-glucan, this may point to involvement in a transglycosidase reaction coupling chitin to β-1,3-glucan.
4. Several members of the Crh family contain a carbohydrate-binding module (CBM 43), implicated in chitin binding, immediately upstream of the GH 16 domain (CAZY; http://afmb.cnrs-mrs.fr/CAZY; Coutinho and Henrissat 1999).
5. *Sch. pombe*, which completely lacks chitin, has no Crh family members.

D. The Ecm33/Sps2 Family

The Ecm33/Sps2 family of GPI proteins is also widely distributed in fungi. *ECM33* deletion mutants in *Sac. cerevisiae*, *Can. albicans* and *A. fumigatus* show strong cell wall-related phenotypes such as increased sensitivity to drugs that interfere with cell wall formation, constitutive activation of the cell wall integrity (CWI) pathway (see Sect. VIII.), and the formation of swollen cells (Martinez-Lopez et al. 2004; Pardo et al. 2004; Yin et al. 2005; Chabane et al. 2006). In addition, the *ecm33*Δ mutant in *Sac. cerevisiae* secretes considerably more β-1,6-glucan-bound cell wall proteins into the medium than wild-type cells, suggesting that cell wall assembly is affected (De Groot et al. 2001). Unfortunately, members of the Ecm33 family do not show homology with proteins with a known enzymatic function.

E. The Bgl2 Family

ScBgl2p is a secretory protein that strongly associates with chitin and β-1,3-glucan and belongs to GH family 17 (CAZY; http://afmb.cnrs-mrs.fr/CAZY/; Mrsa et al. 1993; Coutinho and Henrissat

1999). In vitro studies using purified Bgl2p from *A. fumigatus*, *Can. albicans* and *Sac. cerevisiae* show that it has both endo-β-1,3-glucanase activity and transglucosidase activity, introducing an intrachain β-1,6-linkage in a β-1,3-glucan chain (Mrsa et al. 1993; Yu et al. 1993; Mouyna et al. 1998). Consistent with the ubiquitous nature of β-1,3-glucan in fungal cell walls, Bgl2 family members are widespread in ascomycetes and are present in the basidiomycetes *U. maydis* and *Cry. neoformans* as well (SGD; http://db.yeastgenome.org/; comparison resources, BLASTP vs fungi).

Three Bgl2 family members, Scw4p and Scw10p of *Sac. cerevisiae* and MP65p/Scw1 of *Can. albicans*, are also nonGPI secretory proteins. They are resistant to extraction with hot SDS, but can be released from the wall with mild alkali (De Groot et al. 2004; Yin et al. 2005). As they can be released by β-1,3-glucanase, but not by β-1,6-glucanase, they are thought to be linked to β-1,3-glucan directly; they lack though a DGQJQ sequence (see Sect. V.A.). In mycelial ascomycetes (e.g. *N. crassa*, *Aspergillus* spp), some additional Bgl2 family members have predicted GPI anchors (big-PI Fungal Predictor, available at http://mendel.imp.ac.at/gpi/fungi_server.html; Eisenhaber et al. 2004).

F. The Dfg5/Dcw1 Family

Dcw1p and Dfg5p (GH 76) are a pair of homologous GPI proteins in *Sac. cerevisiae* with similarity to bacterial α-1,6-mannanases (CAZY; http://afmb.cnrs-mrs.fr/CAZY/; Coutinho and Henrissat 1999; Kitagaki et al. 2002).

Immediately upstream of their presumed GPI-anchor addition site, they contain multiple lysine residues; stretches of consecutive serine or threonine residues are also lacking, indicating that these proteins are retained in the plasma membrane (Caro et al. 1997; Frieman and Cormack 2004). A double disruptant of *DCW1* and *DFG5* is synthetically lethal (Kitagaki et al. 2002) and this is also the case in *Can. albicans* (Spreghini et al. 2003), indicating that their function is essential. In *Sac. cerevisiae*, it has been shown that precursor forms of GPI cell wall proteins prior to their incorporation into the wall are cleaved at the plasma membrane between the glucosamine and the first mannose residue of the anchor (Kollar et al. 1997; Fujii et al. 1999). It seems plausible that Dcw1p and Dfg5p are involved in this processing step. Dfg5 and Dcw1 homologues widely occur in ascomycetes, including mycelial species such as *Aspergillus* spp, *M. grisea*, *N. crassa*, the dimorphic fungus *P. brasiliensis*, and in the fission yeast *Sch. pombe* (CAZY; http://afmb.cnrs-mrs.fr/CAZY/). In the basidiomycete *U. maydis*, homologues of Dfg5/Dcw1 are present as well. However, they seem to be lacking in *Cry. neoformans*, which is consistent with the absence of an outer protein layer in their cell wall.

VIII. The Cell Wall Integrity Pathway

To maintain cell wall integrity during stress, such as caused by the presence of cell wall lytic enzymes secreted by plants or by a sudden drop in environmental osmolarity by rain, fungi have developed backup mechanisms. The signaling cascade mediating the cell wall stress response, called the CWI pathway, is particularly well studied in *Sac. cerevisiae* (for a review, see Levin 2005). The cell wall stress response in *Sac. cerevisiae* is characterized by several alterations in the composition and architecture of the cell wall. These include: (1) mobilization of the chitin synthase Chs3p and its transport from internal stores to the plasma membrane, resulting in elevated chitin levels in the lateral walls including the lateral walls of the growing bud (Valdivia and Schekman 2003), (2) increased expression of *GFA1*, which encodes glutamine-fructose-6-phosphate amidotransferase, the first committed enzyme of the chitin biosynthetic pathway (Lagorce et al. 2002), (3) increased expression of *FKS2*, a β-1,3-glucan synthase-encoding gene, (4) increased expression of a characteristic set of cell wall proteins (Jung and Levin 1999; Lagorce et al. 2003; Boorsma et al. 2004; Garcia et al. 2004), and (5) a strong increase in the levels of the CWP–polysaccharide complex CWP → [chitin →] β-1,6-glucan, which is accompanied by increased resistance of intact cells to β-1,3-glucanase (Kapteyn et al. 1997; De Nobel et al. 2000).

In mycelial fungi, the response to cell wall stress has been studied in less detail, but increased deposition of chitin has been described for the cell walls of *A. nidulans* (Katz and Rosenberger 1971) and *A. niger* (Ram et al. 2004); in addition, increased expression of the chitin synthase-encoding genes *csm*A and *csm*B has been observed in *A. nidulans* (Takeshita et al. 2006). The expres-

sion of α-1,3-glucan synthase-encoding genes is also induced in response to cell wall stress, both in *A. niger* and *P. chrysogenum* (Damveld et al. 2005b). This is consistent with the considerable increase in thickness of the inner (skeletal) layer of the cell wall of *A. flavus* and *A. fumigatus* occurring after exposure to an inhibitor of β-1,3-glucan synthesis (Kurtz et al. 1994). Cell wall stress caused by the disruption of chitin synthases is also compensated for by increased synthesis of α-1,3-glucan (Mellado et al. 2003).

The CWI pathway in *Sac. cerevisiae* makes use of the Pkc1p-controlled MAPK cascade. In the case of cell wall stress the MAP kinase of this cascade (Slt2p/Mpk1p) becomes dually phosphorylated (De Nobel et al. 2000). The most important target of activated Slt2p/Mpk1p of this cascade is the MADS box transcription factor Rlm1p (Jung et al. 2002; Lagorce et al. 2003). Recent studies indicate that the cell wall stress response in mycelial fungi is mediated by a similar signaling pathway. Disruption of the *A. oryzae kexB* gene, which encodes the homologue of the Golgi-localized *Sac. cerevisiae* endoprotease Kex2, resulted in phosphorylation of the MpkA protein, which is the homologue of the Slt2p/Mpk1p of *Sac. cerevisiae* (Mizutani et al. 2004; for the role of ScKex2p in cell wall integrity, see Tomishige et al. 2003). Moreover, *kexB* deletion led to induced expression of several cell wall-related genes, including β-1,3-glucan synthase- and chitin synthase-encoding genes, indicating activation of a back-up mechanism to prevent further cell wall damage (Mizutani et al. 2004). In *A. niger* it was shown that deletion of the Rlm1p homologue eliminated the induction of the α-1,3-glucan synthase gene (*agsA*) and reduced the increase in chitin deposition after exposure to cell wall stress (Damveld et al. 2005a). Homologues of the proteins involved in the cell wall integrity pathway are also found in the mycelial fungi *A. nidulans*, *G. zeae*, *N. crassa*, and *M. grisea* (Damveld et al. 2005a), as well in the basidiomycete *Cry. neoformans* (Gerik et al. 2005). Deletion of genes involved in the proposed Pkc1p-controlled signaling cascade in *Cry. neoformans* revealed similar phenotypes as observed for the phenotypes of the corresponding deletion strains in *Sac. cerevisiae* (Kraus et al. 2003; Gerik et al. 2005). However, deletion of members of the Pkc1p-controlled signaling cascade in both *A. niger* and *Cry. neoformans* also resulted in divergent phenotypes, indicating that the CWI pathway was modified (Damveld et al. 2005a; Gerik et al. 2005).

IX. Conclusions and Perspectives

Comparative genomics has a powerful impact on fungal research and thus also on fungal cell wall biology, but this is only the beginning. Not only will it allow comparative analysis of glycosyltransferases and (trans)glycosidases (Campbell et al. 1997; Coutinho and Henrissat 1999; see also the CAZY web site at http://afmb.cnrs-mrs.fr/CAZY/), but it will also provide provisional answers to questions like whether and to what extent the regulatory mechanisms of cell wall biosynthesis are conserved, whether transcription factor binding sites are conserved, and how the gene composition of transcriptional modules might have evolved (Gasch et al. 2004; Nemecek et al. 2006; Xu et al. 2006). The increasing availability of fungal genomes will also boost proteomic analysis of cell wall proteins. On the biochemical level, cell wall analysis is lagging behind. We are still waiting for the definitive identification of most of the cell wall assembly enzymes and for (better) assays of their activity. Assays for several glycan synthases and for most glycosyl transferases are still lacking. Many cell wall analyses do not address the question if and how the separate cell wall components are covalently linked to other cell wall macromolecules. Detailed structural analyses of several cell wall polysaccharides are not available or have only been studied in detail in a single model fungus.

Although the cell wall architecture of *Sac. cerevisiae* and *Sch. pombe* provide the research community with powerful conceptual and technical tools to unravel the molecular structure of the cell wall of many other ascomycetous and basidiomycetous fungi, more model systems might be extremely useful, particularly in the case of the basidiomycetous fungi. In view of the wonderful variety shown by fungi and because entire groups of fungi have hardly been explored, such as the mycobionts of lichens, amphibian pathogens, fish pathogens, insect pathogens, or fungi growing under extreme conditions such as in acidic rivers or in the Antarctic, we may expect numerous surprises.

References

Abruzzo GK, Flattery AM, Gill CJ, Kong L, Krupa D, Pikounis VB, Kropp H, Bartizal K (1995) Evaluation of water-soluble pneumocandin analogs L-733560, L-705589, and L-731373 with mouse models of disseminated aspergillosis, candidiasis, and cryptococcosis. Antimicrob Agents Chemother 39:1077–1081

Ahrazem O, Gomez-Miranda B, Prieto A, Bernabe M, Leal JA (2000) Heterogeneity of the genus *Myrothecium* as revealed by cell wall polysaccharides. Arch Microbiol 173:296–302

Alviano CS, Travassos LR, Schauer R (1999) Sialic acids in fungi: a minireview. Glycoconj J 16:545–554

Banks IR, Specht CA, Donlin MJ, Gerik KJ, Levitz SM, Lodge JK (2005) A chitin synthase and its regulator protein are critical for chitosan production and growth of the fungal pathogen *Cryptococcus neoformans*. Eukaryot Cell 4:1902–1912

Bardalaye PC, Nordin JH (1976) Galactosaminogalactan from cell walls of *Aspergillus niger*. J Bacteriol 125:655–669

Bardalaye PC, Nordin JH (1977) Chemical structure of the galactomannan from the cell wall of *Aspergillus niger*. J Biol Chem 252:2584–2591

Barran LR, Schneider EF, Wood PJ, Madhosingh C, Miller RW (1975) Cell wall of *Fusarium sulphureum*. I. Chemical composition of the hyphal wall. Biochim Biophys Acta 392:148–158

Beauvais A, Bruneau JM, Mol PC, Buitrago MJ, Legrand R, Latgé JP (2001) Glucan synthase complex of *Aspergillus fumigatus*. J Bacteriol 183:2273–2279

Beauvais A, Park S, Morelle W, Tanguy M, Huerre M, Perlin DS, Latge JP (2005) Two α(1-3) glucan synthases with different functions in *Aspergillus fumigatus*. Appl Environ Microbiol 71:1531–1538

Biswas SK, Yamaguchi M, Naoe N, Takashima T, Takeo K (2003) Quantitative three-dimensional structural analysis of *Exophiala dermatitidis* yeast cells by freeze-substitution and serial ultrathin sectioning. J Electron Microsc 52:133–143

Blumenthal HJ, Roseman S (1957) Quantitative estimation of chitin in fungi. J Bacteriol 74:222–224

Boorsma A, Nobel H de, Riet B ter, Bargmann B, Brul S, Hellingwerf KJ, Klis FM (2004) Characterization of the transcriptional response to cell wall stress in *Saccharomyces cerevisiae*. Yeast 21:413–427

Borkovich KA, Alex LA, Yarden O, Freitag M, Turner GE, Read ND, Seiler S, Bell-Pedersen D, Paietta J, Plesofsky N, Plamann M, Goodrich-Tanrikulu M, Schulte U, Mannhaupt G, Nargang FE, Radford A, Selitrennikoff C, Galagan JE, Dunlap JC, Loros JJ, Catcheside D, Inoue H, Aramayo R, Polymenis M, Selker EU, Sachs MS, Marzluf GA, Paulsen I, Davis R, Ebbole DJ, Zelter A, Kalkman ER, O'Rourke R, Bowring F, Yeadon J, Ishii C, Suzuki K, Sakai W, Pratt R (2004) Lessons from the genome sequence of *Neurospora crassa*: tracing the path from genomic blueprint to multicellular organism. Microbiol Mol Biol Rev 68:1–108

Bose I, Reese AJ, Ory JJ, Janbon G, Doering TL (2003) A yeast under cover: the capsule of *Cryptococcus neoformans*. Eukaryot Cell 2:655–663

Boulianne RP, Liu Y, Aebi M, Lu BC, Kues U (2000) Fruiting body development in *Coprinus cinereus*: regulated expression of two galectins secreted by a non-classical pathway. Microbiology 146:1841–1853

Brandhorst T, Klein B (2000) Cell wall biogenesis of *Blastomyces dermatitidis*. Evidence for a novel mechanism of cell surface localization of a virulence-associated adhesin via extracellular release and reassociation with cell wall chitin. J Biol Chem 275:7925–7934

Brandhorst T, Wüthrich M, Finkel-Jimenez B, Klein B (2003) A C-terminal EGF-like domain governs BAD1 localization to the yeast surface and fungal adherence to phagocytes, but is dispensable in immune modulation and pathogenicity of *Blastomyces dermatitidis*. Mol Microbiol 48:53–65

Braun PC, Calderone RA (1978) Chitin synthesis in *Candida albicans*: comparison of yeast and hyphal forms. J Bacteriol 133:1472–1477

Brul S, King A, Van der Vaart JM, Chapman J, Klis F, Verrips CT (1997) The incorporation of mannoproteins in the cell wall of *S. cerevisiae* and filamentous *Ascomycetes*. Antonie Van Leeuwenhoek 72:229–237

Bull AT (1970) Chemical composition of wild-type and mutant *Aspergillus nidulans* cell walls. The nature of polysaccharide and melanin constituents. J Gen Microbiol 63:75–94

Bush DA, Horisberger M, Horman I, Wursch P (1974) The wall structure of *Schizosaccharomyces pombe*. J Gen Microbiol 81:199–206

Cabib E, Duran A (2005) Synthase III-dependent chitin is bound to different acceptors depending on location on the cell wall of budding yeast. J Biol Chem 280:9170–9179

Campbell JA, Davies GJ, Bulone V, Henrissat B (1997) A classification of nucleotide-diphospho-sugar glycosyltransferases based on amino acid sequence similarities. Biochem J 326:929–939

Cao L, Chan CM, Lee C, Wong SS, Yuen KY (1998) *MP1* encodes an abundant and highly antigenic cell wall mannoprotein in the pathogenic fungus *Penicillium marneffei*. Infect Immun 66:966–973

Cappellaro C, Mrsa V, Tanner W (1998) New potential cell wall glucanases of *Saccharomyces cerevisiae* and their involvement in mating. J Bacteriol 180:5030–5037

Caro LHP, Tettelin H, Vossen JH, Ram AFJ, Van den Ende H, Klis FM (1997) *In silico* identification of glycosylphosphatidylinositol-anchored plasma-membrane and cell wall proteins of *Saccharomyces cerevisiae*. Yeast 13:1477–1489

Caro LHP, Smits GJ, Van Egmond P, Chapman JW, Klis FM (1998) Transcription of multiple cell wall protein-encoding genes in *Saccharomyces cerevisiae* is differentially regulated during the cell cycle. FEMS Microbiol Lett 161:345–349

Carotti C, Ragni E, Palomares O, Fontaine T, Tedeschi G, Rodriguez R, Latge JP, Vai M, Popolo L (2004) Characterization of recombinant forms of the yeast Gas1 protein and identification of residues essential for glucanosyltransferase activity and folding. Eur J Biochem 271:3635–3645

Cassone A, Simonetti N, Strippoli V (1974) Wall structure and bud formation in *Cryptococcus neoformans*. Arch Microbiol 95:205–212

Chabane S, Sarfati J, Ibrahim-Granet O, Du C, Schmidt C, Mouyna I, Prevost MC, Calderone R, Latge JP (2006) Glycosylphosphatidylinositol-anchored Ecm33p influences conidial cell wall biosynthesis in *Aspergillus fumigatus*. Appl Environ Microbiol 72:3259–3267

Cole GT, Hung CY (2001) The parasitic cell wall of *Coccidioides immitis*. Med Mycol 39[Suppl 1]:31–40

Cole GT, Sun SH (1985) Arthroconidium-spherule-endospore transformation in *Coccidioides immitis*. In: Szaniszlo PJ (ed) Fungal dimorphism, with emphasis on fungi pathogenic for humans. Plenum, New York, pp 281–333

Cooper DN, Boulianne RP, Charlton S, Farrell EM, Sucher A, Lu BC (1997) Fungal galectins, sequence and specificity of two isolectins from *Coprinus cinereus*. J Biol Chem 272:1514–1521

Coutinho PM, Henrissat B (1999) Carbohydrate-active enzymes: an integrated database approach. In: Gilbert HJ, Davies G, Henrissat B, Svensson B (eds) Recent advances in carbohydrate bioengineering. Royal Society of Chemistry, Cambridge, pp 3–12

Crampin H, Finley K, Gerami-Nejad M, Court H, Gale C, Berman J, Sudbery P (2005) *Candida albicans* hyphae have a Spitzenkorper that is distinct from the polarisome found in yeast and pseudohyphae. J Cell Sci 118:2935–2947

Damveld RA, Arentshorst M, Franken A, vanKuyk PA, Klis FM, Hondel CAMJJ van den, Ram AFJ (2005a) The Aspergillus niger MADS-box transcription factor RlmA is required for cell wall reinforcement in response to cell wall stress. Mol Microbiol 58:305–319

Damveld RA, Vankuyk PA, Arentshorst M, Klis FM, Hondel CA van den, Ram AFJ (2005b) Expression of *agsA*, one of five 1,3-α-D-glucan synthase-encoding genes in *Aspergillus niger*, is induced in response to cell wall stress. Fungal Genet Biol 42:165–177

De Groot PWJ, Ruiz C, Aldana CRV de, Duenas E, Cid VJ, Del Rey F, Rodriguez-Pena JM, Perez P, Andel A, Caubin J, Arroyo J, Garcia JC, Gil C, Molina M, Garcia LJ, Nombela C, Klis FM (2001) A genomic approach for the identification and classification of genes involved in cell wall formation and its regulation in *Saccharomyces cerevisiae*. Comp Funct Genomics 2:124–142

De Groot PWJ, Hellingwerf KJ, Klis FM (2003) Genome-wide identification of fungal GPI proteins. Yeast 20:781–796

De Groot PWJ, Boer AD de, Cunningham J, Dekker HL, Jong L de, Hellingwerf KJ, Koster C de, Klis FM (2004) Proteomic analysis of *Candida albicans* cell walls reveals covalently bound carbohydrate-active enzymes and adhesins. Eukaryot Cell 3:955–965

De Groot PWJ, Ram AF, Klis FM (2005) Features and functions of covalently linked proteins in fungal cell walls. Fungal Genet Biol 42:657–675

De Nobel H, Ruiz C, Martin H, Morris W, Brul S, Molina M, Klis FM (2000) Cell wall perturbation in yeast results in dual phosphorylation of the Slt2/Mpk1 MAP kinase and in an Slt2-mediated increase in *FKS2-lacZ* expression, glucanase resistance and thermotolerance. Microbiology 146:2121–2132

De Nobel H, Sietsma JH, Van den Ende H, Klis FM (2001) Molecular organization and construction of the fungal cell wall. In: Howard RJ, Gow NAR (eds) The Mycota, vol 8. Springer, Berlin Heidelberg New York, pp 181–200

De Nobel JG, Dijkers C, Hooijberg E, Klis FM (1989) Increased cell wall porosity in *Saccharomyces cerevisiae* after treatment with dithiothreitol or EDTA. J Gen Microbiol 135:2077–2084

De Nobel JG, Klis FM, Priem J, Munnik T, Van den Ende H (1990) The glucanase-soluble mannoproteins limit cell wall porosity in *Saccharomyces cerevisiae*. Yeast 6:491–499

Dean N (1999) Asparagine-linked glycosylation in the yeast Golgi. Biochim Biophys Acta 1426:309–322

Depree J, Emerson GW, Sullivan PA (1993) The cell wall of the oleaginous yeast *Trichosporon cutaneum*. J Gen Microbiol 139:2123–2133

Domer JE (1985) *Blastomyces dermatitidis*. In: Szaniszlo PJ (ed) Fungal dimorphism, with emphasis on fungi pathogenic for humans. Plenum, New York, pp 51–67

Ecker M, Deutzmann R, Lehle L, Mrsa V, Tanner W (2006) PIR-proteins of *Saccharomyces cerevisiae* are attached to β-1,3-glucan by a new protein-carbohydrate linkage. J Biol Chem 281:11523–11529

Edson CM, Brody S (1976) Biochemical and genetic studies on galactosamine metabolism in *Neurospora crassa*. J Bacteriol 126:799–805

Eisenhaber B, Schneider G, Wildpaner M, Eisenhaber F (2004) A sensitive predictor for potential GPI lipid modification sites in fungal protein sequences and its application to genome-wide studies for *Aspergillus nidulans*, *Candida albicans*, *Neurospora crassa*, *Saccharomyces cerevisiae* and *Schizosaccharomyces pombe*. J Mol Biol 337:243–253

Eisenman HC, Nosanchuk JD, Webber JB, Emerson RJ, Camesano TA, Casadevall A (2005) Microstructure of cell wall-associated melanin in the human pathogenic fungus *Cryptococcus neoformans*. Biochemistry 44:3683–3693

Feldmesser M, Kress Y, Mednick A, Casadevall A (2000) The effect of the echinocandin analogue caspofungin on cell wall glucan synthesis by *Cryptococcus neoformans*. J Infect Dis 182:1791–1795

Fontaine T, Sinenel C, Dubreucq G, Adam O, Delepierre M, Lemoine J, Vorgias CE, Diaquin M, Latge JP (2000) Molecular organization of the alkali-insoluble fraction of *Aspergillus fumigatus* cell wall. J Biol Chem 275:415–428

Fontaine T, Smith TK, Crossman A, Brimacombe JS, Latgé JP, Ferguson MA (2004) In vitro biosynthesis of glycosylphosphatidylinositol in *Aspergillus fumigatus*. Biochemistry 43:15267–15275

Fraering P, Imhof I, Meyer U, Strub JM, Dorsselaer A van, Vionnet C, Conzelmann A (2001) The GPI transamidase complex of *Saccharomyces cerevisiae* contains Gaa1p, Gpi8p, and Gpi16p. Mol Biol Cell 12:3295–3306

Frieman MB, Cormack BP (2003) The omega-site sequence of glycosylphosphatidylinositol-anchored proteins in *Saccharomyces cerevisiae* can determine distribution between the membrane and the cell wall. Mol Microbiol 50:883–896

Frieman MB, Cormack BP (2004) Multiple sequence signals determine the distribution of glycosylphosphatidylinositol proteins between the plasma membrane and cell wall in *Saccharomyces cerevisiae*. Microbiology 150:3105–3114

Frieman MB, McCaffery JM, Cormack BP (2002) Modular domain structure in the *Candida glabrata* adhesin Epa1p, a β1,6 glucan-cross-linked cell wall protein. Mol Microbiol 46:479–492

Fujii T, Shimoi H, Iimura Y (1999) Structure of the glucan-binding sugar chain of Tip1p, a cell wall protein of *Saccharomyces cerevisiae*. Biochim Biophys Acta 1427:133–144

Fujiwara M, Ichinomiya M, Motoyama T, Horiuchi H, Ohta A, Takagi M (2000) Evidence that the *Aspergillus nidulans* class I and class II chitin synthase genes, *chsC* and *chsA*, share critical roles in hyphal wall integrity and conidiophore development. J Biochem (Tokyo) 127:359–366

Gantner BN, Simmons RM, Underhill DM (2005) Dectin-1 mediates macrophage recognition of *Candida albicans* yeast but not filaments. EMBO J 24:1277–1286

García I, Tajadura V, Martín V, Toda T, Sánchez Y (2006) Synthesis of α-glucans in fission yeast spores is carried out by three α-glucan synthase paralogues, Mok12p, Mok13p and Mok14p. Mol Microbiol 59:836–853

Garcia R, Bermejo C, Grau C, Perez R, Rodriguez-Pena JM, Francois J, Nombela C, Arroyo J (2004) The global transcriptional response to transient cell wall damage in *Saccharomyces cerevisiae* and its regulation by the cell integrity signaling pathway. J Biol Chem 279:15183–15195

Garrison RG (1981) Vegetative ultrastructure. In: Arnold WN (ed) Yeast cell envelopes: biochemistry, biophysics, and ultrastructure, vol 2. CRC, Boca Raton, pp 139–160

Garrison RG (1985) Cytological and ultrastructural aspects of dimorphism. In: Szaniszlo PJ (ed) Fungal dimorphism, with emphasis on fungi pathogenic for humans. Plenum, New York, pp 15–47

Garrison RG, Arnold WN (1981) Atlas of cell morphology. In: Arnold WN (ed) Yeast cell envelopes: biochemistry, biophysics, and ultrastructure, vol 1. CRC, Boca Raton, pp 5–24

Garrison RG, Boyd KS (1973) Dimorphism of *Penicillium marneffei* as observed by electron microscopy. Can J Microbiol 19:1305–1309

Gasch AP, Moses AM, Chiang DY, Fraser HB, Berardini M, Eisen MB (2004) Conservation and evolution of cis-regulatory systems in ascomycete fungi. PLoS Biol 2:2202–2219

Geis PA, Jacobs CW (1985) Polymorphism of *Wangiella dermatitidis*. In: Szaniszlo PJ (ed) Fungal dimorphism, with emphasis on fungi pathogenic for humans. Plenum, New York, pp 205–233

Gemmill TR, Trimble RB (1999) Overview of *N*- and *O*-linked oligosaccharide structures found in various yeast species. Biochim Biophys Acta 1426:227–237

Gerik KJ, Donlin MJ, Soto CE, Banks AM, Banks IR, Maligie MA, Selitrennikoff CP, Lodge JK (2005) Cell wall integrity is dependent on the *PKC1* signal transduction pathway in *Cryptococcus neoformans*. Mol Microbiol 58:393–408

Gomez BL, Nosanchuk JD (2003) Melanin and fungi. Curr Opin Infect Dis 16:91–96

Gow NA, Gooday GW (1982) Growth kinetics and morphology of colonies of the filamentous form of *Candida albicans*. J Gen Microbiol 128:2187–2194

Grün CH, Hochstenbach F, Humbel BM, Verkleij AJ, Sietsma JH, Klis FM, Kamerling JP, Vliegenthart JFG (2005) The structure of cell wall α-glucan from fission yeast. Glycobiology 15:245–257

Haido RMT, Silva MH, Ejzemberg R, Leitão EA, Hearn VM, Evans EGV, Barreto Bergter E (1998) Analysis of peptidogalactomannana from the mycelial surface of *Aspergillus fumigatus*. Med Mycol 36:313–321

Hamada K, Terashima H, Arisawa M, Yabuki N, Kitada K (1999) Amino acid residues in the omega-minus region participate in cellular localization of yeast glycosylphosphatidylinositol-attached proteins. J Bacteriol 181:3886–3889

Hardham AR (2001) Cell biology of fungal infections of plants. In: Howard RJ, Gow NAR (eds) The Mycota, vol 8. Springer, Berlin Heidelberg New York, pp 91–123

Hearn VM, Sietsma JH (1994) Chemical and immunological analysis of the *Aspergillus fumigatus* cell wall. Microbiology 140:789–795

Heath IB (1994) The cytoskeleton in hyphal growth, organelle movements, and mitosis. In: Wessels JGH, Meinhardt F (eds) The Mycota, vol 1. Springer, Berlin Heidelberg New York, pp 43–65

Hochstenbach F, Klis FM, Van den Ende H, Van Donselaar E, Peters PJ, Klausner RD (1998) Identification of a putative α-glucan synthase essential for cell wall construction and morphogenesis in fission yeast. Proc Natl Acad Sci USA 95:9161–9166

Hogan LH, Klein BS (1994) Altered expression of surface α-1,3-glucan in genetically related strains of *Blastomyces dermatitidis* that differ in virulence. Infect Immun 62:3543–3546

Horisberger M, Clerc MF (1988) Ultrastructural localization of anionic sites on the surface of yeast, hyphal and germ-tube forming cells of *Candida albicans*. Eur J Cell Biol 46:444–452

Horisberger M, Rouvet-Vauthey M (1985) Cell wall architecture in the fission yeast *Schizosaccharomyces pombe*. Experientia 41:748–750

Howard RJ, Aist JR (1979) Hyphal tip cell ultrastructure of the fungus *Fusarium*: improved preservation by freeze-substitution. J Ultrastruct Res 66:224–234

Howard RJ, Ferrari MA, Roach DH, Money NP (1991) Penetration of hard substrates by a fungus employing enormous turgor pressures. Proc Natl Acad Sci USA 88:11281–11284

Humbel BM, Konomi M, Takagi T, Kamasawa N, Ishijima SA, Osumi M (2001) In situ localization of β-glucans in the cell wall of *Schizosaccharomyces pombe*. Yeast 18:433–444

Ichinomiya M, Horiuchi H, Ohta A (2002a) Different functions of the class I and class II chitin synthase genes, *chsC* and *chsA*, are revealed by repression of *chsB* expression in *Aspergillus nidulans*. Curr Genet 42:51–58

Ichinomiya M, Motoyama T, Fujiwara M, Takagi M, Horiuchi H, Ohta A (2002b) Repression of *chsB* expression reveals the functional importance of class IV chitin synthase gene *chsD* in hyphal growth and conidiation of *Aspergillus nidulans*. Microbiology 148:1335–1347

Ichinomiya M, Yamada E, Yamashita S, Ohta A, Horiuchi H (2005) Class I and class II chitin synthases are involved in septum formation in the filamentous fungus *Aspergillus nidulans*. Eukaryot Cell 4:1125–1136

Inoue SB, Takewaki N, Takasuka T, Mio T, Adachi M, Fujii Y, Miyamoto C, Arisawa M, Furuichi Y, Watanabe T (1995) Characterization and gene cloning of 1,3-β-D-glucan synthase from *Saccharomyces cerevisiae*. Eur J Biochem 231:845–854

Jaafar L, Moukadiri I, Zueco J (2003) Characterization of a disulphide-bound Pir-cell wall protein (Pir-CWP) of *Yarrowia lipolytica*. Yeast 20:417–426

James PG, Cherniak R, Jones RG, Stortz CA, Reiss E (1990) Cell-wall glucans of *Cryptococcus neoformans* Cap 67. Carbohydr Res 198:23–38

Jeong HY, Chae KS, Whang SS (2004) Presence of a mannoprotein, MnpAp, in the hyphal cell wall of *Aspergillus nidulans*. Mycologia 96:52–56

Jigami Y, Odani T (1999) Mannosylphosphate transfer to yeast mannan. Biochim Biophys Acta 1426:335–345

Jikibara T, Tada K, Takegawa K, Iwahara S (1992a) Studies on the uronic acid-containing glycoproteins of *Fusarium* sp. M7-1: II. The primary structures of the low molecular weight carbohydrate chains of the glycoproteins. J Biochem (Tokyo) 111:230–235

Jikibara T, Takegawa K, Iwahara S (1992b) Studies on the uronic acid-containing glycoproteins of *Fusarium* sp. M7-1: I. Isolation and some properties of the glycoproteins. J Biochem (Tokyo) 111:225–229

Jikibara T, Takegawa K, Iwahara S (1992c) Studies on the uronic acid-containing glycoproteins of *Fusarium* sp. M7-1: III. The primary structures of the acidic polysaccharides of the glycoproteins. J Biochem (Tokyo) 111:236–243

Johnston IR (1965) The composition of the cell wall of *Aspergillus niger*. Biochem J 96:651–658

Jung US, Levin DE (1999) Genome-wide analysis of gene expression regulated by the yeast cell wall integrity signalling pathway. Mol Microbiol 34:1049–1057

Jung US, Sobering AK, Romeo MJ, Levin DE (2002) Regulation of the yeast Rlm1 transcription factor by the Mpk1 cell wall integrity MAP kinase. Mol Microbiol 46:781–789

Kahn JN, Hsu MJ, Racine F, Giacobbe R, Motyl M (2006) Caspofungin susceptibility in *Aspergillus* and non-*Aspergillus* molds: inhibition of glucan synthase and reduction of β-D-1,3 glucan levels in culture. Antimicrob Agents Chemother 50:2214–2216

Kanetsuna F, Carbonell LM (1971) Cell wall composition of the yeastlike and mycelial forms of *Blastomyces dermatitidis*. J Bacteriol 106:946–948

Kapteyn JC, Montijn RC, Dijkgraaf GJP, Van den Ende H, Klis FM (1995) Covalent association of β-1,3-glucan with β-1,6-glucosylated mannoproteins in cell walls of *Candida albicans*. J Bacteriol 177:3788–3792

Kapteyn JC, Montijin RC, Vink E, Cruz J de la, Llobell A, Douwes JE, Shimoi H, Lipke PN, Klis FM (1996) Retention of *Saccharomyces cerevisiae* cell wall proteins through a phosphodiester-linked β-1,3-/β-1,6-glucan heteropolymer. Glycobiology 6:337–345

Kapteyn JC, Ram AF, Groos EM, Kollar R, Montijn RC, Van Den Ende H, Llobell A, Cabib E, Klis FM (1997) Altered extent of cross-linking of β-1,6-glucosylated mannoproteins to chitin in *Saccharomyces cerevisiae* mutants with reduced cell wall β-1,3-glucan content. J Bacteriol 179:6279–6284

Kapteyn JC, Van Egmond P, Sievi E, Van den Ende H, Makarow M, Klis FM (1999) The contribution of the O-glycosylated protein Pir2p/Hsp150 to the construction of the yeast cell wall in wild-type cells and β1,6-glucan-deficient mutants. Mol Microbiol 31:1835–1844

Kapteyn JC, Hoyer LL, Hecht JE, Muller WH, Andel A, Verkleij AJ, Makarow M, Van Den Ende H, Klis FM (2000) The cell wall architecture of *Candida albicans* wild-type cells and cell wall-defective mutants. Mol Microbiol 35:601–611

Kapteyn JC, Riet B ter, Vink E, Blad S, De Nobel H, Van Den Ende H, Klis FM (2001) Low external pH induces *HOG1*-dependent changes in the organization of the *Saccharomyces cerevisiae* cell wall. Mol Microbiol 39:469–479

Katayama S, Hirata D, Arellano M, Perez P, Toda T (1999) Fission yeast β-glucan synthase Mok1 requires the actin cytoskeleton to localize the sites of growth and plays an essential role in cell morphogenesis downstream of protein kinase C function. J Cell Biol 144:1173–1186

Katz D, Rosenberger RF (1971) Hyphal wall synthesis in *Aspergillus nidulans*: effect of protein synthesis inhibition and osmotic shock on chitin insertion and morphogenesis. J Bacteriol 108:184–190

Kitagaki H, Wu H, Shimoi H, Ito K (2002) Two homologous genes, *DCW1* (*YKL046c*) and *DFG5*, are essential for cell growth and encode glycosylphosphatidylinositol (GPI)-anchored membrane proteins required for cell wall biogenesis in *Saccharomyces cerevisiae*. Mol Microbiol 46:1011–1022

Klebl F, Tanner W (1989) Molecular cloning of a cell wall exo-β-1,3-glucanase from *Saccharomyces cerevisiae*. J Bacteriol 171:6259–6264

Klein BS, Jones JM (1994) Purification and characterization of the major antigen WI-1 from *Blastomyces dermatitidis* yeasts and immunological comparison with A antigen. Infect Immun 62:3890–3900

Klimpel KR, Goldman WE (1988) Cell walls from avirulent variants of *Histoplasma capsulatum* lack α-(1,3)-glucan. Infect Immun 56:2997–3000

Klis FM, Boorsma A, De Groot PWJ (2006) Cell wall construction in *Saccharomyces cerevisiae*. Yeast 23:185–202

Klis FM, De Jong M, Brul S, De Groot PWJ (2007) Extraction of cell surface-associated proteins from living yeast cell. Yeast 24:253–258

Klutts J, Yoneda A, Reilly MC, Bose I, Doering TL (2006) Glycosyltransferases and their products: cryptococcal variations on fungal themes. FEMS Yeast Res 6:499–512

Knauer R, Lehle L (1999) The oligosaccharyltransferase complex from yeast. Biochim Biophys Acta 1426:259–273

Kobayashi GS, Medoff G, Maresca B, Sacco M, Kumar BV (1985) Studies on phase transitions in the dimorphic pathogen *Histoplasma capsulatum*. In: Szaniszlo PJ (ed) Fungal dimorphism, with emphasis on fungi pathogenic for humans. Plenum, New York, pp 69–91

Kollar R, Petrakova E, Ashwell G, Robbins PW, Cabib E (1995) Architecture of the yeast cell wall. The linkage between chitin and β(1>3)-glucan. J Biol Chem 270:1170–1178

Kollár R, Reinhold BB, Petráková E, Yeh HJC, Ashwell G, Drgonová J, Kapteyn JC, Klis FM, Cabib E (1997) Architecture of the yeast cell wall. β(1>6)-glucan interconnects mannoprotein, β(1>)3-glucan, and chitin. J Biol Chem 272:17762–17775

Konomi M, Fujimoto K, Toda T, Osumi M (2003) Characterization and behaviour of α-glucan synthase in *Schizosaccharomyces pombe* as revealed by electron microscopy. Yeast 20:427–438

Kopecka M, Fleet GH, Phaff HJ (1995) Ultrastructure of the cell wall of *Schizosaccharomyces pombe* following treatment with various glucanases. J Struct Biol 114:140–152

Kraus PR, Fox DS, Cox GM, Heitman J (2003) The *Cryptococcus neoformans* MAP kinase Mpk1 regulates cell integrity in response to antifungal drugs and loss of calcineurin function. Mol Microbiol 48:1377–1387

Kurtz MB, Heath IB, Marrinan J, Dreikorn S, Onishi J, Douglas C (1994) Morphological effects of lipopeptides against *Aspergillus fumigatus* correlate with activities against (1,3)-β-D-glucan synthase. Antimicrob Agents Chemother 38:1480–1489

Lagorce A, Le Berre-Anton V, Aguilar-Uscanga B, Martin-Yken H, Dagkessamanskaia A, Francois J (2002) Involvement of *GFA1*, which encodes glutamine-fructose-6-phosphate amidotransferase, in the activation of the chitin synthesis pathway in response to cell-wall defects in *Saccharomyces cerevisiae*. Eur J Biochem 269:1697–1707

Lagorce A, Hauser NC, Labourdette D, Rodriguez C, Martin-Yken H, Arroyo J, Hoheisel JRD, Francois J (2003) Genome-wide analysis of the response to cell wall mutations in the yeast *Saccharomyces cerevisiae*. J Biol Chem 278:20345–20357

Latgé JP, Mouyna I, Tekaia F, Beauvais A, Debeaupuis JP, Nierman W (2005) Specific molecular features in the organization and biosynthesis of the cell wall of *Aspergillus fumigatus*. Med Mycol 43[Suppl 1]:S15–S22

Levin DE (2005) Cell wall integrity signaling in *Saccharomyces cerevisiae*. Microbiol Mol Biol Rev 69:262–291

Linder MB, Szilvay GR, Nakari-Setala T, Penttila ME (2005) Hydrophobins: the protein-amphiphiles of filamentous fungi. FEMS Microbiol Rev 29:877–896

Lipke PN, Ovalle R (1998) Cell wall architecture in yeast: new structure and new challenges. J Bacteriol 180:3735–3740

Lloberas J, Querol E, Bernues J (1988) Purification and characterization of endo-β-1,3-1,4-D-glucanase activity from *Bacillus licheniformis*. Appl Microbiol Biotechnol 29:32–38

Loftus BJ, Fung E, Roncaglia P, Rowley D, Amedeo P, Bruno D, Vamathevan J, Miranda M, Anderson IJ, Fraser JA, Allen JE, Bosdet IE, Brent MR, Chiu R, Doering TL, Dontin MJ, D'Souza CA, Fox DS, Grinberg V, Fu JM, Fukushima M, Haas BJ, Huang JC, Janbon G, Jones SJM, Koo HL, Krzywinski MI, Kwon-Chung JK, Lengeler KB, Maiti R, Marra MA, Marra RE, Mathewson CA, Mitchell TG, Pertea M, Riggs FR, Salzberg SL, Schein JE, Shvartsbeyn A, Shin H, Shumway M, Specht CA, Suh BB, Tenney A, Utterback TR, Wickes BL, Wortman JR, Wye NH, Kronstad JW, Lodge JK, Heitman J, Davis RW, Fraser CM, Hyman RW (2005) The genome of the basidiomycetous yeast and human pathogen *Cryptococcus neoformans*. Science 307:1321–1324

Lopes-Bezerra LM, Schubach A, Costa RO (2006) *Sporothrix schenckii* and sporotrichosis. An Acad Bras Cienc 78:293–308

Lu CF, Montijn RC, Brown JL, Klis F, Kurjan J, Bussey H, Lipke PN (1995) Glycosyl phosphatidylinositol-dependent cross-linking of α-agglutinin and β-1,6-glucan in the *Saccharomyces cerevisiae* cell wall. J Cell Biol 128:333–340

Magnelli PE, Cipollo JF, Robbins PW (2005) A glucanase-driven fractionation allows redefinition of *Schizosaccharomyces pombe* cell wall composition and structure: assignment of diglucan. Anal Biochem 336:202–212

Mahadevan PR, Tatum EL (1965) Relationship of the major constituents of the *Neurospora crassa* cell wall to wild-type and colonial morphology. J Bacteriol 90:1073–1081

Mahadevan PR, Tatum EL (1967) Localization of structural polymers in the cell wall of *Neurospora crassa*. J Cell Biol 35:295–302

Maligie MA, Selitrennikoff CP (2005) *Cryptococcus neoformans* resistance to echinocandins: (1,3)β-glucan synthase activity is sensitive to echinocandins. Antimicrob Agents Chemother 49:2851–2856

Manners DJ, Meyer MT (1977) The molecular structures of some glucans from the cell walls of *Schizosaccharomyces pombe*. Carbohydr Res 57:189–203

Manners DJ, Masson AJ, Patterson JC, Björndal H, Lindberg B (1973) The structure of a β-(1>6)-D-glucan from yeast cell walls. Biochem J 135:31–36

Martinez-Lopez R, Monteoliva L, Diez-Orejas R, Nombela C, Gil C (2004) The GPI-anchored protein CaEcm33p is required for cell wall integrity, morphogenesis and virulence in *Candida albicans*. Microbiology 150:3341–3354

Maubon D, Park S, Tanguy M, Huerre M, Schmitt C, Prevost MC, Perlin DS, Latge JP, Beauvais A (2006) *AGS3*, an β(1-3)glucan synthase gene family member of *Aspergillus fumigatus*, modulates mycelium growth in the lung of experimentally infected mice. Fungal Genet Biol 43:366–375

Mellado E, Dubreucq G, Mol P, Sarfati J, Paris S, Diaquin M, Holden DW, Rodriguez-Tudela JL, Latge JP (2003) Cell wall biogenesis in a double chitin synthase mutant (*chs*G^{--}/*chs*E^{--}) of *Aspergillus fumigatus*. Fungal Genet Biol 38:98–109

Mizutani O, Nojima A, Yamamoto M, Furukawa K, Fujioka T, Yamagata Y, Abe K, Nakajima T (2004) Disordered cell integrity signaling caused by disruption of the *kexB* gene in *Aspergillus oryzae*. Eukaryot Cell 3:1036–1048

Montijn RC, Van Wolven P, De Hoog S, Klis FM (1997) β-Glucosylated proteins in the cell wall of the black yeast *Exophiala* (*Wangiella*) *dermatitidis*. Microbiology 143:1673–1680

Montijn RC, Vink E, Muller WH, Verkleij AJ, Van den Ende H, Henrissat B, Klis FM (1999) Localization of synthesis of β1,6-glucan in *Saccharomyces cerevisiae*. J Bacteriol 181:7414–74120

Morrison VA (2006) Echinocandin antifungals: review and update. Expert Rev Anti Infect Ther 4:325–342

Mouyna I, Hartland RP, Fontaine T, Diaquin M, Simenel C, Delepierre M, Henrissat B, Latge JP (1998) A 1,3-β-glucanosyltransferase isolated from the cell wall of *Aspergillus fumigatus* is a homologue of the yeast Bgl2p. Microbiology 144:3171–3180

Mouyna I, Fontaine T, Vai M, Monod M, Fonzi WA, Daiquin M, Popolo L, Hartland RP, Latge JP (2000) Glycosylphosphatidylinositol-anchored glucanosyltransferases play an active role in the biosynthesis of the fungal cell wall. J Biol Chem 275:14882–14889

Mrsa V, Klebl F, Tanner W (1993) Purification and characterization of the *Saccharomyces cerevisiae BGL2* gene product, a cell wall endo-β-1,3-glucanase. J Bacteriol 175:2102–2106

Mrsa V, Seidl T, Gentzsch M, Tanner W (1997) Specific labelling of cell wall proteins by biotinylation. Identification of four covalently linked *O*-mannosylated proteins of *Saccharomyces cerevisiae*. Yeast 13:1145–1154

Mrsa V, Tanner W (1999) Role of NaOH-extractable cell wall proteins Ccw5p, Ccw6p, Ccw7p and Ccw8p (members of the Pir protein family) in stability of the *Saccharomyces cerevisiae* cell wall. Yeast 15:813–820

Müller J (1999) Electron microscopy of *Candida albicans*. Mycoses 42[Suppl 1]:5–11

Munro CA, Gow NA (2001) Chitin synthesis in human pathogenic fungi. Med Mycol 39[Suppl 1]:41–53

Nakajima T, Ballou CE (1974) Characterization of the carbohydrate fragments obtained from *Saccharomyces cerevisiae* mannan by alkaline degradation. J Biol Chem 249:7679–7684

Nakayama K, Feng Y, Tanaka A, Jigami Y (1998) The involvement of *mnn4* and *mnn6* mutations in mannosylphosphorylation of *O*-linked oligosaccharide in yeast *Saccharomyces cerevisiae*. Biochim Biophys Acta 1425:255–262

Nemecek JC, Wuthrich M, Klein BS (2006) Global control of dimorphism and virulence in fungi. Science 312:583–588

Nicholas RO, Williams DW, Hunter PA (1994) Investigation of the value of β-glucan-specific fluorochromes for predicting the β-glucan content of the cell walls of zoopathogenic fungi. Mycol Res 98:694–698

Nombela C, Gil C, Chaffin WL (2006) Non-conventional protein secretion in yeast. Trends Microbiol 14:15–21

Osumi M, Naito M, Yamada N, Yaguchi H, Iwata K (1993) Effects of a new antidermatophytic agent liranaftate on the ultrastructure of *Trichophyton mentagrophytes*. Chemotherapy 41:555–567

Pardo M, Monteoliva L, Vazquez P, Martinez R, Molero G, Nombela C, Gil C (2004) *PST1* and *ECM33* encode two yeast cell surface GPI proteins important for cell wall integrity. Microbiology 150:4157–4170

Pierini LM, Doering TL (2001) Spatial and temporal sequence of capsule construction in *Cryptococcus neoformans*. Mol Microbiol 41:105–115

Ram AFJ, Brekelmans SSC, Oehlen LJWM, Klis FM (1995) Identification of two cell cycle regulated genes affecting the β1,3-glucan content of cell walls in *Saccharomyces cerevisiae*. FEBS Lett 358:165–170

Ram AFJ, Arentshorst M, Damveld RA, Vankuyk PA, Klis FM, Van den Hondel CAMJJ (2004) The cell wall stress response in *Aspergillus niger* involves increased expression of the glutamine: fructose-6-phosphate amidotransferase-encoding gene (*gfaA*) and increased deposition of chitin in the cell wall. Microbiology 150:3315–3326

Rappleye CA, Engle JT, Goldman WE (2004) RNA interference in *Histoplasma capsulatum* demonstrates a role for α-(1,3)-glucan in virulence. Mol Microbiol 53:153–165

Reese AJ, Doering TL (2003) Cell wall α-1,3-glucan is required to anchor the *Cryptococcus neoformans* capsule. Mol Microbiol 50:1401–1409

Reggiori F, Canivenc-Gansel E, Conzelmann A (1997) Lipid remodeling leads to the introduction and exchange of defined ceramides on GPI proteins in the ER and Golgi of *Saccharomyces cerevisiae*. EMBO J 16:3506–3518

Roberson RW, Fuller MS (1990) Effects of the demethylase inhibitor, cyproconazole, on hyphal tip cells of *Sclerotium rolfsii*. II An electron microscope study. Exp Mycol 14:124–135

Rodrigues ML, Dobroff AS, Couceiro JN, Alviano CS, Schauer R, Travassos LR (2002) Sialylglycoconjugates and sialyltransferase activity in the fungus *Cryptococcus neoformans*. Glycoconj J 19:165–173

Rodríguez-Peña JM, Cid VJ, Arroyo J, Nombela C (2000) A novel family of cell wall-related proteins regulated differently during the yeast life cycle. Mol Cell. Biol 20:3245–3255

Rodriguez-Peña JM, Rodriguez C, Alvarez A, Nombela C, Arroyo J (2002) Mechanisms for targeting of the *Saccharomyces cerevisiae* GPI-anchored cell wall protein Crh2p to polarised growth sites. J Cell Sci 115:2549–2558

Roemer T, Delaney S, Bussey H (1993) *SKN1* and *KRE6* define a pair of functional homologs encoding putative membrane proteins involved in β-glucan synthesis. Mol Cell Biol 13:4039–4048

Roh DH, Bowers B, Schmidt M, Cabib E (2002) The septation apparatus, an autonomous system in budding yeast. Mol Biol Cell 13:2747–2759

Roncero C (2002) The genetic complexity of chitin synthesis in fungi. Curr Genet 41:367–378

Rooney PJ, Sullivan TD, Klein BS (2001) Selective expression of the virulence factor BAD1 upon morphogenesis to the pathogenic yeast form of *Blastomyces dermatitidis*: evidence for transcriptional regulation by a conserved mechanism. Mol Microbiol 39:875–889

Ruiz-Herrera J (1992) Fungal cell wall. Structure, synthesis, and assembly. CRC, Boca Raton

Ruiz-Herrera J, Leon CG, Carabez-Trejo A, Reyes-Salinas E (1996) Structure and chemical composition of the cell walls from the haploid yeast and mycelial forms of *Ustilago maydis*. Fungal Genet Biol 20:133–142

San-Blas G, San-Blas F (1977) *Paracoccidioides brasiliensis*: cell wall structure and virulence, a review. Mycopathologia 62:77–86

Schoffelmeer EAM, Kapteyn JC, Montijn RC, Cornelissen BC, Klis FM (1996) Glucosylation of fungal cell wall proteins as a potential target for novel antifungal agents. In: Lyr H, Russel PE, Sisler HD (eds) Modern fungicides and antifungal compounds. Intercept, Andover, pp 157–162

Schoffelmeer EAM, Klis FM, Sietsma JH, Cornelissen BJ (1999) The cell wall of *Fusarium oxysporum*. Fungal Genet Biol 27:275–282

Schoffelmeer EAM, Vossen JH, Van Doorn AA, Cornelissen BJ, Haring MA (2001) FEM1, a *Fusarium oxysporum* glycoprotein that is covalently linked to the cell wall matrix and is conserved in filamentous fungi. Mol Genet Genomics 265:143–152

Shatkin AJ, Tatum EL (1959) Electron microscopy of *Neurospora crassa* mycelia. J Biophys Biochem Cytol 6:423–426

Shaw JA, Mol PC, Bowers B, Silverman SJ, Valdivieso MH, Duran A, Cabib E (1991) The function of chitin synthases 2 and 3 in the *Saccharomyces cerevisiae* cell cycle. J Cell Biol 114:111–123

Sietsma JH, Wessels JGH (1994) Apical wall biogenesis. In: Wessels JGH, Meinhardt F (eds) The Mycota, vol 1. Growth, differentiation and sexuality. Springer, Berlin Heidelberg New York, pp 125–141

Small JM, Mitchell TG (1986) Binding of purified and radioiodinated capsular polysaccharides from *Cryptococcus neoformans* serotype A strains to capsule-free mutants. Infect Immun 54:742–750

Smits GJ, Schenkman LR, Brul S, Pringle JR, Klis FM (2006) Role of cell-cycle-regulated expression in the localized incorporation of cell-wall proteins in yeast. Mol Biol Cell 17:3267–3280

Spreghini E, Davis DA, Subaran R, Kim M, Mitchell AP (2003) Roles of *Candida albicans* Dfg5p and Dcw1p cell surface proteins in growth and hypha formation. Eukaryot Cell 2:746–755

Strahl-Bolsinger S, Gentzsch M, Tanner W (1999) Protein *O*-mannosylation. Biochim Biophys Acta 1426:297–307

Sugawara T, Takahashi S, Osumi M, Ohno N (2004) Refinement of the structures of cell-wall glucans of *Schizosaccharomyces pombe* by chemical modification and NMR spectroscopy. Carbohydr Res 339:2255–2265

Sumita T, Yoko-o T, Shimma Y, Jigami Y (2005) Comparison of cell wall localization among Pir family proteins and functional dissection of the region required for cell wall binding and bud scar recruitment of Pir1p. Eukaryot Cell 4:1872–1881

Suzuki S (1997) Immunochemical study on mannans of genus Candida. I. Structural investigation of antigenic factors 1, 4, 5, 6, 8, 9, 11, 13, 13b and 34. Curr Top Med Mycol 8:57–70

Takeshita N, Yamashita S, Ohta A, Horiuchi H (2006) *Aspergillus nidulans* class V and VI chitin synthases CsmA and CsmB, each with a myosin motor-like domain, perform compensatory functions that are essential for hyphal tip growth. Mol Microbiol 59:1380–1394

Thompson JR, Douglas CM, Li W, Jue CK, Pramanik B, Yuan X, Rude TH, Toffaletti DL, Perfect JR, Kurtz M (1999) A glucan synthase *FKS1* homolog in *Cryptococcus neoformans* is single copy and encodes an essential function. J Bacteriol 181:444–453

Tokunaga M, Kusamichi M, Koike H (1986) Ultrastructure of outermost layer of cell wall in *Candida albicans* observed by rapid-freezing technique. J Electron Microsc (Tokyo) 35:237–246

Tomazett PK, Cruz AH, Bonfim SM, Soares CM, Pereira M (2005) The cell wall of *Paracoccidioides brasiliensis*: insights from its transcriptome. Genet Mol Res 4:309–325

Tomishige N, Noda Y, Adachi H, Shimoi H, Takatsuki A, Yoda K (2003) Mutations that are synthetically lethal with a *gas1*Δ allele cause defects in the cell wall of *Saccharomyces cerevisiae*. Mol Genet Genomics 269:562–573

Travassos LR (1985) *Sporothrix schenckii*. In: Szaniszlo PJ (ed) Fungal dimorphism. With emphasis on fungi pathogenic for humans. Plenum, New York, pp 121–163

Trinel PA, Lepage G, Jouault T, Strecker G, Poulain D (1997) Definitive chemical evidence for the constitutive ability of *Candida albicans* serotype A strains to synthesize β-1,2 linked oligomannosides containing up to 14 mannose residues. FEBS Lett 416:203–206

Uccelletti D, Pacelli V, Mancini P, Palleschi C (2000) *vga* Mutants of *Kluyveromyces lactis* show cell integrity defects. Yeast 16:1161–1171

Utsugi T, Minemura M, Hirata A, Abe M, Watanabe D, Ohya Y (2002) Movement of yeast 1,3-β-glucan synthase is essential for uniform cell wall synthesis. Genes Cells 7:1–9

Valdivia RH, Schekman R (2003) The yeasts Rho1p and Pkc1p regulate the transport of chitin synthase III (Chs3p) from internal stores to the plasma membrane. Proc Natl Acad Sci USA 100:10287–10292

Van der Vaart JM, Caro LHP, Chapman JW, Klis FM, Verrips CT (1995) Identification of three mannoproteins in the cell wall of *Saccharomyces cerevisiae*. J Bacteriol 177:3104–3110

Vink E, Rodriguez-Suarez RJ, Gerard-Vincent M, Ribas JC, Nobel H de, Ende H van den, Duran A, Klis FM, Bussey H (2004) An in vitro assay for (1>6)-β-D-glucan synthesis in *Saccharomyces cerevisiae*. Yeast 21:1121–1131

Weber I, Assmann D, Thines E, Steinberg G (2006) Polar localizing class V myosin chitin synthases are essential during early plant infection in the plant pathogenic fungus *Ustilago maydis*. Plant Cell 18:225–242

Weig M, Jansch L, Gross U, De Koster CG, Klis FM, De Groot PWJ (2004) Systematic identification in silico of covalently bound cell wall proteins and analysis of protein-polysaccharide linkages of the human pathogen *Candida glabrata*. Microbiology 150:3129–3144

Wessels JGH, Sietsma JH (1981) Fungal cell walls: a survey. In: Tanner W, Loewus FA (eds) Plant carbohydrates II. Extracellular carbohydrates. (Encyclopedia of plant physiology, vol 13B) Springer, Berlin Heidelberg New York, pp 352–394

Wheeler RT, Fink GR (2006) A drug-sensitive genetic network masks fungi from the immune system. PLoS Pathog 2:e35

Willer T, Valero MC, Tanner W, Cruces J, Strahl S (2003) *O*-mannosyl glycans: from yeast to novel associations with human disease. Curr Opin Struct Biol 13:621–630

Woo PC, Chong KT, Leung AS, Wong SS, Lau SK, Yuen KY (2003) *AFLMP1* encodes an antigenic cel wall protein in *Aspergillus flavus*. J Clin Microbiol 41:845–850

Wösten HA (2001) Hydrophobins: multipurpose proteins. Annu Rev Microbiol 55:625–646

Xu JR, Peng YL, Dickman MB, Sharon A (2006) The dawn of fungal pathogen genomics. Annu Rev Phytopathol 44:337–366

Yamada E, Ichinomiya M, Ohta A, Horiuchi H (2005) The class V chitin synthase gene *csmA* is crucial for the growth of the *chsA chsC* double mutant in *Aspergillus nidulans*. Biosci Biotechnol Biochem 69:87–97

Yamaguchi M, Biswas SK, Kita S, Aikawa E, Takeo K (2002) Electron microscopy of pathogenic yeasts *Cryptococcus neoformans* and *Exophiala dermatitidis* by high-pressure freezing. J Electron Microsc (Tokyo) 51:21–27

Yin QY, Groot PWJ de, Dekker HL, Jong L de, Klis FM, Koster CG de (2005) Comprehensive proteomic analysis of *Saccharomyces cerevisiae* cell walls: identification of proteins covalently attached via glycosylphosphatidylinositol remnants or mild alkali-sensitive linkages. J Biol Chem 280:20894–20901

Yu L, Goldman R, Sullivan P, Walker G, Fesik SW (1993) Heteronuclear NMR studies of C-13-labeled yeast cell wall β-glucan oligosaccharides. J Biomol NMR 3:429–441

Zlotnik H, Fernandez MP, Bowers B, Cabib E (1984) *Saccharomyces cerevisiae* mannoproteins form an external cell wall layer that determines wall porosity. J Bacteriol 159:1018–1026

5 The Cytoskeleton and Polarized Growth of Filamentous Fungi

R. Fischer[1]

CONTENTS

I. **Introduction** 121
II. **The Hyphal Growth Form and the Spitzenkörper** 121
III. **The Microtubule Cytoskeleton** 123
A. Organization of the Microtubule Cytoskeleton 123
B. Origin of Microtubules 124
C. The Microtubule Plus End 125
D. The MT Lattice 127
E. MT-Dependent Motor Proteins 127
F. Cell End Makers at the Cortex 129
IV. **The Actin Cytoskeleton** 130
A. Organization of the Actin Cytoskeleton . 130
B. The Polarisome 130
C. Actin-Dependent Motor Proteins 131
D. The *swo* Mutants and the Establishment of Polarity 131
V. **Conclusions** 132
References 132

I. Introduction

Polarized growth is the mechanism by which filamentous fungi extend their hyphae. Microtubules (MT) and filamentous actin (F-actin), in combination with their corresponding motor proteins, kinesin, dynein and myosin, play important roles in this process. Actin has an essential role for tip elongation and septation. It is required for vesicle secretion and cell wall extension, and possibly – together with the MT cytoskeleton – for the localization of so-called cell end marker or landmark proteins, which control growth directionality. The exact contribution of the MT cytoskeleton on polarized growth is less clear. Genetic, biochemical and cell biological approaches in *Aspergillus nidulans* and other fungi led to a modified view of many MT-related aspects within the past few years. There is increasing evidence that MT cables, which are visualized by immunostaining or GFP-tubulin fusion proteins, consist of several MTs and their dynamics appears to be different in fast-growing hyphal tips as compared with young germlings. Whereas the spindle pole bodies were considered as the only, or the main, microtubule organizing centres (MTOCs) in filamentous fungi, it appears that additional MTOCs outside the nuclei are responsible for the generation of the complex MT array. In addition to new insights into the MT network and its dynamics, the roles of several kinesins have been elucidated recently and their interplay with dynein investigated. It became clear that MT functions are interwoven with those of the actin cytoskeleton and that three main structures are required for polarized growth: the Spitzenkörper (vesicle supply centre), the polarisome and probably cell end markers at the cortex. We describe a model for polarized growth, where the MT cytoskeleton continuously provides the building material within vesicles to the Spitzenkörper and determines growth directionality by the delivery of cell end marker proteins and the actin cytoskeleton is crucial for the last step of vesicle secretion.

II. The Hyphal Growth Form and the Spitzenkörper

One fascinating aspect of filamentous fungi is their continuous tip elongation. Whereas this phase of polarized growth only lasts a short time in the life cycle of the budding yeast *Saccharomyces cerevisiae*, it is the main growth form of filamentous fungi. Fungi are surrounded by a rigid cell wall and, in order to expand the hyphae, it is assumed that the walls need to be plasticized and new membrane has to be inserted. These two processes are linked because enzymes, which are required outside the cell, are transported towards the tip within vesicles. The process has been reviewed recently (Sietsma and

[1] Max-Planck-Institute for terrestrial Microbiology, Karl-von-Frisch-Str., D-35043 Marburg, Germany and University of Karlsruhe, Institute for Applied Biosciences, Dept. of Applied Microbiology, Hertzstrasse 16, D-76187 Karlsruhe, Germany

Biology of the Fungal Cell, 2nd Edition
The Mycota VIII
R.J. Howard and N.A.R. Gow (Eds.)
© Springer-Verlag Berlin Heidelberg 2007

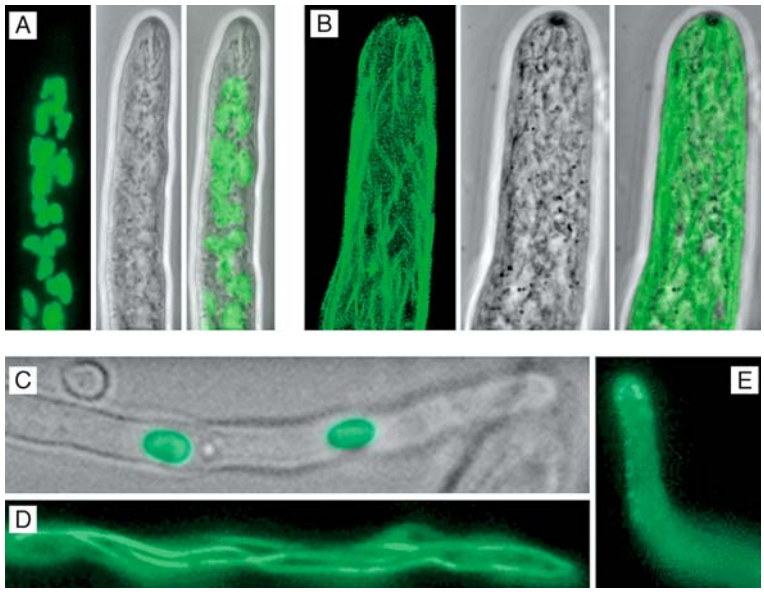

Fig. 5.1. Microtubule, actin and nuclear organization. **a** Hyphal tip of *N. crassa* with GFP-labelled nuclei: *left* GFP, *middle* phase contrast, *right* overlay. **b** GFP-labelled MTs in the tip of *N. crassa*. **c** GFP-tagged nuclei in a hyphal tip of *Asp. nidulans*. **d** GFP-labelled MTs in *Asp. nidulans*. **e** actin in *Asp. nidulans*. Images of *N. crassa* were kindly provided by Rosa R. Mouriño Pérez (Departamento de Microbiologia, Centro de Investigacion Cientifica y Educacion, Ensenada, Mexico). An actin-binding protein GFP construct was kindly provided by Miguel Peñalva (Cesic, Madrid, Spain)

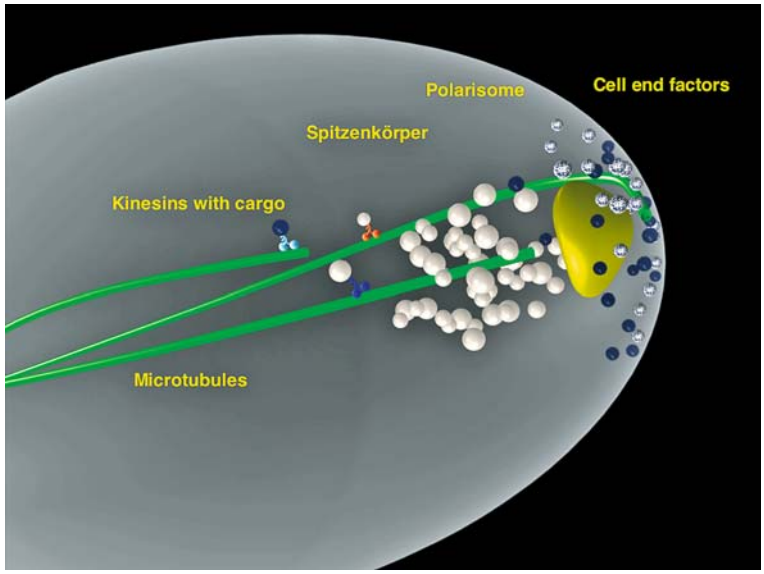

Fig. 5.2. Model of a growing hyphal tip with MTs, cargo-delivering kinesin motor proteins, the Spitzenkörper, the polarisome and cell end markers. Modified after Harris et al. (2005). See text for further explanation

Wessels 2006; Virag and Harris 2006a). The vesicles fuse with the cytoplasmic membrane and thus lead to expansion of the membrane and delivery of their contents (Bartnicki-Garcia et al. 1995). The place where vesicles are generated may be far behind the growing tip (see Chap. 1 in this volume). The involvement of vesicles for polarized growth was proposed many decades ago, when Brunswick observed an accumulation of vesicles in the apical dome of fungal hyphae, using phase contrast microscopy (Brunswick 1924; Girbardt 1957; Fig. 5.1). This structure was named with the German word "Spitzenkörper" (= apical body) or the vesicle supply centre (VSC; Girbardt 1957; Bartnicki-Garcia et al. 1995). The latter name refers to its proposed function as a transit station for vesicles from the hyphal body to the plasma membrane. The position of the organelle determines growth direction (Riquelme et al. 1998). S. Bartnicki-Garcia (Riverside, Calif., USA) and C. Bracker (West Lafayette, Ind., USA) demonstrated fantastically the importance of this organelle for polarized growth.

Tip extension needs to be a well controlled process, because secretion of cell-wall lytic enzymes, required for loosening the cell wall prior to extension, as well as enzymes for cell wall synthe-

sis, may be deleterious for the cell. In addition, new places of polarized growth need to be established for every new branch formed (Riquelme and Bartnicki-Garcia 2004). This shows that tip elongation is likely to require the full equipment of the cellular toolbox. Several organisms are studied extensively to understand the phenomenon at the molecular level. Most importantly are *Sac. cerevisiae* and the closely related but filamentously growing *Ashbya gossypii*, the fission yeast *Schizosaccharomyces pombe*, the basidiomycete and plant pathogen dimorphic *Ustilago maydis*, the human pathogenic *Candida albicans* and several obligate filamentous fungi, such as *Neurospora crassa* and *Asp. nidulans* (Steinberg et al. 2001; Pruyne et al. 2004; Crampin et al. 2005; Harris et al. 2005; Martin and Chang 2005; Philippsen et al. 2005). Research on polarized growth currently has a very high impact, because it is considered as one major target for the development of antifungal drugs.

III. The Microtubule Cytoskeleton

A. Organization of the Microtubule Cytoskeleton

MTs are hollow tubes composed of 13 protofilaments, each of which is made up with the heterodimer αβ-tubulin as the building block. MTs have an inherent instability and continuously elongate at their plus end, where αβ-tubulin dimers are added. One parameter, which determines the elongation rate, is the concentration of dimers in the cell. Both tubulin subunits contain a bound GTP. The nucleotide-binding pocket is located at the interface between the α- and β-tubulin subunits and thus this GTP is rather stable. In contrast, GTP in the β-tubulin subunit is exposed and undergoes easily hydrolysis. Once β-tubulin contains GDP, the assembly is blocked and a catastrophic event occurs.

MTs are visible in fixed cells by immunolocalization light microscopy (Fischer and Timberlake 1995; Czymmek et al. 1996; Bourett et al. 1998) or by electron microscopy (Jung et al. 1998) but these methods do not allow the study of MT behaviour in living cells. This became possible after the advent of the green fluorescent protein (GFP). In *Sac. cerevisiae* interphase cells, short MTs are attached to nuclei and their growth towards the cortex and subsequent shrinkage causes short-distance movement of the nuclei. The situation changes once the yeast cell enters the division cycle. The nuclear spindle pole body divides, the two organelles move to opposite positions of the nucleus and polymerize the spindle MTs. In addition, the spindle pole bodies produce cytoplasmic MTs, which in turn mediate MT–cortex interactions (Hoepfner et al. 2000). In *Sch. pombe* interphase cells contain several cytoplasmic MTs, which span the entire cell. Because they serve as tracks to deliver so-called cell end markers, they determine growth directionality in this yeast (Tran et al. 2001).

In filamentous fungi, GFP-tagged MTs were studied first in *Asp. nidulans* in X. Xiang's laboratory (Bethesda, Md., USA). MTs are quite inflexible structures and their orientation mainly depends on the shape of the fungal cell. Hence, they are mostly aligned parallel to the growth axis and they range in number over 3–6 (Fig. 5.1). *Asp. nidulans* MTs extend with a speed of about 14 µm/min, reach the cortex, pause for some time and undergo a catastrophic event. Subsequently, MTs shrink with a speed of about 30 µm/min and MTs either depolymerize all the way to the MTOC or rescue occurs before this, and MTs elongate again (Han et al. 2001). Slightly different values were recently obtained in the group of B. Heath (Sampson and Heath 2005). They also observed that short MT fragments were able to slide towards the hyphal tip. In *N. crassa* the MT network was first visualized by N. Read's group in Edinburgh (UK) and was analysed recently in more detail (Freitag et al. 2004; Mouriño-Pérez et al. 2006). From observations of the MT cytoskeleton in these two filamentous fungi it is obvious that the organization appears to be quite different. In *N. crassa* the MT cytoskeleton is far more complex than in *Asp. nidulans* and the number of nuclei in one compartment is also very different between the two fungi. Another big difference is the regulation of mitosis. Whereas nuclear division is synchronized in *Asp. nidulans* it is not in *N. crassa* (Suelmann et al. 1997; Freitag et al. 2004).

Investigations of MT arrangements within a cell were done by immunofluorescence and recently by using fluorescently labelled tubulin (Fischer and Timberlake 1995; Ding et al. 1998; Han et al. 2001; Freitag et al. 2004; Czymmek et al. 2005). It appears that the structures, which can be seen after immunostaining or as GFP-labelled filaments, consist of several individual MTs. There is increasing evidence for this organization, especially coming from studies with *Sch. pombe*. Here it was shown recently that the orientation of MTs can be opposite in one bundle and that a kinesin-like

motor protein in combination with dynein is required for sliding of individual MTs within a bundle and maintenance of MT polarity (Carazo-Salas et al. 2005). For *Asp. nidulans* Konzack et al. (2005) reported that the fluorescence intensity of a MT varies dynamically and that the regions with low intensity do recover brightness after some time. Similarly, after bleaching of a given MT at one place, brightness returns quickly (Veith et al. 2005). In addition, thin MT filaments occasionally detach from a MT for some time before they merge again to form a thick MT (R. Fischer, unpublished data). These observations are in agreement with a model that MT filaments consist of a bundle, and that individual MTs within a bundle undergo individual behaviour and dynamics.

B. Origin of Microtubules

MTs cannot efficiently assemble *de novo* in a eukaryotic cell, but require an initiation point, the MTOC. This point is characterized by a protein complex, whose characteristic component is γ-tubulin (Pereira and Schiebel 1997; Job et al. 2003; Aldaz et al. 2005; Doxsey et al. 2005). Originally discovered in *Asp. nidulans*, γ-tubulin was found in all eukaryotes studied and the concept of γ-tubulin-mediated nucleation of MT polymerization is an accepted model (Oakley and Oakley 1989; Oakley et al. 1990; Oakley 1995, 2004). However, the exact mechanism is still under debate. It appears that γ-tubulin in higher eukaryotes forms a 2.2-MDa ring complex consisting of 12 or 13 (different numbers exist in the literature) γ-tubulin subunits associated with other proteins, the so-called γ-tubulin ring complex (γ-TuRC; Aldaz et al. 2005). The γ-TuRC acts as an initiator complex, where 13 tubulin protofilaments emanate. It has been known for a long time that fungal spindle pole bodies (SPBs) are very active MTOCs (Jaspersen and Winey 2004). The SPB is embedded into the nuclear envelope, divides prior to mitosis and, by definition, localizes at the poles of the mitotic spindle. SPBs consist in *Sac. cerevisiae* of an inner and an outer plaque and they are able to polymerize MTs on both sides of the nuclear envelope. During mitosis the outer MTs are called astral MTs, but also in interphase SPBs act as active MTOCs in *Sac. cerevisiae* as well as in filamentous fungi (Heath 1981). Whether the protein composition of the SPB in *Sac. cerevisiae* and in filamentous fungi is largely conserved or more diverse remains to be determined.

It seems that the SPBs are the only places from which the yeast *Sac. cerevisiae* polymerizes MTs (see movies accompanying Hoepfner et al. 2000). However it must be noted that cytoplasmic MTs appear not to play many important roles in *Sac. cerevisiae*, besides the positioning of the nucleus prior to mitosis (Maekawa and Schiebel 2004). The cytoplasmic MT array is not very pronounced and is usually limited to a few MTs growing out of the SPB into the cytoplasm. In contrast, filamentous fungi employ MTs for their fast, polarized growth during interphase (Riquelme et al. 2003; Horio and Oakley 2005; Fig. 5.1). Nevertheless, it was assumed for a long time that SPBs are the only place for MT initiation (Oakley 2004; Czymmek et al. 2005; Sampson and Heath 2005). This assumption was based on the finding that the intracellular αβ-tubulin pool is used for the assembly of spindle MTs as well as for cytoplasmic MTs. Indeed, cytoplasmic MTs are generally disassembled prior to mitosis and regenerate thereafter (Ovechkina et al. 2003; Sampson and Heath 2005). In order to determine the origin of new MTs, re-growth of MTs was observed in *Sch. pombe* after depolymerization of MTs by drugs (Mata and Nurse 1997). These studies revealed that, in fission yeast, MTs are generated from the SPB and other MTOCs around the nucleus and in the cytoplasm. During cell division an equatorial MTOC (EMTOC) becomes very important (Hagan 1998; Sawin et al. 2004; Venkatram et al. 2005). The origin of MTs from the cell centre leads to an orientation with their plus ends towards the growing ends. Recently, another tool was used to determine the origin of MTs. Using MT plus end-localizing proteins, such as homologues of the mammalian EB1, MT initiation was analysed in the plant pathogenic basidiomycete *Ustilago maydis*. It was found that MT nucleation occurs at three places: at dispersed cytoplasmic sites, at a polar MTOC and at the SPB (Straube et al. 2003).

In filamentous fungi, our knowledge of MT organization is restricted to a few species, such as the chytridiomycete *Allomyces macrogynus*, the basidiomycete *U. maydis*, and the ascomycete *Asp. nidulans* which is one of the best studied examples. Whereas Sampson and Heath (2005) reported that MTs emanate only from SPBs, Konzack et al. (2005) demonstrated that MTOCs exist apart from the SPBs. This discrepancy may be due to the different methods used. In the first study, the authors observed GFP-labelled MTs and the location of nu-

clei was determined by the absence of cytoplasmic fluorescence. The authors of the second study used simultaneous labelling of nuclei with a red fluorescent protein and GFP-labelled tubulin. In addition, a plus end-tracking protein, KipA, was used to determine the origin of MTs. MTOCs were found at the SPBs but also in the cytoplasm and at septa of *Asp. nidulans* (Fig. 5.3). This organization recently received further evidence through the characterization of a novel MTOC-associated protein, ApsB (Veith et al. 2005). Here, the authors demonstrated that MTOCs at septa are important for the production of the interphase cytoplasmic MT array (Fig. 5.3). These findings are in good agreement with the results obtained in *Sch. pombe* and *U. maydis*.

It is still an open question whether there are MTOCs at hyphal tips of filamentous fungi. Whereas γ-tubulin can be visualized at the tips of *All. macrogynus* hyphae and thus MTs polymerize from the tip to the back (McDaniel and Roberson 1998), γ-tubulin has not yet been detected at that place in e.g. *Asp. nidulans*. Nevertheless, using the kinesin motor KipA, Konzack et al. (2005) found that sometimes MTs do also polymerize from the tip. It has to be considered that a MT occasionally does not depolymerize upon contact with the cortex but bends along the cortex towards the rear of the hypha. If this MT would continue growth, it could explain the observed comets from the tip to the back of the hypha. In *N. crassa* the situation appears to be far more complicated because of the higher number of MTs and nuclei (Freitag et al. 2004; Mouriño-Pérez et al. 2006). Detailed studies of MT origin have not yet been performed.

C. The Microtubule Plus End

MTs grow and shrink in a treadmilling manner if they are polymerized in vitro. In comparison, in vivo MTs are rather stable at the minus end and dynamics occur mainly at the MT plus end. It is well accepted that this MT end consists of a large protein complex, which is involved in the regulation of MT dynamics as well as in the regulation of interactions with cortical actin, membrane proteins or proteins associated with the kinetochore of chromosomes (Schuyler and Pellman 2001b; Hestermann et al. 2002; Akhmanova and Hoogenraad 2005). Given the diversity of interacting partners, it is obvious that the protein complex composition may vary

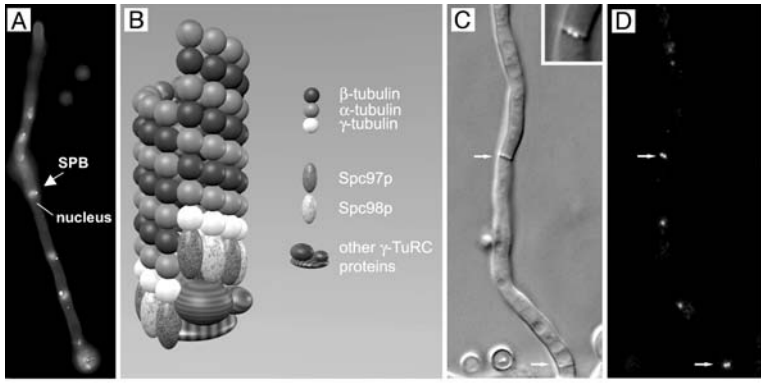

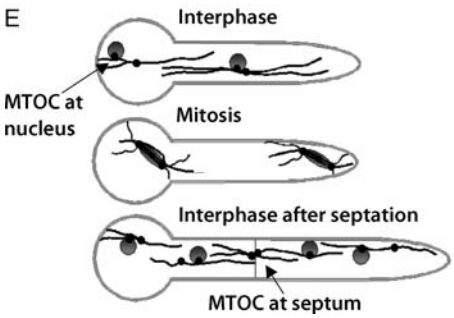

Fig. 5.3. MTOCs in *Asp. nidulans*. **a** Hypha with DAPI-stained nuclei and GFP-labelled spindle-pole body (SPB)-associated ApsB. Nuclei are evenly spaced and at each nucleus a SPB is visible. **b** Scheme of a MTOC with γ-tubulin and other proteins described in *Sac. cerevisiae*. Adapted from Pereira and Schiebel (1997) and Oakley (2000). **c**, **d** MTOCs visualized by GFP-ApsB fusion, at septa: *left* phase contrast, *right* same hypha under fluorescent conditions. *Inset* in **c** Enlargement of the septum and overlay of phase contrast and fluorescent images. **e** MTOCs are found at the nuclei, in the cytoplasm and at septa. Taken from Konzack et al. (2005), with permission

depending on the function of the MT and is likely to be a highly controlled and organized structure. There are three different ways of how proteins can reach the MT plus end and remain associated with it as the MT is growing (Howard and Hyman 2003; Al-Bassam et al. 2006).

In fungi the best studied organisms with respect to the MT plus end are *Sac. cerevisiae* and *Sch. pombe*. In *Sac. cerevisiae* MT–cortex interactions play important roles for the positioning of the mitotic spindle and nuclear migration (Schuyler and Pellman 2001a). One of the most prominent examples of a MT plus end-associated protein is dynein (Fig. 5.4). It localizes to the MT tip and hitchhikes with the growing filament to the cell periphery. Once at the cortex, dynein is activated and pulls the attached MT towards the cortex. This leads to translocation of the nucleus (Schuyler and Pellman 2001a; Maekawa et al. 2003; Sheeman et al. 2003; Maekawa and Schiebel 2004). The kinesin motor protein Kip2 appears to be responsible for the plus end localization of several proteins, e.g. the CLIP170-like protein Bik1 (Carvalho et al. 2004). Similar to the situation in *Sac. cerevisiae*, the CLIP170-like protein of *Sch. pombe*, Tip1, localized to MT plus ends. The responsible motor for this localization was Tea2 (Busch et al. 2004). However MTs do not play such important roles for polarized growth in yeasts, in comparison with filamentous fungi. Only some components have been found which localize at MT plus ends, among them are subunits of the dynein motor complex (Zhang et al. 2002). Interestingly conventional kinesin, KinA, is required for their MT tip localization (Zhang et al. 2003; Fig. 5.4). The CLIP170-like protein, ClipA, in *Asp. nidulans* does also accumulate at MT plus ends and its localization is also dependent on the Tea2/Kip2 homologue KipA (Efimov et al. 2006).

The question is which role do the plus end-localized proteins play for polarized growth. As mentioned above, MT–cortical interactions are necessary for dynein-dependent nuclear positioning prior to mitosis in *Sac. cerevisiae* (Carminati and Stearns 1997). In *Asp. nidulans* dynein is also required for nuclear positioning and migration; and recently Veith et al. showed that the interaction of MT plus ends with the cortex contributes to the dynamics of mitotic spindles (Xiang et al. 1994; Xiang and Fischer 2004; Veith et al. 2005). Whether interphase nuclei are pulled through similar MT–cortex interactions is not clear yet.

Whereas the role of the MT plus end protein complex is quite obvious for force generation to translocate organelles, a role for polarized growth is less obvious. Some new ideas came from observations in growing tips of *Asp. nidulans* and visualization of MTs. Konzack et al. (2005) described that MTs merge into one point in the apex. Given that vesicles constantly travel towards the vesicle supply centre, the position of MT ends determines the vesicle supply centre location. In the *kipA* (*tea2/kip2*) mutant, MTs did not merge into one point and hyphae grew in meandering curves rather than straight. This was explained by the lack of pro-

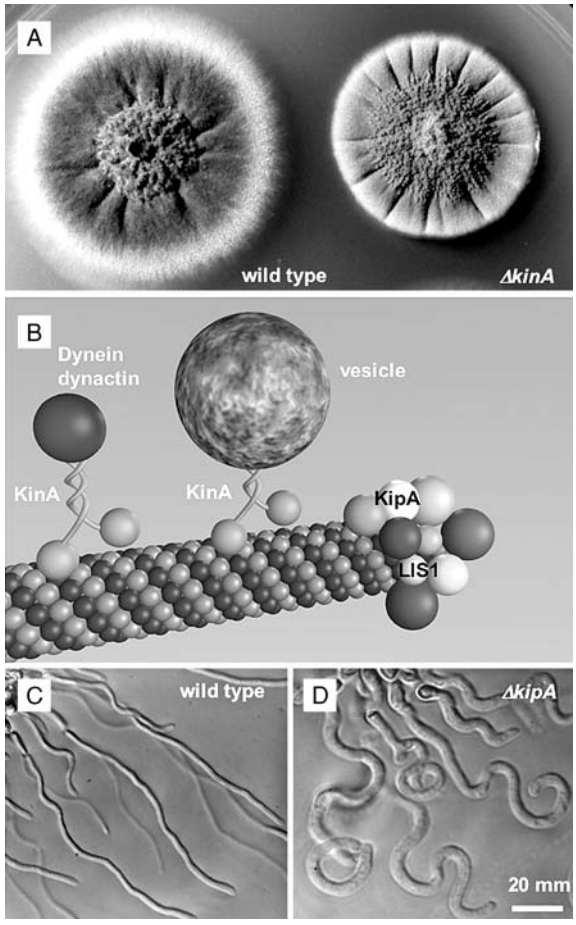

Fig. 5.4. The role of conventional KinA and Kip2 family kinesin KipA. **a** Comparison of a wild type with a conventional kinesin deletion mutant (taken from Requena et al. 2001). **b** Scheme of a MT with the MT plus end complex. This protein complex consists of several proteins, e.g. KipA or LIS1, conventional kinesin transports vesicles and components of the plus end complex, for instance dynein (Zhang et al. 2003). A direct interaction between KinA and dynein or dynactin has not yet been verified. Modified after Hestermann et al. (2002) **c**, **d** When KipA, which is suggested to be involved in the delivery of cell end markers, is missing, hyphae lose directionality. Images taken from Konzack et al. (2005), with permission

teins (normally transported by KipA) at the plus end which mediate cortical contact. There is good evidence for such a situation in *Sch. pombe*. It was shown that the cortex protein Tea1 is transported by Tea2 (Browning et al. 2003; Martin and Chang 2003; Sawin and Snaith 2004). If either of the two genes is deleted, *Sch. pombe* cells appear curved or T-shaped (Snell and Nurse 1994; Browning et al. 2000). Hence Tea1 and other proteins were named cell polarity determinants or cell end marker proteins. However, to prove such a model in *Asp. nidulans*, cargoes of KipA have to be identified and characterized. Another crucial piece in the puzzle is the identification of cortex proteins. Whereas cortical contacts of MTs involved in nuclear migration require the cortical protein ApsA in *Asp. nidulans* (Num1 in *Sac. cerevisiae*; Veith et al. 2005), this interaction appears not to be necessary for polarized growth (Fischer and Timberlake 1995). In *Sch. pombe* a new protein, Mod5, was described as a membrane anchor for the polarized growth machinery (Snaith and Sawin 2003). In filamentous fungi, a protein with significant sequence similarity has not yet been identified. However, a protein serving a similar function as Mod5 is currently under study in our laboratory (Takeshita and Fischer, unpublished)

D. The MT Lattice

MT function and dynamics are not only determined by the plus and minus ends, but also by the filament lattice, which in higher eukaryotes can be decorated with a number of different microtubule-associated proteins (MAPs), which in turn may control the activity of associated motor proteins (Baas et al. 1994; Cassimeris and Spittle 2001; Baas and Qiang 2005; Fig. 5.4). Despite the abundance of those proteins in higher eukaryotes, it is not clear yet whether proteins like Tau exist in filamentous fungi. Proteins such as katanin and spastin could be conserved proteins, because sequences with high similarity can be found in the *Asp. nidulans* and *Asp. fumigatus* genomes (Konzack, unpublished data). Experimental data for the role of this class of MT-associated proteins are not yet available for filamentous fungi.

E. MT-Dependent Motor Proteins

MTs and their dynamics are in principle sufficient to create force and transport cargoes (attached to the growing end) in a cell. However, two classes of motor proteins have evolved which guarantee fast MT-dependent movement in the cell, the minus end-directed dynein and the plus end-directed kinesins (Fig. 5.4). Some kinesins also move in the opposite direction. Both motor classes are characterized by a motor domain in which ATP is hydrolysed (Hirokawa 1998). Within the protein the location of the motor domain can be N- or C-terminal as well as in the middle region. How chemical energy is converted into conformational changes and how force is generated is best understood for conventional kinesin. Interested readers should refer to several recent reviews (Woehlke and Schliwa 2000; Schliwa and Woehlke 2003; Yildiz and Selvin 2005; Adio et al. 2006).

Whereas all fungi employ a single dynein for their transport processes, their genomes usually contain several kinesin-encoding genes. For instance, *Asp. nidulans* harbours 11 and *N. crassa* ten different kinesins (Rischitor et al. 2004; Fuchs and Westermann 2005). BimC kinesin was the first kinesin discovered in *Asp. nidulans* and defines the entire class of BimC-like kinesins (Enos and Morris 1990). The gene was discovered in a screen for temperature-sensitive *Asp. nidulans* mutants with defects in mitosis (bim = block in mitosis). BimC is a C-terminal motor which forms a tetramer with two motor domains opposite to each other. Because every head domain binds to a MT, this arrangement allows cross-linking of adjacent MTs. This feature is very important during mitosis, where mitotic spindle MTs slide along each other to distribute chromosomes (Kapitein et al. 2005). Whereas BimC was discovered in a genetic screen (Morris 1976), four other kinesins were isolated in reverse genetic approaches.

A second motor with functions in mitosis is the C-terminal kinesin-like protein KlpA with similarity to *Sac. cerevisiae* Kar3 kinesin (Prigozhina et al. 2001). The gene was isolated through a PCR approach and subsequently characterized. Deletion of *klpA* kinesin alone did not produce any severe phenotoype but suppressed a *bimC* mutation (O'Connell et al. 1993).

Another kinesin with a function in mitosis is the Kip3 family member KipB kinesin, where the motor domain is localized closer to the N-terminus. Gene deletion did not cause any defect in hyphal extension or organelle movement, but in chromosome segregation (Rischitor et al. 2004). This was surprising, because a similar motor in *Sac. cerevisiae*, Kip3, is involved in nuclear migra-

tion (Miller et al. 1998). However, *Asp. nidulans* KipB results are in good agreement with results for the homologous proteins in *Sch. pombe*, Klp5 and Klp6 (West et al. 2002).

Two motors with N-terminal motor domains and pronounced roles in polarized growth are conventional kinesin, KinA kinesin and the CENP-E family kinesin KipA kinesin. Deletion of *kinA* resulted in slower hyphal growth, which is similar to effects in other fungi (Lehmler et al. 1997; Seiler et al. 1997; Wu et al. 1998; Requena et al. 2001; Fig. 5.4). It is generally accepted that this motor transports vesicles towards the extending tip and provides cell wall components (Seiler et al. 1999). In addition, it appears to be involved in other cellular processes related to polarized growth, namely mitochondrial and nuclear distribution. Whereas nuclear distribution was affected in *N. crassa* and *Asp. nidulans*, mitochondrial distribution was changed in *N. haematococca* (Wu et al. 1998). This may be due to the fact that mitochondrial movement depends on the actin cytoskeleton in *Asp. nidulans* (Suelmann and Fischer 2000) and on the MT cytoskeleton in *N. crassa* (Fuchs et al. 2002; Fuchs and Westermann 2005). Whether mitochondrial distribution is also altered in *N. crassa* conventional kinesin mutants, has not yet been studied. The mechanism of how conventional kinesin may contribute to mitochondrial or nuclear distribution is not yet clear, but it could be that the effects are indirect. It was shown in *Asp. nidulans* that KinA is required for transportation of dynein subunits to the plus end of MTs (Zhang et al. 2003; Fig. 5.4). Dynein is a crucial motor for nuclear migration; and exclusion of dynein from the MT plus ends could cause the observed nuclear clustering (Xiang et al. 1994). In addition, it has to be considered that conventional kinesin may well be involved in delivering other components of the MT plus end complex. Lack of conventional kinesin could thus influence the dynamics of MTs as well as their cortical interaction.

KipA of *Asp. nidulans* is similar to Tea2 in *Sch. pombe* and is characterized by an N-terminal motor domain (Konzack et al. 2005). It accumulates at MT plus ends and appears to reach this place by an intrinsic motor activity. Mutant proteins, in which a crucial residue for ATP hydrolysis was replaced, lost the ability to accumulate at MT tips but decorated them evenly. These findings were in agreement with studies of Tea2 in *Sch. pombe* (Browning et al. 2003). Gene deletion caused a surprising phenotype in *Asp. nidulans*. Delta *kipA* strains grew as well as wild-type strains but the hyphal morphology was changed. In contrast to MTs in the wild type, MTs in the *kipA* deletion strain did not merge into one place at the apex. This was interpreted as a reason why hyphae would meander. If MTs do meet at one point, they would deliver the vesicles, which are transported along them at one place, the Spitzenkörper. Hence, hyphae would grow straight. If MTs do not merge one point, vesicles would be delivered at different places and arbitrarily a majority could be deposited on the left, in the middle or on the right side of the hypha. For instance, if the majority of vesicles were deposited asymmetrically at the left, the hypha would grow to the left. The KipA protein could transport proteins, which are necessary for temporal anchorage of MT at the cortex at a specific point. Those proteins would be crucial for straight growth and, because they labelled the end of the cell, they were named "cell end markers" in *Sch. pombe*. Examples of such a protein in fission yeast are Tea1 and Tip1 (Browning et al. 2003; Busch et al. 2004). However, MT fixation at the cortex through Tea1 has not been shown. Tea1 may indeed be evolutionarily conserved among fungi, because a similar protein has been localized to the growing hyphal tip in *Asp. nidulans* (Konzack, Takeshita and Fischer, unpublished data).

Deletion of any kinesin motor (besides *bimC*) does not cause severe phenotypes. Interestingly even a strain in which KinA, KipA and KipB were deleted was still viable, although hyphal growth and development were quite severely affected (Konzack et al. 2005). This shows that kinesins can substitute for each other to some extent, which was recently shown nicely in the case of the Unc-104 homologues, Nkin-2 kinesin and Nkin-3 kinesin from *N. crassa*. Whereas Nkin-2 associates with mitochondria and connects mitochondria with MTs, Nkin-3 was found in the cytoplasm. Surprisingly, after depletion of Nkin-2, Nkin-3 was upregulated and also bound to mitochondria and MTs (Fuchs and Westermann 2005). Homologues of these two motors do also exist in *Asp. nidulans* and are currently being investigated in our laboratory. It appears that one of them, UncA kinesin, plays role in hyphal tip extension whereas the other one, UncB kinesin, is likely to play a role in the nucleus and during septation (N. Zekert, unpublished data).

As mentioned above, fungi usually contain only a single dynein protein, although in some basidiomycetes the heavy chain is encoded by two genes (Eshel et al. 1993; Xiang et al. 1994; Straube et al.

2001; Yamamoto and Hiraoka 2003; Martin et al. 2004). Dynein has a crucial role in nuclear migration but is also implicated in vesicle transport (Seiler et al. 1999). Because dynein moves towards the MT minus end, it is difficult to imagine that it is directly involved in polarized growth, given that MTs are mainly oriented with their plus ends to the membrane. Indeed, deletion of dynein does not cause an immediate block of hyphal extension and the impact on colony growth could partly be due to the lack of nuclei and other organelles, which are translocated with the help of dynein (Xiang et al. 1994).

Besides the concerted action of the cytoskeleton and associated motor proteins to translocate organelles, cytoplasmic streaming has to be considered as another mechanism to push forward the cytoplasm and organelles. Mouriño-Pérez et al. (2006) showed recently in *N. crassa* that the MT array was able to advance as a unit as the hypha elongates. The basis for this bulk flow has not yet been resolved.

If MTs play a role in vesicle delivery to the growing hyphal tip, the question remains how the places for cell extension are marked. First insights into this process came from studies in *Sch. pombe*.

F. Cell End Makers at the Cortex

One of the first proteins which labelled a growing yeast end was discovered in *Sch. pombe* in a screening for polarity mutants. One of the corresponding genes, which was cloned by complementation, encodes the Tea1 protein (Mata and Nurse 1997). The protein is hitchhiking with growing MT ends and is delivered at the pole, where it associates with the cortex. The second one, Tea2 kinesin, encodes a kinesin-like motor protein (Browning et al. 2000; Fig. 5.5). It was shown recently that the main membrane anchor, which recruits proteins such as Tea1, is Mod5 (Browning et al. 2003; Snaith and Sawin 2003). This protein is posttranslationally modified with a prenyl residue, which confers membrane association. Among the proteins recruited to the Mod5 anchor is also the formin, For3 (Bretscher 2005; Martin et al. 2005; Martin and Chang 2006). This protein initiates the growth of actin filaments away from the growing tip. These cables can be used as tracks for the vesicles necessary for cell extension.

Given that the machinery is largely conserved in filamentous fungi and that a crucial component, similar to Mod5 was identified in *Asp. nidulans*, the question remains what targets Mod5 to the membrane at the pole of the cell rather than along the cell. This points to a key function of the membrane itself. Indeed, it was proposed some time ago that sterol-rich lipid rafts exist which may cause asymmetric distribution of proteins in a membrane (Grossmann et al. 2006; Hancock 2006). There is recent evidence that these membrane domains play a role in polarized growth of filamentous fungi (Martin and Konopka 2004); and the laboratory of S. Harris (Lincoln, USA) has shown that a ceramide synthase is important for hyphal morphogenesis (Li et al. 2006).

Because the installation of the growth machinery at a specific place determines growth directionality, one would expect that external signals influence the architecture of proteins. Indeed recently a kinase, AtmA, with such a potential was described in *Asp. nidulans* (Li et al. 2006). This kinase has a well characterized role in DNA damage response, but Li et al. (2006) found that deletion also affects the establishment of polarized growth. The reason appears to lie in a disorganization of MTs in the apex, similar to the defect in the kinesin mutant Δ*kipA* (Konzack et al. 2005). Whereas MTs merge in one point in the wild type, they are dispersed in the *atmA* and the *kipA* mutants. In both cases the authors argue that MT–cortex interaction might be affected. Two further candidates for regulation of protein activity are Pod6 and Cot1, which were described in *N. crassa*, although they are distributed evenly along the hypha and do not show an accumulation at the growing tip (Seiler et al. 2006).

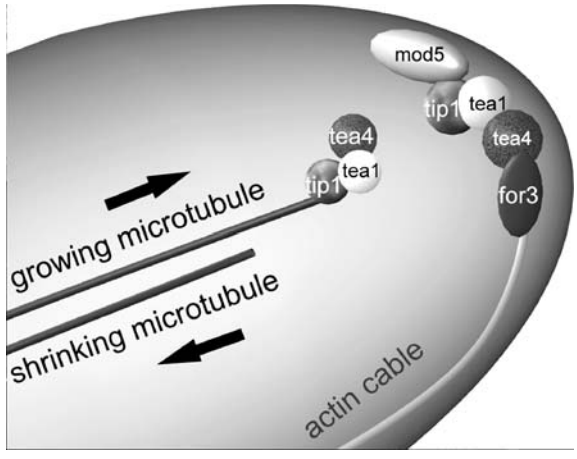

Fig. 5.5. Model of polarized growth in *Sch. pombe*. Reprinted from Martin and Chang (2003), with permission from Elsevier

IV. The Actin Cytoskeleton

A. Organization of the Actin Cytoskeleton

Immunostaining of actin or visualization with phallloidin derivatives revealed a spot-like distribution of the protein along the cortex in many fungi with a high concentration at the tip. In comparison, in *Ash. gossypii* actin cables are frequently seen (Schmitz et al. 2006). Meanwhile, actin was fused to GFP, which allows in vivo studies of the dynamics of actin (B. Oakley, personal communication; Fig. 5.1). Furthermore, Peñalva et al. fused an actin-binding protein with GFP, which is also a nice tool to study actin localization and behaviour in living *Asp. nidulans* cells (M. Peñalva, personal communication). The important role actin plays in polarized growth becomes obvious when depolymerizing agents, such as latrunculin B or cytochalasin, are added to growing hyphae. Sampson et al. showed that addition of latrunculin B causes a fast block in hyphal extension (Sampson and Heath 2005; Fig. 5.6). Likewise, deletion of the myosin gene, *myoA*, is lethal (McGoldrick et al. 1995). There are two likely contributions of the actin cytoskeleton to polarized growth. On the one hand, the actin–myosin cytoskeleton is used for vesicle transportation and secretion and thus the delivery of cell wall components. On the other hand, cortical proteins are brought into place by this system in *Sac. cerevisiae* and guarantee the proper attachment of MTs to the cortex (Schuyler and Pellman 2001b). Because MT attachment sites required for polarized growth seem to be very defined in the apical dome (see below), it is conceivable that the actin cytoskeleton plays a role at this point as well. However, further experiments are required to unravel the exact mechanisms.

As another aspect of polarized growth, we should consider the existence of a Ca^{2+} gradient along the hypha with a high concentration at the tip of *Phyllosticta ampelicida* and *N. crassa* (Shaw et al. 2001; Silverman-Gavrila and Lew 2003; see also Chap. 9 in this volume). In the absence of this gradient, hyphal polarity is affected (Schmid and Harold 1988). Although the effect has been known for a long time, a direct link to the machinery described above has not emerged yet. One explanation for the role of Ca^{2+} ions is the stimulation of vesicle fusion with the membrane. The Ca^{2+} concentration appears to be regulated through a stretch-activated phospholipase C at the tip, which catalyses the formation of inositol (1,4,5)-triphosphate (IP_3) and in turn causes the release of $Ca^{2+}$from special vesicles (Silverman-Gavrila and Lew 2002).

B. The Polarisome

A protein complex related to the actin cytoskeleton is localized at the incipient bud of *Sac. cerevisiae* and is named the polarisome (see Chap. 6 in this volume). This structure is involved in the organi-

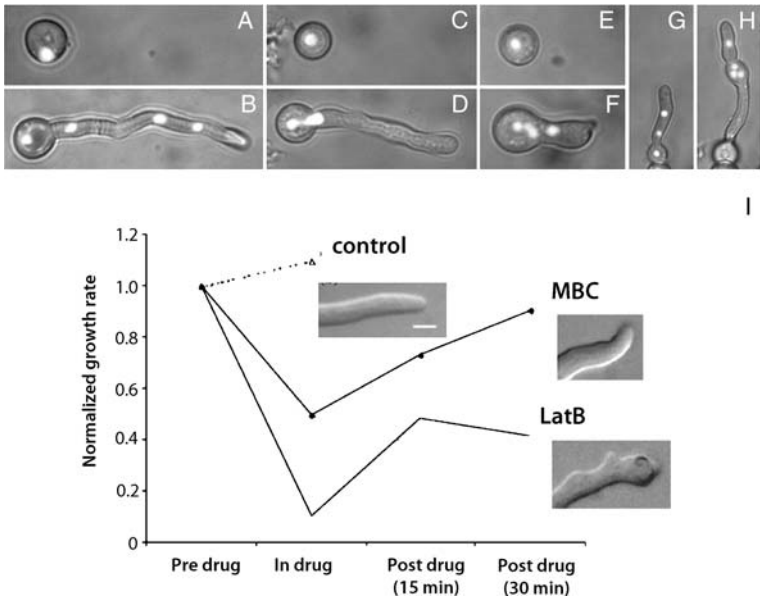

Fig. 5.6. Effect of anti-microtubule and anti-actin drugs on polarized growth of *Asp. nidulans*. **a**, **c** Conidia of a wild-type strain with a GFP-tagged nucleus. **b**, **d** Germlings of the strain in **a**, **c** grown for 10 h at 30 °C in minimal medium (**b**) or minimal medium supplemented with 1.5 µg|ml benomyl. Hyphae elongated and the nucleus divided but nuclei did not migrate into the germtube. **e–h** Germination of a conidium in the presence of 50 µg/ml cytochalasin A. Some spores just swelled but did not form germtubes (**e**) whereas others formed short, more or less deformed hyphae (**f–h**). Nuclear distribution was not specifically affected and sometimes normal (**f**, **h**). **i** Comparison of the growth rate of hyphal tips in the presence of the MT drug MBC or the actin drug latrunculin B (LatB). Taken from Sampson and Heath (2005), with permission

zation of the actin cytoskeleton and its appearance resembles the Spitzenkörper in filamentous fungi (Sagot et al. 2002). There is evidence that this protein complex also exists in filamentous fungi as structure separate from the Spitzenkörper (Harris and Momany 2004). The existence of polarisome components in filamentous fungi was shown first in *Asp. nidulans*. Sharpless and Harris demonstrated that SepA – an orthologue of a key component of the yeast polarisome, Bni1 – colocalize with the Spitzenkörper (Sharpless and Harris 2002). Similarly in *Ash. gossypii*, a filamentous fungus very closely related to *Sac. cerevisiae* (Wendland and Walther 2005), a homologue of the *Sac. cerevisiae* polarisome protein Spa2 was analysed (Knechtle et al. 2003) and recently also the Bni1 orthologue, AgBni1 (Schmitz et al. 2006). Whereas Spa2 is not essential in *Ash. gossypii*, but is necessary for fast polarized growth, deletion of *Agbni1* causes loss of polarization and swelling of the cells to a potato-like appearance. A Spa2 orthologue has been characterized in *C. albicans* as well and its role studied during filamentous growth (Zheng et al. 2003). The protein persistently localizes at hyphal tips and deletion causes defects in polarity establishment. Recently, Crampin et al. suggested that the polarisome and the Spitzenkörper are distinct structures which coexist in hyphae (Sagot et al. 2002; Crampin et al. 2005; Fig. 5.2, see page 122). Similar results for Spa2 (SpaA) have been obtained in *Asp. nidulans*, suggesting that a polarisome or the existence of polarisome components at the growing hyphal tip could be a general theme for filamentous fungi (Virag and Harris 2006b). According to this model, filamentous fungal cells employ both the MT and the actin cytoskeleton and, related to these structural elements, the Spitzenkörper as vesicle supply centre and the polarisome for actin organization.

The machinery discussed so far describes how fungi could extend their hyphae, but this picture does not yet allow any adaptation of the process to external (e.g. nutrient gradients) or internal signals (e.g. the stage of the cell cycle). Little is known so far about the transduction of such signals into e.g. changes of growth direction, although several regulatory proteins have been described which influence polarized growth, probably through an interaction with the actin cytoskeleton. The principle of this possible regulation is best studied in *Sac. cerevisiae* (Tcheperegine et al. 2005) and some of the components appear to be conserved in filamentous fungi. Among those are members of the Rho and Rac families, small GTPases which act as molecular switches (Boyce et al. 2001, 2003, 2005; Guest et al. 2004; Momany 2005; Virag and Harris 2006a). However, a detailed analysis for the exact role in polarized growth in filamentous fungi remains to be done.

C. Actin-Dependent Motor Proteins

The function of the actin cytoskeleton depends on the activity of actin-dependent motor proteins, the myosins. Myosins serve a broad range of cellular functions and are grouped into 18 different classes. In *Asp. nidulans* a class I myosin was identified and shown to be required for protein secretion and polarized growth and with an essential role for viability (McGoldrick et al. 1995). It localizes to the growing hyphal tip (Yamashita et al. 2000).

Given that myosin motors are involved in vesicle transportation towards the cell cortex and vesicle fusion with the cell membrane, it is very interesting that *Asp. nidulans* employs a myosin-derived motor domain for the transportation of class V and class VI chitin synthases, where the motor domain is directly fused to the enzyme (Horiuchi et al. 1999; Takeshita et al. 2005, 2006).

Myosin motor proteins of other classes have been described, e.g. in *Sac. cerevisiae*, where a class V myosin motor is involved in the inheritance of peroxisomes and other organelles (Bretscher 2003; Fagarasanu et al. 2006). A second class V myosin is required for RNA transportation (Bretscher 2003).

D. The *swo* Mutants and the Establishment of Polarity

So far we have discussed polar growth in the sense of maintaining polarized extension by recruiting the cellular machinery for cell wall assembly to the tip of an existing hypha. An interesting remaining question is how polarity is established starting from round spores, such as conidiospores in the case of *Asp. nidulans*. This crucial question has been addressed in *A. nidulans* by the isolation of three temperature-sensitive mutants, *swoC*, *swoD* and *swoF*, in which spores swell at restrictive temperature but do not produce a germ tube (Momany et al. 1999). The SwoC protein displays homology to rRNA pseudouridine synthases of yeast and the role in polarized growth still remains obscure. In contrast SwoF has a high identity with N-myristoyl transferases and it is speculated that a polarity determinant could be the substrate for myristolya-

tion (Shaw et al. 2002). This posttranslational protein modification is found in proteins which switch between membrane-bound and cytoplasmic states (e.g. G protein α-subunits) and could be important for the localization of cell end markers or other landmark proteins, as discussed above (Bathnagar and Gordon 1997). Therefore the identification of prenylated or myristoylated proteins appears to be of prime importance for understanding polarity establishment in filamentous fungi.

V. Conclusions

The past few years have provided many new insights into the role and interplay of actin and the MT cytoskeleton in polarized growth of fungi. It appears that the main function of MTs is to deliver vesicles and cell end markers. Especially the latter function needs much more attention, since only two putative cell end marker protein have been identified in *Asp. nidulans* so far. If homologues of *Sch. pombe* cell end markers exist in filamentous fungi, questions remain: what exactly are their biochemical functions, which downstream events do they trigger to allow straight hyphal growth and which upstream regulatory circuits are integrated? The publication of several fungal genome sequences along with the continuous improvement of molecular and microscopy techniques promise a fruitful future for cytoskeletal research in fungi.

References

Adio S, Reth J, Bathe F, Woehlke G (2006) Regulation mechanisms of Kinesin-1. J Muscle Res Cell Motil 27:153–160

Akhmanova A, Hoogenraad CC (2005) Microtubule plus-end-tracking proteins: mechanisms and functions. Curr Opin Cell Biol 17:47–54

Al-Bassam J, Breugel M van, Harrison SC, Hyman A (2006) Stu2p binds tubulin and undergoes an open-to-closed conformational change. J Cell Biol 172:1009–1022

Aldaz H, Rice LM, Stearns T, Agard DA (2005) Insights into microtubule nucleation from the crystal structure of human gamma-tubulin. Nature 435:523–527

Baas PW, Qiang L (2005) Neuronal microtubules: when the MAP is the roadblock. Trends Cell Biol 15:183–187

Baas PW, Pienkowski TP, Cimbalnik KA, Toyama K, Bakalis S, Ahmad FJ, Kosik KS (1994) Tau confers drug stability but not cold stability to microtubules in living cells. J Cell Sci 107:135–143

Bartnicki-Garcia S, Bartnicki DD, Gierz G, Lopez-Franco R, Bracker CE (1995) Evidence that Spitzenkörper behavior determines the shape of a fungal hypha: a test of the hyphoid model. Exp Mycol 19:153–159

Bathnagar RS, Gordon JI (1997) Understanding covalent modifications of lipids: where cell biology and biophysics mingle. J Cell Biol 7:14–20

Bourett TM, Czymmek KJ, Howard RJ (1998) An improved method for affinity probe localization in whole cells of filamentous fungi. Fungal Genet Biol 24:3–13

Boyce KJ, Hynes MJ, Andrianopoulos A (2001) The CDC42 homolog of the dimorphic fungus *Penicillium marneffei* is required for correct cell polarization during growth but not developmen. J Bacteriol 183:3447–3457

Boyce KJ, Hynes MJ, Andrianopoulos A (2003) Control of morphogenesis and actin localiztion by the *Penicillium marneffei* Rac homolog. J Cell Sci 116:1249–1260

Boyce KJ, Hynes MJ, Andrianopoulos A (2005) The Ras and Rho GTPases genetically interact to co-ordinately regulate cell polarity during development in *Penicillium marneffei*. Mol Microbiol 55:1487–1501

Bretscher A (2003) Polarized growth and organelle segregation in yeast: the tracks, motors and receptors. J Cell Biol 160:811–816

Bretscher A (2005) Microtubule tips redirect actin assembly. Dev Cell 8:458–459

Browning H, Hayles J, Mata J, Aveline L, Nurse P, McIntosh JR (2000) Tea2p is a kinesin-like protein required to generate polarized growth in fission yeast. J Cell Biol 151:15–27

Browning H, Hackney DD, Nurse P (2003) Targeted movement of cell end factors in fission yeast. Nat Cell Biol 5:812–818

Brunswick H (1924) Untersuchungen über die Geschlechts- und Kernverhältnisse bei der Hymenomyzetengattung *Corpinus*. Fisher, Jena

Busch KE, Hayles J, Nurse P, Brunner D (2004) Tea2p kinesin is involved in spatial microtubule organization by transporting tip1p on microtubules. Dev Cell 16:831–843

Carazo-Salas R, Antony C, Nurse P (2005) The kinesin Klp2 mediates polarization of interphase microtubules in fission yeast. Science 309:297–300

Carminati JL, Stearns T (1997) Microbutules orient the mitotic spindle in yeast through dynein-dependent interactions with the cell cortex. J Cell Biol 138:629–641

Carvalho P, Gupta MLJ, Hoyt MA, Pellman D (2004) Cell cycle control of kinesin-mediated transport of Bik1 (CLIP-170) regulates microtubule stability and dynein activation. Dev Cell 6:815–829

Cassimeris L, Spittle C (2001) Regulation of microtubule-associated proteins. Int Rev Cytol 210:163–226

Crampin H, Finley K, Gerami-Nejad M, Court H, Gale C, Berman J, Sudbery P (2005) *Candida albicans* hyphae have a Spitzenkörper that is distinct from the polarisome found in yeast and pseudohyphae. J Cell Sci 118:2935–2947

Czymmek KJ, Bourett TM, Howard RJ (1996) Immunolocalization of tubulin and actin in thick-sectioned fungal hyphae after freeze-substitution fixation and methacrylate de-embedment. J Microsc 181:153–161

Czymmek KJ, Bourett TM, Shao Y, DeZwaan TM, Sweigard JA, Howard RJ (2005) Live-cell imaging of tubulin in the filamentous fungus *Magnaporthe grisea* treated with anti-microtubule and anti-microfilament agents. Protoplasma 225:23–32

Ding DQ, Chikashige Y, Haraguchi T, Hiraoka Y (1998) Oscillatory nuclear movement in fission yeast meiotic prophase is driven by astral microtubules, as revealed by continuous observation of chromosomes and microtubules in living cells. J Cell Sci 111:701–712

Doxsey SJ, McCollum D, Theurkauf W (2005) Centrosomes in cellular regulation. Annu Rev Cell Dev Biol 21:411–434

Efimov V, Zhang J, Xiang X (2006) CLIP-170 homologue and NUDE play overlapping roles in NUDF localization in *Aspergillus nidulans*. Mol Biol Cell 17:2021–2034

Enos AP, Morris NR (1990) Mutation of a gene that encodes a kinesin-like protein blocks nuclear division in *A. nidulans*. Cell 60:1019–1027

Eshel D, Urrestarazu LA, Vissers S, Jauniaux JC, Van Vliet-Reedijk JC, Planta RJ, Gibbons IR (1993) Cytoplasmic dynein is required for normal nuclear segregation in yeast. Proc Natl Acad Sci USA 90:11172–11176

Fagarasanu A, Fagarasanu M, Eitzen GZ, Aitchison JD, Rachubinski RA (2006) The peroxisomal membrane protein Inp2p is the peroxisome-specific receptor for the myosin V motor Myo2p of *Saccharomyces cerevisiae*. Dev Cell 10:587–600

Fischer R, Timberlake WE (1995) *Aspergillus nidulans apsA* (anucleate primary sterigmata) encodes a coiled-coil protein necessary for nuclear positioning and completion of asexual development. J Cell Biol 128:485–498

Freitag M, Hickey PC, Raju NB, Selker EU, Read ND (2004) GFP as a tool to analyze the organization, dynamics and function of nuclei and microtubules in *Neurospora crassa*. Fungal Genet Biol 41:897–910

Fuchs F, Westermann B (2005) Role of Unc104/KIF1-related motor proteins in mitochondrial transport in *Neurospora crassa*. Mol Biol Cell 16:153–161

Fuchs F, Prokisch H, Neupert W, Westermann B (2002) Interaction of mitochondria with microtubules in the filamentous fungus *Neurospora crassa*. J Cell Sci 115:1931–1937

Girbardt M (1957) Der Spitzenkörper von *Polystictus versicolor*. Planta 50:47–59

Grossmann G, Opekarova M, Novakova L, Stolz J, Tanner W (2006) Lipid raft-based membrane compartmentation of a plant transport protein expressed in Saccharomyces cerevisiae. Eukaryot Cell 5:945–953

Guest GM, Lin X, Momany M (2004) *Aspergillus nidulans* RhoA is involved in polar growth, branching, and cell wall synthesis. Fungal Genet Biol 41:13–22

Hagan IM (1998) The fission yeast microtubule cytoskeleton. J Cell Sci 111:1603–1612

Han G, Liu B, Zhang J, Zuo W, Morris NR, Xiang X (2001) The Aspergillus cytoplasmic dynein heavy chain and NUDF localize to microtubule ends and affect microtubule dynamics. Curr Biol 11:19–24

Hancock JF (2006) Lipid rafts: contentious only from simplistic standpoints. Nat Rev Mol Cell Biol 7:456–462

Harris SD, Momany M (2004) Polarity in filamentous fungi: moving beyond the yeast paradigm. Fungal Genet Biol 41:391–400

Harris SD, Read ND, Roberson RW, Shaw B, Seiler S, Plamann M, Momany M (2005) Polarisome meets Spitzenkörper: microscopy, genetics, and genomics converge. Eukaryot Cell 4:225–229

Heath IB (1981) Nucleus-associated organelles in fungi. Int Rev Cytol 69:191–221

Hestermann A, Rehberg M, Gräf R (2002) Centrosomal microtubule plus end tracking proteins and their role in *Dictyostelium* cell dynamics. J Muscle Res Cell Motil 23:621–630

Hirokawa N (1998) Kinesin and dynein superfamily proteins and the mechanism of organelle transport. Science 279:519–526

Hoepfner D, Brachat A, Philippsen P (2000) Time-lapse video microscopy analysis reveals astral microtubule detachment in the yeast spindle pole mutant *cnm67*^{v}. Mol Biol Cell 11:1197–1211

Horio T, Oakley BR (2005) The role of microtubules in rapid hyphal tip growth of *Aspergillus nidulans*. Mol Biol Cell 16:918–926

Horiuchi H, Jujiwara M, Yamashita S, Ohta A, Takagi M (1999) Proliferation of intrahyphal hyphae caused by disruption of *csmA*, which encodes a class V chitin synthase with a myosin motor-like domain in *Aspergillus nidulans*. J Bacteriol 181:3721–3729

Howard J, Hyman AA (2003) Dynamics and mechanics of the microtubule plus end. Nature 422:753–758

Jaspersen SL, Winey M (2004) The budding yeast spindle pole body: structure, duplication, and function. Annu Rev Cell Dev Biol 20:1–28

Job D, Valiron O, Oakley BR (2003) Microtubule nucleation. Curr Opin Cell Biol 15:111–117

Jung MK, May GS, Oakley BR (1998) Mitosis in wild-type and ß-tubulin mutant strains of *Aspergillus nidulans*. Fungal Genet Biol 24:146–160

Kapitein LC, Peterman EJ, Kwok BH, Kim JH, Kapoor TM, Schmidt CF (2005) The bipolar mitotic kinesin Eg5 moves on both microtubules that it crosslinks. Nature 435:114–118

Knechtle P, Dietrich F, Philippsen P (2003) Maximal polar growth potential depends on the polarisome component AgSpa2 in the filamentous fungus *Ashbya gossypii*. Mol Biol Cell 14:4140–4154

Konzack S, Rischitor P, Enke C, Fischer R (2005) The role of the kinesin motor KipA in microtubule organization and polarized growth of *Aspergillus nidulans*. Mol Biol Cell 16:497–506

Lehmler C, Steinberg G, Snetselaar KM, Schliwa M, Kahmann R, Bölker M (1997) Identification of a motor protein required for filamentous growth in *Ustilago maydis*. EMBO J 16:3464–3473

Li S, Du L, Yuen G, Harris SD (2006) Distinct ceramide synthases regulate polarized growth in the filamentous fungus Aspergillus nidulans. Mol Biol Cell 17:1218–1227

Maekawa H, Schiebel E (2004) Cdk1-Clb4 controls the interaction of astral microtubule plus ends with subdomains of the daughter cell cortex. Genes Dev 18:1709–1724

Maekawa H, Usui T, Knop M, Schiebel E (2003) Yeast Cdk1 translocates to the plus end of cytoplasmic microtubules to regulate but cortex interactions. EMBO J 22:438–449

Martin R, Walther A, Wendland J (2004) Deletion of the dynein heavy-chain gene DYN1 leads to aberrant nuclear positioning and defective hyphal development in *Candida albicans*. Eukaryot Cell 3:1574–1588

Martin SG, Chang F (2003) Cell polarity: a new mod(e) of anchoring. Curr Biol 13:R711–R730

Martin SG, Chang F (2005) New end take off: regulating cell polarity during the fission yeast cell cycle. Cell Cycle 4:1046–1049

Martin SG, Chang F (2006) Dynamics of the formin for3p in actin cable assembly. Curr Biol 16:1161–1170

Martin SG, McDonald WH, Yates JR, Chang F (2005) Tea4p links microtubule plus ends with the formin for3p in the establishment of cell polarity. Dev Cell 8:479–491

Martin SW, Konopka JB (2004) Lipid raft polarization contributes to hyphal growth in *Candida albicans*. Eukaryot Cell 3:675–684

Mata J, Nurse P (1997) *tea1* and the microtubular cytoskeleton are important for generating global spatial order within the fission yeast cell. Cell 89:939–949

McDaniel DP, Roberson RW (1998) γ-Tubulin is a component of the Spitzenkörper and centrosomes in hyphal-tip cells of *Allomyces macrogynus*. Protoplasma 203:118–123

McGoldrick CA, Gruver C, May GS (1995) *myoA* of *Aspergillus nidulans* encodes an essential myosin I required for secretion and polarized growth. J Cell Biol 128:577–587

Miller RK, Heller KK, Frisèn L, Wallack DL, Loayza D, Gammie AE, Rose MD (1998) The kinesin-related proteins, Kip2p and Kip3p, function differently in nuclear migration in yeast. Mol Biol Cell 9:2051–2068

Momany M (2005) Growth control and polarization. Med Mycol 43:S23–S25

Momany M, Westfall PJ, Abramowsky G (1999) *Aspergillus nidulans swo* mutants show defects in polarity establishment, polarity maintenance and hyphal morphogenesis. Genetics 151:557–567

Morris NR (1976) Mitotic mutants of *Aspergillus nidulans*. Genet Res 26:237–254

Mouriño-Pérez RR, Roberson RW, Bartnicki-Garcia S (2006) Microtubule dynamics and organization during hyphal growth and branching in *Neurospora crassa*. Fungal Genet Biol 43:389–400

Oakley BR (1995) A nice ring to the centrosome. Nature 378:555–556

Oakley BR (2000) An abundance of tubulins. Trends Cell Biol 10:537–542

Oakley BR (2004) Tubulins in *Aspergillus nidulans*. Fungal Genet Biol 41:420–427

Oakley CE, Oakley BR (1989) Identification of γ-tubulin, a new member of the tubulin superfamily encoded by *mipA* gene of *Aspergillus nidulans*. Nature 338:662–664

Oakley BR, Oakley CE, Yoon Y, Jung KM (1990) γ-Tubulin is a component of the spindle pole body in *Aspergillus nidulans*. Cell 61:1289–1301

O'Connell MJ, Meluh PB, Rose MD, Morris NR (1993) Suppression of the *bimC4* mitotic spindle defect by deletion of *klpA*, a gene encoding a *KAR3*-related kinesin-like protein in *Aspergillus nidulans*. J Cell Biol 120:153–162

Ovechkina Y, Maddox P, Oakley CE, Xiang X, Osmani SA, Salomon ED, Oakley BR (2003) Spindle formation in *Aspergillus* is coupled to tubulin movement into the nucleus. Mol Biol Chem 14:2192–2200

Pereira G, Schiebel E (1997) Centrosome-microtubule nucleation. J Cell Sci 110:295–300

Philippsen P, Kaufmann A, Schmitz H-P (2005) Homologues of yeast polarity genes control the development of multinucleated hyphae in *Ashbya gossypii*. Curr Opin Microbiol 8:370–377

Prigozhina NL, Walker RA, Oakley CE, Oakley BR (2001) γ-tubulin and the C-terminal motor domain kinesin-like protein, KLPA, function in the establishment of spindle bipolarity in *Aspergillus nidulans*. Mol Biol Cell 12:3161–3174

Pruyne D, Legesse-Miller A, Gao L, Dong Y, Bretscher A (2004) Mechanisms of polarized growth and organelle segregation in yeast. Annu Rev Cell Dev Biol 20:559–591

Requena N, Alberti-Segui C, Winzenburg E, Horn C, Schliwa M, Philippsen P, Liese R, Fischer R (2001) Genetic evidence for a microtubule-destabilizing effect of conventional kinesin and analysis of its consequences for the control of nuclear distribution in *Aspergillus nidulans*. Mol Microbiol 42:121–132

Riquelme M, Bartnicki-Garcia S (2004) Key differenences between lateral and apical branching in hyphae of *Neurospora crassa*. Fungal Genet Biol 41:842–851

Riquelme M, Reynaga-Peña CG, Gierz G, Bartnicki-García S (1998) What determines growth direction in fungal hyphae? Fungal Genet Biol 24:101–109

Riquelme M, Fischer R, Bartnicki-Garcia S (2003) Apical growth and mitosis are independent processes in *Aspergillus nidulans*. Protoplasma 222:211–215

Rischitor P, Konzack S, Fischer R (2004) The Kip3-like kinesin KipB moves along microtubules and determines spindle position during synchronized mitoses in *Aspergillus nidulans* hyphae. Eukaryot Cell 3:632–645

Sagot I, Klee SK, Pellman D (2002) Yeast formins regulate cell polarity by controlling the assembly of actin cables. Nat Cell Biol 4:42–50

Sampson K, Heath IB (2005) The dynamic behaviour of microtubules and their contributions to hyphal tip growth in *Aspergillus nidulans*. Microbiology 151:1543–1555

Sawin KE, Snaith HA (2004) Role of microtubules and tea1p in establishment and maintenance of fission yeast cell polarity. J Cell Sci 117:689–700

Sawin KE, Lourenco PCC, Snaith HA (2004) Microtubule nucleation at non-spindle pole body microtubule-organizing centers requires fission yeast centrosomin-related protein mod20p. Curr Biol 14:763–775

Schliwa M, Woehlke G (2003) Molecular motors. Nature 422:759–765

Schmid J, Harold FM (1988) Dual roles for calcium ions in apical growth of *Neurospora crassa*. J Gen Microbiol 134:2623–2631

Schmitz HP, Kaufmann A, Kohli M, Laissue PP, Philippsen P (2006) From function to shape: a novel role of a formin in morphogenesis of the fungus *Ashbya gossypii*. Mol Biol Cell 17:130–145

Schuyler SC, Pellman D (2001a) Search, capture and signal: games microtubules and centrosomes play. J Cell Sci 114:247–255

Schuyler SC, Pellman D (2001b) Microtubule "plus-end-tracking proteins": the end is just the beginning. Cell 105:421–424

Seiler S, Nargang FE, Steinberg G, Schliwa M (1997) Kinesin is essential for cell morphogenesis and polarized secretion in *Neurospora crassa*. EMBO J 16:3025–3034

Seiler S, Plamann M, Schliwa M (1999) Kinesin and dynein mutants provide novel insights into the roles of vesicle traffic during cell morphogenesis in *Neurospora*. Curr Biol 9:779–785

Seiler S, Vogt N, Ziv C, Gorovits R, Yarden O (2006) The STE20/germinal center kinase POD6 interacts with the NDR kinase COT1 and is involved in polar tip extension in *Neurospora crassa*. Mol Biol Cell 17:4080–4092

Sharpless KE, Harris SD (2002) Functional characterization and localization of the *Aspergillus nidulans* formin SEPA. Mol Biol Cell 13:469–479

Shaw BD, Kozlova O, Read ND, Turgeon BG, Hoch HC (2001) Expression of recombinant aequorin as an intracellular calcium reporter in the phytopathogenic fungus *Phyllosticta ampelicida*. Fungal Genet Biol 34:207–215

Shaw BD, Momany C, Momany M (2002) *Aspergillus nidulans swoF* encodes an N-myristoyl transferase. Eukaryot Cell 1:241–248

Sheeman B, Carvalho P, Sagot I, Geiser J, Kho D, Hoyt MA, Pellman D (2003) Determinants of *S. cerevisiae* dynein localization and activation: Implications for the mechanism of spindle positioning. Curr Biol 13:364–372

Sietsma JH, Wessels JG (2006) Apical wall biogenesis. In: Kües U, Fischer R (eds) Growth differentiation and sexuality. Springer, Berlin Heidelberg New York, pp 53–72

Silverman-Gavrila LB, Lew RR (2002) An IP3-activated Ca2+ channel regulates fungal tip growth. J Cell Sci 115:5013–5025

Silverman-Gavrila LB, Lew RR (2003) Calcium gradient dependence of *Neurospora crassa* hyphal growth. Microbiology 149:2475–2485

Snaith HA, Sawin KE (2003) Fission yeast mod5p regulates polarized growth through anchoring of tea1p at cell tips. Nature 423:647–651

Snell V, Nurse P (1994) Genetic analysis of cell morphogenesis in fission yeast – a role for casein kinase II in the establishment of polarized growth. EMBO J 13:2066–2074

Steinberg G, Wedlich-Söldner R, Brill M, Schulz I (2001) Microtubules in the fungal pathogen *Ustilago maydis* are highly dynamic and determine cell polarity. J Cell Sci 114:609–622

Straube A, Enard W, Berner A, Wedlich-Söldner R, Kahmann R, Steinberg G (2001) A split motor domain in a cytoplasmic dynein. EMBO J 20:5091–5100

Straube A, Brill M, Oakley BR, Horio T, Steinberg G (2003) Microtubule organization requires cell cycle-dependent nucleation at dispersed cytoplasmic sites: polar and perinuclear microtubule organizing centers in the plant pathogen *Ustilago maydis*. Mol Biol Cell 14:642–657

Suelmann R, Fischer R (2000) Mitochondrial movement and morphology depend on an intact actin cytoskeleton in *Aspergillus nidulans*. Cell Motil Cytoskel 45:42–50

Suelmann R, Sievers N, Fischer R (1997) Nuclear traffic in fungal hyphae: in vivo study of nuclear migration and positioning in *Aspergillus nidulans*. Mol Microbiol 25:757–769

Takeshita N, Ohta A, Horiuchi H (2005) CsmA, a class V chitin synthase with a myosin motor-like domain, is localized through direct interaction with the actin cytoskeleton in *Aspergillus nidulans*. Mol Biol Cell 16:1961–1970

Takeshita N, Yamashita S, Ohta A, Horiuchi H (2006) *Aspergillus nidulans* class V and VI chitin synthases CsmA and CsmB, each with a myosin motor-like domain, perform compensatory functions that are essential for hyphal tip growth. Mol Microbiol 59:1380–1394

Tcheperegine SE, Gao XD, Bi E (2005) Regulation of cell polarity by interactions of Msb3 and Msb4 with Cdc42 and polarisome components. Mol Cell Biol 25:8567–8580

Tran PT, Marsh L, Doye V, Inoue S, Chang F (2001) A mechanism for nuclear positioning in fission yeast based on microtubule pushing. J Cell Biol 153:397–411

Veith D, Scherr N, Efimov VP, Fischer R (2005) Role of the spindle-pole body protein ApsB and the cortex protein ApsA in microtubule organization and nuclear migration in *Aspergillus nidulans*. J Cell Sci 118:3705–3716

Venkatram S, Jennings JL, Link A, Gould KL (2005) Mto2p, a novel fission yeast protein required for cytoplasmic microtubule organization and anchoring of the cytokinetic actin ring. Mol Biol Cell 16:3052–3063

Virag A, Harris SD (2006a) The Spitzenkörper: a molecular perspective. Mycol Res 110:4–13

Virag A, Harris SD (2006b) Functional characterization of Aspergillus nidulans homologues of *Saccharomyces cerevisiae* Spa2 and Bud6. Eukaryot Cell 5:881–895

Wendland J, Walther A (2005) *Ashbya gossypii*: a model for fungal developmental biology. Nature Rev Microbiol 3:421–429

West RR, Malmstrom T, McIntosh JR (2002) Kinesins *klp5*$^+$ and *klp6*$^+$ are required for normal chromosome movement in mitosis. J Cell Sci 115:931–940

Woehlke G, Schliwa M (2000) Walking on two heads: the many talents of kinesin. Nat Rev Mol Cell Biol 1:50–58

Wu Q, Sandrock TM, Turgeon BG, Yoder OC, Wirsel SG, Aist JR (1998) A fungal kinesin required for organelle motility, hyphal growth, and morphogenesis. Mol Biol Chem 9:89–101

Xiang X, Fischer R (2004) Nuclear migration and positioning in filamentous fungi. Fungal Genet Biol 41:411–419

Xiang X, Beckwith SM, Morris NR (1994) Cytoplasmic dynein is involved in nuclear migration in *Aspergillus nidulans*. Proc Natl Acad Sci USA 91:2100–2104

Yamamoto A, Hiraoka Y (2003) Cytoplasmic dynein in fungi: insights from nuclear migration. J Cell Sci 116:4501–4512

Yamashita RA, Osherov N, May GS (2000) Localization of wild type and mutant class I myosin proteins in *Aspergillus nidulans* using GFP-fusion proteins. Cell Motil Cytoskel 45:163–172

Yildiz A, Selvin PR (2005) Kinesin: walking, crawling or sliding along? Trends Cell Biol 15:112–120

Zhang J, Han G, Xiang X (2002) Cytoplasmic dynein intermediate chain and heavy chain are dependent upon each other for microtubule end localization in *Aspergillus nidulans*. Mol Microbiol 44:381–392

Zhang J, Li S, Fischer R, Xiang X (2003) The accumulation of cytoplasmic dynein and dynactin at microtubule plus-ends is kinesin dependent in *Aspergillus nidulans*. Mol Biol Cell 14:1479–1488

Zheng XD, Wang YM, Wang Y (2003) CaSPA2 is important for polarity establishment and maintenance in *Candida albicans*. Mol Microbiol 49:1391–1405

6 Polarised Growth in Fungi

P. Sudbery[1], H. Court[1]

CONTENTS

I. **Introduction** 137
II. **The Influence of the Cell Cycle** 139
A. *Saccharomyces cerevisiae* 139
B. *Candida albicans* 141
C. Filamentous Fungi 142
III. **The Cytoskeleton** 142
A. Actin 142
B. Septins 143
C. Microtubules 144
1. Tip Growth of the Fission Yeast *Schizosaccharomyces pombe* 144
2. The Role of Microtubules in Hyphal Growth 144
IV. **Polarised Secretion** 145
V. **Rho-type GTPases** 146
A. Activation of Cdc42 146
B. Cdc42 Structure and Mutations 149
C. Cdc42 Effectors 150
1. The Polarisome 150
2. Arp2/3 151
3. PAK Kinases 151
4. Gic1 and Gic2 152
5. Iqg1 152
6. Msb3 and Msb4 152
7. Septins 153
8. Secretory Vesicles and the Exocyst 153
VI. **The Spitzenkörper** 153
A. Localisation of Polarity Proteins During Hyphal Growth 156
B. The Role of Polarity Proteins in Hyphal Growth 156
C. The Role of the Cytoskeleton in Spitzenkörper Function 157
D. The Nature of the Spitzenkörper 158
VII. **Conclusions** 159
References 160

Abbreviations: GAP, GTPase activating protein; GBD, GTPase binding domain; GDI, guanine dissociation inhibitor; GEF, guanosine exhange factor; iMTOC, interphase microtubule organising centre; MEN, mitotic exit network; NETO, new end take off

[1] Department of Molecular Biology and Biotechnology, Sheffield University, Western Bank, Sheffield S10 2TN, UK

Genetic Nomenclature: Where possible the nomenclature used in *Saccharomyces cerevisiae* is employed as follows: *SPA2*, a dominant allele, usually wild type, or the gene itself; *spa2* a recessive allele, usually non-functional, due to a spontaneous or induced mutation; *spa2*Δ a haploid in which the *SPA2* gene has been deleted; *spa2*Δ/Δ, a diploid in which both copies of *SPA2* have been deleted; Spa2, the protein encoded by the *SPA2* gene; Spa2-GFP, a C-terminal fusion between Spa2 and GFP; GFP-Spa2, an N-terminal fusion between Spa2 and GFP. Only where the context is not clear are suffixes such as *Sc*, *Ca Ag* etc. added, e.g. *CaSPA2* = the *Candida albicans* homologue of *SPA2*. In some fungi, such as *Aspergillus nidulans* and *Neurospora crassa*, a different nomenclature is used. Thus the *Asp. nidulans* homologue of the *Sac. cerevisiae SPA2* is *spaA* which encodes the SpaA protein. The Δ symbol is still used to denote a deletion allele, e.g. *spaA*Δ.

I. Introduction

To accommodate new biomass generated through growth, all cells must by necessity increase their surface area. In fungal cells this means expanding the plasma membrane and cell wall, and is achieved by the fusion of membrane-bound secretory vesicles with the existing plasma membrane – the membranes of the incoming secretory vesicles provide the wherewithal for the expansion of the plasma membrane, while their contents contain the raw materials and enzymes for the manufacture of new cell wall. In *Saccharomyces cerevisiae*, lesions in the secretory pathway that block this process result in cells of increasing density and are ultimately lethal (Novick et al. 1980). If the secretory vesicles fused evenly without restriction to the whole of the surface area, then cells would grow isotropically – that is, growth would

Biology of the Fungal Cell, 2nd Edition
The Mycota VIII
R.J. Howard and N.A.R. Gow (Eds.)
© Springer-Verlag Berlin Heidelberg 2007

proceed evenly in all directions. However, fungal cells often grow in a highly polarised fashion where growth in confined to a small part of their total surface area. Such polarized growth requires that the flow of secretory vesicles, and their fusion with the plasma membrane, is directed towards the site of growth.

The growth of fungal hyphae can be dramatically polarised. For example, hyphae of *Neurospora crassa* can extend at a rate of 16 μm min^{-1} (Trinci 1973), which requires a flow of 37,000 vesicles min^{-1} to arrive and fuse with the growing apex (Collinge and Trinci 1974). Yeast cells also show polarised growth, but at a rate that is two orders of magnitude slower than this. Young buds of *Sac. cerevisiae* grow in a polarised fashion from the bud tip before a switch to isotropic growth occurs in late G2 (Kron and Gow 1995; Figs. 6.1, 6.3). During cytokinesis polarised growth is directed to the bud neck to produce the secondary septum (Kron and Gow 1995; Cabib 2004). During nitrogen-limited growth a delayed onset of apical/isotropic switch together with an absence of cell separation after cytokinesis results in chains of elongated cells called pseudohyphae (Gimeno et al. 1992; Kron et al. 1994). When haploid cells are exposed to their cognate mating pheromone polarised growth results in a mating projection or "shmoo" which allows the cells to grow towards the cell of opposite mating type that is producing the pheromone (Bücking-Throm et al. 1973; Segall 1993; Fig. 6.1). The fission yeast *Schizosaccharomyces pombe* grows from the cell pole distant from the division plane before growth is also initiated from the other pole, a process termed new end take off (or NETO; Mitchison and Nurse 1985). The cotton pathogen *Ashbya gossypii* grows exclusively in the hyphal mode, even though it is related to the budding yeast, *Sac. cerevisiae* (Philippsen et al. 2005; Wendland and Walther 2005). Some fungi are dimorphic or polymorphic, being able to grow as both yeast and hyphae according to the environmental conditions. For example, the human fungal pathogen *Candida albicans* can switch between yeast, pseudohyphal and hyphal growth patterns (Odds 1985; Sudbery et al. 2004; Walther and Wendland 2007; Fig. 6.1) and, when exposed to mating pheromone, produces long thin mating projections (Lockhart et al. 2003; Fig. 6.1). Another human fungal pathogen, *Penicillium marneffei*, grows in a hyphal form at 25 °C and as yeast at 37 °C.

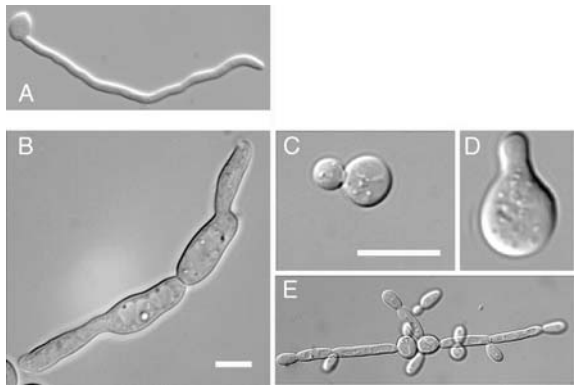

Fig. 6.1. Examples of polarised growth in fungi. **A** *C. albicans* hyphae, **B** *C. albicans* mating projection, **C** *Sac. cerevisiae* yeast, **D** *Sac. cerevisiae* mating projection, **E** *C. albicans* pseudohyphae. *Bars* 5 μm

The budding yeast, *Sac. cerevisiae* and the fission yeast, *Sch. pombe* serve as models for the investigation of the molecular mechanisms that drive polarised growth and a detailed picture has now emerged (Fig. 6.2). Sites of polarised growth are characterised by cortical markers. In budding yeast cells, these markers are deposited by bud site selection pathways and, in shmoos, by the βγ dimer that dissociates from the trimeric G protein complex upon activation of the pheromone receptor. In *Sch. pombe* a kelch repeat protein Tea1 is transported along microtubules by the kinesin motor protein Tea2. At these marked sites the Cdc42 GTPase is activated by its GEF Cdc24. Cdc42 acts as a master regulator of many aspects of cell growth and morphogenesis (Adams et al. 1990a; Johnson 1999; Etienne-Manneville 2004). As a result of Cdc42 action actin cables are nucleated at sites of polarised growth by a surface protein complex called the polarisome (Sheu et al. 1998; Sagot et al. 2002; Evangelista et al. 2002). Post-Golgi secretory vesicles are transported along these actin cables to dock with a second protein complex called the exocyst before fusion with the plasma membrane (Terbush et al. 1996; Schott et al. 1999).

This chapter first reviews how these processes operate in yeast cells. As in most processes associated with the cell cycle, polarised growth is ultimately controlled by the cyclin-dependent kinase – Cdc28 in *Sac. cerevisiae*, Cdc2 in *Sch. pombe*. Thus, the influence of the cell cycle and the cyclin regulators of Cdc28 is reviewed first. This is followed by a consideration of the actin, microtubular and septin cytoskeletons which form an essential part

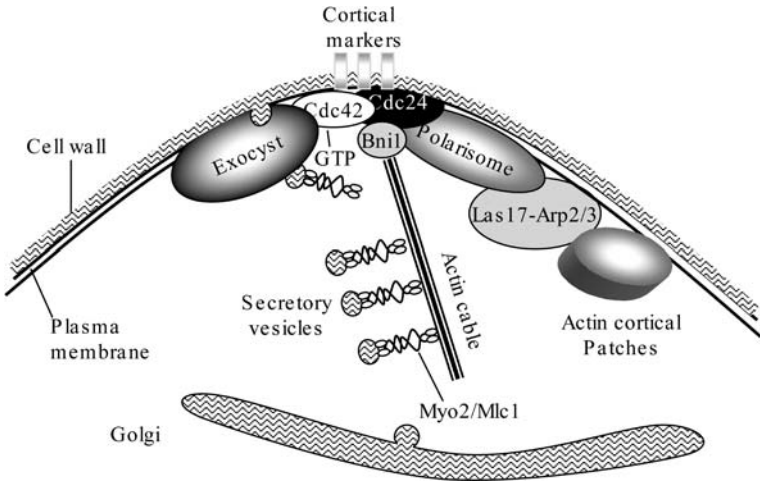

Fig. 6.2. Overview of polarised growth in budding yeast. At sites of polarised growth, indicated by cortical markers, Cdc42 is localised and activated to its GTP-bound state by Cdc24. Cdc42-GTP promotes the localisation and activation of Bni1 and the polarisome, the exocyst and the Las17-Arp2/Arp3 complex. Bni1 nucleates the formation of actin cables which form tracks for the transport of secretory vesicle, by Myo2/Mlc1, which bleb off from late Golgi compartments. On arrival at sites of polarised growth the secretory vesicles dock with the exocyst and fuse with the plasma membrane

of the polarised growth machinery. The subsequent sections review what is known about the transport of secretory vesicles from the Golgi along actin cables to their fusion with the exocyst, and then consider the role of Cdc42 and other Rho-type GTPases which orchestrate many of the processes involved in polarised growth. This includes a consideration how sites of polarised growth are marked by the bud site selection pathways leading to the activation of Cdc42 and the multitude of downstream Cdc42 effectors.

The growth of yeast buds is clearly different from the extension of hyphal tips, and a key question is whether the yeast paradigm is applicable in a modified form to hyphal growth or whether fundamentally different mechanisms are operating. An indication that the budding yeast paradigm requires substantial modification is the presence of a structure called the Spitzenkörper, an accumulation of secretory vesicles at or just behind hyphal tips, for which there does not appear to be a counterpart in *Sac. cerevisiae* (Girbardt 1957, 1969; Harris et al. 2005, Virag and Harris 2006b). Investigations into the molecular composition of the Spitzenkörper are still at a relatively early stage, but it has been clear for a long time that it plays a central role in driving the extension of hyphal tips (Bartnicki-Garcia et al. 1995). The present review concludes by considering how the detailed knowledge of polarised growth in *Sac. cerevisiae* may apply in fungi that can grow in a hyphal form, and in particular the nature of the Spitzenkörper and its relationship to the various complexes and molecular mechanisms that operate in yeast, the workings of which we have at least some understanding.

II. The Influence of the Cell Cycle

A. *Saccharomyces cerevisiae*

In *Sac. cerevisiae* the pattern of growth is strictly regulated by the cell cycle (reviewed by Kron and Gow 1995). Once a mother cell reaches a critical size and forms a bud, growth for the remainder of the cell cycle is confined to the bud (Fig. 6.3A). Young buds grow in a polarised fashion from their tip but switch to isotropic growth in G2. This switch is delayed in a pseudohyphal cell, resulting in the elongated shape of the daughter bud. After mitosis and the formation of the primary septum, growth is re-directed to the bud neck to form the secondary septa either side of the primary septum.

Passage through the cell cycle is regulated by the cyclin dependent kinase, Cdc28, which at various times is partnered by a family of three G1 cyclins (Cln1–Cln3) and six G2 cyclins (Clb1–Clb6; for reviews see Futcher 2002; Jorgensen and Tyers 2004). The following brief summary provides a background for discussion of the influence of the cell cycle on polarised growth. When mother cells grow to an appropriate cell size and in the presence of suitable nutrients, *Start* is initiated by the G1 cyclin, Cln3 (Sudbery et al. 1980; Cross 1988; Nash et al. 1988). This results in a program of transcription of several hundred genes involved in DNA and cell wall synthesis. Among this gene set are two further G1 cyclins, Cln1 and Cln2. In association with these cyclins, Cdc28 then mediates the critical processes necessary for Start, including the destruction of Sic1, an inhibitor of Cdc28 when associated with the Clb family of G2 cyclins. The G1 transcriptional program also results in the expres-

sion of a pair of functionally redundant forkhead transcription factors, Fkh1 and Fkh2, which transcribe the G2 cyclins Clb1–Clb6 (Zhu et al. 2000). These G2 cyclins mediate the shut-off of G1 cyclin transcription and promote the degradation of G1 cyclin proteins (Amon et al. 1993). Cdc28 in association with the Clb cyclins then orchestrates DNA synthesis and the onset of mitosis. To exit mitosis the Clbs must be destroyed and Sic1 re-stabilised as cells enter G1 of the next cycle. Thus there is a wave of G1 cyclin expression followed by a wave of G2 cyclin expression.

The apical growth immediately after bud emergence is promoted by G1 cyclins, while the apical/isotropic growth switch in G2 is co-incident with the rise of G2 cyclins Clb1/Clb2 and the disappearance of the G1 cyclins (Lew and Reed 1993). The ways in which the Cln-Cdc28 kinase promotes polarised growth are still unclear, although some clues are emerging, such as the Cdc28-dependent phosphorylation of Bem1 and Far1 (discussed further below). In *Sac. cerevisiae* cyclin levels may play a role in regulating pseudohyphal growth, which involves increased polarised growth and a delayed apical/isotropic growth switch (Kron et al. 1994; Ahn et al. 2001). Cells lacking Cln1 and Cln2 are defective in pseudohyphal growth, while cells lacking Cln3 show an enhanced pseudohyphal response. Thus, Cln1 and Cln2 promote pseudohyphal growth and Cln3 is a negative regulator (Loeb et al. 1999a). Activation of Cdc28 by mitotic cyclins leads to isotropic growth, therefore inhibition of or delay of this activation would be expected to enhance pseudohyphal growth. Consistent with this hypothesis, a *clb2*Δ/*clb2*Δ strain showed enhanced pseudohyphal growth, while overexpression of Clb2 abrogated pseudohyphal growth (Ahn et al. 1999). The periodicity of *CLB2* transcription is lost in a *fkh1*Δ/Δ *fkh2*Δ/Δ mutant and such cells show constitutive pseudohyphal growth (Zhu et al. 2000).

It is clearly important that mitosis does not occur if the bud has not formed properly. Genetic lesions or environmental perturbations that interfere with the proper formation and growth of the bud triggers the morphogenesis checkpoint which de-

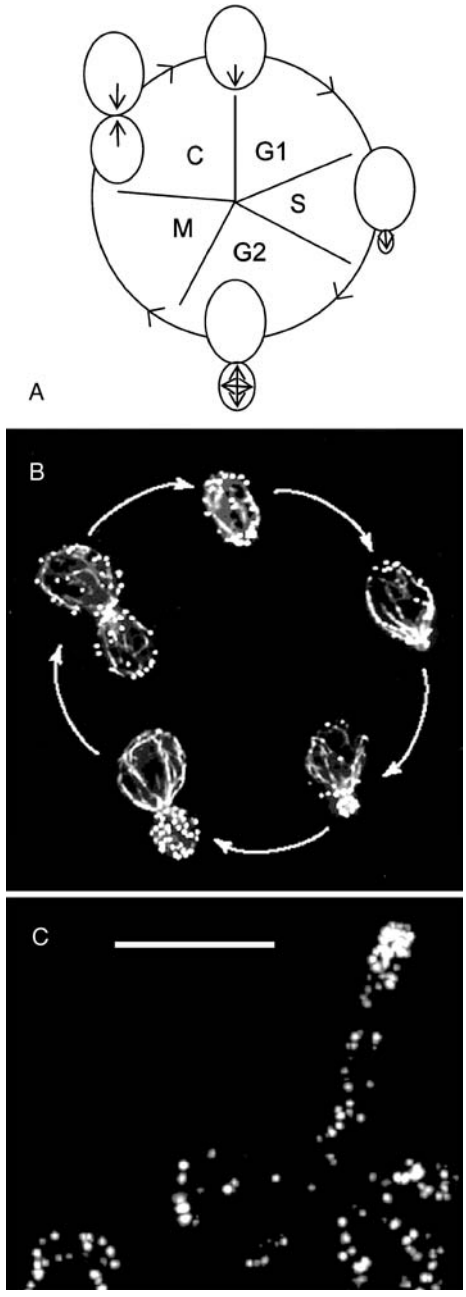

Fig. 6.3. Actin and cell growth polarisation. **A** Polarised growth follows the pattern of actin polarisation: growth is confined to the bud and the pattern of growth switches from apical to isotropic in G2. After mitosis (*M*), during cytokinesis (*C*), growth is directed to the mother cell bud neck to form the secondary septum. **B** Polarisation of the actin cytoskeleton in the cell cycle of *Sac. cerevisiae*. In unbudded cells, actin cortical patches congregate at the incipient bud site to which actin cables are orientated. In small buds, the cables are orientated to the bud tip where the cortical patches congregate. In cells with larger buds, actin cables are directed to the bud neck in mother cells – the actin cables and patches are not polarised in the bud. After mitosis cables and patches are polarised to the mother-bud neck (Phalloidin-TRITC; K. Ayscough). **C** Polarisation of actin cortical patches in *C. albicans* hyphae. (Abp-YFP; H. Crampin, unpublished data). *Bar* 5 μm

lays but does not permanently prevent mitosis (Lew and Reed 1995). The checkpoint operates through the Swe1 kinase, the homologue of the Wee1 kinase first identified in *Sch. pombe*. Swe1 inhibits the Clb2-Cdc28 by phosphorylation of Tyr19 in the active site (Sia et al. 1996). Inhibition of Cdc28 prevents mitosis and also prevents the switch from polarised to apical growth. As a result of operation of the morphogenesis check point buds often become elongated and can resemble pseudohyphae. This has caused much confusion in the literature because pseudohyphae, induced by nitrogen-limited growth, do not depend on Swe1 (Ahn et al. 1999). For example, branched-chain alcohols such as isoamyl alcohol induce a pseudohypha-like phenotype, but this is Swe1-dependent and so is likely to result from some form of interference during bud formation (Martínez-Anaya et al. 2003).

B. *Candida albicans*

The growth pattern of *C. albicans* yeast and pseudohyphal cells is similar to the corresponding states in *Sac. cerevisiae*. Young yeast buds grow in a polarised fashion from their tips but switch to an isotropic mode late in the cell cycle (Soll et al. 1985). Pseudohyphal cells prolong the phase of polarised growth, however a switch to isotropic growth does eventually occur (Crampin et al. 2005). In contrast to yeast and pseudohyphae, hyphal germ tubes grow continuously in a polarised fashion and no switch to isotropic growth occurs, even during mitosis (Soll et al. 1985; Crampin et al. 2005).

In this fungus there is a single homologue of the *Sac. cerevisiae CLN1/CLN2* gene pair, called *HGC1* (Zheng et al. 2004), and a single homologue of *Sac. cerevisiae CLN3* (Chapa y Lazo et al. 2005; Bachewich et al. 2005). There is a third G1 cyclin called *CCN1*. This gene is not the closest *C. albicans* homologue of either *Sac. cerevisiae CLN1/CLN2* or *CLN3*, so its status is unclear. Two G2 cyclins have been identified in *C. albicans*, which are homologues of the *Sac. cerevisiae* Clb2 and Clb4 genes (Bensen et al. 2005).

Note there is some confusion in the *C. albicans* literature concerning G1 cyclin nomenclature. Initially two G1 cyclins were identified. Whiteway and co-workers identified a gene homologous to *Sac. cerevisiae* G1 cyclins and assigned it the name *CCN1* (Whiteway et al. 1992). Sherlock and colleagues isolated two G1 cyclins and assigned them the names *CLN1* and *CLN2*, despite the fact that *CLN1* was known to be the same gene as *CCN1*. For a while *CLN1* was used in the literature by others, for example Loeb and co-workers (1999b). However, it is now clear that *CLN1* is not the closest homologue of *Sac. cerevisiae CLN1* and the standard name has now reverted to the original *CCN1* (Braun et al. 2005). The gene originally named *CLN2* by Sherlock and co-workers is probably the homologue of *Sac. cerevisiae CLN3* and it has now been so re-named. The *C. albicans* genome sequence revealed a third G1 cyclin, which is the closest homologue of the *Sac. cerevisiae CLN1/2* gene pair. For a while this gene was called *CLN21* until its identification as a hyphal specific cyclin, when it was re-named *HGC1* (Zheng et al. 2004).

Cyclins have also been shown to play an important role in the regulation of polarised growth in *C. albicans*. *HGC1* is not expressed in yeast cells but is expressed for a short period upon hyphal induction and is required for hypha formation (Zheng et al. 2004). In contrast to *Sac. cerevisiae*, Cln3 is essential for budding – when Cln3 is depleted using the conditional *MET3* promoter, unbudded mother cells increase in size without budding before spontaneously evaginating hyphal germ tubes (Bachewich and Whiteway 2005; Chapa y Lazo et al. 2005). Thus the G1 cyclins have acquired morphology-specific functions: Cln3 is required for yeast growth and may negatively regulate hyphal growth; Hgc1 is not required for yeast growth, but it is required for hyphal growth; Ccn1 is not required for germ tube formation, but it is required for long-term maintenance of germ tubes (Loeb et al. 1999b). Loss of either of the G2 cyclins, Clb2 and Clb4, leads to constitutive pseudohyphal growth, with loss of Clb2 having the more pronounced effect (Bensen et al. 2005). Loss of the forkhead transcription factor Fkh2, responsible for the periodic transcription of the G2 cyclins, also results in pseudohyphal growth (Bensen et al. 2002).

The hyphal growth resulting from loss of the G1 cyclins and the pseudohyphal growth resulting from loss of the G2 cyclins are examples of the remarkable relationship between polarised growth and cell cycle arrest in *C. albicans*. There have been many reports of cell cycle blocks resulting in polarised growth – further examples are as follows:

- Strains in which the only copy of *CDC28* is under the control of the *MET3* promoter constitutively form a mixture of hyphae and pseudohyphae during growth under *MET3*-repressing conditions (Umeyama et al. 2006).

- A *cdc34*Δ/Δ mutant grows constitutively as hyphae. In *Sac. cerevisiae*, Cdc34 acts as a ubiquitin ligase targetting phosphorylated Sic1, leading to its degradation. Sic1 is an inhibitor of Cdc28 when complexed to the Clb family of G2 cyclins. Destruction of Sic1 is essential for cells to pass Start. Thus, like cells depleted of Cln3, which also form hyphae constitutively, cells lacking Cdc34 are arrested in G1. There is no obvious homologue of *SIC1* in the *C. albicans* genome, but a possible functional counterpart called *SOL1* has been identified (tir-Lande et al. 2005).
- Inhibition of DNA synthesis by hydroxyurea treatment results in pseudohyphal growth (Bachewich et al. 2005).
- Depletion of the polo kinase Cdc5 results in hyper-polarised growth. Cdc5 is required for mitotic exit and cytokinesis in *Sac. cerevisiae* (Bachewich et al. 2005).
- Cells treated with nocadazole, which disrupts the mitotic spindle also show hyper-polarised growth (Bai et al. 2002).
- Cells lacking Gin4, or the related Hsl1 kinase, form pseudohyphae constitutively (Wightman et al. 2004; Umeyama et al. 2005). It is not clear whether this treatment does cause a cell cycle block. However, in *Sac. cerevisiae* Gin4 plays multiple roles in cell cycle progression, including a requirement for septin ring formation (Longtine et al. 1998), failure of which triggers the Swe1-dependent morphogenesis checkpoint (Lew and Reed 1995). The pseudohyphal growth in a *gin4*Δ/Δ mutant is not wholly a result of this checkpoint as it still occurs in a *gin4*Δ/Δ *swe1*Δ/Δ double mutant. Moreover, septin ring formation occurs normally in an *hsl1*Δ/Δ mutant, but constitutive pseudohyphal formation is still observed.

A consistent theme that emerges from these studies is that cell cycle arrest results in polarised growth. Interestingly in the case of Cdc5 depletion and nocadazole treatment, removal of the relevant checkpoint, mediated by Bub5 and Mad2 respectively, which allows the cell cycle to be resumed, also abrogates the polarised growth response (Bai et al. 2002; Bachewich et al. 2005). Thus cell cycle progression itself may be the factor that links these diverse conditions. Cells impaired in progress through G1 form hyphae (Cln3 depletion, *cdc34*Δ/Δ) while cells blocked or impaired in transit through S, G2 and M form pseudohyphae (HU, Clb2 or Clb depletion, *fkh1*Δ/Δ. nocadazole and possibly *gin4*Δ/Δ and *hsl1*Δ/Δ). In this regard it is intriguing that the evagination of hyphal germ tubes from unbudded yeast cells occurs before the *Start* of the cell cycle, as judged by the initiation of S-phase and spindle pole duplication (Hazan et al. 2002). A close parallel is the formation of a shmoo in *Sac. cerevisiae*, where the cell cycle is halted in G1 by Far1 (Peter and Herskowitz 1994).

C. Filamentous Fungi

The hyphae of filamentous fungi grow continuously in a polarised fashion from their tip; and this growth is cell cycle-independent. However in a very short times scale tip growth has been seen to occur in discrete pulses (Lopez-Franco et al. 1994). Filamentous fungi such as *Asp. nidulans* do show a phase of isotropic growth during ascospore swelling before switching to polarised apical growth as the germ tube grows out of the mother cell. This isotropic apical switch is delayed if the first mitosis is blocked in cells growing on rich medium, but not on poor medium (Harris 1999). Thus in this case, and in contrast to *C. albicans*, polarised growth depends on cell cycle progression. However, this relationship is modulated by the nutritional status of the environment.

III. The Cytoskeleton

The actin, tubulin and septin cytoskeletons are all involved in polarised growth in fungi (see also Chaps. 1, 2, 5, 10, 11 in this volume).

A. Actin

The actin cytoskeleton has three components: actin cables, actin cortical patches and a contractile actomyosin ring at the site of septum formation (Adams and Pringle 1983; Lippincott and Li 1998; Fig. 6.3B). In both yeast and filamentous fungi the cortical patches are clustered at sites of polarised growth and the cables orientated towards these sites (Adams and Pringle 1983; Anderson and Soll 1986; Heath 1988; Hazan et al. 2002; Fig. 6.3C). As the mode of growth changes from apical to isotropic during bud growth in *Sac. cerevisiae* the polarisation of both actin cables and cortical patches disappears. After mitosis the actin cytoskeleton becomes polarised to the site

of septum formation (Adams and Pringle 1983; Pruyne and Bretscher 2000a; (Fig. 6.3B). During hyphal growth of *C. albicans* the actin cytoskeleton is polarised continuously to the tip; in contrast to yeast and pseudohyphae, tip-orientated cables and cortical patches persist throughout the cell cycle (Anderson and Soll 1986; Hazan et al. 2002).

Actin cables are nucleated at sites of polarised growth and form tracks for the transport of secretory vesicles by a class V myosin, which in *Sac. cerevisiae* is encoded by *MYO2* (Adams and Pringle 1983; Schott et al. 1999). Subcellular organelles such as the Golgi apparatus, mitochondria, vacuoles and peroxisomes are also transported by Myo2 along actin cables into the daughter bud (Pruyne et al. 2004). Actin cables also form tracks for the asymmetric localisation of some mRNA molecules, such as *ASH1*, to the daughter cell (Sil and Herskowitz 1996). In this case transport is driven by a second-class V myosin encoded by *MYO4* (Bobola et al. 1996).

In *Sac. cerevisiae* actin cables are also required for the orientation of the mitotic spindle across the bud neck. Astral microtubules are guided by actin cables to the cortex of the daughter bud, resulting in the positioning of the mitotic spindle (Segal and Bloom 2001). In this process, a connection between microtubules and actin cables is established through an interaction between Bim1, which decorates the plus ends of microtubules, and Kar9 which associates with Myo2 (Bloom 2000). Capture of microtubules at the bud cortex also involves Bud6, a polarisome component (see below; Segal et al. 2000). Arrival of microtubules at the daughter cell cortex results in the release of Lte1, the GEF for the Tem1 GTPase. Activated Tem1 in turn activates the mitotic exit network (MEN) which is necessary for the completion of mitosis (Seshan and Amon 2004). This mechanism ensures that anaphase cannot be initiated until the spindle is properly positioned across the bud neck.

Actin cortical patches are composed of highly branched actin chains complexed to a large number of actin associated proteins (Winder and Ayscough 2005). They congregate around sites of polarised growth in a wide variety of fungal species, including *Sac. cerevisiae* (Adams and Pringle 1983), *C. albicans* (Anderson and Soll 1986; Hazan et al. 2002; Fig. 6.3B), *Ash. gossypii* (Wendland and Walther 2005) and filamentous fungi (Heath 1988). However, it not clear that they directly promote polarised growth as they are thought to be sites of endocytosis (Geli and Riezman 1998; Matheos et al. 2004; Ayscough 2005). One possibility is that endocytosis is necessary to re-cycle components, such v-SNARES, required for vesicle traffic to sites of polarised growth.

An actomyosin ring forms at the site of septation. This consists of a complex between filamentous actin and the class II myosin encoded in *Sac. cerevisiae* by *MYO1* (Lippincott and Li 1998). Contraction of the ring is thought to guide the formation of the primary septum composed of chitin synthesised by the chitin synthase, Chs2, which is attached to the contractile ring (Vallen et al. 2000; Schmidt et al. 2002; Cabib 2004).

B. Septins

In *Sac. cerevisiae* formation of the contractile ring and a variety of other functions involved in cytokinesis depends on the septin cytoskeleton, which is composed of a family of five related proteins: Cdc3, Cdc10, Cdc11, Cdc12 and Shs1 (Pringle et al. 1995; Gladfelter et al. 2001b; Douglas et al. 2005). They form a single ring at the site of the incipient bud emergence, which is maintained at the bud neck after bud emergence. Later in the cycle the ring elongates to form an hourglass shape before splitting into two rings just before mitosis. During the cell cycle the septin ring transits between a form in which its subunits are in dynamic equilibrium with a cytoplasmic pool and a stable form in which no subunit exchange occurs (Caviston et al. 2003; Dobbelaere et al. 2003). The transition occurs around the time in which the ring elongates to the hourglass shape and is mediated by the Gin4 kinase. Septins act as a scaffold for a variety of functions involved in cytokinesis. Early in the cycle the septin ring localises the chitin synthase encoded by Chs3 which mediates the formation of the external chitin ring that forms the bud scar after the daughter bud separates from the mother cell (Santos and Snyder 1997; Cabib 2004). Also early in the cycle Myo1 and a regulatory light chain Mlc2, localises to the septin ring (Lillie and Brown 1994; Luo et al. 2004). During mitosis this complex successively recruits another regulatory light chain Mlc1, followed by Iqg1 and finally actin (Lippincott and Li 1998; Boyne et al. 2000; Shannon and Li 2000). After formation of the primary septum, the septin rings are required for re-polarisation of growth to the bud neck for the formation of secondary septa. After cell separation in haploid cells, the septin rings on both the mother and daughter cells act as landmarks for the locali-

sation of the axial bud site markers Bud3, Bud4 and Bud10, which mark the site of bud emergence in the next cycle (Chant 1999). Septin rings also form at sites of septation in other fungi. Interestingly the rings only form during or after mitosis in both *Sch. pombe* and *Asp. nidulans* and are unlikely to be part of the mechanism that marks the site where the septum will form (Longtine et al. 1996; Momany et al. 2001). As well as programming cytokinesis, septins serve other roles. First, they act as barriers to diffusion of proteins through the cortex, thus delineating cortical domains (Dobbelaere et al. 2003). Second, they program polarise growth away from the bud neck in young buds, resulting in the characteristic constriction between the mother cell and the daughter bud (Gladfelter et al. 2005). Septins may play other roles during hyphal growth. A band of longitudinal septin bars form at the base of *Sac. cerevisiae* shmoos and *C. albicans* germ tubes (Sudbery 2001; Warenda and Konopka 2002). The role of these structures is not known, but in *C. albicans* they are clearly distinct from the septin rings that also form within the germ tube and their formation is Gin4-independent, in contrast to the septin rings that form within the germ tube (Wightman et al. 2004). Septin caps have been observed at the tips of shmoos and *C. albicans* germ tubes; and again the function of these caps remains obscure (Warenda and Konopka 2002).

C. Microtubules

1. Tip Growth of the Fission Yeast *Schizosaccharomyces pombe*

Microtubules are not required for polarised growth in *Sac. cerevisiae*, however they do play an central role in the polarised growth of other fungi. In the fission yeast *Sch. pombe*, three to six pairs of microtubule bundles run the length of the linear cylindrical cells. These microtubules are nucleated by an interphase microtubule organising centre (iMTOC) located near the nuclear envelope; the plus ends of the microtubules are located at the cell poles and the minus ends are anchored near the iMTOC, thus forming an antiparallel region in the centre of the bundle. The plus ends of the microtubules constantly grow towards the cell poles and shrink back due to depolymerisation when they touch the pole. The microtubules are required for accurate positioning of the growth site. Four proteins, Tea1, Tea2, Tip1 and Mal3, have been identified that are involved in this process. Mutations affecting these proteins result in T-shaped cells due to growth from ectopic sites (Verde et al. 1995). Tea1, a kelch repeat protein, marks the growth site itself (Mata and Nurse 1997). Its functions include the localisation of the *Sac. cerevisiae* Bud6 homologue, which promotes the polarisation of the actin cytoskeleton (Glynn et al. 2001), and Pom1, a kinase required for the initiation of bipolar growth from each cell pole (Bahler and Pringle 1998). Tea1 is delivered to the cell poles on the tips of the microtubules (Mata and Nurse 1997). Tea2, a kinesin motor protein, transports Tip1 and Tea1 along microtubules to their plus end (Behrens and Nurse 2002; Busch et al. 2004). Tip1, a member of the CLIP-170 protein family, is an essential part of the guidance mechanism that maintains the microtubules parallel to the long axis of the cell (Brunner and Nurse 2000). In the absence of Tip, microtubules undergo catastrophic depolymerisation if their tips contact the cell cortex whereas, in the presence of Tip1, the ends are deflected back into the cell and only undergo depolymerisation when they touch the cell pole. Mal3, a member of the EB1 family of microtubule tracking proteins, associates with Tip1 and is required to retain Tip1 at the microtubule tips (Busch et al. 2004). As they arrive at the cell poles on the tips of microtubules, Tea1, Tea2 and Tip1 are transferred to the cell cortex where they accumulate in a mutually interdependent fashion.

2. The Role of Microtubules in Hyphal Growth

In the hyphae of both *C. albicans* and *Asp. nidulans*, long microtubules are orientated along the axis of the hyphae (Barton and Gull 1988; Han et al. 2001). As well as being required for movement of nuclei, they are also required for polarised growth as treatment with microtubule-destabilising drugs slows or halts hyphal extension (Crampin et al. 2005; Horio and Oakley 2005). However, there is an interesting difference between the effects of drugs that destabilise the actin cytoskeleton and those which destabilise the microtubular cytoskeleton. Cytochalisin A, which specifically targets actin cables, and latrunculin A, which has a general destabilising action on filamentous actin, both result in tip swelling, which has been shown to be due to a switch to isotropic growth (Grove and Sweigard 1980; Akashi et al. 1994; Torralba et al. 1998; Heath et al. 2003; Crampin et al. 2005), while destabilising microtubules simply slows or abolishes tip growth (Akashi et al. 1994; Crampin et al. 2005; Horio and Oakley 2005). One interpretation of this

result is that microtubules promote long-distance vesicle transport to the tip while actin cables mediate their short distance distribution to the tip. An alternative, not necessarily incompatible, explanation for the tip swelling is that actin cables tether the Spitzenkörper to the tip (see below).

IV. Polarised Secretion

Secretory vesicles which bleb off from the trans Golgi Network are transported along actin cables to dock with a multi-protein structure called the exocyst at sites of polarised growth (Terbush et al. 1996; Fig. 6.4). Vectorial movement of secretory vesicles from the Golgi to sites of polarised growth depends on the Rab GTPase Sec4, which promotes the exit of secretory vesicles from the late Golgi, their transit to sites of apical growth and docking to the exocyst subunit, Sec15 (Walworth et al. 1992; Guo et al. 1999). Sec4 is essential for viability in both *Sac. cerevisiae* and *C. albicans* (Mao et al. 1999), but possibly not in *Aspergillus niger* (Punt et al. 2001). Sec4 cycles between a GDP and GTP-bound state, mediated by its GEF, Sec2 (Walch-Solimena et al. 1997), and a pair of redundant GAPs, Msb3 and Msb4 (Albert and Gallwitz 2000). Polarised localisation of Sec4 depends on Sec2, but Sec2 localisation is independent of Sec4, thus Sec2 may play a central role in regulating the traffic of secretory vesicles (Walch-Solimena et al. 1997). A pair of redundant Rab GTPases, Ypt31/Ypt32, loads Sec2 onto nascent secretory vesicles forming in late Golgi compartments. Sec2 then recruits Sec4, which allows vesicles to leave the Golgi (Ortiz et al. 2002). Cells lacking Msb3 or Msb4 or mutant forms of Sec4 locked in the GTP-bound state are defective in secretion (Walworth et al. 1992; Gao et al. 2003). Thus Sec4 action requires active cycling between the GTP and GDP-bound states.

The motive force for the transport of secretory vesicles along actin cables is supplied by the class V myosin Myo2, which is complexed to its regulatory light chain Mlc1 (Schott et al. 1999). Both Myo2 and Mlc1 show polarised localisation to sites of growth. Genetic and biochemical evidence suggest that Myo2, Mlc1, Sec2, Sec4 and Ypt31/Ypt32 interact on secretory vesicle membranes, resulting in the activation of Myo2 (Bielli et al. 2006). Once vesicles have docked with the exocyst, vesicle fusion with the plasma membrane is mediated through the interaction of the v-SNARE, Snc1, and the t-SNARE consisting of Sso1 or Sso2 complexed to Sec9, a process that is facilitated by Sec1 (for a review, see Pelham 2001). Docking and fusion of secretory vesicles involves the formation of a ternary complex consisting of one α helix from Snc1, one

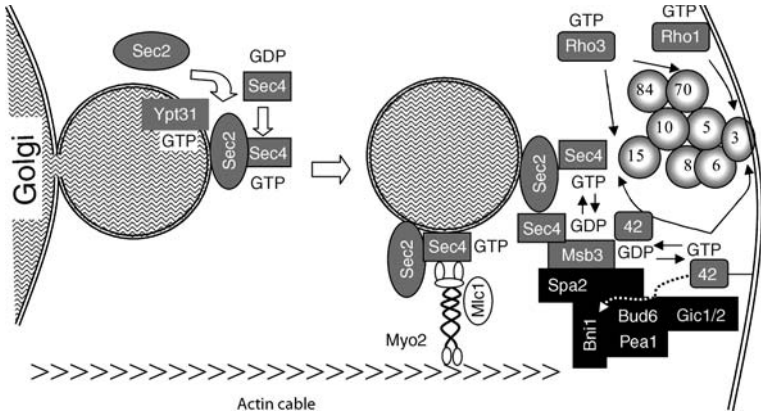

Fig. 6.4. Polarised secretion. Secretory vesicles are transported from the Golgi to dock with the exocyst (*grey spheres*) along actin cables nucleated by the polarisome (*black boxes*). Exit from the Golgi depends upon Ypt31-dependent loading of Sec2 onto secretory vesicles. In turn, Sec2 activates Sec4. The motive force for vesicle movement is provided by Myo2/Mlc1, which forms a complex with Sec2/Sec4 on the surface of the secretory vesicle. Docking of secretory vesicles with the exocyst involves the interaction of Sec4 with exocyst component Sec15. Rho1-GTP co-operates with Cdc42-GTP to localise the exocyst landmark, Sec3. Rho3-GTP co-operates with Cdc42-GTP to promote docking of secretory vesicles. Msb3 provides a connection between the exocyst and the polarisome and also tethers Cdc42-GDP to sites of polarised growth to provide a pool ready to be reactivated to the GTP-bound form. *Numbers* in the exocyst are abbreviations for Sec components, e.g. Sec3 etc, exceptions 70 Exo70, 42 Cdc42

α helix from Sso1 or Sso2 and two α helices from Sec9. Homologues of the Sso1/2 t-SNARE have also been shown to be essential for polarised growth of *Neurospora crassa* hyphae. Polarised localisation of Sec4 occurs at the restrictive temperature of a *sec9* temperature-sensitive (ts) mutation, so vesicle fusion is thought to be downstream from vesicle docking (Walch-Solimena et al. 1997).

V. Rho-type GTPases

Polarised growth in fungi is dependent on a number of different small GTPases of the Rho-Rac family. In *Sac. cerevisiae*, many of the processes of polarised growth including nucleation of actin cables and cortical patches, docking of secretory vesicles with the exocyst and their fusion with the plasma membrane, and formation of the septin ring are orchestrated by the Rho-type GTPase Cdc42 (Hartwell et al. 1974; Johnson and Pringle 1990; Adams et al. 1990a; Johnson 1999; Etienne-Manneville 2004). *cdc42* ts mutants arrest as large multinucleate, unbudded cells with a completely depolarised actin cytoskeleton and random distribution of chitin (Hartwell et al. 1974; Adams et al. 1990b). The continued isotropic growth of these cells suggests that Cdc42 is essential for bud formation and polarised growth, but not for isotropic growth. A similar phenotype is seen in ts mutants of *CDC24* that encodes the activating Cdc24 GEF (see below).

The homologues of Cdc42 and Cdc24 have been found to be essential in all fungi examined to date, including *C. albicans* (Ushinsky et al. 2002; Bassilana et al. 2003), *Ash. gossypii* (Wendland and Philippsen 2001), *Sch. pombe* (Miller and Johnson 1994) and *P. marneffei* (Boyce et al. 2001). In *C. albicans* a low level of expression from the regulatable *MET3* promoter showed that a low level of Cdc42 that was sufficient for viability, was insufficient to sustain hyphal growth – indicating that more Cdc42 is required for the polarised growth of hyphae compared to yeast (Bassilana et al. 2003). Moreover, in *C. albicans* Cdc42 and Cdc24 were shown to be required for the expression of hyphal specific genes (Bassilana et al. 2005). In *P. marneffei* expression of a dominant negative allele resulted in a loss of polarity in both hyphal and yeast forms (Boyce et al. 2001). Thus Cdc42 has conserved and essential roles in orchestrating polarised growth in fungi.

Other Rho-GTPases also play essential roles in polarised growth. In *Sac. cerevisiae*, Rho1 plays multiple roles in cell integrity and polarised growth including:

- the activation of Pkc1, the upstream activator of the cell-integrity MAP kinase pathway (Nonaka et al. 1995),
- acting through Pkc1 to re-polarise actin after a shift to 37 °C (Nonaka et al. 1995; Kohno 1996; Schmidt et al. 1997; Drgonova et al. 1999),
- the activity of β(1-3)-D-glucanase, which synthesises a major component of the cell wall (Drgonova et al. 1996; Qadota et al. 1996),
- together with Cdc42, Rho1 localises the exocyst landmark protein, Sec3 (Guo et al. 2001; Zhang et al. 2001).

In *Sac. cerevisiae* Rho3 promotes the localisation of the exocyst component Exo70 and the fusion of secretory vesicles with the exocyst, a role it shares with Cdc42 (Adamo et al. 2001). Rho3, together with Rho4 also acts on the formins to polarise the actin cytoskeleton (Dong et al. 2003). In *Ash. gossypii* loss of the Rho3 homologue results in a severe defect of polarised growth in which growth of the hyphal tips becomes isotropic, resulting in swollen tips. Polarised growth often re-initiates at these tips, but with a different axis from that of the initial hypha (Wendland and Philippsen 2001).

There are no members of the Rac GTPase family in *Sac. cerevisiae*. However, Rac-type GTPases have been identified in *C. albicans* and *P. marneffeii*. In *C. albicans* loss of Rac1 has a subtle phenotype, affecting hypha formation only when induced by growth when embedded in matrix (Bassilana and Arkowitz 2006). In *P. marneffeii* loss of the Rac GTPase, CflB, results in a defect in hyphal growth and an inability to undergo the developmental program leading to conidiation (Boyce et al. 2003).

A. Activation of Cdc42

Rho-GTPases act as molecular switches that cycle between a GDP-bound off-state and a GTP-bound on-state (Fig. 6.5). In *Sac. cerevisiae*, Cdc42 is activated to its GTP-bound state by its GEF Cdc24 and returned to its inactive GDP-bound state by the GTPase activating proteins (GAPs) Rga1, Rga2 and Bem3 (Zheng et al. 1994; Stevenson et al. 1995; Smith et al. 2002; Caviston et al. 2003). To be active, Cdc42 is attached to the inner surface of the plasma membrane (and possibly

other membranes) through prenylation at its C-terminus. Further regulation of Cdc42 may be imposed by the Rho-guanine dissociation inhibitor (Rho-GDI), Rdi1. Rho-GDIs extract their targets from membranes and maintain them in the cytosol, block the dissociation of GDP necessary for the exchange of GDP for GTP and may interfere with association of the GTPase with its targets (DerMardirossian and Bokoch 2005). Rdi1 is the only *Sac. cerevisiae* GDP Rho-GDI and it co-immuneprecipitates with both Cdc42 and Rho1, so it may regulate both of these GTPases. However, its deletion has no obvious phenotypic effects (Masuda et al. 1994; Koch et al. 1997).

Sac. cerevisiae cells show a unique axis of polarisation. In the budding cycle a single bud emerges and subsequent growth is confined to this bud (Fig. 6.3). Upon pheromone stimulation a single mating projection forms. Although upon prolonged exposure more than one mating projection may form, only one will exhibit active growth. Thus there is a unique axis of polarisation, which is determined by local Cdc42 recruitment and activation, in response to internal cues that dictate the location of the incipient bud site and the formation of primary and secondary septa, or external cues such as the formation of a mating projection.

In budding yeast cells Cdc42 localisation sites are marked by the cortical landmarks that result from bud site selection pathways (Chant 1999; Pruyne and Bretscher 2000b; Casamayor and Snyder 2002; Chang and Peter 2003; Pruyne et al. 2004; Fig. 6.6). In haploid yeast cells bud emergence follows an axial pattern where each generation of daughter buds form at a site adjacent to the previous bud scar (Fig. 6.7). The septin ring that remains after the previous division recruits Bud3, Bud4 and Bud10 that serve as cortical landmarks for bud emergence. In diploid cells, bud emergence follows a bipolar budding pattern where daughter cells bud at the pole distal to their birth pole while mother cells can bud at either pole. Null alleles in the genes encoding these cortical landmarks result in corresponding changes in the budding pattern. Thus mutations in septins and *bud3*, *bud4*, and *axl2* (*bud10*) alleles result in haploid cells showing a bipolar budding pattern. Diploid *bud8*Δ/Δ cells bud only from the pole distal from the birth scar, while *bud9*Δ/Δ diploids bud only from the proximal pole. Both the axial and bipolar cortical landmarks localise Bud2 and Bud5 which are the GAP and GEF, respectively, for the Rsr1 (Bud1) GTPase and which is thus locally activated (Fig. 6.6A; Zheng et al. 1995; Park et al. 1997, 1999, 2002). The effector domain of Rsr1 binds

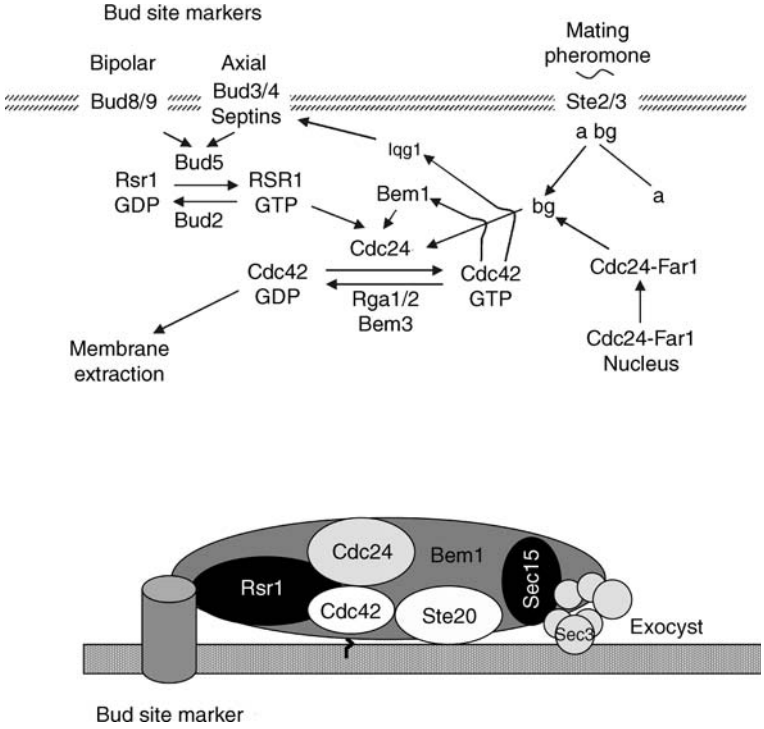

Fig. 6.5. Activation of Cdc42. *Top* Circuits controlling Cdc42 activity. During budding, axial and bipolar bud site selection proteins localise Bud5 and Bud2, which localise and activate the small GTPase Rsr1 (also known as Bud1). Rsr1 localises Cdc24 which activates Cdc42. Bem1 provides a scaffold for the Cdc24/Cdc42 interaction and is itself a downstream effector of Cdc42. When mating pheromone interacts with the 7-transmembrane surface receptor, the trimeric β protein complex dissociates into a βγ dimer and α subunit. The βγ dimer localises Cdc24-Far1 which is released from the nucleus as a result of the action of the MAP kinase signalling pathway (see Fig. 6.8). The return of Cdc42 to the GDP bound form is mediated by the GAPs Bem3 and Rga1/2. The Rho-GDI, Rdi, may maintain Cdc42 in the GDP-bound state and extract Cdc42 from membranes where it is active. *Bottom* Bem1 acts as scaffold protein for the formation of a Cdc42-activating complex on the inner side of the plasma membrane

to the C-terminal of Cdc24 in a GTP-dependent manner. However, the GDP-bound form of Rsr1 interacts with Bem1. Thus, cycling of Rsr1 between GDP and GTP-bound states may be important for its function (Park et al. 1997). The C-terminus of Cdc24 contains an auto-inhibitory domain that is thought to be relieved upon Rsr1 binding (Shimada et al. 2004). In this way Rsr1 localises and activates Cdc24, which in turn activates Cdc42. Rsr1 also physically interacts directly with Cdc42 (Kozminski et al. 2004). Furthermore, Bem1 is an effector for Cdc42, and *bem1*Δ and *rsr1*Δ alleles are synthetically lethal. Finally, Bem1 interacts physically with the exocyst component Sec15 (France et al. 2006). Taken together these observations suggest that Bem1 acts as scaffolding protein for the formation of a Cdc42-activating complex at the cell cortex, which is located by bud site selection markers and may interact with the exocyst (Fig. 6.5B).

In the absence of bud site selection markers buds still emerge, but in a random fashion. In this situation, Cdc42 is evenly located around the cell cortex. However, local stochastic variations in Cdc42 activity are amplified in a self-sustaining feedback loop that results in a signal strong enough to bring about bud emergence. There may be two separate processes both of which operate in a robust feedback circuit (Fig. 6.7 Wedlich-Soldner et al. 2004). One is actin-dependent and is specific to Cdc42 loaded with GTP (Wedlich-Soldner et al. 2003); the other is Bem1-dependent and actin-independent (Irazoqui et al. 2003). The actin-dependent feedback loop is thought to promote the long-term stability of polarisation because Cdc42-GTP activates the nucleation of actin cables and, independently, promotes the formation of the exocyst and the docking of secretory vesicles to the exocyst (see below). Since Cdc42 transport to the cortex is dependent on actin cables and a functioning secretory pathway (Zajac et al. 2005), this results in further delivery of Cdc42 to the local site where Cdc42 was first activated. However, endocytosis, promoted by actin cortical patches, acts to disperse Cdc42 polarity. As a result patches of polarised Cdc42 move around the cortex before bud emergence in the absence of Rsr1 (Irazoqui et al. 2005; Ozbudak et al. 2005).

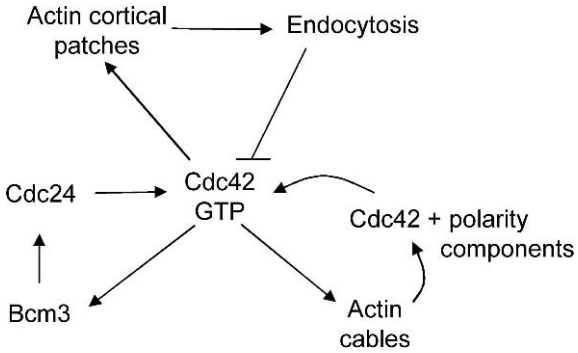

Fig. 6.7. Cdc42 feedback loops. Locally elevated Cdc42-GTP levels, arising by stochastic variation, activate Bem3 which in turn localises Cdc24 to mediate the formation of Cdc42-GTP. Over a longer time-scale, Cdc42-GTP also promotes formation of actin cables and activation of the exocyst, leading to the delivery of more Cdc42 and further polarity components which nucleate more actin cables. The cycle of Cdc42 activation is eventually interrupted by the formation of actin cortical patches, leading to endocytosis of Cdc42

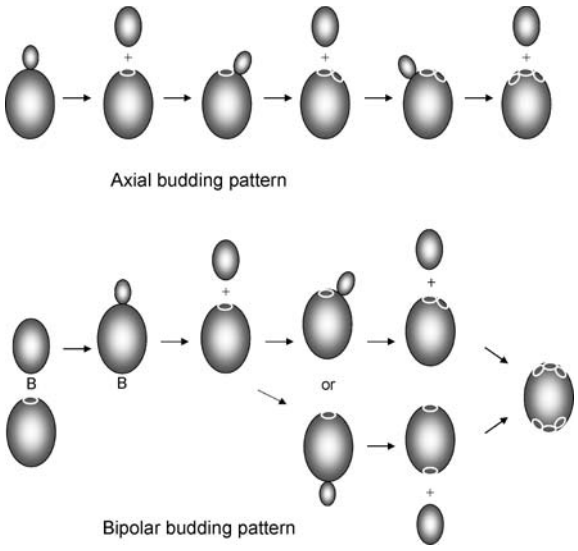

Fig. 6.6. Bud site selection in *Sac. cerevisiae*. *Top* Axial budding pattern in haploids. When the daughter bud separates, it leaves a bud scar on the mother cell (*white circle*). The next bud forms adjacent to this bud scar. After several cell cycles bud scars accumulate at one pole of the cell. *Bottom* Bipolar budding. The first bud to appear on a daughter cell forms at the pole opposite the birth pole (*B*). Subsequent buds can appear at either pole resulting in bud scars accumulating at both poles

The symmetry-breaking role of Bem1 occurs because Bem1 not only acts as a scaffold for Cdc24 to activate Cdc42, but also acts as an effector for activated Cdc42 (Peterson et al. 1994; Bose et al. 2001). Bem1 also physically interacts with the exocyst and so may link the two arms of the feedback process (Zajac et al. 2005; France et al. 2006). Thus Cdc42 is already primed to activate polarised growth and, rather than being absolutely required, the localisa-

tion cues influence this activation to take place at a specific site.

Haploid cells respond to the presence of the cognate mating pheromone by formation of a mating projection. Polarised growth directed against the gradient of mating pheromone allows cells of opposite mating type to meet, fuse and generate a diploid cell (Bücking-Throm et al. 1973; Segall 1993). The mating pheromone interacts with a G protein-coupled 7-transmembrane receptor protein encoded by *STE2* in a-mating type cells and *STE3* in α-mating type cells (Fig. 6.8; for reviews, see Kurjan 1993; Leberer et al. 1997a; Bardwell 2005). Upon interaction of the receptor with its ligand, the tripartite G protein complex dissociates, resulting in a free α subunit and a βγ heterodimer. Consequently, three major cellular responses are initiated: arrest of the cell cycle in G1, activation of transcription program and mating projection formation. The transcriptional program and the G1 arrest result from the activation of a MAP-kinase cascade. G1 arrest results from the phosphorylation of Far1 by the MAP kinase Fus3. Far1 then interacts with and inhibits the Cln2-Cdc28 kinase which is required for initiating the mitotic cell cycle and thus causing cell cycle arrest (Peter et al. 1993; Peter and Herskowitz 1994). However, Far1 is a bi-functional protein that also plays a role in polarised growth (Valtz et al. 1995). It tethers Cdc24 in the nucleus. Upon phosphorylation by Fus3, the Far1-Cdc24 complex leaves the nucleus in an Msn5-dependent fashion (Shimada et al. 2000). Far1 then interacts with the βγ dimer which has remained in the vicinity of the activated pheromone receptor (Valtz et al. 1995; Nern and Arkowitz 1999; Wiget et al. 2004). In this way Cdc24 is recruited to the site of pheromone receptor stimulation to activate Cdc42 and initiate polarised growth. Far1 also tethers Cdc24 in the nucleus during G1 of the budding cycle. Phosphorylation of Far1 by the activated Cln-Cdc28 kinase results in its destruction and release of Cdc24 into the cytoplasm where it is free to be recruited to the incipient bud site by the bud-site selection pathway described above (Shimada et al. 2000). Thus the action of Far1 potentially provides a mechanism not only for the initiation of polarised growth upon activation of the Cln1/2-Cdc28 kinase in G1 but also for how polarised growth is re-directed from the incipient bud site to the site of pheromone receptor activation. However, a major problem with this scenario is that Far1 is not expressed in a/α diploid cells. Thus, the main role of Far1 in haploid cells may be to allow the site of polarised growth to be determined according to the presence or absence of mating pheromone. Originally it was thought that the α subunit of the G protein complex was not active, once dissociated from the βγ subunits. However, it is now known that it associates with activated Fus3 to phosphorylate Bni1 (Metodiev et al. 2002; Matheos et al. 2004). This may provide an additional pathway to direct polarised growth to the site of pheromone activation.

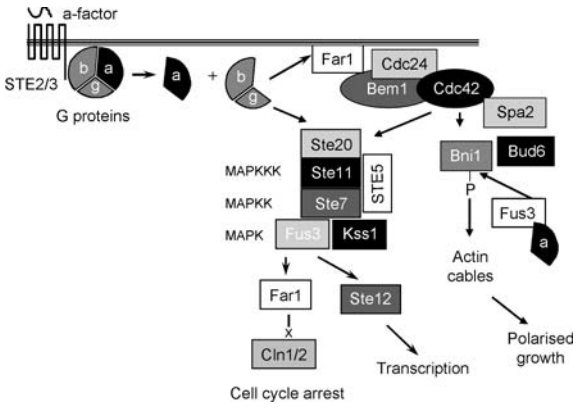

Fig. 6.8. The mating pheromone signal transduction pathway. The βγ dimer, which is released upon mating pheromone interaction with the cognate receptor, recruits and activates Cdc42. This results in the activation of a MAP kinase module through the Cdc42 effector, Ste20. Activated Fus3 MAP kinase activates the Ste12 transcription factor resulting in a transcription program necessary for mating. Fus3 also phosphorylates Far1 which has two roles: (1) it binds and inhibits Cln2-Cdc28 to arrest the cell cycle and (2) it escorts Cdc24 from the nucleus to the βγ dimer at the cell cortex, where it converts Cdc42 to the GTP-bound form. Cdc42-GTP nucleates the formation of actin cables, resulting in polarised growth

B. Cdc42 Structure and Mutations

The structure of Cdc42 and the effect of a large number of Cdc42 point mutations has been reviewed in detail (Johnson 1999). Cdc42 is a member of the Ras superfamily of small GTPases with significant homology to the Ras oncogene. Proteins in this family have a mass of 21 kDa, contain four short blocks of highly homologous sequences implicated in GTP binding and hydrolysis, a 25-residue domain that interacts with effectors, a 10-residue insert that distinguishes Rho-GTPases from Ras-GTPases and a C-terminal sequence required for attachment to the inner leaflet of the plasma membrane by prenylation. The X-ray struc-

ture of the human Cdc42 homologue shows that the effector or switch domain covers a large part of one face of the molecule and provides the surface for interaction with various Cdc42 effectors. Mutations that convert the *H-ras* proto-oncogene into an oncogene decrease the rate of GTP hydrolysis and so lock the protein into the GTP-bound conformation. Corresponding mutations in yeast Cdc42 (*CDC42* G12V, *CDC42 G61L*) are dominant lethals. When conditionally expressed from the GAL promoter, cells become large and multi-budded with aberrant cortical actin structures, showing that constitutive stimulation of polarised growth cannot be tolerated. The H-ras D119A mutation is also oncogenic, but for a different reason – it increases the rate of GDP dissociation. The corresponding yeast Cdc42 D118A is also a dominant lethal, but the terminal phenotype is that of large unbudded cells similar to *cdc42* ts null alleles. It is assumed that this mutant sequesters, but does not activate downstream effectors. Mutations that affect the effector domain allow the different Cdc42 functions to be genetically separated from its function in polarising the actin cytoskeleton (Gladfelter et al. 2001a). For example, *cdc42-20t* and *cdc42-13* specifically affect the localisation of the exocyst landmark Sec3 (Zhang et al. 2001), *cdc42-6* specifically affects the docking of secretory vesicles with the exocyst (Adamo et al. 2001) and *cdc42 V36T*, *K94E* and $cdc42^{Y32H}$ disrupt the organisation of the septin ring (Gladfelter et al. 2002).

C. Cdc42 Effectors

Activated Cdc42 mediates a wide variety of functions involved in polarised growth through its interaction with a number of downstream effectors (Fig. 6.9). These effectors often have a conserved CDC42/Rac interactive binding (CRIB) domain which interacts with Cdc42-GTP (Burbelo et al. 1995). A major role of Cdc42 is the polarisation of the actin cytoskeleton in which separate pathways promote the formation of both actin cortical patches and actin cables. In addition, Cdc42 is required for the formation of septin rings and directly promotes the formation of the exocyst and the docking and fusion of secretory vesicles. These additional roles of Cdc42 can be genetically separated from each other and from its role in actin polarisation by specific point mutations in the effector domain which specifically affect one function while leaving others unaffected.

1. The Polarisome

A cap of proteins, known as the polarisome, consists of Bni1, Spa2, Bud6 and Pea1 and localises to a surface crescent at the incipient bud site and to the tip of small buds (Snyder 1989; Sheu et al. 1998; see also Chap. 5 in this volume). Spa2, Bud6 and Pea1 co-sediment as a 12s complex upon sucrose density centrifugation. Spa2 interacts physically and genetically with other members of the polarisome as well as proteins such as Rho1, Slt2, Msb3/Msb4 and Gic1/Gic2 (see below) and possibly others (Fujiwara et al. 1998; Jaquenoud and Peter 2000; Tcheperegine et al. 2005). Spa2 may therefore act as a scaffold. During cytokinesis, the polarisome relocates to the bud neck followed by formation of the secondary septa. The polarisome is also present at the tips of mating projections.

The polarisome is believed to link Cdc42 signalling to the assembly of actin cables. Loss of polarisome components causes defects in polarised growth and also disrupts bipolar bud site selection (Sheu et al. 2000). The polarisome is required for the action of Bni1 and Bnr1, members of the evolu-

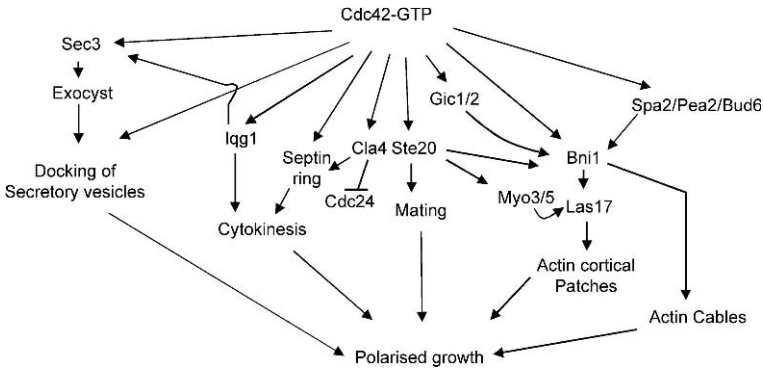

Fig. 6.9. The downstream effectors of activated Cdc42. Cdc42-GTP activates docking of secretory vesicles with the exocyst, the formation of the septin ring, the PAK kinases Cla4 and Ste20, Gic1/Gic2, the polarisome and Bni1. The combined action of these effectors results in polarised growth

tionarily conserved formin family of proteins that mediate the formation of actin cables and cortical patches (Lechler et al. 2001; Sagot et al. 2002; Evangelista et al. 2002). Bni1 interacts physically with Cdc42, Rho1, Bud6 and Spa2. Bni1 localises to the tip of young buds and shmoos, and relocates to the actomyosin ring during anaphase (Evangelista 1997; Imamura 1997). It plays multiple roles in polarised growth, in bud site selection and in cytokinesis where it is required for the contraction of the actomyosin ring. Bnr1 interacts with Rho4, but not with Cdc42 or other GTPases (Imamura 1997), and with Hof1, a protein required for cytokinesis. Bnr1 localises to the mother side of the bud neck throughout the cell cycle and functions primarily in cytokinesis. However, there is clearly some overlap as *bni1*Δ is synthetically lethal with *bnr1*Δ. A *bni1*Δ *bnr1*Δ mutant is defective in cytokinesis and completely lacks actin cables (Vallen et al. 2000; Sagot et al. 2002; Evangelista et al. 2002). The two formin proteins contain a region called the GTPase binding domain (GBD) through which they interact with Cdc42. In addition, two formin homology domains, FH1 and FH2, and a regulatory region called the dia-autoinhibitory domain (DAD) are present in the C-terminal portion of the protein (Evangelista et al. 2003). Interaction of Bni1 with activated Rho-GTPase disrupts an inhibitory intramolecular interaction between the DAD and GBD domains and opens the formin to an active form (Alberts 2001). Activated Bni1 together with Bud6 and Pfy1 (profilin), which is an actin monomer binding protein, nucleates actin cables in vitro and a detailed molecular mechanism for this reaction has now been described (Moseley et al. 2004). Bni1 localises to the bud tip during polarised growth through interactions with the polarisome component Spa2 (Evangelista 1997; Sheu et al. 1998). This localisation is Cdc42-dependent, but still occurs in the absence of the GBD domain (Jaquenoud and Peter 2000; Ozaki-Kuroda et al. 2001). Thus, while Cdc42 directly interacts with Bni1 to activate the nucleation of actin cables, the influence of Cdc42 on Bni1 localisation is probably indirect and occurs through the Cdc42-dependent formation of the polarisome.

As well as displaying synthetic lethality with *bni1*Δ, loss of Bnr1 function is synthetically lethal with loss of Myo1 which, together with actin, forms the contractile actomyosin ring that guides the formation of the primary septum (Vallen et al. 2000). An attractive model is that Bnr1 nucleates actin cables that are necessary for polarised growth – which, in turn, is necessary for the formation secondary septa – while Bni1 is necessary for the contraction of the actomyosin ring. As the bud neck is narrow, secondary septa may still form despite defects in the actomyosin ring. However, this cannot occur if secondary septa formation is also compromised by loss of Bnr1.

2. Arp2/3

Formation of actin cortical patches is nucleated by a dimer of two actin-related proteins, Arp2/3. The Arp2/3 dimer is activated by a complex consisting of Las17 (Bee1), Vrp1 and the type I myosins Myo3 and Myo5 (Lechler and Li 1997; Naqvi et al. 1998; Lechler et al. 2000, 2001; Pruyne and Bretscher 2000a). Las17 is the yeast homologue of the human Wiskott–Aldrich syndrome protein, WASP. Vrp1 is a proline-rich protein known as verprolin, which is a homologue of the mammalian WASP-interacting protein (WIP). Las17 does not appear to interact directly with Cdc42 and it does not contain a CRIB domain, unlike the mammalian WASP. Instead, Vrp1 and Las17 form a stable complex that is recruited to sites of activated Cdc42 through a stable interaction with the formin Bni1. Myo3 and Myo5 interact with the Las17-Vrp1 complex upon phosphorylation by the p21 activated kinases (PAKs) Cla4 and Ste20 (see below; Wu et al. 1997). Thus Myo3/5 recruitment is indirectly dependent on activated Cdc42.

3. PAK Kinases

Cdc42 interacts with and activates a pair of related kinases called Ste20 and Cla4 which show homologies with a family of mammalian p21 activated kinases (PAK). Ste20 was isolated as a multi-copy suppressor of a null allele of *STE4* which encodes the β subunit of the trimeric G protein complex (Leberer et al. 1992). *CLA4* was identified in a synthetic lethal screen with a *cln1*Δ *cln2*Δ mutant (Cvrckova et al. 1995). Both kinases localise to sites of polarised growth in a Cdc42-dependent fashion (Cvrckova et al. 1995; Peter et al. 1996). They each have separate identifiable functions, but a *cla4*Δ *ste20*Δ mutant is non-viable, implying that they are redundant for an essential function. Both proteins have a kinase domain in the C-terminal portion of the protein. In the N-terminal extension to the kinase domain there is a conserved CRIB domain which is also found in the PAK family. The CRIB domain of Ste20 is essential for polarised localisa-

tion and for the essential function shared with Cla4 (Peter et al. 1996; Leberer et al. 1997b).

Ste20 functions in the pheromone response signalling pathway, activating Ste11 which is a mitogen-activated protein (MAP) kinase kinase kinase. Elements of the signalling pathway, including Ste20, are also required for pseudohyphal formation and invasive growth of haploids (Liu et al. 1993). The kinase domain is required for its role in signalling. The CRIB domain is auto-inhibitory and its negative effect on kinase activity is relieved by Cdc42-GTP binding. Cla4 phosphorylates septins (Versele and Thorner 2004). In the absence of Cla4, septin bars form rather than a true ring – a phenotype that is enhanced when a *cla4*Δ mutation is combined with *gin4*Δ and/or *nap1*Δ alleles (Longtine et al. 2000). Cla4 also acts in a negative feedback loop to down-regulate Cdc42 activity. Its activity peaks just after bud emergence, presumably through the action of Cdc42. However, once activated Cla4 phosphorylates and inactivates Cdc24 (Gulli et al. 2000).

The essential functions shared between Cla4 and Ste20 may involve polarisation of both actin cortical patches and cables. As described above, phosphorylation of Myo3/Myo5 is required for the formation of actin cortical patches. Polarisome function and activation of Bni1 are also dependent on phosphorylation by one of the PAKs (Goehring et al. 2003). This conclusion was suggested by a synthetic lethal screen initiated with a *cla4*Δ mutant. Two independent screens identified mutations in genes encoding the polarisome components Spa2, Bud6 and Pea1. Moreover, Bni1 is phosphorylated in vivo and this phosphorylation is reduced, but not abolished, in a *ste20* mutant. Interestingly, the systematic genome-wide screen for mutations that are synthetically lethal with *cla4*Δ identified mutations in 65 different genes mediating a variety of cell functions. In contrast, a screen for mutants that are lethal with *ste20*Δ identified only *CLA4*. Thus, Cla4 may be involved in a wider range of other cell functions than Ste20.

4. Gic1 and Gic2

Gic1 and Gic2 are a pair of redundant proteins that interact through a CRIB domain with Cdc42 specifically in its GTP-bound form (Chen et al. 1997; Brown et al. 1997). *Gic1*Δ *gic2*Δ cells are nonviable at 37 °C, arresting with completely depolarised actin cytoskeletons similar to the phenotype of ts *cdc42* alleles at the restrictive temperature. Since Gic2 localises to presumptive bud sites slightly before polarisome components and is synthetically lethal with *bni1*Δ, one might suggest that they constitute a parallel pathway for the formation of actin cables (Bi et al. 2000; Tcheperegine et al. 2005). However, the demonstration of extensive physical and genetic interactions with other polarisome components led to an alternative hypothesis – that the polarisome, Bni1 and Gic1/2 associate together to form a large complex that mediates the formation of actin cables (Jaquenoud and Peter 2000).

5. Iqg1

Iqg1 shows homology to the mammalian IQGAP family. It contains an N-terminal calponin homology domain that binds actin, followed by a region that binds calmodulin, multiple IQ motifs that bind Mlc1 and a GAP domain that shows a two-hybrid interaction with Cdc42-GTP (Lippincott and Li 1998; Osman and Cerione 1998; Osman et al. 2002). Iqg1 is required for the formation of the contractile actomyosin ring, where it is recruited by Mlc1 and in turn recruits actin to the ring (Lippincott and Li 1998; Boyne et al. 2000; Shannon and Li 2000). Iqg1 also plays a role in the establishment of bud site and polarised growth. It physically interacts with the axial bud site marker Bud4, the exocyst landmark protein Sec3 and it helps localise the septin Cdc12 (Osman et al. 2002). These diverse interactions suggest that Iqg1 serves to co-ordinate the polarised secretion necessary for bud growth and formation of the secondary septum, with the establishment and maintenance of landmark proteins necessary to specify where this secretion should occur.

6. Msb3 and Msb4

Msb3 and Msb4 are multi-copy suppressors of *cdc24* and *cdc42* ts mutations required for actin polarisation (Bi et al. 2000). They also act as GAPS for Sec4 and this activity is necessary for efficient exocytosis (Albert and Gallwitz 2000). They interact with Cdc42 but, unusually for Cdc42 effectors, the specificity is for the GDP-bound form of Cdc42 (Tcheperegine et al. 2005). Msb3/Msb4 localise to regions of polarised growth by binding directly to the N-terminal region of Spa2; *msb3*Δ *msb4*Δ alleles show a moderate defect in polarised growth and are synthetically lethal with *gic1*Δ

*gic2*Δ alleles. These diverse interactions lead to a model in which Msb3/Msb4 links the polarisome and exocyst complexes. First, Msb3/Msb4 facilitate exocytosis by the cycling of Sec4 between GTP and GDP-bound forms. Second, it tethers Cdc42-GDP to Spa2 where it can be locally activated to the GTP-bound form. The activated Cdc42-GTP then activates Bni1, which is also bound to Spa2, resulting in the nucleation of actin cables.

7. Septins

Septin recruitment to a patch at the incipient bud site is a Cdc42-dependent process (Pringle et al. 1995). The role of Cdc42 in septin recruitment can be genetically separated from the role of Cdc42 in polarisation of the actin cytoskeleton by point mutations in the effector domain that specifically affect the formation of the septin rings, leaving actin polarisation apparently unaffected (Gladfelter et al. 2002; Caviston et al. 2003). One of these mutations, $Cdc42^{V36T,K94E}$, resulted in an altered Cdc42 protein that had 40% less intrinsic GTPase activity (Gladfelter et al. 2002). In this mutant septin rings were wider than normal and in some cells formed in ectopic positions. This phenotype was rescued by overexpression of the GAP protein Rga1. In a separate study, overexpression of Rga1 was found to rescue the septin defect of a ts *cdc12-6* allele. In cells lacking all Cdc42 GAPs, septin ring formation was severely disturbed (Caviston et al. 2003). Abnormal septin structures formed at the bud neck and septin caps were present at the tips of highly elongated, tube-like buds that lacked the normal constriction at the bud neck. True septin rings often eventually formed. Growth of the bud distal to these rings was more isotropic. Taken together, the observations described above suggest that Cdc42 GAPs have positive roles in septin ring formation, even though GAPs are normally considered as negative regulators of GTPases. Two explanations are advanced for this unexpected conclusion. First, Cdc42 cycling between GTP- and GDP-bound forms may be required for proper septin ring formation (Gladfelter et al. 2002). Second, besides acting to regulate Cdc42, GAPs may participate directly in the formation of septin rings (Caviston et al. 2003). These explanations are not mutually exclusive.

The observation that the presence of the septin ring is necessary for the normal swelling of the yeast bud, away from the bud neck led to the suggestion that septins can act as a focus for polarised growth (Gladfelter et al. 2005). If this is the case, then the septin cap that is present at the tips of *C. albicans* germ tubes may play a role in directing their intensely polarised growth. Furthermore, septin rings that form along the length of germ tubes do not result in a swelling. Thus, there must be an important difference in the properties of septin rings at the bud neck of yeasts and pseudohyphae, compared with hyphae.

8. Secretory Vesicles and the Exocyst

Localisation of exocyst components, such as Sec15, depend on actin cables and their localisation is thus indirectly dependent on Cdc42 (Zajac et al. 2005). Cdc42, together with the Rho-GTPases Rho1 and Rho3, also act to promote exocytosis directly through two further processes, which are independent of actin cable formation. First, Cdc42 and Rho1 physically interact with an N-terminal domain of Sec3 to promote its localisation (Zhang et al. 2001). Second, Cdc42 and Rho3 promote the fusion of secretory vesicles with the exocyst (Adamo et al. 2001). Cdc42 acts mainly in small buds, while Rho3 acts in large buds. Rho3-GTP interacts with the exocyst component Exo70; and mutants defective in this interaction show that it is necessary for the promotion of vesicle fusion (Roumanie et al. 2005).

VI. The Spitzenkörper

The previous sections describe our increasingly detailed knowledge of the molecular mechanisms of polarised growth in budding yeast cells. However, a problem remains in that the rate of tip extension in a fungal hypha can be up to two orders of magnitude greater than the rate of bud growth (see Introduction). Clearly, while the yeast paradigm is a powerful model for the study of fungal growth, it cannot provide the full picture. An essential difference in the hyphal form of cell expansion is reflected by the presence of a structure called the Spitzenkörper at the tips of hyphae, which is not present in vegetative yeast buds. A full description of Spitzenkörper structure is presented elsewhere in this volume (Chaps. 1, 5, 11). It was first identified as a dark spot in phase contrast microscopy at the tips of the hyphae from a wide variety of fungal species (Brunswick 1924; Girbardt 1957). Subsequent ultrastructure studies showed that it was rich in microfilaments, ribosomes, secretory vesicles and chitosomes (Girbardt 1969; Grove and

Bracker 1970; Grove et al. 1970; Bracker et al. 1976; Howard and Aist 1980; Howard 1981). However, it not is a discrete membrane-bound organelle and can be highly dynamic in its structure (Fischer-Parton et al. 2000).

The Spitzenkörper can be conveniently visualised using fluorescence microscopy following a brief pulse of FM4-64 (Fischer-Parton et al. 2000). This amphiphilic styryl dye is usually used as a marker of endocytosis and vacuolar membranes (see Chaps. 1 and 2 in this volume). However, with brief treatment, the Spitzenkörper is visualised as a spot at the hyphal tip before the vacuoles become visible (Fig. 6.10). This probably comes about through endocytic vesicles being re-sorted to the secretory pathway (Read and Hickey 2001). Fig. 6.11A shows the use of FM4-64 staining in *N. crassa* to visualise the Spitzenkörper. Recently, the presence of a Spitzenkörper in *C. albicans* was revealed by FM4-64 staining and by localisation of Mlc1-YFP to a sub-apical spot (Fig. 6.11C; Crampin et al. 2005).

A model for the role of the Spitzenkörper in polarised growth of hyphae has been elaborated in which it acts as a vesicle supply centre to focus the supply of the secretory vesicles to the hyphal tip (Bartnicki-Garcia et al. 1989; Gierz and Bartnicki-Garcia 2001; Fig. 6.12). According to this model secretory vesicles are manufactured throughout the hyphal cytoplasm and transported to the Spitzenkörper, where they accumulate.

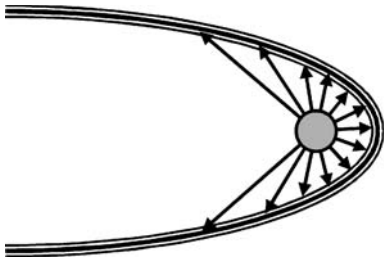

Fig. 6.10. The vesicle supply centre model for the action of the Spitzenkörper. If vesicles exit the Spitzenkörper in every direction equally, a greater concentration per unit area encounters the tip than subapical regions. This results in the characteristic shape of the hyphal tip

From the Spitzenkörper they radiate out in all directions at equal velocities to fuse with the plasma membrane. A greater number of vesicles per unit surface area per unit time fuse with the hyphal apex, compared with subapical regions. If the Spitzenkörper moves forward with a constant velocity, a simple mathematical model predicts that this generates a hyphoid curve that recapitulates the characteristic shape of hyphal tips. This model successfully predicts the dimensions of hyphae and a computer program, Fungus Simulator, allows the path of hyphal growth to be predicted from the position of the Spitzenkörper (Bartnicki-Garcia et al. 1995).

This model has been successfully tested in a number of studies. First, the growth of

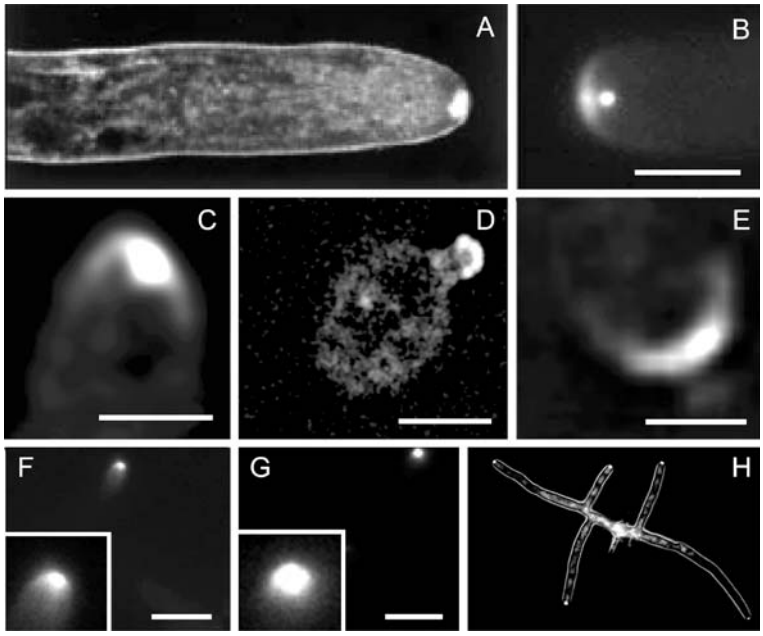

Fig. 6.11. Images of the Spitzenkörper and localisation of polarity proteins. **A** FM4-64 localises to an apical spot in the hyphae of *N. crassa*. **B–D** SepA (**B**) and Mlc1-YFP (**C**) localise to an apical spot and surface crescent in *N. crassa* and *C. albicans* hyphae respectively. **D, E** Mlc1-YFP localises to a surface crescent in *C. albicans* yeast (**D**) and pseudohyphae (**E**). **F–H** Spa2 localises to a spot at the hyphal tip of *A. gossypii* (**H**) and *A. nidulans* (**F**), but in *A. nidulans* the SpaA signal is broader and slightly more apically located compared to FM4-64 (**G**). Cell outlined in **H** is traced from the DIC the image. *Bars* **B** 3 µm; **C,E** 1 µm; **D** 3 µm; **F, G** 10 µm. *Sources* **A** Fischer-Parton et al. (2000); **B** Sharpless and Harris (2002); **C** H Crampin and P Sudbery, unpublished; **D, E** Crampin et al (2005); **F, G** Virag and Harris (2006a); **H** Knechtle et al (2003)

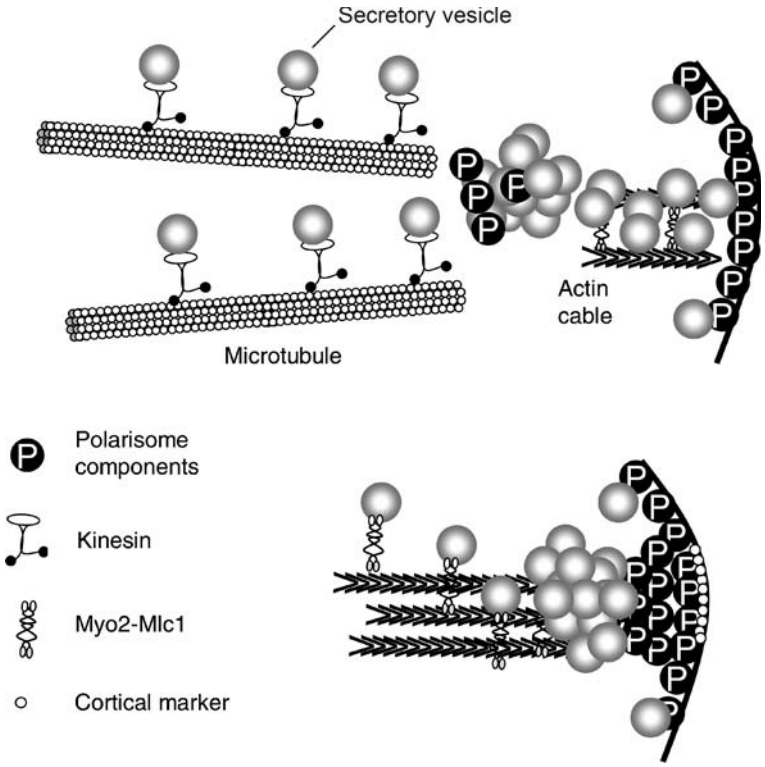

Fig. 6.12. Two views of the Spitzenkörper. *Top* The Spitzenkörper is a switching station where secretory vesicles are deposited by microtubule-mediated transport before onward transport to the tip by actin cable-mediated transport. According to the vesicle supply centre model, most vesicles hit the apex of the hyphal tip, but some fuse at off-centre regions of the polarisome. *Bottom* Polarisome components are localised to a surface crescent and, perhaps because of some form of cortical marker, they become more concentrated at the very tip. This nucleates tip-directed actin cables resulting in the accumulation of secretory vesicles at the centre compared with off-centre regions

Rhizoctonia solani was examined by live-cell video microscopy (Bartnicki-Garcia et al. 1995). After a mild disturbance caused by moving the microscope slide, the Spitzenkörper was observed to withdraw from its polar location. This resulted in the fungal tip becoming spherical rather than hyphoid in shape. After a brief delay the Spitzenkörper returned to its polar location and polarised hyphal growth resumed, leaving a permanent bulge in the hyphal walls. The hyphal profile and direction of growth throughout these events was accurately predicted by the Fungus Simulator program. In another study the position of the Spitzenkörper within the tip was observed to change during hyphal growth of *N. crassa*. Changes in the direction of hyphal growth were shown to be correlated with changes in the Spitzenkörper location (Riquelme et al. 1998). The position of the Spitzenkörper can be experimentally manipulated using laser tweezers. Shortly after the position of the Spitzenkörper was moved to one side, the direction of hyphal growth changed according to its new position (Bracker et al. 1997). Finally, time-lapse videos showed the presence of satellite Spitzenkörper near the tip that were associated with bulges in the hyphal wall. When these satellites fused with the main Spitzenkörper a pulse of tip growth occurred, which was consistent with the previously observed pulsatile growth of fungal hyphae (Lopez-Franco et al. 1994, 1995).

The role of the Spitzenkörper in polarised growth in hyphae raises three inter-related questions. First, what is its molecular composition? Second, what is the relationship of the Spitzenkörper to the polarisome and exocyst complexes of *Sac. cerevisiae*? Third, what regulates the formation of the Spitzenkörper? The importance of the last question is underlined by the hyphal growth *C. albicans* and *Ash. gossypii* that are related to *Sac. cerevisiae* and, at least in the case of *C. albicans*, generate a Spitzenkörper (Crampin et al. 2005; Martin et al. 2005). Are the same components of polarised growth machinery used but in different ways to generate yeast and hyphae, or are additional components employed during hyphal compared to yeast growth? The ability of *C. albicans* to grow as both yeast and hyphae provides a particularly fascinating opportunity to study this issue. *Ash. gossypii* is closely related to *Sac. cerevisiae*, to the extent that extensive synteny is maintained. Thus it would be particularly interesting if *Ash. gossypii* uses only components that are part of the machinery that drives polarised growth in *Sac. cerevisiae.*

A. Localisation of Polarity Proteins During Hyphal Growth

It is not possible to physically isolate the Spitzenkörper, so the most promising route to study its molecular composition is the use of protein fusions to GFP and its derivatives. The *Sac. cerevisiae* paradigm has been used in a number of studies to inform the selection of proteins for study, particularly homologues of the polarisome proteins. A striking pattern is emerging that such proteins can localise either to an apical/subapical spot, or to a surface crescent. In some cases both a spot and a crescent are present in the same hypha. The first example of this was the localisation of SepA in *Asp. nidulans*, a formin family protein that is the homologue of *Sac. cerevisiae* Bni1 (Sharpless and Harris 2002). A subapical spot and a surface crescent are clearly distinguishable (Fig. 6.11B).

In *C. albicans*, Mlc1-YFP and YFP-Cdc42 also localise to a spot and a crescent at hyphal tips (Fig. 6.11C; Crampin et al. 2005). The Mlc1-YFP spot co-localises with FM4-64 and so is likely to be a Spitzenkörper component (Crampin et al. 2005). In yeast and pseudohyphae, Mlc1 localises only to a surface crescent (Fig. 6.11D,E). Since a Spitzenkörper is not present in yeast and pseudohyphae, this suggests that the crescent is the polarisome. Computer modelling based on the information contained with a Z-stack shows that both Mlc1 and FM4-64 form a 3-D ball within the hyphal tip (Crampin et al. 2005). Two further differences between hyphae compared to yeast and pseudohyphae are apparent in *C. albicans* (Crampin et al. 2005). First, Mlc1 is continuously located at the tips of hyphae, provided they are actively growing. After mitosis a ring of Mlc1 also appears and contracts at the septation site. Thus the Mlc1 in the cytokinetic ring co-exists with Mlc1 in the Spitzenkörper. In yeast and pseudohyphae, the Mlc1 crescent disappears from the bud tip before it reappears in the cytokinetic ring. Second, the concentration of Mlc1-YFP in the spot, as measured by fluorescence intensity, is approximately four-fold greater than in the crescent.

The localisation of Spa2 and Bud6 in *C. albicans* hyphae were more difficult to evaluate. Both localised predominantly to a surface crescent or to a cap surrounding the tip region (Crampin et al. 2005). In some cells a spot and a crescent or a crescent with a patch of more intense fluorescence were visible. High resolution restoration microscopy showed that Spa2 did not exactly co-localise with either Mlc1 or FM4-64. Rather Spa2 formed a cap to the 3-dimensional aggregation of FM4-64 and Mlc1 (Crampin et al 2005). Again in yeast and pseudohyphal buds both Spa2 and Bud6 localised to a surface crescent. In *Ash. gossypii* and *Asp. nidulans* hyphae the Spa2 homologue (called SpaA in *Asp. nidulans)* localised to a spot (Knechtle et al. 2003; Virag and Harris 2006a; Fig. 6.11F-H). However, in *Asp. nidulans*, co-localisation of SpaA and FM4-64 again revealed that SpaA took a more crescent-like form as a cap to the FM4-64 spot (Fig. 6.11F,G). Thus while the evidence is equivocal, it seems that Spa2 localises predominantly to a surface crescent or cap that is spatially separate from the FM4-64 spot. An interesting corollary to this observation is that it differs from the Bni1/SepA localisation pattern. In *C. albicans* hyphae Bni1-YFP localises to an apical dot (Crampin et al. 2005; Martin et al. 2005). This is surprising because Bni1 and Spa2 physically interact in *Sac. cerevisiae*. Interestingly, in *Asp. nidulans*, SpaA has been shown unnecessary for SepA localisation (Virag and Harris 2006a), thus it is possible that Spa2 and Bni1 are not so intimately associated in hyphae as they are in the polarisome of yeast buds. In *Ash. gossypii* however, Bni1 was observed to be located in a surface crescent (Schmitz et al. 2006). Thus in three different organisms the formin that nucleates actin cables localises to: an apical dot (*C. albicans*), a dot and crescent (*Asp. nidulans*) and solely as a crescent *(Ash. gossypii*).

B. The Role of Polarity Proteins in Hyphal Growth

Loss of polarity components causes defects in polarised growth of varying severity. Loss of Bni1/SepA in *Asp. nidulans* and *C. albicans* results in abnormally wide hyphae and, in the case of *C. albicans*, a failure to maintain hyphal growth. There is also a severe cytokinesis defect in both fungi (Sharpless and Harris 2002; Martin et al. 2005). Loss of Bni1 is lethal in *Ash. gossypii*, where spores lacking Bni1 germinate to form giant peanut-shaped cells (Schmitz et al. 2006). Deletion of the auto-inhibitory domain of *Ag*Bni1, resulting in an activated protein, causes an increase in tip-directed actin cables and hyphal tip splitting. This affirms that a key role is played by the formin in hyphal growth and suggests that hyphal tip splitting is regulated by the rate of vesicle flow to the hyphal tip. In *C. albicans spa2*Δ/Δ and

*bud6*Δ/Δ mutations resulted in broad hyphae that resembled the shape of pseudohyphae (Zheng et al. 2003; Crampin et al. 2005). Consistent with this phenotype the Spitzenkörper disappeared and Mlc1-YFP was localised only as a surface crescent. In *Ash. gossypii*, loss of Spa2 did not prevent hyphal formation, however hyphae were broader and their extension rates were reduced (Knechtle et al. 2003). *Asp. nidulans* mutants lacking SpaA, the homologue of Spa2, were still able to form hyphae containing a Spitzenkörper, possibly because localisation of the Bni1 homologue, SepA, was not dependent on SpaA (Virag and Harris 2006a).

A defining characteristic of hyphal growth is the continued polarisation of the hyphal tip. The establishment of polarity in *Sac. cerevisiae* depends upon cortical cues supplied by the bud site selection machinery. Homologues of Rsr1 were identified in *Ash. gossypii* and Rsr1 and Bud2 in *C. albicans* (Yaar et al. 1997; Bauer et al. 2004; Hausauer et al. 2005). In *Sac. cerevisiae*, these proteins acted downstream of both bipolar and axial bud site markers to localise Cdc24 and thus activated Cdc42. Loss of these proteins caused a similar phenotype in both fungi. Hyphae were slower growing and wider, and frequent bends along their length apparently were evidence for an inability to maintain a stable direction of growth. In the case of *C. albicans* hyphal branching was promiscuous, while in *Ash. gossypii* frequent abortive branching events gave rise to bulges in the hyphal walls. The slow growth was shown to be due to pauses or shorter periods of growth. During these pauses Spa2-YFP was either lost from the tip or moved from side to side within the hyphal tip so that Spa2 would be positioned to program growth along a new axis when it resumed. Patches of Spa2-YFP also appeared at sites of abortive branches in *Ash. gossypii*. Taken together these observations showed that, in the fungi of the yeast group that produce hyphae, the Rsr1-GTPase module acted to stabilise the axis of growth, presumably by stabilising Cdc42 at the hyphal tip.

In *Asp. nidulans* and other filamentous fungi genes encoding these proteins were either poorly conserved or completely absent (Harris and Momany 2004) which led to speculation that polarised hyphal growth may depend on self-organising Cdc42-feedback loops that occur in *Sac. cerevisiae* in the absence of bud site selection markers (Harris and Momany 2004). However, recently it was shown that hyphae of *Asp. nidulans kipA*Δ mutants grow in a conspicuously wavy shape and the Spitzenkörper moves from side to side within the hyphal tip, a phenotype reminiscent of the *Ash. gossypii* and *C. albicans* mutants lacking bud site selection markers (Konzack et al. 2005). KipA is the *Asp. nidulans* homologue of *Sch. pombe* Tea2, which is a member of the kinesin family plus end-directed microtubule motors. Tea2 delivers Tea1 along microtubules to the cortex at the cell poles where it may provide a landmark for polarised growth (Chang and Peter 2003). Tea1 is also required for the proper organisation of microtubules as in tea1Δ mutants, microtubules curl around the ends of cells. In *Asp. nidulans kipA*Δ mutants, microtubules fail to converge at a single point as they do in wild type cells, but instead are dispersed and mobile. Thus *Asp. nidulans* hyphae may also rely on cortical markers to stabilise the axis of growth. Moreover, microtubules may fix the Spitzenkörper in its position in the centre of the hyphal tip.

C. The Role of the Cytoskeleton in Spitzenkörper Function

Both the actin and microtubular cytoskeleton are essential for normal hyphal growth and Spitzenkörper function (see Chaps. 2 and 5 in this volume, for further discussion). Inhibitors of the actin cytoskeleton – such as cytochalasin A or latrunculin – or actin mutations, cause apical swelling and loss of the Spitzenkörper (Heath et al. 2003; Virag and Griffiths 2004; Crampin et al. 2005). In *C. albicans* this was shown to be due to the pattern of growth switching from polarised to isotropic (Crampin et al. 2005). In *Ash. gossypii*, deletion of a pair of redundant genes *BOI1* and *BOI2*, or *RHO3*, resulted in the periodic loss of actin cables which was accompanied by tip swelling (Knechtle et al. 2006). Boi1/Boi2 and Rho3 were shown to interact physically. Moreover, a constitutively active allele of Rho3, but not a constitutively negative allele, interacted with Bni1. These data suggested that Rho3 together with Boi1/Boi2 provide an alternative, Cdc42-independent, route for the activation of Bni1 and thus the formation of actin cables. It is striking that the loss of actin cables by deletion of *AgBOI1/AgBOI2* or *AGRHO3* results in the tip swelling in a fashion similar to the effect of chemical inhibitors of actin cables described above. Clearly, actin cables are required to maintain polarised growth during hyphal growth and, importantly, in their absence the tip undergoes isometric growth.

Long microtubules run the length of hyphae (Han et al. 2001; Riquelme et al. 2002), which in *C. albicans* are specific to the hyphal form and are not present in the yeast or pseudohyphal form (Barton and Gull 1988; Hazan et al. 2002; Crampin et al. 2005). Disruption of microtubules reduces hyphal growth, but does not cause the tip to swell as seen after loss of actin cables (Akashi et al. 1994; Crampin et al. 2005; Horio and Oakley 2005). Kinesins are motor proteins that are directed towards the plus ends of microtubules, which in hyphae are tip-directed and thus mediate anterograde transport (Konzack et al. 2005). Kinesin-deficient mutants of *Neurospora crassa* are defective in polarised growth and lack a Spitzenkörper (Seiler et al. 1999).

The current view is that microtubules are used for long-distance transport of vesicles to the Spitzenkörper, while actin cables mediate the short-distance dispersal of the vesicles to the cell surface. Thus the Spitzenkörper acts as a switching station between these different modes of transport (Virag and Harris 2006b). This model explains different effects of disruption of the microtubular and actin cytoskeletons. The loss of microtubules halts the flow of vesicles to the tip, so growth ceases. With a functioning microtubular cytoskeleton, vesicles continue to arrive at the tip region; but, in the absence of actin cables to focus the delivery to the tip, they diffuse randomly to the cell surface, producing isotropic tip growth. In addition, or alternatively, the actin and tubular cytoskeletons may play a role in positioning the Spitzenkörper at the tip. Holding the Spitzenkörper at a fixed distance from the tip is an essential postulate of the vesicle supply model. Since the tip is continually moving forward, an active mechanism is required to achieve this. Microtubules may act to push the Spitzenkörper into position from behind and/or actin cables could tether it to the cell cortex. The phenotype of the KipA mutant described above is consistent with a role of microtubules in positioning the Spitzenkörper (Konzack et al. 2005).

D. The Nature of the Spitzenkörper

Research into the mechanisms of polarised growth in budding yeast has revealed the central role played by Cdc42 and other Rho-GTPases in orchestrating polarised growth and illuminated the roles of three different protein complexes:

- The polarisome nucleates actin cables and possibly actin cortical patches.
- The exocyst complex provides a platform for secretory vesicles to dock and fuse with the plasma membrane.
- The Las17/Arp2/Arp3 complex mediates the formation of actin cortical patches.

The distinction between three separate complexes may be artificial, arising from the focus of different research fields on different aspects of polarised growth. It may well be that these complexes represent different facets of a larger supercomplex. Physical interactions between these complexes have already been documented. For example Msb3/Msb4 acts as a GAP for Sec4 on secretory vesicles as they dock with the exocyst and interacts physically with Spa2 (Gao et al. 2003). Bem1, which is part of the polarity complex, co-immune precipitates with Sec15 and Sec8, which are exocyst components (Zajac et al. 2005; France et al. 2006). Bni1 interacts physically with Spa2 and nucleates actin cables, but is also part of the Arp2/Arp3 complex that mediates the production of actin cortical patches (Lechler et al. 2001). One difficulty with a budding yeast model is the small size of the bud when it shows polarised growth, which makes cytology difficult – it not possible realistically to resolve whether these complexes are spatially separate. For brevity in the following discussion the term "polarisome" is used to encompass all these components of the polarised growth machinery in budding yeast.

What then is the relationship between the Spitzenkörper and the polarisome? Central to this question is whether the Spitzenkörper is a separate entity or whether it is a hyperactive polarisome (Fig. 6.12). The first view is based on observations that proteins such as SepA in *Asp. nidulans* and Mlc1, Bni1 and Cdc42 in *C. albicans* clearly distinguish two discrete structures: an internal spot and surface crescent at the hyphal tip (Sharpless and Harris 2002; Crampin et al. 2005). In *C. albicans*, the Mlc1-YFP spot co-localises with FM4-64 and represents the Spitzenkörper, while the crescent – which is also present in yeast and pseudohyphae – represents the polarisome. According to this view, the Spitzenkörper may be a region where secretory vesicles are deposited at the ends of microtubules before being ferried to the hyphal tip along actin cables. Polarisome components are mainly located in a surface crescent, nucleating actin cables for the transport of vesicles from the Spitzenkörper to the tip. Consistent with this model, high-resolution fluorescence microscopy shows that Spa2 localises

slightly towards the tip compared with FM4-64 in both *C. albicans* and *Asp. nidulans* (Crampin et al. 2005; Virag and Harris 2006a). According to the second view, the polarisome complex is distributed around the hyphal tip where it acts to nucleate the formation of actin cables and promote the docking of secretory vesicles. Through an as yet unidentified mechanism, the polarisome complex becomes more concentrated in the central region, giving the illusion of a distinct structure. This aggregation could back up into the hypha, giving the appearance of an internal 3-D structure, which could even eventually separate to produce a physically distinct internal ball and surface crescent.

There are problems with both models. The Spitzenkörper-as-switching-station model does not fully explain why proteins such as Mlc1 are found in the Spitzenkörper. Perhaps Myo2-Mlc1 is involved with transporting vesicles to the Spitzenkörper as well as beyond – to the tip. The Spitzenkörper-as-hyperactive-polarisome model begs the question as to why there should be an apparently discontinuous density in the polarisome complex, resulting in a separate structure visible in both phase contrast and electron microscopy, FM4-64 staining and localisation of proteins such Bni1/SepA and Mlc1. In *C. albicans*, as mentioned above, the intensity of Mlc1-YFP staining in the spot has been measured to be around four-fold greater than the crescent (Crampin et al. 2005) – presumably reflecting some mechanism that locally concentrates or activates Cdc42. However, in *C. albicans*, while YFP-Cdc42 co-localises with FM4-64 in the Spitzenkörper, the intensity of fluorescence is greater in the surface crescent (Crampin et al. 2005). Furthermore, the model does not explain why the Spitzenkörper persists throughout the cell cycle while the polarisome disappears from the tip in G2 (Crampin et al. 2005).

Whatever the relationship of the polarisome and Spitzenkörper, it remains the case that EM, phase contrast microscopy and FM4-64 staining all reveal a small discrete circular structure at or just behind the tip of most actively growing hyphae. Some proteins such as Bni1/SepA and Mlc1 co-localise with this spot. Thus, use of the term Spitzenkörper remains a useful descriptor of this structure. However, fundamental questions remain regarding its relationship with the polarisome, its interaction with the microtubule and actin cytoskeletons and the mechanisms that regulate its formation.

VII. Conclusions

Research using the budding yeast *Sac. cerevisiae* and the fission yeast *Sch. pombe* has revealed much about the mechanism of polarised growth in fungi. Sites of polarised growth are manifest by cortical markers. In *Sac. cerevisiae* these arise from bud site selection pathways in vegetative cells and from the βγ subunit released from the mating pheromone receptor–G protein complex upon pheromone stimulation. In *Sch. pombe* the site of growth is marked by the delivery of Tea1 along microtubules to the cell poles. Marking the sites of polarised growth activates the Cdc42 GTPase, which in *Sac. cerevisiae* leads to the formation of the polarisome which nucleates actin cables leading to the delivery and docking secretory vesicles originating from trans-Golgi membranes. Activated Cdc42-GTP has a number of other effectors, which together orchestrate morphogenic processes required for the orderly formation and growth of the daughter bud. These include the formation of the exocyst complex where the secretory vesicles dock and the formation of the septin ring which co-ordinates formation of the primary septum.

In the model yeasts, the molecular nature of these processes and their regulation are becoming known in ever more detail. What is still uncertain is the way in which these processes are modified in hyphal growth. Hyphae can grow at rates that far exceed the growth of a yeast bud. This rapid growth depends upon, and is orchestrated by, the Spitzenkörper. This apical body is rich in secretory vesicles, which leads to the hypothesis that it acts as a vesicle supply centre – a model which provides a satisfying explanation for hyphal growth and morphology. However, it is important to remember that the Spitzenkörper is not just a collection of vesicles but has a complex structure including ribosomes and microfilaments. The presence of ribosomes may indicate asymmetric localisation of mRNAs and thus translation of key proteins at the sites of polarised growth, a process that has been well documented at the tips of nerve axons in higher organisms. The actin microfilaments may be acting to transport vesicles to the cell surface or they may act to tether the Spitzenkörper so that it remains at the tip, a key requirement of the vesicle supply model.

Molecular characterisation of the Spitzenkörper is at an early stage and, for the present, leans heavily on the underpinning provided by the yeast model. A key question for the present is the rela-

tionship of the polarisome and the Spitzenkörper. Are these two separate structures, with the Spitzenkörper acting as an advanced store of vesicles that are transported on to the cell surface by actin cables nucleated by the polarisome located at the cell surface? Alternatively, is the Spitzenkörper a modified polarisome in which the polarisome components are somehow concentrated to a narrow area at the centre of the hyphal tip and therefore focus the delivery of vesicles to a small area, resulting in much more highly polarised growth than occurs in a yeast bud. A question which perhaps has been less investigated in the present chapter is the role of endocytosis in polarised growth, exemplified by the clustering of actin cortical patches, which mediate endocytosis, to sites of polarised growth in yeast and hyphae. A further question which remains to be investigated is the role of lipid rafts which are also polarised to sites of polarised growth.

The impressive rates of hyphal extension may ultimately be understood by modifications of the yeast paradigm. However, given the very large differences in the rates of polarised growth between yeast cells and hyphae, and the apparent complex structure of the Spitzenkörper, we may anticipate that novel mechanisms will yet be revealed and there is much that remains to be discovered.

References

Adamo JE, Moskow JJ, Gladfelter AS, Viterbo D, Lew DJ, Brennwald PJ (2001) Yeast Cdc42 functions at a late step in exocytosis, specifically during polarized growth of the emerging bud. J Cell Biol 155:581–592

Adams A, Pringle J (1983) Relationship of actin and tubulin distribution to bud growth in wild type and morphogenetic-mutant *Saccharomyces cerevisiae*. J Cell Biol 98:934–945

Adams A, Johnson D, Longnecker R, Sloat B, Pringle J (1990a) CDC42 and CDC43, two additional genes involved in budding and the establishment of cell polarity in the yeast *Saccharomyces cerevisiae*. J Cell Biol 111:131–142

Adams AE, Johnson DI, Longnecker RM, Sloat BF, Pringle JR (1990b) CDC42 and CDC43, two additional genes involved in budding and the establishment of cell polarity in the yeast Saccharomyces cerevisiae. J Cell Biol 111:131–142

Ahn SH, Acurio A, Kron SJ (1999) Regulation of G2/M progression by the STE mitogen-activated protein kinase pathway in budding yeast filamentous growth. Mol Biol Cell 10:3301–3316

Ahn SH, Tobe BT, Gerald JNF, Anderson SL, Acurio A, Kron SJ (2001) Enhanced cell polarity in mutants of the budding yeast cyclin- dependent kinase Cdc28p. Mol Biol Cell 12:3589–3600

Akashi T, Kanbe T, Tanaka K (1994) The role of the cytoskeleton in the polarized growth of the germ tube in *Candida albicans*. Microbiology 140:271–280

Albert S, Gallwitz D (2000) Msb4p, a protein involved in Cdc42p-dependent organization of the actin cytoskeleton, is a Ypt/Rab-specific GAP. Biol Chem 381:453–456

Alberts AS (2001) Identification of a carboxyl-terminal diaphanous-related formin homology protein autoregulatory domain. J Biol Chem 276:2824–2830

Amon A, Tyers M, Futcher B, Nasmyth K (1993) Mechanisms that help the yeast cell cycle clock tick: G2 cyclins transcriptionally activate G2 cyclins and repress G1 cyclins. Cell 74:993–1007

Anderson J, Soll DR (1986) Differences in actin localization during bud and hypha formation in the yeast *Candida albicans* . J Gen Microbiol 132:2035–2047

Ayscough KR (2005) Defining protein modules for endocytosis. Cell 123:188–190

Bachewich C, Whiteway M (2005) Cyclin Cln3p links G1 progression to hyphal and pseudohyphal development in *Candida albicans*. Eukaryot Cell 4:95–102

Bachewich C, Nantel A, Whiteway M (2005) Cell cycle arrest during S or M phase generates polarized growth via distinct signals in *Candida albicans*. Mol Microbiol 57:942–959

Bahler J, Pringle JR (1998) Pom1p, a fission yeast protein kinase that provides positional information for both polarized growth and cytokinesis. Genes Dev 12:1356–1370

Bai C, Ramanan N, Wang YM, Wang Y (2002) Spindle assembly checkpoint component CaMad2p is indispensable for *Candida albicans* survival and virulence in mice. Mol Microbiol 45:31–44

Bardwell L (2005) A walk-through of the yeast mating pheromone response pathway. Peptides 26:337–1476

Bartnicki-Garcia S, Hergert F, Gierz G (1989) Computer-simulation of fungal morphogenesis and the mathematical basis for hyphal (tip) growth. Protoplasma 153:46–57

Bartnicki-Garcia S, Bartnicki DD, Gierz G, Lopez-Franco R, Bracker CE (1995) Evidence that Spitzenkörper behavior determines the shape of a fungal hypha – a test of the hyphoid model. Exp Mycol 19:153–159

Barton R, Gull K (1988) Variation in cytoplasmic microtubular organisation and spindle length between the two forms of the dimorphic fungus *Candida albicans*. J Cell Sci 91:211–220

Bassilana M, Arkowitz RA (2006) Rac1 and Cdc42 have different roles in *Candida albicans* development. Eukaryot Cell 5:321–329

Bassilana M, Blyth J, Arkowitz RA (2003) Cdc24, the GDP-GTP exchange factor for Cdc42, is required for invasive hyphal growth of *Candida albicans*. Eukaryot Cell 2:9–18

Bassilana M, Hopkins J, Arkowitz RA (2005) Regulation of the Cdc42/Cdc24 GTPase module during *Candida albicans* hyphal growth. Eukaryot Cell 4:588–603

Bauer Y, Knechtle P, Wendland J, Helfer H, Philippsen P (2004) A Ras-like GTPase is involved in hyphal growth guidance in the filamentous fungus *Ashbya gossypii*. Mol Biol Cell 15:4622–4632

Behrens R, Nurse P (2002) Roles of fission yeast tea1p in the localization of polarity factors and in organizing the microtubular cytoskeleton. J Cell Biol 157:783–793

Bensen ES, Filler SG, Berman J (2002) A forkhead transcription factor is important for true hyphal as well as yeast morphogenesis in *Candida albicans*. Eukaryot Cell 1:787–798

Bensen ES, Clemente-Blanco A, Finley KR, Correa-Bordes J, Berman J (2005) The mitotic cyclins Clb2p and Clb4p affect morphogenesis in *Candida albicans*. Mol Biol Cell 16:3387–3400

Bi EF, Chiavetta JB, Chen H, Chen GC, Chan CSM, Pringle JR (2000) Identification of novel, evolutionarily conserved Cdc42p- interacting proteins and of redundant pathways linking Cdc24p and Cdc42p to actin polarization in yeast. Mol Biol Cell 11:773–793

Bielli P, Casavola EC, Biroccio A, Urbani A, Ragnini-Wilson A (2006) GTP drives myosin light chain 1 interaction with the class V myosin Myo2 IQ motifs via a Sec2 RabGEF-mediated pathway. Mol Microbiol 59:1576–1590

Bloom K (2000) It's a kar9ochore to capture microtubules. Nat Cell Biol 2:E96–E98

Bobola N, Jansen RP, Shin TH, Nasmyth K (1996) Asymmetric accumulation of ASH1p in postanaphase nuclei depends on a myosin and restricts yeast mating-type switching to mother cells. Cell 84:699–709

Bose I, Irazoqui JE, Moskow JJ, Bardes ESG, Zyla TR, Lew DJ (2001) Assembly of scaffold-mediated complexes containing Cdc42p, the exchange factor Cdc24p and the effector Cla4p required for cell cycle-regulated phosphorylation of Cdc24p. J Biol Chem 276:7176–7186

Boyce KJ, Hynes MJ, Andrianopoulos A (2001) The *CDC42* homolog of the dimorphic fungus *Penicillium marneffei* is required for correct cell polarization during growth but not development. J Bacteriol 183:3447–3457

Boyce KJ, Hynes MJ, Andrianopoulos A (2003) Control of morphogenesis and actin localization by the *Penicillium marneffei* RAC homolog. J Cell Sci 116:1249–1260

Boyne JR, Yosuf HM, Bieganowski P, Brenner C, Price C (2000) Yeast myosin light chain, Mlc1p, interacts with both IQGAP and Class II myosin to effect cytokinesis. J Cell Sci 113:4533–4543

Bracker CE, Ruizherrera J, Bartnicki-Garcia S (1976) Structure and transformation of chitin synthetase particles (chitosomes) during microfibril synthesis *in vitro*. Proc Natl Acad Sci USA 73:4570–4574

Bracker CE, Murphey DJ, Lopez-Franco R (1997) Laser microbeam manipulation of cell morphogenesis in growing hyphae. In: Farkas DL, Tromberg BJ (ed) Functional imaging of optical manipulation of living cells. (Proceedings of SPIE) International Society for Optical Engineering, Bellingham, Wash.

Braun BR, Hoog MV, d'Enfert C, Martchenko M, Dungan J, Kuo A, et al (2005) A human-curated annotation of the *Candida albicans* genome. PloS Genet 1:36–57

Brown JL, Jaquenoud M, Gulli MP, Chant J, Peter M (1997) Novel Cdc42-binding proteins Gic1 and Gic2 control cell polarity in yeast. Gene Dev 11:2972–2982

Brunner D, Nurse P (2000) CLIP170-like Tip1p spatially organizes microtubular dynamics in fission yeast. Cell 102:695–704

Brunswick H (1924) Untersuchungen uber Geschlechts- und Kern- verhaltnisse bei der Hymenomzetengattung *Coprinus*. Fisher, Jena

Bücking-Throm E, Duntze W, Hartwell LH, Manney TR (1973) Reversible arrest of haploid yeast-cells at Initiation of DNA-Synthesis by a diffusible sex factor. Exp Cell Res 76:99–110

Burbelo PD, Drechsel D, Hall A (1995) A conserved binding motif defines numerous candidate target proteins for both Cdc42 and Rac GTPases. J Biol Chem 270:29071–29074

Busch KE, Hayles J, Nurse P, Brunner D (2004) Tea2p kinesin is involved in spatial microtubule organization by transporting Tip1p on microtubules. Dev Cell 6:831–843

Cabib E (2004) The septation apparatus, a chitin-requiring machine in budding yeast. Arch Biochem Biophys 426:201–207

Casamayor A, Snyder M (2002) Bud-site selection and cell polarity in budding yeast. Curr Opin Microbiol 5:179–186

Caviston JP, Longtine M, Pringle JR, Bi E (2003) The role of Cdc42p GTPase-activating proteins in assembly of the septin ring in yeast. Mol Biol Cell 14:4051–4066

Chang F, Peter M (2003) Yeasts make their mark. Nat Cell Biol 5:294–299

Chant J (1999) Cell polarity in yeast. Annu Rev Cell Dev Biol 15:365–391

Chapa y Lazo B, Bates S, Sudbery PE (2005) *CLN3* regulates hyphal morphogenesis in *Candida albicans*. Eukaryot Cell 4:90–94

Chen GC, Kim YJ, Chan CSM (1997) The Cdc42 GTPase-associated proteins Gic1 and Gic2 are required for polarized cell growth in *Saccharomyces cerevisiae*. Gene Dev 11:2958–2971

Collinge AJ, Trinci APJ (1974) Hyphal tips of wild-type and spreading colonial mutants of *Neurospora crassa*. Arch Microbiol 99:353–368

Crampin H, Finley K, Gerami-Nejad M, Court H, Gale C, Berman J, Sudbery PE (2005) *Candida albicans* hyphae have a Spitzenkörper that is distinct from the polarisome found in yeast and pseudohyphae. J Cell Sci 118:2935–2947

Cross FR (1988) *DAF1*, a mutant gene affecting size control, pheromone arrest, and cell-cycle kineticsof *Saccharomyces cerevisiae*. Mol Cell Biol 8:4675–4684

Cvrckova F, Devirgilio C, Manser E, Pringle JR, Nasmyth K (1995) Ste20-like protein-kinases are required for normal localization of cell-growth and for cytokinesis in budding yeast. Gene Dev 9:1817–1830

DerMardirossian C, Bokoch GM (2005) GDIs: central regulatory molecules in Rho GTPase activation. Trends Cell Biol 15:356–363

Dobbelaere J, Gentry MS, Hallberg RL, Barral Y (2003) Phosphorylation-dependent regulation of septin dynamics during the cell cycle. Dev Cell 4:345–357

Dong YQ, Pruyne D, Bretscher A (2003) Formin-dependent actin assembly is regulated by distinct modes of Rho signaling in yeast. J Cell Biol 161:1081–1092

Douglas LM, Alvarez FJ, McCreary C, Konopka JB (2005) Septin function in yeast model systems and pathogenic fungi. Eukaryot Cell 4:1503–1512

Drgonova J, Drgon T, Tanaka K, Kollar R, Chen GC, Ford RA, Chan CSM, Takai Y, Cabib E (1996) Rho1p, a yeast protein at the interface between cell polarization and morphogenesis. Science 272:277–279

Drgonova J, Drgon T, Roh DH, Cabib E (1999) The GTP-binding protein Rho1p is required for cell cycle progression and polarization of the yeast cell. J Cell Biol 146:373–388

Etienne-Manneville S (2004) Cdc42 – the centre of polarity. J Cell Sci 117:1291–1300

Evangelista M (1997) Bni1p, a yeast formin linking Cdc42p and the actin cytoskeleton during polarized morphogenesis. Science 276:118–121

Evangelista M, Pruyne D, Amberg DC, Boone C, Bretscher A (2002) Formins direct Arp2/3-independent actin filament assembly to polarize cell growth in yeast. Nature Cell Biol 4:32–41

Evangelista M, Zigmond S, Boone C (2003) Formins: signaling effectors for assembly and polarization of actin filaments. J Cell Sci 116:2603–2611

Fischer-Parton S, Parton RM, Hickey PC, Dijksterhuis J, Atkinson HA, Read ND (2000) Confocal microscopy of FM4-64 as a tool for analysing endocytosis and vesicle trafficking in living fungal hyphae. J Microsc 198:246–259

France YE, Boyd C, Coleman J, Novick PJ (2006) The polarity-establishment component Bem1p interacts with the exocyst complex through the Sec15p subunit. J Cell Sci 119:876–888

Fujiwara T, Tanaka K, Mino A, Kikyo M, Takahashi K, Shimizu K, Takai Y (1998) Rho1p-Bni1p-Spa2p interactions: implication in localization of Bni1p at the bud site and regulation of the actin cytoskeleton in *Saccharomyces cerevisiae*. Mol Biol Cell 9:1221–1233

Futcher B (2002) Transcriptional regulatory networks and the yeast cell cycle. Curr Opin Cell Biol 14:676–683

Gao XD, Albert S, Tcheperegine SE, Burd CG, Gallwitz D, Bi EF (2003) The GAP activity of Msb3p and Msb4p for the Rab GTPase Sec4p is required for efficient exocytosis and actin organization. J Cell Biol 162:635–646

Geli MI, Riezman H (1998) Endocytic internalization in yeast and animal cells: similar and different. J Cell Sci 111:1031–1037

Gierz G, Bartnicki-Garcia S (2001) A three-dimensional model of fungal morphogenesis based on the vesicle supply center concept. J Theor Biol 208:151–164

Gimeno CJ, Ljungdahl PO, Styles CA, Fink GR (1992) Unipolar cell divisions in the yeast *Saccharomyces cerevisiae* lead to filamentous growth: regulation by starvation and RAS. Cell 68:1077–1090

Girbardt M (1957) Der Spitzenkörper von *Polystictus versicolor*. Planta 50:47–50

Girbardt M (1969) Ultrastructure of apical region of fungal hyphae. Protoplasma 67:413–441

Gladfelter AS, Moskow JJ, Zyla TR, Lew DJ (2001a) Isolation and characterization of effector-loop mutants of CDC42 in yeast. Mol Biol Cell 12:1239–1255

Gladfelter AS, Pringle JR, Lew DJ (2001b) The septin cortex at the yeast mother-bud neck. Curr Opin Microbiol 4:681–689

Gladfelter AS, Bose I, Zyla TR, Bardes ESG, Lew DJ (2002) Septin ring assembly involves cycles of GTP loading and hydrolysis by Cdc42p. J Cell Biol 156:315–326

Gladfelter AS, Kozubowski L, Zyla TR, Lew DJ (2005) Interplay between septin organization, cell cycle and cell shape in yeast. J Cell Sci 118:1617–1628

Glynn J, Lustig R, Berlin A, Chang F (2001) Role of bud6p and tea1p in the interaction between actin and microtubules for the establishment of cell polarity in fission yeast. Curr Biol 11:836–845

Goehring AS, Mitchell DA, Tong AHY, Keniry ME, Boone C, Sprague GF (2003) Synthetic lethal analysis implicates Ste20p, a p21-activated protein kinase, in polarisome activation. Mol Biol Cell 14:1501–1516

Grove SN, Bracker CE (1970) Protoplasmic organization of hyphal tips among fungi: vesicles and Spitzenkörper. J Bacteriol 104:989–1009

Grove SN, Sweigard JA (1980) Cytochalasin A inhibits spore germination and hyphal tip growth in *Gilbertella persicaria*. Exp Mycol 4:239–250

Grove SN, Bracker CE, Morre DJ (1970) An ultrastructural basis for hyphal tip growth in *Pythium ultimum*. Am J Bot 57:245–266

Gulli MP, Jaquenoud M, Shimada Y, Niederhauser G, Wiget P, Peter M (2000) Phosphorylation of the Cdc42 exchange factor Cdc24 by the PAK- like kinase Cla4 may regulate polarized growth in yeast. Mol Cell 6:1155–1167

Guo W, Roth D, Walch-Solimena C, Novick P (1999) The exocyst is an effector for Sec4p, targeting secretory vesicles to sites of exocytosis. EMBO J 18:1071–1080

Guo W, Tamanoi F, Novick P (2001) Spatial regulation of the exocyst complex by Rho1 GTPase. Nat Cell Biol 3:353–360

Han GS, Liu B, Zhang J, Zuo WQ, Morris NR, Xiang X (2001) The *Aspergillus* cytoplasmic dynein heavy chain and NUDF localize to microtubule ends and affect microtubule dynamics. Curr Biol 11:719–724

Harris SD (1999) Morphogenesis is coordinated with nuclear division in germinating *Aspergillus nidulans* conidiospores. Microbiology 145:2747–2756

Harris SD, Momany M (2004) Polarity in filamentous fungi: moving beyond the yeast paradigm. Fungal Genet Biol 41:391–400

Harris SD, Read ND, Roberson RW, Shaw B, Seiler S, Plamann M, Momany M (2005) Polarisome meets Spitzenkorper: microscopy, genetics, and genomics converge. Eukaryot Cell 4:225–229

Hartwell LH, Cullotti J, Pringle JR, Reid BJ (1974) Genetic control of the cell division cycle in yeast. Science 183:46–51

Hausauer DL, Gerami-Nejad M, Kistler-Anderson C, Gale CA (2005) Hyphal guidance and invasive growth in *Candida albicans* require the Ras-like GTPase Rsr1p and its GTPase-activating protein Bud2p. Eukaryot Cell 4:1273–1286

Hazan I, Sepulveda-Becerra M, Liu HP (2002) Hyphal elongation is regulated independently of cell cycle in *Candida albicans*. Mol Biol Cell 13:134–145

Heath IB (1988) Evidence against a direct role for cortical actin arrays in saltatory organelle motility in hyphae of the fungus *Saprolegnia Ferax*. J Cell Sci 91:41–47

Heath IB, Bonham M, Akram A, Gupta GD (2003) The interrelationships of actin and hyphal tip growth in the ascomycete *Geotrichum candidum*. Fungal Genet Biol 38:85–97

Horio T, Oakley BR (2005) The role of microtubules in rapid hyphal tip growth of *Aspergillus nidulans*. Mol Biol Cell 16:918–926

Howard RJ (1981) Ultrastructural analysis of hyphal tip cell growth in fungi: Spitzenkörper, cytoskeleton and endomembranes after freeze-substitution. J Cell Sci 48:89–103

Howard RJ, Aist JR (1980) Cytoplasmic microtubules and fungal morphogenesis: ultrastructural effects of methyl benzimidazole-2-ylcarbamate determined by freeze-substitution of hyphal tip cells. J Cell Biol 87:55–64

Imamura H (1997) Bni1p and Bnr1p: downstream targets of the Rho family of small GTPases which interact with profilin and regulate actin cytoskeleton in *Saccharomyces cerevisiae*. EMBO J 16:2745–2755

Irazoqui JE, Gladfelter AS, Lew DJ (2003) Scaffold-mediated symmetry breaking by Cdc42p. Nat Cell Biol 5:1062–1070

Irazoqui JE, Howell AS, Theesfeld CL, Lew DJ (2005) Opposing roles for actin in Cdc42p polarization. Mol Biol Cell 16:1296–1304

Jaquenoud M, Peter M (2000) Gic2p may link activated Cdc42p to components involved in actin polarization, including Bni1p and Bud6p (Aip3p). Mol Cell Biol 20:6244–6258

Johnson DI (1999) Cdc42: An essential Rho-type GTPase controlling eukaryotic cell polarity. Microbiol Mol Biol Rev 63:54–105

Johnson DI, Pringle JR (1990) Molecular characterization of cdc42, a *Saccharomyces cerevisiae* gene involved in the development of cell polarity. J Cell Biol 111:143–152

Jorgensen P, Tyers M (2004) How cells coordinate growth and division. Curr Biol 14:R1014–R1027

Knechtle P, Dietrich F, Philippsen P (2003) Maximal polar growth potential depends on the polarisome component AgSpa2 in the filamentous fungus *Ashbya gossypii*. Mol Biol Cell 14:4140–4154

Knechtle P, Wendland J, Philippsen P (2006) The SH3/PH domain protein AgBoi1/2 collaborates with the Rho-Type GTPase AgRho3 to prevent nonpolar growth at hyphal tips of *Ashbya gossypii*. Eukaryot Cell 5:1635–1647

Koch G, Tanaka K, Masuda T, Yamochi W, Nonaka H, Takai Y (1997) Association of the Rho family small GTP-binding proteins with Rho GDP dissociation inhibitor (Rho GDI) in *Saccharomyces cerevisiae*. Oncogene 15:417–422

Kohno H (1996) Bni1p implicated in cytoskeletal control is a putative target of Rho1p small GTP binding protein in *Saccharomyces cerevisiae*. EMBO J 15:6060–6068

Konzack S, Rischitor PE, Enke C, Fischer R (2005) The role of the kinesin motor KipA in microtubule organization and polarized growth of *Aspergillus nidulans*. Mol Biol Cell 16:497–506

Kozminski KG, Beven L, Angerman E, Tong AH, Boone C, Park HO (2004) Interaction between a Ras and a Rho GTPase couples selection of a growth site to the development of cell polarity in yeast. Mol Biol Cell 15:355A

Kron SJ, Gow NAR (1995) Budding yeast morphogenesis: signaling, cytoskeleton and cell-cycle. Curr Opin Cell Biol 7:845–855

Kron SJ, Styles CA, Fink GR (1994) Symmetrical cell-division in pseudohyphae of the yeast *Saccharomyces cerevisiae*. Mol Biol Cell 5:1003–1022

Kurjan J (1993) The pheromone response pathway in *Saccharomyces cerevisiae.* Annu Rev Genet 27:147–179

Leberer E, Dignard D, Harcus D, Thomas DY, Whiteway M (1992) The protein kinase homologue Ste20p is required to link the yeast pheromone response G-protein beta-gamma subunits to downstream signalling components. EMBO J 11:4815–4824

Leberer E, Thomas DY, Whiteway M (1997a) Pheromone signalling and polarized morphogenesis in yeast. Curr Opin Genet Dev 7:59–66

Leberer E, Wu CL, Leeuw T, FourestLieuvin A, Segall JE, Thomas DY (1997b) Functional characterization of the Cdc42p binding domain of yeast Ste20p protein kinase. EMBO J 16:83–97

Lechler T, Li R (1997) *In vitro* reconstitution of cortical actin assembly sites in budding yeast. J Cell Biol 138:95–103

Lechler T, Shevchenko A, Shevchenko A, Li R (2000) Direct involvement of yeast type I myosins in Cdc42-dependent actin polymerization. J Cell Biol 148:363–373

Lechler T, Jonsdottir GA, Klee SK, Pellman D, Li R (2001) A two-tiered mechanism by which Cdc42 controls the localization and activation of an Arp2/3-activating motor complex in yeast. J Cell Biol 155:261–270

Lew DJ, Reed SI (1993) Morphogenesis in the yeast cell cycle: regulation by Cdc28 and cyclins. J Cell Biol 120:1305–1320

Lew DJ, Reed SI (1995) A cell-cycle checkpoint monitors cell morphogenesis in budding yeast. J Cell Biol 129:739–749

Lillie SH, Brown SS (1994) Immunofluorescence localisation of the unconventional myosin, Myo2p, and the putative kinesin related protein, Smy1p, to the same regions of polarised growth in *Saccharomyces cerevisiae*. J Cell Biol 125:825–842

Lippincott J, Li R (1998) Sequential assembly of myosin II, an IQGAP-like protein, and filamentous actin to a ring structure involved in budding yeast cytokinesis. J Cell Biol 140:355–366

Liu H, Styles CA, Fink GR (1993) Elements of the yeast pheromone response pathway required for filamentous growth of diploids. Science 262:1741–1744

Lockhart SR, Daniels KJ, Zhao R, Wessels D, Soll DR (2003) Cell biology of mating in *Candida albicans*. Eukaryot Cell 2:49–61

Loeb JDJ, Karentseva TA, Pan T, Sepulveda-Becerra M, Liu HP (1999a) *Saccharomyces cerevisiae* G1 cyclins are differentially involved in invasive and pseudohyphal growth independent of the filamentation mitogen-activated protein kinase pathway. Genetics 153:1535–1546

Loeb JJ, Sepulveda-Becerra M, Hazan I, Liu HP (1999b) A G1 cyclin is necessary for maintenance of filamentous growth in *Candida albicans*. Mol Cell Biol 19:4019–4027

Longtine MS, DeMarini DJ, Valencik ML, Al-Awar OS, Fares H, De Virgilio C, Pringle JR (1996) The septins: roles in cytokinesis and other processes. Curr Opin Cell Biol 8:106–119

Longtine MS, Fares H, Pringle JR (1998) Role of the yeast Gin4p protein kinase in septin assembly and the relationship between septin assembly and septin function. J Cell Biol 143:719–736

Longtine MS, Theesefield CL, McMillan JN, Weaver E, Pringle JR, Lew DJ (2000) Septin-dependent assembly of a cell cycle-regulatory module in *Saccharomyces cerevisiae*. Mol Biol 20:4049–4061

Lopez-Franco R, Bartnicki-Garcia S, Bracker CE (1994) Pulsed growth of fungal hyphal tips. Proc Natl Acad Sci USA 91:12228–12232

Lopez-Franco R, Howard RJ, Bracker CE (1995) Satellite Spitzenkorper in growing hyphal tips. Protoplasma 188:85–103

Luo JY, Vallen EA, Dravis C, Tcheperegine SE, Drees B, Bi EF (2004) Identification and functional analysis of the essential and regulatory light chains of the only type II myosin Myo1p in *Saccharomyces cerevisiae*. J Cell Biol 165:843–855

Mao YX, Kalb VF, Wong B (1999) Overexpression of a dominant-negative allele of *SEC4* inhibits growth and protein secretion in *Candida albicans*. J Bacteriol 181:7235–7242

Martin R, Walther A, Wendland J (2005) Ras1-induced hyphal development in *Candida albicans* requires the formin Bni1. Eukaryot Cell 4:1712–1724

Martínez-Anaya C, Dickinson JR, Sudbery PE (2003) In yeast, the pseudohyphal phenotype induced by isoamyl alcohol results from the operation of the morphogenesis checkpoint. J Cell Sci 116:3423–3431

Masuda T, Tanaka K, Nonaka H, Yamochi W, Maeda A, Takai Y (1994) Molecular-cloning and characterization of yeast-Rho GDP dissociation inhibitor. J Biol Chem 269:19713–19718

Mata J, Nurse P (1997) Tea1 and the microtubular cytoskeleton are important for generating global spatial order within the fission yeast cell. Cell 89:939–949

Matheos D, Metodiev M, Muller E, Stone D, Rose MD (2004) Pheromone-induced polarization is dependent on the Fus3p MAPK acting through the formin Bni1p. J Cell Biol 165:99–109

Metodiev MV, Matheos D, Rose MD, Stone DE (2002) Regulation of MAPK function by direct interaction with the mating-specific G alpha in yeast. Science 296:1483–1486

Miller PJ, Johnson DI (1994) Cdc42P GTPase is involved in controlling polarized cell growth in *Schizosaccharomyces pombe*. Mol Cell Biol 14:1075–1083

Mitchison JM, Nurse P (1985) Growth in cell length in the fission yeast *Schizosaccharomyces pombe*. J Cell Sci 75:357–376

Momany M, Zhao J, Lindsey R, Westfall PJ (2001) Characterization of the *Aspergillus nidulans* septin (asp) gene family. Genetics 157:969–977

Moseley JB, Sagot I, Manning AL, Xu YW, Eck J, Pellman D, Goode BL (2004) A conserved mechanism for Bni1- and mDia1-induced actin assembly and dual regulation of Bni1 by Bud6 and profilin. Mol Biol Cell 15:896–907

Naqvi SN, Zahn R, Mitchell DA, Stevenson BJ, Munn AL (1998) The WASp homologue Las17p functions with the WIP homologue End5p/verprolin and is essential for endocytosis in yeast. Curr Biol 8:959–962

Nash R, Tokiwa G, Anand S, Erikson K, Futcher AB (1988) The WHI1+ gene of *Saccharomyces cerevisiae* tethers cell division to cell size and is a cyclin homolog. EMBO J 7:4335–4346

Nern A, Arkowitz RA (1999) A Cdc24p-Far1p-G beta gamma protein complex required for yeast orientation during mating. J Cell Biol 144:1187–1202

Nonaka H, Tanaka K, Hirano H, Fujiwara T, Kohno H, Umikawa M, Mino A, Takai Y (1995) A downstream target of Rho1 small GTP-binding protein is Pkc1, a homolog of Protein Kinase C, which leads to activation of the map kinase cascade in *Saccharomyces cerevisiae*. EMBO J 14:5931–5938

Novick P, Field C, Schekman R (1980) Identification of 23 complementation groups required for post-translational events in the yeast secretory pathway. Cell 21:205–215

Odds FC (1985) Morphogenesis in *Candida albicans*. Crit Rev Microbiol 12:45–93

Ortiz D, Medkova M, Walch-Solimena C, Novick P (2002) Ypt32 recruits the Sec4p guanine nucleotide exchange factor, Sec2p, to secretory vesicles; evidence for a Rab cascade in yeast. J Cell Biol 157:1005–1015

Osman MA, Cerione RA (1998) Iqg1p, a yeast homologue of the mammalian IQGAPs, mediates Cdc42p effects on the actin cytoskeleton. J Cell Biol 142:443–455

Osman MA, Konopka JB, Cerione RA (2002) Iqg1p links spatial and secretion landmarks to polarity and cytokinesis. J Cell Biol 159:601–611

Ozaki-Kuroda K, Yamamoto Y, Nohara H, Kinoshita M, Fujiwara T, Irie K, Takai Y (2001) Dynamic localization and function of Bni1p at the sites of directed growth in Saccharomyces cerevisiae. Mol Cell Biol 21:827–839

Ozbudak EM, Becskei A, Oudenaarden A van (2005) A system of counteracting feedback loops regulates Cdc42p activity during spontaneous cell polarization. Developmental Cell 9:565–571

Park HO, Bi EF, Pringle JR, Herskowitz I (1997) Two active states of the Ras-related Bud1/Rsr1 protein bind to different effectors to determine yeast cell polarity. Proc Natl Acad Sci USA 94:4463–4468

Park HO, Sanson A, Herskowitz I (1999) Localization of Bud2p, a GTPase-activating protein necessary for programming cell polarity in yeast to the presumptive bud site. Genes 13:1912–1917

Park HO, Kang PJ, Rachfal AW (2002) Localization of the Rsr1/Bud1 GTPase involved in selection of a proper growth site in yeast. J Biol Chem 277:26721–26724

Pelham HRB (2001) SNAREs and the specificity of membrane fusion. Trends Cell Biol 11:99–101

Peter M, Herskowitz I (1994) Direct inhibition of the yeast cyclin-dependent kinase Cdc28-Cln by Far1. Science 265:1228–1231

Peter M, Gartner A, Horecka J, Ammerer G, Herskowitz I (1993) FAR1 links the signal transduction pathway to the cell cycle machinery in yeast. Cell 73:747–750

Peter M, Neiman AM, Park HO, vanLohuizen M, Herskowitz I (1996) Functional analysis of the interaction between the small GTP binding protein Cdc42 and the Ste20 protein kinase in yeast. EMBO J 15:7046–7059

Peterson J, Zheng Y, Bender L, Myers A, Cerione R, Bender A (1994) Interactions between the bud emergence proteins Bem1p and Bem2p and RHO-type GTPases in yeast. J Cell Biol 127:1395–1406

Philippsen P, Kaufmann A, Schmitz HP (2005) Homologues of yeast polarity genes control the development of multinucleated hyphae in *Ashbya gossypii*. Curr Opin Microbiol 8:370–377

Pringle J, Bi E, Harkins HA, Zahner JE, De Virgilio C, Chant J, Corrado K, Fares H (1995) Establishment of cell polarity in yeast. Cold Spring Harbor Symp Quant Biol 60:729–744

Pruyne D, Bretscher A (2000a) Polarization of cell growth in yeast II. The role of the actin cytoskeleton. J Cell Sci 113:571–585

Pruyne D, Bretscher A (2000b) Polarization of cell growth in yeast. I. Establishment and maintenance of polarity states. J Cell Sci 113:365–375

Pruyne D, Legesse-Miller A, Gao LN, Dong YQ, Bretscher A (2004) Mechanisms of polarized growth and organelle segregation in yeast. Annu Rev Cell Dev Biol 20:559–591

Punt PJ, Seiboth B, Weenink XO, Zeijl C van, Lenders M, Konetschny C, Ram AFJ, Montijn R, Kubicek CP, Hondel CAMJ van den (2001) Identification and characterization of a family of secretion-related small GTPase-encoding genes from the filamentous fungus *Aspergillus niger*: a putative *SEC4* homologue is not essential for growth. Mol Microbiol 41:513–525

Qadota H, Python CP, Inoue SB, Arisawa M, Anraku Y, Zheng Y, Watanabe T, Levin DE, Ohya Y (1996) Identification of yeast Rho1p GTPase as a regulatory subunit of 1,3-beta -glucan synthase. Science 272:279–281

Read ND, Hickey PC (2001) The Vesicle trafficking network and tip growth in fungal hyphae. In: Cell Biology of plant and fungal tip growth, ed. A.Geitman. IOS Press. 137–147.

Riquelme M, Reynaga-Pena CG, Gierz G, Bartnicki-Garcia S (1998) What determines growth direction in fungal hyphae? Fungal Genet Biol 24:101–109

Riquelme M, Roberson RW, McDaniel DP, Bartnicki-Garcia S (2002) The effects of ropy-1 mutation on cytoplasmic organization and intracellular motility in mature hyphae of *Neurospora crassa*. Fungal Genet Biol 37:171–179

Roumanie O, Wu H, Molk JN, Rossi G, Bloom K, Brennwald P (2005) Rho GTPase regulation of exocytosis in yeast is independent of GTP hydrolysis and polarization of the exocyst complex. J Cell Biol 170:583–594

Sagot I, Klee SK, Pellman D (2002) Yeast formins regulate cell polarity by controlling the assembly of actin cables. Nat Cell Biol 4:42–50

Santos B, Snyder M (1997) Targeting of chitin synthase 3 to polarised growth sites in *Saccharomyces cereivisiae requires* Chs5p and Myo2p. J Cell Biol 136:95–110

Schmidt A, Bickle M, Beck T, Hall MN (1997) The yeast phosphatidylinositol kinase homolog TOR2 activates RHO1 and RHO2 via the exchange factor ROM2. Cell 88:531–542

Schmidt M, Bowers B, Varma A, Roh DH, Cabib E (2002) In budding yeast, contraction of the actomyosin ring and formation of the primary septum at cytokinesis depend on each other. J Cell Sci 115:293–302

Schmitz HP, Kaufmann A, Kohli M, Laissue PP, Philippsen P (2006) From function to shape: a novel role of a formin in morphogenesis of the fungus *Ashbya gossypii*. Mol Biol Cell 17:130–145

Schott D, Ho J, Pruyne D, Bretscher A (1999) The COOH-terminal domain of Myo2p, a yeast myosin V, has a direct role in secretory vesicle targeting. J Cell Biol 147:791–807

Segal M, Bloom K (2001) Control of spindle polarity and orientation in *Saccharomyces cerevisiae*. Trends Cell Biol 11:160–166

Segal M, Bloom K, Reed SI (2000) Bud6 directs sequential microtubule interactions with the bud tip and bud neck during spindle morphogenesis in *Saccharomyces cerevisiae*. Mol Biol Cell 11:3689–3702

Segall JE (1993) Polarization of yeast-cells in spatial gradients of alpha-mating factor. Proc Natl Acad Sci USA 90:8332–8336

Seiler S, Plamann M, Schliwa M (1999) Kinesin and dynein mutants provide novel insights into the roles of vesicle traffic during cell morphogenesis in *Neurospora*. Curr Biol 9:779–785

Seshan A, Amon A (2004) Linked for life: temporal and spatial coordination of late mitotic events. Curr Opin Cell Biol 16:41–48

Shannon KB, Li R (2000) A myosin light chain mediates the localization of the budding yeast IQGAP-like protein during contractile ring formation. Curr Biol 10:727–730

Sharpless KE, Harris SD (2002) Functional characterization and localization of the *Aspergillus nidulans* formin SEPA. Mol Biol Cell 13:469–479

Sheu YJ, Barral Y, Snyder M (2000) Polarized growth controls cell shape and bipolar bud site selection in *Saccharomyces cerevisiae*. Mol Cell Biol 20:5235–5247

Sheu YJ, Santos B, Fortin N, Costigan C, Snyder M (1998) Spa2p interacts with cell polarity proteins and signaling components involved in yeast cell morphogenesis. Mol Cell Biol 18:4053–4069

Shimada Y, Gulli MP, Peter M (2000) Nuclear sequestration of the exchange factor Cdc24 by Far1 regulates cell polarity during yeast mating. Nat Cell Biol 2:117–124

Shimada Y, Wiget P, Gulli MP, Bi ER, Peter M (2004) The nucleotide exchange factor Cdc24p may be regulated by auto-inhibition. EMBO J 23:1051–1062

Sia RAL, Herald HA, Lew DJ (1996) Cdc28 tyrosine phosphorylation and the morphogenesis checkpoint in budding yeast. Mol Biol Cell 7:1657–1666

Sil A, Herskowitz I (1996) Identification of an asymmetrically localized determinant, Ash1p, required for lineage-specific transcription of the yeast HO gene. Cell 84:711–722

Smith GR, Givan SA, Cullen P, Sprague GF (2002) GTPase-activating proteins for Cdc42. Eukaryot Cell 1:469–480

Snyder M (1989) The spa2 protein of yeast localizes to sites of cell-growth. J Cell Biol 108:1419–1429

Soll DR, Herman MA, Staebell MA (1985) The involvement of cell wall expansion in the two modes of mycelium formation of *Candida albicans*. J Gen Microbiol 131:2367–2375

Stevenson BJ, Ferguson B, Devirgilio C, Bi E, Pringle JR, Ammerer G, and Sprague GF (1995) Mutation of Rga1, which encodes a putative GTPase-activating protein for the polarity-establishment protein Cdc42p, activates the pheromone-response pathway in the yeast *Saccharomyces cerevisiae* . Gene Dev 9:2949–2963

Sudbery PE (2001) The germ tubes of *Candida albicans* hyphae and pseudohyphae show different patterns of septin ring localisation. Mol Microbiol 41:19–31

Sudbery PE, Goodey AR, Carter BLC (1980) Genes that control cell proliferation in the yeast *Saccharomyces cerevisiae*. Nature 288:401–404

Sudbery PE, Gow NAR, Berman J (2004) The distinct morphogenic states of *Candida albicans*. Trends Microbiol 12:317–324

Tcheperegine SE, Gao XD, Bi E (2005) Regulation of cell polarity by interactions of Msb3 and Msb4 with Cdc42

and polarisome components. Mol Cell Biol 25:8567–8580

Terbush DR, Maurice T, Roth D, Novick P (1996) The exocyst is a multi-protein complex required for exocytosis in *Saccharomyces cerevisiae*. EMBO J 15:6483–6494

tir-Lande A, Gildor T, Kornitzer D (2005) Role for the SCF CDC4 ubiquitin ligase in candida albicans morphogenesis. Mol Biol Cell 16:2772–2785

Torralba S, Raudaskoski M, Pedregosa AM, Laborda F (1998) Effect of cytochalasin A on apical growth, actin cytoskeleton organization and enzyme secretion in *Aspergillus nidulans*. Microbiology 144:45–53

Trinci APJ (1973) Growth of wild-type and spreading colonial mutants of *Neurospora crassa* in batch culture and on agar medium. Arch Mikrobiol 91:113–126

Umeyama T, Kaneko A, Nagai Y, Hanaoka N, Tanabe K, Takano Y, Niimi M, Uehara Y (2005) *Candida albicans* protein kinase CaHsl1p regulates cell elongation and virulence. Mol Microbiol 55:381–395

Umeyama T, Kaneko A, Niimi M, Uehara Y (2006) Repression of CDC28 reduces the expression of the morphology-related transcription factors, Efg1p, Nrg1p, Rbf1p, Rim101p, Fkh2p and Tec1p and induces cell elongation in *Candida albicans*. Yeast 23:537–552

Ushinsky SC, Harcus D, Ash J, Dignard D, Marcil A, Morchhauser J, Thomas DY, Whiteway M, Leberer E (2002) *CDC42* is required for polarized growth in the human pathogen *Candida albicans*. Eukaryot Cell 1:95–104

Vallen EA, Caviston J, Bi E (2000) Roles of Hof1p, Bni1p, Bnr1p, and Myo1p in cytokinesis in *Saccharomyces cerevisiae*. Mol Biol Cell 11:593–611

Valtz N, Peter M, Herskowitz I (1995) FAR1 is required for oriented polarization of yeast cells in response to mating pheromones. J Cell Biol 131:863–873

Verde F, Mata J, Nurse P (1995) Fission yeast cell morphogenesis – identification of new genes and analysis of their role during the cell cycle. J Cell Biol 131:1529–1538

Versele M, Thorner J (2004) Septin collar formation in budding yeast requires GTP binding and direct phosphorylation by the PAK, Cla4. J Cell Biol 164:701–715

Virag A, Griffiths AJF (2004) A mutation in the *Neurospora crassa* actin gene results in multiple defects in tip growth and branching. Fungal Genet Biol 41:213–225

Virag A, Harris SD (2006a) Functional characterization of *Aspergillus nidulans* homologues of *Saccharomyces cerevisiae* Spa2 and Bud6. Eukaryot Cell 5:881–895

Virag A, Harris SD (2006b) The Spitzenkorper: a molecular perspective. Mycol Res 110:4–13

Walch-Solimena C, Collins RN, Novick PJ (1997) Sec2p mediates nucleotide exchange on Sec4p and is involved in polarized delivery of post-golgi vesicles. J Cell Biol 137:1495–1509

Walther A, Wendland J (2007) Hyphal growth and virulence. In: Brakhage A (ed) The Mycota: hyphal growth and virulence. Springer, Berlin Heidelberg New York

Walworth NC, Brennwald P, Kabcenell AK, Garrett M, Novick P (1992) Hydrolysis of GTP by Sec4 protein plays an important role in vesicular transport and is stimulated by a GTPase-activating protein in *Saccharomyces cerevisiae*. Mol Cell Biol 12:2017–2028

Warenda AJ, Konopka JB (2002) Septin function in *Candida albicans* morphogenesis. Mol Biol Cell 13:2732–2746

Wedlich-Soldner R, Altschuler S, Wu L, Li R (2003) Spontaneous cell polarization through actomyosin-based delivery of the Cdc42 GTPase. Science 299:1231–1235

Wedlich-Soldner R, Wai SC, Schmidt T, Li R (2004) Robust cell polarity is a dynamic state established by coupling transport and GTPase signaling. J Cell Biol 166:889–900

Wendland J, Philippsen P (2001) Cell polarity and hyphal morphogenesis are controlled by multiple Rho-protein modules in the filamentous ascomycete *Ashbya gossypii*. Genetics 157:601–610

Wendland J, Walther A (2005) *Ashbya gossypii*: a model for fungal developmental biology. Nat Rev Microbiol 3:421–429

Whiteway M, Dignard D, Thomas DY (1992) Dominant negative selection of heterologous genes – isolation of *Candida albicans* genes that interfere with *Saccharomyces cerevisiae* mating factor-induced cell-cycle arrest. Proc Natl Acad Sci USA 89:9410–9414

Wiget P, Shimada Y, Butty AC, Bi ER, Peter M (2004) Site-specific regulation of the GEF Cdc24p by the scaffold protein Far1p during yeast mating. EMBO J 23:1063–1074

Wightman R, Bates S, Amnorrattapan P, Sudbery PE (2004) In *Candida albicans*, the Nim1 kinases Gin4 and Hsl1 negatively regulate pseudohypha formation and Gin4 also controls septin organization. J Cell Biol 164:581–591

Winder SJ, Ayscough KR (2005) Actin-binding proteins. J Cell Sci 118:651–654

Wu C, Lytvyn V, Thomas D, Leberer E (1997) The phosphorylation site for Ste20p-like protein kinase is essential for the function of myosin-I in yeast. J Biol Chem 272:30623–30626

Yaar L, Mevarech M, Koltin Y (1997) A *Candida albicans* RAS-related gene (CaRSR1) is involved in budding, cell morphogenesis and hypha development. Microbiology 143:3033–3044

Zajac A, Sun XL, Zhang J, Guo W (2005) Cyclical regulation of the exocyst and cell polarity determinants for polarized cell growth. Mol Biol Cell 16:1500–1512

Zhang XY, Bi EF, Novick P, Du LL, Kozminski KG, Lipschutz JH, Guo W (2001) Cdc42 interacts with the exocyst and regulates polarized secretion. J Biol Chem 276:46745–46750

Zheng X, Wang Y, Wang Y (2003) *CaSPA2* is important for polarity establishment and maintenance in *Candida albicans*. Mol Microbiol 49:1391–1405

Zheng X, Wang Y, Wang Y (2004) Hgc1, a novel hypha-specific G1 cyclin-related protein regulates *Candida albicans* hyphal morphogenesis. EMBO J 23:1845–1856

Zheng Y, Cerione R, Bender A (1994) Control of the yeast bud-site assembly GTPase Cdc42 – catalysis of guanine-nucleotide exchange by Cdc24 and stimulation of GTPase activity by Bem3. J Biol Chem 269:2369–2372

Zheng Y, Bender A, Cerione R (1995) Interactions among proteins involved in bud-site selection and bud-site assembly in Saccharomyces cerevisiae. J Biol Chem 270:626–630

Zhu GF, Spellman PT, Volpe T, Brown PO, Botstein D, Davis TN, Futcher B (2000) Two yeast forkhead genes regulate the cell cycle and pseudohyphal growth. Nature 406:90–94

7 Signal Transduction and Morphogenesis in *Candida albicans*

A.J.P. Brown[1], S. Argimón[2], N.A.R. Gow[1]

CONTENTS

I. Introduction 167
II. Cell Morphology 168
III. Morphogenetic Signals 170
IV. Morphogenetic Pathways 172
A. Positive Regulation 172
1. MAPK Pathway 172
2. cAMP Signaling Pathway 175
3. pH Signaling Pathway 178
4. Additional Pathways 180
B. Negative Regulation 181
C. Calcium Signaling 183
V. Other Outputs of Morphogenetic Pathways 185
VI. Conclusions 186
References 186

I. Introduction

There are several well studied model systems of fungal growth and morphogenesis. These include *Saccharomyces cerevisiae*, *Schizosaccharomyces pombe*, *Aspergillus nidulans* and *Neurospora crassa*, all of which are tractable to both classical and molecular genetics. In these systems developmental and signaling pathways have been identified, often via the analysis of mutants that exhibit developmental arrest. Subsequently the cognate genes have been defined and examined at the molecular level. Many of these pathways are conserved in fungi and in other organisms, although the signals and outputs from the pathways may differ significantly. Identification of conserved components of such pathways provides one experimental route to establishing their role in other less genetically tractable organisms. The availability of multiple complete genome sequences from a wide range of fungi facilitates the identification of orthologous genes in these organisms and enables the evolution of signaling pathways to be analyzed in the context of their ecology and morphological diversity.

The major systemic fungal pathogen of humans, *Candida albicans*, on which this review focuses, is a case in point. The major tool for understanding key aspects of the morphogenesis and pathogenesis of this fungus has undoubtedly been the resource and insights provided by analysis of *S. cerevisiae*. This is now paying handsome dividends not only because it furthers our understanding of conserved aspects of the biology of *C. albicans*, but also because it enables our investigation of the unique and contrasting properties of this organism that are not features of model fungi. Indeed, the intensity of research effort on *C. albicans* in recent years means that insights gained from the study of this fungus are now explaining features of *S. cerevisiae* biology.

This review describes progress that has been made in understanding a central aspect of the biology of most fungi – their ability to growth either by isodiametric expansion of spheres (yeast cells, spores, spherules, vesicular bodies, etc.) or by apical expansion of hyphal tips. In *C. albicans* and many other fungi growth can occur either in a budding yeast form or as branching hyphae. These fungi are said to be "**dimorphic**". *C. albicans* can also generate a morphological form called a pseudohypha that consists of elongated, conjoined buds. Pseudohyphae were originally thought to represent an intermediate form sharing properties of hyphae and buds. However, the pseudohypha is now known to be a distinct form that is different from both true hyphae and yeast cells (Berman and Sudbery 2002; Sudbery et al. 2004; Wightman et al. 2004). *C. albicans* exhibits at least three vegetative growth forms and so it is more correctly termed "**pleiomorphic**". This review focuses on these growth forms. It does not address other morphologies (white/opaque switching, chlamydospores) which are reviewed elsewhere (Johnson

[1] School of Medical Sciences, Institute of Medical Sciences, University of Aberdeen, Foresterhill, Aberdeen, AB25 2ZD, UK
[2] School of Medical Sciences, University of Aberdeen Current address: Department of Microbiology, Columbia University, Hammer Building, 701 West 168th Street, New York, NY 10032, USA

Biology of the Fungal Cell, 2nd Edition
The Mycota VIII
R.J. Howard and N.A.R. Gow (Eds.)
© Springer-Verlag Berlin Heidelberg 2007

2003; Martin et al. 2005; Staib and Morschhauser 2005).

The regulation of morphogenesis in *C. albicans*, and other fungi, can be reduced to a question of how growth (more specifically expansion of the cell surface) is polarized. Cell polarity is a highly regulated and much studied aspect of cellular physiology (see Chaps. 5 and 6 in this volume). We focus on signal transduction leading to polarized growth rather than the mechanism of polarized growth per se.

Part of the impetus behind the considerable efforts made in recent years to establish the molecular mechanisms underlying dimorphic regulation in *C. albicans* is the notion that hyphal growth is an attribute of pathogenesis, or even a *bona fide* virulence factor (Ryley and Ryley 1990; Cutler 1991; Lo et al. 1997; Saville et al. 2003; Zheng et al. 2004). Hyphae are commonly observed in biopsies of *C. albicans*-infected organs (Odds 1988) and tip growth of hyphae seems well suited to a role for penetrating host tissues (Gow et al. 2002; see also Chap. 10 in this volume). Studies of more-or-less filamentous natural isolates or heavily mutagenized strains that are debilitated in hyphal development showed that such strains are poorer in establishing infections in animal models (Martin et al. 1984; Sobel et al. 1984; Shepherd 1985; Ryley and Ryley 1990). Evidence from earlier literature that hypha development is a virulence factor remained equivocal because clinical lesions with remarkably few hyphal forms were also reported and because random methods of mutagenesis that existed at that time almost certainly generated mutations at a wide range of other loci that encoded potential virulence factors. Also, there is no absolute relationship between hyphal growth and pathogenesis in clinically relevant fungi because many important human pathogens, including *Histoplasma capsulatum*, *Paracoccidioides brasiliensis* and *Coccidioides immitis*, are pathogenic in the yeast form and saprophytic in the hyphal form (Kwon-Chung and Bennett 1992). A range of *Candida* species, including those such as *C. glabrata*, which is not able to generate true filamentous forms, can cause infections and so again no absolute correlation between hyphal development and *Candida* disease is observed. More recently the creation of hypha-deficient mutants with deletions in transcription factors or cyclins that regulate hyphal morphogenesis reinforced the view that hypha formation, or the ability to switch reversibly between different morphological forms, is an important component of the repertoire of virulence attributes of this fungus (e.g. Lo et al. 1997; Saville et al. 2003; Zheng et al. 2004).

C. albicans now represents the third or fourth most common agent of microbial septicemia in United States hospitals and in western hospitals and has outstripped many bacterial infections in terms of incidence and morbidity (Beck-Sagué and Jarvis 1993; Jamal et al. 1999; Tortorano et al. 2004; Almirante et al. 2005). *C. albicans* is a classic opportunistic agent of infection and septicemia is almost always associated with some underlying immune deficiency, such as treatment for cancer or immunosuppression following bone marrow or organ transplantation. It is much more commonly seen as a mucosal pathogen of the oral or vaginal cavity where the disease is called thrush or a "yeast infection".

Prior to the era of molecular genetic analysis of hypha morphogenesis in *C. albicans* an enormous effort was expended on attempting to characterize the environmental conditions that were conducive and stimulatory to dimorphic switching. Unfortunately, strain variability and the lack of systems to perform targeted mutagenesis or mutant screens obscured the data that emerged. In the new era, the construction of isogenic mutants allowed the functional dissection of morphogenetic signaling pathways and hence the mechanisms that are essential for yeast–hypha conversion. This review focuses on these developments.

II. Cell Morphology

Most studies of C. albicans morphogenesis have focused on the transition from the budding, yeast-like form to the hyphal growth form. Although this transition is reversible, little work has addressed hypha-to-yeast morphogenesis. Furthermore, the yeast and hyphal forms represent the morphological extremes that C. albicans is able to manifest. However, this fungus can grow in various filamentous forms, collectively termed pseudohyphae and true hyphae (Merson-Davies and Odds 1989; Fig. 7.1). Pseudohyphae display constrictions at their septa, whereas true hyphae do not. Merson-Davies and Odds (1989) described the morphology index (Mi; based on the relative length and the maximum and septal diameters of cellular compartments) that provides a definitive guide to cell shape in C. albicans. The Mi of bud-

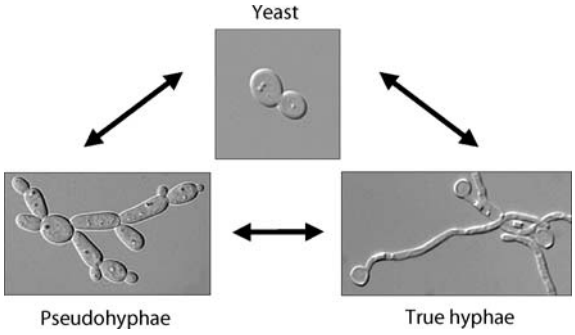

Fig. 7.1. Morphogenesis in *Candida albicans*, a pleiomorphic fungus that undergoes reversible morphological transitions between yeast, pseudohyphal and hyphal growth forms (see Sect. II.). Modified with permission from Berman and Gow (2004)

ding and hyphal cells are approximately 1.5 and 4.0, respectively, while pseudohyphal cells display a range of Mi values from about 2.0 to 3.5. Hyphal cells are generally narrower than pseudohyphal, having maximum diameters of about 2 µm and 5 µm, respectively (Sevilla and Odds 1986). Specific media promote the growth of pseudohyphal cells as opposed to hyphae (Merson-Davies and Odds 1989). Pseudohyphal cells may form in response to moderate morphogenetic signals, whereas hyphal development might be triggered by more extreme morphogenetic conditions.

It is therefore attractive to view pseudohyphal cells as intermediates between budding and hyphal cells, but the weight of evidence from morphological studies and studies of the cell cycle and of signal transduction now firmly suggests that this is not the case and instead suggests that pseudohyphal cells represent a distinct form (for reviews, see Berman and Sudbery 2002; Berman and Gow 2004; Sudbery et al. 2004; see also Chap. 6 in this volume; Figs. 7.1, 7.2). Pseudohyphal cells divide synchronously, whereas hyphal cells grow asynchronously, indicating that there are clear differences in the cell cycle of these two growth forms (Kron and Gow 1995; Gow 1997, 2002). In hyphae, nuclear division takes place within the germ tube, while in both yeast and pseudohyphal forms mitosis occurs in the position of the neck of the mother and daughter cells (Fig. 7.2). Consequently the site of formation of septins, which mark the site of evagination of buds and the plane of cytokinesis, also differ in the true hyphae and the two budding forms (Sudbery 2001; Berman and Sudbery 2002; Berman and Gow 2004; Sudbery et al. 2004). In both yeast cells and pseudohyphae the evagination event is tightly coupled to the cell cycle controls that are described by the START function, while in hyphae evagination occurs before START and is therefore independent of this aspect of cell cycle regulation (Hazan and Liu 2002). In addition, a cell cycle-dependent cyclin (Hgc1) has been described that is expressed in a hypha-specific manner and which is necessary for hyphal development (Zheng et al. 2004). Finally the hyphal form alone has a Spitzenkörper that is reminiscent of the apical body of vesicles seen in true fungi (see Chaps. 5 and 6 in this volume), whereas neither yeast cells nor pseudohyphae have this structure (Crampin et al. 2005).

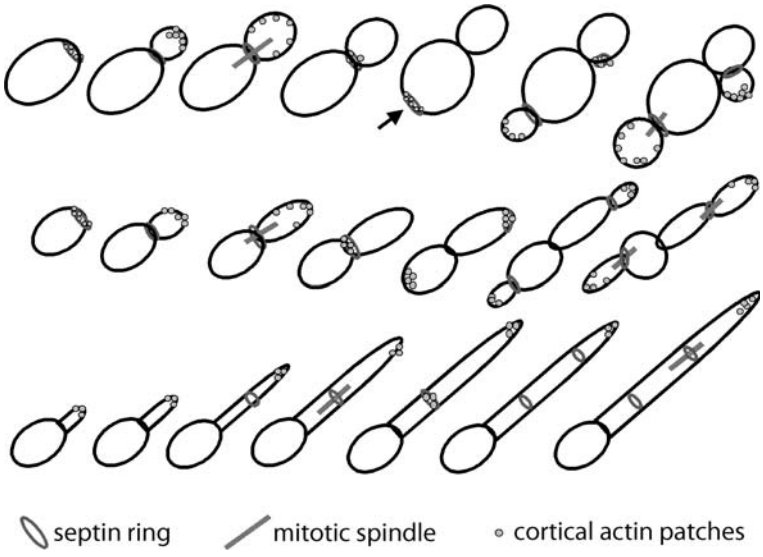

Fig. 7.2. Characteristic features of cell division for the yeast (*top*), pseudohyphal (*middle*) and true hyphal (*bottom*) growth forms of *C. albicans*. Cortical actin patches, the position of the mitotic spindle and the septin rings are shown during the progression of the cell cycles of each morphogenetic form. Modified with permission from Berman and Gow (2004)

Also, hypha-defective and yeast-defective *C. albicans* mutants can grow as pseudohyphae (Braun and Johnson 1997; Stoldt et al. 1997; and see below), suggesting that these growth forms are genetically distinct.

III. Morphogenetic Signals

Yeast–hypha morphogenesis in *C. albicans* can be triggered by numerous different treatments in vitro (Odds 1988). These in vitro conditions presumably reflect the various signals that promote hyphal growth in vivo. Temperatures above 37 °C, serum, ambient pH above 6.5, low dissolved O_2 concentrations and elevated CO_2 concentrations all promote hyphal development, while high cell densities inhibit hyphal development (Odds 1988; Brown et al. 1999; Sonneborn et al. 1999; Klengel et al. 2005). It was suggested that hypha-stimulating conditions were associated with the imposition of an environmental stress; and indeed some stresses such as some rapid changes in ambient temperature or pH and nutrient starvation do stimulate morphogenesis (Brown and Gow 1999, 2001). However, not all hypha-inducing conditions are associated with an environmental stress and not all stresses stimulate morphogenesis. For example, hyperosmotic stresses inhibit hyphal development (Monge et al. 1999). Therefore, whilst environmental stresses do appear to influence hyphal development, morphogenetic signaling pathways are generally considered to be distinct from stress signaling pathways. It has become clear that several morphogenetic signaling pathways exist in *C. albicans*. Although specific pathways appear to mediate responses to distinct sets of environmental triggers, there appears to be overlap between pathways as some share common signaling components (Fig. 7.3; Sect. IV.).

Serum is the most powerful inducer of hyphal development. When serum addition is combined with an increase in temperature, from 25 °C to 37 °C, within 60 min more that 95% of *C. albicans* cells form germ tubes – the progenitors of true hyphae. It is argued that serum is composed mainly of proteins that represent an inaccessible nutrient source until they are hydrolyzed and, hence, that serum addition imposes nitrogen starvation (Brown and Gow 1999). However, serum addition still stimulates hyphal growth when combined with a rich source of nutrients, such as YPD (2% glucose, 2% bacteriological peptone, 1% yeast extract; Swoboda et al. 1994). This indicates that something other than nitrogen starvation is responsible for serum-stimulated morphogenesis.

Fink and co-workers showed that a serum filtrate can stimulate hyphal development efficiently (Feng et al. 1999), suggesting that serum might contain a low molecular weight morphogen(s). This was confirmed by Hudson and co-workers (2004) who reported that glucose was (one of) the active agent(s) present in serum that stimulates morphogenesis. These authors also showed that glucose concentrations of between 0.01% and 0.3% are optimal for the stimulation of hyphal development in liquid assays. Van Dijck's group subsequently showed similar effects on solid medium. Glucose concentrations of between 0.025% and 0.25% are optimal for the stimulation of hyphal development on agar plates (Maidan et al. 2005); and they demonstrated that other fermentable carbon sources can stimulate hyphal growth under these conditions. What is clear is that glucose is a morphogen in *C. albicans* and glucose signaling must be intimately linked with morphogenetic signaling at some mechanistic level.

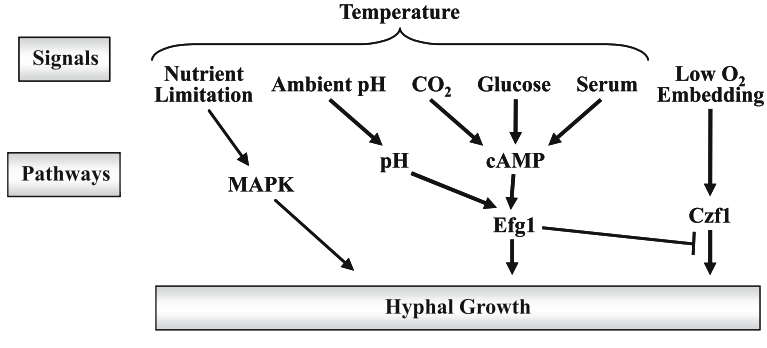

Fig. 7.3. Distinct environmental signals promote morphogenesis via specific signaling pathways in *C. albicans*. Environmental signals include nutrient limitation, ambient pH, CO_2, glucose, serum, low O_2 and embedding in a physical matrix. Additional morphogenetic signals are discussed in Sect. III.. The efficacy of some of these signals is increased by temperature elevation to 37 °C. Specific signaling pathways appear to mediate the responses to these signals (see Sect. IV.). There appears to be some functional overlap between some of these pathways

However, glucose is not the only morphogen in serum. Serum filtrates or glucose do stimulate morphogenesis, but not at the high rates observed for serum itself (Feng et al. 1999; Hudson et al. 2004). Therefore additional serum components are thought to contribute to the potency of this stimulus – ambient pH signaling is likely to contribute, because the addition of serum generally raises the ambient pH towards neutrality (see below). Also, Hudson and co-workers (2004) reported that a non-dialyzable, trichloroacetic acid-precipitable inducer exists in serum. The nature of this presumably large molecular weight component has not been established. Additional small molecular species may contribute to the serum stimulus. For example exogenous human hormones such as oestrodiol and progesterone have been reported to enhance hyphal development (Kinsman et al. 1988; Bramley et al. 1991, Zhao et al. 1995) and *C. albicans* expresses hormone-binding proteins (Williams et al. 1990; Malloy et al. 1993). A combination of (some of) these factors is likely to account for the potency of the serum stimulus.

The related media M199 and RPMI are commonly used to promote the yeast–hypha transition (Lo et al. 1997; Sharkey et al. 1999; Staab et al. 1999). These media and serum may stimulate morphogenesis by similar mechanisms. This view is supported by the observation that numerous *C. albicans* morphogenetic mutants display similar responses to M199 and serum (Lo et al. 1997; Davis et al. 2000).

It has been known for some time that the ambient H^+ concentration (pH) strongly influences *C. albicans* morphogenesis. A shift from acidic (pH 4.5) to more alkaline conditions ($\geq$pH 6.5) promotes hyphal growth when combined with a shift in temperature from 25 °C to 37 °C (Lee et al. 1975; Buffo et al. 1984). These conditions also promote a rise in internal pH that is shown to be a strong correlate of yeast–hypha morphogenesis and may act as a signal transduction system in its own right (Stewart et al. 1988, 1989). A distinct pH signaling pathway is primarily responsible for mediating the effects of pH (Porta et al. 1999; Davis et al. 2000). As described above, changes in ambient pH probably contribute to the efficacy of other hypha-inducing conditions. For example the addition of 10% serum, or serum filtrate, can increase the pH of YPD-based media from about pH 5.0 to pH 6.5. This might complicate the interpretation of much published data.

The physical environment of *C. albicans* cells is reported to influence yeast–hypha morphogenesis. Cells embedded in agar form hyphae, irrespective of chemical composition of the growth medium (Brown et al. 1999), suggesting that *C. albicans* can respond to physical cues to regulate its morphology. This is an attractive idea because previous work demonstrated that *C. albicans* responds to physical cues perhaps via stretch-activated channels to control the direction of hyphal growth (Sherwood et al. 1992; Watts et al. 1998). Most interestingly, embedded *C. albicans* cells form hyphae even at 25 °C, whereas most other stimuli only promote morphogenesis at temperatures above 37 °C (Brown et al. 1999). It was suggested that low oxygen concentrations present in the agar represent the true stimulus that promotes filamentous growth under embedding conditions, but Kumamoto's group went to some lengths to exclude this (Brown et al. 1999). Nevertheless, low oxygen concentrations (or hypoxia) are also able to promote hyphal development (Doedt et al. 2004).

There are also clear links between amino acid metabolism and morphogenesis. Proline has been known for some time to stimulate morphogenesis (Odds 1988). More recently, methionine has been shown to be important for the activation of morphogenesis under certain conditions (Maidan et al. 2005). Amino acid starvation also stimulates pseudohyphal development in *C. albicans*, in a Gcn4-dependent manner (Tripathi et al. 2002; Tournu et al. 2005). Defects in amino acid sensing, caused either by inactivation of the sensor Csy1 or by inactivation of the endoplasmic reticulum chaperone Csh3, also lead to morphogenetic defects (Brega et al. 2004; Martínez and Ljungdahl 2004). A number of observations suggest that the cAMP signaling pathway triggers hyphal development in response to changes in amino acid metabolism (Sect. 2.). For example Gcn4 mediates its effects upon *C. albicans* morphogenesis through Efg1 (Tripathi et al. 2002). In addition, the activation of morphogenesis by methionine is dependent upon Gpr1 (Maidan et al. 2005).

More recently another potent inducer of morphogenesis was confirmed by Muhlschlegel's group. They reported that physiologically relevant concentrations of 5% CO_2/bicarbonate promote the pseudohyphal growth of *C. albicans* on a range of different media (Klengel et al. 2005). These authors went on to define the signaling pathway that mediates this morphogenetic response (Sect. IV.A.) and showed that this pathway is conserved in *Cryptococcus neoformans*. These observations, which significantly extended an earlier report that 25 mM

bicarbonate induces filamentation in *Candida albicans* (Mock et al. 1990), are exploited in clinical diagnostic tests that distinguish *C. albicans* from other *Candida* species (Seth et al. 2005).

Prior nutrient limitation of *C. albicans* cells – for example, for several hours in H_2O – increases the inducibility of yeast cells to form hyphae upon exposure to morphogenetic conditions, but starved cells form hyphae less quickly than metabolically active yeast cells (Buchan and Gow 1991). The use of growth media containing only low concentrations of serum, which therefore may expose cells to both starvation and morphogenetic signals, efficiently promotes hyphal development (Gow 1997). Media containing only a poor carbon and nitrogen source, such as *N*-acetylglucosamine, induce the yeast–hypha transition (Mattia et al. 1982; Torosantucci et al. 1984). Supplementing serum or Glc-Nac medium with amino acids and glucose causes hyphae to revert to yeast cells. This led to the suggestion that starvation contributes significantly to the hyphal stimulus. This might indeed be true. However, more recent data suggest that intimate links between glucose and other nutrient signaling pathways might contribute to these effects upon morphogenesis (Maidan et al. 2005). Such links have been reported in *S. cerevisiae*, for example through Snf1 protein kinases and the repressors Nrg1 and Nrg2 (Vyas et al. 2001, 2003).

It has become increasingly clear that *C. albicans* responds to a variety of environmental cues to regulate yeast–hypha morphogenesis (Fig. 7.3). However, one factor that appears to overlay most of these conditions is temperature: an increase in temperature to about 37 °C is required before most of the above conditions can affect morphogenesis. The basis for this remains obscure. Physical triggers appear to be a possible exception to this "rule", since embedded colonies form hyphae when grown at 25 °C (Brown et al. 1999). However, since cells undergo a heat shock during the embedding process, the possible activation of a temperature switch cannot be excluded entirely.

IV. Morphogenetic Pathways

A. Positive Regulation

Several morphogenetic signaling pathways have been identified in *C. albicans*. Molecular analysis of these pathways was hampered by various features of this fungus: (a) it is diploid (Magee 1998), (b) it displays an alternative genetic code (Santos et al. 1993) and (c) although it carries a mating type-like locus (*MLT*; Hull and Johnson 1999) and strains can be engineered to mate (Gow et al. 2000; Hull et al. 2000; Magee and Magee 2000; Miller and Johnson 2002), no full sexual cycle or meiotic behavior has yet been identified. A parasexual cycle has been developed (Bennett and Johnson 2003), but this tool has not been fully exploited. For these reasons, most experimental approaches toward the identification of signaling components in *C. albicans* initially exploited the genetically tractable model, *S. cerevisiae*. Screens exploited the ability of *C. albicans* genes to complement or suppress mutations in the corresponding *S. cerevisiae* genes (Liu et al. 1994; Clark et al. 1995) or to interfere with or constitutively activate the corresponding signaling pathways in *S. cerevisiae* (Whiteway et al. 1992; Stoldt et al. 1997). Also, the functional analysis of *C. albicans* signaling genes initially relied heavily upon *S. cerevisiae* because the corresponding regulatory hierarchies are better characterized in this organism. However, more recently *C. albicans* genome sequencing facilitated the direct isolation of signal transduction genes from *C. albicans* on the basis of sequence similarities (Braun et al. 2005; d'Enfert et al. 2005). Also, the development of a wider range of molecular tools for *C. albicans* facilitated the functional analysis of signaling genes in this fungus, for example by epistasis experiments and other molecular analyses (Berman and Sudbery 2002; Doedt et al. 2004; Bassilana et al. 2005; Su et al. 2005).

Both positive and negative signaling pathways regulate the yeast–hypha transition in *C. albicans*. The MAPK, cAMP, pH and Czf1 pathways stimulate hyphal development. These are discussed in this section below. Factors, such as Tup1, that repress hyphal development are discussed in Sect. IV.B..

1. MAPK Pathway

The first morphogenetic signaling components to be identified in *C. albicans* were members of a mitogen-activated protein (MAP) kinase pathway analogous to the pheromone signaling (Ste) pathway in *S. cerevisiae* (Alonso-Monge et al. 2006). It should be noted that, like *S. cerevisiae* (Gustin et al. 1998), *C. albicans* has several MAP kinase signaling pathways,including a morphogenetic signaling pathway, a cell integrity pathway and a stress activated kinase pathway (Liu et al. 1993; Roberts and Fink 1994; Navarro-García et al.

1998; Alonso-Monge et al. 2003; Smith et al. 2004; Enjalbert et al. 2006). For the purposes of this discussion, when referring to the MAPK pathway, we mean the morphogenetic signaling pathway. This pathway is often defined experimentally using *C. albicans cph1* null mutants, which lack Cph1, the homologue of the *S. cerevisiae* transcription factor Ste12 (Liu et al. 1994).

Several screens were initially employed (Whiteway et al. 1992; Liu et al. 1994; Clark et al. 1995), each exploiting the detailed understanding of the mating pathway in *S. cerevisiae* (Kurjan 1993). At the time of isolation of the first MAPK pathway components from *C. albicans*, this fungus was thought to be asexual. However, in *S. cerevisiae*, the pheromone response pathway was known to share components with the pseudohyphal signaling pathway (Liu et al. 1993; Roberts and Fink 1994; Kron and Gow 1995). Therefore, components of the *C. albicans* MAPK pathway were initially isolated in *S. cerevisiae* and then their function investigated by examining the phenotype of *C. albicans* null mutants and overexpressing strains.

MAPK pathway mutants display characteristic phenotypes. Null mutants, in which this pathway is blocked, are unable to form hyphae on solid Spider medium (which contains the poor carbon source, mannitol), but they still undergo morphogenesis in response to other stimuli (serum, pH) and in liquid media, including Spider medium (e.g. Liu et al. 1994; Leberer et al. 1996). Constitutive activation of the MAPK pathway, for example by inactivation of the negative regulator Cpp1 (Csank et al. 1997) or overexpression of components of the MAP kinase module (Leberer et al. 1996), promotes constitutive hyphal development. Taken together, these data suggest that the MAPK pathway might activate morphogenesis in response to nutrient limitation (Fig. 7.3). Parallel pathways promote hyphal development in response to other stimuli and, in general, it is thought that there may be some functional overlap between these pathways and the MAPK pathway.

Consistent with these in vitro observations, the MAPK pathway displays functional specialization in vivo. Inactivation of the MAPK pathway attenuates virulence in the mammary glands of lactating mice, preventing tissue colonization (Guhad et al. 1998). However, MAPK pathway mutants retain their virulence in the mouse model of systemic candidosis (Leberer et al. 1996; Lo et al. 1997). Hence, the MAPK pathway is only required for infection in certain specific environments in vivo.

Mep2, a transmembrane ammonium permease, was recently found to be required for the switch from yeast to hyphal growth in response to nitrogen starvation on a solid surface. When ammonium is limiting, Mep2 activates both the MAPK and cAMP pathways in a Ras1-dependent fashion. Thus, Mep2 has a specific function in nitrogen starvation-induced morphogenesis (Biswas and Morschhäuser 2005). By analogy with *S. cerevisiae* (Lorenz and Heitman 1997), a Ras protein is thought to activate both the MAPK and cAMP pathways (Fig. 7.4); and the phenotypes of a *C. albicans ras1* null mutant are consistent with this model. Like a *cph1*, *efg1* double mutant (Lo et al. 1997), this *ras1* null mutant is unable to develop hyphae in response to serum stimulation, whereas single *cph1* and *efg1* mutants are able to develop some hyphae under these conditions (Feng et al. 1999).

By analogy with the *S. cerevisiae* pseudohyphal pathway, one would expect the signal to be passed from Ras2 to the MAPK pathway via a G protein module and 14-3-3 (Bmh1) proteins (Mosch et al. 1996; Roberts et al. 1997). A single essential *BMH1* gene exists in *C. albicans* and this gene does play a role in morphogenetic signaling (Cognetti et al. 2002; Palmer et al. 2004). Similarly, a Cdc42/Cdc24 GTPase module has been identified in *C. albicans*. Both components are highly conserved with their *S. cerevisiae* homologues and both are essential for viability (Mirbod et al. 1997; Ushinsky et al. 2002; Bassilana et al. 2003). Partial depletion of Cdc24, the GDP-GTP exchange factor for Cdc42, causes similar phenotypes to Cdc42 inhibition (Bassilana et al. 2003, 2005), which is consistent with the idea that these proteins act in the same GTPase module. Cdc42 is required for polarized growth, both in yeast and hyphal cells (Ushinsky et al. 2002). *CDC42* mRNA levels differ and a GFP-Cdc42 fusion protein is differentially localized in yeast and hyphae (Mirbod et al. 1997; Hazan and Liu 2002). The ectopic expression of a hyperactive allele of Cdc42 is lethal, but this phenotype is rescued by the inactivation of *CST20* (Ushinsky et al. 2002). Also, Cdc42 binds to a Cst20 motif in vitro (Su et al. 2005). These observations lend considerable weight to the idea that the Cdc42/Cdc24 GTPase module is regulated during morphogenesis and that it operates through the MAPK pathway. Interestingly, *cdc24* mutants with defects in hyphal growth are less able to damage endothelial cells (van den Berg et al. 2004).

The Cdc42/Cdc24 GTPase module is thought to pass the morphogenetic signal to Cst20, a member

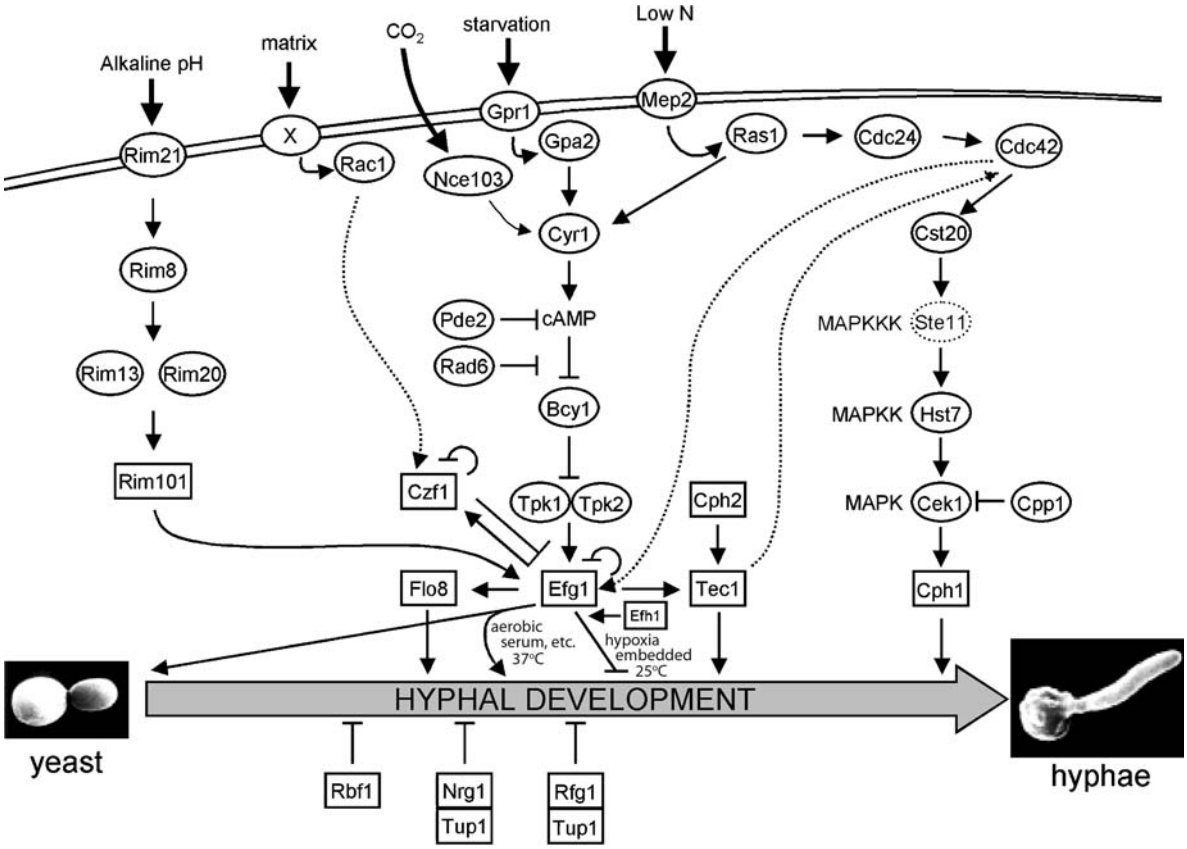

Fig. 7.4. Morphogenetic signaling in *C. albicans*. MAPK, cAMP, pH, alternative conditions (embedding/hypoxia) and other pathways promote hyphal development in *C. albicans* (see Sect. IV.). Many of these pathways depend upon the transcription factor Efg1 for their normal operation. A number of additional factors negatively regulate hyphal development

of the Ste20/p65^{PAK} family of protein kinases, which has been shown to lie on the MAPK pathway (Köhler and Fink 1996; Leberer et al. 1996). Unlike other MAPK pathway mutants, a *C. albicans cst20* null mutant displays attenuated virulence in systemic infections (Leberer et al. 1996), suggesting that Cst20 probably executes additional functions on top of its role in the MAPK pathway. By analogy with *S. cerevisiae* Ste20, Cst20 might integrate morphogenetic signaling with the control of cell polarity.

At the core of the MAPK pathway lies a MAP kinase module that is activated by Cst20 (Fig. 7.4). A homologue of *S. cerevisiae STE11*, which presumably encodes the MAP kinase kinase kinase in this module, has been annotated (Braun et al. 2005), but to our knowledge this *C. albicans STE11* gene has not been functionally dissected. The MAP kinase kinase Hst7 (Clark et al. 1995; Köhler and Fink 1996; Leberer et al. 1996) and MAP kinase Cek1 (Whiteway et al. 1992; Csank et al. 1998) have been characterized and their relative positions on the pathway established by epistasis analyses (Leberer et al. 1996; Csank et al. 1998). The activity of the MAP kinase appears to be negatively regulated by the tyrosine phosphatase, Cpp1, since the constitutive hyphal development observed in a *cpp1* null mutant is inhibited by inactivation of Cek1 (Csank et al. 1997). Cpp1 might also regulate other signaling pathways in *C. albicans* because other protein phosphatases are known to have multiple substrates. Indeed Cpp1 also seems to have a role in the regulation of gene transcription at 37 °C. This role is Cek1-independent and appears to be linked to a pathway that acts through Efg1 (Schröppel et al. 2000).

The function of the MAP kinase module is dependent on the transcription factor Cph1 (Liu et al. 1994). As described above, *C. albicans cph1* null mutants are often used to define this MAPK path-

way experimentally. *C. albicans* Cph1 is a functional homologue of *S. cerevisiae* Ste12 (Liu et al. 1994). In *S. cerevisiae*, Ste12 acts in concert with Tec1 to stimulate the transcription of genes containing the filamentous response element (FRE; Madhani and Fink 1997). A Tec1 homologue has been identified in *C. albicans* and it is involved in morphogenetic regulation (Schweizer et al. 2000). However, Tec1 does not seem to function on the MAPK pathway and hence this factor is discussed below (Sect. 2.). In *S. cerevisiae*, the activation of Ste12-Tec1 by the MAP kinase module is mediated by the inhibition of the repressors Dig1 and Dig2 (Cook et al. 1996). However, no Dig1 or Dig2 homologues in *C. albicans* have been annotated (Braun et al. 2005; d'Enfert et al. 2005). This raises the possibility that the regulation of hyphal development in *C. albicans* by Cph1 might operate via subtly different mechanisms compared with the regulation of *S. cerevisiae* pseudohyphal development by Ste12.

The gene targets of the MAPK pathway, and hence the specific role(s) of this pathway in morphogenesis and virulence, remain obscure. No hypha-specific *C. albicans* genes have been identified, whose expression is dependent on this pathway (Sharkey et al. 1999; Brown et al. 2000). However, the degree of activation of some hypha-specific genes is slightly reduced in *cph1* cells (Leng et al. 2001; Argimón 2006). This is consistent with the idea that the activities of multiple morphogenetic signaling pathways are integrated at hypha-specific promoters (Braun and Johnson 2000; Brown et al. 2000; Brown 2002a).

It is generally accepted that the MAPK pathway is involved in morphogenetic regulation (Brown and Gow 1999; Whiteway 2000; Liu 2001; Berman and Sudbery 2002; Brown 2002a). However, is this really the case? The only morphogenetic phenotype displayed by *C. albicans* null mutants that have a defective MAPK module is the formation of smooth colonies, rather than wrinkly wild-type colonies, on solid Spider medium after about one week of growth (Liu et al. 1994; Köhler and Fink 1996; Leberer et al. 1996). These mutants do not display morphogenetic phenotypes on other solid media or in liquid media. The formation of smooth colonies by MAPK mutants on solid Spider medium is generally interpreted as reflecting a defect in hypha formation; and hence it is inferred that the MAPK pathway contributes to hyphal development. However, Ernst (2000) pointed out the large temporal difference in morphogenesis assays performed using solid and liquid media, and that the interpretation of morphogenetic phenotypes based on colony morphologies could be misleading. Interestingly, our microscopic analyses of MAPK mutants revealed that these cells do form hyphae within hours of plating on solid Spider medium, although they form smooth colonies in the long term (Budge and Brown, unpublished data). Therefore, in our view, the role of the MAPK pathway in hyphal development is not clear. In contrast, this MAPK signaling pathway plays a clear role in the mating response of *C. albicans*. Pheromone receptors have been identified which are presumed to activate the MAPK pathway during the mating response (Bennett et al. 2003; Janiak et al. 2005). More to the point, mutations in the MAPK pathway block mating (Chen et al. 2002; Magee et al. 2002). Constitutive activation of the MAPK pathway does promote filamentous growth (Leberer et al. 1996). However, this might reflect the formation of mating shmoos rather than *bona fide* hyphae. Hence, the general presumption that the MAPK pathway is involved in morphogenetic regulation needs to be questioned.

2. cAMP Signaling Pathway

Ernst and co-workers were the first to identify a component of a second morphogenetic signaling pathway in *C. albicans* (Stoldt et al. 1997). They first identified *EFG1* on the basis that its expression *e*nhances *f*ilamentous *g*rowth in *S. cerevisiae*. Significantly, the morphogenetic phenotypes of *C. albicans efg1* mutants are stronger than those for MAPK pathway null mutants (Lo et al. 1997; Stoldt et al. 1997). This first indicated that Efg1 defines a major morphogenetic pathway in *C. albicans* that is distinct from the MAPK pathway (Fig. 7.3). An *efg1* null mutant displays hyphal defects on solid and liquid serum-containing media and a range of media that might be expected to impose starvation (Lo et al. 1997; Sonneborn et al. 2000). This indicates that serum stimulation and activation on solid surfaces depend specifically upon Efg1 (Fig. 7.3). However, the stimulation of morphogenesis by other signals, such as starvation, pH and CO_2, is also shown to depend upon Efg1, the transcriptional regulator with the broadest contribution to morphogenesis known to date. Efg1 activity is regulated by the cAMP pathway. Therefore in *C. albicans* the cAMP-Efg1 pathway seems to act as a hub that coordinates the input from several types of environmental signals (Fig. 7.3). Several homologues of *S. cerevisiae* cAMP-dependent pathway components have been identified in *C. al-*

bicans, including the receptor Mep2, the G-protein coupled receptor Gpr1, the Gα protein Gpa2, the G-protein Ras1, the adenylyl cyclase Cdc35, the cAMP-dependent protein kinase A and the transcriptional activator Flo8 (Fig. 7.4).

Mep2, a transmembrane ammonium permease, was recently found to be required for the transition from yeast to hyphal growth in response to nitrogen starvation on a solid surface. When ammonium ions are limiting, Mep2 activates both the MAPK and cAMP signaling pathways in a Ras1-dependent fashion (Biswas and Morschhäuser 2005). Thus, Mep2 has a specific function in nitrogen starvation-induced morphogenesis.

It is reported that a single *RAS* locus exists in *C. albicans* (Feng et al. 1999). The deletion of this *RAS1* gene in *C. albicans* is not a lethal event (Feng et al. 1999; Leberer et al. 2001). Interestingly, a second *RAS2* locus has been annotated in the *C. albicans* genome (Braun et al. 2005). Therefore, despite the prevailing view that Ras is not essential in *C. albicans*, it is entirely possible that a *C. albicans ras1 ras2* double mutant is non-viable, like its *S. cerevisiae* counterpart (Kataoka et al. 1984). However, to our knowledge, this has not yet been tested.

C. albicans ras1 mutants are impaired in hyphal growth under a wide range of inducing conditions (Feng et al. 1999; Leberer et al. 2001). Also, a dominant active RAS^{V13} allele enhances hyphal development, whereas a dominant negative RAS^{V13} allele reduces hyphal growth (Feng et al. 1999). The morphogenetic defect of *ras1* cells can be reversed by supplementing the growth medium with cAMP or by overexpressing components of the MAPK cascade (Leberer et al. 2001). Therefore, Ras1 is thought to regulate *C. albicans* morphogenesis by contributing to both the cAMP pathway and the MAPK pathways, like Ras2 in *S. cerevisiae*. The transcript profiling data of Harcus and co-workers (2004) are consistent with this view. They showed that Ras1 regulates a subset of the genes that are controlled by the adenylyl cyclase Cdc35 (see below). However, they also found *C. albicans* genes that were regulated by Cdc35 in a Ras1-independent fashion. These genes may be associated with the activation of the cAMP pathway via Gpr1/Gpa2 signaling (Maidan et al. 2005).

In *C. albicans*, the receptor Gpr1 and its coupled Gα protein Gpa2 are both required for morphogenesis on various solid media, but they only have minor effects upon hyphal development in liquid media (Sánchez-Martínez and Pérez-Martín 2002; Miwa et al. 2004; Maidan et al. 2005). The C-terminal tail of Gpr1 was shown to interact with Gpa2 in a two-hybrid assay (Miwa et al. 2004). Gpa2 functions downstream of Gpr1, leading to the activation of the cAMP pathway (Miwa et al. 2004; Maidan et al. 2005), but not the MAPK pathway as was initially suggested (Sánchez-Martínez and Pérez-Martín 2002). Micromolar concentrations of specific amino acids, such as methionine or isoform, appear to be important for the activation of morphogenesis through Gpr1 (Maidan et al. 2005).

C. albicans has a single homologue of the *S. cerevisiae* adenylyl cyclase Cyr1/Cdc35, encoded by the gene *CDC35* (Rocha et al. 2001). *C. albicans cdc35* cells are viable but grow more slowly than wild type cells, are avirulent in a mouse model of infection and are unable to form hyphae in most liquid and solid hypha-inducing media. The morphogenetic defect can be rescued by exogenous cAMP, which points to a role for Cdc35 in the activation of the cAMP pathway (Rocha et al. 2001). By analogy with the dual regulation of *S. cerevisiae* adenylyl cyclase by Ras2 and Gpa2, and with some supporting experimental evidence, it was suggested that *C. albicans* Cdc35 might also be regulated by Ras1 and Gpa2 (Leberer et al. 2001; Rocha et al. 2001; Maidan et al. 2005).

The adenylate cyclase-associated protein Cap1/Srv2 was shown to interact with Ras and adenylyl cyclase in non-pathogenic fungi to increase cAMP levels under specific environmental conditions. The inactivation of *C. albicans* Cap1/Srv2 causes a similar phenotype to Cdc35 inactivation, that is, impairment of hyphal development on various liquid and solid media and avirulence in the mouse model of systemic candidiasis (Bahn and Sundstrom 2001). Moreover, a peak in the intracellular levels of cAMP is observed one hour after hyphal induction in wild-type *C. albicans* cells. This peak is abolished in *cap1/srv2* cells, establishing a role for Cap1/Srv2 in cAMP-dependent morphogenetic signaling (Bahn and Sundstrom 2001).

C. albicans senses CO_2/bicarbonate levels via adenylyl cyclase (Klengel et al. 2005). These authors demonstrated that CO_2/bicarbonate induces *C. albicans* filamentation through direct stimulation of adenylyl cyclase. Interestingly, this was observed at concentrations of CO_2/bicarbonate that are observed in the mammalian host (about 5%). Also, they showed that the equilibration of CO_2 and bicarbonate levels via carbonic anhydrase (Nce103) is essential for the virulence of *C. albicans* in niches where CO_2 concentrations are limited. Further-

more, this signaling mechanism is conserved in another major fungal pathogen of humans, *Cryptococcus neoformans* (Klengel et al. 2005; Mogensen et al. 2006). Clearly CO_2/bicarbonate signaling via the cAMP pathway is important in the context of fungal morphogenesis and virulence.

Low- (*PDE1*) and high-affinity (*PDE2*) phosphodiesterases have been identified in *Candida albicans* (Hoyer et al. 1994; Bahn et al. 2003; Jung and Stateva 2003). The inactivation of *PDE2* causes hyperfilamentation, presumably through an increase in the intracellular levels of cAMP (Bahn et al. 2003; Jung and Stateva 2003). Therefore, Pde2 is viewed as a negative regulator of cAMP signaling. Significantly, these hyperfilamentous mutants are avirulent in a mouse model of systemic candidiasis (Bahn et al. 2003).

C. albicans protein kinase A (PKA) is composed of regulatory and catalytic subunits. The regulatory subunit is encoded by the *BCY1* gene (Staab et al. 2003; Cassola et al. 2004), whereas there are two catalytic isoforms encoded by *TPK1* and *TPK2* (Sonneborn et al. 2000; Bockmühl et al. 2001). A homozygous *C. albicans bcy1/bcy1* null strain could not be constructed, suggesting that *BCY1* is an essential gene in *C. albicans*. A *bcy1 tpk2* double mutant displays constitutive PKA activity, driven by Tpk1. Surprisingly, this mutant grows normally in the yeast form and develops hyphae normally under inducing conditions (Cassola et al. 2004). A strain overexpressing *BCY1* is defective in hyphal growth in both solid and liquid media (Staab et al. 2003). Both Tpk isoforms in *C. albicans* are positive regulators of hyphal morphogenesis and overexpression of one isoform can complement the deletion of the other (Sonneborn et al. 2000; Bockmühl et al. 2001). Interestingly, Tpk1 and Tpk2 seem to have differential effects upon morphogenesis under different inducing conditions. *C. albicans tpk1* cells show defective filamentation on solid media, but their filamentation remains almost unaffected in liquid media. In contrast, *tpk2* cells display a severe filamentation defect in liquid media, but only a partial defect on solid media. In addition, only *tpk2* mutants are defective in agar invasion (Bockmühl et al. 2001). Epistasis analyses place both Tpk1 and Tpk2 downstream of Ras1 (Bockmühl et al. 2001).

As described above, the cAMP pathway is thought to operate mainly via Efg1. Efg1 contains a putative phosphorylation site for PKA (T206) which is essential to promote hyphal induction under certain inducing conditions (Bockmühl and Ernst 2001). Hence, the activity of this regulator is thought to be modulated by phosphorylation. However, the ability of PKA to phosphorylate Efg1 in vitro has not been formally demonstrated.

Efg1 is a member of the APSES family of fungus-specific transcriptional regulators, which includes *S. cerevisiae* Phd1 and Sok2 (Sonneborn et al. 2000; Tebarth et al. 2003). The depletion of Efg1 results in the impairment of hyphal growth under inducing conditions (Lo et al. 1997; Stoldt et al. 1997), which suggests that Efg1 is an activator of morphogenesis. However, a number of observations now indicate that Efg1 can also act as a repressor. Cells depleted in Efg1 do not grow as normal yeast cells under inducing conditions, but display a pseudohyphal phenotype, with elongated, rod-like cells that often remain attached to one another (Lo et al. 1997; Stoldt et al. 1997). Efg1 overexpression promotes pseudohyphal growth, not hyphal growth, under non-inducing conditions. In addition, *EFG1* transcript levels are quickly downregulated upon hyphal development (Stoldt et al. 1997). These results indicate that Efg1 is regulated at a transcriptional as well as a post-translational level. They also suggest that Efg1 could also be acting as a repressor of elongated, pseudohyphal growth and pointed to a dual role for this transcription factor in morphogenesis (Stoldt et al. 1997). *EFG1* expression is repressed by a Sin3-dependent autoregulation mechanism in response to hyphal stimulation, with both Efg1 and Sin3 (from the Sin3/HDAC histone deacetylase complex) situated at the Efg1 promoter (Tebarth et al. 2003). Efg1 was shown to behave as a repressor in *C. albicans*, using a one-hybrid system (Doedt et al. 2004; Russell and Brown 2005). Taken together, these results are consistent with the idea that Efg1 is a repressor.

Another transcription factor that interacts with Efg1 in vivo was recently identified (Cao et al. 2006). Flo8 is required for morphogenesis under all conditions tested, as well as for virulence. Transcript profiling experiments showed that Flo8 controls a subset of Efg1-regulated genes. Interestingly, *C. albicans flo8*, *efg1* and *cdc35* null mutants all display enhanced filamentation under microaerophilic conditions. Altogether these results imply that Flo8 may function downstream of the cAMP pathway and, together with Efg1, regulate morphogenesis (Cao et al. 2006).

The activity of the cAMP pathway is negatively regulated by Rad6 (Leng et al. 2000). Rad6 depletion enhances pseudohyphal development, whereas Rad6p overexpression inhibits hyphal

development. Rad6 is a ubiquitin-conjugating enzyme that might target a component of the Efg1p pathway for ubiquitination-mediated protein degradation in the absence of a hypha-inducing signal (Leng et al. 2000). Also, recent evidence suggests a link between Efg1 and elements upstream of the MAPK pathway. vanderBerg and co-workers (2004) showed that the expression of *SAP6*, *ECE1* and *HWP1*, three genes that are expressed during morphogenesis and activated in an Efg1-dependent manner (Brown 2002b), was severely reduced in the *cdc42* mutants they tested. This implies that Cdc42 has an additional signaling function that might operate via Efg1, but the mechanism is not known.

How does activation of the cAMP pathway mediate changes in cell shape? In *S. cerevisiae*, the cAMP pathway contributes to the regulation of *FLO11* (*MUC1*), which encodes a cell surface glycoprotein protein, the expression of which appears necessary and sufficient for pseudohyphal development and invasive growth (Lambrechts et al. 1996; Lo and Dranginis 1998; Rupp et al. 1999). In *C. albicans*, Efg1 is required for the expression of hypha-specific genes such as *HWP1*, *HYR1*, *ECE1* and *ALS3* (Sharkey et al. 1999; Brown et al. 2000; Leng et al. 2001; Brown 2002b) – *ALS3* was formerly known as *ALS8* (Zhao et al. 2004). Many of these Efg1 gene targets encode hypha-specific cell wall components and adhesion factors (Birse et al. 1993; Bailey et al. 1996; Staab et al. 1999; Leng et al. 2001; Dieterich et al. 2002; Sohn et al. 2003). It is suggested that Efg1 might interact directly with the promoters of these hypha-specific genes to regulate their expression (Leng et al. 2001), but this remains to be confirmed. However, these Efg1 targets do not appear to mediate the changes in cell shape required for hyphal development because none of these Efg1 gene targets are essential for hyphal development or virulence (Brown 2002b; Sundstrom et al. 2002). The key to the regulation of cell morphology by Efg1 seems to be the *HGC1* gene, which encodes a hypha-specific cyclin that is essential for hyphal development (Zheng et al. 2004). *HGC1* expression is dependent upon Efg1 (and negative regulators of hyphal development; see Sect. IV.B.) and the inactivation of *HGC1* blocks hyphal development. The key question now is how Hgc1 regulates cell form.

Consistent with the strong morphological phenotypes observed in vitro, *efg1* null mutants display significantly attenuated virulence and hyphal development in systemic infections (Lo et al. 1997), suggesting that the cAMP pathway plays an important role in pathogenesis. Efg1 exerts more significant effects upon host invasion and adhesion than Cph1, suggesting that the MAPK pathway is less significant in regulating these virulence attributes than the cAMP pathway (Dieterich et al. 2002). Furthermore cAMP signaling exerts stronger effects upon the *C. albicans* transcriptome than MAPK signaling, at least under the conditions tested (Nantel et al. 2002; Harcus et al. 2004). However, Efg1 is not required for the development of candidosis in all microenvironments in vivo. *Efg1* mutants can form hyphae and retain their virulence in infections of the tongues of immunosuppressed gnotobiotic pigs (Riggle et al. 1999), an infection model that is thought to reflect stimulation via physical cues in the environment (Sect. 4.).

3. pH Signaling Pathway

It has been known for some time that increases in pH, combined with elevated temperatures, promote yeast–hypha morphogenesis (Buffo et al. 1984; Soll 1986). Screens for *C. albicans* genes that are regulated during pH-stimulated morphogenesis led to the identification of *PHR1* and then *PHR2*, which encode pH-regulated glucosidases involved in maintaining cell wall structure and cell shape (Saporito-Irwin 1995; Muhlschlegel and Fonzi 1997; Fonzi 1999). The inactivation of the alkaline-expressed gene *PHR1* causes pH-conditional defects in the polarity of growth and reduced virulence in systemic infection models, whereas null mutations in the acid-expressed gene *PHR2* block growth at pH 4 and attenuate virulence in vaginal infections (Ghannoum et al. 1995; Saporito-Irwin 1995; Muhlschlegel and Fonzi 1997; De Bernardis et al. 1998). Constitutive expression of Phr1 from a *TEF-PHR1* fusion rescues the *phr2* mutant phenotype, indicating that Phr1 and Phr2 are functionally equivalent.

The pH signaling pathways have been characterized in the greatest detail in *Aspergillus nidulans* (Denison et al. 1998; Mingot et al. 1999); and this pathway is conserved in other fungi, including *S. cerevisiae* (Fig. 7.5; see Ramon et al. 1999; Davis et al. 2000; Davis 2003; and references therein). In *A. nidulans*, an alkaline ambient pH is probably detected by the integral membrane proteins, PalH and PalI, whose functions have not been established. This stimulus is then transduced by a signaling cascade involving PalA, PalB, PalC and PalF, which leads to the activation of the zinc finger transcription factor, PacC. This PacC activation in-

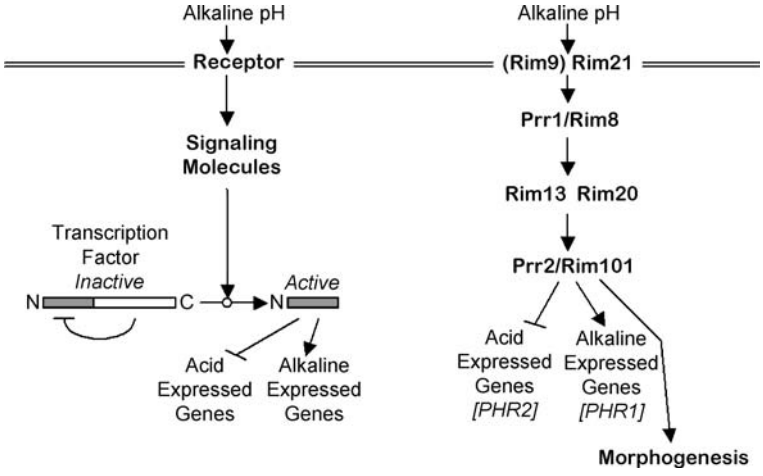

Fig. 7.5. A conserved signal transduction pathway mediates responses to ambient pH in *C. albicans* (see Sect. 3.). Adapted from Davis (2003)

volves a specific cleavage to remove the inhibitory C-terminal region, allowing the N-terminal region to activate the expression of alkaline expressed genes and repress the transcription of acid expressed genes (Fig. 7.5; Mingot et al. 1999). The cleavage of PacC involves a cysteine protease and *palB* encodes a protein with similarity to cysteine proteases (Denison et al. 1995).

Homologues of these pH regulators have been identified in *C. albicans* (Fig. 7.5; Porta et al. 1999; Ramon et al. 1999; Wilson et al. 1999; Davis et al. 2000; Davis 2003; Kullas et al. 2004; Li et al. 2004). Rim21, which is required for the activation of the transcription factor Rim101/Prr2, is thought to act as the sensor of alkaline pH (Davis 2003). Rim8/Prr1 also lies upstream of Rim101/Prr2, as is required for its activation (Porta et al. 1999; Davis et al. 2000). Rim13 is thought to be the protease that cleaves off the C-terminal of Rim101/Prr2 region to activate it in response to alkaline pH (Li et al. 2004), whilst Rim20 is thought to interact with Rim101/Prr2, acting as a scaffold to facilitate the proteolytic cleavage by Rim13 (Kullas et al. 2004).

Mutants that prevent the activation of the transcription factor Rim101/Prr2 display related phenotypes (Porta et al. 1999; Davis et al. 2000; Davis 2003; Li et al. 2004). For example, alkaline-expressed genes (e.g. *PHR1*) are no longer induced and acid-expressed genes (e.g. *PHR2*) are no longer repressed in these mutants. Interestingly, *rim101*/*prr2* and *rim8*/*prr1* mutants also display morphogenetic defects. On solid media at slightly alkaline pH (pH 7.5–8.0), hyphal growth and invasion are blocked on serum and M199 medium and are reduced on Spider and Lee's medium. In liquid media at similar pHs, these null mutants can form hyphae in serum but not in M199, Spider or Lee's media (Porta et al. 1999; Ramon et al. 1999; Wilson et al. 1999; Davis et al. 2000). Similarly, a *rim20* mutant displays a hyphal defect in M199, but not upon serum stimulation in liquid media (Davis et al. 2000). The expression of a C-terminally truncated version of Rim101/Prr2 – equivalent to the removal of the inhibitory C-terminal region of this transcription factor (Fig. 7.5) – suppresses the filamentous defects of *rim8*/*prr1* and *rim20* mutants at alkaline pH and induces constitutive filamentation (Davis et al. 2000; El Barkani et al. 2000). These data confirmed the epistatic relationship between these genes on the Prr2 pathway, as well as the role of this pathway in controlling pH-regulated morphogenesis.

Therefore, both morphogenesis and pH regulated gene expression are controlled by this pH signaling pathway. Interestingly, these phenotypes are separable. For example, expression of the hypha-specific gene HWP1 is not affected by inactivation of RIM8/PRR1, indicating that different control mechanisms can mediate hypha-specific and pH-regulated gene expression (Porta et al. 1999). Also, constitutive expression of Phr1 does not rescue the hyphal defects of rim101/prr2 or rim8/prr1 null mutants, indicating that it is not the lack of Phr1 that prevents hyphal development in these strains (Porta et al. 1999). Hence in C. albicans, there appears to be bifurcation of the pH response pathway at Rim101/Prr2, one fork involved in the control of pH-regulated gene expression and the other fork activating yeast–hypha morphogenesis. Most significantly, the ability of dominant alleles of RIM101/PRR2 to constitutively activate morphogenesis is dependent upon Efg1 (El Barkani

et al. 2000). Therefore, the pH signaling pathway acts through Efg1 to stimulate hyphal development (Figs. 7.3, 7.4).

4. Additional Pathways

The identification and characterization of the *CZF1* gene defined an alternative morphogenetic pathway in *C. albicans* (Brown et al. 1999). This gene was identified on the basis that ectopic expression of *CZF1* promotes hyphal development when *C. albicans* cells are embedded in agar. An *efg1 cph1* double mutant retains the ability to form hyphae under embedding conditions, which may be comparable with the environment of fungal cells during deep tissue invasion (Riggle et al. 1999). This observation strengthened the view that Czf1 defines an alternative pathway, a unique aspect of which is that it appears to respond to physical cues in the environment, rather than chemical cues such as pH, morphogens or starvation (Brown et al. 1999). There might be significant overlap between this "embedding" pathway and the alternative "hypoxia" pathway which is being investigated by Ernst and co-workers (Ernst 2000; Doedt et al. 2004). This pathway is also referred to as the "alternative pathway".

The inactivation of *CZF1* leads to a moderate defect in hyphal growth under embedded conditions (Brown et al. 1999), whilst the inactivation of EFG1 promotes enhances filamentation under similar conditions (Giusani et al. 2002). *CZF1* overexpression in a *cph1* background accelerates the production of filamentous colonies, but overexpression in an *efg1 cph1* double mutant does not generate this phenotype. This suggests that Czf1 promotes filamentous growth by relieving Efg1-mediated repression (Giusani et al. 2002). However, Efg1 binds to *CZF1* promoter and the deletion of *EFG1* abolishes *CZF1* expression (Vinces et al. 2006). Also, Efg1 and Czf1 interact physically in the yeast two-hybrid system (Giusani et al. 2002). Furthermore, ectopic expression of *CZF1* downregulates its own expression. These data indicate that a complex autoregulatory loop involving *EFG1* and *CZF1* regulates morphogenesis under embedding conditions. The current model suggests that, under these conditions, Czf1 negatively regulates its own expression by binding the *CZF1* promoter close to Efg1, thus antagonizing Efg1-mediated activation of *CZF1* (Vinces et al. 2006).

An Efg1 homologue has been identified in *C. albicans* (Efh1), thereby defining second member of the APSES family in this fungus (Doedt et al. 2004). *C. albicans efh1* cells display weak phenotypes during morphogenesis under standard inducing conditions, but they display hyperfilamentation in an *efg1* background under embedded or hypoxic conditions (Doedt et al. 2004), suggesting that Efh1 contributes to the alternative morphogenetic pathway. Genome-wide transcript profiling revealed that Efg1 and Efh1 regulate partially overlapping sets of genes associated with filament formation. However, Efh1 behaves as an activator in the *C. albicans* one-hybrid system, unlike Efg1 which acts as a repressor under these conditions (Doedt et al. 2004; Russell and Brown 2005). Taken together, the data suggest that Efh1 supports the regulatory functions of the main regulator Efg1 in the alternative morphogenetic pathway.

Other components of this alternative signaling pathway(s) remain to be identified. However, Cao and co-workers (2006) showed recently that *C. albicans cdc35* and *flo8* cells display hyperfilamentation under embedded conditions, though the morphology of the filaments is slightly different than that of the *efg1* mutant. This observation implicates the cAMP pathway and Flo8 in the inhibition of *C. albicans* morphogenesis under embedding conditions. However, further experiments are required to better understand the connections between Flo8, Efg1 and Czf1. Another recent study raised the possibility that another G protein may regulate morphogenesis under embedded conditions via Czf1 (Bassilana and Arkowitz 2006). A highly conserved homologue of *S. cerevisiae RAC1* was identified in *C. albicans*. Rac1 is required for filamentous growth under embedded conditions, a *rac1* mutant displaying similar morphogenetic defects as *czf1* cells.

An additional morphogenetic pathway is defined by the factors Cph2, Tec1 and Bcr1. Cph2 (***C****andida* **p**seudo**h**yphal regulator) is a basic helix-loop-helix transcription factor of the Myc subfamily. Cph2 was found to be required for hyphal development in liquid and solid Lee's medium and in serum-containing solid media (Lane et al. 2001b). *CPH2* overexpression induces pseudohyphal growth under conditions that favor the yeast form. *TEC1* transcription is highest in Lee's medium, but is severely reduced in *cph2* cells under these conditions. Furthermore, ectopic *TEC1* expression suppresses the *cph2* defect in hyphal development. Nevertheless, phenotypic differences do exist between wild-type cells and *cph2* cells overexpressing *TEC1*. Taken together, these results suggest that Cph2 mediates its

morphogenetic effects at least partly through Tec1 (Lane et al. 2001b). Finally, epistasis studies between *EFG1*, *CPH1* and *CPH2* revealed that Cph2 functions independently from the MAPK and cAMP signaling pathways (Lane et al. 2001b).

Tec1 is a member of the TEA/ATTS transcription factor family, which was found to regulate hyphal development in *C. albicans* (Schweizer et al. 2000). Tec1 is not involved in the MAPK pathway, as was predicted on the basis of its homology with *S. cerevisiae* Tec1. The deletion of Tec1 results in pseudohyphal growth under strong inducing conditions, such as the addition of serum at 37 °C, and in attenuated virulence. *TEC1* mRNA levels are upregulated during serum-induced hyphal induction (Schweizer et al. 2000), but are down-regulated in an *efg1* null mutant (Lane et al. 2001a). These data suggest that Tec1 is an activator of hyphal development and that Efg1 regulates *TEC1* transcription (Fig. 7.4). *EFG1* overexpression does not suppress the morphogenetic defects of a *tec1* mutant (Schweizer et al. 2000). *TEC1* overexpression promotes hyphal growth at 30 °C, but only pseudohyphal growth in an *efg1* background (Lane 2001a). These results suggest that Tec1 is a downstream effector of Efg1. Interestingly, Bassilana and coworkers (2005) have shown that, in response to serum, *CDC24* transcript levels transiently increase in a Tec1-dependent fashion, suggesting the existence of a positive feedback loop between Cdc24 and Tec1 that contributes to an increase in active Cdc42.

Nobile and Mitchell (2005) identified the *TEC1* and *BCR1* genes in a screen for transcription factor gene mutants that affect biofilm formation in *C. albicans* (Nobile and Mitchell 2005). *TEC1* had been identified previously as a morphogenetic regulator (Schweizer et al. 2000). However, *BCR1* turned out to be a novel regulator of hyphal cell surface adhesins. This led Nobile and Mitchell to suggest that the adherence of hyphal cells is critical for the development of *C. albicans* biofilms (Nobile and Mitchell 2005). Significantly, Nobile and coworkers (2006) then showed that Bcr1 and Tec1 act together to regulate the expression of hyphal adhesin genes such as *HYR1*, *HWP1*, *RBT5*, *HWP1* and *ALS3*. The expression of these genes is blocked in both *tec1* and *bcr1* mutants. However, this defect in *tec1* cells can be suppressed by the ectopic expression of *BCR1*. Therefore, Bcr1 acts downstream of Tec1 to activate the expression of these hyphal adhesins (Nobile et al. 2006).

B. Negative Regulation

The above pathways generally activate hyphal or pseudohyphal development in response to morphogenetic signals. However, other pathways repress hyphal and/or pseudohyphal growth in the absence of a morphogenetic signal (Fig. 7.4).

Tup1p was the first repressor of hyphal development to be identified in *C. albicans* (Braun and Johnson 1997). *C. albicans tup1* null mutants are locked in an elongated pseudohyphal growth form even under conditions that normally promote growth in the yeast form. Phenotypic analyses of *tup1 efg1*, *tup1 cph1* and *chp1 efg1* double mutants and comparison with a *tup1 efg1 cph1* triple mutant suggested that Cph1, Efg1 and Tup1 act in an additive fashion on separate morphogenetic pathways (Braun and Johnson 2000). Seven Tup1-repressed genes were identified in a search for targets of Tup1 (Braun et al. 2000). Five of these targets were induced during morphogenesis (*RBT1*, *RBT4*, *RBT5*, *HWP1*, *WAP1*), two of which were implicated in virulence (*RBT1*, *RBT4*). The other two Tup1 targets were not related to morphogenesis (*RBT2*, *RBT7*), which together with the phenotypic analysis of the *tup1* mutant, suggested that Tup1 has additional roles in repression other than filamentous growth. This was confirmed subsequently by several genome-wide transcript profiling studies (Murad et al. 2001a, b; Garcia-Sanchez et al. 2005; Kadosh and Johnson 2005). For example, Tup1 is involved in the regulation of metabolic and stress functions as well as in morphogenesis.

In *S. cerevisiae*, Tup1 interacts physically with Ssn6 to form a global corepressor complex that actively represses the transcriptional machinery thus inhibiting the transcription of many genes with various functions. Tup1-Ssn6 is targeted to the promoters of these genes through interactions with DNA-binding proteins (Keleher et al. 1992; Smith and Johnson 2000). *C. albicans* expresses homologues to both Ssn6 (Hwang et al. 2003; García-Sánchez et al. 2005) and the DNA-binding proteins that target the Tup1-Ssn6 corepressor complex to the promoter of genes involved in morphogenesis (Braun et al. 2001; Kadosh and Johnson 2001; Khalaf and Zitomer 2001; Murad et al. 2001a). Unexpectedly, Ssn6 is not required for the Tup1-mediated repression of hypha-specific genes during the growth of *C. albicans* in the yeast form (García-Sánchez et al. 2005). This does not exclude the possibility that Ssn6 is present in Tup1-containing repression complexes.

C. albicans Nrg1 was initially identified by our laboratory in a screen for factors that interact specifically with the promoter element C_4T (Murad et al. 2001a). At the same time, *NRG1* was identified independently by the Johnson group whilst searching for proteins that confer Tup1 repression in *C. albicans* (Braun et al. 2001). A single *NRG* locus is present in the *C. albicans* genome sequence, whereas two *NRG* genes exist in *S. cerevisiae* (Park et al. 1999; Braun et al. 2001; Vyas et al. 2001). *NRG1* encodes a 310-amino-acid, 34-kDa zinc finger DNA-binding protein. *In silico* analysis of Nrg1-Tup1-responsive promoters identified by transcript profiling, combined with mutagenesis of a Nrg1-Tup1-responsive promoter in *C. albicans* defined the Nrg1 response element (NRE) as $(A/C)(A/C/G)C_3T$ (Murad et al. 2001a).

Genetic and transcript profiling data are consistent with the idea that Nrg1 might target the global repressor Tup1 to a subset of *C. albicans* promoters, like its homologues in *S. cerevisiae* (Murad et al. 2001a, b; García-Sánchez et al. 2005; Kadosh and Johnson 2005). The deletion of *NRG1* derepresses filamentous growth, *nrg1* cells growing in filamentous forms under conditions that normally promote the growth of yeast cells. This phenotype is related to that observed for *tup1* mutants. Also, the overexpression of *NRG1* represses hyphal development. This phenotype is dependent on Tup1, which is consistent with the idea that Nrg1 is a Tup1-targeting protein (Braun et al. 2001). Also, the inactivation of *NRG1* or *TUP1* dramatically attenuates the virulence of *C. albicans* in a mouse model of systemic candidiasis (Braun et al. 2001; Murad et al. 2001a). Finally, transcript profiling has revealed that hypha-specific genes exist in the subset of *C. albicans* genes that are co-regulated by Nrg1 and Tup1 (Murad et al. 2001a, b; García-Sánchez et al. 2005; Kadosh and Johnson 2005).

NRG1 transcript levels decrease following exposure to serum (Braun et al. 2001). Recent data indicate that Nrg1 activity is also regulated at a post-translational level (Argimón 2006). In response to a morphogenetic signal, Nrg1 activity appears to be down-regulated by the cAMP signaling pathway, thereby releasing the Nrg1-Tup1-mediated repression of hyphal development.

C. albicans Rfg1 is related to the *S. cerevisiae* hypoxic regulator Rox1. Rfg1 was identified independently by two groups as a negative regulator of hyphal development (Kadosh and Johnson 2001; Khalaf and Zitomer 2001). *RFG1* can complement the defects of a *S. cerevisiae rox1* mutant in the Tup1-dependent repression of hypoxic genes. However, Khalaf and Zitomer (2001) showed that the hypoxic gene *HEM13* is not regulated by Rfg1 in *C. albicans*, suggesting that Rfg1 is not a hypoxic repressor in this fungal pathogen. In the absence of a morphogenetic signal, the *rfg1* cells display a mixture of yeast, pseudohyphae and true hyphae in liquid medium (Khalaf and Zitomer 2001). *Rfg1* cells also display hyperfilamentation on solid media and this is correlated with nutrient starvation (Kadosh and Johnson 2001). The expression of some Tup1-repressed genes is derepressed in the *rfg1* mutants. However, the corresponding molecular and morphogenetic phenotypes of *tup1* cells are significantly more dramatic than of *rfg1* mutants (Kadosh and Johnson 2001). These data suggest that Rfg1 contributes to the transcriptional repression of morphogenetic genes by recruiting the Tup1 complex to their promoters. However, Nrg1 appears to play the greater role in Tup1-mediated repression (Kadosh and Johnson 2001, 2005).

Rbf1 was isolated on the basis that it interacts with the RPG box (Ishii et al. 1997a). This short DNA sequence plays an important role in the regulation of several classes of *S. cerevisiae* genes, including ribosomal proteins, transcription, translation and glycolytic genes. Rbf1 exerts a negative effect upon hyphal development in *C. albicans*, since *rbf1* mutants form hyphae constitutively (Ishii et al. 1997b). The mechanism by which Rbf1p mediates this regulatory effect is not clear, but it might act indirectly to inhibit morphogenesis, for example by affecting *C. albicans* metabolism.

It has been known for some time that *C. albicans* morphogenesis is inhibited at high cell densities (Odds 1988). The molecular basis for this effect became apparent when it was found that *C. albicans* responds to quorum-sensing molecules (Hornby et al. 2001). In this study Hornby and coworkers identified farnesol as the quorum-sensing molecule that is responsible for the inoculum size effect in *C. albicans*. Farnesol inhibits the development of new hyphae, but not the growth of existing germ tubes (Mosel et al. 2005), suggesting that this quorum-sensing molecule might block a morphogenetic commitment step. More recently, farnesol was shown to inhibit the expression of hypha-specific genes in *C. albicans* (Enjalbert and Whiteway 2005). Quorum-sensing mechanisms are likely to be important during infections in the host because they have been shown to influence the interactions of *C. albicans* with bacteria in mixed microbial communities as well as the formation of

C. albicans biofilms (Hogan and Kolter 2002; Ramage et al. 2002; Hogan et al. 2004). Recent work from the Hogan laboratory suggests that farnesol might influence morphogenesis by inhibiting the cAMP signaling pathway (Hogan 2006). However, the impact of quorum-sensing upon *C. albicans* morphogenesis might be complex because another quorum-sensing molecule, tyresol, is reported to promote hyphal development (Chen et al. 2004).

A range of additional factors influence *C. albicans* morphogenesis, some of which might play roles in the integration of morphogenetic signaling with changes in cell polarity. For example, Cla4 is a Ste20-like protein that is required for hyphal growth under all conditions tested (Leberer et al. 1997). *S. cerevisiae* Cla4p is a protein kinase that activates myosin 1 and interacts with the G protein Cdc42p. Hence Cla4p presumably exerts its effects upon *C. albicans* morphogenesis through roles in cytoskeletal organization. Inactivation of *C. albicans* Int1 inhibits hyphal development and adhesion (Gale et al. 1998). Int1 associates with the septin ring in yeast and hyphal cells (Gale et al. 2001), and hence like Cla4, Int1 might coordinate morphogenetic signaling pathways with changes in cell polarity. Similarly the forkhead transcription factor Fkh2, the inactivation of which promotes pseudohyphal growth in *C. albicans*, is proposed to act downstream of the main cAMP and MAPK signaling pathways (Bensen et al. 2002).

C. Calcium Signaling

Changes in the concentration of free cytoplasmic calcium ions act as a signal that regulates many aspects of eukaryotic cell biology (e.g. see Chap. 9 in this volume), including fungal morphogenesis, the response to various stresses and tolerance to antifungal drugs. In *S. cerevisiae* and in *C. albicans* calcium ions enter the cell via a calcium channel complex that is composed of two subunits: Cch1 and Mid1. The Cch1 protein shows homology to mammalian α1 voltage-gated calcium channels in its transmembrane segments (Paidhungat and Garrett 1997). The Mid1 accessory protein may modulate the properties of this channel so it becomes responsive to membrane stretch, or it may act as a stretch-activated channel in its own right (Kanzaki et al. 1999). Calcium ions that enter the cytoplasm bind calcium-binding proteins such as calmodulin that in turn modulate the activity of a number calmodulin-dependent protein kinases, resulting in new cellular responses (Fig. 7.6). Calmodulin binds to and blocks the autoinhibitory domain to the calcineurin phosphatase, resulting in its activation (Rusnak and Mertz 2000). This protein desphosphorylates a number of proteins, including the Crz1 transcription factor Crz1, which can then enter the nucleus and activate the expression of a range of genes (Strathopoulos and Cyert 1997; Strathopoulos-Gerontides et al. 1999; Santos and de Larrinoa 2005; Karababa et al. 2006). This pathway regulates a number of important processes in *C. albicans* and other fungi (Blankenship et al. 2003; Kraus and Heitman 2003; Blankenship and Heitman 2005).

The tolerance of *C. albicans* and fungi to azoles and other classes of antifungal drugs has been shown to be regulated by this pathway and calcineurin mutants are hyper-susceptible to azole treatment, so that normally fungistatic agents such as fluconazole become fungicidal in the presence of calcineurin inhibitors such as FK506 or cyclosporin A and in a *cna1* (calcineurin catalytic subunit) mutant background (Edlind et al. 2002; Sanglard et al. 2003). Calcineurin was shown to affect the colony morphology and hence the extent of filamentation on certain solid media (Sanglard et al. 2003) but calcineurin is not essential for filamentous growth, germ tube formation and the penetration and damage of host cells (Blankenship et al. 2003; Bader et al. 2006). Calcineurin is however critical for the ability of *C. albicans* to survive the calcium stress imposed by growth in serum-containing media (Blankenship et al. 2003; Sanglard et al. 2003; Blankenship and Heitman 2005). Hence it is unsurprising that calcineurin is also essential for the virulence of *C. albicans* (Blankenship et al. 2003; Sanglard et al. 2003). The Crz1-mediated calcium signal was also demonstrated to be important for the response to alkaline conditions and membrane stresses (Santos and de Larrinoa 2005). In addition, it was shown recently that the calcium signaling pathway also participates in the cell wall salvage pathway which leads to elevation of the chitin content of the cell wall, via the activation of chitin synthase gene expression and chitin synthesis, in response to damage or depletion of β-1,3-glucan in the wall (Munro and Gow, unpublished data). Therefore calcium signaling plays vital roles in the response of *C. albicans* to various stresses – in particular cell membrane, cell wall stress and ion stresses (Fig. 7.6).

The calcium signaling pathway was also implicated in the regulation of hyphal orientation responses (Sherwood et al. 1992; Lever et al. 1994;

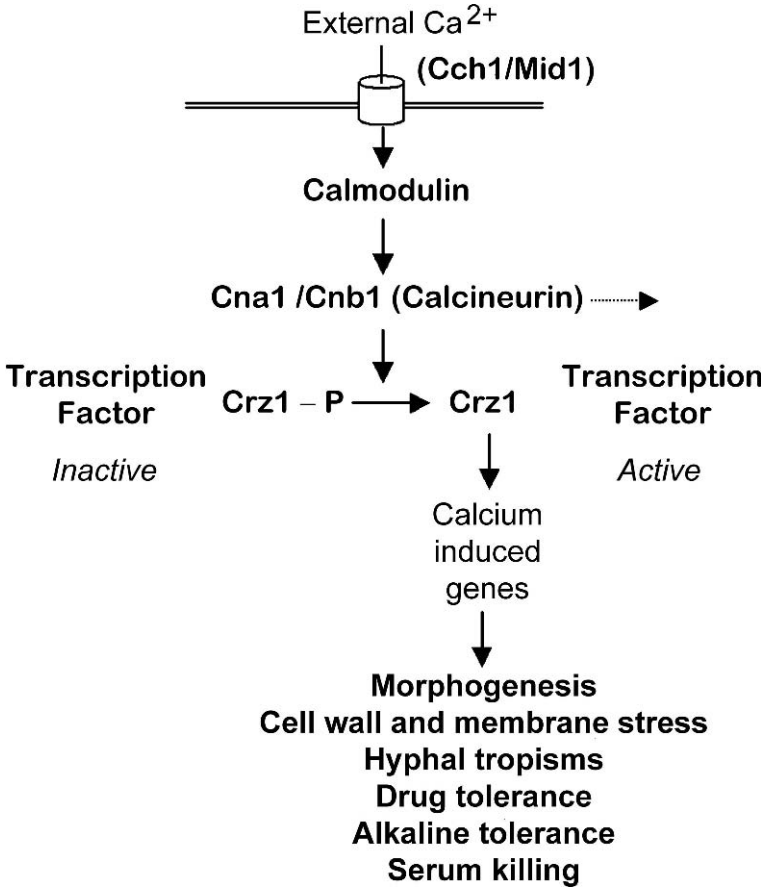

Fig. 7.6. Calcium signaling pathway in which calcium ions pass through a channel complex of Cch1 and Mid1 and bind to calmodulin which activates the calcineurin phosphatase, which in turn dephosphorylates Crz1 transcription factor. Dephosphorylated Crz1 enters the nucleus and activates the expression of a wide range of genes

Watts et al. 1998; Gow 2004). Calcium deprivation or the addition of calcium channel blockers led to a reduced ability of hyphae of *C. albicans* to turn in response to either an imposed electrical field or upon contact with a ridge or a groove (Watts et al. 1998). This suggests that calcium ion uptake in the apical region of the hypha may influence the site at which secretory vesicles fuse with the cell surface, or that a calcium ion gradient is required in some other way to perceive and orient the molecular apparatus that drives cell extension.

Calcium can also bind and affect the activity of some protein kinases directly, such as Ca^{2+}/calmodulin-dependent protein kinase (Dhillon et al. 2003) and protein kinase C. However, disruption of the *C. albicans PKC1* gene does not seem to affect yeast–hypha morphogenesis (Paravicini et al. 1996). The release of calcium ions from stores such as the vacuole and mitochondria is influenced by other signaling molecules such as inositol 4,5-tri-phosphate, which is a product of phospholipase C action on phosphatidylinositol in the plasma membrane. In *C. albicans* three phospholipase C genes have been identified (Kunze et al. 2005). These lack the normal calcium-binding EF hand at the N-terminus of the predicted protein (Bennett et al. 1998). *PLC1* may be an essential gene and mutants that were depleted for the encoded protein were sensitive to osmotic stress, growth on low-carbon-containing media or at low or high temperature. Mutants in *PLC1*, *PLC2* and *PLC3* had a reduced ability to form hyphae under certain conditions but were fully virulent in a mouse systemic model of infection (Kunze et al. 2005). The importance of calcium, calmodulin and inositol phosphate signaling in yeast–hypha morphogenesis has not yet been fully explored but there is some evidence for a role for calcium signaling in yeast–hypha regulation. For example, the yeast-to-hypha transition is known to be inhibited by calmodulin inhibitors (Roy and Datta 1987; Sabie and Gadd 1989; Buchan et al. 1993) and calcium ion uptake is suggested to have a repressing effect on mycelium formation (Holmes et al. 1991). Calmodulin levels are also reported as being elevated in mycelial

forms (Paranjape et al. 1990), although this is not reflected in differential levels of expression of the calmodulin gene *CMD1* (Saporito and Sypherd 1991). Recent evidence suggests that some of these effects may be due to indirect effects on the cell cycle and on lipid and phospholipids metabolism since phenothiazine inhibitors of calmodulin were shown to induce cell cycle arrest in *C. albicans* and to lead to a decline in the cellular lipid pool (Sharma et al. 2001).

V. Other Outputs of Morphogenetic Pathways

Downstream substrates of the morphogenetic signaling pathways listed above are much less clear. In order to achieve a change in cell shape a number of physiological functions must be modulated, including cell polarity, the cell cycle and, ultimately, cell wall biosynthesis. Mechanistically, changes in cell shape are mediated via alterations in the vectorial synthesis of cell wall. This in turn is controlled by actin microfilaments and the secretory pathway that delivers the membrane vesicles required for expansion of the plasma membrane and the enzymes for elaboration of the new cell wall. The molecular machinery that brings about polarized cell wall growth involves several protein complexes, including the polarisome, exocyst, Arp2/3 and Spitzenkörper complexes (for reviews, see Virag and Harris 2006; and Chaps. 5 and 6 in this volume). Considerable advances have been made in our understanding how formin proteins and rho GTPases orchestrate the initiation and assembly of actin at sites of tip growth. This morphogenetic machinery is also tightly coupled to the cell cycle clock, which allows DNA synthesis and nuclear division to be triggered or arrested under appropriate or unfavorable conditions (Wightman et al. 2004). Hyphal cells exhibit polarized cell growth, in which cell expansion is confined to the apex of the hypha, throughout the cell cycle (Staebell and Soll 1985; Anderson and Soll 1986). In yeast cell growth the new bud grows initially by apical expansion, and finally by isotropic growth (Staebell and Soll 1985; see also Chap. 6 in this volume).

In *S. cerevisiae* the transition from apical to isotropic growth of buds was shown to be regulated at a morphogenetic checkpoint at the G2/M interface of the cell cycle (Lew and Reed 1995). Activation of the Cdc28 cyclin-dependent protein kinase by specific cyclins plays a key role in cellular polarity responsible for both triggering polarized bud development in G1 and then regulating the transition from polarized to isotropic bud development at G2/M (Lew and Reed 1993, 1995). The G1 cyclins Cln1, Cln2 and Cln3 are required for activation of polarized growth and the mitotic cyclins Clb1 and Clb 2 are required for depolarization of growth (Lew and Reed 1995).

In *C. albicans* the Cln1 G1 cyclin exhibits cell cycle-dependent expression and is required for the maintenance of filamentous growth, since *cln1* mutants revert more quickly to the yeast form (Loeb et al. 1999). This mutant was deficient in hyphal formation on several solid media but was still competent to form hyphae in liquid media. This suggests that CaCln1 regulation of hyphal growth may be coordinated with specific signal transduction pathways that operate under specific environmental conditions (Loeb et al. 1999). CaCln3p is an essential G_1 cyclin that is important for size regulation of the START function in the cell cycle and is important for morphogenesis. When Cln3p is depleted, buds expand and ultimately form filaments whose continued development depends on the richness of the medium (Bachewich and Whiteway 2005; Lazo et al. 2005). This suggests that Cln3p has a role in coupling the cell cycle to morphogenesis. *C. albicans* has two G2 cyclins, Clb2p and Clb4p, which both negatively regulate the formation of polarized filamentous cells (Bensen et al. 2005). However, Clb2 is probably essential and depleted cells eventually arrest as binucleated elongated and parallel-sided projections reminiscent of true hyphae. In contrast, *CaCLB4*-deleted cells are viable and form constitutive pseudohyphae (Bensen et al. 2005).

In *S. cerevisiae* the regulation of filamentous growth by Cdc28 is modulated by a protein kinase cascade involving Elm1, Hsl1 and Swe1 (Edgington et al. 1999). This suggests that a complex phosphorylation cascade lies upstream of the events that ultimately regulate cell shape by modulating the organization of the actin cytoskeleton and the secretory apparatus (see Chaps. 5 and 6 in this volume).

In *S. cerevisiae* the MAP kinase pathway that activates Ste12 is involved in the regulation of polarized shmoo formation during mating (Fig. 7.5). Until relatively recently *C. albicans* was not thought to mate and was believed to be constitutively diploid. However, the genome sequencing project identified a mating-type locus reminiscent of that in *S. cere-*

visiae and rapid advances in the past five years uncovered a vestigial mating system in *C. albicans* that can be as efficient as that in *S. cerevisiae* (Johnson 2003; and Chap. 8 in this volume). This work clearly showed that regulatory circuits that involve mating and the cell cycle also regulate the phenomena of phenotypic switching and hyphal morphogenesis.

Finally, it is possible or even likely that virulence attributes other than filamentous growth are regulated by these signaling pathways. Mutants in many transcription factors are less virulent than the isogenic parents (e.g. Lo et al. 1997; Schweizer et al. 2000; Murad et al. 2001a, b; Saville et al. 2003; Karababa et al. 2006). This may indicate that these transcription factors regulate multiple virulence factors, including the expression of cell surface adhesions and immunoregulatory molecules, the synthesis of secreted aspartate proteinases, lipases, phospholipases and other hydrolytic enzymes in addition to playing a role in yeast–hypha morphogenesis (Brown and Gow 1999; Gow et al. 2002). It is also clear that these signaling pathways do not operate in isolation and that cross-talk between these pathways exists under certain environmental conditions (Murad et al. 2001a, b; Doedt et al. 2004; Garcia-Sanchez et al. 2005). Virulence and morphogenesis is also coupled to central metabolism and so a network of connections exists between the signals and outputs of the pathways that have been described which can be further modulated by a wide range of environmental conditions. Therefore the outputs of the morphogenetic pathways described here are complex and involve regulation of a wide range of factors important for pathogenesis in *C. albicans*.

VI. Conclusions

Twenty years ago organisms such as *C. albicans* were considered insufficiently tractable for research to make a significant contribution to our understanding of basic mechanisms in cell biology and pathogenesis. However, in the past five years we entered an exciting era in fungal cell biology, particularly for genetically recalcitrant species. New, widely applicable molecular tools and methodologies are being developed rapidly for the functional analysis of fungal genes and fungal genomes. These are being combined with genomic tools that are being built on the platform created by fungal genome sequencing programs. Furthermore, these sequencing projects greatly facilitate the identification, isolation and analysis of genes in genetically recalcitrant fungal species. Hence, significant advances have been made in our understanding of fungal morphogenesis in the past five years. Morphogenetic signaling pathways have been elaborated in more detail. Also, it is becoming clear that these signaling pathways play broader cellular roles than were initially envisaged, for example in the fine-tuning of other virulence factors, metabolism and cell defense mechanisms. However, there are still large gaps in our knowledge. The molecular nature of some morphogenetic signals still remains obscure. Our understanding of morphogenetic signaling is based largely on reverse genetics and genomics: the structure of these pathways remains to be confirmed biochemically. Also, the mechanistic relationship between the morphogenetic signaling events that regulate developmental changes in gene expression and the cell cycle events that mediate changes in cell polarity still remain to be elucidated. A complete understanding of the regulation of morphogenesis and its contribution to *C. albicans* pathogenesis is dependent upon answers to these questions.

Acknowledgements. A.J.P.B., S.A. and N.A.R.G. are supported by the UK Biotechnology and Biological Sciences Research Council, the Wellcome Trust, the Medical Research Council and the European Commission.

References

Almirante B, Rodriguez D, Park BJ, Cuenca-Estrella M, Planes AM, Almela M, Mensa J, Sanchez F, Ayats J, Gimenez M, Saballs P, Fridkin SK, Morgan J, Rodriguez-Tudela JL, Warnock DW, Pahissa A (2005) Epidemiology and predictors of mortality in cases of *Candida* bloodstream infection: results from population-based surevillance, Barcelona, Spain, from 2002–2003. J Clin Microbiol 43:1829–1835

Alonso-Monge R, Navarro-García F, Roman E, Negredo AI, Eisman B, Nombela C, Pla J (2003) The Hog1 mitogen-activated protein kinase is essential in the oxidative stress response and chlamydospore formation in *Candida albicans*. Eukaryot Cell 2:351–361

Alonso-Monge RA, Román E, Nombela C, Pla J (2006) The MAP kinase signal transduction network in *Candida albicans*. Microbiology 152:905–912

Anderson J, Soll DR (1986) Differences in actin localisation in bud and hypha formation in the yeast *Candida albicans*. J Gen Microbiol 132: 2035–2047

Argimón S (2006) Regulation of *ALS3* and *NRG1* during *Candida albicans* morphogenesis. PhD thesis, University of Aberdeen

Bachewich C, Whiteway M (2005) Cyclin Cln3p links G1 progression to hyphal and pseudohyphal development in *Candida albicans*. Eukaryot Cell 4:95–1102

Bader T, Schröppel K, Bentink S, Agabian N, Köhler G, Morschhäuser J (2006) Role of calcineurin in stress resistance, morphogenesis, and virulence of a *Candida albicans* wild-type strain. Infect Immun 74:4366–4369

Bahn YS, Sundstrom P (2001) *CAP1*, an adenylate cyclase-associated protein gene, regulates bud-hypha transitions, filamentous growth, and cyclic AMP levels and is required for virulence of *Candida albicans*. J Bacteriol 183:3211–3223

Bahn YS, Staab J, Sundstrom P (2003) Increased high-affinity phosphodiesterase *PDE2* gene expression in germ tubes counteracts *CAP1*-dependent synthesis of cyclic AMP, limits hypha induction and promotes virulence of *Candida albicans*. Mol Microbiol 50:391–409

Bailey DA, Feldmann PJF, Bovey M, Gow NAR, Brown AJP (1996) The *Candida albicans HYR1* gene, which is activated in response to hyphal development, belongs to a gene family encoding yeast cell wall proteins. J Bacteriol 178:5353–5360

Bassilana M, Arkowitz RA (2006) Rac1 and Cdc42 have different roles in *Candida albicans* development. Eukaryot Cell 5:321–329

Bassilana M, Blyth J, Arkowitz RA (2003) Cdc24, the GDP-GTP exchange factor for Cdc42, is required for invasive hyphal growth of *Candida albicans*. Eukaryot Cell 2:9–18

Bassilana M, Hopkins J, Arkowitz RA (2005) Regulation of the Cdc42/Cdc24 GTPase module during *Candida albicans* hyphal growth. Eukaryot Cell 4:588–603

Beck-Sagué CM, Jarvis WR (1993) National nosocomial infections surveillance system. Secular trends in the epidemiology of nosocomial fungal infections in the United States, 1980–1990. J Infect Dis 167:1247–1251

Bennett DE, McCreary CE, Coleman DC (1998) Genetic characterization of phospholipase C gene from *Candida albicans*: presence of homologous species in *Candida* species other than *Candida albicans*. Microbiology 144:55–72

Bennett RJ, Johnson AD (2003) Completion of a parasexual cycle in *Candida albicans* by induced chromosome loss in tetraploid strains. EMBO J 22:2505–2515

Bennett RJ, Uhl MA, Miller MG, Johnson AD (2003) Identification and characterization of a *Candida albicans* mating pheromone. Mol Cell Biol 23:8189–8201

Bensen ES, Filler SG, Berman J (2002) A forkhead transcription factor is important for true hyphal as well as yeast morphogenesis in *Candida albicans*. Eukaryot Cell 1:787–798

Bensen ES, Clemente-Blanco A, Finley KR, Correa-Bordes J, Berman J (2005) The mitotic cyclins Clb2p and Clb4p affect morphogenesis in *Candida albicans*. Mol Biol Cell 16:3387–3400

Berman J, Gow NAR (2004) Cell cycle of fungal pathogens. In: San-Blas G, Calderone RA (eds) Pathogenic fungi: structural biology and taxonomy. Caister Academic, Wydmondham, pp 101–127

Berman J, Sudbery PE (2002) *Candida albicans*: a molecular revolution built on lessons from budding yeast. Nat Rev Genet 3:918–930

Birse CE, Irwin MY, Fonzi WA, Sypherd PS (1993) Cloning and characterization of *ECE1*, a gene expressed in association with cell elongation of the dimorphic pathogen *Candida albicans*. Infect Immun 61:3648–3655

Biswas K, Morschhäuser J (2005) The Mep2p ammonium permease controls nitrogen starvation-induced filamentous growth in *Candida albicans*. Mol Microbiol 56:649–669

Blankenship JR, Hietman J (2005) Calcineurin is required for *Candida albicans* to survive calcium stress in serum. Infect Immun 73:5767–5774

Blankenship JR, Wormley FL, Boyce MK, Schell WA, Filler SG, Perfect JR, Heitman J (2003) Calcineurin is essential for *Candida albicans* survival in serum and virulence. Eukaryot Cell 2:422–430

Bockmühl DP, Ernst JF (2001) A potential phosphorylation site for an A-type kinase in the Efg1 regulator protein contributes to hyphal morphogenesis of *Candida albicans*. Genetics 157:1523–1530

Bockmühl DP, Krishnamurthy S, Gerads M, Sonneborn A, Ernst JF (2001) Distinct and redundant roles of the two protein kinase A isoforms Tpk1p and Tpk2p in morphogenesis and growth of *Candida albicans*. Mol Microbiol 42:1243–1257

Bramley TA, Menzies GS, Williams RJ, Kinsman OS Adams DJ (1991) Binding sites for LH in *Candida albicans*: comparison with the mammalian corpus luteum LH receptor. J Endocrinol 130:177–190

Braun BR, Johnson AD (1997) Control of filament formation in *Candida albicans* by the transcriptional repressor *TUP1*. Science 277:105–109

Braun BR, Johnson AD (2000) *TUP1*, *CPH1* and *EFG1* make independent contributions to filamentation in *Candida albicans*. Genetics 155:57–67

Braun BR, Head WS, Wang MX, Johnson, AD (2000) Identification and characterisation of *TUP1*-regulated genes in *Candida albicans*. Genetics 156:31–44

Braun BR, Kadosh D, Johnson AD (2001) *NRG1*, a repressor of filamentous growth in *C. albicans*, is down-regulated during filament induction. EMBO J 20:4753–4761

Braun BR, Hoog http://genetics.plosjournals.org/perlserv/?request=get-document&doi=10.1371/ - aff2 M van het, d'Enfert C, Martchenko M, Dungan J, Kuo A, Inglis DP, Uhl MA, Hogues H, Berriman M, Lorenz M, Levitin A, Oberholzer U, Bachewich C, Harcus D, Marcil A, Dignard D, Iouk T, Zito R, Frangeul L, Tekaia F, Rutherford K, Wang E, Munro CA, Bates S, Gow NAR, Hoyer LL, Köhler G, Morschhäuser J, Newport G, Znaidi S, Raymond M, Turcotte B, Sherlock G, Costanzo M, Ihmels J, Berman J, Sanglard D, Agabian N, Mitchell AP, Johnson AD, Whiteway M, Nantel A (2005) A human-curated annotation of the *Candida albicans* genome. PLoS Genetics 1:36–57

Brega E, Zufferey R, Ben Mamoun C (2004) *Candida albicans* Csy1p is a nutrient sensor important for activation of amino acid uptake and hyphal morphogenesis. Eukaryot Cell 3:135–143

Brown AJP (2002a) Morphogenetic signaling pathways in *Candida albicans*. In: Calderone RA (ed) *Candida and candidiasis*. ASM, Washington, D.C., pp 95–106

Brown AJP (2002b) Expression of growth form-specific factors during morphogenesis in *Candida albicans*. In: Calderone RA (ed) *Candida and candidiasis*. ASM, Washington, D.C., pp 87–93

Brown AJP Gow NAR (1999) Regulatory networks controlling *Candida albicans* morphogenesis. Trends Microbiol 7:333–338

Brown AJP, Gow NAR (2001) Signal transduction and morphogenesis in *Candida albicans*. In: Howard RJ, Gow NAR (eds) The Mycota, vol VIII. Biology of the fungal cell, 1st edn. Springer, Berlin Heidelberg New York, pp 55–71

Brown AJP, Barelle CJ, Budge S, Duncan J, Harris S, Lee PR, Leng P, Macaskill S, Abdul Murad AM, Ramsdale M, Wiltshire C, Wishart JA, Gow NAR (2000) Gene regulation during morphogenesis in *Candida albicans*. In: Ernst JF, Schmidt A (eds) Contributions to microbiology: dimorphism in human pathogenic and apathogenic yeasts, vol 5. Karger, Basel, pp 112–125

Brown DH, Giusani AD, Chen X, Kumamoto CA (1999) Filamentous growth of *Candida albicans* in response to physical environmental cues and its regulation by the unique *CZF1* gene. Mol Microbiol 34:651–662

Buchan ADB, Gow NAR (1991) Rates of germ tube formation from growing and non-growing yeast cells of *Candida albicans*. FEMS Microbiol Lett 81:15–18

Buchan ADB, Kelly VA, Kinsman OS, Gooday GW, Gow NAR (1993) Effect of trfluoperazine on growth, morphogenesis and pathogenicity of *Candida albicans*. J Med Vet Mycol 31:427–433

Buffo J, Herman MA, Soll DR (1984) A characterization of pH regulated dimorphism in *Candida albicans*. Mycopathologia 86:21–30

Cao F, Lane S, Raniga PP, Lu Y, Zhou Z, Ramon K, Chen J, Liu H (2006) The Flo8 transcription factor is essential for hyphal development and virulence in *Candida albicans*. Mol Biol Cell 17:295–307

Cassola A, Parrot M, Silberstein S, Magee BB, Passeron S, Giasson L, Cantore ML (2004) *Candida albicans* lacking the gene encoding the regulatory subunit of Protein kinase A displays a defect in hyphal formation and an altered localization of the catalytic subunit. Eukaryot Cell 3:190–199

Chen H, Fujita M, Feng Q, Clardy J, Fink GR (2004) Tyrosol is a quorum-sensing molecule in *Candida albicans*. Proc Natl Acad Sci USA 101:5048–5052

Chen J, Chen J, Lane S, Liu H (2002) A conserved mitogen-activated protein kinase pathway is required for mating in *Candida albicans*. Mol Microbiol 46:1335–1344

Clark KL, Feldmann PJF, Dignard D, Larocque R, Brown AJP, Lee MG, Thomas DY, Whiteway M (1995) Constitutive activation of the *Saccharomyces cerevisiae* mating response pathway by a MAP kinase kinase from *Candida albicans*. Mol Gen Genet 249:609–621

Cognetti D, Davis D, Sturtevant J (2002) The *Candida albicans* 14-3-3 gene, *BMH1*, is essential for growth. Yeast 19:55–67

Cook JG, Bardwell L, Kron SJ, Thorner J (1996) Two novel targets of the MAP kinase Kss1 are negative regulators of invasive growth in the yeast *Saccharomyces cerevisiae*. Genes Dev 10:2831–2848

Crampin H, Finley K, Gerami-Nejad M, Court H, Gale C, Berman C (2005) Candida albicans hyphae have a Spitzenkörper that is distinct from the polarisome found in yeast and pseudohyphae. J Cell Sci 118:2935–2947

Csank C, Makris C, Meloche S, Schroppel K, Rollinghoff M, Dignard D, Thomas DY, Whiteway M (1997) Derepressed hyphal growth and reduced virulence in a VH1 family-related protein phosphatase mutant of the human pathogen *Candida albicans*. Mol Biol Cell 8:2539–2551

Csank C, Schroppel K, Leberer E, Harcus D, Mohamed O, Meloche S, Thomas DY, Whiteway M (1998) Roles of the *Candida albicans* mitogen-activated protein kinase homolog, Cek1p, in hyphal development and systemic candidosis. Infect Immun 66:2713–2721

Cutler JE (1991) Putative virulence factors of *Candida albicans*. Annu Rev Microbiol 45:187–218

Davis D (2003) Adaptation to environmental pH in *Candida albicans* and its relation to pathogenesis. Curr Genet 44:1–7

Davis D, Wilson RB, Mitchell AP (2000) *RIM10*-dependent and -independent pathways govern pH responses in *Candida albicans*. J Bacteriol 20:971–978

De Bernardis F, Muhlschlegel FA, Cassone A, Fonzi WA (1998) The pH of the host niche controls gene expression in and virulence of *Candida albicans*. Infect Immun 66:3317–3325

d'Enfert C, Goyard S, Rodriguez-Arnaveilhe S, Frangeul L, Jones L, Tekaia F, Bader O, Castillo L, Dominguez A, Ernst J, Fradin C, Gaillardin C, Garcia-Sanchez S, de Groot P, Hube B, Klis F, Krishnamurthy S, Kunze D, Lopez M-C, Mavor A, Martin N, Moszer I, Onésime D, Perez Martin J, Sentandreu R, Brown AJP (2005) CandidaDB: a genome database for *Candida albicans* pathogenomics. Nucleic Acids Res 33:D353–D357

Denison SH, Orejas M, Arst HN Jr (1995) Signalling of ambient pH in *Aspergillus* involves a cysteine protease. J Biol Chem 270:28519–28522

Denison SH, Negrete-Urtasun S, Mingot JM, Tilburn J, Mayer WA, Goel A, Espeso EA, Penalva MA, Arst HN Jr (1998) Putative membrane components of signal transduction pathways for ambient pH regulation in *Aspergillus* and meiosis in *Saccharomyces* are homologous. Mol Microbiol 30:259–264

Dhillon NK, Sharma S, Khuller GK (2003) Biochemical characterization of Ca^{2+}/calmodulin dependent protein kinase from *Candida albicans*. Mol Cell Biochem 252:183–191

Dieterich C, Schandar M, Noll M, Johannes F-J, Brunner H, Graeve T, Rupp S (2002) In vitro reconstructed human epithelia reveal contributions of *Candida albicans EFG1* and *CPH1* to adhesion and invasion. Microbiology 148:497–506

Doedt T, Krishnamurthy S, Bockmühl DP, Tebarth B, Stempel C, Russell CL, Brown AJP, Ernst JF (2004) APSES proteins regulate morphogenesis and metabolism in *Candida albicans*. Mol Biol Cell 15:3167–3180

Edgington NP, Blacketter MJ, Bierwagen TA, Myers AM (1999) Control of *Saccharomyces cerevisiae* filamentous growth by cyclin-dependent kinase Cdc28. Mol Cell Biol 19:1369–1380

Edlind T, Smith L, Henry K, Katiyar S, Nickels J (2002) Antifungal activity in *Saccharomyces cerevisiae* is modulated by calcium signaling. Mol Microbiol 46:257–268

El Barkani A, Kurzai O, Fonzi WA, Ramon A, Porta A, Frosch M, Muhlschlegel FA (2000) Dominant active alleles of *RIM101* (*PRR2*) bypass the pH restriction on filamentation of *Candida albicans*. Mol Cell Biol 20:4635–4647

Enjalbert B, Whiteway M (2005) Release from quorum-sensing molecules triggers hyphal formation during *Candida albicans* resumption of growth. Eukaryot Cell 4:1203–1210

Enjalbert B, Smith DA, Cornell MJ, Alam I, Nicholls S, Brown AJP, Quinn J (2006) Role of the Hog1 stress-activated protein kinase in the global transcriptional response to stress in the fungal pathogen *Candida albicans*. Mol Biol Cell 17:1018–1032

Ernst JF (2000) Transcription factors in *Candida albicans* – environmental control of morphogenesis. Microbiology 146:1763–1774

Feng Q, Summers E, Guo B, Fink G (1999) Ras signalling is required for serum-induced hyphal differentiation in *Candida albicans*. J Bacteriol 181:6339–6346

Fonzi WA (1999) *PHR1* and *PHR2* of *Candida albicans* encode putative glycosidases required for proper cross-linking of β-1,3- and α-1,6-glucans. J Bacteriol 181:7070–7079

Gale CA, Bendel CM, McClellan M, Hauser M, Becker JM, Berman J, Hostetter MK (1998) Linkage of adhesion, filamentous growth, and virulence in *Candida albicans* to a single gene, *INT1*. Science 279:1355–1358

Gale C, Gerami-Nejad M, McClellan M, Vandoninck S, Longtine MS, Berman J (2001) *Candida albicans* Int1p interacts with the septin ring in yeast and hyphal cells. Mol Biol Cell 12:3538–3549

García-Sánchez S, Mavor AL, Russell CL, Argimón S, Dennison P, Enjalbert B, Brown AJP (2005) Global roles of Ssn6 in Tup1- and Nrg1-dependent gene regulation in the fungal pathogen, *Candida albicans*. Mol Biol Cell 16:2913–2925

Ghannoum MA, Spellberg B, Saporito-Irwin SM, Fonzi WA (1995) Reduced virulence of *Candida albicans PHR1* mutants. Infect Immun 63:4528–4530

Giusani AD, Vinces M, Kumamoto CA (2002) Invasive filamentous growth of *Candida albicans* is promoted by Czf1p-dependent relief of Efg1p-mediated repression. Genetics 160:1749–1753

Gow NAR (1997) Germ tube growth in *Candida albicans*. Curr Topics Med Mycol 8:43–55

Gow NAR (2002) Cell biology and cell cycle of *Candida*. In: Calderone RA (ed) *Candida* and candidiasis. ASM, Washington, D.C.,pp 145–158

Gow NAR (2004) New angles in mycology: studies in directional growth and directional motility. Mycol Res 108:5–13

Gow NAR, Brown AJP, Odds FC (2000) Candida's arranged marriage. Science 289:256–257

Gow NAR, Brown AJP, Odds FC (2002) Fungal morphogenesis and host invasion. Curr Opin Microbiol 5:366–371

Guhad FA, Jensen HE, Aalbaek B, Csank C, Mohamed O, Harcus D, Thomas DY, Whiteway M, Hau J (1998) Mitogen-activated protein kinase-defective *Candida albicans* is avirulent in a novel model of localized murine candidosis. FEMS Microbiol Lett 166:135–139

Gustin MC, Albertyn J, Alexander M, Davenport K (1998) MAP kinase pathways in the yeast *Saccharomyces cerevisiae*. Microbiol Mol Biol Rev 62:1264–1300

Harcus D, Nantel A, Marcil A, Rigby T, Whiteway M (2004) Transcription profiling of cyclic AMP signaling in *Candida albicans*. Mol Biol Cell 15:4490–4499

Hazan I, Liu H (2002) Hyphal tip-associated localization of Cdc42 is F-Actin dependent in *Candida albicans*. Eukaryot Cell 1:856–864

Hogan DA (2006) Molecular analysis of bacterial–fungal interactions within biofilms. Proc Congr Int Soc Human Anim Mycol 16:77

Hogan DA, Kolter R (2002) *Pseudomonas–Candida* interactions: an ecological role for virulence factors. Science 296:2229–2232

Hogan DA, Vik A, Kolter R (2004) A *Pseudomonas aeruginosa* quorum-sensing molecule influences *Candida albicans* morphology. Mol Microbiol 54:1212–1223

Holmes AR, Cannon RD, Shepherd MG (1991) Effect of calcium ion uptake on *Candida albicans* morphology. FEMS Microbiol Lett 77:187–194

Hornby JM, Jensen EC, Lisec AD, Tasto JJ, Jahnke B, Shoemaker R, Dussault P, Nickerson KW (2001) Quorum sensing in the dimorphic fungus *Candida albicans* is mediated by farnesol. Appl Environ Microbiol 67:2982–2992

Hoyer LL, Cieslinkski LB, McLaughlan MM, Torphy TJ, Shatzman AR, Livi GP (1994) A *Candida albicans* cyclic nucleotide phosphodiesterase: cloning and expression in *Saccharomyces cerevisiae* and biochemical characterization of the recombinant enzyme. Microbiology 140:1533–1542

Hudson DA, Sciascia QL, Sanders RJ, Norris GE, Edwards PJB, Sullivan PA, Farley PC (2004) Identification of the dialysable serum inducer of germ-tube formation in *Candida albicans*. Microbiology 150:3041–3049

Hull CM, Johnson AD (1999) Identification of a mating type-like locus in the asexual pathogenic yeast *Candida albicans*. Science 285:1271–1275

Hull CM, Raiser RM, Johnson AD (2000) Evidence for mating of the "asexual" yeast *Candida albicans* in a mammalian host. Science 289:307–310

Hwang C-S, Oh J-H, Huh W-K, Yim H-S, Kang S-O (2003) Ssn6, an important factor of morphological conversion and virulence in *Candida albicans*. Mol Microbiol 47:1029–1043

Ishii N, Yamamoto M, Lahm HW, Iizumi S, Yoshihara F, Nakayama H, Arisawa M, Aoki Y (1997a) A DNA binding protein from *Candida albicans* that binds to the RPG box of *Saccharomyces cerevisiae* and the telomeric repeat sequence of *Candida albicans*. Microbiology 143:417–427

Ishii N, Yamamoto M, Yoshihara F, Arisawa M, Aoki Y (1997b) Biochemical and genetic characterisation of Rbf1p, a putative transcription factor of *Candida albicans*. Microbiology 143:429–435

Jamal WY, El-Din K, Rotimi VO, Chugh TD (1999) An analysis of hospital-acquired bacteraemia in intensive care unit patients in a university hospital in Kuwait. J Hosp Infect 43:49–56

Janiak AM, Sargsyan H, Russo J, Naider F, Hauser M, Becker JM (2005) Functional expression of the *Candida albicans* alpha-factor receptor in *Saccharomyces cerevisiae*. Fungal Genet Biol 42:328–338

Johnson AD (2003) The biology of mating in *Candida albicans*. Nat Rev Microbiol 1:106–116

Jung WH, Stateva LI (2003) The cAMP phosphodiesterase encoded by *CaPDE2* is required for hyphal development in *Candida albicans*. Microbiology 149:2961–2976

Kadosh D, Johnson AD (2001) Rfg1, a protein related to the *Saccharomyces cerevisiae* hypoxic regulator Rox1, controls filamentous growth and virulence in *Candida albicans*. Mol Cell Biol 21:2496–2505

Kadosh D, Johnson AD (2005) Induction of the *Candida albicans* filamentous growth program by relief of transcriptional repression: a genome-wide analysis. Mol Cell Biol 16:2903–2912

Kanzaki M, Nagasawa M, Kojima I, Sato C, Naruse K, Sokabe M, Iida H (1999) Molecular identification of a eukaryotic, stretch-activated nonselective cation channel. Science 285:882–886

Karababa M, Valentino A, Pardini G, Costs AT, Bille J, Sanglard D (2006) *CRZ1*, a target of the calcineurin pathway in *Candida albicans*. Mol Microbiol 59:1429–1451

Kataoka T, Powers S, McGill C, Fasano O, Strathern J, Broach J, Wigler M (1984) Genetic analysis of yeast *RAS1* and *RAS2* genes. Cell 37:437–445

Keleher CA, Redd MJ, Schultz J, Carlson M, Johnson AD (1992) Ssn6-Tup1 is a general repressor of transcription in yeast. Cell 68:709–719

Khalaf RA, Zitomer RS (2001) The DNA binding protein Rfg1 is a repressor of filamentation in *Candida albicans*. Genetics 157:1503–1512

Kinsman OS, Pitblado K, Coulson CJ (1988) Effect of mammalian steroid hormones and luteinizing hormone on the germination of *Candida albicans* and implications for vaginal candidosis. Mycoses 31:617–626

Klengel T, Liang W-J, Chaloupka J, Ruoff C, Schroppel K, Naglik JR, Eckert SE, Mogensen EG, Haynes K, Tuite MF, Levin LR, Buck J, Muhlschlegel FA (2005) Fungal adenylyl cyclase integrates CO_2 sensing with cAMP signalling and virulence. Curr Biol 15:2021–2026

Köhler JR, Fink GR (1996) *Candida albicans* strains heterozygous and homozygous for mutations in mitogen-activated protein kinase signaling components have defects in hyphal development. Proc Natl Acad Sci USA 93:13223–13228

Kraus PR, Heitman J (2003) Coping with stress: calmodulin and calcineurin in model pathogenic fungi. Biochem Biophys Res Commun 311:1151–1157

Kron SJ, Gow NAR (1995) Budding yeast morphogenesis: signalling, cytoskeleton and cell cycle. Curr Opin Cell Biol 7:845–855

Kullas AL, Li M, Davis DA (2004) Snf7p, a component of the ESCRT-III protein complex, is an upstream member of the RIM101 pathway in *Candida albicans*. Eukaryot Cell 3:1609–1618

Kunze D, Melzer I, Bennett D, Sanglard D, MacCallum DM, Nörskau J, Coleman DC, Odds FC, Schäfer W, Hube B (2005) Functional analysis of the phospholipase C gene *CaPLC1* and two unusual phospholipase C genes *CaPLC2* and *CaPLC3* of *Candida albicans*. Microbiology 151:3381–3394

Kurjan J (1993) The pheromone response pathway in *Saccharomyces cerevisiae*. Annu Rev Genet 27:147–179

Kwon-Chung KJ, Bennett JE (1992) Medical mycology. Lea and Febiger, Philadelphia.

Lambrechts MG, Bauer FB, Marmur J, Pretorius IS (1996) Muc1, a mucin-like protein that is regulated by Mss10, is critical for pseudohyphal differentiation in yeast. Proc Natl Acad Sci USA 93:8419–8424

Lane S, Birse C, Zhou S, Matson R, Liu H (2001a) DNA array studies demonstrate convergent regulation of virulence factors by Cph1, Cph2, and Efg1 in *Candida albicans*. J Biol Chem 276:48988–48996

Lane S, Zhou S, Pan T, Dai Q, Liu H (2001b) The basic helix-loop-helix transcription factor Cph2 regulates hyphal development in *Candida albicans* partly via Tec1. Mol Cell Biol 21:6418–6428

Lazo B, Bates S, Sudbery P (2005) The G_1 cyclin Cln3 regulates morphogenesis in *Candida albicans*. Eukaryot Cell 4:90–94

Leberer E, Harcus D, Broadbent ID, Clark KL, Dignard D, Ziegelbauer K, Schmit A, Gow NAR, Brown AJP, Thomas DY (1996) Homologs of the Ste20p and Ste7p protein kinases are involved in hyphal formation of *Candida albicans*. Proc Natl Acad Sci USA 93:13217–13222

Leberer E, Ziegelbauer K, Schmidt A, Harcus D, Dignard D, Ash J, Johnson L, Thomas DY (1997) Virulence and hyphal formation of *Candida albicans* require the Ste20p-like protein kinase CaCla4p. Curr Biol 7:539–546

Leberer E, Harcus D, Dignard D, Johnson L, Ushinsky S, Thomas DY, Schroppel K (2001) Ras links cellular morphogenesis to virulence by regulation of the MAP kinase and cAMP signalling pathways in the pathogenic fungus *Candida albicans*. Mol Microbiol 42:673–687

Lee KL, Buckler HR, Campbell CC. (1975) An amino acid liquid synthetic medium for the development of mycelial and yeast forms of *Candida albicans*. Sabouraudia 13:148–153

Leng P, Sudbery PE, Brown AJP (2000) Rad6p represses yeast-hypha morphogenesis in the human fungal pathogen, *Candida albicans*. Mol Microbiol 35:1264–1275

Leng P, Lee PR, Wu H, Brown AJP (2001) Efg1, a morphogenetic regulator in *Candida albicans*, is a sequence-specific DNA binding protein. J Bacteriol 183:4090–4093

Lever M, Robertson B, Buchan ADB, Gooday GW, Gow NAR (1994) pH and Ca^{2+} dependent galvanotropism of filamentous fungi: implications and mechanisms. Mycol Res 98:301–306

Lew DJ, Reed SI (1993) Morphogenesis in yeast cell cycle: regulation by Cdc28 and cyclins. J Cell Biol 120:1305–1320

Lew DJ, Reed SI (1995) A cell cycle checkpoint monitors cell morphogenesis in budding yeast. J Cell Biol 129:739–749

Li M, Martin SJ, Bruno VM, Mitchell AP, Davis DA (2004) *Candida albicans* Rim13p, a protease required for Rim101p processing at acidic and alkaline pHs. Eukaryotic Cell 3:741–751

Liu H (2001) Transcriptional control of dimorphism in *Candida albicans*. Curr Opin Microbiol 4:728–735

Liu H, Styles CA, Fink GR (1993) Elements of the yeast pheromone response pathway required for filamentous growth of diploids. Science 262:1741–1744

Liu H, Köhler JR, Fink GR (1994) Suppression of hyphal formation in *Candida albicans* by mutation of a *STE12* homolog. Science 266:1723–1726

Lo HJ, Köhler JR, DiDomenico B, Loebenberg D, Cacciapuoti A, Fink GR (1997) Nonfilamentous *C. albicans* mutants are avirulent. Cell 90:939–949

Lo WS, Dranginis AM (1998) The cell surface flocculin Flo11 is required for pseudohyphae formation and invasion by *Saccharomyces cerevisiae*. Mol Cell Biol 9:161–171

Loeb JDJ, Sepulveda-Becerra A, Hazan I, Liu H (1999) A G_1 cyclin is necessary for maintenance of filamentous growth in *Candida albicans*. Mol Cell Biol 19:4019–4027

Lorenz MC, Heitman J (1997) Yeast pseudohyphal growth is regulated by *GPA2*, a G protein alpha homolog. EMBO J 16:7008–7018

Madhani HD, Fink GR (1997) Combinatorial control required for the specificity of yeast MAPK signaling. Science 275:1314–1317

Magee BB, Magee PT (2000) Induction of mating in *Candida albicans* by construction of MTLa and MTLα strains. Science 289:310–313

Magee BB, Legrand M, Alarco A-M, Raymond M, Magee PT (2002) Many of the genes required for mating in *Saccharomyces cerevisiae* are also required for mating in *Candida albicans*. Mol Microbiol 46:1345–1351

Magee PT (1998) Analysis of the *Candida albicans* genome. In: Brown AJP Tuite MF (eds) Yeast gene analysis. (Methods in microbiology, vol 26) Academic, New York, pp 395–415

Maidan MM, Thevelein JM, Van Dijk P (2005) Carbon source induced yeast-to-hyphae transition in *Candida albicans* is dependent on the presence of amino acids and on the G-protein-coupled receptor Gpr1. Biochem Soc Trans 33:291–293

Malloy PJ, Zhao X, Madani ND, Feldman D (1993) Cloning and expession of the gene from *Candida albicans* that encodes a high-affinity corticosteroid-binding protein. Proc Natl Acad Sci USA 90:1902–1906

Martin MV, Craig GT, Lamb DJ (1984) An investigation of the role of true hypha production in the pathogenesis of experimental candidosis. J Med Vet Mycol 22:471–476

Martin SW, Douglas LM, Konopka JB (2005) Cell cycle dynamics and quorum sensing in *Candida albicans* chlamydospores are distinct from budding and hyphal growth. Eukaryot Cell 4:1191–1202

Martínez P, Ljungdahl PO (2004) An ER packaging chaperone determines the amino acid uptake capacity and virulence of *Candida albicans*. Mol Microbiol 51:371–384

Mattia E, Carruba G, Angiolella L, Cassone A (1982) Induction of germ tube formation by N-acetyl-D-glucosamine in *Candida albicans*: uptake of inducer and germinative response. J Bacteriol 152:555–562

Merson-Davies LA, Odds FC (1989) A morphology index for characterization of cell shape in *Candida albicans*. J Gen Microbiol 135:3143–3152

Miller MG, Johnson AD (2002) White-opaque switching in *Candida albicans* is controlled by mating-type locus homeodomain proteins and allows efficient mating. Cell 110:293–302

Mingot JM, Tilburn J, Diez E, Bignell E, Orejas M, Widick DA, Sarkar S, Brown CV, Caddick MX, Espeso EA, Arst Jr HN, Penalva MA (1999) Specificity determinants of proteolytic processing of *Aspergillus* PacC transcription factor are remote from the processing site, and processing occurs in yeast if pH signalling is bypassed. Mol Cell Biol 19:1390–1400

Mirbod F, Nakashima S, Kitajima Y, Cannon RD, Nozawa Y (1997) Molecular cloning of a Rho family, *CDC42Ca* gene from *Candida albicans* and its mRNA expression changes during morphogenesis. J Med Vet Mycol 35:173–179

Miwa T, Takagi Y, Shinozaki M, Yun C-W, Schell WA, Perfect JR, Kumagai H, Tamaki H (2004) Gpr1, a putative G-protein-coupled receptor, regulates morphogenesis and hypha formation in the pathogenic fungus *Candida albicans*. Eukaryot Cell 3:919–931

Mock RC, Pollack JH, Hashimoto T (1990) Carbon dioxide induces endotrophic germ tube formation in *Candida albicans*. Can J Microbiol 36:249–253

Mogensen EG, Janbon G, Chaloupka J, Steegborn C, Fu MS, Moyrand F, Klengel T, Pearson DS, Geeves MA, Buck J, Levin LR, Mühlschlegel FA (2006) *Cryptococcus neoformans* senses CO_2 through the carbonic anhydrase Can2 and the adenylyl cyclase Cac1. Eukaryot Cell 5:103–111

Monge RA, Navarro-Garcia F, Molero G, Diez-Orejas R, Gustin M, Pla J, Sanchez M, Nombela C (1999) Role of the mitogen-activated protein kinase Hog1p in morphogenesis and virulence of *Candida albicans*. J Bacteriol 181:3058–3068

Mosch HU, Roberts RL, Fink GR (1996) Ras2 signals via the Cdc42/Ste20/mitogen-activated protein kinase module to induce filamentous growth in *Saccharomyces cerevisiae*. Proc Natl Acad Sci USA 93:5352–5356

Mosel DD, Dumitru R, Hornby JM, Atkin AL, Nickerson KW (2005) Farnesol concentrations required to block germ tube formation in *Candida albicans* in the presence and absence of serum. Applied Environ Microbiol 71:4938–4940

Muhlschlegel FA, Fonzi WA (1997) *PHR2* of *Candida albicans* encodes a functional homolog of the pH-regulated gene *PHR1* with an inverted pattern of expression. Mol Cell Biol 17:5960–5967

Murad AMA, Leng P, Straffon M, Wishart J, Macaskill S, MacCallum D, Schnell N, Talibi D, Marechal D, Tekaia F, d'Enfert C, Gaillardin C, Odds FC, Brown AJP (2001a) *NRG1* represses yeast-hypha morphogenesis and hypha-specific gene expression in *Candida albicans*. EMBO J 20:4742–4752

Murad AMA, d'Enfert C, Gaillardin C, Tournu H, Tekaia F, Talibi D, Merechal D, Marchais V, Cottin J, Brown AJP (2001b) Transcript profiling in *Candida albicans* reveals new cellular functions for the transcriptional repressors CaTup1, CaMig1 and CaNrg1. Mol Microbiol 42:981–993

Nantel A, Dignard D, Bachewich C, Harcus D, Marcil A, Bouin A-P, Sensen CW, Hogues H, Hoog M van het, Gordon P, Rigby T, Benoit F, Tessier DC, Thomas DY, Whiteway M (2002) Transcript profiling of *Candida albicans* cells undergoing the yeast-to-hyphal transition. Mol Biol Cell 13:3452–2365

Navarro-García F, Alonso-Monge R, Rico H, Pla J, Sentandreu R, Nombela C (1998) A role for the MAP kinase gene *MKC1* in cell wall construction and morphological transitions in *Candida albicans*. Microbiology 144:411–424

Nobile CJ, Mitchell AP (2005) Regulation of cell-surface genes and biofilm formation by the *C. albicans* transcription factor Bcr1p. Curr Biol 15:1150–1155

Nobile CJ, Andes DR, Nett JE, Smith FJ, Yue F, Phan Q-T, Edwards JE, Filler SG, Mitchell AP(2006) Critical role of Bcr1-dependent adhesins in *C. albicans* biofilm formation in vitro and in vivo. PLoS Pathogen 2:636–649

Odds FC (1988) *Candida* and candidosis, 2nd edn. Bailliere Tindall, London

Paidhungat M, Garrett, S (1997) A homolog of mammalian, voltage-gated calcium channels mediates yeast pheromone-stimulated Ca^{2+} uptake and exacerbates the cdc1(Ts) growth defect. Mol Cell Biol 17:6339–6347

Palmer GE, Johnson KJ, Ghosh S, Sturtevant J (2004) Mutant alleles of the essential 14-3-3 gene in *Candida albicans* distinguish between growth and filamentation. Microbiology 150:1911–1924

Paranjape V, Roy BG, Datta A (1990) Involvement of calcium, calmodulin and protein phosphorylation in morphogenesis of *Candida albicans*. J Gen Microbiol 136:2119–2154

Paravicini G, Medoza A, Antonsson B, Cooper M, Losberger C, Payton MA (1996) The *Candida albicans PKC1* gene encodes a protein kinase C homolog necessary for cellular integrity but not dimorphism. Yeast 30:741–756

Park SH, Koh SS, Chun JH, Hwang HJ, Kang HS (1999) Nrg1 is a transcriptional repressor for glucose repression of *STA1* gene expression in *Saccharomyces cerevisiae*. Mol Cell Biol 19:2044–2050

Porta A, Ramon AM, Fonzi WA (1999) *PRR1*, a homolog of *Aspergillus nidulans palF*, controls pH-dependent gene expression and filamentation in *Candida albicans*. J Bacteriol 181:7516–7523

Ramage G, Saville SP, Wickes BL, Lopez-Ribot JL (2002) Inhibition of *Candida albicans* biofilm formation by farnesol, a quorum-sensing molecule. Appl Env Microbiol 68:5459–5463

Ramon AM, Porta A, Fonzi WA (1999) Effect of environmental pH on morphological development of *Candida albicans* is mediated via the PacC-regulated transcription factor encoded by *PRR2*. J Bacteriol 181:7524–7530

Riggle PJ, Andrutis KA, Chen X, Tzipori SR, Kumamoto CA (1999) Invasion lesions containing filamentous forms produced by a *Candida albicans* mutant that is defective in filamentous growth in culture. Infect Immun 67:3649–3652

Roberts RL, Fink GR (1994) Elements of a single MAP kinase cascade in *Saccharomyces cerevisiae* mediate two developmental programs in the same cell type: mating and invasive growth. Genes Dev 8:2974–2985

Roberts RL, Mosch HU, Fink GR (1997) 14-3-3 proteins are essential for RAS/MAPK cascade signalling during pseudohyphal development in *S. cerevisiae*. Cell 89:1055–1065

Rocha CR, Schroppel K, Harcus D, Marcil A, Dignard D, Taylor BN, Thomas DY, Whiteway M, Leberer E (2001) Signaling through adenylyl cyclase is essential for hyphal growth and virulence in the pathogenic fungus *Candida albicans*. Mol Biol Cell 12:3631–3643

Roy BG, Datta A (1987) A calmodulin inhibitor blocks morphogenesis in *Candida albicans*. FEMS Microbiol Lett 41:327–329

Rupp S, Summers E, Lo HJ, Madhani H, Fink GR (1999) MAP kinase and cAMP filamentous signalling pathways converge on the unusually large promoter of the yeast *FLO11* gene. EMBO J 18:1257–1269

Rusnak F, Mertz P (2000) Calcineurin: form and function. Physiol Rev 80:1483–1500

Russell CL, Brown AJP (2005) Expression of one-hybrid fusions with *Staphylococcus aureus* lexA in *Candida albicans* confirms that Nrg1 is a transcriptional repressor and that Gcn4 is a transcriptional activator. Fungal Genet Biol 42:676–683

Ryley JF, Ryley NG (1990) *Candida albicans* – do mycelia matter? J Med Vet Mycol 28:225–239

Sabie FT, Gadd GM (1989) Involvement of a Ca^{2+}–calmodulin interaction in the yeast-mycelial (Y-M) transition of *Candida albicans*. Mycopathologia 198:47–54

Sánchez-Martínez C, Pérez-Martín J (2002) Gpa2, a G-protein α subunit required for hyphal development in *Candida albicans*. Eukaryot Cell 1:865–874

Sanglard D, Ischer F, Marchetti O, Entenza J, Bille J (2003) Calcineurin A of *Candida albicans*: involvement of antifungal tolerance, cell morphogenesis and virulence. Mol Microbiol 48:959–976

Santos M, Larrinoa IF de (2005) Functional characterization of the *Candida albicans CRZ1* gene encoding a calcineurin-regulated transcription factor. Curr Genet 48:88–100

Santos MAS, Keith G, Tuite MF (1993) Non-standard translational events in *Candida albicans* mediated by an unusual seryl-tRNA with a 5'-CAG-3' (leucine) anticodon. EMBO J 12:607–616

Saporito SM, Sypherd PS (1991) The isolation and characterization of a calmodulin-encoding gene (*CMD1*) from the dimorphic fungus *Candida albicans*. Gene 106:43–49

Saporito-Irwin SM, Birse CE, Sypherd PS, Fonzi WA (1995) *PHR1*, a pH-regulated gene of *Candida albicans*, is required for morphogenesis. Mol Cell Biol 15:601–613

Saville SP, Lazzell AL, Monteagudo C, Lopez-Ribot JL (2003) Engineered control of cell morphology in vivo reveals distinct roles for yeast and filamentous forms of *Candida albicans* during infection. Eukaryot Cell 2:1053–1060

Schröppel K, Sprößer K, Whiteway M, Thomas DY, Röllinghoff M, Csank C (2000) Repression of hyphal proteinase expression by the mitogen-activated protein (MAP) kinase phosphatase Cpp1p of *Candida albicans* is independent of the MAP kinase Cek1p. Infect Immun 68:7159–7161

Schweizer A, Rupp S, Taylor BN, Rollinghoff M, Schröppel K (2000) The TEA/ATTS transcription factor CaTec1p regulates hyphal development and virulence in *Candida albicans*. Mol Microbiol 38:435–445

Seth CC, Johnson E, Baker ME, Haynes K, Mühlschlegel FA (2005) Phenotypic identification of *Candida albicans* by growth on chocolate agar. Med Mycol 43:735–738

Sevilla M-J, Odds FC (1986) Development of Candida albicans hyphae in different growth media-variation in growth rates, cell dimensions and timing of morphological events. J Gen Microbiol 132:3083–3088

Sharkey LL, McNemar MD, Saporito-Irwin SM, Sypherd PS, Fonzi WA (1999) *HWP1* functions in the morphological development of *Candida albicans* downstream of *EFG1, TUP1* and *RBF1*. J Bacteriol 181:5273–5279

Sharma S, Kaur H, Khuller GR (2001) Cell cycle effects of the phenothiazines: trifluoperazine and the chlorpromazine in *Candida albicans*. FEMS Microbiol Lett 199:185–190

Shepherd MG (1985) Pathogenicity of morphological and auxotrophic mutants of *Candida albicans* in experimental infections. Infect Immun 50:541–544

Sherwood J, Gow NAR, Gooday GW, Gregory DW, Marshall D (1992) Contact sensing in *Candida albicans*: a possible aid to epithelial penetration. J Med Vet Mycol 30:461–469

Smith DA, Nicholls S, Morgan BA, Brown AJP, Quinn J (2004) A conserved stress-activated protein kinase regulates a core stress response in the human pathogen *Candida albicans*. Mol Biol Cell 15:4179–4190

Smith RL, Johnson AD (2000) Turning off genes by Ssn6-Tup1: a conserved system of transcriptional repression in eukaryotes. Trends Biochem Sci 25:325–330

Sobel JD, Muller G, Buckley HR (1984) Critical role of germ tube formation in the pathogenesis of *Candida* vaginitis. Infect Immun 44:576–580

Sohn K, Urban C, Brunner H, Rupp S (2003) *EFG1* is a major regulator of cell wall dynamics in *Candida albicans* as revealed by DNA microarrays. Mol Microbiol 47:89–102

Soll DR (1986) The regulation of cellular differentiation in the dimorphic yeast *Candida albicans.* BioEssays 5:5–11

Sonneborn A, Bockmuhl DP, Ernst JF (1999) Chlamydospore formation in *Candida albicans* requires the Efg1p morphogenetic regulator. Infect Immun 67:5514–5517

Sonneborn A, Bockmuhl DP, Gerads M, Kurpanek K, Sanglard D, Ernst JF (2000) Protein kinase A encoded by *TPK2* regulates dimorphism of *Candida albicans*. Mol Microbiol 35:386–396

Staab JF, Bradway SD, Fidel PL, Sundstrom P (1999) Adhesive and mammalian transglutaminase substrate properties of *Candida albicans* Hwp1. Science 283:1535–1538

Staab JF, Bahn Y-S, Sundstrom P (2003) Integrative, multifunctional plasmids for hypha-specific or constitutive expression of green fluorescent protein in *Candida albicans*. Microbiology 149:2977–2986

Staebell M, Soll DR (1985) Temporal and spatial differences in cell wall expansion during bud and mycelium formation in *Candida albicans*. J Gen Microbiol 131:1079–1087

Staib P, Morschhauser J (2005) Differential expression of the NRG1 repressor controls species-specific regulation of chlamydospore development in *Candida albicans* and *Candida dubliniensis.* Mol Microbiol 55:637–652

Stewart E, Gow NAR, Bowen DV (1988) Cytoplasmic alkalinization during germ tube formation in *Candida albicans.* J Gen Microbiol 134:1079–1087

Stewart ES, Hawser S, Gow NAR (1989) Changes in internal and external pH accompanying growth of *Candida albicans*: studies of non-dimorphic variants. Arch Microbiol 151:149–153

Stoldt VR, Sonneborn A, Leuker C, Ernst JF (1997) Efg1p, an essential regulator of morphogenesis of the human pathogen *Candida albicans*, is a member of a conserved class of bHLH proteins regulating morphogenetic processes in fungi. EMBO J 16:1982–1997

Strathopoulos AM, Cyert MS (1997) Calcineurin acts through the *CRZ1/ TCN1*-encoded transcription factor to regulate gene expression in yeast. Genes Dev 11:3432–3444

Strathopolouos-Gerontides A, Guo JJ, Cyert MS (1999) Yeast calcineurin regulates nuclear localization of the Crz1p transcription factor through dephosphorylation. Genes Dev 13:798–803

Su Z, Osborne MJ, Xu P, Xu X, Li Y, Ni F (2005) A bivalent dissectional analysis of the high-affinity interactions between Cdc42 and the Cdc42/Rac interactive binding domains of signaling kinases in *Candida albicans*. Biochemistry 44:16461–16474

Sudbery PE (2001) The germ tubes of *Candida albicans* hyphae and pseudohyphae show different patterns of septin ring localisation. Mol Microbiol 41:19–31

Sudbery P, Gow NAR, Berman J (2004) The distinct morphogenic states of *Candida albicans*. Trends Microbiol 12:317–325

Sundstrom P, Cutler JE, Staab JF (2002) Reevaluation of the role of *HWP1* in systemic candidiasis by use of *Candida albicans* strains with selectable marker *URA3* targeted to the *ENO1* locus. Infect Immun 70:3281–3283

Swoboda RK, Bertram G, Delbruck S, Ernst JF, Gow NAR, Gooday GW, Brown AJP (1994) Fluctuations in glycolytic mRNA levels during the yeast-to-hyphal transition in *Candida albicans* reflect underlying changes in growth rather than a response to cellular dimorphism. Mol Microbiol 13:663–672

Tebarth B, Doedt T, Krishnamurthy S, Weide M, Monterola F, Dominguez A, Ernst JF (2003) Adaptation of the Efg1p morphogenetic pathway in *Candida albicans* by negative autoregulation and PKA-dependent repression of the *EFG1* gene. J Mol Biol 329:949–962

Torosantucci A, Angiolella L, Caccone A (1984) Antimorphogenetic effcts of 2-deoxy-D-glucose in *Candida albicans*. FEMS Microbiol Lett 24:335–339

Tortorano AM, Peman J, Bernhardt H, Klingspor L, Kibbler CC, Faure O, Biraghi E, Canton E, Zimmermann K, Seaton S, Grillot R (2004) Epidemiology of candidaemia in Europe: results of 28-month European Confederation of Medical Mycology (ECMM) hospital-based surveillance study. Eur J Clin Microbiol Infect Dis 23:317–322

Tournu H, Tripathi G, Bertram G, Macaskill S, Mavor A, Walker L, Odds FC, Gow NAR, Brown AJP (2005) Global role of the protein kinase, Gcn2, in the human pathogen, *Candida albicans*. Eukaryot Cell 4:1687–1696

Tripathi G, Wiltshire C, Macaskill S, Tournu H, Budge S, Brown AJP (2002) CaGcn4 co-ordinates morphogenetic and metabolic responses to amino acid starvation in *Candida albicans*. EMBO J 21:5448–5456

Ushinsky SC, Harcus D, Ash J, Dignard D, Marcil A, Morchhauser J, Thomas DY, Whiteway M, Leberer E (2002) *CDC42* is required for polarized growth in human pathogen *Candida albicans*. Eukaryot Cell 1:95–104

van den Berg AL, Ibrahim AS, Edwards JE, Toenjes KA, Johnson DI (2004) Cdc42p GTPase regulates the budded-to-hyphal-form transition and expression of hypha-specific transcripts in *Candida albicans*. Eukaryot Cell 3:724–734

Vinces MD, Haas C, Kumamoto CA (2006) Expression of the *Candida albicans* morphogenesis regulator gene *CZF1* and its regulation by Efg1p and Czf1p. Eukaryot Cell 5:825–835

Virag A, Harris SD (2006) The Spitzenkörper: a molecular perspective. Mycol Res 110:4–13

Vyas VK, Kuchin S, Carlson M (2001) Interaction of the repressors Nrg1 and Nrg2 with the Snf1 protein kinase in *Saccharomyces cerevisiae*. Genetics 158:563–572

Vyas VK, Kuchin S, Berkey CD, Carlson M (2003) Snf1 kinases with different β-subunit isoforms play distinct roles in regulating haploid invasive growth. Mol Cell Biol 23:1341–1348

Watts HJ, Very AA, Perera THS, Davies JM, Gow NAR (1998) Thigmotropism and stretch activated channels in the pathogenic fungus *Candida albicans*. Microbiology 144:689–695

Whiteway M (2000) Transcriptional control of cell type and morphogenesis in *Candida albicans*. Curr Opin Microbiol 3:582–588

Whiteway M, Dignard D, Thomas DY (1992) Dominant negative selection of heterologous genes: isolation of *Candida albicans* genes that interfere with *Saccharomyces cerevisiae* mating factor-induced cell cycle arrest. Proc Natl Acad Sci USA 89:9410–9414

Wightman R, Bates S, Amornrrattanapan P, Sudbery P (2004) In *Candida albicans*, the Nim1 kinases Gin4 and Hsl1 negatively regulate pseudohypha formation and Gin4 also controls septin organization. J Cell Biol 164:581–591

Williams RJ, Dickinson K, Kinsman OS, Bramley TA, Menzies GS, Adams DJ (1990) Receptor-mediated elevation of adenylate cyclase by luteinizing hormone in *Candida albicans*. J Gen Microbiol 136:2143–2148

Wilson RB, Davis D, Mitchell AP (1999) Rapid hypothesis testing with *Candida albicans* through gene disruption with short homology regions. J Bacteriol 181:1868–1874

Zhao X, Malloy PJ, Ardies CM, Feldman D (1995) Oestrogen-binding protein in *Candida albicans*: antibody development and cellular localization by electron immunocytochemistry. Microbiology 141:2685–2692

Zhao X, Oh S-H, Cheng G, Green CB, Nuessen JA, Yeater K, Leng RP, Brown AJP, Hoyer LL (2004) *ALS3* and *ALS8* represent a single locus that encodes a *Candida albicans* adhesin; functional comparisons between Als3p and Als1p. Microbiology 150:2415–2428

Zheng X, Wang Y, Wang Y (2004) Hgc1, a novel hypha-specific G1 cyclin-related protein regulates *Candida albicans* hyphal morphogenesis. EMBO J 23:1845–1856

8 Mating in *Candida albicans* and Related Species

D.R. Soll[1]

CONTENTS

I. **Introduction** 195
II. **Population Studies Suggest Mating is a Rare Event in *C. albicans* and *C. glabrata*** 196
III. **The Discovery of Mating Systems in *C. albicans* and *C. glabrata*** 196
A. *C. albicans* 196
B. *C. glabrata* 198
IV. **The *MTL* Genotype in Nature** 199
V. **Demonstration of Mating in *C. albicans*, but not *C. glabrata*** 201
VI. **Mating of *C. albicans* Requires White–Opaque Switching** 201
A. The a1-α2 Complex Represses Switching 202
B. The Opaque Phenotype is Exclusively Mating-Competent 203
VII. **Summary of the Fundamental Differences between the Mating Systems of *C. albicans* and *S. cerevisiae*** 203
VIII. **The Cell Biology of Mating in *C. albicans*** . . 204
IX. **Returning to a Diploid State after *C. albicans* Mating** 205
X. **The Role of Mating Type Genes** 207
XI. **The Mating System of *Candida dubliniensis*** 208
XII. **Pheromone and the Cytological Pheromone Response** 209
XIII. **The Pheromone Response Pathway in *C. albicans* Opaque Cells** 210
XIV. **Pheromone and G1 in *C. albicans* Mating** . . 210
XV. **Pheromone-Dependent Gene Expression in *C. albicans* Opaque Cells** 211
XVI. **The Temperature Sensitivity of *C. albicans* Opaque Cells and Mating on Skin** 211
XVII. **Pheromone-Regulated Gene Expression in *C. albicans* White Cells** 212
XVIII. **Pheromone Induces *C. albicans* *MTL*-Homozygous White Cells to Become Highly Cohesive and Form Biofilms** 213
XIX. **Conclusion: Why Should We Concern Ourselves with *Candida* Mating?** 214
References 214

[1] Department of Biological Sciences, The University of Iowa, Iowa City, IA 52242, USA

I. Introduction

Mating has been intensively studied in *Saccharomyces cerevisiae* since the original observation by Winge (1935) that diploid cells emerged from the haploid offspring of a single homothallic cell. Since that time, interest first in the genetics and then in the molecular biology of *S. cerevisiae* mating has resulted in powerful paradigms for studying mating in other fungi and gene regulation, including gene silencing in higher eukaryotes (Sprague 2006; Thorner 2006). For the infectious yeasts, including *Candida albicans* and related species, the mating system of *S. cerevisiae* has been used as a road map for exploring mating and identifying those aspects which follow the paradigm and those aspects that are unique. In the past six years, we have witnessed the identification and detailed dissection of the *C. albicans* mating system and to a lesser extent the *C. glabrata* mating system. Comparative analyses of the mating systems and mating-type genes of *S. cerevisiae*, *Candida* species and other related yeasts provide insights into the evolution of the hemiascomycetes (Tsong et al. 2003; Butler et al. 2004; Bennett and Johnson 2005). However, such interest in the pathogenic fungi will wane if the mating systems do not prove to be directly or at least indirectly involved in pathogenesis, since interest in these organisms ultimately is fueled by a quest for treatments and cures. Because studies of the population structure indicate predominantly clonal modes of reproduction for both *C. albicans* and *C. glabrata* (Pujol et al. 2005), recombination is relegated to a rare event, as is mating, a source of recombination. Hence, while mating may play a role in the long-term survival of the species, it may play no immediate role in the virulence or pathogenesis of the organism. There are however indications, at least in the case of *C. albicans*, that the mating process is intimately intertwined with host–pathogen interactions and may in fact play a role in patho-

Biology of the Fungal Cell, 2nd Edition
The Mycota VIII
R.J. Howard and N.A.R. Gow (Eds.)
© Springer-Verlag Berlin Heidelberg 2007

genesis. Here, the mating systems of *C. albicans* and *C. glabrata* are discussed with this issue in mind.

II. Population Studies Suggest Mating is a Rare Event in *C. albicans* and *C. glabrata*

C. albicans and *C. glabrata* represent the two most common of the yeast pathogens (Odds 1988; Pfaller et al. 1998). Both are carried as commensals by humans, opportunistically increasing in number in response to a change in host physiology, causing inflammation and tissue destruction (Odds 1988; Calderone 2002). In immunocompromised hosts, both species frequently cause life-threatening systemic infections. Both species are found predominantly in animal hosts worldwide. During the past 15 years, a variety of genetic fingerprinting methods were used to characterize the population structure of both organisms, including multilocus enzyme electrophoresis (MCEE), hybridization with complex DNA probes and multilocus sequence typing (MLST; Soll et al. 2003; Pujol et al. 2005). These studies revealed that propagation is primarily clonal and that sexual reproduction, if it occurs, is rare or possibly limited to strains genetically related (Pujol et al. 1993; Gräser et al. 1996; Anderson et al. 2001; Tavanti et al. 2005). Indeed, clades were distinguished that maintain their integrity even within common geographical locales (Soll and Pujol 2003; Tavanti et al. 2005). Recently, Tavanti et al. (2005) performed a haplotype analysis of MLST data for *C. albicans* and found a significant level of recombination, but the source of this recombination was not necessarily sexual. In an MLST analysis of 165 *C. glabrata* isolates, Dodgson et al. (2005) found 14 examples of phylogenetic incompatibility, indicating that recombination did occur during the evolution of *C. glabrata*, but it was not clear from their study how frequently or when it occurred. The rare recombinational events suggested by population studies of *C. albicans* and *C. glabrata* may be the result of mating, but other mechanisms may also be at play. Conversely, mating may occur at much higher frequencies than indicated by population studies, but may be missed because of a decrease in the capacity of the great majority of recombinants to compete with established strains for niches (Lockhart et al. 2005). But what if recombination proves to be a rare event? Obviously, if a species maintains the genes for mating and exhibits functional mating responses or fusion in vitro, it would suggest, regardless of mating frequency, that mating is important for the survival of that species. Over hundreds or thousands or millions of years, rare recombinants may save the species from environmental challenges that eliminate the majority of strains.

III. The Discovery of Mating Systems in *C. albicans* and *C. glabrata*

Through 1998, *C. albicans* was deemed asexual, and through 2002 the same was true for *C. glabrata*. The genome sequencing project ended that perception for *C. albicans*. In 1999, Hull and Johnson (1999) identified a single mating locus in the emerging genome sequence that contained genes homologous to the mating-type genes (*MAT* genes) of *S. cerevisiae*. In the case of *C. glabrata*, both a sequencing project (Wong et al. 2003) and a direct search for *S. cerevisiae* mating-type genes (Srikantha et al. 2003) ended that perception in 2003.

A. *C. albicans*

C. albicans is diploid or near-diploid, heterozygous for a significant proportion of genes located on a number of chromosomes (Whelan et al. 1980,1981; Whelan and Soll 1982; Wu et al. 2005). There is no verified example of a haploid strain, although there are examples of aneuploidy (Selmecki et al. 2005; Chen et al. 2003). Hull and Johnson (1999) identified two DNA fragments from the emerging genome database of the Stanford *C. albicans* sequencing project that contained genes homologous to *MAT* genes in *S. cerevisiae* (*S. c.*). In one DNA fragment, they identified a mating-type-like α1 gene (*MTL*α1) homologous to *S.c. MAT*α1 and an *MTL*α2 gene homologous to *S.c. MAT*α2, and on a second fragment an *MTL***a**1 gene homologous to *S. c. MAT***a**1. Subsequently, Tsong et al. (2003) reported the presence of an *MTL***a**2 gene on the second DNA fragment that was not homologous to *S.c. MAT***a**2, but was homologous to a gene in a number of other fungi, including *Neurospora crassa* (Coppin et al. 1997; Astrom et al. 2000; Debuchy et al. 1993). As shown later in this chapter, this gene plays a fundamental role in the regulation of mating and does not have an ortholog in the mating process of *S. cerevisiae*.

When the *MTL* locus of *C. albicans* was initially compared with that of *S. cerevisiae*, three major differences were immediately apparent that could impact function. First and foremost, *C. albicans* had only one mating-type locus, whereas *S. cerevisiae* had three, one expression locus (*MAT*) that was either *MAT***a** or *MAT*α and that defined mating type in haploids, and two silent loci, *HMR* and *HML*, which contained silent copies of the *MAT***a** and *MAT*α genes, respectively (Fig. 8.1A; Thorner 2006). All three *S. cerevisiae* loci were located on chromosome 3. In a diploid *S. cerevisiae* **a**/α cell, the **a**1-α2 repressor complex suppressed mating. An **a**/α *S. cerevisiae* cell possessed one *MAT***a** and one *MAT*α copy at the mating-type locus on the two homologous copies of chromosome 3 (Fig. 8.1B).

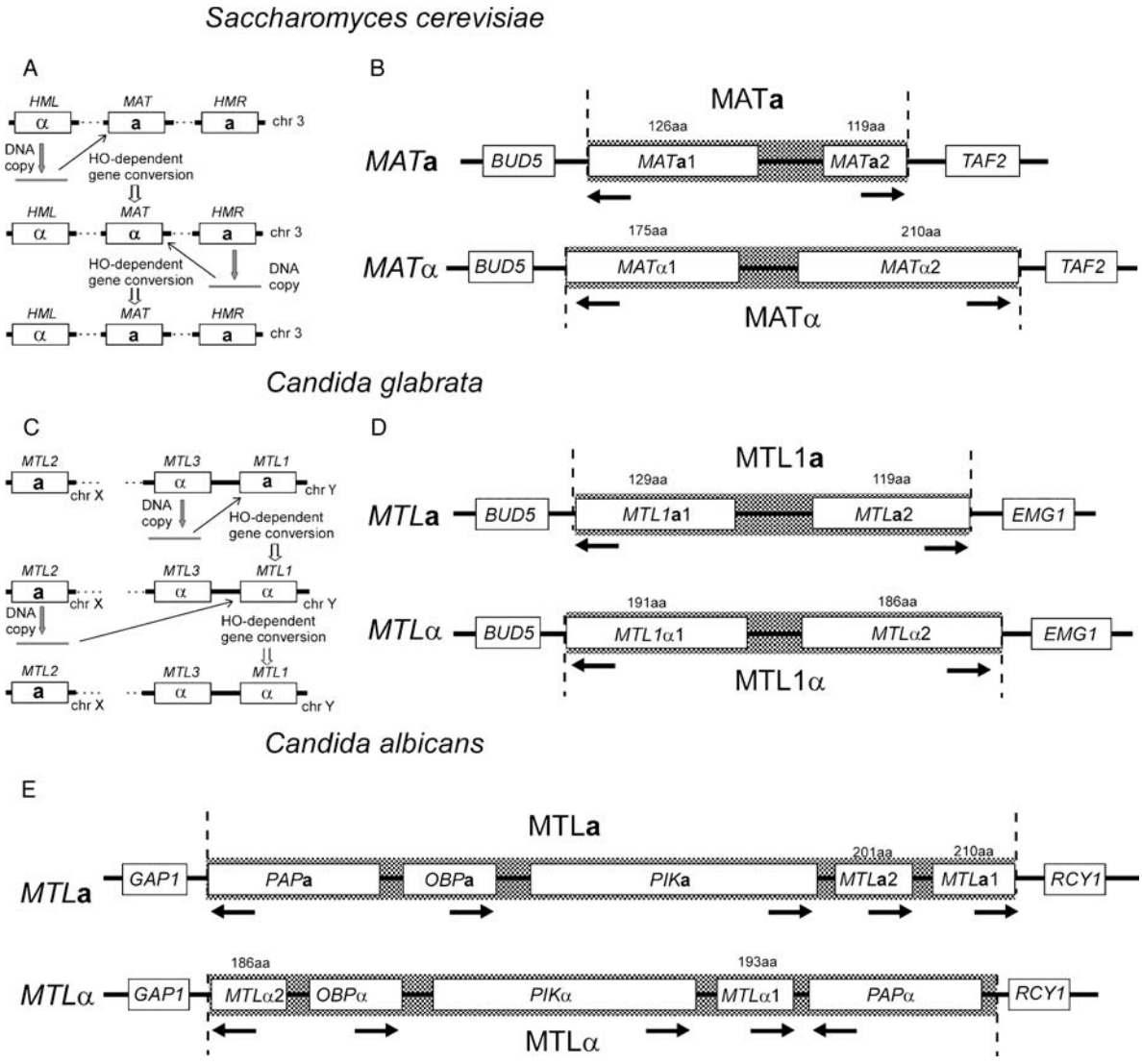

Fig. 8.1. The mating-type loci of *Saccharomyces cerevisiae* (**A**, **B**), *Candida glabrata* (**C**, **D**) and *C. albicans* (**E**). For *S. cerevisiae* and *C. glabrata*, the cassette systems and mating-type switching through gene conversion are described in panels **A** and **C**, respectively. The diploid **a**/α genotype of *C. glabrata* is inferred since only haploid strains have been isolated from nature and no mating (i.e., fusion resulting in the genesis of a diploid) has been identified. The mating-type loci are *hatched* and direction of transcription noted by *arrows* in panels **B**, **D** and **E**. In *C. albicans*, three genes other than mating-type-like genes reside in the *MTL* locus, a phosphotidylinositol kinase (*PIK*), an oxysterol-binding protein-like protein (*OBP*) and a poly(A) polymerase (PAP). See Hull and Johnson (1999) for the *C. albicans* locus; and see Wong et al. (2003) and Srikantha et al. (2003) for the *C. glabrata* loci

To express a mating type and become mating-competent, a diploid **a**/α strain underwent meiosis. In the haploid **a** or α cell, the three mating-type loci represented a cassette system in which the expression locus *MAT* could switch from **a** to α or α to **a** by a gene conversion event in which site specific recombination occurred with a DNA copy of the silent locus of opposite mating type (Fig. 8.1A). Switching was mediated by the *HO* gene, which encoded an endonuclease. Thus, a haploid cell of a homothallic strain of *S. cerevisiae* retained opposite mating-type information when expressing a single mating type. The initial discovery that *C. albicans* contained a single mating-type locus (Hull and Johnson 1999) indicated that things would be different from that of *S. cerevisiae*. *C. albicans* would have to undergo homozygosis to **a**/**a** or α/α, or lose one copy of the mating-type locus to become **a**/– or α/–, to mate. Either way, *C. albicans MTL*-homozygous strains would lose either **a** or α mating-type information when they became mating-competent.

The second major difference between *S. cerevisiae* and *C. albicans* was the content of the mating-type loci. In the *S. cerevisiae MAT***a** copy of the mating-type locus, *MAT***a**1 and *MAT***a**2 were adjacent to each other, separated only by a short intergenic regulatory region harboring no other open reading frames (ORFs; Fig. 8.1B). The same was true for *MTL*α1 and *MTL*α2. The length of the *MAT***a** copy of the locus, defined by the distance between the opposite ends of the two *MAT* genes, was shorter than that of the *MAT*α copy of the locus (Fig. 8.1B). The *MAT***a** genes *MAT***a**1 and *MAT***a**2, as well as the *MAT*α genes *MAT*α1 and *MAT*α2, were transcribed in opposite directions from the Crick–Watson strands of the DNA (Fig. 8.1B). The *MTL***a** genes *MTL***a**1 and *MTL***a**2 of *C. albicans* were also adjacent to each other (i.e., separated only by a non-coding region), but unlike *S. cerevisiae* (Fig. 8.1B), they were transcribed in the same direction (i.e., from the same Crick–Watson strand of DNA; Fig. 8.1E). The *MTL*α genes *MTL*α1 and *MTL*α2 of *C. albicans*, however, were transcribed in opposite directions, like the *MAT*α genes of *S. cerevisiae*, but *MTL*α1 and *MTL*α2 were not adjacent to each other. They were separated by two non-mating-type genes: *OBP*α, which encoded an oxysterol-binding protein-like protein, and *PIK*α, which encoded a phosphtidylinositol kinase (Fig. 8.1E). In addition, a third non-mating-type gene, *PAP*α, which encoded a poly(A) polymerase, resided to the right of *MTL*α1 (Fig. 8.1E). In the *MTL***a** copy of the locus, the three genes *PAP***a**, *OBP***a** and *PIK***a**, were to the left of *MTL***a**2 and *MTL***a**1 (Fig. 8.1E). There may be a reason why both the pair of genes *MAT***a**1 and *MAT***a**2, and the pair of genes *MAT*α1 and *MAT*α2, each shared a common upstream regulatory region in *S. cerevisiae* but not in *C. albicans*. There is an additional characteristic of the alleles of the non-mating-type genes in the *MTL* locus of *C. albicans* that is of interest. They are far more divergent than the alleles of the average gene in the *C. albicans* genome (C. Pujol and D.R. Soll, unpublished data). Furthermore, the divergent alleles exhibit **a**- and α-locus specificity, i.e., an α-allele is usually associated with *MTL*α and an **a**-allele with *MTL***a**, even across clade lines (C. Pujol and D.R. Soll, unpublished data). It is not immediately obvious why the *C. albicans MTL* locus has non-mating-type genes interspersed with mating-type genes, why these particular genes reside in the *MTL* locus, or why the alleles of these three non-mating-type genes are *MTL***a**- and *MTL*α-specific.

The third major difference between *S. cerevisiae* and *C. albicans* was the ploidy of the fusion product. Because *C. albicans* appeared to be an obligate diploid or near diploid, it seemed reasonable to conclude at the time of the discovery of the mating-type locus that it would have to convert to **a**/**a** or α/α to mate and that the fusion product would, therefore, have to be tetraploid. A meiotic reduction division from a tetraploid to a diploid could be complicated, or as we shall see, replaced possibly by an alternative mechanism.

B. *C. glabrata*

C. glabrata has evolved as the second most common *Candida* species isolated from man. It is remarkable in that it colonizes the same human anatomical niches as *C. albicans* and, like *C. albicans*, it lives as a commensal, opportunistically causing infection in response to compromising host conditions. Yet *C. glabrata* is far more closely related to *S. cerevisiae* than it is to *C. albicans* (Barns et al. 1991; Santos et al. 1997; Wong et al. 2002, 2003; Dujon et al. 2004; Kaur et al. 2005). In addition, *C. glabrata* exhibits two high-frequency phenotypic switching systems that are distinct from those of *C. albicans* (Lachke et al. 2000, 2002). And finally, while *C. glabrata* forms pseudohyphae like *C. albicans*, it does not form true hyphae (Lachke et al. 2002). It forms long non-compartmentalized tubes that revert at their apices to the budding growth form. These latter extensions and the process of apical reversion

are surprisingly similar to the conjugation tubes formed by *MTL*-homozygous cells of *C. albicans* responding to pheromone released by cells of the opposite mating type, and the apical reversion of these tubes, respectively.

In 2003, two reports appeared in which the first mating-type genes of *C. glabrata* were described. Wong et al. (2003) constructed a plasmid library with random genomic inserts and sequenced approximately 3000 plasmids representing more than three megabases, roughly 0.2× genome coverage. They used FASTY reciprocal best fits software to identify orthlogs of *S. cerevisiae* genes. They found orthologs of *S. cerevisiae* genes involved in mating, including the mating factor α2 gene, *MF*α2, *STE13* and *STE6*. More importantly, they found orthologs of *S. cerevisiae MAT*α1 and *MAT*α2 that were oriented divergently, as in *S. cerevisiae*. Srikantha et al. (2003) undertook a different approach that resulted in the identification of three loci representing the *C. glabrata* cassette system for mating-type switching (Fig. 8.1C) and the mating-type genes they harbored (Fig. 8.1D). Based on a comparison of two highly conserved regions in Mat**a**2p and Matα2p of *S. cerevisiae* and orthologs in *C. albicans* and *K. lactis*, Srikantha et al. (2003) synthesized degenerate primers that encompassed 125 bp of the *MAT*α2 ORF of *S. cerevisiae* and used them to amplify *C. glabrata* DNA. They cloned three distinct PCR products, one of which contained a sequence spanning the conserved region of *S. c. MAT*α2. The 125-bp DNA fragment was then used to probe a *C. glabrata* genomic library. One clone identified in the screen proved to contain homologs of *S.c. MAT***a**1 and *MAT***a**2. The deduced *C. glabrata MTL***a**1 protein had 28% overall similarity to *S. c.*MAT**a**1p. The deduced *MTL***a**2 protein had 26% overall identity with both *S. c.* MAT**a**2p and *S. c.* MATα2p. To identify a second *MTL***a** locus with different flanking sequences, a negative PCR selection strategy was applied. Using a different strain and the same flanking sequences for the first *MTL***a** locus identified, an *MTL*α locus was identified that contained homologs of *S.c. MAT*α1 and *S.c. MAT*α2. The configuration of the *MTL* genes in the **a** and α loci, including the directions of transcription and even the gene bordering one end of the *C. glabrata MTL* locus, *BUD5* (Fig. 8.1D), were highly similar to that of the *MAT* locus of *S. cerevisiae* (Fig. 8.1B). By analyzing the expression of *MTL* genes in a number of strains that had been separated into three major classes based on the banding patterns in Southern blots of *MTL***a**1, *MTL***a**2 (or *MTL*α2) and *MTL*α1, Srikantha et al. (2003) obtained data suggesting a configuration that included three loci, one of which, *MTL*1, functioned as an expression locus (Fig. 8.1C). In this study, they also found that 40 natural strains of *C. glabrata* were **a**/α/α or **a**/**a**/α, and were either mating-type **a** or mating-type α, respectively, as was the case in *S. cerevisiae*. The configuration on the loci (Fig. 8.1C) was highly similar to that of *S. cerevisiae* (Fig. 8.1A), although all three of the loci comprising the cassette system in *S. cerevisiae* were on chromosome 3, whereas two of the loci of *C. glabrata* were on one chromosome and one on another.

Butler et al. (2004) subsequently demonstrated that *MTL*1**a** and *MTL*1α contained HO endonuclease cleavage sites. Butler et al. (2004) found a homolog in *C. glabrata* to the *S. cerevisiae* HO endonuclease gene, with 57% sequence identity to the *S. cerevisiae* HO gene. Using a PCR amplification strategy, Butler et al. (2004) then demonstrated switching in vitro at the *MTL1* locus in an originally *MTL*1**a** strain, RND13, and an originally *MTL*1α strain, CBS138. Brockert et al. (2003) demonstrated mating-type switching in vivo. They analyzed the *MTL1* genotype of primary isolates from three patients with vaginal candidiasis caused by single *C. glabrata* strains; and they found in one patient (P1) that, although all isolates exhibited similar DNA fingerprints (i.e., represented the same strain), they consisted of a mixture of **aa**α and **a**αα genotypes. *C. glabrata* therefore has a mating-type cassette system that is functional and active in vitro and vivo.

IV. The *MTL* Genotype in Nature

Hull and Johnson (1999) described the *MTL* locus of *C. albicans* in the laboratory strain SC5314, which served as the major strain for gene deletion studies as a result of the pioneering work of Fonzi and co-workers (Fonzi and Irwin 1993). SC5314 was the first *C. albicans* strain sequenced and auxotrophic derivatives of SC5314 were used to generate null mutants of the *MTL* genes and locus (Hull and Johnson 1999). To assess the proportions of *MTL* genotypes in nature, Lockhart et al. (2002) analyzed 220 independent clinical isolates of *C. albicans*. The majority of these strains had been collected in the late 1990s. Their collection included members of the five major clades of *C. albicans* that,

at the time, had been identified by Southern blot hybridization with the complex DNA fingerprinting probe Ca3 (Pujol et al. 1997, 2002; Blignaut et al. 2002; Soll and Pujol 2003). They found that 96.8% were *MTL*-heterozygous (**a**/α) and only 3.2% *MTL*-homozygous (**a**/**a** or α/α). Furthermore, they found that approximately 4% of **a**/α strains underwent *MTL*-homozygosis to **a**/**a** or α/α at high frequencies. Hence, they found that 7% of natural strains were either *MTL*-homozygous or contained significant proportions of *MTL*-homozygous offspring in growing populations. Legrand et al. (2004) subsequently analyzed 120 clinical isolates collected in the 1980s and early 1990s for *MTL* genotype. They found that 90% were *MTL*-heterozygous and 10% either **a**/**a** or α/α, results similar to those of Lockhart et al. (2002). Finally, Tavanti et al. (2005) analyzed 416 isolates of *C. albicans* for *MTL*-zygosity and found that 89.4% were heterozygous (**a**/α) and 10.6% homozygous (**a**/**a** or α/α), again results similar to those of Lockhart et al. (2002). It therefore seems reasonable to conclude that in nature approximately 90% of *C. albicans* strains are **a**/α and approximately 10% **a**/**a** or α/α.

Tavanti et al. (2005) analyzed the frequency of *MTL*-homozygosity in genetically related groups of *C. albicans* identified by multi-locus sequence typing. They found that 14.9% of isolates (N = 155) in clade 1, 5.5% (N = 55) in clade 2, 16.7% in clade 3 and 4.4% in clade 4 were *MTL*-homozygous. Some minor clades exhibited much higher or lower frequencies, but no conclusions could be drawn from these numbers given the low sample sizes.

Lockhart et al. (2005) noted a possible paradox in the maintenance of predominantly **a**/α strains of *C. albicans* in nature and conservation of the sexual cycle. In *S. cerevisiae*, haploid **a** and α cells retain opposite mating-type genes in one of the silent cassettes. Therefore, whether a cell is diploid or haploid, the entire mating system is conserved at a cellular level. This is not the case in *C. albicans*. When **a**/α cells become *MTL*-homozygous, they lose the mating-type genes of the opposite mating type. Since many strains generated **a**/**a** and α/α cells at relatively high frequency (Lockhart et al. 2002; Pujol et al. 2003, Wu et al. 2005) and mating in nature appeared to be a rare event, as suggested by population structure studies, Lockhart et al. (2005) argued that there appeared to be a robust route to *MTL*-homozygosity, but no similar robust route in the reverse direction to *MTL*-heterozygosity. Lockhart et al. (2005) therefore asked why *MTL*-homozygous strains did not accumulate or predominate in nature. Indeed, if one *MTL*-homozygous genotype acquired a competitive advantage over heterozygous strains and the other *MTL*-homozygous genotype, one could imagine the possible loss of the mating system. Lockhart et al. (2005) hypothesized that **a**/α strains may remain dominant because they may be more competitive than their **a**/**a** or α/α offspring for host niches. Wu et al. (2005) demonstrated that the majority of spontaneous **a**/**a** and α/α offspring arose in vitro by the loss of one homolog of chromosome 5 followed by duplication of the retained homolog, leading to homozygosity along the entire length of chromosome 5. Lockhart et al. (2005) isolated spontaneous **a**/**a** and α/α offspring form several natural **a**/α parent strains that underwent high frequency *MTL*-homozygosis in vitro and found that in every case the **a**/α parent strain was more virulent than the *MTL*-homozygous offspring in a mouse model for systemic infection. Analyses by Ibrahim et al. (2005), however, found only a slight difference in the virulence of *MTL*-heterozygous parent strains and *MTL*-homozygous offspring induced by growth or sorbose medium. The difference between the results of the two studies could be due to differences in the manner in which *MTL*-homozygous offspring were obtained, differences in the origin of the **a**/α strains or differences in the resolution of virulence (i.e., the stringency of the model), since Lockhart et al. (2005) used outbred mice, whereas Ibrahim et al. (2005) used inbred mice.

Lockhart et al. (2005) further found that when **a**/α parent cells and **a**/**a** or α/α offspring were mixed and injected into the same mouse, the parent strain always predominated over the *MTL*-homozygous offspring in infected organs. There were two possible explanations for the observations of Lockhart et al. (2005): first that the heterozygosity of *MTL* genes themselves provided a competitive edge, or, second that heterozygosity of genes other than the *MTL* genes along chromosome 5 provided a competitive edge. Work by Wu et al. (2007) indicated both were correct. Deletion of *MTL***a**1 or *MTL*α2 in natural **a**/α strains had a small but significant effect on virulence. Therefore, it seems likely that the competitive edge of parental **a**/α strains over spontaneous *MTL*-homozygous offspring is due primarily to the heterozygosity of genes other than the *MTL* genes along chromosome 5 (Wu et al., 2007). These results do not, however, detract from the argument by Lockhart et al. (2005) that **a**/α strains predominate because they have a competitive edge over

their spontaneous *MTL*-homozygous offspring (Lockhart et al. 2005; Wu et al., in preparation).

In the case of *C. glabrata*, extensive analyses of the *MTL*-genotypes of natural strains have not been performed as in *C. albicans*. Srikantha et al. (2003) did analyze 40 clinical strains and found that each was haploid, 56% **a** and 44% α. This differed from the diploid nature of natural strains of *C. albicans* and *S. cerevisiae*.

V. Demonstration of Mating in *C. albicans*, but not *C. glabrata*

Once the mating-type locus of *C. albicans* was identified, two groups immediately proceeded with similar strategies to test for mating. Both groups generated **a** and α strains with different auxotrophic markers, then selected for fusants by complementation. Hull et al. (2000) created functional α and **a** strains by deleting the *MTL***a**1 gene or the *MTL*α2 gene, respectively, in a laboratory strain. The *MTL***a**1 deletion strain carried an *ade2*$^-$ marker and the *MTL*α2 deletion strain a *ura3*$^-$ marker. Hull et al. (2000) also generated auxotropic strains in which the entire *MTL***a** or *MTL*α locus was deleted. The **a** and α strains were mixed and co-injected into the tail veins of mice. After 24 h, animals were sacrificed, kidneys removed and macerated, and macerates plated on agar lacking adenine and uridine. On such agar, only fusants grew as a result of complementation. Hull et al. (2000) found complemented strains in the kidney macerates. Cells of these strains contained single nuclei, increased DNA content indicative of tetraploids, and **a**/α genotypes. Magee and Magee (2000) generated **a** and α strains by growing an **a**/α strain on sorbose agar, which had been demonstrated to cause the loss of chromosome homologs, most notably one of the two chromosome 5 homologs which harbors the *MTL* locus (Janbon et al. 1999). Magee and Magee cross-streaked auxotropic **a** and α strains on selection agar and analyzed isolates that grew in the absence of uridine and adenine. Magee and Magee (2000) identified **a**/α isolates with increased DNA content. Hence, one year after identification of the *MTL* locus, cell type-dependent mating (i.e., requiring mating-type **a** and α) was demonstrated both in vivo (Hull et al. 2000) and in vitro (Magee and Magee 2000). In early 2003, Lockhart et al. (2003a) described for the first time the in vitro fusion process at the cellular level, and by vitally labeling natural **a**/**a** and α/α strains with different dyes, demonstrated that fusion only occurred between **a**/**a** and α/α cells.

While mating was immediately demonstrated in *C. albicans* after identification of the mating-type locus, it was not immediately demonstrated in *C. glabrata*. When a *ura3*$^-$ derivative of the natural *C. glabrata* **a** strain 35B11 was cross-streaked with *his3*$^-$ derivatives of natural *C. glabrata* α strains PB921 or 1480.47, incubated overnight, and then replicate-plated on selection plates of nutrient agar lacking uracil or histidine, no diploid fusants were recovered (T. Srikantha and D.R. Soll, unpublished data). This first attempt to identify *C. glabrata* mating cannot be considered in any way conclusive since it was of limited scope and provided negative results. A far more extensive, full-scale approach is warranted in which a greater variety of isolates covering the major genetic groups (Dodgson et al. 2005) are tested because of possible incompatibilities that may have arisen between clades. In addition, a more intense search for a natural diploid strain is warranted, and on the same note, the possibility must be explored that diploids generated by mating are very short-lived and hence might go undetected by the standard complementation test used in the initial studies reported here (T. Srikantha and D.R. Soll, unpublished data). Given that *C. glabrata* strains undergo mating-type switching (Brockert et al. 2003; Butler et al. 2004) and given the observation by Dodgson et al. (2005) that *C. glabrata* populations exhibit phylogenetic incompatibilities and thus most likely undergo recombination, there is a possibility that *C. glabrata* may undergo mating.

VI. Mating of *C. albicans* Requires White–Opaque Switching

The results of Hull et al. (2000) and Magee and Magee (2000) suggested that mating of *C. albicans* was a rare event. However, two extraordinary discoveries by Miller and Johnson (2002) changed that impression and revealed a unique relationship between high-frequency phenotypic switching and the mating process. This part of the story began in 1987 with the discovery of the white–opaque transition. Slutsky et al. (1987) discovered a high-frequency reversible transition between two colony phenotypes which they named the "white–opaque transition" (Fig. 8.2) in a strain (WO-1) isolated

from the blood of a patient with a systemic yeast infection. Cells from a streak of strain WO-1, when clonally plated, formed majority "white" colonies and minority "opaque" colonies (Fig. 8.2A), and white colonies with opaque sectors (Fig. 8.2B). The former were near hemispherical and white, and the latter larger, flat and grey. Opaque colonies differentially stained red when phloxine B was introduced into the supporting agar. Cells from the original streak, when clonally plated on nutrient agar, produced 96.6% white colonies, 0.6% opaque colonies and 2.8% sectored colonies (Slutsky et al. 1987). In an analysis of switching performed on over 100 independent *C. albicans* isolates in 1987, it was observed that approximately 8% of strains underwent the white–opaque transition. Cells from a white colony were round with uniform surfaces (Fig. 8.2C, E), while cells from an opaque colony were twice as large as white cells, possessed unique cell wall pimples (Fig. 8.2D, F) and a large vacuole (Fig. 8.2F). In the late 1980s, it was demonstrated that opaque cells expressed opaque-specific antigens, most notably a protein of 14.5 kDa on the cell surface in association with the unique opaque cell pimple (Anderson et al. 1990). In 1992, Morrow et al. identified the first phase-specific gene, *PEP1*, later renamed *SAP1*, for secreted aspartyl proteinase 1, which was expressed only in the opaque phase. In 1993, another opaque-specific gene, *OP4* (Morrow et al. 1993), and a white-specific gene, *WH11* (Srikantha et al. 1993), were identified. From that time, the list of phase-specific genes has grown (Soll 2002, 2003), culminating in a microarray analysis by Lan et al. (2002), which revealed that the white–opaque transition regulated over 300 genes in the *C. albicans* genome, roughly 6% of the genome. In addition, a variety of studies revealed physiological differences between the two phenotypes (Soll 1992, 2002, 2003; Lan et al. 2002) as well as differences in virulence traits, including: (1) environmental constrains on the bud-hypha transition (Anderson et al. 1989), (2) susceptibility to antifungal agents (Soll et al. 1991; Vargas et al. 2000), (3) proteinase secretion (Morrow et al. 1992; White et al. 1993; Hube et al. 1994), and (4) sensitivity to white blood cells and oxidants (Kolitila and Diamond 1990). Finally, Kvaal et al. demonstrated, in 1997, that white cells were far more virulent than opaque cells in the mouse model for systemic infection, and in 1999, that opaque cells were more virulent than white cells in the colonization of skin. But there remained two major paradoxes related to the opaque phenotype. First, why was it originally observed that only ~8% of natural strains underwent the white–opaque transition, when all strains possessed opaque-specific genes? And second, why were opaque cells sensitive to physiological temperature (i.e., 37 °C)? Opaque cells underwent mass conversion from opaque to white when the temperature was raised from 25 °C to >37 °C (Slutsky et al. 1985, 1987; Rikkerink et al. 1988; Srikantha and Soll 1993; Soll 2003).

A. The a1-α2 Complex Represses Switching

In 2002, Miller and Johnson reported that while the parent **a**/α strain CAI4, which is a *ura3*$^{-}$ derivative of laboratory strain SC5314, did not

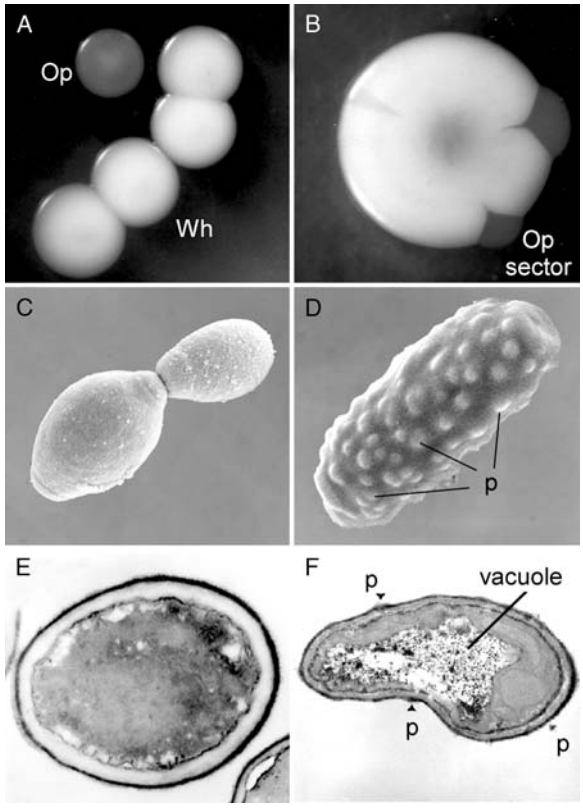

Fig. 8.2. The white–opaque transition in *C. albicans* strain WO-1 (Slutsky et al. 1987). **A** Clonally plated cells from a white colony form majority white (*Wh*) and minority opaque (*Op*) colonies. **B** When a white colony is aged on agar in a plate wrapped with Parafilm to block gas exchange, opaque sectors form at the periphery. **C, D** Scanning electron micrographs of a representative white and opaque cell, respectively. **E, F** Transmission electron micrographs of a representative white and opaque cell, respectively. *p* Pimple. See Anderson and Soll (1987) for ultrastructure of opaque cell

exhibit white–opaque switching, **a** and α strains constructed from CAI4 underwent switching. Srikantha et al. (1998) had previously characterized CAI8, a *ura3*$^{-}$*ade2*$^{-}$ derivative of SC5314, and showed that, while it underwent 3153A-like switching, it did not undergo white–opaque switching. Miller and Johnson (2002) found that, by removing the **a**1-α2 repressor complex through the deletion of either *MTL***a**1 or *MTL*α2, they had de-repressed switching. They demonstrated that the **a** and α derivatives of CAI4, but not **a**/α CAI4, formed opaque sectors and that these sectors contained bona fide opaque cells that did not express the white phase-specific gene *WH11* but did express the opaque phase-specific gene *OP4* (Miller and Johnson 2002). The opaque-specific gene *SAP1* was expressed in the α but not the **a** derivative. To universalize this observation, Lockhart et al. (2002) examined the relationship between the *MTL* genotype and switching in natural strains. First, they found that seven genetically unrelated natural strains of *C. albicans* selected for their capacity to undergo the white–opaque transition were all *MTL*-homozygous, either **a**/**a** or α/α. They then found that, of the seven *MTL*-homozygous strains they identified in 220 analyzed natural strains, five underwent white–opaque switching and the remaining two underwent an aberrant phenotypic transition. In contrast they found that, of 20 randomly selected *MTL*-heterozygous strains, 18 did not undergo switching. The two that did were found to have undergone *MTL*-homozygosis at high frequency before switching. Of the 96.8% of the strains that were *MTL*-heterozygous, approximately 4% were found to undergo *MTL*-homozygosis at high frequency, sometimes as high as one in every ten cell divisions (Lockhart et al. 2003a; Pujol et al. 2003; Wu et al. 2005). The results of Lockhart et al. (2002) therefore generalized the results of Miller and Johnson (2002). These results indicated that the great majority of natural *C. albicans* strains, which are **a**/α, are capable of undergoing white–opaque switching if they first undergo *MTL*-homozygosis.

Pendrak et al. (2004) demonstrated that, when one of the two alleles of *HRB1* was deleted (hemoglobin response gene 1), **a**/α cells underwent switching and produced mating-competent cells, presumably through up-regulation of *MTL*α genes. Their results suggest that, in *C. albicans*, **a**1-α2 repression can be alleviated through host–pathogen interactions.

B. The Opaque Phenotype is Exclusively Mating-Competent

While the first observation by Miller and Johnson (2002) that *MTL* zygosity regulated switching was exciting, their second observation was amazing. Again using complementation as an assay, they found that the efficiency of mating between opaque **a** and opaque α cells was several orders of magnitude greater than between white **a** and white α cells, between white **a** and opaque α cells or between opaque **a** and white α cells. These results indicated that opaque represented the mating-competent phenotype for **a**/**a** and α/α cells and that white was a mating-incompetent phenotype. Lockhart et al. (2003a), using microscopically identified fusions as an assay for mating, tested the generality of this observation in natural strains. They performed 30 independent crosses in which the *MTL* genotype and switch phenotype were varied. These crosses included seven independent natural strains. They found that only crosses between **a**/**a** and α/α cells both expressing the opaque phenotype resulted in fusion. Crosses that included one or both mating types expressing the white phenotype, or crosses with **a**/α cells, generated no fusants. These results generalized the observation by Miller and Johnson (2002) that opaque was the mating-competent phenotype. While Hull et al. (2000) and Magee and Magee (2000) originally used white cells in their demonstration of mating, the frequencies appeared to be very low, suggesting the observed fusions may have been between rare opaque cells that were generated spontaneously in the white populations.

VII. Summary of the Fundamental Differences between the Mating Systems of *C. albicans* and *S. cerevisiae*

The initial characterization of the basic mating process thus revealed fundamental differences between *C. albicans* and *S. cerevisiae* (Fig. 8.3). *S. cerevisiae* diploid **a**/α cells underwent meiosis to generate **a** and α haploid cells that were immediately mating-competent. In contrast, *C. albicans* diploid **a**/α cells underwent *MTL*-homozygosis to produce **a**/**a** or α/α diploid cells, which were not immediately mating-competent. These *MTL*-homozygous cells had to then undergo a phenotypic switch

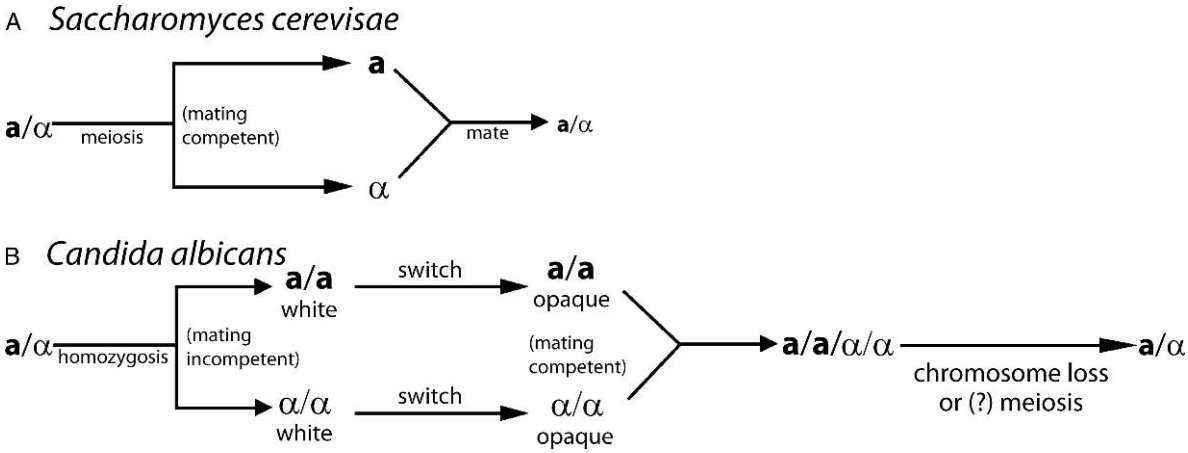

Fig. 8.3. Differences in the mating scenarios of *S. cerevisiae* (**A**) and *C. albicans* (**B**)

from white to opaque to obtain mating competence. When *S. cerevisiae* **a** and α cells mated, they generated a diploid zygote, which could then repeat the mating cycle. When *C. albicans* **a/a** and α/α cells mated, they generated a tetraploid zygote which could then return to the diploid state (see Sect. IX.). These differences are diagrammed in Fig. 8.3.

VIII. The Cell Biology of Mating in *C. albicans*

Miller and Johnson (2002) provided the first images of conjugation tubes in mating mixtures of **a** and α derivatives of the *ura3*$^-$ strain CAI4. Lockhart et al. (2003a) then took advantage of the radical increase in mating frequency obtained when opaque **a** and α cultures were mixed, and when the opaque cells were derived from saturation phase cultures, to analyze the cell biology of mating, including for the first time the process of fusion, between natural **a/a** and α/α strains. By continuously video-recording mixed cultures of **a/a** (P37005) and α/α (WO-1) cells, they documented the dynamics of the fusion event (Fig. 8.4A). They also reconstructed in 3D the fusion event between vitally stained **a/a** and α/α cells within large clumps obtained from suspension cultures using 3D-DIAS software (Wessels et al. 1998; Soll et al. 2000; Fig. 8.4B). This study revealed that the sequence of events during *C. albicans* mating were surprisingly similar to those of *S. cerevisiae*, although they failed to observe nuclear fusion. However, subsequent studies by Bennett et al. (2005) revealed that this failure was due to both the medium employed and the strains analyzed. Bennett et al. (2005) deduced the sequence of nuclear events associated with fusion and development of the first bud from the conjugation tube. In Fig. 8.5, a sequence is presented of the steps in the mating process deduced from several studies (Daniels et al. 2003; Lockhart et al. 2003a; Bennett et al. 2005; Zhao et al. 2005; K. Daniels and D.R. Soll, in preparation). To initiate mating, an opaque **a/a** and an opaque α/α cell release **a**-pheromone and α-pheromone, respectively. As is the case in *S. cerevisiae*, pheromone of one mating type induces polarization and shmooing in cells of the opposite mating type (Fig. 8.5A). The α-pheromone released by an α/α cell forms a gradient decreasing in the direction of an **a/a** cell and vice versa. Through a process referred to as chemotropism (Arkowitz 1999), the evagination on each mother cell (shmoo) elongates in the direction of increasing pheromone concentration, until there is apical contact between the ends of the opposing tubes (Fig. 8.5B). The tubes fuse to form the conjugation bridge (Fig. 8.5C) and the nuclei of the mother cells migrate into the bridge and fuse. At the site of fusion, a daughter cell forms (Fig. 8.5D). As the daughter cell grows, the tetraploid nucleus undergoes mitosis and one daughter nucleus locates in the daughter cell (Fig. 8.5E). When the daughter cell has matured, it in turn buds (Fig. 8.5F). The nucleus left in the bridge divides and the daughter nuclei relocate to the mother cells. Miller and Johnson (2002) found that the colonies formed by tetraploids were white, suggesting, as one might expect, that fusion of the **a/a** and α/α nuclei results in the re-establishment of **a**1-α2 repression

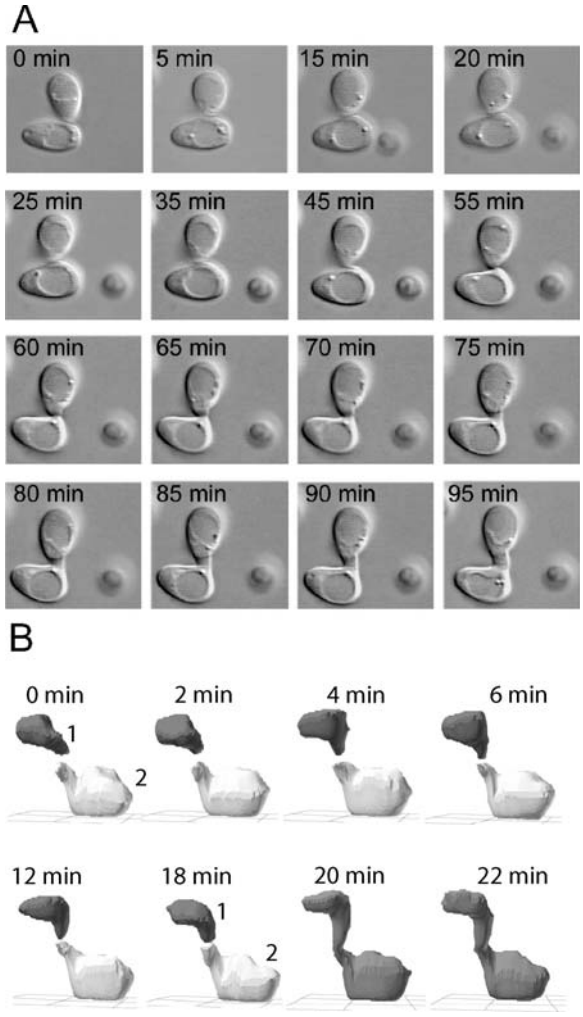

Fig. 8.4. The fusion event during mating of an opaque **a/a** cell (strain P37005) and opaque α/α cell (strain WO-1) of *C. albicans*. **A** Video images of a fusion event on a glass surface viewed through differential interference contrast microscopy. **B** 3D-DIAS reconstruction of fusion of **a/a** and α/α cells in a clump of cells, viewed at 35 °C. Only the fusing cells are reconstructed. See Lockhart et al. (2003a) for details

of switching and re-establishment of the **a/α** white phenotype.

Daniels et al. (2003) stained mixtures of **a/a** and α/α cells with antibody against the hypha-expressed adhesin *HWP1* because the unusual lengths that conjugation tubes attained (Lockhart et al. 2003a, b; Bennett et al. 2005; Zhao et al. 2005) suggested that filamentation-associated genes may be involved. This suggestion was subsequently supported by results obtained in microarray and Northern analyses of gene expression associated with conjugation tube formation (Bennett et al. 2003; Zhao et al. 2005), reviewed in Sect. XV.. Daniels et al. (2003) found that conjugation tubes formed by opaque **a/a** cells, but not opaque α/α cells, expressed HWP1 on their surface. This in turn provided a means for assessing which parent cell contribution (i.e., **a/a** or α/α) to the conjugation tube gave rise to the first daughter cell (i.e., which parent cell was "female"), a distinction that has not been made between the **a** and α mating partners of *S. cerevisiae*. Daniels et al. (2003) found that the first daughter cell emerged from the **a/a**-contributed portion of the bridge, suggesting that the **a/a** partner is female. Daniels et al. (2003) also demonstrated that the HWP1 gene is selectively activated by α-pheromone in opaque **a/a** cells. They showed that HWP1 was expressed in the tubes of three unrelated **a/a** strains (P37005, L26, 12C) undergoing mating with an α/α strain and showed that *HWP1* was not expressed in the conjugation tubes of three unrelated α/α strains (WO-1, 19F, P37037) undergoing mating with an **a/a** strain.

IX. Returning to a Diploid State after *C. albicans* Mating

The original studies by Hull et al. (2000) and Magee and Magee (2000) which demonstrated mating in vivo and in vitro, respectively, included observations indicating that nuclear fusion had occurred, leading to the genesis of a tetraploid nucleus. Bennett et al. (2005), using cytological techniques, then demonstrated that diploid nuclei fused in the conjugation bridge. But how, then, did the tetraploid return to a diploid state? In *S. cerevisiae*, the fusion product of mating was diploid. Diploids returned to the haploid state by meiosis in the process of sporulation (Esperito 2006). The diploid **a/α** cell gave rise to four spores, two **a** and two α. In *C. albicans*, the fusion product was tetraploid (**a/a/α/α**). The outcome of a reduction division would be **a/a**, **a/α** or α/α. This reduction could be accomplished by meiosis or a parasexual process that involved chromosome loss accompanying mitoses. Bennett and Johnson (2003) constructed a tetraploid strain with the following markers on three chromosomes:

Chromosome 1: Δ*gal*/Δ*gal1*/*GAL1*/*GAL1*

Chromosome 3: Δ*ade2*/Δ*ade2*/*ADE2*/*ADE2*

Chromosome 5: *MTL***a**, *MTL*α, Δ*mtla*, Δ*mtl*α1, Δ*mtl*α2

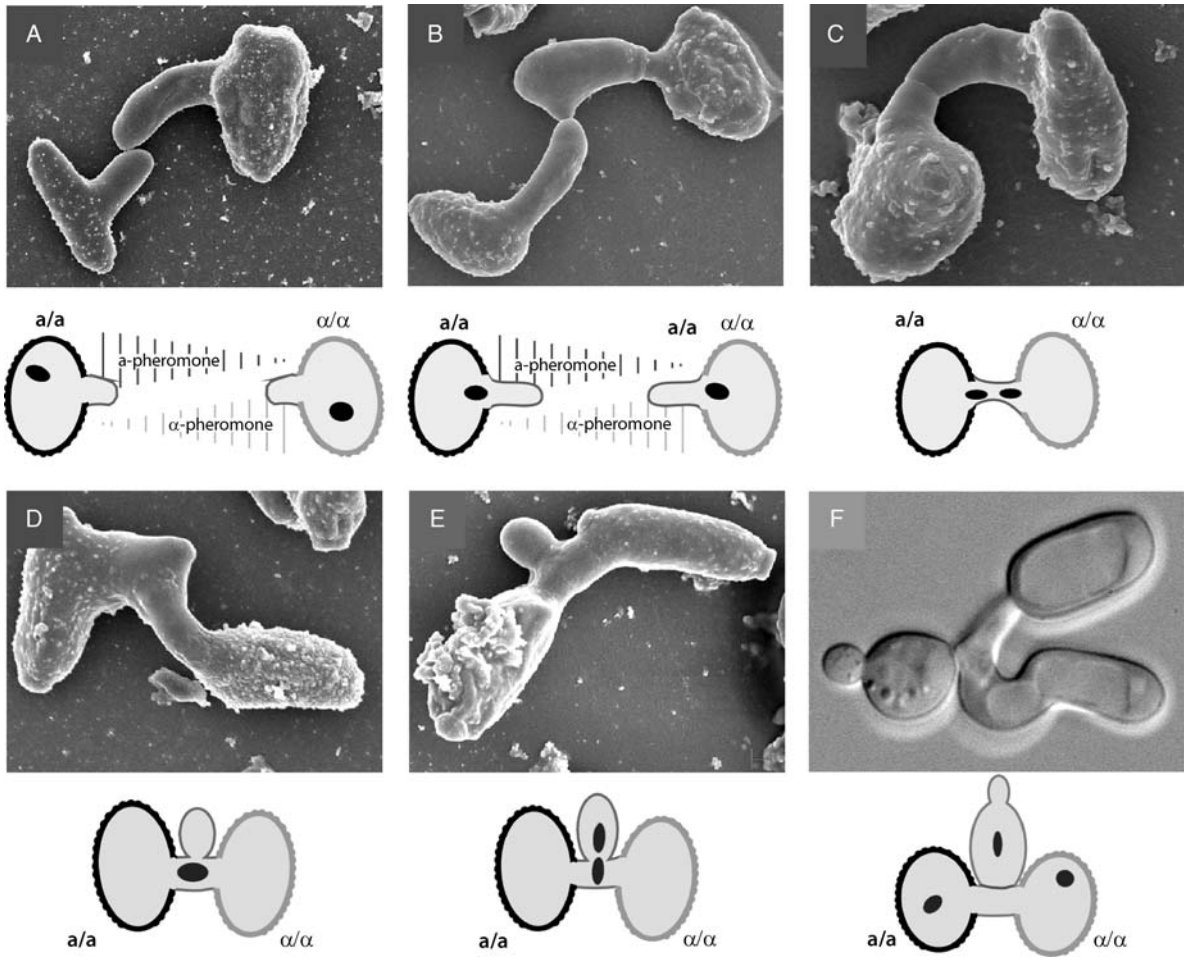

Fig. 8.5. The cell biology of mating in *C. albicans*. **A** An **a/a** cell releases **a**-pheromone, which forms a gradient in the direction of an α/α cell, and an α/α cell releases α-pheromone, which forms a gradient in the direction of the **a/a** cell. Cells respond to the opposite pheromone by arresting in G1, polarizing and shmooing. Evagination is in the direction of the opposite mating type. **B** Conjugation tubes grow up the concentration gradient of the pheromone released by the opposite mating type. Nuclei position at the mother cell-tube junctions. **C** The conjugation tubes fuse end to end, forming the conjugation bridge. Nuclei migrate into the bridge. **D** A bud evaginates from the **a/a** contribution to the conjugation bridge. Nuclei then migrate through the bridge and fuse, probably before nuclear fusion. **E** The bud grows and the nucleus divides. One daughter nucleus enters the bud. **F** A septum forms separating daughter cell from conjugation tube. The nucleus in the tube divides and the daughter nuclei return to the original mother cell. A secondary bud forms on the original daughter cell

The tetraploid strain contained one copy of *URA3* and two copies of *GAL1* and therefore could not grow on medium containing 5-FOA or 2-DOG, but derivatives could if they had lost the one *URA3* allele or the two *GAL1* alleles, respectively. They tested a number of media and found that the pre-sporulation medium used for *S. cerevisiae* resulted in the highest frequency of allelic loss. They found that induced chromosome loss was concerted, i.e., when cells lost two copies of one chromosome, they were more apt to lose copies of other chromosomes. In contrast, diploids grown on pre-sporulation medium did not similarly lose chromosomes. Bennett et al. (2003) further demonstrated that, when tetraploids were grown on sorbose medium (Janbon et al. 1999), chromosome loss was concerted. Growth of tetraploid strains in both pre-sporulation and sorbose medium resulting in diploid or near-diploid offspring. In sporulation medium, some of these offspring became mating-competent (Bennett et al. 2003). While this parasexual reduction from

tetraploidy to diploidy, or near diploid, could be induced on the noted media, one cannot exclude the possibility that meiosis can occur. Tzung et al. (2001) identified in *C. albicans* many homologs of genes involved in meiosis, recombination and the formation of synaptic complexes. There is, therefore, a good chance that meiosis exists, but that the conditions that support meiosis just have not yet been identified.

X. The Role of Mating Type Genes

In diploid **a**/α cells of *S. cerevisiae*, the **a**1-α2 complex represses both **a**- and α-mating competence and α2 represses **a**-specific genes and **a** mating competence. Repression by both the **a**1-α2 complex and α2 occur in conjunction with other factors in the formation of repressor complexes (Sprague 2006). In haploid **a** cells, the expression of **a**-specific genes and the acquisition of **a**-mating competence occur by default. **a** cells are released from **a**1-α2 and α2 repression. In α cells, *MAT*α1 activates α-specific genes and mating competence. Tsong et al. (2003) identified both similarities and differences between *S. cerevisiae* and *C. albicans* with regard to the role of mating-type genes. While the **a**1-α2 complex repressed **a**- and α-mating competence in diploid **a**/α cells of *C. albicans*, *MTL*α2 did not directly repress **a**-specific genes and **a**-mating competence, as the homolog *MAT*α2 did in *S. cerevisiae*. In **a**/**a** cells, **a**-specific genes and **a**-mating competence were positively regulated (activated) by *MTL***a**2, in contrast to a default mechanism in *S. cerevisiae* **a** cells. In α/α cells of *C. albicans*, *MTL*α1 activated α-specific genes and α-mating competence, as in *S. cerevisiae*. These conclusions were based upon the capacity of deletion mutants to mate and upon transcription profiles developed form microarray data. Based on these observations, Tsong et al. (2003) developed a regulatory circuit for transcription of mating-associated genes for the *C. albicans* mating process that incorporated the transition from white to opaque, which is repressed by the **a**1-α2 complex. The circuit included both similarities and major differences to that of the *S. cerevisiae* mating process. Tsong et al. (2003) also generated a phylogenetic tree based upon mating-type loci for the fungi and a model for the evolution of the loss of **a**-specific gene activation in *S. cerevisiae* from an ancestral strain with a general regulatory circuit similar to that of *C. albicans* (Fig. 8.6). The arguments for this elegant model can be found in Tsong et al. (2003). Butler et al. (2004) also derived a phylogenetic tree of the hemiascomycetes that included first the acquisition of the HO gene in the development of a cassette system and then the loss of *MAT***a**2 (*MTL***a**2 in *C. albicans*) and genomic duplication (Fig. 8.6). In this tree, *Yarrowia liploytica* and *C. albicans* branched off early and did not undergo the three landmark events. Thus it seemed to be the general consensus that the regulatory circuits of *C. albicans* may more closely resemble that of the common ancestor than *S. cerevisiae*, or by inference *C. glabrata*. Again, the arguments for this tree can be found in Butler et al. (2004). Interestingly, neither of the models proposed by Tsong et al. (2003) and Butler et al. (2004) included the acquisition and/or loss of white–opaque switching. Either the ancestral strain underwent white–opaque switching and loss of this characteristic occurred soon after *C. albicans* emerged from the phylogenetic tree, or *C. albicans* developed white–opaque switching after it branched from the lineage (Fig. 8.6). In

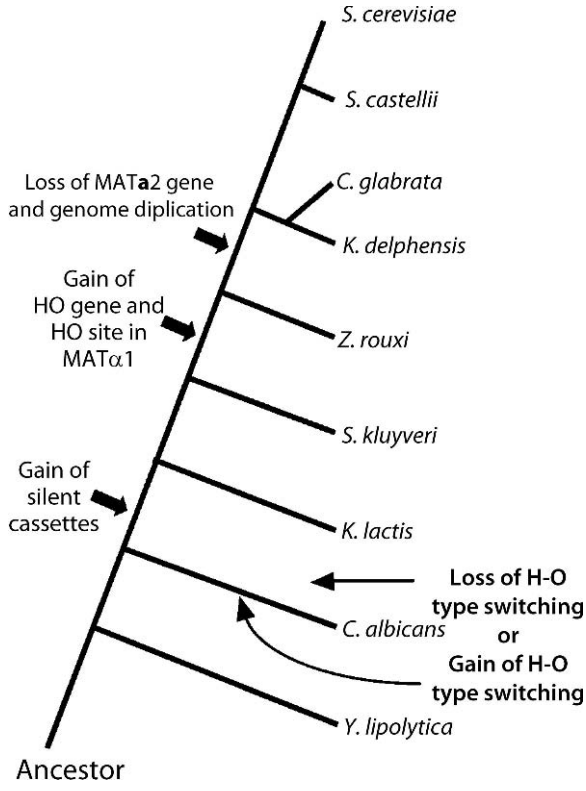

Fig. 8.6. Landmark events in the evolution of *C. albicans*, *C. glabrata* and *S. cerevisiae*. Adapted from Fig. 4 of Butler et al. (2004) and Fig. 6 of Tsong et al. (2003), with the addition of the acquisition or loss of white–opaque switching

this context, it would be interesting to find out if *Yarrowia lipolytica*, which emerged earlier from the lineage than *C. albicans*, undergoes white–opaque switching or possesses orthologs of the *C. albicans* opaque-specific gene *OP4* or the white-specific gene *WH11*.

Because neither mating nor a diploid *C. glabrata* strain has been identified, it is more difficult to assess the functions of the mating-type genes. Srikantha et al. (2003) performed a Northern analysis of *MTL*α1 and *MTL***a**1 and demonstrated that the former was expressed only in cells that were α at the *MTL1* locus and that the latter was expressed only in cells that were **a** at the *MTL1* locus. Given the similarities between the mating loci and the observations that *C. glabrata* like *S. cerevisiae* undergoes mating-type switching, it seems likely that the functional roles of the mating-type genes in the regulation of cell type-specific gene expression and mating will also be similar.

XI. The Mating System of *Candida dubliniensis*

Candida dubliniensis is a close relative of *C. albicans* that was considered in the 1990s a group of atypical strains of the latter species (Odds et al. 1990; Pujol et al. 1997). However, in the mid- to late-1990s, Coleman, Sullivan and co-workers collected a variety of evidence that indicated these strains were in fact members of an independent species closely related to *C. albicans* (Sullivan et al. 1995, 1997; Sullivan and Coleman 1998; Coleman et al. 1997). The genetic data included hybridization with complex DNA fingerprinting probes (Sullivan et al. 1995, 1997; Joly et al. 1999; Odds et al. 1990), hybridization with microsatellite DNA sequences (Sullivan et al. 1993, 1995) and ribosomal DNA sequencing (Sullivan et al. 1995). Perhaps the strongest indication that *C. dubliniensis* evolved as an independent species is the presence of a dispersed mid-repeat sequence that is not present in *C. albicans*, which was utilized as a fingerprinting tool for *C. dubliniensis* (Joly et al. 1999). The closeness of *C. dubliniensis* and *C. albicans*, however, was revealed by the presence of the complex mid-repeat sequence RPS in both species (Joly et al. 2002). Pujol et al. (2004) demonstrated a high level of similarity in the organization of the *MTL*α locus of *C. dubliniensis* and *C. albicans*. A comparison of the *MTL***a** locus from the nucleotide sequences and deduced amino acid sequences provided by the Wellcome Trust Sanger Institute revealed a high level of similarity between the two species (Pujol et al. 2004). Pujol et al. (2004) also demonstrated that, in nature, there are **a**/α, **a**/**a** and α/α strains of *C. dubliniensis*. Of 82 natural strains analyzed, 67% were **a**/α, 21% **a**/**a** and 12% α/α. By DNA fingerprinting with the complex probe Cd25 (Joly et al. 1999), the 82 natural strains separated into two groups, Group I and Group II. Interestingly, while 43% of Group I isolates (N = 61) were **a**/**a** or α/α, only 5% of Group II isolates (N = 21) were **a**/**a** or α/α. The Group II isolates represented a far less inter-related group. Therefore, in nature, the proportion of *MTL*-homozygous isolates was 33%, more than three-fold higher than that of *C. albicans*. The difference probably was due to the increase in genomic instability that was observed in *C. dubliniensis*. *C. dubliniensis* was demonstrated to undergo genomic reorganization which could result in frequent changes in karyotype (Joly et al. 2002), frequent recombinational events at the RPS locus (Joly et al. 2002) and, presumably, high frequency *MTL*-homozygosis (Pujol et al. 2004). Pujol et al. (2004), using microscopically identified fusions as an assay, demonstrated that natural *C. dubliniensis* **a**/**a** and α/α strains readily underwent mating in a cell type-dependent fashion. They demonstrated that *C. dubliniensis* mating included a sequence of cytological events, including nuclear dynamics similar to those of *C. albicans*.

Because the mating system of *C. dubliniensis* was so similar to that of *C. albicans*, Pujol et al. (2004) tested whether the two closely related species could mate. They found that they did, and in a cell type-dependent fashion, at high frequency. One must therefore wonder how these two species have not mixed genetically, given that they colonize and co-colonize the same repertoire of individuals, in particular HIV-positive individuals (Sullivan et al. 1993, 1995, 1997; Coleman et al. 1997; Sullivan and Coleman 1998). DNA fingerprinting studies of isolates from HIV-positive individuals, however, did not indicate the existence of such hybrid species (Odds et al. 1990; Joly et al. 1999), although one could argue that such hybrids were not directly tested for. Mating was also observed between the *Saccharomyces* species *S. cerevisiae* and *S. paradoxus* (Greig et al. 2002). Greig et al. (2002) showed that hybrids are self-fertile, but exhibit lower fertility when back-crossed to either parent. They argued that such hybrids could lead

to new species and that such homoploid hybrid speciation was relatively unique to *Saccharomyces*. Maybe an analogous phenomenon occurs among closely related *Candida* species.

XII. Pheromone and the Cytological Pheromone Response

In 2003, several laboratories simultaneously identified an ortholog of the *S. cerevisiae* mating factor gene, *MF*α1, in the emerging *C. albicans* genome sequence data base (Bennett et al. 2003; Lockhart et al. 2003b; Panwar et al. 2003). No ortholog of the mating factor gene *MF***a** was identified. Both Bennett et al. (2003) and Panwar et al. (2003) constructed *mf*α*1* mutants and found that null mutants that were *MTL*α were incapable of mating. In contrast, null mutants that were *MTL***a** were capable of mating. All three studies revealed that the chemically synthesized 13-mer or 14-mer α-pheromone peptide induced shmooing in **a** cells (Fig. 8.7A). Addition of the 13-mer peptide elicited a stronger response than the 14-mer and is the synthetic pheromone of choice for in vitro studies. Although the **a**-pheromone gene has not yet been identified, Lockhart et al. (2003a) observed that vitally stained α/α cells shmooed when mixed with **a/a** cells, indicating that a potent **a**-pheromone was released by **a/a** cells.

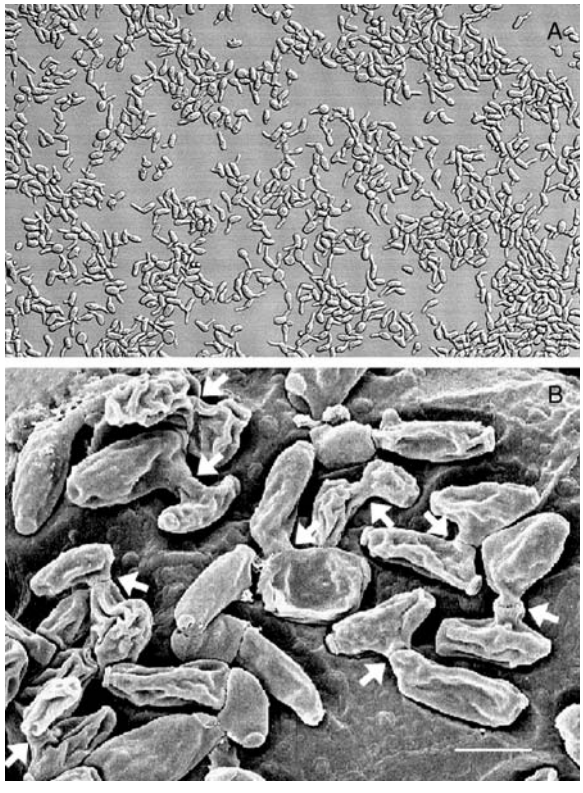

Fig. 8.7. The induction of shmooing by α-pheromone in **a/a** cells derived from saturation phase cultures (**A**); and high-frequency mating between **a/a** and α/α cells on baby mouse skin (**B**). See Zhao et al. (2005) for panel **A** and Lachke et al. (2003) for panel **B**

Pheromone caused opaque cells to polarize, shmoo and extend a conjugation tube, as it does in *S. cerevisiae*. However, the unique shape of opaque cells (Anderson and Soll 1987; Slutsky et al. 1987) appeared to put some restrains on shmooing. General pheromone induction caused conjugation tube evagination at one end of an opaque cell at an angle to the long cell axis, similar to the angle of opaque cell bud formation (Slutsky et al. 1987). In a significant minority of cases the evagination formed along the flank of the elongate cell, which is a rare position for a bud, suggesting dissimilarity. If opaque **a/a** or **a/**– cells were treated with α-pheromone for extended periods of time, in some cases by the re-addition of fresh pheromone at time intervals, the conjugation tubes grew to lengths equivalent to many cell diameters (Bennett et al. 2003; Daniels et al. 2003; Lockhart et al. 2003a; Zhao et al. 2005). Although these tubes were sometimes shaped roughly like true hyphae, they did not compartmentalize through the formation of intermittent septae and the mother cell nucleus did not migrate into the tube and divide. Such conjugation tubes eventually reverted apically to the budding growth form (i.e., a bud formed at the tip of the tube). In these cases, the apical bud received a daughter nucleus and separated from the tube by septation. When reversion occurred at the apex of a long tube, the nucleus migrated into the tube to divide.

C. glabrata also contains an ortholog of the *S. cerevisiae MF*α2 gene, but no recognizable ortholog of the *S. cerevisiae MF***a** gene (Wong et al. 2003; T. Srikantha and D.R. Soll, unpublished data). Since *C. glabrata* contains an ortholog of *S. cerevisiae STE6*, which functions as an exporter of **a**-pheromone, Wu et al. (2005) argued that an *MF***a** gene most probably exists. However, because **a**-pheromone is encoded by an ORF significantly smaller than the α-pheromone ORF in *S. cerevisiae*, it is more difficult to identify the coding region in the genome data base. Rudimentary attempts to stimulate shmoo formation in *C. glabrata* **a** cells by the addition of synthetic α-factor or by mixing **a**

and α cells, have failed (T. Srikantha and D.R. Soll, unpublished data). More work is obviously needed to search for conditions that permit a pheromone response.

XIII. The Pheromone Response Pathway in *C. albicans* Opaque Cells

Given the homologies between *C. albicans* and *S. cerevisiae* for three of the *MTL* genes (Hull and Johnson 1999), it seemed reasonable to expect the signal transduction pathway involved in the pheromone response in *C. albicans* would be similar to that of *S. cerevisiae*. In *S. cerevisiae*, the **a**-or α-pheromone receptor interacts with a trimeric G protein complex (Thorner 2006). Receptor occupancy leads to dissociation of the β from the δ subunit and activation of *STE20*, leading to the activation of a MAP kinase cascade that activates *STE12*, which mediates mating-associated gene transcription, and *FAR1*, which mediates G1 arrest, polarization and shmooing (i.e., conjugation tube evagination). To test whether the pheromone response in *C. albicans* was regulated similarly, Magee et al. (2002) and Chen et al. (2002) analyzed the mating capabilities of null mutants of the *C. albicans* homologs to select genes in the *S. cerevisiae* pathway. As a mating assay, both groups used complementation of auxotrophic markers carried by the **a** and α strains used in the mating mixtures. After generating auxotrophic mutants in **a**/α cells, Magee et al. (2002) generated *MTL*-homozygous derivatives by growth on minimal medium containing sorbose. They found that deletion of *CST20*, the homolog of *S. cerevisiae STE20*, did not affect mating. In *S. cerevisiae*, deletion of *STE20* caused a decrease, but not a block, in mating (Leberer et al. 1996). Deletion of *HST7*, the homolog of *S. cerevisiae STE7*, a MAP kinase, resulted in the loss of mating in both *MTL***a** and *MTL*α cells. And deletion of *CPH1*, the homolog of *S. cerevisiae STE12*, resulted in the loss of mating in both *MTL***a** and *MTL*α cells. Chen et al. (2002) also found that deletion of *CPH1* and *HST7* resulted in a loss of mating and that deletion of *CST20* resulted in a reduction in the frequency of mating. They also found that a double deletion mutant of *CEK1*, the homolog of *S. cerevisiae KSS1*, a MAP kinase, and *CEK2*, a homolog of *S. cerevisiae FUS3*, a MAP kinase that is apparently redundant to *CEK1* in *C. albicans*, resulted in a loss of mating. Chen et al. (2002) further demonstrated that overexpression of *CPH1* in an *MTL***a** background induced expression of genes up-regulated by pheromone in *S. cerevisiae*. Together, these results demonstrated that the pheromone signal in *C. albicans* is transduced through a protein kinase pathway similar to that in *S. cerevisiae*. However, it was not demonstrated that the downstream activation of the *FAR1* homolog regulates the G1 block and polarization in the shmooing process, as it does in *S. cerevisiae*, although it seems likely that it does.

XIV. Pheromone and G1 in *C. albicans* Mating

In *S. cerevisiae*, pheromone blocks cells of the opposite mating type in G1 through the action of *FAR1*, a cyclin-dependent inhibitor of protein kinase (Roberts et al. 2000). While it was initially reported that α-factor did not inhibit cell proliferation by the halo assay (Bennett et al. 2003), Zhao et al. (2005) subsequently performed a kinetic analysis of budding and shmoo formation in mating mixtures of **a**/**a** and α/α cells derived from either exponential or saturation phase cultures. They also quantitated the DNA content of individual nuclei in shmooing and budding cells. Their results indicated that cells, whether in exponential or saturation phase, had simply to be in G1 to respond to pheromone by forming a shmoo and that the response included G1 arrest. Their results also explained why saturation phase cells, which accumulate in G1, are more responsive than exponential phase cells. While roughly 20–40% of cells from exponential phase growth cultures shmoo when treated with pheromone, well over 90% of cells from saturation phase cultures shmoo when treated (Fig. 8.7A; Zhao et al. 2005). Presumably, nuclear fusion after mating fusion occurs between nuclei in G1, and division of the tetraploid nucleus must occur after DNA replication. Either fusion of opposing conjugation tubes releases cells from G1 arrest, or the pheromone block is alleviated by hydrolysis of extracellular pheromone.

In the case of *C. glabrata*, initial attempts to obtain a pheromone response (i.e., shmooing) in mixtures of natural **a** and α strains and in cell cultures treated with two versions of synthetic peptides were unsuccessful (T. Srikantha, K. Daniels,

S. Lachke and D.R. Soll, unpublished data), but were too limited in scope to make firm conclusions.

XV. Pheromone-Dependent Gene Expression in *C. albicans* Opaque Cells

Bennett et al. (2003) analyzed the transcriptional response of opaque **a** cells using a microarray that contained ~11 000 ORFs generated by PCR amplification of sequences based on the Stanford *C. albicans* genome sequence project. They tentatively identified 62 genes up-regulated and four down-regulated by α-pheromone. Fifteen of the up-regulated genes were also up-regulated in *S. cerevisiae*, including the α-receptor gene *STE2*, and genes involved in the MAP kinase pathway, karyogamy, pheromone adaptation, pheromone processing and pheromone export. Bennett et al. (2003) also identified several genes involved in mating that were up-regulated in *C. albicans*, but not in *S. cerevisiae*, including *RAM1*, *RAM2* and *KAR9*. They identified a number of up-regulated genes that were not up-regulated by pheromone in *S. cerevisiae*. Most of these latter genes have not been implicated in mating. Most noteworthy in this category were select filamentation-related genes. Lockhart et al. (2003b) also analyzed gene expression in opaque **a/a** cells in response to α-pheromone by Northern blot hybridization. They also found that the mating-related genes *CAG1*, *STE2*, *STE4*, *FIG1* and *KAR4*, and the filamentation-related gene *HWP1*, were up-regulated by α-pheromone. In addition, they found that three of four opaque-specific genes, *OP4*, *SAP1* and *SAP3*, were down-regulated by α-pheromone. The opaque-specific gene *CDR3* was not similarly down-regulated.

Zhao et al. (2005) subsequently used an oligonucleotide-based microarray to analyze gene expression during mating between natural **a/a** and α/α cells. They identified 56 genes that were up-regulated and 30 that were down-regulated in mating mixtures. They also verified gene expression in mating mixtures by Northern analysis. In addition to many of the mating-associated genes identified as up-regulated by α-pheromone, Zhao et al. (2005) identified *MF*α1, which encodes the α-pheromone, *RCE1*, an ortholog of an *S. cerevisiae* CaaX prenyl proteinase involved in α-pheromone maturation, and *MPT5*, an ortholog of an *S. cerevisiae* gene involved in re-entry into the mitotic cycle. By Northern analysis they found that neither *CST20* nor *FAR1* were constitutively expressed. In addition to the filamentation-associated genes identified by Bennett et al. (2003) as up-regulated, Zhao et al. (2005) identified a number of additional filamentation-associated genes that were up-regulated. Zhao et al. (2005) also identified a gene that was down-regulated during filamentation, *YWP1*, which was also down-regulated in mating mixtures. Furthermore, they found that the white-specific or enriched genes *WH11*, *EFG1* and *TEC1*, were not up-regulated by pheromone when opaque-specific genes were down-regulated, indicating that the down-regulation of opaque-specific genes by α-pheromone was not a result of α-pheromone-induced phenotypic switching. Finally, Zhao et al. (2005) identified a new class of genes that were expressed in the exponential phase of growth, down-regulated when cells entered saturation phase, and up-regulated in response to α-pheromone. The reason for this peculiar regulation pattern is not obvious.

In *S. cerevisiae*, Roberts et al. (2000) demonstrated by microarray analysis that 200 genes were repressed in **a** cells in response to α-pheromone, in most cases as a result of the G1 block. Bennett et al. (2003) did not identify similar down-regulation of a large number of genes in α-pheromone-treated *C. albicans* **a/a** cells, but pointed out that they did not obtain a G1 arrest upon pheromone treatment. This could be due to low levels of shmooing resulting from the use of exponential phase cells, as expected in light of the results of Zhao et al. (2005).Employing saturation phase cells that had accumulated in G1, Zhao et al. (2005) observed down-regulation of 30 genes in mating mixtures, which was more in line with the *S. cerevisiae* results of Roberts et al. (2000).

XVI. The Temperature Sensitivity of *C. albicans* Opaque Cells and Mating on Skin

The discovery that the opaque phenotype was exclusively mating-competent created a paradox. Since *C. albicans* is an opportunistic pathogen that is carried as a commensal in healthy hosts, one might expect mating to occur in the host under the constraints of host–pathogen interactions. But Slutsky et al. (1987), in their initial paper on the

discovery of the white–opaque transition, reported that the opaque phenotype converted to the white phenotype at 37 °C; and a number of subsequent studies verified this observation (Rikkerink et al. 1988; Srikantha and Soll 1993; Soll 2003). Srikantha et al. (1998) further demonstrated that, when the temperature of an opaque culture was raised from 25 °C to greater than 37 °C, cells committed to the white phase after two cell divisions, suggesting an imprinting event (Soll 2003). So how could mating be limited to the opaque phenotype and occur in the host when that phenotype is unstable at physiological temperature? Observations by Kvaal et al. (1999) provided a plausible explanation. They found that opaque cells readily colonized the skin of newborn mice, but white cells did not. The skin temperature of a newborn mouse is 32 °C, a temperature which supports the opaque phenotype. Based on this observation, Lachke et al. (2003) tested whether skin facilitated mating. They found that mixtures of opaque **a/a** and α/α cells underwent shmooing and fusion at high frequency on skin (Fig. 8.7B). In some microscopic fields, over 50% of cells fused. This discovery seemed to provide an explanation for the opaque phenotype, namely that it represented a specialized phenotype for colonizing skin and that skin was, therefore, the mating niche. But this explanation was not completely satisfying. Why would mating be restricted to a very minor site of colonization of the host (Odds 1988)? Moreover, Lachke et al. (2003) observed that, while fusion occurred frequently on skin (i.e., **a/a** and α/α cells readily fused), it rarely culminated in the formation of the first daughter bud. Could it be that **a/a** and α/α cells fused on skin and then had to move to a second body location to complete the mating process? Although plausible, the story was just not that convincing. As we see below, recent observations provide an alternative scenario for the role of the white–opaque transition in mating.

XVII. Pheromone-Regulated Gene Expression in *C. albicans* White Cells

Miller and Johnson (2002) demonstrated that the mating process depended on a switch of both mating types from white to opaque, and Lockhart et al. (2003a) generalized this observation to natural strains. In both studies, it was demonstrated that opaque cells, not white cells, released pheromone and that opaque cells, not white cells, responded to pheromone. It was therefore concluded that opaque cells were exclusively mating-competent and that the *MTL*-homozygous white phenotype was only a transient phenotype spanning the **a/α** "white" to *MTL*-homozygous opaque phenotype. For this reason, when Bennett et al. (2003), Lockhart et al. (2003b) and Zhao et al. (2005) developed transcription profiles of cells treated with pheromone, they employed only opaque cells. Why? Their obvious rationale was based on the fact that only opaque cells responded to pheromone. However, Lockhart et al. (2003b) used α-pheromone-treated white cells as a presumed negative control in their northern analysis of pheromone-induced changes in gene expression. Quite surprisingly, they found that pheromone selectively up-regulated three mating-associated genes in white cells, *CAG1*, *STE4* and *STE2*, just as it did in opaque cells. They found, however, that pheromone-induced up-regulation was selective when compared with the response of opaque cells. α-Pheromone did not similarly up-regulate *FIG1*, *KAR4* or *HWP1* in white cells. In verifying these enigmatic results, Daniels et al. (2006) expanded the list of mating-associated genes that were up-regulated by α-pheromone in white **a/a** cells to include the mating-associated genes, *CEK2* and *SST2*, and added the filamentation-associated genes *RBT1*, *RBT4*, *FGR23* and *CEK1*. They further demonstrated that white **a/a** cells, like opaque **a/a** cells, expressed α-pheromone receptors on their surface (Fig. 8.8A, B, respectively; Daniels et al. 2006). However, the receptors were evenly distributed across the white cell surface (Fig. 8.8A), but clustered at focal points on the opaque cell surface, suggesting localization at opaque cell pimples (Fig. 8.8B). When treated with pheromone, the receptors on both white cells and opaque cells were down-regulated (Fig. 8.8C, D, respectively) but redistribution differed. After down-regulation in white cells, the receptors did not reappear (Fig. 8.8C), whereas in opaque cells, receptors relocalized to the point of conjugation tube evagination in the process of polarization (Fig. 8.8D), as they did in *S. cerevisiae* (Schandel and Jenness 1994; Stefan and Blumer 1999). These results were truly enigmatic. If white cells were mating-incompetent, why did they possess receptors, why did pheromone treatment down-regulated these receptors, and why did pheromone selectively up-regulate mating-associated genes?

XVIII. Pheromone Induces *C. albicans* *MTL*-Homozygous White Cells to Become Highly Cohesive and Form Biofilms

Daniels et al. (2006) speculated on the possible reason why opaque cells might signal white cells. They took into account the observations that: (1) switching to opaque occurred at low frequency at the site of colonization in natural strains that underwent switching (Soll et al. 1987) and were, therefore, presumably *MTL*-homozygous and (2) *C. albicans* has incorporated into its mating program at least a portion of the filamentation program so that conjugation tubes could grow to unusually long lengths (Bennett et al. 2003; Daniels et al. 2003; Zhao et al. 2005). They speculated that in overlapping white **a/a** and α/α populations colonizing the same host niche, a switch to opaque in each overlapping population would be a rare event. For conjugation tubes formed by a rare opaque **a/a** cell and opaque α/α cell to find each other in order to fuse apically, they would have to migrate over long distances. To find each other, the different conjugation tubes would have to assess the gradient of chemoattractant emanating from the opaque cell of opposite mating type. Daniels et al. (2006) reasoned that if the gradients of attractant were soluble, they would dissipate by diffusion and be prone to mechanical destabilization and disruption, given the distances and extended times that would be necessary for chemotropism. Hence, they hypothesized that opaque cells might signal white cells through the release of chemoattractant to form a biofilm that would suppress diffusion and mechanical disruption. They tested several aspects of this hypothesis. First, they demonstrated that α-pheromone induced white **a/a** but not opaque **a/a** cells to become highly cohesive and to form tightly packed monolayers on a substratum. α-Pheromone did not induce a similar response in opaque **a/a** cells (Fig. 8.8E–G). They demonstrated this to be the case for **a**-pheromone induction of white α/α cells as well. Daniels et al. (2006) further demonstrated that as little as 1% opaque cells in a white cell population forming a biofilm stimulated a doubling of biofilm thickness. Finally, they demonstrated that the 3D mature biofilm facilitated chemotropism. The results of Daniels et al. (2006) suggested that the *C. albicans* switching-mating system impacted pathogenesis. The signaling of mating-incompetent white cells by mating competent opaque cells through the release of pheromone was unique among the pathogenic yeast and reminiscent of the inductive events between sex cells and somatic cells in higher eukaryotes. Daniels et al. (2006) suggested that this newly discovered interaction between a mating-competent and mating-incompetent cell that results in the induction of a tissue (biofilm) may represent the ancestral pro-

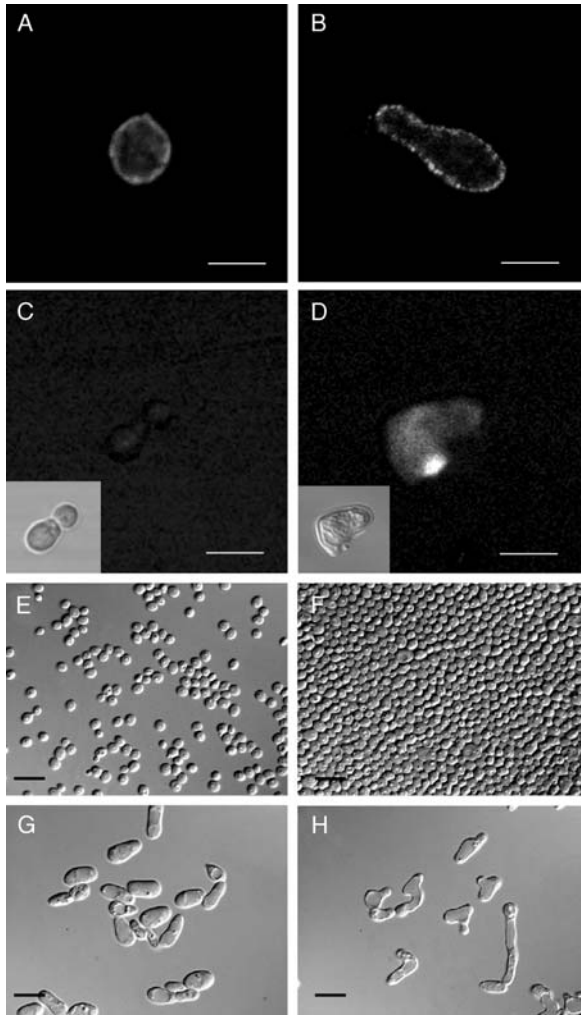

Fig. 8.8. White **a/a** cells possess α-pheromone receptors and respond to α-pheromone by becoming cohesive and forming a biofilm. **A** Staining of α-pheromone receptors on **a/a** white cells. **B** Staining of α-pheromone receptors on **a/a** cells. **C** When white **a/a** cells are treated with α-pheromone, α-pheromone receptors are down-regulated and not relocalized. **D** When opaque **a/a** cells are treated with α-pheromone, α-pheromone receptors are down-regulated and then relocalized to shmoo evagination. **E** Untreated **a/a** white cells are not cohesive. **F** **a/a** white cells treated with α-pheromone become cohesive. **G** Untreated **a/a** opaque cells are not cohesive. **H** α-Pheromone-treated **a/a** opaque cells are not cohesive. See Daniels et al. (2006)

cess in the evolution of higher eukaryotic multicellularity.

XIX. Conclusion: Why Should We Concern Ourselves with *Candida* Mating?

This is not a trivial question. *C. albicans* and *C. glabrata* were considered asexual until quite recently, the former until 1999 and the latter until 2003. In the case of *C. albicans*, the discovery of the mating locus was followed by a number of additional discoveries, most notably a number of characteristics of the *C. albicans* mating system that were unique. These included the discoveries that the Mtl**a**2p was a positive regulator of **a**-specific genes, that the **a**1-α2 complex suppressed switching as well as mating, and that a *MTL*-homozygous cell had to switch from white to opaque to mate. However, studies of the population structure of both *C. albicans* and *C. glabrata* suggested that reproduction was primarily clonal, relegating mating to a rare event for long-term maintenance of the species. Since the primary concern we now have with *C. albicans* is its pathogenesis, why concern ourselves with a rare event that may save the species every million years, but does not play an immediate role in pathogenesis? It may be because of that perception that the number of papers related to *C. albicans* mating has begun to flatten out. The discovery, however, that opaque cells signal white cells and that the outcome of that signaling may be the formation or enhancement of biofilm formation, which is a fundamental virulence factor, may push *C. albicans* mating on stage once again. If mating proves to play a role in pathogenesis, then selective forces – that are related not only to the mating process per se, but to its role in pathogenesis as well – may function to maintain and modify the mating process. This could explain the large proportion of genes that are regulated by the switching-mating process. Although far less attention has been paid to the mating process of *C. glabrata*, it would not be surprising to find that it may also be intimately involved in virulence.

Acknowledgements. The author thanks Dr. K. Daniels for generating figures, Ms. J. Collins for assembling the manuscript, Dr. T. Srikantha for several useful suggestions, and NIH grants AI2392 and DEO14219 for support.

References

Anderson J, Cundiff L, Schnars B, Gao M, Mackenzie I, Soll DR (1989) Hypha formation in the white–opaque transition of *Candida albicans*. Infect Immun 57:458–467

Anderson J, Mihalik R, Soll DR (1990) Ultrastructure and antigenicity of the unique cell wall pimple of the *Candida* opaque phenotype. J Bacteriol 172:224–235

Anderson JB, Wickens C, Khan M, Cowen LE, Federspiel N, Jones T, Kohn LM (2001) Infrequent genetic exchange and recombination in the mitochondrial genome of *Candida albicans*. J Bacteriol 183:865–872

Anderson JM, Soll DR (1987) Unique phenotype of opaque cells in the white–opaque transition of *Candida albicans*. J Bacteriol 169:5579–5588

Arkowitz RA (1999) Responding to attraction: chemotaxis and chemotropism in *Dictyostelium* and yeast. Trends Cell Biol 9:20–27

Astrom SU, Kegel A, Sjostran JO, Rine J (2000) *Kluyveromyces lactis* Sir2p regulates cation sensitivity and maintains a specialized chromatin structure at the cryptic alpha-locus. Genetics 156:81–91

Barns SM, Lane DJ, Sogin ML, Bibeau C, Weisburg WG (1991) Evolutionary relationships among pathogenic *Candida* species and relatives. J Bacteriol 173:2250–2255

Bennett RJ, Johnson AD (2003) Completion of a parasexual cycle in *Candida albicans* by induced chromosome loss in tetraploid strains. EMBO J 22:2505–2515

Bennett RJ, Johnson AD (2005) Mating in *Candida albicans* and the search for a sexual cycle. Annu Rev Microbiol 59:233–255

Bennett RJ, Uhl MA, Miller MG, Johnson AD (2003) Identification and characterization of a *Candida albicans* mating pheromone. Mol Cell Biol 23:8189–8201

Bennett RJ, Miller MG, Chua PR, Maxon ME, Johnson AD (2005) Nuclear fusion occurs during mating in *Candida albicans* and is dependent on the *KAR3* gene. Mol Microbiol 55:1046–1059

Blignaut E, Pujol C, Lockhart S, Joly S, Soll DR (2002) Ca3 fingerprinting of *Candida albicans* isolates from human immunodeficiency virus-positive individuals reveals a new clade in South Africa. J Clin Microbiol 40:826–836

Brockert PJ, Lachke SA, Srikantha T, Pujol C, Galask R, Soll DR (2003) Phenotypic switching and mating type switching of *Candida glabrata* at sites of colonization. Infect Immun 12:7109–7118

Butler G, Kenny C, Fagan A, Kurischko C, Gaillardin C, Wolfe KH (2004) Evolution of the *MAT* locus and its HO endonuclease in yeast species. Proc Natl Acad Sci USA 101:1632–1637

Calderone RA (2002) *Candida* and candidiasis. ASM, Washington, D.C.

Chen J, Chen J, Lane S, Liu H (2002) A conserved mitogen-activated protein kinase pathway is required for mating in *Candida albicans*. Mol Microbiol 46:1335–1344

Chen X, Magee BB, Dawson D, Magee PT, Kumamoto CA (2003) Chromosome 1 trisomy compromises the virulence of *Candida albicans*. Mol Microbiol 51:551–565

Coleman DC, Sullivan DJ, Bennett DE, Moran GP, Barry HJ, Shanley DB (1997) Candidiasis: the emergence of a novel species *Candida dubliniensis*. AIDS 11:557–567

Coppin E, Debuchy R, Arnaise S, Picard M (1997) Mating types and sexual development in filamentous ascomycetes. Microbiol Mol Biol Rev 61:411–428

Daniels KJ, Lockhart SR, Sundstrum P, Soll DR (2003) During *Candida albicans* mating, the adhesin Hwp1 and the first daughter bud localize to the a/a portion of the conjugation bridge. Mol Biol Cell 14:4920–4930

Daniels KJ, Srikantha T, Lockhart SR, Pujol C, Soll DR (2006) Opaque cells signal white cells to form biofilms in *Candida albicans*. EMBO J 25:2240–2252

Debuchy R, Arnaise S, Lecellier G (1993) The mat- allele of *Podospora anserina* contains three regulatory genes required for the development of fertilized female organs. Mol Gen Genet 241:667–673

Dodgson AR, Pujol C, Pfaller MA, Denning DW, Soll DR (2005) Evidence for recombination in *Candida glabrata*. Fungal Genet Biol 42:233–243

Dujon B, Sherman D, Fischer G, Durrens P, Casaregole S, Lafontaine I, De Montigny J, Marck C, Neuveglise C, Talla E, Goffard N, Frangeul L, Aigle M, Anthouard V, Babour A, Barbe V, Barnay S, Blanchin S, Beckerich JM, Beyne E, Bleykasten C, Boisrame A, Boyer J, Cattolico L, Confanioleri F, de Daruvar A, Despons L, Fabre E, Fairhead C, Ferry-Dumazet H, Groppi A, Hantraye F, Hennequin C, Jauniaux N, Joyet P, Kachouri R, Kerrest A, Koszul R, Lemaire M, Lesur I, Ma L, Muller H, Nicaud JM, Nikolski M, Oztas S, Ozier-Kalogeropoulos O, Pellenz S, Potier S, Richard GF, Straub ML, Suleau A, Swennen D, Tekaia F, Wesolowski-Louvel M, Westhof E, Wirth B, Zeniou-Meyer M, Zivanovic I, Bolotin-Fukuhara M, Thierry A, Bouchier C, Caudron B, Scarpelli C, Gaillardin C, Weissenbach J, Wincker P, Souciet JL (2004) Genome evolution in yeasts. Nature 430:35–44

Esperito RE (2006) Meiosis and spore development. In: Linder P, Shore D, Hall MN (eds) Landmark papers in yeast biology. Cold Spring Harbor Laboratory, Cold Spring Harbor, pp 157–192

Fonzi WA, Irwin MY (1993) Isogenic strain construction and gene mapping in *Candida albicans*. Genetics 134:717–728

Gräser Y, Volovsek M, Arrington J, Schönian G, Presber W, Mitchell TG, Vilgalys R (1996) Molecular markers reveal that population structure of the human pathogen *Candida albicans* exhibits both clonality and recombination. Proc Natl Acad Sci USA 93:12473–12477

Greig D, Louis EJ, Borts RH, Travisan M (2002) Hybrid speciation in experimental populations of yeast. Science 298:1773–1775

Hube B, Monod M, Schofield D, Brown A, Gow N (1994) Expression of seven members of the gene family encoding aspartyl proteinases in *Candida albicans*. Mol Microbiol 14:87–99

Hull CM, Johnson AD (1999) Identification of a mating type-like locus in the asexual pathogenic yeast *Candida albicans*. Science 285:1271–1275

Hull CM, Raisner RM, Johnson AD (2000) Evidence for mating of the "asexual" yeast *Candida albicans* in a mammalian host. Science 289:307–310

Ibrahim AS, Magee BB, Sheppard DC, Yang M, Kauffman S, Becker J, Edwards JE Jr, Magee PT (2005) Effects of ploidy and mating type on virulence of *Candida albicans*. Infect Immun 73:7366–7374

Janbon G, Sherman F, Rustcheko E (1999) Appearance and properties of L-sorbose-utilizing mutants of *Candida albicans* obtained on a selective plate. Genetics 153:653–664

Joly S, Pujol C, Rysz M, Vargas K, Soll DR (1999) Development and characterization of complex DNA fingerprinting probes for the infectious yeast *Candida dubliniensis*. J Clin Microbiol 34:1035–1044

Joly S, Pujol D, Soll DR (2002) Microevolutionary changes and chromosomal translocations are far more frequent at RPS loci in *Candida dubliniensis* than in *Candida albicans*. Infect Genet Evol 2:19–37

Kaur R, Domergue R, Zupancic ML, Cormack BP (2005) A yeast by any other name: *Candida glabrata* and its interaction with the host. Curr Opin Microbiol 8:1–7

Kolitila MP, Diamond RD (1990) Effects of neutrophils and in vitro oxidants on survival and phenotypic switching of *Candida albicans* WO-1. Infect Immun 58:1174–1179

Kvaal C, Srikantha T, Soll DR (1997) Misexpression of the white phase-specific gene *WH11* in the opaque phase of *Candida albicans* affects switching and virulence. Infect Immun 65:4468–4475

Kvaal C, Lachke SA, Srikantha T, Daniels K, McCoy J, Soll DR (1999) Misexpression of the opaque phase-specific gene *PEP1* (*SAP1*) in the white phase of *Candida albicans* confers increased virulence in a mouse model of cutaneous infection. Infect Immun 67:6652–6662

Lachke SA, Srikantha T, Tsai L, Daniels K, Soll DR (2000) Phenotypic switching in *Candida glabrata* involves phase-specific regulation of the metallotheionein gene *MT-II* and the newly discovered hemolysin gene *HLP*. Infect Immun 68:884–895

Lachke SA, Joly S, Daniels K, Soll DR (2002) Phenotypic switching and filamentation in *Candida glabrata*. Microbiology 148:2661–2674

Lachke SA, Lockhart SR, Daniels KJ, Soll DR (2003) Skin facilitates *Candida albicans* mating. Infect Immun 71:4970–4976

Lan C, Newport G, Murillo LA, Jones T, Scherer S, Davis RW, Agabian N (2002) Metabolic specialization associated with phenotypic switching in *Candida albicans*. Proc Natl Acad Sci USA 99:14907–14912

Leberer E, Harcus D, Broadbent ID, Clark KL, Dignard D, Ziegelbauer K, Schmidt A, Gow NAR, Brown AJP, Thomas DY (1996) Signal transduction through homologs of the Ste20p and Ste7p protein kinases can trigger hyphal formation in the pathogenic fungus *Candida albicans*. Proc Natl Acad Sci USA 93:13217–13222

Legrand M, Lephart P, Forsche A, Mueller F-MC, Walsh T, Magee PT, Magee BB (2004) Homozygosity at the *MTL* locus in clinical strains of *Candida albicans*: karyotypic rearrangements and tetraploid formation. Mol Microbiol 52:1451–1462

Lockhart SR, Pujol C, Daniels K, Miller M, Johnson A, Soll DR (2002) In *Candida albicans*, white–opaque switchers are homozygous for mating type. Genetics 162:737–745

Lockhart SR, Daniels KJ, Zhao R, Wessels D, Soll DR (2003a) Cell biology of mating in *Candida albicans*. Eukaryot Cell 2:49–61

Lockhart SR, Zhao R, Daniels KJ, Soll DR (2003b) α-Pheromone-induced shmooing and gene regulation require white–opaque switching during *Candida albicans* mating. Eukaryot Cell 2:847–855

Lockhart SR, Wu W, Radke J, Soll DR (2005) Increased virulence and competitive advantage of **a**/α over **a**/**a** or α/α offspring conserves the mating system of *Candida albicans*. Genetics 169:1883–1890

Magee BB, Magee PT (2000) Induction of mating in *Candida albicans* by construction of MTL**a** and MTLalpha strains. Science 289:310–313

Magee BB, Legrand M, Alarco AM, Raymond M, Magee PT (2002) Many of the genes required for mating in *Saccharomyces cerevisiae* are also required for mating in *Candida albicans*. Mol Microbiol 46:1345–1351

Miller MG, Johnson AD (2002) White–opaque switching in *Candida albicans* is controlled by mating-type locus homeodomain proteins and allows efficient mating. Cell 110:293–302

Morrow B, Srikantha T, Soll DR (1992) Transcription of the gene for a pepsinogen, *PEP1*, is regulated by white–opaque switching in *Candida albicans*. Mol Cell Biol 12:2997–3005

Morrow B, Srikantha T, Anderson J, Soll DR (1993) Coordinate regulation of two opaque-specific genes during white–opaque switching in *Candida albicans*. Infect Immun 61:1823–1828

Odds FC (1988) Candida and candidosis, 2nd edn. Bailliere Tindall, London

Odds F, Schmidt J, Soll DR (1990) Epidemiology of *Candida* infections in AIDS. In: Bossche HV (ed) Mycoses in AIDS patients. Plenum, New York, pp 67–74

Panwar SL, Legrand M, Dignard D, Whiteway M, Magee PT (2003) *MF*α*1*, the gene encoding the α mating pheromone of *Candida albicans*. Eukaryot Cell 2:1350–1360

Pendrak ML, Yan SS, Roberts DD (2004) Hemoglobin regulates expression of an activator of mating-type locus α genes in *Candida albicans*. Eukaryot Cell 3:764–775

Pfaller MA, Jones RN, Messer SA, Edmond MB, Wenzel RP, Group SP (1998) National surveillance of nosocomial blood stream infection due to species of *Candida* other than *Candida albicans*: frequency of occurrence and antifungal susceptibility in the SCOPE Program. Diagn Microbiol Infect Dis 30:121–129

Pujol C, Reynes J, Renaud F, Raymond M, Tibayrenc M, Ayala FJ, Janbon F, Mallie M, Bastide JM (1993) The yeast *Candida albicans* has a clonal mode of reproduction in a population of infected human immunodeficiency virus-positive patients. Proc Natl Acad Sci USA 90:9456–9459

Pujol C, Joly S, Lockhart SR, Noel S, Tibayrenc M, Soll DR (1997) Parity among the randomly amplified polymorphic DNA method, multilocus enzyme electrophoresis, and southern blot hybridization with the moderately repetitive DNA probe Ca3 for fingerprinting *Candida albicans*. J Clin Microbiol 35:2348–2358

Pujol C, Pfaller M, Soll DR (2002) Ca3 fingerprinting of *C. albicans* bloodstream isolates from the United States, Canada, South America and Europe reveals a European clade. J Clin Microbiol 40:2729–2740

Pujol C, Messer SA, Pfaller MA, Soll DR (2003) Drug resistance is not directly affected by mating type locus zygosity in *Candida albicans*. Antimicrob Agents Chemother 47:1207–1212

Pujol C, Daniels KJ, Srikantha T, Lockhart SR, Geiger J, Soll DR (2004) The two closely related species *Candida albicans* and *Candida dubliniensis* can mate. Eukaryot Cell 3:1015–1027

Pujol C, Dodgson AR, Soll DR (2005) Population genetics of ascomycetes pathogenic to humans and animals. In press. In: Xu J-P (ed) Evolutionary genetics of fungi. Horizon Scientific, Ipswich, pp 149–188

Rikkerink EH, Magee BB, Magee PT (1988) Opaque-white phenotype transition: a programmed morphological transition in *Candida albicans*. J Bacteriol 170:895–899

Roberts CH, Nelson B, Marton MJ, Stoughton R, Meyer MR, Bennett HA, He YD, Dai H, Walker WL, Hughes TR, Tyers M, Boone C, Friend SH (2000) Signaling and circuitry of multiple MAPK pathways revealed by a matrix of global gene expression profiles. Science 287:873–880

Santos MA, Ueda T, Watanabe K, Tuite MF (1997) The non-standard genetic code of *Candida* spp: an evolving genetic code or a novel mechanism for adaptation? Mol Microbiol 26:423–431

Schandel KA, Jenness DD (1994) Direct evidence for ligand-induced internalization of the yeast α-factor pheromone receptor. Mol Cell Biol 14:7245–7255

Selmecki A, Bergmann S, Berman J (2005) Comparative genome hybridization reveals widespread aneuploidy in *Candida albicans* laboratory strains. Mol Microbiol 55:1553–1265

Slutsky B, Buffo J, Soll DR (1985) High frequency switching of colony morphology in *Candida albicans*. Science 230:666–669

Slutsky B, Staebell M, Anderson J, Risen L, Pfaller M, Soll DR (1987) "White–opaque transition": a second high-frequency switching system in *Candida albicans*. J Bacteriol 169:189–197

Soll DR (1992) High frequency switching in *Candida albicans*. Clin Microbiol Rev 5:183–203

Soll DR (2002) Phenotypic switching. In: Calderone R (ed) *Candida* and candidiasis. ASM, Washington, D.C., pp 123–142

Soll DR (2003) Candida albicans. In: Craig A, Scherf A (eds) Antigenic variation. Academic, London, pp 165–201

Soll DR, Pujol C (2003) DNA fingerprinting *Candida albicans* clades. FEMS Immun Med Microbiol 39:1–7

Soll DR, Langtimm CJ, McDowell J, Hicks J, Galask R (1987) High frequency switching in *Candida* strains isolated from vaginitis patients. J Clin Microbiol 25:1611–1622

Soll DR, Anderson J, Bergen M (1991) The developmental biology of the white–opaque transition in *Candida albicans*. In: Prasad R (ed) *Candida albicans*: cellular and molecular biology. Springer, Berlin Heidelberg New York, pp 20–45

Soll DR, Voss E, Johnson O, Wessels DJ (2000) Three-dimensional reconstruction and motion analysis of living crawling cells. Scanning 22:249–257

Soll DR, Lockhart SR, Pujol C (2003) Laboratory procedures for the epidemiological analysis of microorganisms. In: Murray PR, Baron EJ, Pfaller MA, Tenvver FC, Yoken RH (eds) Manual of clinical microbiology, 8th edn. ASM, Washington, D.C., pp 139–151

Sprague GF (2006) Differentiation: mating and filamentation. In: Linder P, Shsore D, Hall MN (eds) Landmark papers in yeast biology. Cold Spring Harbor Laboratory, Cold Spring Harbor, pp 141–155

Srikantha T, Soll DR (1993) A white-specific gene in the white–opaque switching system of *Candida albicans*. Gene 131:53–60

Srikantha T, Tsai L, Daniels K, Enger L, Highley K, Soll DR (1998) The two-component hybrid kinase regulator *CaNIK1* of *Candida albicans*. Microbiology 144:2715–2729

Srikantha T, Lachke SA, Soll DR (2003) Three mating type-like loci in *Candida glabrata*. Eukaryot Cell 2:328–340

Stefan CJ, Blumer KJ (1999) A syntaxin homolog encoded by *VAM3* mediates down-regulation of a yeast G protein-coupled receptor. J Biol Chem 274:1835–1841

Sullivan D, Coleman D (1998) *Candida dubliniensis*: characteristics and identification. J Clin Microbiol 36:329–334

Sullivan D, Bennett D, Henman M, Harwood P, Flint S, Mulcahy F, Shanley D, Coleman D (1993) Oligonucleotide fingerprinting of isolates of *Candida* species other than *C. albicans* and of atypical *Candida* species from immunodeficiency virus-positive and AIDS patients. J Clin Microbiol 31:2124–2133

Sullivan DJ, Westerneng T, Haynes K, Bennett D, Coleman D (1995) *Candida dubliniensis* sp. nov.: phenotypic and molecular characterization of a novel species associated with oral candidosis in HIV-infected individuals. Microbiology 141:1507–1521

Sullivan DJ, Haynes K, Bille J, Boerlin P, Rodero L, Lloyd S, Henman M, Coleman D (1997) Widespread geographic distribution of oral *Candida dubliniensis* strains in human immunodeficiency virus-infected individuals. J Clin Microbiol 35:960–964

Tavanti A, Davidson AD, Fordyce MJ, Gow NAR, Maiden MCJ, Odds FC (2005) Population structure and properties of *Candida albicans* as determined by multilocus sequence typing. J Clin Microbiol 43:5601–5613

Thorner J (2006) Signal transduction. In: Linder P, Shore D, Hall MN (eds) Landmark papers in yeast biology. CSHL press, Cold Spring Harbor, NY, pp 193–210

Tsong AE, Miller MG, Raisner RM, Johnson AD (2003) Evolution of a combinatorial transcriptional circuit: a case study in yeasts. Cell 115:389–399

Tzung KW, Williams RM, Scherer S, Federspiel N, Jones T, Hansen N, Bivolarevic V, Huizar L, Komp C, Surzycki R, Tamse R, Davis RW, Agabian N (2001) Genomic evidence for a complete sexual cycle in *Candida albicans*. Proc Natl Acad Sci USA 98:3249–3253

Vargas KG, Messer SA, Pfaller MA, Lockhart SR, Stapleton JT, Hellstein J, Soll DR (2000) Elevated phenotypic switching and drug resistance of *Candida albicans* from human immunodeficiency virus-positive individuals prior to first thrush episode. J Clin Microbiol 38:3595–3607

Wessels D, Voss E, Von Bergen N, Burns R, Stites J, Soll DR (1998) A computer-assisted system for reconstructing and interpreting the dynamic three-dimensional relationships of the outer surface, nucleus and pseudopods of crawling cells. Cell Motil Cytoskel 41:225–246

Whelan WL, Soll DR (1982) Mitotic recombination in *Candida albicans*: recessive lethal alleles linked to a gene required for methionine biosynthesis. Mol Gen Genet 187:477–485

Whelan WL, Partridge RM, Magee PT (1980) Heterozygosity and segregation in *Candida albicans*. Mol Gen Genet 180:107–113

Whelan, WL, Beneke ES, Rogers AL, Soll DR (1981) Segregation of 5-fluorocytosine-resistant variants by *Candida albicans*. Antimicrob Agents Chemother 19:1078–1081

White TC, Miyasaki H, Agabian N (1993) Three distinct secreted aspartyl proteinases in *Candida albicans*. J Bacteriol 175:6126–6135

Winge O (1935) On haplophase and diplophase in some *Saccharomyces*. C R Trav Lab Carlsberg Ser Physiol 21:77–111

Wong S, Butler G, Wolfe KH (2002) Gene order evolution and palesopolyploidy in hemiascomycete yeasts. Proc Natl Acad Sci USA 99:9272–9277

Wong S, Fares MA, Zimmermann W, Butler G, Wolfe KH (2003) Evidence from comparative genomics for a complete sexual cycle in the 'asexual' pathogenic yeast *Candida glabrata*. Genome Biol 4:R10

Wu W, Pujol C, Lockhart SR, Soll DR (2005) Mechanisms of mating type homozygosis in *C. albicans*. Genetics 169:1311–1327

Wu W, Lockhart SR, Pujol C, Srikantha T, Soll DR (2007) Heterozygosity of genes in the sex chromosome regulates *Candida albicans* virulence. Molec Micro (in press)

Zhao R, Daniels KJ, Lockhart SR, Yeater KM, Hoyer LL, Soll DR (2005) Unique aspects of gene expression during *Candida albicans* mating and possible G1 dependency. Eukaryot Cell 4:1175–1190

9 Ions Regulate Spore Attachment, Germination, and Fungal Growth

B.D. Shaw[1], H.C. Hoch[2]

CONTENTS

I. **Introduction** 219
II. **Attachment** 219
A. Spore Attachment 219
B. Surface Potential and Attachment 221
C. Ions as Regulators of Spore Attachment 222
D. Induction of Ionic Attachment 224
III. **Germination and Apical Growth** 224
A. Influence of Ions on Germination 225
B. Ion Regulation of Morphogenesis 227
IV. **Morphological Specialization** 228
A. Sporulation 228
B. Zoosporulation and Oosporulation 229
C. Infection-Related Structures 230
V. **Conclusions and Future Directions** 231
References 231

I. Introduction

Fungal cells respond to a multitude of environmental conditions for reproduction, dispersal, attachment to a substratum, growth, and in the case of pathogenic species penetration into host tissues. For phytopathogenic fungi, a set of prerequisite conditions must be met before a successful parasitic relationship can be established. The fungal propagule, usually a spore, is dispersed to the host surface and is secured to that surface in a way that optimizes the likelihood of remaining there until germination and growth occur. Optimally, growth is toward the most appropriate site for entry into the host. The environmental conditions that surround the fungal cell and promote these cell responses vary, but include minimally the availability of moisture, light, nutrients, and physical characteristics of the substratum such as wettability and topography. Salts, and more specifically ions, are also important to attachment, germination, growth, and morphological development of the fungal cell. While many studies have addressed, in part, the influence and importance of ions on fungal cell function, relatively few studies have been directed with these effects as the primary focus. Here, we discuss the importance and role of ions in fungal cell biology. Emphasis, although not exclusively so, is placed on fungal cells derived from spores.

Within this chapter, ions are discussed from the standpoint of their influence on:

1. Spore attachment to the substratum,
2. Initiation of spore germination and subsequent growth,
3. Development of specialized structures such as appressoria and fruit body formation.

A summation of these effects on a number of fungal species is presented in Table 9.1. Most investigations have emphasized cations with the anionic component receiving little attention as an influencing factor.

II. Attachment

A. Spore Attachment

Adhesion of fungal spores is a result of an interaction between both the physiochemical nature of the cell surface and that of the substratum. Processes involved in the adhesion of spores serve as a basis for understanding how ions might be influential in spore attachment to surfaces, and many excellent reviews have been written on the topic of spore and germling adhesion (Nicholson and Epstein 1991; Hardham 1992; Braun and Howard 1994a, b; Jones 1994; Epstein and Nicholson 1997; Tucker and Talbot 2001) and thus the subject is discussed briefly only to serve as a background for the processes involved.

Adhesion of microbial propagules to various substrata involves either specific or non-specific

[1] Department of Plant Pathology and Microbiology, Program for the Biology of Filamentous Fungi, 2132 TAMU, Texas A&M University, College Station, TX 77843, USA
[2] Department of Plant Pathology, Cornell University, New York State Agricultural Experiment Station, Geneva, NY 14456, USA

Biology of the Fungal Cell, 2nd Edition
The Mycota VIII
R.J. Howard and N.A.R. Gow (Eds.)
© Springer-Verlag Berlin Heidelberg 2007

Table. 9.1. Cellular influence of exogenous ions on attachment, growth, and development of fungi and related organisms

Organism	Developmental process	Reference(s)
Alternaria solani	Sporulation	Moretto and Barreto (1995)
Aspergillus sp.	Sporulation	Pitt and Ugalde (1984)
Blastocladiella emersonii	Zoospore encystment and attachment	Soll and Sonneborn (1972)
	Cyst germination	Soll and Sonneborn (1972), Van Brunt and Harold (1980)
Candida albicans	Attachment	O'Shea (1991), Jones and O'Shea (1994)
Colletotrichum gloeosporioides	Spore germination	Kim et al. (1998)
	Appressorium formation	Kim et al. (1998)
Colletotrichum lindemuthianum	Spore attachment	Young and Kauss (1984)
Colletotrichum trifollii	Appressorium formation	Dickman et al. (1995), Warwar and Dickman (1996)
Fusarium graminearum	Hyphal extension and branching, and morphology	Robson et al. (1991a, b)
Metarhizium anisopliae	Spore germination	St. Leger et al. (1989), (1990)
	Appressorium formation	St. Leger et al. (1990), (1991)
Neurospora crassa	Hyphal extension and branching, and morphology	Schmid and Harold (1988), Dicker and Turian (1990), Silverman-Gavrila and Lew (2003)
Penicillium sp.	Sporulation	Pitt and Poole (1981), Pitt and Ugalde (1984), Pitt and Barnes (1993), Roncal et al. (1993), Pascual et al. (1997)
Phyllosticta ampelicida	Spore attachment	Kuo and Hoch (1996), Shaw et al. (1998)
	Germination	Shaw et al. (1998), Shaw and Hoch (2000)
	Appressorium formation	Shaw and Hoch (2000)
Phytophthora cinnamomi	Zoospore encystment and attachment	Gubler et al. (1989), Irving and Grant (1984)
	Cyst germination	Byrt et al. (1982), Irving and Grant (1984)
Phytophthora infestans	Germination and zoosporulation	Hill et al. (1998)
Phytophthora palmivora	Zoospore encystment and attachment	Irving et al. (1984)
	Cyst germination	Grant et al. (1986)
	Appressorium formation	Bircher and Hohl (1999)
Phytophthora parasitica	Zoospore encystment and attachment	Warburton and Deacon (1998)
	Cyst germination	von Broembsen and Deacon (1996), Warburton and Deacon (1998)
Phytophthora sojae	Cyst germination and sporulation	Xu and Morris (1998)
Pythium aphanidermatum	Zoospore encystment and attachment	Donaldson and Deacon (1992)
	Cyst germination	Donaldson and Deacon (1992)
Saccharomyces cerevisiae	Sporulation	Suizu et al. (1994, 1995)
Saprolegnia ferax	Hyphal extension and branching, and morphology	Jackson and Heath (1989)
Sporothrix schenckii	Spore germination	Rivera and Rodriguez (1992)
Trichoderma viride	Sporulation	Krystofova et al. (1995, 1996)
Uromyces appendiculatus	Spore germination	Baker et al. (1987)
	Appressorium formation	Staples et al. (1983), Kaminskyj and Day (1984), Hoch et al. (1987a), Stumpf et al. (1991)
Zoophthora radicans	Appressorium formation	Magalhaes et al. (1991)

mechanisms. **Specific attachment** occurs when the interaction involves molecular 'lock and key' recognitions, e.g. between a ligand and its receptor molecule. Typically, most fungal spores attach to host and artificial substrata *non-specifically*. Spores of *Cochliobolus heterostrophus* (Braun and Howard 1994a, b), *Nectria haematococca* (Kwon and Epstein 1993), and *Magnaporthe grisea*

(Hamer et al. 1988), for example, exhibit little preference for the surface on which they attach – host, non-host, hydrophobic, hydrophilic, etc. Spores of some fungi, however, do attach preferentially to surfaces with specific degrees of wettability, e.g. urediospores of rust fungi (Terhune and Hoch 1993), or with specific surface charge potentials as discussed below. Furthermore, attachment may be either active or passive (Jones 1994). **Active mechanisms** for attachment occur when the cell is stimulated to produce adhesive polymers such as when zoospores sense and respond to a host surface by encysting (Hardham et al. 1991) or as in spores of *N. haematococca* (Kwon and Epstein 1993) where adhesive material is produced in zucchini fruit extract but not in water. For the latter case, the adhesive material is produced within 20 min of exposure to the extract, well before germ tube emergence (3–7 h). Active production of such adhesives is inhibited by various metabolic factors from living or killed spores. Also, active adhesion occurs as the cell becomes more active metabolically and develops a pronounced extracellular matrix (ECM) as it initiates development of a germ tube and begins growth on a substratum. **Passive attachment** occurs when preformed molecules on the spore surface affix the cell to a substratum. Packaging of such 'glues' may be in specially positioned compartments as in the 'spore tip mucilage' of *M. grisea* (Hamer et al. 1988), in 'sheaths' that surround the spore as on pycnidiospores of *Phyllosticta ampelicida* (Kuo and Hoch 1995; Shaw et al. 1998) or on specialized appendages (Jones 1994). Passive attachment is often rapid and is not metabolically dependent. As noted below, cations have in some instances pronounced temporal effects on spore attachment.

Hydrophobicity and hydrophilicity, viz. **wettability**, of the spore surface and the substratum frequently dictate whether or not spores adhere (passively), much less whether attachment is weak or firm. Wettability of spore surfaces is influenced, in part, by the chemical nature of the spore surface, typically including a complex of proteins, e.g. the cysteine-rich hydrophobin polypeptides (Wessels 1996), and carbohydrates, usually as glycoproteins. Ions influence the hydrophobic domain surrounding these molecules. Addition of ions (increase in ionic strength of the surrounding solution) increases hydrophobic adhesion not only because electrostatic interactions are suppressed (Ochoa 1978), but also because the surfaces become less polar as the ordered layer of water molecules is released into the 'bulk' aqueous phase (Rutter and Vincent 1984; Rosenberg and Kjelleberg 1986), leading to an increase in entropy. It is not surprising then that the addition of cations (e.g. Ca^{2+}, H^{+}) to spore suspensions of *P. ampelicida* enhances both the rate and tenacity of attachment to hydrophobic substrata (Kuo and Hoch 1996; Shaw and Hoch 1999), as discussed later. Assessment of fungal spore attachment to substrata of varying wettabilities has been reported for numerous species. In contrast, where a colloid, bacterium, spore, etc., and the substratum are hydrophilic, short-range repulsive forces prevent attachment even with the addition of electrolytes (Harding 1971; Rutter and Vincent 1984). Many fungal and oomycete spores attach well to both hydrophobic and hydrophilic surfaces, e.g. *M. grisea* (Hamer et al. 1988) and *Phytophthora cinnamoni* (Gubler et al. 1989), and some only or preferably to hydrophobic surfaces, e.g. *Uromyces appendiculatus* (Terhune and Hoch 1993), *Botrytis cinerea* (Doss et al. 1993), *Colletotrichum graminicola* (Mercure et al. 1994; Chaky et al. 2001), *Phyllosticta* species (Kuo and Hoch 1996; Shaw et al. 2006) and *Colletotrichum musae* (Sela Burrlage et al. 1991). Where the role of ionic influence on wettability was investigated, attachment of spores was greatly enhanced. However, a simple concept dictating an increase in entropy upon ionic elevation was more often not the case as other factors must also be taken into account, e.g. how ions affect surface potential and counter repulsive effects of like-charged bodies.

B. Surface Potential and Attachment

Most fungal propagules possess net negative charges (Kennedy 1991; O'Shea 1991; Pendland and Boucias 1991; Jones and O'Shea 1994; Kuo and Hoch 1995) due to the ionization of surface groups, e.g. carboxyls, glycolipids, acidic amino acids. Attachment of such propagules likely involves, in part, the physiochemical forces of repulsion/attraction derived from electrostatic and van der Waals forces between the surface charges of the two bodies (spores and the substratum). Together, the attraction–repulsion forces follow the lyophobic colloid theory referred to as the DLVO theory (Dejaguin and Landau 1941; Verwey and Overbeek 1948). It is, in part, the additive effects of the electrostatic repulsive forces and the attraction of the van der Waals forces that determine adhesion of colloids (or spores). Such forces operate

at distances of 1–10 nm, while the hydrophobic forces discussed above influence adhesion at greater distances (Gristina 1987; Israelachvili and McGuiggan 1988). According to DLVO theory initial 'attachment' of a colloid, or in this case a spore, is weak, tenuous, and time-dependent (Rutter and Vincent 1984). The interaction between a charged spore and the substratum is such that, at low electrolyte concentration, a significant free energy barrier needs to be overcome before the spore is able to contact the surface. However, if the electrolyte level is increased, the energy barrier is effectively depleted and a strong net attraction occurs between the spore and the substratum. Such enhanced contact and adhesion of fungal propagules with various charged substrata has been noted in a number of studies (Young and Kauss 1984; Jones and O'Shea 1994; Kuo and Hoch 1996; Shaw and Hoch 1999, 2000). Once the proximity of the spore to the substratum is determined by the physiochemical nature of the two interacting surfaces, biological glues of the propagule assure attachment to the substratum.

Clearly, many factors mediate attachment of spores to substrata: wettability and surface potentials of both the substratum and the spore, electrolyte species and concentration, adhesive nature of the spore 'glue', as well as possibly spore size. All are important in determining proximity when the spore reaches the substratum.

C. Ions as Regulators of Spore Attachment

Ionic mediation of fungal spore attachment to substrata has been reported for a number of genera. Acidification or elevation of the ionic concentration of media enhanced the rate at which conidia of *Phyllosticta ampelicida* attached to hydrophobic substrata (Kuo and Hoch 1996; Fig. 9.1), as well as the number of conidia that attached (Shaw and Hoch 1999). In the latter study, it was also noted that the addition of cations to a suspension of conidia induced attachment, albeit weakly, to hydrophilic surfaces. Normally, spores of *P. ampelicida* do not adhere to hydrophilic surfaces when in ddH_2O or solutions of low ionic strength. This effect was valence-dependent, with La^{3+} inducing higher levels of attachment than Ca^{2+} or Mg^{2+}, which in turn mediated higher levels of attachment than K^+ or Na^+ (Fig. 9.2). In that study Cl^- was the anion common to all cations tested, with the conclusion that it was not directly effecting attachment. Similarly, attachment of *Colletotrichum lindemuthianum* conidia is also enhanced in solutions with elevated levels of various cations including Na^+, K^+, Mg^{2+}, and Ca^{2+}, although no difference was noted between monovalent and divalent cations (Young and Kauss 1984). *Discula umbrinella* conidium attachment is pH-dependent. A low pH (4–5), viz. high H^+ concentrations, promoted maximum attachment while an increase in pH disrupted attachment (Toti et al. 1992). Similarly, adhesion of *Candida albicans* yeast cells is also mediated by the addition of cations to the solution. In these studies divalent cations were 10–100 times more effective than monovalent cations in inducing attachment (O'Shea 1991). This effect was due to a reduction in the electrostatic potential of the *C. albicans* cell (Jones and O'Shea 1994). Acidification of the media also efficiently increased cell attachment. Although anions are frequently overlooked, it is significant that varying the anion valency using Cl^- and SO_4^{2-}, gave no apparent difference (Jones and O'Shea 1994). This is not necessarily surprising since most spores have a net anionic charge.

Cationic enhancement of attachment as described above is likely due, in part, to the attenuation of negatively charged groups on the surface of both spore and substratum. Together, these systems exhibit attachment properties that are influenced as much by the physiochemical nature of the spore and its substratum than by a more specific receptor ligand binding. An additional mechanism of cation-enhanced attachment is suggested by the adhesion of *Arthrobotrys oligospora* to its nematode host (Tunlid et al. 1992), and by zoospore cyst attachment in *Phytophthora cinnamomi* (Gubler et al. 1989). Attachment in each of these cases may involve a Ca^{2+}-mediated reorganization of carbohydrate-containing polymers on the spore surface. A discussion of this and other possible mechanisms for cation mediated attachment is detailed below.

In the Oomycota adhesion of encysted zoospores is clearly enhanced by cationic amendment, particularly Ca^{2+}. In *Blastocladiella emersonii* K^+, Na^+, Rb^+, Mg^{2+}, and Ca^{2+} stimulate encystment of zoospores (Soll and Sonneborn 1972). Encystment of *B. emersonii* zoospores is preceded by a K^+-mediated depolarization of the plasma membrane (Jen and Haug 1981). The effect of many cation species on encystment of *Phytophthora cinnamomi* zoospores has been tested (Byrt et al. 1982; Irving and Grant 1984), with Ca^{2+} being most effective in inducing encystment at mil-

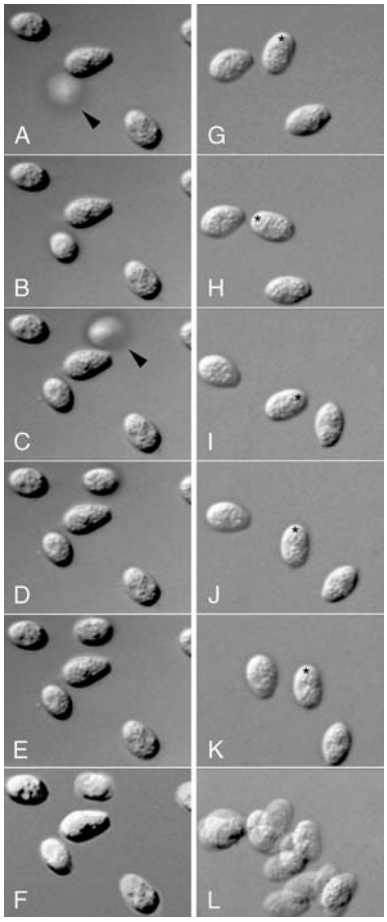

Fig. 9.1. Behavior of *Phyllosticta ampelicida* conidia settling onto hydrophobic (**A–F**) and hydrophilic (**G–L**) substrata as observed using an inverted light microscope. Spores in acidified (pH 4) water attach immediately (<0.03 s) upon contact with a hydrophobic surface. **A** Four spores are already attached and immobile with one 'out-of-focus' spore (*arrowhead*) about to make contact. In **B** and **C**, it made contact and attached immediately. A second spore (*arrowhead*) is about to contact the surface in frame **C**. Contact and attachment of the spore is noted in **D–E**. **F** A composite overlay of frames **A–E** illustrates the non-motile characteristic of attached conidia. Times for frames **A–E** are 3.23 s, 3.23 s, 4.08 s, 4.13 s, 4.15 s, respectively. Conidia in frames **G–K** on highly hydrophilic heat-treated glass do not attach (*asterisk* denotes the same spore). **L** A composite overlay of frames **G–K** illustrates that the conidia did not attach. Frames **G–K** taken at 10-min intervals. Adapted from Kuo and Hoch (1996)

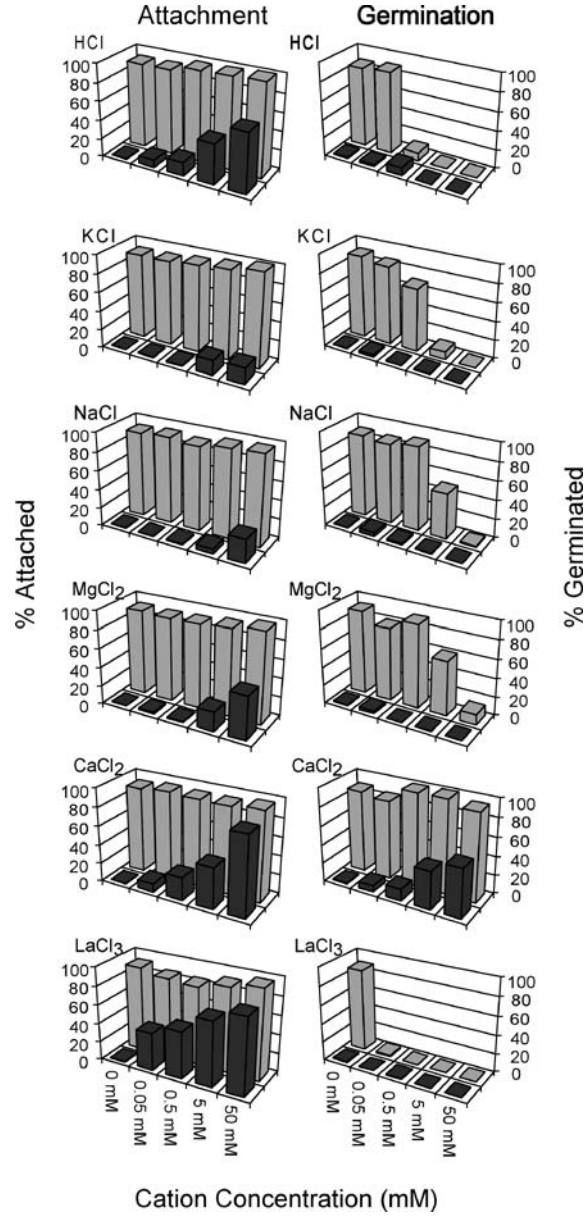

Fig. 9.2. Attachment and germination of pycnidiospores of *Phyllosticta ampelicida* as influenced by various cations of chloride salts. In distilled H_2O neither attachment nor germination occurred on hydrophilic glass substrata, but both occurred at high levels on hydrophobic polystyrene. Efficiency of attachment to hydrophilic substrata was a direct function of cation concentration and valence. All tested cations were inhibitory to germination, however, except Ca^{2+}. Adapted from Shaw and Hoch (1999)

limolar levels. Sr^{2+} could also induce encystment. Among monovalent cations Na^+ and Cs^+ had negligible effects on encystment; while K^+ did induce encystment, it became increasingly inhibitory to germination as its concentration increased (Byrt et al. 1982). In the latter case, it was noted that Ca^{2+} could override this 'germination' toxicity of K^+ (Irving and Grant 1984). The K^+ ionophore, valincomycin, and the Ca^{2+} ionophore, A23187, both induced encystment, indicating that one or both cations are likely involved in the encystment process in *P. cinnamomi*. In one of the few studies

that also analyzed anioinic effects, ions Cl^-, NO^{3-}, SO_4^{2-}, and PO_4^{3-} were all tested as Na^+ salts and no difference in encystment induction was found in *P. cinnamomi* (Byrt et al. 1982). In another study, increasing the concentration of $Ca^{2+}$from 2 mM to 20 mM enhanced attachment of *P. cinnamomi* cysts, while chelation of Ca^{2+} with EGTA completely inhibited cyst adhesion (Gubler et al. 1989). Similarly, adhesion of *Pythium aphanidermatum* cysts was found to be dependent on Ca^{2+} availability, although Mg^{2+} and Sr^{2+} were also able to induce encystment. All other tested cations were either ineffective or toxic (Donaldson and Deacon 1992). This observation is most interesting, considering that *Phytophthora palmivora* zoospores were found to release Ca^{2+} just prior to encystment (Irving et al. 1984). Gubler and colleagues also noted that Mg^{2+} was capable of inducing an 8-fold increase in cyst adhesion and they supported the earlier assertion of Irving and Grant (1984) that the monovalent cation Na^+ had negligible effects on cyst attachment. Additionally, transmembrane Ca^{2+} fluxes were associated with zoospore encystment of *P. parasitica*. From both internal stores and the external environment, Ca^{2+} was essential for zoospore encystment, as determined by the use of channel blockers lanthanum, verapamil, and TMB-8, the fluorescence indicator Fura-2, and by assessing the influx and efflux of $^{45}Ca^{2+}$ (Warburton and Deacon 1998). Recently Gow and colleagues sought to resolve the role of K^+ ions in zoospore biology and found that modulation of cytoplasmic levels of this ion play an important role in zoospore swimming behavior and encystment (Appiah et al. 2005). Furthermore, there were genus-specific effects of K^+ when comparing *Pythium* sp. zoospores with those of *Phytophthora*. High levels of external K^+ reduced swimming speeds, altered swimming patterns, and induced encystment in *Phytophthora palmivora* but had comparatively little effect in *Pythium aphanidermatum*. Additionally, increasing the cytoplasmic K^+ concentration through treatment with ionophores reduced swimming speeds and often led to increased encystment. Taken together, these data all point to the importance of dynamic regulation of K^+ ion to the behavior of oomycete zoopspores.

D. Induction of Ionic Attachment

The mechanism by which cations in the extracellular environment influence spore attachment is not well understood, in part because there are a multitude of interactions possible (viz. electrostatic, van der Waals forces, etc.) in addition to compounding associations of surface wettability and ligands. It is much more difficult to separate these effects in biological systems where surfaces are complex, compared with simplified inert colloidal systems, and arrive at simplified explanations. It is clear, however, that the presence of cations can induce attachment of many microorganisms to the substratum. Possibilities for the role of ions in attachment include: (1) attenuation of the electronegative surface groups on the propagules and substratum (Fletcher 1980; Jones and O'Shea 1994), (2) divalent or trivalent ions bridging two negatively charged groups on the spore and the substratum in the case of pH dependent effects, attenuation of the inherent electronegativity of surface components by protonation of negatively charged groups, thus reducing electrostatic repulsive forces and enhancing attachment (O'Shea 1991; Jones and O'Shea 1994), (3) attenuation of the adhesive material by ions, as suggested in the nematode trapping fungus *A. oligospora* (Tunlid et al. 1991) or in marine algae where cations have been shown to increase the adhesiveness of the spore glue (Cooksey 1981), (4) effects on the thickness of the electrical double layer between adhering surfaces by free ions (Young and Kauss 1984; Jones 1994), and finally, (5) attenuation of surface hydrophobicity by free ions in media (Jones 1994).

III. Germination and Apical Growth

Once the fungal spore has been deposited in a new locale – apart from 'sister spores', sori, and conidiogenous hyphae that may harbor self-germination inhibiting substances – it has the opportunity to initiate restoration of metabolic and physiological activity, a process normally considered a prelude to germination. In the strictest sense, germination begins when the resting stage (dormancy) ends and not when a germ tube is first visible. After all, at what level of resolution or detection should we consider a germ tube visible? Certainly other prerequisite conditions (or lack of) such as light, water, nutrients, aeration, etc. need to be satisfied as well. As will become evident, exogenous ions are frequently equally important in the germination process and in continued extension of the cell.

A. Influence of Ions on Germination

Unlike the studies of ionic influence on adhesion, much of the evidence concerning ions and germination focuses on Ca^{2+}. This is due primarily to the ubiquitous role that Ca^{2+} plays in signaling pathways in eukaryotes (Pitt and Ugalde 1984; Clapham 1995; Rudd and Franklin-Tong 1999; Sanders et al. 1999, 2002; Berridge et al. 2003). Despite the ubiquity of the role of Ca^{2+} in a number of developmental processes, some fungal systems tested thus far require Ca^{2+} availability for germination, while others seem to germinate in its absence, at least to the extent of not added experimentally. Where it is found to be necessary Ca^{2+} likely has two mechanisms in stimulating germination: (1) enhancing attachment or contact of the propagules to its substratum (as discussed above), and/or (2) setting up the tip high gradient of Ca^{2+} ion found at the apex of hyphae (as described below).

Many cations enhanced the attachment of *P. ampelicida* conidia to a substratum, however all except Ca^{2+} were inhibitory of germination (Shaw and Hoch 1999; Fig. 9.2). Availability of external Ca^{2+} was essential for normal germination of *P. ampelicida* conidia. Using a Ca^{2+}-EGTA buffering system (Wayne 1985) to control the amount of free Ca^{2+} (0.1 nM to 1 mM) in the external medium, at 10 µM or higher the cation was found to be essential for normal germination to ensue (Shaw and Hoch 2000; Fig. 9.3). The presence of Ca^{2+} was required for the first 25–60 min following spore attachment to hydrophobic substrata. Conidia of *P. ampelicida* germinate only after they become attached to a hydrophobic surface. Attachment was a prerequisite for initiation of germination while availability of nutrients, normally considered adequate for germination of most fungal spores, had no influence on this fungus (Kuo and Hoch 1995). Some pharmacological agents known to block membrane resident ion channels, e.g. nicardipine and Gd^{3+}, effectively abolished germination of conidia. Additionally, the calmodulin antagonists, compound 48/80 and compound R-24571, completely inhibited germination. Taken together, these data suggest that Ca^{2+} and Ca^{2+}-signaling pathways are essential for *P. ampelicida* pycnidiospore germination and lead us to propose that mechanosensitive Ca^{2+} channels resident in the membrane of the *P. ampelicida* conidium open upon attachment of the spore to a surface. Once open, Ca^{2+} ion enters the cell and sets in motion Ca^{2+}-mediated signaling that leads to spore germination (Fig. 9.4).

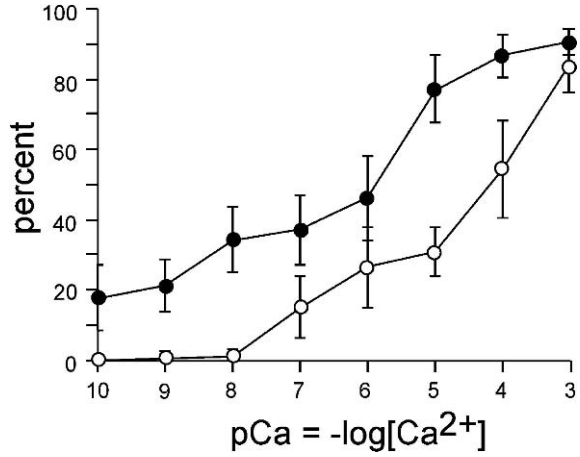

Fig. 9.3. Comparison of germination (*filled circles*) and appressorium formation (*open circles*) in *Phyllosticta ampelicida*, adapted from Shaw and Hoch (2000). This study used the Ca^{2+} buffering systems developed by Wayne (1985). *P. ampelicida* germination and appressorium formation required external free Ca^{2+}

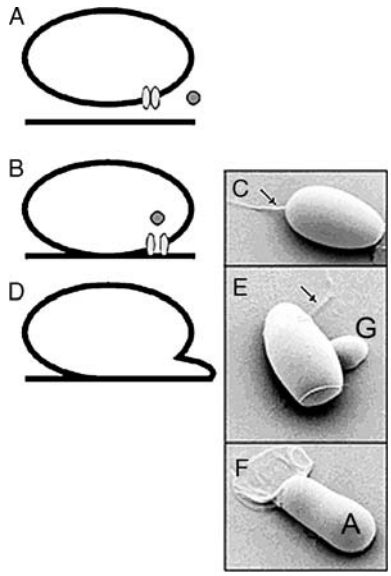

Fig. 9.4. Model for Ca^{2+} induction of spore germination in *Phyllosticta ampelicida.* **a** Unattached conidium does not germinate. Mechanosensitive channel closed. **b**, **c** Spore attachment leads to mechanical stress on the spore wall and membrane; mechanosensitive channel open leading to Ca^{2+} influx. **d**, **e** Elevated internal Ca^{2+} leads to germination within 40–60 minutes of attachment. **f** Mature appressorium, 4–6 h. *G* Germ tube, *A* appressorium and 'collapsed' cytoplasmically emptied spore, *arrow* apical appendage

Ca^{2+}-calmodulin signaling pathways have been implicated in germination of *Metarhizium anisopliae* (St. Leger et al. 1990). Germination occurred in media containing 2 mM EGTA, viz. low

levels of Ca^{2+}, but when the ionophore A23187 was added germination did not occur. This suggests that internal stores of Ca^{2+} are sufficient to allow for germination. Unfortunately, St. Leger and colleagues did not test internal Ca^{2+} channel blockers such as TMB-8 to ascertain this hypothesis. The plasma membrane Ca^{2+} channel blocker La^{3+}, as well as calmodulin antagonists, disrupted germination by interrupting normal protein phosphorylation (St. Leger et al. 1989). Similarly, in *Colletotrichum gloeosporioides* conidia inhibition of calmodulin- and calmodulin kinase-associated processes with compound 48/80 or KN93, respectively, reduced germination (Kim et al. 1998). In the same study chelation of Ca^{2+} with EGTA also reduced germination, as did U73122 inhibition of phopholipase C. Germination of *Sporothrix schenckii* conidia was also dependent on external Ca^{2+} availability, though pharmacological stimulation of protein kinase C could override the requirement for Ca^{2+} (Rivera and Rodriguez 1992). Additionally, germination of *Uromyces* urediospores was enhanced with either Ca^{2+} or Mg^{2+}, but neither K^+ or Na^+ was effective in stimulating germination in water purified with an ion exchange resin (Baker et al. 1987). It seems likely that, at least for some fungal systems, Ca^{2+} dynamics are important regulators of spore germination.

In contrast to the previous discussion, external Ca^{2+} appears to have little or no role in germination in *Colletotrichum trifolli* (Dickman et al. 1995; Warwar and Dickman 1996). Neither Ca^{2+} chelation with EGTA, nor the use of the ionophore A23187 affected germination, which is surprising since both compounds are effectively toxic at high concentrations in many cell systems. It is possible that a more carefully constructed Ca^{2+} buffering system may effectively influence germination, possibly even at low Ca^{2+} concentrations. Additionally, various channel blockers had little effect on the germination of *C. trifollii* conidia (Warwar and Dickman 1996) or the rate of germination in *Zoophthora radicans* (Magalhaes et al. 1991). In *Z. radicans* an EGTA buffering system was used to reduce Ca^{2+} to nanomolar levels. Neither this treatment nor the use of channel blockers reduced germination levels appreciably, although multipolar germination was reported when Nd^{3+} was used to inhibit Ca^{2+} entry into the spores. Appressorium formation, however, was greatly effected in both of these systems (see below). It should be noted that calmodulin inhibitors disrupted germination in both systems. Thus, Ca^{2+} regulation of germination in these systems remains unclear.

In the Oomycota, direct and indirect germination were noted to be influenced by ions, particularly Ca^{2+}. Germination of *Phytophthora infestans* sporangia is associated with Ca^{2+} availability (Hill et al. 1998). Chelation of divalent ions with either BAPTA or EGTA suppressed germination of *P. infestans* sporangia, as did treatment with the Ca^{2+} channel blockers lanthanum and gadolinium. Ca^{2+} was generally more effective than Mg^{2+} in overcoming these treatments, but concentrations of either cation above 1 mM inhibited germination. The developmental fate of germinating *Phytophthora sojae* cysts was dependent on Ca^{2+} availability (Xu and Morris 1998). If >10 mM Ca^{2+} was supplied to cysts, direct germination (emergence of a germ tube) proceeded. If, however, <10 mM Ca^{2+} was provided to cysts, indirect germination (zoospore release) occurred. No other tested ion, including Mg^{2+}, Mn^{2+}, K^+, and Na^+, had this effect on the cysts. Application of the Ca^{2+} channel blocker, verapamil, to *P. sojae* cysts also decreased direct germination and increased secondary zoospore release (Xu and Morris 1998). Encysted zoospores of *Phytophthora parasitica* lost their ability to germinate if they are diluted in H_2O. However, if 50 mM $CaCl_2$ was added to the cysts, germination returns to normal levels (von Broembsen and Deacon 1996). Additionally, transmembrane Ca^{2+} fluxes were associated with cyst germination of *P. parasitica* (Warburton and Deacon 1998). The cations Na^+, Ca^{2+}, and Sr^{2+} induced both encystment and germination of *Phytophthora palmivora* (Grant et al. 1986). However, in a subsequent report, Grant and colleagues confirmed a requirement for Ca^{2+} in germination but could not confirm the requirement for Na^+ (Iser et al. 1989). Ca^{2+} from both internal stores and the external environment was essential for germination, as determined by the use of channel blockers (lanthanum, verapamil, TMB-8), by the fluorescence indicator Fura-2, as well as by influx and efflux dynamics using $^{45}Ca^{2+}$. Warburton and Deacon (1998) demonstrated a net Ca^{2+} influx during zoospore encystment followed by a net efflux, from internal stores, during germination. While any tested cation was effective in inducing encystment of *P. cinnamomi* zoospores, only Ca^{2+} induced germination (Byrt et al. 1982). None of the anions Cl^-, NO^{3-}, SO_4^{2-}, and PO_4^{3-} tested as Na^+ salts showed a detectable difference in induction of germination. In a later study, Ca^{2+} was shown to

be essential for germination of *P. cinnamomi* cysts (Irving and Grant 1984).

In *Pythium aphanidermatum*, germination was enhanced by Ca^{2+}, as well as by Mg^{2+} and Sr^{2+}, while all other tested ions, including K^+, Li^+, Na^+, Ba^{2+}, Mn^{2+}, Fe^{3+}, and Cu^{3+}, either had no effect on germination or were toxic (Donaldson and Deacon 1992). Ca^{2+} flux is essential for both encystment and germination in this system, as Ca^{2+} is released upon encystment and taken up during germination. The results of these studies led Donaldson and Deacon (1992) to propose an 'auto-signaling' hypothesis for a role of Ca^{2+} in encystment and germination of zoospores, and to explain why cysts that maintain contact with a substratum germinate at much higher levels than those kept in suspension. Ca^{2+} secreted by encysting zoospores (Irving et al. 1984; Iser et al. 1989) enhance attachment, possibly through ionic bridging or polymerization of a surface molecule. More recent data suggest that Ca^{2+} is not secreted until the early stages of signaling for germination (Warburton and Deacon 1998). At that time, Ca^{2+} accumulates between the cyst and the substratum and is available for re-absorption by the cyst, possibly enhancing germination. It is clear that a flux of Ca^{2+} is essential for both encystment and germination of zoospores in many of the Oomycota. Knowledge of the role of calcium in encystment and germination in the Oomycota has lead to at least one disease control recommendation (von Broembsen and Deacon 1997). Addition of 10 mM Ca^{2+} to an irrigation system interfered with the normal development of *Phytophthora parasitica* by inducing encystment and germination, without a corresponding shift to indirect germination and zoospore production.

Exogenously supplied K^+, Na^+, Rb^+, Mg^{2+}, and Ca^{2+} were demonstrated to stimulate germination of encysted *Blastocladiella emersonii* zoospores (Soll and Sonneborn 1972; Van Brunt and Harold 1980). The germination stimulus by K^+ may be the result of the depolarization of the membrane by its rapid uptake as determined by reversal of quenching of the fluorophore DiO-C_6 as well as the accumulation of $^{42}K^+$ (Van Brunt and Harold 1980). Using $^{45}Ca^{2+}$ it was shown that Ca^{2+} is not taken up by the spores, but likely binds to external sites. In the same study it was shown that *B. emersonii* zoospores required Ca^{2+} and K^+ to germinate, but were inhibited from germinating (10% germination) if Na^+ was present. Germination of both *Aphanomyces astaci* and *A. eutiches* cysts also was induced by the addition of various cations, including K^+ and Ca^{2+} (Svensson and Unestam 1975; Deacon and Saxena 1998).

B. Ion Regulation of Morphogenesis

Like studies of germination, work on the role of exogenously applied cations in growth and branching of hyphae focused primarily on Ca^{2+}, and included studies with *Fusarium graminearum* (Robson et al. 1991a, b), *Neurospora crassa* (Schmid and Harold 1988), and *Saprolegnia ferax* (Jackson and Heath 1989). In *F. graminearum* the rate of hyphal extension and the extent of branching were both affected directly by the external Ca^{2+} concentration (Robson et al. 1991a, b). Hyphal growth rate increased as Ca^{2+} concentration increased from 48 nM to 10 µM, but concentrations >10 µM had no further effect. In addition, those mycelia that grew in <10 µM Ca^{2+} media had an altered growth habit, with increased branching and bulbous hyphae. Growth rate decreased and branching increased by application of various Ca^{2+} channel blockers (Robson et al. 1991a, b). In addition, apical extension in *Neurospora crassa* (Schmid and Harold 1988) and *Saprolegnia ferax* (Jackson and Heath 1989) was impaired by a decrease in external Ca^{2+} concentration. In both cases growth was accompanied by abnormal bulbous growth. Branching was also enhanced in *N. crassa* when grown in Ca^{2+}-depleted media or exposed to Ca^{2+} channel blockers (Dicker and Turian 1990). In *N. crassa* the rate of apical extension was affected more strongly by a reduction in external, wall-bound $^{45}Ca^{2+}$ than by cytoplasmic $^{45}Ca^{2+}$ (Schmid and Harold 1988).

Like most other tip-growing eukaryotic cell types, filamentous fungi exhibit an internal tip high Ca^{2+} gradient (Robson et al. 1991a, b; Heath 1995). Significant advances by Lew and colleagues have revealed much about the influence of this gradient in *N. crassa*. Depletion of the gradient by injection of the Ca^{2+} chelator BAPTA dissipated the gradient and caused growth to cease (Silverman-Gavrila and Lew 2000). One question raised by this observation is 'How is the Ca^{2+} gradient established?' Though stretch-activated Ca^{2+} channels have been found in *N. crassa* both physiologically (Levina et al. 1995) and through computational approaches (Zelter et al. 2004), there remains no evidence that influx of the ion at the growing tip results in the observed gradient (Lew 1999; Silverman-Gavrila and Lew 2000). Indeed hyphal growth in *N. crassa* can proceed in the presence of Ca^{2+} channel blockers

(Levina et al. 1995), indicating that internal stores may be the most important component for setting up the tip-high Ca^{2+} gradient. Experimental evidence suggests that the gradient may be established by 1,4,5-trisphosphate (IP_3)-activated release of internal Ca^{2+} stores in vesicles found at the hyphal apex (Torralba et al. 2001; Silverman-Gavrila and Lew 2002, 2003). Newer evidence points to a population of tip-concentrated mitochondria (that are not participating in ATP synthesis) in Ca^{2+} sequestration (Levina and Lew 2006). One possible role for this gradient theorized by Silverman-Gavrila and Lew (2002) is that Ca^{2+} enhances vesicle docking. Therefore the tip-high Ca^{2+} results in an increase in fusion of secretory vesicles at the hyphal apex where growth occurs. This is consistent with the presence of the Spitzenkörper, a cloud of secretory vesicles that participates in tip growth (Harris et al. 2005; Virag and Harris 2006) at hyphal apices (see also Chaps. 5 and 6 in this volume).

IV. Morphological Specialization

As in cell germination and growth, exogenous ions affect fungal cell differentiation. A variety of specialized structures including, but not limited to, production of asexual and sexual reproductive structures and their associated propagules (conidia, zoospores, etc.), morphologically distinct structures aiding ingress of the fungus (pathogen) into its host, or in the adsorption of nutrients (appressoria, hyphopodia, haustoria, etc.), are triggered by the presence of certain ions. In some situations the absence of ions are similarly stimulatory. Again, there appears to be in the literature an emphasis on calcium as the dominant ion affecting these events, perhaps because more methods have been developed for its detection and monitoring or, more likely, because calcium is one of the most important molecules in ionic signaling pathways.

A. Sporulation

The molecular genetics of conidiation induction in filamentous fungi have been reviewed recently (Adams et al. 1998; Fischer 2002; Roncal and Ugalde 2003). Additionally, a number of filamentous fungi reportedly initiate sporulation upon exposure to elevated levels of ions, notably calcium. Often, conidiogenous fungi sporulate under conditions of duress such as nutrient depletion and mechanical perturbation, osmotic shock or under certain light regimes. Osmotic stimulation of conidiation has been reported to occur in *A. nidulans* when exposed to 0.8 M NaCl (Lee and Adams 1996) and in *A. oryzae* when exposed to 0.1 M KCl (Song et al. 2001) though the mechanisms of conidiation induction in both cases remain to be elucidated. Conidiation in submerged culture is rare among fungi, however many species of *Penicillium* and a few *Aspergillus* species sporulate in submerged culture when nutrients are depleted (Pitt and Ugalde 1984). When nutrients are plentiful conidiation does not occur. *Penicillium* species including *P. notatum*, *P. griseofulvum*, *P. urticae*, *P. oxalicum*, and *P. cyclopium* have been observed to sporulate when supplied with elevated levels of calcium (1–10 mM), even in nutritionally adequate media (Foster et al. 1945; Hadley and Harrold 1958a, b; Pitt and Poole 1981; Ugalde and Pitt 1983; Roncal et al. 1993; Pascual et al. 1997). The signaling process is not clearly understood, although it was demonstrated that under these conditions relatively short exposures to calcium (0.5–2.0 min) were all that were required for the process to be initiated, that very little calcium was taken up into the cytosol, and that considerable binding of calcium to the plasma membrane occurred (Ugalde and Pitt 1986; Ugalde et al. 1990). In addition, calcium-induced conidiation can be reversed by exposing cells to the chelating agent BAPTA within 2 h (Ugalde et al. 1990). Furthermore, calcium channel blockers appeared to have no effect on the conidiation response to external ion (Roncal et al. 1993). This suggests that calcium is bound primarily to the extracellular domains of the cell, where it possibly signals the conidiation process. Roncal and co-workers (1993) provide compelling evidence that calcium induced alkalinization of cell apices triggers conidiation in *P. cyclopium*. More recent work has indicated that in *P. cyclopium* a conidiation autoinducer, conidiogenol, may be involved. The mechanism of Ca^{2+} induction may be through reducing the concentration of conidiogenol required for induction (Roncal et al. 2002), though the mechanism of this induction remains to be elucidated. Pitt and Barnes (1993) associated calcium-induced conidiation with signaling via calmodulin and protein phosphorylation pathways. The topic of signal transduction pathways and conidiation has been reviewed (Pitt and Kaile 1990; Adams et al. 1998; Fischer 2002; Roncal and Ugalde 2003).

Calcium-induced sporulation also has been reported in other fungi. In *Trichoderma viride* calcium supplied in millimolar quantities promoted conidiation as well as growth (Krystofova et al. 1995, 1996). When calcium was sequestered with EGTA the rate of conidiation was reduced significantly, but so was the rate of growth which may indicate that cell health may have been compromised by the chelation treatment. Enhanced sporulation of *Alternaria solani* has been reported in culture media supplemented with calcium carbonate (Moretto and Barreto 1995); however, since several other variables were introduced into the experimental design of this study, it is difficult to assign a direct effect of calcium on sporulation. In *Fusarium graminearum* formation of conidia was reduced by 98% in 14 nM Ca^{2+}, compared with their formation in 50 µM Ca^{2+} (Robson et al. 1991a, b). In a diploid strain of *Saccharomyces cerevisiae*, meiotic sporulation (ascospore production) was induced when free external Ca^{2+} was reduced and internal cell levels were increased to a 3000 times differential .(Suizu et al. 1995). It was further determined that an influx of external Ca^{2+}, rather than a release of Ca^{2+} from internal stores, initiated meiosis and sporulation in this yeast. In contrast, no marked changes were found in the external or internal levels for other ions, including Mg^{2+}, Na^{+}, or K^{+}. Additionally, sporulation was completely repressed when using media containing no detectable Ca^{2+} or Mg^{2+} (determined by HPLC; .Suizu et al. 1994).

Sodium has been implicated in promoting conidiation in strains of *Aspergillus nidulans* bearing abnormal distributions of nuclei in most cells, including hyphae, phialides, conidia, etc. (Queiroz and Azevedo 1998). When high levels of NaCl (0.5 M) are incorporated into the growth medium, conidiation is significantly increased, although no effect has been noted on nuclear distribution.

B. Zoosporulation and Oosporulation

Sporulation, both asexual and sexual, in the Oomycota is also enhanced, and in some cases dependent, on available Ca^{2+}. In *Saprolegnia* (Fletcher 1979), *Achlya* (Griffith et al. 1988), *Pythium* (Lenny and Klemmer 1966), and *Phytophthora* (Elliot 1972), Ca^{2+} has been implicated in the formation of reproductive structures. *Saprolegnia terrestris* oogonial initials have an increased rate of abortive oogonia under Ca^{2+}-deficient conditions. Ultrastructural analysis showed a decreased density of lipid bodies and an increased density of mitochondria under these conditions (Fletcher 1983). In *Phytophthora palmivora* (Elliott 1986) and *P. cactorum* (Elliott 1988) trifluoperazine, an inhibitor of calmodulin, inhibited oosporogenesis and zoosporogenesis. *Aphanomyces eutiches* oospore formation is also thought to be dependent on Ca^{2+} availability .(Yokosawa et al. 1995). In contrast to these examples, oogonium development in *S. diclina* is reportedly reduced by increasing Ca^{2+} availability (Fletcher 1988).

Micromolar levels of Ca^{2+} are required for sporangium development in *Achlya* sp. (Griffin 1966). Chelation of external Ca^{2+} with EGTA to levels below 0.1 µM blocked sporulation of *Achlya bisexualis* (Thiel et al. 1988). Additionally, the Ca^{2+} channel blockers lanthanum (at 20 µM) and gadolinium (at 50 µM) blocked sporangium development or sporulation in *A. bisexualis*, depending on the developmental maturity at the time of application. Sporulation in sporangia of *Phytophthora infestans* is associated with Ca^{2+} availability (Hill et al. 1998). Either BAPTA or EGTA chelation suppressed zoospore development in *P. infestans* sporangia. Lanthanum and gadolinium also suppressed zoospore formation, which could be overcome by the addition of Ca^{2+}, and in some cases Mg^{2+}; but levels of either cation above 1 mM inhibited development. In another report, zoospore release from *P. infestans* cysts was stimulated by 0.3 mM Ca^{2+} whereas Mg^{2+}, K^{+}, and Na^{+} were each less effective at stimulating zoospore release .(Sato 1994). Recently zoosporogenesis and expression of *pic* genes involved in zoospore cleavage were found to be blocked by inhibitors of phopholipase C and inositol triphosphate receptor-gated calcium channels (Tani et al. 2004).

The release of secondary zoospores from an encysted zoospore, i.e. indirect germination, also may be influenced by Ca^{2+} dynamics. In at least six species of *Aphanomyces*, secondary zoospore emergence was monitored in relation to Ca^{2+} dynamics (Cerenius and Soderhall 1985). If zoospores were exposed to 50 mM Ca^{2+} during the first 15 min of encystment, the cysts developed a germ-tube and differentiated by direct germination. If, however, the zoospores were induced to encyst by physical agitation and were denied Ca^{2+}, they subsequently germinated indirectly. It seems that, at least in *Aphanomyces*, indirect germination is a default pathway that can be disrupted by Ca^{2+}. Similarly, in *Phytophthora sojae* <10 mM free

Ca^{2+} stimulated secondary zoospore release, while >10 mM Ca^{2+} stimulated direct germination (Xu and Morris 1998).

C. Infection-Related Structures

Phytopathogenic fungi often gain access to their plant host through appressoria formed at germ tube or hyphal apices (Emmett and Parbey 1975; Hoch and Staples 1987; Dean 1997; Tucker and Talbot 2001; see also Chaps. 10, 11 in this volume). For most of these fungi, it is not clear what on the host surface serves to signal appressorium development; however, there are many 'all encompassing' vague features that have been identified, including contact with a 'hard surface', a hydrophobic surface, and in some instances a hydrophilic surface, etc. (Lee and Dean 1994; Xiao et al. 1994; Nicholson and Kunoh 1995; Beckerman and Ebbole 1996; Gilbert et al. 1996; Perfect et al. 1999). In rust fungi, urediospore germlings sense sub-micron topographical features that trigger appressorium development (Hoch et al. 1987a, b; Allen et al. 1991). Even so, the next level of signal perception beyond these surface features remains elusive, although there is some evidence for specific signaling pathway involvement, e.g. cAMP (Lee and Dean 1993; Yang and Dickman 1997; Choi et al. 1998). Similarly, ionic signaling mechanisms may be operative in appressorium induction of some fungal systems. Again as already discussed, the ion that has received the most attention is Ca^{2+}.

Concentrations of Ca^{2+} >1 µM, but not K^+ or Cl^-, were required for appressorium formation in *Zoophthora radicans* (Magalhaes et al. 1991). Similarly, appressoria did not form on germlings of *Phyllosticta ampelicida* in a buffer containing <1 µM Ca^{2+} (Fig. 9.3). Appressorium formation approached 100% when 1 mM Ca^{2+} was available (Shaw and Hoch 2000). In both fungal systems, Ca^{2+} channel blockers indicated that both external and internal sources of Ca^{2+} were required for normal appressorium development. Additionally, calmodulin antagonists completely abolished appressorium formation, suggesting that Ca^{2+} signaling pathways may be involved in initiating differentiation in each system. More recently, calmodulin was shown to be upregulated in *M. grisea* just prior to appressorium induction (Liu and Kolattukudy 1999). Similarly, La^{3+} and Gd^{3+} disrupted appressorium formation in *Metarhizium anisopliae* (St. Leger et al. 1991), although earlier work by the same group showed that external Ca^{2+} was not required for normal appressorium formation (St. Leger et al. 1990). St. Leger and colleagues believe that it is the tip-high Ca^{2+} gradient that maintains polarity, and that disruption of this gradient is intimately involved in initiation of appressorium formation (St. Leger et al. 1991).

The addition of EGTA to the medium surrounding *Colletotrichum trifollii* reduced appressorium formation in a concentration-dependent manner (Dickman et al. 1995; Warwar and Dickman 1996). Additionally, the ionophore A23187 reduced appressorium formation. These data indicate that Ca^{2+} is likely involved in appressorium initiation in *C. trifollii*. Furthermore, the Ca^{2+} channel blockers nifedipine, neodymium, and TMB-8 had pronounced effects on appressorium formation, suggesting that more than one type of Ca^{2+} channel may be involved in regulation of appressorium development. Interestingly, when the flux of internal stores of Ca^{2+} was inhibited by TMB-8, normal melanization of appressoria was disrupted. In *C. gloeosporioides* inhibition of calmodulin or calmodulin kinase-associated processes with compound 48/80 or KN93, respectively, reduced appressorium formation (Kim et al. 1998); and those appressoria that did form in the presence of KN93 were greatly reduced in melanin content. Chelation of Ca^{2+} with EGTA also reduced germination and appressorium formation in *C. gloeosporioides*, as did inhibition of phopholipase C with U73122.

In urediospore germlings of the rust fungi, appressorium formation is generally stimulated by surface topographical features (Hoch et al. 1987a, b). Mechosensitive Ca^{2+} channels have been implicated in this response (Zhou et al. 1991). The presence of Ca^{2+}, Mg^{2+}, or K^+ can, however, stimulate appressorium formation on *Uromyces appendiculatus* urediospores germinating on agar or liquid media (Staples et al. 1983; Kaminskyj and Day 1984), however, these appressoria form aerially apart from the surface, a condition much different from in vivo growth on its host (Hoch et al. 1987a, b). On normally inductive topographies, however, the presence of millimolar levels of Ca^{2+}, K^+, or Na^+ inhibited appressorium formation (Stumpf et al. 1991). Sodium, as previously reported (Staples et al. 1983), was especially inhibitory toward appressorium development.

Appressorium formation by germlings in the Oomycota may also be influenced by Ca^{2+}. Reduc-

tion of external free Ca^{2+} with EGTA inhibited appressorium formation in *Phytophthora palmivora* (Bircher and Hohl 1999). Antagonism of calmodulin, in this case with TFP, also inhibited appressorium formation. These data suggest that, as with the many examples above, Ca^{2+} is an integral component of initiating appressorium formation.

V. Conclusions and Future Directions

It becomes clear that a dichotomy exists between studies concerned with the effect of exogenously supplied ions on attachment and the effects on other developmental processes in fungi. In the case of attachment, a variety of ions have been tested and various theories have been developed to describe their role in that process. In studies of germination, growth, and differentiation emphasis usually has been on physiological events in the cytosol and their relationship to signaling cascades. In particular, Ca^{2+} has been the ion most implicated for cellular function(s) and thus has received most attention. Conclusions regarding a specific role for Ca^{2+} in developmental processes perhaps should be made with a degree of caution. For example, Youatt (1994) pointed out, and rightly so, that EGTA is capable of chelating other divalent ions in addition to Ca^{2+}. Thus, one can not be certain which ion effects are responsible for experimental observations. In studies by Youatt, Zn^{2+}, Fe^{2+}, and Mn^{2+} could serve as Ca^{2+} substitutes for the growth of several fungi (Youatt and McKinnon 1993; Youatt 1994).

Assessment of ionic effects on fungal cell function can be advanced significantly using newer technological approaches as well as reconsidering how older methods might be better applied. For the latter, one must use more precise methods for ascertaining whether or not the concentration of the ion in question is well established. This means using appropriate buffering systems, such as Ca^{2+}-EGTA or BAPTA, where the free calcium ion is precisely controlled (Magalhaes et al. 1991; Bers et al. 1994; Shaw and Hoch 2000), rather than simply adding Ca^{2+} as a salt. Studying effects of ions on cells might be accomplished if their delivery could be more precisely targeted rather than bathing the entire cell or thallus in a solution of the ions of interest. Such approaches might include the localized release of ions at selected extracellular regions on a cell using a micropipette delivery system or through caged-ions and their photoactivation and release. More technologically advanced approaches might take advantage of micro- and nanofabrication methods (Hoch et al. 1996). There are many opportunities for applying 'nanobiotechnology' to the study of fungal cell biology in which the substratum can be modified in numerous ways to accommodate nano-size analytical sampling devices, molecular delivery devices, fluidics (pumps, valves, etc.), topographical features, patterning of specific domains (hydrophobic, ligands, caged-ions, etc.), and micro-electronics. Currently there are excellent opportunities to assess ion concentrations and species temporally and spatially, using a variety of methods such as the vibrating ion-specific electrode (Smith et al. 1994; Smith 1995), ion microscopy which detects ion species using a mass spectrometry-based imaging technique (Chandra et al. 1999), and fluorescent probes with affinities for specific ions, e.g. aequorin which emits light upon binding with calcium (Shimomura et al. 1989; Read et al. 1993; Kendall and Badminton 1998; Shaw et al. 2001; Nelson et al. 2004). Other methods will surely become available. Each of these approaches lends tremendous opportunities for gaining a better understanding of fungal cell biology and how it is influenced by the surrounding ionic environment.

References

Adams TH, Wieser JK, Yu J-H (1998) Asexual sporulation in *Aspergillus nidulans*. Microbiol Mol Biol Rev 62:35–54

Allen EA, Hazen BE, Hoch HC, Kwon Y, Leinhos GME, Staples RC, Stumpf MA, Terhune BT (1991) Appressorium formation in response to topographical signals by 27 rust species. Phytopathology 81:323–331

Appiah AA, West P van, Osborne MC, Gow NA (2005) Potassium homeostasis influences the locomotion and encystment of zoospores of plant pathogenic oomycetes. Fungal Genet Biol 42:213–223

Baker CJ, Tomerlin JR, Mock N, Davidson L, Melhuish J (1987) Effects of cations on germination of urediniospores of *Uromyces phaseoli*. Phytopathology 77:1556–1560

Beckerman JL, Ebbole DJ (1996) MPG1, a gene encoding a fungal hydrophobin of *Magnaporthe grisea*, is involved in surface recognition. Mol Plant Microbe Interact 9:450–456

Berridge MJ, Bootman MD, Roderick HL (2003) Calcium signalling: dynamics, homeostasis and remodelling. Nat Rev Mol Cell Biol 4:517–529

Bers DM, Patton CW, Nuccitelli R (1994) A practical guide to the preparation of Ca^{2+} buffers. Methods Cell Biol 40:3–29

Bircher U, Hohl HR (1999) A role for calcium in appressorium induction in *Phytophthora palmivora*. Bot Helv 109:55–65

Braun EJ, Howard RJ (1994a) Adhesion of *Cochliobolus heterostrophus* conidia and germlings to leaves and artificial surfaces. Exp Mycol 18:211–220

Braun EJ, Howard RJ (1994b) Adhesion of fungal spores and germlings to host plant surfaces. Protoplasma 181:202–212

Broembsen SL von, Deacon JW (1996) Effects of calcium on germination and further zoospore release from zoospore cysts of *Phytophthora parasitica*. Mycol Res 100:1498–1504

Broembsen SL von, Deacon JW (1997) Calcium interference with zoospore biology and infectivity of *Phytophthora parasitica* in nutrient irrigation solutions. Phytopathology 87:522–528

Byrt PN, Irving HR, Grant BR (1982) The effect of cations on zoospores of the fungus *Phytophthora cinnamomi*. J Gen Microbiol 128:1189–1198

Cerenius L, Soderhall K (1985) Repeated zoospore emergence as a possible adaptation to parasitism in *Aphanomyces*. Exp Mycol 9:259–263

Chaky J, Anderson K, Moss M, Vaillancourt L (2001) Surface hydrophobicity and surface rigidity induce spore germination in *Colletotrichum graminicola*. Phytopathology 91:558–564

Chandra S, Leinhos GME, Morrison GH, Hoch HC (1999) Imaging of total calcium in urediospore germlings of *Uromyces* by ion microscopy. Fungal Genet Biol 27:77–87

Choi WB, Kang SH, Lee YW, Lee YH (1998) Cyclic AMP restores appressorium formation inhibited by polyamines in *Magnaporthe grisea*. Phytopathology 88:58–62

Clapham DE (1995) Calcium signaling. Cell 80:259–268

Cooksey KE (1981) Requirement for calcium in adhesion of a fouling diatom to glass. Appl Environ Microbiol 41:1378–1382

Deacon JW, Saxena G (1998) Germination triggers of zoospore cysts of *Aphanomyces euteiches* and *Phytophthora parasitica*. Mycol Res 102:33–41

Dean RA (1997) Signal pathways and appressorium morphogenesis. Annu Rev Phytopathol 35: 211–234

Dejaguin BV, Landau L (1941) Theory of the stability of strongly charged lyphobic sols and of the adhesion of strongly charged particles in solutions of electrolytes. Acta Physiochim USSR 14:633–662

Dicker JW, Turian G (1990) Calcium deficiencies and apical hyperbranching in wild type and the frost and spray morphological mutants of *Neurospora crassa*. J Gen Microbiol 136:1413–1420

Dickman MB, Buhr TL, Warwar V, Truesdell GM, Huang CX (1995) Molecular signals during the early stages of alfalfa anthracnose. Can J Bot 73:S1169–S1177

Donaldson SP, Deacon JW (1992) Role of calcium in adhesion and germination of zoospore cysts of *Pythium*: a model to explain infection of host plants. J Gen Microbiol 138:2051–2059

Doss RP, Potter SW, Chastagner GA, Christian JK (1993) Adhesion of nongerminated *Botrytis cinerea* conidia to several substrata. Appl Environ Microbiol 59:1786–1791

Elliot CG (1972) Calcium chloride and growth and reproduction of *Phytophthora cactorum*. Trans Br Mycol Soc 58:169–172

Elliott CG (1986) Inhibition of reproduction of *Phytophthora* by the calmodulin-interacting compounds trifluoperazine and ophiobolin A. J Gen Microbiol 132:2781–2786

Elliott CG (1988) Stages in oosporogenesis of *Phytophthora* sensitive to inhibitors of calmodulin and phosphodiesterase. Trans Br Mycol Soc 90:187–192

Emmett RW, Parbey DG (1975) Appressoria. Annu Rev Phytopathol 13:147–167

Epstein L, Nicholson RL (1997) Adhesion of spores and hyphae to plant surfaces. In: Carroll GC, Tudzynski P (eds) The Mycota, vol V, part A. Springer, Berlin Heidelberg New York, pp 11–25

Fischer R (2002) Conidiation in *Aspergillus nidulans*. In: Osiewacz HD (ed) Molecular biology of fungal development. Dekker, New York, pp 59–86

Fletcher J (1979) Effect of calcium chloride concentration on growth and sporulation of *Saprolegnia terrestris*. Ann Bot 44:589–594

Fletcher J (1983) An analysis of ultrastructural changes during oosphere initial development in oogonia from calcium sufficient and calcium deficient cultures of *Saprolegnia terrestris*. Ann Bot 52:31–38

Fletcher J (1988) Effects of external calcium concentration and of the ionophore A23187 on development of oogonia, oospores and gemmae in *Saprolegnia diclina*. Ann Bot 62:445–448

Fletcher M (1980) Adherence of marine microorganisms to smooth surfaces. In: Beachey E (ed) Bacterial adherence. Chapman and Hall, London, pp 143–374

Foster JW, McDaniel LE, Woodruff HB, Stokes JL (1945) Microbiological aspects of penicillin: V. Conidiospore formation in submerged cultures of *Penicillium notatum*. J Bacteriol 50:365–368

Gilbert RD, Johnson AM, Dean RA (1996) Chemical signals responsible for appressorium formation in the rice blast fungus *Magnaporthe grisea*. Physiol Mol Plant Pathol 48:335–346

Grant BR, Griffith JM, Irving HR (1986) A model to explain ion-induced differentiation in zoospores of *Phytophthora palmivora*. Exp Mycol 10:89–98

Griffin DH (1966) Effect of electrolytes on differentiation in *Achlya* sp. Plant Physiol 41:1254–1256

Griffith JM, Iser JR, Grant BR (1988) Calcium control of differentiation in *Phytophthora palmivora*. Arch Microbiol 149:565–571

Gristina AJ (1987) Biomaterial-centered infection: microbial adhesion versus tissue integration. Science 237:1588–1595

Gubler F, Hardham AR, Duniec J (1989) Characterizing adhesiveness of *Phytophthora cinnamomi* zoospores during encystment. Protoplasma 149:24–30

Hadley G, Harrold CE (1958a) The sporulation of *Penicillium notatum* Westling in submerged liquid culture. I. The effects of calcium and nutrients on sporulation. J Exp Bot 9:408–417

Hadley G, Harrold CE (1958b) The sporulation of *Penicillium notatum* Westling in submerged liquid culture. II. The initial sporulation phase. J Exp Bot 9:418–425

Hamer JE, Howard RJ, Chumley FG, Valent B (1988) A mechanism for surface attachment in spores of a plant pathogenic fungus. Science 239:288–290

Hardham AR (1992) Cell biology of pathogenesis. Annu Rev Plant Physiol Plant Mol Biol 43:491–526

Hardham AR, Gubler F, Duniec J (1991) Ultrastructural and immunological studies of zoospores of *Phytophthora*. In: Lucas JA, Shattock RC, Shaw SS, Cooke LR (eds) *Phytophthora*. Cambridge University, Cambridge, pp 50–69

Harding D (1971) Stability of silica dispersions. J Coll Interface Sci 35:172–174

Harris SD, Read ND, Roberson RW, Shaw BD, Seiler S, Plamann M, Momany M (2005) Polarisome meets spitzenkorper: microscopy, genetics, and genomics converge. Eukaryot Cell 4:225–229

Heath IB (1995) Integration and regulation of hyphal tip growth. Can J Bot 73:S131–S139

Hill AE, Grayson DE, Deacon JW (1998) Suppressed germination and early death of *Phytophthora infestans* sporangia caused by pectin, inorganic phosphate, ion chelators and calcium-modulating treatments. Eur J Plant Pathol 104:367–376

Hoch HC, Staples RC (1987) Structural and chemical changes among the rust fungi during appressorium development. Annu Rev Phytopathol 25:231–247

Hoch HC, Staples RC, Bourett T (1987a) Chemically induced appressoria in *Uromyces appendiculatus* are formed aerially apart from the substrate. Mycologia 79:418–424

Hoch HC, Staples RC, Whitehead B, Comeau J, Wolf ED (1987b) Signaling for growth orientation and cell differentiation by surface topography in *Uromyces*. Science 235:1659–1662

Hoch HC, Jelinski LW, Craighead H (1996) Nanofabrication and biosystems: integrating materials science, engineering and biology. Cambridge Unversity Press, Cambridge.

Irving HR, Grant BR (1984) The effect of calcium on zoospore differentiation in *Phytophthora cinnamomi*. J Gen Microbiol 130:1569–1576

Irving HR, Griffith JM, Grant BR (1984) Calcium efflux associated with encystment of *Phytophthora palmivora* zoospores. Cell Calcium 5:487–500

Iser JR, Griffith JM, Balson A, Grant BR (1989) Accelerated ion fluxes during differentiation in zoospores of *Phytophthora palmivora*. Cell Differ Dev 26:29–38

Israelachvili JN, McGuiggan PM (1988) Forces between surfaces in liquids. Science 241:795–800

Jackson SL, Heath IB (1989) Effects of exogenous calcium ions on tip growth intracellular calcium concentration and actin arrays in hyphae of the fungus *Saprolegnia ferax*. Exp Mycol 13:1–12

Jen CJ, Haug A (1981) Potassium-induced depolarization of the transmembrane potential in *Blastocladiella emersonii* zoospores precedes encystment. Exp Cell Res 131:79–87

Jones EBG (1994) Fungal adhesion. Mycol Res 98:961–981

Jones L, O'Shea P (1994) The electrostatic nature of the cell surface of *Candida albicans*: a role in adhesion. Exp Mycol 18:111–120

Kaminskyj SG, Day AW (1984) Chemical induction of infection structures in rust fungi II. Inorganic ions. Exp Mycol 8:193–201

Kendall JM, Badminton MN (1998) *Aequorea victoria* bioluminescence moves into an exciting new era. Trends Biotechnol 16:216–224

Kennedy MJ (1991) *Candida* blastospore adhesion, association, and invasion of the gastrointestinal tract of vertebrates. In: Cole GT, Hoch HC (eds) The fungal spore and disease initiation in plants and animals. Plenum, New York, pp 157–180

Kim Y-K, Li D, Kolattukudy PE (1998) Induction of Ca^{2+}-calmodulin signaling by hard-surface contact primes *Colletotrichum gloeosporioides* conidia to germinate and form appressoria. J Bacteriol 180:5144–5150

Krystofova S, Varecka L, Betina V (1995) The $^{45}Ca^{2+}$ uptake by *Trichoderma viride* mycelium. Correlation with growth and conidiation. Gen Physiol Biophys 14:323–337

Krystofova S, Varecka L, Betina V (1996) Effects of agents affecting Ca^{2+} homeostasis on *Trichoderma viride* growth and conidiation. Folia Microbiol (Praha) 41:249–253

Kuo KC, Hoch HC (1995) Visualization of the extracellular matrix surrounding pycnidiospores, germlings, and appressoria of *Phyllosticta ampelicida*. Mycologia 87:759–771

Kuo KC, Hoch HC (1996) Germination of *Phyllosticta ampelicida* pycnidiospores: prerequisite of adhesion to the substratum and the relationship of substratum wettability. Fungal Genet Biol 20:18–29

Kwon YH, Epstein L (1993) A 90 kDa glycoprotein associated with adhesion of *Nectria haematococca* macroconidia to substrata. Mol Plant Microbe Interact 6:481–487

Lee BN, Adams TH (1996) *fluG* and *flbA* function interdependently to initiate conidiophore development in *Aspergillus nidulans* through *brlA* beta activation. EMBO J 15:299–309

Lee YH, Dean RA (1993) cAMP regulates infection structure formation in the plant pathogenic fungus *Magnaporthe grisea*. Plant Cell 5:693–700

Lee YH, Dean RA (1994) Hydrophobicity of contact surface induces appressorium formation in *Magnaporthe grisea*. FEMS Microbiol Lett 115:71–75

Lenny JF, Klemmer HW (1966) Factors controlling sexual reproduction and growth in *Pythium graminicola*. Nature 209:1365–1366

Levina NN, Lew RR (2006) The role of tip-localized mitochondria in hyphal growth. Fungal Genet Biol 43:65–74

Levina NN, Lew RR, Hyde GJ, Heath IB (1995) The roles of Ca^{2+} and plasma membrane ion channels in hyphal tip growth of *Neurospora crassa*. J Cell Sci 108:3405–3417

Lew RR (1999) Comparative analysis of Ca^{2+} and H^+ flux magnitude and location along growing hyphae of *Saprolegnia ferax* and *Neurospora crassa*. Eur J Cell Biol 78:892–902

Liu ZM, Kolattukudy PE (1999) Early expression of the calmodulin gene, which precedes appressorium formation in *Magnaporthe grisea*, is inhibited by self-inhibitors and requires surface attachment. J Bacteriol 181:3571–3577

Magalhaes BP, Wayne R, Humber RA, Shields EJ, Roberts DW (1991) Calcium-regulated appressorium formation of the entomopathogenic fungus *Zoophthora radicans*. Protoplasma 160:77–88

Mercure EW, Leite B, Nicholson RL (1994) Adhesion of ungerminated conidia of *Colletotrichum graminicola* to artificial hydrophobic surfaces. Physiol Mol Plant Pathol 45:421–440

Moretto KCK, Barreto M (1995) Influence of some culture media on the growth and sporulation of *Alternaria solani* and of some factors on the infection frequency on tomato. Summa Phytopathol 21:188–191

Nelson G, Kozlova-Zwinderman O, Collis AJ, Knight MR, Fincham JR, Stanger CP, Renwick A, Hessing JG, Punt PJ, van den Hondel CA, Read ND (2004) Calcium measurement in living filamentous fungi expressing codon-optimized aequorin. Mol Microbiol 52:1437–1450

Nicholson RL, Epstein L (1991) Adhesion of fungi to the plant surface: prerequisite for pathogenesis. In: Cole GT, Hoch HC (eds) The fungal spore and disease initiation in plants and animals. Plenum, New York, pp 3–23

Nicholson RL, Kunoh H (1995) Early interactions, adhesion, and establishment of the infection court by *Erysiphe graminis*. Can J Bot 73:S609–S615

Ochoa JL (1978) Hydrophobic (interaction) chromatography. Biochimie 60:1–15

O'Shea P (1991) The role of electrostatic and electrodynamic forces in fungal morphogenesis and host infection. In: Latage JP, Boucias D (eds) Fungal cell wall and immune response. Springer, Berlin Heidelberg New York, pp 85–305

Pascual S, Melgarejo P, Magan N (1997) Induction of submerged conidiation of the biocontrol agent *Penicillium oxalicum*. Appl Microbiol Biotechnol 48:389–392

Pendland JC, Boucias DG (1991) Physiochemical properties of cell surfaces from the different developmental stages of the entomopathogenic hyphomycete *Nomuraea rileyi*. Mycologia 83:264–272

Perfect SE, Hughes HB, O'Connell RJ, Green JR (1999) *Colletotrichum*: a model genus for studies on pathology and fungal-plant interactions. Fungal Genet Biol 27:186–198

Pitt D, Barnes JC (1993) Calcium homeostasis, signaling and protein phosphorylation during calcium-induced conidiation in *Penicillium notatum*. J Gen Microbiol 139:3053–3063

Pitt D, Kaile A (1990) Transduction of the calcium signal with special reference to Ca^{2+}-induced conidiation in *Penicillium notatum*. In: Kuhn PJ, Trinci APJ, Jung MJ, Goosey MW, Copping LG (eds) Biochemistry of cell walls and membranes in fungi. Springer, Berlin Heidelberg New York, pp 283–298

Pitt D, Poole PC (1981) Calcium-induced conidiation in *Penicillium notatum* in submerged culture. Trans Br Mycol Soc 76:219–230

Pitt D, Ugalde UO (1984) Calcium in fungi. Plant Cell Environ 7:467–475

Queiroz MV de, Azevedo JL de (1998) Characterization of an *Aspergillus nidulans* mutant with abnormal distribution of nuclei in hyphae, metulae, phialides and conidia. FEMS Microbiol Lett 166:49–55

Read ND, Shacklock PS, Knight MR, Trewavas AJ (1993) Imaging calcium dynamics in living plant cells and tissues. Cell Biol Int 17:111–125

Rivera RN, Rodriguez DVN (1992) Effects of calcium ions on the germination of *Sporothrix schenckii* conidia. J Med Vet Mycol 30:185–195

Robson GD, Wiebe MG, Trinci APJ (1991a) Involvement of calcium in the regulation of hyphal extension and branching in *Fusarium graminearum* A 3/5. Exp Mycol 15:263–272

Robson GD, Wiebe MG, Trinci APJ (1991b) Low calcium concentrations induce increased branching in *Fusarium graminearum*. Mycol Res 95:561–565

Roncal T, Ugalde U (2003) Conidiation induction in *Penicillium*. Res Microbiol 154:539–546

Roncal T, Ugalde U, Irastorza A (1993) Calcium-induced conidiation in *Penicillium cyclopium*: calcium triggers cytosolic alkalinization at the hyphal tip. J Bacteriol 175:879–886

Roncal T, Cordobes S, Sterner O, Ugalde U (2002) Conidiation in *Penicillium cyclopium* is induced by conidiogenone, an endogenous diterpene. Eukaryot Cell 1:823–829

Rosenberg M, Kjelleberg S (1986) Hydrophobic interactions: role in bacterial adhesion. Adv Microb Ecol 9:353–393

Rudd JJ, Franklin-Tong VE (1999) Calcium signaling in plants. Cell Mol Life Sci 55:214–232

Rutter PR, Vincent B (1984) Physiochemical interactions of the substratum, microorganisms, and the fluid phase. In: Marshall KC (ed) Microbial adhesion and aggregation. Springer, Berlin Heidelberg New York, pp 21–38

Sanders D, Brownlee C, Harper J (1999) Communicating with calcium. Plant Cell 11:681–706

Sanders D, Pelloux J, Brownlee C, Harper JF (2002) Calcium at the crossroads of signaling. Plant Cell 14[Suppl]:S401–S417

Sato N (1994) Effect of some inorganic salts and hydrogen ion concentration on indirect germination of the sporangia of *Phytophthora infestans*. Ann Phytopathol Soc Jpn 60:441–447

Schmid J, Harold FM (1988) Dual roles for calcium ions in apical growth of *Neurospora crassa*. J Gen Microbiol 134:2623–2632

Sela Burrlage MB, Epstein L, Rodriguez RJ (1991) Adhesion of ungerminated *Colletotrichum musae* conidia. Physiol Mol Plant Pathol 39:345–352

Shaw BD, Hoch HC (1999) The pycnidiospore of *Phyllosticta ampelicida*: surface properties involved in substratum attachment and germination. Mycol Res 103:915–924

Shaw BD, Hoch HC (2000) Ca^{2+} regulation of *Phyllosticta ampelicida* pycnidiospore germination and appressorium formation. Fungal Genet Biol 31:43–53

Shaw BD, Kuo KC, Hoch HC (1998) Germination and appressorium development of *Phyllosticta ampelicida* pycnidiospores. Mycologia 90:252–268

Shaw BD, Kozlova O, Read ND, Turgeon BG, Hoch HC (2001) Expression of recombinent aequorin as an intracellular calcium reporter in the phytopathogenic fungus *Phyllosticta ampelicida*. Fungal Genet Biol 34:207–215

Shaw BD, Carroll GC, Hoch HC (2006) Generality of the prerequisite of conidium attachment to a hydrophobic substratum as a signal for germination among *Phyllosticta* species. Mycologia 98:186–194

Shimomura O, Musicki B, Kishi Y (1989) Semi-synthetic aequorins with improved sensitivity to calcium ions. Biochem J 261:913–920

Silverman-Gavrila LB, Lew RR (2000) Calcium and tip growth in *Neurospora crassa*. Protoplasma 213:293–217

Silverman-Gavrila LB, Lew RR (2002) An IP_3-activated Ca^{2+} channel regulates fungal tip growth. J Cell Sci 115:5013–5025

Silverman-Gavrila LB, Lew RR (2003) Calcium gradient dependence of *Neurospora crassa* hyphal growth. Microbiology 149:2475–2485

Smith PJS (1995) The non-invasive probes: tools for measuring transmembrane ion flux. Nature 378:645–646

Smith PJS, Sanger RH, Jaffe LF (1994) The vibrating Ca^{2+} electrode: a new technique for detecting plasma membrane regions of Ca^{2+} influx and efflux. Methods Cell Biol 40:115–134

Soll DR, Sonneborn DR (1972) Zoospore germination in *Blastocladiella emersonii* IV. Ion control over cell differentiation. J Cell Sci 10:315–333

Song MH, Nah J-Y, Han YS, Han DM, Chae K-S (2001) Promotion of conidial head formation in *Aspergillus oryzae* by salt. Biotechnol Lett 23:689–691

St. Leger RJ, Roberts DW, Staples RC (1989) Calcium- and calmodulin-mediated protein synthesis and protein phosphorylation during germination growth and protease production by *Metarhizium anisopliae*. J Gen Microbiol 135:2141–2154

St. Leger RJ, Butt TM, Staples RC, Roberts DW (1990) Second messenger involvement in differentiation of the entomopathogenic fungus *Metarhizium anisopliae*. J Gen Microbiol 136:1779–1790

St. Leger RJ, Roberts DW, Staples RC (1991) A model to explain differentiation of appressoria by germlings of *Metarhizium anisopliae*. J Invertebr Pathol 57:299–310

Staples RC, Grambow HJ, Hoch HC (1983) Potassium ion induces rust fungi to develop infection structures. Exp Mycol 7:40–46

Stumpf MA, Leinhos GME, Staples RC, Hoch HC (1991) The effect of pH and potassium on appressorium formation by *Uromyces appendiculatus* urediospore germlings. Exp Mycol 15:356–360

Suizu T, Tsutsumi H, Kawado A, Murata K, Imayasu S (1994) On the importance of calcium and magnesium ions in yeast sporulation. J Ferment Bioengineer 77:274–276

Suizu T, Tsutsumi H, Kawado A, Suginami K, Imayasu S, Murata K (1995) Calcium ion influx during sporulation in the yeast *Saccharomyces cerevisiae*. Can J Microbiol 41:1035–1037

Svensson E, Unestam T (1975) Differential induction of zoospore encystment and germination in *Aphanomyces astaci*, Oomycetes. Physiol Plant 35:210–216

Tani S, Yatzkan E, Judelson HS (2004) Multiple pathways regulate the induction of genes during zoosporogenesis in *Phytophthora infestans*. Mol Plant Microbe Interact 17:330–337

Terhune BT, Hoch HC (1993) Substrate hydrophobicity and adhesion of *Uromyces* urediospores and germlings. Exp Mycol 17:241–252

Thiel R, Schreurs WJA, Harold FM (1988) Transcellular ion currents during sporangium development in the water mould *Achlya bisexualis*. J Gen Microbiol 134:1089–1098

Torralba S, Heath IB, Ottensmeyer FP (2001) Ca^{2+} shuttling in vesicles during tip growth in *Neurospora crassa*. Fungal Genet Biol 33:181–193

Toti L, Viret O, Chapela IH, Petrini O (1992) Differential attachment by conidia of the endophyte *Discula umbrinella* Berk. and Br. Morelet to host and non-host surfaces. New Phytol 121:469–475

Tucker SL, Talbot NJ (2001) Surface attachment and prepenetration stage development by plant pathogenic fungi. Annu Rev Phytopathol 39:385–417

Tunlid A, Johansson T, Nordbring Hertz B (1991) Surface polymers of the nematode trapping fungus *Arthrobotrys oligospora*. J Gen Microbiol 137:1231–1240

Tunlid A, Jansson HB, Nordbring Hertz B (1992) Fungal attachment to nematodes. Mycol Res 96:401–412

Ugalde UO, Pitt D (1983) Morphology and calcium-induced conidiation of *Penicillium cyclopium* in submerged culture. Trans Br Mycol Soc 80:319–325

Ugalde UO, Pitt D (1986) Calcium uptake kinetics in relation to conidiation in submerged cultures of *Penicillium cyclopium*. Trans Br Mycol Soc 87:199–204

Ugalde UO, Virto MD, Pitt D (1990) Calcium binding and induction of conidiation in protoplasts of *Penicillium cyclopium*. Antonie van Leeuwenhoek J Microbiol Serol 57:43–50

Van Brunt J, Harold FM (1980) Ionic control of germination of *Blastocladiella emersonii* zoospores. J Bacteriol 141:735–744

Verwey EJW, Overbeek JTG (1948) Theory of the stability of lyphobic colloids – the interaction of sol particles having an electric double layer. Elsevier, New York

Virag A, Harris SD (2006) The Spitzenkörper: a molecular perspective. Mycol Res 110:4–13

Warburton AJ, Deacon JW (1998) Transmembrane Ca^{2+} fluxes associated with zoospore encystment and cyst germination by the phytopathogen *Phytophthora parasitica*. Fungal Genet Biol 25:54–62

Warwar V, Dickman MB (1996) Effects of calcium and calmodulin on spore germination and appressorium development in *Colletotrichum trifolii*. Appl Environ Microbiol 62:74–79

Wayne R (1985) The contribution of calcium ions and hydrogen ions to the signal transduction chain in phytochrome-mediated fern spore germination. PhD thesis, University of Massachussetts, Amherst

Wessels JGH (1996) Fungal hydrophobins: proteins that function at an interface. Trends Plant Sci 1:9–15

Xiao JZ, Watanabe T, Kamakura T, Ohshima A, Yamaguchi I (1994) Studies on cellular differentiation of *Magnaporthe grisea*. Physicochemical aspects of substratum surfaces in relation to appressorium formation. Physiol Mol Plant Pathol 44:227–236

Xu C, Morris PF (1998) External calcium controls the developmental strategy of *Phytophthora sojae* cysts. Mycologia 90:269–275

Yang Z, Dickman MB (1997) Regulation of cAMP and cAMP dependent protein kinase during conidial germination and appressorium formation in *Colletotrichum trifolii*. Physiol Mol Plant Pathol 50:117–127

Yokosawa R, Kuninaga S, Sakushima A, Sekizaki H (1995) Induction of oospore formation of *Aphanomyces euteiches* Drechsler by calcium ion. Ann Phytopathol Soc Jpn 61:434–438

Youatt J (1994) The toxicity of metal chelate complexes of EGTA precludes the use of EGTA buffered media for the fungi *Allomyces* and *Achlya*. Microbios 79:171–185

Youatt J, McKinnon I (1993) Manganese reverses the inhibition of fungal growth by EGTA. Microbios 74:181–196

Young DH, Kauss H (1984) Adhesion of *Colletotrichum lindemuthianum* to *Phaseolus vulgaris* hypocotyls and to polystyrene. Appl Environ Microbiol 47:616–619

Zelter A, Bencina M, Bowman BJ, Yarden O, Read ND (2004) A comparative genomic analysis of the calcium signaling machinery in *Neurospora crassa*, *Magnaporthe grisea*, and *Saccharomyces cerevisiae*. Fungal Genet Biol 41:827–841

Zhou XL, Stumpf MA, Hoch HC, Kung C (1991) A mechanosensitive channel in whole cells and in membrane patches of the fungus *Uromyces*. Science 253:1415–1417

10 Biomechanics of Invasive Hyphal Growth

N.P. Money[1]

CONTENTS

I. **Introduction** 237
II. **A Physical View of the Hypha** 237
III. **Experimental Subjects** 239
IV. **Invasive Force** 239
A. Force Measurements from Vegetative Hyphae 239
B. Fluctuations in Hyphal Force 242
V. **Substrate Resistance and Tissue-Degrading Enzymes** 242
VI. **A Simple Model of Invasive Hyphal Growth** 243
A. Outline of Model 243
B. Evidence Supporting the Model 244
1. Turgor Pressure Powers Invasive Growth 244
2. The Cytoskeleton Plays Little, if Any, Mechanical Role in the Exertion of Force by Hyphal Tips 245
3. Significance of Wall Compliance 245
VII. **Appressorial Mechanics** 246
VIII. **Conclusions and Future Research** 247
References 247

I. Introduction

Fungi meet their energetic needs by absorbing nutrients from diverse materials of biological and synthetic origin. Filamentous species elaborate colonies of branched hyphae that penetrate solid substances by a process called invasive growth. This mechanism is one of the defining characteristics of the fungi. As far as we know, the cell biological processes that operate during invasive growth are the same as those that function when fungi colonize surfaces. Polarized synthesis of plasma membrane and cell wall advances the position of the hyphal tips, and new axes of growth emerge in the form of lateral branches to generate networks of interconnected cylinders. During growth, hyphae secrete enzymes that dissolve polymers to release sugars and other small molecules that can be transported through the plasma membrane. Besides liberating nutrients, secreted enzymes are also effective at reducing the physical resistance of the material surrounding the hyphae. Experimental evidence suggests, however, that hyphae do not wholly liquify their food sources. Instead their tips push continuously, overcoming residual barriers to penetration and determining the direction taken by the colonies as they mine their food sources. This chapter is concerned with the role of mechanical factors in the process of invasive hyphal growth.

II. A Physical View of the Hypha

Hyphal growth has been described as a slow form of cellular motility with similarities to amoeboid locomotion (Pickett-Heaps and Klein 1998; Heath and Steinberg 1999). It is valuable to think about hyphae in this way, because many of the cytoskeletal structures used by amoebae to crawl over surfaces are also implemented in hyphal elongation (Geitmann and Emons 2000; Xiang and Plamann 2003). But the analogy is flawed, in the sense that the fungus moves only by growing: pre-existing material cannot move without creating new plasma membrane and cell wall. Only when the tube is extended can cytoplasm flow from elsewhere in the mycelium toward the tip. This process is particularly apparent when older portions of septate hyphae are evacuated as the tip extends and new hyphal compartments are created (Ingold 1986).

In common with all free-living cells, those of fungi are usually saltier and more sugary than their surroundings. This difference in chemical potential across the plasma membrane drives a net flux of water into the cell. If the homeostatic mechanisms that control the osmolality of the cytoplasm minimize the difference in osmotic pressure between the cell and its surroundings, then the influx of water is modest and requires little effort on the part of the

[1] Department of Botany, Miami University, Oxford, OH 45056, USA

Biology of the Fungal Cell, 2nd Edition
The Mycota VIII
R.J. Howard and N.A.R. Gow (Eds.)
© Springer-Verlag Berlin Heidelberg 2007

cell to manage its hydrostatic pressure or export water. As this slightly hypertonic cell grows, it simply remains hydrated by the slow trickle of water through its plasma membrane. If, however, the cell is much more hypertonic than its surroundings it becomes inflated by the sustained water influx and, eventually, it will burst its plasma membrane. But bursting is usually avoided because cells limit water influx in one of two ways. First, many protists export water using contractile vacuoles. Other protists, and many bacteria, plants, and fungi, protect their plasma membranes with an enveloping cell wall. As the walled cell inflates, it pushes its plasma membrane against the inner surface of the wall, and when the wall ceases to yield, the pressure in the cytoplasm rises. A difference in osmolality between the cell and its surroundings of 100 mmol kg^{-1} generates a turgor pressure of 0.25 MPa, or 2.5 atmospheres (atm.), which is comparable to the pressure in a bicycle tire. Fungal hyphae are highly pressurized cells, pumped to a few atmospheres of pressure by osmosis, and the cytoplasm is expelled explosively if the cell wall ruptures. This turgid quality of hyphae has always impressed investigators, but its importance in growth has been an issue of longstanding debate (Reinhardt 1892; see Sect. VI.B.1.).

Turgor exerts an equal force over every portion of the plasma membrane and inner surface of the cell wall. None of this pressure is exerted against the material surrounding the cell – the substrate though which the fungus is growing – unless the wall relaxes and has some freedom to expand. Because cell wall expansion is greatest at the hyphal apex, this is the region where the hypha exerts the highest proportion of its turgor against the substrate. This makes a great deal of mechanical sense, of course, for a cell that acts as an elongated mining device. But it is important to avoid inappropriate metaphors when describing hyphae: they do not operate like needles or drill bits. When a needle is pushed, the force acting along the shaft is concentrated at the tip. In other words, the force per unit area, or pressure, at the tip is far greater than the pressure acting over the wider cross-section of the needle shaft. The sharper the tip, the greater the amplification of pressure. For a hypha, there is no such increase in pressure at the cell apex. If the turgor in the hypha is 0.25 MPa, then the same force per unit area is exerted over every square micron of the cell wall's inner surface. By controlling the plasticity of its wall, this cell has the capacity to exert pressures between zero and 0.25 MPa against the substrate, but never anything greater.

The final consideration in relation to physical principles is the importance of adhesion. Unless the fungal hypha is secured to something behind its apex as it pushes against its food source, extension pushes the filamentous cell away from its growth substrate rather than into it (Money 2004). The adhesion of fungal pathogens to plant cuticle has been studied in some detail (Braun and Howard 1994; Tucker and Talbot 2001), and the strength with which spores and yeast cells bond to mica and glass surfaces has been measured using atomic force microscopy (Bowen et al. 2000a, b; Pouliot et al. 2005). In the AFM experiments by Bowen and colleagues, conidia of *Aspergillus niger* were immobilized on the instrument's cantilever, using glue. The spores were then maneuvered to touch a test surface and were held in contact with this for a few seconds. Finally, the cantilever was retracted and the force required to separate the cell from the surface was measured. This experiment was performed in air and in salt solutions. The adhesive force was substantially greater in air, in which conidia resisted detachment from surfaces until they were disturbed by a force of approximately 45 nanonewtons (nN). Pouliot et al. (2005) made comparable measurements in *Aureobasidium pullulans*, but they determined the force necessary to break contact between the cantilever and the cell surface. Again, the adhesive forces were in the nanonewton range. These experiments quantified the adhesiveness of the spore, and yeast cell surface, in these fungi, but probably underestimated the strength with which spores and germlings of some fungi bond to surfaces prior to invasive growth. For example, in the case of the rice blast fungus, *Magnaporthe grisea*, there are at least three separate steps in the adhesion of the pathogen to the leaf surface prior to invasive growth: (1) mucilage exuded from one end of the conidium sticks the spore to the leaf surface at the moment of contact (Hamer et al. 1998), (2) following germination, secreted adhesive glues the germling to the cuticle, and (3) the appressorium – the organism's infection platform – becomes tightly bonded to the leaf through the formation of a discrete ring of powerful adhesive (Howard and Valent 1996; Ebata et al. 1998). Although *M. grisea* is particularly adept at physical penetration of its host (see Sect. VII.), other fungi execute comparable programs of gluing events as they colonize their food sources.

III. Experimental Subjects

Since the publication of the first edition of this volume of *The Mycota* in 2001, significant progress in understanding the mechanics of invasive growth has come from the extension of experiments on oomycete water molds (Kingdom Straminipila) to species in Kingdom Fungi. The range of hyphal sizes among these microorganisms is illustrated in Fig. 10.1. The first measurements of hyphal turgor pressure using a device called the pressure probe were made from the large hyphae of water molds (Money 1990). The smaller hyphae of ascomycete and basidiomycete fungi represent a significantly greater challenge for investigations with the pressure probe, but Lew and colleagues had success in working with *Neurospora crassa* (Lew et al. 2004). Measurements of the forces exerted by hyphae of water molds and fungi have also been made using strain gauges, and additional inferences about turgor have come from experiments using other techniques. These experiments are detailed in the following section. The available evidence shows that the hyphae of the oomycete water molds and fungi have remarkably similar mechanical properties. This resemblance reflects the deep convergence that occurred during the evolution of hyphal microorganisms (Money et al. 2004).

IV. Invasive Force

A. Force Measurements from Vegetative Hyphae

It is important to underscore the difference between measurements of turgor pressure and measurements of the pressure exerted by hyphal apices. If hyphae of a particular fungus are pressurized to 0.3 MPa (3 atm), then the plasma membrane pushes against every 1 μm^2 patch of the inner surface of the cell wall with a force of 0.3 μN (because 0.3 MPa = 0.3 $\mu N\,\mu m^{-2}$). If the wall is rigid, this internal pressure is not "felt" by the material in contact with the outer surface of the wall. But once the wall yields, some proportion of the turgor is exerted against the substrate. Turgor represents the maximum pressure that a hypha can exert. The hypha can only exert all of its internal pressure during invasive growth if it renders its wall so fluid that it no longer offers any opposition to turgor. In principle, this may happen when the hyphal tip is protected from rupture by the hardness of its surroundings. Wall yielding must be subjected to exquisite control during growth. For the hypha to extend, its wall must yield enough to permit turgor to overcome the resistance of the substrate; but if the wall is loosened beyond the point needed to penetrate the substrate, the hyphal wall may fracture. Errors in this control mechanism can often be seen by looking at agar cultures of fungi that are shocked by transfer from a warm or cool incubator to room temperature: tips burst and hyphae bleed cytoplasm into the medium. The available experiments with strain gauges suggest that modest yielding of the hyphal wall usually occurs at the tip, enabling the fungus to wield up to 50% of its turgor for invasive purposes without bursting. The issue of wall yielding is discussed further in Sect. VI.

Experiments with miniature strain gauges are difficult and the results require careful interpretation. The trickiness comes from the sensitivity of the instruments needed to measure the tiny forces exerted by single microscopic hyphae. The devices used in fungal experiments have a flat silicon beam with a thickness of 0.1 mm and width of 10 mm. The strain gauge is clamped in a vertical orientation and the hypha is allowed to push against the beam (Fig. 10.2A,C). The fact that a hyphal tip with a 10 μm diameter pushes against just 1/1000th of the beam's width with a force of only a few millionths of 1 N illustrates the complexity of the experiments. Nevertheless, using a carefully calibrated strain gauge and a remote-controlled micromanipulator, reproducible measurements of the forces exerted by hyphae have been obtained. For understanding the invasive process, estimates of applied pressure are far more meaningful than those of force, because applied pressures can be compared with turgor measurements and with data on substrate strength. The pressures are estimated from the measured forces by dividing the force (μN) by the contact area (μm^2) between the hypha and the strain gauge. The reliance upon the estimated contact area is a potential source of error, because the region of the cell wall touching the silicon beam is usually obscured by the "vastness" of the beam in comparison with the hypha. For a comparable challenge, consider the difficulty in photographing a finger tip pushing a door bell when you're peering down from the roof of a house.

Table 10.1 provides biomechanical data from the fungus *Mucor hiemalis* (Zygomycota) and the water mold *Thraustotheca clavata* (Oomycota). In

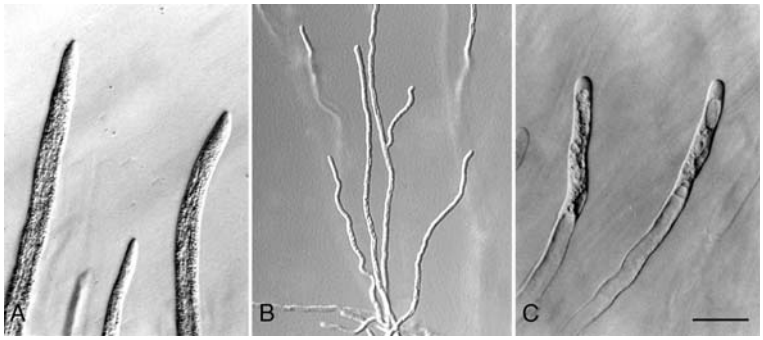

Fig. 10.1. Range of hyphal size among fungi and oomycete water molds. **a** The saprobe *Achlya bisexualis* (Saprolegniaceae, Oomycota) produces non-septate hyphae with acute apices (maximum diameter of the pair of largest hyphae is 23 µm). **b** Hyphae of *Magnaporthe grisea* (Ascomycota), the rice blast fungus, are less than 5 µm in diameter, typical of ascomycete and basidiomycete species. Image kindly supplied by Timothy M. Bourett and Richard J. Howard, DuPont Co. **c** *Basidiobolus microsporus* is a member of the family Entomophthoraceae (Zygomycota) that includes many important insect pathogens. Hyphal diameter in this image is 18 µm. *Bar* 50 µm

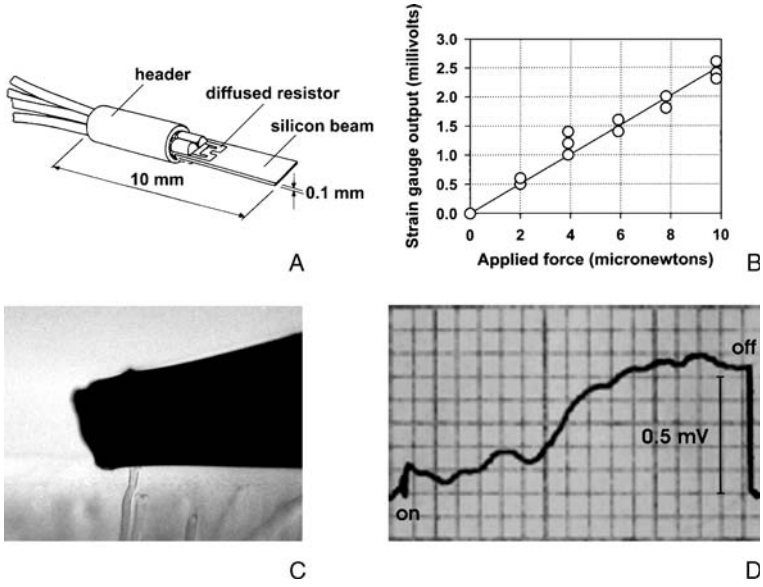

Fig. 10.2. a Diagram of miniature strain gauge used to measure the force exerted by individual hyphae (adapted from technical literature from Sensor One Technologies Corp., Sausalito, Calif.). **b** Calibration curve showing relationship between applied force and strain gauge output voltage. During calibration, force is controlled by placing µg and mg masses on the end of the silicon beam of a strain gauge that is clamped in a horizontal orientation. **c** Hypha of *Allomyces macrogynus* (Chytridiomycota) pushing against the silicon beam of the strain gauge. A single tip of a hypha that is growing within agar has extended from the edge of the solid medium into a well filled with nutrient broth. For scale, note that the width of the silicon beam is 0.1 mm. **d** Example of a force recording from single *Allomyces macrogynus* hypha; *on* marks the time (t = 0) when the hyphal apex contacted the silicon beam; *off* marks the time (t = +3 min) when the strain gauge was moved away from the hypha, resulting in an immediate drop in instrument output to the baseline voltage. In this case, the peak strain gauge output was 0.6 mV, which corresponded to an applied force of 2.4 µN (refer to **b**). Since the area of the hyphal tip in contact with the silicon beam was 80 μm^2, the estimate of applied pressure for this cell was 0.03 N μm^{-2} (= 0.03 MPa = 0.3 atm)

a published survey of 13 species of basidiomycetes, ascomycetes, zygomycetes, chytridiomycetes, and oomycete water molds, hyphal turgor ranged over 0.21–0.85 µN μm^{-2} (or MPa) and mean applied pressures ranged over 0.04–0.09 µN μm^{-2} (Money et al. 2004). These applied pressures represented a maximum of 54% of the available turgor pressure. Smaller hyphae exerted less force than larger cells,

Table. 10.1. Comparison between the biomechanical characteristics of hyphae of a zygomycete fungus and an oomycete water mold. Turgor measurements were made with a pressure probe and by vapor pressure deficit osmometry, and force measurements were made with a miniature strain gauge. Data are shown as means ± standard error, with number of replicates in parentheses. ANOVA showed a significant difference (*) in turgor ($P < 0.005$), but no significant difference (*NS*) between the pressures applied by the two species ($P = 0.37$). From Money (2004), with permission from Elsevier

Organism	Turgor pressure (MPa)	Applied force (μN)	Contact area (μm^2)	Applied pressure ($\mu N\ \mu m^{-2}$ or MPa)[c]	Ratio of applied pressure to turgor
Mucor hiemalis[a] Kingdom Fungi, Phylum Zygomycota	0.58 ± 0.01 (12)	2.1 ± 0.4 (24)	52 ± 13 (24)	0.05 ± 0.01 (24)	0.09
Thraustotheca clavata[b] Kingdom Straminipila, Phylum Oomycota	0.69 ± 0.02 (9)*	9.8 ± 3.5 (21)	166 ± 42 (21)	0.06 ± 0.01 (21)^{NS}	0.09

[a] Cells cultured in potato dextrose agar and broth.
[b] Cells cultured in peptone/yeast extract/glucose agar and broth.
[c] Individual measurements of force were paired with individual measurements of contact area, providing an estimate of applied force for each hypha. Mean values for applied pressure were obtained from these data, not by division of mean force (column 3) by mean contact area (column 4).

but in terms of pressure (force per unit area), differences between species were trivial.

Experiments with strain gauges may underestimate the maximum pressures exerted by hyphae. This possibility is underscored by the observation that hyphal tips change shape when they make contact with the silicon beam of the instrument. Clearly, the mechanical properties of the hyphae are altered by the experiment. If the hyphae of some species are left in contact with the beam for many minutes, they reorient their growth axis, or form branches, and grow around the obstruction. But what is encouraging, given the limitations of the method, is the fact that the estimates of the applied pressure never exceed the levels of turgor pressure. Applied pressures are always some fraction of turgor. If the applied pressures were higher than turgor pressures, we would need to revisit our hypothesis about the origin and control of invasive force.

Besides the strain gauge experiments, other techniques have been used to measure the forces exerted by hyphae. Wright et al. (2005) used optical tweezers to measure the forces applied by hyphal tips of *N. crassa*. In these experiments, polystyrene beads with diameters of 1 μm and 4 μm were positioned in the paths of extending hyphae and trapped using a laser (Fig. 10.3). The force required to push a bead from its trapped location was proportional to its size: a higher force (in the piconewton range) was necessary to disturb a larger bead. Even at full laser power, producing the strongest trap, the hyphae displaced the beads. Because the strength of the optical trap was limited to the piconewton range, the observed displacement of the beads was predictable from the measurement of forces of 0.4–3.2 μN from *N. crassa* hyphae (Money et al. 2004). The optical trapping experiments are significant, however, because they confirmed the exertion of force by single hyphae using an independent method.

Other important experiments that provided new information on hyphal mechanics employed atomic force microscopy. Ma et al. (2005) probed the surface of *Aspergillus nidulans* hyphae and detected differences in structure and viscoelasticity between the growing apex and the distal, mature regions of hyphae. Apical walls were more

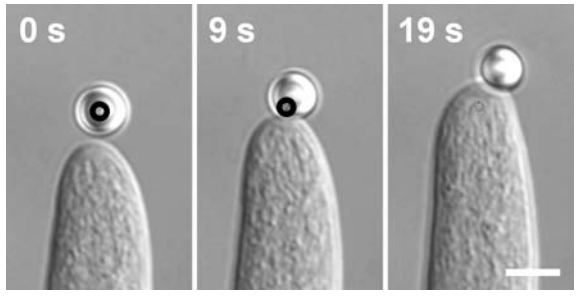

Fig. 10.3. Time course of a growing hypha of *Neurospora crassa* pushing a 4 μm polystyrene bead from a 70 mW laser trap. The *black circle* indicates the position of the trap. *Bar* 5 μm. From Wright et al. (2005)

compliant than sub-apical regions of the cell. These data are consistent with patterns of wall failure observed when hyphae are subjected to osmotic shock or microinjected with silicone oil to measure the tensile strength of their walls (Money and Hill 1997; Walker et al. 2006).

B. Fluctuations in Hyphal Force

Fluctuations in the forces exerted by hyphae have been detected using the strain gauge method described in the previous section (Johns et al. 1999). These changes are most evident in recordings from the large hyphae of oomycete water molds that push against the silicon beam with a maximum force of 100 μN, but they have also been observed in species from Kingdom Fungi. Any pulses in force produced by smaller hyphae are invisible against the background of the recordings because the total force exerted by these cells is so close to the limits of resolution of the instrument. For some time, vigorous debate has surrounded the phenomenon of pulsatile growth in fungi.

There is consensus among plant scientists that pollen tubes grow in a pulsatile fashion, cycling through periods of relatively fast extension interspersed by periods of slower growth (Hepler et al. 2001). Correlations have been observed between these growth pulses and changes in intracellular pH and calcium concentration, though causality in these links is unproven. Pulses in the rate of hyphal extension have also been reported, but some authors suggest that these are artifacts of optical technique rather than evidence of erratic growth (López-Franco et al. 1994; Jackson 2001; Sampson et al. 2003). The force measurements are consistent with the presence of growth pulses among fungi. But, because the hyphal tip is pushing against the strain gauge in these experiments, it is also possible that the fluctuations in force are an abnormal response by cells that are compelled to push against a fixed silicon beam. The demonstration of oscillations in force during basidiome extension is consistent with the proposed growth pulses in hyphal growth, because fruiting bodies are constructed from hyphae, but the possibility of experimental artifact cannot be ruled out in this case either (Money and Ravishankar 2005). Geitmann (2006) has suggested that pulses in force may assist tip-growing cells of plants and fungi in their invasive activities in some fashion comparable to the action of a jackhammer.

V. Substrate Resistance and Tissue-Degrading Enzymes

The synergistic roles of enzyme action and physical penetration in the invasive growth process has been assumed for decades. Long before the twentieth century discovery that enzymes are proteins, Anton de Bary discussed the "secretion of solvents" that would assist parasitic fungi during the penetration of plant cell walls and insect cuticles (de Bary 1866). Reflecting the intense interest in the chemistry of alcoholic fermentation at this time, he likened these solvents to the "ferments" involved in respiration. Manabu Miyoshi (1895) conducted the first experiments to test the importance of mechanical force during the penetration of plant tissues. He showed that *Botrytis cinerea* could penetrate collodion gel (cellulose nitrate), gold leaf, slivers of mica, and other materials (Fig. 10.4). By comparing the strength of these substances with the mechanical properties of onion epidermis and *Tradescantia* leaves, Miyoshi suggested that fungi were capable of direct physical penetration of plant tissues. His 1895 paper provided measurements of substrate strength made by piercing various materials with glass needles: he estimated that a pressure of 0.35 MPa was needed to penetrate onion epidermis; *Tradescantia* leaves were tougher, requiring a pressure of 0.49 MPa; and 0.18-mm-thick collodion gel resisted penetration until the pressure increased to 0.74 MPa. Miyoshi had no idea how hyphae could exert force, only that they must do so to grow invasively. Modern studies support and extend his conclusions. Miyoshi's pressure estimates are somewhat higher than the applied pressures reported by the strain gauge, but they do fit nicely within the range of turgor pressures measured from the hyphae of other fungi (Money et al. 2004). As mentioned earlier (Sect. IV.A.), growth against a fixed silicon beam is an artificial challenge, and hyphae probably apply more of their turgor when they are buried in their natural substrates. The importance of mechanical penetration in *B. cinerea* is further supported by recent experiments showing that mutant strains of the fungus lacking cutinase and cutinolytic lipase activity penetrate intact leaves and flowers of various species and show no reduction in pathogenicity (Reis et al. 2005). Miyoshi's work ranks among the landmarks in the history of plant pathology, both for its technical brilliance and for insightfulness.

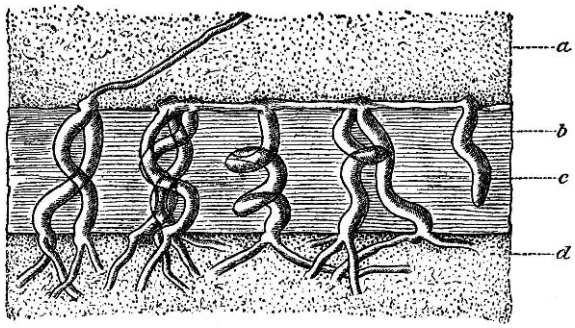

Fig. 10.4. Classic illustration from Miyoshi (1895) showing hyphae of *Botrytis cinerea* (*c*) penetrating a thin film of collodion gel (*b*) sandwiched between layers of gelatin (*a*, *d*). Note that the hyphae show swellings at the interface between the upper layer of gelatin and the collodion. These swellings may be indicative of wall loosening that occurred when the hyphae encountered the collodion barrier. Loosening of the hyphal wall increases the force exerted by the cell

Twenty-first century measurements of substrate resistance have been made by attaching glass probes and steel needles to strain gauges and monitoring the forces required to pierce a variety of tissues (Fig. 10.5). This higher-tech version of Miyoshi's experimental method was used to measure the mechanical resistance of grass roots and mammalian skin tissue to invasion by *Pythium* species. Root epidermal cells of wheat seedlings resisted penetration until pressures of 2.3–11.8 MPa were applied at the tips of glass microprobes; the strength of root epidermis of creeping bentgrass varied from 1.1 MPa to 9.6 MPa (MacDonald et al. 2002). Hyphae of the pathogen *Pythium graminicola* exerted a mean pressure of 0.2 MPa, suggesting that secreted enzymes must effect at least a 10-fold reduction in cell wall resistance to allow invasion. A similar conclusion was reached in the analysis of the mechanical barrier presented by intact human and equine skin to invasion by *Pythium insidiosum* (Ravishankar et al. 2001). While it seems certain that these oomycetes rely upon enzymes to reduce tissue resistance, these experiments also highlighted the significance of wounding of host tissues, and the attendant softening of infection barriers, as a stimulus for colonization. Interestingly, a comparative study of *Pythium* species showed no relationship between their secreted protease activity, preferred carbon sources in culture, and natural growth substrates (Davis et al. 2006). Solomon et al. (2003) pointed out that our understanding of pathogenesis would benefit greatly from studies that identify specific nutrients that sustain the growth of fungi on their hosts.

In summary, the available data suggest that the relative importance of enzymes versus mechanical force varies according to the mechanical obstacles encountered by the growing fungus. This means that hyphae must display considerable mechanical flexibility in response to physical changes in the microenvironment in which they insinuate themselves. This takes us to the following simple model of invasive hyphal growth.

VI. A Simple Model of Invasive Hyphal Growth

A. Outline of Model

The biomechanics of invasive growth can be considered on a number of different levels. If we re-

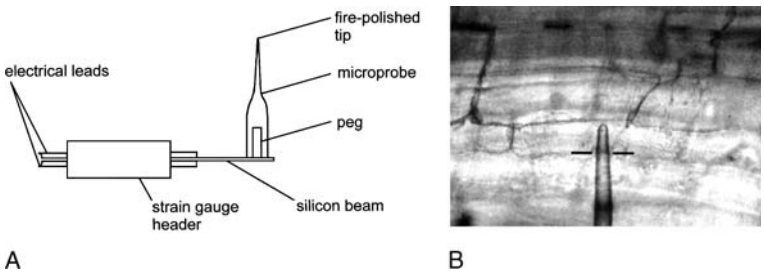

Fig. 10.5. Microprobe system for estimating substrate resistance to hyphal penetration. **A** Microprobe attached to miniature strain gauge system shown in Fig. 10.2A. The silicon beam is shown in profile. A cylindrical peg is glued to the flat surface of the beam and glass microprobes of various sizes are slipped onto its free end as shown. **B** Penetration of a root epidermal cell of a creeping bentgrass seedling with a glass microprobe with tip diameter of 5 µm. The short black lines highlight the position of the plant cell wall surrounding the point where it is pierced by the pipet tip. Adapted from MacDonald et al. (2002)

strict our purview to a straightforward rendering of the primary variables that control how much force, or pressure, a hypha exerts at its tip, the process is easily grasped. The osmotically generated turgor pressure within the hypha (Ψ_p) is the maximum pressure that the cell can exert against its surroundings. The maximum force is determined by the area over which this pressure acts. If a hypha with a turgor pressure of 0.5 MPa, and diameter of 5 µm, pushes against the epidermal cells of a plant over a tip area (A) of 20 µm^2, the total force available to this cell is 10 µN. Because the force that the cell actually exerts (F_{inv}) must be governed by the degree to which the wall at its apex relaxes, it can only employ the full 10 µN if the wall offers zero resistance to expansion. In this hypothetical case, the resistance of the wall, or its yield threshold (Y) is zero. If the wall is less plastic, and does not yield until the pressure exceeds 0.25 MPa (i.e., Y = 0.25 MPa), and then yields completely, then the actual force with which this hypha presses against the substrate is reduced to 5 µN. If we assume that the force exerted by the cytoskeleton is dwarfed by turgor pressure (see Sect. VI.B.2.), then we can reasonably model the invasive pressure (force per unit area) with the following simple equation:

$$P_{inv} = \Psi_p - Y \quad (10.1)$$

In reality, the behavior of the wall is probably more subtle and it continues to dampen the force exerted by the tip, to a greater or lesser degree, after the internal pressure exceeds its yield threshold. For this reason, the model is better expressed with the following equation:

$$P_{inv} = \Psi_p \cdot y \quad (10.2)$$

where y = wall compliance, reflecting the damping of invasive pressure due to the degree of wall yielding (expressed as a fraction). If, for example, the cell wall always absorbs 30% of the turgor before yielding, y = 0.7. Figure 10.6 illustrates this theoretical relationship between turgor and wall compliance. The mechanism is likely complicated further by non-linearity of the relationship between y and turgor (i.e., if Ψ_p and y are dependent variables). Nevertheless, this simple rendering of the model is useful because it focuses attention upon the mechanical variables – namely turgor and wall strength – that are of most practical significance to investigators of invasive growth. A decade after the first exposition of this basic idea (Money 1995), the experimental evidence in its favor has strengthened.

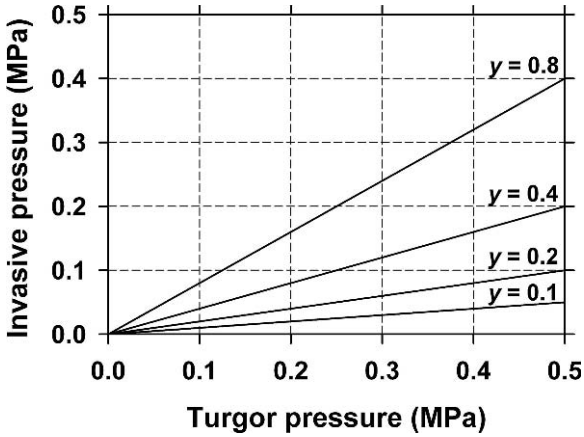

Fig. 10.6. Plot illustrating theoretical relationship between turgor pressure, wall compliance (y), and the pressure exerted by the hyphal apex. Loosening of connections between stress-bearing polymers within the cell wall increases y and boosts the pressure exerted by the hyphal tip, even if turgor remains constant

B. Evidence Supporting the Model

1. Turgor Pressure Powers Invasive Growth

Evidence showing that turgor powers invasive growth comes from a variety of observations. First, osmotic stress experiments, performed on hyphae of the oomycete water mold *Achlya bisexualis*, demonstrated that the force exerted by the hyphal apex is derived from turgor (Money et al. 2004). As a testimonial to the role of turgor this is indirect, because we must infer that the turgor-derived force *is* utilized during invasive growth. But the case is clinched by the observation that osmotic stress, and the accompanying reduction in hyphal turgor pressure, has an inhibitory effect upon invasive growth. The strongest experiments of this kind also involve water molds, whose sluggish response to dehydration allows the investigator to control their turgor by altering the osmolality of their growth medium (Money 1997a; Lew et al. 2004). Hyphae with their usual 0.4–0.7 MPa of turgor seem to push through a solid medium like knives through warm butter. But bereft of pressure, the cells loosen their walls, abandon their usual streamlined form, and squirm, obesely, over the agar surface. Related experiments have quantified the effects of turgor reduction upon the penetration of materials of defined hardness including agar medium of varying gel strength and synthetic materials, including thin Mylar films. These investigations extend the conclusions drawn from the water molds to ascomycetes, including the

rice blast fungus, *M. grisea* (Howard et al. 1991), and the human pathogen *Wangiella dermatitidis* (Brush and Money 1999). Together, these observations serve as critical indicators of the function of hyphal turgor pressure. They establish the fact that only modest pressure (on the order of a few tenths of 1 atm) is necessary to distend the cell surface (once it is loosened) and that the high levels of turgor characteristic of most growing hyphae are needed only for invasive purposes. This argument is detailed by Money (2001). The oft-repeated statement that "turgor drives growth" scratches the surface of an important concept and is responsible for a great deal of misinformation about fungal development. Recent analysis of the importance of turgor in shaping plant and fungal cells is given by Bartnicki-Garcia et al. (2000), Harold (2005) and Mathur (2006). In addition, Charras et al. (2005) present evidence for the generation of cytoplasmic pressure gradients in animal cells, which raises the possibility that turgor may vary along the length of a hypha in response to fluctuations in extension rate and the formation of branches.

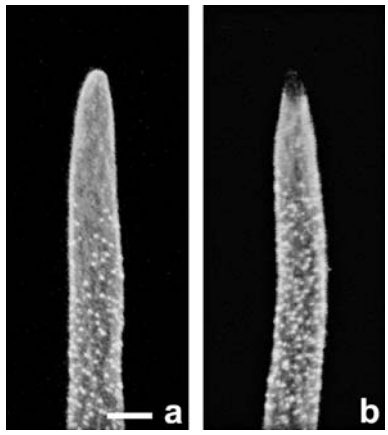

Fig. 10.7. Confocal images of F-actin distribution in hyphae of the oomycete *Achlya bisexualis* growing: **a** non-invasively, **b** invasively. Cells stained with Alexa Fluor 488 conjugated to phalloidin. Most non-invasive cells have a prominent cap of actin at their tips and more diffuse fibrils and plaques in their sub-apical regions (**a**). The apices of most invasive cells lack an actin cap (**b**). *Bar* 10 µm. From Walker et al. (2006), with permission from Elsevier

2. The Cytoskeleton Plays Little, if Any, Mechanical Role in the Exertion of Force by Hyphal Tips

The polarized extension of actin microfilaments accompanies the growth of hyphae (Heath 2000; Walker and Garrill 2006). It has been suggested that this process may play some role in distending the plasma membrane and cell wall, particularly under conditions of low turgor pressure (Money 1997a; Heath and Steinberg 1999). This is supported by altered patterns of actin distribution in the hyphae of water molds subjected to osmotic stress (Harold et al. 1996). But recent work argues for a different conclusion. Walker et al. (2006) compared the actin distribution in fully pressurized hyphae of the oomycetes *Achlya bisexualis* and *Phytophthora cinnamomi* growing invasively, through agar, and non-invasively on the agar surface. They reported that cells growing invasively, and therefore "needing" to exert higher pressures to sustain growth, were more likely to exhibit an actin-free zone at their apices (Fig. 10.7). The authors suggested that this may reflect the cytoskeleton's role in controlling the expansion of the apical cell wall. In other words, the depletion of actin within the tips of invasive cells would result in greater yielding of the wall and the exertion of a higher proportion of the turgor pressure against the material in advance of the hyphal tips. According to these elegant experiments, protrusive force and pressure (F_{inv}, P_{inv}) would increase in proportion to actin depletion rather than enrichment. The role of actin as a restraint for tip expansion is further indicated by the hyphal swelling that follows cytoskeletal disruption in the zygomycete *Gilbertella persicaria* (Grove and Sweigard 1980) and the ascomycete *Geotrichum candidum* (Heath et al. 2003), and by observations on *dis* mutants of *Arabidopsis* that show distorted trichomes (Mathur 2006).

3. Significance of Wall Compliance

The compliance of the cell wall governs the amount of the internal turgor that acts upon the material surrounding the cell apex. Theoretically, this exerted pressure can range between zero and 100%. In experiments, variations in wall compliance between different species apply 9–54% of the available turgor against the flat silicon beam of a strain gauge but, as argued earlier, it seems likely that this percentage can rise further under more natural conditions. The control of hyphal wall compliance is best understood in oomycete water molds (Money and Hill 1997). Yielding of their cellulosic walls is controlled, at least in part, by secreted 1,4-β-D-glucan glucan hydrolases. These enzymes are thought to cleave cross links between the cellulose microfibrils in the wall.

VII. Appressorial Mechanics

The tips of the hyphae of many pathogenic fungi are transformed into specialized invasive structures called appressoria on the surfaces of plant and invertebrate hosts. Appressoria often form at the tips of germ tubes shortly after spore germination, but similar structures also develop from branches within a vegetative mycelium. According to some researchers, the latter cells should be called hyphopodia, but this distinction is not accepted by everyone. In most respects, the invasive mechanism employed by appressoria duplicates the penetration of mechanical obstacles by vegetative hyphae: the pathogen pierces the host surface by exerting force at the tip of a filamentous hypha (see Fig. 11.8 in this volume, Chap. 11). But there are some important differences. The formation of an appressorium allows the fungus to: (1) adhere very tightly to the host surface, (2) re-orient its direction of growth through an angle of 90 °, and (3) exert much larger forces than those wielded by vegetative cells. Appressoria seem to have evolved as a cellular strategy for overcoming particularly resistant barriers to invasion. The melanized appressoria of the rice blast pathogen, *Magnaporthe grisea*, and species of *Colletotrichum*, have been the subject of the majority of studies, but appressoria of other phytopathogens (Pryce-Jones et al. 1999) and invertebrate pathogens (Holland et al. 1999) have also been examined from a biomechanical perspective.

Appressorial development and function has been addressed in a number of excellent reviews (Howard and Valent 1996; Howard 1997; Deising et al. 2000; Talbot 2003; Wang et al. 2005; Hardham, Chap. 11 in this volume). Briefly, the tip of the germ hypha stops extending in response to cues on the host surface, swells, and affixes itself to the host through the secretion of an adhesive. These processes are accompanied by the conversion of insoluble storage carbohydrates and lipids into lower molecular weight compounds, including glycerol, that boost the osmotic pressure of the appressorial cytoplasm (Thines et al. 2000; Weber et al. 2001). In melanized appressoria, pigment is deposited in a discrete layer under the microfibrillar cell wall, greatly reducing the permeability of the cell surface (Howard and Ferrari 1989). The mode of action of the appressorial melanin remains uncertain, but it seems that the presence of the pigment reduces osmolyte leakage from the cytoplasm during a period of increasing hydrostatic pressure (Money 1997b). Finally, a slender hypha – termed the "penetration hypha" or "penetration peg" – elongates from the base of the appressorium and pushes through the underlying host structure. The infection process is referred to as "direct penetration", to distinguish the mechanism from the (presumably) less strenuous "indirect" entry of fungi through stomata or other natural apertures. For the melanized appressoria of *M. grisea* and *Colletotrichum* species there is no clear evidence that host penetration is aided through the secretion of enzymes (Wirsel et al. 2004). The faster penetration of rice leaves in comparison with synthetic materials hints at the significance of enzymes for *M. grisea* (Howard et al. 1991), but it is possible that penetration is a purely mechanical process. Cell wall-degrading enzymes may prove more important for fungi that form non-melanized appressoria. The localized secretion of cellulase by the tips of the penetration hyphae of the powdery mildew *Blumeria graminis* f. sp. *hordei* supports this conclusion (Pryce-Jones et al. 1999).

The enormous pressures generated by appressorial osmosis have been estimated by deflating the cells in polyethylene glycols and other compounds (Howard and Ferrari 1989; Howard et al. 1991) and by determining the melting point of ice crystals within the appressorial cytoplasm (Money and Howard 1996). These experiments suggest that turgor may rise to as much as 8.0 MPa, or 80 atm, in *M. grisea*. This record turgor estimate is consistent with force data derived from laser-based measurements of the depth of impressions made by appressoria in a metal film supported by silicone gel (Bechinger et al. 1999). These experiments show that the penetration hyphae of *C. gramincola* exert an average force of 17 μN, which corresponds to an applied pressure of 5.4 MPa for a flattened tip with a 2 μm diameter (or 8.0 MPa for a 1.6 μm tip). The ability of the fungus to pierce synthetic surfaces of varying composition and hardness provides an independent measure of appressorial strength. Experiments with thin sheets of Mylar showed that *M. grisea* was capable of penetrating substrates with hardnesses ranging from 140 MPa to 250 MPa (Howard et al. 1991). The obvious mismatch between the measurements of Mylar hardness and appressorial turgor presents a conundrum, but it is not clear how the hardness data obtained by macroscopic indentation correspond to the obstacles encountered by fungi on the microscopic scale (Goriely and Tabor 2006).

The unusual mechanical prowess exhibited by foliar pathogens of grasses may reflect the hardness

of the silicified leaves of these plants coupled with their innate resistance to enzymatic digestion. In other words, the durability of cereal leaves may have driven the evolution of high turgor among their pathogens.

VIII. Conclusions and Future Research

From a biomechanical viewpoint, the hyphae of oomycete water molds, basidiomycetes, and other fungal taxa behave in a very similar fashion. Osmosis pressurizes them to the same levels of turgor, and by loosening their cell walls they exert some proportion of their internal pressure against the material in contact with their growing tips. The operation of a common invasive mechanism among water molds and fungi (and, probably, pollen tubes) offers a beautiful example of convergent evolution. The importance of enzymes in reducing the mechanical resistance of the solid materials penetrated by fungi has been quantified in a few instances. This work has provided a reasonably satisfactory picture of the mutual mechanical roles of turgor and enzymes in the fungal colonization of solid substrates. Genomic investigations have greatly accelerated the task of identifying the secreted enzymes that enable fungi to degrade plant polysaccharides and other polymers, but it is unclear which of these proteins has the greatest effect upon the mechanical obstacles to colonization. Many of the secreted enzymes are likely to perform dual roles of barrier-weakening and nutrient solubilization as hyphae permeate their solid food sources.

There are a number of unanswered questions about invasive growth whose inherent interest and practical significance demands study along the lines discussed in this chapter. Further experimentation with instruments such as the atomic force microscope are likely to yield a more detailed picture of the way in which hyphae exert pressure, and mathematical modeling will help clarify how the hyphal wall is modified to govern the exertion of hydrostatic force. The insights about fungal development that have come from investigations on the melanized appressoria of *M. grisea* and *Colletotrichum* species encourage research on the appressoria of other fungi. The process of strand and rhizomorph extension in basidiomycetes is another subject that deserves intensive biomechanical study (Fig. 10.8). The remarkable invasive ability of these multi-hyphal organs is a subject for future experimentation that seems likely to produce data of practical significance. By understanding how hyphae bundle during the formation of these structures, and how they extend in a cooperative fashion, it will be possible to elaborate upon a decade of research on tip growth at the single cell level to understand the spread of wood-decay fungi and phytopathogens through forest soils.

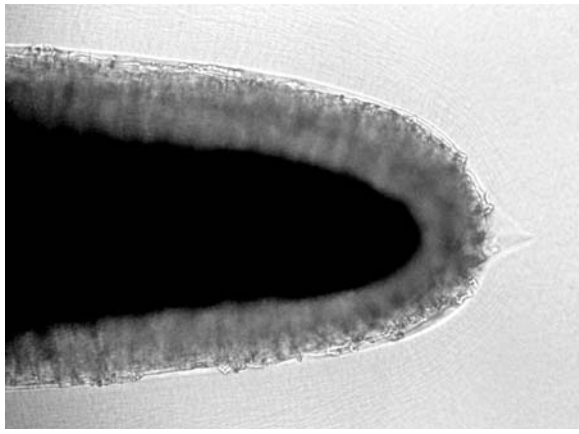

Fig. 10.8. Tip of a 1-mm diameter rhizomorph of *Armillaria mellea* growing though agar medium

Acknowledgements. The author acknowledges support from the National Institutes of Health and the National Science Foundation for support of research on invasive hyphal growth.

References

Bartnicki-Garcia S, Bracker CE, Gierz G, López-Franco R, Lu HS (2000) Mapping the growth of fungal hyphae: orthogonal cell wall expansion during tip growth and the role of turgor. Biophys J 79:2382–2390

Bary A de (1866) Morphologie und physiologie der pilze, flechten und myxomyceten. W. Engelmann, Leipzig

Bechinger C, Giebel KF, Schnell M, Leiderer P, Deising HB, Bastmeyer M (1999) Optical measurements of invasive forces exerted by appressoria of a plant pathogenic fungus Science 285:1896–1899

Bowen WR, Lovitt RW, Wright CJ (2000a) Direct quantification of *Aspergillus niger* spore adhesion in liquid using an atomic force microscope. J Colloid Interface Sci 228:428–433

Bowen WR, Lovitt RW, Wright CJ (2000b) Direct quantification of *Aspergillus niger* spore adhesion in air using an atomic force microscope. Colloids Surf A 173:205–210

Braun EJ, Howard RJ (1994) Adhesion of fungal spores and germlings to host plant surfaces. Protoplasma 181:202–212

Brush L, Money NP (1999) Invasive hyphal growth in *Wangiella dermatitidis* is induced by stab inoculation and shows dependence upon melanin biosynthesis. Fungal Genet Biol 28:190–200

Charras GT, Yarrow JC, Horton MA, Mahadevan L, Mitchison TJ (2005) Non-equilibration of hydrostatic pressure in blebbing cells. Nature 435: 365–369

Davis DJ, Lanter K, Makselan S, Bonati C, Asbrock P, Ravishankar JP, Money NP (2006) Relationship between temperature optima and secreted protease activities of three *Pythium* species and pathogenicity toward plant and animal hosts. Mycol Res 110:96–103

Deising HB, Werner S, Wernitz M (2000) The role of fungal appressoria in plant infection. Microbes Infect 2:1631–1641

Ebata Y, Yamamoto H, Uchiyama T (1998) Chemical composition of the glue from appressoria of *Magnporthe grisea*. Biosci Biotechnol Biochem 62:672–674

Geitmann A (2006) Plant and fungal cytomechanics: quantifying and modeling cellular architecture. Can J Bot 84:581–593

Geitmann A, Emons AMC (2000) The cytoskeleton in plant and fungal cell tip growth. J Microsc 198:218–245

Goriely A, Tabor M (2006) Estimates of biomechanical forces in *Magnaporthe grisea*. Mycol Res 110:755–759

Grove SN, Sweigard JA (1980) Cytochalasin A inhibits spore germination and hyphal tip growth in *Gilbertella persicaria*. Exp Mycol 4:239–250

Hamer JE, Howard RJ, Chumley FG, Valent B (1998) A mechanism for surface attachment in spores of a plant pathogenic fungus. Science 239:288–290

Harold FM (2005) Molecules into cells: specifying spatial architecture. Microbiol Mol Biol Rev 69:544–564

Harold RL, Money NP, Harold FM (1996) Growth and morphogenesis in *Saprolegnia ferax*: is turgor required? Protoplasma 191:105–114

Heath IB (2000) Organization and function of actin in hyphal tip growth. In: Staiger CJ, Baluska F, Volkmann D, Barlow PW (eds) Actin: a dynamic framework for multiple plant cell functions. Kluwer, Dordrecht, pp 275–300

Heath IB, Steinberg G (1999) Mechanisms of hyphal tip growth: tube dwelling amebae revisited. Fungal Genet Biol 28:79–93

Heath IB, Bonham M, Akram A, Gupta GD (2003) The interrelationships of actin and hyphal tip growth in the ascomycete *Geotrichum candidum*. Fungal Genet Biol 38:85–97

Hepler PK, Vidali L, Cheung AY (2001) Polarized cell growth in higher plants. Annu Rev Cell Devel Biol 17:159–187

Holland RJ, Williams KL, Khan A (1999) Infection of *Meloidogyne javonica* by *Paecilomyces lilacinus*. Nematology 1:131–139

Howard RJ (1997) Breaching the outer barriers – cuticle and cell wall penetration. In: Carroll G, Tudzynski P (eds) The Mycota, vol V, part A. Plant relationships. Springer, Berlin Heidelberg New York, pp 43–60

Howard RJ, Ferrari MA (1989) Role of melanin in appressorium function. Exp Mycol 13:403–418

Howard RJ, Valent B (1996) Breaking and entering: host penetration by the fungal rice blast pathogen. Annu Rev Microbiol 50:491–512

Howard RJ, Ferrari MA, Roach DH, Money NP (1991) Penetration of hard substrates by a fungus employing enormous turgor pressure. Proc Natl Acad Sci USA 88:11281–11284

Ingold CT (1986) Protoplasmic flow in hyphae. Trans Br Mycol Soc 86:349–351

Jackson SL (2001) Do hyphae pulse as they grow? New Phytol 151:556–560

Johns S, Davis CM, Money NP (1999) Pulses in turgor pressure and water potential: resolving the mechanics of hyphal growth. Microbiol Res 154:225–231

Lew RR, Levina NN, Walker SK, Garrill A (2004) Turgor regulation in hyphal organisms. Fungal Genet Biol 41:1007–1015

López-Franco R, Bartnicki-Garcia S, Bracker CE (1994) Pulsed growth of fungal hyphal tips. Proc Natl Acad Sci USA 91:12228–12232

Ma H, Snook L, Kaminskyj S, Dahms TY (2005) Surface ultrastructure and elasticity in growing tips and mature regions of *Aspergillus* hyphae describe wall maturation. Microbiology 151:3679–3688

MacDonald E, Millward L, Ravishankar JP, Money NP (2002) Biomechanical interaction between hyphae of two *Pythium* species (Oomycota) and host tissues. Fungal Genet Biol 37:245–249

Mathur J (2006) Local interactions shape plant cells. Curr Opin Cell Biol 18:40-p46

Miyoshi M (1895) Die Durchbohrung von Membranen durch Pilzfäden. Jahrb Wiss Bot 28:269–289

Money NP (1990) Measurement of hyphal turgor. Exp Mycol 14:416–425

Money NP (1995) Turgor pressure and the mechanics of fungal penetration. Can J Bot 73[Suppl 1]:S96–S102

Money NP (1997a) Wishful thinking of turgor revisited: the mechanics of fungal growth. Fungal Genet Biol 21:173–187

Money NP (1997b) Mechanism linking cellular pigmentation and pathogenicity in rice blast disease: a commentary. Fungal Genet Biol 22:151–152

Money NP (2001) Functions and evolutionary origin of hyphal turgor pressure. In: Geitmann A, Cresti M, Heath IB (eds) Cell biology of plant and fungal tip growth. Kluwer, Dordrecht, pp 161–170

Money NP (2004) The fungal dining habit: a biomechanical perspective. Mycologist 18:71–76

Money NP, Hill T (1997) Correlation between endoglucanase secretion and cell wall strength in oomycete fungi: implications for growth and morphogenesis. Mycologia 89:777–785

Money NP, Howard RJ (1996) Confirmation of a link between fungal pigmentation, turgor pressure, and pathogenicity using a new method of turgor measurement. Fungal Genet Biol 20:217–227

Money NP, Ravishankar JP (2005) Biomechanics of stipe elongation in the basidiomycete *Coprinopsis cinerea*. Mycol Res 109:628–635

Money NP, Davis CM, Ravishankar JP (2004) Biomechanical evidence for convergent evolution of the invasive growth process among fungi and oomycete water molds. Fungal Genet Biol 41:872–876

Pickett-Heaps JD, Klein AG (1998) Tip growth in plant cells may be amoeboid and not generated by turgor pressure. Proc R Soc Lond Ser B 265:1453–1459

Pouliot JM, Walton I, Nolen-Parkhouse M, Abu-Lail LI, Camesano TA (2005) Adhesion of *Aureobasidium pullulans* is controlled by uronic acid based polymers and pullulan. Biomacromolecules 6:1122–1131

Pryce-Jones E, Carver T, Gurr S (1999) The roles of cellulase enzymes and mechanical force in host penetration by *Erysiphe graminis* f. sp. *hordei*. Physiol Mol Plant Pathol 55:175–182

Ravishankar JP, Davis CM, Davis DJ, MacDonald E, Makselan SD, Millward L, Money NP (2001) Mechanics of solid tissue invasion by the mammalian pathogen *Pythium insidiosum*. Fungal Genet Biol 34:167–175

Reinhardt MO (1892) Das Wachsthum der Pilzhyphen. Jahrb Wiss Bot 23:479–566

Reis H, Pfiffi S, Hahn M (2005) Molecular and functional characterization of a secreted lipase from *Botrytis cinerea*. Mol Plant Pathol 6:257–267

Sampson KN, Lew RR, Heath IB (2003) Time series analysis demonstrates the absence of pulsatile hyphal growth. Microbiology 149:3111–3119

Solomon PS, Tan K-C, Oliver RP (2003) The nutrient supply of pathogenic fungi: a fertile field for study. Mol Plant Pathol 4:203–210

Talbot NJ (2003) On the trail of a cereal killer: exploring the biology of *Magnaporthe grisea*. Annu Rev Microbiol 57:177–202

Thines E, Weber RWS, Talbot NJ (2000) MAP kinase and protein kinase A-dependent mobilization of triacylglycerol and glycogen during appressorium turgor generation by *Magnaporthe grisea*. Plant Cell 12:1703–1718

Tucker SL, Talbot NJ (2001) Surface attachment and prepenetration stage development by plant pathogenic fungi. Annu Rev Phytopathol 39:385–417

Walker SK, Garrill A (2006) Actin microfilaments in fungi. Mycologist 20:26–31

Walker SK, Chitcholtan K, Yu Y-P, Christenhusz GM, Garrill A (2006) Invasive hyphal growth: an F-actin depleted zone is associated with invasive hyphae of the oomycetes *Achlya bisexualis* and *Phytophthora cinnamomi*. Fungal Genet Biol 43:357–365

Wang Z-Y, Jenkinson JM, Holcombe LJ, Soanes DM, Veneault-Fourrey C, Bhambra GK, Talbot NJ (2005) The molecular biology of appressorium turgor generation by the rice blast fungus *Magnaporthe grisea*. Biochem Soc Trans 33:384–388

Weber RWS, Wakley GE, Thines E, Talbot NJ (2001) The vacuole as central element of the lytic system and sink for lipid droplets in maturing appressoria of *Magnaporthe grisea*. Protoplasma 216:101–112

Wirsel GR, Reimann S, Deising HB (2004) Genetics of phytopathology: fungal morphogenesis and plant infection. Prog Bot 65:147–178

Wright GD, Arlt J, Poon WCK, Read ND (2005) Measuring fungal growth forces with optical tweezers. Proc SPIE 5930:F1–F7

Xiang X, Plamann M (2003) Cytoskeleton and motor proteins in filamentous fungi. Curr Opin Microbiol 6:628–633

11 Cell Biology of Fungal and Oomycete Infection of Plants

A.R. Hardham[1]

CONTENTS

I. **Introduction** 251
II. **Reaching the Plant Surface** 252
III. **Adhesion** 253
A. Spore Adhesion to the Plant Surface . . . 254
B. Molecular Characterisation of Adhesive Molecules 255
IV. **Growth on the Plant Surface** 257
A. Spore Germination 257
B. Hyphal Growth on the Plant Surface . . . 260
C. The Influence of the Plant Surface on Hyphal Growth 262
V. **Penetration of the Plant** 263
A. The induction of Appressorium Differentiation 263
B. Appressorium Development and Function 265
VI. **Acquisition of Nutrients from the Plant** . . . 269
A. Haustoria and Intracellular Hyphae of Biotrophic Pathogens 269
B. Colonisation of Plant Tissues: the Role of Cell Wall-Degrading Enzymes 274
VII. **Conclusions** 276
References 276

I. Introduction

Plants are, in general, resistant to the attempts of potential pathogens to infect them. Pathogens that do succeed, however, cause widespread environmental damage and economic losses. In order to establish infection, pathogens must overcome highly effective, constitutive physical and chemical barriers to pathogen ingress. They must avoid inducing additional host defences, and they must deploy mechanisms for obtaining from the plant the nutrients they need for growth and reproduction. In order to meet all these requirements, successful pathogens employ a range of different infection strategies. The strategies may be specific to a particular pathogen species or they may differ according to the nature of the plant surface or the prevalent environmental conditions. Despite the differences, there are a number of key steps common to most infection strategies, including adhesion to the plant surface, penetration into the plant and acquisition of nutrients from the plant cells.

Basic aspects of the development of plant diseases have been known for a long time but recent studies have greatly increased our understanding of the cellular and molecular mechanisms that underlie the infection process. We now have more information on the nature of pathogen adhesives, on the role of the cytoskeleton in hyphal growth and differentiation and on signalling molecules that regulate the development and function of a variety of specialised infection structures. The new information not only contributes to our understanding of the biology of eukaryotic cells but also provides a framework for the future development of improved control methods for use in the management of plant disease in agriculture and natural ecosystems. Advances in technologies that allow broad-scale gene discovery and determination of gene function are bringing with them an explosion in our knowledge of genes and proteins involved in plant infection. In this chapter, these new data are reviewed in the context of our understanding of the cell biology of the infection process, from the arrival of a pathogen spore at the plant surface, through to the establishment of feeding structures within the plant tissues. The pathogens on which the article is focused include both fungi and oomycetes. Organisms in the class Oomycetes form hyphae and other infection structures that are morphologically and functionally similar to those of true fungi. The Oomycetes are, however, phylogenetically quite distinct from the fungi. Analysis of structural, biochemical and molecular characteristics have led to the Oomycetes being grouped with the chromophyte algae, and other taxa that possess tubular flagellar hairs, in an assemblage called the Stramenopiles (Gunderson et al. 1987;

[1] Plant Cell Biology Group, Research School of Biological Sciences, The Australian National University, Canberra, ACT 2601, Australia

Biology of the Fungal Cell, 2nd Edition
The Mycota VIII
R.J. Howard and N.A.R. Gow (Eds.)
© Springer-Verlag Berlin Heidelberg 2007

Barr 1992; Patterson and Sogin 1992; Van de Peer and De Wachter 1997).

Fungal and oomycete pathogens of plants can be divided into two main categories: the biotrophs which obtain the nutrients they need from living plant cells and the necrotrophs which acquire their nutrients from killed plant cells (Oliver and Ipcho 2004). Some pathogens are hemibiotrophs which initially establish a biotrophic interaction with living host cells before killing the plant cells and turning to a necrotrophic life style (Perfect et al. 2001). These different life-styles have considerable bearing on the infection strategies employed by the fungal species involved. In any plant–pathogen interaction, the extent of progress of infection is determined by genetic and epigenetic factors which influence the degree of resistance of the host plant and the degree of virulence of the invading pathogen.

II. Reaching the Plant Surface

Most fungal spores are non-motile (Fig. 11.1A) and reach potential host plants by passive means, including being blown in the wind or transported by insects and animals (Brown and Hovmøller 2002; Aylor 2003). Some fungi and many oomycetes produce motile zoospores that move actively through the action of one or two flagella which project from the spore surface (Fig. 11.1B). The flagella have an internal structure that is typical of eukaryotic flagella, being based on the 9+2 microtubular axoneme, and contain a range of protein components commonly involved in flagellar structure and function (Hardham 1987; Gubler et al. 1990; Harper et al. 1995). Because the oomycetes are a major group of plant pathogens, there has been an effort to understand the mechanisms underlying their directed movement towards potential hosts.

Oomycete zoospores are chemotactically and electrotactically attracted to the surface of potential host plants (Tyler 2002; Gow 2004). In general, these tactic responses are non-specific in that they guide the zoospores to both hosts and non-hosts; however, specific recognition of a chemoattractant produced by a host plant is known to occur. For example, genistein and diadzein, two isoflavones secreted by soybean roots, serve as potent chemoattractants for zoospores of the soybean pathogen, *Phytophthora sojae*, but not for zoospores of several other species of *Phytophthora* and *Pythium* that are not soybean pathogens (Morris and Ward

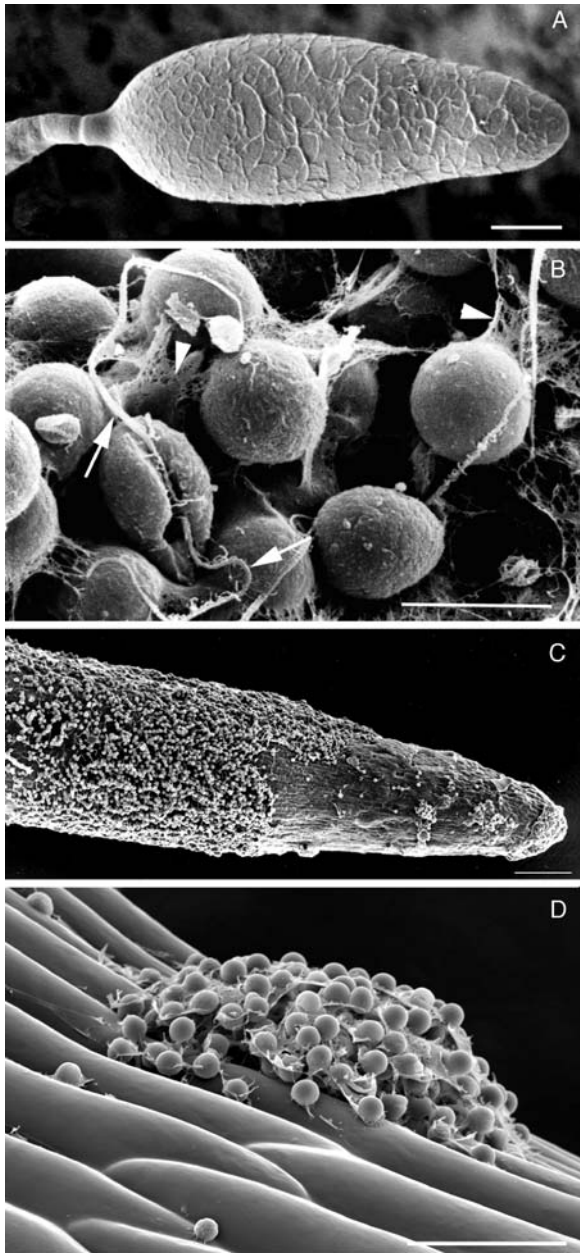

Fig. 11.1. Fungal and oomycete spores. **A** Cryoscanning electron micrograph (cryoSEM) of a developing conidium of *Magnaporthe grisea* (Howard 1994). *Bar* 2.5 µm. **B** SEM of a zoospore and cysts of *Phytophthora cinnamomi* on the surface of an onion root. Two flagella (*arrows*) emerge from the centre of a groove on the ventral surface of the zoospores. During encystment, the cells round up and secrete extracellular matrix and adhesive material (*arrowheads*; Hardham et al. 1994). *Bar* 10 µm. **C** SEM of *P. cinnamomi* zoospores after preferential chemotactic attraction and adhesion to the elongation zone but not the root tip of an onion root. *Bar* 100 µm. **D** CryoSEM of *P. nicotianae* cysts on the surface of a tobacco root. *Bar* 50 µm

1992). Specific attraction mechanisms are also capable of directing zoospore movement to particular regions of the plant. Zoospores of a number of soil-borne *Phytophthora* species swim to the root elongation zone and avoid root cap and root hair regions (Fig. 11.1C). Targetting can also be specific for a particular pathogen species. Thus, zoospores of *Pythium aphanidermatum* are attracted to the root hair zone of rye grass roots while zoospores of *Phytophthora palmivora* are attracted to the elongation zone of the same roots (Van West et al. 2002). Zoospores swim towards wounds and also show auto-aggregation phenomena (Fig. 11.1D). There is evidence that targeting of zoospores to these different locations involves electrotaxis to anodic or cathodic regions of the roots (Van West et al. 2002). At an even finer spatial scale, oomycete zoospores may be preferentially attracted to the grooves between adjacent epidermal cells (Fig. 11.1D) or to stomata (Hardham 2001, 2005; Kiefer et al. 2002; Soylu et al. 2003).

While the flagella of oomycete zoospores have an internal structure typical of eukaryotic flagella, their surface structure is quite distinct. The shorter, anterior flagellum possesses two rows of tubular mastigonemes whose motion during wave propagation along the flagellum reverses the thrust of flagellar beat and pulls the zoospore forward (Cahill et al. 1996). The longer, posterior flagellum trails behind the zoospore and appears to act like a rudder, occasionally flicking and changing swimming direction. In *Phytophthora nicotianae*, immunocytochemical studies have revealed that the shaft of the mastigonemes is composed of a 40-kDa glycoprotein (Robold and Hardham 1998) but little other molecular information is known of the composition of mastigonemes or the identity of chemotaxis or electrotaxis receptors on the zoospore surface in this or any other Stramenopile organism. Integrated cellular and molecular approaches have, however, begun to provide some new information on the signalling pathways involved in zoospore motility and taxis. In two recent studies, silencing of genes encoding the α-subunit of a trimeric G protein (Latijnhouwers et al. 2004) and a bZIP transcription factor (Blanco and Judelson 2005) led to the inhibition of *Phytophthora infestans* zoospore motility. In both categories of mutants, the zoospores turned more frequently and spun on the spot. Studies aimed to determine downstream targets of the G protein may reveal further details of the signal transduction pathway involved in zoospore motility (Dong et al. 2004). Because silencing of these two genes also produced aberrations in infection structure development, it was not possible to use these mutants to assess the contribution of zoospore motility and taxis to pathogen virulence.

Oomycete zoospores are able to swim in water for hours or even days, using endogenous energy supplies thought to be predominantly carbohydrates and lipids. While inhibitor experiments suggested that mRNA and protein synthesis are not required (Penington et al. 1989), it is now clear that gene expression and protein production does occur in zoospores. Zoospores inherit many, perhaps the majority, of their proteins from the sporangium but in vivo labelling studies have shown that new proteins are synthesised in *Phytophthora infestans* zoospores (Krämer et al. 1997) and proteomic analyses have revealed polypeptides that are more abundant in zoospores than in any other stage of the lifecycle of *Phytophthora palmivora* (Shepherd et al. 2003). In addition, genes that are preferentially expressed in *Phytophthora* zoospores have also been identified (Ambikapathy et al. 2002; Škalamera et al. 2004; Connolly et al. 2005; Judelson and Blanco 2005). Exactly when these newly synthesised molecules are active remains to be determined. Some, such as P5CR, an enzyme involved in proline biosynthesis, or Pdr1, an ABC transporter, could function in the motile zoospores while others, such as cell wall-degrading enzymes, may be synthesised in readiness for secretion from germinated cysts during infection.

III. Adhesion

In the majority of cases, infection is initiated by pathogen spores that become attached to the plant surface. Adhesion of pathogen cells to the surface of potential hosts plays an important role in a number of aspects of pathogenesis (Kunoh et al. 1991; Nicholson and Epstein 1991; Braun and Howard 1994b; Nicholson 1996; Epstein and Nicholson 1997; Tucker and Talbot 2001). Adhesion prevents spores from being dislodged by wind or rain before they have a chance to penetrate the plant. Adhesion and close contact of spores and germ tubes with the underlying plant facilitates the reception of signals that guide pathogen growth on the plant surface and that initiate differentiation of infection structures during pathogenesis. Strong adhesion of appressoria enables penetration of plant cell walls by specialised penetration pegs.

A. Spore Adhesion to the Plant Surface

Spore adhesives are generally non-specific and will attach spores to substrata with a range of properties, although preferential binding to hydrophobic surfaces may occur as shown by conidia of the leaf pathogens *Magnaporthe grisea*, *Colletotrichum graminicola*, *Uromyces appendiculatus* and *Phyllosticta ampelicida* (Hamer et al. 1988; Terhune and Hoch 1993; Mercure et al. 1994b; Shaw and Hoch 1999). The timing of the onset of adhesiveness of fungal or oomycete spores varies widely. In some cases, the spore is already adhesive when it reaches the plant. Uredospores of *Uromyces fabae*, for example, adhere immediately to hydrophobic surfaces, probably through hydrophobic interactions (Clement et al. 1994). In other cases, adhesive material is rapidly released after the spore reaches the plant surface. Contact of conidia of *Blumeria graminis* with a hydrophobic surface stimulates release of extracellular matrix material within seconds (Carver et al. 1999). Conidia of *Magnaporthe grisea* release adhesive from the periplasmic space between the plasma membrane and cell wall at the tip of the conidium 15–20 min after inoculation on the leaf surface (Fig. 11.2A, B; Hamer et al. 1988). Adhesion of *Magnaporthe grisea* conidia is not inhibited by treatment with azide or cycloheximide, indicating that neither respiration nor protein synthesis is required; adhesive release is a result of the rupture of the conidial cell wall on spore hydration. Motile oomycete zoospores secrete adhesive material from cortical vesicles and become attached within 2 min of docking at the plant surface (Fig. 11.2C, D; Bartnicki-Garcia and Sing 1987; Gubler et al. 1989; Hardham and Gubler 1990; Cope et al. 1996).

The strength and nature of pathogen adhesion to the host surface often changes as infection proceeds. Adhesion of the spores themselves may progress from an initial weak attachment to a more tenacious adhesion (Deising et al. 1992; Tucker and Talbot 2001). Often an increase in the strength of adhesion coincides with spore germination and results from changes in the quantity and/or compo-

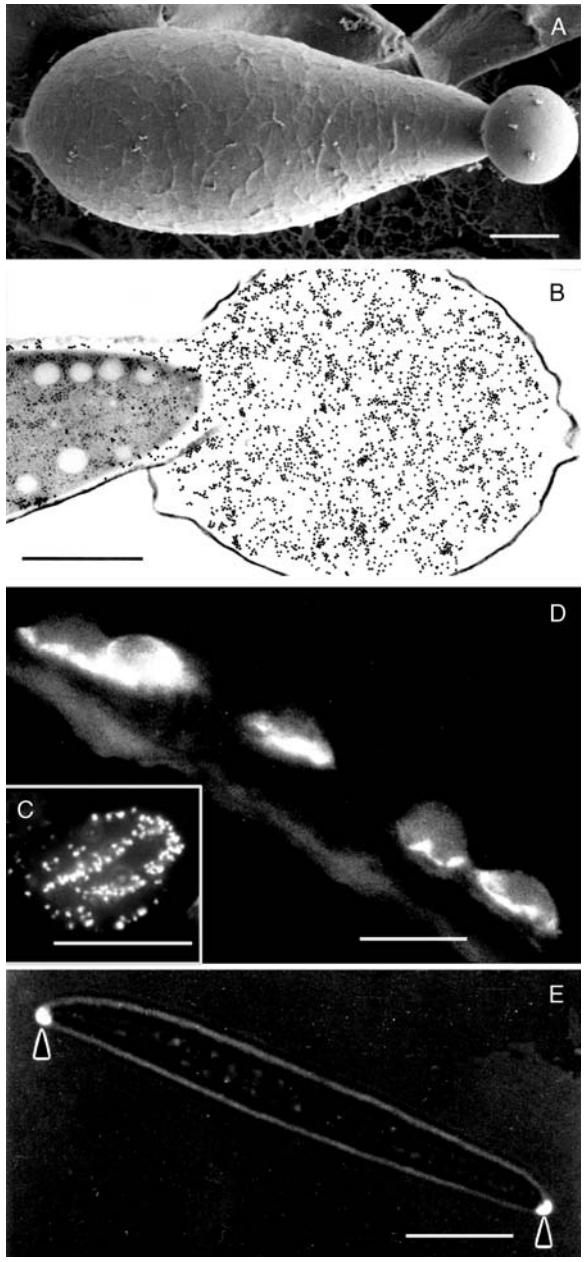

Fig. 11.2. Spore adhesion. **A** CryoSEM of a conidium of *Magnaporthe grisea* after release of adhesive mucilage material from the apex of the spore (Braun and Howard 1994b). *Bar* 2.5 µm. **B** Transmission electron micrograph (TEM) of a conidium of *M. grisea* after release of adhesive material from the periplasmic space between the spore wall and the plasma membrane. The section has been labelled with Concanavalin A-gold that reacts with the spore tip mucilage (Howard et al. 1991a). *Bar* 1 µm. **C** Immunofluorescence micrograph of *Phytophthora cinnamomi* zoospore labelled with Vsv-1, a monoclonal antibody that reacts with the contents of ventral vesicles in the zoospore cortex. *Bar* 10 µm. **D** Cryosection of *P. cinnamomi* cysts 5 min after settling onto a root of *Eucalyptus seiberi*. The section is labelled with Vsv-1 antibody which reacts with the PcVsv1 adhesin secreted from the zoospore ventral vesicles and forms a pad between the spores and the root surface (Hardham et al. 1991). *Bar* 10 µm. **E** Mucilage material released from the tips of a macroconidium of *Nectria haematococca* labelled with Concanavalin A-FITC (Kwon and Epstein 1993). *Bar* 20 µm

sition of material being secreted (Doss et al. 1995; Watanabe et al. 2000; Apoga et al. 2001; Carzaniga et al. 2001; Wright et al. 2002). In the downy mildew pathogen, *Hyaloperonospora parasitica*, there is no extracellular matrix material associated with the conidia but germ tubes and appressoria of this Oomycete release a fibrillar matrix containing β-1,3-glucans confined to the cell–substratum interface and a proteinaceous matrix which spreads beyond the contact zone (Carzaniga et al. 2001).

The timing of production of adhesive molecules and the speed with which adhesive material is released is likely to reflect the requirements of the pathogen involved. In the case of pathogens in aquatic environments, the release of adhesive may need to be rapid to prevent the spore from being swept away from the plant surface. In this case, the adhesive would need to be pre-formed and stored in the spores. For leaf pathogens, initial weak adhesion may successfully retain the spore in place until it has time to synthesise adhesive molecules which are then secreted to achieve a stronger attachment prior to and during germ tube growth and plant penetration.

B. Molecular Characterisation of Adhesive Molecules

Despite recognition of the importance of adhesion in pathogenesis, molecules responsible for the adhesion of fungal plant pathogens have yet to be fully identified and characterised. Analysis of extracellular matrix material secreted by fungal cells has documented the presence of a range of components, including proteins, glycoproteins, carbohydrates and lipids (Doss 1999; Hutchinson et al. 1996, 2002; Sugui et al. 1998; Apoga et al. 2001) and shown differences in the composition of material secreted by spores, germ tubes and appressoria (Fig. 11.3A–C; O'Connell et al. 1996a, b; Pain et al. 1996; Zelinger et al. 2004). In addition to adhesion, extracellular matrices are thought to serve a variety of functions, including roles in cell protection against desiccation or toxins and in communication and signalling (Nicholson and Epstein 1991; Deising et al. 1992; Moloshok et al. 1993; Viret et al. 1994; Görnhardt et al. 2000). The presence of enzymes in

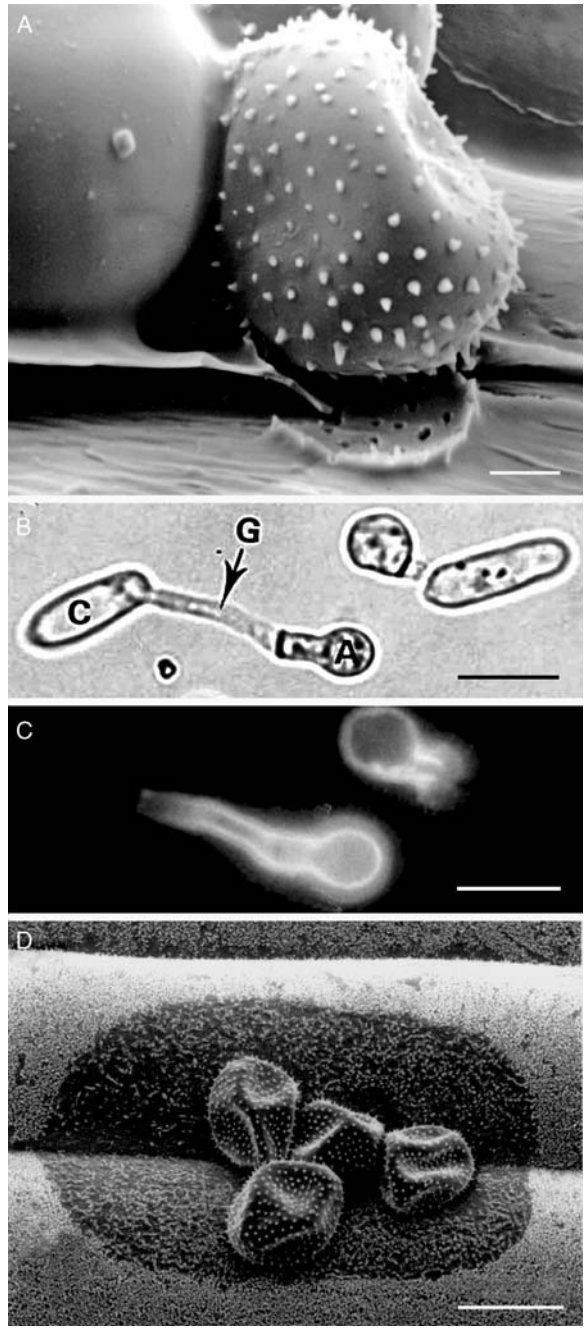

Fig. 11.3. Spore extracellular matrix material. **A** CryoSEM of uredospore of *Uromyces viciae-fabae* (*right*) and glass bead (*left*) on leaf of *Vicia faba*. The pattern of spines of the uredospore has been left in the adhesive pad of mucilage material secreted by the spore (Clement et al. 1997). *Bar* 20 µm. **B**, **C** Germinating conidia of *Colletotrichum lindemuthianum* viewed using bright field (**B**) and fluorescence (**C**) microscopy UB26 monoclonal antibody labels the surface of germ tubes (*G*) and appressoria (*A*) but not conidia (*C*; Hutchinson et al. 2002). *Bar* 10 µm. **D** CryoSEM of uredospores of *Puccinia hordei* on the surface of a barley leaf. Wax on the leaf surface surrounding the spores appears eroded, possibly through the action of enzymes secreted by the ungerminated spores (Read 1991). *Bar* 20 µm

the extracellular matrix secreted by fungal cells also suggests that they may alter the properties of the leaf surface (Fig. 11.3D; Read 1991; Mercure et al. 1994a; Nicholson 1996). The extracellular matrix secreted by uredospores of *Uromyces fabae* and by conidia of *Blumeria graminis*, *Pestalotia malicola* and *Uncinula necator* contains cutinase and other esterases, the activity of which could change surface hydrophobicity and enhance spore adhesion (Deising et al. 1992; Pascholati et al. 1992; Nicholson et al. 1993; Suzuki et al. 1998; Gevens et al. 2001; Rumbolz et al. 2002). Indeed, chemical inhibition of esterase activity results in reduced adhesion of *Uromyces fabae* spores (Deising et al. 1992).

Although the adhesive molecules within the extracellular matrix material secreted by fungal cells are yet to be identified, in a number of instances, incubation with the lectin Concanavalin A was shown to inhibit spore adhesion, indicating that the adhesive molecules contain mannosyl or glucosyl residues (Fig. 11.2B,E; Hamer et al. 1988; Viret et al. 1994; Kwon and Epstein 1997; Shaw and Hoch 1999). In *Nectria haematococca*, the adhesive material is released from the tips of the macroconidia and the active component has been shown to be a 90-kDa glycoprotein (Fig. 11.2E; Kwon and Epstein 1993, 1997). A monoclonal antibody which reacts with a number of polypeptides on the surface of conidia of *Colletotrichum lindemuthianum*, including a predominant 110-kDa glycoprotein, is also capable of inhibiting spore adhesion (Hughes et al. 1999). Despite the fact that these observations were made some time ago, no gene encoding an adhesive protein from a fungal plant pathogen has yet been cloned and we have little understanding of the nature of any phytopathogenic fungal adhesive.

In contrast to the lack of characterisation of adhesive molecules produced by fungal plant pathogens, a number of genes encoding putative adhesives of oomycete plant pathogens were recently cloned and characterised. The first encodes a 34-kDa glycoprotein that is synthesised and secreted by hyphae and cysts of *Phytophthora nicotianae* (Séjalon-Delmas et al. 1997; Villalba Mateos et al. 1997). The 34-kDa glycoprotein contains two cellulose-binding domains and is an elicitor of the defence response in tobacco plants. Silencing of the expression of this gene results in a decrease in hyphal adhesion to cellulose, although the transformants do not show reduced pathogenicity when host tobacco plants are inoculated with mycelia (Gaulin et al. 2002). A second group of genes encoding cyst-germination-specific acid repeat (Car) proteins was cloned from *Phytophthora infestans* (Görnhardt et al. 2000). The *Car* genes contain multiple copies of an octapeptide repeat, a motif found in mucin proteins in mammals. Members of the *Car* gene family are expressed during cyst germination and appressorium development; and the Car proteins occur on the surface of the germlings. It is suggested that the Car mucins may protect the germlings from desiccation and other forms of physical or chemical damage as well as contributing to germling adhesion to the leaf surface (Görnhardt et al. 2000).

The third class of adhesive gene was cloned from *Phytophthora cinnamomi* and encodes an approximately 220-kDa protein, designated PcVsv1, that resides in cortical vesicles underlying the ventral surface of the zoospores (Fig. 11.2C; Robold and Hardham 2005). Immunocytochemical studies of the Vsv1 protein have documented its rapid secretion during zoospore encystment and its presence in the adhesive pad that is deposited between the cyst and the adjacent surface (Fig. 11.2D; Hardham and Gubler 1990). The Vsv1 proteins are synthesised during asexual sporulation and packaged into small vesicles which are randomly distributed in the cytoplasm of the multinucleate sporangia but which are transported to the ventral surface as of zoospores form during sporangial cytokinesis (Hyde and Hardham 1993; Dearnaley et al. 1996). A cDNA-encoding PcVsv1 was isolated by screening an expression library constructed from mRNA from sporulating hyphae with antibodies directed towards the PcVsv1 protein (Robold and Hardham 2004, 2005). *PcVsv1* is 7.4 kb in length and contains no introns. Apart from short N- and C-terminal sequences, the bulk of the PcVsv1 protein is composed of 47 copies of a domain approximately 50 amino acids in length that shows homology to thrombospondin type 1 repeats (TSR1s) found in a number of adhesive extracellular matrix proteins in animals (Adams and Tucker 2000) and secreted adhesins in apicomplexan malarial parasites (Tomley and Soldati 2001). *PcVsv1* expression is up-regulated after the induction of sporulation, consistent with the appearance of ventral vesicles at this time. Homologues of PcVsv1 occur in *Phytophthora sojae*, *P. ramorum*, *P. infestans* and *P. nicotianae* (Robold and Hardham 2005) and immunolabelling with Vsv1 antibodies shows that the Vsv1 adhesin also occurs in *Pythium*, *Albugo* and *Plasmopara*, suggesting that it is widespread across the Oomycetes.

IV. Growth on the Plant Surface

A. Spore Germination

Spores are designed for dispersal and survival under potentially adverse conditions. In many cases, spores undergo a period of dormancy, during which time their metabolic activity is low, allowing them to survive until conditions suitable for germination are encountered. Dormancy may be maintained by compounds secreted by the spores themselves or by other microbes (Hegde and Kolattukudy 1997; Staples and Hoch 1997; Thines 2004; Wang and Higgins 2005) or by the absence of specific cues for germination. Most fungal spores need water to hydrate before germination can take place, but oomycete spores such as sporangia, cysts or chlamydospores are not desiccated and do not undergo rehydration before germination. Commonly spores of saprophytic fungi require an external nutrient source before they germinate, however, spores of many plant pathogenic fungi will germinate in the absence of exogenous nutrients, relying on endogenous resources within the spore. This nutritional independence during germination and early germling growth is advantageous for phytopathogens because external energy resources may be limited until the pathogen has penetrated the plant surface, especially in the case of foliar pathogens. Spore germination is induced by both physical and chemical properties of the plant surface (Shaw and Hoch 1999; Staples and Hoch 1997; Chaky et al. 2001; Osherov and May 2001; Barhoom and Sharon 2004). Important factors often include contact with a hydrophobic and solid surface, cuticular waxes and adhesion to the underlying substratum (Shaw and Hoch 2000; Shaw et al. 2006; see also Chap. 9 in this volume).

There is evidence for the participation of three different signal transduction pathways in the germination of fungal conidia, namely pathways involving G proteins, MAP kinase and cAMP (Kinane et al. 2000; Osherov and May 2001; Doehlemann et al. 2006). In *Colletotrichum lagenarium*, both the cAMP and MAP kinase pathways are required for germination on host leaves (Yamauchi et al. 2004) and disruption of the MAP kinase gene, *CMK1*, inhibits conidial germination (Takano et al. 2000). In *Colletotrichum trifolii*, *Ctg-1* transcripts encoding the α-subunit of heterotrimeric G proteins increase in abundance during conidial germination and gene knockout experiments show that the Gα protein is required for germination to occur (Truesdell et al. 2000). Small GTP-binding proteins, such as Cdc42, may also be required for spore germination (Chen et al. 2006). Current data suggest that the pathway activated during spore germination may depend on the nature of the inductive signals. In *Colletotrichum gloeosporioides*, for example, plant surface signals induce conidial germination in a cAMP-independent manner but cAMP is required for germination under saprophytic conditions (Barhoom and Sharon 2004).

Many spores are able to germinate from multiple sites on the spore surface (Fig. 11.4A, B). In these cases, the site at which germination actually occurs may be influenced by environmental factors, such as light, oxygen, nutrients or adhesion to the underlying substratum (Gold and Mendgen 1991; Lee and Dean 1994; Kuo and Hoch 1996; Staples and Hoch 1997; Shaw et al. 1998). Contact with another spore or proximity to a plant cell can also have a marked effect on the sites of germination. Conidia of *Geotrichum candida*, for example, form a germ tube at a site remote from the site of contact with another spore (Robinson 1973). Spores of *Idriella bolleyi* germinate on the side of the spore facing away from living root hairs of cereals, but towards dead root hairs (Allan et al. 1992). The signals that stimulate germination, and the type of germination that ensues, influence the subsequent development of the pathogen and its pathogenicity. In both *Blumeria graminis* and *Colletotrichum gloeosporioides*, for example, conidial germination results in subsequent appressorium formation when contact is made with the plant surface (Wright et al. 2000; Barhoom and Sharon 2004). Germination can occur under other circumstances but does not lead to appressorium formation.

For some spores, the site of germination occurs at a predictable location. In *Cochliobolus heterostrophus*, germination occurs at the ends of the crescent-shaped conidia (Braun and Howard 1994a) and in *Magnaporthe grisea* it occurs at the apical and/or basal cells of the pear-shaped conidia (Fig. 11.4A; Hamer et al. 1988). Uredospores, but not basidiospores (Gold and Mendgen 1991), of rusts germinate from a germination pore, a specialised area in which the spore wall is thinner than in other regions (Deacon 1997). In the oomycetes, while no structural organisation indicative of the site of germination in the cyst has been recognised, there is evidence that this location is pre-determined because cysts of *Phytophthora* and *Pythium* germinate from a region in the centre of what was the ventral groove of the zoospores

(Mitchell and Deacon 1986; Paktitis et al. 1986; Hardham and Gubler 1990). In this case, the region of germ tube emergence is pre-aligned towards the plant as a result of the orientation of the motile zoospores before they encyst and adhere to the plant surface (Fig. 11.2D; Mitchell and Deacon 1986; Hardham and Gubler 1990).

The first morphological sign of germination is the accumulation of apical vesicles with a range of sizes (typically 40–400 nm diam.) and morphologies, beneath the site of germ tube emergence (Fig. 11.4C–E). The apical vesicles fuse with the overlying plasma membrane in the apical dome, thus generating localised surface growth. As well as contributing to the expanding plasma membrane, the vesicles contain substrates and enzymes required for cell wall formation and molecules that protect the germ tube and attach it to the underlying surface. Exocytosis of these materials is accompanied by endocytic retrieval of excess plasma membrane and membrane receptors (Atkinson et al. 2002; Fuchs et al. 2006).

Localised outgrowth of the spore surface establishes the polarity of growth of the germling. There is some evidence that microtubules may be involved, perhaps through their role in organelle distribution (Riemann et al. 2002; Mourino-Perez et al. 2006). There is, however, more evidence demonstrating the role of actin microfilaments in development of the polar outgrowth. Filamentous actin typically forms longitudinal bundles in the hyphal cytoplasm and extends into the apical dome at the tip of the germ tubes and hyphae (Gow 1995). Radial arrays of actin microfilaments form in germinating cysts and hyphal branches before germ tube or branch formation (Fig. 11.4F; Bachewich and Heath 1998). Experimental removal of actin microfilaments through treatment with cytochalasins or latrunculin B, inhibits germ tube formation in germinating spores (Bachewich and Heath 1998; Riemann et al. 2002). Consistent with the involvement of actin in this process is the observation that myosin is required for the establishment of polarised growth and secretion in *Aspergillus* germlings (McGoldrick et al. 1995). Actin could direct establishment of polar outgrowth during spore germination and hyphal branching by facilitating

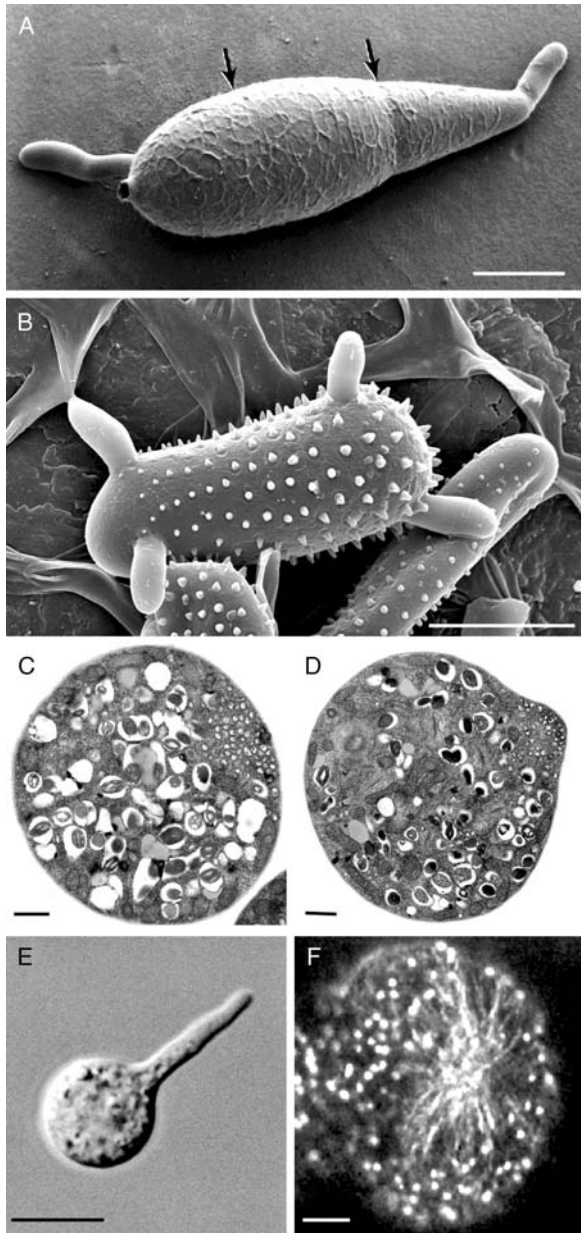

Fig. 11.4. Spore germination. **A** CryoSEM of a germinated conidium of *Magnaporthe grisea*. *Arrows* indicate cross-walls between the three cells of the conidium (Money and Howard 1996). *Bar* 5 µm. **B** CryoSEM of a uredospore of poplar rust pathogen (*Melampsora larici-populina*) that has germinated from four locations (micrograph by courtesy of Roger Heady, Australian National University, Canberra, Australia). *Bar* 10 µm. **C** TEM of a *Phytophthora cinnamomi* cyst in which a cluster of apical vesicles has formed in the cell cortex at a location presumed to be the future site of germination. *Bar* 1 µm. **D** TEM of a *P. cinnamomi* cyst with a cluster of apical vesicles at the site of spore germination. *Bar* 1 µm. **E** Germinated cyst of *P. cinnamomi*, 60 min after encystment. *Bar* 10 µm. **F** Hypha of *Saprolegnia ferax* labelled with rhodamine-phalloidin, showing a radial array of actin microfilaments at a point of branch formation in a cell recovering from treatment with latrunculin B (Bachewich and Heath 1998). *Bar* 5 µm

the transport of apical vesicles to the germination or branch site or by targeting vesicle fusion at that site through regulation of the distribution or activity of ion channels or docking receptors in the plasma membrane (Levina et al. 1994; Ayscough et al. 1997). The facts that interference with Ca^{2+} homeostasis inhibits spore germination (Shaw and Hoch 2000; Warwar and Dickman 1996) and variations in Ca^{2+} concentration precede and influence the site of spore germination and branch formation (Hyde and Heath 1995) support this hypothesis (Grinberg and Heath 1997). It is suggested that Ca^{2+} ion fluxes could be responsible for organising filamentous actin into the radial arrays (Bachewich and Heath 1998).

The germination of fungal and oomycete spores is accompanied by extensive changes in gene expression and the production of new proteins. Over the past few years, several studies identified cohorts of genes whose expression is upregulated during spore germination (Thomas et al. 2002; Avrova et al. 2003; Dilger et al. 2003; Sacadura and Saville 2003; Takano et al. 2003, Shan et al. 2004; Both et al. 2005; Grenville-Briggs et al. 2005; Posada-Buitrago and Frederick 2005; Zahiri et al. 2005). Proteomic studies also showed that many proteins are present at higher concentrations in germinating spores than at other stages in the pathogen's lifecycle (Krämer et al. 1997; Shepherd et al. 2003; Ebstrup et al. 2005; Cooper et al. 2006). The proteins that increase in abundance perform a wide spectrum of cellular functions and include proteins involved in basic metabolism: DNA, RNA and protein synthesis, signalling, cell structure and growth. In general, these broad-ranging gene and protein discovery projects do not provide information that identifies proteins that play key spore germination-specific roles, although a number of studies highlight the abundance of heat-shock and other proteins that may contribute to protection against oxidative and other stresses encountered as part of the plant's defensive response (Görnhardt et al. 2000; Avrova et al. 2003). It is, however, an exciting time as these gene discovery projects serve as a springboard for more in-depth characterisation of selected genes and their encoded proteins.

Many spores can germinate and sustain growth of the germ tube for at least a short time in the absence of exogenous nutrients (Lucas and Knights 1987; Barbosa et al. 2006), indicating that they use endogenous supplies of carbon and nitrogen to support this early growth and development. Lipids and carbohydrates are thought to be the most important sources of energy in fungal and oomycete spores (Fig. 11.5A–F). Lipid is found in the form of lipid globules surrounded by a single membrane. Lipid droplets are abundant in fungal conidia

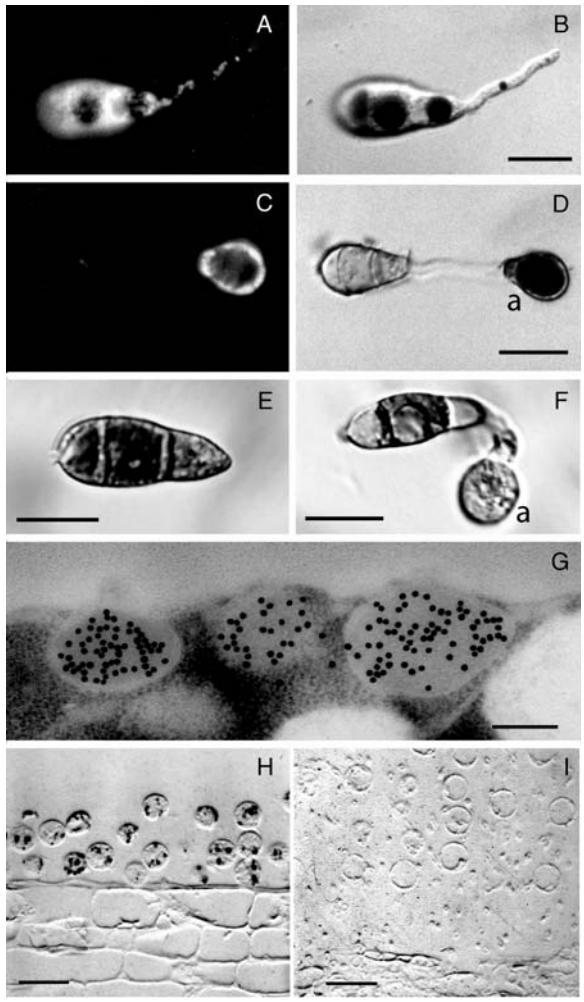

Fig. 11.5. Spore nutrient reserves. **A**, **B** Staining of lipid with Nile Red (**A**) and vacuoles with Neutral Red (**B**) in conidial germling of *Magnaporthe grisea* 2 h post-germination. **C**, **D** Staining of lipid with Nile Red (**C**) and vacuoles with Neutral Red (**D**) in conidium and appressorium of *M. grisea* 36 h post-germination. **E**, **F** Staining of glycogen in conidia and appressorium of *M. grisea*. Dense deposits of glycogen are present in ungerminated conidia (**E**) but are reduced during appressorium formation (**F**). Unpublished micrographs in **A–F** are by courtesy of Dr. R.W.S. Weber. *Bars* 10 µm. **G** Immunogold labelling of *Phytophthora cinnamomi* zoospore with monoclonal antibody Lpv-1-Au_{18} that reacts with high molecular weight glycoproteins in large peripheral vesicles in the zoospore cortex (Hardham 1995). *Bar* 0.25 µm. **H**, **I** Immunogold-silver enhanced light microscope labelling with Lpv-1 of large peripheral vesicles in cysts of *P. cinnamomi* fixed 1 h (**H**) and 4 h (**I**) after infection of a root of *Eucalyptus seiberi* (Gubler and Hardham 1991). *Bar* 20 µm

and are mobilised during conidial germination (Fig. 11.5A–D; Thines et al. 2000; Weber et al. 2001; Both et al. 2005; Barbosa et al. 2006). Enzymes involved in lipid breakdown via the glyoxylate cycle have been shown to be up-regulated in germinating conidia and disruption of the genes encoding glyoxylate cycle enzymes delay or inhibit conidial germination (Wang et al. 2003; Solomon et al. 2004; Both et al. 2005). In fungal conidia, storage carbohydrates are often in the form of glycogen aggregates (Thines et al. 2000; Weber and Davoli 2002; Tsuji et al. 2003). Cytochemical staining revealed the breakdown of glycogen deposits during conidial germination and genetic studies confirmed that this process is required for normal conidial germination (Fig. 11.5E) Both et al. 2005). In oomycete cysts, such as those of *Phytophthora*, storage β-1,3-glucans called mycolaminarins occur in abundant vesicles with characteristic lamellations (Powell and Bracker 1977; Wang and Bartnicki-Garcia 1980).

Fungal and oomycete spores also contain protein stores (Van Etten et al. 1979; Bullock et al. 1980; Russo et al. 1982; Gubler and Hardham 1990). In *Botryodiplodia theobromae* pycnidia (Van Etten et al. 1979) and *Sclerotinia sclerotiorum* sclerotia (Russo et al. 1982), 20-kDa and 36-kDa polypeptides, respectively, form the major storage proteins. In *Phytophthora cinnamomi*, the storage proteins are large glycoproteins over 500 kDa relative molecular mass (Fig. 11.5G, H; Gubler and Hardham 1988; Marshall et al. 2001). In each case, the proteins are deposited in cytoplasmic vesicles (Fig. 11.5G). During germination and germling development, these protein-containing vesicles become dilated and their contents become increasingly electron-lucent as they are degraded (Bullock et al. 1983; Gubler and Hardham 1990). In *Phytophthora cinnamomi* germlings, the storage protein is no longer detectable immunocytochemically by 3–4 h after cyst germination (Fig. 11.5H, I).

B. Hyphal Growth on the Plant Surface

The mode of growth established by germinating spores continues as hyphae grow across the plant surface. Hyphae extend by tip growth, a process in which surface expansion is restricted to the apical dome of the hypha. This is achieved by localised fusion of cytoplasmic vesicles with the plasma membrane in the dome. Surface expansion is highest at the very apex of the dome and decreases rapidly subapically. The cylindrical walls of the hypha subtending the apex are rigid and do not expand.

The exact shape of the hyphal apex and the organisation of organelles within the apical regions of the hypha vary in different species of fungus or oomycete; however, it seems likely that the basic mechanism responsible for tip growth is similar in all cases. Details of the interplay between wall extensibility, the cytoskeleton and cell turgor pressure which achieve this precisely regulated apical expansion have given rise to a number of models of hyphal tip growth (Bartnicki-Garcia 1996; Heath and Steinberg 1999; see also Chap. 10 in this volume). Some envisage that the newly formed wall at the hyphal apex is easily expandable and, in a controlled fashion, yields to the forces of turgor pressure (Sietsma and Wessels 1994). The absence of cellulose from the wall of the hyphal apex of *Achlya ambisexualis* would be consistent with this model (Shapiro and Mullins 2002). Others suggest that turgor pressure may not participate in the extension of narrow tubes such as hyphae (Pickett-Heaps and Klein 1998; Heath and Steinberg 1999). Some view the newly formed wall to be so pliable that actin microfilaments are invoked to form a stabilising and regulatory network on the cytoplasmic face of the plasma membrane in the apex (Heath 1994; Money 1994; Kaminskyj and Heath 1996). Others see the need for degradative enzymes to loosen the structure of the newly formed wall at the apex to allow expansion to occur (Bartnicki-Garcia 1973; Bartnicki-Garcia et al. 1989; Loprete and Hill 2002). In all these models, the numerous small vesicles in the apical cytoplasm play a central and indispensable role in the delivery of wall components and membrane to the expanding apical surface.

In many cases, apical vesicles are aggregated into a cluster known as the Spitzenkörper, a structure which is visible in the light microscope (Fig. 11.6A–C; Girbardt 1969; Grove and Bracker 1970; Grove et al. 1970). The important role of the Spitzenkörper in tip growth was recognised soon after its discovery; and studies using confocal and video-enhanced microscopy techniques support this contention (López-Franco and Bracker 1996; Riquelme et al. 1998; Dijksterhuis 2003). The Spitzenkörper acts as a vesicle supply centre from which vesicles move out and fuse with the plasma membrane within the apical dome. Bartnicki-Garcia and co-workers developed a mathematical model that accurately describes hyphal growth and that highlights two important parameters, namely the rate of movement of the vesicle supply centre

and the rate of vesicle release from the centre (Bartnicki-Garcia et al. 1989, 1990; Bartnicki-Garcia 2002; Diéguez-Uribeondo et al. 2004). The values of these two parameters determine hyphal extension rate and hyphal diameter. Cessation of movement of the vesicle supply centre results in spherical tip expansion, such as occurs during appressorium formation; asymmetric positioning or duplication of the Spitzenkörper gives rise to bending or branching of the hypha (Dijksterhuis 2003; Riquelme and Bartnicki-Garcia 2004).

The size and morphology of the vesicles in the hyphal apex vary widely, a feature considered likely to reflect differences in vesicle contents and function. To date, we have little understanding of the basis for these differences, the range of constituents in any one vesicle type, or the distinct functions different vesicle types might serve (Harris et al. 2005). Some vesicles contain wall precursors and enzymes involved in wall construction and modification (Hill and Mullins 1980; Ayscough et al. 1997). Some enzymes are secreted into the wall where they generate or cleave glycosidic bonds within or between wall components (Loprete and Hill 2002). Others, such as chitin and cellulose synthetases, are incorporated into the membrane of the vesicles so that, on fusion at the cell surface, the enzymes are incorporated into the plasma membrane (Bracker et al. 1976). Other vesicles contain proteases and other degradative enzymes whose function is to digest the plant cell wall, to allow invasion and nutrient acquisition. Continued growth of the hypha means that proteins incorporated into plasma membrane at the apex are swept backwards and soon located in the cylindrical, non-expanding part of the hypha. These proteins may be retrieved by endocytosis and recycled via an endosome-based membrane system (Hoffmann and Mendgen 1998; Read and

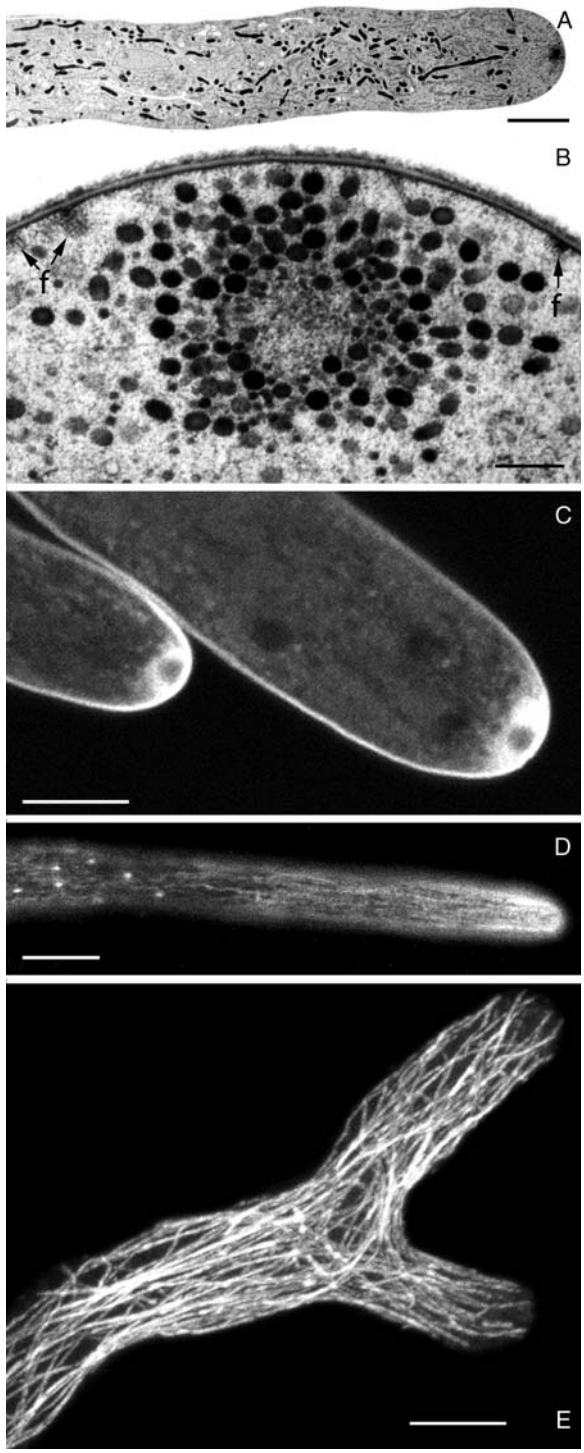

Fig. 11.6. Hyphal tip growth. **A** Hyphal apex of *Sclerotium rolfsii*, showing zonation of organelles along the hypha. The extreme apex contains a Spitzenkörper and is free of large organelles; mitochondria and ER occur in the subapical cytoplasm; vacuoles and nuclei are positioned further back from the apex (Roberson and Fuller 1988). *Bar* 4 µm. **B** Spitzenkörper in the apex of a hypha of *S. rolfsii*. A cluster of apical vesicles surrounds a vesicle-free core. Filasomes (*f*) occur near the plasma membrane (Roberson and Fuller 1988). *Bar* 0.25 µm. **C** Hyphae of *Botrytis cinerea* labelled with Concanavalin A. The plasma membrane and components of the endomembrane system, including apical vesicles, are labelled. The core of the Spitzenkörper is unlabelled (Bourett et al. 1998). *Bar* 5 µm. **D** Longitudinally oriented actin microfilaments and peripheral plaques of filamentous actin stained with rhodamine-phalloidin in a hypha of *Saprolegnia ferax* (Jackson and Heath 1990). *Bar* 10 µm. **E** Labelling of hyphae of *Rhizoctonia oryzae* with anti-tubulin antibodies to reveal the distribution of microtubules (Bourett et al. 1998). *Bar* 5 µm

Hickey 2001; Read and Kalkman 2003; Fuchs and Steinberg 2005; see also Chap. 1 in this volume).

The continuous supply of vesicles to the apical cluster is critical for tip growth and is dependent upon the efficient transport of vesicles from their site of production in the Golgi apparatus (or Golgi equivalent in fungi lacking recognisable Golgi stacks; Welter et al. 1988; Mendgen et al. 1995; Satiat-Jeunemaitre et al. 1996; see Chap. 1 in this volume) in the subapical cytoplasm. Vesicle transport is dependent upon cytoskeletal elements, actin microfilaments and microtubules. Actin microfilaments form longitudinally oriented cables and fine filaments in the cytoplasm extending, in some cases, into the apical dome (Fig. 11.6D). They also form peripheral plaques (filasomes) and are part of the core of the Spitzenkörper (Fig. 11.6B; Jackson and Heath 1990; Kwon et al. 1991b; Heath 1994, 1995b; Czymmek et al. 1996; Srinivasan et al. 1996 Heath and Steinberg 1999; Harris et al. 2005). Microtubules are longitudinally oriented and usually do not extend into the apical dome (Fig. 11.6E; Bourett and Howard 1991; Heath 1994, 1995b; Roberson and Vargas 1994; Czymmek et al. 1996, 2005; Bourett et al. 1998). Disruption of the function of either actin microfilaments or microtubules, through drug treatments or disruption of genes encoding cytoskeleton-associated proteins, causes variable effects on vesicle transport and tip growth (Heath 1995a; Langford 1995; Lehmler et al. 1997; Inoue et al. 1998; Riquelme et al. 1998; Yamashita and May 1998; Czymmek et al. 2005). These studies suggest that microtubule arrays are mainly concerned with long-distance transport of cell components, including vesicles, early endosomes and nuclei (Wedlich-Söldner et al. 2002b; Steinberg and Fuchs 2004; Fuchs et al. 2005; Lenz et al. 2006). As part of this role, microtubules direct the transport of apical vesicles to the Spitzenkörper, thus ensuring a ready supply of vesicles for redistribution (Schuchardt et al. 2005). Actin microfilaments are involved in movement of the apical vesicles from the Spitzenkörper or vesicle supply centre and their fusion with the plasma membrane in the expanding hyphal apex. The role of cytoskeletal elements in polarised growth is further considered in Chaps. 5 and 6 in this volume.

Another aspect of hyphal structure with which the cytoskeleton is involved is the stratification of organelles along the hypha (Fig. 11.6A). Apart from the small vesicles and cytoskeletal elements, the apical dome is largely free of other organelles (Fig. 11.6A, C). Beneath the dome are zones rich in mitochondria or nuclei and thereafter the hypha becomes increasingly vacuolate. Golgi bodies and endoplasmic reticulum (ER) occur throughout the cytoplasm, with the ER network in some cases showing a gradient of distribution with more dense arrays near the hyphal apex (Maruyama et al. 2006). Hyphae also contain a system of tubular and spherical vacuoles that function in the transport of material (e.g. phosphate) from the apex to more distal regions of the mycelium (Shepherd et al. 1993; Allaway et al. 1998; Cole et al. 1998; Hyde et al. 2002; see also Chap. 2 in this volume). Microtubules are responsible for the movement of nuclei, ER and tubular vacuoles, for the reorganisation of the ER network and for the trafficking of vesicles between the ER and Golgi apparatus (Hyde et al. 1999; Wedlich-Söldner et al. 2002a).

C. The Influence of the Plant Surface on Hyphal Growth

Many fungi grow across the surface of the plant in an apparently unguided fashion. However, others are capable of detecting and reacting to chemical and/or topographical signals from the plant (Wynn 1981; Hoch and Staples 1991). Hyphae of *Rhizoctonia* and other fungal species grow towards and along the grooves overlying the anticlinal walls of epidermal cells (Fig. 11.7A; Armentrout et al. 1987). It is thought that this polarity is due to the leakiness of the area to exudates from within the leaf (Hoch and Staples 1991). Many pathogens that invade the leaf surface through stomatal pores show preferential growth towards stomata. This guidance may be derived from chemical signals but is also achieved by the recognition of and response to the surface topography of the leaf. The growing hypha is able to detect the ridges and grooves on the substratum and orients its growth accordingly, a process called thigmotropism. This phenomenon has been studied in detail in species of rusts. Many *Puccinia* species, for example, grow perpendicularly to the rows of epidermal cells (Fig. 11.7B, C). It was demonstrated that hyphae respond to a physical signal and not a chemical one – inert replicas of the leaf surface or even artificial gratings induce the same thigmotropic response (Wynn 1976; Dickinson 1979; Hoch et al. 1987a). This growth pattern is thought to enhance the chances of hyphae encountering stomata which, in graminaceous plants, occur in longitudinal rows (Fig. 11.7C). The dimensions of the topographical features to which hyphae

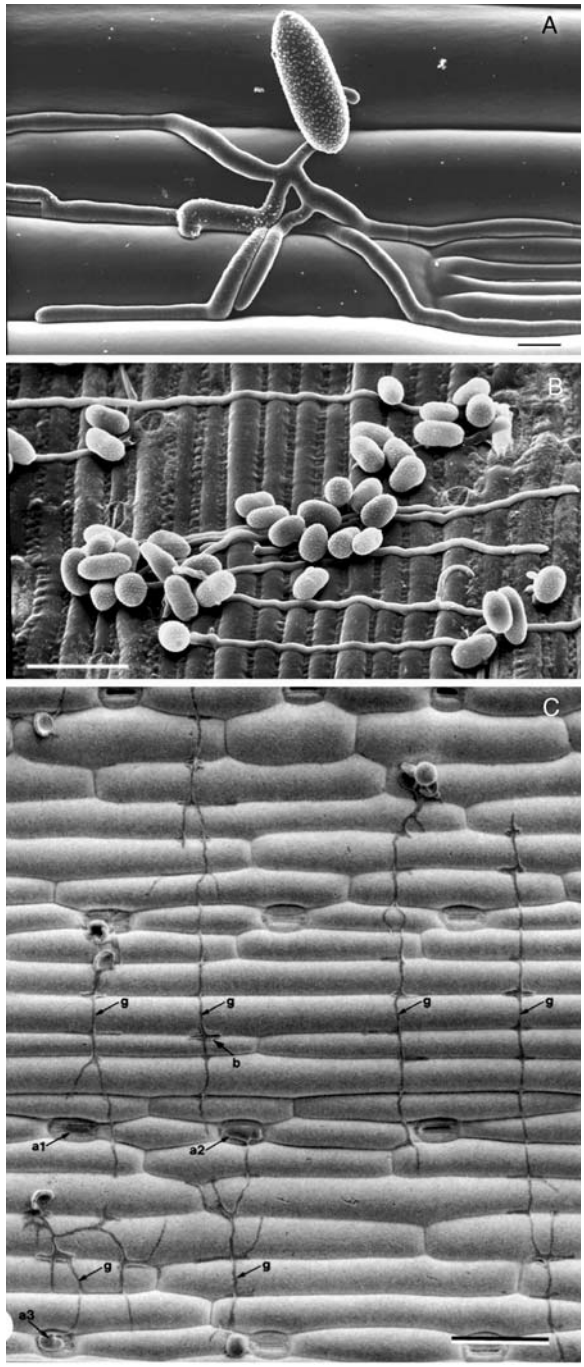

Fig. 11.7. Thigmotropic growth of fungal germlings. **A** CryoSEM of hyphae of *Blumeria graminis* f.sp. *avenae* grow along the grooves formed by the anticlinal walls of the epidermal cells on an oat leaf (Carver et al. 1995). *Bar* 10 µm. **B** CryoSEM of hyphae produced by germinated uredospores of *Puccinia graminis* f.sp. *tritici* grow perpendicular to the ridges and grooves on the leaf surface (Staples and Hoch 1997). *Bar* 50 µm. **C** Uredospores of *P. hordei* on the surface of a barley leaf. Primary germ tubes grow at right angles to the grooves formed by the anticlinal walls of the epidermal cells. On encountering a stoma, the hyphal apex differentiates into an appressorium over the stomatal pore (Read et al. 1992). *Bar* 100 µm

respond were determined with great precision for germlings of *Uromyces appendiculatus*. Maximum response was shown to ridges or grooves spaced 0.5–15.0 µm apart (Hoch et al. 1987a).

The mechanisms by which hyphae achieve directed growth are still not fully understood. The position of the Spitzenkörper or vesicle supply centre in the hyphal apex is clearly involved in bringing about directed growth, but how are the topographical signals perceived and the signals transduced to bring about appropriate changes in the position of the Spitzenkörper? We do know that firm adhesion of the hypha to the substratum is mandatory (Epstein et al. 1985). However, it was established that the topographical signals are perceived in an area of the hypha in contact with the substratum, 0–10 µm from the hyphal apex (Corrêa and Hoch 1995). Studies of *Uromyces appendiculatus* led to the suggestions that the cytoskeleton (Hoch et al. 1986, 1987b; Bourett et al. 1987; Hoch and Staples 1991) and/or the operation of an integrin-like protein might be involved in either signal reception or transmission (Corrêa et al. 1996). These chemical and physical signals not only influence the polarity of hyphal growth, but they may also induce the hyphal apex to differentiate into specialised infection structures which penetrate the host surface.

V. Penetration of the Plant

A. The induction of Appressorium Differentiation

Signals from the plant surface not only guide the growing germ tube or hypha but also trigger the development of infection structures capable of penetrating the host surface (Fig. 11.8A–C). In some pathogens, the infection structures are highly specialised appressoria that invade the underlying plant epidermis through the production of a fine penetration peg. Both physical and chemical signals play a role in the induction of appressorium differentiation (Emmett and Parbery 1975; Deising et al. 2000; Kamakura et al. 2002). Factors shown to trigger appressorium differentiation include the topography, hardness and hydrophobicity of

the substratum and the chemical composition of the surface. In some cases, a single factor may apparently be sufficient to trigger differentiation (Mendgen et al. 1996; Dean 1997); in other cases, multiple signals are required (Collins and Read 1997; Collins et al. 2001).

Hydrophobicity of the substratum influences appressorium induction but its exact role is still unclear. Some studies of *Magnaporthe grisea*, for example, found a correlation between surface hydrophobicity and appressorial differentiation (Jelitto et al. 1994; Lee and Dean 1994) and found that a hydrophobic surface is sufficient for appressorial induction in the absence of other cues (Gilbert et al. 1996). Other studies of *M. grisea*, however, found that the requirement is for a hard surface, whether hydrophilic or hydrophobic (Xiao et al. 1994) and that the response is modulated by conidial density (Hegde and Kolattukudy 1997). These observations suggest that other factors, including some that are as yet not documented, may be involved. Surface hardness, topography and degree of hydrophobicity do, for example, influence the ability of hyphae to adhere to the substratum; and attachment or close association of the germling to the underlying surface is consistently an important requirement for appressorial differentiation (Emmett and Parbery 1975; Read et al. 1992; Liu and Kolattukudy 1999; Yamaoka and Takeuchi 1999). Studies of the development of *Colletotrichum graminicola* growing on microfabricated silicon substrata showed that at least 4 µm of continuous contact of the germ tube with the hydrophobic substratum is required for the induction of appressoria in this species (Apoga et al. 2004). The ability of the pathogen to adhere to the plant surface is affected by the properties of the hyphal surface and there is evidence that surface characteristics of germ tubes and appressoria may be different from those of the conidium (Fig. 11.3B, C; Hutchison et al. 2002).

One class of hyphal surface molecules that have been extensively studied and have the capacity to influence attachment is the hydrophobins. Hydrophobins are small cysteine-rich proteins that self-assemble on the cell surface and modify sur-

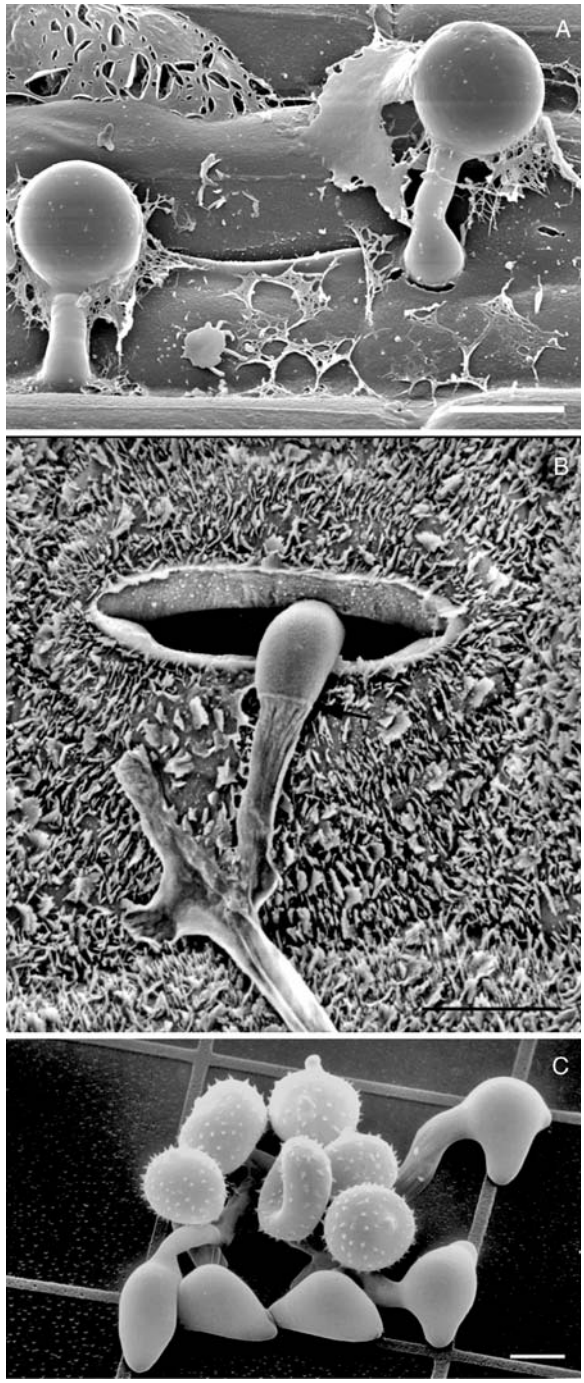

Fig. 11.8. Thigmotropism and appressorium formation. **A** Germinated cysts of *Phytophthora cinnamomi* penetrating along anticlinal wall junctions of the epidermis of an alfalfa root. The hyphae form appressorium-like swellings at the point of invasion. *Bar* 10 µm. **B** CryoSEM of hypha of *Melampsora lini* (flax rust pathogen) growing on the surface of a flax leaf. The hypha has differentiated into an appressorium over a stoma. The hypha has collapsed behind the septum (*arrow*) delineating the appressorium (micrograph courtesy of CSIRO Plant Industry, Australia). *Bar* 10 µm. **C** Uredospores of *Uromyces appendiculatus* growing on a polystyrene replica containing ridges 0.5 µm in height. Appressoria differentiated when the hyphal apex encountered a ridge (Hoch and Staples 1991). *Bar* 10 µm

face hydrophobicity (Wessels 1996, 1999; Kershaw and Talbot 1998). They are likely to have a marked influence on recognition (Beckerman and Ebbole 1996) and adhesion phenomena (Talbot et al. 1996). *MPG1* and *MHP1* genes that encode class I and class II hydrophobins, respectively, in *M. grisea* are both highly expressed during early infection structure differentiation (Soanes et al. 2002; Kim et al. 2005). *MHP1* null mutants undergo the initial step in appressorium induction, swelling and hook formation, but do not form appressoria on surfaces that are normally inductive (Talbot et al. 1993). *MHP1* null mutants have a greatly reduced ability to form appressoria (Kim et al. 2005). Another *M. grisea* gene that encodes a small extracellular matrix protein and whose expression is upregulated during appressorium development is *EMP1* (Ahn et al. 2004). Appressorium formation and pathogenicity are greatly reduced in *EMP1* null mutants. *Sclerotinia sclerotiorum* hyphae also secrete a low molecular weight protein that functions like a hydrophobin and promotes the formation of aerial hyphae (Lugones et al. 2004). Together, these results point to the importance of pathogen surface characteristics in growth and the induction and development of infection structures on the plant surface.

Various chemicals, including cutin monomers, surface waxes and leaf alcohols, can induce appressorial differentiation (Read et al. 1992; Gilbert et al. 1996; Collins et al. 2001) and there is evidence of species-specificity in these interactions. Waxes from barley leaves are more effective inducers of appressorium formation by *Blumeria graminis* f. sp. *hordei* than are waxes from non-host plants (Tsuba et al. 2002). Plant surface waxes are also able to overcome the suppression of appressorial development by self-inhibitors which diffuse from the conidia when at high densities (Hegde and Kolattukudy 1997; Liu and Kolattukudy 1999).

Some pathogens, such as rust fungi in the genera *Puccinia*, *Uromyces* and *Melampsora*, invade leaves by forming an appressorium over a stomatal pore (Fig. 11.8B). Germlings of these species can distinguish the ridges associated with the lip of the guard cells. They also respond to stomatal impressions on plastic replicas of leaf surfaces and to ridges and grooves of similar dimensions on inert surfaces, indicating once again that surface topography can induce the response (Fig. 11.8; Hoch et al. 1987a; Collins and Read 1997; Read et al. 1997). The dimensions of the topographical features that induce appressorium development have been defined precisely for the bean rust fungus, *Uromyces appendiculatus*. A change in elevation on the substratum of 0.5 μm is optimal to trigger appressorium development, a height similar to that of ridges associated with the stomal lip (Hoch et al. 1987a; Kwon and Hoch 1991). The site of signal reception lies on the surface of the hyphae in contact with the substratum, <20 μm from the hyphal apex (Kwon and Hoch 1991; Corrêa and Hoch 1995).

B. Appressorium Development and Function

In *Magnaporthe grisea*, the first morphological sign of the initiation of appressorium development is the swelling and bending of the conidial germ tube into a hook-like structure which proceeds to enlarge to form a domed appressorium (Fig. 11.9A). Ultrastructural studies show that the onset of appressorium formation is associated with the dispersal of the apical cluster of vesicles (Hoch and Staples 1987; Dijksterhuis 2003) or with the displacement of the cluster to a position close to the substratum (Mims and Richardson 1989; Bourett and Howard 1990; Howard et al. 1991a; Kwon et al. 1991a). The linear arrays of microtubules in the hyphae become reorganised in the germ tube tip as it begins to differentiate (Kwon et al. 1991a; Takano et al. 2001). Some appressoria appear to be simple swellings of the hyphae as they attempt to penetrate the plant surface (Fig. 11.8A). Others, for example those formed by *Puccinia graminis* f. sp. *tritici* over a stoma, may be bi- or multi-lobed (Collins et al. 2001). Appressoria that have received the greatest attention are highly specialised dome-shaped cells such as those produced by *M. grisea* and species of *Colletotrichum* and *Uromyces* (Figs. 11.9, 11.10). Biomechanical modelling recently showed that this basic design is robustly consistent with a bioelastic shell that maintains its shape under very high turgor pressures (Tongen et al. 2006).

The properties of the appressorium surface are critical to appressorium function. In *M. grisea*, a wall approximately 150–200 nm in thickness is present over the domed portion of the cell, but is absent from the base of the appressorium (Fig. 11.9C, D; Howard and Ferrari 1989; Bourett and Howard 1990; Howard et al. 1991a). Part of the *M. grisea* appressorium wall is a layer of melanin that reduces the porosity of the wall to less than 1 nm and renders the wall impermeable to most compounds except water (Howard et al. 1991a; Howard 1997). The appressorial pore at the base of the appressorium lacks both chitin and melanin and is surrounded by

a ring of wall material that adheres tightly to the underlying substratum and is presumed to function as a seal between the two surfaces (Figs. 11.9, 11.10). Differentiation of the appressorial wall relative to this pore has also been demonstrated immunocytochemically in *Colletotrichum lindemuthianum* (Pain et al. 1995) and can be recognised as a light spot in light microscopy (Diéguez-Uribeondo et al. 2003). The melanised wall is impermeable to glycerol, an osmoticum that builds up to high concentrations within the appressorium. A concentration of 3.2 M has been measured in appressoria of *M. grisea* (deJong et al. 1997). The high glycerol concentration generates turgor pressures as high as 8 MPa in *M. grisea* (Howard et al. 1991b; deJong et al. 1997), 2.6 MPa in *C. kahawae* (Chen et al. 2004) and 0.35 MPa in *Uromyces appendiculatus* (Terhune et al. 1993). This latter pressure is still sufficient to deform the lips of the underlying guard cells. The importance of melanin in host penetration was demonstrated in studies of the effects of inhibitors of melanin biosynthesis and of mutants deficient in melanin biosynthetic enzymes (Chumley and Valent 1990; Perpetua et al. 1996; Kawamura et al. 1997). Such mutants of *M. grisea* build up much lower concentrations of glycerol (deJong et al. 1997), develop a lower turgor pressure (Money and Howard 1996) and, in both *M. grisea* and *C. lagenarium*, exhibit markedly reduced pathogenicity (Chumley and Valent 1990; Perpetua et al. 1996).

Appressorium development and maturation is supported by nutrients stored within the conidium and transported from the conidium along the germ tube. In *M. grisea*, the main storage reserves in the conidium are glycogen, trehalose and lipids. At the end of appressorium development, a septum separates the appressorium from the germ tube and conidium; the conidium and germ tube are depleted of reserves and cytoplasm, and collapse (Fig. 11.9A, B). A number of recent studies investigated the process of nutrient transport from the conidium and its degradation in the developing appressorium and its importance for the generation of turgor pressure and effective function of the appressorium.

The role of trehalose metabolism has been shown through targeted gene replacement of trehalose synthetic or degradative enzymes in *M. grisea* (Foster et al. 2003). Null mutants lacking the trehalose-6-phosphate synthase gene, *TPS1*, cannot synthesise trehalose and do not develop full turgor pressure within the appressorium. Enzymes involved in trehalose breakdown, in contrast, are not required for appressorium development and maturation but are needed for later stages of colonisation. Glycogen is another storage product that is accumulated in fungal conidia and mobilised during conidial germination and appressorium development (Fig. 11.5E, F; Thines et al. 2000; Weber et al. 2001; Weber and Davoli 2002; Tsuji et al. 2003). Analysis of patterns of gene expression showed that transcript ion of genes encoding

Fig. 11.9. (left column on page 267) Appressorium differentiation. **A** CryoSEM of germinated conidia of *Magnaporthe grisea*. The germ tube of each conidium has differentiated into an appressorium (*A*). The cytoplasm in the basal and middle cells of the three-celled conidia has been degraded to support growth of the appressorium; these two cells of each conidium have subsequently collapsed (*arrows*; *s* septum; Money and Howard 1996). *Bar* 5 µm. **B** CryoSEM of mature appressorium of *M. grisea* which has been sealed off from the subtending conidium and germ tube by a septum. The contents of the conidium and germ tube have been degraded and these cells have collapsed (Braun and Howard 1994b). *Bar* 2 µm. **C** TEM of a mature *M. grisea* appressorium (freeze-substituted cell). The electron dense layer of melanin (*M*) covers most of the appressorial surface but not the surface in contact with the substratum. The latter area is the appressorium pore (between *arrowheads*) and, at this stage of development, consists of a plasma membrane and appears to lack any cell wall (Howard et al. 1991a). *Bar* 1 µm. **D** High magnification TEM image of the appressorium pore of *M. grisea* (freeze-substituted cell). The section has been labelled with wheat germ agglutinin-gold to localise chitin in the fungal cell wall. No labelling is evident across the pore, reflecting the lack of cell wall material in this region (Howard et al. 1991a). *Bar* 1 µm

Fig. 11.10. (right column on page 267) Penetration peg production by the appressorium. **A** Young penetration peg formed at the appressorium pore in an appressorium of *Magnaporthe grisea* (TEM of freeze-substituted cell). The pore region is defined by the perimeter of the appressorium wall (*arrowheads*) and is covered by an overlay of wall material (*o*; Bourett and Howard 1992). *Bar* 0.5 µm. **B** Appressorium of *M. grisea* that has produced a penetration peg that has grown over 6 µm into the underlying substratum (TEM of a freeze-substituted cell; Howard et al. 1991a). *Bar* 1 µm. **C** CryoSEM of lower surface of an appressorium of *M. grisea* that has been detached from the substratum. The appressorium pore is shown in the centre of the appressorium base; the hole that was torn during detachment marks the site of the penetration peg. A ring (between *arrowheads*) encircles the appressorium pore (between *arrows*; Howard et al. 1991b). *Bar* 1 µm. **D** The base of an appressorium of *M. grisea* adhering to a substratum as viewed from the inside of the appressorium after rupture of the appressorium by sonication. The hole (*arrowhead*) is an impression left in the Mylar substratum at the site of the penetration peg. Appressorium pore is between *arrows*; *m* extracellular matrix material (Howard et al. 1991b). *Bar* 1 µm

enzymes involved in glycogen breakdown is high during in germinating conidia (Thomas et al. 2002; Both et al. 2005). Accompanying histochemical labelling also showed breakdown of glycogen stores in the conidia after germination (Thines et al. 2000; Both et al. 2005).

During conidial germination, lipid bodies are quickly mobilised and accumulate in the germ tube apex and developing appressorium (Fig. 11.5A–D; Thines et al. 2000). During appressorium maturation and turgor pressure generation, the lipid is converted to glycerol. The lipid bodies disappear, apparently coalescing and being taken up by vacuoles and triacylglycerol lipase enzyme activity in-

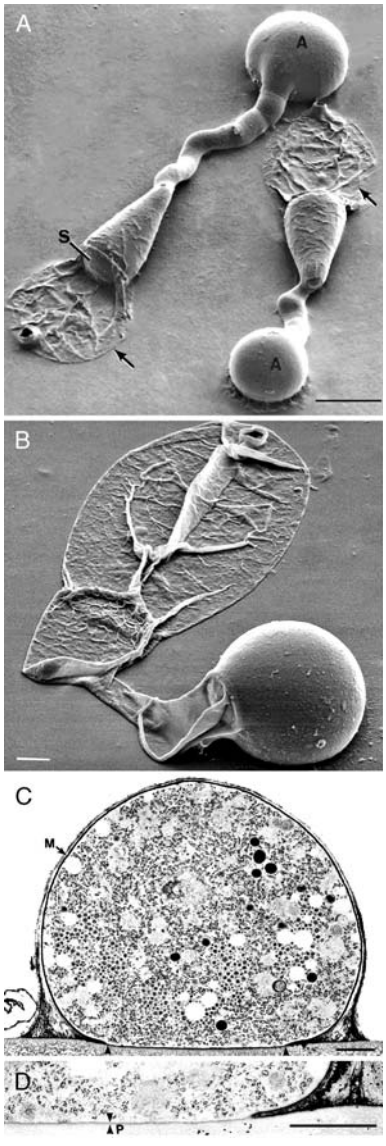

Fig. 11.11.

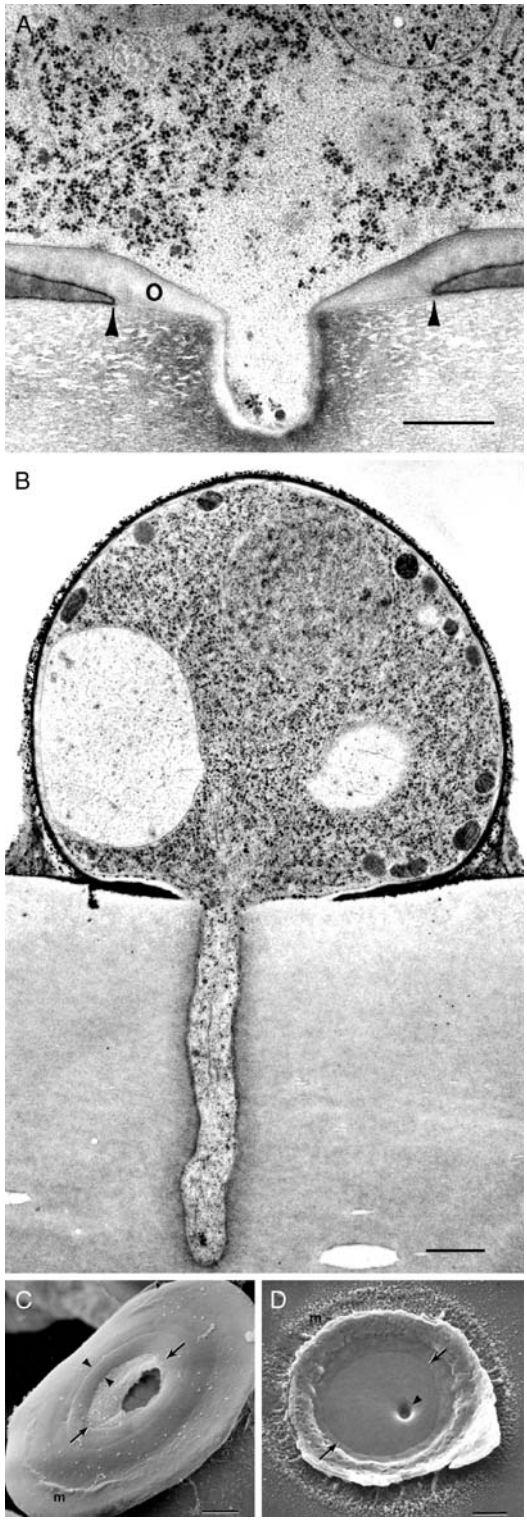

Fig. 11.12.

creases (Thines et al. 2000). Conversion of lipid to glycerol leads to fatty acid synthesis and a requirement for fatty acid β-oxidation, operation of the glyoxylate cycle and gluconeogenesis (Wang et al. 2005). In fungi, β-oxidation is carried out in the peroxisomes and recent studies produced evidence for an important role of these organelles in appressorium maturation and turgor generation (Kimura et al. 2001; Lu et al. 2005; Bhambra et al. 2006; Ramos-Pamplona and Naqvi 2006).

It is likely that stores of protein in the conidium are also remobilised during appressorium development, although as yet little is known of the operation of this process. In *M. grisea*, targetted deletion of a vacuolar serine protease gene, *SPM1*, reduces appressorium development (Donofrio et al. 2006) and proteasome homologues, Mgp1 and Mgp5, have been identified in proteomic studies of developing appressoria (Kim et al. 2003).

In *M. grisea*, after melanisation of the appressorial wall, an overlay of wall material is deposited over the appressorial pore (Fig. 11.10A; Bourett and Howard 1990). A fine penetration peg, about 0.7 μm in diameter, forms on the pore surface and grows through the epidermal cell wall of the host (Fig. 11.10; Howard and Valent 1996). The cytoplasm of the penetration peg is generally devoid of organelles but contains a bundle of actin microfilaments (Bourett and Howard 1991). Visualisation of microtubule arrays in appressoria is facilitated by GFP-tagging of tubulin. Both linear and randomly organised microtubule arrays have been observed in developing appressoria (Takano et al. 2000; Czymmek et al. 2005) but in mature appressoria a novel population of microtubules oriented vertically, i.e. perpendicular to the leaf surface, has been imaged in addition to the cortical array (Park et al. 2004). Targetted deletion of a transcription factor (*MST12*) in *M. grisea* results in failure of penetration peg formation and penetration (Park et al. 2002); and in this mutant both the vertical actin and microtubule arrays are disrupted (Park et al. 2004). Further analysis of the genes regulated by *MST12* promises to help characterise the roles of these cytoskeletal elements in penetration peg formation and function.

With a turgor pressure of 8 MPa, it was calculated that the penetration peg of *M. grisea* appressoria could generate a force of 8–17 μN (Money and Howard 1996), a value in good agreement with that measured using elastic optical waveguides for the force produced by appressorial penetration pegs of *C. graminicola* (Bechinger et al. 1999). The fact that these pressures are sufficient for the penetration peg to force its way through a surface as hard as a plant epidermal cell wall was elegantly demonstrated in *M. grisea* through the use of mylar sheets which are impervious to degradation by fungal enzymes (Howard and Ferrari 1989; Bourett and Howard 1990; Howard et al. 1991a, b). These studies indicated that the fungus is capable of penetrating mylar sheets as hard as or harder than a rice leaf surface by using force alone. However, it was also found that the fungus penetrates the rice leaf more quickly than it does mylar sheets of hardness similar to that of the rice leaf, suggesting that, on the plant surface, the fungus uses both physical force and enzymatic digestion to penetrate the leaf surface (Bastmeyer et al. 2002).

The critical role played by turgor pressure and the development of a structurally sound penetration peg was highlighted by molecular studies of selected genes identified from transcript profiling studies that focused on genes that are expressed during appressorium formation. One such group of proteins is the tetraspanins, small membrane proteins that occur in a variety of plant pathogenic fungi (Veneault-Fourrey et al. 2006). In *M. grisea*, *C. lindemuthianum* and *Botrytis cinerea*, targeted deletion of tetraspanin-encoding genes (*Pls1*, *ClPLS1* and *Bcpls1*, respectively) leads to failure of the pathogen to penetrate the host surface (Clergeot et al. 2001; Gourgues et al. 2004; Veneault-Fourrey et al. 2005). It is believed that disruption of tetraspanin synthesis causes abnormalities in the structure or location of the penetration peg. Targeted deletion of the *PDE1* gene encoding a P-type ATPase resident in the plasma membrane of germinating conidia and developing appressoria also inhibits the development of penetration hyphae (Balhadere and Talbot 2001).

Two other proteins shown to be required for normal penetration peg development are cyclophilin and metallothionein. Cyclophilin, a peptidyl prolyl isomerase that aids protein folding, is conserved throughout the eukaryotes. In *M. grisea*, a single cyclophilin gene, *Cyp1*, encodes two mRNA transcripts that give rise to cytosolic and mitochondrial proteins (Viaud et al. 2002). *Cyp1* is highly expressed during infection. Targetted deletion or disruption of the cyclophilin genes in *M. grisea* and *B. cinerea* impairs penetration peg formation and turgor pressure generation and reduces pathogen virulence (Viaud et al. 2002, 2003). Metallothionins are small antioxidant proteins found in all eukaryotes. In *M. grisea*, studies

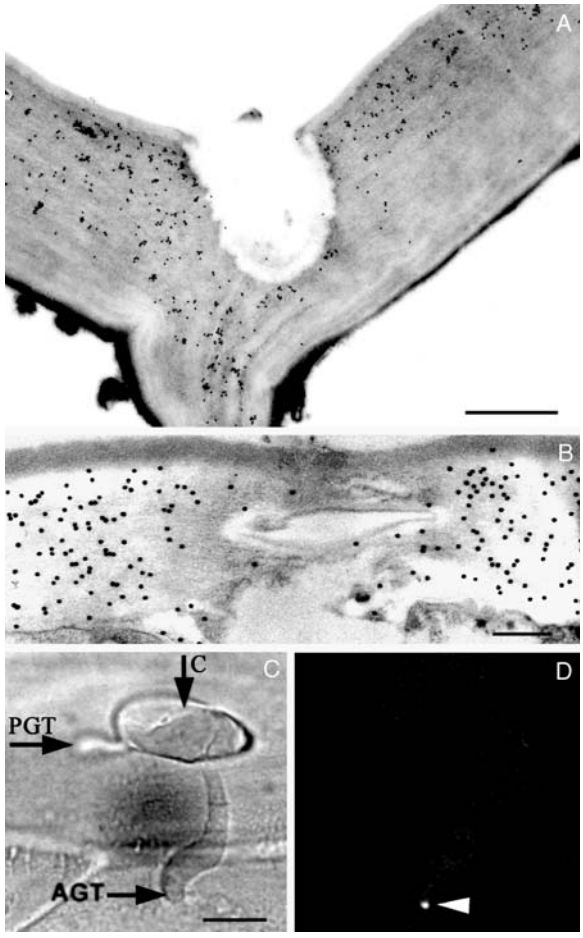

Fig. 11.13. Enzyme secretion at the point of plant cell wall penetration. **A** Cavity in an epidermal cell wall produced by the penetration peg of an appressorium of *Cochliobolus sativus* on a leaf of barley. The section was immunogold labelled with JIM5, a monoclonal antibody specific for polygalacturonic acid. The erosion of the wall suggests that wall-degrading enzymes were secreted by the penetration peg. The plant cell wall contains less polygalacturonic acid near the edges of the cavity than in regions further away (Clay et al. 1997). *Bar* 1 µm. **B** Outer epidermal wall of *Vicia faba* breached by a penetration peg formed by an appressorium of *Uromyces vignae*. The section was labelled with JIM 7, a monoclonal antibody specific for methylesterified pectin. The wall close to the penetration site has lower pectin content than in other regions. Material prepared by high pressure freezing and freeze-substitution (Xu and Mendgen 1997). *Bar* 0.2 µm. **C, D** Germinated conidium of *Blumeria graminis* f.sp. *hordei* on the surface of a barley leaf labelled with a monoclonal antibody specific for cellobiohydrolase shown in bright field (**C**) and fluorescence illumination (**D**). A highly localised area at the tip of the appressorial germ tube was labelled by the antibody (*arrowhead*). *C* Conidium, *PGT* primary germ tube, *AGT* apppressorial germ tube (Jones et al. 1998). *Bar* 10 µm

of appressorial gene expression showed that transcripts encoding metallothioneins are abundant in appressoria (Ebbole et al. 2004). The metallothionein proteins becomes localised on the inner side of the cell wall of the appressorium (Tucker et al. 2004). Targetted disruption of the *MMT1* gene leads to failure of the pathogen to penetrate the plant cuticle, perhaps because of abnormalities in the appressorial or penetration peg cell wall.

After breaching the cuticle, the penetration peg grows through the wall of the infected plant cell. The lack of compression, indicative of mechanical force, and the localised degradation of wall structure surrounding the penetration peg produced by appressoria and haustorial mother cells are taken as evidence of the action of fungal enzymes (Fig. 11.13). Molecular cytochemical studies give evidence of both localised reduction in individual components in the plant cell wall at the penetration site, and of temporally and spatially restricted production and secretion of wall degrading enzymes. Reductions in pectin, cellulose and xyloglucan were reported adjacent to appressorial penetration pegs produced by *Cochliobolus sativus* and *Uromyces vignae* (Fig. 11.13A, B; Clay et al. 1997; Xu and Mendgen 1997). Extensive studies of the activity of cell wall-degrading enzymes during infection structure formation in *U. fabae* revealed a cascade of enzyme activities, with pectin methylesterase and cellulase activities coinciding with the differentiation of infection hyphae and haustorial mother cells (Deising and Mendgen 1992; Frittrang et al. 1992; Heiler et al. 1993; Deising et al. 1995a, b; Mendgen et al. 1996). Localisation studies showed polygalacturonase in germ tubes and appressoria penetration pegs of *Colletotrichum lindemuthianum* (Dumas et al. 1999) and cellobiohydrolase at the appressorial penetration peg of *Blumeria graminis* (Fig. 11.13C, D; Pryce-Jones et al. 1999). Antibodies directed towards subtilisin-like proteases and pectate lyase were also shown to reduce pathogenicity of *M. poae* and *C. gloeosporioides*, respectively (Wattad et al. 1997; Sreedhar et al. 1999).

VI. Acquisition of Nutrients from the Plant

A. Haustoria and Intracellular Hyphae of Biotrophic Pathogens

Phytopathogenic fungi and oomycetes employ a variety of infection strategies in order to gain ac-

cess to the nutrients they need for growth, development and reproduction. The strategy used by necrotrophic fungi is to obtain nutrients by killing the host cells, forming expanding necrotic lesions. The strategy used by biotrophic pathogens is to establish a close and stable relationship with living host cells and to redirect the flow of nutrients from the plant cell into the pathogen. To do this, biotrophic pathogens form specialised feeding structures that take the form of haustoria or differentiated intracellular hyphae.

In some biotrophic pathogens, such as the powdery mildews, the appressorial penetration pegs grow directly through the outer epidermal cell wall and form haustoria within the epidermal cells. In other biotrophic pathogens, such as the rusts, the appressorial penetration peg grows through a stomatal aperture into the substomatal cavity (Fig. 11.14). In this case, the pathogen then develops a substomatal vesicle and infection hyphae which traverse the intercellular spaces in the leaf until contact is made with a parenchyma cell. The apex of the infection hypha then differentiates to form a haustorial mother cell which produces a penetration peg which grows through the wall of the plant cell and develops a haustorium (Fig. 11.15A, C; Mendgen and Deising 1993; Mendgen et al. 1996). The haustorial mother cell on the surface of the leaf parenchyma cell thus plays a similar role to that of the appressorium on the plant surface; however, little is known of the factors that induce haustorial mother cell differentiation or that regulate its function (Mendgen and Hahn 2002). This is due in large part to the difficulties in studying the development of a cell that cannot be observed without sectioning the leaf in order to observe the structures within it. It is generally believed that haustorial mother cells rely on the action of secreted cell wall-degrading enzymes in order to penetrate the mesophyll plant cell wall (Chong et al. 1981; Taylor and Mims 1991). Nevertheless, regardless of the exact mode of invasion, it is important to note that penetration pegs produced by appressoria and haustoria mother cells puncture the plant cell wall but they do not breach the underlying plant cell plasma membrane. In both cases, the plant plasma membrane is invaginated but remains intact and surrounds the expanding haustorium or intracellular hypha (Fig. 11.15C).

The degree of structural and functional specialisation of the nutrient-absorbing haustoria and intracellular hyphae is variable (Manners and Gay 1983). The body of the haustorium, often subtended from a narrow neck region (Fig. 13A, C), is approximately spherical or lobed in the oomycete downy mildews and dikaryotic rust spore infections (Fig. 11.15C) but is filamentous and unbranched in the monokaryotic rust spore infections. Haustoria of the powdery mildews have a high surface to volume ratio as a result of multiple projections from the haustorial body (Fig. 11.15B; Manners and Gay 1983). The extensions may project outwards (as in *Blumeria graminis*) or they may wrap around the haustorial body. Hemibiotrophic fungi, such as species of *Colletotrichum* which grow biotrophically for a period of time before becoming necrotrophic, produce an infection vesicle and primary hyphae that together constitute the intracellular hyphae (Fig. 11.16C). The wall and plasma membrane of the haustorium or intracellular hyphae are continuous with the wall and plasma membrane of the hyphal cell on the outside of the invaded plant cell. In the powdery mildews, the haustorium becomes delineated from the appressorium by a septum in the neck, but in the downy mildews and rust fungi a septum is not formed (Manners and Gay 1983).

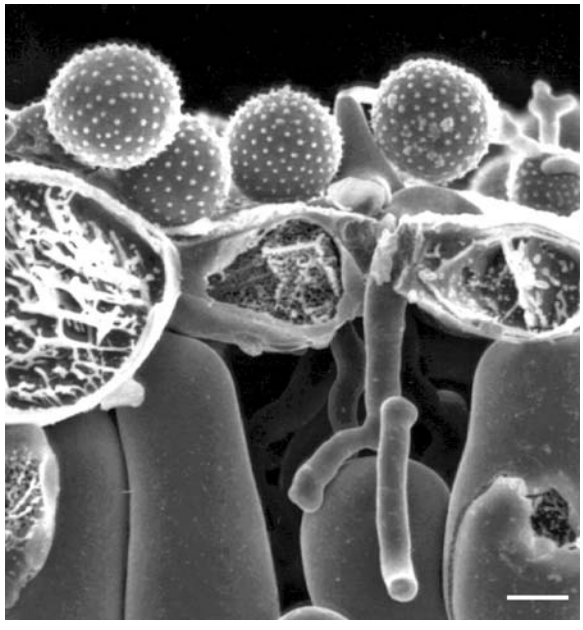

Fig. 11.14. Leaf penetration through a stomatal aperture. CryoSEM image of uredospores of *Melampsora lini* that germinated on the surface of a flax leaf and penetrated the leaf through a stoma. An infection hyphae within the leaf has made contact with a mesophyll cell (Hardham and Mitchell 1998). *Bar* 1 μm

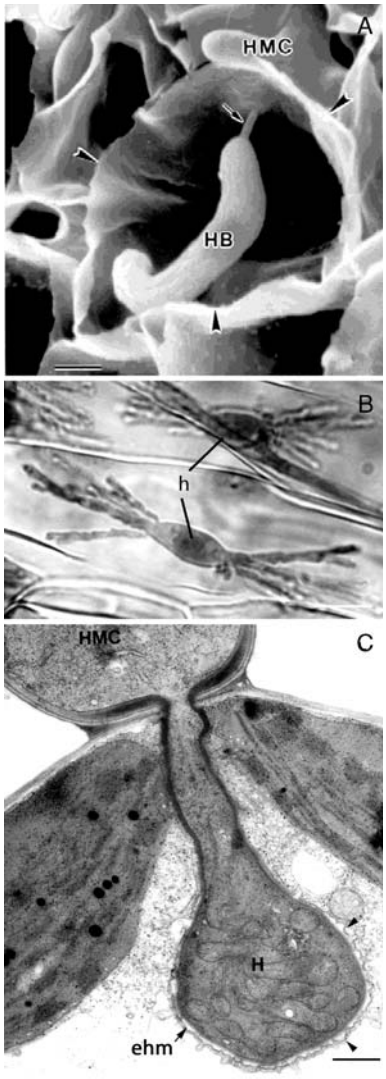

Fig. 11.15. Formation of haustoria and intracellular hyphae. **A** CryoSEM of dikaryotic haustorium of *Puccinia arachidis* in a mesophyll cell of peanut. *Arrow* Haustorial neck, *HB* haustorial body, *HMC* haustorial mother cell (Mims et al. 2003). *Bar* 3 µm. **B** Bilateral haustoria (*h*) of *Blumeria graminis* f.sp. *hordei* in barley leaf cell (Takemoto et al. 2006). *Bar* 10 µm **C** TEM image of a haustorial mother cell (*HMC*) and haustorium (*H*) of *Melampsora lini* in a flax leaf mesophyll cell. The haustorium is surrounded by the invaginated host cell plasma membrane (*ehm*). The extrahaustorial matrix (*arrowheads*) lies between the haustorium wall and the host plasma membrane (micrograph by courtesy of L. Murdoch). *Bar* 0.5 µm

The invaginated host plasma membrane surrounding the haustorium is termed the extrahaustorial membrane (Fig. 11.15C). Over most of the haustorium surface, the wall of the haustorium (or intracellular hypha) is separated from the plant plasma membrane by an extrahaustorial or interfacial matrix layer (Fig. 11.15C). In the powdery mildews and dikaryotic rust infections, both the fungal and plant plasma membranes are tightly pressed against the haustorial wall in the neck of the haustorium, an arrangement that results in sealing of the extrahaustorial matrix compartment (Fig. 11.15C; Heath 1976). Structures in the neck region of the downy mildews are not of similar morphology to the neckbands in the powdery mildews and rusts, but are thought to be functionally equivalent (Woods and Gay 1983). With a view to understanding the structure and function of haustoria and intracellular hyphae of the biotrophic phytopathogens, much effort has been directed towards identifying the molecular composition of the plant–pathogen interface. Evidence of molecular specialisations in this interface has accumulated and is believed to be indicative of the role of these infection structures in nutrient uptake.

Ultrastructural studies show that the extrahaustorial membrane formed in rust, powdery mildew and downy mildew infections is morphologically distinct from the plasma membrane in other parts of the cell (Littlefield and Bracker 1972; Aist and Bushnell 1991; Callow and Green 1996; Mims et al. 2003; Celio et al. 2004). The extrahaustorial membrane is thicker than the plant plasma membrane and is heavily glycosylated. This differentiation was exemplified in immunocytochemical studies of pea powdery mildew which showed the segregation of two high molecular weight glycoproteins within the plasma membrane of the infected pea epidermal cells (Roberts et al. 1993). One glycoprotein is excluded from the extrahaustorial membrane as the haustorium develops; the other glycoprotein occurs in the extrahaustorial membrane but not elsewhere in the plant plasma membrane. Cytochemical studies also revealed that the extrahaustorial membrane surrounding powdery mildew and dikaryotic rust haustoria lacks the ATPase activity which is generally seen in the plant plasma membrane and which is still present in the plasma membrane in other parts of the infected cell (Spencer-Phillips and Gay 1981; see also Gay and Woods 1987). In contrast, the extrahaustorial membrane surrounding filamentous haustoria of monokaryotic rust infections contains ATPase activity, although in some cases there is a gradient of reduced ATPase activity towardst the tip of the haustorium, i.e. the end opposite the point of entry into the cell (Woods and Gay 1987; Baka et al. 1995). The plant membrane surrounding intracellular hyphae of *Colletotrichum lindemuthi-*

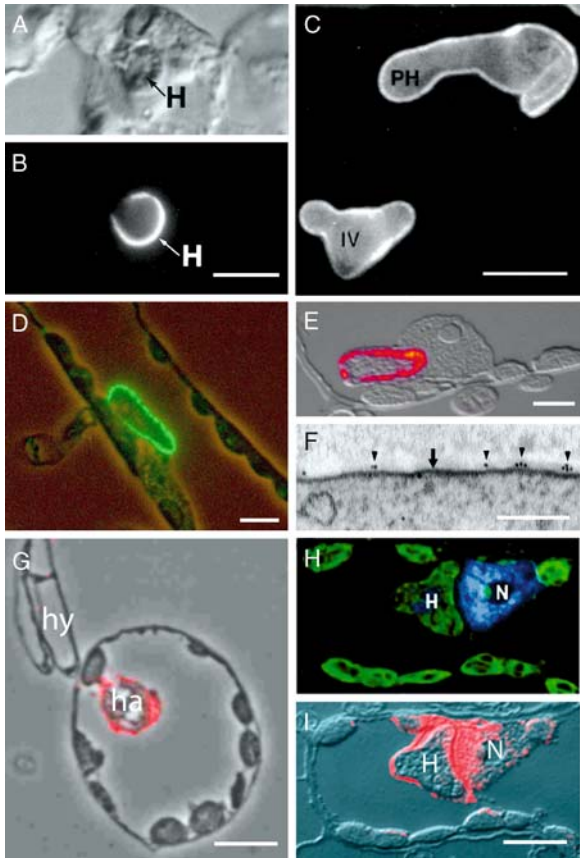

Fig. 11.16. Surface properties of haustoria and intracellular hyphae. **A**, **B** Bright field (**A**) and immunofluorescence (**B**) light micrographs of infection hypha and haustorium (*H*) of *Melampsora lini* in a flax leaf. The wall of the haustorium, but not that of the hypha or plant cell, is labelled with monoclonal antibody, ML-1 (micrographs by courtesy of L. Murdoch). *Bar* 10 µm. **C** Immunofluorescence labelling of primary hypha (*PH*) and infection vesicle (*IV*) produced by *Colletotrichum lindemuthianum* within an epidermal cell of *Phaseolus vulgaris* labelled with monoclonal antibody UB25 that reacts with a 40.5-kDa glycoprotein in the intracellular hyphal walls and interfacial matrix layer (Perfect et al. 1998). *Bar* 10 µm. **D** Immunolabelling of a putative amino acid transporter on the surface of the haustorium of *Uromyces fabae* in a mesophyll cell of a bean leaf (Hahn et al. 1997). *Bar* 3 µm. **E** Immunolabelling of the HXT1p hexose transporter on the surface of a dikaryotic haustorium of *U. fabae* in a mesophyll cell of a bean leaf (Voegele and Mendgen 2003). *Bar* 5 µm. **F** Immunogold labelling of the HXT1p hexose transporter on the plasma membrane (*arrowheads*) of a haustorium of *U. fabae* in a mesophyll cell of a bean leaf. *Arrow* Extrahaustorial membrane (Voegele et al. 2001). *Bar* 0.1 µm. **G** Immunolabelling of the Uf-INV1p invertase around the periphery of a haustorium (*ha*) of *U. fabae* in a bean mesophyll cell. *hy* Intercellular hypha (Voegele et al. 2001). *Bar* 10 µm. **H**, **I** Immunolabelling of the RTP1p protein secreted by a haustorium (*H*) of *U. fabae* and transferred into the cytoplasm and nucleus (*N*) of the infected plant mesophyll cell. Nucleus stained blue with bisbenzimide (**H**) and RTP1p fluorescence shown in red (**I**; Kemen et al. 2005). *Bar* 10 µm

anum also contains ATPase activity and thus lacks this form of specialisation shown by the powdery mildew and dikaryotic rust infections (O'Connell 1987). These results were interpreted as indicating that the haustoria of monokaryotic rusts and the hemibiotroph are less specialised than the dikaryotic haustoria (O'Connell 1987; Baka et al. 1995).

There is still little understanding of the molecular composition of the extrahaustorial or interfacial matrix between the wall of the haustorium or intracellular hypha and the plant plasma membrane. It is clear that the material within the matrix is of both plant and pathogen origin and that it contains carbohydrates (Chard and Gay 1984; O'Connell 1987). Immunolabelling showed the presence of proline- and hydroxyproline-rich glycoproteins similar to those found in plant cell walls (Hippe-Sanwald et al. 1994; Stark-Urnau and Mendgen 1995). A number of N-linked glycoproteins were also demonstrated in the interfacial matrix around *Colletotrichum* infection hyphae in bean (Pain et al. 1994; O'Connell et al. 1996a). One of these, a proline-rich glycoprotein, is specific for the surface of intracellular hyphae growing inside living plant cells during the biotrophic phase of growth, and is absent from the surface of primary hyphae growing intercellularly and from hyphae growing on the plant surface (Pain et al. 1994; O'Connell et al. 1996b; Perfect et al. 1998, 2000).

Immunocytochemical investigations showed that the walls of fungal haustoria contain molecules also found in the walls of mycelia and other cells of the same species (Mackie et al. 1991; Callow et al. 1992; Scott et al. 1997; Murdoch et al. 1998; Perfect et al. 2001), as well as molecules that are specific to the haustorial walls (Fig. 11.16A, B; Murdoch and Hardham 1998; Murdoch et al. 1998). They also produced the first evidence of differences in protein composition between haustorial and mycelial plasma membranes (Callow et al. 1992; Mackie et al. 1993). Further details of the molecular differentiation of the haustorial plasma membrane came from the characterisation of genes that are preferentially expressed in the haustoria of the bean rust fungus, *Uromyces fabae*, and these landmark studies provided the first direct evidence of the central role haustoria play in nutrient uptake.

Molecular characterisation of *Uromyces* haustoria began with the demonstration that the level of ATPase activity in plasma membranes from haustoria is significantly higher than in plasma membranes from ungerminated or germinated uredospores (Struck et al. 1996; Wirsel et al. 2001).

The gene encoding the H^+-ATPase was cloned and analysis of its expression showed that transcript levels do not mirror those of enzyme activity (Struck et al. 1998; Wirsel et al. 2001), indicating that regulation of the *Uromyces fabae* haustorial plasma membrane H^+-ATPase is likely to be under post-translational control. It was envisaged that the Uf-PMA1 ATPase pumps protons out of the haustorium into the extrahaustorial matrix, thereby establishing a proton gradient that could drive uptake of nutrients across the haustorial plasma membrane. Generation of such a gradient would be possible because the extrahaustorial matrix is a sealed compartment (Szabo and Bushnell 2001).

The next advance was the identification of three *in planta*-induced genes that encode putative amino acid transporters (Hahn et al. 1997). One of these proteins was immunolocalised to the haustorial plasma membrane but no transport activity could be demonstrated (Fig. 11.16D; Mendgen et al. 2000). The other two genes, whose amino permease activity has been confirmed, have not yet been localised; however, transcript levels for both are highest in haustoria (Struck et al. 2002, 2004). The latter two proteins, UfAAT1p and UfAAT3p, are similar to symport amino acid permeases which use the transmembrane pH gradient generated by a plasma membrane ATPase to power amino acid uptake. Heterologous expression in *Xenopus* oocytes revealed that they preferentially transport amino acids that are present in low concentrations in infected leaves, with Uf-AAT1p exhibiting a preference for lysine and histidine, and Uf-AAT3p a preference for leucine, methionine and cysteine (Struck et al. 2002, 2004).

The next breakthrough came with the cloning of a gene encoding a hexose sugar transporter with specificity for glucose and fructose (Voegele et al. 2001). The hexose transporter, Uf-HXT1p, was localised to the plasma membrane in the distal tip of monokaryotic haustoria and throughout the body of dikaryotic haustoria (Fig. 11.16E, F; Voegele and Mendgen 2003). It is also a proton symporter.

Sugars are transported around the plant mainly in the form of the disaccharide, sucrose. Thus, in order for Uf-HXT1p to import sugars into the haustorium, sucrose must be broken down into its constituent glucose and fructose units and these monosaccharides made available to the transporter. Potentially, this conversion of sucrose to glucose and fructose could occur in the plant cytoplasm or in the extrahaustorial matrix, and could be achieved through the action of either fungal or plant enzymes. Evidence that a fungal invertase is likely to play an active role in generation of the monosaccharides comes from the cloning and characterisation of an invertase gene, *Uf-INV1*, from *Uromyces fabae* (Voegele et al. 2006). *Uf-INV1* transcript levels are high in haustoria and the Uf-INV1p protein is localised to the extrahaustorial matrix (Fig. 11.16G). Analysis of the expression of three bean invertases showed that one of these is also up-regulated in infected leaves. Current data thus suggest that, as the pathogen reprograms the infected leaf to act as a sink instead of a source of sugars, plant invertase may cleave sucrose in the plant cytosol and fungal invertase may act on sucrose that has moved into the extrahaustorial matrix.

To maintain the flow of sugar from the infected leaf through the extrahaustorial matrix and into the pathogen, it is important for the glucose and fructose taken up by the HXT1p transporter to be removed from the haustorial cytoplasm. Two enzymes that are abundant in haustoria and could be involved in this process are MAD1p, a mannitol dehydrogenase, and ARD1p, a $NADP^+$-dependent D-arabitol dehydrogenase (Link et al. 2005; Voegele et al. 2005). These enzymes may contribute to the conversion of the imported sugars into mannitol and arabitol, both of which accumulate in infected leaves. It is suggested that mannitol and arabitol could serve a number of functions, including roles in carbohydrate storage and translocation, and in the suppression of host defences (Link et al. 2005; Voegele et al. 2005). There is also evidence that glycerol may be an important transferred metabolite in the hemibiotroph, *Colletotrichum gloeosporioides* (Wei et al. 2004).

This evidence of active carbohydrate metabolism is augmented by evidence of other forms of biosynthetic activity in the haustoria. Two highly abundant transcripts in the *Uromyces fabae* haustoria encode enzymes involved in thiamine biosynthesis; others participate in the synthesis of metallothioneins (Hahn and Mendgen 1997; Sohn et al. 2000). Taken together, these exciting new data paint a picture of haustoria as centres of intense metabolic activity that play a pivotal role in the orchestration of nutrient acquisition, biosynthesis and suppression of host defences (Voegele and Mendgen 2003; Jakupovic et al. 2006).

It has been generally accepted for some time that, in order to establish their close and successful interaction with living host cells, biotrophic fungi must induce major changes in host cell metabolism

and organisation. But how this might be achieved remains an enigma. Could pathogen proteins or other complex molecules be secreted into the extrahaustorial matrix and then translocated across the extrahaustorial membrane into the plant cell? The first indications that this might be possible came with the demonstration that avirulence proteins produced by the rice blast and flax rust fungi interact directly with disease resistance proteins located in the plant cell cytoplasm (Jia et al. 2000; Dodds et al. 2004). Now it has been shown that proteins produced by the haustoria of biotrophic pathogens can indeed move into the host cell (Fig. 11.16H, I; Kemen et al. 2005; Catanzariti et al. 2006). While as yet there is no information on the molecular mechanisms responsible for this translocation event in fungal diseases, sequence analysis of avirulence and other secreted proteins in the oomycetes has revealed the presence of an RxLR motif near the N-terminus that potentially could target proteins into the host cytoplasm (Rehmany et al. 2005). A similar motif is used by malarial parasites to target virulence proteins into the cytoplasm of infected mammalian cells (Hiller et al. 2004; Marti et al. 2005) and the *Phytophthora* RxLR-containing leader sequence is capable of effecting protein transfer in transgenic malarial cells (Bhattacharjee et al. 2006). There seems little doubt that more details of this targeting and translocation system in the oomycetes will be elucidated in the near future, while the first information on the equivalent fungal mechanisms remains to be discovered.

B. Colonisation of Plant Tissues: the Role of Cell Wall-Degrading Enzymes

The development of haustoria by biotrophic pathogens requires highly localised wall degradation to allow ingress of the penetration peg through the plant cell wall without causing further disruption which might trigger the plant defence response and death of the infected cell. Details of exactly how wall degradation is restricted to the small area required for penetration are still not known, although it has been suggested that the use of enzymes that have a high molecular weight and that become bound to the cell wall may limit their diffusion away from the site of secretion (Akimitsu et al. 2004). It is also possible that only selected wall components are degraded. Removal of the pectin component of the cell wall but not cellulose or hemicelluloses, for example, occurs during formation of the unusual interaction apparatus produced by *Cymadothea trifolii* during penetration of clover leaf cells (Simon et al. 2005). In this system, instead of the development of a haustorium inside the infected plant cell, the plant plasma membrane is induced to invaginate in the absence of any apparent fungus-derived structures. During establishment of the biotrophic interaction, a linking tube that connects the invaginated plasma membrane bubble in the plant cell with the infection apparatus in the adjacent fungal hyphae forms through the plant cell wall. Polygalacturonases are secreted by the fungus at the site of contact and pectin components are selectively removed from within the linking tube. This partial wall degradation may preserve overall structural integrity while allowing enhanced flow of nutrients from the plant cell or of regulatory molecules from the fungus (Simon et al. 2005). More widespread degradation of pectin and other wall components can occur during a biotrophic interaction, such as exemplified during the infection of grass ovary tissues by *Claviceps purpurea* (Tenberge et al. 1996; Tudzynski and Scheffer 2004).

In contrast to the biotrophs, necrotrophic pathogens do not need to restrict host cell wall degradation to avoid triggering plant cell death (ten Have et al. 2002). Wall digestion during necrotrophic infections was studied by labelling wall components and by localising secreted wall-digesting enzymes. Secretion of pectolytic enzymes and extensive loss of pectin were observed in a range of infections (Centis et al. 1997; Rha et al. 2001; Boudjeko et al. 2006). Reduction in cellulose, hemicellulose and pectin components close to the site of contact with the fungus was observed during infection of wheat spikes with *Fusarium graminearum* (Wanjiru et al. 2002).

Characterisation of pathogen genes encoding cell wall-degrading enzymes revealed that in many cases they constitute large gene families. There are, for example, respectively 12 and over 20 endopolygalacturonase genes in *Sclerotinia* (Li et al. 2004) and *Phytophthora* (Götesson et al. 2002); *F. graminearum* has 32 xyloglucanase genes (Hatsch et al. 2006). In addition, post-translational modifications may give rise to even more isozymes than there are genes (D'Ovidio et al. 2004; Xie et al. 2005; Beliën et al. 2006; Wu et al. 2006). There is a suggestion that gene family size might correlate with host range but this is clearly not always the case (ten Have et al. 2001; Götesson et al. 2002). Given the great molecular complexity of the plant cell wall,

the multiplicity of cell wall-degrading enzymes is likely a reflection of specialisations for the cleavage of particular molecular linkages and for optimal performance under a range of environmental conditions (ten Have et al. 2002; D'Ovidio et al. 2004).

Early studies showed secretion of a cascade of cell wall-degrading enzymes during infection, commonly reporting the early production of pectinases followed by hemicellulases and then cellulases (Jones et al. 1972). Over recent years, much effort focused on elucidating factors that regulate the expression of genes encoding cell wall-degrading enzymes. These studies showed differences not only in the timing of production of different categories of enzymes but also differential expression of individual members within a single gene family. Differential expression of polygalacturonase genes, for example, occurs in a range of pathogens, including *Botrytis cinerea* (Wubben et al. 1999,2000; ten Have et al. 2001), *Colletotrichum lindemuthianum* (Centis et al. 1997) and *Sclerotinia sclerotiorum* (Martel et al. 1996,1998, Li et al. 2004). Transcript analysis highlighted the differential expression of 30 xylanase genes in *Fusarium graminearum* (Hatsch et al. 2006). Glucanase genes in *Phytophthora infestans* are also differentially expressed at different stages of the pathogen's asexual lifecycle (McLeod et al. 2003).

Some genes encoding cell wall-degrading enzymes are constitutively expressed but the majority are induced by the presence of the enzyme's substrate or products of its catalytic activity. Thus, expression of endo- and exo-polygalacturonase genes may be induced by pectin (Centis et al. 1997; Isshiki et al. 2003; Herbert et al. 2004; Li et al. 2004; Yan and Liou 2005), polygalacturonic acid (Wubben et al. 1999; Rha et al. 2001; Ohtani et al. 2003) or galacturonic acid (Rha et al. 2001; ten Have et al. 2001; Li et al. 2004). Expression of genes encoding xylanases are induced by xylan or xylose (Gómez-Gómez et al. 2002; Degefu et al. 2004; Brito et al. 2006). The regulation of gene expression is not always as simple as these data suggest. In *Aspergillus niger*, for example, xylose, a subunit of xyloglucan hemicelluloses, induces expression of the transcriptional regulator, *XlnR* which in turn induces both xylanase and cellulolytic genes (van Peij et al. 1998).

Many genes encoding cell wall-degrading enzymes are also subject to carbon catabolic repression. In this mode of regulation, the presence of readily utilisable sugars such as glucose or sucrose represses gene expression (de Vries et al. 2002; Akimitsu et al. 2004; D'Ovidio et al. 2004). At least in some systems, this response is mediated by the catabolite repressive element A (CreA), a *cis*-acting zinc finger repressor that binds to specific sequences in the gene's promoter (Isshiki et al. 2003; Ohtani et al. 2003; Brito et al. 2006). Enzymes produced by gene family members that are not under catabolic repression may act as "extracellular guards" that monitor the environment for the presence of potential substrates (Wubben et al. 2000; Hatsch et al. 2006). Just as the activity of cell wall-degrading enzymes is influenced by the pH of the solution in which it is functioning, the expression of genes encoding these enzymes may also be affected by ambient pH (Shih et al. 2000; ten Have et al. 2001; Gómez-Gómez et al. 2002; Rollins 2003; Akimitsu et al. 2004). Pathogens have the ability to change the ambient pH, either acidifying or alkalinising the environment, to better suit their degradative requirements (Prusky and Yakoby 2003).

In early studies of the role of cell wall-degrading enzymes in pathogenicity, targeted inactivation or gene knockout experiments failed to demonstrate a requirement for one or more enzymes in the infection process (Walton 1994; Annis and Goodwin 1997). Pathogen virulence was not measurably affected when one or even up to four genes (Kim et al. 2001) were inactivated. Failure of these gene inactivation experiments to decrease pathogen virulence was attributed to residual enzyme activity due to other members of the gene family or to presence of a closely related gene family. However, over the past few years, a growing number of studies demonstrated significant reduction of pathogenicity when one or two genes encoding cell wall-degrading enzymes were inactivated. The majority of these studies focused on polygalacturonases (Tenberge et al. 1996; Shieh et al. 1997; Isshiki et al. 2001) but pectin lyase (Rogers et al. 2000; Yakoby et al. 2001; Oeser et al. 2002; Tudzynski and Scheffer 2004) and xyloglucanase (Brito et al. 2006) are also required for full virulence. In *Cochliobolus carbonum*, the species in which extensive gene knockout experiments had consistently failed to produce any effect on pathogenicity, targeted gene replacement of a regulatory gene, *ccSNF1*, successfully demonstrated the essential role of cell wall degrading enzymes in the infection of plants by this fungus (Tonukari et al. 2000). *ccSNF1* is an orthologue of the yeast protein kinase *SNF1* gene which is required for the expression of catabolite-repressed genes (Celenza and Carlson 1984). In the *C. carbonum* study, deletion

of *ccSNF1* led to down-regulation of the expression of a number of xylanase, pectinase and glucanase genes, and subsequent inhibition in penetration and reduction in lesion development on the maize host (Tonukari et al. 2000). An SNF1 orthologue in *Fusarium oxysporum* was also shown to control expression of cell wall-degrading enzymes and virulence (Ospina-Giraldo et al. 2003).

VII. Conclusions

This chapter reviews our current understanding of the cell biology of the infection of plants by pathogenic fungi and oomycetes. In the six years since the first edition of this volume was prepared, a great deal of exciting new data has emerged from cellular and molecular studies of a range of biotrophic and necrotrophic pathogens. Gene discovery and proteomic studies helped identify cohorts of genes/proteins that are preferentially expressed in hyphae, spores, germlings, appressoria or haustoria; targeted gene disruption, structural and cytochemical studies helped characterise many of these genes/proteins, providing clues to their role in specific stages of the infection process. We now have a much improved understanding of the role of the cytoskeleton in hyphal growth and morphogenesis, including its role in endocytosis and exocytosis. We now have full sequence data on oomycete hyphal and spore adhesive proteins, opening the way for a thorough analysis of the role of adhesion in the infection process. We now have a greatly expanded understanding of the molecular controls of spore germination and appressorium differentiation, including details of nutrient mobilisation and signal transduction pathways that support appressorial development. Amino acid and sugar transporters have been identified in haustorial membranes which, together with the identification of other proteins involved in biosynthesis and sugar metabolism, provide the long-sought after definitive evidence of the central role played by haustoria in nutrient uptake during biotrophic infections. Equally exciting is the unambiguous demonstration of the transfer of haustorial proteins into the cytoplasm and nucleus of the infected plant cell, giving substance to the long-held belief that biotrophic pathogens manipulate the organisation and metabolism of the infected host cell. Extensive evidence for the crucial function of cell wall-degrading enzymes in host penetration has also been gathered from studies of a number of different host–pathogen systems.

Many of the most exciting aspects of the information on plant–pathogen interactions that emerged over the past six years arose from studies that combined modern techniques in molecular genetics and microscopy. Such integrated approaches promise to provide the avenue for a continued explosion in our understanding of the cellular basis of the infection of plants by fungal and oomycete pathogens.

Acknowledgements. I would like to sincerely thank Drs. T.L.W. Carver, R.P. Clay, J.A. Clement, L. Epstein, F. Gubler, S.J. Gurr, I.B. Heath, H.C. Hoch, R.J. Howard, K. Mendgen, C.W. Mims, L.J. Murdoch, R.J. O'Connell, N.D. Read, R.W. Roberson, D. Takemoto and R.W.S. Weber who supplied micrographs for inclusion in this review chapter.

References

Adams JC, Tucker RP (2000) The thrombospondin type 1 repeat (TSR) superfamily: diverse proteins with related roles in neuronal development. Dev Dyn 218:280–299

Ahn N, Kim S, Choi W, Im K-H, Lee Y-H (2004) Extracellular matrix protein gene, *EMP1*, is required for appressorium formation and pathogenicity of the rice blast fungus, *Magnaporthe grisea*. Mol Cells 17:166–173

Aist JR, Bushnell WR (1991) Invasion of plants by powdery mildew fungi, and cellular mechanisms of resistance. In: Cole GT, Hoch HC (eds) The fungal spore and disease initiation in plants and animals. Plenum, New York, pp 321–345

Akimitsu K, Isshiki A, Ohtani K, Yamamoto H, Eshel D, Prusky D (2004) Sugars and pH: a clue to the regulation of fungal cell wall-degrading enzymes in plants. Physiol Mol Plant Pathol 65:271–275

Allan RH, Thorpe CJ, Deacon JW (1992) Differential tropism to living and dead cereal root hairs by the biocontrol fungus *Idriella bolleyi*. Physiol Mol Plant Pathol 41:217–226

Allaway WG, Ashford AE, Heath IB, Hardham AR (1998) Vacuolar reticulum in oomycete hyphal tips: an additional component of the Ca^{2+} regulatory system? Fungal Genet Biol 22:209–220

Ambikapathy J, Marshall JS, Hocart CH, Hardham AR (2002) The role of proline in osmoregulation in *Phytophthora nicotianae*. Fungal Genet Biol 35:287–299

Annis SL, Goodwin PH (1997) Recent advances in the molecular genetics of plant cell wall degrading enzymes produced by plant pathogenic fungi. Eur J Plant Pathol 103:1–14

Apoga D, Jansson H-B, Tunlid A (2001) Adhesion of conidia and germlings of the plant pathogenic fungus *Bipolaris sorokiniana* to solid surfaces. Mycol Res 105:1251–1260

Apoga D, Barnard J, Craighead HG, Hoch HC (2004) Quantification of substratum contact required for initiation of *Colletotrichum graminicola* appressoria. Fungal Genet Biol 41:1–12

Armentrout VN, Downer AJ, Grasmick DL, Weinhold AR (1987) Factors affecting infection cushion development by *Rhizoctonia solani* on cotton. Phytopathology 77:623–630

Atkinson HA, Daniels A, Read ND (2002) Live-cell imaging of endocytosis during conidial germination in the rice blast fungus, *Magnaporthe grisea*. Fungal Genet Biol 37:233–244

Avrova AO, Venter E, Birch PRJ, Whisson SC (2003) Profiling and quantifying differential gene transcription in *Phytophthora infestans* prior to and during the early stages of potato infection. Fungal Genet Biol 40:4–14

Aylor DE (2003) Spread of plant disease on a continental scale: role of aerial dispersal of pathogens. Ecology 84:1989–1997

Ayscough KR, Stryker J, Pokala N, Sanders M, Crews P, Drubin DG (1997) High rates of actin filament turnover in budding yeast and roles for actin in establishment and maintenance of cell polarity revealed using the actin inhibitor latrunculin-A. J Cell Biol 137:399–416

Bachewich C, Heath IB (1998) Radial F-actin arrays precede new hypha formation in *Saprolegnia*: implications for establishing polar growth and regulating tip morphogenesis. J Cell Sci 111:2005–2016

Baka ZA, Larous L, Lösel DM (1995) Distribution of ATPase activity at the host–pathogen interfaces of rust infections. Physiol Mol Plant Pathol 47:67–82

Balhadere PV, Talbot NJ (2001) *PDE1* encodes a P-type ATPase involved in appressorium mediated plant infection by the rice blast fungus *Magnaporthe grisea*. Plant Cell 13:1987–2004

Barbosa AC, Carmo AE do, Graf L, Tomaz R, Fogaça de Souza C, Mendes J, Randi MAF, Buchi D, Schadeck RJG (2006) Morphology and lipid body and vacuole dynamics during secondary conidia formation in *Colletotrichum acutatum*: laser scanning confocal analysis. Can J Microbiol 52:117–124

Barhoom S, Sharon A (2004) cAMP regulation of "pathogenic" and "saprophytic" fungal spore germination. Fungal Genet Biol 41:317–326

Barr DJS (1992) Evolution and kingdoms of organisms from the perspective of a mycologist. Mycologia 84:1–11

Bartnicki-Garcia S (1973) Fundamental aspects of hyphal morphogenesis. In: Ashworth JM, Smith JE (eds) Microbial differentiation. Cambridge University, Cambridge, pp 245–267

Bartnicki-Garcia S (1996) The hypha: unifying thread of the fungal kingdom. In: Sutton BC (ed) A century of mycology. Cambridge University, Cambridge, pp 105–133

Bartnicki-Garcia S (2002) Hyphal tip growth – outstanding questions. In: Osiewacz HD (ed) Molecular biology of fungal development. Dekker, New York, pp 29–58

Bartnicki-Garcia S, Sing VO (1987) Adhesion of zoospores of *Phytophthora* to solid surfaces. In: Fuller MS, Jaworski A (eds) Zoosporic fungi in teaching and research. Southeastern Publishing, Athens, pp 279–283

Bartnicki-Garcia S, Hergert F, Gierz G (1989) Computer simulation of fungal morphogenesis and the mathematical basis for hyphal (tip) growth. Protoplasma 153:46–57

Bartnicki-Garcia S, Hergert F, Gierz G (1990) A novel computer model for generating cell shape: application to fungal morphogenesis. In: Kuhn PJ, Trinci APJ, Jung MJ, Goosey MW, Copping LG (eds) Biochemistry of cell walls and membranes in fungi. Springer, Berlin Heidelberg New York, pp 43–60

Bastmeyer M, Deising H, Bechinger C (2002) Force exertion in fungal infection. Annu Rev Biomol Struct 31:321–341

Bechinger C, Giebel K-F, Schnell M, Leiderer P, Deising HB, Bastmeyer M (1999) Optical measurements of invasive forces exerted by appressoria of a plant pathogenic fungus. Science 285:1896–1899

Beckerman JL, Ebbole DJ (1996) *MPG1*, a gene encoding a fungal hydrophobin of *Magnaporthe grisea*, is involved in surface recognition. Mol Plant Microbe Interact 9:450–456

Beliën T, Van Campenhout S, Robben J, Volckaert G (2006) Microbial endoxylanases: effective weapons to breach the plant cell-wall barrier or, rather, triggers of plant defence systems? Mol Plant Microbe Interact 19:1072–1081

Bhambra GK, Wang Z-Y, Soanes DM, Wakley GE, Talbot NJ (2006) Peroxisomal carnitine acetyl transferase is required for elaboration of penetration hyphae during plant infection by *Magnaporthe grisea*. Mol Microbiol 61:46–60

Bhattacharjee S, Hiller NL, Liolios K, Win J, Kanneganti TD, Young C, Kamoun S, Haldar K (2006) The malarial host-targeting signal is conserved in the Irish potato famine pathogen. PLoS Pathogens 2:453–465

Blanco FA, Judelson HS (2005) A bZIP transcription factor from *Phytophthora* interacts with a protein kinase and is required for zoospore motility and plant infection. Mol Microbiol 56:638–648

Both M, Csukai M, Stumpf MPH, Spanu PD (2005) Gene expression profiles of *Blumeria graminis* indicate dynamic changes to primary metabolism during development of an obligate biotrophic pathogen. Plant Cell 17:2107–2122

Boudjeko T, Andème-Onzighi C, Vicré M, Balangé A-P, Ndoumou DO, Driouich A (2006) Loss of pectin is an early event during infection of cocoyam roots by *Pythium myriotylum*. Planta 223:271–282

Bourett TM, Howard RJ (1990) In vitro development of penetration structures in the rice blast fungus *Magnaporthe grisea*. Can J Bot 68:329–342

Bourett TM, Howard RJ (1991) Ultrastructural immunolocalization of actin in a fungus. Protoplasma 163:199–202

Bourett TM, Howard RJ (1992) Actin in penetration pegs of the fungal rice blast pathogen, *Magnaporthe grisea*. Protoplasma 168:20–26

Bourett T, Hoch HC, Staples RC (1987) Association of the microtubule cytoskeleton with the thigmotropic signal for appressorium formation in *Uromyces*. Mycologia 79:540–545

Bourett TM, Czymmek KJ, Howard RJ (1998) An improved method for affinity probe localization in whole cells of filamentous fungi. Fungal Genet Biol 24:3–13

Bracker CE, Ruiz-Herrera J, Bartnicki-Garcia S (1976) Structure and transformation of chitin synthetase particles (chitosomes) during microfibril synthesis in vitro. Proc Natl Acad Sci USA 73:4570–4574

Braun EJ, Howard RJ (1994a) Adhesion of *Cochliobolus heterostrophus* conidia and germlings to leaves and artificial surfaces. Exp Mycol 18:211–220

Braun EJ, Howard RJ (1994b) Adhesion of fungal spores and germlings to host plant surfaces. Protoplasma 181:202–212

Brito N, Espino JJ, González C (2006) The endo-ß-1,4-xylanase xyn11A is required for virulence in *Botrytis cinerea*. Mol Plant Microbe Interact 19:25–32

Brown JKM, Hovmøller MS (2002) Aerial dispersal of pathogens on the global and continental scales and its impact on plant disease. Science 297:537–541

Bullock S, Ashford AE, Willets HJ (1980) The structure and histochemistry of sclerotia of *Sclerotinia minor* Jagger II. Histochemistry of extracellular substances and cytoplasmic reserves. Protoplasma 104:333–351

Bullock S, Willets HJ, Ashford AE (1983) The structure and histochemistry of sclerotia of *Sclerotinia minor* jagger III. Changes in ultrastructure and loss of reserve materials during carpogenic germination. Protoplasma 117:214–225

Cahill DM, Cope M, Hardham AR (1996) Thrust reversal by tubular mastigonemes: immunological evidence for a role of mastigonemes in forward motion of zoospores of *Phytophthora cinnamomi*. Protoplasma 194:18–28

Callow JA, Green JR (1996) The plant plasma membrane in fungal disease. In: Smallwood M, Knox JP, Bowles DJ (eds) Membranes: specialized functions in plants. Bios Scientific, Oxford, pp 543–562

Callow JA, Mackie A, Roberts AM, Green JR (1992) Evidence for molecular differentiation in powdery mildew haustoria through the use of monoclonal antibodies. Symbiosis 14:237–246

Carver TLW, Thomas BJ, Ingerson-Morris SM (1995) The surface of *Erysiphe graminis* and the production of extracellular material at the fungus-host interface during germling and colony development. Can J Bot 73:272–287

Carver TLW, Kunoh H, Thomas BJ, Nicholson RL (1999) Release and visualization of the extracellular matrix of conidia of *Blumeria graminis*. Mycol Res 103:546–560

Carzaniga R, Bowyer P, O'Connell RJ (2001) Production of extracellular matrices during development of infection structures by the downy mildew *Peronospora parasitica*. New Phytol 149:83–93

Catanzariti A-M, Dodds PN, Lawrence GJ, Ayliffe MA, Ellis JG (2006) Haustorially expressed secreted proteins from flax rust are highly enriched for avirulence elicitors. Plant Cell 18:1–14

Celenza JL, Carlson M (1984) Cloning and genetic mapping of *SNF1*, a gene required for expression of glucose-repressible genes in *Saccharomyces cerevisiae*. Mol Cell Biol 4:49–53

Celio GJ, Mims CW, Richardson EA (2004) Ultrastructure and immunocytochemistry of the host-pathogen interface in poinsettia leaves infected with powdery mildew. Can J Bot 82:421–429

Centis S, Guillas I, Séjalon N, Esquerre-Tugayé MT (1997) Endopolygalacturonase genes from *Colletotrichum lindemuthianum*: cloning of *CLPG2* and comparison of its expression to that of *CLPG1* during saprophytic and parasitic growth of the fungus. Mol Plant Microbe Interact 10:769–775

Chaky J, Anderson K, Moss M, Vaillancourt L (2001) Surface hydrophobicity and surface rigidity induce spore germination. Phytopathology 91:558–564

Chard JM, Gay JL (1984) Characterization of the parasitic interface between *Erysiphe pisi* and *Pisum sativum* using fluorescent probes. Physiol Plant Pathol 25:259–276

Chen C, Ha Y-S, Min J-Y, Memmott SD, Dickman MB (2006) Cdc42 is required for proper growth and development in the fungal pathogen *Colletotrichum trifolii*. Eukaryot Cell 5:155–166

Chen Z, Nunes MA, Silva MC, Rodrigues CJ (2004) Appressorium turgor pressure of *Colletotrichum kahawae* might have a role in coffee cuticle penetration. Mycologia 96:1199–1208

Chong J, Harder DE, Rohringer R (1981) Ontogeny of mono- and dikaryotic rust haustoria: cytochemical and ultrastructural studies. Phytopathology 71:975–983

Chumley FG, Valent B (1990) Genetic analysis of melanin-deficient, nonpathogenic mutants of *Magnaporthe grisea*. Mol Plant Microbe Interact 3:135–143

Clay RP, Bergmann CW, Fuller MS (1997) Isolation and characterization of an endopolygalacturonase from *Cochliobolus sativus* and a cytological study of fungal penetration of barley. Phytopathology 87:1148–1159

Clement JA, Porter R, Butt TM, Beckett A (1994) The role of hydrophobicity in attachment of urediniospores and sporelings of *Uromyces viciae-fabae*. Mycol Res 98:1217–1228

Clement JA, Porter R, Butt TM, Beckett A (1997) Characteristics of adhesion pads formed during imbibition and germination of urediniospores of *Uromyces viciae-fabae* on host and synthetic surfaces. Mycol Res 101:1445–1458

Clergeot P-H, Gourgues M, Cots J, Laurans F, Latorse M-P, Pépin R, Tharreau D, Notteghem J-L, Lebrun M-H (2001) *PLS1*, a gene encoding a tetraspanin-like protein, is required for penetration of rice leaf by the fungal pathogen *Magnaporthe grisea*. Proc Natl Acad Sci USA 98:6963–6968

Cole L, Orlovich DA, Ashford AE (1998) Structure, function, and motility of vacuoles in filamentous fungi. Fungal Genet Biol 24:86–100

Collins TJ, Read ND (1997) Appressorium induction by topographical signals in six cereal rusts. Physiol Mol Plant Pathol 51:169–179

Collins TJ, Moerschbacher BM, Read ND (2001) Synergistic induction of wheat stem rust appressoria by chemical and topographical signals. Physiol Mol Plant Pathol 58:259–266

Connolly MS, Sakihama Y, Phuntumart V, Jiang Y, Warren F, Mourant L, Morris PF (2005) Heterologous expression of a pleiotropic drug resistance transporter from *Phytophthora sojae* in yeast transporter mutants. Curr Genet 48:356–365

Cooper B, Garrett WM, Campbell KB (2006) Shotgun identification of proteins from uredospores of the bean rust *Uromyces appendiculatus*. Proteomics 6:2477–2484

Cope M, Webb MC, O'Gara ET, Philip BA, Hardham AR (1996) Immunocytochemical comparison of peripheral vesicles in zoospores of *Phytophthora* and *Pythium* species. Mycologia 88:523–532

Corrêa A Jr, Hoch HC (1995) Identification of thigmoresponsive loci for cell differentiation in *Uromyces* germlings. Protoplasma 186:34–40

Corrêa A Jr, Staples RC, Hoch HC (1996) Inhibition of thigmostimulated cell differentiation with RGD-peptides in *Uromyces* germlings. Protoplasma 194:91–102

Czymmek KJ, Bourett TM, Howard RJ (1996) Immunolocalization of tubulin and actin in thick-sectioned fungal hyphae after freeze-substitution fixation and methacrylate de-embedment. J Microsc 181:153–161

Czymmek KJ, Bourett TM, Shao Y, DeZwaan TM, Sweigard JA, Howard RJ (2005) Live-cell imaging of tubulin in the filamentous fungus *Magnaporthe grisea* treated with anti-microtubule and anti-microfilament agents. Protoplasma 225:23–32

D'Ovidio R, Mattei B, Roberti S, Bellincampi D (2004) Polygalacturonases, polygalacturonase-inhibiting proteins and pectic oligomers in plant-pathogen interactions. Biochim Biophys Acta 1696:237–244

Deacon JW (1997) Modern mycology. Blackwell Science, Oxford, p. 303

Dean RA (1997) Signal pathways and appressorium morphogenesis. Annu Rev Phytopathol 35:211–234

Dearnaley JDW, Maleszka J, Hardham AR (1996) Synthesis of zoospore peripheral vesicles during sporulation of *Phytophthora cinnamomi*. Mycol Res 100:39–48

Degefu Y, Lohtander K, Paulin L (2004) Expression patterns and phylogenetic analysis of two xylanase genes (*htxyl1* and *htxyl2*) from *Helminthosporium turcicum*, the cause of northern leaf blight of maize. Biochimie 86:83–90

Deising H, Mendgen K (1992) Developmental control of enzyme production and cell wall modification in rust fungi, and defence reactions of the host plant. In: Stahl U, Tudzynski P (eds) Molecular biology of filamentous fungi. VCH, Weinheim, pp 27–44

Deising H, Nicholson RL, Haug M, Howard RJ, Mendgen K (1992) Adhesion pad formation and the involvement of cutinase and esterases in the attachment of uredospores to the host cuticle. Plant Cell 4:1101–1111

Deising H, Frittrang AK, Kunz S, Mendgen K (1995a) Regulation of pectin methylesterase and polygalacturonate lyase activity during differentiation of infection structures in *Uromyces viciae-fabae*. Microbiology 141:561–571

Deising H, Rauscher M, Haug M, Heiler S (1995b) Differentiation and cell wall degrading enzymes in the obligately biotrophic rust fungus *Uromyces viciae-fabae*. Can J Bot 73[Suppl 1]:S624–S631

Deising HB, Werner S, Wernitz M (2000) The role of fungal appressoria in plant infection (Review). Microbes Infect 2:1631–1641

deJong JC, McCormack BJ, Smirnoff N, Talbot NJ (1997) Glycerol generates turgor in rice blast. Nature 389:244–245

Dickinson S (1979) Growth of *Erysiphe graminis* on artifical membranes. Physiol Plant Pathol 15:219–221

Diéguez-Uribeondo J, Förster H, Adaskaveg JE (2003) Digital image analysis of internal light spots of appressoria of *Colletotrichum acutatum*. Phytopathology 93:923–930

Diéguez-Uribeondo J, Gierz G, Bartnicki-Garcia S (2004) Image analysis of hyphal morphogenesis in Saprolegniaceae (Oomycetes). Fungal Genet Biol 41:293–307

Dijksterhuis J (2003) Confocal microscopy of Spitzenkörper dynamics during growth and differentiation of rust fungi. Protoplasma 222:53–59

Dilger M, Felsenstein FG, Schwarz G (2003) Identification and quantitative expression analysis of genes that are differentially expressed during conidial germination in *Pyrenophora teres*. Mol Gen Genet 270:147–155

Dodds PN, Lawrence GJ, Catanzariti A-M, Ayliffe MA, Ellis JG (2004) The *Melampsora lini AvrL567* avirulence genes are expressed in haustoria and their products are recognized inside plant cells. Plant Cell 16:755–768

Doehlemann G, Berndt P, Hahn M (2006) Different signalling pathways involving a G α protein, cAMP and a MAP kinase control germination of *Botrytis cinerea* conidia. Mol Microbiol 59:821–835

Dong W, Latijnhouwers M, Jiang RHY, Meijer HJG, Govers F (2004) Downstream targets of the *Phytophthora infestans* Gα subunit PiGPA1 revealed by cDNA-AFLP. Mol Plant Pathol 5:483–494

Donofrio NM, Oh Y, Lundy R, Pan H, Brown DE, Jeong JS, Coughlan S, Mitchell TK, Dean RA (2006) Global gene expression during nitrogen starvation in the rice blast fungus, *Magnaporthe grisea*. Fungal Genet Biol 43:605–617

Doss RP (1999) Composition and enzymatic activity of the extracellular matrix secreted by germlings of *Botrytis cinerea*. Appl Environ Microbiol 65:404–408

Doss RP, Potter SW, Soeldner AH, Christian JK, Fukunaga LE (1995) Adhesion of germlings of *Botrytis cinerea*. Appl Environ Microbiol 61:260–265

Dumas B, Centis S, Sarrazin N, Esquerré-Tugayé M-T (1999) Use of green fluorescent protein to detect expression of an endopolygalacturonase gene of *Colletotrichum lindemuthianum* during bean infection. Appl Environ Microbiol 65:1769–1771

Ebbole DJ, Jin Y, Thon M, Pan H, Bhattarai E, Thomas T, Dean R (2004) Gene discovery and gene expression in the rice blast fungus, *Magnaporthe grisea*: analysis of expressed sequence tags. Mol Plant Microbe Interact 17:1337–1347

Ebstrup T, Saalbach G, Egsgaard H (2005) A proteomics study of in vitro cyst germination and appressoria formation in *Phytophthora infestans*. Proteomics 5:2839–2848

Emmett RW, Parbery DG (1975) Appressoria. Annu Rev Phytopathol 13:147–163

Epstein L, Nicholson RL (1997) Adhesion of spores and hyphae to plant surfaces. In: Carroll G, Tudzynski P (eds) The Mycota, vol V, part A. Plant relationships. Springer, Berlin Heidelberg New York, pp 11–25

Epstein L, Laccetti L, Staples RC, Hoch HC, Hoose WA (1985) Extracellular proteins associated with induction of differentiation in bean rust uredospore germlings. Phytopathology 75:1073–1076

Foster AJ, Jenkinson JM, Talbot NJ (2003) Trehalose synthesis and metabolism are required at different stages of plant infection by *Magnaporthe grisea*. EMBO J 22:225–235

Frittrang AK, Deising H, Mendgen K (1992) Characterization and partial purification of pectinesterase, a differentiation-specific enzyme of *Uromyces viciae-fabae*. J Gen Microbiol 138:2213–2218

Fuchs U, Steinberg G (2005) Endocytosis in the plant-pathogenic fungus *Ustilago maydis*. Protoplasma 226:75–80

Fuchs U, Manns I, Steinberg G (2005) Microtubules are dispensable for the initial pathogenic development but required for long-distance hyphal growth in the corn

smut fungus *Ustilago maydis*. Mol Biol Cell 16:2746–2758

Fuchs U, Hause G, Schuchardt I, Steinberg G (2006) Endocytosis is essential for pathogenic development in the corn smut fungus *Ustilago maydis*. Plant Cell 18:2066–2081

Gaulin E, Jauneau A, Villalba F, Rickauer M, Esquerré-Tugayé MT, Bottin A (2002) The CBEL glycoprotein of *Phytophthora parasitica* var. *nicotianae* is involved in cell wall deposition and adhesion to cellulosic substrates. J Cell Sci 115:4565–4575

Gay JL, Woods AM (1987) Induced modifications in the plasma membranes of infected cells. In: Pegg GF, Ayers PG (eds) Fungal infection of plants. Cambridge University, Cambridge, pp 79–91

Gevens AJ, Carver TLW, Thomas BJ, Nicholson RL (2001) Visualization and partial characterization of the ECM of *Pestalotia malicola* on artificial and natural substrata. Physiol Mol Plant Pathol 58:277–285

Gilbert RD, Johnson AM, Dean RA (1996) Chemical signals responsible for appressorium formation in the rice blast fungus *Magnaporthe grisea*. Physiol Mol Plant Pathol 48:335–346

Girbardt M (1969) Die ultrastruktur der apikalregion von pilzhyphen. Protoplasma 67:413–441

Gold RE, Mendgen K (1991) Rust basidiospore germlings and disease initiation. In: Cole GT, Hoch HC (eds) The fungal spore and disease initiation in plants and animals. Plenum, New York, pp 67–99

Gómez-Gómez E, Ruiz-Roldan MC, Di Pietro A, Roncero MIG, Hera C (2002) Role in pathogenesis of two endo-ß-1,4-xylanase genes from the vascular wilt fungus *Fusarium oxysporum*. Fungal Genet Biol 35:213–222

Görnhardt B, Rouhara I, Schmelzer E (2000) Cyst germination proteins of the potato pathogen *Phytophthora infestans* share homology with human mucins. Mol Plant Microbe Interact 13:32–42

Götesson A, Marshall JS, Jones DA, Hardham AR (2002) Characterization and evolutionary analysis of a large polygalacturonase gene family in the oomycete plant pathogen *Phytophthora cinnamomi*. Mol Plant Microbe Interact 15:907–921

Gourgues M, Brunet-Simon A, Lebrun M-H, Levis C (2004) The tetraspanin BcPls1 is required for appressorium-mediated penetration of *Botrytis cinerea* into host plant leaves. Mol Microbiol 51:619–629

Gow NAR (1995) Tip growth and polarity. In: Gow NAR, Gadd GM (eds) The growing fungus. Chapman and Hall, London, pp 277–299

Gow NAR (2004) New angles in mycology: studies in directional growth and directional motility. Mycol Res 108:5–13

Grenville-Briggs LJ, Avrova AO, Bruce CR, Williams A, Whisson SC, Birch PRJ, Van West P (2005) Elevated amino acid biosynthesis in *Phytophthora infestans* during appressorium formation and potato infection. Fungal Genet Biol 42:244–256

Grinberg A, Heath IB (1997) Direct evidence for Ca^{2+} regulation of hyphal branch induction. Fungal Genet Biol 22:127–139

Grove SN, Bracker CE (1970) Protoplasmic organization of hyphal tips among fungi: vesicles and Spitzenkörper. J Bacteriol 104:989–1009

Grove SN, Bracker CE, Morré DJ (1970) An ultrastructural basis for hyphal tip growth in *Pythium ultimum*. Am J Bot 57:245–266

Gubler F, Hardham AR (1988) Secretion of adhesive material during encystment of *Phytophthora cinnamomi* zoospores, characterized by immunogold labelling with monoclonal antibodies to components of peripheral vesicles. J Cell Sci 90:225–235

Gubler F, Hardham AR (1990) Protein storage in large peripheral vesicles in *Phytophthora* zoospores and its breakdown after cyst germination. Exp Mycol 14:393–404

Gubler F, Hardham AR (1991) The fate of peripheral vesicles in zoospores of *Phytophthora cinnamomi* during infection of plants. In: Mendgen K, Lesemann D-E (eds) Electron microscopy of plant pathogens. Springer, Berlin Heidelberg New York, pp 197–210

Gubler F, Hardham AR, Duniec J (1989) Characterising adhesiveness of *Phytophthora cinnamomi* zoospores during encystment. Protoplasma 149:24–30

Gubler F, Jablonsky PP, Duniec J, Hardham AR (1990) Localization of calmodulin in flagella of zoospores of *Phytophthora cinnamomi*. Protoplasma 155:233–238

Gunderson JH, Elwood H, Ingold A, Kindle K, Sogin ML (1987) Phylogenetic relationships between chlorophytes, chrysophytes, and oomycetes. Proc Natl Acad Sci USA 84:823–5827

Hahn M, Mendgen K (1997) Characterization of in planta-induced rust genes isolated from a haustorium-specific cDNA library. Mol Plant Microbe Interact 10:427–437

Hahn M, Neef U, Struck C, Göttfert M, Mendgen K (1997) A putative amino acid transporter is specifically expressed in haustoria of the rust fungus *Uromyces fabae*. Mol Plant Microbe Interact 10:438–445

Hamer JE, Howard RJ, Chumley FG, Valent B (1988) A mechanism for surface attachment in spores of a plant pathogenic fungus. Science 239:288–290

Hardham AR (1987) Microtubules and the flagellar apparatus in zoospores and cysts of the fungus *Phytophthora cinnamomi*. Protoplasma 137:109–124

Hardham AR (1995) Polarity of vesicle distribution in oomycete zoospores: development of polarity and importance for infection. Can J Bot 73[Suppl 1]:S400–S407

Hardham AR (2001) Cell biology of fungal infection of plants. In: Howard RJ, Gow NAR (eds) The Mycota, vol VII. Biology of the fungal cell. Springer, Berlin Heidelberg New York, pp 91–123

Hardham AR (2005) *Phytophthora cinnamomi*. Molec Plant Pathol 6:589–604

Hardham AR, Gubler F (1990) Polarity of attachment of zoospores of a root pathogen and pre-alignment of the emerging germ tube. Cell Biol Int Rep 14:947–956

Hardham AR, Mitchell HJ (1998) Use of molecular cytology to study the structure and biology of phytopathogenic and mycorrhizal fungi. Fungal Genet Biol 24:252–284

Hardham AR, Gubler F, Duniec J, Elliott J (1991) A review of methods for the production and use of monoclonal antibodies to study zoosporic plant pathogens. J Microsc 162:305–318

Hardham AR, Cahill DM, Cope M, Gabor BK, Gubler F, Hyde GJ (1994) Cell surface antigens of *Phytophthora*

spores: biological and taxonomic characterization. Protoplasma 181:213–232
Harper JDI, Gubler F, Salisbury JL, Hardham AR (1995) Centrin association with the flagellar apparatus in spores of *Phytophthora cinnamomi*. Protoplasma 188:225–235
Harris SD, Read ND, Roberson RW, Shaw B, Seiler S, Plamann M, Momany M (2005) Polarisome meets Spitzenkörper: microscopy, genetics, and genomics converge. Eukaryot Cell 4:225–229
Hatsch D, Phalip V, Petkovski E, Jeltsch J-M (2006) *Fusarium graminearum* on plant cell wall: no fewer than 30 xylanase genes transcribed. Biochem Biophys Res Commun 345:959–966
Have A ten, Breuil WO, Wubben JP, Visser J, van Kan JAL (2001) *Botrytis cinerea* endopolygalacturonase genes are differentially expressed in various plant tissues. Fungal Genet Biol 33:97–105
Have A ten, Tenberge KB, Benen JAE, Tudzynski P, Visser J, van Kan JAL (2002) The contribution of cell wall degrading enzymes to pathogenesis of fungal plant pathogens. In: Kempken F (ed) The Mycota, vol XI. Agricultural applications. Springer, Berlin Heidelberg New York, pp 341–358
Heath IB (1994) The cytoskeleton in hyphal growth, organelle movements, and mitosis. In: Wessels JGH, Meinhardt F (eds) The Mycota, vol I. Growth, differentiation and sexuality. Springer, Berlin Heidleberg New York, pp 43–65
Heath IB (1995a) Integration and regulation of hyphal tip growth. Can J Bot 73[Suppl 1]:S131–S139
Heath IB (1995b) The cytoskeleton. In: Gow NAR, Gadd GM (eds) The growing fungus. Chapman and Hall, London, pp 99–134
Heath IB, Steinberg G (1999) Mechanisms of hyphal tip growth: tube dwelling amebae revisited. Fungal Genet Biol 28:79–93
Heath MC (1976) Ultrastructural and functional similarity of the haustorial neckband of rust fungi and the casparian strip of vascular plants. Can J Bot 54:2484–2489
Hegde Y, Kolattukudy PE (1997) Cuticular waxes relieve self-inhibition of germination and appressorium formation by the conidia of *Magnaporthe grisea*. Physiol Mol Plant Pathol 51:75–84
Heiler S, Mendgen K, Deising H (1993) Cellolytic enzymes of the obligately biotrophic rust fungus *Uromyces viciae-fabae* are regulated differentation-specifically. Mycol Res 97:77–85
Herbert C, O'Connell R, Gaulin E, Salesses V, Esquerre-Tugayé MT, Dumas B (2004) Production of a cell wall-associated endopolygalacturonase by *Colletotrichum lindemuthianum* and pectin degradation during bean infection. Fungal Genet Biol 41:140–147
Hill TW, Mullins JT (1980) Hyphal tip growth in *Achlya*. I. Cytoplasmic organization. Can J Microbiol 26:1132–1140
Hiller NL, Bhattacharjee S, van Ooij C, Liolios K, Harrison T, Lopez-Estaño C, Haldar K (2004) A host-targeting signal in virulence proteins reveals a secretome in malarial infection. Science 306:1934–1937
Hippe-Sanwald S, Marticke KH, Kieliszewski MJ, Somerville SC (1994) Immunogold localization of THRGP-like epitopes in the haustorial interface of obligate, biotrophic fungi on monocots. Protoplasma 178:138–155
Hoch HC, Staples RC (1987) Structural and chemical changes among the rust fungi during appressorium development. Annu Rev Phytopathol 25:231–247
Hoch HC, Staples RC (1991) Signaling for infection structure formation in fungi. In: Cole GT, Hoch HC (eds) The fungal spore and disease initiation in plants and animals. Plenum, New York, pp 25–46
Hoch HC, Bourett TM, Staples RC (1986) Inhibition of cell differentiation in *Uromyces* with D_2O and taxol. Eur J Cell Biol 41:290–297
Hoch HC, Staples RC, Whitehead B, Comeau J, Wolf ED (1987a) Signaling for growth orientation and cell differentiation by surface topography in *Uromyces*. Science 235:1659–1662
Hoch HC, Tucker BE, Staples RC (1987b) An intact microtubule cytoskeleton is necessary for mediation of the signal for cell differentiation in *Uromyces*. Eur J Cell Biol 45:209–218
Hoffmann J, Mendgen K (1998) Endocytosis and membrane turnover in the germ tube of *Uromyces fabae*. Fungal Genet Biol 24:77–85
Howard RJ (1994) Cell biology of pathogenesis. In: Zeigler RS, Leong SA, Teng PS (eds) Rice blast disease. CAB International, Wallingford, pp 3–22
Howard RJ (1997) Breaching the outer barriers – cuticle and cell wall penetration. In: Carroll G, Tudzynski P (eds) The Mycota vol V, part A, plant relationships. Springer, Berlin Heidleberg New York, pp 43–60
Howard RJ, Ferrari MA (1989) Role of melanin in appressorium function. Exp Mycol 13:403–418
Howard RJ, Valent B (1996) Breaking and entering: host penetration by the fungal rice blast pathogen *Magnaporthe grisea*. Annu Rev Microbiol 50:491–512
Howard RJ, Bourett TM, Ferrari MA (1991a) Infection by *Magnaporthe*: an in vitro analysis. In: Mendgen K, Lesemann D-E (eds) Electron microscopy of plant pathogens. Springer, Berlin Heidleberg New York, pp 251–264
Howard RJ, Ferrari MA, Roach DH, Money NP (1991b) Penetration of hard substrates by a fungus employing enormous turgor pressures. Proc Natl Acad Sci USA 88:11281–11284
Hughes HB, Carzaniga R, Rawlings SL, Green JR, O'-Connell RJ (1999) Spore surface glycoproteins of *Colletotrichum lindemuthianum* are recognized by a monoclonal antibody which inhibits adhesion to polystyrene. Microbiology 145:1927–1936
Hutchinson KA, O'Connell RJ, Pain NA, Green JR (1996) A bean epicuticular glycoprotein is present in the extracellular matrices around infection structures of the anthracnose fungus, *Colletotrichum lindemuthianum*. New Phytol 134:579–585
Hutchinson KA, Green JR, Wharton PS, O'Connell RJ (2002) Identification and localization of glycoproteins in the extracellular matrices around germ-tubes and appressoria of *Colletotrichum* species. Mycol Res 106:729–736
Hyde GJ, Hardham AR (1993) Microtubules regulate the generation of polarity in zoospores of *Phytophthora cinnamomi*. Eur J Cell Biol 62:75–85
Hyde GJ, Heath IB (1995) Ca^{2+}-dependent polarization of axis establishment in the tipgrowing organism, *Saprolegnia ferax*, by gradients of the ionophore A23187. Eur J Cell Biol 67:356–362

Hyde GJ, Davies D, Perasso L, Cole L, Ashford AE (1999) Microtubules, but not actin microfilaments, regulate vacuole motility and morphology in hyphae of *Pisolithus tinctorius*. Cell Motil Cytoskeleton 42:114–124

Hyde GJ, Davies D, Cole L, Ashford AE (2002) Regulators of GTP-binding proteins cause morphological changes in the vacuole system of the filamentous fungus, *Pisolithus tinctorius*. Cell Motil Cytoskeleton 51:133–146

Inoue S, Turgeon BG, Yoder OC, Aist JR (1998) Role of fungal dynein in hyphal growth, microtubule organization, spindle pole body motility and nuclear migration. J Cell Sci 111:1555–1566

Isshiki A, Akimitsu K, Yamamoto M, Yamamoto H (2001) Endopolygalacturonase is essential for citrus black rot caused by *Alternaria citri* but not brown spot caused by *Alternaria alternata*. Mol Plant Microbe Interact 14:749–757

Isshiki A, Ohtani K, Kyo M, Yamamoto H, Akimitsu K (2003) Green fluorescent detection of fungal colonization and endopolygalacturonase gene expression in the interaction of *Alternaria citri* with citrus. Phytopathology 93:768–773

Jackson SL, Heath IB (1990) Evidence that actin reinforces the extensible hyphal apex of the oomycete *Saprolegnia ferax*. Protoplasma 157:144–153

Jakupović M, Heintz M, Reichmann P, Mendgen K, Hahn M (2006) Microarray analysis of expressed sequence tags from haustoria of the rust fungus *Uromyces fabae*. Fungal Genet Biol 43:8–19

Jelitto TC, Page HA, Read ND (1994) Role of external signals in regulating the prepenetration phase of infection by the rice blast fungus, *Magnaporthe grisea*. Planta 194:471–477

Jia Y, McAdams SA, Bryan GT, Hershey HP, Valent B (2000) Direct interaction of resistance gene and avirulence gene products confers rice blast resistance. EMBO J 19:4004–4014

Jones AL, Im K-H, Savka MA, Wu M-J, DeWitt NG, Shillito R, Binns AN (1998) Auxindependent cell expansion mediated by overexpressed auxin-binding protein-1. Science 282:1114–1117

Jones TM, Anderson AJ, Albersheim P (1972) Host–pathogen interactions. IV. Studies on the polysaccharide-degrading enzymes secreted by *Fusarium oxysporum* f. sp. *lycopersici*. Physiol Plant Pathol 2:153–166

Judelson HS, Blanco FA (2005) The spores of *Phytophthora*: weapons of the plant destroyer. Nat Rev Microbiol 3:47–58

Kamakura T, Yamaguchi S, Saitoh K, Teraoka T, Yamaguchi I (2002) A novel gene, *CBP1*, encoding a putative extracellular chitin-binding protein, may play an important role in the hydrophobic surface sensing of *Magna porthe grisea* during appressorium differentiation. Mol Plant Microbe Interact 15:437–444

Kaminskyj SGW, Heath IB (1996) Studies on *Saprolegnia ferax* suggest the general importance of the cytoplasm in determining hyphal morphology. Mycologia 88:20–37

Kawamura C, Moriwaki J, Kimura N, Fujita Y, Fuji S, Hirano T, Koizumi S, Tsuge T (1997) The melanin biosynthesis genes of *Alternaria alternata* can restore pathogenicity of the melanin-deficient mutants of *Magnaporthe grisea*. Mol Plant Microbe Interact 10:446–453

Kemen E, Kemen AC, Rafiqi M, Hempel U, Mendgen K, Hahn M, Voegele RT (2005) Identification of a protein from rust fungi transferred from haustoria into infected plant cells. Mol Plant Microbe Interact 18:1130–1139

Kershaw MJ, Talbot NJ (1998) Hydrophobins and repellents: proteins with fundamental roles in fungal morphogenesis. Fungal Genet Biol 23:18–33

Kiefer B, Riemann M, Büche C, Kassemeyer H-H, Nick P (2002) The host guides morphogenesis and stomatal targeting in the grapevine pathogen *Plasmopara viticola*. Planta 215:387–393

Kim H, Ahn J-H, Görlach JM, Caprari C, Scott-Craig JS, Walton JD (2001) Mutational analysis of β-glucanase genes from the plant-pathogenic fungus *Cochliobolus carbonum*. Mol Plant Microbe Interact 14:1436–1443

Kim S, Ahn IP, Rho HS, Lee YH (2005) *MHP1*, a *Magnaporthe grisea* hydrophobin gene, is required for fungal development and plant colonization. Mol Microbiol 57:1224–1237

Kim ST, Cho KS, Yu S, Kim SG, Hong JC, Han CD, Bae DW, Myung AE, Kang KY (2003) Proteomic analysis of differentially expressed proteins induced by rice blast fungus and elicitor in suspension-cultured rice cells. Proteomics 3:2368–2378

Kimura A, Takano Y, Furusawa I, Okuno T (2001) Peroxisomal metabolic function is required for appressorium-mediated plant infection by *Colletotrichum lagenarium*. Plant Cell 13:1945–1957

Kinane J, Dalvin S, Bindslev L, Hall A, Gurr S, Oliver R (2000) Evidence that the cAMP pathway controls emergence of both primary and appressorial germ tubes of barley powdery mildew. Mol Plant Microbe Interact 13:494–502

Krämer R, Freytag S, Schmelzer E (1997) In vitro formation of infection structures of *Phytophthora infestans* is associated with synthesis of stage specific polypeptides. Eur J Plant Pathol 103:43–53

Kunoh H, Nicholson RL, Kobayashi I (1991) Extracellular materials of fungal structures: Their significance at prepenetration stages of infection. In: Mendgen K, Lesemann D-E (eds) Electron microscopy of plant pathogens. Springer, Berlin Heidleberg New York, pp 223–234

Kuo KC, Hoch HC (1996) Germination of *Phyllosticta ampelicida* pycnidiospores: prerequisite of adhesion to the substratum and the relationship of substratum wettability. Fungal Genet Biol 20:18–29

Kwon YH, Epstein L (1993) A 90-kDa glycoprotein associated with adhesion of *Nectria haematococca* macroconidia to substrata. Mol Plant Microbe Interact 6:481–487

Kwon YH, Epstein L (1997) Involvement of the 90 kDa glycoprotein in adhesion of *Nectria haematococca* macroconidia. Physiol Mol Plant Pathol 51:287–303

Kwon YH, Hoch HC (1991) Temporal and spatial dynamics of appressorium formation in *Uromyces appendiculatus*. Exp Mycol 15:116–131

Kwon YH, Hoch HC, Aist JR (1991a) Initiation of appressorium formation in *Uromyces appendiculatus*: organization of the apex, and the responses involving microtubules and apical vesicles. Can J Bot 69:2560–2573

Kwon YH, Hoch HC, Staples RC (1991b) Cytoskeletal organization in *Uromyces* urediospore germling apices during appressorium formation. Protoplasma 165:37–50

Langford GM (1995) Actin- and microtubule-dependent organelle motors: interrelationships between the two motility systems. Curr Opin Cell Biol 7:82–88

Latijnhouwers M, Ligterink W, Vleeshouwers VGAA, Van West P, Govers F (2004) A G α subunit controls zoospore motility and virulence in the potato late blight pathogen *Phytophthora infestans*. Mol Microbiol 51:925–936

Lee Y-H, Dean RA (1994) Hydrophobicity of contact surface induces appressorium formation in *Magnaporthe grisea*. FEMS Microbiol Lett 115:71–76

Lehmler C, Steinberg G, Snetselaar KM, Schliwa M, Kahmann R, Bölker M (1997) Identification of a motor protein required for filamentous growth in *Ustilago maydis*. EMBO J 16:3464–3473

Lenz JH, Schuchardt I, Straube A, Steinberg G (2006) A dynein loading zone for retrograde endosome motility at microtubule plus-ends. EMBO J 25:2275–2286

Levina NN, Lew RR, Heath IB (1994) Cytoskeletal regulation of ion channel distribution in the tip-growth organism *Saprolegnia ferax*. J Cell Sci 107:127–134

Li RG, Rimmer R, Buchwaldt L, Sharpe AG, Séguin-Swartz G, Hegedus DD (2004) Interaction of *Sclerotinia sclerotiorum* with *Brassica napus*: cloning and characterization of endo- and exo-polygalacturonases expressed during saprophytic and parasitic modes. Fungal Genet Biol 41:754–765

Link T, Lohaus G, Heiser I, Mendgen K, Hahn M, Voegele RT (2005) Characterization of a novel $NADP^+$-dependent D-arabitol dehydrogenase from the plant pathogen *Uromyces fabae*. Biochem J 389:289–295

Littlefield LJ, Bracker CE (1972) Ultrastructural specialization at the host–pathogen interface in rust-infected flax. Protoplasma 74:271–305

Liu ZM, Kolattukudy PE (1999) Early expression of the calmodulin gene, which precedes appressorium formation in *Magnaporthe grisea*, is inhibited by self-inhibitors and requires surface attachment. J Bacteriol 181:3571–3577

López-Franco R, Bracker CE (1996) Diversity and dynamics of the Spitzenkörper in growing hyphal tips of higher fungi. Protoplasma 195:90–111

Loprete DM, Hill TW (2002) Isolation and characterization of an endo-(1,4)-β-glucanase secreted by *Achlya ambisexualis*. Mycologia 94:903–911

Lu J-P, Liu T-B, Lin F-C (2005) Identification of mature appressorium-enriched transcripts in *Magnaporthe grisea*, the rice blast fungus, using suppression subtractive hybridization. FEMS Microbiol Lett 245:131–137

Lucas J, Knights I (1987) Spores on leaves: endogenous and exogenous control of development. In: Pegg GF, Ayres PG (eds) Fungal infection of plants. Cambridge University, Cambridge, pp 45–59

Lugones LG, de Jong JF, de Vries OMH, Jalving R, Dijksterhuis J, Wosten HAB (2004) The SC15 protein of *Schizophyllum commune* mediates formation of aerial hyphae and attachment in the absence of the SC3 hydrophobin. Mol Microbiol 53:707–716

Mackie AJ, Roberts AM, Callow JA, Green JR (1991) Molecular differentiation in pea powdery-mildew haustoria. Planta 183:399–408

Mackie AJ, Roberts AM, Green JR, Callow JA (1993) Glycoproteins recognised by monoclonal antibodies UB7, UB8 and UB10 are expressed early in the development of pea powdery mildew haustoria. Physiol Mol Plant Pathol 43:135–146

Manners JM, Gay JL (1983) The host-parasite interface and nutrient transfer in biotrophic parasitism. In: Callow JA (ed) Biochemical plant pathology. Wiley–Interscience, Chichester, pp 163–195

Marshall JS, Wilkinson JM, Moore T, Hardham AR (2001) Structure and expression of the genes encoding proteins resident in large peripheral vesicles of *Phytophthora cinnamomi* zoospores. Protoplasma 215:226–239

Martel M-B, Létoublon R, Fèvre M (1996) Purification of endo polygalacturonases from *Sclerotinia sclerotiorum*: multiplicity of the complex enzyme system. Curr Microbiol 33:243–248

Martel M-B, Létoublon R, Fèvre M (1998) Purification and characterization of two endopolygalacturonases secreted during the early stages of the saprophytic growth of *Sclerotinia sclerotiorum*. FEMS Microbiol Lett 158:133–138

Marti M, Baum J, Rug M, Tilley L, Cowman AF (2005) Signal-mediated export of proteins from the malaria parasite to the host erythrocyte. J Cell Biol 171:587–592

Maruyama J-I, Kikuchi S, Kitamoto K (2006) Differential distribution of the endoplasmic reticulum network as visualized by the BipA-EGFP fusion protein in hyphal compartments across the septum of the filamentous fungus, *Aspergillus oryzae*. Fungal Genet Biol 43:642–654

McGoldrick CA, Gruver C, May GS (1995) *myoA* of *Aspergillus nidulans* encodes an essential myosin I required for secretion and polarized growth. J Cell Biol 128:577–587

McLeod A, Smart CD, Fry WE (2003) Characterization of 1,3-β-glucanase and 1,3;1,4-β-glucanase genes from *Phytophthora infestans*. Fungal Genet Biol 38:250–263

Mendgen K, Deising H (1993) Infection structures of fungal plant pathogens – a cytological and physiological evaluation. New Phytol 124:193–213

Mendgen K, Hahn M (2002) Plant infection and the establishment of fungal biotrophy. Trends Plant Sci 7:352–356

Mendgen K, Bachem U, Stark-Urnau M, Xu H (1995) Secretion and endocytosis at the interface of plants and fungi. Can J Bot 73[Suppl 1]:S640–S648

Mendgen K, Hahn M, Deising H (1996) Morphogenesis and mechanisms of penetration by plant pathogenic fungi. Annu Rev Phytopathol 34:367–386

Mendgen K, Struck C, Voegele RT, Hahn M (2000) Biotrophy and rust haustoria. Physiol Mol Plant Pathol 56:141–145

Mercure EW, Kunoh H, Nicholson RL (1994a) Adhesion of *Colletotrichum graminicola* conidia to corn leaves: a requirement for disease development. Physiol Mol Plant Pathol 45:407–420

Mercure EW, Leite B, Nicholson RL (1994b) Adhesion of ungerminated conidia of *Colletotrichum graminicola* to artificial hydrophobic surfaces. Physiol Mol Plant Pathol 45:421–440

Mims CW, Richardson EA (1989) Ultrastructure of appressorium development by basidiospore germlings of the rust fungus *Gymnosporangium juniperi-virginianae*. Protoplasma 148:111–119

Mims CW, Celio GJ, Richardson EA (2003) The use of high pressure freezing and freeze substitution to study host-pathogen interactions in fungal diseases of plants. Microsc Microanal 9:522–531

Mitchell RT, Deacon JW (1986) Chemotropism of germtubes from zoospore cysts of *Pythium* spp. Trans Br Mycol Soc 86:233–237

Moloshok TD, Leinhos GME, Staples RC, Hoch HC (1993) The autogenic extracellular environment of *Uromyces appendiculatus* urediospore germlings. Mycologia 85:392–400

Money NP (1994) Osmotic adjustment and the role of turgor in mycelial fungi. In: Wessels JGH, Meinhardt F (eds) The Mycota, vol I. Growth, differentiation and sexuality. Springer, Berlin Heidelberg New York, pp 67–88

Money NP, Howard RJ (1996) Confirmation of a link between fungal pigmentation, turgor pressure, and pathogenicity using a new method of turgor measurement. Exp Mycol 20:217–227

Morris PF, Ward EWB (1992) Chemoattraction of zoospores of the soybean pathogen, *Phytophthora sojae*, by isoflavones. Physiol Mol Plant Pathol 40:17–22

Mourino-Perez RR, Roberson RW, Bartnicki-Garcia S (2006) Microtubule dynamics and organization during hyphal growth and branching in *Neurospora crassa*. Fungal Genet Biol 43:389–400

Murdoch LJ, Hardham AR (1998) Components in the haustorial wall of the flax rust fungus, *Melampsora lini*, are labelled by three anti-calmodulin monoclonal antibodies. Protoplasma 201:180–193

Murdoch LJ, Kobayashi I, Hardham AR (1998) Production and characterisation of monoclonal antibodies to cell wall components of the flax rust fungus. Eur J Plant Pathol 104:331–346

Nicholson RL (1996) Adhesion of fungal propagules. In: Nicole M, Gianinazzi-Pearson V (eds) Histology, ultrastructure and molecular cytology of plant-microorganism interactions. Kluwer Academic, Dordrecht, pp 117–134

Nicholson RL, Epstein L (1991) Adhesion of fungi to the plant surface. In: Cole GT, Hoch HC (eds) The fungal spore and disease initiation in plants and animals. Plenum, New York, pp 3–23

Nicholson RL, Kunoh H, Shiraishi T, Yamada T (1993) Initiation of the infection process by *Erysiphe graminis*: conversion of the conidial surface from hydrophobicity to hydrophilicity and influence of the conidial exudate on the hydrophobicity of the barley leaf surface. Physiol Mol Plant Pathol 43:307–318

O'Connell RJ (1987) Absence of a specialized interface between intracellular hyphae of *Colletotrichum lindemuthianum* and cells of *Phaseolus vulgaris*. New Phytol 107:725–734

O'Connell RJ, Pain NA, Bailey JA, Mendgen K, Green JR (1996a) Use of monoclonal antibodies to study differentiation of *Colletotrichum* infection structures. In: Nicole M, Gianinazzi-Pearson V (eds) Histology, ultrastructure and molecular cytology of plant–microorganism interactions. Kluwer Academic, Dordrecht, pp 79–97

O'Connell RJ, Pain NA, Hutchison KA, Jones GL, Green JR (1996b) Ultrastructure and composition of the cell surfaces of infection structures formed by the fungal plant pathogen *Colletotrichum lindemuthianum*. J Microsc 181:204–212

Oeser B, Heidrich PM, Müller U, Tudzynski P, Tenberge KB (2002) Polygalacturonase is a pathogenicity factor in the *Claviceps purpurea*/rye interaction. Fungal Genet Biol 36:176–186

Ohtani K, Isshiki A, Katoh H, Yamamoto H, Akimitsu K (2003) Involvement of carbon catabolic repression on regulation of endopolygalacturonase gene expression in citrus fruit. J Gen Plant Pathol 69:120–125

Oliver RP, Ipcho SVS (2004) *Arabidopsis* pathology breathes new life into the necrotrophs-vs.-biotrophs classification of fungal pathogens. Mol Plant Pathol 5:347–352

Osherov N, May GS (2001) The molecular mechanisms of conidial germination. FEMS Microbiol Lett 199:153–160

Ospina-Giraldo M, Mullins E, Kang S (2003) Loss of function of the *Fusarium oxysporum SNF1* gene reduces virulence on cabbage and *Arabidopsis*. Curr Genet 44:49–57

Pain NA, O'Connell RJ, Mendgen K, Green JR (1994) Identification of glycoproteins specific to biotrophic intracellular hyphae formed in the *Colletotrichum lindemuthianum*-bean interaction. New Phytol 127:233–242

Pain NA, O'Connell RJ, Green JR (1995) A plasma membrane-associated protein is a marker for differentiation and polarisation of *Colletotrichum lindemuthianum* appressoria. Protoplasma 188:1–11

Pain NA, Green JR, Jones GL, O'Connell RJ (1996) Composition and organisation of extracellular matrices around germ tubes and appressoria of *Colletotrichum lindemuthianum*. Protoplasma 190:119–130

Paktitis S, Grant B, Lawrie A (1986) Surface changes in *Phytophthora palmivora* zoospores following induced differentiation. Protoplasma 135:119–129

Park G, Xue GY, Zheng L, Lam S, Xu J-R (2002) *MST12* regulates infectious growth but not appressorium formation in the rice blast fungus *Magnaporthe grisea*. Mol Plant Microbe Interact 15:183–192

Park G, Bruno KS, Staiger CJ, Talbot NJ, Xu J-R (2004) Independent genetic mechanisms mediate turgor generation and penetration peg formation during plant infection in the rice blast fungus. Mol Microbiol 53:1695–1707

Pascholati SF, Yoshioka H, Kunoh H, Nicholson RL (1992) Preparation of the infection court by *Erysiphe graminis* f.sp. *hordei*: cutinase is a component of the conidial exudate. Physiol Mol Plant Pathol 41:53–59

Patterson DJ, Sogin ML (1992) Eukaryote origins and protistan diversity. In: Hartman H, Matsuno K (eds) The origin and evolution of the cell. World Scientific, Singapore, pp 13–46

Peij NNME van, Gielkens MMC, Vries RP de, Visser J, Graaff LH de (1998) The transcriptional activator XlnR regulates both xylanolytic and endoglucanase gene expression in *Aspergillus niger*. Appl Environ Microbiol 64:3615–3619

Penington CJ, Iser JR, Grant BR, Gayler KR (1989) Role of RNA and protein synthesis in stimulated germination of zoospores of the pathogenic fungus *Phytophthora palmivora*. Exp Mycol 13:158–168

Perfect SE, O'Connell RJ, Green EF, Doering-Saad C, Green JR (1998) Expression cloning of a fungal proline-rich glycoprotein specific to the biotrophic interface formed in the *Colletotrichum*-bean interaction. Plant J 15:273–279

Perfect SE, Pixton KL, O'Connell RJ, Green JR (2000) The distribution and expression of a biotrophy-related gene, *CIH1*, within the genus *Colletotrichum*. Mol Plant Pathol 1:213–221

Perfect SE, Green JR, O'Connell RJ (2001) Surface characteristics of necrotrophic secondary hyphae produced by the bean anthracnose fungus, *Colletotrichum lindemuthianum*. Eur J Plant Pathol 107:813–819

Perpetua NS, Kubo Y, Yasuda N, Takano Y, Furusawa I (1996) Cloning and characterization of a melanin biosynthetic *THR1* reductase gene essential for appressorial penetration of *Colletotrichum lagenarium*. Mol Plant Microbe Interact 9:323–329

Pickett-Heaps JD, Klein AG (1998) Tip growth in plant cells may be amoeboid and not generated by turgor pressure. Proc R Soc Lond Ser B 265:1453–1459

Posada-Buitrago ML, Frederick RD (2005) Expressed sequence tag analysis of the soybean rust pathogen *Phakopsora pachyrhizi*. Fungal Genet Biol 42:949–962

Powell MJ, Bracker CE (1977) Isolation of zoospore organelles from *Phytophthora palmivora*. Proc Int Mycol Congr 2:533

Prusky D, Yakoby N (2003) Pathogenic fungi: leading or led by ambient pH? Mol Plant Pathol 4:509–516

Pryce-Jones E, Carver T, Gurr SJ (1999) The roles of cellulase enzymes and mechanical force in host penetration by *Erysiphe graminis* f.sp *hordei*. Physiol Mol Plant Pathol 55:175–182

Ramos-Pamplona M, Naqvi NI (2006) Host invasion during rice-blast disease requires carnitine-dependent transport of peroxisomal acetyl-CoA. Mol Microbiol 61:61–75

Read ND (1991) Low-temperature scanning electron microscopy of fungi and fungus-plant interactions. In: Mendgen K, Lesemann D-E (eds) Electron microscopy of plant pathogens. Springer, Berlin Heidelberg New York, pp 17–29

Read ND, Hickey PC (2001) The vesicle trafficking network and tip growth in fungal hyphae. In: Geitmann A, Cresti M, Heath IB (eds) Cell biology of plant and fungal tip growth. IOS, Amsterdam, pp 137–148

Read ND, Kalkman ER (2003) Does endocytosis occur in fungal hyphae? Fungal Genet Biol 39:199–203

Read ND, Kellock LJ, Knight H, Trewavas AJ (1992) Contact sensing during infection by fungal pathogens. In: Callow JA, Green JR (eds) Perspectives in plant cell recognition. Cambridge University, Cambridge, pp 137–172

Read ND, Kellock LJ, Collins TJ, Gundlach AM (1997) Role of topography sensing for infection – structure differentiation in cereal rust fungi. Planta 202:163–170

Rehmany AP, Gordon A, Rose LE, Allen RL, Armstrong MR, Whisson SC, Kamoun S, Tyler BM, Birch PRJ, Beynon JL (2005) Differential recognition of highly divergent downy mildew avirulence gene alleles by RPP1 resistance genes from two Arabidopsis lines. Plant Cell 17:1839–1850

Rha E, Park HJ, Kim MO, Chung YR, Lee C-W, Kim JW (2001) Expression of exo-polygalacturonases in *Botrytis cinerea*. FEMS Microbiol Lett 201:105–109

Riemann M, Büche C, Kassemaeyer H-H, Nick P (2002) Cytoskeletal responses during early development of the downy mildew of grapevine (*Plasmopara viticola*). Protoplasma 219:13–22

Riquelme M, Bartnicki-Garcia S (2004) Key differences between lateral and apical branching in hyphae of *Neurospora crassa*. Fungal Genet Biol 41:842–851

Riquelme M, Reynaga-Peña CG, Gierz G, Bartnicki-García S (1998) What determines growth direction in fungal hyphae? Fungal Genet Biol 24:101–109

Roberson RW, Fuller MS (1988) Ultrastructural aspects of the hyphal tip of *Sclerotium rolfsii* preserved by freeze substitution. Protoplasma 146:143–149

Roberson RW, Vargas MM (1994) The tubulin cytoskeleton and its sites of nucleation in hyphal tips of *Allomyces macrogynus*. Protoplasma 182:19–31

Roberts AM, Mackie AJ, Hathaway V, Callow JA, Green JR (1993) Molecular differentiation in the extrahaustorial membrane of pea powdery mildew haustoria at early and late stages of development. Physiol Mol Plant Pathol 43:147–160

Robinson PM (1973) Oxygen – positive chemotropic factor for fungi? New Phytol 72:1349–1356

Robold AV, Hardham AR (1998) Production of species-specific monoclonal antibodies that react with surface components on zoospores and cysts of *Phytophthora nicotianae*. Can J Microbiol 44:1161–1170

Robold AV, Hardham AR (2004) Production of monoclonal antibodies against peripheral vesicle proteins in zoospores of *Phytophthora nicotianae*. Protoplasma 223:121–132

Robold AV, Hardham AR (2005) During attachment *Phytophthora* spores secrete proteins containing thrombospondin type 1 repeats. Curr Genet 47:307–315

Rogers LM, Kim Y-K, Guo WJ, Gonzáles-Candelas L, Li D, Kolattukudy PE (2000) Requirement for either a host- or pectin-induced pectate lyase for infection of *Pisum sativum* by *Nectria hematococca*. Proc Natl Acad Sci USA 97:9813–9818

Rollins JA (2003) The *Sclerotinia sclerotiorum pac1* gene is required for sclerotial development and virulence. Mol Plant Microbe Interact 16:785–795

Rumbolz J, Kassemeyer HH, Steinmetz, V, Deising HB, Mendgen K, Mathys D, Wirtz S, Guggenheim R, (2000) Differentiation of infection structures of the powdery mildew fungus *Uncinula necator* and adhesion to the host cuticle. Can J Bot 78:409–421

Russo GM, Dahlberg KR, Van Etten JL (1982) Identification of a development-specific protein in sclerotia of *Sclerotinia sclerotiorum*. Exp Mycol 6:259–267

Sacadura NT, Saville BJ (2003) Gene expression and EST analyses of *Ustilago maydis* germinating teliospores. Fungal Genet Biol 40:47–64

Satiat-Jeunemaitre B, Cole L, Bourett T, Howard R, Hawes C (1996) Brefeldin A effects in plant and fungal cells: something new about vesicle trafficking? J Microsc 181:162–177

Schuchardt I, Assmann D, Thines E, Schuberth C, Steinberg G (2005) Myosin-V, kinesin-1, and kinesin-3 cooperate in hyphal growth of the fungus *Ustilago maydis*. Mol Biol Cell 16:5191–5201

Scott V, Sherwin T, Gull K (1997) gamma-Tubulin in trypanosomes: molecular characterisation and localisation to multiple and diverse microtubule organising centres. J Cell Sci 110:157–168

Séjalon-Delmas N, Villalba Mateos F, Bottin A, Rickauer M, Dargent R, Esquerré-Tugayé MT (1997) Purification, elicitor activity, and cell wall localization of a glycoprotein from *Phytophthora parasitica* var. *nicotianae*, a fungal pathogen of tobacco. Phytopathology 87:899–909

Shan W, Marshall JS, Hardham AR (2004) Stage-specific expression of genes in germinated cysts of *Phytophthora nicotianae*. Mol Plant Pathol 5:317–330

Shapiro A, Mullins JT (2002) Hyphal tip growth in *Achlya bisexualis*. II. Distribution of cellulose in tip elongating and non-elongating regions of the wall. Mycologia 94:273–279

Shaw BD, Hoch HC (1999) The pycnidiospore of *Phyllosticta ampelicida*: surface properties involved in substratum attachment and germination. Mycol Res 103:915–924

Shaw BD, Hoch HC (2000) Ca^{2+} regulation of *Phyllosticta ampelicida* pycnidiospore germination and appressorium formation. Fungal Genet Biol 31:43–53

Shaw BD, Kuo KC, Hoch HC (1998) Germination and appressorium development of *Phyllosticta ampelicida* pycnidiospores. Mycologia 90:258–268

Shaw BD, Carroll GC, Hoch HC (2006) Generality of the prerequisite of conidium attachment to a hydrophobic substratum as a signal for germination among *Phyllosticta* species. Mycologia 98:186–194

Shepherd SJ, Van West P, Gow NAR (2003) Proteomic analysis of asexual development of *Phytophthora palmivora*. Mycol Res 107:395–400

Shepherd VA, Orlovich DA, Ashford AE (1993) A dynamic continuum of pleomorphic tubules and vacuoles in growing hyphae of a fungus. J Cell Sci 104:495–507

Shieh M-T, Brown RL, Whitehead MP, Cary JW, Cotty PJ, Cleveland TE, Dean RA (1997) Molecular genetic evidence for the involvement of a specific polygalacturonase, P2c, in the invasion and spread of *Aspergillus flavus* in cotton bolls. Appl Environ Microbiol 63:3548–3552

Shih J, Wei Y, Goodwin PH (2000) A comparision of the pectate lyase genes, *pel-1* and *pel-2*, of *Colletotrichum gloeosporioedes* f. sp. *malvae* and the relationship between their expression in culture and during necrotrophic infection. Gene 243:139–150

Sietsma JH, Wessels JGH (1994) Apical wall biogenesis. In: Wessels JGH, Meinhardt F (eds) The Mycota, vol I. Growth, differentiation and sexuality. Springer, Berlin Heidelberg New York, pp 125–141

Simon UK, Bauer R, Rioux D, Simard M, Oberwinkler F (2005) The intercellular biotrophic leaf pathogen *Cymadothea trifolii* locally degrades pectins, but not cellulose or xyloglucan in cell walls of *Trifolium repens*. New Phytol 165:243–260

Škalamera D, Wasson AP, Hardham AR (2004) Genes expressed in zoospores of *Phytophthora nicotianae*. Mol Genet Genomics 270:549–557

Soanes DM, Kershaw MJ, Cooley RN, Talbot NJ (2002) Regulation of the *MPG1* hydrophobin gene in the rice blast fungus *Magnaporthe grisea*. Mol Plant Microbe Interact 15:1253–1267

Sohn J, Voegele RT, Mendgen K, Hahn M (2000) High level activation of vitamin B1 biosynthesis genes in haustoria of the rust fungus *Uromyces fabae*. Mol Plant Microbe Interact 13:629–636

Solomon PS, Lee RC, Wilson TJG, Oliver RP (2004) Pathogenicity of *Stagonospora nodorum* requires malate synthase. Mol Microbiol 53:1065–1073

Soylu S, Keshavarzi M, Brown I, Mansfield JW (2003) Ultrastructural characterisation of interactions between *Arabidopsis thaliana* and *Albugo candida*. Physiol Mol Plant Pathol 63:201–211

Spencer-Phillips PTN, Gay JL (1981) Domains of ATPase in plasma membranes and transport through infected plant cells. New Phytol 89:393–400

Sreedhar L, Kobayashi DY, Bunting TE, Hillman BI, Belanger FC (1999) Fungal proteinase expression in the interaction of the plant pathogen *Magnaporthe poae* with its host. Gene 235:121–129

Srinivasan S, Vargas MM, Roberson RW (1996) Functional, organizational, and biochemical analysis of actin in hyphal tip cells of *Allomyces macrogynus*. Mycologia 88:57–70

Staples RC, Hoch HC (1997) Physical and chemical cues for spore germination and appressorium formation by fungal pathogens. In: Carroll G, Tudzynski P (eds) The Mycota, vol V, part A. Plant relationships. Springer, Berlin Heidelberg New York, pp 27–40

Stark-Urnau M, Mendgen K (1995) Sequential deposition of plant glycoproteins and polysaccharides at the host–parasite interface of *Uromyces vignae* and *Vigna sinensis*. Evidence for endocytosis and secretion. Protoplasma 186:1–11

Steinberg G, Fuchs U (2004) The role of microtubules in cellular organization and endocytosis in the plant pathogen *Ustilago maydis*. J Microsc 214:114–123

Struck C, Hahn M, Mendgen K (1996) Plasma membrane H^+-ATPase activity in spores, germ tubes, and haustoria of the rust fungus *Uromyces viciae-fabae*. Fungal Genet Biol 20:30–35

Struck C, Siebels C, Rommel O, Wernitz M, Hahn M (1998) The plasma membrane H^+-ATPase from the biotrophic rust fungus *Uromyces fabae*: molecular characterization of the gene (*PMA1*) and functional expression of the enzyme in yeast. Mol Plant Microbe Interact 11:458–465

Struck C, Ernst M, Hahn M (2002) Characterization of a developmentally regulated amino acid transporter (AAT1p) of the rust fungus *Uromyces fabae*. Mol Plant Pathol 3:23–30

Struck C, Mueller E, Martin H, Lohaus G (2004) The *Uromyces fabae UfAAT3* gene encodes a general amino acid permease that prefers uptake of *in planta* scarce amino acids. Mol Plant Pathol 5:183–189

Sugui JA, Leite B, Nicholson RL (1998) Partial characterization of the extracellular matrix released onto hydrophobic surfaces by conidia and conidial germlings of *Colletotrichum graminicola*. Physiol Mol Plant Pathol 52:411–425

Suzuki S, Komiya Y, Mitsui T, Tsuyumi S, Kunoh H, Carver TLW, Nicholson RL (1998) Release of cell wall degrading enzymes from conidia of *Blumeria graminis* on artifical substrata. Ann Phytopathol Soc Jpn 64:160–167

Szabo LJ, Bushnell WR (2001) Hidden robbers: the role of fungal haustoria in parasitism of plants. Proc Natl Acad Sci USA 98:7654–7655

Takano Y, Kikuchi T, Kubo Y, Hamer JE, Mise K, Furusawa I (2000) The *Colletotrichum lagenarium* MAP kinase gene *CMK1* regulates diverse aspects of fungal pathogenesis. Mol Plant Microbe Interact 13:374–383

Takano Y, Oshiro E, Okuno T (2001) Microtubule dynamics during infection-related morphogenesis of *Colletotrichum lagenarium*. Fungal Genet Biol 34:107–121

Takano Y, Choi W, Mitchell TK, Okuno T, Dean RA (2003) Large scale parallel analysis of gene expression during infection-related morphogenesis of *Magnaporthe grisea*. Mol Plant Pathol 4:337–346

Takemoto D, Jones DA, Hardham AR (2006) Reorganization of the cytoskeleton and endoplasmic reticulum in the *Arabidopsis pen1-1* mutant inoculated with the non-adapted powdery mildew pathogen, *Blumeria graminis* f. sp. *hordei*. Mol Plant Pathol (in press)

Talbot NJ, Ebbole DJ, Hamer JE (1993) Identification and characterization of *MPG1*, a gene involved in pathogenicity from the rice blast fungus *Magnaporthe grisea*. Plant Cell 5:1575–1590

Talbot NJ, Kershaw MJ, Wakley GE, De Vries OMH, Wessels JGH, Hamer JE (1996) *MPG1* encodes a fungal hydrophobin involved in surface interactions during infection-related development of *Magnaporthe grisea*. Plant Cell 8:985–999

Taylor J, Mims CW (1991) Fungal development and host cell responses to the rust fungus *Puccinia substriata* var. *indica* in seedling and mature leaves of susceptible and resistant pearl millet. Can J Bot 69:1207–1219

Tenberge KB, Homann V, Oeser B, Tudzynski P (1996) Structure and expression of two polygalacturonase genes of *Claviceps purpurea* oriented in tandem and cytological evidence for pectinolytic enzyme activity during infection of rye. Phytopathology 86:1084–1097

Terhune BT, Hoch HC (1993) Substrate hydrophobicity and adhesion of *Uromyces* urediospores and germlings. Exp Mycol 17:241–252

Terhune BT, Bojko RJ, Hoch HC (1993) Deformation of stomatal guard cell lips and microfabricated artificial topographies during appressorium formation by *Uromyces*. Exp Mycol 17:70–78

Thines E (2004) Mycol Res 108:374–383

Thines E, Weber RWS, Talbot NJ (2000) MAP kinase and protein kinase A-dependent mobilization of triacylglycerol and glycogen during appressorium turgor generation by *Magnaporthe grisea*. Plant Cell 12:1703–1718

Thomas SW, Glaring MA, Rasmussen SW, Kinane JT, Oliver RP (2002) Transcript profiling in the barley mildew pathogen *Blumeria graminis* by serial analysis of gene expression (SAGE). Mol Plant Microbe Interact 15:847–856

Tomley FM, Soldati DS (2001) Mix and match modules: structure and function of microneme proteins in apicomplexan parasites. Trends Parasitol 17:81–88

Tongen A, Goriely A, Tabor M (2006) Biomechanical model for appressorial design in *Magnaporthe grisea*. J Theor Biol 240:1–8

Tonukari NJ, Scott-Craig JS, Walton JD (2000) The *Cochliobolus carbonum SNF1* gene is required for cell wall-degrading enzyme expression and virulence on maize. Plant Cell 12:237–247

Truesdell GM, Yang Z, Dickman MB (2000) A G-α subunit gene from the phytopathogenic fungus *Colletotrichum trifolii* is required for conidial germination. Physiol Mol Plant Pathol 56:131–140

Tsuba M, Katagiri C, Takeuchi Y, Takada Y, Yamaoka N (2002) Chemical factors of the leaf surface involved in the morphogenesis of *Blumeria graminis*. Physiol Mol Plant Pathol 60:51–57

Tsuji G, Fujii S, Tsuge S, Shiraishi T, Kubo Y (2003) The *Colletotrichum lagenarium* Ste12-like gene CST1 is essential for appressorium penetration. Mol Plant Microbe Interact 16:315–325

Tucker SL, Talbot NJ (2001) Surface attachment and prepenetration stage development by plant pathogenic fungi. Annu Rev Phytopathol 39:385–417

Tucker SL, Thornton CR, Tasker K, Jacob C, Giles G, Egan M, Talbot NJ (2004) A fungal metallothionein is required for pathogenicity of *Magnaporthe grisea*. Plant Cell 16:1575–1588

Tudzynski P, Scheffer J (2004) *Claviceps purpurea*: molecular aspects of a unique pathogenic lifestyle. Mol Plant Pathol 5:377–388

Tyler BM (2002) Molecular basis of recognition between *Phytophthora* pathogens and their hosts. Annu Rev Phytopathol 40:137–167

Van de Peer Y, De Wachter R (1997) Evolutionary relationships among the eukaryotic crown taxa taking into account site-to-site rate variation in 18S rRNA. J Mol Evol 45:619–630

Van Etten JL, Freer SN, McCune B (1979) Presence of a major (storage?) protein in dormant spores of the fungus *Botryodiplodia theobromae*. J Bacteriol 138:650–652

Van West P, Morris BM, Reid B, Appiah AA, Osborne MC, Campbell TA, Shepherd SJ, Gow NAR (2002) Oomycete plant pathogens use electric fields to target roots. Mol Plant Microbe Interact 15:790–798

Veneault-Fourrey C, Parisot D, Gourgues M, Lauge R, Lebrun MH, Langin T (2005) The tetraspanin gene *ClPLS1* is essential for appressorium-mediated penetration of the fungal pathogen *Colletotrichum lindemuthianum*. Fungal Genet Biol 42:306–318

Veneault-Fourrey C, Lambou K, Lebrun M-H (2006) Fungal Pls1 tetraspanins as key factors of penetration into host plants: a role in re-establishing polarized growth in the appressorium?. FEMS Microbiol Lett 256:179–184

Viaud MC, Balhadère PV, Talbot NJ (2002) A *Magnaporthe grisea* cyclophilin acts as a virulence determinant during plant infection. Plant Cell 14:917–930

Viaud M, Brunet-Simon A, Brygoo Y, Pradier J-M, Levis C (2003) Cyclophilin A and calcineurin functions investigated by gene inactivation, cyclosporin A inhibition and cDNA arrays approaches in the phytopathogenic fungus *Botrytis cinerea*. Mol Microbiol 50:1451–1465

Villalba Mateos F, Rickauer M, Esquerré-Tugayé MT (1997) Cloning and characterization of a cDNA encoding an elicitor of *Phytophthora parasitica* var. *nicotianae* that shows cellulose-binding and lectin-like activities. Mol Plant Microbe Interact 10:1045–1053

Viret O, Tott L, Chapela IH, Petrini O (1994) The role of the extracellular sheath in recognition and attachment of conidia of *Discula umbrinella* (Berk. & Br.) Morelet to the host surface. New Phytol 127:123–131

Voegele RT, Mendgen K (2003) Rust haustoria: nutrient uptake and beyond. New Phytol 159:93–100

Voegele RT, Struck C, Hahn M, Mendgen K (2001) The role of haustoria in sugar supply during infection of broad bean by the rust fungus *Uromyces fabae*. Proc Natl Acad Sci USA 98:8133–8138

Voegele RT, Hahn M, Lohaus G, Link T, Heiser I, Mendgen K (2005) Possible roles for mannitol and mannitol dehydrogenase in the biotrophic plant pathogen *Uromyces fabae*. Plant Physiol 137:190–198

Voegele RT, Wirsel S, Moll U, Lechner M, Mendgen K (2006) Cloning and characterization of a novel invertase from the obligate biotroph *Uromyces fabae* and analysis of expression patterns of host and pathogen invertases in the course of infection. Mol Plant Microbe Interact 19:625–634

Vries RP de, Jansen J, Aguilar G, Parenicova L, Joosten V, Wulfert F, Benen JAE, Visser J (2002) Expression profiling of pectinolytic genes from *Aspergillus niger*. FEBS Lett 530:41–47

Walton JD (1994) Deconstructing the cell wall. Plant Physiol 104:1113–1118

Wang J, Higgins VJ (2005) Nitric oxide has a regulatory effect in the germination of conidia of *Colletotrichum coccodes*. Fungal Genet Biol 42:284–292

Wang M-C, Bartnicki-Garcia S (1980) Distribution of mycolaminarans and cell wall β-glucans in the life cycle of *Phytophthora*. Exp Mycol 4:269–280

Wang Z-Y, Thornton CR, Kershaw MJ, Li D, Talbot NJ (2003) The glyoxylate cycle is required for temporal regulation of virulence by the plant pathogenic fungus *Magnaporthe grisea*. Mol Microbiol 47:1601–1612

Wang Z-Y, Jenkinson JM, Holcombe LJ, Soanes DM, Veneault-Fourrey C, Bhambra GK, Talbot NJ (2005) The molecular biology of appressorium turgor generation by the rice blast fungus *Magnaporthe gasea*. Biochem Soc Trans 33:384–388

Wanjiru WM, Zhensheng K, Buchenauer H (2002) Importance of cell wall degrading enzymes produced by *Fusarium graminearum* during infection of wheat heads. Eur J Plant Pathol 108:803–810

Warwar V, Dickman MB (1996) Effects of calcium and calmodulin on spore germination and appressorium development in *Colletotrichum trifolii*. Appl Environ Microbiol 62:74–79

Watanabe K, Parbery DG, Kobayashi T, Doi Y (2000) Conidial adhesion and germination of *Pestalotiopsis neglecta*. Mycol Res 104:962–968

Wattad C, Kobiler D, Dinoor A, Prusky D (1997) Pectate lyase of *Colletotrichum gloeosporioides* attacking avocado fruits: cDNA cloning and involvement in pathogenicity. Physiol Mol Plant Pathol 50:197–212

Weber RWS, Davoli P (2002) Autophagocytosis of carotenoid-rich lipid droplets into vacuoles during aeciospore ageing in *Puccinia distincta*. New Phytol 154:471–479

Weber RWS, Wakley GE, Thines E, Talbot NJ (2001) The vacuole as central element of the lytic system and sink for lipid droplets in maturing appressoria of *Magnaporthe grisea*. Protoplasma 216:101–112

Wedlich-Söldner R, Schulz I, Straube A, Steinberg G (2002a) Dynein supports motility of endoplasmic reticulum in the fungus *Ustilago maydis*. Mol Biol Cell 13:965–977

Wedlich-Söldner R, Straube A, Friedrich MW, Steinberg G (2002b) A balance of KIF1A-like kinesin and dynein organizes early endosomes in the fungus *Ustilago maydis*. EMBO J 21:2946–2957

Wei YD, Shen WY, Dauk M, Wang F, Selvaraj G, Zou J (2004) Targeted gene disruption of glycerol-3-phosphate dehydrogenase in *Colletotrichum gloeosporioides* reveals evidence that glycerol is a significant transferred nutrient from host plant to fungal pathogen. J Biol Chem 279:429–435

Welter K, Müller M, Mendgen K (1988) The hyphae of *Uromyces appendiculatus* within the leaf tissue after high pressure freezing and freeze substitution. Protoplasma 147:91–99

Wessels JGH (1996) Fungal hydrophobins: proteins that function at an interface. Trends Plant Sci 1:9–14

Wessels JGH (1999) Fungi in their own right. Fungal Genet Biol 27:134–145

Wirsel SGR, Voegele RT, Mendgen KW (2001) Differential regulation of gene expression in the obligate biotrophic interaction of *Uromyces fabae* with its host *Vicia faba*. Mol Plant Microbe Interact 14:1319–1326

Woods AM, Gay JL (1983) Evidence for a neckband delimiting structural and physiological regions of the host plasma membrane associated with haustoria of *Albugo candida*. Physiol Plant Pathol 23:73–88

Woods AM, Gay JL (1987) The interface between haustoria of *Puccinia poarum* (monokaryon) and *Tussilago farfara*. Physiol Mol Plant Pathol 30:167–185

Wright AJ, Carver TLW, Thomas BJ, Fenwick NID, Kunoh H, Nicholson RL (2000) The rapid and accurate determination of germ tube emergence site by *Blumeria graminis* conidia. Physiol Mol Plant Pathol 57:281–301

Wright AJ, Thomas BJ, Carver TLW (2002) Early adhesion of *Blumeria graminis* to plant and artificial surfaces demonstrated by centrifugation. Physiol Mol Plant Pathol 61:217–226

Wu S-C, Halley JE, Luttig C, Fernekes LM, Gutiérrez-Sanchez G, Darvill AG, Albersheim P (2006) Identification of an *endo*-β-1,4-D-xylanase from *Magnaporthe grisea* by gene knockout analysis, purification, and heterologous expression. Appl Environ Microbiol 72:986–993

Wubben JP, Mulder W, ten Have A, van Kan JAL, Visser J (1999) Cloning and partial characterization of endopolygalacturonase genes from *Botrytis cinerea*. Appl Environ Microbiol 65:1596–1602

Wubben JP, Have A ten, Kan JAL van, Visser J (2000) Regulation of endopolygalacturonase gene expression in *Botrytis cinerea* by galacturonic acid, ambient pH and carbon catabolite repression. Curr Genet 37:152–157

Wynn WK (1976) Appressorium formation over stomates by the bean rust fungus: response to a surface contact stimulus. Phytopathology 66:136–146

Wynn WK (1981) Tropic and taxic responses of pathogens to plants. Annu Rev Phytopathol 19:237–255

Xiao J-Z, Watanabe T, Kamakura T, Ohshima A, Yamaguchi I (1994) Studies on cellular differentiation of *Magnaporthe grisea*. Physicochemical aspects of substratum surfaces in relation to appressorium formation. Physiol Mol Plant Pathol 44:227–236

Xie M, Krooshof GH, Benen JAE, Atwood III JA, King D, Bergmann C, Orlando R (2005) Post-translational modifications of recombinant *B. cinerea* EPG 6. Rapid Commun Mass Spectrom 19:3389–3397

Xu H, Mendgen K (1997) Targeted cell wall degradation at the penetration site of cowpea rust basidiosporelings. Mol Plant Microbe Interact 10:87–94

Yakoby N, Beno-Moualem D, Keen NT, Dinoor A, Prusky D (2001) *Colletotrichum gloeosporioides pel*B is an important virulence factor in avocado fruit-fungus interaction. Mol Plant Microbe Interact 14:988–995

Yamaoka N, Takeuchi Y (1999) Morphogenesis of the powdery mildew fungus in water (4) The significance of conidium adhesion to the substratum for normal appressorium development in water. Physiol Mol Plant Pathol 54:145–154

Yamashita RA, May GS (1998) Motoring along the hyphae: molecular motors and the fungal cytoskeleton. Curr Opin Cell Biol 10:74–79

Yamauchi J, Takayanagi N, Komeda K, Takano Y, Okuno T (2004) cAMP-PKA signalling regulates multiple steps of fungal infection cooperativity with Cmk1 MAP kinase in *Colletotrichum lagenarium*. Mol Plant Microbe Interact 17:1355–1365

Yan H-Z, Liou R-F (2005) Cloning and analysis of *pppg1*, an inducible endopolygalacturonase gene from the oomycete plant pathogen *Phytophthora parasitica*. Fungal Genet Biol 42:339–350

Zahiri AR, Babu MR, Saville BJ (2005) Differential gene expression during teliospore germination in *Ustilago maydis*. Mol Genet Genom 273:394–403

Zelinger E, Hawes CR, Gurr SJ, Dewey FM (2004) An immunocytochemical and ultra-structural study of the extracellular matrix produced by germinating spores of *Stagonospora nodorum* on natural and artificial surfaces. Physiol Mol Plant Pathol 65:123–135

12 Fair Trade in the Underworld: the Ectomycorrhizal Symbiosis

F. Martin[1]

CONTENTS

I. Introduction 291
II. Biology of the Ectomycorrhizal Symbiosis . 292
A. Trading in the Underground 292
III. Symbiosis Development 293
A. Building the Symbiosis 293
B. Cross-Talk in the Ectomycorhizosphere 294
IV. Genomics of Ectomycorrhizal Symbioses . . 296
A. Genome Sequence of the Ectomycorrhizal Basidiomycete *Laccaria bicolor* 296
B. The Transcriptome of Ectomycorrhizal Fungi 298
1. Transcripts Expressed in Free-Living Mycelium 298
2. Transcripts Expressed in Symbiotic Tissues 299
3. Early-Transcriptionally Responsive Genes to Symbiosis Formation 299
4. Middle- and Late-Transcriptionally Responsive Genes to Symbiosis Formation 300
5. Functional Specialization of the Hyphal Web Compartments . . 302
6. Plant Responses upon Symbiosis Development 302
C. Ectomycorrhizal Mutants 302
V. Future Research 303
References 304

I. Introduction

Biological diversity is often exclusively considered at the level of plants and animals, whereas the bulk of global biodiversity is in fact at the microbial level. Although it is clear that the ecology of our planet is driven by microbial ecosystems, we are severely hampered by our limited understanding of the diversity and function of such microbial ecosystems. Living in the vicinity of weathered rock and growing on mineral particles and decaying organic matter are a cast of hundreds of fungal species. Within the rhizosphere which hosts large and diverse communities of prokaryotic and eukaryotic microorganisms that compete and interact with each other and with plant roots, mycorrhizal fungi are almost ubiquitous. These species are no marginal oddity, having been shown to account for half of the fungal species in most temperate, montane and boreal forests (Fierer et al. 2005). The symbiotic relationship between roots and these fungi is one of the most prevalent associations in all terrestrial ecosystems. Knowing which processes these soil fungi are responsible for, and how, is thus increasingly important for understanding the inputs and outputs in forest ecosystems.

The hyphae of mycorrhizal fungi and plant short roots form a novel composite organ, the so-called mycorrhiza, which is the site of nutrient and carbon transfer between the two symbiotic partners. This interaction allows terrestrial plants to grow efficiently in suboptimal environments (Brundrett 2002; Read and Perez-Moreno 2003). The first mycorrhizal associations must have been derived from earlier types of plant–fungus interaction, such as endophytic fungi in the bryophyte-like precursors of vascular plants (Redecker et al. 2000). Structures similar to arbuscular mycorrhiza have been observed in plant fossils from the Early Devonian (Selosse and Le Tacon 1998), whereas fossil ectomycorrhiza have been found in the middle Eocene (Le Page et al. 1997). Mycorrhizal associations are found on most annual and perennial plants (probably >90%). About two-thirds of these plants, mostly herbaceous species, are symbiotic with arbuscular mycorrhizal (AM) glomalean fungi (Glomeromycota). Ericoid mycorrhizas are ecologically important as efficient organic matter (OM) degraders, but are mainly restricted to heathlands (Read and Perez-Moreno 2003). While a relatively small number of plants, ca. 8000, form ectomycorrhizas (ECM), their ecological importance is amplified by their wide occupancy of biomes. Trees of Betulaceae, Cistaceae, Dipterocarpaceae, Fagaceae,

[1] UMR INRA/UHP 1136 'Interactions Arbres/Micro-Organismes', IFR 110, Centre INRA de Nancy, 54280 Champenoux, France

Biology of the Fungal Cell, 2nd Edition
The Mycota VIII
R.J. Howard and N.A.R. Gow (Eds.)
© Springer-Verlag Berlin Heidelberg 2007

Pinaceae, Myrtaceae, Salicaceae and several tribes in Fabaceae are ectomycorrhizal plants, dominating boreal, temperate, mediterranean and some subtropical forest ecosystems (Read and Perez-Moreno 2003). Through mutualistic symbioses with ECM fungi, these tree species have been able to acquire metabolic capabilities that in turn have allowed the utilization of otherwise unavailable ecological niches. Despite their obvious importance, still little is known about the biology and ecology of most ECM species. For example, we still do not understand the importance of key ecological processes, such as the spatial and temporal scales at which root colonization occurs, the role of sexual versus vegetative reproduction in the spread of ECM fungi or how the mycobionts participate to the fitness of their host trees. An understanding of these ecological processes requires a better knowledge of the underlying molecular mechanisms (Martin 2001).

After a brief description of the biology of ectomycorrhizal fungi, the present review focuses on the molecular processes involved in the development of this ectomycorrhizal symbiosis. Recent reviews (Harrison 2005; Hause and Fester 2005; Paszkowski 2006) summarize the progress made in understanding arbuscular mycorrhizal symbiosis.

II. Biology of the Ectomycorrhizal Symbiosis

Within days after their emergence in the upper soil profiles (e.g. organic humus and mor layer), up to 95% of the short roots of most conifers and deciduous trees are colonized by ectomycorrhizal mycobionts (Taylor et al. 2000). The ectomycorrhizal basidiomycetes (e.g. agarics, boletes) and ascomycetes (e.g. truffles) are not a phylogenetically distinct group, but an assemblage of very different fungal species that have independently developed a symbiotic lifestyle over the past 130–180 million years (Hibbett et al. 2000; Brundrett 2002). The switch between saprobic and mycorrhizal lifestyles probably happened convergently, and perhaps many times, during evolution of these fungal lineages (Hibbett et al. 2000). This may have facilitated the evolution of ectomycorrhizal lineages with a broad range of physiological and ecological functions, reflecting partly the activities of their disparate saprotrophic ancestors. Whereas a few Basidiomycota clades are exclusively ectomycorrhizal (e.g. bolets), most clades comprise both ectomycorrhizal and saprobic species (e.g. Tricholomataceae), suggesting that the symbiotic ability involved a limited number of (master) genes or key enzyme activities.

Although it was thought that ectomycorrhizal fungi present a low specificity, the use of DNA-based genotyping methods recently modified our understanding of the specificity of mycorrhizal fungi towards their host plants. For example, observations indicated that the host range of ericoid mycorrhizal fungi may be extended also to ectomycorrhizal plants in nature (Bergero et al. 2000; Vrålstad et al. 2000; Tedersoo et al. 2006). In contrast, *Rhizoctonia* spp were reported until recently as the dominant mycorrhizal symbionts of orchids, but direct amplification of fungal DNA from mycorrhizal roots of achlorophyllous and green forest orchids demonstrated that the main symbionts are unculturable fungi that belong to known ectomycorrhizal taxa (Selosse et al. 2002). Therefore, the current anatomical classification of mycorrhizal associations does not take into account the plasticity of the different fungal groups in forming ectomycorrhizal interactions.

A. Trading in the Underground

Pivotal to the success of these ectomycorrhizal interactions is the fair trade of nutrients between the symbionts and their host trees. The prospecting and absorbing extraradical hyphal web captures soil minerals (P, N, water, micronutrients; Smith and Read 1997) and organic nitrogen (Chalot and Brun 1998), assimilating and translocating a large proportion of them to the growing plant (Simard et al. 1997a, b; Chalot et al. 2006). Ectomycorrhizal fungi affect not only mineral and water uptake, but also adaptation to adverse soil chemical conditions (Meharg and Cairney 2000) and susceptibility to diseases (Smith and Read 1997), and substantially contribute to plant growth and productivity (Grove and Le Tacon 1993). Further, the fungus within the root is insulated from competition with other soil microorganisms and, therefore, is a preferential user of the plant carbon (ca. 10–20% of the host photoassimilates; Rygiewicz and Andersen 1994; Högberg et al. 2001). As a result, mycorrhizas that represent a large carbon drain for their host (i.e. ectomycorrhizal tips with a thick mantle and/or species producing large and abundant fruiting bodies) may represent less than optimal

mutualistic associations and the cost and benefits may fluctuate according to environmental and biotic factors. Natural populations of mycorrhizal plants show large differences in growth responses (including depression) and no simple relationship is considered likely as nutritional benefits in the field are difficult to demonstrate.

Mycorrhizal fungi constitute links in the chain of transfers by which carbon and nitrogen may move between plant and soil compartments (Simard et al. 1997a, b) and can thus influence carbon and nitrogen cycling rates in host plants and forest ecosystems (Read and Perez-Moreno 2003). A major contributing factor in nutrient acquisition by ectomycorrhizal trees is the existence and continued growth of the extramatrical mycelium into soil horizons. It provides the contact between the root system and soil resources which may be discontinuously distributed over large distances from the root. This extramatrical mycelium thus fulfills the essential role of foraging for and exploiting the nutrient resources of the soil and then translocating them to the ectomycorrhizal mantle where storage takes place. Extramatrical hyphæ extend far beyond the depletion zone surrounding the root and thus improve root exploitation of a given soil volume (up to 1000 m of hyphae per 1 m of root; Rousseau et al. 1994). This hyphal network extends through humified forest soils as a prospecting fan which provides optimal efficiency in foraging the patchily distributed resources. Intensive development of mycelial mats is induced by the occurrence of litter organic residues (Bending 2003). The occurrence of this series of interconnected fungal compartments (Hartig net, mantle, rhizomorphs, fungal mats), with different physiological activities, suggests the functional specialization of the different hyphal webs (Cairney and Burke 1996) and a tight coordination of the gene expression and metabolic activities between these compartments. It should be realized that the mycelial mats colonizing OM-rich soil patches with their saprotrophic activities and the hyphae of the Hartig net proliferating in the plant apoplast are highly contrasting, Janus-faced entities with opposite physiological activities. How the different fungal compartments (i.e. fan-like mycelium degrading OM, rhizomorphs transporting nutrients, symbiotic tissues) coordinate their activities and synchronize them with the host plant metabolism and development is one of the challenging questions for future research. While analysis of metabolic activities in ECM systems has been a mainstay of mycorrhizal research, investigation of dynamic changes in the symbiosis metabolic networks in situ (Martin 2001) has become the new focus of the postgenomic effort (Morel et al. 2005; Wright et al. 2005). The major challenges now are to understand how changes in nutrient availability and environment are sensed and signalled and to understand the nature of the subsequent metabolic reconfiguration.

III. Symbiosis Development

A. Building the Symbiosis

Development of a mature ectomycorrhiza proceeds through a programmed series of events. Morphological, anatomical and cytological changes that accompany symbiosis development have been described in great detail in several ectomycorrhizal associations [e.g. *Picea abies*/*Amanita muscaria* (Köttke and Oberwinkler 1986, 1987); *P. abies*/*Hebeloma crustuliniforme* (Brunner and Scheidegger 1995); *Eucalyptus*/*Pisolithus* (Chilvers 1968; Massicotte et al. 1987; Horan et al. 1988; Dexheimer et al. 1994); *Alnus rubra*/*Alpova diplophloeus* (Massicotte et al. 1986, 1989a, b); *Dryas integrifolia*/*Hebeloma cylindrosporum* (Melville et al. 1988); and *Betula pendula*/*Paxillus involutus* (Brun et al. 1995)]. The mature organization of ectomycorrhiza varies with the host and fungal species, generating hundreds of different morphotypes (Agerer 1993). In addition, a survey of almost any natural fungal progeny (Wong et al. 1989, 1990) and population (Gay et al. 1993) will reveal a considerable range of symbiotic phenotypes. However, although some of the details vary, early stages of ectomycorrhiza development have well characterized similar morphological developmental transitions.

Fungal hyphae emerging from a soil propagule (spores, sclerotia) or an older mycorrhiza tip growth in the rhizosphere make contact with the root surface, penetrate the root cap cells and grow through them. Backwards from the tip, the invasion of root cap cells proceeds inwards until the hyphae reach the epidermal cells (Horan et al. 1988). After contact, hyphal growth on the root surface initiates swelling of the hyphal tips, leading to pad-like structures and the formation of dense finger-like structures. The development of the mantle and the Hartig net (Fig. 12.1), characterized by labyrinthine branching of hyphae grow-

ing in the root apoplast (Massicotte et al. 1989c), is linked to pivotal events at the hyphal tip. Progression from the strongly rhizomorphic outgrowth of the free-living mycelium to the plectenchymatous structure of the ectomycorrhizal sheath and the coenocytic Hartig net hyphæ is associated with a lack of septation, a loss of apical coherence and intimate juxtaposition of hyphæ (Köttke and Oberwinkler 1987; Massicotte et al. 1987). Interestingly, several mycorrhiza-defective mutants of the ectomycorrhizal basidiomycete *Hebeloma cylindrosporum* seem to be affected at these earliest stages of symbiosis development (Combier et al. 2004). Mutants 2A9 and 10F11 burst and released their cellular content when in contact with the host root, suggesting that they are altered in the plant signal sensing and/or transduction pathways required for a proper interaction. After attachment onto epidermal cells, hyphae multiply to form a series of layers several hundred microns thick which differentiate to form the mature mantle (Horan et al. 1988). An outward network of hyphae prospecting the soil and gathering nutrients irradiate from the outer layers of the mantle (Fig. 12.1). These morphological studies of the processes leading to the mature ectomycorrhiza have shown a fairly complex influence of the root on the fungus, including a general growth stimulus, a trophic response directing hyphal growth inwards towards the plant tissues and a morphogenetic effect leading to compact hyphal mantle development. In addition to yet unidentified morphogenetic molecules, the supply of carbon-rich nutrients and vitamins and the presence of a physical support likely play a role in the mantle differentiation (Martin and Tagu 1999). In return, fungal hyphae stimulate lateral root formation, dichotomy of the apical meristem in conifer species and cytodifferentiation of root cells (radial elongation, root hair decay; Fig. 12.1; Massicotte et al. 1987, 1989b; Horan et al. 1988; Dexheimer and Pargney 1991; Ditengou et al. 2000).

B. Cross-Talk in the Ectomycorhizosphere

For optimal development of the symbiosis, partners evolve complex coordinated developmental processes and, at the same time, sense and respond to physiological factors and environmental cues (Martin et al. 2001). To understand molecular communication between host plants and soil fungi, one of the most pressing questions is the chemical structure of the signals that induce symbiosis-related gene expression and subsequent morphogenetic processes in plant roots and fungal hyphae.

Both ectomycorrhizal partners probably possess one to many types of signal receptors/sensors that may bind with several (or a number of) rhizospheric excreted signals (Horan and Chilvers 1990; Martin et al. 2001; Jambois et al. 2005). In turn, signals/sensors complexes are thought to trigger expression of downstream genes including components of the signalling and hormonal pathways. Molecules that control the interactions between ECM partners are likely involved in:

1. Tropism of hyphae for host tissues (e.g. rhizospheric signals),

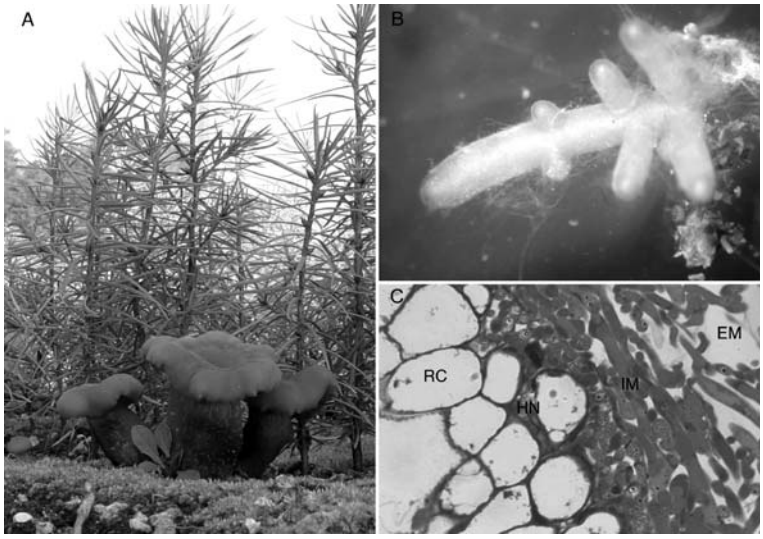

Fig. 12.1. The ectomycorrhizal symbiosis. **A** Seedlings of Douglas fir (*Pseudotsuga menziesii*) colonized by the ectomycorrhizal basidiomycete *Laccaria bicolor*. The fungal mycelium has developed ectomycorrhizas on the root system and has produced a fruiting body above ground. Photograph courtesy of D. Vairelles. **B** Short roots of beech (*Fagus sylvatica*) ensheathed by the mycelium of *Laccaria amethystina*. Photograph courtesy of M. Buée. **C** Transverse section of a *Eucalyptus*/*Pisolithus* ectomycorrhiza showing the external (*EM*) and internal (*IM*) mantles: the fungal hyphae have begun to penetrate between the epidermal cells of the root cortex (*RC*) to form the Hartig net (*HN*). Epidermal cells are radially enlarged

2. Attachment and invasion of host tissues by hyphae, such as adhesins and carbohydrate active hydrolytic enzymes,
3. Induction of organogenetic programmes in both fungal and root cells (hormones and secondary signals, such as calcium or nitric oxide),
4. Facilitation of *in planta* mycobiont survival faced to the plant defense responses,
5. Coordinating the metabolic trafficking for exchanging carbon, nitrogen, phosphate and other metabolites.

For both symbionts, the period prior to physical contact involves the recognition and attraction of appropriate partners and other events promoting the interaction. The multiplicity of identified signals (auxins, ethylene, alkaloids, cytokinins, flavonols) can act in a synergistic (rutine/zeatine) or antagonistic (indole-3-acetic acid/hypaphorine) manner (Ditengou and Lapeyrie 2000; Jambois et al. 2005). In the vicinity of a host root, fungal morphology shifts towards enhanced hyphal growth and extensive hyphal branching. Such a response can be triggered by host root exudates, such as rutin and zeatin (Lagrange et al. 2001), suggesting that the fungus perceives positional information through sensing host-derived signals (e.g. 'branching factor') leading to intensified hyphal ramification that is likely to increase the probability of contact with a host root. In eucalypt ectmycorrhizas, host-released metabolites such as the flavonol, rutin, and the cytokinin, zeatin, strikingly modified the hyphal morphology of the ECM *Pisolithus microcarpus* (Lagrange et al. 2001). Rutin stimulated hyphal growth when present in the growth medium at a very low level, whereas the cytokinin, zeatin, modified the hyphal branch angle. These rhizospheric molecules are therefore able to induce morphological changes similar to those observed during actual ectomycorrhizal development (Köttke and Oberwinkler 1987; Horan et al. 1988). In AM symbiosis, a recent breakthrough was the identification of a branching factor, 5-deoxy-strigol, released by *Lotus japonicus* and able to stimulate pre-symbiotic hyphal growth and branching (Akiyama et al. 2005). Strigolactones strongly and rapidly stimulated cell proliferation of the AM fungi *Gigaspora rosea*, *Glomus intraradices* and *Gl. claroideum* at concentrations as low as 10^{-13} M. This was also associated with a rapid increase in mitochondrial density and respiration, as shown with *Gl. intraradices* (Besserer et al. 2006). Strigolactones have been isolated from a wide range of mono- and dicotyledonous plants and were found previously to stimulate seed germination of parasitic weeds such as *Striga* and *Orobanche*. The concentration of strigolactones in root exudates coincides with the host specificity of AM fungi (Akiyama et al. 2005). This widespread strigolactone perception system suggests that the earliest land plants already used this class of molecules to communicate with their symbiotic partners (Brachman and Parniske 2006). It remains to be determined whether the evolutionary younger ectomycorrhizal basidiomycetes and ascomycetes are responsive to these rhizospheric strigolactones. The current body of data also points toward a central symbiosis signalling pathway in plants which has been recruited repeatedly by symbionts of different evolutionary age (Brachman and Parniske 2006).

Root exudates and zeatin also trigger an enhanced accumulation of fungal molecules, such as the betaine of tryptophan, hypaphorine (Béguiristain and Lapeyrie 1997). This fungal alkaloid is the major indolic compound isolated from the ectomycorrhizal fungus *P. microcarpus* (Béguiristain et al. 1995) and is produced in larger amounts by this fungus during mycorrhiza development (Béguiristain and Lapeyrie 1997). Competitive antagonism between host endogenous indole-3-acetic acid (IAA) and the secreted fungal indole alkaloid hypaphorine must contribute to regulate symbiosis ontogenesis (Ditengou and Lapeyrie 2000; Jambois et al. 2005). Special interest has been paid for many years to the role of IAA in the formation of ectomycorrhizal tissues. Pine inoculated with a mutant of *Hebeloma cylindrosporum* strain overproducing IAA produced an increased number of ectomycorrhizal roots (Gay et al. 1994) which presented a strikingly altered morphology (i.e. multiseriate Hartig net; Gea et al. 1994; Tranvan et al. 2000) confirming that some morphogenetic steps controlling the mycorrhiza development are regulated by secreted fungal IAA. In contrast, inhibitors of polar auxin transport, such as 2,3,5-triiodobenzoic acid (TIBA), restrict the stimulation of lateral root formation and the colonization of the tap-root cortex of conifer seedlings by ectomycorrhizal fungi (Karabaghli-Degron et al. 1998). Exogenous IAA secreted by most ectomycorrhizal fungi likely alters the root IAA homeostasis by unknown mechanisms. The impact of fungal invasion on auxin transporters and transport facilitators remains to be investigated.

Although the above summarizes the scarce current knowledge on signalling processes in plant–ectomycorrhizal fungi associations, it does not explain why a particular tree establishes a symbiosis with a certain type of mycobiont, or why most host plants can interact with dozen of fungal species. Most probably the solutions to these puzzles lie in the nature of signals and receptors themselves. Once the fungal hyphae are within the root, other trophic and developmental inputs, from both symbionts, are likely necessary for successful symbiosis. In entering its novel niche, the colonizing hyphae need to adjust to their new environment, i.e. the root apoplast. One essential modification is the alteration of the cell surface, leading to the insulation of the mycobiont facing plant defense molecules and/or leading to changes in the permeability of the cell surface allowing the symbiotic traffic.

IV. Genomics of Ectomycorrhizal Symbioses

Mycobionts, belonging to a wide range of ascomycetous and basidiomycetous species, induce similar symbiotic structures (i.e. mantle and Hartig net) in widely diverse conifer and hardwood species, suggesting that ectomycorrhizal symbioses have likely evolved by recruiting some common core genetic programs in their partners. The latter hypothesis is supported by various genetic and molecular studies (Martin et al. 2001; Wiemken and Boller 2002).

Major alterations in patterns of gene expression occur during, and are likely required for, ectomycorrhiza development (Martin et al. 2001). As I postulated 15 years ago, the basic regulatory mechanism likely involves hierarchies of nuclear gene expression (Martin and Hilbert 1991). At the top level would be a set of master genes whose activity mediates the developmental switch from the indeterminate, apical growth pattern of vegetative mycelium to the highly organized pattern of the ectomycorrhiza. The activity of these genes would be necessary and sufficient to induce a regulatory cascade that is partially responsible for ectomycorrhiza ontogeny. These genes would respond to rhizospheric and apoplastic signals released by the host plant (Jambois et al. 2005), positional information mediated by sensory molecules and nutritional cues (e.g. concentration of N and C metabolites). These genes would then activate the mycorrhiza development program and reinforce decisions during most phases of the ectomycorrhiza ontogeny. At lower levels in the regulatory hierarchy would be genes (e.g. hydrophobins, enzymes) that regulate the details of symbiosis development (e.g. aggregation of hyphae), which are likely to differ among mycorrhizal fungal species and host trees. To date, hundreds of genes preferentially expressed in symbiotic tissues have been identified by transcript profiling (Voiblet et al. 2001; Podila et al. 2002; Polidori et al. 2002; Peter et al. 2003; Johansson et al. 2004; Menotta et al. 2004; Duplessis et al. 2005, Le Quéré et al. 2005), but the master genes mediating the symbiosis development have not yet been identified.

Whereas master regulatory genes controlling the ectomycorrhiza development await identification, legume mutants have been key tools for the genetic dissection of AM development (Parniske 2004). In *Medicago*, *Lotus* and *Pisum*, the impaired genes are collectively referred to as the 'common' *SYM* genes. These genes define a partial overlap between the genetic programs for the AM endosymbiosis and the nitrogen-fixing root nodule symbiosis. The evolutionary implication is that the younger bacterial symbiosis has recruited functions from the ancient AM symbiosis. It is tempting to speculate that the recent ectomycorrhizal symbioses (~180 million years) have also recruited the AM symbiosis *SYM* genes, i.e. *SYMRK/NORK/DMI2* receptor kinase, *DMI1* ion channel and *DMI3* calcium- and calmodulin-dependent kinase. The quest for these and additional symbiosis factors is currently carried out using a series of complementary approaches, including comparative genomics, transcriptomics, metabolomics, proteomics and reverse genetics.

A. Genome Sequence of the Ectomycorrhizal Basidiomycete *Laccaria bicolor*

Molecular phylogeny has shown that saprotrophic, parasitic and symbiotic fungi are found in many taxonomic groups, which suggests that these life histories have evolved repeatedly within the Mycota kingdom (Hibbett et al. 2000). On the genomic level, there are basically three compatible mechanisms that can account for the multiple emergence and adaptations to parasitic and symbiotic growth in fungi (Tunlid and Talbot 2002). They are as follows:

1. Parasitism and symbiosis are associated with the presence of novel genes. Such genes may have a specific role during host infection and could be acquired by gene duplication or horizontal gene transfer.
2. Adaptations to the parasitic or symbiotic habits may result from differences in the regulation of gene expression through the activity of a core set of transcription factors.
3. Parasitism and symbiosis are associated with gene loss and deletions.

It can be expected that the mechanism(s) involved will be identified in the coming years, because a large amount of information from the genome sequences of fungal saprotrophs, pathogens and symbionts will shortly become available through the Fungal Genome Initiative at the Broad Institute (http://www.broad.mit.edu/annotation/fungi/fgi/) and the Community Sequencing Program of the United States Department of Energy Joint Genome Institute (http://www.jgi.doe.gov/CSP/index.html); in total, there are currently 115 completed or ongoing fungal genome projects (Genomes Online Database, http://www.genomesonline.org/; Galagan et al. 2005; Xu et al. 2006).

If there is a basic repertoire of fungal symbiotic genes, it can likely be identified by comparing whole genomes of saprobic species (e.g. *Coprinopsis cinerea*, *Pleurotus ostreatus*) and pathogenic species (e.g. *Ustilago maydis*, *Melampsora larici-populina*, *Heterobasidion annosum*) with mycorrhizal genomes. The availability of genome sequences from ecologically and taxonomically diverse fungi will not only allow ongoing genome-scale research on those species, but will also enhance the value of other sequences through comparative studies of gene evolution, genome structure, metabolic and regulatory pathways, and symbiosis/pathogenesis/saprotrophism. Within the framework of the *Populus* genome sequencing project, we proposed the draft sequencing of several known fungal associates of this perennial tree species (Martin et al. 2004): the ectomycorrhizal fungus *Laccaria bicolor*, the endomycorrhizal fungus *Glomus intraradices* and the rust fungus *Melampsora larici-populina*, to decifer the complex biological interactions that evolve from these plant–microbial associations. The sequencing of the genome of the symbiotic basidiomycete *Laccaria bicolor* was accomplished using the whole-genome shotgun (WGS) approach by the United States Department of Energy Joint Genome Institute (http://genome.jgi-psf.org/Lacbi1/Lacbi1.home.html) and the *Laccaria* Genome Consortium (http://mycor.nancy.inra.fr/IMGC/LaccariaGenome/) and publicly released in July 2006.

The *Laccaria* genome is much larger (ca. 65 Mb) than that of the other basidiomycetes whose genomic sequences have been published (Martinez et al. 2004; Loftus et al. 2005; Kämper et al. 2006). The v1.0 assembly was based on a 9.9-fold redundant WGS dataset in paired-end reads from plasmid and fosmid genomic DNA libraries. The *L. bicolor* genome shows no evidence for a recent whole-genome duplication, but is rich in repeated sequences, multigene families and transposable elements (J. Labbé, H. Quesneville and J. Wuyts, unpublished data). Only a very limited degree of gene synteny was observed between *L. bicolor* and the other sequenced basidiomycetes (B Cänbäck, unpublished data). A substantial motivation for sequencing the *Laccaria* genome was to study protein-coding genes. Besides being the first step in accurately defining the *L. bicolor* proteome, this fundamental data set yielded insights into differences between this symbiotic basidiomycete and other basidiomycete species with a complete genome sequence. A total of ~20,000 genes encoding proteins (i.e. 37% of the whole genome sequence) was identified using an annotation pipeline mainly based on the EUGENE and FGENESH/FGENESH+ programs, which combined both intrinsic (*ab initio* prediction) and extrinsic data [cDNA/expressed sequence tag (EST), protein matches]. Predicted genes, supporting evidence, structural and functional annotations are available through interactive visualization and analysis tools from the JGI Genome Portal (http://genome.jgi-psf.org/Lacbi1/Lacbi1.home.html). Up to 44,000 ESTs were also sequenced from cDNA libraries of free-living mycelia, ectomycorrhizas and fruiting bodies to train the gene predictors, confirm the gene models and investigate *Laccaria* transcriptome. Annotation of these assembled ESTs is available from the INRA *Laccaria* EST database (http://mycor.nancy.inra.fr/IMGC/LaccariaGenome/LaccariaDB/index.php?table=search&start=0&search=&order=Contig_Name).

A striking result of preliminary analysis of the *Laccaria* gene space is the finding that 30% of the gene models in the *Laccaria* genome are of unknown function. *Laccaria* open reading frames showed a complex gene structure with many short introns and alternative splicing of these introns. The gene organization in *L. bicolor* is thus con-

siderably more complex than that of ascomycetes for which genome sequence is available and is comparable with that observed in *Cryptococcus neoformans* (Loftus et al. 2005), *Phanerochaete chrysosporium* (Martinez et al. 2004) and *C. cinerea* (http://www.broad.mit.edu/annotation/genome/coprinus_cinereus/Home.html).

Most of the gene family expansion in the *Laccaria* genome as compared with the saprotrophic *C. cinerea* and *P. chrysosporium* was found to have occurred in those predicted to have roles in signal transduction mechanisms (e.g. 10-fold higher number of alpha GTPases), heterokaryon incompatibility (HI) and autophagic- or apoptotic-type programmed cell death. In addition to their role in HI, several of the latter proteins appear to be involved in the regulation of cell cycle, development and sexual differentiation and are likely expressed on exposure to developmental signals, stress factors and antifungal agents (Federova et al. 2005). Several secreted small cysteine-rich proteins showed a significant similarity to effector proteins and haustoria expressed secreted proteins (HESP) of *Magnaporthe oryzea*, *Melampsora lini* and *Uromyces fabae* involved in pathogenesis (Kulkarni et al. 2003; Kemen et al. 2005; Catanzariti et al. 2005). It is tempting to speculate that this rich assortment of effector small proteins may interact with or manipulate host plants during infection and subsequent symbiosis, as suggested for *Phytophthora* species (Kamoun 2006) and *Toxoplasma gondii* (Zhou et al. 2005).

L. bicolor is diverse in its catabolic capabilities. Present in its genome are proteases, lipases, phytases and ~315 carbohydrate-active enzymes (Coutinho and Henrissiat 1999), including glucanases, cellulases, polygalacturonases and chitinases, which are involved in the degradation and modification of polymers commonly found in organic horizons of the soil. In comparison with other soil basidiomycete and ascomycete saprotrophs, *Laccaria* has a very low repertoire of cellulolytic and hemicellulolytic genes, suggesting a reduced ability to modify cellulose. The set of encoded enzymes might however be sufficient for a limited saprophyte lifestyle, but with a limited ability to alter the plant cell wall structure (Coutinho, Danchin and Henrissiat, unpublished data). However, their expression might have advantages in the extraradical mycelial mats colonizing litter substrates rich in organic matter. The *L. bicolor* genome also contains catabolic ability for more complex compounds, including aromatic derivatives and long-chain hydrocarbons (nitroalkanes, fatty acids), commonly found in plant tissues and soil organic matter.

This genome sequence from a major mycorrhizal clade reveals an organism equipped to take advantage of transient occurrences of high-nutrient niches within a bulk low-nutrient environment. The roots of the host plant, but also dead organic matter and microscale 'hot spots' of the rhizospheric soil might provide such niches. The JGI has released the genome sequence of the lignocellulose-degrading *P. chrysosporium* (Martinez et al. 2004). Together with ectomycorrhizal fungi, the latter basidiomycetous white-rot is a key member of the suite of microorganisms that exist around trees. With the genomes of the saprotrophic *P. chrysosporium*, symbiotic *L. bicolor* and pathogenic *M. larici-populina* (pending; http://www.jgi.doe.gov/sequencing/why/CSP2006/poplarrust.html) in hand, we would be poised to achieve a deeper understanding of the processes by which basidiomycetous fungi colonize wood, interact with the host trees in their ecosystem and perform vital functions in the carbon and nitrogen cycles.

B. The Transcriptome of Ectomycorrhizal Fungi

1. Transcripts Expressed in Free-Living Mycelium

In the free-living mycelia of *L. bicolor*, *P. microcarpus*, *Paxillus involutus*, *H. cylindrosporum* and *Tuber borchii* grown on agar medium, the majority of the most abundant transcripts were novel genes for which no function could be assigned (Peter et al. 2003; Johansson et al. 2004; Lambillotte et al. 2004; Gabella et al. 2005). This suggests that they code for functions not expressed in model systems and/or laboratory growth conditions. The majority of the 15 most expressed genes of *L. bicolor*, *P. microcarpus* and *P. involutus*, for example, have only been found in the respective species so far. Among the 15 highly expressed transcripts of *L. bicolor*, only one transcript (CipC-related protein) was also detected in *P. microcarpus*, *P. involutus* (Johansson et al. 2004) and *Hebeloma cylindrosporum* (Lambilliotte et al. 2004) ESTs. Among the prominent transcripts with known function, two were involved in carbon metabolism (cytochrome C oxidase, 1,4-benzoquinone reductase) and one coded for a ribosomal protein. In *P. microcarpus* mycelium, several of the most abundant transcripts coded for

structural proteins such as the hydrophobins and the secreted SnodProt1 protein. The latter displays a strong similarity to the hydrophobin-related cerato-platanin, a phytotoxin from the ascomycete *Ceratocystis fimbriata* (Pazzagli et al. 1999). Other abundant transcripts showed strong similarity to metallothionein-related cysteine-rich proteins, which are likely involved in metal transport, cellular detoxication and stress response.

2. Transcripts Expressed in Symbiotic Tissues

Ectomycorrhiza development influences gene expression in the host plant and the colonizing fungus in a pleiotropic manner. The global gene expression analyses of several ectomycorrhizal associations (e.g. *Betula*/*Paxillus*, *Eucalyptus*/*Pisolithus*, *Pinus*/*Laccaria*, *Tilia*/*Tuber*; Voiblet et al. 2001; Podila et al. 2002; Polidori et al. 2002; Peter et al. 2003; Johansson et al. 2004; Menotta et al. 2004; Duplessis et al. 2005; Le Quéré et al. 2005) provided new insights to existing models of ectomycorrhiza development and identified hundreds of ECM-regulated genes. As expected from previous studies (Hilbert et al. 1991; Tagu et al. 1996; Nehls et al. 1998a, b, 2001a, b; Niini et al. 1996; Kim et al. 1998; Tarkka et al. 1998; Wright et al. 2000; Sundaram et al. 2001; Charvet-Candela et al. 2002), many cellular functions were found to be involved in symbiosis development, including genes involved in cell growth, differentiation and signaling, synthesis of cell wall and extracellular matrices, and primary metabolism (Fig. 12.2). Gene profiling based on cDNA arrays showed that developmental reprogramming takes place in roots and hyphae, although the magnitude of transcriptome alteration appears to be much larger in the mycelium than in the root cells (Voiblet et al. 2001; Johansson et al. 2004; Duplessis et al. 2005; Le Quéré et al. 2005). Marked changes in the gene expression in ectomycorrhizal roots are observed at multiple levels: (1) a general activation of the fungal protein synthesis machinery and respiration, probably supporting an intense cell proliferation, (2) an increased accumulation of transcripts coding for cell-surface proteins in fungal hyphae (hydrophobins, mannoproteins, chitin synthase), probably involved in the mantle and symbiotic interface formation, and (3) the upregulation of defense reactions and hormone metabolism in colonized roots. The induction of common gene networks takes place in various ectomycorrhizal systems, as several of these cellular functions are similarly regulated in the various investigated symbiotic models. At the different developmental stages studied, the development of the symbiosis between *Pisolithus*/*Eucalyptus*, *Paxillus*/*Betula*, *Pisolithus*/*Populus*, *Laccaria*/*Populus* and *Laccaria*/*Pseudotsuga* does not induce the expression of ectomycorrhiza-specific genes (Voiblet et al. 2001; Johansson et al. 2004; Le Quéré et al. 2005; A. Kohler, V. Pereda and M. Peter, unpublished data). A survey of up to 9500 unique transcripts (i.e. 20% of the total gene set) of *Populus* confirmed the lack of host ectomycorrhiza-specific genes (A. Kohler, V. Pereda and F. Martin, unpublished data). The apparent lack of ectomycorrhiza-specific gene is striking and suggests that ontogenic and metabolic programs leading to symbiosis development are mostly driven by differential expression of pre-existing transcription factors and/or transduction pathways, rather than the specific expression of symbiosis-specific gene arrays. A more complete analysis of this crucial question will await the completion of larger sets of ectomycorrhiza expression profiles on a wider range of associations, using whole-genome microarrays and high-throughput quantitative PCR of transcription factors.

3. Early-Transcriptionally Responsive Genes to Symbiosis Formation

Prior contact between partners, the upregulation of genes coding for the glyoxylate pathway enzyme, malate synthase (Balasubramanian et al. 2002) and the autophagy-involved *LB-AUT7* (Kim et al. 1999) suggest that there is a rapid catabolism and recycling of existing fungal material, such as lipids, and channeling toward biosynthesis of new cell components during the early phase of the interaction. This metabolic shift may reflect the transition from a saprobic mode to the symbiotic mode of growth. During the following phase, among the most abundantly expressed transcripts in developing ectomycorrhiza are many genes expected to be involved in synthesis of the fungal cell wall and symbiosis interfacial matrix (Martin et al. 1999). Proteins accumulating in *Pisolithus* cell walls, including different hydrophobins and mannoproteins (Tagu et al. 1996; Laurent et al. 1999; Voiblet et al. 2001; Peter et al. 2003), are found in increased amounts in symbiotic tissues. The corresponding transcripts are strongly activated in the early stages of development of *Pisolithus* and *Paxillus* mycorrhiza when the root tips are colonized and mantle formation is taking place. They then return to their constitutive

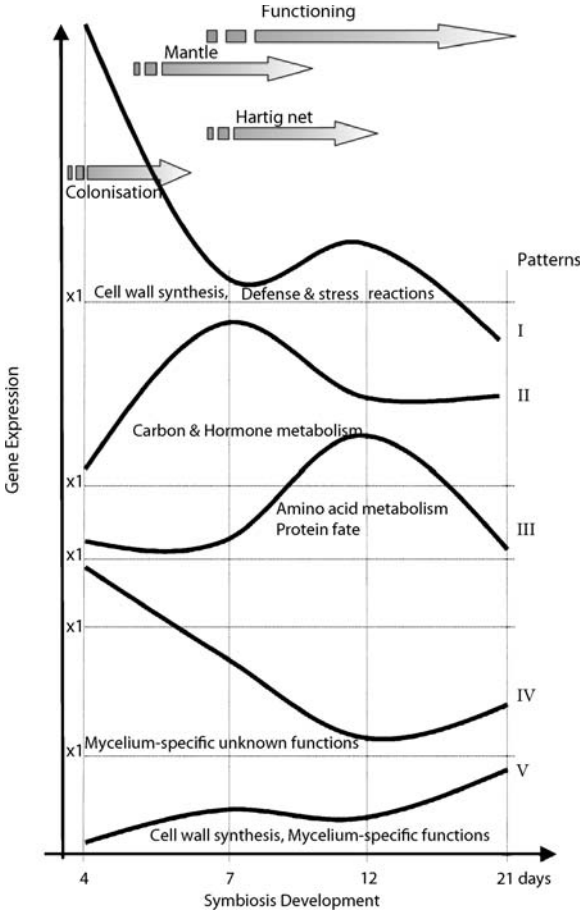

Fig. 12.2. Schematic drawing describing the five major gene expression patterns of plant and fungal symbiosis-regulated genes during the development of the *Eucalyptus–Pisolithus* mycorrhiza (after Duplessis et al. 2005)

level in the maturing mycorrhiza (Fig. 12.2; Duplessis et al. 2005; Le Quéré et al. 2005). Increased expression of hydrophobin and mannoprotein transcripts during the early stages of ectomycorrhizal development is suggestive of direct participation of the corresponding proteins in morphogenetic events related to the fungus adhesion to root surfaces. The SRAP32 polypeptides of *P. microcarpus* first appeared at contact and their synthesis increased during mycorrhizal formation, suggesting a role in mycorrhizal development most likely as structural proteins (Burgess et al. 1995). Upregulation of the synthesis of these fungal symbiosis-related polypeptides was tightly correlated to the infectivity of the fungal strain (Burgess et al. 1995). In addition to mannoproteins, adhesins and hydrophobins, which show preferential expression during symbiosis development (Laurent et al. 1999; Martin et al. 1999), enzymatic proteins may also be located at the novel fungus–plant symbiotic interface. TbSP1 is a secreted and surface-associated phospholipase A2 showing an upregulated expression in C- or N-deprived free-living mycelia from the ectomycorrhizal ascomycete *Tuber borchii*. This enzyme, likely involved in nutrient sensing, also showed an upregulated expression in *Cistus incanus*/*Tuber borchii* ectomycorrhiza (Soragni et al. 2001). TbSP1 was located on the fungal wall, mostly on the branched Hartig net hyphae (Miozzi et al. 2005). Alteration of the concentration of secreted proteins may be a way to regulate the symbiosis morphogenesis by changing the chemical structure of cell wall polymers. As a consequence, the mechanical properties of the cell walls and extracellular matrix involved in the symbiotic interface may be strongly modified. A prerequisite for the ectomycorrhizal sheath development around the host root is the tight contact between neighboring cells. Hence, structural cysteine-rich proteins, such as hydrophobins, and enzymes that can covalently cross-link polysaccharides are likely candidates for extracellular proteins with a promotive role in morphogenesis.

4. Middle- and Late-Transcriptionally Responsive Genes to Symbiosis Formation

As expected from an alliance aimed to better exploit the scarce nutrients of soil horizons, symbiosis induces dramatic changes in nutrient content and metabolic fluxes in root and fungal tissues (Blaudez et al. 1998; Martin et al. 1998; Laczko et al. 2003). To survive *in planta*, the developing mycobiont must express the channels, pumps and transporters at the appropriate time, the correct location and at the right levels. It must also activate and regulate the anabolic and catabolic enzymes needed to deal with nutritional and growth requirements over a sustained period in order to complete its life cycle. It is a general observation that these metabolic alterations are accompanied by mineral- and nutrient-related changes in gene expression, i.e. regulation of genes coding for transporters and assimilative enzymes. When the symbiotic interface is differentiated, it has been observed that transporters of monosaccharides, nitrate, ammonium, peptides and water from symbionts are differentially expressed (Nehls et al. 1998a, 1999b, 2000, 2001b; Wright et al. 2000; Jargeat et al. 2003; Javelle et al. 2003a, b; Grunze et al. 2004; Marjanovic et al. 2005; Selle et al. 2005; Chalot et al. 2006). This

likely reflects the intense metabolite fluxes taking place between the partners.

Isotopic labelling showed that mycelium metabolism is dramatically influenced by mycorrhizal colonization, with a greater allocation of carbon to short-chain polyols and trehalose (Martin et al. 1998) used for translocating carbon through the hyphal webs (Söderström et al. 1988). Expression of several fungal genes controlling assimilation of carbon compounds is upregulated in ectomycorrhiza (Nehls et al. 1999a, 2001a, b). For example, several fungal transcripts coding for enzymes in the glycolysis, tricarboxylic acid cycle and the mitochondrial electron transport chain are upregulated in developing symbiotic tissues (Patterns II and III in Fig. 12.2), confirming a general stimulation of the glucose respiration pathways. Both transcriptomics (Wright et al. 2005) and metabolite profiling (Martin et al. 1998) suggest the activity of anaplerotic pathways, via the concerted action of fatty acid β-oxidation and the glyoxylate cycle in ectomycorrhiza. Growth in the host apoplastic space, together with the proliferation of hyphae forming the coenocytic Hartig net, may explain the highest demand in carbon metabolites and the accompanying upregulation of transcripts encoding enzymes of the glucose respiration pathways.

Whereas an intense flux of carbon metabolites moves from the root tissues to the fungal hyphae, an opposite flux of nitrogen and phosphate compounds takes place from the soil to the plant through the mycelial web. This leads to the regulation of several N-metabolism genes (Botton and Dell 1994; Javelle et al. 2003b). The regulation observed is in agreement with an efflux of amino acids, mainly glutamine, from fungal cells and a subsequent uptake by root cells, although recent data suggest a significant role for NH_4^+ efflux, through ammonia diffusion and/or Ato-like fungal efflux systems (Selle et al. 2005; Chalot et al. 2006), and NO_3^- (Kohler, Pereda and Martin, unpublished data) in the N-transfer between partners. Transcripts coding for the nitrate reductase, NADP-glutamate dehydrogenase, aspartate aminotransferase and other N-metabolism enzymes are upregulated in symbiotic tissues (Duplessis et al. 2005; Le Quéré et al. 2005; Morel et al. 2005; Wright et al. 2005) in agreement with the increased amino acid synthesis observed using ^{13}C NMR (Martin et al. 1998).

In mycorrhizal associations, the host plant mainly derives its inorganic phosphate (Pi) from the fungus (Smith and Read 1997). Pi in soil solutions is easily taken up by ECM hyphae and then translocated to the host roots. Its absorption and efflux are probably regulated by intracellular Pi and inorganic polyphosphate (PolyP) pools. Excess intracellular Pi is stored as PolyP by most ECM fungi. These PolyP are mainly oligophosphates with an average chain length of ten phosphate residues (Martin et al. 1994). NMR comparisons of PolyP in vivo with those in model solutions suggest that they are low-soluble aggregates in ECM fungi (Martin et al. 1985). PolyP are the only macromolecular anions in the fungal vacuole (Martin et al. 1985; 1994); and their roles in basic amino acid and cation retention and osmoregulation have been demonstrated both in vivo and in vitro in yeasts and postulated in ECM fungi (Martin 1985). Several low- and high-affinity Pi transporters have been identified in the genomes of *L. bicolor* (F. Martin, unpublished data) and *H. cylindrosporum* (C. Plassard, personal communication), but the molecular processes controlling Pi uptake in ECM fungi are so far unknown. It is assumed that a plant Pi transporter is expressed specifically on the peri-arbuscular membrane in endomycorrhizal symbioses (Harrison 2005) and on the plasmamembrane of host cortical cells in contact with the fungal Hartig net in ectomycorrhiza. Amongst its 13 low- and high-affinity Pi transporters, a transporter of *Populus trichocarpa* is expressed specifically in endomycorrhiza, whether another transporter is preferentially expressed in ectomycorrhizal root tips (V. Pereda, unpublished data). A question that has been repeatedly asked in the literature is what the plant does to make a mycorrhizal associate lose its P into the cortical apoplast. Fitter (2006) postulated that, when an AM fungus develops an arbuscule inside a root cell and begins to move Pi ions across the peri-arbuscular membrane, the plant detects this increased Pi flux which then stimulates increased carbon allocation and subsequent hexose transfer to the mycobiont. The phosphate/carbohydrates exchange in ectomycorrhizal symbioses is also tightly regulated. In a *Populus tremula* × *Populus alba*/*Laccaria* ectomycorrhiza, shading of the plant, which reduced the carbohydrate supply to the mycobiont, resulted in a decrease in phosphate absorption by the ectomycorrhizal roots (Bücking and Heyser 2001). Microautoradiography after pulse-labelling with ^{33}Pi and $^{14}CO_2$ suggested a correlation between the Pi amount translocated from the mycelium to the host plant and the amount of carbohydrate transferred from the plant to the fungus.

5. Functional Specialization of the Hyphal Web Compartments

In microcosms mimicking the forest soil conditions, Wright et al. (2005) identified striking differential expression in the various fungal compartments (mycelial patches, rhizomorphs, ectomycorrhizal tips) of the *Betula*/*Paxillus* association. The pattern of differential expression of genes encoding key N-assimilating enzymes may be influenced by multiple factors, such as the level of NH_4^+ within the nutrient patch, the extent of NH_4^+ translocation versus assimilation within the extramatrical mycelium and the microenvironment in which the rhizomorph and mycorrhizal root tips are situated. Interestingly, Morel et al. (2005) detected no significant differential expression for genes encoding components involved in the glutamine synthetase/glutamate synthase cycle, urea or arginine biosynthetic pathways in a comparison between the extramatrical mycelium and mycorrhizal root tips of the *B. pendula*/*P. involutus* association grown under N-limited conditions. However, these authors showed that urea was the principal N compound in hyphae, and suggested that urea-producing pathways may be activated in extramatrical mycelium of *P. involutus* under N-limited conditions. This clearly confirmed the physiological heterogeneity and functional specialization among the different compartments of the fungal webs (Cairney and Burke 1996). Whether gene expression of metabolic genes is controlled by sugar- and amino acid-dependent regulation, as reported for free-living mycelium (Nehls et al. 2001a), by symbiosis-related developmental signals (Martin et al. 2001) or by the external microenvironment (Morel et al. 2005; Wright et al. 2005) is not known.

6. Plant Responses upon Symbiosis Development

The ability of poplar trees to form ectomycorrhizas is under genetic control (Tagu et al. 2001). Heritability of the ectomycorrhizal trait was investigated in *Pinus elliottii* (Rosado et al. 1994) and a strong narrow-sense heritability was found (0.81) for the percentage of ectomycorrhizas formed. A similar experiment was performed on poplar (Tagu et al. 2005) and a heritability value of 0.49 was found. This indicates that genetic traits are involved in the ectomycorrhizal phenotype in tightly controlled growth conditions and genetic variability exists between half-sib progenies. One putative quantitative trait locus (QTL) was positioned on the genetic map of each parental genotype, *P. trichocarpa* and *P. deltoides*. The QTL on the male *P. trichocarpa* genetic map was localized close to a locus previously shown to be involved in the interaction between *Populus* and the foliar rust fungus *Melampsora larici-populina* (Dowkiw and Bastien 2004), providing a genetic indication that the ectomycorrhizal trait could be associated with loci and genes that might be common to the interaction with mutualistic root and pathogenic leaf fungi. As emphasized by Mendgen and Hahn (2002), host cellular responses upon contact with plant-invading biotrophic microorganisms are very similar whatever the outcome of the association.

As shown by whole-genome oligoarray analysis, changes in transcript concentration in host root tissues are limited (<2% of the total transcripts in *Populus trichocarpa*; A. Kohler, V. Pereda and F. Martin, unpublished data). Most ectomycorrhiza-regulated host genes are involved in auxin metabolism, calcium signalling pathways and transcriptional regulation. Some non-specific, broad-spectrum defenses (e.g. chitinases, peroxidases) are clearly mounted in plant hosts when ectomycorrhizal fungi penetrate directly into the root and digests a way through the apoplastic space (Pattern I in Fig. 12.2; Duplessis et al. 2005; Le Quéré et al. 2005). These induced defense responses may limit the fungal invasion of root tissues. Future research should explore the molecular mechanisms that orchestrate the escape of the symbionts from the host defense system. Modulation of host vesicle trafficking by secreted effector proteins, as recently shown for bacterial pathogens (Nomura et al. 2006), may create a host environment favorable for hyphal survival and proliferation.

C. Ectomycorrhizal Mutants

Variation in mycorrhizal structures appears to be genetically determined in the mycobiont (Wong et al. 1989, 1990), which should make it possible to identify the loci that contribute to this variation. It is therefore crucial to identify plant and fungal phenotypic mutants altered in the development of the ectomycorrhiza structure. This would allow one to follow the specification events that take place during the different stages of symbiosis development. Primary targets for gene inactivation are the ectomycorrhiza-regulated genes identified by transcriptomics (see Sect. IV.B.). Unfortunately, procedures for knocking-out genes

by homologous recombination are not yet feasible in ECM fungi. Hence, polyethylene glycol- and *Agrobacterium*-mediated transformations were used for random insertional mutagenesis to generate mutants of the ectomycorrhizal basidiomycete *H. cylindrosporum* impaired in their symbiotic capability (Combier et al. 2004). Following restriction enzyme-mediated integration or plasmid insertion, a total of 29 non-mycorrhizal (*myc*$^-$) agrotransformants were identified. Light and scanning electron microscopy observations of pine roots inoculated with *myc*$^-$ mutants suggested that these mutants were blocked at early stages of interaction, confirming that key genes are essential for symbiosis development. Sequencing of the tagged loci is on-going and preliminary results have identified genes coding for hypothetical proteins, tubulin and aspartic protease (R. Marmeisse, personal communication).

V. Future Research

Advances of recent years have provided insights on the molecular basis of ectomycorrhiza morphogenesis and functioning. Several studies using large-scale EST sequencing (Voiblet et al. 2001; Podila et al. 2002; Peter et al. 2003), mRNA displays (Kim et al. 1998; Polidori et al. 2002; Menotta et al. 2004) and cDNA arrays (Voiblet et al. 2001; Johansson et al. 2004; Duplessis et al. 2005; Le Quéré et al. 2005; Morel et al. 2005) have characterized the expression of hundreds of genes in a few ectomycorrhizal model systems. It is apparent from these expression profiling studies that there is a vast complexity of genetic programs with overlapping and coordinated expression of gene networks. The products encoded by these regulated genes are involved in the attachment of hyphae to host surfaces and penetration into root tissues, plant defense reactions, hormonal metabolism, morphogenetic switches of the fungal hyphae and novel metabolic patterns in both partners. The sequence information generated from gene-profiling studies provide the starting point for understanding how transcript/protein networks are altered during mycorrhizal development via the high-throughput functional analysis of the plant and fungal sensors, signalling pathways and transcription factors.

Considering the tissue and cellular complexity of the symbiosis, one has to conclude that the analysis of whole mycorrhizas done so far is an approach with low resolution for the analysis of cellular function during development and functioning. Gene expression profiles should now be performed on purified or at least enriched samples from specific cell populations and tissues (e.g. Hartig net or mantle cells). The analysis of the differential expression of hexose-regulated fungal genes within the different symbiotic tissues of the *Amanita*/*Populus* ectomycorrhiza (Nehls et al. 2001b) have shown that this innovative approach is within reach and will be facilated by the use of laser microdissection systems, together with gene profiling of extraradical regions of the soil mycelial networks.

The genomes of the host tree, *P. trichocarpa*, and the ectomycorrhizal *Laccaria bicolor* have now been deciphered, which has opened avenues for comparative genomics and genome-wide gene transcript profilings in perennial trees and basidiomycetes. A wealth of data is now available to researchers by way of a number of dedicated web sites. These new tools will have an important impact on the mycorrhiza research confirming the complexity of the interaction between trees and their soil partners. Our understanding is still limited as to how parasitic and symbiotic fungi infect their hosts, including the mechanisms of host recognition, development of infection structures, control of host defense reactions and penetration and colonization of the host tissues. Analysis of the genome sequences of symbiotic and pathogenic fungi will provide new insights into these processes and further clarify the molecular and physiological bases of plant–microbe interactions. There is much room for exciting discoveries, especially when it is considered that approximately 50% of the gene models in the *Laccaria* genome are of unknown function.

Acknowledgements. I would like to thank A. Kohler and S. Duplessis for their long-standing and efficient support, and former and current PhD students and postdocs for their collaboration. Investigations carried out in my laboratory were supported by grants from the INRA (projects Lignome and Genome Sequencing of Poplar and Associated Micro-organisms), the Génoscope (project ForEST) and the Région Lorraine. The Laccaria genome project is a collaborative effort involving: DOE Joint Genome Institute (coordinator, P. Richardson), INRA-Nancy (UMR IaM, F. Martin et al.), University of Alabama–Huntsville (Department of Biological Sciences, G. Podila et al.), Gent University (Bioinformatics & Evolutionary Genomics Division, P. Rouzé et al.) and DOE Oak Ridge National Laboratory (J. Tuskan et al.). This project was performed under the auspices of the U.S. Department of Energy's Office of Science, Biological and Environmental Research Program and by the University of California, Lawrence Livermore National Laboratory, Lawrence Berkeley National Laboratory and Los Alamos National Laboratory.

References

Agerer R (1993) Colour atlas of ectomycorrhizae, 7th edn (1993–1998). Einhorn, Schwäbisch Bmünd

Akiyama K, Matsuzaki K, Hayashi H (2005) Plant sesquiterpenes induce hyphal branching in arbuscular mycorrhizal fungi. Nature 435:824–827

Balasubramanian S, Kim SJ, Podila GP (2002) Differential expression of a malate synthase gene during the preinfection stage of symbiosis in the ectomycorrhizal fungus *Laccaria bicolor*. New Phytol 154:517–528

Béguiristain T, Lapeyrie F (1997) Host plant stimulates hypaphorine accumulation in *Pisolithus tinctorius* hyphae during ectomycorrhizal infection while excreted fungal hypaphorine controls root hair development. New Phytol 136:525–532

Béguiristain T, Côté R, Rubini P, Jay-Allemand C, Lapeyrie F (1995) Hypaphorine accumulation in hyphae of the ectomycorrhizal fungus, *Pisolithus tinctorius*. Phytochemistry 40:1089–1091

Bergero R, Perotto S, Girlanda M, Vidano G, Luppi AM (2000) Ericoid mycorrhizal fungi are common root associates of a Mediterranean ectomycorrhizal plant (*Quercus ilex*). Mol Ecol 9:1639–1649

Bending GD (2003) Litter decomposition, ectomycorhizal roots and the 'Gadgil' effect. New Phytol 15:228–229

Besserer A, Puech-Page V, Kiefer P, Gomez-Roldan V, Jauneau A, Roy S, Portais JC, Roux C, Bécard G, Séjalon-Delmas (2006) Strigolactones stimulate arbuscular mycorrhizal fungi by activating mitochondria. PLoS Biol 4:1239–1247

Blaudez D, Chalot M, Dizengremel P, Botton B (1998) Structure and function of the ectomycorrhizal association between *Paxillus involutus* and *Betula pendula* II. Metabolic changes during mycorrhiza formation. New Phytol 138:543–552

Botton B, Dell B (1994) Expression of glutamate dehydrogenase and aspartate aminotransferase in eucalypt ectomycorrhizas. New Phytol 126:249–257

Brachmann A, Parniske M (2006) The most widespread symbiosis on Earth. PLoS Biol 4:1111–1112

Brun A, Chalot M, Finlay RD, Söderström B (1995) Structure and function of the ectomycorrhizal association between *Paxillus involutus* (Batsch) Fr. and *Betula pendula* (Roth.). I. Dynamics of mycorrhiza formation. New Phytol 129:487–493

Brundrett M (2002) The co-evolution of mycorrhizas and roots of land plants: evaluation of the structure and function of ancient and modern associations. New Phytol 154:275–304

Brunner I, Scheidegger C (1995) Effects of high nitrogen concentrations on ectomycorrhizal structure and growth of seedlings of *Picea abies* (L.) Karst. New Phytol 129:83–95

Bücking H, Heyser W (2001) Microautoradiographic localization of phosphate and carbohydrates in mycorrhizal roots of *Populus tremula* x *Populus alba* and the impli cations for transfer processes in ectomycorrhizal associations. Tree Physiol 21:101–107

Burgess T, Laurent P, Dell B, Malajczuk N, Martin F (1995) Effect of fungal-isolate aggressivity on the biosynthesis of symbiosis-related polypeptides in differentiating eucalypt ectomycorrhizas. Planta 195:407–417

Cairney JWG, Burke RM (1996) Physiological heterogeneity within fungal mycelia: an important concept for a functional understanding of the ectomycorrhizal symbiosis. New Phytol 134:685–695

Catanzariti AM, Dodds PN, Lawrence GJ, Ayliffe MA, Ellis JG (2005) Haustorially expressed secreted proteins from flax rust are highly enriched for avirulence elicitors. Plant Cell 18:243–256

Chalot M, Brun A (1998) Physiology of organic nitrogen acquisition by ectomycorrhizal fungi and ectomycorrhizas. FEMS Microbiol Rev 22:21–44

Chalot M, Blaudez D, Brun A (2006) Ammonia: a candidate for nitrogen transfer at the mycorrhizal interface. Trends Plant Sci 11:263–266

Charvet-Candela V, Hitchin S, Ernst D, Sandermann H Jr, Marmeisse R, Gay G (2002) Characterization of an *Aux/IAA* cDNA up-regulated in *Pinus pinaster* roots in response to colonization by the ectomycorrhizal fungus *Hebeloma cylindrosporum*. New Phytol 154:769–778

Chilvers GA (1968) Low power electron microscopy of the root cap region of eucalypt mycorrhizas. New Phytol 67:663–668

Combier JP, Melayah D, Raffier C, Pépin R, Marmeisse R, Gay G (2004) Nonmycorrhizal (Myc-) mutants of *Hebeloma cylindrosporum* obtained through insertional mutagenesis. Mol Plant Microbe Interact 17:1029–1038

Coutinho PM, Henrissat B (1999) Carbohydrate-active enzymes:an integrated database approach. In: Gilbert HG, Davies G, Henrissat B, Svensson B (eds) Recent advances in carbohydrate bioengineering. Royal Society of Chemistry, Cambridge, pp 3–12

Dexheimer J, Pargney JC (1991) Comparative anatomy of the host-fungus interface in mycorrhizas. Experientia 47:312–320

Dexheimer J, Gerard J, Genet P (1994) Study of transformations of the root system of *Eucalyptus globulus* associated with *Pisolithus tinctorius*. I. Aptitude to mycorrhization of different kinds of roots. Phytomorphology 44:235–245

Ditengou FA, Lapeyrie F (2000) Hypaphorine from the ectomycorrhizal fungus *Pisolithus tinctorius* counteracts activities of indole-3-acetic acid and ethylene but not synthetic auxins in eucalypt seedlings. Mol Plant Microbe Interact 13:151–158

Ditengou FA, Béguiristain T, Lapeyrie F (2000) Root hair elongation is inhibited by hypaphorine, the indole alkaloid from the ectomycorrhizal fungus *Pisolithus tinctorius*, and restored by indole-3-acetic acid. Planta 211:722–728

Dowkiw A, Bastien C (2004) Characterization of two major genetic factors controlling quantitative resistance to *Melampsora larici-populina* leaf rust in hybrid poplars: strain specificity, field expression, combined effects, and relationship with a defeated qualitative resistance genotype. Phytopathology 94:1358–1367

Duplessis S, Courty PE, Tagu D, Martin F (2005) Transcript patterns associated with ectomycorrhiza development in Eucalyptus globulus and *Pisolithus microcarpus*. New Phytol 165:599–611

Fedorova ND, Badger JH, Robson GD, Wortman JR, Nierman WC (2005) Comparative analysis of programmed cell death pathways in filamentous fungi. BMC Genomics 6:177

Fierer N, Jackson JA, Vilgalys R, Jackson RB (2005) Assessment of soil microbial community structure by use of taxon-specific quantitative PCR assays. Appl Environ Microbiol 71:4117–4120

Fitter A (2006) What is the link between C and P fluxes in arbuscular mycorrhizas? A null hypothesis for symbiotic function. New Phytol 172:3–6

Gabella S, Abba S, Duplessis I, Montanini B, Martin F, Bonfante P (2005) Expressed sequence tags and cDNA arrays reveal novel marker genes controlling fruit body formation in *Tuber borchii*. Eukaryot Cell 4:1599–1602

Galagan JE, Henn MR, Li-Jun MA, Cuomo CA, Birren B (2005) Genomics of the fungal kingdom:Insights into eukaryotic biology. Genome Res 15:1620–1631

Gay G, Marmeisse R, Fouillet P, Bouletreau M, Debaud JC (1993) Genotype/nutrition interactions in the ectomycorrhizal fungus *Hebeloma cylindrosporum* Romagnesi. New Phytol 123:335–343

Gay G, Normand L, Marmeisse R, Sotta B, Debaud JC (1994) Auxin overproducer mutants of *Hebeloma cylindrosporum* Romagnési have increased mycorrhizal activity. New Phytol 128:645–657

Gea L, Normand L, Vian B, Gay G (1994) Structural aspects of ectomycorrhiza of *Pinus pinaster* (Ait.) Sol. formed by an IAA-overproducer mutant of *Hebeloma cylindrosporum* Romagnési. New Phytol 128:659–670

Grove TS, Le Tacon F (1993) Mycorrhiza in plantation forestry. Adv Plant Pathol 9:191–227

Grunze N, Willmann M, Nehls U (2004) The impact of ectomycorrhiza formation on monosaccharide transporter gene expression in poplar roots. New Phytol 164:147–155

Harrison M (2005) Signaling in the arbuscular mycorrhizal symbiosis. Annu Rev Microbiol 59:19–42

Hause B, Fester T (2005) Molecular and cell biology of arbuscular mycorrhizal symbiosis. Planta 221:184–196

Hibbett DS, Gilbert LB, Donoghue MJ (2000) Evolutionary instability of ectomycorrhizal symbioses in basidiomycetes. Nature 407:506–508

Hilbert JL, Costa G, Martin F (1991) Ectomycorrhizin synthesis and polypeptide changes during the early stage of eucalypt mycorrhiza development. Plant Physiol 97:977–984

Högberg P, Nordgren A, Buchmann N, Taylor AFS, Ekblad A, Högberg MN, Nyberg G, Ottosson-Löfvenius M, Read DJ (2001) Large-scale forest girdling shows that current photosynthesis drives soil respiration. Nature 411:789–792

Horan DP, Chilvers GA (1990) Chemotropism; the key to ectomycorrhizal formation? New Phytol 116:297–301

Horan DP, Chilvers GA, Lapeyrie FF (1988) Time sequence of the infection process in eucalypt ectomycorrhizas. New Phytol 109:451–458

Jambois A, Dauphin A, Kawano T, Ditengou FA, Bouteau F, Legué V, Lapeyrie F (2005) Competitive antagonism between IAA and indole alkaloid hypaphorine must contribute to regulate ontogenesis. Physiol Plant 123:120–129

Jargeat P, Rekangalt D, Verner MC, Gay G, Debaud JC, Marmeisse R, Fraissinet-Tachet L (2003) Characterisation and expression analysis of a nitrate transporter and nitrite reductase genes, two members of a gene cluster for nitrate assimilation from the symbiotic basidiomycete *Hebeloma cylindrosporum*. Curr Genet 43:199–205

Javelle A, André B, Marini AM, Chalot M (2003a) High-affinity ammonium transporters and nitrogen sensing in mycorrhizas. Trends Microbiol 11:53–55

Javelle A, Morel M, Rodriguez-Pastrana BR, Botton B, André B, Marini AM, Brun A, Chalot M (2003b) Molecular characterization, function and regulation of ammonium transporters (Amt) and ammonium-metabolizing enzymes (GS, NADP-GDH) in the ectomycorrhizal fungus *Hebeloma cylindrosporum*. Mol Microbiol 47:411–430

Johansson T, Le Quéré A, Ahren D, Söderström B, Erlandsson R, Lundeberg J, Uhlen M, Tunlid A (2004) Transcriptional responses of *Paxillus involutus* and *Betula pendula* during formation of ectomycorrhizal root tissue. Mol Plant Microbe Interact 17:202–215

Kamoun S (2006) A catalogue of the effector secretome of plant pathogenic oomycetes. Annu Rev Phytopathol 44:41–60

Kämper J, Kahmann R, Bölker M, Ma L-J, Brefort T, Saville BJ, Banuett F, Kronstad JW, Gold SE, Müller O, et al (2006) Insights from the genome of the biotrophic fungal plant pathogen *Ustilago maydis*. Nature 444:97–101

Karabaghli-Degron C, Sotta B, Bonnet M, Gay G, Le Tacon F (1998) The auxin transport inhibitor 2,3,5-triiodobenzoic acid (TIBA) inhibits the stimulation of in vitro lateral root formation and the colonization of the tap-root cortex of Norway spruce (*Picea abies*) seedlings by the ectomycorrhizal fungus *Laccaria bicolor*. New Phytol 140:723–733

Kemen E, Kemen AC, Rafiqi M, Hempel U, Mendgen K, Hahn M, Voegele RT (2005) Identification of a protein from rust fungi transferred from haustoria into infected plant cells. Mol Plant Microbe Interact 18:1130–1139

Kim SJ, Hiremath ST, Podila GK (1998) Cloning and identification of symbiosis-regulated genes from the ectomycorrhizal *Laccaria bicolor*. Mycol Res 103:168–172

Kim SJ, Bernreuther D, Thumm M, Podila GK (1999) *LB-AUT7*, a novel symbiosis-regulated gene from an ectomycorrhizal fungus, *Laccaria bicolor*, is functionally related to vesicular transport and autophagocytosis. J Bacteriol 181:1963–1967

Köttke I, Oberwinkler F (1986) Root–fungus interactions observed on initial stages of mantle formation and Hartig net establishment in mycorrhizas of *Amanita muscaria* on *Picea abies* in pure culture. Can J Bot 64:2348–2354

Köttke I, Oberwinkler F (1987) The cellular structure of the Hartig net: coenocytic and transfer cell-like organization. Nord J Bot 7:85–95

Kulkarni RD, Kelkar HS, Dean RA (2003) An eight-cysteine-containing CFEM domain unique to a group of fungal membrane proteins. Trends Biochem Sci 28:118–121

Laczko E, Boller T, Wiemken V (2003) Lipids in roots of *Pinus sylvestris* seedlings and in mycelia of *Pisolithus tinctorius* during ectomycorrhiza formation: changes in fatty acid and sterol composition. Plant Cell Environ 27:27–40

Lagrange H, Jay-Allemand C, Lapeyrie F (2001) Rutin, the phenolglycoside from eucalyptus root exudates, stimulates *Pisolithus* hyphal growth at picomolar concentrations. New Phytol 149:349–355

Lambilliotte R, Cooke R, Samson D, Fizames C, Gaymard F, Plassard C, Tatry MV, Berger C, Laudié M, Legeai F, Karsenty E, Delseny M, Zimmermann S, Sentenac H (2004) Large-scale identification of genes in the fungus *Hebeloma cylindrosporum* paves the way to molecular analyses of ectomycorrhizal symbiosis. New Phytol 164:505–513

Laurent P, Voiblet C, Tagu D, De Carvalho D, Nehls U, De Bellis R, Balestrini R, Bauw G, Bonfante P, Martin F (1999) A novel class of ectomycorrhiza-regulated cell wall polypeptides in *Pisolithus tinctorius.* Mol Plant Microbe Interact 12:862–871

LePage BA, Currah RS, Stockey RA, Rothwell GW (1997) Fossil ectomycorrhizae from the middle Eocene. Am J Bot 84:410–412

Le Quéré A, Wright D, Söderström B, Tunlid A, Johansson T (2005) Global patterns of gene regulation associated with the development of ectomycorrhiza between birch (*Betula pendula* Roth.) and *Paxillus involutus* (Batsch) Fr. Mol Plant Microbe Interact 18:659–673

Loftus BJ, Fung E, Roncaglia P, Rowley D, Amedeo P, Bruno D, Vamathevan J, Miranda M, Anderson IJ, Fraser JA, et al (2005) The genome of the basidiomycetous yeast and human pathogen *Cryptococcus neoformans*. Science 307:1321–1324.

Marjanovic Z, Uehlein N, Kaldenhoff R, Zwiazek JJ, Weiß M, Hampp R, Nehls U (2005) Aquaporins in poplar: what a difference a symbiont makes! Planta 222:258–268

Martin F (1985) ^{15}N-NMR studies of nitrogen assimilation and amino acid biosynthesis in the ectomycorrhizal fungus *Cenococcum graniforme.* FEBS Lett 182:350–354

Martin F (2001) Frontiers in molecular mycorrhizal research – genes, loci, dots and spins. New Phytol 150:499–507

Martin F, Hilbert JL (1991) Morphological, biochemical and molecular changes during ectomycorrhiza development. Experientia 47:321–330

Martin F, Tagu D (1999) Developmental biology of a plant–fungus symbiosis: the ectomycorrhiza. In: Varma A, Hock B (eds) Mycorrhiza: structure, molecular biology and function, 2nd edn. Springer, Berlin Heidelberg New York, pp 51–73

Martin F, Marchal JP, Timinska A, Canet D (1985) The metabolism and physical state of polyphosphates in ectomycorrhizal fungi. A ^{31}P nuclear magnetic resonance study. New Phytol 101:275–290

Martin F, Rubini P, Côté R, Kottke I (1994) Aluminium polyphosphate complexes in the mycorrhizal basidiomycete *Laccaria bicolor:* a ^{27}Al NMR study. Planta 19:241–246

Martin F, Boiffin V, Pfeffer PE (1998) Carbohydrate and amino acid metabolism in the *Eucalyptus globulus–Pisolithus tinctorius* ectomycorrhiza during glucose utilization. Plant Physiol 118:627–635

Martin F, Laurent P, De Carvalho D, Voiblet C, Balestrini R, Bonfante P, Tagu D (1999) Cell wall proteins of the ectomycorrhizal basidiomycete *Pisolithus tinctorius*: Identification, function, and expression in symbiosis. Fungal Genet Biol 27:161–174

Martin F, Duplessis S, Ditengou F, Lagrange H, Voiblet C, Lapeyrie F (2001) Developmental cross talking in the ectomycorrhizal symbiosis: signals and communication genes. New Phytol 151:145–154

Martin F, Tuskan GA, DiFazio SP, Lammers P, Newcombe G, Podila GK (2004) Symbiotic sequencing for the *Populus* mesocosm. New Phytol 161:330–335

Martinez D, Larrondo LF, Putnam N, Sollewijn Gelpke MD, Huang K, Chapman J, Helfenbein KG, Ramaiya P, Detter JC, Larimer F, Coutinho PM, Henrissat B, Berka R, Cullen D, Rokhsar D (2004) Genome sequence of the lignocellulose degrading fungus *Phanerochaete chrysosporium* strain RP78. Nature Biotechnol 22:695–700

Massicotte HB, Peterson RL, Ackerley CA, Piché Y (1986) Structure and ontogeny of *Alnus crispa-Alpova diplophloeus* ectomycorrhizae. Can J Bot 64:177–192

Massicotte HB, Peterson RL, Ackerley CA, Ashford AE (1987) Ontogeny of *Eucalyptus pilularis-Pisolithus tinctorius* ectomycorrhizae. II. Transmission electron microscopy. Can J Bot 65:1940–1947

Massicotte HB, Peterson RL, Melville LH (1989a) Ontogeny of *Alnus rubra- Alpova diplophloeus* ectomycorrhizae. I. Light microscopy and scanning electron microscopy. Can J Bot 67:191–200

Massicotte HB, Ackerley CA, Peterson RL (1989b) Ontogeny of *Alnus rubra- Alpova diplophloeus* ectomycorrhizae. II. Transmission electron microscopy. Can J Bot 67:201–210

Massicotte HB, Peterson RL, Melville LH (1989c) Hartig net structure of ectomycorrhizae synthesized between *Laccaria bicolor* (Tricholomataceae) and two hosts: *Betula alleghaniensis* (Betulaceae) and *Pinus resinosa* (Pinaceae). Am J Bot 76:1654–1667

Meharg AA, Cairney JWG (2000) Co-evolution of mycorrhizal symbionts and their hosts to metal-contaminated environments. Adv Ecol Res 30:69–112

Melville LH, Massicotte HB, Ackerley CA, Peterson RL (1988) An ultrastructural study of modifications in *Dryas integrifolia* and *Hebeloma cylindrosporum* during ectomycorrhiza formation. Bot Gaz 149:408–418

Mendgen K, Hahn M (2002) Plant infection and the establishment of fungal biotrophy. Trends Plant Sci 7:352–356

Menotta M, Amicucci A, Sisti D, Gioacchini AM, Stocchi V (2004) Differential gene expression during presymbiotic interaction between *Tuber borchii* Vitad. and *Tilia americana* L. Curr Genet 46:158–165

Miozzi L, Ballestrini R, Bolchi A, Novero M, Ottonello S, Bonfante P (2005) Phospholipase A2 up-regulation during mycorrhiza formation in *Tuber borchii.* New Phytol 167:229–238

Morel M, Jacob C, Kohler A, Johansson T, Martin F, Chalot M, Brun A (2005) Identification of genes differentially expressed in extraradical mycelium and ectomycorrhizal roots during *Paxillus involutus–Betula pendula* ectomycorrhizal symbiosis. Appl Environ Microbiol 71:382–391

Nehls U, Wiese J, Guttenberger M, Hampp R (1998a) Carbon allocation in ectomycorrhizas: identification and expression analysis of an *Amanita muscaria* monosaccharide transporter. Mol Plant Microbe Interact 11:167–176

Nehls U, Béguiristain T, Ditengou F, Lapeyrie F, Martin F (1998b) The expression of a symbiosis-regulated gene in eucalypt roots is regulated by auxins and

hypaphorine, the tryptophan betaine of the ectomycorrhizal basidiomycete *Pisolithus tinctorius*. Planta 207:296–302

Nehls U, Ecke M, Hampp R (1999a) Sugar- and nitrogen-dependent regulation of an *Amanita muscaria* phenylalanine ammonium lyase gene. J Bacteriol 181:1931–1933

Nehls U, Kleber R, Wiese J, Hampp R (1999b) Isolation and characterization of a general amino acid permease from the ectomycorrhizal fungus *Amanita muscaria*. New Phytol 144:343–349

Nehls U, Wiese J, Hampp R (2000) Cloning of a *Picea abies* monosaccharide transporter gene and expression – analysis in plant tissues and ectomycorrhizas. Trees 14:334–338

Nehls U, Mikolajewski S, Magel E, Hampp R (2001a) Carbohydrate metabolism in ectomycorrhizas: gene expression, monosaccharide transport and metabolic control. New Phytol 150:533–541

Nehls U, Bock A, Ecke M, Hampp R (2001b) Differential expression of hexose-regulated fungal genes *AmPAL* and *AmMst1* within *Amanita*/*Populus* ectomycorrhizas. New Phytol 150:583–589

Niini S, Tarkka MT, Raudaskoski M (1996) Tubulin and actin patterns in Scots pine (*Pinus sylvestris*) roots and developing ectomycorrhiza with *Suillus bovinus*. Physiol Plant 96:186–192

Nomura K, DebRoy S, Lee YH, Pumplin N. Jones J, He SY (2006) A bacterial virulence protein suppresses host innate immunity to cause plant disease. Science 313:220–223

Parniske M (2004) Molecular genetics of the arbuscular mycorrhizal symbiosis. Curr Opin Plant Biol 7:414–421

Paszkowski U (2006) A journey through signaling in arbuscular mycorrhizal symbioses 2006. New Phytol 172:35–46

Pazzagli L, Cappugi G, Manao G, Camici G, Santini A, Scala A (1999) Purification, characterization, and amino acid sequence of cerato-platanin, a new phytotoxic protein from *Ceratocystis fimbriata* f. sp. *platani*. J Biol Chem 274:24959–24964

Peter M, Courty PE, Kohler A, Delaruelle C, Martin D, Tagu D, Frey-Klett P, Duplessis S, Chalot M, Podila G, Martin F (2003) Analysis of expressed sequence tags from the ectomycorrhizal basidiomycetes *Laccaria bicolor* and *Pisolithus microcarpus*. New Phytol 159:117–129

Podila GK, Zheng J, Balasubramanian S, Sundaram S, Hiremath S, Brand J, Hymes M (2002) Fungal gene expression in early symbiotic interactions between *Laccaria bicolor* and red pine. Plant Soil 244:117–128

Polidori E, Agostini D, Zeppa S, Potenza L, Palma F, Sisti D, Stocchi V (2002) Identification of differentially expressed cDNA clones in *Tilia platyphyllos-Tuber borchii* ectomycorrhizae using a differential screening approach. Mol Genet Genomics 266:858–864

Read DJ, Perez-Moreno J (2003) Mycorrhizas and nutrient cycling in ecosystems – a journey towards relevance? New Phytol 157:475–492

Redecker D, Kodner R, Graham LE (2000) Glomalean fungi from the Ordovician. Science 289:1920–1921

Rosado SCS, Kropp BR, Piché Y (1994) Genetics of ectomycorrhizal symbiosis. I. Host plant variability and heritability of ectomycorhizal and root traits. New Phytol 126:105–110

Rousseau JVD, Sylvia DM, Fox AJ (1994) Contribution of ectomycorrhiza to the potential nutrient absorbing surface of pine. New Phytol 128:639–644

Rygiewicz PT, Andersen CP (1994) Mycorrhizae alter quality and quantity of carbon allocated below ground. Nature 369:58–60

Selle A, Willmann M, Grinze N, Geßler A, Weiß M, Nehls U (2005) The high-affinity poplar ammonium importer PttAMT1.2 and its role in ectomycorrhizal symbiosis. New Phytol 168:697–706

Selosse M-A, Le Tacon F (1998) The land flora: a phototroph-fungus partnership? Trends Ecol Evol 13:15–20

Selosse MA, Weiß M, Jany JL, Tillier A (2002) Communities and populations of sebacinoid basidiomycetes associated with the achlorophyllous orchid *Neottia nidus-avis* (L.) L.C.M. Rich. and neighbouring tree ectomycorrhizae. Mol Ecol 11:1831–1844

Simard SW, Perry DA, Jones MD, Myrold DD, Durall DM, Molina R (1997a) Net transfer of carbon between ectomycorrhizal tree species in the field. Nature 388:579–582

Simard SW, Jones MD, Durall DM, Perry DA, Myrold DD, Molina R (1997b) Reciprocal transfer of carbon isotopes between ectomycorrhizal *Betula papyrifera* and *Pseudotsuga menziesii*. New Phytol 137:529–542

Smith SE, Read, DJ (1997) Mycorrhizal symbiosis, 2nd edn. Academic, London

Söderström B, Finlay RD, Read DJ (1988) The structure and function of the vegetative mycelium of ectomycorrhizal plants. IV. Qualitative-analysis of carbohydrate contents of mycelium interconnecting host plants. New Phytol 109:163–166

Soragni E, Bolchi A, Balestrini R, Gambaretto C, Percudani R, Bonfante P, Ottonello S (2001) A nutrient-regulated, dual localization phospholipase A(2) in the symbiotic fungus *Tuber borchii*. EMBO J 20:5079–5090

Sundaram S, Kim SJ, Suzuki H, McQuattie CJ, Hiremath ST, Podila, GK (2001) Isolation and characterization of a symbiosis-regulated *ras* from the ectomycorrhizal fungus *Laccaria bicolor*. Mol Plant Microbe Interact 14:618–628

Tagu D, Nasse B, Martin F (1996) Cloning and characterization of hydrophobins-encoding cDNAs from the ectomycorrhizal basidiomycete *Pisolithus tinctorius*. Gene 168:93–97

Tagu D, Faivre-Rampant P, Lapeyrie F, Frey-Klett P, Vion P, Villar M (2001) Variation in the ability to form ectomycorrhizas in the F1 progeny of an interspecific poplar (*Populus* spp) cross. Mycorrhiza 10:237–240

Tagu D, Bastien C, Faivre-Rampant P, Garbaye J, Vion P, Villar M, Martin F (2005) Genetic analysis of phenotypic variation for ectomycorrhiza formation in an interspecific F1 poplar full-sib family. Mycorrhiza 15:87–91

Tarkka M, Niini SS, Raudaskoski M (1998) Developmentally regulated proteins during differentiation of root system and ectomycorrhiza in Scots pine (*Pinus sylvestris*) with *Suillus bovinus*. Physiol Plant 104:449–455

Taylor AFS, Martin F, Read DJ (2000) Fungal diversity in ectomycorrhizal communities of Norway spruce [*Picea abies* (L.) Karst.] and beech (*Fagus sylvatica* L.) along north-south transects in Europe. In: Schulze ED (ed) Carbon and nitrogen cycling in European forest ecosystems. (Ecological studies, vol 142) Springer, Berlin Heidelberg New York, pp 343–365

Tedersoo L, Hansen K, Perry BA, Kjøller R (2006) Molecular and morphological diversity of pezizalean ectomycorrhiza. New Phytol 170:581–596

Tranvan H, Habricot Y, Jeannette E, Gay G, Sotta B (2000) Dynamics of symbiotic establishment between an IAA-overproducing mutant of the ectomycorrhizal fungus *Hebeloma cylindrosporum* and *Pinus pinaster*. Tree Physiol 20:123–129

Tunlid A, Talbot NJ (2002) Genomics of parasitic and symbiotic fungi. Curr Opin Microbiol 5:513–519

Voiblet C, Duplessis S, Encelot N, Martin F (2001) Identification of symbiosis-regulated genes in *Eucalyptus globulus-Pisolithus tinctorius* ectomycorrhiza by differential hybridization of arrayed cDNAs. Plant J 25:181–191

Vrålstad T, Fossheim T, Schumacher T (2000) *Piceirhiza bicolorata* – the ectomycorrhizal expression of the *Hymenoscyphus ericae* aggregate? New Phytol 145: 549–563

Wiemken V, Boller T (2002) Ectomycorrhiza: gene expression, metabolism and the wood-wide web. Curr Opin Plant Biol 5:355–361

Wipf D, Benjdia M, Tegeder M, Frommer WB (2002) Characterization of a general amino acid permease from *Hebeloma cylindrosporum*. FEBS Lett 528:119–124

Wong KKY, Piché Y, Montpetit D, Kropp BR (1989) Differences in the colonization of *Pinus banksiana* roots by sib-monokaryotic and dikaryotic strains of ectomycorrhizal *Laccaria bicolor*. Can J Bot 67:1717–1726

Wong KKY, Montpetit D, Piché Y, Lei J (1990) Root colonization by four closely related genotypes of the ectomycorrhizal basidiomycete *Laccaria bicolor* (Maire) Orton – comparative studies using electron microscopy. New Phytol 116:669–679

Wright DP, Scholes JD, Read DJ, Rolfe SA (2000) Changes in carbon allocation and expression of carbon transporter genes in *Betula pendula* Roth. colonized by the ectomycorrhizal fungus *Paxillus involutus* (Batsch) Fr. Plant Cell Environ 23:39–49

Wright DP, Johansson T, Le Quéré A, Söderström B, Tunlid A (2005) Spatial patterns of gene expression in the extramatrical mycelium and mycorrhizal root tips formed by the ectomycorrhizal fungus *Paxillus involutus* in association with birch (*Betula pendula*) seedlings in soil microcosms. New Phytol 167:579–596

Xu JR, Peng YL, Dickman MB, Sharin A (2006) The dawn of fungal pathogen genomics. Annu Rev Phytopathol 44:337–366

Zhou XW, Kafsack BFC, Cole RN, Beckett P, Shen RF, Carruthers VB (2005) The opportunistic pathogen *Toxoplasma gondii* deploys a diverse legion of invasion and survival proteins. J Biol Chem 280:34233–34244

13 Network Organisation of Mycelial Fungi

M. Fricker[1], L. Boddy[2], D. Bebber[1]

CONTENTS

I. **Introduction** 310
II. **Conceptual Frameworks for Network Analysis** 312
A. Experimental Analysis of Mycelia as Networks 312
B. Common Network Measures 317
C. Predicted Transport Characteristics . . . 319
D. Predicted Network Resilience 320
III. **Comparison with Other Representations of Mycelial Structure and Growth** 320
A. Continuous Models 321
B. Cellular Automata Models 322
C. Vector Models 322
D. Abstracted Networks – Hub and Spoke Models 323
IV. **Nutrient Transport Through the Network** . 323
A. Transport at the Micron to Millimetre Scale 324
B. Transport at the Millimetre to Centimetre Scale 325
V. **Conclusion: Future Prospects** 327
References 327

I. Introduction

Filamentous fungi grow out from a spore or an inoculum, by apical extension of slender hyphae that then branch sub-apically to form a fractal, tree-like mycelium. In ascomycetes and basidiomycetes, tangential hyphal fusions or anastomoses occur as the colony develops to form an interconnected mycelial network (Rayner et al. 1994, 1999; Glass et al. 2000, 2004). The basic sequence of morphological events leading to fusion has been well described, most notably by Buller (1931, 1933; summarised by Gregory 1984), and details of the underlying cellular and molecular events are beginning to be elucidated in model systems such as *Neurospora* and *Colletotrichum* (Glass et al. 2000, 2004; Hickey et al. 2002; Roca et al. 2003, 2004, 2005a, b; Fleissner et al. 2005). In the larger, more persistant saprotrophic and ectomycorrhizal basidiomycetes, the network architecture develops further as the colony grows with the formation of specialised high-conductivity channels, termed cords, through aggregation and limited differentiation of hyphae (Cairney 2005). Cords tend to be well insulated from the environment and are able to translocate nutrients between separate food resources or to and from the foraging margin (Boddy 1999; Leake et al. 2004). At the same time as cords form, the intervening regions of the mycelium regress and are presumably recycled to support new growth. The resulting structure and scale of the corded networks vary between species, and give rise to qualitatively different, recognisable network architecture (Fig. 13.1). These networks are not static, but are continuously reconfigured in response to local nutritional or environmental cues, damage or predation, through a combination of new growth, branching, fusion or regression (Boddy 1999; Leake et al. 2004). Furthermore, a single genetically identical individual network (genetic mycelial unit, or GMU *sensu* Olsson 2001) can undergo quantum shifts in size through fragmentation, leading to several separate functional mycelial units (FMU; Olsson 1999, 2001). Conversely, fusion of separate FMUs in the following growth season can rapidly (re-)generate a more expansive network (Rayner et al. 1994; Boddy 1999; Leake et al. 2004).

Whilst the largest mycelial networks that are typically grown in laboratory microcosms range over 0.1–1.0 m^2, in an undisturbed forest ecosystem almost all trees and fallen plant parts are interconnected by a diverse population of mycelial systems forming an extensive network over a much larger physical scale termed the 'wood wide web' (WWW; Read 1997; Simard et al. 1997; Simard and Durall 2004). There is considerable evidence for extensive nutrient uptake and exchange through the WWW (Simard et al. 1997; Read and Perez-Moreno 2003; Leake et al. 2004; Simard and Durall 2004).

[1] Department of Plant Sciences, University of Oxford, South Parks Road, Oxford, OX1 3RB, UK
[2] Cardiff School of Biosciences, Cardiff University, Cardiff, CF10 3US, UK

Biology of the Fungal Cell, 2nd Edition
The Mycota VIII
R.J. Howard and N.A.R. Gow (Eds.)
© Springer-Verlag Berlin Heidelberg 2007

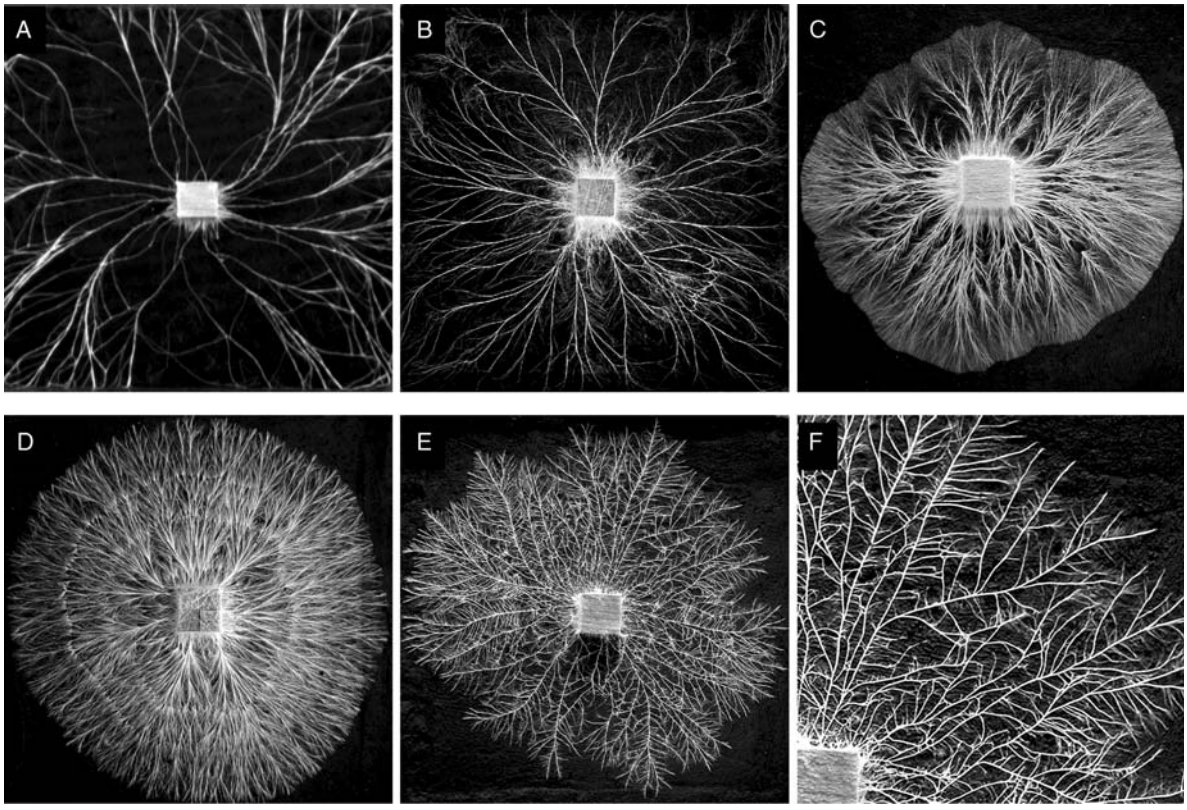

Fig. 13.1. Colony morphology and network architecture for different species of saprotrophic basidiomycetes. **A–F** Mycelial systems of *Resinicium bicolor* (**A**), *Phanerochaete velutina* (**B**), *Hypholoma fasciculare* (**C**), *Coprinus picaceous* (**D**) and *Phallus impudicus* (**E, F**) growing from wood blocks of 2 cm side in 24×24 cm trays of compressed non-sterile soil to illustrate the range of network architecture shown by different species. Photos courtesy of G. Tordoff

Fungi, like any other organisms, must partition limited resources among competing requirements. For example, a very dense, highly connected network might have high transport capacity and resilience to damage or attack because of multiple transport pathways. However, it would incur a large material cost of construction per unit area of explored space and would cover new ground slowly. Conversely, a sparse system could extend further for the same material cost, but would risk missing resources and have fewer alternate routes to survive damage and disconnection (Boddy 1993, 1999; Rayner et al. 1994, 1999). We do not know what factors have been most significant in shaping each strategy in evolutionary terms (Pringle and Taylor 2002) or how organisation and integration of such networks can emerge without centralised control (Rayner 1991; Rayner et al. 1994, 1999). However, as a starting point we might envisage that the resulting networks represent an effective balance between cost, exploration, exploitation, transport efficiency and resilience to damage. Subtle shifts in the developmental process for different species may have effectively weighted the relative importance of each these aspects to adapt to different spatial and temporal patterns of resource availability and environmental conditions, giving rise to a set of foraging strategies for each species (Boddy 1999). However, there has been relatively little explicit analysis of the structure of the networks formed, their dynamic behaviour and how both impact on these proposed functions.

In this chapter we explore this relatively uncharted middle ground between the microscopic cellular level dominated by discrete tubular hyphae (reviewed in this series by Trinci et al. 1994) and the macroscopic level of intact colonies (reviewed in this series by Olsson 2001), to see the extent that it is possible to characterise the network aspect of mycelial growth. A few years ago this would have been a daunting task as there was no coherent conceptual framework to describe, meas-

ure, summarise and compare such complex networks. In the 1990s, fractal measures were introduced as useful tools to capture aspects of the network structure as a metric (Ritz and Crawford 1990; Crawford et al. 1993; Donnelly et al. 1995; Mihail et al. 1995; Boddy et al. 1999; Crawford et al. 1999; Boddy and Donnelly 2006). However, a single summary value can only express a small fraction of the complexity in the system, even with subsampling of different regions. Recently, considerable advances have been made in network analysis, using concepts and tools emerging from graph theory and statistical mechanics (Strogatz 2001; Albert and Barabasi 2002; Dorogovtsev and Mendes 2002; Newman 2003; Amaral and Ottino 2004). These techniques have been applied to a swathe of complex systems, including biological networks such as protein–protein interactions or food webs, and may provide a useful conceptual framework for quantitative analysis of fungal mycelia. We therefore provide an introduction to some of the theory and terminology used to analyse networks, translated as far as we are able into mycological language. We then evaluate its application to analyse the dynamics, efficiency, resilience and adaptation of self-organised fungal networks at different spatial scales. We also try to set network analysis in context with other approaches to measure and model fungal behaviour, with the expectation that a combination of approaches will be required to understand fungal growth over the enormous range of length scales needed.

II. Conceptual Frameworks for Network Analysis

To use network analysis tools to analyse fungal mycelia, it is necessary to translate the morphological structures observed into an appropriate network representation (Bebber et al., submitted). Our starting assumption is that the fungal mycelium can be represented as a graph by classifying junctions (branch-points and anastomoses) as nodes and the hyphae or cords between nodes as links. It is possible to (manually) extract the network from images of mycelial systems taken at appropriate resolution. We illustrate the process and results using the classic microscopic image of *Coprinus sterquilinus* from Buller (1931; Fig. 13.2A) and images of *Phanerochaete velutina* from our own work (Fig. 13.2C). We have developed a simple software interface to simplify extraction of the network that is available on request.

At the moment nodes have to be manually chosen as automated segmentation algorithms are not yet sufficiently robust to extract the network unsupervised. Each node is given a unique identifier and stored as a list together with its Cartesian (x, y) co-ordinates. Links are stored interchangeably either as an adjacency matrix or in a list format that can be imported into a wide range of freely available software packages, such as Pajek (http://vlado.fmf.uni-lj.si/pub/networks/pajek/). As links vary in length (l) and cross-sectional area (a), the links are weighted, i.e. they differ in their connection strength. The diameter and hence area of each cord can be determined using image analysis tools. The material construction cost of each link can be estimated from the volume ($l \times a$), i.e. longer, thicker hyphae or cords are more costly to produce in terms of the mass of material required to build them. Similarly, the predicted transport flux through the network is expected to increase with increasing cross-sectional area, but decrease with link length. The precise relationship between flow and area is less clear. For the extreme case of laminar flow through individual hyphal tubes, flow can scale with r^4 in accordance with the Hagen–Poiseuille equation:

$$\text{Volume flow rate per hub} = -\frac{\pi r^4}{8\eta}\frac{\partial P}{\partial x} \qquad (13.1)$$

where r is the radius of the tube, η is the viscosity of the fluid, and $-\delta P/\delta x$ is the negative gradient of the hydrostatic pressure. In multi-hyphal aggregates such as cords, the structure is more akin to a cylinder packed with individual hyphae in parallel. In this case, flow can scale with the area, i.e. r^2, although it is recognised that the internal structure of cords can be more complex, with both larger vessel hyphae increasing potential flow and fibre hyphae that do not contribute to transport.

A. Experimental Analysis of Mycelia as Networks

The *C. sterquilinus* colony (Fig. 13.2A) captures the essence of fungal network formation on a microscopic scale. A sparse branching tree-like structure forms in the peripheral growth zone from tip growth and sub-apical branching, whilst secondary growth and fusion of hyphae in the centre of the colony forms an interconnected network with

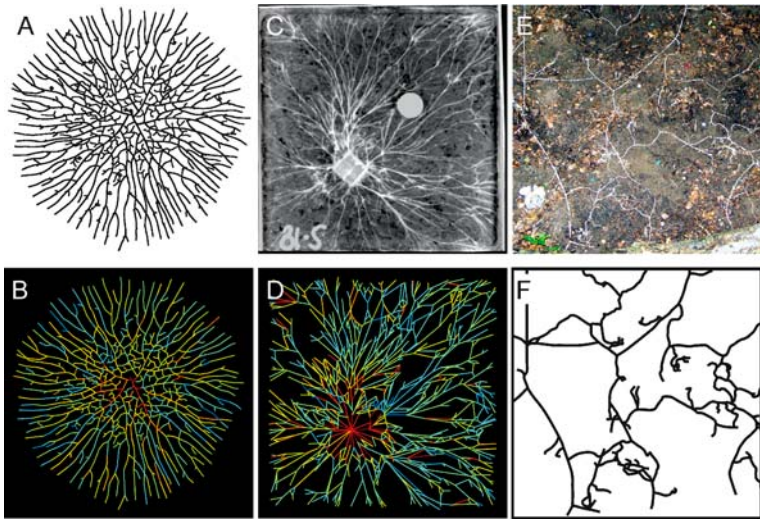

Fig. 13.2. Analysis of mycelial network structures over different length scales. **A** Drawing of a young colony of *Coprinus sterquilinus* showing the development of an anastomosing network in the colony interior. The colony is around 380 µm in diameter (modified from Buller 1931). **B** Network representation of the same colony in which the link weight is colour coded on a rainbow scale, with red representing the thickest hyphae. **C** Mycelial system of *P. velutina* grown from 4 cm^3 beech wood inocula on a 24×24 cm tray of non-sterile soil with an inert bait (*grey circle*) after 39 days. Digital images were obtained from photographs taken by R. Bolton. **D** Network representation of the same colony in which the link weight is colour coded on a rainbow scale with red representing the thickest cord. **E** A 75×75 cm portion of an extensive network of the saprotrophic fungus *Megacollybia platyphylla* growing from a log in Wytham Wood, Oxfordshire, UK. **F** A schematic representation of the *M. platyphylla* network

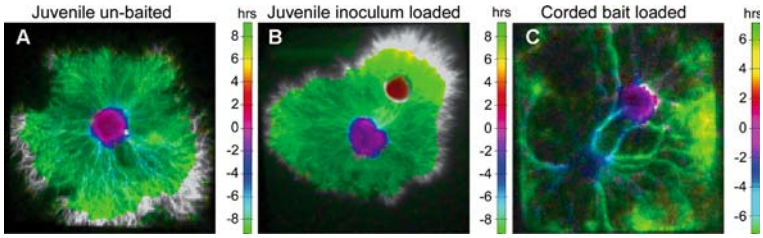

Fig. 13.3. Establishment of oscillatory phase domains in colonies of *P. velutina*. Pseudo-colour-coded images showing the relative phase of the oscillatory component of labelled aminoisobutyrate (^{14}C-AIB) transport determined pixel-by-pixel using Fourier analysis. The colour represents the phase difference in hours (*hrs*) according to the adjacent scale for each image from the oscillation recorded at the loading site. Only regions with the same frequency are colour-coded. Regions with a different frequency or where the Fourier analysis was not possible, such as the growing colony margin, are coded in grey-scale. The period of the oscillation ranged from 18.3 h (**A**, **B**) to 14.2 h (**C**), depending on the growth temperature with a Q_{10} of around 2. **A** Control colony grown for 240 h, showing distinct phase domains in the inoculum and foraging mycelium with ~7 h phase difference. **B** Development of an additional phase domain in the bait of a juvenile colony. The bait lags the inoculum by ~3.5 h. **C** Phase map of a 35-day-old colony following loading at the bait, showing distinct phase domains in the bait, inoculum, connecting cords and foraging mycelium

many cycles (Fig. 13.2A). The extracted network representation contains 579 nodes and 656 links (Table 13.1), each with an associated measure of its length and diameter that can be combined to give an estimate of the volume (cost) or predicted resistance to flow (Fig. 13.2B). In theory, larger networks than this can be captured using large-scale mycelial mapping (LSMM; Crawford et al. 1993; Ritz et al. 1996) and analysed at the level of an individual hypha. However, it becomes increasingly difficult to distinguish fusions from overlapping hyphae as the colonies become denser; and the sheer number of

Table. 13.1. A summary of common network measures and their application to fungal mycelia

Topology Measure	Symbol	Description	Example networks *Coprinus sterquilinus*	*Phanerochaete velutina*
Nodes (vertices)	N	The total number of connected entities. In the mycelium, these are the branch points, fusions, or tips.	579	986
Links (edges)	M	The total number of connections. In the mycelium, the number of cords or hyphae that connect the vertices. Links can be directed, i.e. flow occurs only in one direction.	656	1351
Node degree	k	The number of links attached to a node. Often used as a measure of the connectedness of networks, especially the frequency distribution of k. This measure is less useful for mycelia as k is usually either 3 (for junctions) or 1 (for tips). Mean k (excluding the highly-connected wood block) is given on the right. Node strength (see below) is more appropriate for weighted networks.	2.26	2.71
Subgraphs	g	If the network is broken up, the number of disconnected parts. Of interest when considering resilience of the mycelium to attack.	1	1
Cyclomatic number (Haggett and Chorley 1969)	$M-N+g$	The number of closed loops or cycles in the network. This gives an indication of the number of redundant pathways in the mycelium.	78	366
α−index (Haggett and Chorley 1969)	$\alpha = \frac{M-N+g}{2N-5}$	The number of cycles normalised by the possible maximum (assuming no overlapping links), taking values from 0 to 1 to allow comparison of networks of different sizes. This measure has been described as 'meshedness' (Buhl et al. 2004).	0.07	0.19
Clustering coefficient (Watts and Strogatz 1998)	C	A measure of the number of cycles, or loops, of length 3 (i.e. triangles) in the network. Takes values from 0 to 1. Useful for describing the connectedness of some types of network, but less so for fungal networks and many other spatial networks, as their construction often precludes the formation of triads.	0.01	0.11
Spatial structure				
Spatial extent	A	The area covered by the mycelium. Calculated as the area of the convex hull of the node positions in space or by segmentation of the colony outline.	0.11 mm^2	51,050 mm^2
Node density	NA^{-1}	The number of junctions per unit area of space covered by the mycelium. This is a measure of the branching/fusing density. It is likely that this varies through space and time, indicating the responses of mycelial branching to local conditions. Data may be aggregated using spatial interpolation techniques such as Kriging (Isaaks and Srivastava 1989).	5185 mm^{-2}	0.019 mm^{-2}
Link weight	w	A measure relating to the properties of a link, for example its physical length l or cross-sectional area a. Measures can be combined to predict other properties, such as resistance to transport or volume of cords (see below). Estimating link weight is fundamental to other, more complex, calculations of network properties. Mean a is given on the right.	0.000033 mm^2	0.03 mm^2
Node strength (Barthelemy et al. 2005)	$s = \sum_{i=1}^{k} w_i$	A measure of the importance of a node, calculated by summing the link weights w of all the k links connected to a node. For example, the (trimmed) mean value of the node strengths (ignoring the central wood block), calculated as the sum of link cross-sectional areas, is given on the right. This measure is regarded as more informative than node degree for weighted networks.	0.000075 mm^2	0.09 mm^2
Total length	$L = \sum_{i=1}^{L} l_i$	The total length of links in the network, calculated by summing the lengths of all links in the network.	12.2 mm	12,600 mm

Topology Measure	Symbol	Description	Example networks *Coprinus sterquilinus*	*Phanerochaete velutina*
Total volume (cost)	$V = \sum_{i=1}^{L} l_i a_i$	An estimate of the material construction cost of the network, calculated summing the estimated volumes (la) of each link. Actual mass can be estimated if the density of cords is known. This could be extended to the mass of carbon, nitrogen, or other components making up the mycelium.	0.00038 mm^3	391 mm^3
Volume density	VA^{-1}	The amount of mycelium per unit area. Gives an estimate of the efficiency of the mycelium in covering space.	0.017 $\frac{mm^3}{mm^2}$	0.008 $\frac{mm^3}{mm^2}$
K-function (Ripley 2004)	$K(t) = nAN^{-1}$	The K-function provides an estimate of the spatial clustering of points, in this case nodes. K for a particular radius t around a node is the average number of nodes within t of that node, divided by the total node density. $K(t)$ can be compared with expected values for a completely random (Poisson) distribution to detect clustering of nodes at different spatial scales.	–	–
Mass fractal dimension	$n(s) \approx cs^{-d}$	Mycelia can be described as fractals over certain length scales, as they fill space more than a line but less than a continuous plane (Boddy and Donnelly 2006). The *box counting* method overlays a series of grids of square boxes with side length s onto an image of the network. The number of boxes that intersect the image $n(s)$ is related to s via the fractal dimension d.	–	–
Transport Resistance	$r \propto la^{-1}$	Resistance is a measure of the difficulty transporting material through a link, proportional to length divided by cross-sectional area, so that long, thin links have greater resistance. Resistance can be thought of as analogous to expected travel time in road networks, or electrical resistance in electrical networks of resistors. The inverse of resistance is conductance (al^{-1}). Resistance is a fundamental measure in estimating transport through the network. Resistance can be used in electrical resistance network models to provide estimates of flux through the mycelium. Mean resistance for the fungal network is given on the right.	690 $\frac{mm}{mm^2}$	585 $\frac{mm}{mm^2}$
Shortest path (see Dorogovtsev and Mendes 2002)	$d_{ij} = \sum_{h=1}^{g} r_h$	The shortest path, or geodesic path, between nodes i and j is the path of least resistance. There are g links in the shortest path. There may be more than one path with the smallest sum of resistances, and several paths with sums of resistances very close to the smallest sum. We expect the maximum rate of transport of material along the shortest path. The shortest path is a fundamental measure of network transport. However, it fails to take into account parallel pathways in predicting flux which may be captured better using electrical circuit analogues (see above).	–	–
Diameter (see Dorogovtsev and Mendes 2002)	$D = \max(d_{ij})$	The diameter of the network is the longest shortest path. Although widely used in graph theoretic approaches for unweighted networks, in fungal networks this measure is highly sensitive to the presence of a very long, thin connection, usually a peripheral cord in the case of a mycelial network.	14,818 $\frac{mm}{mm^2}$	18,980 $\frac{mm}{mm^2}$
Average shortest path	$\ell = \frac{1}{N(N-1)} \sum_{i \neq j} d_{ij}$	The average shortest path provides a measure of the overall transport efficiency of the network. Networks of similar physical extent which have smaller average shortest paths have a more efficient transport system.	5061 $\frac{mm}{mm^2}$	5474 $\frac{mm}{mm^2}$

Topology Measure	Symbol	Description	Example networks *Coprinus sterquilinus*	*Phanerochaete velutina*
Global efficiency (Latora and Marchiori 2001, 2003)	$E_{glob} = \frac{1}{N(N-1)} \sum_{i \neq J} \frac{1}{d_{ij}}$	The *efficiency* measure was introduced (Latora and Marchiori 2001) to overcome a difficulty with the average shortest path, namely that for disconnected networks the shortest path could be infinite (i.e. for two nodes in separated subgraphs). In the efficiency calculation, the mean reciprocal of the shortest path is calculated; and the reciprocal for disconnected nodes is defined as zero.	0.00028 $\frac{mm^2}{mm}$	0.00032 $\frac{mm^2}{mm}$
Betweenness centrality (Freeman 1977)	$B_u = \sum_{ij} \frac{\sigma_{iuj}}{\sigma_{ij}}$	Betweenness centrality is a measure of the importance of a node or link to transport. The betweenness centrality of a node or link u is the proportion of all shortest paths between pairs of nodes i and j, σ_{ij}, that pass through u, σ_{iuj}. Loss of the node or link with the highest betweenness centrality leads to the most increases in shortest path lengths.	–	–
Central point dominance (Freeman 1977)	$CPD = \frac{1}{N-1} \sum_i (B_{max} - B_i)$	Central point dominance (CPD) measures the relative importance of the node with the largest betweenness centrality (B_{max}), compared with all other nodes. For a star-like network CPD = 1, because all shortest paths pass through the central node and only one shortest path through all other nodes.	0.50	0.62
Resilience				
Relative diameter	$D_{rel} = D^* / D$	Removal of nodes or links should increase the shortest paths in the network, thereby increasing the diameter (and mean shortest path). Relative diameter is the diameter of a disturbed network D^* scaled by the original diameter D. However, fragmentation of the network into subgraphs leads to infinite shortest paths, making this measure difficult to apply in many circumstances.	–	–
Vulnerability (Gol'dshtein et al. 2004)	$V = \frac{E_{glob} - E^*_{glob}}{E_{glob}}$	When nodes or links are removed from a network, the length of shortest paths and number of disconnected nodes is expected to increase, and therefore the global efficiency decreases. Scaling the efficiency of a disturbed network () by the original efficiency gives a measure of the disturbance. Calculating V for removal of a single node or link gives the vulnerability for that node or link.	–	–
Reachability (availability; Ball and Provan 1983)	$R = \frac{2P}{N(N-1)}$	Reachability is the number of paths between nodes that exist in the network P, divided by the possible number of paths (i.e. $N(N-1)/2$). Fragmentation of the network into subgraphs decreases P. Unlike relative efficiency, the measure is independent of the length of shortest paths.	–	–

nodes and links makes manual extraction of the network prohibitively time-consuming. In the future it may be possible to sub-sample segments of the entire colony if suitable methods are developed to deal with the connectedness of nodes and links at the artificial boundaries that this introduces.

The next appropriate level of resolution in practical terms are microcosms in the centimetre to metre range where the dominant structure is a corded mycelium (Figs. 13.1, 13.2C,D). In the case of the *P. velutina* grown in a 24-cm square microcosm, the size of the corded experimental networks reaches around 500–1500 nodes (Fig. 13.2C; Bebber et al., submitted). It might be appropriate to consider the links to be directed on the basis of their initial growth direction. However, in practice, the physiological direction of nutrient fluxes is more important and does not have to follow the developmental connection sequence. Unfortunately, we cannot predict *a priori* which direction the flux may move in and, indeed, we expect it to vary depending on the source–sink relationships within the network. In the future, the techniques to map fluxes described below (Sect. IV.) may provide this information, but at this stage it is simpler to assume that links are undirected and capable of moving nutrients in either direction. The reader is referred to the chapter by Ashford and Allaway (Chap. 2 in this volume) for a discussion of the possible role of vacuolar transport mechanisms for trans-cellular movement of materials over long distances.

In theory, the same approaches can be used for networks in the field. However, the structure is more difficult to capture from simple photographs (Fig. 13.2E) as the network requires careful excavation and additional on-site notes to define contiguous cords. Thus, at this stage it is relatively easy to extract a schematic representation of the network (Fig. 13.2F), but rather more difficult to perform a robust quantitative analysis.

B. Common Network Measures

Once the weighted network has been digitised, a wide range of network parameters can be calculated. Some of the most common ones are given in Table 13.1. These values either have a straightforward biological meaning in their own right or they provide a comparison with network structures in other domains. As the data are embedded in Euclidean space, a number of basic morphological measures can be readily derived. An insight into the behaviour of the mycelial network can then be gleaned by following the trajectory for each parameter over time (Bebber et al., submitted). For example, the area covered by the colony can be estimated from the convex hull (effectively the polygon formed by stretching an elastic band around the outermost points), provided the network is not too sparse (Fig. 13.4A). The sum of the link lengths gives the total length of mycelium present (Fig. 13.4B), whilst including the cross-sectional area of the links gives an estimate of the volume of the fungus that, with appropriate calibration, can be related to the wet or dry weight. Early development in *P. velutina* is characterised by initial diffuse growth and branching of individual hyphae, which then resolve into cords as the growing front moves outward (Fig. 13.2C). Thus global network size measures, such as area, number of nodes and number of links, increase through time (Fig. 13.4A, B). However, the local scale network evolution is characterised by selective loss of connections and thinning out of the fine mycelium and weaker cords that gives rise to a decrease in the network density (cost per unit area) with increasing colony area (Fig. 13.4C). Although these measures provide a compact summary of the whole colony, they disguise any local variations in structure. There are a number of spatial averaging techniques, such as Kriging (Isaaks and Srivastava 1989), to interpolate between the very fine information at the level of each node and the overall colony metrics; and this approach may also facilitate comparison between different replicates and treatments.

A number of different quantities are typically measured for a network to understand its properties better. The degree (k) of each node is given by the number of links associated with that node. Thus tips have a degree of 1 as they are only connected to the previous node and branch points typically have a degree of 3, because the growth processes forming the network tend to give a single branch or a single fusion at each point. Initially overlapping cords often subsequently fuse, which generates $k = 4$ nodes. It is unlikely that there will be any loops where a link curls back around on itself to re-join the same node, although multiple parallel links between two nodes are possible. As the fine structure of the mycelium within a food resource, such as an agar inoculum or wood block, cannot be resolved, each of these is represented as a node with many links, resembling a hub in other network systems.

Considerable emphasis has been placed on the frequency distribution of node degree

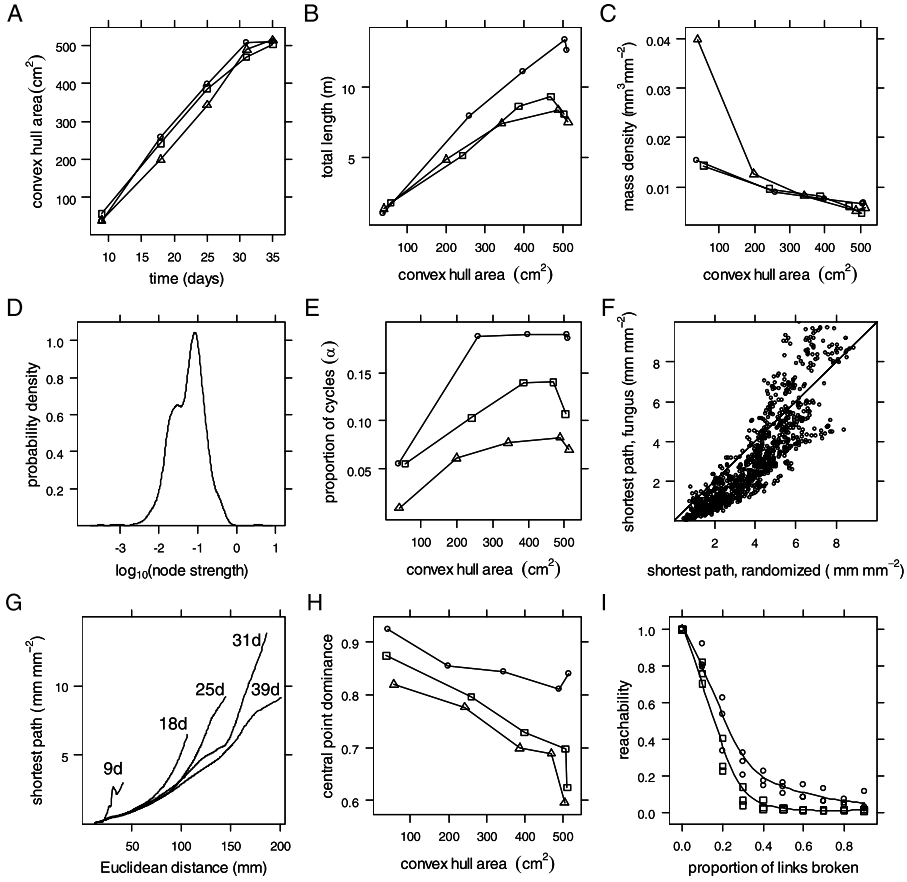

Fig. 13.4. Network measures for colonies of *P. velutina*. Mycelial systems of *P. velutina* were grown from 4 cm^3 beech wood blocks in 24×24 cm trays of non-sterile soil and photographed at intervals up to 39 days. The weighted network was manually extracted from digitised images and a range of network parameters calculated for three independent time-series. **A** The change in area, measured as the convex hull, with growth of the colonies. **B** The change in mycelium total length as the area increases. **C** The mass density taking into account the varying diameter of the cords. **D** The probability distribution of $\log_{10}$ node strength. **E** The change in the proportion of fundamental cycles (α) with increasing area. **F** Comparison of the shortest path (in 1000s) from the inoculum to every node for the weighted network plotted against the same network with the weights distributed evenly across the links. Points below the diagonal indicate that the fungus is performing better than expected for this null model. **G** Average shortest path distances (in 1000s) plotted against the Euclidean distance from the inoculum for all nodes at the time points indicated. Only means fitted by Friedman's smoother are shown for clarity. Mean values for later stages are smaller than those for earlier stages at a given Euclidean distance, showing that the network increases transport capacity as it develops. **H** The central point dominance (CPD) gives a measure of the decrease in the importance of the inoculum as the network becomes better connected. **I** Change in the reachability of all nodes in the network with progressive removal of links to simulate the effect of grazing. The resilience of the weighted network (*open circles*) is greater than the same network with the weights distributed evenly as a null model (*open squares*)

in other networks, following the discovery of scale-free distributions in networks from many different domains (Barabasi and Albert 1999). However, the degree distributions for fungal networks are not very informative because of the constraints imposed by the developmental process and crowding effects restricting the maximum number of possible connections, as with other spatial networks (Barrat et al. 2005). In weighted networks, the weighted degree distribution of node strength, measured as the sum of link cross-sectional areas per node, is regarded as a more informative measure to take into account the varying importance of the connections to each node (Barrat et al. 2004). For the *P. velutina* networks, the frequency distribution of node strength follows an approximately log-normal distribution (Fig. 13.4D).

The next level of organisation up, from a consideration of individual nodes and their summary statistics, is a consideration of the properties of their local neighbourhood. There are several measures that describe how well each node and its neighbours are interconnected. One of the most common is the mean clustering coefficient, C (Watts and Strogatz 1998), defined as the proportion of links connecting a node's immediate neighbours out of the maximum possible number of links. However, C is restricted to the case of cycles with three links forming triads, which is not appropriate to all classes of network, including fungal mycelia, as their construction effectively precludes formation of triads. In practice, the network forms an interconnected reticulate system with many 4-, 5- or 6-node rings spreading away from the central inoculum. Thus more general measures have been proposed to capture the structure of larger cycles (Alon et al. 1997; Caldarelli et al. 2004). The meshedness coefficient was recently introduced to address this point for planar graphs of ant galleries (Buhl et al. 2004; Cardillo et al. 2006). However, the meshedness coefficient is actually a re-discovery of the alpha coefficient originally proposed by the geography community in the 1960s (Haggett and Chorley 1969). Thus we prefer this latter original terminology and measure of closed loops as it has a historical precedent over meshedness (Fig. 13.4E). The shift from essentially a radial tree during early growth to a more reticulate network with increased cross-linking is reflected in an increasing value of the alpha index (Fig. 13.4E). Thus these fungal networks progress from a branching tree to a weakly connected lattice-like network behind the growing margin through a process of fusion and reinforcement to form loops and selective removal and recycling of excess redundant material (Bebber et al., submitted).

C. Predicted Transport Characteristics

To determine the efficiency of nutrient translocation in the mycelial network, the predicted transport performance was assessed. The typical metric used in network analysis is based on the shortest distance between any two nodes and is summarised either as the average, to give the average shortest path through the network, or as the longest shortest path which is termed the diameter of the network. A small average shortest path or a low diameter implies that it is easy to transport material anywhere in the network. However, in weighted mycelial networks, the network diameter is a highly unstable measure of network size as it is extremely sensitive to thin links with very high resistance at the mycelial margin. Thus we have not yet found this a useful network statistic, even for comparison with networks from other domains.

In a spatial graph, the average shortest path and the network diameter are expected to increase as the colony gets bigger, simply because they are defined by the physical distances between the nodes. However, including the predicted consequences of the varying cross-sectional area can significantly alter this view. Thus, thickening of some routes, effectively increasing their transport capacity, reduces the apparent shortest transport path (Bebber et al., submitted). In isolation, it is difficult to attribute meaning directly to this measure. However, one way to assess the significance of the organisation of the weighted links is to compare the actual network with one in which the weights have been either randomised between the links or distributed evenly across all links. Although results from such an analysis can be summarised as the mean shortest path or the diameter, it has proved more informative to consider how the performance changes with radius, not least because this maps onto the developmental sequence of network formation. Thus, over most of the physical radius of the colony, the structure built by the fungus has a lower shortest path than the equivalent structure with the same total material spread evenly across the network (Fig. 13.4F). Near the boundary the two systems become equivalent and right at the margin, where the very fine hyphae are located, the real colony performs much worse than the homogeneous network. As the network grows, previously peripheral nodes, which originally had a long shortest path, become better connected to the inoculum by the development of stronger links (Fig. 13.4G). Thus the branching margin resolves down to a more efficient transport system through thinning out of some links, coupled with reinforcement of retained routes and an increase in their transport capacity (Bebber et al., submitted).

The importance of any node, as a transport hub, can be estimated from the proportion of shortest paths that pass through it, in a measure termed the *betweenness centrality* that was originally used in the social sciences (Freeman 1977). A more specific measure derived from the betweenness centrality is the *central point dependence* (CPD), which focuses solely on the relative importance of the node with

the greatest betweenness centrality. In fungal networks this corresponds typically to the inoculum. Thus the CPD declines from ~90% to ~70% in control networks (Fig. 13.4H) and to ~55% in networks with an additional added wood resource (Bebber et al., submitted). This suggests that the network becomes more decentralised as it grows, forming cross-links that bypass the original inoculum.

Although these network measures provide some indication of the predicted transport efficiency of the mycelial systems, network analysis based on graph theory does not readily capture the importance of many potential parallel pathways for flux through the network, as they are dominated by measures that highlight single (shortest) paths. We have also examined alternative approaches using well developed tools for solving current flow through complex resistor networks (e.g. Hankin 2006). The weighted adjacency matrix from the mycelial network is already in an appropriate form to be recast as an electrical circuit analogue, with the additional constraint that flux (current) through the network can only be calculated if a driving force (voltage) is applied to certain points in the network. This allows what-if type examinations of the expected flux as source–sink patterns change. For example, a map of the predicted current flow from the inoculum to the hyphal tips can be calculated if a voltage is applied at the inoculum and all the tips are grounded.

D. Predicted Network Resilience

Whilst the architecture of the weighted network clearly improved transport efficiency, in nature the same system also has to resist accidental damage or targeted attack by grazers.

In many networks, the probability of node or link removal is unlikely to be random, and may also show a high degree of correlation between adjacent nodes. For example, in the case of fungi, grazing by soil invertebrates may occur at specific locations in the network (Harold et al. 2005). This is because some regions are more palatable or accessible than others. One measure to characterise the vulnerability of the network is to examine the effect of link breakage on global efficiency (E), where E is measured as the sum of the inverse of all shortest paths (Latora and Marchiori 2001). This measure is more appropriate than just changes in the mean shortest path as it can handle disconnection of parts of the network. In other network analyses it is often the nodes that are attacked. However, for fungal mycelia we believe that discussion of link breakage has more biological relevance. Thus, in a targeted attack, we assume that the probability of link breakage is proportional to length and inversely proportional to area [$P(b) \sim l/a$], i.e. longer, thinner cords are more likely to break. To highlight the importance of the organisation of the weighted links in the network, this can be compared with a model in which the breakage probability is proportional to length alone. The relative global efficiency, $E/E_{\max}$, where $E_{\max}$ is the efficiency of the unbroken network, is consistently greater for a given proportion of links broken, when link weighting is taken into account. Thus the distribution of link diameters in the fungal networks significantly increases their resilience to attack. One disadvantage of the vulnerability measure for a weighted network is that consistent removal of the weakest links naturally biases the measure of efficiency, so the decrease in network performance is perhaps not as marked as expected. An alternative measure, termed *reachability* (Ball and Provan 1983), provides an unbiased measure as it only considers the proportion of paths remaining, without reference to their transport capacity (Fig. 13.4H).

Whilst a single metric, such as 50% of the maximum efficiency or number of paths, provides a succinct summary of the resilience of the network, it disguises much of the subtlety in the full response of the fungal systems to attack. Thus the reachability of the weighted network does not decay with a simple function, but is eroded down to a core that is very much harder to destroy than equivalent networks with evenly distributed weights or randomised weights. This suggests that the same core architecture that gives the network good predicted transport properties (see Sect. II.C.) also gives it good resilience. Interestingly, the predicted pattern following this type of simulated attack closely matches the observed pattern for real mycelial systems of *P. velutina* under attack by particular species of *Collembola* (Fig. 13.5A, B). It is also worth noting that part of the resilience of such a biological network may not be just the architecture of the network prior to damage, but the ease and efficiency with which the network can reconnect itself following attack. In this respect, a self-organising spatial network may have considerable advantages over a random network in the cost, consistency and efficacy of the rewiring process needed to re-establish a functioning system.

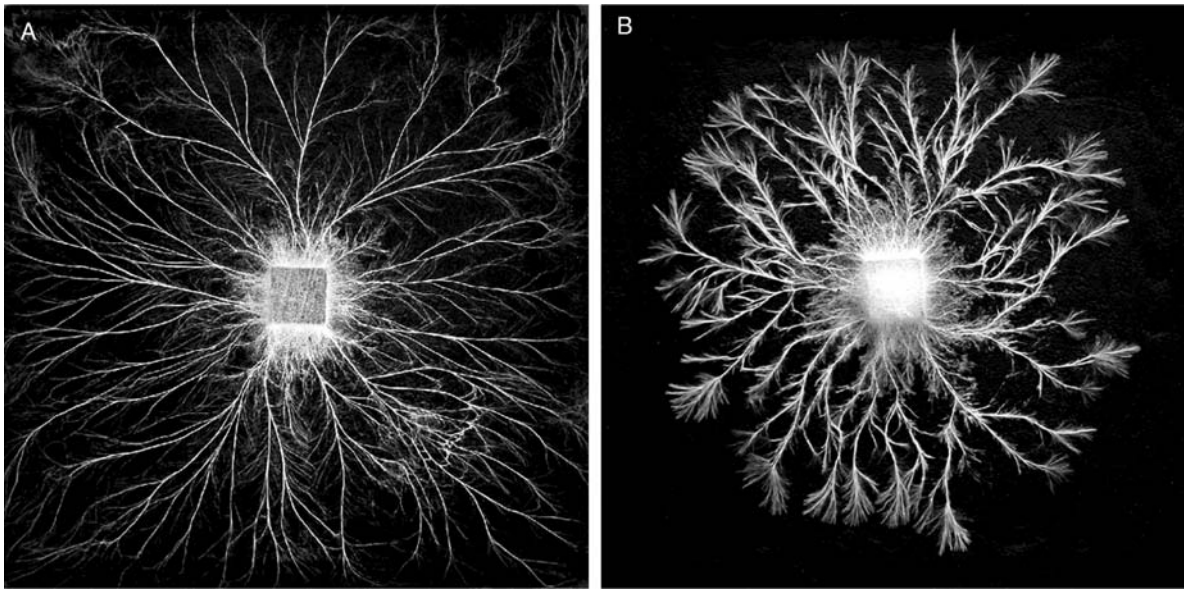

Fig. 13.5. The effect of *Collembola* grazing on networks of *P. velutina*. Mycelial systems of *P. velutina* grown from 4 cm^3 beech wood inocula on 24×24 cm trays of non-sterile soil after 21 days in the absence (**A**) and presence (**B**) of *Collembola*. In the presence of grazing, the network is trimmed down to a central core and the frequency of circumferential links increases. In addition there is a profusion of new fine mycelia from the damaged tips. Digital images were obtained from photographs taken by G. Tordoff

III. Comparison with Other Representations of Mycelial Structure and Growth

Network analysis provides a compact description of the fungal mycelium drawn from experimental systems and may provide insights into the underlying developmental processes. However, it is not a mathematical model of the fungal growth process *per se*. In an ideal world it might be possible to infer network construction algorithms from the network structure which would be of use to biologists and may also inform the design and construction of anthropogenic infrastructure networks. Whilst this is still an aspiration, it is instructive to compare the results and expectations of the experimentally derived network representation with other models of colony growth.

A. Continuous Models

There is an extensive literature describing both the cell biology of hyphal tip growth (see the chapters by Bourett et al., Fischer, and Sudbery and Court; respectively Chaps. 1, 5 and 6 in this volume) coupled with increasingly sophisticated mathematical models based around the vesicle supply centre (VSC) model (Bartnicki-Garcia et al. 1989; reviewed by Prosser 1995a, b; Geitmann 2006; see also Sudbery and Court, Chap. 6 in this volume), including extension to three-dimensional models (Gierz and Bartnicki-Garcia 2001; Tindemans et al. 2006). These models provide the raw material for developing models of colony branching patterns, but do not yet include anastomoses. Furthermore, they are probably pitched at too fine a resolution to consider scaling-up to a working model of network formation.

At the level of the colony, a range of different modelling approaches have been applied (Bezzi and Ciliberto 2004). There are several 'continuous models' that seek to model the collective attributes of the mycelium, rather than the growth of individual hyphae, but include morphological features such as tip growth, branching, anastomosis and cell death within the equations (Edelstein 1982; Edelstein and Segel 1983; Edelstein et al. 1983; Edelstein-Keshet and Ermentrout 1989; Davidson et al. 1996, 1997; Davidson and Park 1998; Davidson and Olsson 2000; Boswell et al. 2002, 2003a; Jacobs et al. 2004). In such models growth is driven by nutrient concentration derived from uptake and internal passive or active transport. The most advanced

partial differential equation (PDE) model has been developed for *Rhizoctonia solani* and has been calibrated against experimental measurements of key parameters (Davidson et al. 1997; Davidson 1998; Davidson and Olsson 2000; Boswell et al. 2002, 2003a). Predictions from the model match experimental observations for systems growing on tessellated heterogeneous resources (Jacobs et al. 2004), but the equations are difficult to solve mathematically (Boswell et al. 2003b) and effectively limit computation to a simulation of growth over a few centimetres and a few hours. Nevertheless, these models provide good descriptions of mass and substrate distributions for growth in both homogeneous and heterogeneous environments. One of the disadvantages of this basic PDE approach is that it can only describe the architecture of the mycelium through its average properties, such as branches and fusions per unit area, since it does not have an explicit morphological representation of the colony structure. This makes it more difficult to understand the impact that the network structure might have on transport properties and colony growth.

B. Cellular Automata Models

The first attempts to capture a direct representation of the morphology of the colony were based on cellular automata (CA) operating in discrete time, space and state. Although CA models are discretised, 'growth' is typically controlled through interaction with continuous fields of nutrients or signalling molecules (Ermentrout and Edelstein-Keshet 1993; Liddell and Hansen 1993; Regalado et al. 1996; Lopez and Jensen 2002). CA models can generate crude spatial representations of mycelial structure (Fig. 13.6A), but are heavily constrained by the regular, often two-dimensional lattice used in the simulation. One more recent approach to unite the aspirations of the different types of modelling is to make a hybrid model that captures the most pertinent biological behaviourr in a PDE model, but allows the PDE model to run on a discrete framework that simulates the discrete behavior of individual hyphae and the network structure of the mycelium. This approach has been pioneered by Davidson and colleagues with impressive results (Boswell et al. 2006).

C. Vector Models

An alternative approach to achieve greater morphological realism is to develop models based upon (empirical) rules that govern the growth rate and branching characteristics of vectors representing the hyphae. The rules may include stochastic sampling of experimentally determined parameter distributions of, for example, tip and branch angles, branching frequency or internode length (Hutchinson et al. 1980; Yang et al. 1992a, b; Lejeune and Baron 1995, 1997, 1998; Lejeune et al. 1995). Rather than prescribe these growth and branching parameters, Meškauskas and colleagues (2004a, b) developed a Neighbour Sensing (NS) model in which the growth vector of each virtual hyphal tip is cal-

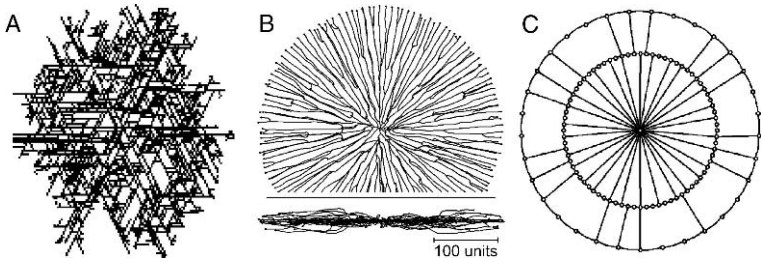

Fig. 13.6. Morphological models of colony growth. **A** The typical output from a cellular automaton model running on a hexagonal grid in which the growth direction and branching probability have a limited degree of stochasticity (M.D. Fricker, unpublished data). **B** Visualizations produced by the neighbour-sensing model of hyphal growth, assuming a negative autotropic reaction and density-dependent branching (branching probability 40% per iteration), with the density field being generated by all of the mycelium. An additional horizontal plane tropism restricts growth to a thin horizontal zone analogous to a circular colony grown on agar (viewed from above, *upper visualization*) with a narrow profile (side view, *lower visualization*; Meškauskas et al. 2004a). **C** An analytically solvable model showing radial connections from peripheral nodes to an effective hub. The average shortest path can be calculated with varying cost-functions for systems with multiple concentric rings (Jarrett et al. 2006)

culated taking into account the potential influence of the surrounding virtual mycelium (Fig. 13.6B). Thus in this model branching probability, position and orientation are determined directly by evaluation of local density-dependent fields, rather than through random stochastic processes. The model outputs various colony statistics, such as total mycelial length and internode length, that assist in comparison with real experimental data (Meškauskas et al. 2004a, b).

Other visually realistic simulations have been produced using 'Lindenmayer' (or L) systems. L-Systems are string rewriting rules (productions) operating on a component (predecessor) and converting it to a successor according to the rule(s), so that a complex object can be developed by successive replacement of parts of a simpler object. They were formulated by Lindenmayer (1968) as an axiomatic theory of biological development. L-Systems operate with a string notation which has been given increasing levels of complexity and simulation power over the years (Prusinkiewicz and Lindenmayer 1990; Prusinkiewicz 2004; Prusinkiewicz and Rolland-Lagan 2006; see also the 'visual models of morphogenesis' website at http://www.cpsc.ucalgary.ca/Research/bmv/vmm-deluxe/index.html).

Although branching fungal mycelia fit well with the L-system framework, there has been little application of L-systems to modelling fungi (Liddell and Hansen 1993; Soddell et al. 1995; Tunbridge and Jones 1995). The most sophisticated stochastic context-sensitive parametric L-system so far developed (Tunbridge and Jones 1995) implements the underlying cellular processes originally put forward by Prosser and Trinci (1979). Thus tip growth is dependent on vesicle supply from sub-apical compartments. Once sufficient growth occurs, nuclear division and septum formation take place. If sufficient vesicles subsequently accumulate in subapical segments, branch formation is initiated. Iteration of these rules generates a string describing the branching structure, but with no explicit two- or three-dimensional representation. To produce realistic two-dimensional images, additional stochastic operations are included during visualisation of the structure, such as random selection of branching direction, variation in branching angle, curved hyphal shape and preferential radial growth. The authors note that more realistic graphical depiction would require the introduction of geometrical information into the simulation so that the stochastic elements form part of the developmental rules rather than just affecting visualisation of the structure.

These models all produce branching trees, where the emphasis is to achieve a representative simulation of the structure formed or to investigate plausible mechanisms based on the underlying physiological processes that may control growth. However, none of the vector models include anastomoses, not least because hyphal contact is difficult to calculate in three-dimensional space and cycles are difficult to capture within the hierarchical data structure of either the NS-model or L-model. Thus, none of the current morphological models help to provide any insight into the importance of the network structure. Furthermore, it is not possible to perform much quantitative comparison between the extracted network representations described here and the model simulations in the absence of anastomoses.

D. Abstracted Networks – Hub and Spoke Models

An alternative approach to understand the behaviour of fungal networks is to abstract the essence of a mycelial network and re-cast it in a form that permits more rigorous mathematical analysis. Thus the interplay between radial expansion and lateral connections can be captured in a 'hub and spoke' model of the developing fungal mycelium (Ashton et al. 2005; Jarrett et al. 2006; see Fig. 13.6C). This is a generalised topology applicable to several different (non-biological) transport systems and allows exactly solvable solutions to questions of nutrient flows under different cost scenarios (Ashton et al. 2005; Jarrett et al. 2006). The formula for the average shortest path length across the network comprising a central hub with varying connections (spokes) to a ring of nodes can be calculated and exhibits non-trivial behaviour when different cost functions are imposed on transport through the hub, for example. It is possible to extend this model further to consider a more complicated model of a biological system which contain a ring and hub embedded within another ring, with the original ring–hub motif functioning now as a hub. This process may then be repeated to whatever extent is required by 're-normalising' each ring–hub combination as a hub for the next outer ring, with a cost for using this hub equivalent to the average shortest path of the original ring–hub motif (Jarrett et al. 2006). This enables analysis

of increasingly complex networks by collapsing multiple rings around a very central hub into one structure albeit with a complicated cost function.

IV. Nutrient Transport Through the Network

Although the network architecture is of considerable interest, it only defines which connections are possible at any given time, but not the strength or direction of nutrient transport or signalling fluxes flowing on the network. The precise mechanisms underlying nutrient translocation in fungi are not yet characterised in detail, but are thought to include mass flow, diffusion, generalised cytoplasmic streaming and specific vesicular transport (Jennings 1987; Olsson and Jennings 1991; Olsson and Gray 1998; Cairney 2005; Darrah et al. 2006; see also the chapter by Ashford and Allaway, Chap. 2 in this volume).

A. Transport at the Micron to Millimetre Scale

At the cellular level, many organelles are known to move by motor-driven transport predominantly along the microtubule cytoskeleton, primarily to keep pace with the extending hyphal tip in the apical septal compartment (Fischer 1999; Steinberg 2000; Suelmann and Fischer 2000; Westermann and Prokisch 2002; Hickey et al. 2005; see also the chapters by Fischer and by Sudbery and Court, respectively Chaps. 5 and 6 in this volume). Occasionally much more rapid movements can be observed and may be driven by association with different classes of motor protein (Suelmann and Fischer 2000). For example, during normal growth, migration of the most apical nuclei follows tip elongation, at speeds of 0.1–1.2 $\mu m\ min^{-1}$, with progressive slowing and eventually arrest sub-apically (Suelmann et al. 1997; Fischer 1999). However, during formation of a dikaryon, nuclear migration can be orders of magnitude higher (Suelmann and Fischer 2000) and nuclei can spread over long distances throughout the whole mycelium of the compatible partner. Whilst the nucleus is not normally considered in discussion of nutrient movement, it has been suggested that mobilisation of N and P from DNA can act as a valuable source of nutrients from an osmotically inactive precursor that can be exploited under resource limitation or during secondary branch formation in more mature hyphae (Maheshwari 2005).

Movement of material in vesicles along a cytoskeletal system is perhaps a more traditional mechanism to translocate nutrients over long distances. However, at this stage there is little quantitative information documenting the role of vesicle movement in sub-apical compartments, as most research has focussed on vesicle trafficking events at the tip, particularly the evidence for (or against) endocytosis (e.g. Cole et al. 1997; Hoffmann and Mendgen 1998; Fischer-Parton et al. 2000; Atkinson et al. 2002; Torralba and Heath 2002; Read and Kalkman 2003; Steinberg and Fuchs 2004; Harris and Kwang 2006; see also the chapter by Bourett et al., Chap. 1 in this volume). Motor-driven transport along microtubules can operate at speeds of 1–3 $\mu m\ s^{-1}$ (Steinberg 1998, 2000), which is more than sufficient velocity to bring material to an elongating tip, although the flux depends on the volume of the vesicles and the concentration of the nutrients. To be an effective transport system over several septal compartments or even over a whole colony, a microtubule-based system would require persistent polarised arrays extending over a considerable physical distance. Although there is increasing evidence of a role for microtubules in organelle movement (Xiang and Plamann 2003), only a few studies have documented microtubule arrays over the physical scales needed to explain nutrient transport throughout a colony (see, for example Timonen et al. 2001). Likewise, actin microfilaments are essential for polarised growth and septation, and are involved in organelle movement in apical cells (Steinberg 1998, 2000; Czymmek et al. 2005; Harris and Kwang 2006; see also the chapter by Sudbery and Court, Chap. 6 in this volume), but their role has not been studied in the long-distance transport of vesicles on a millimetre scale or higher.

In addition to small vesicle transport, it has been proposed that the highly dynamic pleiomorphic vacuolar system might have a role in long-distance nutrient translocation (Ashford 1998; Ashford and Allaway 2002; Chap. 2 in this volume). This extensive organelle system is present in filamentous fungi of all the major fungal taxonomic groups so far examined (Ashford 1998; Ashford and Allaway 2002). Several mechanisms have been suggested, including diffusion through connected vacuole compartments, directed transport of small vesicles, 'crawling' of large vacuoles and even peristaltic-like contractions (Ashford 1998; Cole et al. 1998; Bago et al. 2001; Ashford and Allaway

2002; Cairney 2005; see the chapter by Ashford and Allaway, Chap. 2 in this volume). We recently used confocal fluorescence recovery after photobleaching (FRAP) of an internalised fluorescent marker to quantify diffusive transport for different levels of vacuolar organisation moving away from the tip, in combination with a predictive simulation model from these data to determine the transport characteristics of the system over an extended length scale (Darrah et al. 2006). This combined imaging and modelling approach reveals that the vacuole system can have a major impact on solute transport on a millimetre-to-centimetre scale. There is also a strong predicted interaction between vacuolar organisation, available nutrient levels, the predicted diffusion transport distances and the architecture of the branching colony margin. For example, an unbranched hypha possessing a continuous tubular vacuole system can sustain growth over a transport distance ~12–24 mm solely by diffusion through the vacuole system. Conversely, diffusion alone in a maximally branched system would only be sufficient to supply enough resources to the tip over a few millimetres (Darrah et al. 2006).

This poise between translocation being sufficient or insufficient depending on the amount of hyphal branching and status of the vacuolar network suggests that nutrient supply through the vacuolar system could be an important route to co-ordinate tip growth and branching. It is possible that regulation of the connectivity of the vacuolar system could change its translocation capacity according to the local nutrient demand. The system could thus shift between increasing transport to tips, to preventing unnecessary nutrient mobility by isolating tips. Alternatively, and equally likely, is that the vacuolar system translocates material acquired by the tips back into the main colony, against the mass flow component in the cytoplasm needed for tip extension, particularly when growing over an inert substrate (Fig. 13.7). This problem becomes progressively more acute moving basipetally from the tip, as the acropetal flow through the parent hypha has to increase with the number of tips supported. Some reduction in the flow velocity can be achieved by increasing the diameter of the hypha, particularly as volume flow scales with r^4 (see Eq. 13.1). However, fluorescence labelling of the vacuoles and mitochondria in these regions shows that they are anchored in place and buffeted by a cytoplasmic flow (Ashford 1998; Darrah et al. 2006).

It should be noted that the vacuole model does not preclude additional solute translocation pathways that may operate in parallel in the cytoplasm. We are currently working on the measurement and modelling of cytoplasmic and apoplastic diffusion and mass flow pathways, with a view to building an extended model with all compartments represented. It is expected that this will yield useful predictive results for relatively simple branched mycelial systems in the peripheral growth zone. However, there is still remarkably little understanding on how these might interface with the develop-

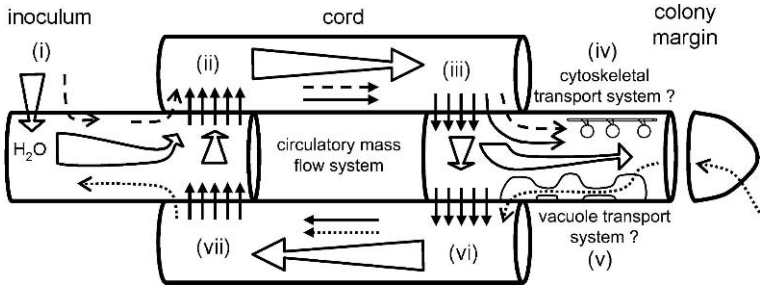

Fig. 13.7. Schematic diagram of possible transport pathways operating in corded mycelial systems. (*i*) Water (*open arrows*) and nutrients (*dashed line*) are initially taken up at the inoculum. *(ii)* An osmotically active solute (*solid arrows*) is loaded into a vessel hypha within a cord to generate an acropetal pressure-driven mass flow that also carries other solutes towards the tips. *(iii)* The osmotic gradient is maintained by solute unloading at the base of the peripheral growth zone. *(iv)* Nutrients needed for growth move towards the tip through a combination of cytoplasmic diffusion, mass flow, vesicle transport and/or diffusion through the vacuole system. Nutrients taken up at the tip have to move backwards against the prevailing direction of mass flow, possibly through the vacuole system (*v*). *(vi)* The majority of the osmotically active solute is loaded into a second vessel hypha to generate a mass flow in the opposite direction to facilitate basipetal transport. *(vii)* Unloading of the solute at the inoculum completes the cycle needed for rapid bi-directional solute movement

ing sub-marginal anastomosis network and cord formation behind the growth front. Clearly an area for future research is to provide detailed anatomical descriptions of the hyphal organisation in these key areas of the colony, to link cell biological investigations at the hyphal level to flux-based measurements at the colony level.

B. Transport at the Millimetre to Centimetre Scale

Detailed temporal and spatial analysis of nutrient fluxes in individual mycelia uses non-invasive mapping of radioisotopes, mainly ^{14}C and ^{32}P. Typically, the final radiolabel distribution is visualised using autoradiography techniques, phosphor-imaging or analysis by destructive harvesting of the tissues followed by scintillation counting. The emerging picture for C and P dynamics is complex, with evidence from studies in microcosms for highly responsive shifts in nutrient allocation depending upon the size and quality of resource units, the sequence of their encounter and the presence of other competing organisms (Boddy 1999). In general, substantial levels of isotope are taken up, but with varying amounts retained at the loading site (Clipson et al. 1987; Olsson and Gray 1998). Net allocation of the remainder through the network is a complex function of multiple competing source–sink relationships (Wells et al. 1995, 1998, 1999). Movement can be bi-directional (Granlund et al. 1985; Olsson and Gray 1998; Lindahl et al. 2001; Nielsen et al. 2002), with features similar to the operation of a circulatory system (Wells et al. 1998).

Absolute rates of translocation vary over at least two orders of magnitude, from 1.8 mm h^{-1} (Olsson and Gray 1998) to 200 mm h^{-1} (Brownlee and Jennings 1982), depending upon the degree that specific transport pathways, such as cords and rhizomorphs, have developed. The most likely system driving transport over these length scales is mass flow, although how the driving force is established and the precise anatomy, connectivity and control of flux through the conduits are not clear. Unlike a cytoskeletal/motor-driven system, the velocity of movement in a mass flow system is relatively uninformative *per se*, as it is a function of the relative cross-sectional area of the different pipes at each level in the branching hierarchy. For example, the water flow rate through a single cord growing out across an inert surface has to scale linearly with the number of growing tips supported and inversely with the cross-sectional area of conducting tissue in the cord in relation to the cross-sectional area of the individual hyphae. In other branching systems there is typically conservation of cross-sectional area at all levels of the branching hierarchy, giving a constant flow rate (West et al. 1997, 2001). We infer that this is not the case in fungal networks, as the diameter of the cords increases at a lower rate than predicted by an area-preserving relationship and conversely the measured (nutrient) velocities are all significantly greater than the tip extension rate. There is also a major conceptual difficulty in setting up a plausible mass flow model that can accommodate bi-directional movement without extremely tight coupling between inflow and outflow at each end of the system. One solution might be to have specialised cells cycling an osmotically active molecule, such as trehalose, at both ends of two adjacent but insulated conduits to generate anti-parallel mass flow (Fig. 13.7). Other nutrients could be loaded and unloaded at any point of the circulating stream as local source–sink patterns change. Interestingly, the rate of solute movement in the cords in such a circulatory mass flow model could be completely uncoupled from the rate of tip growth.

In comparison to C and P, even less information is available for N dynamics, as there is no suitable radioisotope tracer. However, some progress has been made using ^{14}C-aminoisobutyrate (^{14}C-AIB) as a non-metabolised marker for soluble amino acids (Kim and Roon 1982; Watkinson 1984; Lilly et al. 1990; Olsson and Gray 1998; Tlalka et al. 2002, 2003). ^{14}C-AIB shows rapid uptake, bi-directional transport and movement through specific transport pathways in undifferentiated mycelia on agar (Olsson and Gray 1998). Recently, using photon-counting scintillation imaging (PCSI), we showed that N allocation is extremely dynamic, with rapid, preferential N-resource allocation to C-rich sinks, induction of bi-directional transport on cord formation and abrupt switching between different pre-existing transport routes (Tlalka et al. 2002, 2003). These results suggested that our predictions of transport based solely on the network architecture (see Sect. II.C.) are too simplistic. However, we believe that the mismatch between predictions from the simple network model and the experimental data will be a productive area for future research and may give much greater insights into the strategy used by the fungus to control fluxes.

Whilst indeterminate growth and flexible resource allocation are of great benefit in exploiting a patchy resource environment (Boddy 1999; Ettema and Wardle 2002; Watkinson et al. 2006), coordination of these activities poses a considerable challenge within an interconnected, but locally responsive, network (Rayner et al. 1994). In this context, it is interesting to note that there is a significant pulsatile component to N-transport, with evidence for differential behaviour between the assimilatory and foraging mycelia. The pulsatile component can be analysed using Fourier techniques to show that signals from the assimilatory hyphae in the inoculum, new resources and the foraging hyphae all oscillate as distinct domains that are locally synchronised, but are out of phase with each other (Fig. 13.3, see page 312; Tlalka et al., submitted). At this stage we do not know what significance to attribute to the emergence of oscillatory phase domains in terms of global co-ordination within the colony. However, there is an extensive literature on the emergent properties of coupled oscillatory systems (see, for example Strogatz 2001) and it is tempting to speculate that coupled oscillatory behaviour may reflect underlying pattern formation in basidiomycete fungi, as with other simple microbial systems (Gerisch 1987; Dormann et al. 2002; Ueda 2005). This may represent a general principle used by self-organising biological systems to achieve global co-ordination and solve complex routing problems (Nakagaki et al. 2000, 2004; Tero et al. 2006).

V. Conclusion: Future Prospects

The past few years have seen massive advances in the technology available to address fundamental questions in fungal biology. Live cell imaging, molecular techniques and green fluorescent protein fusions are set to revolutionise our understanding of sub-cellular dynamics in a similar manner to results in the plant field (Brandizzi et al. 2002; Fricker et al. 2006; see also the chapters by Ashford and Allaway, and Bourett et al., respectively Chaps. 1 and 2 in this volume). New radioisotope imaging techniques are adding dynamics to our understanding of nutrient fluxes at the colony level (Gray et al. 1995; Timonen et al. 1996; Olsson and Gray 1998; Lindahl et al. 2001; Tlalka et al. 2002, 2003), whilst tools from graph theory may start to provide insights into the crucial network organisation and behaviour within the colony. Indeed, it is not impossible that detailed characterisation of such self-organised, adaptive networks and their dynamical behaviour may inform strategies to improve the design of anthropogenic infrastructure networks. Finally, a range of mathematical models is being developed that have the potential to draw together results from all these disparate strands and synthesise a coherent picture of colony growth and function for the first time.

Acknowledgements. Research in the authors' laboratories has been supported by BBSRC (43/P19284), NERC (GR3/12946, NER/A/S/2002/882), EPSRC (GR/S63090/01), EU Framework 6 (STREP No. 12999), the Oxford University Research Infrastructure Fund and the University Dunston Bequest. We thank A. Ashford, K. Burton, P.R. Darrah, D.P. Donnelly, D. Eastwood, J. Efstathiou, J. Hynes, N. Johnson, F. Reed-Tsochas, M. Tlalka, G.M. Tordoff, S.C. Watkinson and members of CABDyN for stimulating discussion.

References

Albert R, Barabasi AL (2002) Statistical mechanics of complex networks. Rev Mod Phys 74:47–97

Alon N, Yuster R, Zwick U (1997) Finding and counting given length cycles. Algorithmica 17:209–223

Amaral LAN, Ottino JM (2004) Complex networks – augmenting the framework for the study of complex systems. Eur Phys J B 38:147–162

Ashford AE (1998) Dynamic pleiomorphic vacuole systems: are they endosomes and transport compartments in fungal hyphae? Adv Bot Res 28:119–159

Ashford AE, Allaway WG (2002) The role of the motile tubular vacuole system in mycorrhizal fungi. Plant Soil 244:177–187

Ashton DJ, Jarrett TC, Johnson NF (2005) Effect of congestion costs on shortest paths through complex networks. Phys Rev Lett 94:1–4

Atkinson HA, Daniels A, Read ND (2002) Live-cell imaging of endocytosis during conidial germination in the rice blast fungus, *Magnaporthe grisea*. Fungal Genet Biol 37:233–244

Bago B, Pfeffer P, Shachar-Hill Y (2001) Could the urea cycle be translocating nitrogen in the arbuscular mycorrhizal symbiosis? New Phytol 149:4–8

Ball MO, Provan JS (1983) Calculating bounds on reachability and connectedness in stochastic networks. Networks 13:253–278

Barabasi AL, Albert R (1999) Emergence of scaling in random networks. Science 286:509–512

Barrat A, Barthelemy M, Pastor-Satorras R, Vespignani A (2004) The architecture of complex weighted networks. Proc Natl Acad Sci USA 101:3747–3752

Barrat A, Barthelemy M, Vespignani A (2005) The effects of spatial constraints on the evolution of weighted complex networks. J Stat Mech 5:49–68

Barthelemy M, Barrat A, Pastor-Satorras R, Vespignani A (2005) Characterization and modeling of weighted networks. Physica A 346:34–43

Bartnicki-Garcia S, Hergert F, Gierz G (1989) Computer-simulation of fungal morphogenesis and the mathematical basis for hyphal (tip) growth. Protoplasma 153:46–57

Bezzi M, Ciliberto A (2004) Mathematical modelling of filamentous microorganisms. http://arxivorg/abs/q-bio/0402004

Boddy L (1993) Saprotrophic cord-forming fungi – warfare strategies and other ecological aspects. Mycol Res 97:641–655

Boddy L (1999) Saprotrophic cord-forming fungi: meeting the challenge of heterogeneous environments. Mycologia 91:13–32

Boddy L, Donnelly DP (2006) Fractal geometry and microorganisms in the environment. In: Senesi N, Wilkinson K (eds) Fractal structures and processes in the environment. IUPAC, London

Boddy L, Wells JM, Culshaw C, Donnelly DP (1999) Fractal analysis in studies of mycelium in soil. Geoderma 88:301–328

Boswell GP, Jacobs H, Davidson FA, Gadd GM, Ritz K (2002) Functional consequences of nutrient translocation in mycelial fungi. J Theor Biol 217:459–477

Boswell GP, Jacobs H, Davidson FA, Gadd GM, Ritz K (2003a) Growth and function of fungal mycelia in heterogeneous environments. Bull Math Biol 65:447–477

Boswell GP, Jacobs H, Davidson FA, Gadd GM, Ritz K (2003b) A positive numerical scheme for a mixed-type partial differential equation model for fungal growth. Appl Math Comp 138:321–340

Boswell GP, Jacobs H, Ritz K, Gadd GM, Davidson FA (2006) The development of fungal networks in complex environments. Bull Math Biol. DOI 10.1007/s11538-005-9056-6

Brandizzi F, Fricker M, Hawes C (2002) A greener world: the revolution in plant bioimaging. Nature Rev Mol Cell Biol 3:520–530

Brownlee C, Jennings DH (1982) Long-distance translocation in *Serpula lacrimans* – velocity estimates and the continuous monitoring of induced perturbations. Trans Br Mycol Soc 79:143–148

Buhl J, Gautrais J, Sole RV, Kuntz P, Valverde S, Deneubourg JL, Theraulaz G (2004) Efficiency and robustness in ant networks of galleries. Eur Phys J B 42:123–129

Buller AHR (1931) Researches on fungi, vol 4. Longmans Green, London

Buller AHR (1933) Researches on fungi, vol 5. Longmans Green, London

Cairney JWG (2005) Basidiomycete mycelia in forest soils: dimensions, dynamics and roles in nutrient distribution. Mycol Res 109:7–20

Caldarelli G, Pastor-Satorras R, Vespignani A (2004) Structure of cycles and local ordering in complex networks. Eur Phys J B 38:183–186

Cardillo A, Scellato S, Latora V, Porta S (2006) Structural properties of planar graphs of urban street patterns. Phys Rev E 73:066107

Clipson NJW, Cairney JWG, Jennings DH (1987) The physiology of basidiomycete linear organs.1. Phosphate-uptake by cords and mycelium in the laboratory and the field. New Phytol 105:449–457

Cole L, Hyde GJ, Ashford AE (1997) Uptake and compartmentalisation of fluorescent probes by *Pisolithus tinctorius* hyphae: evidence for an anion transport mechanism at the tonoplast but not for fluid-phase endocytosis. Protoplasma 199:18–29

Cole L, Orlovich DA, Ashford AE (1998) Structure, function, and, motility of vacuoles in filamentous fungi. Fungal Genet Biol 24:86–100

Crawford JW, Ritz K, Young IM (1993) Quantification of fungal morphology, gaseous transport and microbial dynamics in soil – an integrated framework utilizing fractal geometry. Geoderma 56:157–172

Crawford JW, Pachepsky YA, Rawls WJ (1999) Integrating processes in soils using fractal models. Geoderma 88:103–107

Czymmek KJ, Bourett TM, Shao Y, DeZwaan TM, Sweigard JA, Howard RJ (2005) Live-cell imaging of tubulin in the filamentous fungus *Magnaporthe grisea* treated with anti-microtubule and anti-microfilament agents. Protoplasma 225:23–32

Darrah PR, Tlalka M, Ashford A, Watkinson SC, Fricker MD (2006) The vacuole system is a significant intracellular pathway for longitudinal solute transport in basidiomycete fungi. Eukaryot Cell 5:1111–1125

Davidson FA (1998) Modelling the qualitative response of fungal mycelia to heterogeneous environments. J Theor Biol 195:281–292

Davidson FA, Olsson S (2000) Translocation induced outgrowth of fungi in nutrient-free environments. J Theor Biol 205:73–84

Davidson FA, Park AW (1998) A mathematical model for fungal development in heterogeneous environments. Appl Math Lett 11:51–56

Davidson FA, Sleeman BD, Rayner ADM, Crawford JW, Ritz K (1996) Context-dependent macroscopic patterns in growing and interacting mycelial networks. Proc R Soc Lond Ser B 263:873–880

Davidson FA, Sleeman BD, Rayner ADM, Crawford JW, Ritz K (1997) Travelling waves and pattern formation in a model for fungal development. J Math Biol 35:589–608

Donnelly DP, Wilkins MF, Boddy L (1995) An integrated image-analysis approach for determining biomass, radial extent and box-count fractal dimension of macroscopic mycelial systems. Binary 7:19–28

Dormann D, Vasiev B, Weijer CJ (2002) Becoming multicellular by aggregation; The morphogenesis of the social amoebae *Dicyostelium discoideum*. J Biol Phys 28:765–780

Dorogovtsev SN, Mendes JFF (2002) Evolution of networks. Adv Phys 51:1079–1187

Edelstein L (1982) The propagation of fungal colonies – a model for tissue-growth. J Theor Biol 98:679–701

Edelstein L, Segel LA (1983) Growth and metabolism in mycelial fungi. J Theor Biol 104:187–210

Edelstein L, Hadar Y, Chet I, Henis Y, Segel LA (1983) A model for fungal colony growth applied to *Sclerotium rolfsii*. J Gen Microbiol 129:1873–1881

Edelstein-Keshet L, Ermentrout B (1989) Models for branching networks in 2 dimensions. SIAM J Appl Math 49:1136–1157

Ermentrout GB, Edelstein-Keshet L (1993) Cellular automata approaches to biological modeling. J Theor Biol 160:97–133
Ettema CH, Wardle DA (2002) Spatial soil ecology. Trends Ecol Evol 17:177–183
Fischer R (1999) Nuclear movement in filamentous fungi. FEMS Microbiol Rev 23:39–68
Fischer-Parton S, Parton RM, Hickey PC, Dijksterhuis J, Atkinson HA, Read ND (2000) Confocal microscopy of FM4-64 as a tool for analysing endocytosis and vesicle trafficking in living fungal hyphae. J Microsc 198:246–259
Fleissner A, Sarkar S, Jacobson DJ, Roca MG, Read ND, Glass NL (2005) The *so* locus is required for vegetative cell fusion and postfertilization events in *Neurospora crassa*. Eukaryot Cell 4:920–930
Freeman LC (1977) Set of measures of centrality based on betweenness. Sociometry 40:35–41
Fricker M, Runions J, Moore I (2006) Quantitative fluorescence microscopy: from art to science. Annu Rev Plant Biol 57:79–107
Geitmann A (2006) Plant and fungal cytomechanics: quantifying and modeling cellular architecture. Can J Bot 84:581–593
Gerisch G (1987) Cyclic-AMP and other signals controlling cell-development and differentiation in *Dictyostelium*. Annu Rev Biochem 56:853–879
Gierz G, Bartnicki-Garcia S (2001) A three-dimensional model of fungal morphogenesis based on the vesicle supply center concept. J Theor Biol 208:151–164
Glass NL, Jacobson DJ, Shiu PKT (2000) The genetics of hyphal fusion and vegetative incompatibility in filamentous ascomycete fungi. Annu Rev Genet 34:165–186
Glass NL, Rasmussen C, Roca MG, Read ND (2004) Hyphal homing, fusion and mycelial interconnectedness. Trends Microbiol 12:135–141
Gol'dshtein V, Koganov GA, Surdutovich GI (2004) Vulnerability and hierarchy of complex networks. http://arXivorg/abs/cond-mat/0409298
Granlund HI, Jennings DH, Thompson W (1985) Translocation of solutes along rhizomorphs of *Armillaria mellea*. Trans Br Mycol Soc 84:111–119
Gray SN, Dighton J, Olsson S, Jennings DH (1995) Real-time measurement of uptake and translocation of Cs-137 within mycelium of *Schizophyllum commune* Fr by autoradiography followed by quantitative image-analysis. New Phytol 129:449–465
Gregory PH (1984) The fungal mycelium: an historical perspective. Trans Br Mycol Soc 82:1–11
Haggett P, Chorley RJ (1969) Network analysis in geography. Arnold, London
Hankin RKS (2006) The resistor array package. http://wwwcranr-projectorg
Harold S, Tordoff GM, Jones TH, Boddy L (2005) Mycelial responses of *Hypholoma fasciculare* to collembola grazing: effect of inoculum age, nutrient status and resource quality. Mycol Res 109:927–935
Harris SD, Kwang WJ (2006) Cell polarity in filamentous fungi: shaping the mold. Int Rev Cytol 251:41–77
Hickey PC, Jacobson DJ, Read ND, Glass NL (2002) Live-cell imaging of vegetative hyphal fusion in *Neurospora crassa*. Fungal Genet Biol 37:109–119
Hickey PC, Swift SR, Roca MG, Read ND (2005) Live-cell imaging of filamentous fungi using vital fluorescent dyes and confocal microscopy. Methods Microbiol 34:63–87
Hoffmann J, Mendgen K (1998) Endocytosis and membrane turnover in the germ tube of *Uromyces fabae*. Fungal Genet Biol 24:77–85
Hutchinson SA, Sharma P, Clarke KR, Macdonald I (1980) Control of hyphal orientation in colonies of *Mucor hiemalis*. Trans Br Mycol Soc 75:177–191
Isaaks EH, Srivastava RM (1989) Applied geostatistics. Oxford University Press, New York
Jacobs H, Boswell GP, Scrimgeour CM, Davidson FA, Gadd GM, Ritz K (2004) Translocation of carbon by *Rhizoctonia solani* in nutritionally-heterogeneous microcosms. Mycol Res 108:453–462
Jarrett TC, Ashton DJ, Fricker M, Johnson NF (2006) Interplay between function and structure in complex networks. Phys Rev D 74:026116
Jennings DH (1987) Translocation of solutes in fungi. Biol Rev 62:215–243
Kim KW, Roon RJ (1982) Transport and metabolic effects of alpha-aminoisobutyric-acid in *Saccharomyces cerevisiae*. Biochim Biophys Acta 719:356–362
Latora V, Marchiori M (2001) Efficient behavior of small-world networks. Phys Rev Lett 87:198701
Latora V, Marchiori M (2003) Economic small-world behavior in weighted networks. Eur Phys J B 32: 249–263
Leake JR, Johnson D, Donnelly DP, Muckle GE, Boddy L, Read DJ (2004) Networks of power and influence: the role of mycorrhizal mycelium in controlling plant communities and agroecosystem functioning. Can J Bot 82:1016–1045
Lejeune R, Baron GV (1995) On the use of morphological measurements for the quantification of fungal growth. Biotechnol Tech 9:327–328
Lejeune R, Baron GV (1997) Simulation of growth of a filamentous fungus in 3 dimensions. Biotechnol Bioeng 53:139–150
Lejeune R, Baron GV (1998) Modeling the exponential growth of filamentous fungi during batch cultivation. Biotechnol Bioeng 60:169–179
Lejeune R, Nielsen J, Baron GV (1995) Morphology of *Trichoderma reesei* QM-9414 in submerged cultures. Biotechnol Bioeng 47:609–615
Liddell CM, Hansen D (1993) Visualizing complex biological interactions in the soil ecosystem. J Vis Comp Anim 4:3–12
Lilly WW, Higgins SM, Wallweber GJ (1990) Uptake and translocation of 2-aminoisobutyric acid by *Schizophyllum commune*. Exp Mycol 14:169–177
Lindahl B, Finlay R, Olsson S (2001) Simultaneous, bidirectional translocation of ^{32}P and ^{33}P between wood blocks connected by mycelial cords of *Hypholoma fasciculare*. New Phytol 150:189–194
Lindenmayer A (1968) Mathematical models for cellular interaction in development, parts I and II. J Theor Biol 18:280–315
Lopez JM, Jensen HJ (2002) Generic model of morphological changes in growing colonies of fungi. Phys Rev E 65:021903
Maheshwari R (2005) Nuclear behavior in fungal hyphae. FEMS Microbiol Lett 249:7–14
Meškauskas A, Fricker MD, Moore D (2004a) Simulating colonial growth of fungi with the Neighbour-Sensing model of hyphal growth. Mycol Res 108:1241–1256

Meškauskas A, McNulty LJ, Moore D (2004b) Concerted regulation of all hyphal tips generates fungal fruit body structures: experiments with computer visualizations produced by a new mathematical model of hyphal growth. Mycol Res 108:341–353
Mihail JD, Obert M, Bruhn JN, Taylor SJ (1995) Fractal geometry of diffuse mycelia and rhizomorphs of *Armillaria s*pecies. Mycol Res 99:81–88
Nakagaki T, Yamada H, Toth A (2000) Maze-solving by an amoeboid organism. Nature 407:470–470
Nakagaki T, Yamada H, Hara M (2004) Smart network solutions in an amoeboid organism. Biophys Chem 107:1–5
Newman MEJ (2003) The structure and function of complex networks. SIAM Rev 45:167–256
Nielsen JS, Joner EJ, Declerck S, Olsson S, Jakobsen I (2002) Phospho-imaging as a tool for visualization and noninvasive measurement of P transport dynamics in arbuscular mycorrhizas. New Phytol 154:809–819
Olsson S (1999) Nutrient translocation and electrical signalling in mycelia. In: Gow NAR, Robson GD, Gadd GM (eds) The fungal colony. Cambridge University Press, Cambridge, pp 25–48
Olsson S (2001) Colonial growth of fungi. In: Howard RJ, Gow NAR (eds) The Mycota, vol VIII. Biology of the fungal cell. Springer, Berlin Heidelberg New York, pp 125–141
Olsson S, Gray SN (1998) Patterns and dynamics of ^{32}P-phosphate and labelled 2-aminoisobutyric acid (^{14}C-AIB) translocation in intact basidiomycete mycelia. FEMS Microbiol Ecol 26:109–120
Olsson S, Jennings DH (1991) Evidence for diffusion being the mechanism of translocation in the hyphae of 3 molds. Exp Mycol 15:302–309
Pringle A, Taylor JW (2002) The fitness of filamentous fungi. Trends Microbiol 10:474–481
Prosser JI (1995a) Kinetics of filamentous growth and branching. In: Gow NAR, Gadd GM (eds) The growing fungus. Chapman and Hall, London, pp 301–318
Prosser JI (1995b) Mathematical modelling of fungal growth. In: Gow NAR, Gadd GM (eds) The growing fungus. Chapman and Hall, London, pp 319–336
Prosser JI, Trinci APJ (1979) Model for hyphal growth and branching. J Gen Microbiol 111:153–164
Prusinkiewicz P (2004) Modelling plant growth and development. Curr Opin Plant Biol 7:79–83
Prusinkiewicz P, Lindenmayer A (1990) The algorithmic beauty of plants. Springer, Berlin Heidelberg New York
Prusinkiewicz P, Rolland-Lagan AG (2006) Modeling plant morphogenesis. Curr Opin Plant Biol 9:83–88
Rayner ADM (1991) The challenge of the individualistic mycelium. Mycologia 83:48–71
Rayner ADM, Griffith GS, Ainsworth AM (1994) Mycelial interconnectedness. In: Gow NAR, Gadd GM (eds) The growing fungus. Chapman and Hall, London, pp 21–40
Rayner ADM, Watkins ZR, Beeching JR (1999) Self-integration – an emerging concept from the fungal mycelium. In: Gow NAR, Robson GD, Gadd GM (eds) The fungal colony. Cambridge University Press, Cambridge, pp 1–24
Read D (1997) Mycorrhizal fungi – the ties that bind. Nature 388:517–518
Read DJ, Perez-Moreno J (2003) Mycorrhizas and nutrient cycling in ecosystems – a journey towards relevance? New Phytol 157:475–492
Read ND, Kalkman ER (2003) Does endocytosis occurr in fungal hyphae? Fungal Genet Biol 39:199–203
Regalado CM, Crawford JW, Ritz K, Sleeman BD (1996) The origins of spatial heterogeneity in vegetative mycelia: a reaction-diffusion model. Mycol Res 100:1473–1480
Ripley BD (2004) Spatial statistics. Wiley, New York
Ritz K, Crawford J (1990) Quantification of the fractal nature of colonies of *Trichoderma viride*. Mycol Res 94:1138–1141
Ritz K, Millar SM, Crawford JW (1996) Detailed visualisation of hyphal distribution in fungal mycelia growing in heterogeneous nutritional environments. J Microbiol Methods 25:23–28
Roca MG, Davide LC, Mendes-Costa MC, Wheals A (2003) Conidial anastomosis tubes in *Colletotrichum*. Fungal Genet Biol 40:138–145
Roca MG, Davide LC, Davide LMC, Schwan RF, Wheals AE (2004) Conidial anastornosis fusion between *Colletotrichum* species. Mycol Res 108:1320–1326
Roca MG, Arlt J, Jeffree CE, Read ND (2005a) Cell biology of conidial anastomosis tubes in *Neurospora crassa*. Eukaryot Cell 4:911–919
Roca MG, Read ND, Wheals AE (2005b) Conidial anastomosis tubes in filamentous fungi. FEMS Microbiol Lett 249:191–198
Simard SW, Durall DM (2004) Mycorrhizal networks: a review of their extent, function, and importance. Can J Bot 82:1140–1165
Simard SW, Perry DA, Jones MD, Myrold DD, Durall DM, Molina R (1997) Net transfer of carbon between ectomycorrhizal tree species in the field. Nature 388:579–582
Soddell F, Seviour R, Soddell J (1995) Using Lindenmayer systems to investigate how filamentous fungi may produce round colonies. Complexity Int 2
Steinberg G (1998) Organelle transport and molecular motors in fungi. Fungal Genet Biol 24: 161–177
Steinberg G (2000) The cellular roles of molecular motors in fungi. Trends Microbiol 8:162–168
Steinberg G, Fuchs U (2004) The role of microtubules in cellular organization and endocytosis in the plant pathogen *Ustilago maydis*. J Microsc 214:114–123
Strogatz SH (2001) Exploring complex networks. Nature 410:268–276
Suelmann R, Fischer R (2000) Nuclear migration in fungi – different motors at work. Res Microbiol 151:247–254
Suelmann R, Sievers N, Fischer R (1997) Nuclear traffic in fungal hyphae: in vivo study of nuclear migration and positioning in *Aspergillus nidulans*. Mol Microbiol 25:757–769
Tero A, Kobayashi R, Nakagaki T (2006) Physarum solver: a biologically inspired method of road-network navigation. Physica A 363:115–119
Timonen S, Finlay RD, Olsson S, Soderstrom B (1996) Dynamics of phosphorus translocation in intact ectomycorrhizal systems: non-destructive monitoring using a beta-scanner. FEMS Microbiol Ecol 19:171–180
Timonen S, Smith FA, Smith SE (2001) Microtubules of the mycorrhizal fungus *Glomus intraradices* in symbiosis with tomato roots. Can J Bot 79:307–313
Tindemans SH, Kern N, Mulder BM (2006) The diffusive vesicle supply center model for tip growth in fungal hyphae. J Theor Biol 238:937–948

Tlalka M, Watkinson SC, Darrah PR, Fricker MD (2002) Continuous imaging of amino-acid translocation in intact mycelia of *Phanerochaete velutina* reveals rapid, pulsatile fluxes. New Phytol 153:173–184

Tlalka M, Hensman D, Darrah PR, Watkinson SC, Fricker MD (2003) Noncircadian oscillations in amino acid transport have complementary profiles in assimilatory and foraging hyphae of *Phanerochaete velutina*. New Phytol 158:325–335

Torralba S, Heath IB (2002) Analysis of three separate probes suggests the absence of endocytosis in *Neurospora crassa* hyphae. Fungal Genet Biol 37:221–232

Trinci APJ, Wiebe MG, Robson GD (1994) The mycelium as an integrated entity. In: Wessels JGH, Meinhardt F (eds) Growth, differentiation and sexuality. Springer, Berlin Heidelberg New York, pp 175–193

Tunbridge A, Jones H (1995) An L-Systems approach to the modeling of fungal growth. J Vis Comp Anim 6:91–107

Ueda T (2005) An intelligent slime mold: a self-organizing system of cell shape and information. In: Armbruster D, Kaneko K, Mikhailov AS (eds) Networks of interacting machines: production organisation in complex industrial systems and biological cells. World Scientific, Singapore, pp 1–35

Watkinson SC (1984) Inhibition of growth and development of *Serpula lacrimans* by the non-metabolized amino-acid analog alpha-aminoisobutyric-acid. FEMS Microbiol Lett 24:247–250

Watkinson SC, Bebber D, Darrah PR, Fricker MD, Tlalka M, Boddy L (2006) The role of wood decay fungi in the carbon and nitrogen dynamics of the forest floor. In: Gadd GM (ed) Fungi in biogeochemical cycles. Cambridge University Press, Cambridge, pp 151–181

Watts DJ, Strogatz SH (1998) Collective dynamics of 'small-world' networks. Nature 393:440–442

Wells JM, Boddy L, Evans R (1995) Carbon translocation in mycelial cord systems of *Phanerochaete velutina* (Dc, Pers) Parmasto. New Phytol 129:467–476

Wells JM, Harris MJ, Boddy L (1998) Temporary phosphorus partitioning in mycelial systems of the cord-forming basidiomycete *Phanerochaete velutina*. New Phytol 140:283–293

Wells JM, Harris MJ, Boddy L (1999) Dynamics of mycelial growth and phosphorus partitioning in developing mycelial cord systems of *Phanerochaete velutina*: dependence on carbon availability. New Phytol 142:325–334

West GB, Brown JH, Enquist BJ (1997) A general model for the origin of allometric scaling laws in biology. Science 276:122–126

West GB, Brown JH, Enquist BJ (2001) A general model for ontogenetic growth. Nature 413:628–631

Westermann B, Prokisch H (2002) Mitochondrial dynamics in filamentous fungi. Fungal Genet Biol 36:91–97

Xiang X, Plamann M (2003) Cytoskeleton and motor proteins in filamentous fungi. Curr Opin Microbiol 6:628–633

Yang H, King R, Reichl U, Gilles ED (1992a) Mathematical-model for apical growth, septation, and branching of mycelial microorganisms. Biotechnol Bioeng 39:49–58

Yang H, Reichl U, King R, Gilles ED (1992b) Measurement and simulation of the morphological development of filamentous microorganisms. Biotechnol Bioeng 39:44–48

Biosystematic Index

Achlya ambisexualis, 260
Achlya bisexualis, 229, 240, 244, 245
agarics, 292
Agrobacterium, 303
Albugo, 256
Allomyces macrogynus, 240
Alternaria solani, 229
Arabidopsis thaliana, 34, 75
ascomycetes, 292
Ascomycota, 28
Ashbya gossypii, 138, 143, 146, 156
Aspergillus, 51, 107, 108, 111, 258
Aspergillus flavus, 100, 103, 112
Aspergillus fumigatus, 2, 103, 104, 108–112
Aspergillus kawachii, 103
Aspergillus nidulans, 2, 4, 6, 7, 10, 11, 14, 16, 18, 22–37, 39, 59, 63, 90, 100, 103, 108, 109, 111, 112, 137, 144, 156, 157, 167, 241
Aspergillus niger, 23, 32, 103, 104, 109, 112, 145, 238, 275
Aspergillus oryzae, 51, 54, 55, 58, 63, 73, 90, 103, 112
Aureobasidium pullulans, 238

Basidiobolus microsporus, 240
basidiomycetes, 292
Basidiomycota, 25, 26, 28, 49, 50, 61, 292
Blastomyces dermatitidis, 100, 101, 107, 109
Blumeria graminis, 107, 254, 256, 257, 270
Blumeria graminis f. sp. *hordei*, 246, 265, 269, 271
Blumeria graminis f.sp. *avenae*, 263
boletes, 292
Botryodiplodia theobromae, 260
Botrytis cinerea, 4, 6, 10, 14, 18, 22, 242, 243, 261, 268, 275

Candida, 108
Candida albicans, 32, 100, 106, 107, 109–111, 137, 138, 141, 143, 144, 167
Candida glabrata, 100, 106, 168
Candida guilliermondii, 32
Candida lusitaniae, 32
Candida tropicalis, 100
Chaetomium globosum, 4, 6, 10, 14, 18, 22
Claviceps purpurea, 274
Coccidioides immitis, 4, 6, 10, 14, 18, 22, 102, 103, 168
Cochliobolus carbonum, 275
Cochliobolus heterostrophus, 220, 257
Cochliobolus sativus, 269
Collembola, 319
Colletotrichum, 246, 247, 265, 270, 272
Colletotrichum carbonum, 276
Colletotrichum gloeosporioides, 257, 269, 273
Colletotrichum graminicola, 40, 53, 221, 246, 254, 264, 268
Colletotrichum kahawae, 266
Colletotrichum lagenarium, 257, 266
Colletotrichum lindemuthianum, 32, 222, 255, 256, 266, 268, 269, 271, 272, 275
Colletotrichum trifollii, 226, 230, 257
Coprinopsis cinerea, 297
Coprinus cinerea, 107
Coprinus sterquilinus, 311–315
Cryptococcus neoformans, 4, 6, 10, 14, 18, 22, 65, 102, 104, 105, 108–112, 171, 298
Cymadothea trifolii, 274

Debaryomyces hansenii, 107

Entamoeba, 28
Escherichia coli, 66
Eucalyptus pilularis, 70, 72
Eucalyptus seiberi, 254, 259
Exophiala (Wangiella) dermatitidis, 65, 100, 109, 245
Exophiala dermatitidis, 65, 109

Fusarium acuminatum, 100
Fusarium graminearum, 42, 109, 227, 274, 275
Fusarium oxysporum, 100, 102, 276
Fusarium sulphureum, 100
Fusarium verticillioides, 25

Geotrichum candidum, 245, 257
Giardia, 28
Gibberella zeae, 103, 107, 109, 112
Gigaspora margarita, 50, 70
Gigaspora rosea, 295
Gilbertella persicaria, 38, 39, 245
Glomus claroideum, 295
Glomus intraradices, 50, 65, 70, 74, 295, 297

Hanseniaspora osmophila, 100
Hansenula anomala, 100
Hebeloma cylindrosporum, 294
Helicobasidium mompa, 28
Heterobasidion annosum, 297
Histoplasma capsulatum, 100–102, 168
Homo sapiens, 5–10, 12–22, 26, 27, 29, 31, 32, 34–37, 39, 41
Hyaloperonospora parasitica, 255

Idriella bolleyi, 257

Kluyveromyces lactis, 100, 107
Kluyveromyces waltii, 24

Laccaria bicolor, 76, 296

Lotus japonicus, 295

Magnaporthe, 52
Magnaporthe grisea, 4, 6, 10, 14, 18, 22, 25, 32, 38–40, 52, 90, 103, 107, 109, 111, 112, 220, 221, 230, 238, 240, 245–247, 252, 254, 257–259, 264–266, 268
Magnaporthe poae, 269
Megacollybia platyphylla, 312
Melampsora, 265
Melampsora larici-populina, 258, 297
Melampsora lini, 264, 270–272
Metarhizium anisopliae, 230
Mucor hiemalis, 239, 241

Nectria haematococca, 63, 220, 221, 254, 256
Neolecta, 93
Neurospora, 51, 52, 72
Neurospora crassa, 4, 6, 10, 11, 14, 18, 22, 52, 62, 63, 67, 88, 100, 103, 104, 107, 109, 111, 112, 137, 138, 146, 158, 167, 227, 239, 241

Oomycota, 50, 58, 61
orchids, 292

Paracoccidioides brasiliensis, 101, 168
Paxillus involutus, 74, 75
Penicillium chrysogenum, 112
Penicillium marneffei, 100, 102, 103, 138, 146
Penicillium variotii, 109
Pestalotia malicola, 256
Phanerochaete, 49, 51, 54, 57, 58
Phanerochaete chrysosporium, 34, 298
Phanerochaete velutina, 49, 54, 55, 57, 68, 73, 311–317, 319
Phaseolus vulgaris, 272
Phialocephala fortinii, 66
Phialophora fortinii, 73
Phyllosticta ampelicida, 221, 222, 254
Phytophthora, 252, 253, 257, 260, 274
Phytophthora cinnamomi, 221, 222, 245, 252, 254, 256, 258–260, 264
Phytophthora infestans, 226, 229, 253, 256, 275
Phytophthora nicotianae, 252, 256
Phytophthora palmivora, 224, 226, 229, 253
Phytophthora parasitica, 226
Phytophthora ramorum, 256
Phytophthora sojae, 252, 256
Pichia angusta, 107
Pichia membranaefaciens, 100
Pichia pastoris, 28, 29, 38
Pisolithus, 49–51, 54, 57, 58, 65
Pisolithus microcarpus, 49, 70, 295
Pisolithus tinctorius, 49, 52, 54, 59, 62, 66, 67, 72, 73, 76
Plasmopara, 256
Pleurotus ostreatus, 297

Puccinia, 262, 265
Puccinia arachidis, 271
Puccinia graminis f. sp. *tritici*, 263, 265
Puccinia hordei, 255, 263
Pythium, 243, 252, 256, 257
Pythium aphanidermatum, 227, 253
Pythium graminicola, 243
Pythium insidiosum, 243

Rhizoctonia, 262, 292
Rhizoctonia oryzae, 4, 6, 10, 14, 22, 31, 261
Rhizoctonia solani, 155, 321

Saccharomyces cerevisiae, 4, 6, 7, 10, 11, 14, 16, 18, 22–27, 29–37, 39, 41, 50–54, 56, 58, 60–64, 66–68, 70–76, 98, 100, 106–112, 137–143, 167
Saccharomyces rouxii, 100
Saprolegnia ferax, 62, 227, 258, 261
Schizophyllum commune, 100
Schizosaccharomyces pombe, 29, 32, 62, 63, 75, 99, 107–110, 138, 141, 144, 146, 167
Sclerotinia, 274
Sclerotinia sclerotiorum, 4, 6, 10, 14, 18, 22, 260, 265, 275
Sclerotium rolfsii, 100, 261
Sporothrix schenckii, 101, 104, 109

Thraustotheca clavata, 239, 241
Trichoderma viride, 28, 33
Tricholomataceae, 292
Trichophyton mentagrophytes, 100
Trichosporon cutaneum, 105
Trigonopsis variabilis, 100
truffles, 292

Uncinula necator, 256
Uromyces, 265, 272
Uromyces appendiculatus, 221, 254, 263–266
Uromyces fabae, 52, 254, 256, 269, 272, 273
Uromyces phaseoli, 62
Uromyces viciae-fabae, 255
Uromyces vignae, 269
Ustilago maydis, 26, 32, 37, 42, 52–54, 61–63, 104–106, 108–111, 297

Vicia faba, 255, 269

Wangiella dermatitidis, 245

Xenopus, 273

Yarrowia lipolytica, 106

Zoophthora radicans, 230
Zygomycota, 1

Subject Index

^{14}C-aminoisobutyrate, 325
5-deoxy-strigol, 295

a1-α2 complex, 207
acridine orange, 51
actin, 26, 34, 37, 38, 63, 142, 185, 258
  actomyosin ring, 140–142, 149, 150
  anti-actin drugs, 62
  cables, 138, 142
  caps, 62
  cortical patches, 142
  cytoskeleton, 142
  filasome, 37, 38
  microfilaments, 258, 323
  plaques, 62
actomyosin ring, 151
ade2, 51, 52, 57
adenylyl cyclase, 176
adhesins, 300
adhesion, 101, 178, 183, 219–225, 238, 253–257
affinity probes, 24
Alexa dyes, 53
alkaline phosphatase, 53, 60, 73
α-1,3-glucan, 99, 101, 102, 104, 105, 112
α-1,6-galactan, 106
α-factor, 71
α-tubulin, 62
AmCyan, 53, 56
amino acid permeases, 273
amino acid starvation, 171
amoeboid locomotion, 237
anaplerotic pathway, 301
anastomoses, 309, 311
anastomosis, 320, 321
aniline blue, 105
antibiotic
  macrolide, 68
antibody, 66
  exopolyphosphatase, 66
AoVam3p, 51, 54
AP-3 adaptor protein, 73
AP-3 complex, 53
apical vesicles, 33, 52, 53, 258–262
appressoria, 37, 90, 228, 230, 238, 246, 253–270
ApsA, 127
APSES family, 177
arbuscular mycorrhiza, 291
ARF-GAP, 10, 24, 31, 41
ARF-GEF, 10, 21, 31, 32
arginine, 67
armadillo repeats, 54
Arp1, 63
Arp2/3, 151
ASH1, 143
atmA, 129
atomic force microscopy, 238, 241, 247
ATP, 67, 68
  driven chaperone, 60
  hydrolysis, 60, 68
  synthase, 68
ATPase, 67
  Mg^{2+}-ATPases, 75
  plasma membrane H^+-ATPase, 68
  V-ATPase, 67, 68
  vacuolar H^+, 67
attachment, 219, 221, 254, 255, 264, 294
auto-signaling hypothesis, 227
autophagosome, 73
autophagy, 54
  macroautophagy, 64, 73
auxins, 295
axl2, 147

bafilomycin, 68
Bary, Anton de, 242
BCECF, 67
Bem1, 140, 147, 148
Bem3, 146, 147
β-1,3-glucan, 98–103, 108, 183
β-1,4-glucan, 109
β-1,6-glucan, 98, 99, 103–105
Bim1, 143
biofilm, 183
biofilms and mating, 213
biotrophic, 26, 70, 269–275, 302
biotrophs, 252
Bni1, 131, 139, 150–152, 156
Bnr1, 150
BOI1, 157
BOI2, 157
branching factor, 295
brefeldin A, 30, 39
  BODIPY, 54
bud, 57, 58, 63
  clathrin-coated, 59
  developing (in yeast), 50
bud site marker, 143
  Bud3, 143
  Bud4, 143
  Bud10, 143
Bud1, 147
Bud2, 147, 157

Bud3, 147
Bud4, 147, 152
Bud5, 147
Bud6, 143, 150–152, 156
budding, 168
  vacuole bounding membrane, 72
butyl methyl methacrylate embedment, 56

Ca
  localization, 67
Ca^{2+}, 51, 67, 225
Ca^{2+} gradient, 130
cables, 143
CAD1, 75
cadmium, 75
calcineurin, 183
calcium, 60
calcium channel, 183
calcium signaling, 183
calmodulin, 60, 183
cAMP, 257
cAMP pathway, 175
cAMP signaling, 171
capsule, 105
carbohydrate-active enzymes, 298
carboxy-DFFDA, 50–52, 54, 55, 68
carboxyfluorescein, 51, 67
carboxypeptidase Y, 54, 70
carboxySNAFL, 67
catabolic repression, 275
CCN1, 141
Cdc12, 152
Cdc2, 138
Cdc24, 138, 139, 146–149, 173
Cdc28, 138–141, 149
Cdc34, 142
Cdc42, 138, 139, 145–149, 151–153, 173
Cdc5, 142
CDCF, 67
CDF, 75
cell, 50, 52, 56, 59
  animal, 52, 58, 70–72, 74
  cycle, 51, 58
  eukaryote, 50, 60, 72
  expansion, 71
  fixation, 56
  fractions, 65
  freeze-substituted, 72
  guard, 58
  hyphal, 62
  hyphal tip, 49, 59, 74
  live, 64
  living, 49, 51, 53–55, 57, 66, 76
  logarithmic, 67
  mammalian, 73, 74
  penultimate, 58, 67
  periphery, 63
  plant, 53, 73, 75
  preservation, 56
  stationary, 67
  surface, 71
  tip, 2, 26, 50, 57, 58, 67, 69
  to cell, 69
  wild-type, 53, 67, 74
  zinc-depleted, 74
cell cycle, 99, 169, 185
cell end makers, 129
cell polarity, 20, 127, 168, 185
cell tracker, 76
  reagents, 51
cell wall, 52, 65, 72
cell wall biosynthesis, 185
cell wall construction genes
  AGS1, 109
  Ags1p, 99
  agsA, 112
  Bgl2, 107, 110
  CHS, 108, 109
  Crh, 110
  Dcw1, 111
  Dfg5, 111
  Ecm33, 110
  FKS1, 106, 108
  FKS2, 111
  Gas, 110
  Gel, 110
  Hoc1, 108
  Kre6, 104, 105, 109
  MOK1, 109
  MOK11, 109
  MOK12, 109
  MOK13, 109
  MOK14, 109
  Phr, 110
  Sps2, 110
cell wall expansion, 238
cell wall extension, 245
cell wall integrity pathway, 111
cell wall morphology, 98–100
  yeast walls, 105
cell wall polysaccharides
  α-1,3-glucan, 99, 101, 102, 104, 105, 112
  α-1,6-galactan, 106
  α-glucan, 101
  β-1,3-glucan, 98, 102
  β-1,4-glucan, 101, 109
  β-1,6-glucan, 98, 99, 103–105
  chitin, 98, 102, 105
  galactomannan, 103
  galactosaminogalactan, 103
  glucuronoxylomannan, 105, 106
  poly-N-acetylgalactosamine, 103
cell wall proteins
  Bad1, 107
  Bad1p, 101
  GPI-CWP, 98
  PIR cell wall protein, 106
  PIR proteins, 98
cell wall-degrading enzymes, 246, 274
cellular automata models, 321
cellular compartmentalization, 1
  biochemistry of, 24
cerato-platanin, 299
CFDA, 51, 52, 54, 70
chemical fixation, 49, 55, 56, 58, 65, 70
chemotaxis, 252
chitin, 100, 183
chitin synthase, 108, 183

chloride channel, 30
chloromethyl dyes, 52, 76
Chs2, 143
Cla4, 150–152
clathrin, 2, 18, 31, 36, 38, 41, 56, 59, 72, 73
  associated proteins, 17
  binding proteins, 17, 36
  light chain, 36
CLB2, 140
CLIP170, 126
ClipA, 126
Cln1, 139–141
Cln2, 139–141
Cln3, 139–141
CMAC, 51, 52, 54, 55, 76
CMFDA, 51, 52, 55, 76
CO_2, 170
cobalt, 74
COG complex, 11, 15, 17, 34, 36
comparative genomics, 22
concanamycin, 68
concanavalin A, 24, 25, 28, 39, 40, 56
confocal laser scanning microscopy, 11
conidia, 52, 53
conidiation, 228
conidiophores, 53
cord, 309, 316, 319, 325
cortical actin, 125
cortical markers, 138
cortical patches, 143
Cot1p, 74
Cph1, 173
CPY, 70, 73
  pathway, 73
cryofixation, 56, 65, 66
cryosections, 59
Cvt pathway, 73
CWI pathway, 112
cyclin, 185
  hypha-specific, 180
cyclophilin, 268
cyst
  germination, 256
cysteine protease, 179
cysts, 226
cytochalasin, 62, 130
cytodifferentiation, 294
cytoplasm, 64, 66–69, 73, 74, 76
  tip, 58
  to vacuole pathway, 73
cytoplasmic streaming, 50, 58, 70
cytoskeleton, 23, 26, 51, 56, 61–63, 70, 76, 123, 142, 244, 245, 276
  vacuolar integrity, 26

diffusion, 64, 68–70, 74, 76
  coefficient, 69
$DiOC_6(3)$, 55
DLVO theory, 221
DNM1, 59
DSL1, 34
dynactin, 63
dynamin, 6, 17, 18, 37, 59, 61
  related proteins, 18, 24, 37, 41
dynein, 62, 63, 127, 128
  cytoplasmic, 63

EB1, 124
ectomycorrhiza, 299
ectomycorrhizal mantle, 293
ectomycorrhizal mutant, 302
Efg1, 175
EGFP, 51, 54
electron microscopy, transmission, 24
  three-dimensional imaging, 24
electrotaxis, 252
embedding, 171
embedding pathway, 180
EMTOC, 124
encysted, 226
encysted zoospore, 229
encystment, 227
endocytic compartment
  early, 71
endocytic pathway, 52, 53, 56, 70–72
endocytosis, 2, 13, 16, 31, 36–38, 41, 52, 53, 59, 71, 72, 143, 148, 154, 261, 323
endomembrane, 56
endomembrane system, 1
endoplasmic reticulum, 23, 24, 54, 55
  cisternal sheets, 25
  comparative genomics, 3
  COPII proteins, 8–11
  ER-Golgi anterogade pathway, 8, 30, 31
  ER-Tracker^{TM}, 54
  filamentous fungi vs. yeast, 26
  motility, 26
  peripheral network, 25, 40
  proteins, 3, 4
    luminal, 3
    membrane, 3
  smooth, 25
  tubular–vesicular network, 26
endosomal pathway, 72
endosome, 11, 16, 36–39, 51–54, 61, 62
  early, 52, 63, 70, 71
  late, 19–21, 35, 38, 39, 54, 70, 71
  membrane proteins, 21
  prevacuolar, 70
  prevacuolar compartment, 20
  proteins, 19–22
  recycling to Golgi, 20
  sorting, 71
  sorting complexes, 19
  transport, 20
environmental stress, 170
enzyme, 53, 56, 60, 67, 68, 73
  hydrolytic, 67
ER-Tracker^{TM}, 19, 54
esterases
  cytoplasmic, 52
Exo70, 145, 146, 153
exocyst, 138, 145, 148, 153, 185
exocytosis, 22, 32, 53, 72, 153, 276
  proteins, 19–22
extracellular matrix, 221, 255
extrahaustorial matrix, 271
extrahaustorial membrane, 271

extramatrical mycelium, 293

Far1, 140, 142, 147, 149
farnesol, 183
filasome, 23, 28, 37, 38, 261, 262
fission yeast, 144
Fkh2, 141
flagella, 252
flow cytometry, 54
fluorescence recovery after photobleaching (FRAP), 49, 64, 68, 324
fluorescent probes, 49, 51, 54, 55, 57, 64, 67, 73, 76
  dextrans, 52, 72
  FuraZin-1, 74
  LysoSensor, 51
  LysoTracker, 51
  membrane-impermeant, 52
fluorescent proteins, 2, 25, 26, 32, 41, 51, 53, 90, 123, 125
  reef coral FP, 40, 53
FM1-43, 52, 53
FM4, 53
FM4-64, 51–55, 61, 71, 72, 156
For3, 129
foraging strategies, 310
freeze substitution, 24, 28, 33, 38–40, 49, 55–57, 65, 66, 70, 72, 73, 269
  vacuolar diffusive, 69
freeze-dried, 65
freeze-drying, 66
frozen bulk specimens, 66
frozen section, 65, 66, 70
frozen-hydrated, 66
fruiting body, 292
functional complementation, 11
functional mycelial unit, 309
Fus3, 149
Fzo1, 59
Fzo1p, 59

G protein, 253
G protein complex, 149
G1 arrest and mating, 210
G1 cyclin, 139, 140
G2 cyclin, 139, 140
galactosamine, 104
galectins, 107
ɣ-tubulin, 124
GARP complex, 19
gene
  deletion, 7, 11
  expansions, 41
  targeting, 2, 7
genetic mycelial unit, 309
genome, 297
germ tube, 50, 52, 70, 169, 253, 258
germination, 26, 224–230, 238, 257–260
GET complex, 31
GFP (green flourescent protein), 51, 53–56, 59–63, 73, 76
Gic1, 150, 152
Gic2, 150, 152
Gin4, 142–144
Glomeromycota, 291
glucose, 170
glutamine, 301
glutamine synthetase/glutamate synthase cycle, 302
glutathione, 51, 52, 75, 76
glycogen, 38, 259, 260, 266, 267
glycoproteins
  galactomannoproteins, 99, 100, 104
  mannoproteins, 98
glyoxylate pathway, 299
Golgi, 1, 28–34, 53, 54, 57, 59, 62, 72, 107, 112, 139, 143, 145, 262
Golgi apparatus, 5, 24, 27, 41
  concanavalin A binding sites, 28
  COPI proteins, 8–11
  fenestrated cisternae, 28
  Golgi-ER retrogade pathway, 8, 9, 19, 30
  matrix proteins, 29
  proteins, 5–7, 29–32
    resident, 5, 6
    retention, 6
  stacked membranes, lack of, 27, 29, 41
Golgi vesicles, 51
golgins, 6, 29
GORASPs, 6, 29
grazing, 319, 320
growth, 49, 58, 69
  bipolar, 62
  conditions, 66
  form, 51
  inhibiting conditions, 58
  logarithmic, 67
  medium, 54
  microtubule, 54
  rate, 52, 55
  tip, 2, 41, 72, 142, 144, 155, 185, 227, 260, 262, 320, 322
GTP, 59, 60
GTPɣS, 59
GTPase, 60, 61, 173

Hartig net, 72, 293
haustoria, 228, 269
haustoria expressed secreted proteins, 298
haustorial mother cells, 269
HDEL/KDEL receptors, 27, 41
hemibiotrophs, 252
heterokaryon incompatibility, 298
HEX-1, 89–92
  alternative splicing, 90
  crystal lattice, 91, 92
  immuno-gold detection, 89
  peroxisome targeting signal (PTS-1), 90
  self-assembly, 90
hex-1, 93
  mRNA transcripts, 93
  phylogenetic distribution, 93
HGC1, 141
histone deacetylase, 177
Hof1, 151
homotypic vacuole fusion, 50, 52, 54, 59–61, 73
HOPS complex, 19
Hsl1, 142
hydrophobicity, 221, 254
hydrophobins, 264, 296
hydroxyurea, 142
hypaphorine, 295
hypha

anastomosis, 87
evolution, 87
mycelium, 87
hypha-to-yeast morphogenesis, 168
hyphae, 167
hyphal apex, 23, 33, 125, 130, 154, 155, 260, 261
hyphal development, 172
hyphal growth rate, 227
hyphal orientation, 184
hyphal tip cell, 2, 22, 23
hyphopodia, 228
hypoxia, 171
hypoxia pathway, 180

immunocytochemistry, 25, 38, 55, 56, 72, 266, 271, 272
immunofluorescence, 56, 60, 71
immunogold, 56, 59
immunolocalization, 62, 123, 273
inducible promoters, 22
infection strategies, 251
infection vesicle, 270
inositol phosphate signaling, 184
interfacial matrix, 272
invertase, 100, 272, 273
ion
and phytochelatins, 75
distribution, 76
extraction, 74
redistribution, 65, 66
retaining, 55
sequestration in vacuoles, 74
toxic, 74
transport, 67
Iqg1, 152
isoamyl alcohol, 141
isotropic growth, 138

Kar9, 143
Kin1, 62
kin2, 53
kin3, 62, 63
kinesin, 62, 63, 127, 158
KipA, 126, 157, 158

L-systems, 322
lanthanum, 72, 224, 226, 229
latrunculin B, 62, 130, 144, 157, 258
lipid raft, 129
LMA1, 60
Lucifer Yellow, 52, 71
LY-CH, 52, 53, 55, 72
lysosomal compartment, 19, 38, 39

magnesium, 67
Mal3, 144
mannoproteins, 299
mannose-6-phosphate receptors, 38
mannosyl-phosphate, 108
MAP kinase, 257
MAPK pathway, 172
mass fractal dimension, 314
mastigonemes, 253
mathematical models, 320
mating
Candida albicans, 195
Candida dubliniensis, 208
Candida glabrata, 198
mating on skin, 209
mating pheromone, 71, 149
mating type like (MTL) locus, 197
MDY-64, 51
mechosensitive Ca^{2+} channel, 230
melanin, 98, 106, 230, 246, 265
membrane
cell, 49
channel, 68
domain, 56
dynamics, 56
endosomal, 73
flow, 55, 56
fusion, 50, 59, 60, 73
immobilization, 56
impermeant, 52
inner mitochondrial, 59
interaction, 55
internalisation, 71, 72
invagination, 61, 64, 73
label, 51, 53
outer mitochondrial, 59
permeant ester, 67
plasma, 52, 53, 59, 65, 71–74
potential, 51
recycling assay, 52
retrieval, 70, 72
scission, 59
selective dyes, 52
target, 60
targeting, 71
transfer, 70
transport, 76
vacuole, 50–54, 61, 67, 68, 71–74
vesicle, 60
membrane fusion, 36
metallothionein, 268, 273, 299
Mgm1p, 59
microelectrodes, 65
microscopy
confocal, 49–51, 53, 56, 57, 61, 66
differential interference contrast (DIC), 49, 51, 55
electron, 49, 55–57, 59, 65, 70–72
fluorescence, 50, 57
light, 55
video, 51
microtubule, 63, 144, 258
and tubular vacuole network, 59
and vacuolar tubules, 62
depolymerisation, 62
drugs, anti-, 58, 62, 74
elongating, 62
gliding, 63
growth, 54
longitudinal, 62
motility, 63
motors, 54, 60, 62, 63
Ni^{2+} disruption, 74
tracks, 62, 63
microtubule cytoskeleton, 323
microtubule plus end, 125

microtubules, 26, 37, 49
mitochondria, 53, 54, 59, 62, 143
  fusion and fission, 58
  inheritance, 59
  microfilament, 63
  movement, 63
  movement of, 62
  network, 74
  positioning, 63
  tubular, 54
  tubular networks, 58, 59
mitochondrial, 56
  outer membrane, 59
mitogen-activated protein (MAP) kinase pathway, 172
mitotic exit network, 143
Miyoshi, Manabu, 242
Mlc1, 139, 145, 152, 156, 159
Mn, 74
Mod5, 127, 129
morphogenetic checkpoint, 185
morphogenetic signaling pathway, 170
motility, 74
  actin filament-based, 63
  effects of zinc and nickel on, 74
  endosome, 62
  larger vacuoles, 74
  organelle, 62
  transport along the vacuolar conduit, 74
  tubule, 76
  vacuole, 49, 51, 55, 58, 61–63, 68, 69, 76
Msb3, 145, 150, 152
Msb4, 145, 150, 152
MTOC, 124
multiphoton microscopy, 11
multivesicular bodies, 38, 39, 56, 71–73
mutant
  class E vacuole protein sorting, 70
MVB, 71, 72
mycelial network, 49, 309
  adjacency matrix, 311, 319
  α−index, 313
  alpha coefficient, 318
  betweenness centrality, 315, 318
  central point dependence, 318
  central point dominance, 315, 317
  clustering coefficient, 313, 318
  control, 310
  coordination, 326
  cost, 310, 312, 314
  cyclomatic number, 313
  diameter, 314, 318
  electrical circuit analogue, 319
  global efficiency, 315, 319
  graph theory, 311
  hub and spoke models, 322
  link weight, 313, 318, 319
  meshedness coefficient, 318
  node degree, 313, 316
  node strength, 313, 317
  reachability, 315, 317, 319
  resilience, 310, 315, 317, 319
  shortest path, 314, 317, 318
  topology, 313
  transport, 310, 314, 318, 319, 323
  vulnerability, 315, 319
  weighted, 311
mycelium, 88
  peripheral growth zone, 88
mycorrhiza, 66, 69, 75, 291
  arbuscular, 50, 70
  ecto-, 49, 65, 67, 70, 72, 76
MYO1, 143
Myo2, 63, 139, 143, 145
MYO4, 143
myosin, 7, 29, 63, 109, 121, 130, 131, 143, 151, 183, 258

N-acetylglucosamine, 172
N-glycosylation, 107
nanogold
  internalisation of, 71
neckbands, 271
necrotrophs, 252
negative regulation, 181
NETO, 138
neutral red, 51
nickel, 74
nitrogen, 74
  starvation, 73
  storage of, 67
  supply, to growing hyphal tips, 69
  transport, 69
NKIN, 63
NMR, 65–67, 76
nocadazole, 142
nonconventional export, 107
NSF, 60
Num1, 127
nutrient, 58
  micro-, 75
nutrient acquisition, 293
nutrient mobilisation, 276
nutrient transport, 70, 318, 323
  bi-directional movement, 325
  diffusion, 324
  mass flow, 324, 325
  non-invasive mapping, 325
  phase domains, 326
  pulsatile component to N-transport, 326
Nyv1p, 60

O-glycosylation, 107
oestrodiol, 171
Oomycetes, 251
  phylogenetically, 251
optical tweezer, 241
Oregon Green, 51
organic nitrogen, 292
osmolality, 237, 238, 244
osmotic pressure, 237
osmotic stress, 244, 245
oxygen, 170, 300

PacC, 179
PAK kinase, 151
pathway
  diffusive, 69
  vacuolar, 69
Pea1, 150

penetration peg, 246, 253, 268
Pep12, 54, 71
peripheral growth zone, 311, 324
peroxisomes, 143
pH, 54, 71
  ambient, 171
  cytoplasmic, 67
  intracellular, 51
  vacuolar, 73
  vacuole, 49, 67
pH signaling, 171
pH signaling pathway, 178
pheromone, 209–212
pheromone response pathway, 173
phosphate, 67, 69, 74
phosphodiesterases, 177
phospholipase, 300
phospholipase C, 184
phosphorus, 66, 67, 74, 301
photon-counting scintillation imaging, 325
Pkc1, 146
plasma membrane, 36
PO_4^{3-}, 74
Poiseuille equation, 311
polarisome, 130, 138, 150, 158–160, 185
polarity, 262
polarized growth, 168
polarized secretion, 145
polyphosphate, 64–67, 73, 76, 301
Pom1, 144
potassium, 66, 67, 74
prenyl residue, 129
pressure probe, 239, 241
prevacuolar compartment, 11, 20, 54, 70, 73
primary septum, 143
probenecid, 52
progesterone, 171
protease, 60, 243, 298
protein kinase A (PKA), 177
protein kinases, 174
protein(s)
  basic, 67
  endomembrane, 3–22
  glycosylation, 33
  localisation, 60
  motor, 63
  multidrug resistance-associated, 75
  retrieval, 72
  secretion, 32
  sorting, 67, 70, 71, 76
  sorting pathway, 54
  targeting, 49, 61, 67, 70, 71
  transport, 1
  turnover, 72
  vacuole fusion, 54
proteolytic processing, 67
proteomic, 253
protoplast, 71
pseudohypha, 167
pulsatile growth, 242
punctate structures, 52, 54
PVE, 70

Q-SNAREs, 12, 60
quantitative trait locus, 302
quinacrine, 51
quorum-sensing, 182

R-SNAREs, 12, 60
Rab, 59–61
RAB BAPs, 13
RAB GAPs, 12–16, 34
RAB GEFs, 12–16, 34, 35
RAB GTPase, 12–16, 33, 34, 41, 145
Rac, 131
Rac GTPase, 146
  CflB, 146
  Rac1, 146
Ras1, 176
ratio, 61
  -metric analysis, 54, 74
  imaging, 67
RCY1, 71
rcy1, 71
Rdi1, 147
receptors, 294
repression, 181
Rga, 146, 147, 153
rhizomorphs, 247, 293, 302
Rho, 131
Rho1, 146, 150, 151, 153
RHO3, 157
Rho3, 145, 153
Rho4, 146, 151
rhodamine 123, 54
Rhodamine B, 54
Rsr1, 147, 148, 157

SAR1 GTPase, 9, 32
Sec2, 145
Sec3, 145
Sec4, 145, 146, 152
Sec9, 146
Sec12, 32
Sec15, 145, 153
Sec17p, 60
Sec18p, 60
secreted enzymes, 237, 243, 247
secretory pathway, 24, 32–36
secretory vesicles, 137, 139, 143, 145, 153
segregation structure, 50, 57, 58, 63, 70
SepA, 131, 156
septa, 50, 87, 98, 138, 143, 168
septal pore cap, 25, 26, 40, 87
septins, 143, 153, 169, 183
  Cdc10, 143
  Cdc11, 143
  Cdc12, 143
  Cdc3, 143
  Shs1, 143
septum, 50
serum, 170
shmoos, 138, 144
Sic1, 139, 140
signal transduction, 257
signals, 294
Slt2, 150
SNAP, 60

SNARE, 12–16, 33, 34, 53, 59–61
  complex, 60, 73
  mediators, 12
  regulators, 60
SNARF, 67
Snc1, 53
SOL1, 142
SPA2, 137
Spa2, 150–152, 156
SpaA, 131, 156, 157
spindle pole body, 122, 124
Spitzenkörper, 2, 52, 53, 89, 100, 121, 139, 153, 158–160, 185, 228, 260
spore, 252
  dormancy, 257
  germination, 256, 259
spore tip mucilage, 221, 254
START, 185
Start, 139
Ste11, 152
Ste2, 71, 149
Ste20, 150–152
Ste20/p65^{PAK} family, 174
Ste3, 149
sterol biosynthesis, 27
stomata, 262, 265
strain gauge, 239–243, 245
stretch-activated channel, 171, 183, 227
strigolactones, 295
structure
  cellular, 56
styryl dyes, 51
sugar transporter, 273
surface topographical feature, 230
Swe, 141
switching and mating competence, 203
swoD, 131
swoF, 131
symbioses, 292
synteny, 297

t-SNARE, 51, 54, 59–61, 71, 145
  Sec9, 145
  Sso1, 145
  Sso2, 145
Tea1, 127, 129, 144, 157
Tea2, 126, 138, 144, 157
Tem1, 143
temperature, 170
tetraspanin, 268
thermal dimorphism, 101
thigmotropism, 262
tip growth, 144, 155, 260, 320
tip high Ca^{2+} gradient, 225, 227
Tip1, 126, 144
tissue-degrading enzymes, 242
Tlg1p, 71
Tlg2p, 71
tomography, electron, 24
tonoplast, 52
topography, 263
Tpk isoform, 177
transcript profiling, 182
transcription factor, 173, 253
transcriptome, 298
transformation, 303
transport
  basic amino acids, 67
  diffusive, 69, 73
  endosome, 63, 72
  glutathione-conjugate, 75
  long-distance, 49
  longitudinal, 64, 68
  microtubules, 63
  nitrogen, 67, 68, 76
  nutrient, 50, 74–76, 309
  organelle, 60, 62
  organic anion, 52
  phosphate, 67–69, 76
  phytochelatin-Cd complex, 75
  protein, 69, 72
  proton, 68
  rate, 69
  retrograde, 61
  sugar, 69, 70
  tubule, 57, 61, 68, 69, 76
  vacuole, 49, 64, 65, 68–70, 74–76
  vacuole content, 57
  vesicle, 57, 60, 69
  zinc, 75
transporter, 71, 300
  ABC, 75
  ATP-binding cassette, 75
  cation, 74
  CDF, 74
  efflux, 74, 75
  glutathione, 52
  influx, 74
  sugar, 274
  vacuole membrane, 74
  zink, 74
transposable elements, 297
TRAPP complex, 8, 26
trimeric G protein, 138
tubule, 50, 53–59, 61, 64, 68, 69, 72–74, 76
tubulin, 74
Tup1-Ssn6 corepressor, 181
turgor pressure, 238, 260
tyresol, 183

ubiquitin, 178
ubiquitination, 71
ugo, 59
Ugo1p, 59
ultrastructure, 55, 56, 72, 76
urea, 302

v-SNARE, 60, 145
  Snc1, 145
Vac8, 54
Vac8p, 61
vacuole(s), 11, 19, 38, 49–76, 143
  acidification, 67, 68, 74
  amino acids in, 67
  detoxifying, 49, 74–76
  differentation, 49
  differentiation, 51, 55, 68, 73, 75
  motile, 49–76

protein, 19–22
solute transport, 324
spherical, 49, 50, 54, 55, 61, 62, 69, 73, 74
system, 323
transport, 51
tubular, 49–76
Vam3, 54
Vam3p, 54, 59, 60, 71, 73
Vam7p, 61
vesicle(s), 53, 55–59, 62, 63, 65, 71–73, 76
apical, 52, 53
coated, 51, 59, 72
COPI, 8–11, 30
COPII, 8–11, 30
docking, 60
fusion, 60, 61, 69
movement, 323
supply centre, 122, 261
targeting, 73
trafficking, 31, 33, 56
virulence factor, 168
Vph1p, 61
VPS
pathway, 73
vps, 70, 71
Vps1, 59
VSC, 122

wall degrading enzymes, 269
Wee1, 141
white–opaque switching, 201
whole-genome duplication event, 24, 27
whole-genome shotgun, 297
wood wide web, 309
Woronin body
as adaptation, 93
function, 90
genesis, 91
inheritance, 93
purification, 89
turgor pressure, 91
ultrastructure, 88

X-ray microanalysis, 65, 66, 74

yeast, 50–54, 56, 57, 59–61, 63–65, 67, 70–76
yeast–hypha morphogenesis, 171
Yeb3, 54
Ypt31, 145
Ypt32, 145
Ypt7, 59–61
Yup1, 61

zinc, 74, 75
zinc shock, 74, 75
-depleted cell, 74
zoospores, 252
motility, 253
zoosporogenesis, 229
Zrc1p, 74
Zrt3p, 74, 75